→1st Symposium on Space Educational Activities

1ST SYMPOSIUM
SPACE / EDUCATIONAL / ACTIVITIES
PADOVA - 9/12 December 2015



Università degli Studi di Padova
CISAS G. Colombo
Dipartimento di Fisica e Astronomia Galileo Galilei
esa European Space Agency
agenzia spaziale italiana
Space Generation Advisory Council
Patrocinio del Comune di Padova

European Space Agency

CONTENTS

Introduction from CISAS Director

Introduction from ESA Education Office

Introduction from the Symposium Chairman and the Organizing Committee

1stSSEA program

SESSION 1: A - Nanosat Programs (Wednsday 09th - 11.30) Chairman: Prof. Alessandro Francesconi

1	Andris Slavinskis	THE ESTONIAN STUDENT SATELLITE PROGRAMME: PROVIDING SKILLS FOR THE MODERN ENGINEERING LABOUR MARKET
2	Raffaele Mozzillo	CUBESAT TEAM OF POLITECNICO DI TORINO: PAST, PRESENT AND FUTURE PROJECTS
3	Rasmus Gundorff Sæderup	AAUSAT5 - AN EVALUATION OF A STUDENT-RUN CUBESAT PROJECT
4	Ignacio Barrios Tascón	QBITO DEVELOPMENT AND STUDENTS INVOLVEMENT
5	Marcello Valdatta	ELEONORA: A INTERNATIONAL SATELLITE PROJECT FOE THE CANADIAN SATELLITE DESIGN CHALLANGE
6	Aleksander Lidtke	ENHANCING SPACEFLIGHT SAFETY WITH UOS3 CUBESAT

SESSION 2: G - Test Platforms & Facilities (Wednsday 09th - 17.30) Chairman: Dr. Francesco Sansone – Dr. Livia Savioli

1	Mattia Mazzucato	DEVELOPMENT OF A GROUND-BASED COOPERATING SPACECRAFT TESTBED FOR RESEARCH AND EDUCATION
2	Sebastiano Chiodini	MORPHEUS: A FIELD ROBOTICS TESTBED FOR SOIL SAMPLING AND AUTONOUMUS NAVIGATION
3	Lennart Kryza	DEVELOPING TECHNOLOGIES FOR SPACE ON A TERRESTRIAL SYSTEM: A COST EFFECTIVE APPROACH FOR PLANETARY ROBOTICS RESEARCH
4	Bence Góczán	BALLOON PLATFORM FOR HIGH ALTITUDE RESEARCH
5	Marco Barbetta	ARCADE EXPERIMENT ON BOARD BEXUS 13 AND 17: DESIGN, INTEGRATION AND FLIGHT OF A TECHNOLOGY TEST PLATFORM WITHIN A STUDENT BALLOON PROGRAMME

SESSION 3: F - Hyper-gravity & Low-gravity Experiments (Thursday 10th - 09.30) Chairman: Dr. Natacha Callens

1	Davide Petrillo	FELDS EXPERIMENT: A NEW FLEXIBLE SOFT DOCKING CONCEPT
2	Francesco Creatini	PHOS EXPERIMENT: THERMAL RESPONSE OF A LARGE DIAMETER PULSATING HEAT PIPE ON BOARD REXUS 18 ROCKET
3	Ágota Simon	INTERACTION OF LASER EXPOSED NON-ANTIBIOTIC SOLUTIONS WITH TARGET SURFACES IN HYPERGRAVITY CONDITIONS: ESA “SPIN YOUR THESIS!” CAMPAIGN
4	Zafiro Aspridou	EFFECT OF HYPERGRAVITY ON BACTERIAL MOTILITY AND HEAT RESISTANCE
5	Marcello Valdatta	FROM REDEMPTION TO ARTICA. THE ROAD FROM AN EDUCATIONAL PROJECT TO AN ACTUAL DEVICE
6	Miriam Manzoni	SPIN YOUR THESIS! 2013: A PULSATING HEAT PIPE ON THE LARGE DIAMETER CENTRIFUGE

SESSION 5: D - Educational Programs & Strategies 2 (Thursday 10th - 11.30) Chairman: Prof. Michéle Lavagna

1	Federico Curiano'	EDUCATIONAL ACTIVITY OF SAPIENZA SPACE SYSTEMS AND SPACE SURVEILLANCE LABORATORY – S5LAB
2	Dario Modenini	SPACE ENGINEERING AND SMALL SATELLITES EDUCATIONAL ACTIVITIES AT UNIVERSITY OF BOLOGNA
3	Alexander Biebricher	ON THE STUDENT ROCKET PROGRAM AT ANDØYA SPACE CENTER

SESSION 5: E - Atmospheric & Planetary Experiments (Thursday 10th - 17.00) Chairman: Prof. Anton Ivanov

1	Encarnación Serrano Castillo	AEROSOLS AND CLOUDS FORMATION RESEARCH IN A5-UNIBO EXPERIMENT ONBOARD BEXUS 18- LESSONS LEARNED
2	Sascha Wizemann	MICRO-REENTRY-CAPSULE-2 REXUS
3	Timo A Stein	THE COSMIC PARTICLE TELESCOPE PROJECT – FIRST RESULTS
4	Sebastiano Chiodini	MISSUS EXPERIMENT SENSORS DATA ANALYSIS
5	Daniel Nilsson	SALACIA REXUS PROJECT
6	Matteo Duzzi	SCRAT EXPERIMENT: A STUDENT EXPERIENCE
7	Davide Paganini	POLARIS EXPERIMEN: STRATOSPHERIC FLIGHT OUTCOMES AND EXPERIENCE GAINED FROM THE REXUS-BEXUS PROGRAMME

SESSION 6: C - Educational Programs & Strategies 1 (Friday 11th - 09.30) Chairman: Dr. Riccardo Rando

1	Kartik Kumar	EDUCATIONAL OPPORTUNITIES THROUGH MARS ANALOG RESEARCH
2	Lawrence Reeves	THE CANADIAN SATELLITE DESIGN CHALLENGE: BUILDING FUTURE SPACE CAPABILITY IN CANADA
3	Johannes Gutsmiedl	PROVIDING HANDS-ON SPACE EDUCATION BY INVOLVEMENT OF COLLABORATING SELF-RELIANT STUDENT TEAMS
4	Ana Raposo	SPACE GENERATION ADVISORY COUNCIL PROJECT GROUPS- EDUCATIONAL ACTIVITIES IN AN INTERNATIONAL NETWORK

SESSION 7: B - Nanosat Technologies (Thursday 11th - 11.30) Chairman: Prof. Anton Ivanov

1	Lasse Bromose	TOWARDS A COLLABORATIVE DISTRIBUTED GROUND STATION FOR SMALL CUBESAT TEAMS
2	Tom Hoppenbrouwers	ICE CUBES – A FAST TRACK, LOW COST SERVICE FOR SMALL EXPERIMENTS TO THE ISS
3	Arthur Scharf	HORIZON ACQUISITION FOR ATTITUDE DETERMINATION USING IMAGE PROCESSING ALGORITHMS - HORACE ON REXUS 16 – AN EDUCATIONAL PROJECT
4	Damien Watremetz	DEVELOPMENT AND TESTING OF THE ON-BOARD SOFTWARE FOR QB50 NANOSATELLITE IP2SAT
5	Boris Segret	AUTONOMOUS NAVIGATION FOR DEEP-SPACE CUBESATS
6	Olga Mamoutova	ON DESIGN FOR RELIABILITY OF ELECTRONICS IN NANOSATELLITE

SESSION 8: I - Students Rocketry (Friday 11th - 15.00) Chairman: Prof. Michèle Lavagna

1	Christian Bach	SOUNDING ROCKET DEVELOPMENT WITH LIQUID PROPELLANTS WITHIN THE DLR STERN PROGRAMME
2	Matteo Poli	IMPROVING A SOUNDING ROCKET TECHNOLOGY DEMONSTRATOR FOR STUDENT EXPERIMENTAL ACTIVITIES
3	Aureliano Rivolta	LOW COST MEMS IMU CALIBRATION FOR AEROSPACE STUDENT ACTIVITIES
4	Danylo Malyuta	ACTIVE MODEL ROCKET STABILIZATION VIA COLD GAS THRUSTERS
5	Giovanni Pandolfi	PRIMO: AN ULTRALIGHT LAUNCH VEHICLE FOR NANO AND MICROSATELLITES
6	Hamed Gamal	DESIGN, SIMULATIONS AND ANALYSIS OF AN AIR LAUNCH ROCKET FOR HUNTING LOW EARTH ORBIT'S SPACE DEBRIS

SESSION 9: H - Students Research (Friday 11th - 17.30) Chairman: Prof. Alessandro Francesconi

1	Alvaro Tomàs Soria Salinas	CONVECTIVE HEAT TRANSFER MEASUREMENTS AT THE MARTIAN SURFACE
2	Lorenzo Bucci	ROBOTIC REFUELING SYSTEM FOR ON ORBIT SERVICING
3	Gilberto Grassi	MODELING A NEW CONCEPT OF TETHER DEPLOYER WITH RETRIEVABLE CAPABILITY FOR SPACE APPLICATIONS
4	Alessandro Serboli	LARGE DEPOT TO SERVICE MANNED MARS MISSIONS
5	Simon Olvhammar	SOFTWARE-DEFINED DICKE-SWITCHED RADIOMETRY USING ETTUS USRP AND GNU RADIO

Poster Session (Thursday 10th - 15.00)

1	Sebastian Hettrich	ANALOGUE PLANETARY RESEARCH AS A TOOL FOR EFFECTIVE SPACE EDUCATION
2	Sergio Erculiani	SEARCHING FOR LIFE FINGERPRINTS IN THE LABORATORY
3	Zoe Lola	"SO... YOU WANT TO LEAVE THE EARTH" THE NECESSITY OF ASTRONAUTS PSYCHOSOCIAL SUPPORT
4	Cem Avsar	BENEFITS AND CHALLENGES OF STUDENT DRIVEN SPACE PROJECTS: A SURVEY ON HANDS-ON EDUCATION AT TU BERLIN
5	Avishek Ghosh	A STUDY AND APPROACH TO USE LUNAR REGOLITH FOR 3D PRINTING IN MICROGRAVITY ENVIRONMENT
6	Renato Macchietto	ZERO ROBOTICS: THE EXPERIENCE OF A HIGH SCHOOL TEAM FACING REAL SPACE PROBLEMS

Introduction from CISAS Director

With great pleasure, I am introducing the proceedings of the 1st Symposium on Space Educational Activities, on behalf of the University of Padova ad in particular of the Center of Studies and Activities for Space CISAS "Giuseppe Colombo".

In such a context, the "peaceful co-operation in space on a world-wide scale" - Prof. Giuseppe Colombo, Padova 1981- is extremely topical, as well as his brilliant ideas and concepts: tethered space elevators, solar reflectors and solar sails (MIT, 1979).

Since 1982, following the ethic and scientific legacy of Bepi Colombo, our Centre has participated to several international space projects and missions such as Giotto, Cassini-Huygens, Rosetta, MarsExpress, VenusExpress, ExoMars 2016, BepiColombo, Solar Orbiter, JUICE, promoting and developing the inspiration and the heritage of his contributions.

Furthermore, CISAS is deeply involved in the formation of the next generation of space experts supporting the Aerospace Engineering courses and thanks to the Ph.D. school on Sciences, Technologies and Measurements for Space, and our students are involved in a wide number of international projects, on the footsteps of prof. Colombo's international and interdisciplinary career.

Our PhD Students launched the exciting idea of the 1st Symposium on Space Educational Activities, an international event conceived as a showcase for the educational and hands-on activities as well as a place for them to meet with colleagues, experts and educators. The CISAS direction has been proud to encourage and support such initiative, advising them in the co-ordination phase but leaving to the students the whole organization of the event, trusting their skills and capabilities for a successful symposium.

The results are self-explicatory: more than two hundred attendees from Europe, Middle East and America, several scientific sessions and invited lectures. The special participation of Samantha Cristoforetti "launched in orbit" the Symposium, thanks to her own witness on the 199 days on board of the International Space Station.

The success of the 1st SEEA shall be found in the dedication and in the hard work of the Organizing Committee, as well as in the support of all the involved institutions, in particular the European Space Agency and the University of Padova, and in the enthusiasm of all the young attendees.

The important outcomes of this 1st SEAA edition are a very significant proof that the new generations of students must be continuously encouraged, stimulated and supported for applying to Space research , giving them the opportunity to learn from the experts, compare themselves and discuss with their colleagues, in the framework of future space programs and of future editions of the Symposium.



Prof. Stefano Debei
Director of CISAS "Giuseppe Colombo"

Introduction from ESA Education Office

The Education Office of the European Space Agency welcomed immediately the proposal made by the University of Padova and the Center of Studies and Activities for Space CISAS "Giuseppe Colombo" who proposed to organise a symposium on space-related programmes and activities conducted by university students. This type of symposium was recognised as offering the chance to fill an evident vacuum. The ESA Education Office decided to support the organisers, and a very constructive collaboration started. The 1st Symposium on Space Educational Activities was therefore confirmed and several other important organisations active in the space sector soon demonstrated a considerable appreciation for the initiative and offered their support in addition to ESA Education's involvement. These not only included national space agencies such as ASI, DLR, and the SNSB, but also research organisations, industry, public Italian institutions, and obviously also a number of institutions linked to Academia. Many of these partners contributed in various forms to the organisation and to the good success of the event.

The preparation of the symposium progressed well: a large number of abstracts were submitted and evaluated professionals from academic, institutional and industrial institutions accepted the invitation and the number of registrations to participate in the event exceeded the best expectations. During the symposium, presentations of a broad range of student activities from different countries were offered to the audience. This whole package of successful student projects demonstrated the value of educational hands-on opportunities. Typically these projects originate from educational scopes but in reality, for the students, they constitute a bridge to transition from their university studies to professional work. In many cases the student activities overlap with cutting-edge scientific or technological research, sometimes achieving the quality attained by professionals. Students at all levels of their university studies (Bachelor, Master and PhD candidates) presented in an international environment the content and the results of their work. This was for them an important experience in their educational and professional growth.

In addition to the thankfulness owed to the organisers of the Symposium and to those that offered their support, tribute should also to be paid to all the organisations and institutions which intelligently foster university students, offering them the chance to engage in the execution of real space programmes. This commendation is addressed, especially to professors and personnel in academia who, day by day, mentor, supervise, support and motivate the students. Their efforts clearly require plenty of personal dedication, and they are clearly based on utmost passion for their work as educators. Their day by day activities deserve the highest appreciation.

ESA Education Office as well as all organisations and personnel active in creating and supporting opportunities to allow students to engage in real space related programmes are well aware that these efforts will soon reap rewards: the university students of today are the next generation of space professionals.



Piero Galeone
Head of Tertiary Education Unit
ESA Education and Knowledge Management Office
ESA Director General's Services - Strategy Department

Introduction from the Symposium Chairman and the Organizing Committee

The proceedings collected in this book are the final stage of the 1st Symposium on Space Educational Activities, that we had the pleasure to host in Padova, Italy, on December 9th-12th, 2015. The symposium was born from the desire of a group of PhD students to create a dedicated showcase for space-related educational projects and programs; the farsightedness of ESA Education Office as well as the willingness of the Center of Studies and Activities for Space CISAS "Giuseppe Colombo" to support them allowed the concept to evolve in a bright international event with more than two hundred registered attendees from twenty different countries.

The 1st SSEA would not have been possible without the efforts of the local team that managed the whole symposium from registrations to check-outs and social events: we want to thank them all for their outstanding work. Many thanks to Piero Galeone and Natacha Callens from ESA, for their support and continuous assistance in the event planning, and to the whole Technical Committee for their commitment in the selection and organization of the technical contributions.

The 1st SSEA was more than just a collection of presentation sessions, as the attendees had the possibility to participate to dedicated lectures from NASA, ESA and ELGRA representatives, as well as to meet Captain Samantha Cristoforetti less than six months after the end of her mission *Futura* on board the International Space Station. Furthermore, the event allowed students, researchers and educators to meet and share their experiences, expanding their networks and creating new contacts at the venue and during the social events managed by the local organization.

The main contribution to the 1st SSEA was from the attendees, and we want to thank all these students and young professionals for sharing their experiences and ideas related to many interesting and innovative experiments and concepts. The papers they presented at the Symposium were divided in eight sessions plus a poster session, as reported in these proceedings. The main topics were related to ground and laboratory experiments, as well as missions in space and other relevant environments, and two sessions were dedicated to the discussion of educational programs and strategies. This proceedings book contains many reports on works still in progress, and even though few of them may include some naivety justified by the authors' young age, many papers address subjects and introduce novel ideas of outstanding value, regardless of the fact they originate from student teams.

Looking forward to a second edition of the Symposium on Space Educational Activities to further discover and display the works of these young attendees, we wish them all a long and fruitful space career.



Prof. Alessandro Francesconi
Symposium Chairman



Dr. Lorenzo Olivieri
Organizing Committee

1st Symposium on Space Educational Activities

DECEMBER 9th DETAILED PROGRAM

TIME	PROGRAM
08:30 – 09.30	**Registrations**
09:30 – 11.00	**OPENING CEREMONY** **9:30 – 10:00 Welcoming addresses** Prof. Alessandro Francesconi – Symposium Chairman Prof. Marcella Bonchio – University of Padova, Vice Rector for Research Dr. Carlo Pasqualetto – Padova Municipality Councillor Dr. Natacha Callens – Administrator European Space Agency Academy – Training and Learning Centre Prof. Ugo Galvanetto – University of Padova, President of the Study Course in Aerospace Engineering Prof. Stefano Debei – University of Padova, CISAS "G. Colombo" Director **10.00 – 11.00 CISAS Space Activities** Prof. Stefano Debei
11:00 – 11.30	**Coffee Break**
11:30 – 13:00	**SESSION 1: Nanosat Programs** Chairman: Prof. Enrico C. Lorenzini, University of Padova
13:00 – 14:15	**Lunch**
14:15 – 15:00	**Lecture: ESA Academy** Dr. Natacha Callens – Administrator ESA Academy – Training and Learning Centre
15:00 – 17:00	**Meet an Astronaut event** Samantha Cristoforetti – ESA/ASI Astronaut, Italian Air Force
17:00 – 17.30	**Coffee Break**
17:30 – 19:00	**SESSION 2: Test Platforms & Facilities** Chairman: Dr. Francesco Sansone – University of Padova Dr. Livia Savioli – University of Padova

1st Symposium on Space Educational Activities

DECEMBER 10th DETAILED PROGRAM

TIME	PROGRAM
08:45 – 09.30	**Lecture: Giuseppe Colombo** Prof. E. C. Lorenzini – University of Padova
09:30 – 11.00	**SESSION 3: Hyper-gravity & Low-gravity Experiments** Chairman: Dr. Natacha Callens – Administrator ESA Academy – Training and Learning Center
11:00 – 11.30	**Coffee Break**
11:30 – 13:00	**SESSION 4: Educational Programs & Strategies 2** Chairman: Prof. Anton Ivanov – École Polytechnique Fédérale de Lausanne
13:00 – 14:15	**Lunch**
14:15 – 15:00	**Lecture: Rosetta Mission** Mr. Sylvain Lodiot – Rosetta Operation Manager, European Space Agency
15:00 – 16:00	**POSTER SESSION & SMALL TALKS**
16:00 – 16.30	**Coffee Break**
16:30 – 17:00	**Lecture: ELGRA Activities** Prof. Monica Monici – ELGRA President – University of Florence
17:00 – 19:00	**SESSION 5: Atmospheric & Planetary Experiments** Chairman: Prof. Michéle Lavagna – Politecnico di Milano

1st Symposium on Space Educational Activities

DECEMBER 11th DETAILED PROGRAM

TIME	PROGRAM
09:00 – 09.30	**Lecture: ESA Education Hands-On Experiments Opportunities** Dr. Natacha Callens – Administrator ESA Academy – Training and Learning Centre
09:30 – 11.00	**SESSION 6: Educational Programs & Strategies** Chairman: Dr. Riccardo Rando – University of Padova
11:00 – 11.30	**Coffee Break**
11:30 – 13:00	**SESSION 7: Nanosat Technologies** Chairman: Prof. Anton Ivanov – École Polytechnique Fédérale de Lausanne
13:00 – 14:15	**Lunch**
14:15 – 15:00	**Lecture: NASA: Plans and Programs** Dr. David J. Thompson – Goddard Space Flight Center, National Aeronautics and Space Administration
15:00 – 16:30	**SESSION 8: Students Rocketry** Chairman: Prof. Michéle Lavagna – Politecnico di Milano
16:30 – 17.00	**Coffee Break**
17:00 – 17:30	**Lecture 7: ESA Education Hands-On Satellite Opportunities** Mr. Piero Galeone – Head of the Tertiary Education Unit, Education Office, European Space Agency
17:30 – 19:00	**SESSION 9: Students Research** Chairman: Prof. Alessandro Francesconi – University of Padova
19:00 – 20:00	**CLOSING CEREMONY** **"CISAS G. Colombo" BEST PAPER AWARD**

SESSION 1: A - Nanosat Programs

(Wednsday 09th - 11.30)

Chairman: Prof. Alessandro Francesconi

THE ESTONIAN STUDENT SATELLITE PROGRAMME: PROVIDING SKILLS FOR THE MODERN ENGINEERING LABOUR MARKET

Andris Slavinskis, Karl Reinkubjas, Karoli Kahn, Hendrik Ehrpais, Katrīna Kalniņa, Erik Kulu, Mihkel Pajusalu, Urmas Kvell, Indrek Sünter, Henri Kuuste, Viljo Allik, Silver Lätt, Riho Vendt, and Mart Noorma

Tartu Observatory, Space Technology Department, Observatooriumi 1, Tõravere, 61602, Tartu county, Estonia

University of Tartu, Institute of Physics, Ravila 14c, 50411, Tartu, Estonia

ABSTRACT

In this study, we analyse the Estonian Student Satellite Programme (ESTCube Programme) from the point of view of Future Work Skills 2020 (published by the Institute for the Future, 2011). The ESTCube Programme started in 2008 with the first project ESTCube-1 which is a one-unit CubeSat, launched in May 2013. The main scientific objective of the satellite was to demonstrate components of the electric solar wind sail technology in low Earth orbit. The main socioeconomical objective of the ESTCube Programme is to provide hands-on education to young engineers (secondary school and university level) through development of space technology. Members of the ESTCube team have also contributed to Aalto-1 development, are developing the European Student Earth Orbiter optical payload, are developing ESTCube-2 satellite, have established start-up companies and are providing hands-on education to school pupils.

1. INTRODUCTION

It is widely recognized that the higher education landscape is in the middle of global transformation. As one of the situation analyses, the Institute for the Future published in 2011 an analysis of the key drivers, reshaping the labor market in the future until 2020. Six drivers of change, shaping the future of the world, were described as follows: extreme longevity, rise of smart machines and systems, computational world, new media ecology, superstructured organizations, and globally connected world [1]. From those drivers of change the following ten skills, important for the people to cope with the changes, were derived [1]:

1. sense-making,
2. social intelligence,
3. novel and adaptive thinking,
4. cross-cultural competency,
5. computational thinking,
6. new media literacy,
7. transdisciplinarity,
8. design mindset,
9. cognitive load management,
10. virtual collaboration.

In order to cope with the global trends, the universities have to provide their students with appropriate learning tools and environment to develop those skills. It is even more difficult in the countries like Estonia, where the popularity of careers in science or engineering among the high school graduates is low. Thus new educational approaches and tools for both science popularization and higher education have to be adopted. Even more, with the concept of life-long learning starting from kindergarten and reaching to retirement ages, there is a need for inspiring educational programmes, which provide opportunities for all age groups of people interested in self-development.

Space has always inspired people and the space outreach activities have historically been among the most successful tools for general science popularization. At the same time, the educational space projects at the university level have been mostly designed to prepare the new work force mostly for the space sector. High costs have prevented adoption of that kind of projects in general science and engineering education. Nowadays, after the dawn of the era of nanosatellites, the space technology development has become more and more accessible for universities around the world. Thus it can be used by the educational space programmes for supporting the general science and engineering education.

In this paper, we study how an educational space technology programme, the Estonian Student Satellite Programme (ESTCube Programme), performs in the role of a nation-wide booster for the science and engineering education, engaging learners from the first grade of primary school up to doctoral level. We present the educational

design of the programme and compare the learning outcomes of the programme with the list of the Future Work Skills 2020. Based on the analysis, we describe the characteristics an educational space programme should have in order to support development of such skills.

2. ESTONIAN STUDENT SATELLITE PROGRAMME

2.1. Background

Estonian Student Satellite Programme was established in 2008. About the same time Estonia was moving towards the status of a European Cooperating State at the European Space Agency (the status was achieved in 2009). At that time, the space technology had never been taught at Estonian universities before. The programme started as an initiative of a group of students of physics, supported by the researchers from Tartu Observatory and the University of Tartu.

As the aim of the ESTCube Programme is to develop subsystems from ground up, this has lead to more than 20 master theses and more than 30 bachelor theses being written within the programme. The team has published ten peer-reviewed journal articles where students are first authors [2–11] and about ten conference papers. In total, more than 250 students have worked in the ESTCube Programme. At one time, 20-30 students are active in the team. The core team consists of about 10 students and four advisors. Three PhD students work in the team and one has graduated [12]. More than 60 presentations have been given at scientific and engineering conferences, workshops and seminars. The team has international trainees, as well as international members acquiring a degree. In total, more then 30 internationals come from Latvia, Lithuania, Ukraine, Finland, Germany, the USA, Slovenia, Canada, Spain Vietnam, Turkey and India.

2.2. Objectives

The main objective of the programme was to provide students with practical experiences in their fields of study, following the concept of Problem Based Learning [13]. At the same time, the importance of the need for training in transferable skills, like management, team work, time management, public relations, public presentation etc. was clearly recognized. The project was also meant to inspire Estonian youngsters to consider their future careers in exact sciences and engineering and to show that even the most complicated systems, like a spacecraft, can be develop in their homeland. The later one is an important aspect in the current socio-economic context of Estonia, where people are eager to look for better jobs with higher salaries abroad, mostly in the older member states of the European Union.

2.3. Projects of the ESTCube Programme

The flagship project of the programme has been development of the first Estonian satellite ESTCube-1 [9]. ESTCube-1 is a one-unit CubeSat with the mission objective to demonstrate components of electric solar wind sail (E-sail) technology [14, 15] in the Earth's ionosphere. The satellite bus worked successfully but tether deployment was non successful [11].

The successor, ESTCube-2, is currently under development with the main mission to effectively deorbit the satellite using the plasma brake [16, 17]. Such experiment would also continue to test E-sail components, since both technologies differ only by the polarity of the charge applied to the tether. In the case of ESTCube-2, new technologies for tether deployment and tether production will be demonstrated.

The ESTCube team has contributed to development of the Finnish Aalto-1 satellite which will also demonstrate plasma brake technology which is based on and improved upon ESTCube-1 payload. The satellite is planned to be launched in March 2016.

The ESTCube team participates in the European Student Earth Orbiter (ESEO) project for which an optical payload is being developed.

The programme provides cooperation opportunities for primary school pupils in form of Space Club Estronauts (weekly meetings held since 2007) and for high school students in the form of a summer work camp "Teadusmalev" (Science Task Force) (since 2012) where they are presented with a scientific or engineering problems and given freedom to solve it on their own. Since the summer of 2015, Science Task Force has become international with nine students from Estonia and three from Latvia.

2.4. Guiding Principles

While there are many different practices to set up a student satellite projects, the most convenient one from the instructional point of view is to involve a group of students in the research of a single lab under the supervision of the lab personnel. In the case of the ESTCube Programme, however, the students are in charge of the project. Students taking the responsibility and leading their own work is the first key principle of the Programme. Involvement of students from many universities is the second key principle. Involvement of an international consortium of research institutes and companies in the activities of the programme is the third key principle. The results of the student projects also give a significant contribution to the science.

3. COMPARISON WITH THE FUTURE WORK SKILLS 2020

While the Estonian Student Satellite stared three years before the list of the Future Work Skills 2020 was published, the intended learning outcomes of the programme have not been intentionally aligned with the list. However, as the authors believe the Future Work Skills 2020 is an appropriate reference to the global trends, we have analysed the activities of the Estonian Student Satellite Programme in this framework.

3.1. Sense-making

Sense-making is defined as the ability to determine the deeper meaning or significance of what being expressed [1]. In the ESTCUbe Programme, the participants are forced to develop the sense-making skills through the need to find their own way for solving problems in all the fields of activities of the project. The role of instructors is only to support the learning process and not to provide solutions.

3.2. Social Intelligence

Social Intelligence is defined as the ability to connect to others in a deep and direct way, to sense and stimulate reactions and desired interactions [1]. This ability is developed through the work in diverse teams. In all projects of ESTCube Programme, satellite subsystems are developed in multinational groups of students with different backgrounds. This skill is developed even further by the need to advocate the need for space exploration for general audience and media, when the students are forced to understand the needs of the other people in order to put their reasoning into the appropriate context.

3.3. Novel and Adaptive Thinking

Nanosatellite development is an extremely rapidly developing field of technology. As one of the key principles of the ESTCube Programme is to always aim for a significant contribution to the science, the mission objectives of the projects are highly innovative, for example, to test novel propulsion technology which would allow for record-fast Solar System exploration and enable new missions [18]. Most of the satellite subsystems have to be developed in-house using many original solutions.

3.4. Cross-Cultural Competency

The ESTCube Programme involves students from different nations with research partners from all over the world. In order to meet the project objectives and deadlines in time, the mutual understanding and tolerance are essential. Through the long term cooperation in the diverse setting, this skill is actively developed. Students are always invited to join the team already during the first year of their studies and to continue until the end of their graduate or post-graduate studies. Furthermore, some of the most active student have joined the ESTCube Programme even before, during their studies at high school. For most of the participants, this is their first experience of working in an international team.

3.5. Computational Thinking

This skill is defined as an ability to translate vast amounts of data into abstract concepts and to understand data-based reasoning [1]. As this is one of the most important professional skills of scientists and engineers, it is clearly developed for the participants of the Programme during their studies anyway.

3.6. New-Media Literacy

New Media Literacy is defined as an ability to critically assess and develop content that uses new media forms, and to leverage these media for persuasive communication [1]. The students currently attending universities belong the generation, which has grown up with the user-generated media, like YouTube, Facebook, Twitter, etc. However, the need for effective outreach of the space technology projects has forced the participant of the Programme to find optimal solutions using text, audio, and video to deliver the messages to different audiences: school children, pensioners at popularization events, researchers and other students at the scientific conferences. The ESTCube Facebook page is regularly updated by students and has more than 5000 followers.

3.7. Transdisciplinarity

Transdisciplinarity is defined as an ability to understand concepts across multiple disciplines [1]. In space projects, it has always been important not to focus only on the mission design and engineering, but also understand the applications, fundraising, media relations and public perception. This provides opportunities for students from different study programmes. In the ESTCube Programme, students from journalism, economics, management, law and even from linguistics and arts have written their theses. During regular joint reporting meetings, issues of different research are shared and thus the understanding of other fields of research is supported for participants.

3.8. Design Mindset

Design mindset is defined as an ability to represent and develop tasks and work processes for desired outcomes [1]. While this skill might be somewhat less related to the learning outcomes of the ESTCube Programme, it could be related to understanding of the difference the work environment can cause to the result. In space projects, the positive effect of Concurrent Design Facilities for mission design and conducting the reviews is well acknowledged.

3.9. Cognitive Load Management

Cognitive Load Management is defined as an ability to discriminate and filter information for importance, and to understand how to maximize cognitive functioning using a variety of tools and techniques [1]. In this respect, a space technology project, as most of other research projects, requires participants to effectively conduct literature review and synthesis of earlier research data. This ability is actively developed during the filtering of the most important sources.

3.10. Virtual Collaboration

The Estonian Student Satellite Programme, relying on cooperation of partners from many different physical international locations, is built on virtual collaboration. Several software and communication tools, like Skype, Hangouts, Confluence, JIRA, DropBox, Google Docs etc. are used to conduct regular meetings, manage tasks, and share resources.

4. RESULTS

The current status of the projects of the Estonian Student Satellite Programme is the following.

The ESTCube-1 CubeSat was launched to space on board the Vega rocket in May 2013. The satellite worked as expected; except for the following issues — a larger than expected decrease in energy production during the mission; a need for in-orbit recalibration of attitude determination sensors; ferromagnetic materials aligning the satellite frame with the geomagnetic field; and problems with reeling out the tether. However, from developing all subsystems in-house and operating the satellite, the team has gained valuable experience that could decrease the development time and improve the overall quality of the follow-up missions [11].

The next satellite mission, ESTCube-2 is in development stage — prototypes of subsystems have been and are being built. In addition to technical developments, the team is working on fundraising. At this point, the satellite is being developed in a way that it can be scaled, depending on the available funding. A one-unit CubeSat would be able to host the plasma brake experiment. A two-unit CubeSat could also test a miniaturised camera, as well as a C band communication system. The miniaturised camera could be used for monitoring on larger satellites and for proximity operations. A three-unit CubeSat could host a propulsion system for attitude control. While ESTCube-2 can use magnetorquers for satellite spin up, which provides the centrifugal force for tether deployment, such approach could not be used with follow-up mission in the solar wind, hence other means of attitude control will be required. In an ideal case, ESTCube-2 would be developed as a platform which can be used for future missions.

The Aalto-1 payload has been delivered and the satellite is planned to be launched in March 2016. A member of the ESTCube team developed motor control electronics.

For the ESEO optical payload, the team is working towards finishing engineering models. The payload consist of two cameras. Primary camera based on ESTCube-1 camera and secondary camera with improved optics, resolution and data processing unit.

The ESTCube team consist of students from the following study programmes: physics, computer science, computer engineering, measurement science, information technology, electronics, product development, mechanics, communications, navigation, aerospace engineering, economics, law, managements, linguistics and media arts.

Every summer Tartu Observatory hosts a summer training programme which invites local students, as well as international students. Many of the international students have been supported by Erasmus+ training scholarship.

More than 50 primary school pupils have participated in the activities of the Space Club Estronauts. More than 20 secondary school pupils have participated in summer work camp Science Task Force. For example, in the summer of 2015, pupils built a three-axis Helmholtz coil. Some pupils from the Science Task Force chose to study in some of the exact science fields and re-join the ESTCube team as students.

ESTCube projects appear on regular bases in all conventional media channels including evening news and the cover pages of the leading daily newspapers in Estonia. It has been widely covered by leading international news agencies.

Former members of the ESTCube team have established five start-up companies which develop space and consumer products. Co-founders of companies were active members of the core team during the time they worked on ESTCube-1. It suggests that an educational space programme might inspire students to be entrepreneurs and take other challenges. Founders of one of the companies first built up a competence in synthetic aperture radar image processing (two PhD theses) and lately established

the company.

5. CONCLUSIONS

The Estonian Student Satellite Programme is an example of an inspiring space technology exercise, useful for different age groups and supporting education in many traditional non-space curricula. A comparison with one of the visions of the work skills gaining more and more importance in the future, the Future Work Skills 2020, demonstrates that an educational space technology project could provide opportunities to develop at least nine out of ten of those skills. The important elements of educational design of such a space technology programme are the following.

1. Use of Problem Based Learning methodology.
2. Long-term engagement of the participants.
3. International consortium of developers.
4. Multiple geographical locations of development teams.
5. Engagement of participants from different fields of studies to perform supporting tasks of the Programme.
6. Engagement of participants in outreach activities.
7. Active internal communication of different groups inside the project team.
8. Provide the participants with feedback on process.

REFERENCES

[1] A. Davies, D. Fidler, and M Gorbis. Future Work Skills 2020. Research Institute Report SR-1382A, Institute for the Future for University of Phoenix, 2011.

[2] M. Pajusalu, R. Rantsus, M. Pelakauskas, A. Leitu, E. Ilbis, J. Kalde, H. Lillmaa, R: Reinumägi, K. Voormansik, K. Zalite, V. Allik, M. Noorma, and S. Lätt. Design of the Electrical Power System for ESTCube-1 satellite. *Latvian Journal of Physics and Technical Sciences*, (3):16–24, 2012.

[3] Andris Slavinskis, Urmas Kvell, Erik Kulu, Indrek Sünter, Henri Kuuste, Silver Lätt, Kaupo Voormansik, and Mart Noorma. High spin rate magnetic controller for nanosatellites. *Acta Astronaut.*, 95:218–226, 2014.

[4] Urmas Kvell, Marit Puusepp, Franz Kaminski, Jaan-Eerik Past, Kristoffer Palmer, Tor-Arne Grönland, and Mart Noorma. Nanosatellite orbit control using MEMS cold gas thrusters. *Proc. Estonian Acad. Sci.*, 63(2S):279–285, 2014.

[5] Henri Kuuste, Tõnis Eenmäe, Viljo Allik, Ants Agu, Riho Vendt, Ilmar Ansko, Kaspars Laizāns, Indrek Sünter, Silver Lätt, and Mart Noorma. Imaging system for nanosatellite proximity operations. *Proc. Estonian Acad. Sci.*, 63(2S):250–257, 2014.

[6] Andris Slavinskis, Erik Kulu, Jaan Viru, Robert Valner, Hendrik Ehrpais, Tõnis Uiboupin, Markus Järve, Endel Soolo, Jouni Envall, Tobias Scheffler, Indrek Sünter, Henri Kuuste, Urmas Kvell, Jaanus Kalde, Kaspars Laizāns, Erik Ilbis, Tõnis Eenmäe, Riho Vendt, Kaupo Voormansik, Ilmar Ansko, Viljo Allik, Silver Lätt, and Mart Noorma. Attitude determination and control for centrifugal tether deployment on ESTCube-1 nanosatellite. *Proc. Estonian Acad. Sci.*, 63(2S):242–249, 2014.

[7] Mihkel Pajusalu, Erik Ilbis, Taavi Ilves, Mihkel Veske, Jaanus Kalde, Henri Lillmaa, Ramon Rantsus, Martynas Pelakauskas, Ahto Leitu, Kaupo Voormansik, Viljo Allik, Silver Lätt, Jouni Envall, and Mart Noorma. Design and testing of the electrical power system for ESTCube-1. *Proc. Estonian Acad. Sci.*, 63(2S):232–241, 2014.

[8] Kaspars Laizāns, Indrek Sünter, Karlis Zālīte, Henri Kuuste, Martin Valgur, Karl Tarbe, Viljo Allik, Georgi Olentšenko, Priit Laes, Silver Lätt, and Mart Noorma. The design of fault tolerant command and data handling subsystem for ESTCube-1. *Proc. Estonian Acad. Sci.*, 63(2S):222–231, 2014.

[9] Silver Lätt, Andris Slavinskis, Erik Ilbis, Urmas Kvell, Kaupo Voormansik, Erik Kulu, Mihkel Pajusalu, Henri Kuuste, Indrek Sünter, Tõnis Eenmäe, Kaspars Laizāns, Kārlis Zālīte, Riho Vendt, Johannes Piepenbrock, Ilmar Ansko, Ahto Leitu, Andres Vahter, Ants Agu, Elo Eilonen, Endel Soolo, Hendrik Ehrpais, Henri Lillmaa, Ivar Mahhonin, Jaak Mõttus, Jaan Viru, Jaanus Kalde, Jana Šubitidze, Jānis Mucenieks, Jānis Šate, Johan Kütt, Juris Poļevskis, Jürgen Laks, Kadi Kivistik, Kadri-Liis Kusmin, Kalle-Gustav Kruus, Karl Tarbe, Katrin Tuude, Katrīna Kalniņa, Laur Joost, Marko Lõoke, Markus Järve, Mart Vellak, Martin Neerot, Martin Valgur, Martynas Pelakauskas, Matis Averin, Mats Mikkor, Mihkel Veske, Ott Scheler, Paul Liias, Priit Laes, Ramon Rantsus, Reimo Soosaar, Risto Reinumägi, Robert Valner, Siim Kurvits, Sven-Erik Mändmaa, Taavi Ilves, Tanel Peet, Tavo Ani, Teet Tilk, Timothy Henry Charles Tamm, Tobias Scheffler, Toomas Vahter, Tõnis Uiboupin, Veigo Evard, Andreas Sisask, Lauri Kimmel, Olaf Krömer, Roland Rosta, Pekka Janhunen, Jouni Envall, Petri Toivanen, Timo Rauhala, Henri Seppänen, Jukka Ukkonen, Edward Haeggström, Risto Kurppa, Taneli Kalvas, Olli Tarvainen, Janne Kauppinen, Antti Nuottajärvi, Hannu Koivisto, Sergiy Kiprich, Alexander Obraztsov, Viljo Allik, Anu Reinart, and Mart Noorma. ESTCube-1 nanosatellite for electric solar wind sail in-orbit technology demonstration. *Proc. Estonian Acad. Sci.*, 63(2S):200–209, 2014.

[10] Andris Slavinskis, Hendrik Ehrpais, Henri Kuuste, Indrek Sünter, Jaan Viru, Erik Kulu, Johan Kütt, and

Mart Noorma. Flight results of ESTCube-1 attitude determination system. *Accepted for publishing in Journal of Aerospace Engineering*, 2015.

[11] Andris Slavinskis, Mihkel Pajusalu, Henri Kuuste, Erik Ilbis, Tõnis Eenmäe, Indrek Sünter, Kaspars Laizāns, Hendrik Ehrpais, Paul Liias, Erik Kulu, Jaan Viru, Jaanus Kalde, Urmas Kvell, Johan Kütt, Karlis Zalite, Karoli Kahn, Silver Lätt, Jouni Envall, Petri Toivanen, Jouni Polkko, Pekka Janhunen, Roland Rosta, Taneli Kalvas, Riho Vendt, Viljo Allik, and Mart Noorma. ESTCube-1 in-orbit experience and lessons learned. *IEEE Aerosp. Electron. Syst. Mag.*, 30(8):12–22, 2015.

[12] Andris Slavinskis. *ESTCube-1 attitude determination*. PhD thesis, University of Tartu, 2015.

[13] C. E. Hmelo-Silver. Problem-Based Learning: What and How Do Students Learn? *Educational Psychology Review*, 16(3):235–266, 2004.

[14] P. Janhunen and A. Sandroos. Simulation study of solar wind push on a charged wire: basis of solar wind electric sail propulsion. *Ann. Geophys.*, 25:755–767, 2007.

[15] P. Janhunen, P. K. Toivanen, J. Polkko, S. Merikallio, P. Salminen, E. Hæggström, H. Seppänen, R. Kurppa, J. Ukkonen, S. Kiprich, G. Thornell, H. Kratz, L. Richter, O. Krömer, R. Rosta, M. Noorma, J. Envall, S. Lätt, G. Mengali, A. A. Quarta, H. Koivisto, O. Tarvainen, T. Kalvas, J. Kauppinen, A. Nuottajärvi, and A. Obraztsov. Electric solar wind sail: Toward test missions. *Rev. Sci. Instrum.*, 81:111301:1–11, 2010.

[16] Pekka Janhunen. Simulation study of the plasma brake effect. *Ann. Geophys.*, 32:1207–1216, 2014.

[17] Pekka Janhunen. Electrostatic plasma brake for deorbiting a satellite. *J. Propul. Power*, 26:370–372, 2010.

[18] Pekka Janhunen, Petri Toivanen, Jouni Envall, Sini Merikallio, Giuditta Montesanti, Jose Gonzalez del Amo, Urmas Kvell, Mart Noorma, and Silver Lätt. Overview of electric solar wind sail applications. *Proc. Estonian Acad. Sci.*, 63(2S):267–278, 2014.

CUBESAT TEAM OF POLITECNICO DI TORINO: PAST, PRESENT AND FUTURE PROJECTS

Raffaele Mozzillo[(1)], Loris Franchi[(2)], Lorenzo Feruglio[(3)], Fabrizio Stesina[(4)], Sabrina Corpino[(5)]

[(1)]Politecnico di Torino, Corso Duca degli Abruzzi 24 - Torino (Italy), Email: raffaele.mozzillo@polito.it
[(2)]Politecnico di Torino, Corso Duca degli Abruzzi 24 - Torino (Italy), Email: loris.franchi@polito.it
[(3)]Politecnico di Torino, Corso Duca degli Abruzzi 24 - Torino (Italy), Email: lorenzo.feruglio@polito.it
[(4)]Politecnico di Torino, Corso Duca degli Abruzzi 24 - Torino (Italy), Email: fabrizio.stesina@polito.it
[(5)]Politecnico di Torino, Corso Duca degli Abruzzi 24 - Torino (Italy), Email: sabrina.corpino@polito.it

ABSTRACT

The CubeSat Team is a student team of Politecnico di Torino involved in the design and development of small platforms for scientific space missions and for testing new technologies in orbit. The team was created in 2008 on the initiative of students and professors of the Aerospace Engineering course. More than 150 students got involved in the program since then. The CubeSat Team is coordinated by the Systems and Technologies for Aerospace Research team of the Mechanical and Aerospace Engineering Department, under the supervision of Professor Sabrina Corpino.
The objectives of the program are summarised in the following mission statement: "To educate aerospace-engineering students on systems development, management, and team work. To achieve insight in the development of scenarios and enabling technologies for future space missions"
In these years, the CubeSat Team reached great achievements, above all the launch of the e-st@r-I spacecraft, one of the two first Italian CubeSats in orbit. Students got involved in the design, development, and verification effort and participated actively in the integration and launch campaign. At the moment, two other CubeSats are being developed at the Systems and Technologies for Aerospace Research laboratory (STARLab): e-st@r-II, and 3-STAR, which are respectively part of the ESA "Fly Your Satellite!" and GEOID programs. The primary scientific payload of e-st@r-II is an active Attitude Determination and Control System for which innovative determination algorithms have been developed. The CubeSat successfully completed the environmental test campaign on June 2015 at ESA-ESTEC. 3-STAR is a 3U CubeSat that will take part in the GEOID constellation for the validation of the GENSO network through the HumSat communication payload. In addition, 3-STAR carries a remote sensing GNSS-based payload. This experiment will open the door to several applications, from Earth monitoring to civil protection warning services, and eventually military missions.
The team is also working on the definition of new mission concepts to define innovative solutions targeted to establish low-cost/fast-delivery space assets for science and exploration of the Solar system. The aim of these missions is to increase the scientific and technological knowledge with unprecedented measurements and by exploiting the potentialities of interplanetary CubeSats as distributed systems. At the present moment, two main destinations are considered: Mars and Near Earth Asteroids. For these studies, two important international collaborations have been established, with MIT and NASA's JPL.
All these activities will be described into the details in the paper.

1. Introduction

The CubeSat Team is a student team which deals with the design and development of space missions carried out by small platforms, in collaboration with other universities and research centers, international agencies and industry. The group consists of undergraduate and PhD students led by Prof. Sabrina Corpino and works in the Systems and Technologies for Aerospace Research Laboratory (STARLab), located inside the Department of Mechanical and Aerospace Engineering of Politecnico di Torino (DIMEAS). The core of the team consists of Aerospace Engineering students, but also students from different courses of study (e.g. Mechanical Engineering, Electronics and Telecommunications) are an important part of the team.
The Team is officially recognized as a student team of Politecnico di Torino. This gives the opportunity for students to be granted their participation in the team with credits, with which they can replace one of the exams of the study plan. Moreover, the Team receives financial support by the university through the committee "Fondi Progettualità Studentesca" (Funds for Students Projects), which basically reinvests part of the annual fees paid by students, by financing projects of the students themselves.
The Team has an official website (www.polito.it/cubesat-team) where is possible to find all the information on the projects, the collaborations and the team members. In addition, the outreach planning relies greatly on social networks (i.e. Facebook, facebook.com/CubeSatTeam, and Twitter, twitter.com/CubeSatTeam) to raise awareness of our research and to attract, at the same time, both new students and new sponsors.

2. Research activities

The CubeSat Team was created on 2008 with the objective of giving hands-on experience opportunities to university students, by establishing different research lines. Since the beginning, the Team focuses its activities on working on CubeSats missions and platforms, mainly as educational programs but also for technology demonstration and scientific purposes. Specifically, it conducts mission studies, design, development, integration and launch of CubeSats, which are a type of miniaturized and standardized satellite greatly appreciated worldwide, as demonstrated by the significant increase of platforms launched in recent years [1].

Programs developed by the Team have a common mission statement, which sums up the basic idea of research and education:

"To educate aerospace-engineering students on systems development, management, and team work. To achieve insight in the development of scenarios and enabling technologies for future space missions."

The hands-on-practice approach is considered a good mean to achieve our objectives as technical University, and this is the main reason why a structured permanent education and research program based on CubeSat has been established at Politecnico di Torino. The program is based on the idea that Universities shall take up the technological challenges issued by the scientific community and industries, in order to gain knowledge necessary for future space mission.

As Figure 1 illustrates, a space mission carried out by a University is driven first of all by the relevance that the mission has both for the research and the education purposes, being at the same time constrained by limited budget and resources.

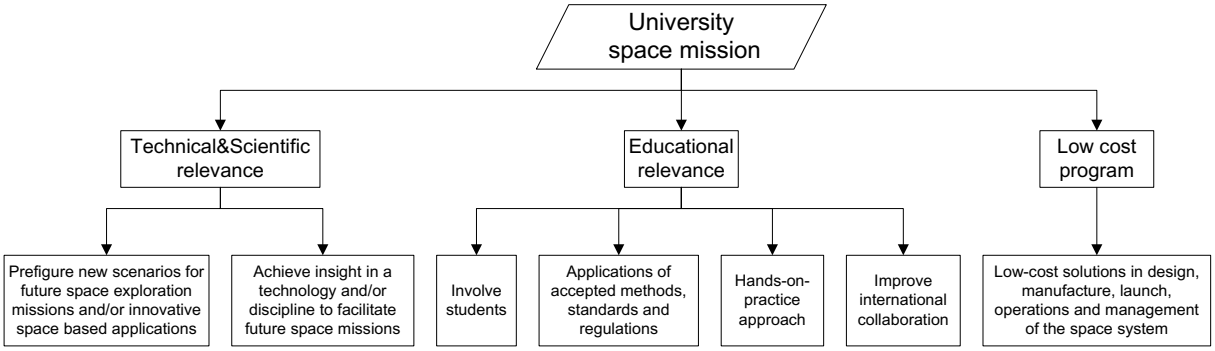


Figure 1: University space mission guidelines

The main program guidelines have been assumed as high level objectives and constraints for the research program. They can be listed as follows:

- WHAT/1: To inspire and prepare future space-professionals: students are the end users of the mission
- WHAT/2: To improve knowledge in space science and engineering: real world shall take advantages of our missions
- WHY: To meet stakeholders' needs. Stakeholders are: students & civil society, scientific community, industry
- HOW: To carry out a space program from the design to in-orbit operations, completely managed by students.

Since our research program has educational relevance, students must learn how to build a space mission from the very beginning throughout the project development, dealing with all the aspects related to a space program. The project is entirely carried out by the Team coordinated by the Team Leader, who is responsible for the whole program. The team is organized according to a defined work breakdown structure, which takes into account both technical and non-technical aspects. Students learn by practice how to:

- Design, manufacture, verify and test, and operate a space system
- Manage, control and document the development process according to current regulations and applicable standards (e.g. ECSS)
- Prepare technical documentation to report the project
- Team working and collaborate in an international multicultural environment
- Disseminate the results of the program
- Promote the program within the suitable stakeholders.

The educational purpose of the program is pursued at several levels:

- Undergraduate CubeSat program consists of class works developed during regular courses of the Aerospace Engineering Bachelor degree. Assignments are usually related to equipment-subsystem of the CubeSat. Undergraduate students also join the CubeSat Team for the preparation of

their final work, or for the mandatory internship. About 20 students participate in the activity every year

- Graduate students are involved in the CubeSat program during regular courses of the Master of Science in Aerospace Engineering and for the preparation of their final thesis. Master students works on the definition of the mission and of the system, as well as on the development and verification phases according to their talent and program schedule. Some of them join the CubeSat Team for 6 to 12 months to study in depth particular subjects and to develop their final work. Several students that have joined the team during the Bachelor degree then remained within the team until the completion of the Master of Science degree. About 40 students participate in the class work activity every year, and about 10% out of them remain in the team for the preparation of the thesis
- Postgraduate program. The CubeSat Team consists mainly of PhD students, who are usually the leaders of single units and coordinate the group of under-graduate and graduate students within the same unit. One PhD student is the System Engineer of the CubeSat project and coordinates all the technical activities. PhD students deal with CubeSat-related technology development and methodologies definition. At the moment, three PhD students are working on the CubeSat program full time.

2.1. Satellite programs

Currently, two CubeSat programs are being developed by the Team: e-st@r program, based on 1U platforms, and 3-STAR program, which instead aims at developing a 3U.

2.1.1. E-st@r

E-st@r program was born on 2008 in response to an initiative of the Education Office of the European Space Agency (ESA). The first platform developed within this program is e-st@r-I, a 1U CubeSat [2]. The project was selected among other ESA state members' universities to be launched on VEGA Maiden Flight as secondary payloads [3]. Finally, it was launched on February 2012 with other six platforms and it has been one of the first two Italian CubeSats to reach the space.

The payload was an active Attitude Determination and Control Subsystem (ADCS) aimed at demonstrating autonomous attitude control capabilities based on magnetic actuation [4].

The development of the first CubeSat led to achieving remarkable technical results:

- A platform for satellites CubeSat class was developed, tested on the ground and in orbit. This can accommodate different payloads and be adopted as the reference bus future projects. Many devices and components manufactured and tested precisely for e-st@r-I (e.g. ADCS board, magnetic torquers, antenna deployment system [5], etc.) could be easily integrated in next projects
- A mobile Ground Control Station (GCS) was built and it was very useful especially during the verification phase, system tests and as a backup of the main GCS during in-orbit operations
- Methodologies, design tools and verification procedures were developed and established, and they are still adopted in the current projects [6].

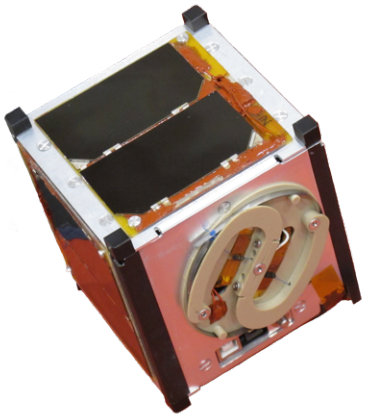


Figure 2: e-st@r-I CubeSat

Several lessons learned were collected during e-st@r-I design and AIV phases. However, the educational objectives were successfully achieved but the technical mission was not totally accomplished. In fact, even if the CubeSat successfully passed all verifications, in orbit it intermittently transmitted just only few days after the launch. Low battery voltage was targeted as the most possible reason for this failure.

Thanks to these results, lessons learned, the interest of students and the dedication of researchers and professors of the team, continuity was given to the work of the CubeSat Team with the launch of new initiatives: the project e-st@r-II and the program 3-star.

The development of e-st@r-II took advantage of the experience gained from its predecessor through the improvement of all subsystems, both hardware and software [7]. The development of the satellite started soon after the launch of the previous project, and then, in the first semester of 2013 it was selected for the ESA's "Fly Your Satellite!" (FYS!) initiative [8]. The payload is again the ADCS, with a major focus on a determination algorithm developed precisely for e-st@r-II. The aim is to demonstrate the capability of performing the estimation of the attitude even only with Earth Magnetic Field vector and angular velocities measurements. Secondary mission objectives are the test in orbit of COTS technology and in-house developed hardware (e.g. UHF communication system) and software (e.g. command and data handling software), which will demonstrate the students' skills and capabilities.

The "Fly Your Satellite!" program is an exciting initiative from the Education and Knowledge Management Office of ESA focused on CubeSat projects run by university students. The program is one of the several hands-on opportunities offered by ESA Education and provides experience of the full life-cycle of a space project. ESA provides the CubeSat teams with direct support from ESA technical specialists and access to state-of-the-art environmental test facilities. ESA will also procure a launch opportunity for selected CubeSat(s).
The satellite was selected to participate in Phase 1 ("Build your satellite!", with the review of the design conducted by ESA's experts) and Phase 2 ("Test your satellite!", with an environmental test campaign at ESA ESTEC, performed on May and June 2015 [9]), and it is waiting for gaining the "Ticket to Orbit!" (Phase 3) and to operate soon in space (Phase 4, "CubeSats in Space!").

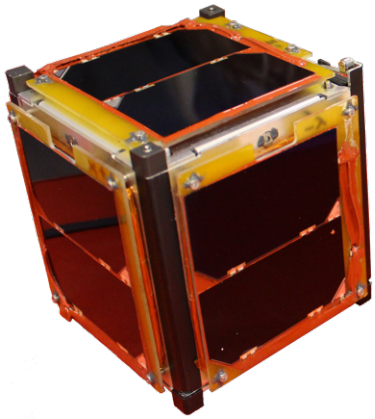


Figure 3: e-st@r-II CubeSat

2.1.2. 3-STAR

3-STAR program was born as a reaction to GEOID (GENSO Experimental Orbital Initial Demonstration) ESA Education Office in 2010. This initiative promotes:

- The creation of a constellation of CubeSat in Low Earth Orbit to validate the network of ground stations GENSO
- The development of the first set for the demonstration project HumSAT (Humanitarian SATellite) supported by European Space Agency and by the United Nations, which aims to improve the communication skills in developing countries and in countries affected by natural disasters or catastrophic events.

Within this program the CubeSat Team is designing and developing a 3U CubeSat form, 3-STAR [10], which is the evolution of the e-st@r platform. One of the payloads is developed in collaboration with students of the group Remote Sensing Department of Electronics and Telecommunications of the Politecnico di Torino, and so, from this point of view, the 3-STAR program is strongly multidisciplinary. The payload is P-GRESSION (Payload for GNSS Remote Sensing and Signal detectION) and the objective is to perform radio-occultation and reflectometry experiments. Currently, the program is in Phase B (Preliminary definition).

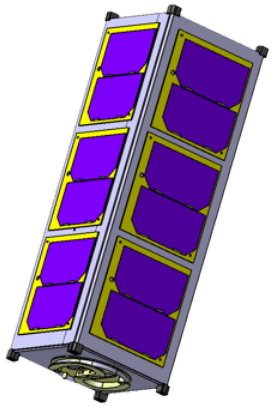


Figure 4: 3-STAR CubeSat (preliminary CAD model)

2.2. Mission design

One of the fields that our team is very involved in (similarly to satellite hardware integration and testing), is mission analysis and design. This is a wide category, and includes very different subjects:

- Tradespace exploration (for example Multi Attribute Utility Theory, a methodology with which great number of different possible designs are evaluated with respect to mission objectives and stakeholder needs)
- Detailed budget of the different subsystems (the "budgets" are a set of equations and formulas specific to the various subsystems that allow to define general and high level characteristics and that serve as basis to proceed with the detailed satellite design that is usually carried out in later stages)
- Analytical analysis such as astrodynamics (manoeuvres, trajectories and spaceflight) and architectures designs (telecommunications, distributed systems, and so on).

All these activities fall under the specified category of mission analysis and preliminary design. The students involved in these collaborations often have to deal with challenging problems, due to the fact that little is known of the mission and the system that will carry it out, and to the fact that the possible design choices are an enormous number.
Therefore, usually the students are assigned to a very specific task, often related to a reference mission that is used to allow the training of the new students.
The students principally are focusing their efforts in different fields: 1) Preliminary design 2) Coverage analysis 3) Mission architecture and concept 4) mission autonomy 5) Tradespace exploration (multi-attribute utility theory).

In these cases, the missions used as reference involve two technologies that are on the leading edge of the research effort in the small satellite field: distributed systems and interplanetary small satellites.

3. The role of the students and the opportunities offered to them

Many students have been involved in the programs of the CubeSat Team participating in every stage of the design (Figure 5), thus experiencing first-hand a real project and teamwork. The integration of components, the manufacturing operations of the devices, the mechanical tests, vibration, thermal vacuum, functional tests, simulations Hardware-In-The-Loop, have enabled dozens of students to express their ability in parallel the theoretical study, and to develop the System Engineer attitude, which will prove useful during the professional career. Indeed, many former members of the team are having the chance to work in companies with similar roles to those they had in the team, thus allowing them to exercise the skills acquired during their collaborations within the team. Some examples are shown in Tab. I.

Table I: Current jobs of some former members of the team

Former role in the team	Present job
System and AIV Engineer	Test Engineer @ Airbus DS
System Engineer	System Engineer @ Tyvak International
System Engineer	Innovation Engineer @ Heerema Marine Contractors
ADCS Engineer	GNC Engineer @ ELV
OBC engineer	Software Developer @ Magneti Marelli
OBC engineer	Data Handling Engineer @ Thales Alenia Space
OBC engineer	Software Engineer @ Airbus DS
GCS Engineer	Ground Systems Engineer @ SES Techcom

In several cases, the students finish off the work of months through the publication of scientific papers and internal reports, or theses (sometimes prepared within student exchange programs with other universities). In general, each student leaves the team with a Curriculum enriched by activities that are not commonly offered within the typical study plans. In addition, participation in workshops and meetings allowed them to get in touch with students from other countries, in international and multidisciplinary contexts (in Figure 6, many of the conferences and workshops attended by members of the Team are shown).

Over the past years more than 150 students have participated in the creation and development of CubeSat programs, including those have helped with project work and exercises, while being enrolled in the courses of the Bachelor and Master of Science. Some results:

- 25 thesis completed
- 20 publications in Proceedings of international conferences and workshops
- 3 manuscript accepted on international journals
- 22 works presented at events and conferences.
- 5 members involved in student exchange programs.

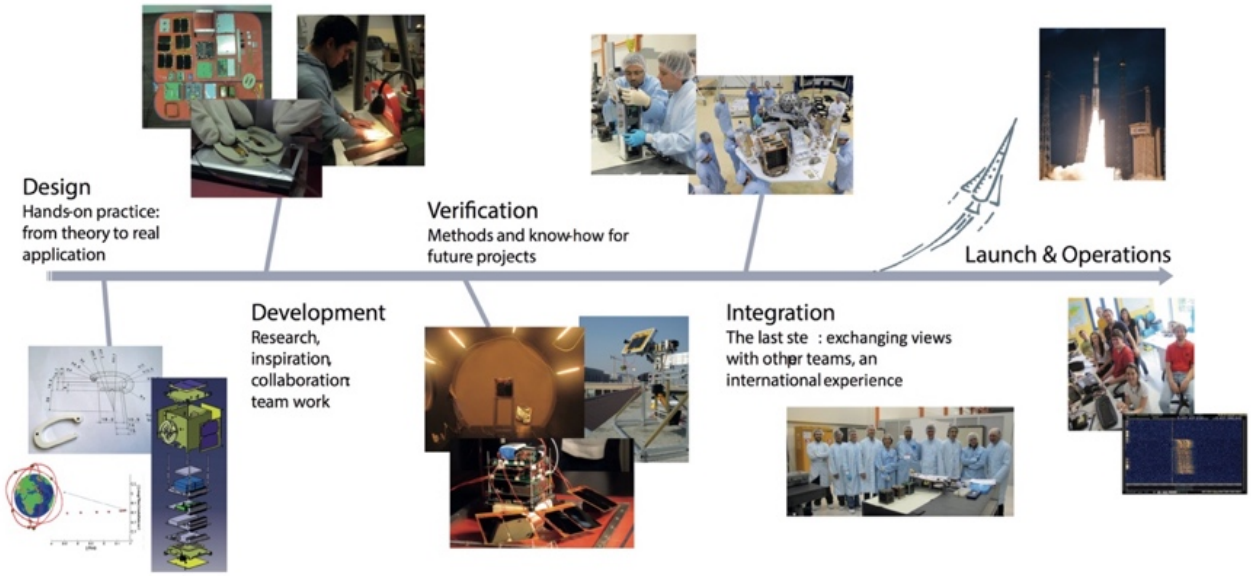


Figure 5: Phases of e-st@r missions in which the students have been involved

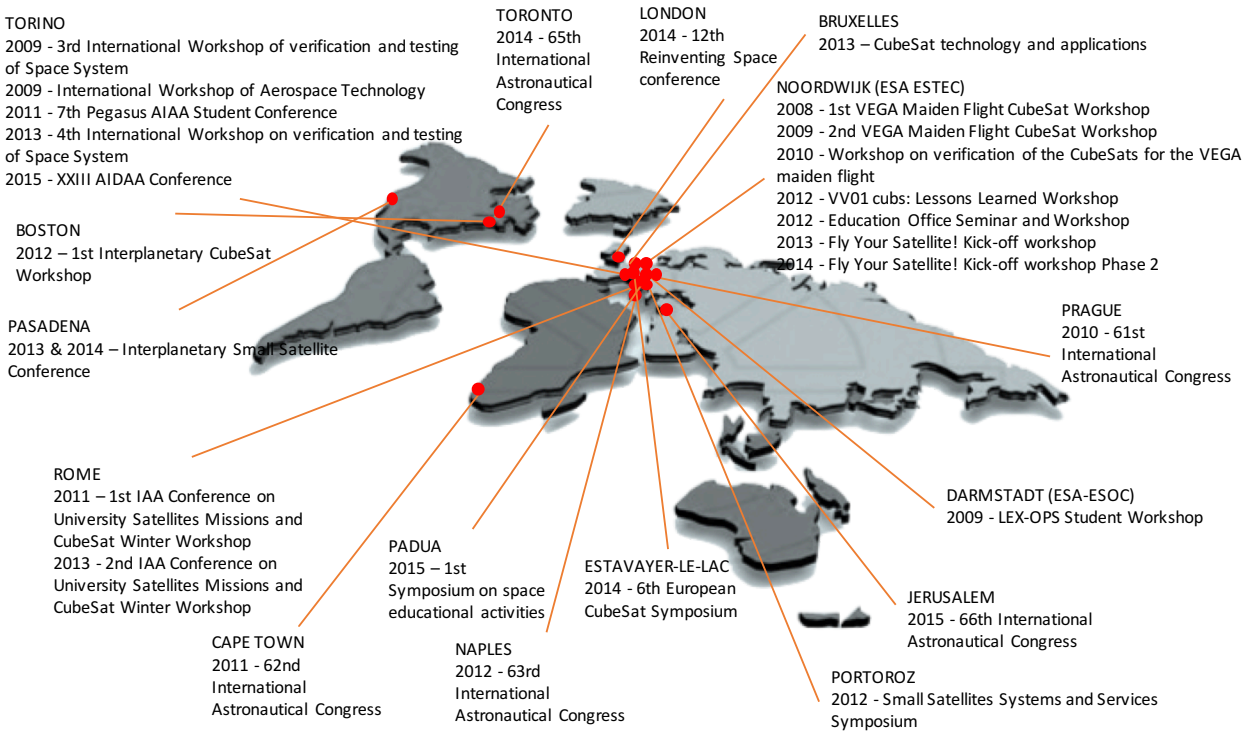


Figure 6: Conferences and workshops attended by members of the CubeSat Team

A very important event, both from the educational and technical point of view, is represented by the participation of the Team into the FYS! initiative.
The opportunity provided by ESA Education Office resulted to be very important for the students involved in all the phases of the initiative. Being in touch with the top experts in the field, first by email and teleconferences, and then side by side in the laboratories, is one of the best ways to acquire knowledge and to prove oneself in a professional context. Other key elements were the meetings and reviews between the Team and the ESA experts and managers, which represented a great outcome for all the students involved into the project. In fact, they have allowed to experience first-hand the project management related aspects.

4. Next projects and collaborations

The Team is always focused on the future, and of course the research activities are strongly influenced by the roadmaps established by space agencies.
The future research will investigate three principal branch of study, that are 1) innovative scientific missions, 2) optimal system design and 3) autonomous systems, relying on the relevant increase of the Technology Readiness Level of CubeSat-related technology.
As regards the scientific mission, the Team is looking at the new paradigm of interplanetary CubeSat [11] with two main destinations, Mars and Near Earth Asteroids (NEA). Both the missions take into account the possibilities offered by constellations and formations flying.
The objectives of a mission to Mars are to establish a low-cost/fast-delivery space asset to investigate specific phenomena that may affect the future human exploration of the planet and to provide the scientific community with unprecedented measurements to support the long term vision of human exploration of Mars. Three mission concepts for orbit, atmosphere and surface exploration were preliminary designed:

- Mars Orbital Environment Exploration (MOEX), which studies orbital particulate environment and dust climatology, focusing on micrometeoroids and dust rings by using CubeSat platforms. The MOEX mission concept is shown in Figure 7

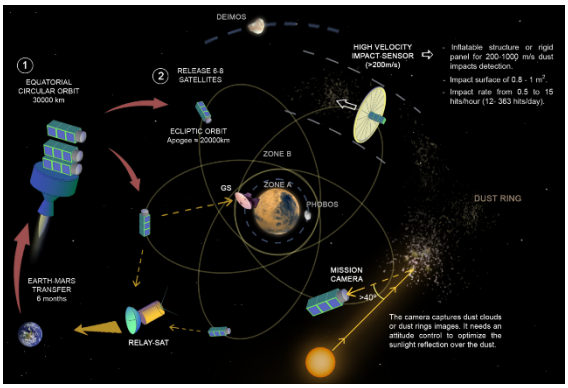


Figure 7: MOEX mission concept

- Mars Atmosphere Research with In situ Operations (MARIO), which investigates upper and lower atmosphere in order to characterize and study atmospheric features and processes of Martian atmosphere and its interaction with future human in situ missions. It consists of orbiters and swarm of CubeSats, and landers with deployable tethered balloons

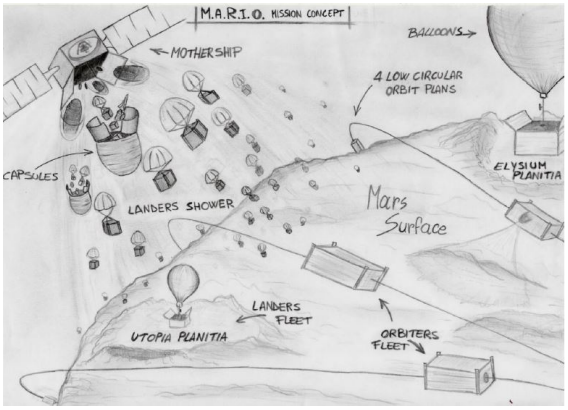


Figure 8 MARIO mission concept

- Spacecraft to Analyse Life-evidences Underneath Soil (SALUS). It searches for evidences on Martian (sub) surface that could represent hazard for human exploration, together with understanding if past/present life existed/exists on Mars. Space Penetrator System are the key elements of this mission, and they are based on CubeSat-sized technology

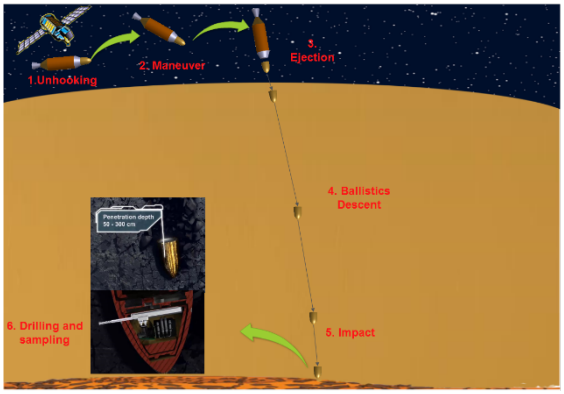


Figure 9 SALUS mission concept

NEA missions were identified by the International Space Exploration Coordination Group (which includes in practice the most important space agencies) as a potential pathway toward the driving goal of human exploration of Mars. The mission designed by the Team has the objective to deploy & operate a CubeSat-based space asset at a NEA, providing unprecedented measurements and data about the asteroid targeted to Solar System studies and knowledge-gap-filling activities, to the study of the consequences of an impact on an asteroid, and to the demonstration of key-technologies.

Going into details, the reference mission is a CubeSat mission to a binary asteroid, Didymos. The system will be object of a joint mission between ESA and NASA, that will launch each one spacecraft. The NASA one is going to impact the smaller component of the binary system, while ESA spacecraft will monitor the change in numerous parameters due to the impact of the other spacecraft.

Key objectives of the CubeSats under study are to enhance and support the science activities of the ESA spacecraft (measuring composition, type, properties and their changes post impact) and to explore and implement interesting and promising technologies that are currently at a lower technology readiness level (TRL).

A challenging aspect for the interplanetary mission is represented by the autonomy of the system. Indeed, the long distance from the Earth and the less available communication windows (if compared to LEO missions), entails the need for autonomous systems.

In the recent years, thanks to the increase of the know-how on machine-learning techniques and the advance of the computational capabilities of on-board processing, algorithms involving artificial intelligence (i.e. neural networks and fuzzy logics) have begun to spread even in the space applications. Nowadays, thanks to these reasons, the implementation of such techniques is becoming possible even on smaller platforms, such as CubeSats. In this context, the Team is also investigating the feasibility of a total autonomous system, by using Neural Networks, Fuzzy Logic and Genetic Algorithms. For instance, thanks to the adaptability of these algorithms, it is possible to identify a failure and recover it not via active/passive hardware redundancy (as usually done) but only via software (e.g. by redistributing the control torques [12]).

The Team is also investigating the use of early design techniques in the development of CubeSat and related missions, focusing principally on the Concurrent Design (CD) methodology. This design methodology is relative young, in fact a first case study was provided by the CESAR mission assessment in March 1999, and is nowadays under study within the ESA and NASA's JPL facilities.

There are many definitions for Concurrent engineering but the ESA's preferred definition [13] best describes the Team idea too:

"Concurrent engineering is a systematic approach to integrated product development that emphasizes the response to customer expectations. It embodies team values of cooperation, trust and sharing in such a manner that decision making is by consensus, involving all perspectives in parallel, from the beginning of the product life-cycle."

The application of this new methodology within the Team will allow all the team members to learn from the others and to cooperate each other. One of the goals of our methodology is also to create a highly motivated and multidisciplinary team able to perform the design tasks in almost real time. Reaching these objectives is more difficult than it might first appear, but it can provide many benefits in terms of velocity and performance of the conceptual design and in the learning quality of the members.

Various partnerships are currently active and / or under development for the coming years. The most relevant are with Massachusetts Institute of Technology (MIT) and NASA Jet Propulsion Laboratory (JPL).

The collaboration with MIT was carried out during 2014 and it has been possible thanks to Intesa San Paolo, that through a public call, selected worthy projects and sponsored them. The people involved were two PhD students from Politecnico di Torino (that went to Boston) and three PhD students from MIT that were hosted in Torino. The subject of the collaboration was "CubeSat for space exploration: a new paradigm for planetary science mission", and has been a fruitful joint effort between an engineering team (CubeSat Team) and a science one (EAPS department, Sara Seager's group). The research field was about distributed system on Mars, and the main task has been:

- To develop one or more mission concepts involving the use of CubeSat-like systems to perform distributed science on the planet
- To increase our knowledge about the environment and its dynamics, and gathering new data that would help the scientific community to prepare the way for human missions at Mars.

In this sense, the different background of the two participating teams was a positive and key aspect of the activity. MIT group provided the scientific knowledge necessary to characterize the initial structure of the mission. Indeed, helping to analyse into details the scientific problems related to it and to define with remarkable rigor the methodology used to explore the scientific part, was fundamental for the successful definition of the mission aspects. On the other side, CubeSat Team members were precious to provide the engineering knowledge that helped to define concept that were not only feasible, but also very appealing from the engineering research point.

The fundamental aspect of this collaboration was centred on the MEPAG (Mars Exploration Program Analysis Group) documents, which allowed us to select relevant scientific objectives that ensures actuality for our mission design effort. On this subject, after having defined the aforementioned characteristics, the teams defined the possible payloads, and from these the science traceability matrix for the mission, therefore exploring and tracing the link from the mission goals (and objectives) to the requirements (instrument, project, and mission).

Analysis were carried out on various different disciplines, all involving early mission design. Going into details, the main focus of this second part has been performing concurrent design activities, allowing to define the mission concept with details compatible with a Phase A status, in a quick and efficient way. Moreover, on this subject, tradespace exploration (and in this Multi Attribute Utility Theory, MAUT) was addressed, and more detailed analysis on the mission were performed (mass, link, power and propulsion budgets, entry descent and landing).

The students at the end of the collaboration were extremely satisfied, and learned traversal skills thanks to the diverse teams that were participating. The professors involved were also a key part of this project, as they performed related educational activities during the periods as guest in the respective hosting universities.

As regards the collaboration between Politecnico di Torino and JPL/Caltech, it is being carried out during 2015, and involves two graduate students from the CubeSat Team that were hosted for months in Pasadena, California, in the renowned laboratory that is one of the excellence institutes in the space engineering and research (Earth Science and Interplanetary). The subjects of the collaboration are "Development of mission architecture concept study for a CubeSat asteroid mission" and "Design of the Thermal Control System of a CubeSat satellite", and are all carried out under the JPL Visiting Student Research Program (JVSRP). The students are staying abroad for a period of 6 months each, and each student is having the chance to work on a similar and related field with respect to the one they were addressing when in Torino. This opportunity has been made possible because the JPL yearly selects a relatively small number of students and allows them to work as interns in their facilities, followed by mentors that add to the collaboration further aspects for the personal and professional growth of the students.

In addition to the environment being extremely interesting and motivating, because of all the space activities that are daily carried out in the laboratory, JPL puts a considerable effort in making the student stay as fruitful as possible. Guided tours of the laboratories and numerous conferences make the students very exposed to several state of the art practices.

Moreover, depending on the mentor that are assigned to, the students can be assigned to work also on secondary projects, enhancing the networking skills and allowing the students to interact more deeply with the current activities in the laboratory.

5. Conclusions

The CubeSat Team is a student team of Politecnico di Torino, which deals with the design and development of space missions carried out by small platforms. The group consists of a leading professor and undergraduate and PhD students, and works in the STARLab. The core of

the team consists of Aerospace Engineering students, but also students from different courses of study are an important part of the team.

The main activities of the Team are the two CubeSat programs, e-st@r and 3-STAR, and the missions design studies. To date, a 1U CubeSat (e-st@r-I) was launched within ESA's "CubeSats on VEGA Maiden Flight" initiative on 2012, and another 1U platform (e-st@r-II) is participating in ESA's "Fly Your Satellite!" initiative and after having successfully passed the environmental test campaign at ESTEC is now close to gain its ticket to orbit. In addition, a 3U CubeSat (3-STAR), is in the preliminary definition phase. Several scientific mission are being investigated, with two main destinations, that are Mars and Near Earth Asteroids.

The Team collaborates with other universities and research centres, international agencies and industry, and some other partnerships are being planned. At the moment, the most important collaborations are with MIT (the subject of the collaboration is "CubeSat for space exploration: a new paradigm for planetary science mission") and NASA's JPL (the subjects of the collaboration are "Development of mission architecture concept study for a CubeSat asteroid mission" and "Design of the Thermal Control System of a CubeSat satellite").

6. References

[1] Gunter's Space Page, CubeSat, *http://space.skyrocket.de/doc_sat/cubesat.htm*, last access: November 2015

[2] S. Corpino, S. Chiesa, F. Stesina, N. Viola, *CubeSat development at Politecnico di Torino: the e- st@r program*, Proceedings of the 61st International Astronautical Congress, Prague (CZ), 27 September–1 October 2010

[3] ESA website, CubeSat Teams, http://www.esa.int/Education/CubeSat_teams, last access: November 2015

[4] F. Stesina, S. Corpino, R. Mozzillo, G. Obiols-Rabasa, *Design of the Active Attitude Determination and Control System for the e-st@r CubeSat*, Proceeding of 63rd International Astronautical Congress, Naples (Italy), October 2012, pp.4585-4594.

[5] G. Fanchini, D. Gagliostro, *The e-st@r CubeSat: Antennas system*, Acta Astronautica, Volume 69, Issues 11-12, December 2011, Pag. 1089 – 1095, DOI: 10.1016/j.actaastro.2011.06.009

[6] S. Corpino, F. Stesina, *Verification of a CubeSat via Hardware-in-the-loop Simulation*, IEEE Transactions on Aerospace and Electronic Systems, Vol. 50, No. 4, 2014, DOI. No. 10.1109/TAES.2014.130370

[7] G. Obiols Rabasa, S. Corpino, R. Mozzillo, F. Nichele, *E-st@r-I experience: valuable knowledge for improving the e-st@r-II design*, Proceedings of the 65th International Astronautical Congress, Toronto (CA), 29 September - 3 October 2014

[8] ESA website, Fly Your Satellite! CubeSat Teams, http://www.esa.int/Education/Fly_Your_Satellite!_CubeSat_teams, last access: November 2015

[9] G. Obiols Rabasa, S. Corpino, R. Mozzillo, F. Nichele, *Lessons learned of a systematic approach for the e-st@r-II CubeSat environmental test campaign*, Proceedings of the 66th International Astronautical Congress, Jerusalem (IL), 12 - 16 October 2015

[10] G. Ridolfi, S. Corpino, F. Stesina, R. Notarpietro, M. Cucca, F. Nichele, *Constellation of cubesats: 3-star in the humsat/geoid mission*, In: Proceedings of the 62nd International Astronautical Congress, Cape Town, South Africa, October 2011

[11] M.A. Viscio, N. Viola, S. Corpino, F. Stesina, S. Fineschi, F. Fumenti, C. Circi, *Interplanetary CubeSats system for space weather evaluations and technology demonstration*, Acta Astronautica Vol. 104, Issue 2, November-December 2014, pages 516-525, DOI. No. 10.1016/j.actastro.2014.06.005

[12] L. Feruglio, L. Franchi, R. Mozzillo, F. Stesina, S. Corpino, *Autonomous neuro-fuzzy solution for fault detection and attitude control of a 3U CubeSat*, Proceedings of the 66th International Astronautical Congress, Jerusalem (IL), 12 - 16 October 2015

[13] M. Bandecchi, B. Melton, F. Ongaro, *Concurrent Engeneering applied to space mission assessment and design*, Esa bulletin 99, September 1999, page 1

QBITO DEVELOPMENT AND STUDENTS INVOLVEMENT

Ignacio Barrios Tascón [(1)], Ana Laverón Simavilla [(1)], Efrén Moreno Benavides [(1)]

(1) Universidad Politécnica de Madrid,
E-USOC, Spanish User Support and Operations Centre
Centro de Investigación y Desarrollo Aeroespacial
Campus de Montegancedo, UPM
28223, Pozuelo de Alarcón
Madrid, SPAIN,
Email: ibarrios@eusoc.upm.es

ABSTRACT

QBITO is the first CubeSat developed by Universidad Politécnica de Madrid (UPM). It is a 2U CubeSat and is one of the satellites that compound the project QB50 lead by Von Karman Institute (VKI) in Belgium. The main task of QBITO will be to operate the Ion Neutral Mass Spectrometer (INMS) which is the primary payload on-board the CubeSat and which will study the properties of the lower thermosphere. The most outstanding feature of QBITO is the amount of new in-house developments that are present in the design. These include the Structural Subsystem, the Electrical Power Subsystem, the Communications Subsystem and a novel Antenna Deployment Mechanism. These new developments are complemented with Commercial Off-The-Shelf units in order to reach a robust, yet innovative, architecture.

Apart from the INMS, QBITO will carry three other payloads in order to take advantage of the mission as much as possible. The first is an experiment that will assess the performance of the Docosane as a Phase Change Material. It is being developed in collaboration with the Belgian company Wallopt. The second experiment, the Medium Wave Infrared Detector, is developed by the Spanish company New Infrared Technologies and aims at testing a novel kind of uncooled detectors, in space conditions. Finally, the third additional payload, developed at UPM is the Experimental Software. It implements an attitude determination and control algorithm based on fuzzy control theory. The purpose is to test the suitability of this kind of control technique for spacecraft attitude control applications.

The CubeSat has been integrated and tested by QBITO team which includes UPM staff, professors and students and it will be ready for the launch scheduled in 2016. The environmental tests have been performed in the Spanish company SENER and in AIRBUS Defense and Space.

One of the objectives of the project has been to involve university students in all the phases of the project, from design to validation. Being able to work in a real project allow the students to complement their academic training and gain a valuable experience.

An overview of the space engineering educational activities carried on at UPM, QBITO mission, the in-house developments for this project and the students' involvement will be presented.

1. INTRODUCTION

In recent years, a transformation in teaching and learning methods in European universities has taken place, aiming at increasing active learning. The transition from an education system based on teaching to a system based on learning, making the student the center of the educational process, is being pursued.

The application of these new models particularly benefits engineering education, because training in engineering has an essential practice component. In particular, subjects in the second cycle of the degree, which have a very technological and systematic nature, are more suited to implement active learning methods. Active learning methods enhance not only the students' acquisition of competences specific of each subject, but also the development of generic competences as communication, team work, leadership, etc., that are increasingly valued in the professional field.

Since the academic year 2009/10, several innovation activities have been performed in space engineering education at the UPM. In 2012 the QB50 project was announced and it was considered an opportunity for the university to involve the students in a real project where they could gain valuable experience. The UPM was awarded with the development of one of the 50 CubeSats that will compound the project. The development of this CubeSat, called QBITO, has been performed by the Spanish User Support and Operations Center (E-USOC, www.eusoc.upm.es), a center in the UPM delegated by the European Space Agency (ESA)

to operate scientific experiments on board the International Space Station (ISS); it supports fluid science experiments performed within the European Columbus Laboratory and experiments in the Microgravity Science Glovebox in the U.S. Destiny module of the ISS.

This paper presents the different active learning activities carried out by the UPM in space engineering education, stressing the ones performed in the frame of QBITO project.

2. ACTIVE LEARNING ACTIVITIES AT UPM

Several active learning activities are currently being performed in space engineering education at UPM. These are presented below.

2.1. Demonstrator satellites

During the 2010/11 academic year a new laboratory was created, where students work in groups to carry out the integration and validation of the subsystems of a microsatellite. The educational microsatellite serves to demonstrate the basic functionalities of a satellite, and it is having great success among the students.

The subsystems which the students have to integrate and validate are: power, data handling, communications, attitude control and thermal control. Some of the activities performed by the students are the verification of:

- The solar panels, obtaining their P-I and V-I profiles.
- The peak power tracker performance in different illumination conditions.
- The electrical voltages and currents for different load profiles.
- The power switches functionality.
- The mass properties of all subsystems and of the integrated satellite.
- The telemetry measurements calibration.
- The telemetry data rates, and verification of the telecommands.
- The attitude determination and control sensors and actuators.
- The attitude control algorithms.

A set of manuals and procedures were developed, making an effort in presenting and conducting these practices in a way as close as possible to real satellite verification tests: the satellite and each of its subsystems are first presented so that students are familiar with their design, features and specifications; after that, procedural steps have to be followed carefully, assessing the results against the applicable specifications; finally the students prepare the test reports and fill a requirements validation matrix.

Each subsystem is verified individually before assembling it with the previously verified modules and performing an integrated verification. Once all modules have been tested and assembled, the complete satellite is tested in its final configuration.

The groups have to work as a team and organize each of their members' tasks in order to ensure an efficient use of time and resources, and the proper level of safety; the latter is supported by a lecturer monitoring their work.

Students are able to get in close contact with practical aspects of satellite design, development and operation:

- They are able to see, use and perform a series of tests and measurements on a functioning satellite and its components. This allows them to get familiar with satellite components and their performances, as well as with laboratory test equipment and procedures.
- They are able to communicate with the satellite and gain experience with some of the capabilities and limitations related to remote operation and monitoring.
- They get a first hands-on contact with integration and verification activities as they are performed in space industry (within the limitations imposed by the demonstrator satellite itself, by the laboratory environment and by organizational aspects such as duration of the lessons and number of students); these activities have a big impact in the overall cost of a satellite project and are usually not well understood when studied only from a theoretical perspective.

With this activity several topics in the "Conceive Design Implement Operate" (CDIO) syllabus have been implemented, among them are: Team Operation; Communication Strategy and Structure; Written Communication; System Engineering, Modeling and Interfaces; Hardware Software Integration; Test, Verification, Validation, and Certification.

2.2. Conceptual design of a satellite mission

Students work in groups to develop the conceptual design of a satellite mission. Each group member adopts a specific role and they have to work and communicate as an engineering team to define their mission requirements, derive the system and subsystem requirements, design the different subsystems in accordance with those requirements and ensure the consistency and feasibility of the overall design.

The mission statement of each project is defined by the respective team. Some examples of the projects developed are:

- Provide images of high latitude oceans of interest for sea transport. The images should allow the analysis of the ice caps melting to assess the feasibility and safety of maritime routes in high latitudes.
- Achieve a microgravity platform to perform material science experiments in microgravity.
- Obtain a map of the celestial sphere in the near ultraviolet and far ultraviolet frequencies.
- Achieve a global monitoring system for the low frequency variations of the Earth magnetic field preceding the earthquakes, in order to provide earthquakes early warning.

The change of the teaching and learning model has required obtaining educational licenses of the following software tools, widely used in the space industry:

- The mission analysis software STK (Satellite Tool Kit).
- The satellite thermal control system design software ESARADESATAN.

2.3. Development of a satellite tracking ground station

Nowadays there are many educational satellites orbiting the Earth and sending telemetry accessible to any ground station that meets the required specifications, such as the Delfi-C3 (http://www.delfispace.nl/). In addition to this type of satellites, important observation satellites such as NOAA (National Oceanic and Atmospheric Administration, http://www.goes.noaa.gov/) also offer open telemetry. These fact together with the intended CubeSat activity in the university led to the construction of a ground station (see Fig. 1) to allow the communication with open satellites, downlinking their data and processing it on ground. The station was installed at the E-USOC.



Figure 1. Satellite tracking ground station antenna

The set-up of the station and its Monitoring and Control System was carried out through several student Final Theses. The results of these works were validated by acquiring and interpreting telemetry from several operational university satellites.

Thanks to the set-up of the ground station, students can now perform training activities which allow them to learn:

- How to communicate with satellites.
- How to download telemetry and how to process the data.

Students have downlinked data from several satellites and provided them to their respective teams, who have a system set-up to collect it. The satellites tracked so far are Compass One (beacon and housekeeping in Morse CW), Hope One (beacon and housekeeping in Morse CW), O/Oreos (data uploaded to the mission web page: beacon and housekeeping in AFSK 1200 bps), Swiss Cube (science data automatically forwarded to the SwissCube MCS: BPSK AX.25, 1200 bps), Eyesat AO-27 (APSK AX.25, 1200 bps), PolyItan (GFSK AX.25, 9600 bps), QB50 precursor flights (data uploaded to the mission web page: housekeeping BPSK AX.25 1200 bps and CW beacon).

Working with real satellites allows addressing the work in a more realistic way, which is very motivating for the students.

2.4. Development of a laboratory satellite

The demonstrator satellites acquired in previous years are good for conducting laboratory practices in the subject, but do not provide adequate flexibility for students to engage in new hardware and software developments. Therefore, the development of a self-designed demonstrator satellite was started through Final Theses in 2012.

Five students have been involved in this activity carrying out their theses: two in the Electric Power System design, two in the Attitude Control System design, and one in the Mechanical design and overall integration.

The development is currently in its final stage and it has being used since the first semester of 2015/16. Having an in-house development will also allow to have more units and to significantly reduce costs.

2.5. QB50 project

QB50 is a project funded by the European Commission inside the 7th Framework Program to launch and operate an international network of 50 CubeSats. Their mission is dedicated to the acquisition of multi-point in-situ measurements of key components of the thermosphere and lower ionosphere, and to the research

of the re-entry into the atmosphere. It will be the first big network of CubeSats on orbit, a concept that has attracted much interest in recent years, but so far no university, institution or space agency had taken the initiative to create and coordinate.

A team of UPM professors submitted a proposal to the QB50 project, which was selected and has been carried out during the 2012-16 timeframe. The overall objectives of the proposal are the design, development, construction, launch and operation of one of the two-unit CubeSats of the network, which will carry an atmospheric sensors kit provided by the consortium.

The project has a high educational, scientific and technological value for universities. It allows UPM to be part of an international group of more than 50 universities worldwide working and sharing knowledge for a successful mission. In addition, a ground stations network to support the operations of the satellite constellation and maximize the amount of scientific data downlinked is being created.

The 7th Framework Programme funds 75% of the launch cost, as well as the development and manufacture of the scientific sensors and the procurement of a few Attitude Determination and Control Units. The remaining 25% of the launch cost, and the design, manufacture and operation cost of the CubeSats and ground stations of the network must be funded by the project participants.

The UPM satellite is called QBITO. The project is being designed and manufactured by final-year students of the degree, led by lecturers and E-USOC staff. It has been very challenging to be able to develop such a project with a high participation of students, since attending other courses was not always compatible with the project schedule and its fixed milestones. Only their very high motivation and commitment with the project makes it possible.

3. QB50 PROJECT

QB50 is a European 7FP project aiming to put into orbit an international network of 50 CubeSats for multi-point, in-situ measurements in the lower thermosphere and re-entry research. This concept has been under discussion for several years but, so far, no university, institution or space agency has taken the initiative to set up and coordinate such a powerful network.

QB50 mission consists of a network of 50 CubeSats in a 'string-of-pearls' configuration. The CubeSats will be launched from the International Space Station. The starting point of the mission will be a circular orbit at around 400 km altitude and 52º inclination, and due to atmospheric drag, the CubeSat orbits will decay until the spacecraft burn in the atmosphere. The separation distance between CubeSats will increase during the mission, eventually leading to a non-uniform distribution of satellites all the way around the Earth. This happens due to atmosphere density variations along the orbit and variations in the individual CubeSat orientations, mass distributions, etc. The expected lifetime of individual CubeSats is between three and six months, depending on the launch schedule and sun activity.

The characterization of the lower thermosphere and ionosphere properties has been studied before by means of highly elliptical orbit satellites and sounding rocket flights, providing measurements during very small times and in small regions at a time. Also, powerful remote-sensing instruments have been used, which are not ideally suited for exploring the lower thermosphere because the atmosphere is so rarefied that the return signal is weak.

QB50 idea is to acquire in-situ and long-duration measurements of key parameters and constituents of the lower thermosphere and ionosphere. This implementation is more complicated than the first two solutions, but results to be the best approach to study these atmospheric layers. The combination of a large number of CubeSats with identical sensors launched at the same time into a network will provide multi-point measurements that allow the separation of spatial and temporal variations of lower thermosphere/ionosphere characteristics.

The main reasons that lead the definition of such special mission, instead of other more common higher orbit missions, are:

- Scientific interest in the very low orbit atmospheric layers.
- The lifetime of the CubeSats in a very low-Earth orbit will be a few months only, which is much less than the 25 years stipulated by international requirements related to space debris. In addition, the educational objectives will be also met with a short mission duration.
- A very low-Earth orbit allows high data rates because of the short communication distances involved.
- In very low-Earth orbits, the CubeSats will be below the Earth's radiation belts, which is advantageous because CubeSats use low-cost Commercial-off-the-shelf (COTS) components which are not radiation hardened.

The 50 CubeSats will comprise about 40 atmospheric double CubeSats with standardized sensors and about

10 double or triple CubeSats for science and technology demonstration.

QBITO's objective is to accomplish the design, development, building, testing, launch and operation of one of the 40 double CubeSat carrying as main payload the Ion and Neutral Mass Spectrometer (INMS).

3.1. Schedule

November 2011 was the kick-off date for QB50 project. At that time the call for proposals was made public for the interested institutions to apply. QBITO proposal was submitted by the team in April 2012. After being selected, the team was required to pass the Preliminary Design Review (PDR) in May 2013. The design made a successful PDR. The Critical Design Review (CDR) for QBITO was passed in September 2014. From that moment on, the development activities continued with the emphasis put on testing and integration activities. The Assembly, Integration and Test (AIT) Readiness Review was accepted in February 2015. Currently these testing activities are being carried out in order to pass the Flight Readiness Review which is due February 2016.

After being accepted for flight, QBITO will be sent to Innovative Solutions in Space (ISIS), in the Netherlands, in order for the main payload, the INMS, to be integrated. This will happen in April 2016. Payload integration activities will be done at ISIS premises, before the CubeSats are delivered to Nanoracks, QB50 launch provider, in the USA. Launch window will be opened in July 2016 and will last for several months. The main milestones of the project are presented in Tab. 1.

Table 1. Schedule for QB50 project.

Call for Proposals	November 2011
Submission of Proposal	April 2012
PDR	May 2013
CDR	September 2014
AIT Readiness Review	February 2015
FRR	February 2016
Shipment for Main Payload Integration	April 2016
Launch window start	July 2016

In May 2014, two precursor CubeSats were launched in order to test critical equipment that will have a great impact on QB50 performance. The precursor flight flew, among other equipment, an INMS unit and a Surrey Space Centre ADCS Bundle. These two units, as shown below will be part of QBITO, so a valuable feedback for the mission is being currently analysed.

3.2. Mission goals

QBITO mission encloses different goals related to both the QB50 project and university related advantages. Among the principal goals, the next can be found:

- Comply with QB50 mission requirements.
- Operate secondary payloads included by QBITO team.
- Gain spacecraft engineering experience for staff at Universidad Politécnica de Madrid.
- Involve university students in the design and development of the CubeSat.
- Test in-house developed equipment in real space mission conditions.

QB50 mission requirements were identified by QB50 consortium as the baseline to be followed by the teams. These requirements are based on the CubeSat standard and the main payload restrictions as presented in [1], [2] and [3].

4. QBITO

4.1. System overview

QBITO design choices have been based on the search of functional robustness. QBITO is a two-unit (2U) CubeSat and redundancy has not been pursued due to constraints of volume and mass. The symmetry and the most favourable geometry configuration in terms of air drag torque in nominal attitude for the INMS operation have been taken into account.

The Electrical Power System (EPS) is in charge of setting the power supply commanded by the On-Board Computer (OBC). It provides with 3V3 and 5V power levels and also with the batteries power level.

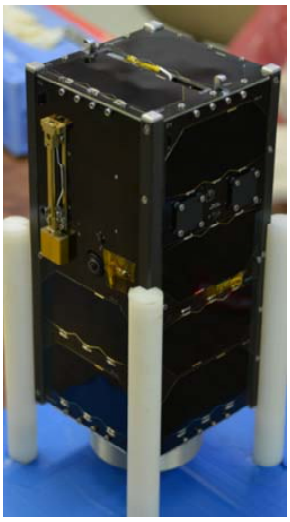


Figure 2. QBITO

Three I2C data buses are present in QBITO architecture:

- System I2C: this is the main internal communications bus in QBITO. The OBC will act as the master of this bus at all times during the mission. The slaves will be different subsystems that need communication with the OBC.
- ADCS I2C: the ADCS includes its own internal communication bus. In here, the ADCS CubeComputer will act as the master and the rest of the ADCS equipment will act as slaves.
- EPS I2C: the EPS includes an internal I2C that is used to communicate the EPS microprocessor (master) with the batteries board (slave).

Other communication buses are used in the design. The OBC has been required to use UART communication protocol in order to communicate with the primary payload, the INMS, and SPI bus has been selected for communicating the OBC and the COM subsystem.

Apart from these communication buses there are certain lines that will be used to get or monitor certain information. These are:

- Analogue lines: the OBC will acquire analogue measures of certain parameters by means of these connections.
- Digital lines: different digital lines will be used as interrupting lines for the OBC and as enable lines for the antenna deployment mechanism.
- RF lines: these lines will transmit the RF signals from the COM PCB to the UHF and VHF antennas.

Most of the data and the power lines will be routed through the PC104 bus that will go across the PCB stack inside the CubeSat.

4.2. Payloads

4.2.1. INMS

This is the main payload of QBITO. It will be in charge of taking in-situ measurements to characterize the composition of ions and neutral particles and their spatial variation in the lower thermosphere. This will provide key measurements that will improve significantly the determination of atmospheric variables and will provide with key inputs for atmospheric models.

The INMS is a miniaturised analyser designed for sampling of low mass ionised and neutral particles in the spacecraft ram direction with the instrument resolutions optimised for resolving the major constituents in the lower thermosphere, i.e., O, O2, N2. The INMS development is being carried out by Mullard Space Science Laboratory (MSSL) and the flight unit will be integrated in QBITO at ISIS premises, prior to launch.



Figure 3. Ion Neutral Mass Spectrometer

4.2.2. MWIRD

The MWIRD is an experiment that will test the behaviour in space of an uncooled medium wave infrared detector based on the new Vapour Phase Deposited (VPD) PbSe technology. The experiment has been designed by New Infrared Technologies, a Spanish company developer of this technology. Two detectors will be tested in QBITO. One will point towards nadir and the other towards zenith direction.

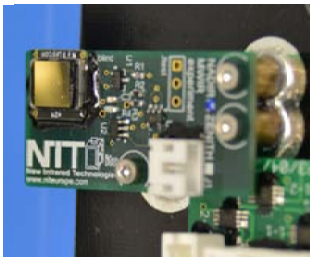


Figure 4. Medium Wave Infrared Detector

4.2.3. PCM

The PCM experiment aims at testing the performance of n-Octadecane as a useful phase change material for future use in space thermal control systems. The experiment has been developed by the UPM in collaboration with the Belgian company Wallopt. A flight experiment is mandatory to increase the TRL of this technology. A differential test experiment has been designed where an identical thermal environment will be imposed to two experimental cells, one as a witness cell (in fact a thermal spreader) and another one as a cell equipped with a PCM. The thermal evolution of the cells will be recorded and compared to each other.



Figure 5. Phase Change Material experiment

4.2.4. ESW

The experimental software (ESW) is an attitude determination and control software that will be tested on QBITO taking advantage of the hardware included in Surrey's QB50 ADCS Bundle. It will aim at demonstrating novel fuzzy logic algorithms use for attitude control. It is capable of performing full attitude determination and control, tailored for QBITO mission.

It is expected to validate separately the orbit and attitude determination module and the attitude control module. Among the benefits that can be expected from the ESW development there is the consecution of a more powerful controller, which deals easily with inaccuracies of the satellite model and that can be quite easily adaptable to other missions. Also, it is expected that it will improve the performances while reducing the power consumption of the whole subsystem, see [5].

4.2.5. Payloads operation

The operation of the INMS has been required to be managed by the OBC by means of uploaded scripts generated by the mission scientific team. These scripts will include both direct payload commands and time tagged commands which will define the functioning of the instrument. This philosophy has been also adopted for the operation of the secondary payloads. Therefore, the PCM and ESW experiments will be managed with the same kind of commands scripts.

The MWIRD experiment will not follow this method and will be active at all times, since the power required to operate is very low.

5. IN-HOUSE DEVELOPMENTS

5.1. Structure

The structure has been developed in-house with the purpose of getting a lightweight multi-mission configurable structure. It was conceived for the mission when QBITO was selected to be part of QB50 project in April 2012.

QBITO structure can be divided into primary and secondary structures. The first one comprises an aluminium alloy skeleton which includes the rails that interface with the deployer system, two main squared frames at the top and bottom of the CubeSat (Z axis), and FR4 laminate side panels.

The skeleton and the side panels act as a whole in order to provide global stiffness and load-bearing capacity. The secondary structure includes the subsystems PCBs and the spacers that connect these PCBs to the main structure.

The technique used to do the conceptual design was based on applying the design theory "Entropy-Based Design" described in [8], which aims at selecting a concept that keeps as low as possible the number of internal dependencies. The result of applying this theory led to a solution that has the following characteristics:

- Maximum useful volume for subsystems.
- Maximum number of degrees of freedom, which is related to the possibility of changing the design.
- Maximum flexibility, which is related to the possibility of adding new components.
- Maximum number of translational and rotational symmetries, which is related to the possibility of moving components.
- Maximum modularity which is related to the possibility of changing a component.
- Minimum number of components, which is related to improvements in mass, cost, reliability, and power.
- Maximum number of equal components, which is related to the reduction of cost.

The result can be seen in Fig. 6 where arrows remember that it allows three different 90º rotations, one translation along Z-axis and one symmetry around Z-axis. The result is a modular configuration with enough flexibility to satisfy the requirements of quite different missions.

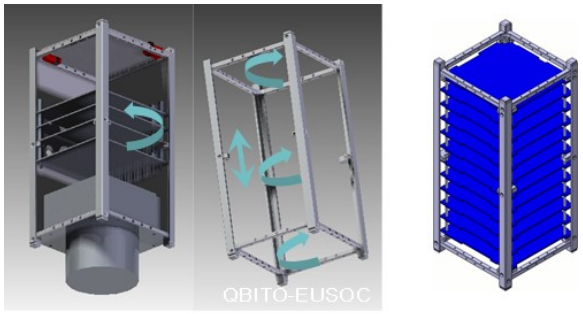


Figure 6. QBITO structure

Finally, the side panels act not only as load-bearing structural members, but are an integral part of the electrical power system. They support the solar panels that provide the power to the satellite and have copper tracks that act as power buses. The FR4 laminate employed is highly-available in the market and is heavily used as a substrate for printed circuit boards because of its excellent electrical, mechanical and thermal properties.

5.2. EPS

The EPS is in charge of managing the power supply on-board. The power is obtained from the solar radiation by means of solar panels that will be installed in the exterior lateral panels. Five faces of the satellite will be covered by a total of 16 solar cells, leaving one of the faces free to be used by the INMS. Triple junction GaAs AzurSpace's 3G30C Advanced solar cells have been selected due to their efficiency of 30%.

The EPS will optimize the power received using five Maximum Power Point Trackers (MPPT). This power will be regulated to the proper voltage levels required by the different equipment (3V3 and 5V) and distributed using dedicated switches. For some units such as the antenna deployment mechanism this voltage level will not be regulated and the power will be drawn from the batteries directly. Finally, the EPS will be in charge of managing the charge and discharge processes of the set of two batteries (2.5 Ah, each) selected for the mission. The rest of the subsystem has been designed and will be developed in-house

The EPS has five pairs of controlled switches. Each pair is able of switching on/off a 3V3 line and a 5V line, both protected by a dedicated thermal fuse. All the logic is an in-house development that runs in an ultralow consumption microcontroller manufactured by Texas Instruments.

5.3. COM

QBITO COM is based on a full duplex architecture with UHF for downlink and Beacon, and VHF for reception. Transmission rates are 9600 and 1200 bps for downlink and uplink, respectively. The subsystem makes use of programmable transceivers which are configured by the OBC. The COM board is divided into two main parts, transmission (it includes the beacon) and reception. The COM status is monitored by the OBC. The data interface is through the SPI bus, with power lines of 3.3 V and 5 V.

Regarding the antennas, a four monopole turnstile will be used for downlink achieving circular polarization and omnidirectional pattern, whereas a VHF monopole is used for the uplink.

5.4. Antenna Deployment Mechanisms

The antennas will be deployed with a novel deployment mechanism designed and developed in-house. Four equal mechanisms will be used for the deployment of the four monopoles that compound the UHF antenna. Another mechanism scaled to a larger dimension will be used for the deployment of the VHF antenna.

This mechanism is an optimized antenna deployment mechanism that fulfils the next requirements:

- Minimum impact in the lateral faces.
- Minimum impact in volume, mass and cost.
- Minimum number of parts in order to have maximum reliability.
- Minimum number of manufacture tolerance.

The mechanism is based on a torsional spring which is previously rolled inside a cylinder. This results in the antenna being pushed out and deployed. Special care has been taken into account for mitigating the problems derived from the friction between the antenna and the walls of the cylinder.

5.5. TCS

The thermal control will be carried out by a control system based on thermal coatings and paints. The thermal control design also includes two heaters that will be in charge of maintaining the batteries within their operational temperature range. This will cope with all the thermal loads which have been identified for the different operating scenarios for QBITO mission.

6. STUDENTS CONTRIBUTION

From the beginning of the project the educational objective has been present. The participation of students has been pursued from the very start of the design phase. Students have worked in different subsystems, always supervised by university professors and engineers. The assignation to the respective subsystems has been always based on the students' interests and project needs. Tab. 2 shows the number of students that have worked on the different parts of the project so far.

When joining the team every student was given a general introduction to the project both from the technical and management points of view. After this they started working on the relevant subsystem with their supervisors. Most of the students have taken advantage of the work carrying it out in the frame of their final thesis to finish the university studies.

QBITO project is having an important implication from students. The opportunity to work in QBITO increases their hands-on experience since they work in and see the main aspects of a real space project.

Table 2. Student participation in QBITO.

Work group	Professor	Engineer/PhD	Student
System Engineering		1	1
EPS	0.5	1	4
OBC		1	5
ADCS	1	2	4
COM	1		3
Structure	0.5	1	3
TCS		1	1
Payloads		1	
Ground Segment		2	3
AIT		2	1
		TOTAL	25

Some students were able to participate in the initial phase of the project, more focused on the design; others in the procurement, manufacturing and validation phase, having direct interaction with the industries where the tests are being performed (i.e. SENER and AIRBUS DS); and others have been able to participate in all the phases.

Not only does the project allows them to apply the knowledge they have acquired in the university courses but it also gives them the opportunity to develop certain skills necessary to work in future projects such as the team work or the time management. It also shows them how important the international cooperation is to accomplish most of the projects in the space field.

7. CONCLUSIONS

This paper has presented the different active learning activities carried on in space engineering at UPM. Different activities have been presented where the students get hands-on experience in real space projects.

The most important project at the moment among the ones presented is QBITO, the first CubeSat of UPM. It is part of the European project QB50 and is now in the AIT phase. The mission together with the students' contribution has been presented.

The next steps in QBITO project are related to the Flight Readiness Review. The environmental tests will be done in the coming months, so that the QB50 project deadlines are met. Students will continue working in the project until the operation phase.

REFERENCES

[1] Riki Munakata, CubeSat Design Specification, Rev. 12, California Politechnic State University, 8th January, 2009

[2] A. Denis, QB50 System Requirements and Recommendations, Issue 7, 13th February, 2015.

[3] R.A. Chaudery, QB50 INMS Science Unit Interface Control Document, Issue 7, University College London, 4th December, 2013.

[4] I. Barrios et al., QBITO, the first CubeSat by Universidad Politecnica de Madrid, Small Satellites Systems and Services Symposium, 26th – 30th May, 2014, Porto Petro, Majorca, Spain.

[5] D. Calvo et al., Fuzzy attitude control for a nanosatellite in LEO orbit, 40th COSPAR Scientific Assembly 2014.

[6] J. J. Fernandez et al., The QBITO CubeSat: Applications in Space Engineering Education at Technical University of Madrid, 40th COSPAR Scientific Assembly 2014.

[7] E. Moreno, et al. QBITO EPS and Structure as Technology Demonstrators for Students, Oral presentation, 5th European CubeSat Symposium, Brussels, June, 2013.

[8] E. Moreno, Advanced Engineering Design: An integrated approach, 1st Edition, Woodhead Publishing, 2012.

[9] QB50 Project Website: www.qb50.eu

[10] Universidad Politécnica de Madrid Website: www.upm.es

[11] E-USOC Website: www.eusoc.upm.es

AAUSAT5 - AN EVALUATION OF A STUDENT-RUN CUBESAT PROJECT

Rasmus Gundorff Sæderup[1,3] **and Joakim Bruslund Haurum**[2,3]

[1]*BSc student, 5th semester, Electronic Engineering and IT, Aalborg University, E-mail: rsader13@student.aau.dk, Phone: +45 20931467*
[2]*BSc student, 5th semester, Medialogy, Aalborg University, E-mail: jhauru13@student.aau.dk, Phone: +45 31614628*
[3]*Mailing address: Damstræde 143, 1, 9220 Aalborg Øst, Denmark*

ABSTRACT

AAUSAT5 is a 1U cubesat designed and built by engineering students at Aalborg University (AAU). It is part of a new pilot project from the European Space Agency (ESA) called *Fly Your Satellite from the ISS!* (FYS). The program allows students to get hands-on experience with working in the space industry by designing, constructing, testing and launching a satellite. AAUSAT5 was deployed in the fall of 2015, with an expected mission lifetime of 3-8 months.
In this article, the experiences acquired during the 18 month long production, qualification and testing phase of the AAUSAT5 cubesat is evaluated and discussed. Based on these observations and the conclusions obtained, several suggestions are formulated on how the work-flow of an educational satellite program can be improved. The proposed work-flow is compared to the methodology used on previous student-built cubesat projects from AAU as well as the FYS methodology.
These suggestions cover subjects such as how to optimize the development of the satellite including documentation and tests. This was done by the use of extensive knowledge sharing tools and the use of a distributed structural and functional architecture in the cubesat, allowing subteams to work on different subsystems at the same time.

It is discussed and evaluated how the Problem Based Learning (PBL) approach at AAU has influenced the AAUSAT5 project. Resource management, teamwork, project planning and educational planning are discussed more in detail.
The educational and work-flow aspects of participating in the FYS program are analyzed. Being part of FYS has been a positive experience and a great opportunity to be a part of the space industry. However, FYS being a pilot project in the workings, means that there are elements of the project that can be improved upon. This is in particular the planning of the overall course of the program and the cooperation between the various stakeholders in the project such as ESA, NASA, NanoRacks and AAU.

Key words: AAUSAT5, Aalborg University, AAU, cubesat, education, problem-based learning, PBL, ESA, FYS, ISS, resource management, planning, teamwork.

1. INTRODUCTION

Satellites are often seen as something only governmental space agencies and large companies had the technology and funding to develop, build and launch. However, with the reduced cost of rocket launches and the reduced size and cost of electronic components, space exploration has become more accessible than ever. This has enabled university students, among others, from around the world to build satellites and get hands-on experience with space technology. This inspired the creation of the cubesat standard, to increase the accessibility to space for students (Cal Poly SLO & The CubeSat Program 2014). The cubesat standard makes it possible for both students and companies to develop and produce relatively cheap satellites in a very short time frame, compared to traditional satellites. The standard thus makes it easier to build satellites, by defining a common platform on which satellites with many different purposes can be made. Also, the standard makes it easier for launch providers to integrate cubesats, which in turn makes the launch cheaper.

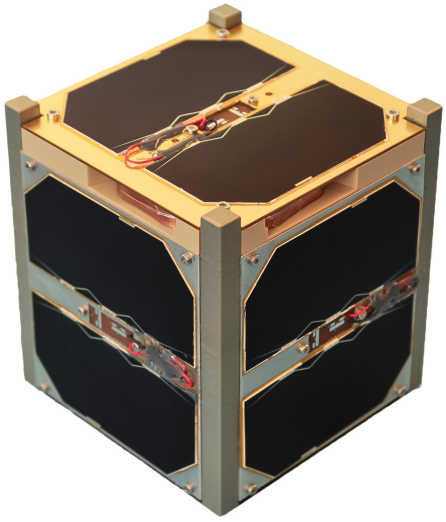


Figure 1. The AAUSAT5 satellite.

The Education office of the European Space Agency has also helped spread the knowledge and interest in this topic, by providing students opportunities regarding space exploration by means of projects such as *Fly Your Satellite!*, *Drop Your Thesis!*, *Fly your Thesis!* etc. (Walker et al. 2010). Furthermore, with all these student-based satellite projects, a lot of experiences are gained that can be used in future projects and by other student teams. This article aims at evaluating the AAUSAT5 satellite project, and listing the things that can be learned and improved upon from the project. This includes project management, documentation and knowledge sharing among others. A photo of the AAUSAT5 satellite is shown in Figure 1.

2. AAU STUDENT SPACE

In the summer of 2001, a group of students at Aalborg University started building a cubesat, "giving the students an unique chance to experience a real engineering project with real engineering problems" (AAU Student Space 2003). This group of students has since evolved into what is now known as AAU Student Space. AAU Student Space is run by students, meaning that it is the students that design, build and test the satellites.
An associate professor at AAU is the manager of AAU Student Space, taking care of funding, facilities, as well as outreach such as press releases. An important aspect of AAU Student Space is the fact that it is run 100 % on a voluntary basis, meaning that the students are not getting any academic credits for their participation in the project, as it is a spare-time project and not a part of their curriculum. However, students doing satellite-related semester projects do get credits for their projects. Despite not getting credits from being part of AAU Student Space, students still learn a lot from the project, as they get to work with things outside the scope of the study curriculum.

The students are primarily electronic engineering students, but software- , robotics- and mechanical engineering students are also part of the project. It is both bachelor and master students who work on the project, giving the opportunity for bachelor students to learn from the master students and utilize their knowledge and experience. It also means that a lot of different people with different kinds of backgrounds and technical knowledge contribute to the same project. This results in a problem being viewed from different angles, which restricts tunnel vision and therefore allows for a better solution.

As of the writing of this article, five cubesats have been designed and built at Aalborg University by students, namely AAU Cubesat, AAUSAT-II, AAUSAT3, AAUSAT4 and AAUSAT5, see Figure 2. Of these, four have been launched, since AAUSAT4 is still pending its ticket to orbit.
The purpose of the satellites has ranged from observing the earth with a camera or measuring gamma radiation, to receiving and decoding AIS signals. AIS (Automatic Identification System) signals are sent out by ships and by

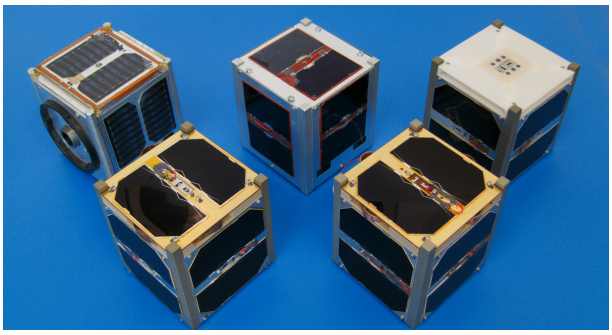


Figure 2. From left to right: AAU Cubesat, AAUSAT4, AAUSAT-II, AAUSAT5 and AAUSAT3.

decoding these signals, one is able to track the ship traffic. For AAUSAT3, it is primarily the ship traffic in the arctic regions, particularly Greenland that is monitored, as AAUSAT3 is sponsored by the Danish Maritime Authorities who would like to monitor ships in Danish waters (AAU Student Space 2013). All launched satellites designed in Aalborg have functioned in space - AAUSAT-II was operational for more than 12 months, and AAUSAT3 was operational for more than 18 months. Additionally, all of the satellites were built primarily using off-the-shelf components when possible, as to demonstrate that it is possible to build a working satellite without having to pay for space grade parts.

When ESA Education launched the FYS-program in 2013, the AAU Student Space team applied for the program with the AAUSAT4 satellite, which at the time was under construction. The *Fly Your Satellite!* (FYS) program is a ESA Education project for university students, aiming at giving students hands-on experience with working in the space industry by designing, constructing, testing and launching a satellite (ESA Education 2015b). The FYS program has primarily been focused on the documentation and testing aspects of a satellite. This is to give students insight into these essential parts of the workflow of building a satellite and ensuring that it is functional in space, in the same way as is done for a commercial satellite. Therefore, FYS has primarily been a program for already designed and built satellites, that were ready, or almost ready, for testing (ESA Education 2013).
AAUSAT4 was selected for the program in June 2013, along with five other university student teams (ESA Education 2015b). The design and payload of AAUSAT4 was largely based on AAUSAT3, but with a new and improved AIS receiver. The AAUSAT4 satellite made the foundations for AAUSAT5, which is described in the following section.

3. AAUSAT5

In the spring of 2014, ESA invited AAU Student Space to contribute with a satellite, AAUSAT5, that would be launched in conjunction with ESA astronaut Andreas

Mogensen's mission to the International Space Station (ISS), who was also set to be the first Danish astronaut. This was partly done to increase public interest in space, but AAUSAT5 would also act as ESA's pilot project for a variant of the FYS program called *Fly your satellite from the ISS!*, as AAUSAT5 would be the first ever ESA satellite launched from the ISS. The AAUSAT5 mission is therefore partly sponsored by ESA, who have provided access to its testing facilities at ESTEC, guidance from their experts, sponsored additional tests at private companies, and sponsored the HTV-5 launch to the ISS.

As the satellite had to be built, tested and be ready for launch within a year and a half, it was not realistic to design a new satellite. Instead, it was decided to base the design on the AAUSAT4 satellite. This proved advantageous, since AAUSAT5 was to be built primarily by students new to AAU Student Space. Thus, it was determined that it would be beneficial for these students to get an introduction to space technology by building a previously designed satellite with flight heritage from AAUSAT3, which most of the AAUSAT4/5 design is identical to, before designing a new satellite.

Compared to the AAUSAT3 orbit and the desired AAUSAT4 orbit, the ISS orbit has some major differences. First off, the altitude is different: AAUSAT3 has an orbit altitude of about 800 km (NY2O 2015a), whereas AAUSAT5 only has an altitude of approximately 400 km. Due to the low altitude of AAUSAT5, the atmospheric drag will be more prominent, resulting in a shorter mission lifetime. The mission duration is estimated to range from three to eight months after deployment (ESA Education 2015a), before AAUSAT5 will burn up in the atmosphere. Additionally, the orbit of ISS has a rather low inclination of $51.6°$ (NY2O 2015b), whereas AAUSAT3 has an inclination of $98.6°$ (NY2O 2015a). This means that AAUSAT5 will not be able to pass over the arctic, as AAUSAT3 can. Thus, AAUSAT5, unlike AAUSAT3, is not able to monitor ships in the arctic regions.

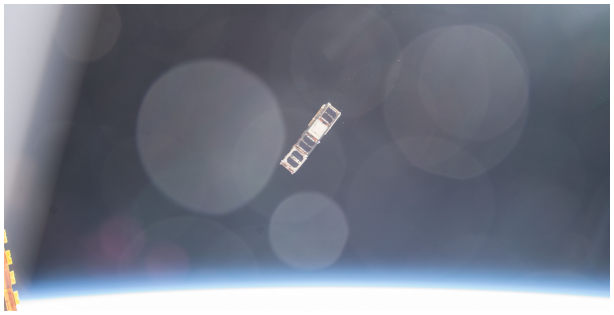


Figure 3. A photo of AAUSAT5 and GOMX-3 shortly after deployment. Credit: NASA

Compared to AAUSAT4, the design of AAUSAT5 is very similar, apart from a few changes. Due to time restrictions, the experimental Attitude Determination and Control System 2 (ADCS2) subsystem was not implemented, and the solar sensors used by this subsystem were therefore not included either. Also, some changes had to be done to the kill switch circuit and power supply, to ensure no undesired booting of the satellite could take place on board the space station.

AAUSAT5 was launched to the ISS on board the HTV-5 spacecraft on August 19, 2015, and was deployed from the ISS October 5th, see Figure 3. After deployment, two-way communication to the satellite has been obtained, however the signals from the satellite are weaker than expected. In the following section, the architecture of AAUSAT5 is explained, with a focus on the distributed architecture utilized.

4. ARCHITECTURE

AAUSAT5 utilizes a distributed structure, meaning that there is not just one On Board Computer (OBC) on which all commands are executed. Instead, multiple subsystems are located in the satellite, which communicate on a common bus. Both hardware and software subsystems exist, which each have their own purpose, functionalities as well as their own processing unit. This can be seen on Figure 4, where the different subsystems on AAUSAT5 are illustrated. The satellite consists of the four hardware subsystems: Electronic Power Supply (EPS), Radio (COM), Attitude Determination and Control System (ADCS) and the payload (AIS). There are also two software subsystems, namely the Flight Planner (FP) and the log (LOG).

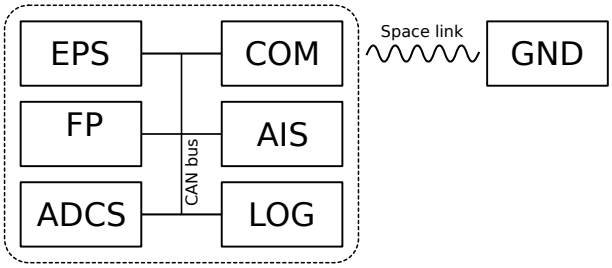


Figure 4. The distributed architecture of AAUSAT5.

This distributed architecture has multiple advantages: First of, the satellite is less vulnerable to hardware and software failures, mostly regarding the OBC, since a failure in a single processing unit on a single subsystem might not render the entire satellite inoperable, which would be more likely with a single OBC. So, if for instance the ADCS breaks down, the rest of the satellite can still operate as normal.

It also allows for easier development, since each subsystem can be developed independently of the others, as long as the mutual interfaces have been defined in advance. Because of this, smaller groups of people can work on multiple subsystems, thus allowing parallel work. From a manufacturing point of view it is also advantageous, since each subsystem can be soldered and tested independently, leading to a more time efficient manufacturing

phase. It is also relatively easy to change a certain subsystem or add new ones, as long as they comply with the set interfaces.

A lot of care has to be taken when utilizing a distributed architecture, as the interfaces have to be defined in advance. These interfaces include electrical (SPI, I^2C, CAN, etc.), communication interfaces (e.g. package size, header content), and of course a clear definition of what each subsystem is responsible for. For instance, should the ADCS be allowed to change the current to the magnetorquers in order to change the attitude of the satellite, or should the EPS do it because it is power-related? If this is not done thoroughly, use-cases might exits where the satellite will not behave as desired.

However, despite using a distributed architecture, if the COM breaks down, it would most likely result in a mission end due to the loss of communication link with the satellite. In the case of the EPS breaking down, the mission will also end due to the loss of power to the subsystems. These concerns are however present in most, if not all, cubesat designs by nature, unless duplicate systems are used to increase redundancy. In the following section, the learning methodology at AAU is explained, as this is also the methodology used at AAU Student Space.

5. PROBLEM BASED LEARNING

Aalborg University differs from most universities in regards to its learning methodology (Aalborg University 2015). At AAU, a problem based learning (PBL) approach is applied. This means that students, instead of only getting a theoretical knowledge about a certain topic through their courses, also get to use their knowledge to understand and solve a real world problem. Some contextual investigation has to be done in this regard, in order to find out how a solution based on the acquired knowledge can fit into a real world problem. This gives hands-on experience with solving a problem, meaning that students are prepared for the reality that meets them when they graduate, as most jobs in some way require problem-solving skills.

At AAU, this PBL approach is implemented by means of semester projects. Here, half the semester study time is allocated for courses, and the other half for a project related to the curriculum of the semester. Groups of two to seven people work together on each semester project, meaning that students will also get a great deal of experience regarding cooperation and working in a team, project management, as well as solving conflicts in the group.

The working methodology in AAU Student Space is very similar to the one in the semester project. A problem is found, e.g. *how can ship traffic be monitored from space?*, and a solution is developed, in this case a cubesat. However, there are some differences, especially the fact that the project duration of a cubesat is many times greater than a semester project, which only lasts five months. Also, there are more people working on a satellite than at a semester project. This means that the planning and structuring of the project is more complicated than what the students are used to, however experience shows that the students, through their semester projects, have obtained the tools needed to administrate this task.

Also, the AAUSAT5 project has demonstrated practical application of the things learned in the courses at AAU, such as modulation theory, software design and communication protocols. Students have also learned things which are not part of their study curriculum when building AAUSAT5, such as how to do space grade soldering, how attitude determination and control works in space and how to design a space grade power supply. From a learning perspective, this is of great value, since the students obtain more knowledge and hands-on experience with various topics, which is of great value for potential employers. Now that the AAU PBL methodology has been explained, the FYS methodology can be described and evaluated.

6. FLY YOUR SATELLITE!

Being part of ESA Educations FYS program has been a great learning experience and a great opportunity for the students to learn how to test a satellite and work with an industry leading organization. The students have also learned how much documentation is needed for a satellite as well as the level of detail required for the documentation. Also, it made it possible to work with experts in different fields such as mechanical engineering and thermodynamics, which the AAUSAT5 team otherwise would not have been able to.

Since the *Fly Your Satellite from the ISS!* program is still a pilot project, there are a few places where improvements of the program can be made. This is especially regarding coordination of requirements. For instance, there were initially a lot of requirements from ESA regarding the satellite, which the cubesat team was to document how the satellite was compliant with. However, almost a year after the program was started, it turned out that a lot of the requirements were superseded by the launch provider, NanoRacks, and that the cubesat thus did not need to be compliant with the requirements set by ESA. Therefore, more information about deadlines and requirements that the satellite has to comply with should be given to the cubesat team as early as possible. This is especially important if these requirements require testing, as testing can be a time-consuming process. The FYS team should also strive towards making sure that the information given to the cubesat team regarding these things should ideally not be changed at a later point. To accommodate this, better coordination between ESA, NASA, the cubesat team and launch provider is suggested. This is to make sure that all parts as early as possible agree on what needs to

be done throughout the project and what the responsibilities are for each stakeholder.

The mutual understanding of deadlines should be improved between ESA and the cubesat team. From the cubesat team's side, the team has to recognize that the FYS team has to handle the documentation over to review boards and launch providers and that the documentation therefore has to be made within deadlines. From the FYS team's side, the team has to recognize that the students have semester projects to look after, which means that the number of students working on the cubesat project at a time varies.Also, since the project is run by students, the time to work on satellite-related tasks during the exam period and the time up to project hand-ins is also limited. On the other hand, the students are willing to put the time into the project in their spare time, so deadlines can be met. From the PBL and FYS methodologies, methods for project structuring can be utilized, as described in the following section.

7. PROJECT STRUCTURING AND RESOURCE MANAGEMENT

At AAU Student Space, a horizontal project management is employed, meaning that the project is a collaborate effort on equal terms for all team members, i.e. a flat hierarchy. Due to the satellite's architecture, where the subsystems are independent from one another, it is possible for the cubesat team to split into small groups which each focus on their own subsystem. This way, the development and manufacturing process is parallelized, speeding up the entire process. Major success has been experienced with this group structure, due to its resemblance to the semester group projects at AAU, which the students are used to and comfortable with.
As a result of the horizontal project management structure at AAU Student Space, the students have a weekly meeting, where decisions are made in plenum. Here, the team discusses how the current progress of each subsystem is, and what the course of action should be for the future. This is done to ensure that all subsystems are ready for the deadlines imposed on the team. This involves making a schedule for when each team uses the single clean-room available, when subsystems should be completely soldered, when individual subsystem tests should be performed etc.
By using this structure, the team members are given a flexible work schedule, which means that they are not forced to shift focus away from their semester projects. Instead, they can plan when they work on the subsystems themselves, as long as they meet the agreed upon deadlines.
When manufacturing the subsystems, several performance and module tests are performed, so that any potential errors or problems are revealed before the entire subsystem has been soldered. This allows the team to try either correcting the errors or starting over on the subsystem, without having wasted time working on a faulty board. However, time for problem fixing should also be allocated, as the students otherwise would have a stressful time trying to manage semester projects and satellite projects simultaneously.

However, for the mission test (MT), vibration test (VT) and thermal-vacuum test (TV) of the satellite, it is required that the team allocates more time than usual. This is due to the length of the tests, which ranges from 2 days to 2 weeks, with the TV and VT requiring specialized equipment, and requires the presence of several team members to conduct the test and write the necessary test reports. These tests should be planned well in advance, as to avoid a rush period before test start. This was not the case before the AAUSAT5 TV, which took place at the ESTEC facilities in the Netherlands. This meant that for 4 days before the test start, the team worked extensively on getting the satellite ready for testing, and making sure that every subsystem worked nominally. This was partly due to unlucky scheduling, as it was not possible to get final confirmation of when the test could take place until a few weeks in advance due to scheduling conflicts. It was however primarily due to the EPS requiring more thorough testing than the previous satellites' EPS, which the team had not taken into consideration when doing the project planning.

Furthermore, when manufacturing the subsystems, the team experienced several times that the previous AAU Student Space teams had made changes in either the design or implementation, without documenting it, or that the AAUSAT5 team did not have access to the documentation. This resulted in delays when soldering and testing, as it had to be discussed and verified with the members of previous satellite teams whether the documentation accessible to was correct. This had for example the effect that the readability of most of the code was low due to the lack of comments or the fact that the GUI code for the ground station software is currently difficult to modify, as a result of the lack of documentation of the code.

To help with the organization of the tests, the team should utilize timetables such as a Gannt chart to keep track of deadlines. However, the current work distribution should be maintained, due to the architecture of the satellite and the size of the team. Furthermore, it is recommended to reduce testing times by developing automatized testing software for each test. This would require less human interaction during the test, thereby minimizing the potential human errors and influences. Additionally, the test software should be capable of filling out a standard test report, to minimize the workload for team members. This would allow the conductor to start the test and hereafter work on other pressing matters, or conduct several tests at the same time on different subsystems. A vital part of making a satellite, and testing it is the documentation. This aspect of a cubesat program is discussed in the following section.

8. DOCUMENTATION

The documentation required for AAUSAT5, and especially AAUSAT4, has been greater than what was previously done for e.g. AAUSAT3. This is due to the FYS-project, where the required documentation needed to be very detailed and thorough. This was partly to give students a glimpse of the documentation needed for a commercial satellite, but also to make sure that the satellites fulfill the requirements set. Because of this, some of the documentation is not seen as essential as others by the cubesat team, possibly because it has not been properly adapted for a small cubesat. We would therefore advise that the amount of documentation that student cubesat teams have to provide as part of FYS is reconsidered. Also, it should be evaluated if the documents are necessary for the mission to be a success, to ensure that the necessary documentation fits the scope of a cubesat project for students, especially when considering the new students lack of experience regarding space technology. For new students participating in AAU Student Space, it can be difficult to understand the communication between the cubesat team and ESA, due to the large amount of abbreviations used. In fact, it can be difficult to keep track of, even for long-term team members.

Generally, it can be difficult to keep track of the referencing of requirements and tests, to indicate which tests show compliance with the requirements. To make this easier, it would be advised to do this referencing, e.g. by the use of a compliance matrix, when designing the requirements and tests, so that the tests are designed with the requirements strongly in mind.

The level of documentation performed on previous satellites has been rather limited, and has mostly been regarding mechanical stability as well as radio licensing, to be delivered to the launch provider. Also, most of the documentation has not been properly migrated to where documentation is currently stored. This means that the reasoning behind old design choices originating from previous satellites is either lost or will have to be passed by word of mouth to new cubesat members.

The requirements set by ESA to the satellite as part of the FYS-project are listed in the *Fly Your Satellite! interface Design Specification* (FDS). These requirements are, together with the cubesat teams own requirements listed in the *System Specification Document* (SSD), put in the *Verification Control Document* (VCD) tool in the FYS portal, see Figure 5. The FYS portal is a shared drive where both ESA and the cubesat team can upload files and comment on files and requirements, and is used to document compliance with the requirements.

However, the VCD-tool can be difficult to use, especially for new students who have not used the tool previously. Firstly, it is problematic that it is possible for the cubesat team to edit text fields that the team is not allowed to edit. The layout of the website used to interface with the portal has a non-intuitive layout, which decreases readability and makes it difficult to find what one is looking

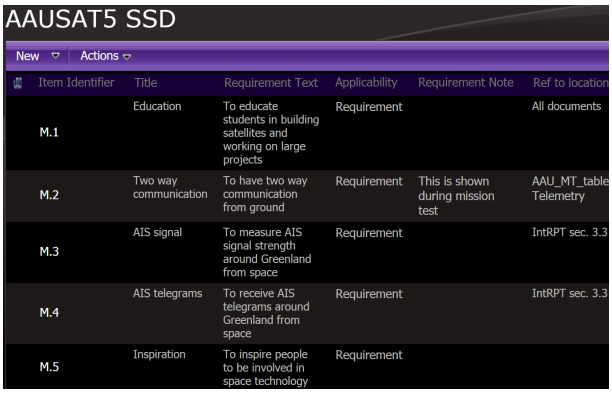


Figure 5. An excerpt from the FYS portal.

for. The FYS team is notified when changes occur in the portal, whereas notifications for the cubesat team is only implemented in parts of the FYS portal - it would be advantageous if this was implemented fully, as it would reduce the feedback time from the cubesat team. Dates for when changes are made in the portal also needs to be added manually, which can be tedious and is often forgotten, which reduces traceability. Also, it is not possibly to link/reference to documents uploaded to the FYS drive, and thus referencing has to be done for each individual requirement by mentioning the name of the referenced document or attaching the relevant document to the requirement. A direct link to the document on the FYS drive is thus not possible to have, resulting in the same documents being uploaded several different places, or in some cases only some places, resulting in lack of traceability.

We therefore propose that the FYS portal is updated with a more user friendly and intuitive design, in which user restrictions are employed, so that the teams can only edit what they are supposed to have access to. The updated design should also automatically keep track of which changes are made by which team and create a user- and time stamp after each change. Finally, the portal should utilize a centralized documentation repository, which the cubesat teams upload their documents to. This repository should be easily accessible from the requirements sections, from which the user can easily reference the document so that it is accessible from the requirement page, without uploading the document again. By using a centralized repository, only one copy of each document is uploaded, and the traceability of the documents is not jeopardized. Having a centralized repository eases the sharing of knowledge between team members, which is described in more detail in the following section.

9. KNOWLEDGE SHARING

An essential part of any engineering project is the sharing of knowledge between the members of the team working on the project. This can be done in multiple ways, some of which have been used in the AAUSAT5 project. For

version control of schematics, software and documentation, Git and Github has been used. This is practical since previous versions of the files can be located if important features are deleted. Also, it is possible for multiple people to work on the same files at the same time on different PC's, since Git handles the merging of the files. Another feature of Git is that different branches of the same repository can be made, meaning that a new feature can be implemented in the code in a new branch, without changing the code that the other developers are using. When the feature is implemented and working, the branches can be merged.

However, for general communication between team members regarding meeting dates, development statuses and minutes of meetings, a different platform is needed. Here, different methods have been used during the AAUSAT5 development phase. Initially, Trac was used, an open source wiki, project management and bug/issue tracking system. However, Trac was abandoned after a few months - partly because it was not used by the entire team and became a part of the routine to use, but also because it was not as user-friendly as it could be.
Instead, the AAUSAT5-mailing list was used, which all members of the AAUSAT5 team were a part of. The mailing list is fast and easy to use, and since everyone at the university use their email anyways, the response time is very fast. However, the mailing list is not ideal for saving information such as test results, since the information can quickly get lost, due to the amount of emails that are sent. When using the mailing list, all members are notified whenever a mail is sent, no matter its relevance for all team members.

For a short period, Slack was also used. Slack is a messaging app for teams, which allows multiple people from the same team to create multiple *channels*, i.e. multiple chats. This enables easier, faster and less formal communication than via email, and allows integration with other tools such as Twitter and Github. It also enables team members from different subsystems to see what is going on in other channels, to have an idea of the progress of other subsystems. However, Slack was also abandoned, because it was not used by the entire team and the response time was too long compared to when sending emails, because all university students already use their email daily. Slack was therefore a website that team members had to visit to see if there was a message which required their attention. A mobile app and push notifications do exist for Slack, but these were not used to the full extent by the entire team.
From these experiences, it can be concluded that information can easily get lost if there are too many channels of communications, and different parts of the team use different channels and to different extents.

For future projects, the project management tool and bug/issue tracking system should first and foremost be quick and easy to use. A wiki-like functionality is needed to save information about how things are done, or how things work. But a fast and easily accessible communication channel should also be available, for quick information sharing between team members. Finally, a version control software such as Git should be used for schematics and software. Documentation in the form of reports, such as test reports, could also be put in the version control software, but could also be done in the wiki and then exported when needed, which would allow for easier, faster updates.

It should be decided at an early point in the project which tools are used and for what, and an introduction of the tools should be made to all team members, to ensure that everyone knows how to use them. This ensures that the tools will in fact be used by all members of the team, which is the most important factor for ensuring a proper knowledge sharing. Whatever project management tool is chosen, the knowledge from previous satellites should ideally be migrated to this tool, to prevent the loss of information between "generations" of AAU Student Space members, as discussed in the *Project structuring and resource management* section. Many lessons have been learned after the launch of AAUSAT5 with regards to troubleshooting among other things. This is described in the following.

10. EXPERIENCES LEARNED AFTER LAUNCH

After the launch of AAUSAT5, a lot of work was put into getting the radio link up and running. It turned out that the signal strength of signals transmitted by AAUSAT5 was not as strong as expected, which meant that the signals could not be received and decoded in Aalborg. Therefore, a systematic problem detection had to be initiated, to find the cause of the problem with the purpose of solving it. A ground station had been sent to Lars Mehnen in Austria before the deployment, as it was known in advance that the signal strength in Aalborg would not be as strong as that a smaller latitudes, due to the inclination of the satellite. Signals were received in Austria, but they were not as strong as expected either. The signals received were too weak to be decoded, but the Morse beacons transmitted by the satellite could be decoded, indicating a battery voltage of 7.9-8.0 V and a temperature of 21° C (AAU Student Space 2015, p. 4).

Mike Rupprecht, a radio amateur in Germany, had some rather strong signals, and forwarded IQ-recordings of those signals to the AAUSAT5 team, for decoding. When the first data beacon was decoded, it showed that the satellite was in good condition with the expected subsystems powered on (AAU Student Space 2015, p. 4). The first decoded data beacon can be seen in Figure 6.

A pass log was introduced on the mailing list, where a brief summary of each pass was written, containing info about signal strength, beacons received and data/requests sent to the spacecraft. This is necessary as a part of the knowledge sharing between team members, Mike Rupprecht and Lars Mehnen. It can also be used for backtracking issues, as a record of the steps taken to resolve a problem should always be kept.

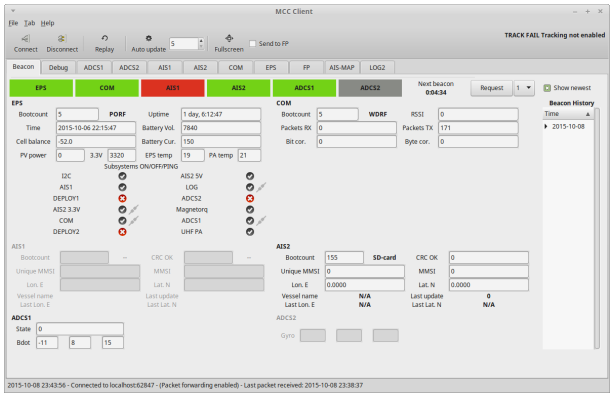


Figure 6. The first decoded data beacon from AAUSAT5.

Since the deployment, different data has been requested from the ground station, to assist in the troubleshooting. As of the writing of this, the cause of the low signal strength has not been identified, but a strong suspect is that the antennas have not fully deployed. This would also explain why no AIS data has been received.

From this, it is clear that a lot of work has to be put into troubleshooting a spacecraft, and that the task is not made easier when the passes only occur 3 times a day and has a duration of only 10-15 minutes. However, students have learned a lot from troubleshooting, for instance regarding how radio receivers and ground station works. So, from a learning perspective, the communication issues have in fact been beneficial, and has required much more work from the team than if the satellite was operating nominally.

From the launch event, it was clear that multiple outreach responsible are needed for a cubesat project that has caught the media's interest. It turned out that the media's interest for the project was bigger than expected, which meant that more team members could be used for interviews etc. Also, more work should be put into maintaining a social media profile on e.g. Facebook and Twitter, since the interest for the satellite, especially in the time around launch, is rather big. But as every member of the AAUSAT5 team was busy during the launch with various mission critical tasks and media outreach, social media was down-prioritized.

For the next satellite to be made at AAU, the possible causes for the low signal strength should be found, and fail safe mechanisms should be introduced and improved to prevent a similar problem from occurring again.

11. CONCLUSION

To conclude on the experiences learned from the AAUSAT5 project, we propose that future student-run cubesat teams utilize a workflow, which is heavily influenced by the AAU Student Space and FYS workflow.

When managing a student-run cubesat-project, we propose utilizing the group structure, which has been utilized for all AAU cubesats. This structure allows for several groups researching, developing, testing and documenting independently of each other. However, for this structure to work it requires that the satellite supports the possibility of having several groups working on several subsystems at a time. The team should also remember to add time to solve potential problems before a deadline, as they otherwise will experience stressful periods where they try to fulfill deadlines, but have to redo an entire subsystem after having found a fatal error. This especially applies to the weeks before any major test.

This methodology also sets some requirements for the participants, as it requires that they are capable of managing their own time, taking responsibility, and working together in a group. This may not be as intuitive to students from universities that employ more traditional learning methods than AAU. Nonetheless, we recommend this group structure, as it also prepares the students for the job market, where they have to work in groups or small teams, and be able to rely on each other and solve potential group problems.

For resource management, we propose that the team sets up a central hub, such as a websie, where all information regarding deadlines, documentation, timelines etc. is easily attainable. Here, the user should be able to check e.g. whether the cleanroom is booked, without having to struggle with a nonintuitive interface. If this is not the case, important information is scattered around on different e-mails, websites and is ultimately lost.

The website should also be utilized for project management, where the user should have access to a set amount of tools such as a bug/issue tracking system, a wiki for writing and exporting documentation, a communication channel between team members, integration with a version control system (Git, SVN) etc. It is especially important that it is easy and intuitive for the user to manage and add to the documentation.
This can partly be done by automatizing the test procedure so that a piece of software performs the test and creates a document describing whether each test was nominal, who the test conductor was, test date etc. This way, all test reports are standardized, and can then be stored on the website.
The version control system should be used primarily for schematics of the satellite and for software. This way, the team is able to work on several tasks on the same software, or test different implementations, without the fear of losing valuable data. The change log of this system should be accessible from the website, to retain the de-

sired central hub structure, allowing the user to get all necessary information from one place.

When writing documentation, we propose that the user should settle for a midpoint between the amount that the AAU Student Space teams has normally written, and the amount required as a part of the FYS-program. Every meaningful change to the satellite, either software or hardware, should be properly documented and stored, but the amount of documentation that has to be written should also match the scope of the project. The team should therefore, in our opinion, not be required to document the student-built cubesat as if it was a commercial satellite. However, this is not always the team's decision. Therefore, we also strongly advice any team that works with a sponsor or launch partner to agree upon the scope of documentation and deadlines in advance. This also includes informing one another about ones working conditions, such as the fact that in the case of AAU Student Space, everything on the satellite is made by voluntary students in their spare time.

ACKNOWLEDGMENTS

The authors would like to thank the European Space Agency, for their great help with the testing and documentation of the AAUSAT4 and AAUSAT5 satellites, as part of the FYS program. We would especially like to thank Mr. Piero Galeone and the team associated with the FYS-program for their assistance throughout the entire project. ESA has also assisted in sponsoring the authors trip to the 1st Symposium on Space Educational Activities, of which the authors are grateful for. A thanks also goes to the Study Board for Electronics and IT at AAU, which has also helped fund the trip.
Associate professors Jens Dalsgaard Nielsen and Jesper Abildgaard Larsen are also thanked for their great involvement in the AAU Student Space project, and their willingness to always assist in any way possible.
All sponsors and other companies who has been of assistance regarding the AAUSAT5 satellite are also thanked, especially Hytek and ZARM, for their great help with the vibration testing. All the radio amateurs who has helped with detecting beacons from AAUSAT5, specially Lars Mehnen (OE3HMW), Mike Rupprecht (DK3WN), Jan Van Gils (PE0SAT), Edson W. R. Pereira (PY2SDR) and Lars-Christian Hauer (DJ3BO) for their help with receiving the signals from AAUSAT5, and thus showing that the satellite was alive and well. We would especially like to thank Lars Mehnen (OE3HMW) who let us use his antenna as a ground station and Mike Rupprecht (DK3WN) who let us use his ground station to listen with.
Finally, the authors would like to thank all members of AAU Student Space, both students and former students, for their high level of enthusiasm and willingness to put the work into the project that is needed. You guys are the best.

REFERENCES

Aalborg University. 2015, The Aalborg Model For Problem Based Learning, http://www.en.aau.dk/about-aau/aalborg-model-problem-based-learning/

AAU Student Space. 2003, AAU cubesat, http://www.space.aau.dk/cubesat

AAU Student Space. 2013, AAUSAT3 Mission Description, http://www.space.aau.dk/aausat3/index.php?n=Main.AAUSAT3MissionDescription

AAU Student Space. 2015, AAUSAT5 LEOP Status Report

Cal Poly SLO & The CubeSat Program. 2014, CubeSat Design Specification Rev. 13, http://333.cubesat.org/images/developers/cds_rev13_final2.pdf

ESA Education. 2013, Call For Proposals: Fly Your Satellite!, http://www.esa.int/Education/Call_for_Proposals_Fly_Your_Satellite

ESA Education. 2015a, AAUSAT5 Mission, http://www.esa.int/Education/CubeSats_-_Fly_Your_Satellite/AAUSAT5_mission

ESA Education. 2015b, Fly Your Satellite! Programme, http://www.esa.int/Education/CubeSats_-_Fly_Your_Satellite/Fly_Your_Satellite!_programme

NY2O. 2015a, AAUSAT3, http://www.n2yo.com/satellite/?s=39087

NY2O. 2015b, SPACE STATION, http://www.n2yo.com/satellite/?s=25544

Walker, R., Galeone, P., Page, H., et al. 2010, in Education Engineering (EDUCON), 2010 IEEE, 1699–1708

ELEONORA: A INTERNATIONAL SATELLITE PROJECT FOR THE CANADIAN SATELLITE DESIGN CHALLANGE

Marcello Valdatta[(1)], Lawrence Reeves[(2)], Jacopo Panerati[(3)], Constance Fodè[(4)], Niccolò Bellini[(5)], Davide Rastelli[(6)], Stefano Naldi[(7)]

(1) University of Bologna, Aerospace Eningeering, Via Fontanelle, 40, Forlì FC, Italy; Marcello.valdatta@gmail.com
(2) Canadian Satellite Design Challenge Management Society, 5050 Elgin St.,Vancouver, B.C. CANADA LReeves@csdcms.ca
(3) Ecole Polytechnique de Montreal, Canada; École Polytechnique de Montréal C.P. 6079, Succ. Centre-Ville Montréal (Qc), H3C 3A7 Canada; jacopo.panerati@polymtl.ca
(4)Ecole Polytechnique de Montreal, Canada, PolyOrbite society; École Polytechnique de Montréal C.P. 6079,. Centre-Ville Montréal (Qc), H3C 3A7 Canada; constance.fode@gmail.com
(5) N.P.C. New Production Concept, Via Errico Malatesta, 27-29, 40026 Imola BO; niccolo.bellini@gmail.com
(6)N.P.C. New Production Concept, Via Errico Malatesta, 27-29, 40026 Imola BO; rastelli.dav@gmail.com
(7)N.P.C. New Production Concept, Via Errico Malatesta, 27-29, 40026 Imola BO; naldi.ste@gmail.com

ABSTRACT

The Canadian Satellite Design Challenge (CSDC) is a competition, focused on educational purposes, for teams of university students (both undergraduate and graduate) to design and build a "Cubesat" satellite, which will conduct a science mission. Eleonora is a 3U cubesat designed by PolyOrbite, a joint team from Polytechnique Montreal (Quebec, Canada) and the University of Bologna (Italy) to compete in the 2012-2014 edition of the CSDC. The Eleonora mission had a timeline of 20 months and followed the key reviews of a space project, including workshops organized by the CSDC panel, and concluded with the vibration tests at David Florida Laboratories (DFL) of the Canadians Space Agency (CSA). The two teams worked in their respective country but had regular meetings, via teleconference or in person, to review the project. During the initial period of the competition, the two teams worked together to define the mission, then designed, produced, integrated, and tested the 3U cubesat. The Eleonora mission had two principale objects: the first objective was to use a camera to take photos of the Canadian Arctic for the Geocryolab (Laboratory of Geotechnics and Geomorphology of Cold Regions) of the University of Montreal; the second objective was to test in flight and validate a deorbiting system consisting in a deployable sail, suitable for cubesats, in order to avoid, in the future, the proliferation of space debris. Eleonora obtained third overall place among teams coming from ten of the major Canadian universities. The paper describes the CSDC competition and explains the work made by the members of the teams with different backgrounds and preparation level. The paper show how the work was organized, the scientific motivations, the technical description of the satellites, organizational issues and lessons learned, and how the members gained experience during the competition, with a view to the future of the programme.

.

1. CANADIAN SATELLITE DESIGN CHALLANGE

The Canadian Satellite Design Challenge (CSDC) is a Canada-wide competition for teams of university students to design and build a 3U cubesat (or "triple cubesat") satellite. The CSDC has the ultimate objective of launching the winning satellite in order to conduct its science mission.

The CSDC is structured like a real-world space mission; the CSDC management assumes the role of the Customer, and each participating team assumes the role of a Prime Contractor. Teams are issued requirements documents at the beginning of the competition, and have documentation delivery milestones, and a comprehensive Critical Design Review, all of which are reviewed by a panel of experience space industry professionals.

The CSDC is present a significant learning and career development opportunity for the participants, who acquire interdisciplinary technical, teamwork, leadership, and management skills. Not only do the participants gain a wealth of knowledge and experience about spacecraft design and engineering, but also project management. It is hoped, and intended, that the experience and leadership skills they acquire will help them to achieve success in their post-university careers, and benefit equally the organisations at which they pursue their careers.

2. TECHNICAL SOCIETY POLYORBITE

Thanks to the contact with the director of the CSDC a group of student of University of Bologna had the possibility to join the team of Polytechnique Montreal for the 2012 – 2014 edition of the contest.

As usual in the Canadian universities, the student of Montreal founded a technical society named of PolyOrbite.
At the École Polytechnique de Montréal (EPM), technical societies ("sociétés techniques" in French) are student associations that offer to the student body the chance to apply their personal talents and classroom knowledge to concrete engineering projects.
In most cases, these technical societies aim at validating their prototypes (whether they consist of a solar car or an hybrid rocket or else) on the stage of national and international competitions, representing EPM and their sponsors with pride.
The involvement with technical societies allows students to foster their technical knowledge and to demonstrate soft skills such as: teamwork, leadership and management, that also play an important role in an engineering career.
Founded at EPM in 2012, PolyOrbite is one of these societies, as well as the only one dedicated the development of space applications.
Since its creation, PolyOrbite helped promoting interest in space-related activities among students and faculty and it is now regarded as a major asset for EPM.

The Canadian Satellite Design Challenge (CSDC) is a two years competition organized by a "federally-incorporated not-for-profit organisation" [1] now at its third iteration.
The goal of the CSDC is to bring together teams of graduate and undergraduate students from Canadian and international universities and let them confront one another in the development of a nano-satellite with affordable materials and technologies.
The work of PolyOrbite's CSDC team is supervised by a single project manger (fig 1) and it is split among seven different teams. Six of these teams are purely technical in nature and they are in charge of the design and development of the six subsystems of the satellite (structure, payload, power management, data-handling, telecommunication, and attitude control).
The seventh team is the "financial team" whose task is to raise and manage the budget required by all the other teams.

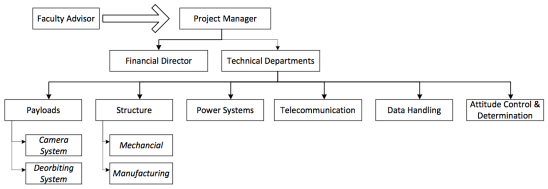


Fig1 Team Organitations

In order to raise enough money, the financial director of this team has to build good relationships (i.e. partnerships and sponsorships) with local companies working in the aerospace field, banks, research foundations, and anyone else who values and wants to support the project.
In order to maximize the probability of a financial agreement being renewed, it is also important to keep in touch with all sponsoring organizations by sending them monthly newsletters regarding the progress of PolyOrbite and how their money was spent.

PolyOrbite's demographic consists, for the most part, of undergraduate students---this is a common trait of all technical societies at EPM---from several different engineering fields (e.g. mechanical, aerospace, computer, physical and electrical engineering).
It is also worth mentioning that the majority of them did not have previous expertise in space and space-related technology.
A limited number of graduated students cover major roles (e.g. team leaders) and can provide guidance and share knowledge with the entire team.
A faculty advisor, in the person of professor Giovanni Beltrame from the EPM's Department of Computer Engineering, supervises the team and acts as an external counselor.
Once a year, the team leaders and the project manager of PolyOrbite invite interested people to join the society conducting a recruiting session.
The selection process usually weights the motivation factor just as much than the technical skills possessed by an aspiring candidate.

Student of Polytechnique Montre´al and students of University of Bologna composed the team that participated to the project. The two teams worked in their respective country but had regular meetings, via teleconference or in person, to review the project. The major challenge was to prepare two different sets of hardware in two different places (the CubeSat structure in Canada and the deorbiting system in Italy). It means that when the two teams met for the integration, before the planned vibrations test, all the parts had to be assembled without deep modification. To succeed in such a challenge, the details need to be planned in advance, including the alternative strategies. It was necessary to foreseen the problematic, even from the practical and logistic point of view (necessary tools, spare parts, transportation, etc.). One of the strategies from the Bologna team was to prepare the mechanical connection ad hoc for the structure prepared in Montreal, but with the possibility to change the attach point to the structure in order to provide, in the future, the possibility to use it with different structure. This planning phase resulted very important because for technical reason independent from University of Montreal, it was not possible to use the ad hoc structure and it was necessary to use a commercial one (Figures 3 and 4). The integration projects took some hours but it was possible to build the

CubeSat and perform successful vibration test at David Florida Laboratory (DFL) of Canadian Space Agency (CSA).

3. SCIENTIFIC MOTIVATION

Eleonora satellite was design to provide data on global warming effects. One of the problems caused by the increase of the temperature is the effect on permafrost and glaciers and their consequently reduction. Even if is clear to understand the effect of the rise of temperature on ice, it is difficult to quantify this effect. For example is important to to recollect the data necessary to study and understand how the increase in average temperatures, the recession of ice landforms and transformation of periglacial areas correlate with the changes that can be observed in the biodiversity (i.e. the number of species living in the ecosystem) of the affected areas. These kind of data are crucial for the research of Geocryolab of University of Montreal, in particular for the Canadaian Artic Area (fig 2). For this Eleonora was provided with a camera to transmit to the ground photos of the situation of the artic ice. In particular the ice coverage reduction on the Bylot and Baffin island over the period going from early April to late October [2].

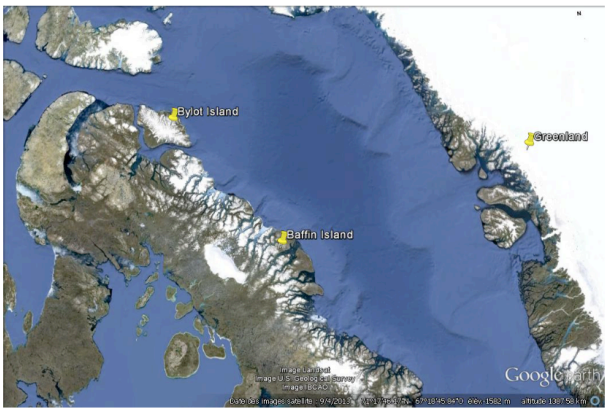


Fig 2 The area of research in Canadian Artic

Eleonora has then a limited life both in the mission and both in the hardware, as like cubesat the life expectation it is short. In other hands the orbit foreseen for the mission is between 600km and 800km. This means that the orbit lifetime of the spacecraft could have a length of even 100 years versus maximum 1 year of mission whit the possibility to grow the population of space debris [10]. From the point of view of the space debris IADC (Inter-Agency Space Debris Coordination Committee) guidelines [3] this is not an acceptable configuration. For this Eleonora was provided also with a deorbiting device designed, built and integrated by the group of Bologna. This passive device, based on a sail, will allow the satellite to respect the space debris mitigation guidelines. This deorbital device was also designed to be plug and play, this means that if working in future could be easily integrated to every cubesat. The second object of the mission is to test in flight a standardized deorbiting system for cubesat.

4. SATELLITE DESCRIPTION AND PAYLOADS

The satellite design is based on 3Unit cubesat standard [4]. The structure was based on off the shelf material readapted to host the deorbiting device. The internal architecture of the satellite was also based on commercial components for contain the costs and the time of development but with ad hoc designed elements where needed. In particular the principal subsystems of the spacecraft includes an EPS (Electrical Power System), C&DH (Command and Data Handling), an Attitude Control and Determination System (ACDS) and the payloads. The Montreal team designed and realized the solar panel and managed its integration with a commercial EPS; designed part of the C&DH, in particular for the data processing; the design of ACDS. The satellite is also provided with a GPS/GLONASS receiver in order to determinate the position [1]. The structure itself of the satellite needed to be modified to host the deorbiting system from 3U to 2.5U.

4.1 Camera payloads.

The camera is based on CMOS sensor with a resolution of 50 Mpixel able to scan an area of 1000 km by1000 km region. The challenge was to take pictures of the interaction between ice and permafrost and send them to the ground. To do so, the camera lens needed to capture four pictures every two weeks during the summer. Moreover, the quantity of pictures taken cannot be the same every season since the polar night does not permit it. The payload was designed to send compressed pictures of 1.6 MB. The major technological issue that expected to encounter is the limited data budget of the down link connection on such a small satellite. This problem will be made even worse by the power budget restrictions that are, likewise, imposed by the satellite size. For this was decided to mitigate this problem performing on-board data pre processing using low-power high-performance dedicated FPGA hardware. This pre processing has the dual goal of merging multiple pictures and compressing the information to be transmitted. A machine learning application was evaluated to optimize this process in order to pre select the important images from the large raw of data [5].

4.2 Deorbiting sail.

The deorbiting sail was the part developed from Bologna. The system is named ARTICA (Aerodynamic Re-entry Technology In CubeSat Application) [6][7]

and is thought to be plug and play and totally autonomous form the rest of the satellite. It works like an other spacecraft attached to the bottom of the principal satellite. The structure of the system is based on a box of the dimension of 0.5 cubesat. In this box is content the sail, the on board computer (OBC) of the system and the batteries. When the OBC command the start of the operation, the box is opened and the sail released. The sail work increasing the aspect mass ratio of the satellite, the drag sail accelerates the deorbiting rate of the satellite, reducing its lifetime in orbit. In this way is possible to meet the recommendations on space debris mitigation (25 year lifetime) even from critical altitudes. The sail increase the surface of the satellite and reduce the disposal time according to the following formula:

$$(t_f - t_0) = \frac{H}{B\sqrt{\mu r}} \frac{1}{\rho_{(r_0)}} \qquad (1)$$

$$B = c_d \frac{A}{m} \qquad (2)$$

Where (tf−t0) is the orbit time life, H is the scale length of the parameterization of the atmosphere, μ is the gravitational constant, r is radius of the orbit, ρ(r0) is the atmospheric density at the initial point and B is the inverse of ballistic parameter. The sail is used to increase the A/m ratio and in that way B parameter (eq. 2) that permits to reduce the orbit lifetime (eq. 1).

The results of the simulation taking in consideration a circular 700 km orbit with an inclination of 98° are showed in simulations in fig 2 and fig 4

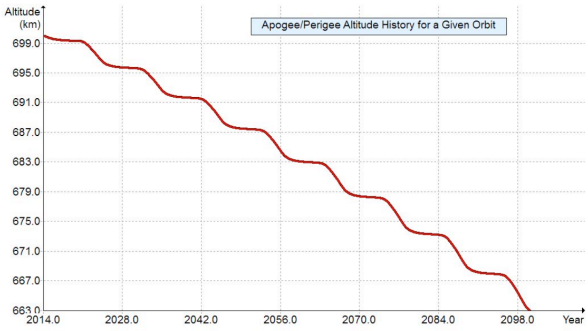


Fig 3 Natural orbit lifetime (about 70 years)

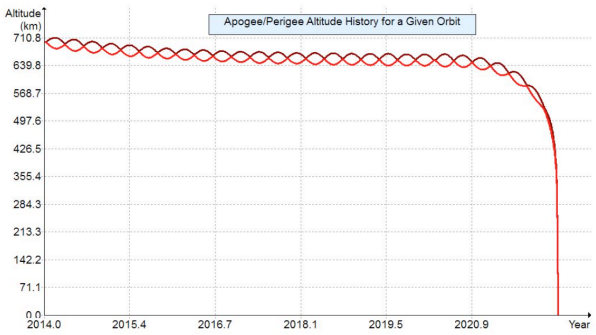


Fig 4 Sail deployed lifetime (respect the 25 years)

The system was successfully integrated in Eleonora and designed to be applicable, in future, on every cubesat. (fig 5, fig 6, fig 7)

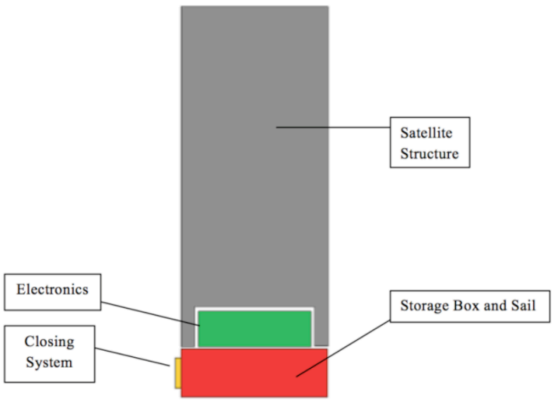


Fig 5 the set up of the satellite

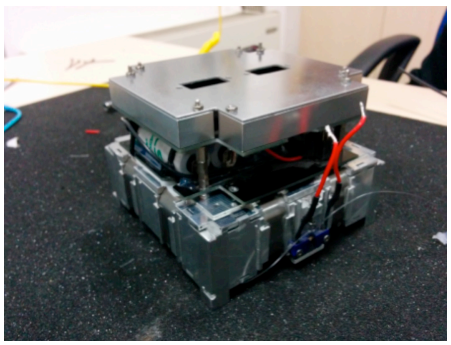


Fig 6 the deorbiting system ready to be integrated



Fig 7 the Eleonora Satellite fully integrated

5. PROGECT LIFE CYCLE

The CSDC is structured following a normal mission lifecycle on 20 months with mid term reviews and tests (fig 8). The whole team in order to advance in the competition (and in the mission) had to work in two different continents. Beside the distance between the two team, the modern telecommunication systems helped to keep in schedule and exchange information and documentation, drawing ecc. A weekly telecom was schedule between the teams to keep track and discuss of the project. Moreover the whole team had face to face team during the principal reviews of the mission and during the vibration tests.

The PDR (preliminary design review) was the fist review in which the team was all-together in Canada. The project was presented to a panel of expertise including Canadian Space Agency (CSA) and private industries. The PDR was at MDA headquarter. The team collected feedback to improve the project and to prepare the Critical Design Review (CDR).

During the CDR part of the team was involved in the presentations of the project to the IAC of Beijing and participated to the review thanks to setting a teleconference. The result of CDR was positive and the team collected useful feedback to complete the design of the satellite.

The last step of the project was the integration and the preparation for the vibration tests. The object of the test was to qualify the satellite to survive to the launch vibrations.

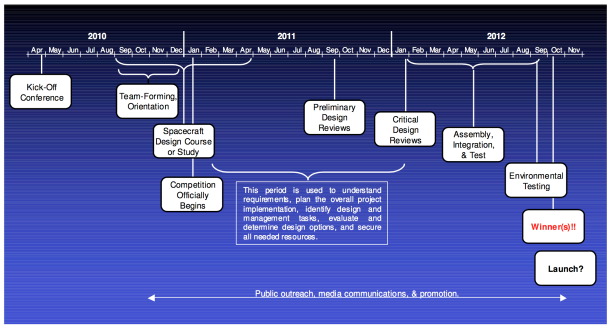


Fig 8 CSDC timeline

6. FINAL INTEGRATION AND VIBRATION TEST

The final integration was performed at the facilities of the EPM University. To succeed in such a challenge, working in different state, the details need to be planned in advance, including the alternative strategies. It was necessary to foreseen the problematic, even from the practical and logistic point of view (necessary tools, spare parts, transportation, etc.). One of the strategies from the Bologna team was to prepare the mechanical connection ad hoc for the structure prepared in Montreal, but with the possibility to change the attach point to the structure in order to provide, in the future, the possibility to use it with different structure. This planning phase resulted very important because for technical reason independent from University of Montreal, it was not possible to use the ad hoc structure and it was necessary to use a commercial one (Fig 9 and 10). The integration projects took some hours but it was possible to build the CubeSat.



Fig 9 The integration with a commercial structure

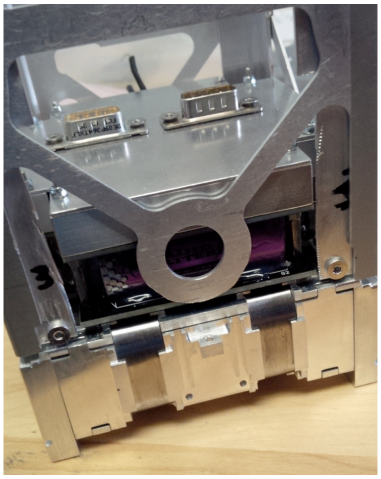


Fig 10 Detail of the integrations

The vibration test was performed at David Florida Laboratory (DFL) of Canadian Space Agency (CSA). The tests aim at qualifying the structure with respect to launch mechanical loads. The satellite was excited using a shaker and with the spacecraft closed inside a T-pod (fig 11), in all three directions (the vibrating table could move both in plane and out of plane), and for each of them the following procedure in terms of vibration was applied:

- low level sine sweep in the range 5 – 2000Hz

- High frequency random vibration 5- 2000 Hz (Dnepr PSD profile)

- Low level sine sweep in the range 5 – 2000Hz

In the post processing phase the results obtained before and after random vibration excitation in terms of amplitude vs frequency were compared in order to detect shifts in the resonant peaks which could denote a loosening in the fastening or a structural alteration. A visual inspection was carried on after the test campaign: no structural alterations or damages were detected: the retaining wire appeared to be still in position and tight keeping the deorbiting box in the closed configuration. The results was positive whit minor shifting but still plenty in the tolerance range.

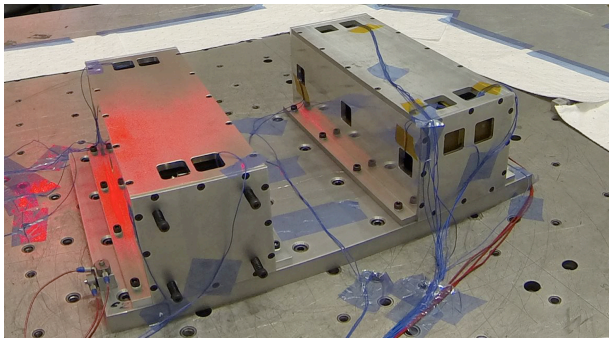


Fig 11. The vibration test at DFL of CSA

7. CONCLUSION

After the vibration test, the CSDC was declared concluded. The PolyOrbite team won the Third Prize. The result need to be considered very positive because for the team of EPM was the first time that was facing with a whole space mission. Many members were studying for the first time the problematic of the space project. Sometimes the general inexperience brings to an underestimation of the problematic connected with the design and the integrations. Moreover for the Bologna team was sometime difficult to communicate or have information about the on-going of the design of the spacecraft with Canadian team because the turnover inside PolyOrbite. In other hand both team gained a lot of experience in general design and develop of space mission and actual space hardware.
From the scientific point of view the experience had demonstrate the possibility to use the deorbiting system like plug and play unit for all cubesats. In the last configurations, next to the case of Eleonora the dimensions of the systems were reduced in order to make it suitable for smallest spacecraft. The vibration test showed that the mechanical system is reliable, as well like the design of all satellite, and the data collected are very important because will be a good start point for the continuation of PolyOrbite and for Artica. [8] [9]
An other important point was the collaboration between two students team with different cultural environment and different level of preparation. This teach to the both side how to relate with an other colleagues, whit a different point of view of an issues, in proficient way whit the only aim to reach the best design and best solution possible.
In the end new friendships and collaborations are set and in the future will be possible to start new project and research even outside from competition background. Figure 12 and fig 13



Fig 12. The team during the vibration tests



Fig 13 The award for the third prize in the competition

8. REFERENCE

[1] IAC-15,E1,3,8,x30090 ELEONORA, A 3U CUBESAT FOR THE CANADIAN SATELLITE DESIGN CHALLENGE - Constance Fodé Alexandre Guay, Prescilia Desroches, Mathieu Lalonde, Jacopo Panerati, Mark Smyth, Marcello Valdatta, Niccolò Bellini, Davide Rastelli, Stefano Naldi, Giovanni Beltrame)

[2] IAC-14,B1,6,3,x24258 A NANO-SATELLITE TO MONITOR ARCTIC GEOSYSTEM CHANGES AFFECTING BIODIVERSITY IN THE CANADIAN ARCTIC Jean-Romain Roy, Vincent Bougie, E´tienne Bourbeau, Nicolas Cloutier, Alexandre Guay, Mathieu Lalonde, Jacopo Panerati, Mark Smyth, Maxime Tousignant, Daniel Fortier, Giovanni Beltrame

[3]“ IADC-02-01 iadc space debris mitigation guidelines,” 2007. [Online]. Available: http://www.iadc-online.org/Documents/

[4] Cubesat Standard. http://www.cubesat.org/index.php/documents/developers

[5] IAC-13, E2, 3-V.4.4x18640 3U CUBESAT FOR THE CANADIAN SATELLITE DESIGN CHALLENGE: A POLYTECHNIQUE MONTRE´AL AND UNIVERSITY OF BOLOGNA COOPERATION Mark Smyth Etienne Bourbeau, Jacopo Panerati, Niccolo` Bellini, Alexandra Labbe´, Anthony Buffet, Alexandre Guay, Alfredo Locarini, Stefano Naldi, Davide Rastelli, Marcello Valdatta

[6] N. Bellini, A. Locarini, S. Naldi, D. Rastelli, M. Valdatta, and F. Piergentili, “A space debris cleaner kit based on polyuretanic foam,” in IAC-13, A6, P.29.x17013, 64nd International Astronautical Congress, Beijing, China, October 2013.

[7] M. Valdatta, N. Bellini, A. Locarini, S. Naldi, and D. Rastelli, “A compact storage deorbiting sail for cubesat applications,” in IAC-14, A6, 4.2.x25439, 65nd International Astronautical Congress, Toronto, Canada, October 2014.

[8] IAC-15- A6,IP,30,x30649 A.R.T.I.C.A. DEORBITING SYSTEM: THE NEW DESIGN AND PROTOTYPE OF A COMPACT DEORBITING SAIL ON BOARD CUBESAT “URSA MAIOR” , Niccolò Bellini , Stefano Naldi , Davide Rastelli, Marcello Valdatta

[9] Fodè, Panerati, Desroches, Valdatta, Beltrame; "Monitoring glaciers from space using cubesat"; IEEE Communications Magazine volume 53, Issues 5, page 208-210, ISSN: 0163-6804, INSPEC: 15125480, DOI: 10.1109/MCOM.2015.7105665; may2015

[10] J.-C. Liou and N. L. Johnson, “A sensitivity study of the effectiveness of active debris removal in {LEO},” Acta Astronautica, vol. 64, no. 23, pp. 236 – 243, 2009

ENHANCING SPACEFLIGHT SAFETY WITH UOS3 CUBESAT

Aleksander A. Lidtke[(1)], Clemens Rumpf[(1)], Adrian Tatnall[(1)], Hugh G. Lewis[(1)], Scott J. Walker[(1)], Mia Taylor[(2)], Robert C. Fear[(3)], Alex S. Weddell[(4)], Robert G. Maunder[(5)], James R.B. Bantock[(6)]

(1) Aeronautics and Astronautics, University of Southampton, SO17 1BJ, Southampton, UK, al11g09@soton.ac.uk

(2) Winchester School of Art, University of Southampton, SO23 8DL, Winchester, UK, mt1v08@soton.ac.uk

(3) School of Physics and Astronomy, University of Southampton, SO17 1BJ, Southampton, UK, R.C.Fear@soton.ac.uk

(4) Electronics and Electrical Engineering, University of Southampton, SO17 1BJ, Southampton, UK, asw@ecs.soton.ac.uk

(5) Southampton Wireless Group, University of Southampton, SO17 1BJ, Southampton, UK, R.G.Maunder@soton.ac.uk

(6) Electronics and Software Systems, University of Southampton, SO17 1BJ, Southampton, UK, jrbb1g11@ecs.soton.ac.uk

ABSTRACT

Earth orbits are becoming increasingly congested. This will not only impact future space operations but also become a concern for the population on the ground; with more spacecraft being flown, more objects will re-enter the atmosphere in an uncontrolled fashion. Parts of these satellites can reach Earth surface and endanger the ground population (e.g. ROSAT or UARS satellites). A student-run project from the University of Southampton aims to build a 1U cubesat (approx. 10 by 10 by 10 cm satellite), which will gather data that will improve the accuracy of re-entry predictions. The cubesat will record and deliver its position and attitude during the orbital decay, thus providing validation data for re-entry prediction tools. This will reduce the risk to the ground population because more accurate prognoses will allow mitigation measures to be implemented in the areas at risk. The mission could also allow the risk of collision between spacecraft to be estimated more accurately thanks to improvement of the atmospheric models. This would give the decision makers more complete information to use, for instance, in collision avoidance manoeuvre planning.

1 INTRODUCTION

The first spacecraft, Sputnik 1, was launched on 4 Oct 1957 [1]. More spacecraft have been launched since, many of which have been left on-orbit [2]. The fact that more spacecraft are being launched than are being removed from orbit has led to an increase in the number of objects orbiting the Earth. This is because spacecraft at high altitudes are relatively unaffected by atmospheric drag, which is the major force that makes spacecraft naturally leave orbit and re-enter the atmosphere [3]. Until mid-October 2015, the catalogue of space objects that can be tracked and whose positions were made publicly available through www.space-track.org [4] has grown to 15 268. This increase in the number of tracked objects was also caused by collisions and fragmentations, which produce small objects that are unlikely to survive re-entry. However, entire spacecraft are still being left on-orbit and will eventually re-enter in an uncontrolled manner.

It is impossible to accurately predict how many new spacecraft will be launched, at what rate, into what orbital regimes, and how many of them will be deliberately manoeuvred out of orbit [2]. This affects predictions of the total number of objects on-orbit by orders of magnitude [5]. However, if any spacecraft are launched into low-Earth orbit, some of them will eventually decay under the influence of atmospheric drag and re-enter Earth's atmosphere. Depending on the design and composition of the re-entering spacecraft, up to 40% of its original mass could survive the re-entry and reach Earth's surface [6].

The frequent re-entries of spacecraft (approx. one large object per week [6]) raise concerns about potential ground casualties that such events could cause. This has led to several institutions and countries implementing standards, e.g. NASA [7], and legislation, e.g. France [8], that address this risk.

Being able to predict re-entry in advance enables mitigation measures to be implemented to reduce the risk to the ground population. However, at present, re-entry can be predicted with an accuracy of 2 to 28% of the remaining lifetime in orbit [6]. A "rule of thumb" relative re-entry prediction uncertainty of ±20% is recommended by Pardini and Anselmo [6].

For a spacecraft located in a circular orbit of radius r around a planet with gravity parameter μ ($398600\ \mathrm{km}^3/sec^2$ for Earth), the orbital period is given by Eq. (1) [3].

$$\tau = 2\pi \sqrt{\frac{r^3}{\mu}}. \qquad (1)$$

For a spacecraft in a circular, 200 km altitude orbit, the orbital period is approx. 1.5 hours. Even with 2% re-entry prediction error bound, 24 hours before the re-entry the prediction is accurate to 33% of the orbital period, i.e. 29 minutes. For longer lead times, the time window, in which the spacecraft might re-enter, is larger. In the above example, 74 hours before the re-entry, the spacecraft could re-enter anywhere along its orbit. This means that the satellite could reach Earth's surface over any latitude it flies over, which is given by the inclination of the orbit [9]. For many orbits used by earth observation satellites, namely Sun-synchronous orbits, that implies all latitudes with the exceptions of the poles [3]. That

being said, the re-entry will take place along the satellite's ground track. Therefore, the satellite cannot impact any location on the globe. The possible re-entry locations from the above 200 km circular orbit example, 74 hours before the re-entry, are shown in Fig. 1.

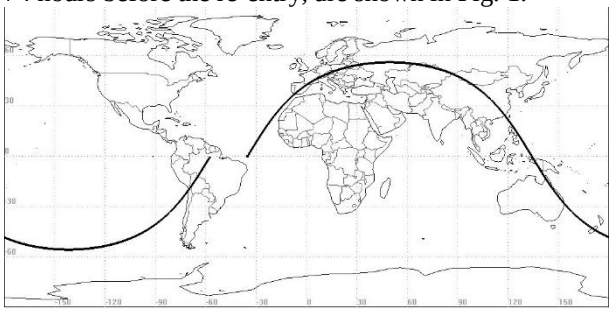


Figure 1: Possible re-entry locations of a satellite in a circular, 200 km altitude orbit with inclination of 55°. Predicted 74 hours before the re-entry with 2% uncertainty.

Such low accuracy of re-entry prediction makes implementing efficient risk mitigation measures difficult because of the large area over which the spacecraft might re-enter [6]. This large area means that for every specific location at risk, e.g. a city, the probability that the satellite will impact this specific point is extremely low. This low probability, combined with relatively small area that can be affected due to limited size of the debris, makes it irrational to issue a decision to implement mitigation measures. In other words, current re-entry predictions do not provide information that is actionable. However unlikely, a re-entry could cause casualties nonetheless. Therefore, improving the accuracy of re-entry prediction, and thus enabling actionable re-entry warnings to be issued, is of importance to both the decision makers and the ground population that is potentially at risk.

The inaccuracies associated with re-entry prediction have several different origins, which are well reviewed by Pardini and Anselmo [9] and references therein. These uncertainties are largely associated with modelling of the acceleration due to atmospheric drag, a_D, an object of mass m, cross-sectional area A, and drag coefficient C_D, moving through a fluid of density ρ at speed v, will experience. This acceleration is given in Eq. 2 [3].

$$a_D = \frac{1}{2}\rho v^2 \frac{A}{m} C_D. \qquad (2)$$

The specific sources of re-entry prediction uncertainty include:

1. sparse or imprecise satellite tracking data, which mean that re-entry prediction might have to be done based on inaccurate satellite ephemerides
2. unknown satellite shape and altitude, which affects the area A in Eq. 2
3. inaccuracies in modelling the spatial and temporal variability of atmospheric density ρ
4. possible variations in solar activity that cannot be forecast far in advance, which could unexpectedly change the atmospheric density ρ
5. modelling interactions between the spacecraft and the atmosphere particles, which are captured by the drag coefficient C_D

Four out of five mentioned sources of re-entry prediction uncertainty (points 2, 3, 4, and 5) are associated with modelling of the atmospheric drag; either directly (2, 3, and 5) or indirectly (4). These sources of uncertainty may interact and thus result in different overall re-entry prediction error for a specific re-entry case, even if the same models and practices, which gave highly-accurate predictions for other cases, are used [9].

Accuracy of the satellite drag modelling also affects the confidence with which possible on-orbit collisions can be forecast. This is because drag modelling affects the accuracy of the ephemerides [10], which in turn impacts how accurately the probability that two objects will collide can be estimated [11]. Thus, improving drag modelling accuracy would directly increase the safety of space assets by helping to prevent their destruction during collisions. Preventing orbital collisions, through better collision forecasts and avoidance manoeuvres, reduces the number of pieces of debris added into the environment. Collision avoidance is not the most effective space debris mitigation measure; however, it is one of the means to limit the growth of the number of space debris. If the quantity of debris does not increase significantly, the collision risk of all the satellites will not increase much further, thus enabling the continued use of the resource of space [12].

Thus, improving the accuracy of satellite drag modelling could improve the safety of the ground population, as well as the safety of the space assets themselves.

Fundamentally, theories, for example predicting the atmospheric drag or solar activity, can only be improved by corroborating them further [13]. This is to say by comparing theories to experimental data in a process that is often referred to as validation [14].

Due to the fact that every re-entry is different, e.g. as far as solar activity or the initial orbit are concerned, [9] and physical properties of the re-entering objects are not always known, such validation data for re-entry prediction are scarce. Thus, the safety of spaceflight could be improved by recording the re-entry profile of an object and comparing them to predictions. This object should have well-defined geometry and drag coefficients, as well as known attitude. Its position and attitude should be recorded throughout the decay with as high accuracy as possible.

Table 1: Mission objectives of UOS³ and corresponding success criteria.

ID	Objective statement	Success criteria		
		Minimum	Nominal	Full
1	Design, build, test and operate a CubeSat using primarily resources from the University of Southampton.	Successful flight qualification test according to launch provider specification requirements.	Deployment of CubeSat in Space with subsequent radio contact.	Delivery of at least one photograph as well as position and attitude time history for nominal mission duration.
2	Obtain visible-band photographs of Europe and transmit them to the ground for public relations and outreach purposes.	Successful operation of camera and photo downlink capability demonstrated in laboratory conditions.	Take a photograph in space and downlink it at least partially.	Take a photograph in space with Earth at least partially visible and downlink it completely.
3	Generate data to validate space object re-entry prediction tools.	Successfully demonstrate correct experiment operations in laboratory conditions.	Record and downlink at least one data point after deployment.	Record and downlink experiment data for nominal mission duration.

Such a need could be met by a spacecraft capable of recording its orbital position, ideally with accuracy better and spatial resolution higher than the publicly available ephemerides, i.e. two line element sets (TLEs) [15]. Such a mission should also be capable of recording its attitude at a sufficient frequency to allow reconstruction of the attitude profile between consecutive attitude measurements. The spacecraft fulfilling this mission should be small enough to enable its drag coefficients to be easy to characterise in hypersonic wind tunnels that are available in Europe, i.e. should have diameter smaller than approx. 0.2-0.6 m [16]. Finally, if the spacecraft is relatively inexpensive, several instances of it could be flown in multiple missions and thus generate the validation data in a range of space weather conditions, increasing the robustness of the validation.

The University of Southampton has decided to address this scientific need by flying a 1U cubesat, approx. 10 by 10 by 10 cm satellite [17], the University of Southampton Small Satellite, or UOS³ [18]. Ideally, a satellite used to generate re-entry validation data should be spherical, which would simplify modelling of its interaction with the atmosphere. However, few actual satellites are spheres and so the UOS³ will present a more representative test case. The more challenging shape of the satellite is offset by the fact that it will carry on-board position sensors. If such sensors were to be accommodated in a spherical satellite, the craft would need to be larger, and thus more expensive to launch.

This mission will be described in more detail in section 2. The UOS³ project has been conceived and is being carried out mostly by the students of the University. The involvement of the different student groups, the backgrounds of which extend beyond aerospace engineering or, in fact, science and technology, is described in section 3. Even though the UOS³ is still being constructed, several lessons have been learnt by the team over the duration of the project. These will be summarised in section 4.

2 THE UNIVERSITY OF SOUTHAMPTON SMALL SATELLITE, UOS³

The University of Southampton Small Satellite was conceived to address the above mentioned need to improve re-entry prediction tools. Since its inception, the UOS³ has sparked world-wide interest and five institutions, including the European Space Agency, have expressed formal interest in accessing the data that the cubesat will gather.

Furthermore, this satellite will be the first one built at the University of Southampton; this is deemed a considerable achievement and hence one of its primary mission objectives is to return a photograph of the Earth taken from orbit, which will be used for publicity purposes.

The mission objectives of UOS³, together with different levels of success criteria for each, are given in Tab. 1. They represent the intent of flying the satellite in-orbit but, even should this not take place, UOS³ will be deemed a success nonetheless, thanks to the gain in expertise of the participants.

The origins of this mission and organisation of the programme will now be briefly described. Then, the suite of sensors, capable of delivering the data that will address the set mission objective number 3, will be presented, together with an outline of the satellite platform that will be used to fly the proposed sensors.

2.1 HISTORY AND ORGANISATION

The UOS³ programme was started in the second quarter of 2014. The discussion about building UOS³ was prompted by attendance at the ESEO Lecture Course organised by the European Space Agency [19]. This workshop brought together students from across Europe, some of whom had built cubesats in the past. It was a unique opportunity to learn about organising such projects in a university environment. Two further workshops, one organised by the UK Space Agency and one by the UK organisation for Amateur Radio Satellites

(AMSAT-UK), played a major role in the UOS^3 programme as well.

These workshops exposed the project leads to more people who had been involved or interested in building cubesats, some of whom were also members of the University but were unknown to the project leads due to the size of the institution. These workshops enabled collaboration and knowledge transfer, and eventually contributed to the start of the UOS^3 project.

The biggest constraints for UOS^3 were the overall cost and duration of the project. Unless the project generated sufficient interest and gathered enough supporters, it would likely not be continued once its initiators have left the University. Moreover, no budget was allocated for the project at its outset and, without sufficient support, financial backing would not be gained.

Complexity of the satellite had to be kept low due to the fact that no complete cubesat has ever been built at the University of Southampton. Consequently, designs of only parts of such satellites were available to build upon. Moreover, the fact that UOS^3 will be the first University of Southampton cubesat meant that few processes were in place to enable intra-University collaboration on a project of this scale. It was clear that students from many different faculties would need to be involved, for example aerospace and electronics engineering. Due to the structure and legislation of the University, running a single, assessed project with students from multiple faculties is currently impossible. Thus the work has to be split into several smaller projects, each specific to one faculty. Reducing the complexity and number of on-board interfaces simplifies the organisation of student groups to design and produce the satellite, as less configuration control has to be put in place. This not only makes interface control easier, but also reduces the schedule overhead associated with it.

2.2 PAYLOAD

The orbital decay trajectory has to be recorded using on-board sensors to give a higher temporal resolution (frequency of measurements) than could be achieved by, for example, tracking the spacecraft using ground sensors. In order to provide satisfactory spatial accuracy, star sensors or global navigation satellite system (GNSS) receivers had to be used.

Initial launch-provider enquiries revealed that it was unreasonable to hope that sufficient funding for the launch of a satellite larger than a 1U cubesat would ever become available. Due to volume and associated power constraints that are inherent to such spacecraft, star sensors were not considered for navigation any further.

The only commercially-available GNSS receiver that appeared feasible to be flown on a 1U cubesat platform due to its relatively low power consumption, was the OEM615 by NovAtel [20]. The GNSS receiver distributor recommended using it in conjunction with an active antenna by Antcom [21].

The peak power consumption of the GNSS receiver is up to 1 W when using only the GPS satellite constellation. This necessitates covering as much of the external surface area of the satellite with solar cells as possible, thus restricting the use of Earth horizon sensors or photodiodes. Therefore, it was decided to use a relatively low-power magnetometer (AK9863 by Asahi Kasei Microdevices [22]) to estimate the attitude of the craft. It is augmented with sun-vector sensing performed by measuring the solar array currents [23]. Such a combination of sensors limits the complexity of the spacecraft and reduces the net power consumption of the payload, while satisfying the 5º attitude knowledge requirement [23].

The attitude of the spacecraft will be stabilised using a passive magnetic system, which consists of a permanent magnet that aligns one of the cubesat axes with the local magnetic field, as well as hysteresis rods that dampen the oscillations [24]. Such an attitude control subsystem (ACS) choice reduces the number of interfaces on board UOS^3. However, it also necessitates calibration of the magnetometer to be able to extract useful attitude knowledge in the presence of a strong, self-induced magnetic field. Similar spacecraft have flown before [25]; therefore, it is expected that UOS^3 mission objectives can be met with the proposed design.

The final piece of payload of UOS^3 is a camera, which will deliver images that will be used for publicity and outreach purposes. Following a similar trade-off to that performed for ICUBE-1 [26], the same camera was selected for UOS^3. Namely, the µCAM-II by 4D Systems [27] will be flown. Unfortunately, the signal from ICUBE-1 has never been received [28]; therefore, the selected camera does not have any flight heritage. However, it is hoped that any camera faults would have been discovered during ICUBE-1's testing or will be identified during the UOS^3 test campaign.

2.3 SYSTEM DESIGN

Due to the mentioned budget and schedule constraints, the UOS^3 design philosophy favours the use of flight-proven hardware. This allows less testing to be performed on the component level without increasing the mission failure risk beyond what is deemed acceptable. This reasoning has influenced the selection of the payload sensor suite, camera, as well as attitude control subsystem architecture, which were described in section 2.2.

The same rationale was applied to the selection of the UOS^3 bus design. Moreover, wherever possible, manufacturing the assemblies and subsystems at the University of Southampton is favoured. This enables exposing as many students to the project as possible, thus increasing the educational return of the mission. It also reduces the cost of the cubesat.

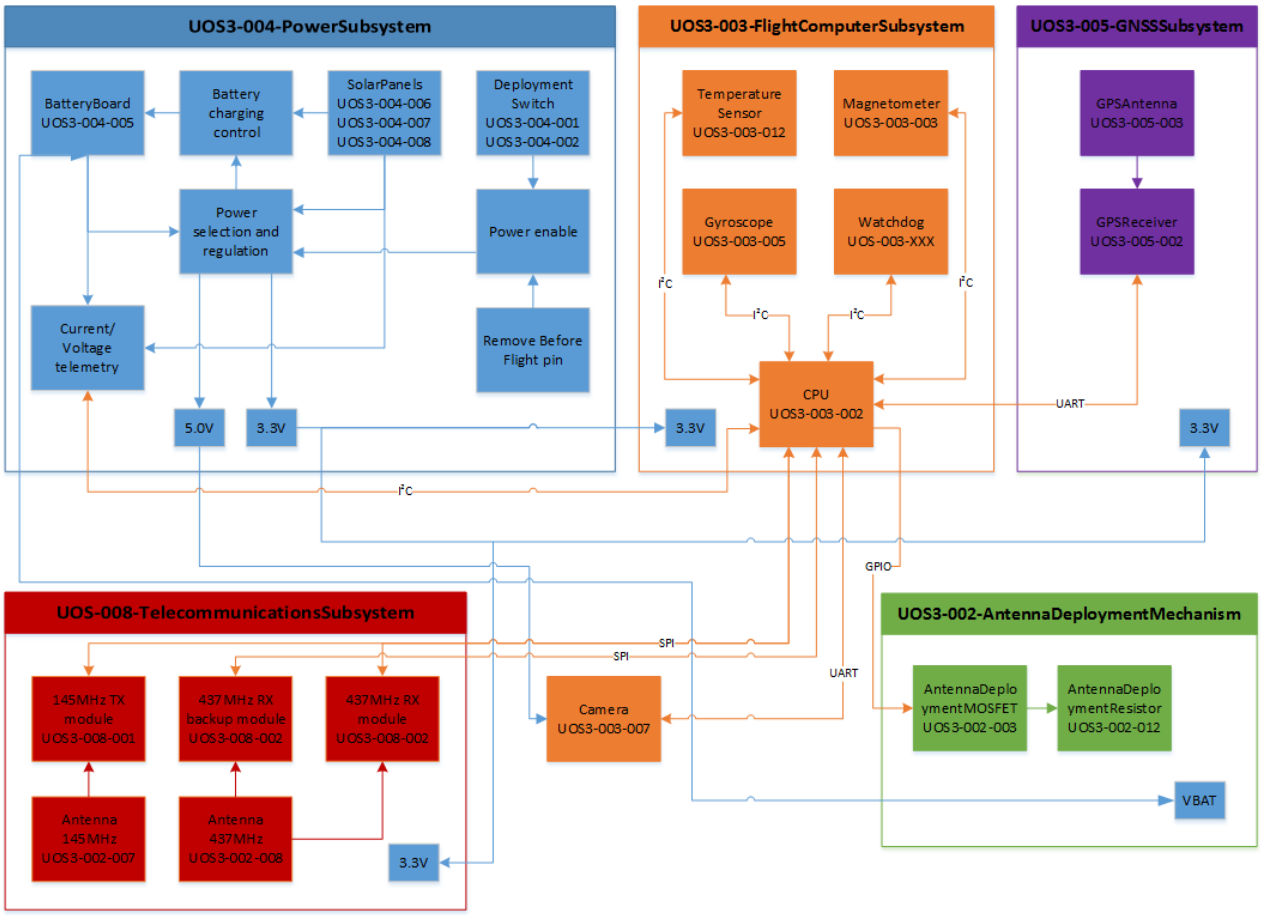


Figure 2: Block diagram of the UOS[3] cubesat system. Passive components, such as structure or attitude control subsystem, have been intentionally omitted for clarity.

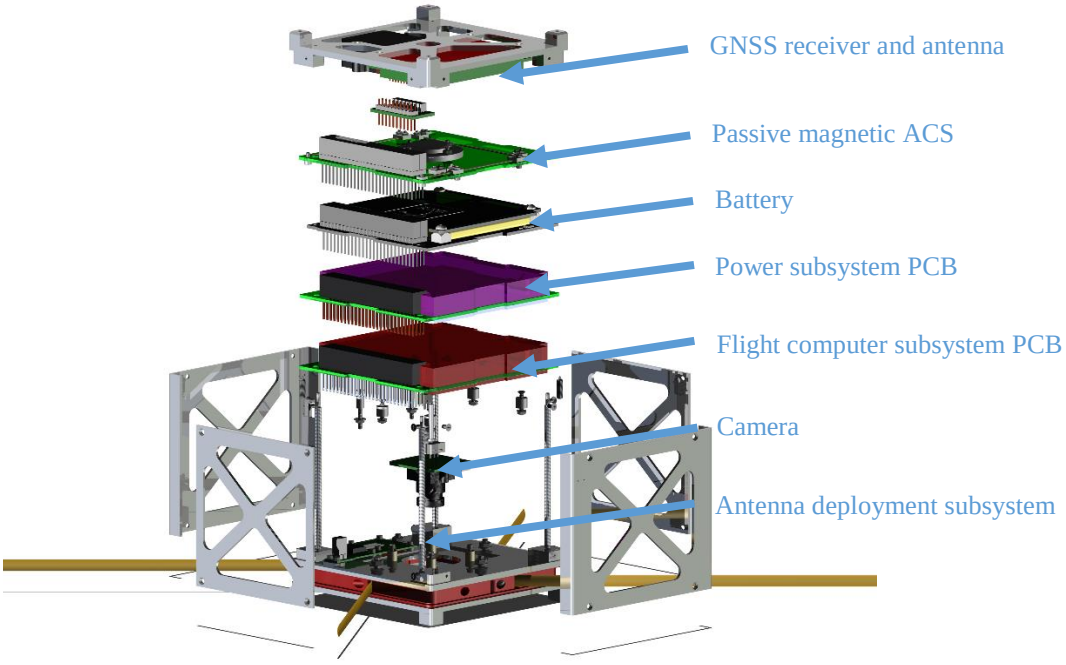


Figure 3: Exploded view of UOS[3]. Solar panels, located on the surfaces of the structural panels, have been omitted for clarity.

Furthermore, utilising the University's expertise and facilities was set as the first UOS^3 mission objective. The University of Southampton can boast a broad base of expertise in space activities. This base extends across many faculties and includes both upstream capabilities, e.g. development of space technology or spacecraft design, and downstream capabilities, e.g. exploitation of technology, communications, earth observation and navigation. What has been missing in the past is a catalyst to bring all these activities together and the UOS^3 cubesat programme is that catalyst, which is reflected by this mission objective.

The block diagram of the UOS^3 satellite system is shown in Fig. 2. Passive components, such as the load-bearing structure and passive magnetic ACS, have been omitted from the figure for clarity.

The on-board computer subsystem, which also includes all the sensors except for the GNSS receiver and antenna, is based around a 32-bit ARM® processor, namely the TM4C123GH6PM [29] by Texas Instruments. Most on-board communications are realised over an I^{2}C bus, with an exception of several SPI and UART connections. This reduces the number of connections that have to be routed on the printed circuit boards (PCBs), limited in size by the cubesat form factor. Use of I^{2}C also simplifies connecting PCBs to each other, and removes the need to have a dedicated general purpose input-output (GPIO) pin of the main microcontroller assigned to only one sensor. A dedicated GPIO pin would be required if the communications were realised over an SPI bus, for example. In order to limit the complexity of the entire spacecraft, only one main microcontroller will be used and that has a limited number of GPIO pins.

The power subsystem gathers energy using custom-built solar panels supplied by DHV Technology [30]. Each of the panels houses two triple-junction, GaAs solar cells, manufactured by AZUR SPACE Solar Power [31]. The custom shape of the solar panels enables them to interface with an in-house manufactured load-bearing structure. The energy gathered by the panels is stored for use in eclipses in a 10 Wh battery manufactured by a UK-based company, Clyde Space [32]. The solar cells' output is maximised by implementing a maximum power point tracking algorithm.

The UOS^3 structure houses all the subsystems in a configuration that provides optimum mission performance. The accuracy of the attitude sensing is improved by maximising the physical separation between the magnetometer and the ACS magnet, thus reducing the strength of the self-induced magnetic field. The chosen spacecraft configuration also enables the GNSS antenna to be pointed along the zenith, thus providing the best positioning accuracy.

Telecommand uplink is achieved at a frequency of 437 MHz. A hot-redundant receiver is incorporated into the telecommunications design to cope with failures of the primary receiver. Spacecraft telemetry, experimental data (position and attitude measurements), as well as images will be downlinked over 145 MHz. Use of these frequencies was decided upon because they are commonly used by radio amateurs around the World and thus many ground stations should readily be available for UOS^3 to use. Also, a simplified and faster frequency coordination process can be followed for these amateur frequencies, thus reducing the overall programme duration and cost.

Accommodating the antennae, one pair of which spans 978 and the other 316 mm, in the 10 by 10 cm cubesat envelope is a challenge. This is normally overcome by deploying the antennae after the cubesat is released from the launch vehicle. It was decided to use tape spring antennae, similar to what was successfully used by F-1 and M^3 cubesats [33, 34]. These will be stowed inside the allowed cubesat envelope by wrapping them around a 3D printed plastic structure and restraining them from accidental deployment using a nylon wire. Once the UOS^3 is deployed in space, this wire will be split by the heat generated by running current through a resistor. The accumulated strain energy of the antennae will cause them to deploy once the restraint of the wire is removed. This mechanism is based on the design that was successfully used on-board the Xatcobeo cubesat [35].

All the above mentioned subsystems have been accommodated in the 1U cubesat envelope according to the arrangement shown in Fig. 3. The solar panels are bolted onto the structural panels, which have been exploded in Fig. 3. Solar panels were excluded from the figure for clarity.

3 STUDENT INVOLVEMENT

Over the timespan of the academic year 2014/15, UOS^3 involved 15 students in the final year of their undergraduate programmes, who worked on it as their final projects. In the year 2015/16 it involves 12 new final-year undergraduate students and two Master students. As the development of the mission progresses, more students benefit from being able to take part in this large collaborative project.

This section describes the student groups that are involved in the project, how they benefit from it, and how the collaboration between various groups is achieved. The lessons learnt in the process are considered valuable to other universities that wish to develop cubesats because most University projects focus on students working individually or in small groups with similar background. Thus, enabling several projects to work in a larger programme that spans many different disciplines and involves multiple individuals or small groups of students may prove challenging in the university environment.

3.1 ENGINEERING

Most cubesat projects tend to involve students from various areas of engineering. This is understandable, given that spacecraft are complex autonomous systems.

Consequently, their design and manufacture requires many hours of skilled labour.

The UOS^3 is no different in this respect, as it primarily involves mechanical, aerospace, and electronic engineering students. They have been taking part in all design, manufacture and verification phases of UOS^3, except for definition of the top-level requirements and architecture. The latter tasks were performed by volunteer postgraduate students and staff of the University.

The structure of an integrated Master of Engineering (MEng) course at a UK university, such as Southampton, can involve a group design project (GDP). In a GDP, a number of students from the same discipline would typically design, manufacture and test a piece of hardware [36]. At the University of Southampton, the GDP takes place in the final year of the MEng course. UOS^3 involves students from several GDPs at any given time. Flow of information is facilitated by postgraduate students that oversee the programme, and serve as project managers and system engineers. Their involvement also ensures continuity of knowledge throughout the course of the programme. This is because postgraduate studies last several years, whereas MEng students are only involved for up to one academic year.

Unlike most GDPs, the students working on UOS^3 have to collaborate with other groups working on different pieces of hardware and software that will form part of the same system. This exposes the students to an industry-like situation, because few large-scale engineering projects are carried out by a single group of people. It necessitates stricter configuration control, because decisions taken by one group of students affect others. Moreover, the software and hardware interfaces between the products delivered by each group have to be looked after more carefully. Lastly, schedules of the different groups have to be synchronised to ensure that every group will have access to the assembled cubesat hardware to conduct the integration and verification of their product. Finished designs of certain groups are inputs to the work conducted by others, which also has to be coordinated. Even though the responsibility for this systems engineering and programme management rests on postgraduate students, students from all the GDPs are naturally exposed to it. Therefore, they have an insight into how such tasks are carried out, which is a unique educational experience.

3.2 PHYSICS AND ASTRONOMY

Apart from engineering students, UOS^3 also involves final-year Physics and Astronomy students that calibrate the magnetometer, which will be flown aboard the craft. The two students who chose this project are enrolled on the Physics with Space Science degree programme, which combines a core physics degree with specialist options on space-based applications (e.g. remote sensing, study of the interaction between the solar wind and Earth, and space-based astronomy) and courses on spacecraft engineering. These students have to understand how UOS^3 is designed and what the self-induced magnetic field will be in order to make sure that the calibration is meaningful. Furthermore, the students gain an insight into how the satellite will be operated. Lastly, because the calibration is being carried out in parallel with the satellite design and manufacture, the students gain an insight into actual engineering and project management. These are unique opportunities, which are not normally given to most Physics students, but which capitalise on the courses taken as part of the Physics with Space Science degree. These opportunities will, therefore, definitely be useful to the students when they pursue their careers and begin to work on larger-scale space missions or in other fields of science and engineering.

This group of students also prepares the method of processing the data that the UOS^3 mission will gather, such that higher-level data products may be distributed to the scientific community. In the case of UOS^3, this will be attitude history rather than just histories of the solar array currents and raw magnetometer readings, for example. Understanding such data processing chains is crucial for students who aim to work in the field of space science, because in their future careers they will work in one of the steps of this chain. Being able to understand the whole process, having already experienced it in its entirety, allows the students to better understand where they fit in the big picture. Working on UOS^3 might be the only opportunity for them to gain such insights.

3.3 FINE ART

Being able to experience the satellite creation process has been a stimulus for fine art and graphic arts students at the Winchester School of Art (WSA). The remainder of this section gives examples of how satellites can be interpreted and serve as an inspiration for an artistic process. Having an insight into this perspective may prove valuable to other institutions wishing to expand how they use space for tertiary education.

Students at WSA were first introduced to the cubesat project through Deep Highly Eccentric, a group exhibition of artwork that explored ideas of abstraction and distance in relation to artificial satellites. Lectures were scheduled alongside the exhibition, covering aspects of satellite history, their relation to surveillance, our geopolitical sphere and their influence on culture. Art students were invited to develop art works in response to the UOS^3 cubesat, which has become an extracurricular project where student participation is voluntary.

The UOS^3 project proposes a valuable professional experience within an art and science context. It enables art students to engage with different disciplines and their methodologies and invites them to consider alternative forms of communication and dissemination of the project themes. One of such invaluable and unique insights is witnessing aspects of the engineering process as well as learning about space debris.

To encourage a breadth of thinking around the subject matter and foster creativity, the project was further introduced by combining astronautics, cultural and associative perspectives. To a non-specialist, satellites may appear to be relatively mysterious objects: photographic images of satellites are scarce and selectively shot. Most representations are "artist impressions" and illustrate satellites floating in space like science-fiction spacecraft from another world or future. A lack of information around them adds to a sense of their technological abstraction, which is amplified through their physical distance. This absence of information potentially opens up space for different interpretations – such as a mythologizing of satellites: imagining them as contemporary gods of communication that influence our lives from afar. Not unlike the Greek god Hermes or the Roman adaptation, Mercury, who are said to represent themes of trade, travel, trickery and thieves and guide souls to the underworld. Like these gods, satellites cross geographical and metaphorical boundaries as they bridge the journey between worlds.

If anthropomorphized, the Pleiades satellite image of the Envisat satellite also takes on a different reading – a form of caring interaction, one satellite literally looking out for another. Or when the Philae lander accidentally captured one of its legs in the shot when taking photographs of the Comet 67P/Churyumov-Gerasimenko, it unwittingly followed contemporary trends and produced a "satellite selfie".

Satellites also offer a different way of seeing; by producing images that are multispectral and panchromatic, bringing new material and expanding dialogue around lens based history and landscape photography.

Additionally, the influence of satellite technology on artists and authors can be seen in works such as "Olympic Rainbow", made in 1988 by Nam Jun Paik and involved satellites around the world transmitting images and sounds which the artist edited in real time and re-transmitted back across the planet. Similarly, artist Trevor Paglen drew upon satellite positioning data to locate and photograph secret spy satellites, using long exposures to reveal what is not supposed to exist.

Although it is not yet known how students will respond to UOS^3 in detail, it is an exciting proposition that invokes thinking about the future and space within an art context and is a rich resource for creative potential.

3.4 OTHER STUDENT GROUPS

Students from virtually any discipline can volunteer to work on the UOS^3 in their spare time. Their work is overseen by one of the University's many societies (the University of Southampton Spaceflight Society [37]). This society, a student-run organisation, is tasked with building the ground station that will be used for UOS^3 operations. The Society has undertaken similar projects with high-altitude balloons, and is thus one of the groups within the University that is best prepared for this task.

On the other hand, the nature of the society enables any student to participate in the UOS^3 programme by working on hardware that directly interfaces with the satellite. It thus gives a broad range of students an opportunity to gain direct insight into the cubesat hardware as well as programme structure; an experience that would not otherwise be possible during any university project.

UOS^3 has also sparked interest in the student-run newspaper at the University of Southampton, the Wessex Scene [38]. The involved students decided to track the progress of the satellite development and publish regular updates. This exposes these students to technical journalism, and further disseminates information about UOS^3. This exposes more students to how the project is run, and the satellite designed and manufactured.

Lastly, UOS^3 is a case study indicating the beginning of a new space era. It was used in this context in several lectures given to history students, allowing them to appreciate the fact that, unlike a few decades ago, not only select few countries can now build and operate satellites.

4 CONCLUSIONS

The UOS^3 programme would likely never have happened had it not been for workshops that exposed its initiators to individuals who had worked on similar projects. This has made the current project leads realise that starting a project to build and launch an educational satellite might not be easy, but certainly is achievable. This proves that workshops like this are definitely beneficial and bring the intended results.

Space is often used in tertiary education of students with science and technology backgrounds. However, it can be useful in enhancing the education of other students, for example history or fine art. Involvement of the Winchester School of Art in the UOS^3 programme shows this and serves as an example to other educational institutions that space can be used to educate many more students than traditionally done. One area where the UOS^3 programme could still improve is involving law students to interpret the international laws governing spaceflight, e.g. the liability convention, or marketing students to work on branding of the project.

The most important lesson that has been learnt over the course of the programme is how crucial it is to involve postgraduate students and staff to ensure continuity of knowledge over the several years that the programme is likely to take. What also proved beneficial in this respect was employing some of the students, who were or will be involved in the programme, as interns.

Overall, the UOS^3 cubesat programme is an example of how a relatively simple mission can bring large benefits to both the host educational institution, by enabling its students to work on a large, collaborative project, as well as the scientific community. The interest of major research institutions around the world in the data delivered by the UOS^3 mission proves that this project addresses an important scientific need.

5 ACKNOWLEDGEMENTS

The authors would like to express their gratitude to Dr Wendell Bailey from the Cryogenics Department for helping with heat-treatment of the hysteresis rods, which form part of the attitude control subsystem of the UOS^3.
Big thanks also go to the staff of the Engineering and Design Manufacturing Centre, who have manufactured the satellite structure, and assisted in work done on other subsystems.
The authors would also like to express they gratitude to Dr Ke Li from Electronics and Electrical Engineering for the assistance in measuring the impedance of the UOS^3 telecommunications subsystem, and the design of the radiofrequency equipment.
Lastly, big thanks to the staff of the electronics workshop at the Institute of Sound and Vibration Research, who have been sharing their expertise in the field of electronics, and provided lab space for manufacturing of many components of the UOS^3.

6 REFERENCES

1 - Garber, S., "Sputnik and the dawn of the space age," 2007. URL: www.history.nasa.gov/sputnik/, last accessed 12 Oct 2015.
2 – Klinkrad, H., "Space Debris: Models and Risk Analysis", Chichester, UK, Praxis Publishing, 2006.
3 – Vallado, D., "Fundamentals of Astrodynamics and Applications; Fourth Edition", Microcosm Press, 2013.
4 – Space-Track, URL: www.space-track.org, last accessed 12 Oct 2015.
5 – White, A., Lewis, H.G., "The many futures of active debris removal", Acta Astronautica, no. 95, pp. 189-197, 2014.
6 – Pardini, C., Anselmo, L., "Reentry predictions of three massive uncontrolled spacecraft", 23rd International Symposium on Space Flight Dynamics, Pasadena, CA, USA, 2012.
7 – National Aeronautics and Space Administration, "NASA-STD-8719.14A: Process for Limiting Orbital Debris", 25 May 2012. URL: http://www.hq.nasa.gov/office/codeq/doctree/871914.pdf, last accessed 12 Oct 2015.
8 – Lazara, B., "Technical Regulations for Space Operations", COPUOS STSC, Vienna, Austria, 2014.
9 – Pardini, C., Anselmo, L., "Re-entry predictions for uncontrolled satellites: results and challenges", 6th IAASS Conference – Safety is Not an Option, Montreal, Canada, 2013.
10 – Pardini, C., Kent Tobiska, W., Anselmo, L., "Analysis of the orbital decay of spherical satellites using different solar flux proxies and atmospheric density models", Advances in Space Research, pp. 392-400, 2006.
11 – Alfano, S., "Relating Position Uncertainty to Maximum Conjunction Probability", The Journal of the Astronautical Sciences, vol. 53, no. 2, pp. 193-205, 2005.
12 – Lewis, H.G., White, A., Crowther, R., Stokes, H., "Synergy of debris mitigation and removal," Acta Astronautica, vol. 81, pp. 62-68, 2012.
13 – Popper, K., "The Logic of Scientific Discovery", London, UK, Taylor & Francis Group, 2014.
14 – Definition of "validate", Oxford University Press, URL: www.oxforddictionaries.com/definition/english/validate, last accessed 1 Nov 2015.
15 – Oltrogge, D., Ramrath, J. "Parametric Characterization of SGP4 Theory and TLE Positional Accuracy", Advanced Maui Optical and Space Surveillance Technologies Conference, Wailea, Maui, HI, USA, 2014.
16 – Gouder, K., "Imperial College London Hypersonic Gun Tunnel", URL: www.nwtf.ac.uk, last accessed 1 Nov 2015.
17 – Pumpkin, Inc., "Begin your CubeSat Mission with the CubeSat Kit", URL: www.cubesatkit.com, last accessed 1 Nov 2015.
18 – Lidtke, A.A., Rumpf, C., "University of Southampton Small Satellite: Home" URL: www.generic.wordpress.soton.ac.uk/uos3, last accessed 24 Nov 2015.
19 – ESA Education, "Students: apply for the second session of ESEO courses", 18 Nov 2013, URL: http://www.esa.int/Education/Students_apply_for_the_second_session_of_ESEO_courses, last accessed 14 Oct 2015.
20 – NovAtel, "OEM615 Dual-Frequency GNSS Receiver",
URL: http://www.novatel.com/products/gnss-receivers/oem-receiver-boards/oem6-receivers/oem615/, last accessed 2015 Oct 13.
21 – Huynh, S., "Active L1/L2 GPS Antenna, P/N: 1.2G1215A4-12NRMM-4 Rev B", 11 Mar 2005, URL: http://antcom.com/productsheets/1.2G1215A4-12NRMM-4_D.pdf, last accessed 13 Oct 2015.
22 – Asahi Kasei Microdevices Corporation, "AK8963 3-axis electronic compass IC", 2015, URL: http://www.akm.com/akm/en/product/datasheet1/?partno=AK8963, last accessed 13 Oct 2015.
23 – Burton, R., Rock, S., Springmann, J., Cutler, J., "Online Attitude Determination of a Passively Magnetically Stabilized Spacecraft", Advances in the Astronautical Sciences Spaceflight Mechanics, vol. 148, 2013.
24 – Santoni, F., Zelli, M., "Passive magnetic attitude stabilization of the UNISAT-4 microsatellite", Acta Astronautica, vol. 65, p. 792–803, 2009.
25 – Springmann, J., Cutler, J., Bachivan, H., "Magnetic Sensor Calibration and Residual Dipole Characterization for Application to Nanosatellites", AIAA/AAS Astrodynamics Specialist Conference, Toronto, Canada, 2010.
26 – Khurshid, K., Mahmood, R., Islam, Q., "A survey of camera modules for CubeSats - Design of imaging payload of ICUBE-1", 6th International Conference on

Recent Advances in Space Technologies (RAST), Istanbul, Turkey, 2013.
27 - 4D Systems, "Micro CAM 2 (uCAM-II)",URL: http://www.4dsystems.com.au/product/uCAM_II/, last accessed 13 Oct 2015.
28 – Krebs, G., "ICube 1," Gunter's Space Page, URL: http://space.skyrocket.de/doc_sdat/icube-1.htm, last accessed 13 Oct 2015.
29 – Texas Instruments, "TM4C123GH6PM", URL: http://www.ti.com/product/tm4c123gh6pm, last accessed 13 Oct 2015.
30 – DHV Technology, "Manufacturing solar panels for small satellites. Our design team will ensure the solar panel meets with your satellite structure", URL: http://dhvtechnology.com/?page_id=1302, last accessed 13 Oct 2015.
31 – AZUR SPACE Solar Power GmbH, "30% Triple Junction GaAs Solar Cell Assembly Type: TJ Solar Cell Assembly 3G30A", 19 Nov 2012, URL: http://www.azurspace.com/images/pdfs/0003401-00-00_DB_3G30A.pdf, last accessed 13 Oct 2015.
32 – Clyde Space, "CubeSat Standalone Battery CS-SBAT3-10", URL: http://www.clyde-space.com/cubesat_shop/batteries/16_cubesat-standalone-battery, last accessed 13 Oct 2015.
33 – AMSAT-UK, "TechEdSat FITSAT-1 WE-WISH F-1", URL: http://amsat-uk.org/satellites/non-operational/techedsat-f-1-fitsat-1-we-wish/, last accessed 13 Oct 2015.
34 – European Space Agency, "M3 / M-Cubed", URL: https://directory.eoportal.org/web/eoportal/satellite-missions/m/m3-mcubed, last accessed 13 Oct 2015.
35 – Encinas Plaza, J.M., Vilan Vilan, J.A., Aquado Agelet, A., Brandiaran Mancheno, J., Lopez Estevez, M., Martinez Fernandez, C., Sarmiento Ares, F., "Xatcobeo: Small Mechanisms for CubeSat Satellites - Antenna and Solar Array Deployment", 40th Aerospace Mechanisms Symposium, Cocoa Beach, FL, USA, 2010.
36 – Zervos, A., "FEEG6013 Group Design Project", University of Southampton, 23 Apr 2015, URL: http://www.southampton.ac.uk/engineering/postgraduate/taught_modules/feeg6013_group_design_project.page, last accessed 13 Oct 2015.
37 – "Southampton University Spaceflight Society", URL: www.susf.co.uk, last accessed 13 Oct 2015.
38 – Oliver, M., "The Final Frontier: How a Group of University of Southampton Students Aim to Get a Satellite into Space", URL: https://www.wessexscene.co.uk/science/2015/10/17/the-final-frontier-how-a-group-of-university-of-southampton-students-aim-to-get-a-satellite-into-space/, last accessed 28 Nov 2015.

SESSION 2: G - Test Platforms & Facilities

(Wednsday 09th - 17.30)

Chairman: Dr. Francesco Sansone – Dr. Livia Savioli

DEVELOPMENT OF A GROUND-BASED COOPERATING SPACECRAFT TESTBED FOR RESEARCH AND EDUCATION

Mattia Mazzucato[1*], Sergio Tronco[1], Andrea Valmorbida[1], Fabio Scibona[2], and Enrico C. Lorenzini[2]

[1] *Center of Studies and Activities for Space Giuseppe Colombo (CISAS), University of Padova*
[2] *Department of Industrial Engineering, University of Padova*
[*] *mattia.mazzucato.1@studenti.unipd.it*

ABSTRACT

Todays single satellites are limited by both the launchers capacity to deliver the whole satellite mass into a proper orbit (2 - 7 tons for European launchers), and the available volume of the launcher fairings (4 m in diameter and 5 - 7.5 m in height). This constrains the capabilities of telescopes, interferometers, coronagraphs, etc., since their performances are strongly related to focal length, mirror surfaces, aperture sizes and mass. By distributing a single large satellite capabilities over an equivalent multiple cooperating space vehicles system, these mass and volume constraints can be overcome, leading also to new capabilities and more flexible and robust to failures systems. However, this new concept requires a high level of autonomy, resulting in stringent requirements on the Guidance Navigation and Control (GNC) system.

New technologies in the fileds of relative navigation and control strategies are required, and ground-based testbed can be sucessfully used to develop and validate these required advancements both in hardware and software. In this paper, we describe the innovative aspects of a cooperating spacecraft testbed under development at the Center of Studies and Activities for Space (CISAS) and the Department of Industrial Engineering of the University of Padova. We also present and discuss experimental activities carried out by PhD and Master's Degree student, including attitude navigation and control strategies.

Key words: spacecraft testbed, MEMS gyroscopes for attitude navigation, Kalman filtering, quaternion-based PID control.

1. INTRODUCTION

The idea of using a group of autonomous small space vehicles cooperating with each other in place of a single larger spacecraft has become an important field of research among the space community worldwide in the last 15 years. The distribution of functions and paylods among coordinated small units overcomes some important limitations of a traditional monolithic satellite: (1) mass and volume constraints posed by today's launchers can be overcome (2) mission capabilities can be modified through the reconfiguration of the satellite formation (flexibility); (3) the development cost is lower; (4) the loss of a spacecraft doesn't lead to a failure of the whole mission (robustness): a malfunctioning satellite can be replaced or the formation can be reconfigured. Despite these benefits, however, a distributed space system poses several significant design challenges and requires new technologies, including: (1) new relative navigation sensors and actuators; (2) limited on board resources; (3) inter-satellite communication; and (4) a high level of autonomy.

These advanced technologies both in hardware and software can be developed and validated using ground-based testbeds. The research Group for Measurement and Space Technology (GMTS) of the Center of Studies and Activities for Space (CISAS) and the Department of Industrial Engineering of the University of Padova is developing a ground-based testbed called SPARTANS, i.e. cooperating SPAcecRraft Testbed for Autonomous proximity operatioNs experimentS. In particular, SPARTANS is a testbed for the development and verification on the ground of relative navigation sensors and coupled position and attitude proximity control strategies. The hardware is designed to conduct advanced research activities for several applications, as for instance Automated Rendezvous and Docking or Capture (ARD/C) and Satellite Formation Flying (SFF).

The paper is organized as follows. In the fisrt part, after a brief description of our hardware simulator main features, we present some preparatory experimental activities to characterize the SPARTANS testbed. After that, the attitude navigation system is presented along with some experimental tests performed to characterize and validate the navigation approach. To conclude, a quaternion-based Proportional-Integral-Derivative regulator is presented and its performances are displayed through the execution of attitude maneuvers in two different scenarios.

2. THE SPARTANS PROJECT

The final aim of our SPARTANS project is to design, realize and validate a representative facility to carry out both research and educational activities mainly in the fields of SFF and ARD/C. In its final configuration, the SPARTANS testbed consists of two or more Spacecraft Simulators representing the units of a satellite formation and a Control Station (external computer) (Figure 1).

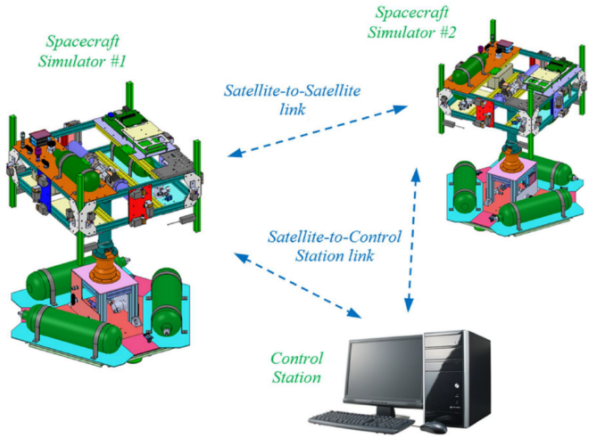


Figure 1. SPARTANS testbed overview.

Each Simulator is made of an Attitude Module (AM) with three rotational degrees of freedom provided by mechanical gimbals and a Translational Module (TM) with two position degrees of freedom that translates on a glass-covered plane using a low friction air cushion system. This separated-vehicles testbed will provide a representative dynamic environment for the development and verification on the ground of coupled position and relative attitude Guidance Navigation and Control (GNC) algorithms [1]. This kind of facility is also designed with some flexibility in changing the onboard configuration, so that it can be used for educational purposes in the fields of space robotics, satellite navigation, space instrumentations, automatic controls and space systems.

The SPARTANS project started in 2010 and it is currently carried forward by Aerospace Enginnering Master's Degree students, PhD students and Post-Doc researchers. At the current state of the project, a first prototype of the AM is fully developed and operative (Figure 2). A second version of the AM, a first prototype of the TM and a glass-covered table, over wich the simulators can move at low frictin, have been designed and are planned to be built and tested in the very near future. The main subsystems of the AM are briefly described in the following subsections.

2.1. The Attitude Module main features

The Attitude Module consists of five main subsystems: (1) the Structural Subsystem, (2) the Propulsion Subsystem, (3) the Attitude Determination and Control Subsystem, (4) the Electric and Power Subsystem and (5) the Communication and Data Handling Subsystem. The synergy of all subsystems allows the autonomous execution of attitude maneuvers.

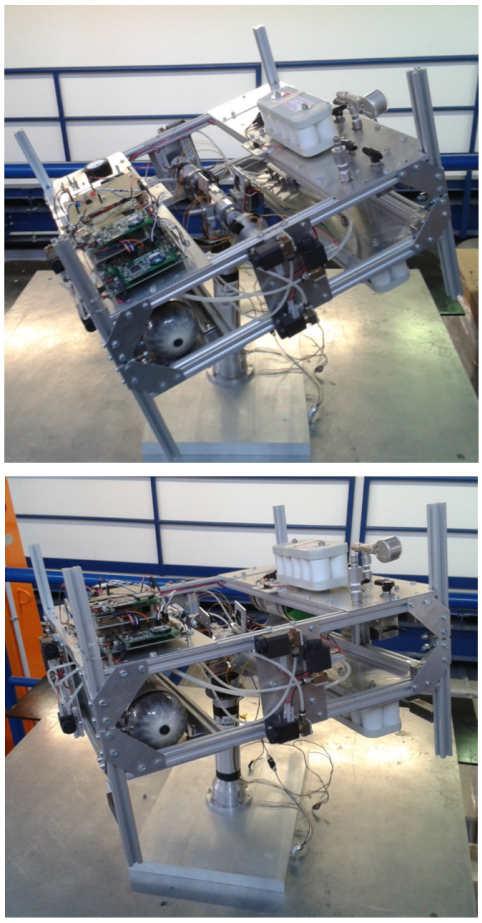


Figure 2. The first prototype of the Attitude Module.

1) *The Structural Subsystem*

The structural subsystem is composed of two modules: the structure itself and the cardanic joint system. The structure aims to provide an hardware platform where instrumentation can be positioned: an external rigid frame is formed by aluminum profile beams which support four aluminum plates where on board instrumentation is mounted. The configuration is designed to be sufficiently rigid and lightweight. The cardanic joint system provides three rotational degrees of freedom as shown in Fig. 3: the AM can freely rotate about the yaw axis, while rotations about roll and pitch axes are mechanically limited to the range $[-40$ deg, $+40$ deg$]$.

2) *The Propulsion Subsystem*

The propulsion subsystem consists of two parts: the high pressure and the low pressure sections. The high pressure section comprises (a) two tanks with a total capacity of 2 liters at a maximum pressure of 200 bar, (b) a fill and vent system for the pneumatic system load and depletion

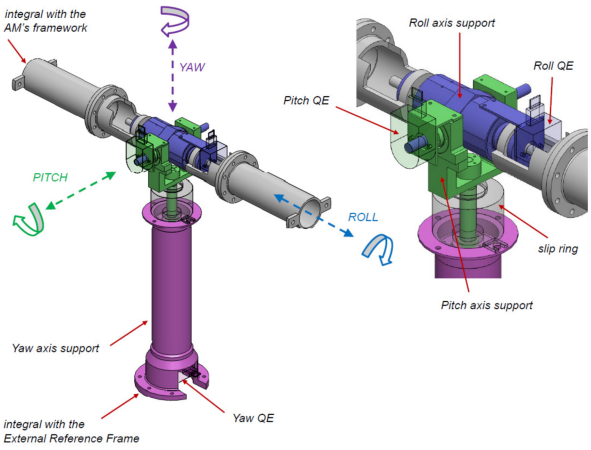


Figure 3. The Cardanic Joints System with roll axis in blue, pitch axis in green and yaw axis in violet.

and (c) a pressure regulator to provide the low pressure section the correct operative conditions. The low pressure section consists of (a) six pairs of thrusters, (b) a flexible polymer pipe system and (c) two six-way manifolds whose task is to make the pressured gas available to all thrusters. Each thruster is provided with a solenoid valve and a convergent nozzle with 0.75 mm diameter outlet. The thrust provided by the propulsion system is controlled by a Pulse Width Modulation (PWM) approach.

3) *The Attitude Determination and Control Subsystem*

The Attitude Determination and Control Subsystem (ADCS) includes attitude sensors and on board microcontroller. Two different kind of attitude sensors are currently present on board the AM: three quadrature encoders (QE) mounted at the cardanic joint interface and an Inertial Measurement Unit (IMU). Both the QE and IMU are used to determine the AM attitude with respect to the Local Vertical - Local Horizontal (LVLH) External Reference Frame. The IMU provides high rate estimations which are though subjected to drift as time increases. Since QE accuracy is far better than the one achievable with IMU, the QE are used as reference to evaluate the deterioration of the inertial estimations.
The on board electronics handles GNC tasks as it recieves informations from sensors, computes the control actions to be actuated by means of the thruster system and manage all the communication processes between the AM and the Control Station.

4) *The Electric and Power Subsystem*

The electrical power is made available by means of two rechargable 12 V Ni-Cd batteries, connected in series, with an overall capacity of 8 Ah. A DC/DC converter is used to reduce the available voltage to feed each electric device with the required operative voltage.

5) *The Communication and Data Handling Subsystem*

An external laptop is used as a control station to boot the simulator, to load the software and to recieve and store telemetry data.

All the on board processes are handled by a dedicated software, written in Dynamic C and organized into 6 main libraries: (1) Sensors; (2) Position and Attitude Determination System; (3) Controller; (4) Propulsion; (5) Communication; and (6) Housekeeping. Each library corresponds to an on board process. Fig. 4 shows the main processes managed by the on board microcontroller. The on board micro-controller is able to manage two different types of processes: (1) Periodic Interrupt Processes, which are time dependent periodic operations such as GNC operations and thrusters firing time computation; (2) Event-driven tasks, which implement time independent operations such as initialization of the system, test definition and execution.

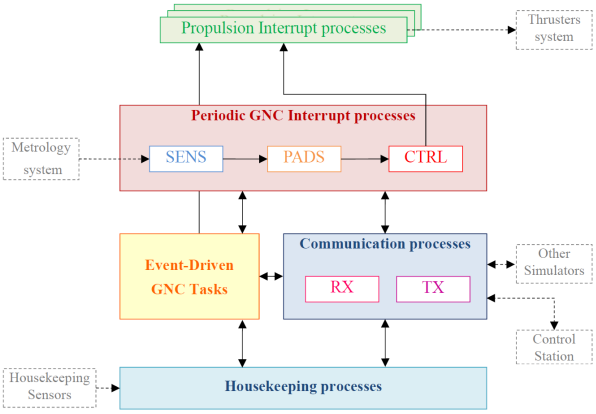


Figure 4. Micro-controller main processes and data flow.

In a SPHERES-like approach [2], the software is provided with a section for students and guest researchers who are free to implement algorithms and control strategies in a safe, fault tolerant software environment. The control station is provided with a GUI which allows the experimenter to set control parameters, to initialize and execute tests and to check in real time the state of the simulator, including data of the test under execution.

3. PREPARATORY EXPERIMENTAL ACTIVITIES

A series of preparatory experimental activities were carried out by PhD and Master Degree students of the SPARTANS team, in order to have all the elements required to test some specific attitude control maneuvers using the first AM prototype. In particular, three main activities were carried out: (1) AM mass balancing, (2) estimation of the force actuated by the onboard thrusters, and (3) determination of the AM inertia tensor.

3.1. Mass balancing

First of all, the AM was set in a mass balancing condition in which its center of mass is as close as possible to the Joints System center of rotation, obtaining a platform whose attitude is (almost) independent on perturbing torques due to gravity. This condition was reached through a first proper AM design where group of components with similar mass are placed in simmetric locations with respect to the joints center of rotation. A finer mass balance was then achieved by placing trimming masses in proper locations through a trial and error procedure.

3.2. Thrusters force estimation

The characterization of the on board thrusters was performed by means of a Torque Balance system. The overall system is composed of: (a) a steel wire, whose rotational stiffnes k was previously determined as shown in [3]; (b) a pair of AM thrusters positioned at the end of a profile beam, at the same distance $b/2$ from the wire and with opposite thrust directions; (c) two lasers at the ends of the profile beam; and (d) an external goniometer with resolution 0.5 deg to detect the angular position θ of the Torque Balance, and placed under the Torque Balance system with its center maintained along the wire axis.

The thrusters are activated and, once the system reaches its equilibrium configuration, the angular position of the Torque Balance is measured and the thrust is estimated as:

$$S = k\frac{\theta_{eq}}{b}. \tag{1}$$

Several tests were conducted in order to estimate the AM thrusters force as a function of the total pressure of the air supplying the thrusters nozzles. The tests were performed for a total pressure in the range of 1.5 bar to 10 bar, and the resulting force profile as a function of the total pressure showed with good approximation a linear trend. For the nominal operational pressure of 10 bar, a thrust of $S = (0.389 \pm 0.007)N$ was estimated with a coverage factor of 2.

3.3. Inertia tensor estimation

The characterization of the AM inertial properties was performed by means of a Torque Pendulum. The setup consists of: (a) the vertical steel wire; (b) the horizontal profile beam provided with two lasers at its ends; (c) a structure of profile beams and plates to support the AM in the required orientation with the wire axis passing through the AM center of mass; and (d) a photoresistance, connected to an acquisition system, to measure the oscillations of the pendulum by observing the passage of the laser beam.

The AM moment of inertia $I_{m,i}$ about an i^{th} direction passing through the AM center of mass can be computed as:

$$I_{m,i,tot} = I_{m,i} + I_{m,i,frame} = k\frac{T^2}{4\pi^2} \tag{2}$$

where $I_{m,i,frame}$ is the moment of inertia of the supporting system with known value, and $I_{m,i,tot}$ is the moment of inertia of the overall system, evaluated from measurements of the oscillation period T of the Torque Pendulum. The AM inertia tensor accuracy is strongly dependent on both the measurement directions with respect to the AM Body reference frame and the number of measurement directions taken into account. A preliminary analysis was carried out to identify the measurement directions that could lead to a better estimation of the AM inertia tensor, using past moment of inertia measurements and test results and considering also the AM geometry.

Given the inertial measurements, the AM interia tensor in its Body reference frame was determined as the solution of a linear system dependent on the measurement directions. As a result, the inertial properties of the AM were determined with an uncertanty of 4% for a 2σ confidence level.

4. THE ATTITUDE NAVIGATION SYSTEM

The Attitude Navigation System was developed with the main objective of determining the angular position of the AM Body reference frame with respect to an external Global reference frame. The Attitude Navigation System is based on low cost MEMS inertial sensors and an extended formulation of a quaternion-based Indirect Kalman Filter (IKF) algorithm. In particular, two different type of sensors were used: (1) a 3 axis MEMS gyroscope MPU-6050; (2) a star sensor, wich was simulated using optical Quadrature Encoders (QEs) that directly measure roll, pitch and yaw angles of the AM.

The development of the Attitude Navigation System followed three main steps: (1) characterization of the random noises of the inertial sensors, (2) implementation of a calibration procedure to compensate deterministic error sources, and (3) development and validation of the IKF algorithm through both computer simulations and experimantal tests.

4.1. Random noises characterization

The gyroscope sensor provides measurments of the AM angular velocity vector $\boldsymbol{\omega}$ projected in the AM Body reference frame at high frequency, therefore in theory it whould be possible to compute the current attitude of the platform knowing its initial attitude and propagating gyroscope measurements. However, gyroscopic measurements $\boldsymbol{\omega}_m$ are affected by a bias $\mathbf{b}$ and a high frequency white zero mean Gaussian noise $\mathbf{n}_w$:

$$\boldsymbol{\omega}_m = \boldsymbol{\omega} + \mathbf{b} + \mathbf{n}_w \tag{3}$$

The bias term for the gyroscope is non-static and it can be modeled as a low frequency white zero mean Gaussian noise accumulation process $\mathbf{n}_b$:

$$\dot{\mathbf{b}} = \mathbf{n}_b \tag{4}$$

On the other hand, the star tracker is a really affordable sensor, but provides measurements at a lower frequency when compared to the gyroscope sensor:

$$\mathbf{q}_m = \mathbf{q} + \mathbf{n}_q \tag{5}$$

where, considering the value of $\mathbf{n_q}$ sufficiently small, we may define it as a white Gaussian noise with zero mean.

In order to estimate the AM attitude state, it is required to know the measurements noise levels of the real sensor. The Allan variance analysis [4] was conducted in order to determine the gyroscope Angular Random Walk (ARW) coefficient N for the high frequency measurements noise $\mathbf{n}_w$ and the Rate Random Walk (RRW) coefficient K for the low frequency bias noise $\mathbf{n}_b$, whose values are reported in Table 1. The Allan deviation curves for the MPU-6050 MEMS gyroscope are shown in Fig. 5.

Axis	**N**	**B**	**K**
	$\left[(^\circ/\mathrm{s})/\sqrt{Hz}\right]$	$[^\circ/\mathrm{s}]$	$\left[(^\circ/s)\sqrt{Hz}\right]$
X	7.867E-3	1.241E-3	1.111E-4
Y	9.281E-3	1.418E-3	1.389E-4
Z	7.389E-3	1.117E-3	1.111E-4

Table 1. Noise coefficients for the gyroscope ($100\,Hz$ *sampling rate). N si the ARW coefficient, B is the Bias Instability coefficient and K is the RRW coefficient.*

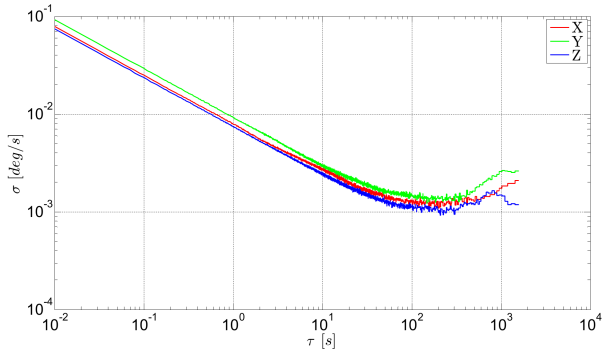


Figure 5. Allan deviation curves for the gyroscope MPU-6050 (100 Hz sampling rate).

4.2. Calibration procedure

To improve the attitude estimation accuracy, the calibration procedure proposed in [5] was implemented to compensate deterministic error sources due to gyroscope misallignments, scale factors and zero rate bias. Using a spline interpolation applied to QEs measurements, a fiducial reference of the AM orientation has been defined and calibration matrices were computed adopting a least square minimization procedure.

4.3. Navigatyion algorithm development and validation

An extended formulation of an Indirect Kalman Filter [6] was used to fuse the attitude measurements provided by the two sensors (the gyroscope and the simulated star sensor), using the star sensor to correct the attitude error caused by the white noise integration on gyroscopic measurements. In addition, an extended formulation of the filter allows to linearize the attitude dynamics of the platform about the current estimation of its attitude state, simplifying the computational cost of the Kalman Filter when applied to a process governed by a non-linear stochastic difference equation with a non linear-stochastic measurement equation:

$$\mathbf{x}_k = f(\mathbf{x}_{k-1}, \mathbf{u}_{k-1}, \mathbf{w}_{k-1}) \tag{6}$$

$$\mathbf{z}_k = h(\mathbf{x}_k, \mathbf{v}_k) \tag{7}$$

where $\mathbf{x}_k$ is the attitude state, $\mathbf{u}_k$ is the control torque, $\mathbf{z}_k$ is the measurements vector and $\mathbf{w}_k$ and $\mathbf{z}_k$ represent respectively the process and measurement noises. An attitude rapresentation based on quaternions or Euler parameters allows a low cost and singularity-free attitude computation, and has been used in the propagation equations of the filter.

Several numerical simulations were first conducted in MATLAB to evaluate the IKF performance for different operative frequencies and an approximated formulation of the filter equations, in order to reduce the computational cost of the algorithm when run in a real time application. A navigation unit was then realized using an Arduino DUE microcontroller that receives measurements form sensors and implements the IKF algorithm in a 84 MHz clock speed ARM processor (Fig. 6). Several experimental tests were then conducted to validate the proposed Attitude Navigation System with: (1) an imposed motion particularly irregular, (2) a state update phase of the IKF executed at a frequency of 100 Hz, and (3) a star sensor measurement update phase executed every 3 seconds. Experimental results showed in Fig. 7 and listed in Table 2 show that the estimation accuracy on the Euler angles can be considered always lower than 0.5 deg. Moreover, the estimation accuracy of the angular velocity components is mainly related to the gyroscope white noise and it is comprised in a band of uncertainty of ± 0.3 deg/s with a 3σ confidence level.

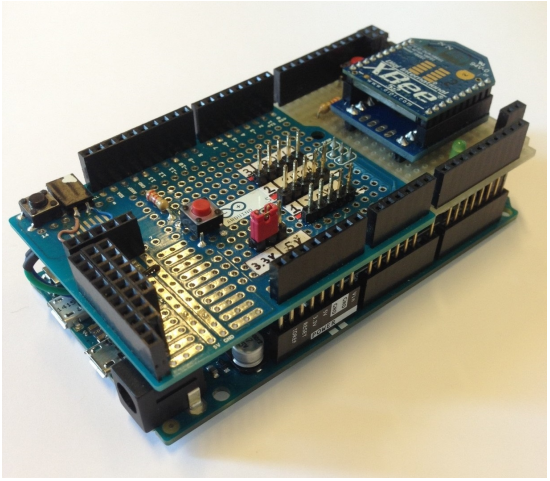


Figure 6. The Navigation Unit for the SPARTANS Attitude Module, realized using an Arduino Due board.

Test number	RMS errors on Euler Angles		
	ϕ_{error}	θ_{error}	ψ_{error}
TEST 1	0.062°	0.049°	0.058°
TEST 2	0.063°	0.048°	0.039°
TEST 3	0.059°	0.052°	0.057°
TEST 4	0.068°	0.058°	0.047°

Table 2. RMS errors of the Euler angles estimated with the IKF.

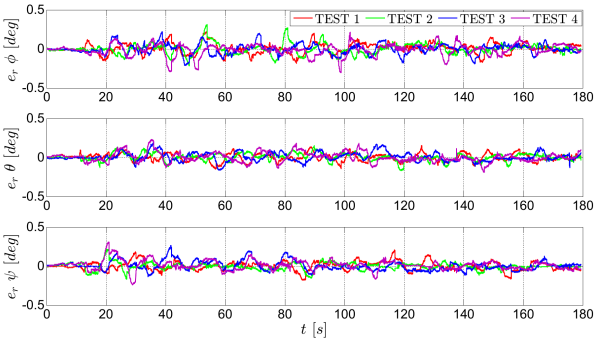


Figure 7. Time profiles of the Euler angles estimation errors.

5. CONTROL MANEUVERS

The development of advanced and efficient control strategies is crucial in formation flight operations. The SPARTANS project provides a facility which eases the implementation and testing of control algorithms in a space representative environment. Both advanced research and educational activities are supported by the facility.

In the current section, a quaternion-based PID controller for attitude maneuvers is presented as a result of a student project. The PID regulator includes proportional and derivative kick avoidance and an anti-reset windup feedback scheme to properly manage the actuators nonlinear behaviors introduced by saturation. A first order low pass filter is used to minimize the noise level introduced by the derivative component of the controller. The resulting equations are discretized in the domain of time by means of a backward difference scheme for the derivative action, and a forward difference scheme for the integral action. Further details can be found in [7]. The adopted PID controller scheme is shown in Fig. 8. The PID regulator is tuned following a trial and error approach by means of software simulations.

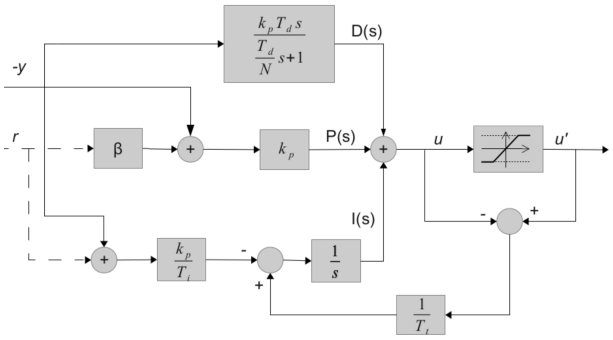


Figure 8. Block diagram of a PID control scheme with proportional and derivative kick avoidance, anti-reset wind up and low pass filter. Only 1 DoF is considered for simplicity.

In order to evaluate the real performances of the controller and to validate the control strategy, two different types of attitude maneuvers were performed. In the first scenario the AM is required to perform a set point reaching maneuver in which the desired attitude is described in terms of roll, pitch and yaw angles: $\Theta_d = [\phi_d,\ \theta_d,\ \psi_d] = [5,\ 7.5,\ 25]$ deg (Fig. 9). The second scenario consists in the execution of a repointing maneuver: the reference trajectory (Fig. 10) is obtained by means of pseudospectral optimization methods for a coarse repointing maneuver with active constraints on the attitude state trajectory [8].

Fig. 9 and Fig. 11 respectively show the overall results of the set point reaching maneuver and the pointing errors associated with the repointing maneuver. The concordance between simulations and test results validates the software simulation environment. The tracking error is always lower than 0.5 deg for both dynamic and steady state conditions.

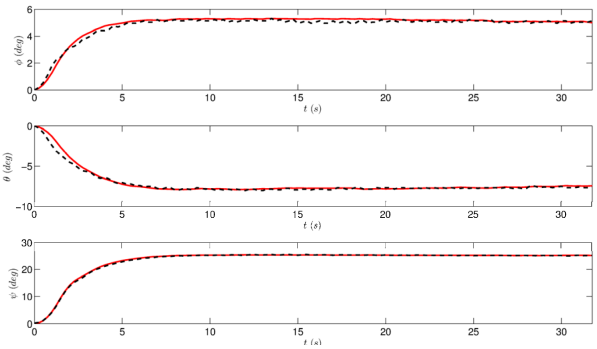


Figure 9. Comparison between simulation results (in continuous red line) and experimental results (in dashed black line) in terms of roll ϕ , pitch θ and yaw ψ angles time profiles for the quaternion-based PID controller applied to a set point reaching maneuver.

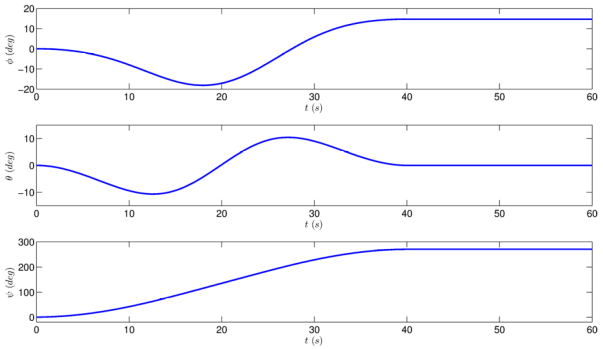


Figure 10. Roll ϕ , pitch θ and yaw ψ reference time profiles for the 3 DoF attitude trajectory tracking test.

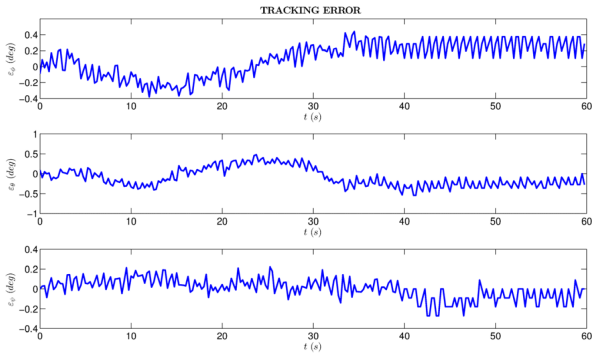


Figure 11. Roll ϕ , pitch θ and yaw ψ trajectory tracking error time profiles for the 3 DOF attitude trajectory tracking test.

6. CONCLUSIONS

In this paper we discussed the experimental activities carried out by PhD and Master's Degree students of the Group for Measurements and Space Technology at the University of Padova, aimed at developing and testing of the Attitude Module (AM) for the SPARTANS project.

One of the innovative aspects of the SPARTANS AM is the use of a custom-made low friction mechanical joints system that allows a free rotation of the AM about the yaw direction, while both roll and pitch motions are mechanically limited to the range $[-40$ deg, $+40$ deg$]$. Also, the use of optical quadrature encoder to directly measure the rotations of the joints system allows to evaluate and compensate for drifts and bias on the attitude state estimated with the on board low cost IMU.

Three main preparatory experimental activities were carried out to: (1) make the AM center of mass as close as possible to the joints system center of rotation (mass balancing), reproducing an attitude dynamics which is typical of the space environment, i.e. free of perturbing torques due to gravity; (2) evaluate the force actuated by the on board thrusters; and (3) estimate the AM inertia tensor. We used a simple and low cost rotational system in two configurations, Torque Balance and Torque Pendulum, in which a metallic wire acting as a torsional spring is the sensitive element. After the estimation of the wire torsional stiffness with a relative uncertainty of 1.8% (2σ), we estimated the force actuated by the thrusters on board the AM with a relative uncertainty of 1.8% (2σ) and the AM inertial tensor components with a maximum relative uncertainty of 4% (2σ).

After that, we discussed the development and validation of an Attitude Navigation System for the AM based on a low cost MEMS IMU, the three QEs used to simulate a star sensor, and an extended formulation of the Indirect Kalman Filter (IKF) algorithm. Random noises of the IMU were first characterized through the Allan variance analysis, and a calibration procedure was then implemented to compensate sensors deterministic error sources due to misalignments, scale factors and bias. Numerical simulations were carried out to evaluate the IKF performance for different operative frequencies and an approximated formulation of the filter equations in order to reduce the computational cost of the algorithm when run in a real time application. A navigation unit was realized using an Arduino Due microcontroller that receives measurements form sensors and implements the IKF algorithm. Several experimental tests were conducted to validate the proposed Attitude Navigation System with an imposed motion particularly irregular. Experimental results showed that the estimation accuracy on the Euler angles and angular velocity is 0.5 deg and 0.3 deg/s respectively.

We concluded this paper showing experimental results of specific attitude control maneuvers carried out on our hardware simulator using a discrete-time quaternion-based PID control law. In particular, two scenarios were considered: a set point reaching maneuver and a tracking maneuver of a pre-computed reference attitude trajectory. Experimental results showed that the tracking errors are always lower than 0.5 deg for both dynamic and steady state conditions.

REFERENCES

[1] A. Valmorbida, M. Mazzucato, S. Tronco, S. Debei and E. C. Lorenzini, "SPARTANS A cooperating spacecraft testbed for autonomous proximity operations experiments", Instrumentation and Measurement Technology Conference (I2MTC), 2015 IEEE International.

[2] `http://ssl.mit.edu/spheres/guestScientistProgram.html`

[3] A. Valmorbida, F. Scarpa, M. Mazzucato, S. Tronco, S. Debei and E. C. Lorenzini, "Attitude Module Characterization of the Satellite Formation Flight Testbed", IEEE Metrology for Aerospace 2014.

[4] IEEE Std 647-2006. IEEE Standard Specification Format Guide and Test Procedure for Single-Axis Laser Gyros. 2006.

[5] B. Peter. Development of an automatic IMU calibration system. Master's thesis, Swiss Federal Institute of Technology, 2011.

[6] N. Trawny and S. I Roumeliotis. Indirect Kalman Filter for 3D attitude estimation. University of Minnesota, Dept. of Comp. Sci. & Eng., Tech. Rep, 2, 2005.

[7] A. Visioli, "Practical PID Control", Springer, 2006.

[8] A. Valmorbida, M. Mazzucato, A. Aboudan and S. Tronco, "Test of attitude control maneuvers with a Satellite Formation Flight testbed," in Metrology for Aerospace (MetroAeroSpace), 2014 IEEE , pp. 439-444, 29-30 May 2014.

MORPHEUS: A FIELD ROBOTICS TESTBED FOR SOIL SAMPLING AND AUTONOUMUS NAVIGATION

S. Chiodini[(1)], A. Carron[(2)], M. Pertile[(1)], M. Todescato[(2)], E. Bertolutti[(3)], A. Bilato[(3)], A. Boscardin[(3)], G. Corrà[(3)], A. Correnti[(3)], R. Dalla Vecchia[(3)], N. Dal Lago[(3)], M. Fadone[(3)], S. Fogarollo[(3)], H. Ghassabian[(3)], E. Mion[(3)], D. Paganini[(3)], F. Quadrelli[(3)], G. Soldà[(3)], A. Todescan[(3)], E. Toffanin[(3)], S. Debei[(1)]

[(1)]CISAS "Giuseppe Colombo", Via Venezia 15, 35131 Padova (ITALY), Email: sebastiano.chiodini@studenti.unipd.it,
[(2)]Department of Information Engineering, Via Gradenigo 6/B, 35131 Padova (ITALY),
[(3)]University of Padova,Via Venezia 15, 35131 Padova (ITALY)

ABSTRACT

MOPRHEUS (Mars Operative Rover of Padova Engineering University Students) is a planetary like rover under development at the University of Padova. It has been designed by a team of students as a testbed for planetary robotic exploration technologies, like soil and rocks extraction and sampling, and autonomous navigation in unstructured environment. The team would like to test the rover capabilities in international competitions as the European Rover Challenge, which guidelines has been adopted in the rover design phase.
The rover, which is remotely controlled, drives in skid steering configuration and has six motorized wheels connected to the chassis through three rockers. A robotic arm, with an interchangeable end-effector, and a sample extraction drill are used for soil sampling. Rover hardware have been designed to be modular, extensible and maintainable.
Autonomous navigation capabilities are achieved thanks to a suite of sensors: stereo-camera, GPS, IMU, wheel encoders and ultrasonic sensors, which operates in a sensor fusion approach. Stereo-camera images are processed by means of a Visual Odometry algorithm in order to obtain the rover pose.
MORPHEUS relies on two control boards: JETSON TK1, an NVIDIA embedded platform which provides the computational capabilities to process stereo-camera images for navigation purposes and manages communication with rover base station, and UDOO board, a microcontroller which manages the motion of the rover and process ultrasonic sensor signal. The software architecture is based on ROS (Robot Operating System) framework, in order to obtain high flexibility and modularity.
In this paper, MORPHEUS overall design is described, control simulations and Visual Odometry algorithm performances are presented.

1. INTRODUCTION

MORPHEUS is a planetary like rover designed by a team of engineering students of University of Padova. The team would like to test the rover capabilities in international competitions as the European Rover Challenge, which guidelines has been adopted in the rover design phase [1]. Competitions like the European Rover Challenge and the University Rover Challenge [2] offer to University students from a wide range of disciplines to gain real-world experience in both ''hard'' engineering skills such as mechanical and electronic design, fabrication, and testing, and ''soft'' skills such as project management, system level thinking, creative problem solving, and interpersonal skills [3]–[6].
MORPHEUS is designed to be a functional rover, capable to perform different tasks similar to ones that will support the future manned Mars exploration. It is controlled remotely by a human operator. In detail, the rover will be able to sample surface soil and rocks, to drill, to autonomously drive in harsh terrains and to operate assistant and maintenance tasks. The rover has six wheels, connected to the chassis through three rockers, and it is able to drive using a skid steering configuration. It will feature a robotic arm (with three hot swappable manipulators for different tasks), a sample extraction drill, a stereoscopic vision system and an omnidirectional antenna for communications. All parts are easily exchangeable thanks to the various joints and multiple connectors. The overall design has been focused on systems modularity to allow fast repairs and quick configuration changes. An accessible red emergency stop button guarantees safety for operators.

2. ROVER MECHANICS

2.1. Rover Locomotion

MORPHEUS rover is a six wheeled skid-steer mobile rover [7]. Each wheel has its own brushless motor and a transmission belt mechanism for the connection system; this configuration improves the security, reliability and performance of the motion system. The rover is designed to reach a maximum speed of 1m/s (3.6km/h) within 5s on a soil with a slope of 15° (acceleration of 0.2m/s^2) and to tolerate a max 50° roll angle. Thanks to the skid steering configuration, the rover is able to turn around itself. Rover dimensions are 820x130x1000mm, and the total mass is around 50kg.
The drive system is composed by off-the-shelf components (Maxon motors):

- Planetary Gearhead GP 32 HP Ø32 mm, 4.0 - 8.0 Nm, metal version, High Power.

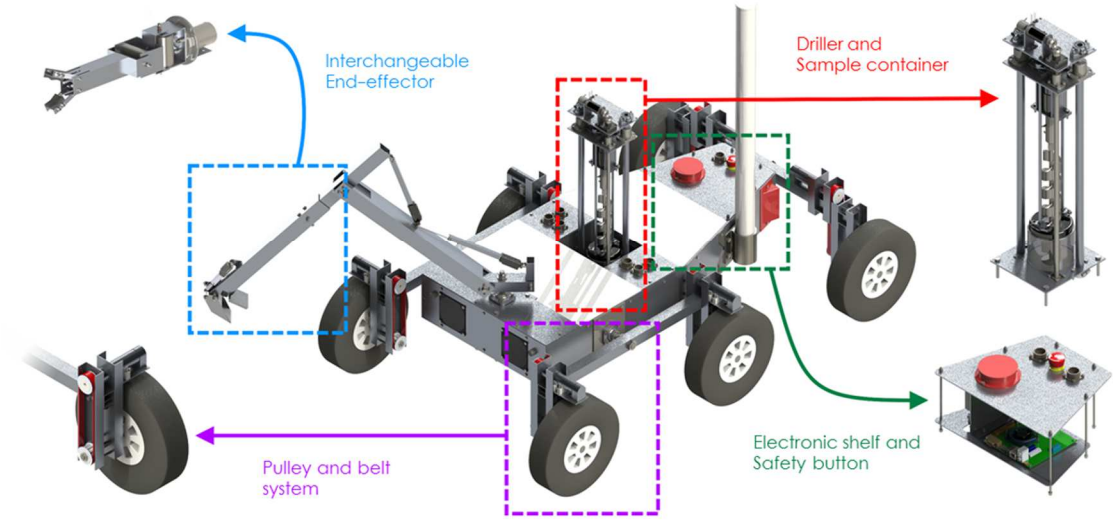


Figure 1. MORPHEUS overview.

- EC-max 30 Ø30 mm, brushless, 60 Watt, with Hall's sensors.
- Encoder HEDL 5540, 500 CPT, 3 channels, with Line Driver RS 422.
- DEC Module 50/5, Digital Amplifier 1-Q-EC 50 V / 5 A, Speed Control, PWM output.

The configuration with three rockers, everyone equipped with two wheels, has been chosen to guarantee sufficient adherence to the soil.
The belts and pulleys system is composed by off-the-shelf compomemts (Poggi Trasmissioni Meccaniche):

- 34H0410012 belt
- 31T 10/12-6F pulleys

MORPHEUS rover is sustained by a chassis, which bears all the structural loads, and the rover coverage. The chassis is composed by a steel tubular welded structure (20x20x1mm squared section). The coverage permits to mount many components (PCB, fans, connectors, etc.) and also acts as protection against the external environment.
Fig. 1 shows and overview of MORPHEUS rover, the pull and belt system, the arm with the interchangeable end-effector, the driller and the electronic case. Fig 2 shows a detail of MORPHEUS.

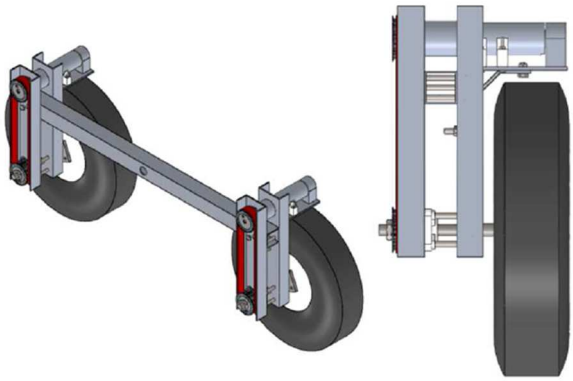


Figure 2. Side rockers detail.

2.2. Robotic Arm and Driller

MORPHEUS Arm is designed to face the European Rover Challenge Science, Maintenance and the Assistance Tasks [1][8]; the arm is removable. This subsystem has two different end-effectors Fig. 3, the first one is for the Science task (3 DOF arm) and the second one for the Maintenance and Assistance Task (6 DOF arm).

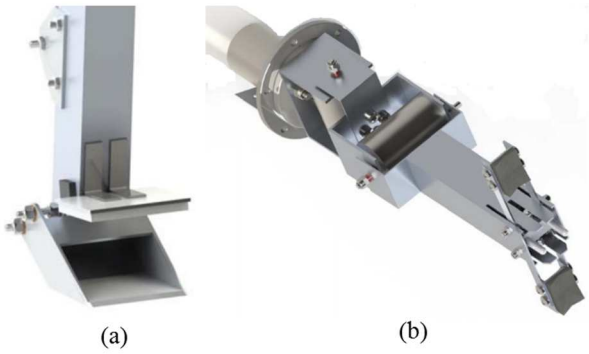


Figure 3. Rover arm end effectors. (a) Science task; (b) Manipulator - Maintenance task.

The motors used in the arm subsystem are:

- PS150 24 125-2S, Base motor
- Firgelli L16, 1st/2nd arm actuator
- Firgelli L12, End-effector actuator
- BS138F 12 208-2S, Wrist Motors (manipulator)

Firgelli linear actuators are embedded with a potentiometer that gives back information about actuator position. Fig 4. shows the 3DOF robotic arm.
A series of simulation has been performed to test the 3DOF behavior under operative condition: follow a path from user input, dig test and transport of soil and rocks. A PID (proportional - integral - derivative controller with position feedback) control loop has been implemented in order to control the arm. The first control strategy that has been implemented is decentralized control: in this case, the arm is characterized by three independent systems, so we can control each joint axis as a single input/single output system. Coupling effects between joints during motion are treated as disturbance inputs [9]. Fig. 5 shows the used 3DOF robotic arm decentralized control scheme in Simulink.



Figure 4. Rover 3DOF robotic arm.

A Drill has been designed in order to collect a 25g soil sample from a layer 15cm below the surface. Two optical switch are used to check the tip motion limits. A button load cell is embedded into the drill subsystem in order to detect the tip axial loads and to prevent damages to the subsystem. Since driller shaft can sustain a maximal axial load of 120N the load cell threshold is 100N.

3. ROVER ELECTRONICS

JETSON TK1 and UDOO are the rover control boards. The first one is a NVIDIA embedded platform whereas the other one is a singleboard computer. The JETSON is the rover main board: it checks the sensors, processes the images for the stereovision system and manages the communication between the rover and the base station. The UDOO microcontroller manages the motion of the rover through the motor drivers. The rover power supply is provided by 4 commercial off-the-shelf 12V 9Ah Lead Crystal rechargeable batteries; this should provide 1h of working time. A custom power supply board delivers the following voltage values: 3.3V-5V- 12V-24V.



Figure 5. Rover driller subsystem.

For telecommunications will be used a system of two AirMax Omni AMO-5G10 omnidirectional antenna, one for the rover and one for the base station. Each of them is connected to a RocketM5 module. The communication will be in Wifi on 5.6GHz. The range is 1km.
The NVIDIA JETSON TK1 is the rover core, it exploits a 4-PLUS-1 Cortex A15 “r3” CPU. This board manages housekeeping (motors and rover temperatures) and navigation data (GPS signal, IMU signal, sonar senor data, stereo-images) and Webcam for public outreach. Texas Instruments LM73 checks motors and rover temperature. IMU InvenSense MPU-6050 and GPS

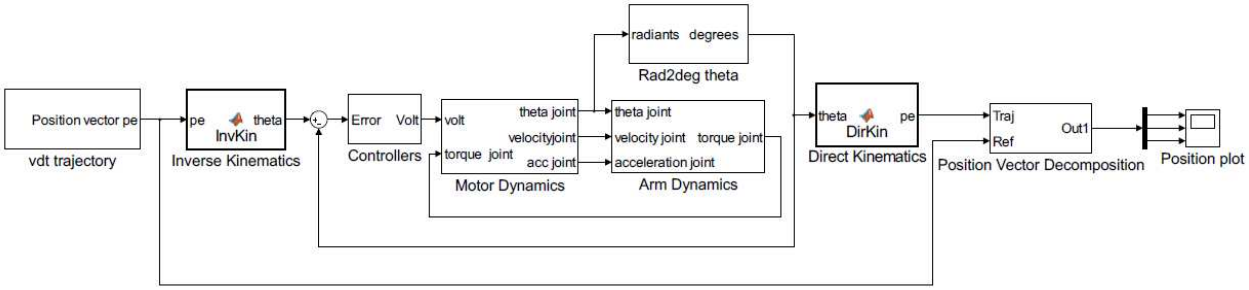


Figure 6. 3DOF robotic arm decentralized control scheme in Simulink.

GlobalSat EM-506 are used for the rover motion and localization. All of the sensors are connected via I2C bus. There are three Logitech HD Webcam C310 (1280x720 pixel): two of them for the Arm control and the other one is used for the Drill. Moreover, two Raspberry-PI camera modules and a Raspberry- PI compute module compose the stereovision system for autonomous motion control. Lastly two load cells (capacitance 5kg±0,05%) are connected to JETSON board through a Phidget-Bridge. The voltages and power consumption are constantly read by the JETSON to prevent excessive battery drain. In this way functional and irregular conditions can be filled in real time by the rover, checked and handling.

The other core of the rover is a UDOO board, which implements a microcontroller (Atmel SAM3X8E ARM Cortex-M3 CPU) and a Dual-Core processor (CPU Freescale i.MX 6 ARM Cortex-A9 Dual core 1GHz) working together. The function of this board is to control the Arm and the rover motion motors. The UDOO is connected to several PCBs that manage the interface between motors and the components

There are three PCBs for the motion: two positioned on the lateral sides and another one on the back side. Every board is composed by two proprietary decoders, which control two motors by setting their speed and direction while two encoders return the feedback to the UDOO.

PCBs for the Arm and Drill are mounted directly on each subsystem. The Drill is controlled by a custom board which is realized with two lmd18200 drivers. Every driver returns a voltage feedback to the UDOO proportional to the current consumption of the motor. The Drill has a supply voltage of 24V and a maximum power consumption of 33W.

For the Arm base there is a motor which controls the rotation through a custom driver with an lmd18200. The limbs motion is performed by three Firgelli linear motor (two L-16 and L-12 at the end) and they are controlled by three proprietary drivers.

At the end, four LV-MaxSonar® -EZ ultrasonic sensors are being used to detect targets around the rover for collision avoidance. They are two in front of the rover and two in the lateral sides, transmitting with the UDOO through a PWM modulation.

4. ROVER SOFTWARE

The rover's software is designed to then be modular, extensible and maintainable. According to these principles, the software has been divided into six major modules: HAL (Hardware Abstract Layer, contains the drivers), Control (contains classes to perform the tasks), Core (manages the rover during the tasks), GSE, Telemetry (stores and manages tracking) and Watchdog (check that the boards and processes do not lock). The languages used are C/C ++ and Python.

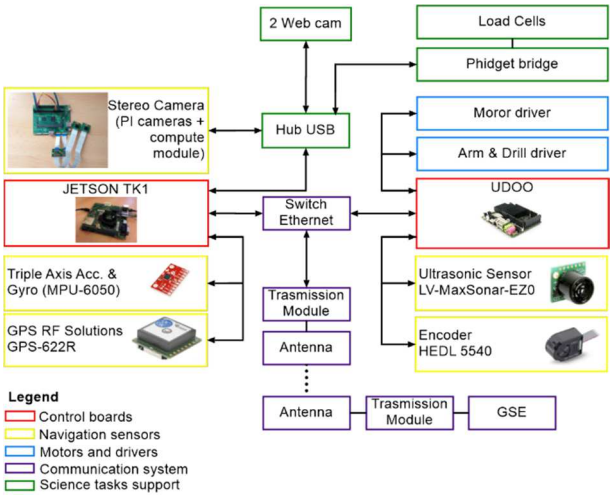


Figure 7. Rover functional scheme, sensors, drivers and communication subsystem.

Modules are interconnected each other thank to a robotic open source platform Robot Operating System (ROS).

The rover orientation and relative position is provided by a sensor fusion algorithm which uses GPS, IMU and visual odometry data. During navigation task for collision avoidance, the rover exploits four ultrasonic sensors.

All activities of the rover are monitored through computer screens. The team uses a multi-thread software and GUI written in C++ (with QT libraries). The GUI is able to broadcast all the needed data with an interval of about a 0.5s while ensuring great precision and security.

The rover is remotely controlled by means of a joystick for a real-time feedback to the user.

4.1. Navigation

The pose of the rover will be estimated through the measurements collected by a GPS module and an IMU (accelerometers and gyroscopes). This algorithm provides an estimate of the vehicle position and orientation that is far more accurate than the one obtained by the GPS and the IMU separately. Indeed the weaknesses of the former are compensated by the latter and vice versa: while the GPS provides only a rough estimate of the position with low update frequency, the IMU gives more precise data with high update frequency; on the other hand the accelerometers and gyroscopes can only give a relative measure with an error that increases over time (due to the integration of the accelerations and velocities) whereas the GPS measure is absolute, as it doesn't depend on the motion of the rover.
The sensor fusion algorithm will be implemented using a Kalman filter, which will compute the optimal solution to the problem and will give reliable values for the position and the orientation of the rover [10].

4.2. Visual Odometry

The rover will use Visual Odometry (VO) to determine its motion examining the changes that motion induces on the images of the vehicle on-board cameras. It is planned to use a stereo camera system consisting of two pi camera attached to the rover chassis. The cameras capture two synchronous images partially overlapped and send it to the board computer. Here a software processes the images in real time and determine the vehicle pose. VO does not suffer from wheel slip in uneven terrain or other adverse conditions and is therefore an useful support to wheel odometry and to other navigation systems such as global positioning system (GPS) and inertial measurement units (IMUs).
For our purpose we need a real-time long-run implementation with a robust outlier rejection scheme. To do that we implement a software in C++ using OpenCV and OpenGV libraries [11].
Following the approach proposed by [12] we choose to compute the relative motion as a 3D-to-2D camera-pose estimation problem (see scheme below). We tested three different algorithm (Kneip [13], Gao [14] and EPnP [15]) inside a sample consensus framework (RANSAC) and then completed the methods by non-linear optimization [16].
For the y-axis rotation with 5° steps we obtained an error lower than 0.3% with the Gao algorithm. We intend to test this software on a ground similar to that of the competition to find the best camera configuration for our purpose.

5. PROJECT STATUS AND CONCLUSIONS

A planetary like rover has been designed by a team of engineering students of University of Padova. The team would like to test the rover capabilities in international competitions as the European Rover Challenge, which guidelines has been adopted in the rover design phase. The platform will be uses as a testbed for planetary robotic exploration technologies: soil extraction and classification and autonomous navigation.
The project is on-going, in the near future rover mechanical assembling phase, and custom electronic board manufacturing will be done. The code developed for rover and arm control, autonomous navigation will be integrated in the rover main software.

REFERENCES

[1] Mars Society Polska, "European Rover Challenge 2015 Rules," 2015.

[2] Mars Society, "University Rover Challenge." [Online]. Available: http://urc.marssociety.org/home. [Accessed: 28-Nov-2015].

[3] M. A. Post and R. Lee, "Lessons learned from the York University Rover Team (YURT) at the University Rover Challenge 2008-2009," *Acta Astronaut.*, vol. 68, pp. 1343–1352, 2011.

[4] S. Meszyński and M. Józefowicz, "Analog Mars Rover Service as a Robotic Hardware and Team Building Platform," in *Aerospace Robotics II*, 2015, pp. 145–161.

[5] M. K. Shafin, K. L. Kabir, I. Ridwan, T. A. Fuad, S. Bardhan, M. I. H. Raju, A. Tahira, I. Afrin, S. Mondal, S. N. Tumpa, A. Ahmed, M. A. Badhon, M. T. I. Jony, F. H. Khan, M. M. Karim, and M. A. Hossain, "Mongol Barota: A next generation rover," in *The 8th International Conference on Software, Knowledge, Information Management and Applications (SKIMA 2014)*, 2014, pp. 1–8.

[6] A. G. M. B, J. Timmis, and A. F. T. Winfield, "Towards Autonomous Robotic Systems," *Taros*, vol. 8069, pp. 429–430, 2014.

[7] A. Mandow, J. L. Martínez, J. Morales, J. L. Blanco, A. García-Cerezo, and J. González, "Experimental kinematics for wheeled skid-steer mobile robots," in *IEEE International Conference on Intelligent Robots and Systems*, 2007, pp. 1222–1227.

[8] E. Bertolutti, "Studio, analisi e progettazione di un braccio robotico ridondante per l'esplorazione planetaria," Università degli Studi di Padova, 2015.

[9] E. Toffanin, "Cinematica, Dinamica e Controllo del Braccio Robotico per il Rover D'Ateneo MORPHEUS," Università degli Studi di Padova, 2015.

[10] F. Caron, D. Pomorski, and P. Vanheeghe, “GPS/IMU data fusion using multisensor Kalman ltering: introduction of contextual aspects,” *Inf. Fusion*, vol. 7, pp. 221–230, 2006.

[11] L. Kneip and P. Furgale, “OpenGV: A unified and generalized approach to real-time calibrated geometric vision,” in *2014 IEEE International Conference on Robotics and Automation (ICRA)*, 2014, pp. 1–8.

[12] D. Nister, O. Naroditsky, and J. Bergen, “Visual odometry,” in *Proceedings of the 2004 IEEE Computer Society Conference on Computer Vision and Pattern Recognition, 2004. CVPR 2004.*, 2004, vol. 1, pp. 652–659.

[13] L. Kneip, D. Scaramuzza, and R. Siegwart, “A novel parametrization of the perspective-three-point problem for a direct computation of absolute camera position and orientation,” *Proc. IEEE Comput. Soc. Conf. Comput. Vis. Pattern Recognit.*, pp. 2969–2976, 2011.

[14] Xiao-Shan Gao, Xiao-Rong Hou, Jianliang Tang, and Hang-Fei Cheng, “Complete solution classification for the perspective-three-point problem,” *IEEE Trans. Pattern Anal. Mach. Intell.*, vol. 25, no. 8, pp. 930–943, Aug. 2003.

[15] V. Lepetit, F. Moreno-Noguer, and P. Fua, “EPnP: An Accurate O(n) Solution to the PnP Problem,” *Int. J. Comput. Vis.*, vol. 81, no. 2, pp. 155–166, 2009.

[16] G. Soldà, “Implementation and Experimental Verification of a 3D-to-2D Visual Odometry Algorithm for Real Time Measurements of a Vehicle Pose,” Università degli Studi di Padova, 2015.

DEVELOPING TECHNOLOGIES FOR SPACE ON A TERRESTRIAL SYSTEM: A COST EFFECTIVE APPROACH FOR PLANETARY ROBOTICS RESEARCH

Lennart Kryza, Sascha Kapitola, Cem Avsar, and Klaus Briess

Technische Universität Berlin, Department of Aeronautics and Astronautics, Marchstrasse 12, 10587 Berlin, Germany

ABSTRACT - The exploration of space relies heavily on robotics. Planetary rovers form the backbone of remote scientific activities on celestial bodies. These systems fulfill many different tasks, ranging from mapping a designated area with highest precision to collecting and analyzing soil samples. This paper introduces the possibilities of conducting scientific research in the field of space robotics embedded in a terrestrial system. The rover developed at the TU Berlin resembles a terrestrial system, consisting of hardware which is mostly not qualified for space. However, technologies, competencies and methods developed for it are predestined for space application. Prime examples for the competitive results are machine autonomy, object recognition and navigation. SEAR shows the benefits of using a terrestrial platform for the research of new and unqualified technology which might proof a valid solution for space exploration in the future.

1. INTRODUCTION

Developing space technology is an interminable and expensive process. The development and qualification of hardware for space applications is costly. This results in challenges for the education of young engineers, as well as the research process. Systems can rarely be tested under the operation conditions, hands-on experience with flight hardware is uncommon for most students.

During the SEAR project, a planetary rover was developed in order to compete at the SpaceBot Cup which was initiated and organized by the German Aerospace Center (DLR). Over 50 students in more than two years were involved in designing and testing the robot, gaining in-depth knowledge about the system and leading to several theses.

Robotics offers unique possibilities to conduct research on hardware which is not qualified for space operations. A systems can be designed and tested for the operation in a planetary exploration scenario. This allows to conduct research on Earth without the need to invest in space proven components.

The diversity and complexity of planetary robotics results in two major challenges: Cost of development and demanding operation procedures. Controlling a system which is to be maneuvered through an unknown terrain over timely delayed communication poses both risks for the mission and challenges for the operator. Communication is delayed and only possible during not more than one quarter of operation time. This leads to the central requirement of an autonomous system, which is able to achieve most of the mission goals on its own. Methods of achieving such autonomy are presented in this paper, as well as other aspects which can be researched on with a terrestrial system, pointing out methods for simulating such scenarios, as well as presenting first results.

2. PROJECT SEAR AND THE SPACEBOT CAMP 2015

The SEAR (Small Exploration Assistant Rover) project began in 2013 when the first DLR SpaceBot Cup was announced. Robotic systems were to explore an unknown environment, only provided with a rough map of the field. Two objects had to be autonomously found, identified and collected. These object were then to be transported to a third one in order to assemble a complete system. [1]. The development of technologies capable of autonomously complete such mission scenario was the main driver for the German Aerospace Center (DLR) to host and support the competition [2].

Figure 1 shows the two objects which were to be collected and the station for assembling on the right: The cup was to be put on a scale on top of the basis, while the battery had to be moved into an

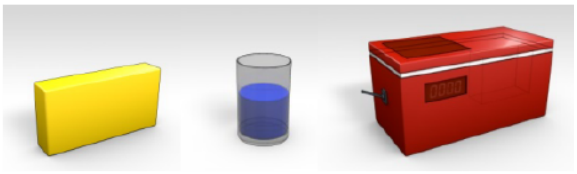


Figure 1. The three objects for manipulation during the SpaceBot Cup, Source: DLR

opening on the side of it. Then a lever on the other side was to be pulled.
The Chair of Space Technology of the TU Berlin decided to participate in the contest and started the development of the rover SEAR in April 2013. The TU Berlin's space research is normally focused around the development of pico- and nanosatellites, as can be seen in table 1, where some of the active satellite missions and developments are listed. Up to this date, 10 satellites developed at the TU Berlin have successfully been launched.

Mission	**Launch**	**Mission purpose**
BEESAT-2	2013	Demonstration of 3-axis stabilized CubeSat
BEESAT-3	2014	Hands-on education, Demonstration of a 1 Mbit/s SBand Transmitter
BEESAT-4	2016	Demonstration of a CubeSat with GPS capability
TUBIN	2016	Earth Observation with a COTS infrared camera
S-NET	2016	Intersatellite communication in S-Band (Four Satellites)
TechnoSat	2017	Technology demonstration of miniaturized components

Table 1. Satellite Developments at the TU Berlin

Many of the students participating in the rover team were also involved in the satellite projects, which led to a bidirectional synergy in the developments. The goal was to create a system which is able to fulfill all the requirements of the contest, but at the same time serves as an educational platform for students. In the future, miniaturization expertise of the Chair of Space Technology would be used in order to extend the functionalities of the rover and integrate miniaturized systems into it.

Work began with a budget of only 50 000 EUR in April 2013 and within six months, a rover was built. SEAR in its configuration from 2013 can be seen in figure 2. Student ambition is the main reason that

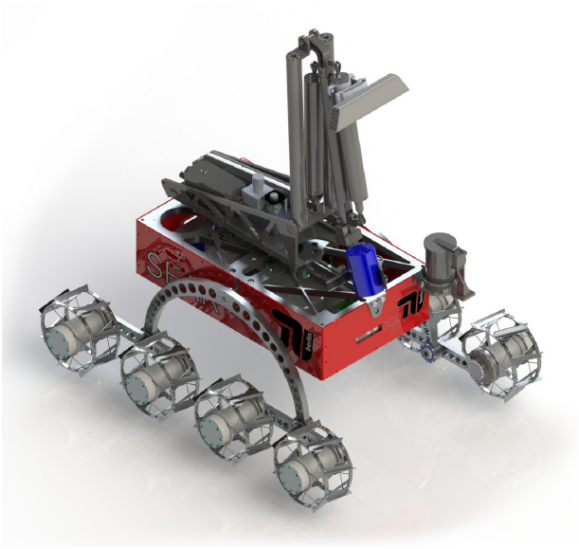


Figure 2. SEAR 2013 configuration

this system could be built in such short amount of time. However, performance of the system during the cup 2013 was characterized by problems in the communication between ground station and rover. Therefore this subsystem was revised after the cup and will be explained in more detail in section 3.5.

All other teams had similar issues and the competition ended without a winner. However, a new SpaceBot Cup was announced in 2015 and team SEAR applied and was selected to participate as well. In the light of the events of 2013, a qualification was to be passed two month prior the actual cup. Only if four teams would pass the qualification, the competition would take place. Team SEAR was one of only three teams who was able to pass the qualification (10 teams competed) and thus the SpaceBot Cup was canceled. However, it was replaced by the SpaceBot Camp 2015, where all 10 teams could present their systems during the mission scenario.

3. SIMULATING SPACE OPERATION ON A TERRESTRIAL SYSTEM

Space hardware is not specifically needed in order to create a system on which mission scenarios can be simulated and trained. However, a rover must have the same capabilities it would have in a real space mission, in order for it to be an appropriate testing platform. Among these capabilites are the following:

1. **Processing** - Planetary rovers must be capable to execute complex operations and fulfill various tasks, such as navigating rough terrain and conduct scientific experiments without direct human interaction.
2. **Sensors** - In order to safely navigate, sensors are required which allow the rover to percept its environment.
3. **Locomotion** - A planetary rover must be able to overcome obstacles, climb hills and pass slopes up to a certain degree. A robust and capable locomotion system represents the basis for that.
4. **Communication** - Communication with Earth or satellites is important for rovers in order to be operable and transfer data. Long distances represent a severe challenge, when data transmission can take several minutes.
5. **(partial) Autonomy** - Due to high delay in communication, at least partial autonomy is required. Operation of a planetary rover is not always possible, and vast distances make interaction nearly impossible.

If these requirements are met by a rover, it becomes a system on which planetary scenarios can be simulated as in the case of SEAR.

3.1. Mechanical Design

SEAR was designed in order to compete at the SpaceBot Cup 2013. While the mission scenario was the primary design driver, the system was also planned in coherence with space system design standards.

The basis of the rover forms the chassis, which allows to navigate rough terrain and inclines of up to 30°. A Rocker-Bogie systems was chosen, in order to guarantee safe and robust navigation. The conceptual design can be seen in figure 3. Each of the eight wheels is driven by an individual motor in order to guarantee enough force. The motors were integrated into the wheels, which are depicted in figure 4.

The sturdy design in combination with the extensions, allows the rover to overcome different kinds of grounds, such as stone, rocks or sand. Brush-less DC Motors by Faulhaber were chosen as main gearing system.

The same principles were used for by designing the corpus of the rover. Figure 5 shows the basic structure and the results of a mechanical load analysis which was conducted. The ground plate can withstand loads of up to 160 N, which is more than

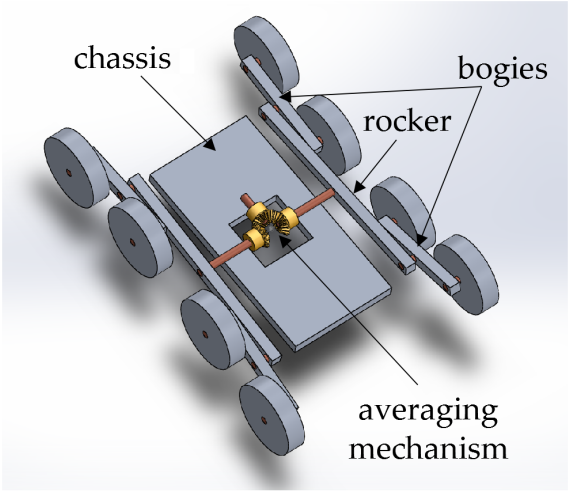


Figure 3. Rocker-bogie system of SEAR - Concept

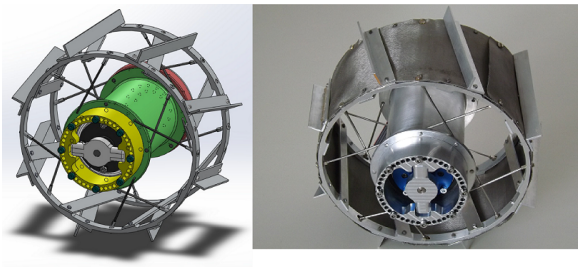


Figure 4. Wheel of the SEAR locomotion system

sufficient for all of the rover's components. It is not designed to support the whole of the weight, since the suspension system is distributed over several points. Only the electronics, the OCB (On-Board Computer) and peripheral computing systems are placed on it. The top of the corpus was tested with up to 250 N, since the main stressed is induced at the outer parts of the construction. Aluminum was

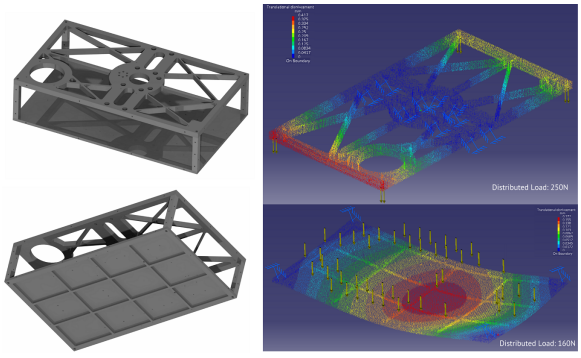


Figure 5. SEAR corpus design and mechanical load analysis

used as main material for all structural components. This results in a relatively light build, but increased production effort.

3.2. Electronics and Communication

The electrical design is kept relatively simple, but reliable. As energy source a LiFePO4 battery is used, which has a capacity of 20 Ah and provides 24 V of voltage. These 24 V are then converted by DC/DC-converters in order to create the two main buses: A 12 V and a 5 V bus. The eight motor controllers of the locomotion system are directly connected to the battery.

The communication subsystem of SEAR uses commercial solutions only. Local Area Networks are used for transferring data and interacting with the rover, both wired and wireless versions. In case of the wireless network, 5 GHz are used as carrier frequency.

3.3. Sensors

SEAR relies mostly on optical sensors. In order to perceive its surrounding, ASUS Xtion Cameras are used [3]. These sensors do not only provide RGB images, but also have depth image capabilities. Infrared sensors and common RGB cameras are additionally used for collecting information.

3.4. Software Design

The software design of SEAR is based on the operating system ROS (Robot Operating System). ROS is an open source project which is used by universities and research institutions around the world. It provides a software platform and packages which can be used for the development and operation of a robot. The benefit for the SEAR project was that some parts of the robot's implementation could be used rather than developed. This would save time and allow the team to focus on internal developments in regard to the mission scenario which was to be fulfilled.

Figure 6 shows the general software architecture which is used on the rover and during development. While almost the complete software is running within the ROS environment and some packages are used, the internal implementation was centered around the mission scenario.
Benefits of this procedure not only includes an decreased development time for the rover software, but also educational aspects. Students working on the project not only gain experience in rover software, but also the ROS system, which is widely used in robotics.

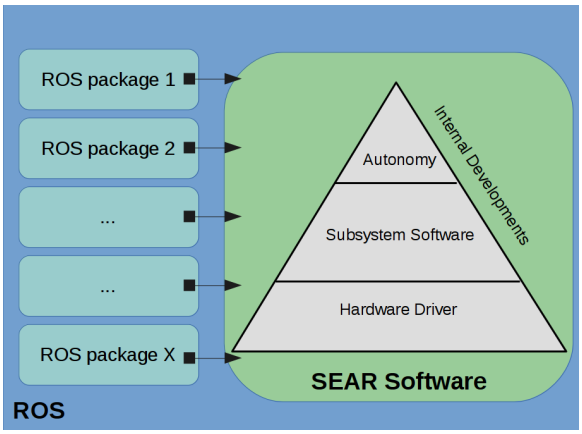


Figure 6. General software architecture of SEAR

3.5. Mission related software developments

In order to compete at the SpaceBot Cup, software specific to the tasks had to be developed. The following five software packages are internal developments and have been written by students:

1. **ROS-Faulhaber Driver**
2. **Object Recognition**
3. **Inter ROS Master UDP Communication**
4. **Several GUIs for ground station operation**
5. **Autonomy / Task Management**

The **ROS-Faulhaber Driver** was written in order to control the chassis motors via ROS. The software is commandable via ROS, takes velocity commands and translates into messages which can be understood by the motor controllers. The basic data flow is illustrated in figure 7. While the ROS

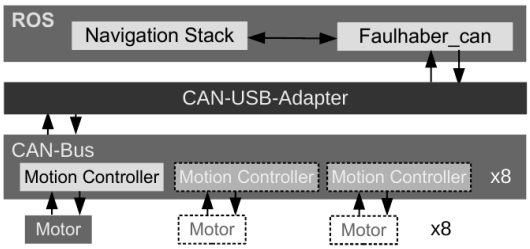


Figure 7. Data flow of the motor control software [5]

Navigation Stack is used in order to create the velocity commands based on the desired navigation, the Faulhaber_can uses these data in order to communicate the motor commands with the motor controllers via a CAN-bus. The controllers in turn then translate these into the right current for the

motors. The CAN-bus is used in order to create a stable and reliable data transmission platform. It is also used in many satellite projects at the Chair of Space Technology.

In order to able to collect the desired object autonomously during the mission, the rover has to be able to identify these objects on its own. The **Object Recognition** software uses the all available parameter in order to search and find the three objects in the camera images. The approach is based on blob detection and uses in first instance mainly the objects' colors.

Other aspects which are taken into considera-

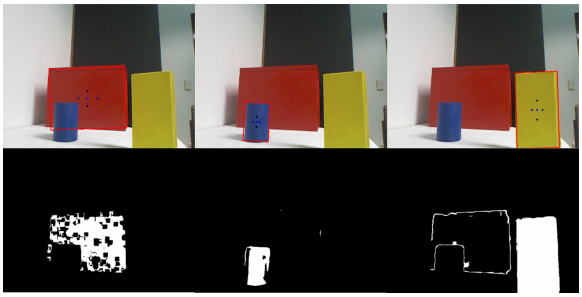


Figure 8. Object recognition software results

tion are the size and aspect ratios of the recognized color blobs. Additionally, a cascade machine learning algorithm is used to double check object candidates based on geometrical relations. Results of the object recognition can be seen in figure 8. Objects are clearly identified and the negative image only shows the recognized objects in white. For the complete process, Xtion camera images are used. Since these sensors also provide depth data, it is even possible for the rover to identify the exact distance and orientation of the objects towards itself.

The communication software of SEAR was revised after the cup in 2013. although its basic functionality stayed the same. In order to operate SEAR in the mission scenario, two ROS Masters are needed. ROS Masters provide registration and management services for the different ROS nodes (i.e. programs) which are running on a ROS system [6]. Due to the delay in the communication, one ROS Master is needed for the ground and space segment each. The general communication architecture can be seen in figure 9. Two nodes are involved in the communication between the two segments. Telemetry data is collected by the node in the space segment and sent via the gateway to the ground station. Telecommandos are transferred to via the ground node to the space segment and then initialized by the space segment node. In 2013, the used transfer protocol between all systems was TCP, which led to severe problems in the communication. Data would not be sent to the ground station before the reception of preceding data packages were not

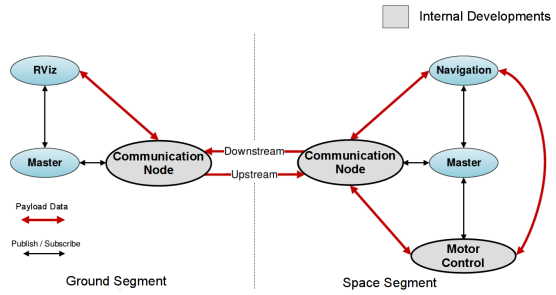


Figure 9. SEAR communication architecture ([7], edited)

confirmed. This led to an ever growing amount of telemetry which was not transferred, which in turn increased the effective delay significantly. The software was revised in 2015 and the access point now communicates via a UDP based protocol with the gateway. This led to the prevention of detectable increase in the delay, making the communication between SEAR and the operators stable.
The characteristics of the communication line, such as the delay or temporary loss of communication are induced by the network emulator. This communication layout is illustrated in figure 10.

The access point represents a lander and is

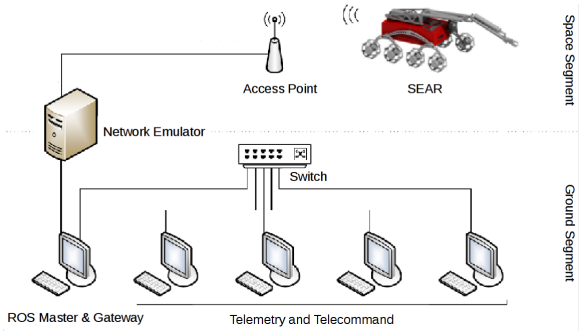


Figure 10. Communication layout

simulated in the project by the lander PC, which is a common laptop. The lander PC provides a wireless LAN, in which it communicates with the rover. Connection between the access point and the network emulator, as well as the network emulator and the gateway in the ground station, are wired LAN connections.
The **autonomy and task management** system of SEAR will be discussed in more detail in section 4.

3.6. SEAR system in 2015

SEAR has undergone some changes since 2013. These were made in order improve the rover's capabilities of competing at the SpaceBot Cup successfully, at the same time the guideline to construct a system which can theoretically be used

in space application was kept. The system of 2015 can be seen in figure 11.

The number of cameras could be increased

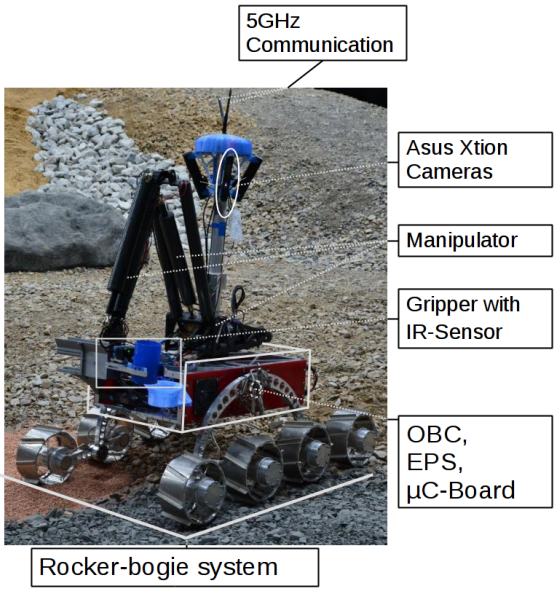


Figure 11. SEAR 2015 ([10], edited)

by constructing a camera mast. The system now uses up to 6 Xtion cameras in order to create an image of its surroundings. While USB bus limits prevent SEAR of operating all cameras of the same time, it was possible to switch between five of the cameras periodically and thus generate all around view over time. The sixth camera is turned on all of the time, because it is used for the localization of the rover, which is achieved by SLAM (Simultaneous Localization and Mapping).

The gripper was also revised and was internally developed and produced. It improves the safety of the grasping process. The gripper could also be equipped with a camera to its infrared sensor. This way it was possible to implement an autonomous grasping process, where the rover scans its the near environment where it thinks an object should be and then uses both the IR-sensor and camera in order to confirm the exact position.
Minor changes include OBC-housing, wireless communication devices and transport container for the objects.

3.7. Analogies between the terrestrial design and a planetary exploration rover

The SEAR rover resembles a planetary rover in many aspects and the main aspect of it is appropriate for space application. The chassis has proven to be reliable during the qualification and the SpaceBot Camp 2015. Further, although commercial sensors are used for the navigation of SEAR, the principle does not differ from actual rover missions. While stereo images are commonly used ([8],[9]), the same kind of data can be generated with Xtion Cameras. The depth images are converted to point clouds, which can be used for obstacle avoidance and mapping. Figure 12 shows an example of the mapping capabilities of SEAR.

The communication characteristics are also

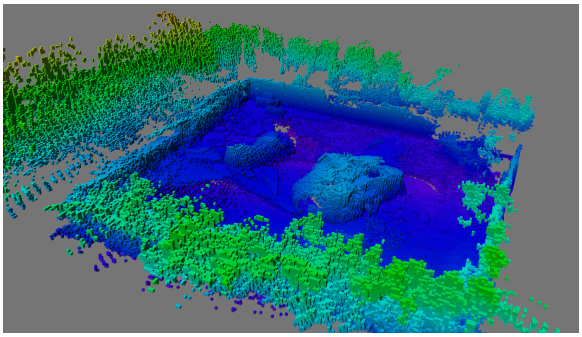


Figure 12. SEAR mapping results

similar to an actual planetary mission. This does not only include effects which are created by the network emulator, such as the delay. Due to interferences, package loss in the wireless network is a possibility and the data rate is restricted, too. These things had to be taken under consideration during the development and form strong parallels to a space mission.
When these aspect are brought together during the operation, one of the most obvious analogies can be observed: The operation itself. Mission operations were put in focus of the project during a lecture in late 2014. During this time, many GUIs were developed in order to improve the control and monitoring of the system.

4. DEVELOPMENT OF A METHODICAL AUTONOMY FOR A PLANETARY ROVER

Autonomy is an important aspect of planetary robotics. In the SEAR project it was a design driver in order to compete at the SpaceBot Cup.
The autonomy system of SEAR is designed hierarchically. The top level is represented by the task management and focuses on the decision making process. Other autonomous processes are implemented within the subsystem software, such as the grasping process or the autonomous navigation.
The autonomy of SEAR is methodical, because it is strongly connected to the mission scenario for which is was created. The system cannot - and is not supposed to - operate autonomously under any condition. It is even required to wait for operator input

in case undefined states are reached.
The autonomy approach for SEAR's task management system makes use of behaviour trees. Behaviour trees are based in the computer game industry and used in order to create artificial intelligence for non-player characters. They offer unique and dynamical possibilities to create complex behaviours flexibly. Most importantly, it is possible to design an autonomy in a very defined way, enabling an engineer to predict the robot's decision very accurately. Behaviour trees consist of different logic blocks which themselves represent behaviour trees also. They can result in one of three states:

1. Success
2. Failure
3. Running

The first two indicate the completion of the respective tree, while the third reports an active process. Two of the most fundamental blocks are the sequence and the selector. In a sequence, children elements are triggered until one of it reports a failure, then the complete sequence fails. Only if all children are successful, this element returns a success. This logic can be seen in figure 13.

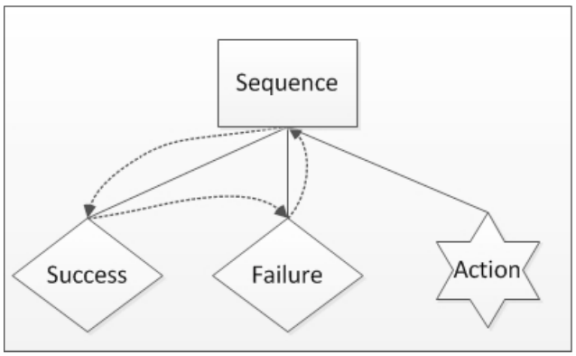


Figure 13. Principal of the behaviour tree sequence [11]

Another important element is the selector which works the other way around. It triggers its children until one of them succeeds and only fails if all of them fail. This principal is illustrated in figure 14.

It was possible to use these and other elements in order to create a complex behaviour tree which follows the priorities set by the mission scenario. An excerpt of the created behaviour tree can be seen in figure 15. The main approach is to let the rover first initialize all of its subsystems before it starts operation. It then checks whether objects for grasping are available. If that is not the case,

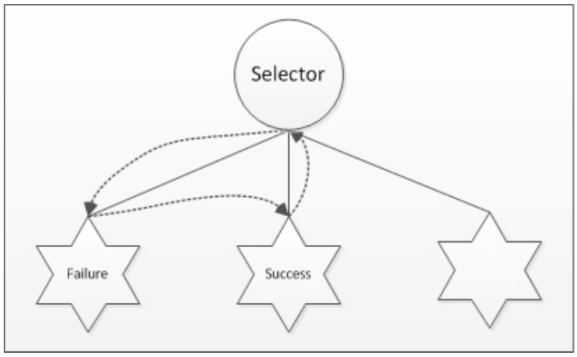


Figure 14. Principal of the behaviour tree Selector [11]

it checks whether it has already picked up objects and is able to start assembling or if it has already finished all of its tasks and can go home. Most of the operational time, all of these checks will report failure, which will lead to the robot exploring its surroundings (in order to find objects for grasping and the station for assembling). As it can be seen, the task management system must be aware of many information. This leads to the requirement to create interface between it and almost every subsystem, resulting in a vast amount of data which change constantly.

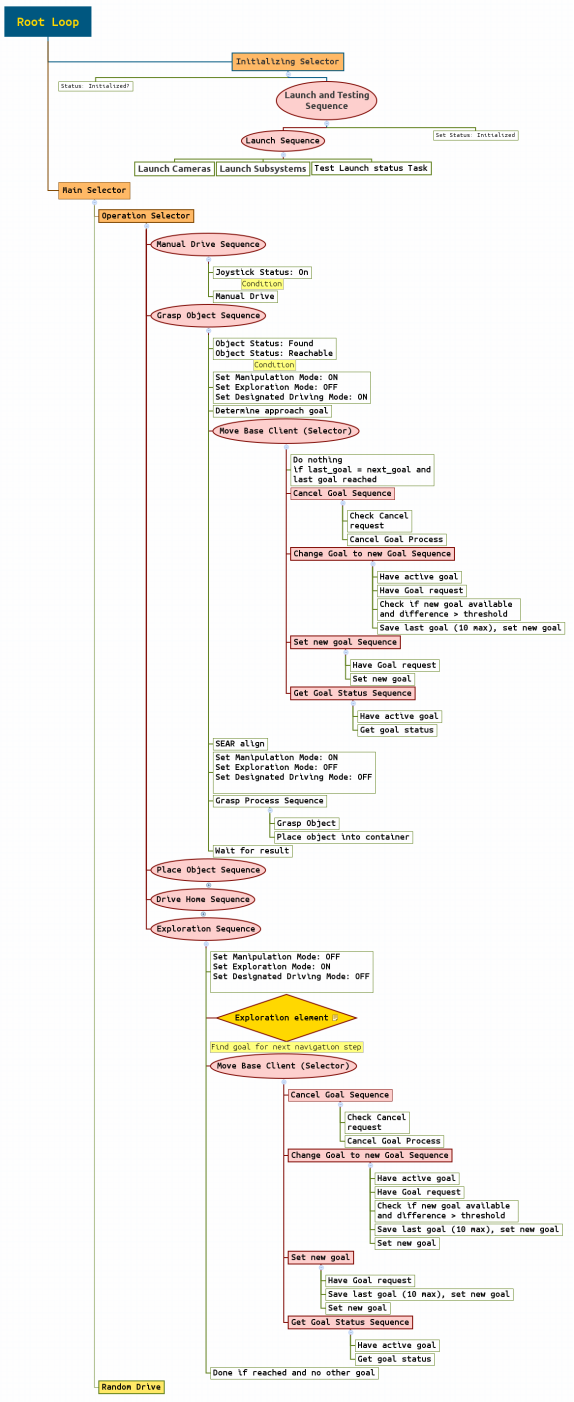


Figure 15. SEAR behaviour tree

5. CONCLUSION

It was shown that specific topics of planetary robotics can be researched on a terrestrial system. The SEAR rover has not only to be proven to be an excellent educational platform, but also to offer possibilities of simulating a planetary mission under defined conditions.

The result of this research project is a system which is able to autonomously explore its environment, and to locate and grasp specific objects. The operation concept has shown to be reliable and appropriate for this scenario.

Future work will focus on extending the autonomy system of SEAR and expand its capabilities. It is also planned to integrate satellite hardware into the system and thus slowly converting the rover to an actual space system.

ACKNOWLEDGMENT

The SEAR project is funded by the German Aerospace Center (DLR) with funds from the Federal Ministry of Economics and Technology (BMWi) on the basis of a decision of the German Bundestag (Grant No.: 50RA1314; Grant No.: 50RA1420).

REFERENCES

1. DLR SpaceBot Cup robot race on artificial planet. 13 November 2013. Press release of the German Aerospace Center. [Online] http://www.dlr.de/dlr/presse/en/desktopdefault.aspx/tabid-10308/471_read-8688/year-2013/#/gallery/12905
2. DLR-"SpaceBot Cup" geht in die heie Phase. 15 March 2013. Press release of the German Aerospace Center. [Online] http://www.dlr.de/dlr/presse/desktopdefault.aspx/tabid-10308/471_read-6551/year-all/#/gallery/9146
3. ASUS Xtion PRO.[Online] https://www.asus.com/3D-Sensor/Xtion_PRO/
4. The Robot Operating System. [Online] http://www.ros.org/
5. Fahrwerkansteuerung und -simulation von planetarem Rover SEAR. Hadi Albalkhi. November 8 2014.
6. ROS wiki entry: Master [Online] http://wiki.ros.org/Master
7. Kommunikation der Softwarekomponenten beim Small Exploration Assistant Rover (SEAR). Sascha Kapitola. November 6 2014.
8. Autonomy for Mars Rovers: Past, Present, and Future. Max Bajracharya, Mark W. Maimone, and Daniel Helmick. 2008. [Online] http://users.etown.edu/w/wunderjt/ITALY_2009/PUBLICATION_MARS_SPIRIT_ALL_PATH_PLANNING_JPL.pdf
9. Over-the-Horizon, Autonomous Navigation for Planetary Exploration. Ioannis Rekleitis, Jean-Luc Bedwani, and Erick Dupuis. 2007. [Online] http://cim.mcgill.ca/~yiannis/Publications/IROS_2007.pdf
10. Image by: Christopher-Eyk Hrabia
11. Behavior Trees for Hierarchical RTS AI. Stephan Delmer. [Online] https://www.smu.edu/~/media/Site/guildhall/Documents/Theses/Delmer_Stephan_Thesis_Final.ashx?la=en

BALLOON PLATFORM FOR HIGH ALTITUDE RESEARCH

Bence Dávid Góczán [(1)], Levente Pápay [(1)], Márk Németh [(1)], Patrik Bélteky [(1)]

[(1)]Simonyi Károly College for Advanced Studies at BUDAPEST UNIVERSITY OF TECHNOLOGY AND ECONOMICS (BME), Budapest, HUNGARY
Email: goczan.bence@simonyi.bme.hu, papay.levente@simonyi.bme.hu, nemeth.mark@simonyi.bme.hu, belteky.patrik@simonyi.bme.hu

ABSTRACT

The upper atmosphere continues to be an area of significant interest to the scientific community. The most cost-effective way to reach the stratosphere is using a high altitude balloon. Developing a reliable telemetry unit for balloon flight could take a lot of time and engineering resources which university projects and small research groups usually do not possess.
Commercial tracking devices could be used, but often they just don't meet the requirements of a science project. Another solution could be participating in organized balloon flights (i.e. BEXUS [1]). These kinds of programs are not so frequent and the costs of the flight and the selection process are not always affordable for smaller (student) research groups.
This paper describes our solution of an affordable balloon platform for high altitude research.

1. INTRODUCTION

Our team of university students is working on a modular, reliable balloon platform for high altitude research. Our goal is to develop an easily configurable and expendable flight computer that provides telemetry data and manages the science payload. Also we are working on a ground station with an automated radio station and a mission control room.
The Reusable High Altitude Balloon (ReHAB) probe is designed to be a service module for various balloon missions while only minimal maintenance is needed between flights. The purpose of the ReHAB module is to ensuring access for smaller university research groups into the stratosphere. Beside the technological infrastructure our team is also able to provide payload testing, flight planning, launch and mission control and recovery services.
This document is covering the operational environment requirements and development objectives in section two. Section three is presenting the detailed system design of the sub-modules. The current version of the system is briefed in section four. Section five and six are about testing and upcoming development plans.

2. OBJECTIVES AND SYSTEM REQUIREMENTS

The main objective of ReHAB program is to deliver up to 3kg science payload to an altitude of 25000 meters or above.
The ReHAB module should be able to monitor and control the science payload. There should be an option for visual feedback of the science payload via still images or video stream (i.e. TV camera downlink or integrated still image camera).
The service module should provide the telemetry and house-keeping data during flight for live tracking and system management.
The flight team also provides various services:

- Third party science payload testing and qualifying for high altitude flights
- Mission planning: flight plan, paperwork, launch planning, recovery planning
- Launch site equipment and launch operations
- Mission control: radio station management, mission control operators, flight management
- Recovery: tracking and recovering the balloon
- Cooperation in post flight data analysis

The planned flights are on between 25000 and 35000 meters altitude. In near space environment the module faces with low temperature, low pressure and increased radiation. The electronics should be designed and properly protected against these conditions.
The lowest temperature is in the tropopause layer of the atmosphere and it can reach -56°C according to NASA Atmospheric Model [2]. In these conditions a proper insulation and heating system should be designed for the service module and the scientific payload to protect the electronic sub-systems and increase battery life.
In the stratosphere air pressure could drop 1/100 of the surface pressure. The service module has in an unpressurized capsule so the electronic and mechanical components should be qualified to operate in such low air pressure conditions.
Sun radiation (heat and UV radiation) increases during ascent. Effects of heat radiation could be decreased by an MLI insulation coat. UV redundant electronic components should be selected or should be shielded. Mechanical components (i.e. 3D printed parts) should be properly surface treated against UV aging.
Third party science payloads should be tested and qualified for these conditions prior flight.

3. SYSTEM DESIGN

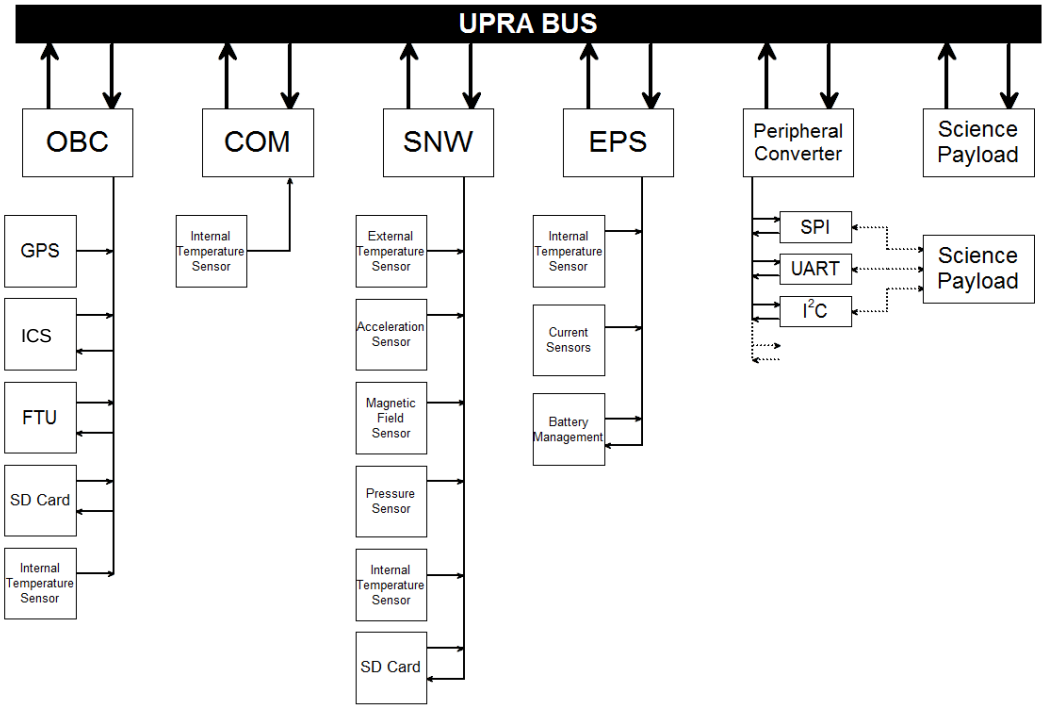


Figure 1. Block diagram of the UPRA flight computer

The telemetry system is the modular UPRA flight computer designed by our team. The modules connect via an internal system bus which based on CAN-BUS. CAN is selected because of its reliable properties. Standard CAN lines are expanded with a BUS_BUSY line as an extra indicator for large dada flow (e.g. pictures).

The modules are realized on a small, 70x75mm PCB with stackable 40 pin connector (UPRA Standard on Fig.2.). Each module has their own diagnostics and programming lines connected to the 40 pin connector for easy access after integration. That helps testing and debugging without the disassembly of the flight computer.

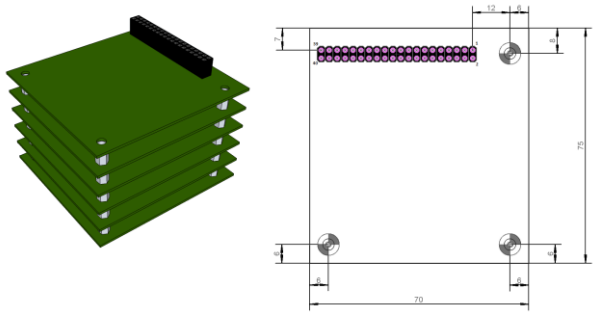


Figure 2. UPRA Standard

3.1. On-Board Computer (OBC)

The functions of the On-Board Computer are to synchronize the sub-modules and overview the execution of the flight plan. During the mission it processes and logs the telemetry and house-keeping data, manages the GPS module, communicates with the sub-modules via the System Bus and manages the scientific payload and cameras.

The OBC is based on an STM32F4 AMR cortex microcontroller which was chosen by its wide variety of integrated peripherals: CAN, UART, DCMI, SDIO, RTC, ADC, temperature sensor.

The system time is provided by the Real Time Clock (RTC) of the STM controller. RTC is used to synchronize the automated functions and to follow the flight plan. The system time is also used to label the pictures taken by the integrated camera and the data stored in the system log.

The GPS module connected to the OBC via UART port and communicates with NMEA protocol. We use $GPGGA message to get geo coordinates and altitude. The timestamp from the NMEA messages is used to synchronize the system time which tend to slip due to the temperature drop during flight.

House-keeping data (HK) is gathered from the other modules via the system bus. HK contains the module temperatures, bus voltage, battery voltage, current consumption and module status words. OBC gets its module temperature from the integrated temperature sensor of the STM microcontroller.

The processed telemetry and house-keeping data is used to create various radio communication packages for real time tracking and stored in the system log.

The OBC has an SD Card slot and accept memory cards up to 2GB storage size. OBC can manage FAT

filesystem that provides easy access to the flight data during post flight analysis.
In normal operation mode the OBC collects the house-keeping data, reads the GPS module, stores the processed data on the SD card and sends the telemetry data via radio. Taking pictures with the integrated camera is less frequent, but still part of the normal operation mode.
If a control command is received the OBC change to 'Control' mode and execute the control command. During 'Control' mode the normal operation is suspended.
In picture download mode the OBC reads the last picture from the SD card and sends it to the COM as radio packets. During picture download the normal operation is suspended.
Beacon mode is activated when the balloon reaches 500m altitude during descent. In this mode the OBC only reads the GPS module and sends telemetry packets to the COM in two second periods. This helps the recovery team to find the probe after landing. Beacon mode can switch back to normal operation mode if the altitude is over 500m again or a control command sent by the mission control operators.

3.2. Integrated Camera System (ICS)

A modified STM32DIS-CAM module is used as the Integrated Camera System. This off the shelf module has been supplemented with an oscillator circuit to be able to operate on its own and connected to the OBC via DCMI port.



Figure 3. STM32DIS-CAM

The module is able to work with both OV9655 [3] and OV2640 [4] camera chip. OV2640 is preferred because of its better resolution and native JPEG output.
Both camera chips are configured via the two-wire Serial Camera Control Bus (SCCB). SCCB provides access to the controlling registers. The camera can be reconfigured during flight with control commands sent from by mission control. This provides the capability to use the correct settings to take a proper image. Also this allows taking high resolution pictures for post flight analysis and low resolution images for radio download.
The image data is sent via the Digital Video Port which is a 10-bit parallel connection to the OBC. The current design only uses 8-bit connection mode, which can be configured via SCCB.
OV9655 has a maximum resolution of 1280x1024 pixels. It has no integrated image compressor unit which means proper amount of RAM is needed to process maximum resolution images.
OV2640 has a maximum resolution of 1600x1200 pixels. The chip has integrated image compressing coprocessor with JPEG output. This means smaller temporary storage space can be used for image capture.
Both camera chips equipped with a lens that has 65° field of view. The camera mount is designed to be able to accept different extra lenses. The current configuration is equipped with a 180° FOV fish-eye lens.
Images taken by the ICS are stored on the SD card of the OBC. The name of the image files contains the time when the picture is taken to help post flight analysis.

3.3. Communication Module (COM)

The Communication Module is designed around an SI4461 FSK transceiver integrated circuit produced by Silicon Laboratories. The module is configured to meet the standards of HAM radios so the balloon can be tracked by amateur radio operators. The transmit frequency is set in the ISM range near the 70cm band to meet the European amateur radio standards. For the telemetry transmission we use 625bps data rate and 625 kHz deviation. To increase the spectral efficiency, Gaussian FSK modulation is used. Since the communication is done via an additive noisy channel, it is necessary to filter out the erroneous packets, so they are supplemented with CRC error code.
For larger data flow (e.g. pictures or scientific data) the module can be configured to high speed transmission.
Due to the continuous change of the probe orientation the antenna should broadcast in all directions as far as possible. Thus, a monopole antenna is connected the probe. Because, according to the ISM standard limited radiated power, the resulting SLOS is compensated by the antenna unit of ground station.
64-byte data packages are used for radio communication. Different packet structures are used for designated message types.
Real time tracking packages are formed to meet the standards of UKHAS message structure [5] which is widely used among European amateur balloon operators. Using UKHAS message format can provide easy trackability as multiple ground stations can be configured operated by the members of the amateur radio community.
For house-keeping data and large data flow we use our own packet structure since these data should only be managed by the qualified operators of the mission.
The COM is also preprocess the control commands from the GND and generates an internal message to alert the OBC about the incoming radio message.

Module temperature of the COM is measured by the internal temperature sensor of SI4461 and is sent to the OBC via internal system bus as house-keeping data.

3.4. Sensor Network (SNW)

The Sensor Network module collects the environmental data of the balloon: external temperature, pressure, inertial data, and also manages the house-keeping sensor data of a third party science payload.
The SNW is designed around an STM32F3 ARM microcontroller which was chosen by its wide variety of integrated peripherals: CAN, UART, SPI, I^2C, SDIO, RTC, ADC, temperature sensor.
The integrated Real Time Clock (RTC) provides the module time which is regularly synchronized to the system clock of OBC. RTC is used to synchronize the SNW functions and provides the timestamp of the raw sensor data stored on the module's own SD Card.
Inertial sensors, accelerometer and magnetic field sensor are connected to the controller via I^2C. Inertial sensors are used to read orientation data of the probe which can be used in post flight data clarification: picture processing, directional sensor data analysis, probe trajectory analysis.
Pressure sensor is also connected via I^2C bus and the data can be used to determine altitude more accurate.
External temperature is measured by a PT100 sensor connected to the microcontrollers A/D converter (ADC).
The module temperature is measured by the internal sensor of the microcontroller also is connected to the ADC and is sent to the OBC via internal system bus as house-keeping data.
Additional ADC, SPI, UART and I^2C lines are available for connecting extra sensors which can be used to monitor third party science payload environmental conditions or extra sensors for smaller missions.

3.5. Electric Power System (EPS)

The Electric Power System provides the proper bus voltage for each module and monitors the power consumption and battery level.
The EPS is built around a switching power supply circuit configured to provide stable 3.3V voltage for the subsystems. Each module has its own power line which makes every subsystem being monitored individually.
EPS has an STMF3 microcontroller that collects the current consumption of the modules, shuts malfunctioned subsystems down and sends the data to the OBC via system bus.
The module uses ADM4073 Current-Sense Amplifier IC for current measuring. If the circuit detects overcurrent on any module it can shut it down automatically. The microcontroller then tries to restart the module. If overcurrent detected again the module is shut down permanently.
Battery level and temperature is also monitored by the EPS. If the battery level drops under dangerous level most of the subsystems are shut down. Only the OBC and the COM module would be kept alive in power saving mode. If the battery temperature drops to dangerous level battery heating would be turn on until it stabiles the temperature.
Three AA dry cell batteries are used as power source. The batteries are placed in some extra insulation to increase efficiency in cold temperatures.

3.6. Structure (STRU)

A plastic frame is designed with 3D printable parts to secure the electronics, antenna and insulation. The frame has a 1U CubeSat form factor as a proof of concept for further development. Also the 1U CubeSat has a desirably small size. By reducing the weight of ReHAB module the flight became more efficient: less gas or smaller balloon would be enough to reach the desired flight altitude or more science payload can be attached to the balloon during missions.

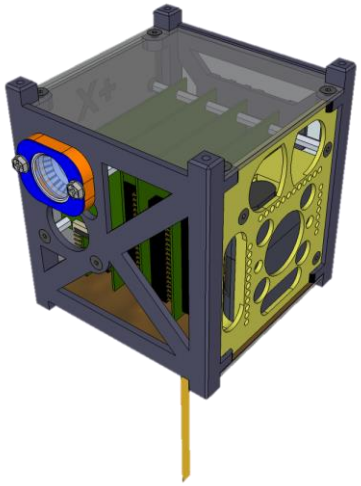


Figure 4. 1U CubeSat STRU CAD plan

The 1U CubeSat frame is placed in a Styrofoam insulation box with 20mm wall-thickness. This Styrofoam box is the primary thermal insulation for the ReHAB module.

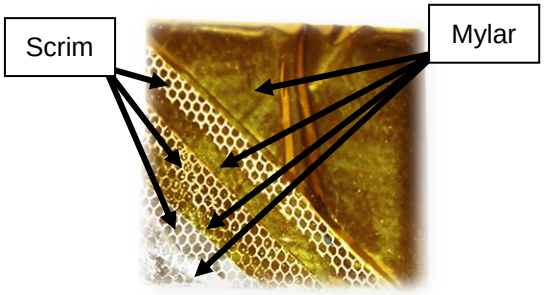


Figure 5. Cross-section of the MLI

The secondary insulation is a four layer MLI coating produced from Mylar and scrim with adhesive

technology in our workshop. The hatch area of the MLI coat is secured with Velcro stripes. This two level insulation system provides a suitable temperature for the electronics without additional heating system.

3.7. Ground Station (GND)

Our Ground Station consists of two parts: the automated radio station and the mission control room. The GND is under development right now. Until it is not in service we use the *Satellite Tracking Station* of Budapest University of Technology and Economics (BME-GND) [6]

Automated Radio Station (ARS)

The ARS is designed to operate in the 430-440 MHz band as we use amateur radio frequencies for balloon tracking. The controller computer is a Raspberry Pi single card Linux based computer [7]. The radio transceiver is based on an SI4464 FSK transceiver integrated circuit produced by Silicon Laboratories and connected to the Raspberry Pi via SPI port. The controller computer is connecting to the internet/local intranet through Ethernet and can be remote controlled from different locations.
The tasks of the controller computer:

- Controlling the radio transceiver: Mode switch to high speed transmission for large data flow (e.g. picture download) or low speed transmission for telemetry and commanding.
- Telemetry data processing: reception, demodulation, CRC check, data storing and Ethernet-based digital data transmission to the mission control server.
- Controlling the antenna rotator: developed for later infrastructural upgrades of the antenna system.
- Balloon path prediction for the antenna rotator using the current telemetry data and pre-flight simulation data.

The antenna system is placed on the top of *Schönherz Zoltán Student Hostel* of Budapest University of Technology and Economics (SCH-BME). It is a 19 stories high building located in the urban area of Budapest. Right now an Omni-directional antenna is mounted which according to our tests meets our mission requirements.
The radio station will be placed at the service room of the *HA5KFU University HAM Radio Club* [8] which is located at the 19th floor of SCH-BME. The room has an Ethernet connection with optical link to the computer network of the building. The optical link is needed to fulfill lightning protection regulations.

Mission Control Room (MC)

Mission Control is also located in SCH-BME. For smaller missions the MC is built up in the *Robotics and Embedded Systems Lab* with maximum four work station (projector is optional). For more complex missions the *Computer Room* is available with up to fifteen workstations and a projector. Both places are under the supervision of *Simonyi Károly College for Advanced Studies* [9]. The mission control server is hosted by the *Computer Science Department* of SCH-BME.
For tracking and mission control a web based application is used. The flight and science data is stored on the mission control server. Each workstation can download and display the necessary information they need.
Central display is showing the route, geo-coordinates and the altitude of the balloon. This information is also available for the public on our website with the latest downloaded image added.
The Radio Workstation is monitoring the ARS via direct contact and managing the controlling commands sent to the balloon.
The Telemetry Workstation is monitoring the route and altitude of the balloon. The operator is compares the various simulation data with the live telemetry and meteorological information.
The House-keeping Workstation is monitoring the environmental data and probe life-signs. The operator is reporting the changes of sub-module status, internal temperature, battery level and other crucial information.
The Science Workstations are operating the science payload. The operators are in contact with the science team and developing the flight plan prior launch.

3.8. Other modules

There are additional modules under development to expand the abilities of the main telemetry system. These modules are the Flight Termination Unit (FTU), Advanced External Camera System (AECS), Interface Module (IM) and an Offline Backup Module (OBM).

Flight Termination Unit (FTU)

This module is placed outside the probe, its purpose is to cut the tether of the balloon and/or destroy the balloon itself. Since we use latex balloons the envelope is not needed to be destroy, it is enough to cut off the payload. The FTU should be able to recognize if the cut was not successful and signal to the OBC. In the current blueprints we use Nichrome wire to cut and optogates to measure the presence of the cord.

Advanced External Camera System (AECS)

This module can be used to connect high definition offline cameras to the payload. These could be compact or professional third party cameras with external control port (data port or external shutter connection). The AECS connects to the telemetry system via the UPRA system bus and generates control messages (e.g. Canon CHDK) or simulate pushbuttons for external shutter release.

Interface Module (IM)

Interface Module would allow third party (science) payload to be connected to the telemetry system. The IM has an UPRA system bus connection to the flight computer, several communication ports (I^2C, UART, SPI) and GPIO ports to the payload. This module is needed if the science payload didn't designed to be connected to UPRA telemetry, but is needed to be controlled through the flight (e.g. sending back measurement data, receiving commands, automated/timed functions should be generated by flight computer)

Offline Backup Module (OBM)

This module is placed and connected to the payload train in a smaller capsule. Its purpose is to serve as a backup beacon in total system failure making the recovery possible. Also it is planned when water landing occurs this capsule serves as a floating beacon. It has a commercial GPS-GSM tracker with a SIM card and as response for a call it sends back its current geo-coordinates. It is also able to record the flight path under 18km altitude.

4. CURRENT VERSION OF THE PLATFORM

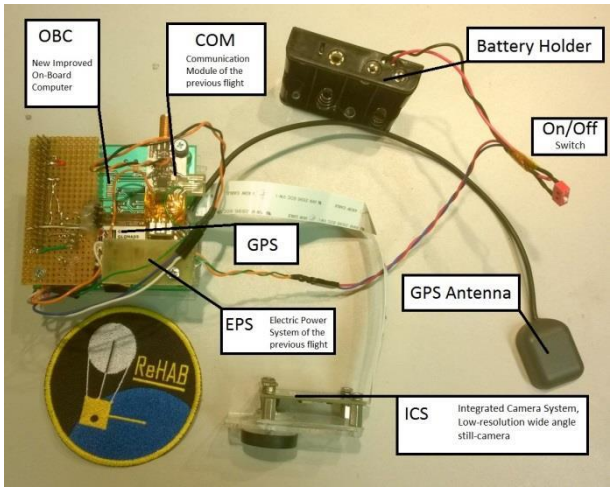


Figure 6. ReHAB-150 ver.1.x telemetry system

4.1. OBC v1.5

- STM32F407VGT6 32-bit ARM Cortex-M4F microcontroller, 1 MB Flash, 192 KB RAM, TQFP100 package
- System Clock: Real Time Clock (RTC)
- ADC + internal temperature sensor
- GPS port (UART RX only)
- CAN controller + CAN transceiver
- DCMI port for integrated camera control (30pin FFC/FCP)
- Micro SD-card slot (SDIO)
- Diagnostic port (UART)
- ECS port (2pin GPIO)
- 2×20 pin stackable UPRA-BUS connector

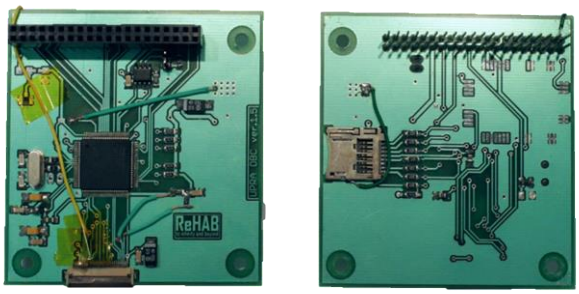


Figure 7. OBC ver.1.5 flight version

In ReHAB-150 v1.x the COM module was connected to the OBC via the diagnostic UART port. Two GPIO pins are used to connect third party camera (ECS). A modified Polaroid PDC 3070 digital camera is used as an external camera for taking high resolution images. The ECS controlled by the OBC but it has its own power source (four AAA batteries). The frame rate of the camera depends on the altitude. In higher altitudes pictures are taken more frequent.
For geo-tracking an NV08C-CSM GPS module is used. This model can operate up to 50km altitude by default configuration. The GPS is connected to the OBC via UART, but only the RX line was used since the module run on factory configurations. For better performance an external antenna is connected to the GPS module.



Figure 8. GPS module of ReHAB-150 ver.1.x

4.2. ICS v1.0

- OV9655 1.3 megapixel CMOS camera chip
- 24kHz oscillator
- 1.8V step down voltage converter
- 3.3V voltage regulator
- 30pin FFC/FPC DCMI connector

A modified STM32DIS-CAM module is used as the Integrated Camera System. This off the shelf module has been supplemented with an oscillator circuit to be able to operate on its own and connected to the OBC via DCMI port.
The OV9655 is configured to take RGB-555 images in 320x196 pixel resolution. The small resolution is due to the limited RAM capacity of the OBC v1.5.



Figure 9. Test image taken by the ICS v1.0

As the OV9655 chip camera has 65° field of view (FOV) it has been equipped with a 180° FOV fisheye lens in a configuration seen on Fig.10.

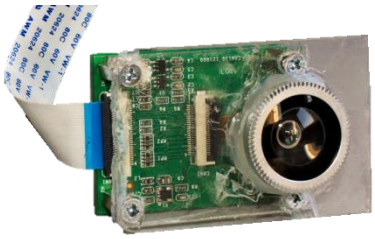


Figure 10. ICS v1.0 with fisheye lens

4.3. COM v0.1 (proto)

- SI4461 FSK transceiver
- C8051F326 microcontroller
- SMA antenna connector
- UART port

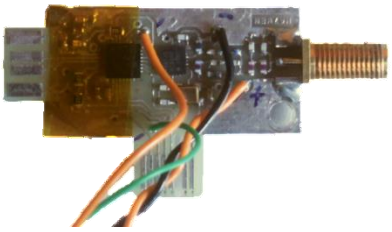


Figure 11. COM v0.1 proto

In ReHAB-150 v1.x module the prototype of the COM is used. COM v0.1 is a heavily modified version of a development circuit originally designed for a course of *Department of Broadband Infocommunications and Electromagnetic Theory* of Budapest University of Technology and Economics (BME HVT). Hardware changes were implemented to connect the module to the OBC via UART. The firmware is completely designed by the UPRA team for UPRA/ReHAB missions.

4.4. SNW v1.0 (development version)

- PIC24HJ128GP504 microcontroller
- CAN controller + CAN transceiver
- MAG3110 3-Axis Digital Magnetometer Sensor
- MPU6050 3-Axis Accelerometer
- Micro SD-card slot (SPI)
- Diagnostic port (UART)

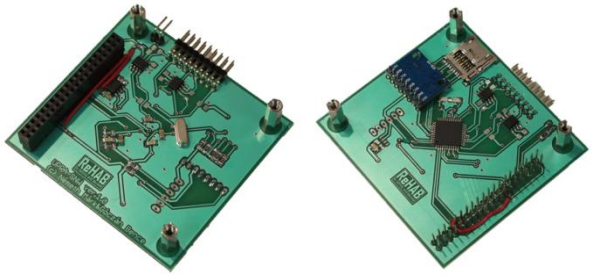


Figure 12. SNW v1.0 dev

This version of the SNW has never reached flight readiness due to development issues. The PIC24HJ128GP504 controller has some issues with its SPI and CAN peripheral which we couldn't overcome during firmware development. Due to these setbacks the further development with PIC24HJ128 controller was suspended and new microcontroller family was chosen.

4.5. EPS v0.1 (proto)

The power supply module is a simple switching step down converter with no monitoring functions. Its only purpose is to provide stable 3.3V voltage for the electronics.



Figure 13. EPS v0.1 proto

Three AA dry cell batteries are used as power source. The batteries are placed in some extra insulation to increase efficiency in cold temperatures.

4.6. STRU v1.1

The current version of the ReHAB capsule has an aluminum frame for support. The frame makes a 150x150x150mm cube with four support rings for the parachute cord.
For thermal insulation 20mm thick Styrofoam panels are used. Inside the thermal capsule there is 110x110x110mm space for the electronics. The capsule also has a four layer MLI insulation coat produced from Mylar and scrim with adhesive technology in our workshop.



Figure 14. Styrofoam insulation and MLI coat

The antenna is secured on the bottom (Z-) side of the fully assembled capsule. The antenna is made of measuring tape and precisely calibrated for the 70cm band we use for radio communication.

4.7. Ground station

While our ground station is under development we use the *Satellite Tracking Station* of Budapest University of Technology and Economics (BME-GND [6]). The station was primary designed for the tracking of MASAT-1 CubeSat, but also able to track other satellites and high altitude balloons.
The station is controlled by a Raspberry PI microcomputer that manages the automatic antenna rotator and the radio transceiver. Raspberry PI is connected to the mission control room via Ethernet and can be configured from any remote location with an internet connection.



Figure 15. Polarized antenna of BME-GND

For balloon tracking the station uses rotary cross-Yagi antenna system on Fig.15. In order to avoid cross-attenuation they were used in circularly polarized mode.

5. TESTS AND ANALYSIS

Our team had two test-flights and intensive bench testing during development. The first test-flight was performed with an early development prototype which was a one flight mockup of the system. Since then the testing is ongoing with ReHAB-150 ver.1.x system described in the previous section.

5.1. ReHAB 150 proto test-flight

The test-flight was performed at XI. Simonyi Károly Conference in cooperation with MASAT-1 team. The prototype of the telemetry system was used in this test. As ground station and mission control BME-GND [6] station was used.

Mission objectives:
- Perform a balloon launch
- Collect telemetry data
- Stream back telemetry data and live tracking
- Send control commands to the probe
- Take pictures with the ICS
- Download images via radio
- Recovering the probe

The test went according to plans until T+0:30:15. Due to a software error the telemetry system switched to Beacon Mode and started streaming only the last coordinates. At T+0:40:33 due to a GPS malfunction and another software issue communication was lost with balloon. Mission control operators continued to calculate the landing site according to simulations and meteorological information until T+2:10:00. A recovery team searched the predicted landing area without success. The probe claimed lost at T+5:00:00.
The probe was found and recovered by civilian reporting. The landing site was about 30kms off course.
Post flight analysis revealed several issues in the embedded software including altitude processing errors and watchdog and timeout configuration errors.
Data logging, image capturing and radio communication methods proved to be working.
Using the collected data the flight software was improved, GPS hardware was reassembled and retested in the further development of the telemetry system.

Lessons learned:
- GPS simulation test environment should be assembled for telemetry data processing tests
- Long-term operation tests shuld be performed before flight
- Backup tracking system shuld be implemented

5.2. ReHAB 150 ver.1.0 test-flight

The test-flight performed as an entry for *Global Space Balloon Challenge 2015* (GSBC) [10]. ReHAB 150 ver.1.0 was used in the test and the ground station was BME-GND. The system was expanded with a GSM based backup tracking system.

Mission objectives:
- Perform a balloon launch
- Collect telemetry data
- Stream back telemetry data and live tracking
- Send control commands to the probe
- Take pictures with the ICS
- Download images via radio
- Recovering the probe

The communication was lost at T+0:5:32 shortly after launch due to a software error and the mission control switched to emergency tracking operations. The balloon was tracked based on the data of the backup tracking system. At T+3:34:12 mission control received a landing signal and the recovery team took off. Thanks to the backup tracking system the probe was recovered by the team about 60kms off course.
Post flight analysis revealed further issues with the watchdog configurations. Pre-flight integration tests didn't reveal this type of error. Data logging and image collection worked fine until the system malfunction.
The large drift of the flight trajectory was caused by a cold front reached the airspace in mid-flight.

Lessons learned:
- Pre-flight tests shuld be extended and improved
- Launch window management and launch date selection shuld be improved
- Mid-flight simulations and meteorological data analysis shuld be improved
- Recovery trainings shuld be performed to improve the work of the Recovery Team

5.3. COM module test

A long range radio communication test was performed before the first test-flight in cooperation with MASAT-1 team. Balloon probe was secured on top of a fifty meters high antenna tower 10kms away from the radio station. The ground station was controlled remotely from the test tower.

Test objectives:
- Stream telemetry data
- Send control commands to the probe
- Download images via radio

The COM module performed as expected during test. All objectives passed, the COM hardware, embedded software and ground station software was certified flight ready.

5.4. Telemetry data processing test

GPS module was substituted with a PC interface for this test. NMEA message flow was generated from various simulation data and sent to the telemetry system via UART port.

Test objectives:
- Simulate high altitude GPS data
- Simulate GPS signal loss
- Process and log telemetry data on-board
- Stream telemetry data via radio

First tests revealed issues in altitude depending functions which have been fixed.
In the latest tests telemetry system performed as expected and telemetry processing methods was certified flight ready.

5.5. Environmental tests

Low temperature performance was tested since the team only had access to a cooling chamber so far. Individual sub-systems and the integrated telemetry system were placed to a -25°C environment without insulation for the minimum of three hours.

Test objectives:
- Monitoring system functions in low temperature environment

Test results:
- Clock synchronization passed
- Module temperature measurement passed
- Radio communication passed
- Data storage passed

5.6. Long-term operation test

For long-term operation test an Arduino [11] based automated test-radio station was used. The test station logged the received data and periodically sent controlling commands to the telemetry system.

Test objectives:
- Test long-term operation stability without operator interaction
- Test watchdog and timeout configurations
- Test on-board storage capacity and reliability

Different time periods were set for tests from typical flight length to five days of continuous operation.
Sending poorly synchronized controlling commands can lead to a COM module stop. In these cases COM and OBC perform a synchronized restart. Both modules continue operation as expected.
Synchronizing radio uplink messages by radio operator or automatic algorithms could prevent restarts and increase operation stability. Current watchdog and timeout configurations proved to be able to prevent full system shutdowns. On-board storage capacity and reliability fulfilled the calculated requirements.
According to the tests ReHAB 150 ver.1.1 was certified flight ready.

6. FUTURE DEVELOPMENT

Next step in the development is to deploy our own ground station. The automated radio station is close to production and the web based mission control application is already in development. We have already installed and tested the antenna system.

The aluminum frame of the probe will be replaced with a 3D printed CubeSat sized plastic frame. CAD planning has already been finished. Right now the selection of the constructor is in progress.

Development of the new EPS is passed hardware component selection state. Right now schematic and PCB design is in progress.

The new COM and SNW modules are in an early development stage. We would like to flight-test at least one of these modules in summer of 2016.

In the future we are planning to organize trainings for the mission control operators, launch crew and recovery team.

After some test-flights in spring, 2016 we would like to start the scientific work in cooperation with university research groups. Our plan is to establish a schedule for regular flights with open payload capacity for various university research projects.

7. REFERENCES

[1] "REXUS/BEXUS – Rocket and Balloon Experiments for University Students," [Online]. Available: http://rexusbexus.net/. [Accessed 10. 11. 2015.].

[2] NASA, "Earth Atmospheric Model (Metric)," [Online]. Available: https://www.grc.nasa.gov/www/k-12/airplane/atmosmet.html. [Accessed 10. 11. 2015.].

[3] OMNIVISION, "OV9655/OV9155 Datasheet," OmniVision Technologies, Inc., 1341 Orleans Drive Sunnyvale, CA USA, 2006.

[4] OMNIVISION, "OV2640 Datasheet," OmniVision Technologies, Inc., 1341 Orleans Drive Sunnyvale, CA USA, 2006.

[5] "UKHAS Communications Protocol," [Online]. Available: https://ukhas.org.uk/communication:protocol. [Accessed 10. 11. 2015.].

[6] "BME-GND Home," [Online]. Available: http://gnd.bme.hu/. [Accessed 10. 11. 2015.].

[7] "Raspberry Pi Home," [Online]. Available: https://www.raspberrypi.org/. [Accessed 10. 11. 2015.].

[8] "HA5KFU," [Online]. Available: http://ha5kfu.sch.bme.hu/. [Accessed 10. 11. 2015.].

[9] "Simonyi Károly Szakkollégium Weblapja," [Online]. Available: http://simonyi.bme.hu/. [Accessed 10. 11. 2015.].

[10] "Global Space Balloon Challenge 2015," [Online]. Available: https://balloonchallenge.org/. [Accessed 10. 11. 2015.].

[11] "Arduino Home," [Online]. Available: https://www.arduino.cc/. [Accessed 10. 11. 2015.].

ARCADE EXPERIMENT ON BOARD BEXUS 13 AND 17: DESIGN, INTEGRATION AND FLIGHT OF A TECHNOLOGY TEST PLATFORM WITHIN A STUDENT BALLOON PROGRAMME

Marco Barbetta[(1)], Francesco Branz[(2)], Andrea Carron[(3)], Lorenzo Olivieri[(2)], Francesco Sansone[(4)], Livia Savioli[(4)], Fabio Spinello[(3)], Alessandro Francesconi[(4)]

[(1)] 2045Tech, Via della Croce Rossa, 112 – 35129 Padova, Italy, barbettamarco@gmail.com
[(2)] Centre of Studies and Activities for Space (CISAS) – "G. Colombo", University of Padova, Italy
[(3)] Department of Information Engineering, University of Padova, Italy
[(4)] Department of Industrial Engineering, University of Padova, Italy

ABSTRACT

ARCADE, Autonomous Rendezvous, Control And Docking Experiment, is a technology demonstrator aiming to prove automatic attitude determination and control, rendezvous and docking capabilities for small scale spacecraft and aircraft. The experiment embodies a simplified scenario in which an autonomous vehicle mock-up performs automatic rendezvous and docking operations with a fixed complementary unit. The system features a relative infrared navigation sensor, an attitude control system based on a reaction wheel and a small-scale docking mechanism. Moreover, it is equipped with pressure and temperature sensors, and wind probes to monitor the external environmental conditions.

ARCADE was developed in the framework of REXUS/BEXUS programme, which is a programme for European students resulting from a collaboration between DLR, SNSB and ESA. It allows students to propose an experiment to fly on a stratospheric balloon, face a selection based on many technical and organizational metrics, deal with project reviews, design and integration, and finally with a launch campaign. Arcade flew on board the BEXUS-13 stratospheric Balloon (2011), but due to a critical software failure the experiment was not able to perform the required task; a second selection in the REXUS/BEXUS programme allowed the experiment to fly again on board the BEXUS-17 balloon (2013). During the flight, several navigation-control-docking sequences at different altitudes were performed and environmental data was collected; the latter allowed to estimate the IR sensor accuracy and the different control techniques evaluated various combinations of actuators, algorithms and sensors.

In this paper the design components of ARCADE are described but the main focus will be on the development of the project within the framework of the programme from the preliminary design to the two launches. Result obtained from the second balloon flight are then presented, both from the technical and from the educational point of view.

1. INTRODUCTION

The ARCADE Experiment was born from the idea of four university students of gathering the topics of their master's thesis in a single concept that could be tested in a relevant environment like a stratospheric flight. The common background is the execution of autonomous navigation, attitude control and docking operations between independent small vehicles. Over the last decades, an increasing interest arose about operations based on fleets of small cooperative vehicles. On one hand, miniature satellites (in the micro/nano range) begun to represent effective solutions to improve the execution and the capabilities of new kinds of space missions, including 1) on-orbit automated inspection and servicing of larger satellites, in order to extend their operational lifetime, replace their payloads or perform orbital manoeuvres [1][2]; 2) on-orbit assembly of low-cost large modular spacecraft, that would significantly benefit from standardization and miniaturization of the used modules, as well as from the possibility of launching them as piggybacks [3][4]; 3) debris capture and active removal [5][6]. On the other hand, advanced cooperative Micro Aerial Vehicles (MAVs) are increasingly employed in several atmospheric applications, such as remote observation of hazardous or otherwise unreachable areas, i.e. toxic regions, urban canyons or interior of buildings, and evaluation, rescue and surveillance operations.

The main issue related to the development of these new concepts was represented by the miniaturization of the technologies involved for proximity operations, attitude control and docking between small autonomous vehicles. While they had already been developed for large spacecraft or aerial vehicles, there was still a lack of applicable solutions for miniaturized automatic systems [7]-[10].

In this framework, the idea to develop a technology demonstrator to prove automatic proximity navigation, attitude control and docking between small vehicles was born. The possibility of a balloon flight, offered by the REXUS/BEXUS Programme [11], represented a good opportunity for the students to test the whole experiment in a relevant environment, as well as a

unique opportunity to experience the development of a real space mission.
The project started in December 2010, when the experiment was selected at the selection workshop. Less than one year later, at the end of September, 2011, ARCADE was launched on board BEXUS 13. Unfortunately, it was not possible to perform all the planned test operations because of a critical failure few minutes after the take-off. The experiment was proposed for a second flight two years later and launched again on board BEXUS 17 in 2013. The second launch was successful: several autonomous docking manoeuvres were performed, allowing to test the technologies developed by the students, also in critical conditions, such as very low pressure and temperature.
ARCADE Experiment represent one of the technologies developed at the Centre of Studies and Activities for Space (CISAS) "G. Colombo" - University of Padova, in the wider framework of researches on automatic docking and relative navigation technologies [12][13][14][15][16][17].
The paper is organized as follows: the description of the main subsystems of the ARCADE Experiment is presented in section 2; section 3 is dedicated to the evolution of the experiment, from the concept, through its realization and the final flight configuration. The flight results are presented in section 4 and section 5 is dedicated to an important aspect that characterizes the experience within a REXUS/BEXUS Programme: the lessons learned during the evolution of the activity. They are presented at different levels, from the design of the experiment to the launch campaigns, as well as from team working and organization point of view.

2. ARCADE EXPERIMENT DESCRIPTION

ARCADE aims to test different technologies for aerial and space vehicles navigation, rendezvous and docking in the extreme environmental conditions (low temperature and temperature gradients, low pressure) of a stratospheric flight. The experiment is composed by a small external vehicle (SMAV - SMAll Vehicle) and its parent unit (PROXBOX - PROXimity BOX). The PROXBOX is mounted on the structure lifted by the balloon, which is called gondola, along with all the other experiments sharing the BEXUS flight. The SMAV is supported by an external rigid structure, called STRUT (STRUcTure), and has two degrees of freedom respect to the PROXBOX: a rotational one, around the vertical yaw axis, and a translational one, towards the gondola (Figure 1). As visible in the logic diagram reported in figure two, the SMAV, representing the chaser in the experimental docking scenario, is a fully independent vehicle from the power point of view, with dedicated navigation, control and docking devices and on-board batteries; data processing is however managed by the PROXBOX flight computer.

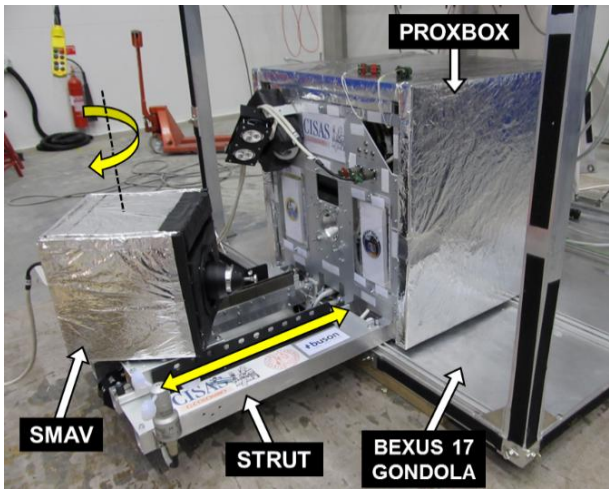


Figure 1. ARCADE main parts: the fixed PROXimity BOX containing the electronics and the support hardware, the independent SMall Aerial Vehicle with its degrees of freedom, and the supporting STRUcTure.

The PROXBOX acts as the target, and contains the docking interface and navigation components, as well as the main battery pack and the on-board computer. It determines the data sampling, receives commands, sends telemetry/data to the ground station, provides data storage and manages all the experiment's devices and sensors.

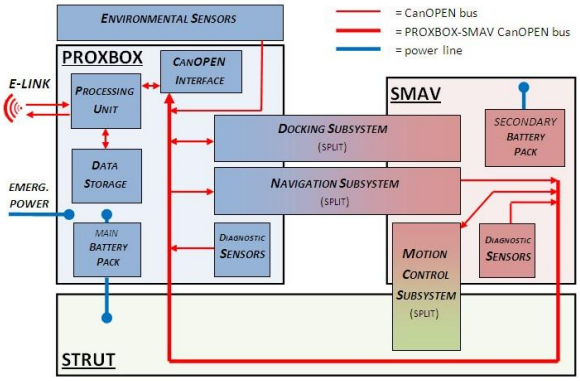


Figure 2. ARCADE top-level logic, showing the main subsystem and power and data lines.

2.1. Docking Mechanism

ARCADE docking mechanism (Figure 3) is a gender-mate, small-scale simplified version of the Russian Soyuz and European ATV one [18]. It is composed by two parts, a conic probe (a) with a magnetic tip (b) fixed on a spring-damper device (c) on the SMAV side, and a drogue with a movable capturing electromagnet (d - for soft docking) and three locking solenoids (f - for hard docking) on the PROXBOX. During soft docking, the mechanical conic shape helps the SMAV to align with the PROXBOX, and the magnetic tip is captured by the drogue electromagnet; residual misalignments up to 5°

are tolerated by this system. To allow the locking solenoids to create the hard docking, the joined bodies are pulled backward by a linear motor (e), reaching the final mated configuration. Last, a spring-mounted disk on the SMAV side (g) is loaded during the procedure, allowing to both create a compressive force that further secures the joint in the "hard docking" configuration and to push away the SMAV during the release phase.

2.2. Attitude Control

The ARCADE-R2 Control Subsystem accomplishes the main task of actively control the yaw movements of the SMAV. A correct attitude is required while approaching the PROXBOX in order to successfully complete the docking manoeuvres, though the docking mechanism was designed to tolerate a maximum misalignment of ±5 deg.

The SMAV rotation can be actuated by two alternative solutions: (1) a custom reaction wheel (RW) on board the SMAV and (2) a brushless DC motor directly connecting the SMAV to the support plate. The first is the nominal actuator for realistic operations, while the second is a backup solution.

For what concerns the motion control software two different techniques are implemented: (1) a state-space control and (2) a simple PID control law. The control algorithms are designed considering the SMAV angular position/velocity and the reaction wheel speed.

To measure the attitude of the systems two options are also implemented in the experiment: (1) the custom IR navigation sensor and (2) an optical encoder coupled with the backup motor. Figure 4 illustrates the forces and torques considered in the model. The differential equation that governs the SMAV angular acceleration is reported in Eq. 1.

$$I\ddot{\vartheta} = mge\left[\sin\alpha\cdot\sin(\psi-\psi_0-\pi)+\sin\beta\cdot\sin\left(\psi+\psi_0-\frac{\pi}{2}\right)\right] + \tau_w - \mu_f\dot{\vartheta} \quad (1)$$

where I is the moment of inertia of the SMAV, m is the mass of the SMAV, g is the gravity acceleration, α is the gondola pitch misalignment, β is the gondola roll misalignment, ψ is the SMAV yaw rotation, ψ_0 is the centre of mass angular position of the SMAV, e is the centre of mass eccentricity, τ_W is the wind disturbance torque, μ_f is the viscous friction coefficient, τ_m is the input torque provided by the reaction wheel. The SMAV dynamic system, Σ_C, was written in continuous state-space form neglecting the disturbances. Given the following specifications:

- rise time t_r = 3 s
- settling time t_s = 4 s
- maximum overshoot m_p = 5%

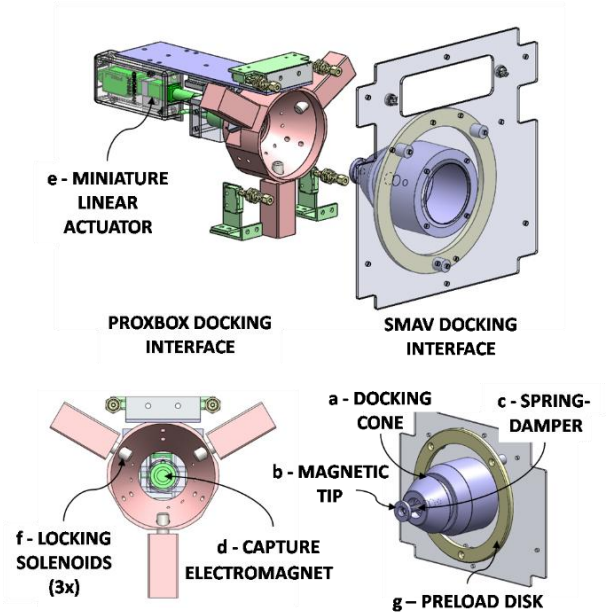


Figure 3. ARCADE docking system: the gender-mate mechanism is composed by two interfaces (the drogue on the PROXBOX, the probe on the SMAV) actuated by miniature linear actuators; three solenoids create the solid joint in hard-docking configuration.

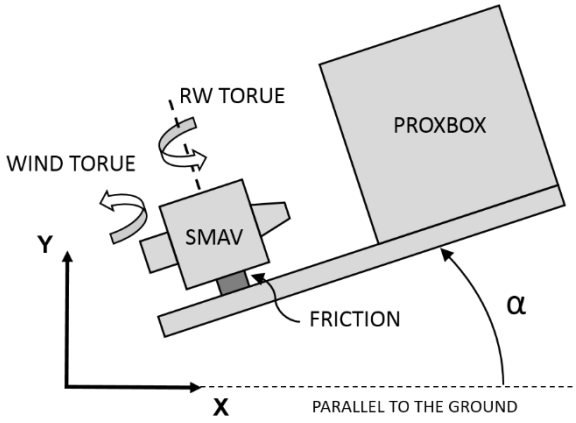


Figure 4. Illustration of the forces and the torques involved in the ARCADE dynamic model.

it is possible to derive the poles for the closed loop continuous system. The system Σ_C can be discretized and the computed poles are converted using the zero-pole matching technique. Finally the loop is closed using the discrete integral control technique where the state is estimated using a standard Luenberger observer. The complete control system scheme is shown in Figure 5.

The second solution for the SMAV motion control is a simple discrete PID. The parallel structure is chosen for its simplicity. The three PID gains, proportional, derivative and integral are computed through analytical computations and then tuned manually.

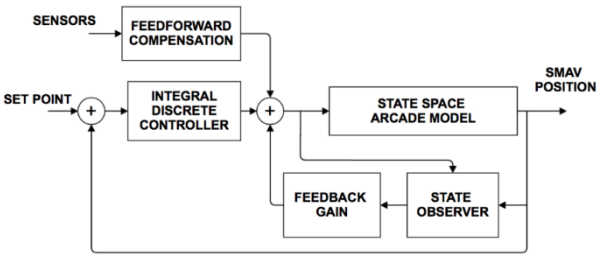


Figure 5. Logic scheme of the state space controller.

2.3. Relative Navigation

The experiment is provided with a custom relative navigation sensor for the determination of the SMAV linear position and yaw rotation, with respect to the PROXBOX docking interface. The sensor design aims at compactness and simplicity, both in terms of hardware components and software computational burden. In particular, the sensor is conceived as an alternative to systems based on image processing or LIDARs [19]-[22].

As a result, the sensor is composed by a beacon infrared LED on-board the PROXBOX and two infrared photodiode receivers mounted on the face of the SMAV containing the docking mechanism (see Figure 6).

The working principle is very simple: the photodiodes output voltages generated by the LED beacon are modulated by the SMAV-PROXBOX relative position and attitude and are measured with high accuracy; then, a dedicated algorithm based on the LED emission model and the experiment geometry determines the SMAV position and attitude relative to the PROXBOX from the measured signals. The distance between the two infrared receivers was set in order to generate a significant difference in the photodiode voltages due to rotation, while keeping them within the emission lobe of the beacon in the whole workspace of the SMAV.

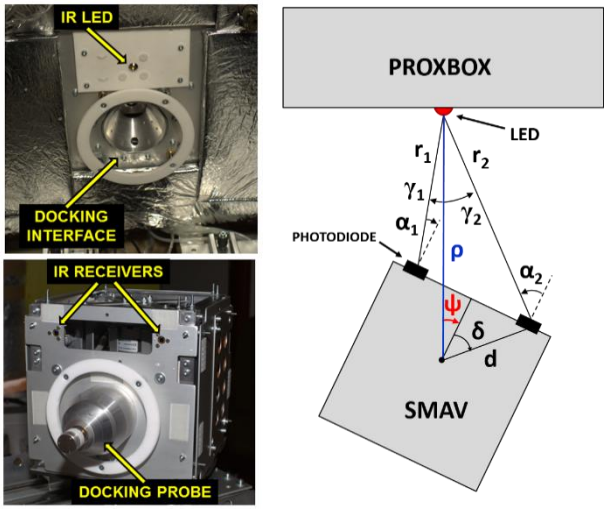


Figure 6. Elements of the IR sensor on the PROXBOX (top left) and on the SMAV (bottom left) and geometrical parameters of the sensor model (right).

The photodiode output voltages V_i (i=1,2) are described in Eq. 2-3; they depend on the power emitted by the LED P_{LED}, the LED-photodiode distance r_i, the photodiode sensitive area A_i, the photodiode photosensitivity k_i, the angle of incidence α_i, the angle γ_i between the LED optical axis and the line joining the LED to the i-th photodiode, and the amplification gain of the receivers conditioning electronics e_i. The term $f(\gamma)$ represents the ratio between the LED radiant intensity (Wsr^{-1}) at a given γ and the radiant intensity at $\gamma = 0$. Both $f(\gamma)$ and $g(r)$ were determined experimentally by fitting the photodiode outputs that were measured during laboratory tests prior the launch campaign. Moreover, the amplification contribution of the acquisition channel of each infrared receiver can be defined as $C_i = P_{LED} A_i k_i e_i$. Such terms are independent from the SMAV position and attitude; however, they are modified by the environment temperature variation, as the latter affects the photodiode sensitivity k and the forward voltage of the LED. For this reason, the C_i parameters are periodically calibrated during test operations. As the translational motion of the SMAV can occur only along the LED central axis direction, the parameters r_i, α_i and γ_i result from simple geometrical relations involving the SMAV distance ρ and yaw rotation ψ relative to the PROXBOX. The values of d and δ are known from the geometry of the SMAV. Thus, it is possible to express V_1 and V_2 as functions of solely the SMAV distance ρ and yaw rotation ψ. The flight software of the experiment exploits a damped-least-square iterative algorithm to determine ρ and ψ from the measured photodiode voltages $V_{1,m}$, $V_{2,m}$.

$$V_1 = P_{LED} A_1 k_1 e_1 f(\gamma_1) g(r_1) \cos\alpha_1 = C_1 f(\gamma_1) g(r_1) \cos\alpha_1 \quad (2)$$

$$V_2 = P_{LED} A_2 k_2 e_2 f(\gamma_2) g(r_2) \cos\alpha_2 = C_2 f(\gamma_2) g(r_2) \cos\alpha_2 \quad (3)$$

From the hardware point of view, particular attention was paid to the rejection of ambient light that could affect the sensor measurements. For this reason, photodiodes with daylight filter are exploited and the beacon emission is distinguished from direct sunlight by modulating the LED drive current with a 10 kHz sinusoid. The receiver conditioning boards use amplifiers with a narrow band-pass filter centred at 10 kHz followed by precision envelope detector.

Temperature issues affecting gain stability are taken into account in both transmitter and receiver electronics design. The LED emission level is kept constant thanks to a precision sinusoidal current source featuring a power op-amp with current shunt feedback as output stage; the shunt is characterized by high temperature stability. The gain of the receiver section can be adjusted in order to match the signal dynamics due to

distance and yaw angle ranges. In order to assure high receiver gain stability, the photodiode conditioning boards employ high-stability op-amp integrated circuits, precision feedback resistors, and high op-amp feedback. As a back-up solution for the determination of the SMAV yaw rotation, two custom MEMS gyroscopes were installed inside the SMAV and the PROXBOX respectively, allowing a differential yaw rate measurement. Their exploitation was conceived to provide an alternative feedback measurement for the attitude control system.

2.4. Thermal Control

Because of the extreme environment conditions that are expected during a balloon flight up to the stratosphere, particular attention was paid to the design of a robust thermal control. In fact, as shown by data retrieved by experiments that participated to the BEXUS programme before ARCADE [23], the floating phase of the flight is characterized by very low temperatures and pressure, respectively down to -80 °C and 10 mbar. The chosen thermal control strategy was oriented to provide each critical component / subsystem with a proper insulation from the rest of the experiment, so that its temperature remained within operational limits exploiting internal heat generation. In case this was absent, or not sufficient, heaters were added to warm the component / subsystem. A series of PT100 temperature sensors were placed in the critical spots inside the experiment to provide real-time feedback for the thermal control operator through telemetry during the flight. In order to determine the required thickness of the foam insulation layer for each component / subsystem, as well as the thermal power to be generated by the heaters, a detailed numerical thermal model of the whole experiment was developed. This model describes the ARCADE hardware as a series of thermal nodes that exchange thermal power both towards each other and the surrounding environment through conductive, convective and radiative links. Each node is characterized by physical (mass, density, specific heat, thermal conductivity, emissivity) and geometrical (volume, area) properties. Figure 7 shows a map of the thermal links between the nodes. The numerical tool, developed in the *Matlab* environment, is able to simulate the temperature profile of the nodes as a function of time and environment conditions (air temperature, pressure and density, sun radiation, ground radiation).

2.5. Support Hardware

The electronic system was conceived keeping in mind the need to control many types of actuators, and to acquire different types of physical measurements. Therefore, an industrial CANopen bus solution was adopted. Most of the selected devices are CANopen compatible and are queried by the main intelligence of the system, an x86-based PC104 single-board computer (SBC). The SBC board contains a real-time QNX OS, which executes management, telecommand and telemetry tasks. All the data acquisition (sensors, diagnostic currents, voltages, switch status) and actuation (motors, transmitters and latches) is performed through industrial automation modules and motor drivers connected to the SBC through the CANopen bus. An analog sine wave generator followed by an impressed-current driver powers the LED emitter on board of the PROXBOX. Signal from the Photodiode receiver on board of the SMAV is conditioned, demodulated and acquired by CANopen compatible modules.

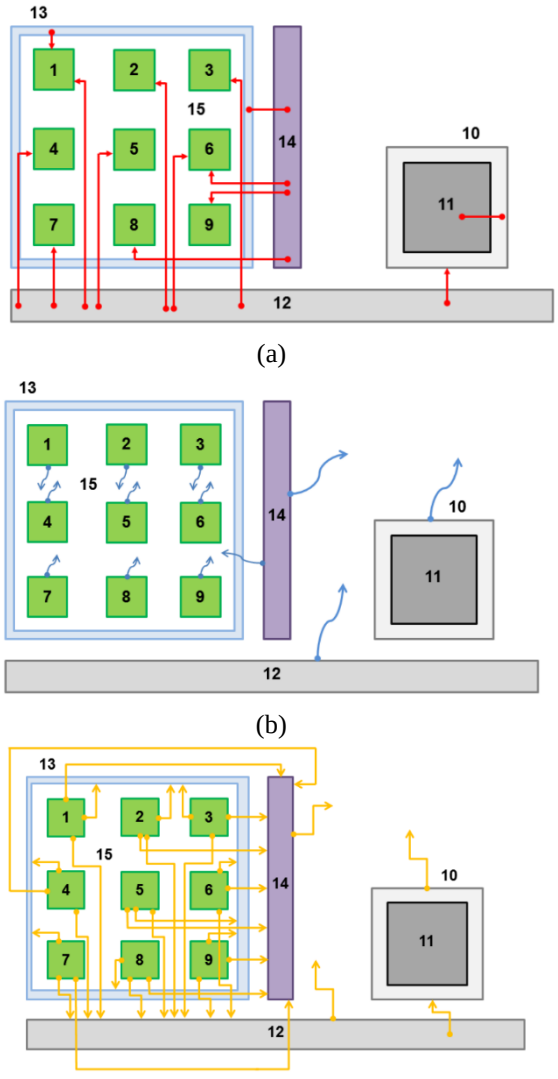


Figure 7. Map of the conductive (a), convective (b) and radiative (c) links between the nodes of the thermal model of ARCADE.

Because of the mechanical structure of the experiment, the power systems of PROXBOX and SMAV are isolated and totally independent. The power source consisted of Li-$SOCl_2$ (Lithium Thionyl-Chloride) battery packs (total energy 1.3 kWh, nominal).
Both the SMAV and the PROXBOX power systems are equipped with current and voltage diagnostics in order to monitor the battery and subsystem voltages and the current consumption.

3. EXPERIMENT EVOLUTION

The design of ARCADE was a continuously evolving process, which started from scratch and resulted in a fully-functional experiment through different steps. Following the REXUS/BEXUS programme schedule, the first iteration of this design process was the experiment proposal that was presented at the Selection Workshop at ESTEC, Noordwijk, The Netherlands, in December 2010. After the selection of the project by the REXUS/BEXUS board, the experiment design developed through the Preliminary Design Review (PDR), the Critical Design Review (CDR), the Interim Progress Review (IPR) and the Early Acceptance Review (EAR), between February 2011 and September 2011. Figure 8 shows the layout of the experiment at each milestone; it can be seen that the design changed significantly between the Selection Workshop and the PDR, while it remained basically the same after that, facing only minor changes.

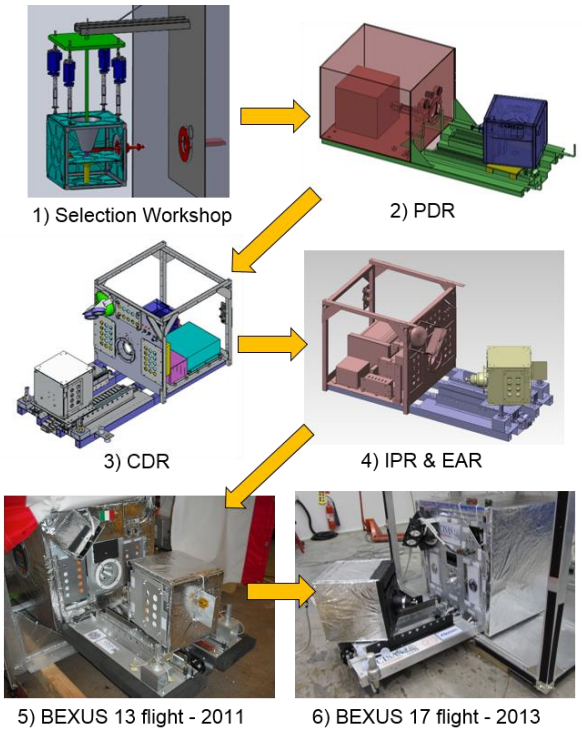


Figure 8. ARCADE evolution through BEXUS 12/13 and BEXUS 16/17 programmes.

The design of ARCADE-R2 resulted in minor modifications of the final design of ARCADE, consisting in (1) substitution of damaged or obsolete hardware (PC104, wind velocity and direction probes), in (2) replacement of heavy components with lighter ones, aiming at reducing the overall experiment mass, (3) improvement of the docking mechanism geometry and in (4) a complete re-design of the software and ground segment.

4. FLIGHTS RESULTS

In this section, the main results of the test operations carried out during the BEXUS 17 flight are described.

4.1. Docking Mechanism

During the BEXUS-17 integration, the docking mechanism was subjected to several tests, to calibrate the automatic docking procedure and to check residual misalignments from the shipment to ESRANGE Space Centre. To limit transient vibrations and loads during the BEXUS balloon release, ARCADE was launched in mated configuration; during the flight, the experiment successfully performed three complete release operations and two docking procedures (Figure 9).

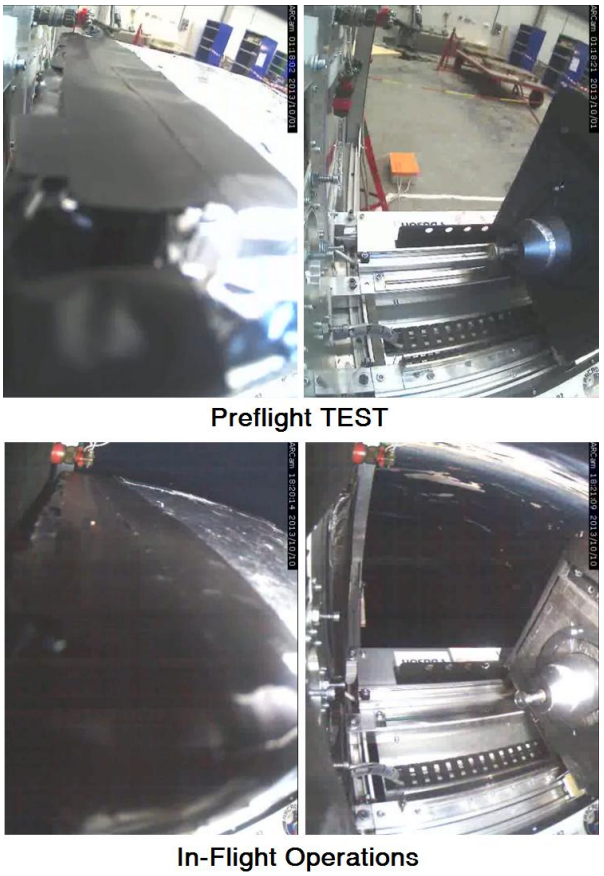


Figure 9. Images form ARCADE on board camera showing docking procedures during BEXUS 17 pre-launch test (top) and flight operations (bottom).

During the first docking procedure in the ascent phase, it was observed that the drogue electromagnet was not able to capture the probe magnet, due to small thermal deformation caused by the temperature drop (about 1.55°C per minute for the first 30 minutes from launch). Increasing the miniature linear actuator set point allowed to solve the issue. The flight and the successive landing demonstrated the mechanism intrinsic robustness: the interfaces survived to the second flight with no visible damage. The whole design process and the data collected during the flight gave important suggestions for similar docking systems developed at CISAS in the framework of small satellites docking system development [12][13][14].

4.2. Attitude Control

As described in the previous sections, many different options are available on ARCADE-R2 regarding the SMAV yaw actuation, the feedback sensors and the control algorithm. Table 1 lists in horizontal lines the four tested combinations of these options during BEXUS-17 flight (#1 to #4). The gyroscopes option is not enlisted because they were not tested during the actual flight as one of them failed prior to launch day and it was not possible to repair or replace it. The feedback loop on the backup motor is a PID position loop internal to the motor driver, however it is not possible to control it with the custom controllers developed for ARCADE-R2. Unluckily, IR sensor combined with the SS controller showed to be unreliable during pre-flight tests and, for this reason, was not included within the flight operations. During the mission, the backup motor positioning always worked properly.
Several homing and pointing manoeuvres were executed during the flight (test #1, see Table 1) and the accuracy was always within the target performances. Figure 10 shows the results of an example manoeuvre. The reaction wheel showed a good behaviour both with the PID (test #2) and the SS (test #3) controllers. A ±4 deg dead band is implemented in order to avoid the saturation of the RW. Figure 11 shows the pointing angle with RW actuation, encoder feedback and PID controller, while Figure 12 shows the pointing with SS controller.

Table 1 Matrix of motion tests executed during BEXUS-17 flight: RW = reaction wheel, BM = backup motor, IR = infrared sensor, E = optical encoder, SS = state-space controller, PID = PID controller.

	Actuation		**Sensors**		**Algorithm**	
	RW	BM	IR	E	SS	PID
#1		X		X	-	-
#2	X			X		X
#3	X			X	X	
#4	X		X			X

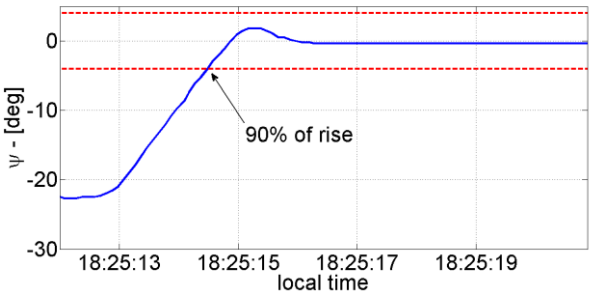


Figure 10. SMAV pointing manoeuvre: backup motor on encoder feedback (test #1).

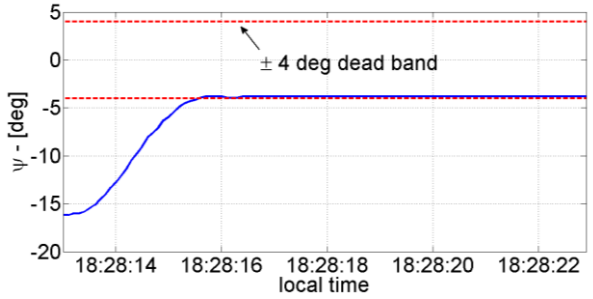


Figure 11. SMAV pointing manoeuvre reaction wheel on encoder feedback, PID controller (test #2).

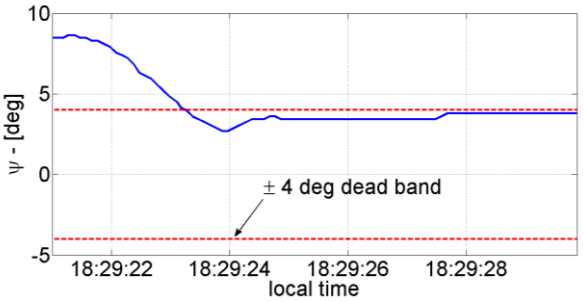


Figure 12. SMAV pointing manoeuvre: reaction wheel on encoder feedback, SS controller (test #3).

4.3. Relative Navigation

The infrared navigation sensor was tested during various automatic procedures that were executed by the experiment during the flight. At the beginning of each of them, the calibration constants of the photodiode receiver acquisition channels, C_1 and C_2, were determined automatically. This solution was adopted as both the LED emitter and the photodiode receivers are sensitive to temperature variations, requiring a periodic calibration during the whole flight. Then, data collected during the flight were analysed in post processing. The inversion algorithm was applied to the receivers voltages measured and recorded during the flight. Figure 13 shows the results of the estimation process compared to the values of SMAV position and attitude provided by the encoders, and indicates the instants when the calibration constants were determined. The

sensor performance is expressed in terms of standard deviation σ_ρ, σ_ψ of the estimates of ρ and ψ with respect to reference values given by the linear and rotary encoders mounted on the experiment. The uncertainty of the estimates of ρ and ψ is 5 mm and 1.5 deg, respectively. These are average values of σ_ρ and σ_ψ; a worsening of sensor performance of ~50% is noticed for ψ approaching its range limits (±40 deg) and for low values of ρ (0.23 m), which means the SMAV tip is being captured by the drogue. In both cases, the photodiode receivers are close to the lateral limits of the LED lobe, which causes signal attenuation. For low values of ψ and higher values of ρ, the uncertainty is better than the average values (~50%).

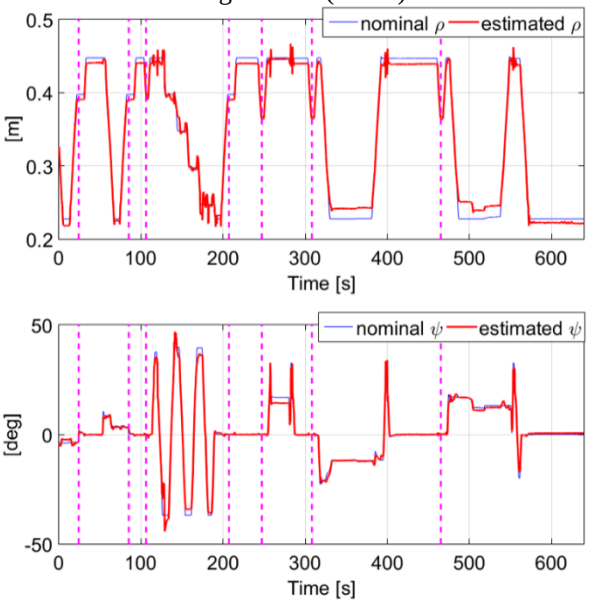


Figure 13. Estimates of the SMAV-PROXBOX relative distance (top) and yaw rotation (bottom) compared to the reference values measured by the linear and rotary encoders. Vertical dotted lines indicate when the calibrations constants were determined.

4.4. Thermal Control

During the flight, the temperature of some critical spots inside the experiment was monitored, enabling active thermal control of such spots from the ground station by turning on and off the heaters when needed. The temperature values were recorded from three hours before the flight until three hours after landing and are shown in Figure 14 - Figure 15. The recorded values are compared to simulated values obtained with the described numerical tool, exploiting the actual flight conditions data (external air temperature and pressure, wind gusts velocity, altitude). In Figure 15, the simulated temperature of the interior of the SMAV is compared to the average value of the temperature of three monitored devices, as in the thermal model the SMAV interior is composed by one single node. It is important to notice that during the ascent and floating phases, the temperature of the monitored devices remained well within their operational ranges (typically: -20°C to 50°C). Moreover, the simulated temperature profile match quite well with the measured data, with maximum discrepancies below 5°C in most cases.

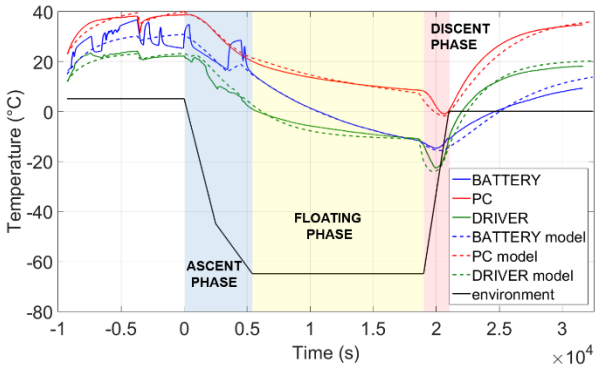


Figure 14. Measured and simulated temperatures inside the PROXBOX, and external air temperature.

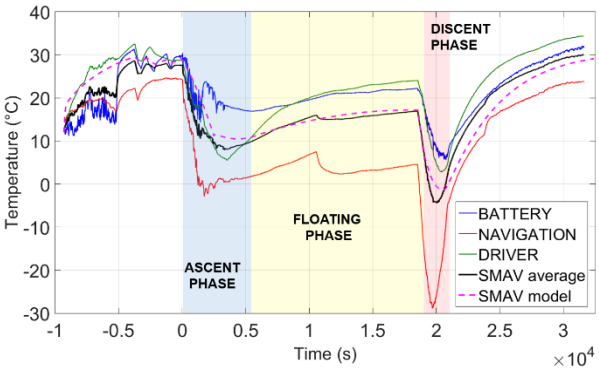


Figure 15. Measured and simulated temperatures inside the SMAV.

4.5. Support Hardware

The electronic system experienced no failures during BEXUS-17 flight, neither on signal conditioning nor actuator operation. Also, the power system sustained the power needs of each experiment subsystem as expected, and the reserve power on the batteries kept the SBC running until recovery.

5. LESSONS LEARNED

The scientific results coming from the experiments are only part of what the team got from this whole experience. While facing all the phases, challenges and issues of this project, the team had the opportunity to make lots of errors. But also some good things and decisions. From the formers, the team learnt the most and every teammate made up a know-how that will for sure help them when facing their next challenges and issues. Advice from ESA experts was for sure highly valuable and helped to anticipate many of the potential

problems or – why not – improve many aspects of the design. However only the issues you personally face teach you the best.

5.1. Experiment Design

As described in the article, the overall experiment design initially proposed was very different from the CDR design. This was because severe simplification was advised by the selection board. At early stage of design, the designers hardly foresee the probable issues that some high-level choices will imply. In the framework of REXUS/BEXUS, it was more important to succeed in a part of a less ambitious experiment than completely fail a big challenge. The first lesson then is: do not fall in love with an idea but consider what you want to get from it, and show that idea to people who already have experience on it, and listen to their feedback.

Moreover, many solutions to design problems were found while discussing with ESA experts, or also experts from University labs. In the end, the simpler (even if less elegant) solution was the one which probably best served for the purpose. So always opt for a proven and already well-known solution for your problem if that fits your needs. That can be easily seen in the redesign of the wind probes: the initial pressure probe design was superseded by the simpler anemometer solution. Also: the yaw control motor was initially designed to be a hollow-shaft model to let wires pass through the rotary joint. In the end, such solution was so expensive that a simple motor was used, and room was cleverly found to let the wires pass without interfering with the movement.

Furthermore, in the initial design of the experiment, many subsystems – mostly electronics – were supposed to be self-built: acquisition boards and power distribution units. However, the time for the realization of such design was underestimated, and the reliability of such solutions hardly reached the one of commercial/industrial alternative solutions, even if their often bigger size caused some space allocation problems. Although, some parts still were self-built, mostly those for which a valid COTS alternative was not found. However, some others, like CAN-bus acquisition boards for Navigation receivers, were still self-built and posed some severe reliability issues during the first ARCADE flight preparation. For this reason they were eventually replaced with COTS alternatives that the team wisely brought at the launch campaign. It's very important to use as much commercial components as possible: they will cost more and be bigger, and power hungry, but they will be more likely to work, withstand harsh environments, be more ready to use and easy to replace.

Finally, it is worth to mention that the first ARCADE flight early failed due to an operating system crash. Although the failure analysis revealed no precise failure mode nor reason, it was clear that software developing time was underestimated during integration, and priority was wrongly assigned to hardware, when it was better to test software thoroughly with incomplete hardware that having the full hardware with not enough tested software to drive it. So never underestimate software developing time and never cause the software engineer work on a deadline-induced panic.

5.2. Launch Campaign

During ARCADE launch campaign, the first two days at least were spent to assemble the experiment and actually finalize some tests and fixes which were on late schedule. However, in general this is the moment in which many unsuspected problems arise, and the deadline prevents engineers to reach the performance to set everything up. From our observations, this was not only the case of our experiment team. So we learnt that finalization deadline should be at least one month before the launch campaign, and that should be as if what works one month before is the same subset of things that will work at the launch, and nothing more. It's better to drop some part of the experiment, rather than frantically trying to get everything working, possibly touching some other things that were working before. This leads to one more lesson, which is avoiding to make any kind of changes at last, particularly in the subsystem which is the easier to change because it needs no direct intervention: the software. During ARCADE preparation, a potential improvement on the telemetry software was deployed on the board, but this led to worse performances of all the telemetry responsiveness. So after some time spent trying to understand what was not working as expected, the team decided to roll back the deployment and restore the original software. If the reason of the malfunction were not identified in this update, probably the flight software would be affected of that through the whole flight.

Moreover, during ARCADE preparation, a self-built gyroscope failed. Some time was spent to try to identify and solve the issue, without success. Being the part not available off the shelf, there was no way to replace it and so the part was deactivated in the flight configuration, reducing the experiment success expectation right before the flight. Such failure happened during the second flight: that means that the parts survived to a flight and two years of tests. Nonetheless, it failed at last. If a spare part were built for that, replacement would have saved the subsystem: so we learned that spare parts, even if they are a cost, are fundamental to avoid such problems that are easy to solve – and do not require engineering – if you thought about that before.

Actually, even if that part were available, replacement would have taken not less than three hours, being the part in the core central section of the SMAV. This was mainly due to the volume requirements, which

prevented to make a design easy to disassemble and service: moreover, most of the bolts were thread-locked for flight, which made the servicing even more difficult. This happened also for many other subsystems that were inspected/tested before flight. So another lesson is: make things bigger or less elegant but easy serviceable because this will save your time and let you use it to solve real problems.
Lastly for this section, we recall that during the first ARCADE flight, telecommand failed due to the crash of the SBC operating system, which gave us only 15 minutes online. During the second flight, telecommand was interrupted due to the under-temperature failure of the E-Link system, which gave us about 1h30 of link. The experiment was designed to perform automatic sequences in that case, however during the first flight the crash prevented everything from working in the software subsystems, during the second flight the automatic procedures run, but they were not able to overcome some problems due to harsh conditions (motor force/torque, thermal control) and so they were not much useful. So we learnt to give more importance to software autonomy, and be sure that most part of the test results can be obtained without telecommand, as this was proven not to be very reliable for different reasons.

5.3. Procurement

The REXUS/BEXUS programme gives chance to change the bill of materials (BOM) of the experiments and define the final components up to the CDR. Considering the lead time of some critical components, in some cases this time can be not even sufficient to have all the components available when the integration phase begins. During ARCADE procurement, the motor drivers had more than 2 months of lead time, and due to misunderstandings with the university buyer office, this time became more than 3 months. This caused a severe delay to the testing and software developing phase, for which the motor drivers were necessary. This underlines the importance to freeze the BOM as early as possible, in order to get all the needed components in time, and also consider that institutions can have some bureaucratic times that increase the overall lead time of the components.
Using parts available from big distributors – when possible - always helps, because they are often available quickly, they can deliver anywhere in the world (so even to the launch site) and often institutions have quicker dedicated channels to buy from them. This was observed during ARCADE procurement phase: the first components delivered were the one from big electronics distributors.
Finally, it is important to speak about the primary Lithium batteries, largely used in BEXUS experiments due to the unleashed performances in harsh temperature conditions. Those batteries also have long lead times, and their transport is subject to hazmat regulations. During both ARCADE and ARCADE-R2 procurements, big issues were registered because of such batteries. The small numbers of available distributors, together with the long lead time, caused them to arrive quite late in both cases. Then, the ADR shipment to the launch site was not easy to organize, as in general express couriers never accept hazmat shipping from unexperienced customers. Specialized couriers have to be used, but reliability and freight times are often disappointing. For ARCADE-R2 flight, there was the risk for the batteries not to arrive on time at the launch site, so the team had to organize the necessary measures to bring the batteries with them on the flight to Kiruna, which was the only chance to bring them on time for the launch campaign. This underlines the importance to buy the batteries at earliest, and organize the shipping with good advance, being sure that there are not misunderstandings with the courier on the kind of hazmat goods and freight times.

5.4. Testing

During testing, most of the potential issues of design were discovered, and this helped the team a lot to find reliable solutions in time. However, in some cases it was hard to test all subsystems in flight configurations, and this prevented the discovery of other latent problems. For example, the STRUT cable guide was tested in low temperature with a lower number of cabling passing through it, and this did not spot out the problem causing the cables to become harder when they freeze, making very difficult for the linear motor to move the STRUT carriage. This results in unexpected problems of movement during flight and made much harder to operate the experiment. Testing in flight configuration is then very important. In fact, any difference between test and flight configuration can lead to a total invalidation of the test itself even if reasoned assumptions are made.
It is not always easy or possible, but it is very worth to try. Finally, the number of possible tests is very high, especially when the experiment is complicated and rich in subsystems. Time can be not enough to perform all the tests, so it is fundamental to give the tests a priority, and test before things that, in the designer's mind, are less likely to work, in order to have more time to correct them, and leave "confirmation tests" only at last. This was seen during ARCADE test phase, in which the most complicated subsystems, as they were integrated at last, were less tested. More effort should have been made in finalizing them in advance to have more time to be confident with their reliability.

5.5. Outreach and Funding

Comparing with the results of other student teams, ARCADE team was not fully satisfied of the outreach

results obtained in terms of visibility and partnerships. Outreach is a required activity by REXUS/BEXUS programme, but moreover it is very important not only for the experiment visibility but also for funding. ARCADE had not funding problems, because all activities were paid by University of Padova funds or freely offered by an industry consortium affiliated with the University. However, the outreach itself results in good visibility, articles and radio appearances, but not in new partnerships or funding. Based on the team's opinion, this was due to the fact that a full-time person was not available for outreach - as engineering work needed all possible effort – whereas other teams devoted even two people to this task. So a final lesson is to include people dedicated to outreach from the beginning, and devoted to that task only.

6. CONCLUSIONS

This paper presented the whole experience of the ARCADE experiment, from its conception to the realization and testing. ARCADE is a technology demonstrator developed by a student team of the University of Padova that participated to two stratospheric balloon flights in the framework of the BEXUS programme, in 2011 and 2013. Critical technologies for autonomous relative navigation, attitude control and docking between miniature space and aerial vehicles were developed and tested in extreme environment conditions, giving the team members the incomparable opportunity to participate to a small scale space mission, get in touch with international experts and gain a huge know-how through hands-on activities.

In the first half of this paper, the ARCADE experiment is described in details, considering both its final configuration and the design process that lead from the conception to the integration and testing. Moreover, the main results obtained from the flight test operations are presented. Then, the second half of the paper summarizes all the experience and lessons learned by the team during the whole programme, which make, together with the scientific results, the most valuable outcome of the programme.

BIBLIOGRAPHY

[1] On-Orbit Satellite Servicing Study, Project Report, NASA (2010),

[2] Saleh J.H., Lamassoure E., Hastings D.E.: Space System flexibility provided by on-orbit servicing: part I. Journal of Spacecraft and Rockets 39 (4), 551-560 (2001)

[3] Rodgers L.: Concepts and technology development for the autonomous assembly and reconfiguration of modular space systems. Master Thesis, Massachusetts Institute of Technology (2005)

[4] Gralla E.L.: Strategies for launch and assembly of modular spacecraft. Master Thesis, Massachusetts Institute of Technology (2006)

[5] Nishida S.I., Kawamoto S., Okawa Y., Terui F., Kitamura S.: Space debris removal system using a small satellite

[6] Kaplan M.H.: Space debris realities and removal. Proc. of the 16th Improving Space Operations Workshop (2010)

[7] Miller D. Saenz-Otero A., Wertz J. et al.: SPHERES: A testbed for long duration satellite formation flying in micro-gravity conditions. Proc. of the AAS/AIAA Space Flight Mechanics Meeting (2000)

[8] Rodgers L., Hoff N., Jordan E., Heiman M., Miller D.W.: A universal interface for modular spacecraft. Proc. of 19th Annual AIAA/USU Conference on Small Satellites (2005)

[9] Tchoryk P., Hays A.B., Pavlich J.C.: A docking solution for on-orbit satellite servicing: part of the responsive space equation. Proc. 1st Responsive Space Conference (2003)

[10] Ui K, Matunaga S., Satori, S., Ishikawa T.: Microgravity experiments of nano-satellite docking mechanism for final rendezvous approach and docking phase. Microgravity - Science and Technology 17 (3), 56-63 (2005)

[11] Fittock M. REXUS/BEXUS: launching student experiments a step towards a stronger space science community, 38th COSPAR Scientific Assembly, July 2010.

[12] Olivieri L., Francesconi A.: Design of a docking mechanism for small spacecraft. Proc. 63rd International Astronautical Congress (2012)

[13] Olivieri L., Branz F., Savioli L., Francesconi, A.: Conceptual design of small spacecraft docking mechanism actuated by electroactive polymers. Proc. 2nd IAA Conference on University Satellites Missions and Cubesat Winter Workshop (2013)

[14] Olivieri L., Antonello A., Savioli L., Francesconi A.: Dynamic behavior of a semi-androgynous small satellite docking interface. Proc. 65rd International Astronautical Congress (2014)

[15] Sansone F., Branz F., Francesconi A., Barbetta M., Pelizzo M.G.: 2D Close Range Navigation Sensor for Miniature Cooperative Spacecraft. IEEE Transactions on Aerospace & Electronic Systems 50 (1), 160-169, 2014

[16] Sansone F., Olivieri L., Branz F., Francesconi A.: Low-cost Relative Navigation Sensors for Miniature Spacecraft and Drones. 2nd IEEE International Workshop on Metrology for Aerospace, Benevento, Italy, 2015

[17] Sansone F., Olivieri L., Branz F., Francesconi A.: Proximity Relative Navigation Sensors for Small-scale Spacecraft and Drones. 66th International Astronautical Congress, Jerusalem, Israel, 2015

[18] Boesso A., Francesconi A.: ARCADE small-scale

docking mechanism for microsatellites. Acta Astronautica, 86, 77-87 (2013)
[19] Wenzel K. E., Masselli A., Zell A.: Automatic take-off, tracking and landing of a miniature UAV on a moving carrier vehicle. Journal of Intelligent & Robotic Systems, 61, 221-238 (2010)
[20] Meier L., Tanskanen P., Fraundorfer F., Pollefeys M.: Pixhawk: a system for autonomous flight using onboard computer ision. Proc. IEEE International Conference Robotics and Automation (2011)
[21] Kendoul F., Fantoni I., Nonami K.: Optic flow-based vision system for autonomous 3D localization and control of small aerial vehicles. Robotics and Autonomous Systems 57, 591-602 (2009)
[22] Grzonka S., Grisetti G., Burgard W.: Towards a navigation system for autonomous indoor fying. Proc. IEEE International Conference on Robotics and Automation (2009)
[23] Chiaradia M., et al.: A Student Experiment from Stratospheric Ballon BEXUS 10: SCRAT from Concept to Launch, 20th ESA Symposium on European Rocket and Balloon Programmes and Related Research, France, May 2011

SESSION 3: F - Hyper-gravity & Low-gravity Experiments

(Thursday 10th - 09.30)

Chairman: Dr. Natacha Callens

SPIN YOUR THESIS! 2013: A PULSATING HEAT PIPE ON THE LARGE DIAMETER CENTRIFUGE

M. Manzoni[(1)], M.Mameli[(2)]

[(1)]Università degli Studi di Bergamo, Dept. of Eng. and Applied Science, Viale Marconi 5, 24044 Dalmine (BG), Italy; University of Brighton, School of Computing, Eng. & Math., BN2 4GJ, Brighton, UK, Email: miriam.manzoni@unibg.it
[(2)] Università di Pisa, DESTEC, Largo Lazzarino 2, 56122 Pisa, Italy, Email: mauro.mameli@unibg.it

ABSTRACT

The present work reports the results of the experimental campaign performed during the ESA Educational program Spin Your Thesis! 2013. A bottom heated mode Pulsating Heat Pipe (PHP) has been investigated on the ESA-ESTEC Large Diameter Centrifuge under different hyper-gravity levels (up to 20g) and different heat loads (50W, 70W, 100W): for the first time, a capillary PHP with circular cross section channels has been fully thermally characterized in such conditions. Comparisons with a novel lumped parameters model are presented: the numerical tool showed very high capability in accurately reproducing the experimental data both in terms of temperature and pressure.

1. INTRODUCTION

The present industry demand of high heat transfer capability, as well as cheap components, leads to the evolution of novel two-phase passive systems. The latent heat associated to phase changes is indeed a very efficient means of absorbing or releasing heat at small temperature differences. Pulsating Heat Pipes (PHPs) are recent and promising two-phase heat transfer devices, suitable for moderately high heat flux applications (up to 30 W/cm^2), that allow efficient thermal control in space and reduction of moving mechanical elements.

Patented in its most common assessment by Akachi [1,2], a PHP usually consists of a capillary tube closed end-to-end, evacuated and partially filled with a working fluid, which results as an alternation of vapor bubbles and liquid slugs. When heat power is provided to the evaporator section, the thin liquid film, which surrounds each vapor plugs, evaporates, bubbles expand and push the adjacent fluid towards the condenser zone where heat is rejected to a cold source and condensation occurs within the vapor plugs nearby the wall surface.

In spite of the simple structure, PHPs working principles are complex: nowadays, there are no models able to fully describe and predict the actual behavior of PHPs both in transient and in pseudo-steady state operation. Moreover, a reliable database which contemplates a large variety of operating conditions, including gravity modifications, cannot be easily found in literature. In particular, the behavior in hyper-gravity of PHPs has never been studied in detail [3-7], even if hyper-gravity may arise in several applications from automotive to aerospace, from chemical reactors to material synthesis. The lack of a full range characterization with respect to hyper-gravity leads to a series of interesting questions: how hyper-gravity affects PHPs thermal hydraulic behaviour? Could hyper-gravity be beneficial for the device performance and in what ranges? Is it possible to develop a numerical model able to simulate PHPs under such conditions?

The present work reports the results of the experimental campaign performed during ESA Spin Your Thesis! 2013 on a copper PHP filled with FC-72. The bottom heated configuration has been investigated on the ESA-ESTEC Large Diameter Centrifuge (LDC) under different hyper-gravity levels (from 1g to 20g) and different heat loads (50W, 70W and 100W). For the first time, a capillary PHP with circular cross section channels, equipped with 14 thermocouples (TCs) and a pressure transducer has been thermally characterized in such conditions. In addition comparison with a novel, lumped parameter code able to simulate confined PHPs operation will be reported to demonstrate the capability of this new numerical tool in predicting PHPs thermal performance even in modified gravity conditions.

2. EXPERIMENTAL SET-UP

The PHP structure (Fig. 1) consists of a copper tube (ID/OD 1.1/2.0mm) folded in 32 parallel channels, closed end-to-end, evacuated down to 0.3mPa and finally filled of degassed FC-72 with a volumetric filling ratio of 0.5±0.03. The incondensable gas content is estimated less than 6PPM. The PHP is heated up making use of electric resistors (*Thermocoax® Single core 1 Nc Ac*) wrapped around the evaporator bends, while the condenser section is embedded into an heat sink and cooled by forced convection (air fans ebmpapst.co.uk® 8412N/2GH-214). The effect of hyper-gravity on the fans speed has been proven to be negligible (<0.9%) if the load is applied perpendicular with respect to the rotational axes.

A pressure transducer (Kulite®, ETL/T 312, 1.2bar A) is plugged just outside the condenser section. The PHP is equipped with 14 T TCs (wire diameter 0.127mm, accuracy of ±0.1°C after calibration): 9 are tin soldered on the external tube surface 6mm above the evaporator (adiabatic TCs); 4 are placed in the condenser region

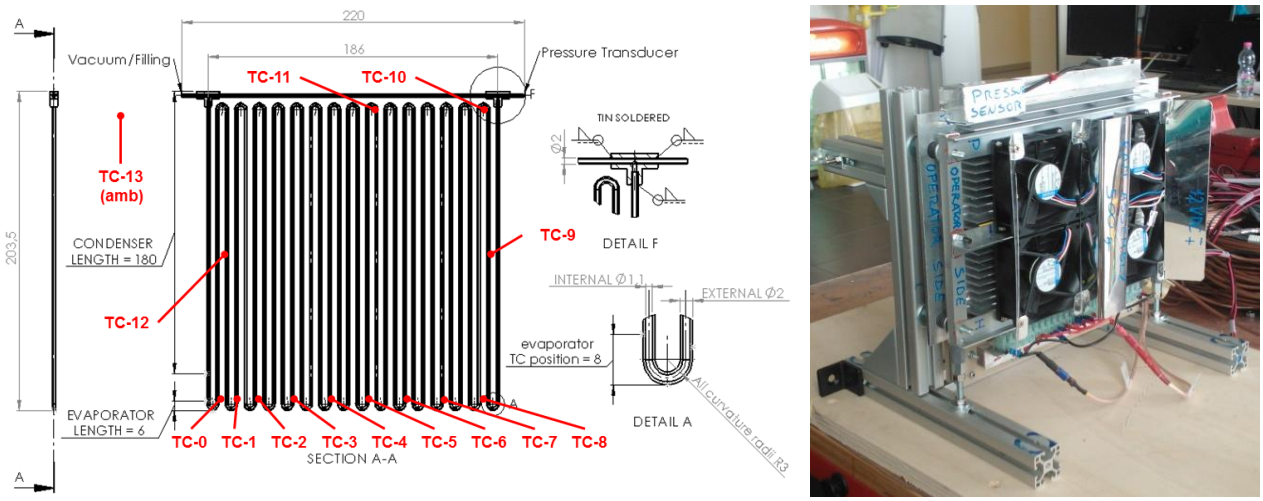


Figure 1. On the left, technical sketch of the PHP; on the right PHP cell in vertical bottom heated mode

(condenser TCs); the last one measures the environmental temperature.

The PHP is also equipped with a g-sensor (Analog Devices® ADXL326) located on one side of the heat sink. All these transducers are connected to a data acquisition system (NI-cRIO-9073, NI-9214®) and the signals are recorded at 16Hz.

Only the PHP test cell is located in the gondola while the peripheral facilities are located in the LDC hub in order to avoid hyper-gravity on the electronic equipment: shielded wires pass through the LDC branch to connect the test cell to the hardware in the hub. There are no mechanical connections between the gondola floor and the PHP support since the LDC is a passive swing out system meaning that the gondola will orient such that the gravity vector is always perpendicular to its floor [8].

3. EXPERIMENTAL RESULTS

3.1. Experimental procedure

Every experiment has been carried out with the following procedure: first, the PHP test rig is placed inside one of the LDC gondolas in bottom heat mode configuration; then the gondola is closed and the gravity vs. time profile is set. Afterwards, the initial heat input level is set and the experiment is powered up at normal gravity (1g) to warm-up the PHP for at least 8 minutes even if the system is able to reach the pseudo-steady-state, which means that all temperature signals show an average value constant in time, in about 180s; even though every test is performed with a peculiar gravity and heat power history, every heat input or gravity level step is kept for 8 minutes. Finally the heating power supply is switched off and a cool down phase of 15 minutes is performed at normal gravity so that all the temperatures reach the room conditions. Repeatability tests have been performed for almost every testing condition.

3.2. Hyper-gravity tests

The first series of test is carried out by changing the heat input (50W→70W→100W) at constant gravity level, in order to understand to what extent gravity may assist or inhibit the flow motion.

Results are presented in terms of temperature and pressure time evolutions. Warm colors represent the hotter temperatures (adiabatic zone close to the evaporator), cold colors the condenser temperatures, while the external environment is characterized in green.

When the PHP is oriented in the vertical bottom heated position, the acceleration vector is parallel to the flow path, from the condenser to the evaporator zone. Thus, gravity helps the liquid flowing down from the condenser to the evaporator section; this, theoretically, enhances the whole fluidic motion inducing high circulation of the fluid within the tube. High circulation means improved heat transfer capacities. The experimental data at 2g (Fig. 2), indeed, show that the PHP is working with slightly better thermal performance at 2g: direct comparisons are possible at 50W and 100W and in both cases the temperatures near the evaporator zone are evidently lower. Furthermore the 2g acceleration prevents the occurrence of local dry-outs at 100W. At normal gravity and high heat input levels, indeed, some PHP channels may undergo a sudden thermal crisis, characterized by higher temperatures, probably due to fluid motion dampening or local dryouts. Fig. 2 shows that at 100W all the recorded temperatures remain within a narrow range till the LDC stops and only at this moment one temperature signal raises underlining the dry-out appearance. All these results are comparable with the ones achieved on the same apparatus tested during the hyper-gravity phases (1.8g) of parabolic flights [9].

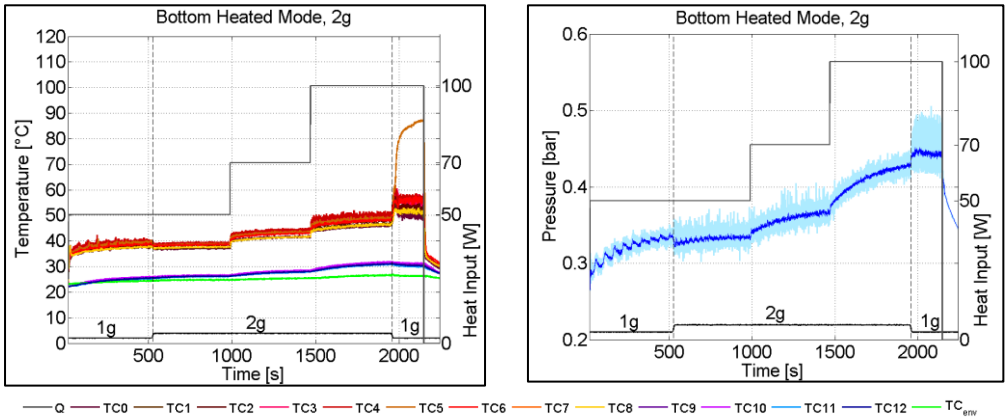


Figure 2. 2g test: on the left, wall temperatures; on the right, local fluid pressure. Solid lines represent the filtered data, while colored ranges the non filtered pressure. For the TCs positions refer to Fig. 1

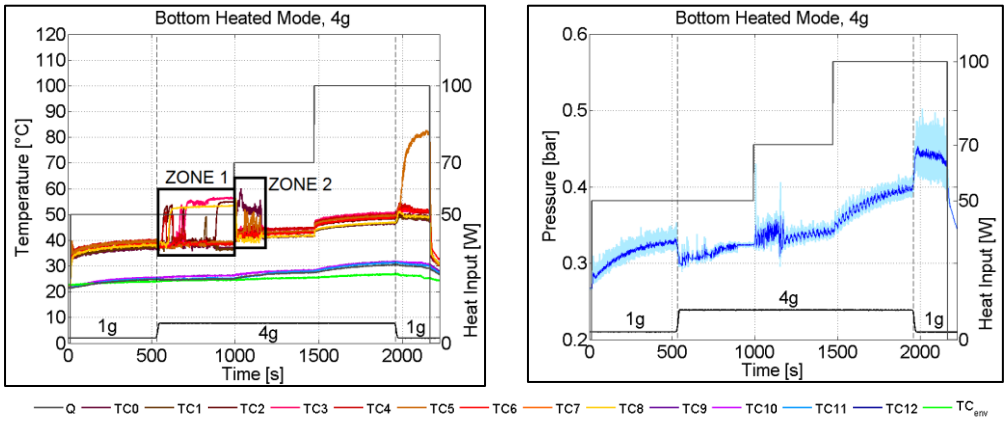


Figure 3. 4g test: on the left, wall temperatures; on the right, local fluid pressure. Solid lines represent the filtered data, while colored ranges the non filtered pressure. For the TCs positions refer to Fig. 1

Fig. 3 shows that at 4g acceleration strongly inhibits the fluid motion, as underlined by the pressure diagram, at 50W and many locations in the evaporator undergo local fluid dry-outs with temperature increase (Thermal Crisis - zone 1). While at 70W another kind of thermal instability, characterized by a more frequent stopover phenomena, resulting in large amplitude and less regular temperature and pressure oscillations, occurs (Transient Thermal Instability - zone 2). Nevertheless the system is able to resettle, after about 120s, and afterwards it keeps a stable and efficient operation. No local thermal instabilities are detected at 100W.

At 6g (Fig. 4) the first unstable zone 1 covers a wider heat input range: neither the 50W nor the 70W heat input levels provide enough thermal diving force to promote a stable fluid oscillation. Only at 100W the vapor expansion is strong enough to compete with the gravity acceleration, indeed after a long settlement period characterized by frequent stopovers phenomena and large amplitude temperature and pressure oscillations (zone 2), a stable behavior is finally reached.

At 10g (Fig.5) zone 1 again covers the 50 and 70W period but, at 100W, the device is not able anymore to recover from the second transient thermal instability.

In addition tests are performed increasing the acceleration level at constant heat input (Fig. 6). As expected, the two different thermal instabilities detected in the previous tests (zones 1 and 2) occur in these experiments too. A peculiar behavior can be observed for the 50W test: at 4g, after a very small period of transient thermal instability (zone 2), the device undergoes a very long thermal crisis (zone 1) and the number of dried-out channel increases with the acceleration level but, interestingly, their temperature level slightly decreases. Furthermore when the LDC stops spinning, the PHP is not able to recover the stable operation. At 70W, as expected, the transition between 1, 2, and 4g enhances the performances of the PHP. Then at 5 and 6g a transient thermal instability occurs driving the PHP to a complete thermal crisis regime. This is comparable with what has been previously observed for 50W. Therefore, it seems that the transient thermal instability is, actually, a transition between a stable mode, where performances are also enhanced by the hyper-gravity, and a thermal crisis regime. Notice that at 100W, the transition between zone 2 and zone 1 is not so evident at least for the tested gravity levels.

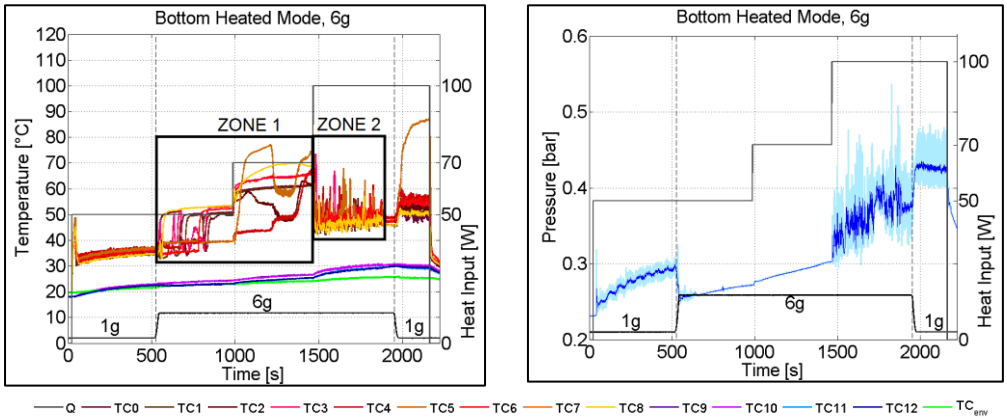


Figure 4. 6g test: on the left, wall temperatures; on the right, local fluid pressure. Solid lines represent the filtered data, while colored ranges the non filtered pressure. For the TCs positions refer to Fig. 1

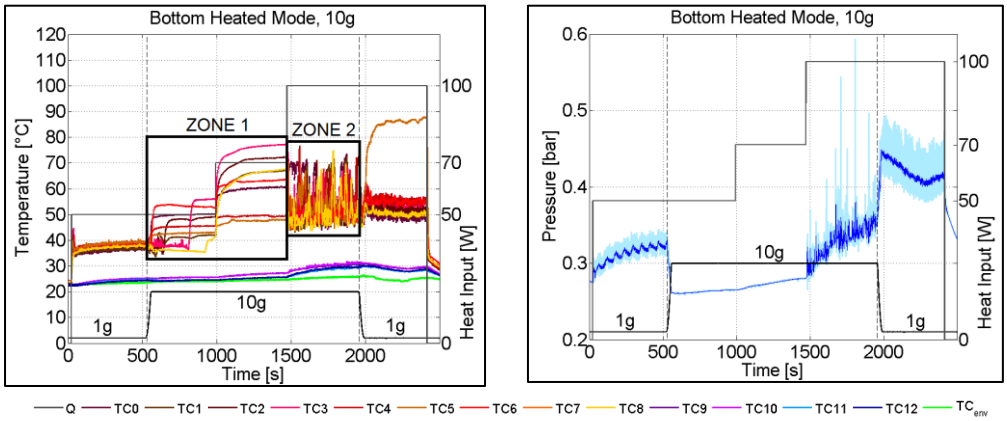


Figure 5. 10g test: on the left, wall temperatures; on the right, local fluid pressure. Solid lines represent the filtered data, while colored ranges the non filtered pressure. For the TCs positions refer to Fig. 1

Fig. 6 shows also the theoretical fluid saturation pressure calculated as a function of the environmental temperature (green line). If the fluid is not moving inside the condenser, its temperature will approach the cooling medium temperature. This means that the local fluid pressure approaches the saturation value at room temperature and the PHP is going towards worse working conditions. This is indeed what happens at increasing accelerations after the thermal crisis.

Since the internal flow visualizations could not be performed during the present experimental campaign a possible physical explanation of the above phenomenon may be attempted on the basis of the fluid local pressure. When the PHP is working in the vertical bottom heated mode, the gravity force helps the liquid phase to flow from the condenser section to the evaporator zone. This alternation of evaporation and condensation assists the motion of the fluid inside the capillary tube and, at normal gravity; an alternation of liquid slug and vapor plugs could be achieved. A small increase of the gravity improves the performances of the PHP while, if gravity increases too much, the liquid phase is forced to flow in the evaporator section but the heating power is not any more sufficient to push it up in the condenser. This leads to the formation of a liquid storage in the bottom of the device and a vapor amass in the top section. Since heating power is provided in the evaporator, bubbles may be still generated within the liquid storage causing a local and more chaotic fluid motion observed in the pressure signal that is oscillating in a less regular way with respect to the stable operation. Temperature in the evaporator section also undergoes unstable and incoherent oscillations (zones 2, Transient Thermal Instability). The bubbles generated by the boiling process, however, are inhibited by a further increase of the gravity acceleration until the system reaches the overall thermal crisis (zones 1). In this case pressure oscillations are damped and moreover, when gravity increases, the pressure signal shows a step reduction comparable with the gravity step enhancement. Finally, it is assumed that at very high gravity levels bubbles collapse as soon as they are formed because of the very high hydraulic pressure. In this condition, the system reaches an equilibrium state, and saturation pressure can be measured in the top vapor.

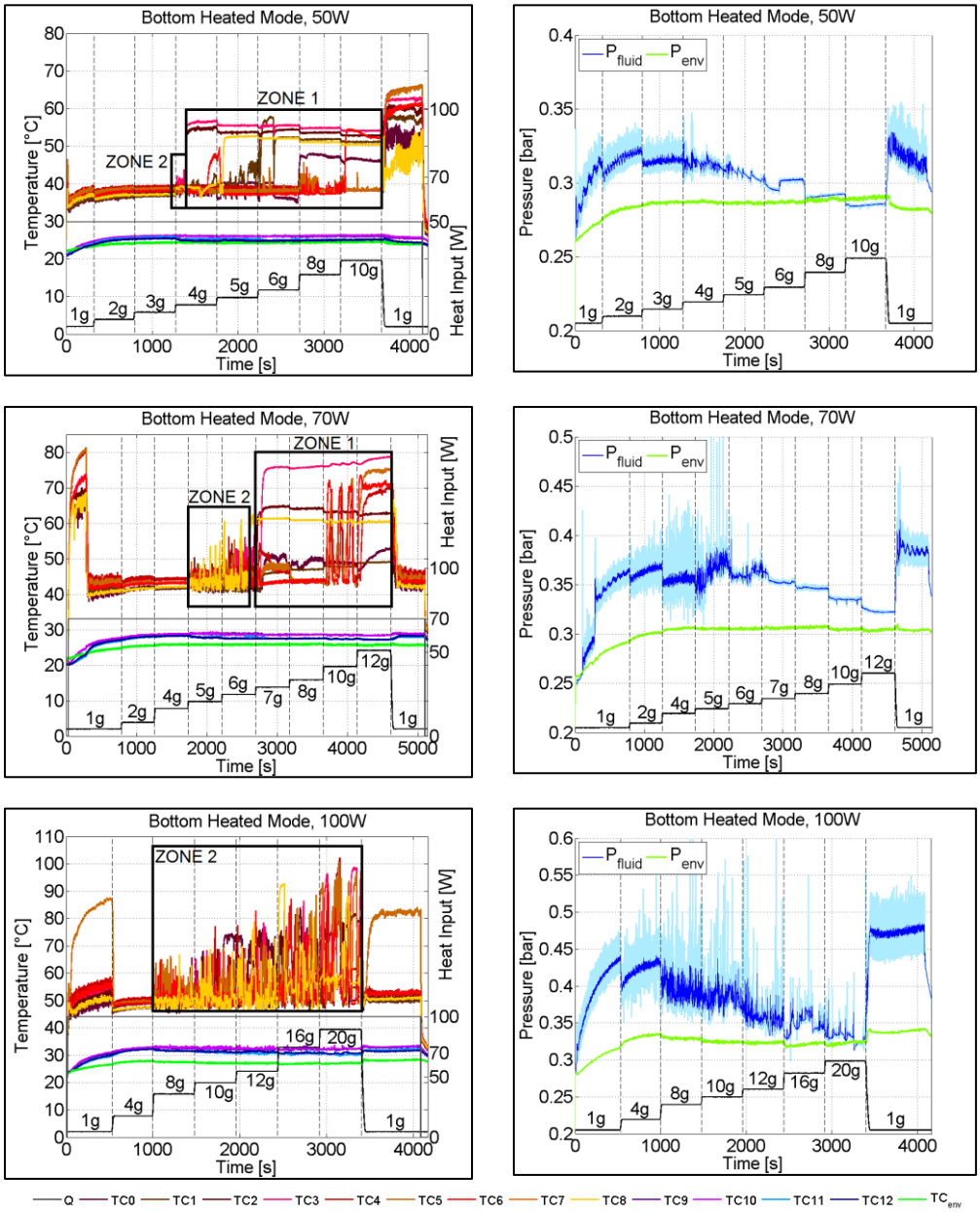


Figure 6. 50W (a), 70W (b) and 100W (c) tests: on the left, wall temperatures; on the right, local fluid pressure. Solid lines represent the filtered data, while colored ranges the non filtered pressure. For the TCs positions refer to Fig. 1

4. NUMERICAL RESULTS

4.1. The numerical model

A novel lumped parameters numerical model has been developed [10]. It can be applied to PHPs in a confined operational mode and it uses an advanced numerical technique to allow fast simulations extending sensitivity analysis and device designs.

Even if lumped parameter models are not a novelty for such systems [11-12], for the first time this kind of numerical tools has been applied to simulate transient operative conditions removing physical simplified assumptions and embedding, directly, phase changes. Besides, the code has two main blocks: an Eulerian model for the external tube and a Lagrangian model for the internal two-phase flow. A dedicate matrix allows communication between fix and moving domains. Mass, momentum and energy balances are solved for liquid and vapor through a novel hierarchical method: for each time step, first the heterogeneous phase changes are solved, then the homogenous evaporation/condensation phenomena through the interface are accounted for, finally all the other phenomena (e.g. sensible heat exchange with the wall, axial conduction, etc.) are computed.

The final mathematical model results in an ODE system which is solved numerically by means of a blocked algorithm consisting of a combination of Adams Bashforth schemes of order one and two with the

Störmer-Verlet method. The use of the latter one for the discretization of the system block descending from the momentum equation was driven by its well known properties in capturing the long term dynamics of second order ODE systems in an accurate and stable way. Such choice, which represents a novelty with respect to the previous simulation tools, has been shown to be extremely effective in preventing unphysical phenomena such as the overlapping of adjacent fluidic domains.

For the implementation of the numerical method an interpreted code written in GNU Octave was chosen in order to allow for agile development of model modifications and extension; by suitably optimizations, its efficiency was enhanced to reduce global simulation time to a level comparable with more complex tools.

Tab. 1 resumes the principal inputs given to the numerical tool to perform the simulations shown in the following section.

Table 1. Principal physical and numerical inputs

Input parameter	**Value**
Working fluid	FC-72
Volumetric filling ratio	0.5
Tube material	Copper
ID/OD	1.1/2.0 mm
Surface roughness	50 μm
Total length	6.62 m
No. of evaporator bends	16
*External HTC	400 W/m^{2}K
*Film Thickness	50 μm
*ΔT superheat	2.5 °C
*ΔT cooling	0.01 °C
*No. of slug/plug at $t = 0$	20
*No. of wall grids	400

* Values are guessed in feasible ranges. Sensitivity analyses showed independency of the numerical results.

4.2. Comparison with experimental data

The proposed numerical model is applicable to slug flow operating regime. In order to satisfy this assumption, the Bond number criterion [13] should be satisfied: for the tested PHP, theoretically, the transition between confined and unconfined flow should occur between 2g and 3g. Thus simulations have been limited up to 2g only.

The comparison between experimental and numerical results in term of local spatial average wall temperature is reported in Fig. 7, while Fig. 8 shows the recorded and predicted fluidic pressure. It is clearly visible that the model is able to reproduce the experimental data for the tested conditions; even the slightly improvement of the thermal performance when passing from 1g to 2g at 50W and 100W is correctly computed. The maximum error in term of wall temperature is less than 6%; in addition the numerical temperatures fit within the experimental dispersion range, apart for the 70W results that are little over-estimated (~3K).

Moreover, the model is able to reproduce the transition of about 10s between the different operative conditions (power and gravity levels); an under-prediction of the start up time is, instead, visible: the reason of that lies in the fact that the thermal inertia of the peripheral elements, in particular the heat sink at the condenser section, is not yet modelled.

5. CONCLUSIONS

A multi-turn, bottom heated mode PHP with standard 2D geometry has been experimentally investigated in hyper-gravity conditions on the LDC at the ESA-ESTEC center. The temporal trend of the wall temperature and the local fluid pressure signal show that the PHP thermal response is strongly and rapidly affected by the variation of the gravity field. In particular gravity may either assists or inhibits the flow motion depending on the heat input level.

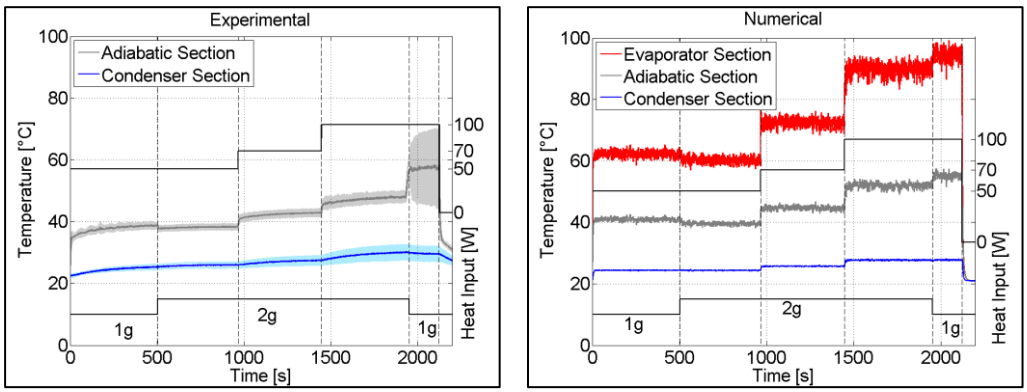


Figure 7. Comparison between experimental (left) and numerical (right) wall temperatures for a bottom heated mode PHP at different heat inputs and gravity levels. Solid lines represent the local spatial average wall temperature; colored ranges on the experimental results indicate the standard deviation on the recorded data.

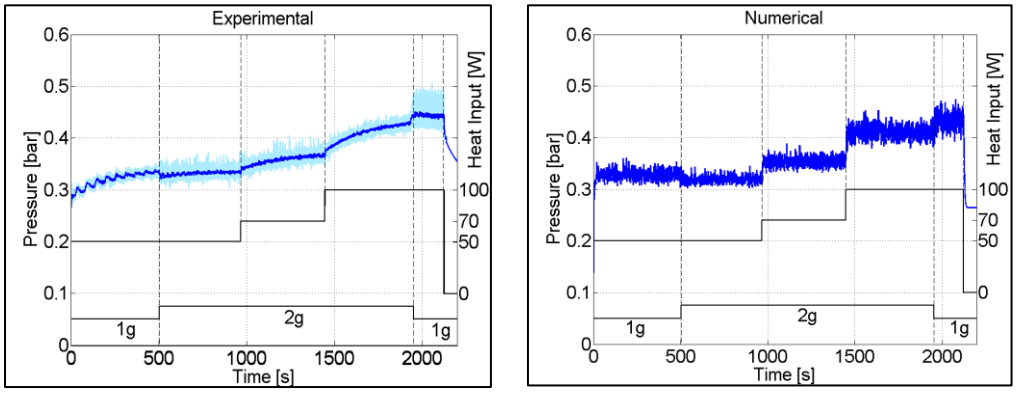


Figure 8. Comparison between experimental (left) and numerical (right) pressure for a bottom heated mode PHP at different heat inputs and gravity levels. Solid lines represent the filtered data, colored ranges on the experimental results the non filtered pressure

Two different local thermal crisis has been detected: if the fluid pumping forces, resulting from the heating power, can compete with the acceleration forces the system only undergoes local frequent stopover phenomena (Transient Thermal Instability), while, if the pumping forces are completely damped in some channels because of the acting acceleration, wall temperature increases and settles to a higher level (Thermal Crisis).

In addition, the experimental data from the 2g test have been compared with the numerical predictions from a novel lumped parameters model: this new numerical tool showed very high simulating capability, being able to reproduce with remarkable accuracy the experimental data for all the operative conditions.

6. ACKNOWLEDGEMENTS

The present work has been carried out in the framework of the project ESA-AO-2009 "Microgravity investigations of a novel two phase thermal management device for the ISS" financed by the Italian Space Agency (ASI-DOLFIN-II). A thanks is needed to ESA's Spin You Thesis!2013 organizers and LIS engineers for the support in the hyper-gravity experimental campaign, as well as to the MSc thesis student C. Roncelli for his help in the experimental assessment. Thank to Dr. O. Minster and Dr. B. Toth for their interest and support to PHP**s** activities and to all the members of the Pulsating Heat Pipe International Scientific Team, led by Prof. M. Marengo, for their contribution in the pushing of the PHP technology for real space applications. Finally the authors acknowledge Prof. M. Petridis and the School of Computing, Engineering and Mathematics of the University of Brighton for the financial support.

NOMENCLATURE

ASI	Italian Space Agency
ESA	European Space Agency
ID	Internal Diameter
ISS	International Space Station
LDC	Large Diameter Centrifuge
OD	Outer Diameter
ODE	Ordinary Differential Equation
PHP	Pulsating Heat Pipe
TC	Thermocouple

REFERENCE

[1] Akachi, H., Structure of a heat pipe. US Patent 4,921,041 (1990).

[2] Akachi, Structure of micro-heat pipe. US Patent 5,219,020 (1993).

[3] Gu J., Kawaji M., Futamaca R., "Microgravity performance of micro pulsating heating pipe", *Microgravity Science and Technology* 16-1 (2005).

[4] Gu J., Kawaji M., Futamaca R., "Effect of gravity on the performance on pulsating heating pipe", *J. of Thermophysics and Heat Transfer*, 18-3 (2004).

[5] Kiseev, V.M. , Zolkin, K.A., "The Influence of acceleration on the performance of Oscillating Heat Pipe", *Proc. of the 11th International Heat Pipe Conference*, Tokyo, Japan (1999).

[6] Ma, H., Thompson, S.M. , Hathaway, A.A., Smoot, C.D., Wilson, C.A., "Experimental investigation of a Flat-Plate Oscillating Heat Pipe during high-gravity loading", *Processing of the ASME 2011 International Mechanical Engineering Congress & Exposition IMECE2011-64821*, Denver, Colorado, USA, (2011).

[7] Van Es, J., Woering, A.A., "High-acceleration performance of the Flat Swinging Heat Pipe", *NLR-TP-2000-265*, (2000).

[8] Van Loon, J. J. W. A., Krouse J., Kunha, U., Goncalves, J., Almeida, H., Schiller, P., "The Large Diameter Centrifuge, LDC, for life and physical sciences and technology", *Proc. of the Life in Space for Life on Earth Symposium*. Angers, France (2008).

[9] Mameli, M., Araneo, L., Filippeschi, S., Marelli, L., Testa, R., Marengo, M., "Thermal response of a closed loop pulsating heat pipe under variable

gravity field", *Int. J. of Thermal Sciences*, 80, pp.11-22 (2014).
[10] Manzoni, M., Mameli, M., Andromidas, S., de Falco, C., Araneo, L., Filippeschi, S., Nikas, K.-S., Marengo, M., "Sensitivity analysis of a capillary Pulsating Heat Pipe: influence of the tube characteristics", *Proceeding of the 14th UK Heat Transfer Conference*, Edinburgh, UK (2015).
[11] Zhang, Y., Faghri, A., "Advances and unsolved issues in pulsating heat pipes", *Heat Transfer Engineering*, 29, pp. 20-44 (2008).
[12] Tang, X., Sha, L., Zhang, H., Ju, Y., "A review of recent experimental investigations and theoretical analyses for Pulsating Heat Pipes", *Front. Energy*, 7, pp.161-173 (2013).
[13] Baldassari C., Marengo M., "Flow boiling in microchannels and microgravity", *Progress in Energy and Combustion Science*, 39-1, pp. 1-36 (2013).

FELDS EXPERIMENT: A NEW FLEXIBLE SOFT DOCKING CONCEPT

Davide Petrillo[1], Alessandro Cavinato[1], Marco Gaino[1], Marco Buonomo[2], Federico Chiariotti[2], Lorenzo Olivieri[4], Francesco Branz[4], Francesco Sansone[1], Riccardo Mantellato[1], Guus Borst[3], and Alessandro Francesconi[1-4]

[1]*Department of Industrial Engineering (DII), University of Padova, Italy*
[2]*Department of Information Engineering (DEI), University of Padova, Italy*
[3]*Airbus Defence and Space Netherlands, Leiden, The Netherlands*
[4]*Center for Studies and Activities for Space (CISAS), University of Padova, Italy*

1. Abstract

Flexible Electromagnetic Leash Docking system (FELDs) is a technology demonstrator whose main objective is to test an electromagnetic soft docking system that guarantees a mechanical connection between two spacecraft through the use of a flexible cable. Docking is performed by launching a ferromagnetic probe towards the target, which attracts it with a static magnetic field. Since the connection between the probe and the launching spacecraft is flexible, the system is self-adjusting, with no need for precise positioning and attitude control; this represents a significant advantage over the existing mechanical docking systems, which require a high level of navigation accuracy. The experiment consists of a prototype of the proposed docking system; measurements are collected to study the magnetic attraction between the two interfaces in microgravity, and so to verify the effectiveness of this new docking technology.
The prototype comprises two main subsystems, the launcher (GUN) and the receiving interface (SEC). The design of the SEC is based on empirical measurements and simulations of the magnetic field, as its effect on the probe is fundamental to the docking. Load cells and dampers are placed on the SEC mountings, both to reduce the effect of the impact and measure the system response. Further empirical measurements are collected to validate the two-body vibrational model used for its design.
Some studies on friction effects and other tests on specific components were conducted to optimize the design of the GUN subsystem for the microgravity behavior, and a stereoscopic video system was set up and calibrated to measure the probe trajectory and gauge the strength of the capture effect of the magnetic field.
The setup was tested in microgravity at the ZARM Drop Tower in Bremen as part of the ESA Education-sponsored Drop Your Thesis! 2014 program. Five drops were performed, with different system parameters.
The first three drops were performed with perfect alignment between the two spacecraft, and the docking attempts were successful. The last two drops were performed with a significant misalignment; in these cases, the probe did not reach the target due to snags in the tether release system. The drop results show the magnitude of the capture effect; the probe was guided towards the receiving interface by the magnetic field. Further studies should be performed on the release system, due to the strong effect of tether friction in microgravity conditions, but the prototype shows significant advantages over existing docking technologies.

2. Introduction

Obtaining a physical connection between two spacecraft is fundamental for several important activities, such as crew, fuel and material transfer. Docking is the last phase of a rendez-vous between the involved objects, in which the actual physical link is established. Docking mechanisms quickly evolved from a simple mechanical interface to much more sophisticated technologies, enabling crew members to move between two vehicles in a shirt-sleeve environment and the transfer of electric power and propellants between linked ships. A simple example of a general docking configuration is depicted in Fig. 1.

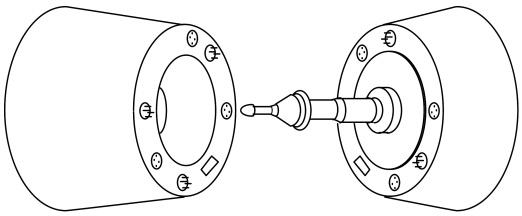


Figure 1. Classic Docking system

One example is represented by the Soyuz docking mechanism [1], which consists of an active docking assembly and a passive docking assembly. This type of docking system is called the probe and cone, or ”Classic”, type and is shown in Fig. 2.
This docking mechanism is attached to the transfer hatch of the Soyuz vehicle. It corrects initial vehicle misalignments and dampens the impact energy; the probe can be extended and retracted by the docking mechanism drive. The head of the front probe has four latches, which

are extended and retracted by the latch drive. The moment when the probe head first touches the cone is called “touchdown”, and once the probe head latches are locked in the socket, the docking mechanism draws both vehicles together and mutually aligns them.

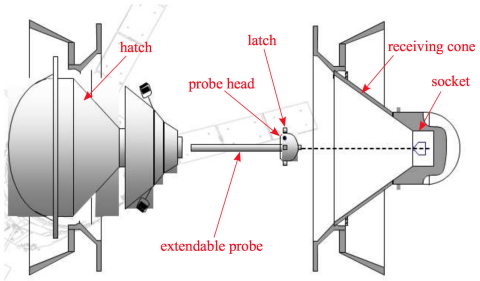


Figure 2. Soyuz Docking system

Although the classical mechanical approach guarantees structural rigidity through the strong link between the involved objects, significant drawbacks make this solution very challenging: the mechanical complexity and strict pointing/control requirements of traditional docking mechanisms are well known, and they constrain the operation flexibility of the whole system, as well as being extremely massive and unwieldy for small satellites.
Only a few other connection systems for small-scale spacecraft have been developed to date, mostly based on the probe-receptacle configuration.
One example is given by the ARCADE Experiment docking system (Fig. 3) [2] that is based on a concept similar to the Soyuz docking system but for smaller vehicles. The CISAS ”G.Colombo” research group (University of Padova) developed ARCADE in the framework of the REXUS/BEXUS program, an SNSB/DLR campaign (in collaboration with ESA) that allows students from universities and higher education colleges across Europe to carry out scientific and technological experiments on research rockets and balloons.
The ARCADE docking mechanism is composed of a probe with a steel tip, which is captured by an electromagnet placed at the end of the drogue; a linear actuator pulling action performs the docking maneuver until three latches lock the probe in position.

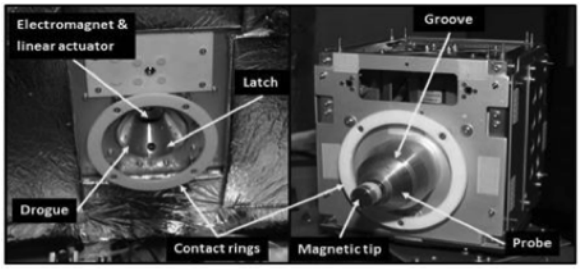


Figure 3. ARCADE Experiment

The CISAS ”G. Colombo” group also developed another novel small-scale docking system (Fig. 4) that uses a semi-androgynous shape-shifting mechanism [4]; one of the two interfaces shifts into a ”drogue” configuration, letting the other port penetrate and close around it to create a solid joint.

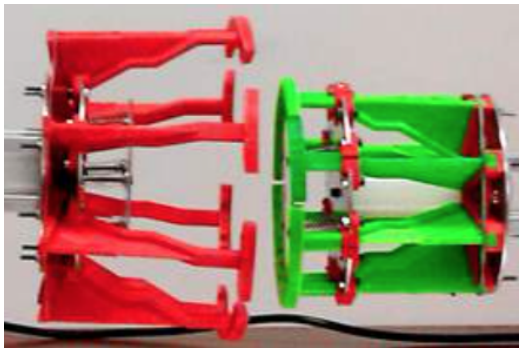


Figure 4. CISAS Semi androgynous docking system

Magnetic docking mechanisms for small satellites have never been tested before; large-scale androgynous magnetic soft docking system was studied and patented [3] by NASA (Fig. 5), but its structure is not easily adaptable to smaller sizes. Its original function was the docking of visiting spacecraft and the berthing of the Crew Return Vehicle at the International Space Station. The system is composed of an active subsystem on one spacecraft and a passive subsystem on the other spacecraft. In preparation for docking, one spacecraft would move to a position near the other spacecraft, with the docking ports of the two spacecraft in approximate alignment. Then, while one spacecraft maintains an approximately constant position relative to the other spacecraft, the actuators of the active subsystem would extend the ring, gently pushing the guide petals and magnetic striker plates: in effect, the active subsystem would reach out, attract, and grab the passive subsystem.

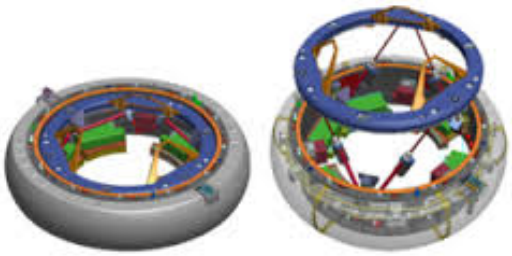


Figure 5. ISS NASA Docking system (Courtesy of NASA)

In this framework, a new approach to overcome some of the drawbacks listed above (accurate attitude and aligning control, close distances for approach) was conceived by the FELDs team building an electromagnetic docking system that guarantees the mechanical connection by using a flexible wire (Fig. 7) and it was tested in microgravity conditions. The docking is performed by launching a ferromagnetic probe (linked with the wire) towards the target, which attracts it with a static magnetic field. As the connection between the probe and the launching spacecraft is flexible, the system is self-adjusting, with no need for precise positioning

and attitude control. Another advantage of this kind of system over traditional docking mechanisms is the low impact force: as the probe mass is almost negligible when compared to the target satellite mass (1-5 %), the soft docking attempt does not disturb the target spacecraft trajectory and its attitude. After the successful soft docking, the target can be reeled in by retracting the wire and a traditional hard dock can be performed, controlling the tether tension to dampen the residual relative motion of the two spacecraft. This would allow for unmanned docking even with a non-cooperative target spacecraft, a maneuver considered extremely challenging.
The FELDs experiment has two main objectives: the first is to test and validate the performance of the FELDs docking system, while the second is to study the dynamics of the target system and the chaser during and after the impact. In order to achieve these objectives, the dynamics of the encounter events are monitored during the experiment (e.g., forces and torques between the probe and the target) and the kinematics of the probe/tether system and the approach system are studied using a set of dedicated sensors and camcorders in relation to the operating conditions.
The results are extremely useful to understand the in-orbit behaviour of a free-floating spacecraft touched by a tethered probe in the framework of a docking maneuver and to evaluate the system concept feasibility and the possible limitations of the proposed technology.
The rest of the article is organized as follows: sections 3 and 5 give an introduction and a description of the Drop Your Thesis! campaign, while sections 4 and 6 describe the experiment and the results we obtained. Finally, section 7 contains the conclusions.

3. Drop Your Thesis!

The FELDs Experiment has been selected for The Drop Your Thesis! 2014 program [5] that gives university students the opportunity to perform scientific or technological research in microgravity conditions. This is possible through the use of the ZARM Drop tower [6], in which the gravity acceleration on the experiment capsule is 10^{-6} g for about 5 to 10 seconds.
The ZARM Drop Tower is 146 metres high. The experiment is mounted into a capsule and released from a height of 120 meters, achieving microgravity conditions for approximately 4.74 seconds in a vacuum. A catapult launch mode is also possible, in which the experiment capsule is launched from the bottom of the tower; this extends the duration of microgravity to 9.3 seconds. At the end of the experiment the capsule is decelerated rapidly to 50g. This setup allows for a wide range of microgravity experiments to be performed in the Drop Tower.
The experiment objectives were accomplished with the Drop mode by performing five docking attempts in realistic orbital conditions through the use of the ZARM Drop Tower; the experiment consists of a model of the docking system, with two subsystems that represent the two spacecraft. As the LEO orbit environment is similar to the microgravity conditions during a ZARM drop, the experiment was a realistic test of the technology and the dynamics measurements will be applicable in future studies and prototypes. The team, once received the final selection for Drop Your Thesis! 2014, has begun to face a number of issues for the realization of the experiment, one of these is the feasibility of the proposed technology through a series of dynamic analyses like the electromagnet sphere of influence of attraction, the dynamics of the tethered system to the target and the response of the target after the probe's impact. Other important topics were a number of critical aspects for the success of the mission such as budget management, outreach and the typical problem solving engineering issues.



Figure 6. ZARM Drop tower (Courtesy of ESA)

4. Experiment layout

Since the experiment goal was to study the behavior of the electromagnetic attraction in low gravity conditions, the experiment had to have the receiving interface generating the electromagnetic force on one side, a simple docking interface in the middle (a ferromagnetic sphere), free to move in space, and a launching system on the other side (Fig. 7). The receiving and the launching subsystems, called SEC and GUN, were mounted on two parallel platforms integrated in the ZARM drop capsule. They were separated by a specific distance, so they were not too close, avoiding problems in the visualization of the ascent phase, but close enough to ensure the docking to end before the capsule reaches the ground. This distance was the first parameter that was determined. The dynamic simulation in Matlab considered a free-falling time of 4.7 seconds and given electromagnetic force and probe mass.

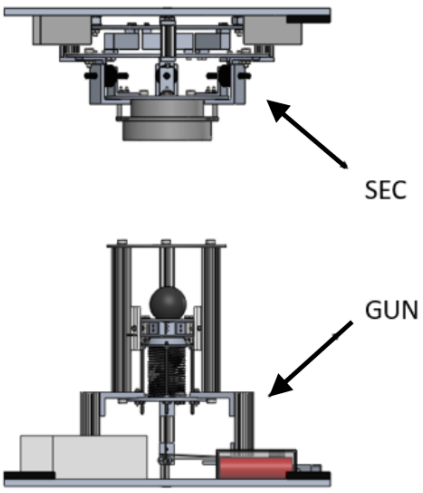


Figure 7. FELDs Experiment

This first part of the design was approached in a systematic way: in order to choose the correct sizes and distances and to consider the correct force field of the electromagnet and velocity of the probe in the ascent phase, several physical tests and simulations were performed. The explanation of the experimental design method is presented separately for each subsystem for additional clarity.

4.1. SEC System

The SEC subsystem represents the target interface of the docking mechanism; the major function of this subsystem is to damp and measure the impact of the probe during the last phase of the soft docking procedure. In the first phase of the design, this subsystem was expected to have a low stiffness coefficient, letting the receiving interface move and simulating the motion of the target in free space. This subsystem was redesigned from scratch later, introducing the damping effect and an increased stiffness in order to simulate the response of real target system of a docking mechanism and to study any possible effect in the surrounding area. This new version of the receiving interface was the one adopted in the detailed design of the SEC subsystem, and describes its actual function in the complete experiment.
The experiment receiving interface consists of a multi-layered structure (Fig. 8) connected to the upper capsule platform; it is composed of three aluminum plates, an electromagnet, three shear beam load cells, three shear dampers, spacers, connectors and a safety-block substructure to prevent any damage to the system during the capsule landing. The layered structure, together with the dampers' action, models the typical features of a real target interface; the data from the load cells can be exploited for future technology development.

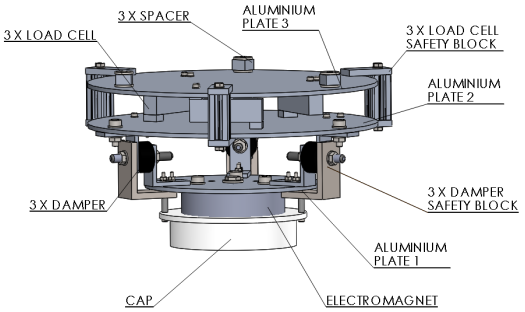


Figure 8. SEC System

This subsystem can be approximated as a two-body vibrational model: the first body is the plate connecting the load cells to the dampers and the second body is the electromagnet. The simulation based on the model took into account the rigidity of the load cells and the effect of the dampers, and their output was used to dimension both the load cells and the dampers.

4.2. GUN System

The GUN subsystem (Fig. 9) is the launch unit of the docking mechanism. It is composed of a mechanical aluminum structure, which allows the sliding of the spring firing mechanism (two aluminum disks guided by three low friction teflon guides), and a Regulation System (Fig. 10).

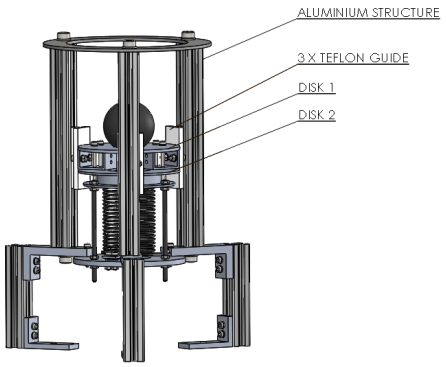


Figure 9. GUN System

The Regulation System's aim is to keep the tether tense before the drop and to adjust the spring compression so as to provide the desidered momentum to the probe (in relation to the desired probe impact velocity with the electromagnet).

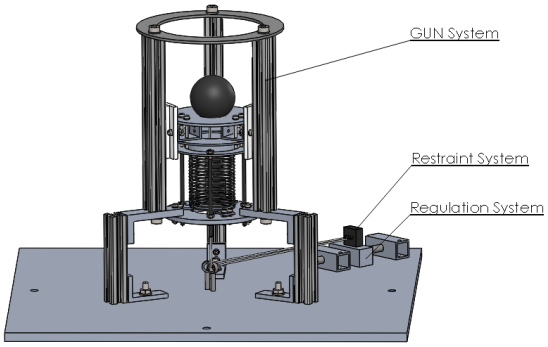


Figure 10. GUN System and Regulation System

The Regulation System is provided of a restraint system connected to a constantan wire, which burns in about 0.2 seconds when a peak current of 50 A is applied to it, thus allowing an istantaneous spring decompression and a smooth release of the probe.

4.3. Measurement systems

The experiment collected two data sets, to evaluate both the efficiency of the docking and the effects on the receiving system.
In order to evaluate the dynamics of the tethered system, four high-speed cameras were placed along the trajectory of the probe (Fig. 11). Two cameras were placed at the same height, and at a right angle to each other; the other two were placed 20 cm below the first pair in order to capture the whole trajectory. We considered each image separately and applied the Hough transform [7] in order to find the spherical probe, which shows as a circle in recorded images at all angles; interpolating the physical location of the probe was then a simple matter of Euclydean geometry.
The position data obtained by the camera covered the full trajectory of the probe, and allowed us to calculate both the capture and guide effect of the magnet and possibly harmful influences, e.g., friction on the tether.
The other data from the experiment were obtained by placing three shear load cells on the SEC; the load cells measured the force of the impact with a sampling frequency of 1 kHz, capturing all relevant dynamics and allowing us to derive the SEC impulse response.

5. Drop Campaign

The DYT! 2014 campaign was at the ZARM Drop Tower, and lasted two weeks. The first (3-7 nov 2014) was the integration week, during which the experiment was tested and set up in the drop capsule, integrating its systems with



Figure 11. Measurement camera system

the capsule interfaces. The five drops were performed during the second week (10-14 nov 2014).

5.1. Integration week

The preparation for the drops consisted of several activities, which went on in parallel.
The first task was the preparation and assembly of the experimental setup; this was delicate and important work, as the whole experiment had to be completely disassembled and reassembled inside the 1.7 m high capsule. The system tests were performed in normal gravity conditions, so the setup was different from the one that was to be used in microgravity; it had to use a stronger GUN spring, with a 2530 N/m elastic coefficient. It also mounted tougher load cells with a 5 kg capacity.
Communication with the ZARM engineers was extremely important in this phase, as the experiment had to be refined and perfectly integrated with the drop capsule. Their microgravity experience was useful for several minor adjustments, such as smoothing the Bosch profiles' surfaces to reduce friction in the GUN.
After mounting the main mechanical subsystems and setting up the wiring and electronics, the final system checks and gravity tests were performed; the results were used to calibrate the load cells.
All the tests were performed without mounting the

microgravity release system, as its spring was too weak for the gravity tests.
After the tests, the planning for the drop sequence started, as well as the preparation of the system for microgravity conditions. In order to do that, the two main subsystems were removed from the capsule and re-assembled for the drop. The GUN was reassembled with a weaker spring (80 N/m) and the friction between the guides was retested. The 3 kg load cells were mounted on the SEC, and the electromagnet was switched with a new one to avoid system failures.
The stereoscopic camera system was also set up during the first week, using the supports and lights provided by ZARM to ensure the cameras had the correct alignment and a clear view of the probe's trajectory, without reflections or shadows.
During this phase, there were some very stimulating discussions with the ZARM engineers, which led to some improvements to the release system and to the addition of a cylindrical plastic tube between the release system and the GUN to act as a guide for the tether after the release.
At the end of integration week the final experiment modifications were made inside the capsule to optimize it for the drops and finally mounted and secured the cameras.
All the subsystems were tested one more time in order to be sure that the electronics, the mechanical components and the interfaces with the capsule worked correctly. Finally, a rigorous launch checklist was developed.

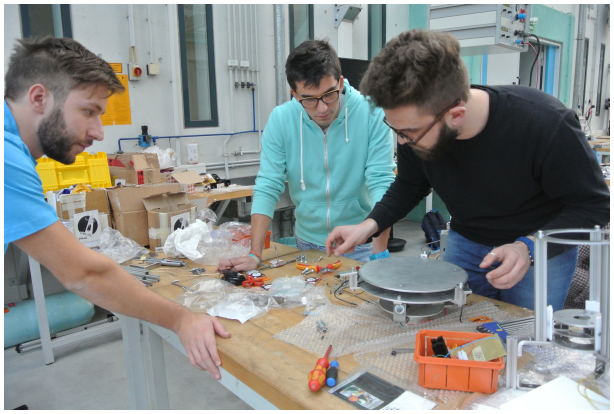


Figure 12. Integration week

5.2. Drop week

During the second week there was a scheduled drop per day. The experiment capsule was transported to the top of tower and then dropped; the free fall-induced microgravity lasted 4.7 s. A test was considered successful if the probe was captured by the SEC; the main test parameters are listed below.

- Misalignment between GUN and SEC subsystems (angle θ);
- Spring compression and so the estimated probe velocity (S);
- Distance between SEC and GUN (D);
- Release system type ($R.type$); release system type I used a torsion spring, directly connected to the constantan wire, while type II used a textile thread with low friction.



Figure 13. ZARM Drop Tower control room

The drops were scheduled in the morning, so the setup for next day was decided after evaluating the drop results. The appropriate changes or adjustments to the system were made while following a general roadmap; the main concept behind the roadmap was to change the system parameters one at a time to evaluate their effect on the docking procedure.
The first drop was a general proof of concept, with perfect alignment ($\theta = 0$). In case of success, the plan was to gradually increase the angle so that a straight trajectory would take the probe farther and farther from the centre of the SEC 3-5 cm in the second drop and 6-7 cm in the third. The plan in case of failure was to add the bumper (like a sort of cone put around of the elctromagnet thath through a rebound of the probe to bumper is able to provide the docking also with relative high misalignment) or reduce the velocity of the probe by decreasing the spring compression.
The first three drops were the real test of the system; in case of success, we planned to use the last two drops to estimate some of the more important effects. The planned fourth drop had the same misalignment as the third, but a lower velocity, in order to magnify the guiding effect of the magnetic field. The fifth drop was a stress test, with increased distance and initial velocity in order to evaluate the tether dynamics in more difficult conditions.
The parameters that were used in each drop are summarized in Table 1.
During the first drop, which had a higher spring compression, the probe successfully hit the SEC and bounced on the electromagnet before docking. In this launch a small misalignment between the GUN and SEC ($2.5\,^\circ$ offset) appeared in the data analisys, probably because of manufacturing inaccuracies in the components.

Drop	θ [deg]	S [mm]	D [cm]	$R.type$	Result
1	0	21	34	I	Y
2	0	12	34	I	Y
3	0	12	34	I	Y
4	2.5	12	34	I	N
5	2.5	12	41	II	N

Table 1. Review of the nominal parameters for each drop. The last column displays the results of the tests (Y for success, N for failure).

In the second drop, the spring compression (and, consequently, the probe velocity) was reduced in order to obtain clearer data in the same situation: the reduced velocity highlighted the electromagnet's capture effect and its sphere of influence.
The third drop was used to increase the confidence on the data, so it was decided to stray from the roadmap, maintaining the same parameters as in the second drop.
The first three drops were successful, but the last two were not, as Table 1 shows. It was decided to increase the misalignment in the fourth drop by adding spacers to two of the three GUN supports, tilting the subsystem. The idea was to obtain a precise vertical alignment between the SEC and GUN, correcting the manufacturing error. Due to problems in the release system, the docking attempt was not successful; the tether got stuck in the middle of the GUN, and the resulting friction slowed the probe down and stopped it before it could reach the electromagnet. The data from the release system camera showed that the energy of the torsion spring sent the tether towards the centre of the GUN too fast, bunching it up between the central screw and the acrylic glass tube and increasing its friction.
The last drop used a simpler release system to avoid the problem that made the previous one fail; the torsion spring was removed in order to unwind the tether more slowly, using a thin wire to connect the constantan and the tether.The distance between GUN and SEC was also increased, as planned in the roadmap.
The 5^{th} drop also failed because of release system complications; the tether release was still too quick, getting the tether stuck between the central screw and the Plexiglas tube like in the 4^{th} drop.

6. Results

The data we collected from the camera system and the load cells were analyzed after the drop campaign, and were fundamental to determine some important parameters of the system model, such as the friction force on the tether after the release, the real force field of the electromagnet, and the dynamic behavior of the receiving interface, as well as providing a qualitative vision of the phenomenon.
The processed video data was used to verify the theoretical model of the probe's behavior in its ascent phase by comparing its trajectory to a simulated one (Fig. 14). The position data was used twice, first to compare the vertical ascent of the probe to the model, then to model both its vertical motion and the misalignment.

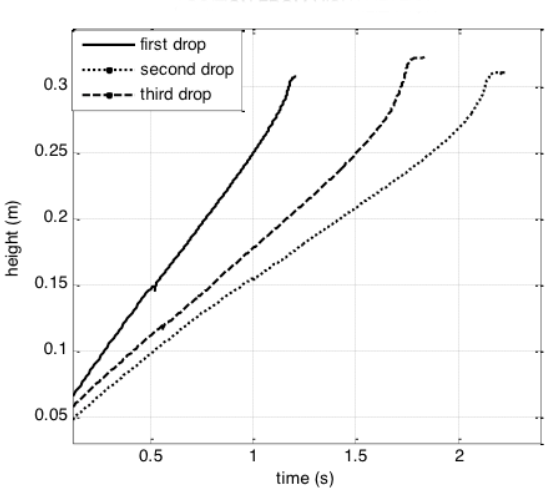


Figure 14. Position of the probe over time, first three drops

The simulation was based on a simple differential equation:

$$m\frac{d^2x}{dt^2} + C\frac{dx}{dt} + F(x) = 0 \qquad (1)$$

where the first term is the inertial force, the second the friction force and the last one the Electromagnetic force in the given position.
This simulation needed the initial position of the probe and its initial velocity as inputs (which were known from the characteristics of the spring in the GUN subsystem, considering an eventual misalignment), and calculated the position (vertical position and misalignment) of the probe calculated from the previous equation. The friction acting on the tether was not known beforehand, so the parameters were derived from the real data. The calculated friction for the five drops is given in Table 2. The load cell data showed that the system response was as expected; the maximum peak was collected from the load cells for every successful drop and the damping time was comparable to the time from the simulation, ending the response before the capsule reached the ground.
The simulations were used to compare the real forces and the ones we expected from the theoretical model. The two trends were comparable, justifying the design choices in terms of stiffness and damping parameters and confirming the descriptive power of the model (Fig. 15). There was one important difference between the real trend and the expected response: a secondary frequency in the force oscillation. This frequency was not accounted for in the

Drop	θ [deg]	v_i [cm/s]	T [s]	$F_{friction}$ [N]
1	0	23.5	1.19	0.009
2	0	13	2.13	0.005
3	0	14.3	1.76	0.002
4	2.5	11.5	nd	0.006*
5	2.5	11.06	nd	0.005*

*Table 2. Drop data: *this value of friction is correct for the first part of the ascent phase; after a certain time, the friction started to increase, stopping the sphere in its ascent phase and causing the failure.*

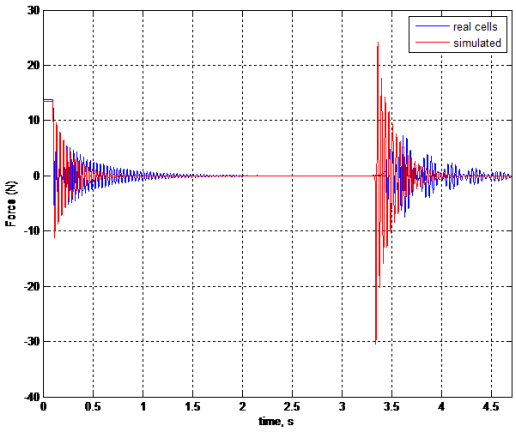


Figure 15. Load cells response: simulated (red) and real (blue)

model, and the analysis showed that the torsion of the receiving interface, which was not included in the model, had a substantial effect on the response. Even accounting for this phenomenon, the general analysis still holds.

7. Conclusions

In conclusion, the design and building process of the experiment was an important learning experience; the progression from the first preliminary design to the complete experiment was long and full of challenges, but most of them were met with a systematic approach and overcome. The design process was made harder by the unintuitive nature of motion in microgravity; the absence of the Earth's gravity made even very small forces significant. Problems due to this were mostly averte for the first three drops, but were the major cause of the failure of the last two; the release system was less resilient than we expected, and future experiments will certainly have to consider that.



Figure 16. FELDs, best student team project IAC 2015

The attention to all details, even the most minute, and the ability to think in terms of all possible negative outcomes are part of the standard toolbox of an engineer, especially one who works in research, but actual experience with complicated systems that can fail in unexpected ways is the best way to develop and grow these skills.
Despite all the problems, the success of the experiment turned out to be the most educational part: the good results we obtained had to be analyzed carefully, distinguishing the relevant data from the measurement noise and spotting the trends and their physical causes. Thanks to the massive theoretical work in the design phase, we just had to account for a few factors to fit our model of the system to the empirical data; the knowledge of the system we acquired, both analytical and intuitive, will be very helpful in the design of future developments of the technology.
The experimental results also proved very encouraging: the three successful drops demonstrated the capability of the technology, and the data agreed with the theoretical model. This experiment was the first test of the FELDs technology, and its success is the first step towards a full space-viable implementation of the system; in order to achieve this ambitious goal, further study will be needed on the release system, which will have to unwind the tether with negligible friction and rewind it smoothly and in a controlled manner.
The idea behind FELDs and the encouraging results were met with considerable interest by the aerospace research community; we presented the experiment at the International Astronautical Conference (IAC) [8], winning the Hans von Muldau award for best student team paper and receiving several interesting feedback comments and helpful ideas for continuing the development of the system (Fig. 16).

Acknowledgments

Firstly, we would like to thank ESA Education and all the people who worked on the *Drop Your Thesis! 2014* program for giving us the opportunity to make our idea a reality.
All the CISAS team also deserves our gratitude, as their help has been invaluable throughout the whole experiment, from the early design phase to the result analysis; the Department of Industrial Engineering and the University of Padova in general provided us with the space and means to work. The same goes for ELGRA and our mentor Guus Borst, who proved very helpful in the final design phases.
A special mention should go to ZARM and their engineers, whose insight and experience were critical during the campaign.
Finally, we would like to thank all our private sponsors for their generosity; their contribution was fundamental in building the actual experiment.

References

[1] Hinman, Elaine M., and David M. Bushman. "Soviet automated rendezvous and docking system overview." *Automated Rendezvous and Capture Review. Executive Summary.* Vol. 1. 1991.

[2] Boesso, A., and A. Francesconi. "ARCADE small-scale docking mechanism for micro-satellites." *Acta Astronautica* 86 (2013): 77-87.

[3] Lewis, James L., et al. "Advanced Docking System With Magnetic Initial Capture." (2004).

[4] Olivieri, L., Antonello, A., Savioli, L., Francesconi, A., Dynamic behavior of a Semi-Androgynous small satellite docking interface. *65th IAC, Toronto, Canada*, 29 September 03 October 2014

[5] Callens, Natacha, et al. "Esa parabolic flights, drop tower and centrifuge opportunities for university students." *Microgravity Science and Technology* 23.2 (2011): 181-189.

[6] Dittus, Hansjörg. "Drop tower Bremen: a weightlessness laboratory on Earth." *Endeavour* 15.2 (1991): 72-78.

[7] VC, Hough Paul. "Method and means for recognizing complex patterns." *U.S. Patent No. 3,069,654.* 18 Dec. 1962.

[8] Petrillo, Davide et al. "FELDs experiment from design to microgravity testing." *66th IAC, Jerusalem, Israel*, 12 16 October 2015

PHOS EXPERIMENT: IMPLEMENTATION AND TEST OF A LARGE DIAMETER PULSATING HEAT PIPE ON BOARD REXUS-18

F. Creatini [(1)], G. Becatti [(1)], F. Belfi [(1)], G. Cicero [(1)], D. Fioriti [(1)], D. Di Prizio [(1)], S. Piacquadio [(1)], G. M. Guidi[(1)], G. Orlandini [(1)], A. Frigerio [(1)], S. Fontanesi [(1)], P. Nannipieri [(1)], M. Rognini [(1)], N. Morganti [(1)], S. Filippeschi [(1)], P. Di Marco [(1)], L. Fanucci [(1)], F. Baronti [(1)], M. Mameli [(1)], M. Manzoni [(2)] M. Marengo [(2)]

[(1)] University of Pisa, Largo Lucio Lazzarino 2, 56122 Pisa, Italy, Email: giuliabecatti92@gmail.com
[(2)] University of Bergamo, Viale Guglielmo Marconi 5, 24044 Dalmine (BG), Italy, Email: mauro.mameli@unibg.it

ABSTRACT

In the present work, the results of two Closed Loop Pulsating Heat Pipes (CLPHPs) tested on board REXUS-18 sounding rocket in order to get experimental data over a relatively broad reduced gravity period (about 90 s) are thoroughly discussed. The CLPHPs are partially filled with refrigerant FC-72 and have, respectively, an inner tube diameter larger (3.0 mm) and slightly smaller (1.6 mm) than a critical diameter defined on Earth gravity conditions. On ground, the small diameter CLPHP works as a real Pulsating Heat Pipe (PHP): the typical capillary slug flow pattern forms inside the device and the heat exchange is triggered by self-sustained thermally driven oscillations of the working fluid. Conversely, the large diameter CLPHP behaves like a two-phase thermosyphon in vertical position while does not operate in horizontal position as the working fluid stratifies within the tube. Then, the idea to test the CLPHPs under reduced gravity conditions: as soon as gravity reduces, buoyancy becomes less intense and the typical capillary slug flow pattern appears. Moreover, this allows to increase the heat transfer rate and, consequently, to decrease the overall thermal resistance. Even though it was not possible to experience the expected reduced gravity conditions due to a failure of the yo-yo de-spin system, the thermal response to the peculiar acceleration field (hyper-gravity) experienced on board is thoroughly described.

1 INTRODUCTION

Pulsating Heat Pipe (PHP) is a promising two-phase passive heat transfer device for the thermal management of electronic components in space application. Derived as an implementation of the well-known Heat Pipes, PHPs were patented by Akachi [1-2] and consist of a serpentine capillary tube close end-to-end in a loop. The tube is first evacuated and then partially filled with a working fluid, which naturally resides in the form of liquid plugs alternated to vapor slugs. In order to obtain the desired liquid slug/vapor plug flow regime, a small critical diameter is required. The PHP fluid motion is activated when input heat power is provided to the evaporator section, which guarantees the expansion of the vapor bubbles and the push of the adjacent liquid plugs to the condenser section, where the heat is released to the cold source and the condensation process occurs.

The design of the PHPs is based on the so-called Bond number confinement criterion, which states that a capillary slug flow pattern can form inside the tube when the ratio between surface tension forces and buoyancy forces is smaller than four, that occurs if the inner tube diameter is smaller than a critical diameter formulated on Earth gravity conditions, i.e. $d_{cr} = 2\sqrt{\sigma/g(\rho_l - \rho_v)}$. Considering the static Bond criterion, it seems that under reduced gravity conditions, the inner tube diameter may be increased to the bitter end. Actually, both Gu et al [3] and Mameli et al [4] asserted that viscous and inertial effects always play a significant role in the definition of the flow pattern within the device that can not be discounted. Considering the recent formulation of the dynamic confinement criterion based on the Weber and Garimella numbers, it seems that a two-phase loop device may works as a PHP under reduced gravity conditions with an inner tube diameter larger than the one evaluated on static Earth gravity conditions. Therefore, in order to evaluate the validity of such assumption experimental verification is fundamental, to decouple completely the inertial effects from buoyancy.

Based on the above considerations, Mangini et al. [6] tested a planar Closed Loop Pulsating Heat Pipe (CLPHP), with an inner tube diameter (3 mm) much larger than the critical diameter value defined on static Earth gravity conditions (1.7 mm at 20 °C for refrigerant FC-72), both on ground and in the micro-gravity conditions, experienced during the 61st ESA Parabolic Flight Campaign. On ground, the device works as a closed loop two-phase thermosyphon when gravity assisted and as a pure conductive medium when placed in a horizontal position. When the gravity level decreases, visualization studies reveal a sudden transition of the flow pattern from stratified to slug flow. Then, the oscillations of the working fluid suddenly activate and the device is also able to work as a PHP when placed in horizontal position.

The milli-gravity condition available during a parabolic flight is approximately 20 s, not enough time for the device to reach an operational pseudo-steady-state. In order to characterize the overall thermal performance of a PHP, the requirement of an extended reduced gravity environmental is basic. Alternative methods to obtain a longer reduced gravity period are on board a sounding rocket or a satellite in an orbit around the Earth.

The aim of the present work is to investigate the thermal response of two CLPHPs with an inner tube diameter smaller and larger than the critical one on Earth, respectively, in the gravity conditions experienced on board REXUS-18 sounding rocket. The reduced gravity period is expected to last around 90 s according to preliminary calculations based on the foreseen overall mass of the payload. The flight test results are compared with the results obtained on ground with the devices both in vertical Bottom Heat Mode (BHM) and horizontal orientations.

2 EXPERIMENTAL SET-UP

The test-cell and the peripheral systems are mounted inside a cylindrical module, which constitutes the REXUS-18 sounding rocket casing, according to the system architecture sketched in Fig. 1. The geometrical features of the module are given in the REXUS sounding rocket user manual.

The test-cell consists of two CLPHPs and a phase change material, which acts as a heat sink. The CLPHPs condenser sections are embedded in an airtight box, referred to as experiment box in Fig.1, in order to prevent phase change material leakages that may result in a serious hazard from launch safety point of view. The battery cells that provide the input heat power to the CLPHPs evaporator sections are assembled in the battery pack. The electronic boards for the management of the data from the sensors and input heat power are mounted inside the on-board data handling and power management boxes, respectively.

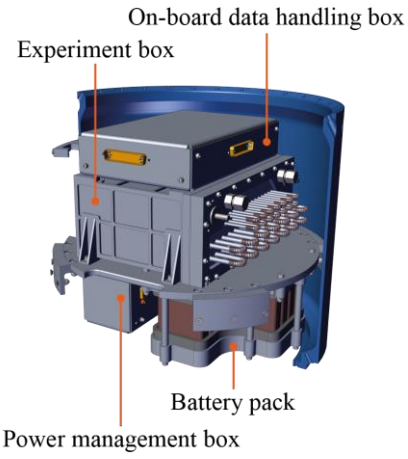


Figure 1. PHOS experimental set-up.

2.1 Test-cell

The geometrical features of both CLPHPs are summarized in Tab. 1. The basic devices structure, as sketched in Fig. 2, consists of an aluminium tube folded in a double-layer configuration with 14 curves constituting the evaporator section. Two T-junction close the tube in a loop and in addition allow for obtaining two ports: the former is used for the emptying and filling procedure; the latter hosts a pressure transducer (Kulite®, XCQ-093-1.7BAR-A). Both devices are equipped with T-type thermocouples that have a post-calibration accuracy of ±1 K. The thermocouples are thermally linked to the aluminium tube by means of a high conductive paste. The thermocouples position on the large diameter CLPHP is sketched in Fig. 2 and is symmetrical on the upper and bottom planes, respectively. The thermocouples position on the small diameter CLPHP is exactly the same except in the evaporator section, where the thermocouples are mounted on the curves in an alternate fashion. The thermocouples position is selected in order to make assumptions about the circulation of the working fluid within the device.

Table 1. Geometrical features.

	Small Diameter CLPHP	Large Diameter CLPHP
Internal Diameter (mm)	1.6	3
Outer Diameter (mm)	3.2	5
Radius of Curvature (mm)	4.8	7.5
Overall Length (mm)	192.8	200
Evaporator Length (mm)	6.4	10
Condenser Length (mm)	145	145
Overall Width (mm)	128	200
Overall Height (mm)	12.8	20

The CLPHPs are first evacuated by a two-stage vacuum pump (Edwards®, XDS35i and EXT255H) until a pressure level of approximately 10^{-4} Pa is reached. The selected working fluid, i.e. FC-72, is separately degassed in a secondary loop by a continuous boiling process: the incondensable gases first accumulate in the free volume of a tank and then are vented away by successive suction cycles. Then the devices are partially filled with a volumetric ratio of 0.5 ± 0.025 and permanently sealed. The residual incondensable gases content results in an overpressure slightly above the saturation temperature of FC-72 and included within the margin of accuracy of the pressure transducer.

The output signals are managed by a microcontroller integrated over an electronic board specifically designed in order to meet the experimental objectives. The temperatures and pressure signals are acquired with a frequency of 5 and 10 Hz, respectively.

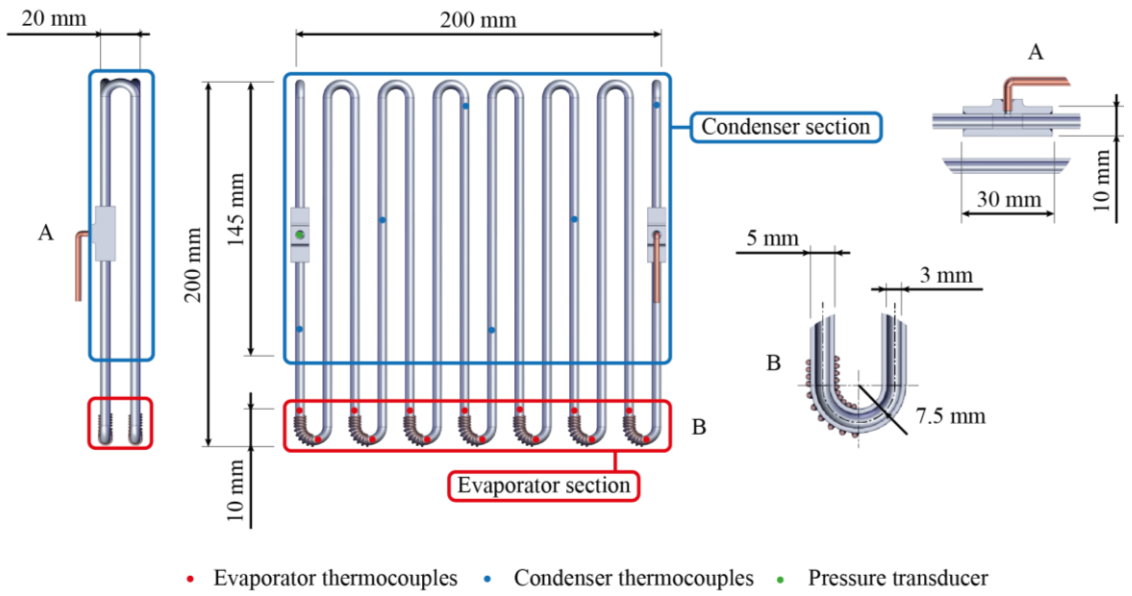


Figure 2. Large diameter CLPHP: structure.

2.1.1 Evaporator section

The CLPHPs evaporator sections consist of 2 wire-shaped heating elements (Thermocoax®, 1 Nc I) 1.6 m long that have a 1 mm external diameter and an equivalent line resistance of 12 Ω/m. The heating elements are connected in parallel and wrapped around the evaporator curves as shown in Fig. 2: the asymmetrical position with respect to the curves is intended to promote the working fluid circulation in a preferential direction. The evaporator sections temperature is limited to 150 °C by 2 thermal protectors (DMP®, 11MP 160L 007E) placed in contact to the aluminium tube. The heating elements are powered up to 400 W by 14 battery cells (SAFT®, MP176065): 8 DC/DC converters, each that consist of a PRM regulator (Vicor®, P024F048T12AL) and a VTM current multiplier (Vicor®, VTM48EF480T006A00) regulate the voltage and current in order to supply with the power profiles represented in Fig. 3 the large and small diameter CLPHPs, respectively.

The nominal power values provided to the heating elements are selected in order to supply to the evaporator sections of both CLPHPs an input heat flux larger than a threshold value. Since it has been proven that there may exist a critical start up heat flux value below which the device shows an unstable behaviour and it can not reach a pseudo-steady [7], the heat flux input levels are chosen above a safety threshold value of 5 W/cm^2 (red line in Fig. 3). The nominal power values are sized so as to result in an input heat flux of 15 W/cm^2. The nominal power values are preceded by peak values intended to rapidly overcome the thermal inertia attributed to aluminium tubes in order to allow the achievement of an operational pseudo-steady-state.

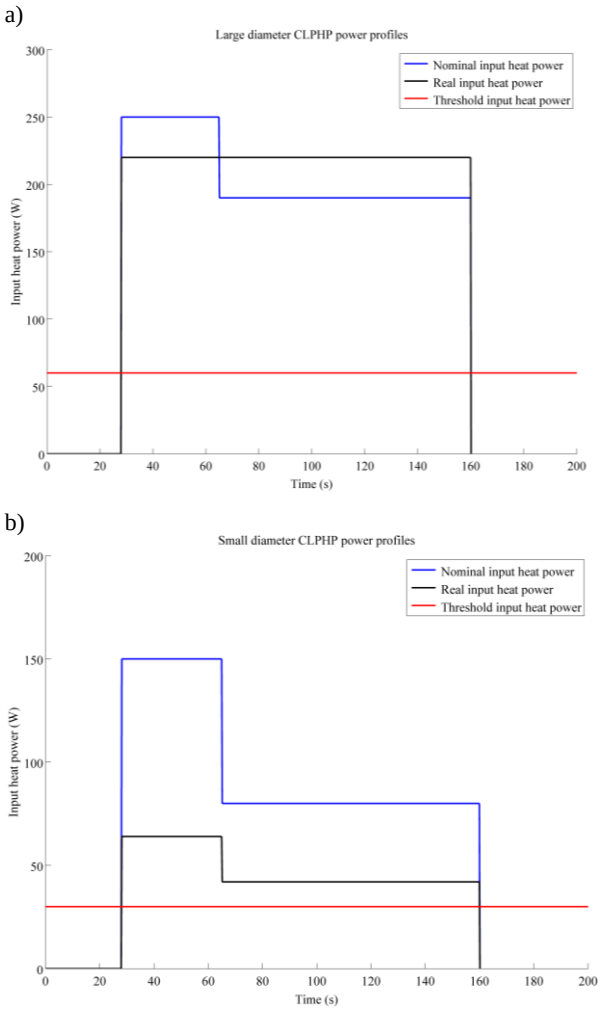


Figure 3. Power profiles: a) large diameter and b) small diameter CLPHPs.

The power is evaluated by combining voltage and current measurements with the values of the duty cycle imposed via software. Voltage and currents measurements are carried out by an instrumental amplifier (Analog Devices®, AD8221) with an accuracy of ±10 % of the imposed power values and acquired with a frequency of 1 Hz.

2.1.2 Condenser section

The heat sink consists in a phase change material in contact with the condenser section. The phase change material is an n-octadecane paraffin wax, whose properties are summarized in Tab. 2.

Table 2. Paraffin was thermal properties.

Thermal Properties	
Melting Point Temperature (K)	301.15
Boiling Point Temperature (K)	591.05
Specific Heat (J kg^{-1} K^{-1})	2160
Latent Heat of Fusion (kJ kg^{-1})	244
Thermal Conductivity (W m^{-1} K^{-1})	0.15

Theoretically, the paraffin wax should absorb heat via latent heat of fusion so as to keep constant the condenser temperature. However, as the thermal conductivity of the paraffin wax is small, after an initial phase during which it absorbs heat via latent heat of fusion, the melting front stops and heat is only dissipated by sensible heat, thus leading to an increase of the condenser temperature. The aforementioned phenomenon should be carefully taken into account and may be likely overcome by embedding a highly conductive structure inside the paraffin wax, i.e. an aluminium honeycomb structure.

The paraffin wax temperature, as clearly highlighted by the condenser temperature trends in Section 3.2, continuously rises without ever reaching the melting point. In fact, the low ambient temperature experienced during the launch countdown lowers the paraffin wax temperature. The problem could be overcome by heating the experiment box external walls prior to launch in order to keep the paraffin wax temperature within the allowable temperature limits.

2.2 Experiment box

The CLPHPs condenser sections are embedded in the experiment box, whose exploded artistic view is sketched in Fig. 4. The CLPHPs are constrained by two polycarbonate supports, each constituted of five separate drilled segments so as to ensure the correct positioning of the devices. The external support is glued with the aluminium cover, which in turn is pressed against an O-ring in order to seal the system.

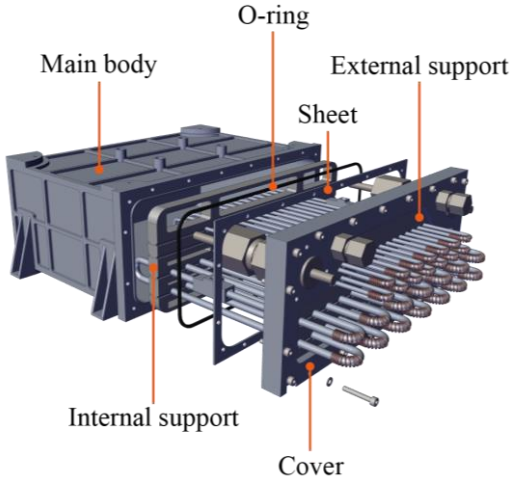


Figure 4. Experiment box exploded view.

The different coefficient of thermal expansion of aluminium and polycarbonate during thermal testing caused the inception of cracks mainly along the mating surface between the aluminium cover and the polycarbonate segments and, consequently, the occurrence of paraffin wax leakages. The cracks were plugged with an extra layer of glue although a more reliable solution based on the more accurate selection of materials and coupling methods should be defined in view of a re-flight opportunity.

3 EXPERIMENTAL RESULTS

The experimental results are presented in terms of temperatures and pressure temporal trends. In the graphs represented below, the tubes wall average evaporator and condenser temperatures are sketched together with the local working fluid pressure on the secondary ordinate axis. The input heat power provided to the heating elements is also reported.

The flight results are compared to that obtained on ground with the devices in vertical BHM and horizontal positions in order to provide comparison between the devices thermal performances under different operational conditions. The performed tests are summarized in Tab. 3.

Table 3. List of the performed tests.

	Small Diameter CLPHP	Large Diameter CLPHP
Ground Tests -Vertical		
Peak Power (W)	64.5	218
Nominal Power (W)	42.5	218
Ground Tests -Horizontal		
Peak Power (W)	64.5	218
Nominal Power (W)	42.5	218
Flight Tests		
Peak Power (W)	64.5	218
Nominal Power (W)	42.5	218

3.1 Ground tests

The ground tests results relative to the small diameter CLPHP are reported in Fig. 5.

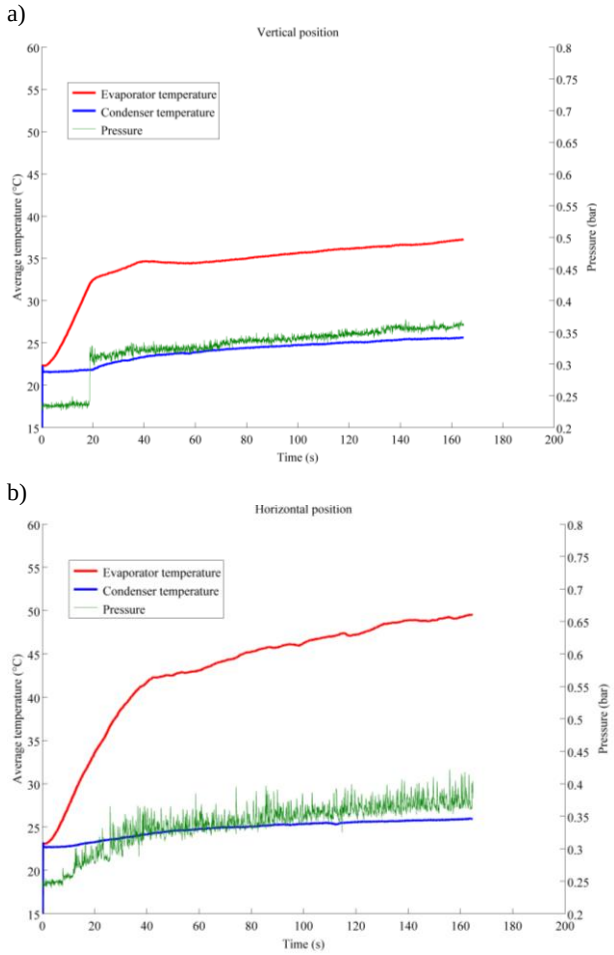


Figure 5. Small diameter CLPHP: a) vertical and b) horizontal ground tests.

The pressure temporal trends relative to the small diameter CLPHP in vertical (Fig. 5a) and horizontal (Fig. 5b) positions evidence some peculiar characteristics: in the former case pressure oscillations have smaller amplitude and higher frequency, in the latter larger amplitude and lower frequency. The reason lies in the different orientation of the device with respect to the gravity vector. In vertical position, the gravity vector acts along the flow path direction, i.e. the longitudinal axis of the tube, and assists the working fluid motion. Therefore, even a small pressure change is sufficient to overcome the inertial effects and push vapour bubbles and adjoining liquid plugs towards the condenser section: the vapour bubbles rise rather easily and the pressure oscillation frequency is high. In horizontal position, the gravity vector acts on a plane perpendicular to the flow path direction. A large pressure change is needed in order to displace the liquid plugs and the working fluid motion is least frequent. The nature of pressure oscillations results in a different start-up behaviour. In vertical position, the start-up occurs suddenly as soon as a sufficient pressure difference is set between the evaporator and condenser sections. In horizontal position, the start-up takes slightly more time, as gravity has not an influence on the working fluid motion.

The working fluid motion inside the CLPHP in different orientations also affects the overall thermal performance. The heat transport capability is higher when gravity assists the working fluid motion as more liquid reaches the condenser section and releases sensible heat. Then, the average evaporator temperature tends towards a lower value when the device is in vertical than in horizontal position.

The ground tests results relative to the large diameter CLPHP are reported in Fig. 6. In order to provide the readers with an understanding of the results, the sketches representing the working fluid distribution with the device in vertical and horizontal positions are provided in Fig. 7.

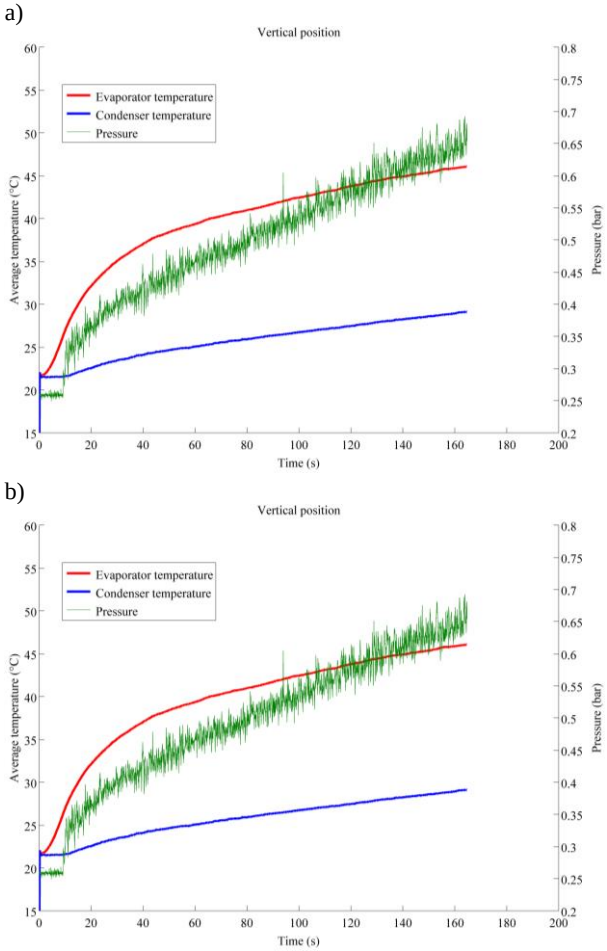


Figure 6. Large diameter CLPHP: a) vertical and b) horizontal ground tests.

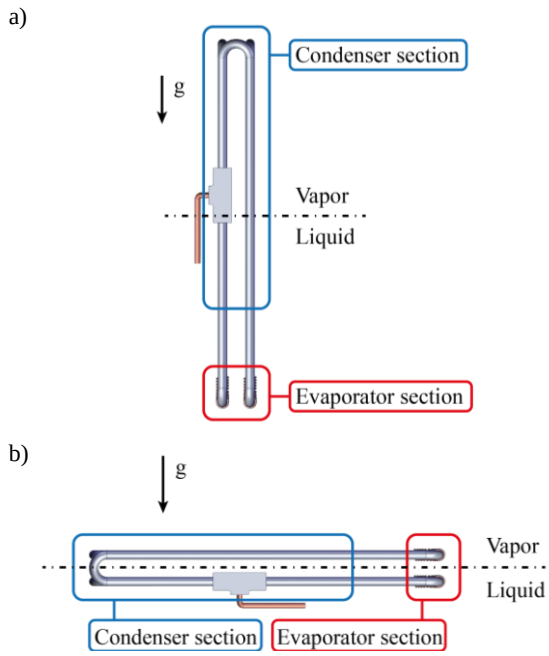


Figure 7. Working fluid distribution: a) vertical and b) horizontal ground tests.

The pressure temporal trends relative to the large diameter CLPHP in vertical (Fig. 6a) and horizontal (Fig. 6b) positions are rather similar to the ones discussed above, although the physical phenomena that occur inside the device are completely different. In vertical position, the device operates as a two-phase thermosyphon, with the liquid phase in the evaporator section and the vapour phase accumulated in the condenser section (Fig. 7a). The liquid phase boils continuously. The generated vapour rises towards the condenser section and, sometimes, drags on with it on some liquid batches in the so-called "bubble lift" mode [8]. As the working fluid distribution inside the device is optimal, even a small pressure difference between the evaporator and condenser sections is able to trigger the working fluid motion. In horizontal position, gravity restrains the liquid phase in the bottom plane of the device while the vapour phase fills the upper plane (Fig. 7b) .The resulting working fluid distribution within the device is not optimal: gravity and the pressure force that ensue from the vapour expansion on the upper plane keep the liquid phase confined to the bottom plane. Therefore, the working fluid is completely immobile until the vapour phase in the upper plane condenses: the associated pressure decrease in the upper plane leads to a vigorous boiling process in the bottom plane. The vapour expansion process is almost instantaneous and traduces in a water hammer associated with high amplitude pressure oscillations. The heat transport process in such a condition is inefficient and results in a higher average evaporator temperature.

3.2 Flight tests

The accelerations experienced during REXUS-18 sounding rocket flight are sketched in Fig. 8. The red and blue lines represent the accelerations along the longitudinal axis of the rocket and on a plane perpendicular to it, respectively. The black vertical lines represent the timeline main events. The one corresponding to the ordinate axis represents the rocket Lift Off (LO) and Start of Experiment (SoE). Then, proceeding to right, at LO +28 s, there occurs the Start of Data Storage (SoDS): from this time, power is provided to the heating elements and data are stored. Finally, power is switched off at LO +160 s.

The black vertical line at LO +70 s corresponds to the instant when the yo-yo system should act and reduce the rotation of the rocket about its longitudinal axis. However, as can be inferred from Fig. 8, the yo-yo system failed and the presence of a residual centrifugal acceleration prevents both CLPHPs to work in a reduced gravity environment. For this reason, the flight results are placed in the context of the hyper-gravity experiments documented in literature.

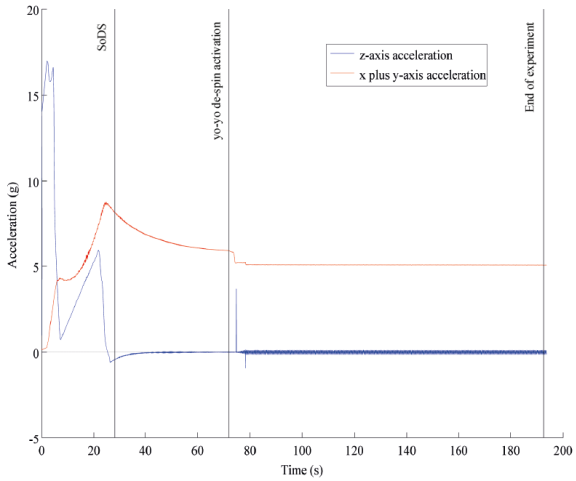


Figure 8. Accelerations.

An image with a series of concentric circles representing the gravity levels that act on the devices depending on their radial distance from the longitudinal axis of the rocket is sketched for clarity in Fig. 9.

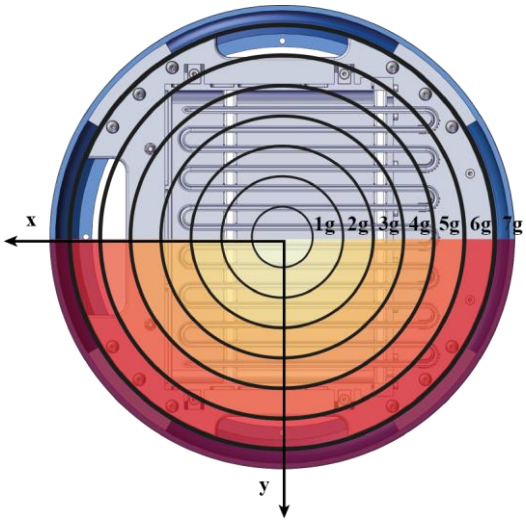


Figure 9. Gravity levels.

The flight test results relative to the small diameter CLPHP are reported in Fig. 10. The centrifugal component of the acceleration promotes the working fluid motion and affects the start-up. However, the acceleration is not oriented from the condenser to the evaporator as in the case when the device is in vertical position but pushes the liquid phase from the central to the peripheral region of the device. The confinement of the liquid phase in the peripheral region of the device results in a detrimental effect on the performance with respect to the vertical ground test but not with respect to the horizontal ground test. The pressure temporal evolution is characterized by the occurrence of random pressure peaks associated with a decrease and increase of the average evaporator temperature, respectively. In fact, when the centrifugal acceleration separates phases, the working fluid motion stops and the heat transport process becomes ineffective. Then, it occurs a decrease of the acceleration level or an increase of pressure in order to allow the working fluid to redistribute properly: the standoff condition is overcome and the device restarts its operation.

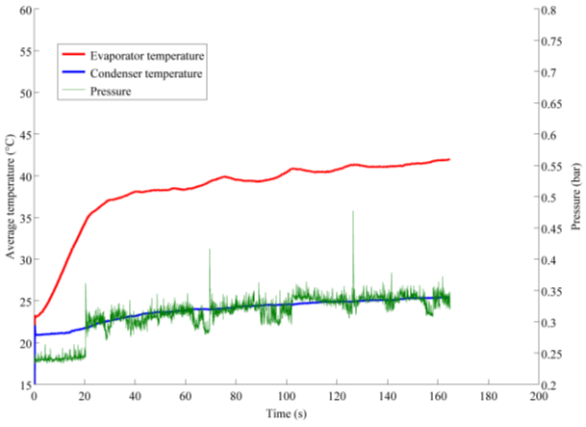


Figure 10. Small diameter CLPHP: flight test.

The flight test results relative to the large diameter CLPHP are reported in Fig. 11. The centrifugal component of the acceleration significantly affects the distribution of the working fluid: the liquid phase is pushed towards the peripheral region of the device while the vapour phase occupies the central region. As such a distribution is not at all optimal, the heat exchange process is not effective and the average evaporator temperature is higher with respect to the vertical case. It is worth to note that, a few moments before the end of the test, a failure in one of the heating elements prevents heat power to be provided to the evaporator section and the average evaporator temperature and pressure decrease.

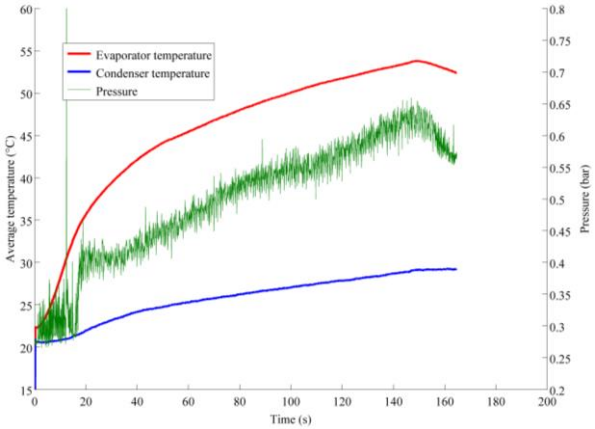


Figure 11. Large diameter CLPHP: flight test.

4 CONCLUSIONS

The thermal response of two tested CLPHPs is investigated on board REXUS 18 sounding rocket. The CLPHPs are made by aluminum tubes folded in a double-layer configuration and filled with FC-72. The difference between the devices regards the inner tube diameter that is larger (3 mm) and slightly smaller (1.6 mm) than a critical diameter defined on static Earth gravity conditions. The experimental test-cell includes: the condenser section, embedded in a phase change material, which absorbs heat via latent heat of fusion in order to keep the evaporator temperature to a nearly constant value; the evaporator section, consisting of wire-shaped heating elements wrapped around the evaporator curves.
Due to a malfunction of the rocket de-spin system, the condition of milli-gravity has not been achieved, so it was not possible to observe the expected net transition in the temperatures and pressure temporal evolutions associated with the occurrence of the slug and plug flow pattern within the device. The following considerations resume the major outcomes of the present work.
The behavior of the small diameter CLPHP confirms the literature results. The centrifugal acceleration from hyper-gravity condition seems to affect positively the thermal performance with respect to horizontal orientation, due to the promotion of the working fluid motion. However, the thermal performance in vertical

position on ground is the best, as gravity acts always from condenser to evaporator.

The overall thermal performance of the large diameter CLPHP in hyper-gravity condition is confirmed better with respect to horizontal position, despite more considerations about the internal motion of the fluid have to be done. The large diameter CLPHP in hyper-gravity condition is more sensitive to the centrifugal acceleration: the liquid and vapor phases hold relatively in the peripheral and central parts of the device. Instead, on ground, the CLPHP is affected by the stratification of the working fluid within the device, as surface tension is not able to balance buoyancy. When in vertical position, the liquid and vapor phases resides in the evaporator and condenser section, respectively and the device behaves like a two-phase thermosyphon. When in horizontal position, the liquid and vapor phases resides in the bottom and upper device planes, respectively, and the device operates intermittently whenever a sufficient temperature gradient arises between the planes to push some liquid in the upper plane.

4.1 Future perspectives

Complete characterization of a large diameter CLPHP needs a long duration milli-gravity environment. The absence of such requirement in REXUS 18 sounding rocket leads the development of a new experiment, an upgraded version of PHOS project, which has been proposed for the 21/22 REXUS campaign. In such experiment, the main aim is still testing a large diameter pulsating heat pipe, however it has the possibility to improve the set-up of PHOS project, starting from its results.

A new design of the large CLPHP is presented, in order to allow more compactness and better performances: instead of a tube with 14 planar turns disposed on a double-layer, the layout will be staggered and an aluminum plate brazed perpendicular to the turns. The aluminum plate interfaces with the box, in order to guarantee the airtight of the box. The new design will be better implemented on board the REXUS rocket and on future applications, in particular the device will allow a better design of the experiment box sealing.

Moreover new accurate studies on the phase change material will be done, in order to improve the thermal conductivity of the paraffin by using a metallic foam. Different types of foam will be tested on ground in order to analyze the characteristic and the best choice.

REFERENCES

1. Akachi, H. (1990). Structure of a heat pipe. *US Patent* 4.921.041.
2. Akachi, H. (1993). Structure of micro-heat pipe. *US Patent* 5.219.020.
3. Zhang, Y. & Faghri, A. (2008). Advances and unsolved issues in pulsating heat pipes. *Heat Transfer Eng.* 29, 20-44.
4. Gu, J., Kawaji, M. & Futamata, R. (2004). Effects of gravity on the performance of pulsating heat pipes. *J. Thermophys. Heat Transfer* 18, 371-378.
5. Mameli, M., Araneo, L., Filippeschi, S., Marelli, L., Testa, R. & Marengo, M. (2014). Thermal response of a closed loop pulsating heat pipe under a varying gravity force. *Int. J. Therm. Sci.* 80, 11-22.
6. Mangini, D., Mameli, M., Georgoulas, A., Araneo, L., Filippeschi, S. & Marengo, M. (2015). A pulsating heat pipe for space applications: ground and microgravity experiments. *Int. J. Therm. Sci.* 95, 53-63.
7. Mameli, M., Marengo, M. & Khandekar, S. (2014). Local heat transfer measurement and thermo-fluid characterization of a pulsating heat pipe. *Int. J. Therm. Sci.* 75, 140-152.
8. Mameli M., Mangini D., Vanoli G., Filippeschi S., Araneo L., Marengo M., Multi-Evaporator Closed Loop Thermosyphon, *7th European Japanese Two Phase Flow Group Meeting*, 11-15 October 2015, Zermatt (CH).

INTERACTION OF LASER EXPOSED NON-ANTIBIOTIC SOLUTIONS WITH TARGET SURFACES IN HYPERGRAVITY CONDITIONS: ESA "SPIN YOUR THESIS!" CAMPAIGN

Ágota Simon[1,2], Alexandru Stoicu[1], Tatiana Tozar[1], Mihail Lucian Pascu[1,2]

[1]Laser Spectroscopy Group, Laser Department, National Institute for Laser, Plasma and Radiation Physics, 409 Atomiștilor, 077125, Măgurele, Ilfov, Romania
[2]Faculty of Physics, University of Bucharest, 405 Atomiștilor, 077125, Măgurele, Ilfov, Romania
agota.simon@inflpr.ro, alexandru.stoicu@inflpr.ro, tatiana.alexandru@inflpr.ro, mihai.pascu@inflpr.ro

ABSTRACT

The present study highlights the HyperMed project, conducted under the aegis of European Space Agency within the "Spin Your Thesis!" 2015 programme.
Experiments have been carried out at the Large Diameter Centrifuge, developed by ESA at ESTEC, Noorwijk, The Netherlands.
The aim of the experiments was to investigate the interaction of unirradiated and laser irradiated medicine solutions with different target surfaces under hypergravity conditions, by means of contact angles of medicine drops formed on the target surfaces, in view of biomedical applications in space.

1. INTRODUCTION

1.1. "Antibiotic revolution"

The discovery of penicillin in 1929 by Alexander Fleming, one of the most significant medical exploit of the 20th century, made possible the arising of antibiotics. They proved to be a life changing factor in the fight against some of the most menacing diseases of the last century. However, not long after the introduction on the market in 1943 of penicillin, reports regarding bacterial resistance pop up [1].
Overuse and misuse of antibiotics has led to increasing rates of drug resistance, multiple drug resistance (MDR) and even extreme drug resistance (XDR) acquired by bacteria. In this way, several pathogenic microorganisms became virtually untreatable [2]. Since the impending modern medicine relies upon more and more effective antibiotics [3], while fewer and fewer new classes are discovered, resistant bacteria have emerged and spread, thus evolving into a serious threat to the public health, requiring urgent action [4,5].
Therefore, it became pressing to uncover alternative treatment solutions: to discover/produce new medicines or to improve the action of the existing ones. Since the advancement of antibiotic resistance, other classes of drugs with antimicrobial activity, like non-antibiotics, were brought into the spotlight. Non-antibiotics may reduce or reverse antibiotics resistance of a variety of pathogenic bacteria [6,7].

Within the "Spin Your Thesis!" 2015 campaign a specific group of non-antibiotics belonging to the phenothiazine family of drugs, known as psychotherapeutic agents, was utilized to perform experiments under hypergravity conditions.

1.2. Why phenothiazines?

Phenothiazines are photosensitive compounds, therefore they can be subjected to modifications at molecular level once exposed to white light or UV radiation. In order to speed up the process of degradation of the parental compound and generation of new photoproducts, a monochromatic and high energy UV laser beam is used [8,9]. The specific exposure of phenothiazines yields new products with increased antibacterial activity compared to the unirradiated initial (parent) compound [8].
Four phenothiazine derivatives have been prepared for hypergravity studies. Chlorpromazine (CPZ) is an antipsychotic drug that has some antimicrobial, fungistatic and fungicidal effects as well [10]. CPZ in ultrapure water solutions exposed to UV laser beam for long time intervals (4-24 h) generated photoproducts with increased antibacterial activity against *Staphylococcus aureus* and *Escherichia coli* [11]. Promazine (PZ), has the potential to improve the cytotoxic activity of doxorubicin against human adenocarcinoma cells [12]. Promethazine (PMZ) can reduce nausea, migraine, allergy, insomnia and, most important, motion sickness in the case of space missions applications. Thioridazine (TZ) is efficient in the therapy of totally drug resistant tuberculosis (TB), investigated by [13,14] and its use in space against TB may be of interest.

1.2.1. Interaction of drug solutions with target surfaces

The aim of the study was to bring into light a new insight about the impact of high g levels on medicine solutions in bulk and on the wettability of hydrophilic and hydrophobic surfaces of drug solutions contained in droplets. A comparison between measured contact angles formed with different target surfaces by

unirradiated and irradiated phenothiazine solutions was possible to be made.
As hydrophilic surfaces, cotton and activated charcoal have been selected in order to perform experiments due to the fact that cotton is one of the main materials used in medical treatments; once impregnated with medicine solutions it may be viewed as a drug delivery system to skin and wounded areas of the infected tissues. The activated charcoal may be utilized to absorb humidity present onboard spacecrafts and to perform pathogenic decontamination on spacecraft's surfaces during long-term space missions. It may also be used on humans as a medicine by itself.
Regarding the hydrophobic surfaces, Parafilm M and aluminum were tested because they can imitate tubing, and respectively cables and spacecraft's walls, for decontamination purposes.

1.3. Why hypergravity conditions?

Time spent in space by humans has increased with the advancement of explorations and microbial infections onboard spacecrafts spawned new medical challenges. Crew member immune dysfunctions can be crucial when it comes to execute long-lasting space missions and astronauts may require treatments against infectious diseases. Since human immune responses are weakened in space, the body is more susceptible to infections. It has been evidenced that several bacteria can survive, proliferate and even are able to turn into more virulent forms at high g- levels, thus threatening the travelers as well as spacecraft hardware [15-17]. Therefore, the interest in developing new methods to treat astronauts and decontaminate spacecraft's surfaces in case of infections, became a more and more relevant issue. An even more important and interesting topic in space exploration may consist in understanding the modifications which may occur in medicines under hypergravity conditions (even temporary). These types of investigations are necessary since the implementation of medicines is always executed after they transit hypergravity conditions at launching and may be needed after gravity variations during the flight. Also, during the flight, the medicines may be used in microgravity conditions, but it has to be taken into consideration the fact that they may already be in an altered form due to the passing through the hypergravity conditions.

2. MATERIALS AND METHODS

2.1. Medicine solutions

Non-antibiotic solutions at 20 mg/mL concentration have been prepared out of four phenothiazine drugs, CPZ ($C_{17}H_{19}ClN_2S$), PZ ($C_{17}H_{20}N_2S$), PMZ ($C_{17}H_{20}N_2S$) and TZ ($C_{21}H_{26}N_2S_2$), by dissolving them in ultrapure water and obtaining solutions as described in [18,19]. Medicines were purchased from Sigma-Aldrich in hydrochloride form, as white to off-white powders with purity ≥ 98%. The representation of the molecules three dimensional structures are shown in Fig. 1.

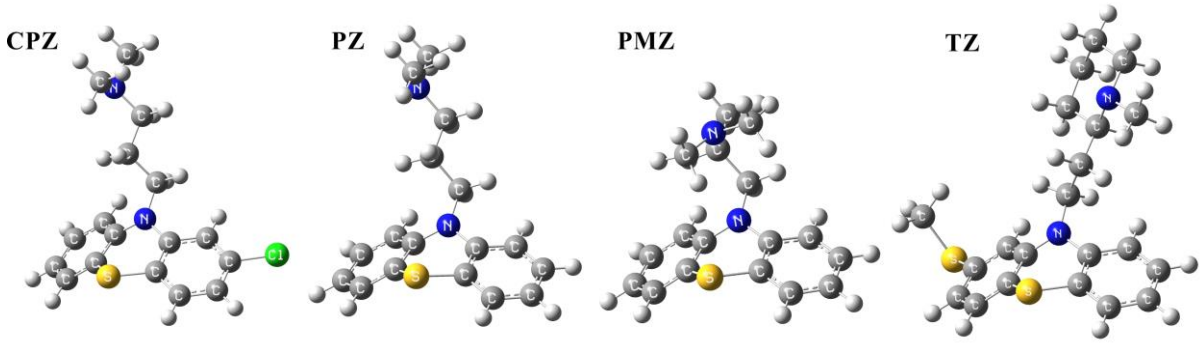


Figure 1. 3D representation of CPZ, PZ, PMZ and TZ with optimised geometry [20].

2.2. Target surfaces

Target surfaces exploited in hypergravity studies consisted of hydrophilic surfaces, such as cotton and activated charcoal, as well as hydrophobic ones, like Parafilm M and aluminum. Cotton test materials were purchased from wfk Testgewebe (DE), pharmacological charcoal products from Biofarm (ROU) and Parafilm M surfaces from Bemis Company (US). Aluminum surfaces have been cut out from raw material and then polished with emery powder and sandpaper. Medicine containing droplets have been brought in contact with the respective surfaces under different high g levels, as illustrated in Fig. 2.

2.3. Laser exposure set-up

The experimental set-up utilized to irradiate phenothiazine aqueous solutions with laser beam is introduced in [21]. CPZ, PZ, PMZ and TZ solutions have been exposed to the laser beam emitted by the forth harmonic generation (FHG) of a Nd:YAG laser with 10 Hz pulse repetition rate for time intervals ranging from 1 to 240 min.

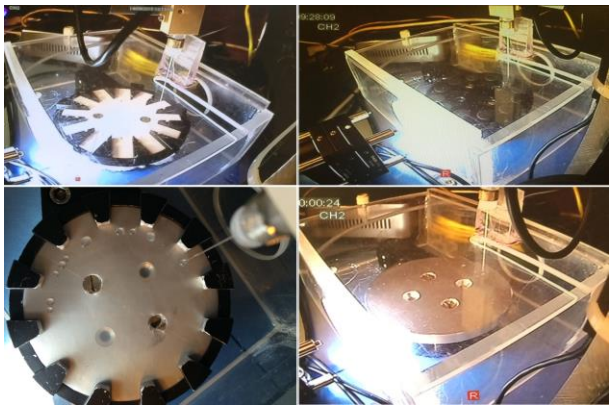


Figure 2. .Cotton, activated charcoal, Parafilm M and aluminum surfaces visualized during experiment inside the gondola of the Large Diameter Centrifuge.

The laser pulse full time width was 10 ns. For each irradiation time 2 mL solution in quartz cuvette was exposed to a beam with 6.5 mJ average energy.

2.4. The Large Diameter Centrifuge

The effect of hypergravity on the interaction of unirradiated and laser irradiated medicine solutions with target surfaces has been investigated by using the Large Diameter Centrifuge (LDC). The LDC, able to induce high g-levels, comprehends 4 rotating arms with a total of 6 swinging gondolas attached, having a maximum diameter of 8 m when gondolas are in full swing-out. Each gondola can be loaded by a maximum of 80 kg, the working space inside being 500x500x720 mm. The maximum hypergravity level which can be attained is 20 g. To seed-up the system from 1 to 20 g takes 60 s.
The system was designed to limit vibrations and at the highest g-level the LDC exhibits a maximum vibration of 0.0712 V_{RMS} within a gondola. [22,23].
Experiments of the HyperMed project were conducted under 2, 5, 10 and 20 g.

2.5. Experimental set-up of the HyperMed project

The HyperMed experiment consisted in droplet generation on target surfaces at various hypergravity levels. Microdroplets containing the studied liquid samples were produced by a programmable Cole-Parmer Compact Syringe Pump 75900-00, 100 µL glass Hamilton Gastight Syringe, a Bürkert 6650-A00 solenoid valve and a Hamilton capillary with the corresponding fittings. Before drop generation, the LDC had to reach the proposed high g-level, to produce the interaction between medicine drops and target surfaces at the settled g-level. Target surfaces were place on a Thorlabs motorized precision rotation stage, controlled by a T-Cube DC servo controller, for acquiring data at all desired g-levels with the same liquid, on the same surface without stopping the LDC. A Phantom Miro 3 high-speed camera recorded drops injection, their impact and interaction with target surfaces. Images obtained were further analysed with ImageJ together with Drop analysis-DropSnake plugin [24]. In order to get good quality images, droplets were illuminated from aside using the backlit illumination technique. This technique provides a dark and sharp silhouette of the drop with a white background, thus facilitating the detection of the contact line and the contour of the sessile drop by the contact angle software.
The full experimental assembly can be seen in Fig. 3.

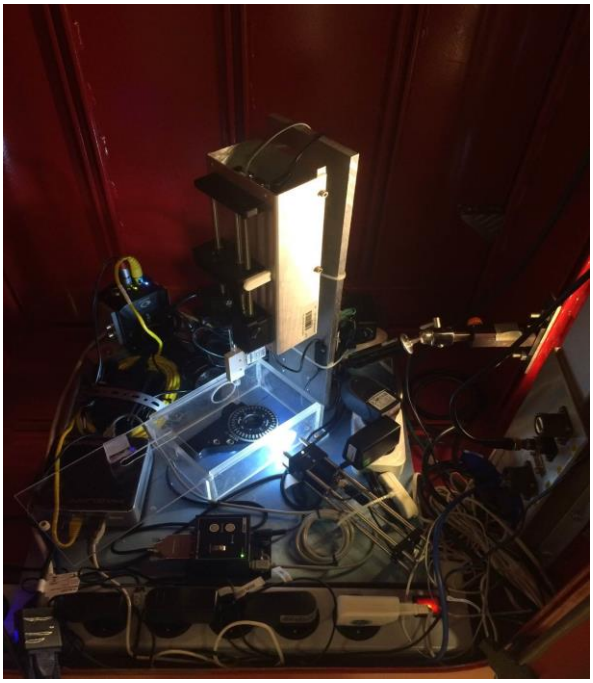


Figure 3. Final integration of the experimental set-up inside the LDC gondola

3. RESULTS

The obtained data within the “Spin Your Thesis!” campaign have shown that dynamic processes dominate the interaction between microdroplets and target surfaces. Experimentally, axial vibrations of the studied drops were observed. In the case of hydrophilic target surfaces, the dynamics presented a continuous evolution, due to the fact that solutions have been absorbed by the surface in time, contact angles undergoing a decrease as a function of time. This process is presented on Fig. 4(A), where the cotton surface had been wetted at 2 g hypergravity level by medicine solution exposed to laser radiation, the solution being almost totally absorbed after 100 ms. Regarding the hydrophobic surfaces, the absorption had been replaced by the evaporation of the drug solutions, contact angles exhibiting relatively constant evolution, as illustrated on Figure 4(B).

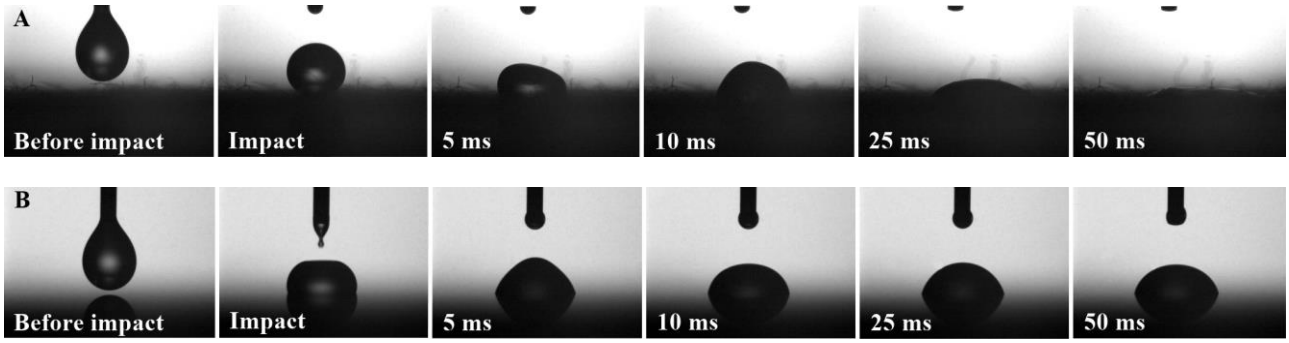


Figure 4. Time evolution of 4 h irradiated CPZ droplets on (A) cotton and (B) aluminum surfaces under 2 g conditions.

Also, a decrease in the generated drops volume under increasing hypergravity conditions was noticed.

Preliminary results have shown that under hypergravity conditions, unirradiated and 4 h irradiated CPZ solutions in microdroplets have better wetting properties on the four studied target surfaces than ultrapure water, in some cases the laser exposed solution proving to presents even better wetting properties.

4. PERSPECTIVES

The application of the laser modified phenothiazines may be conceived in two ways: on one hand to treat human patients in case of infections and on the other, to decontaminate surfaces found in the closed environment of the spacecraft from bacteria and fungi.

ACKNOLEDGEMENTS

The authors acknowledge the financing of the research by CNCS-UEFISCDI by project number PN-II-ID-PCE-2011-3-0922, by the Ministry of Education *via* NUCLEU project PN 0939/2009 and by the European Space Agency Education Office.

The HyperMed team express their gratitude to Jack J.W.A. van Loon and Alan Dowson for their help in hypergravity related issues during the sixth "Spin Your Thesis!" campaign.

The team also would like to express their appreciation for the support of ESA Education Office through Lily Ha, Lucas Pfeiffer and Nigel Savage.

REFERENCES

[1] Azevedo, M.M., Teixeira-Santos, R., Silva, A.P., Cruz, L., Ricardo, E., Pina-Vaz, C. and Rodrigues, A.G., The effect of antibacterial and non-antibacterial compounds alone or associated with antifugals upon fungi, Front. Microbiol. 6(669), 1-7, 2015.

[2] Török, E., Moran, E. and Cooke, F.J., Oxford Handbook of Infectious Diseases and Microbiology, Oxford University Press Inc., New York, 2009.

[3] Coates, A.R.M., Halls, G. and Hu, Y., Novel classes of antibiotics or more of the same?, Br. J. Pharmacol. 163, 184-194, 2011.

[4] Magiorakos, A.-P., Srinivasan, A., Carey, R.B., Carmeli, Y., Falagas, M.E., Giske, C.G., Harbarth, S., Hindler, J.F., Kahlmeter, G., Olsson-Liljequist, B., Paterson, D.L., Rice, L.B., Stelling, J., Struelens, M.J., Vatopoulos, A., Weber, J.T. and Monnet, D.L., Multidrug-resistant, extensively drug-resistant and pandrug-resistant bacteria: an international expert proposal for interim standard definitions for acquired resistance, Clin. Microbiol. Infect. 18, 268-281, 2012.

[5] Obolsky, U., Stein, G.Y. and Hadany, L., Antibiotic Restriction Might Facilitate the Emergence of Multi-drug Resistance, PLoS Comput. Biol. 11(6), 1-15, 2015.

[6] Kristiansen, J.E. and Amaral, L., The potential management of resistant infections with non-antibiotics, J. Antimicrob. Chemother. 40, 319-327, 1997.

[7] Kristiansen, J.E., Thomsen, V.F., Martins, A., Viveiros, M. and Amaral, L., Non-antibiotic Reverse Resistance of Bacteria to Antibiotics, in vivo 24, 751-754, 2010.

[8] Pascu, M.L., Nastasa, V., Smarandache, A., Militaru, A., Martins, A., Viveiros, M., Boni, M., Andrei, I.R., Pascu, A., Staicu, A., Molnar, J., Fanning, S. and Amaral, L., Direct modification of bioactive phenothiazines by exposure to laser radiation, Recent Pat. Antiinfect. Drug Discov. 6(2), 1-13, 2011.

[9] Pascu, M.L., Danko, B., Martins, A., Jedlinszki, N., Alexandru, T., Nastasa, V., Boni, M., Militaru, A., Andrei, I.R., Staicu, A., Hunyadi, A., Fanning, S. and Amaral, L., Exposure of chlorpromazine to 266 nm laser beam generates new species with antibacterial properties: contributions to development of a new process for drug discovery, PLoS ONE 8(2), 1-16, 2013.

[10] Sudeshna, G. and Parimal, K., Multiple non-psychiatric effects of phenothiazines: a review, Eur. J. Pharmacol. 648(1-3), 6-14, 2010.

[11] Alexandru, T., Armada, A., Danko, B., Hunyadi, A., Militaru, A., Boni, M., Nastasa, V., Martins, A.,

Viveiros, M., Pascu, M.L., Molnar, J. and Amaral, L., Biological evaluation of products formed from the irradiation of chlorpromazine with a 266 nm laser beam, Biochem. Pharmacol. 2(1), 1-4, 2013.

[12] Kuzma-Richeret, A., Saczko, J., Choromańska, A., Dumanska, M., Drag-Zalesinska, M., Wysocka, T., Chwilkowska, A., Pola, A., Mosiądz, D., Marcinkowska, A. and Kulbacka, J., The Influence of Phenothiazine Derivatives on Doxorubicin Treatment in Sensitive and Resistant Human Breast Adenocarcinoma Cells, Folia Biol. (Praha) 57, 261-267, 2011.

[13] Amaral, L., Thioridazine: an Old Neuroleptic effective against Totally Drug Resistant Tuberculosis, Acta Med. Port. 25(2), 118-121, 2012.

[14] Amaral, L. and Molnar, J., Why and how thioridazine in combination with antibiotics to which the infective strain is resistant will cure totally drug-resistant tuberculosis, Expert Rev. Anti-Infect. Ther. 10(8), 869-873, 2012.

[15] Guéguinou, N., Huin-Schohn, C., Bascove, M., Bueb, J.L., Tschirhart, E., Legrand-Frossi, C. and Frippiat, J.P., Could spaceflight-associated immune system weakening preclude the expansion of human presence beyond Earth's orbit? J. Leukoc. Biol. 86(5), 1027-1038, 2009.

[16] Taylor, K., Kleinhesselink, K., George, M.D., Morgan, R., Smallwood, T., Hammonds, A.S., Fuller, P.M., Saelao, P., Alley, J., Gibbs, A.G., Hoshizaki, D.K., von Kalm, L., Charles A. Fuller, C.A, Beckingham, K.M. and Kimbrell, D.A., Toll Mediated Infection Response Is Altered by Gravity and Spaceflight in Drosophila, PLoS ONE 9(1), 1-12, 2014.

[17] Wilson, J.W., Ott, C.M., zu Bentrup, K.H., Ramamurthy, R., Quick, L., Porwollik, S., Cheng, P., McClelland, M., Tsaprailis, G., Radabaugh, T., Hunt, A., Fernandez, D., Richter, E., Shah, M., Kilcoyne, M., Joshi, L., Nelman-Gonzalez, M., Hing, S., Parra, M., Dumars, P., Norwood, K., Bober, R., Devich, J., Ruggles, A., Goulart, C., Rupert, M., Stodieck, L., Stafford, P., Catella, L., Schurr, M.J., Buchanan, K., Morici, L., McCracken, J., Allen, P., Baker-Coleman, C., Hammond, T., Vogel, J., Nelson, R., Pierson, D.L., Stefanyshyn-Piper, H.M. and Nickerson, C.A., Space flight alters bacterial gene expression and virulence and reveals a role for global regulator Hfq. Proc. Natl. Acad. Sci. USA 104, 16299-16304, 2007.

[18] Smarandache, A., Kristiansen, J., Christensen, J.B. and Pascu, M.L., Optical studies of the spectral properties of phenothiazines, Lett. Drug Des. Discov. 9(4), 352-360, 2012.

[19] Dinache, A., Boni, M. and Pascu, M.L., Phenothiazine derivatives interaction with laser radiation, Rom. Rep. Phys. 65(3), 1078-1091, 2013.

[20] Frisch, M.J., Trucks, G.W., Schlegel, H.B., Scuseria, G.E., Robb, M.A., Cheeseman, J.R., Scalmani, G., Barone, V., Mennucci, B., Petersson, G.A., Nakatsuji, H., Caricato, M., Li, X., Hratchian, H.P., Izmaylov, A.F., Bloino, J., Zheng, G., Sonnenberg, J.L., Hada, M., Ehara, M., Toyota, K., Fukuda, R., Hasegawa, J., Ishida, M., Nakajima, T., Honda, Y., Kitao, O., Nakai, H., Vreven, T., Montgomery, J.A., Peralta Jr., J.E., Ogliaro, F., Bearpark, M., Heyd, J.J., Brothers, E., Kudin, K.N., Staroverov, V.N., Keith, T., Kobayashi, R., Normand, J., Raghavachari, K., Rendell, A., Burant, J.C., Iyengar, S.S., Tomasi, J., Cossi, M., Rega, N., Millam, J.M., Klene, M., Knox, J.E., Cross, J.B., Bakken, V., Adamo, C., Jaramillo, J., Gomperts, R., Stratmann, R.E., Yazyev, O., Austin, A.J., Cammi, R., Pomelli, C., Ochterski, J.W., Martin, R.L., Morokuma, K., Zakrzewski, V.G., Voth, G.A., Salvador, P., Dannenberg, J.J., Dapprich, S., Daniels, A.D., Farkas, O., Foresman, J.B., Ortiz, J.V., Cioslowski, J. and Fox, D.J., Gaussian 09, Revision C.01. Gaussian Inc., Wallingford, CT, 2010.

[21] Simon, A., Alexandru, T., Boni, M., Damian, V., Stoicu, A., Dutschk, V. and Pascu, M.L., Interaction of solutions containing phenothiazines exposed to laser radiation with materials surfaces, in view of biomedical applications, Int. J. Pharm. 475, e270-281, 2014.

[22] van Loon, J.J.W.A. and Dowson, A., Large Diameter Centrifuge (LDC) Experimenter Users Manual, ESA, 2014.

[23] van Loon, J.J.W.A., Krause, J., Cunha, H., Goncalves, J., Almeida, H. and Schiller, P., The Large Diameter Centrifuge, LDC, for life and physical sciences and technology, Proc. of the "Life in Space for Life on Earth Symposium", Angers, France, 2008.

[24] Stalder, A.F., Kulik, G., Sage, D., Barbieri, L. and Hoffmann, P., A Snake-Based Approach to Accurate Determination of Both Contact Points and Contact Angles, Colloids Surf. A Physicochem. Eng. Asp. 286(1-3), 92-103, 2006.

EFFECT OF HYPERGRAVITY ON BACTERIAL MOTILITY AND HEAT RESISTANCE

Aspridou Zafiro [(1)], Kakagianni Myrsini [(1)], Dimakopoulou- Papazoglou Dafni [(2)], Koutsoumanis Konstantinos [(1)]

[(1)] Lab.of Food Microbiology and Hygiene, Dep. of Food Science and Technology, School of Agriculture, Faculty of Agriculture, Forestry and Natural Environment, Aristotle University of Thessaloniki, Thessaloniki, Greece, PO Box 265 Email: zasprido@agro.auth.gr, mkakagianni@agro.auth.gr, kkoutsou@agro.auth.gr

[(2)] Lab.of Food Engineering and Processing, Dep. of Food Science and Technology, School of Agriculture, Faculty of Agriculture, Forestry and Natural Environment, Aristotle University of Thessaloniki, Thessaloniki, Greece, PO Box 265, Email: ddimakop@agro.auth.gr

ABSTRACT

Microorganisms on Earth surface face several changes in the prevailing environmental conditions through their lifetimes. One of the few constant parameters on our planet over times is gravity. This probably indicates that all living entities have been strongly adapted to it. Gravity, as a mechanical stressful force, can decisively affect basic life processes and possibly induce response mechanisms. The effect of hyper-gravitational field will be studied on two basic aspects of microbial behavior, such as heat resistance and motility. The resistance that microorganisms exhibit to thermal stress determines their survival in their natural habitats and after the application of thermal processing. Heat resistance studies are of great importance for the unraveling of the mechanisms governing gene and protein expression and further microbial responses. Microbial traits, like invasion and virulence for the pathogens, spore germination and outgrowth for the endospore-formers, sensitivity to other stresses, cross protection phenomena and biofilm formation have been found in many cases to be related with heat resistance. Microbial motility benefits bacteria through the capacity to move toward favorable environments and to avoid detrimental conditions, as well as contributes to dispersal and colonization of new niches, thus enabling successful competition with other microorganisms. Motility is generally regarded as a virulence factor and is found critical for biofilm development and maturation contributing indirectly to increased resistance of the motile population. Both these traits are considered crucial for microbial cells in the struggle for survival and growth. Based on the above and the lack of literature data on the effect of low to moderate hyper-gravity levels (<20 g) on these microbial characteristics, the objectives of the present study are the determination of the effects of hyper- gravity on (i) the heat resistance of vegetative cells and spores of bacteria both at population and molecular level as well as (ii) the microbial swimming motility. It is expected that the outcomes of the experiment, beyond the scientific interest, could be valuable tools in order to design new processes, select microorganisms with beneficial technological and functional properties, effectively control microbial load and develop alternative approaches to cope with infections.

1. SCIENTIFIC BACKGROUND

Living organisms and microorganisms on Earth surface face several changes in the prevailing environmental conditions through their lifetimes. One of the few constant parameters on our planet over times is gravity. This probably indicates that organisms have strongly been adapted to it. Since the bloom of space science and the planetary missions (manned or not) new horizons have opened as well as novel possibilities and new problems have emerged. The evolution in these fields introduced this new parameter. Gravity, as a mechanical stressful force, provides a stimulus that decisively affects basic life processes, such as biosynthesis, cell growth and development (Clément, 2006) and possibly induces response mechanisms in the organisms facing differentiated levels of it.

A really decisive property of microorganisms, which determines their survival, is the resistance that exhibit to different stresses both in their natural habitats as well as after the applications of processes aiming at their control. The most widespread action that has been applied so far for the restriction of microbial load is the thermal processing. Inherently, different microbial genera and species exposed to the same heat stress conditions correspond differently (Bacon et al., 2003). Vegetative cells and spores express different susceptibility to thermal stress, while mesophiles are more sensitive than thermophiles microorganisms (Block, 2001). The thermal resistance of a particular microorganism is affected by the various predominant environmental conditions before, during and after the heat treatment (Block, 2001) and the physiological state of the cells (Casadei et al., 2001).

Heat resistance studies are of great importance from a scientific point of view for the unraveling of the mechanisms governing gene and protein expression and further microbial responses. Microbial traits, like invasion and virulence for the pathogens, spore germination and outgrowth for the endospore-formers, sensitivity to other stresses, cross protection phenomena and biofilm formation have been found in many cases to be related with heat resistance (Block, 2001; Sirsat et al., 2011; Wesche et al., 2009). From a safety point of view, quantitative data concerning the heat resistance of various microorganisms could be valuable tools in order

to design thermal processes, or to adjust them, to find combinations of milder processes and interventions with the same effect and effectively control microbial load in several environments. On the other hand, the studied heat resistance of some microorganisms that present beneficial technological and functional properties can be used for their selection and utilization for several terrestrial and extra-terrestrial processes.

Regarding the effect of hyper-gravity on microbial behavior most of the available studies deal with the growth behavior or survival of various microorganisms. To the best of our knowledge, there is only one study concerning the effect of the exposure of a living organism (fruit fly *Drosophila melanogaster*) to hyper-gravity conditions (3-5 g) on the resistance to the subsequent heat stress (Le Bourg and Minois, 1997). The authors have attributed the increased heat resistance of the organism to the mild shock (gravity) applied prior to the severe thermal stress through the induction and expression of heat shock proteins (Minois et al., 1999).

Microbial motility, arguably the most fascinating property of living microorganisms, benefits bacteria through the capacity to move toward favorable environments and to avoid detrimental conditions, as well as contributes to dispersal and colonization of new niches, thus enabling successful competition with other microorganisms (Hibbing et al., 2010). Many bacteria are motile by virtue of peritrichous or polar flagella, and motility is generally regarded as a virulence factor, facilitating the colonization of host organisms or target organs by pathogenic bacteria (Duan et al., 2013). Apart from that, motility is found critical for biofilm development and maturation contributing indirectly to increased resistance of the motile population (Van Houdt and Michiels, 2010). From a health and safety point of view, the study of bacterial motility and specific organelles, such as flagella can help in order to develop organelle and mechanism based approaches to cope with infections.

There are only a few studies about the effect of altered gravity on cellular motility behavior. In the Hypergravity 3000 machine experiment (Johnson and Waldbeser, 2007), human monocyte cultures were exposed to increased gravity levels and their motility was found to be reduced. Regarding bacterial motility, there are data for *Salmonella* Typhimurium behavior which was affected under microgravity conditions (Alexandrov et al., 2009).

Both these traits are considered crucial for microbial cells in the struggle for survival and growth. However, there are no available studies on the effect of low to moderate hyper-gravity levels (<20 g) on these microbial characteristics. Based on the above, the objectives of the present study are the effect of hyper-gravity on: i) microbial heat resistance and ii) microbial swimming motility.

2. EXPERIMENTAL PROCEDURE

The experiment was conducted in the Large Diameter Centrifuge of the European Space Research and Technology Center in Noordwijk, The Netherlands within European Space Agency (ESA) 'SpinYourThesis2015' campaign. The effect of hyper-gravity on i) the heat resistance of vegetative mesophilic cells and spores of thermophilic bacteria and ii) the microbial swimming motility were studied.

Objective 1: Different combinations of hyper- gravity level and temperature were used in order to obtain survival data based on the plating method after certain duration of the trials in order to calculate D values. *Salmonella enterica* ser. Agona and *Geobacillus stearothermophilus* were employed as representative members of vegetative mesophiles and thermophilic spore-formers, respectively. For the mesophiles, two temperature levels and two gravity levels were studied, while for the thermophilic endospore formers, two temperature levels and one gravity level was used (Tab. 1). The temperatures selected and the exposure times were based on literature data, since these are the most frequently used time-temperature combinations for the heat resistance studies of representative members of mesophilic (Humpheson et al., 1998; Juneja et al., 2001; Silva and Gibbs, 2012) and thermophilic (Georget et al., 2014; Iciek et al., 2006; Somavat et al., 2012) microorganisms. Control samples were conducted at 1g.

For this purpose, an oil-bath was loaded on a gondola of the Large Diameter Centrifuge (ESTEC, ESA) in order to perform heat inactivation trials under hyper-gravity conditions. Two runs were conducted for each temperature and gravity level combination. For each run, 4 tubes (as replicates) were used. Just before the run, the rack with the tubes was immersed in the oil-bath with the desired temperature adjusted. The microorganisms faced the thermal stress and the effect of hyper - gravity for a relatively short duration (almost 10 min) of the run. The oil bath was equipped with a temperature indicator and temperature data logger. After the adjustment of the oil bath settings, temperature was maintained stable throughout the experiment without any additional control.

Sample analysis was based on the collection of survival data through the standard plating method in order to calculate D-values. Specifically, the tubes with the samples were analyzed in the LIS laboratory before the run (Initial population: N_0) and immediately after the completion of each run (Final population: $N_{residual}$). Portions (1ml) of each tube were used as samples and properly diluted and surface plated on solid laboratory media. After the incubation of the Petri plates at optimum temperature for 48-72h, the number of the colonies formed on the plate was counted in order to estimate the part of the initial population that survived the treatment. The D value, which is defined as the time for reducing the viable population by 1 decimal

logarithm (90%), is calculated based on the population reduction.

Table 1. Temperature and hyper-gravity level combinations for the objectives

Objective	Type of microorganism	Temperature	Gravity
1	Mesophilic (planktonic)	57 and 65°C	1, 10, 20xg
	Thermophilic (spores)	121 and 125°C	1, 20xg
2	Mesophilic (planktonic)	ambient	1- 20xg

Objective 2: Microscopic examination of *Pseudomonas fluorescens* cells under different hyper-gravity levels at room temperature was conducted in order to monitor their swimming motility behavior. For the motility trials, various gravity levels were studied with the sample being at room temperature. These parameters were kept constant during each run. Motility behavior can be quantified in terms of cell speed, displacement etc.

For this purpose, a z-motorized microscope (Olympus BX61; Olympus) (Fig.1) equipped with a 100x objective and a AVT Pike CCD camera (F- 032B) was connected with a PC and loaded on a gondola of the LDC in order to perform motility trials under hyper-gravity conditions. The microscope was equipped with a temperature controlled stage (Linkam PE60) in order the proper temperature to be maintained in the sample throughout the experiment and a CCD camera was mounted on the microscope for time lapse microscopy experiments. The PC in the central hub of the LDC offered full control on the microscope (Z stage, illumination, imaging, filters e.t.c.) and on the camera. The whole system was remotely controlled. During each run, images were obtained at a rate of 60 frames per second for a total of 1-5 minutes after the selection of the field of view and the focal plane. The sequence of images was analyzed with an image analysis program (ImageProPlus image analysis software version 6.3 (MediaCybernetics Inc., Bethesda, MD)).

3. RESULTS

3.1. Collected data and analysis

Objective 1: Survival data were obtained from the heat inactivation trials. From the colonies counted, after the incubation of the Petri plates, the initial population (Log N_0) and the surviving population after the run (Log $N_{residual}$) were estimated for each temperature and gravity level combination. Control samples were exposed to the same time-temperature combinations at 1xg.



Figure1. Microscope experimental set up

For each combination, 2 runs were conducted and 4 replicate samples were studied in each run. The average population reduction for each run was estimated (n=4).

Objective 2: The motility behavior of *Pseudomonas fluorescens* cells was monitored by phase contrast time lapse microscopy. Images of a selected field of view were obtained at an average rate of 60 frames per second. The motility behavior of the cells was monitored for 1 or 2 minutes under stable hyper-gravity conditions at 2, 4, 10 and 20 xg. The motility behavior was also studied under dynamic gravity conditions. Profiles of increasing or decreasing g levels were also applied. 3000-6000 images were captured for each run. The sequence of images was analyzed with an image analysis program where after the tracking and counting of the cells, the cells' speed, direction and other characteristics were quantified and expressed as distributions (Fig.2).

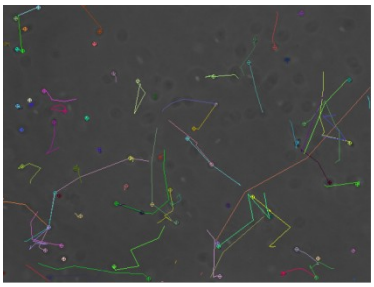


Figure 2. Image analysis- Tracking of the cells

3.2. Expected results

The outcomes of the experiment are expected to provide valuable information about the effect of hyper gravity on microbial behaviour. Beyond the scientific interest, the results of the present study could be used in order to

design new processes, select microorganisms with beneficial technological and functional properties for both terrestrial and extraterrestrial purposes, effectively control microbial load and develop alternative approaches to cope with infections. These data could also be useful in designing new disinfection procedures, even for the support of cleanliness programs for the space missions. Last but not least, exploring the evolutionary mechanisms and environmental limits of microorganism's viability is crucial for evaluating the search for life in extraterrestrial habitats (Des Marais et al., 2008; Fajardo-Cavazos et al., 2007).

4. REFERENCES

Alexandrov, L.B., Alexandrova, S., Usheva, A., 2009. Computer modeling describes gravity-related adaptation in cell cultures. PLoS ONE 4, 8332.

Bacon, R.T., Ransom, J.R., Sofos, J.N., Kendall, P.A., Belk, K.E., Smith, G.C., 2003. Thermal inactivation of susceptible and multiantimicrobial-resistant *Salmonella* strains grown in the absence or presence of glucose. Applied and Environmental Microbiology 69, 4123-4128.

Block, S.S., 2001. Disinfection, sterilization, and preservation. Lippincott Williams & Wilkins.

Casadei, M.A., Ingram, R., Hitchings, E., Archer, J., Gaze, J.E., 2001. Heat resistance of *Bacillus cereus*, *Salmonella typhimurium* and *Lactobacillus delbrueckii* in relation to pH and ethanol. International Journal of Food Microbiology 63, 125-134.

Clément, G., 2006. Introduction to space biology, in: Clément, G., Slenzka, K. (Eds.), Fundamentals of Space Biology. Springer New York, pp. 1-50.

Des Marais, D.J., Allamandola, L.J., Benner, S.A., Boss, A.P., Deamer, D., Falkowski, P.G., Farmer, J.D., Hedges, S.B., Jakosky, B.M., Knoll, A.H., Liskowsky, D.R., Meadows, V.S., Meyer, M.A., Pilcher, C.B., Nealson, K.H., Spormann, A.M., Trent, J.D., Turner, W.W., Woolf, N.J., Yorke, H.W., 2003. The NASA Astrobiology Roadmap. Astrobiology 3, 219-235.

Duan, Q., Zhou, M., Zhu, L., Zhu, G., 2013. Flagella and bacterial pathogenicity. J Basic Microbiol 53, 1-8.

Fajardo-Cavazos, P., Schuerger, A.C., Nicholson, W.L., 2007. Testing interplanetary transfer of bacteria between Earth and Mars as a result of natural impact phenomena and human spaceflight activities. Acta Astronautica 60, 534-540.

Georget, E., Miller, B., Aganovic, K., Callanan, M., Heinz, V., Mathys, A., 2014. Bacterial spore inactivation by ultra-high pressure homogenization. Innovative Food Science & Emerging Technologies 26, 116-123.

Hibbing, M.E., Fuqua, C., Parsek, M.R., Peterson, S.B., 2010. Bacterial competition: surviving and thriving in the microbial jungle. Nature reviews. Microbiology 8, 15-25.

Humpheson, L., Adams, M.R., Anderson, W.A., Cole, M.B., 1998. Biphasic thermal inactivation kinetics in *Salmonella enteritidis* PT4. Applied and Environmental Microbiology 64, 459-464.

Iciek, J., Papiewska, A., Molska, M., 2006. Inactivation of *Bacillus stearothermophilus* spores during thermal processing. Journal of Food Engineering 77, 406-410.

Johnson, C.B., Waldbeser, L.S., 2007. The effect of changes of gravity on human monocyte cell (TUR) phagocytosis. Gravitational and Space Research 19.

Juneja, V.K., Eblen, B.S., Ransom, G.M., 2001. Thermal inactivation of *Salmonella* spp. in chicken broth, beef, pork, turkey, and chicken: Determination of D- and Z-values. Journal of Food Science 66, 146-152.

Le Bourg, E., Minois, N., 1997. Increased longevity and resistance to heat shock in *Drosophila melanogaster* flies exposed to hypergravity. Comptes Rendus de l'Académie des Sciences - Series III - Sciences de la Vie 320, 215-221.

Minois, N., Guinaudy, M.-J., Payre, F., Le Bourg, É., 1999. HSP70 induction may explain the long-lasting resistance to heat of *Drosophila melanogaster* having lived in hypergravity. Mechanisms of Ageing and Development 109, 65-77.

Silva, F.V.M., Gibbs, P.A., 2012. Thermal pasteurization requirements for the inactivation of *Salmonella* in foods. Food Research International 45, 695-699.

Sirsat, S.A., Burkholder, K.M., Muthaiyan, A., Dowd, S.E., Bhunia, A.K., Ricke, S.C., 2011. Effect of sublethal heat stress on *Salmonella* Typhimurium virulence. J Appl Microbiol 110, 813-822.

Somavat, R., Mohamed, H.M.H., Chung, Y.-K., Yousef, A.E., Sastry, S.K., 2012. Accelerated inactivation of *Geobacillus stearothermophilus* spores by ohmic heating. Journal of Food Engineering 108, 69-76.

Van Houdt, R., Michiels, C.W., 2010. Biofilm formation and the food industry, a focus on the bacterial outer surface. J Appl Microbiol 109, 1117-1131.

Wesche, A.M., Gurtler, J.B., Marks, B.P., Ryser, E.T., 2009. Stress, sublethal injury, resuscitation, and virulence of bacterial foodborne pathogens. J Food Prot 72, 1121-1138.

5. ACKNOWLEDGEMENTS

We acknowledge European Space Agency Education Office and Aristotle University of Thessaloniki for their support for the participation of MAH team in 'Spin your Thesis!' 2015. Furthermore, we acknowledge ESA for the scholarship of the first author/presenter of the paper.

FROM REDEMPTION TO ARTICA. THE ROAD FROM AN EDUCATIONAL PROJECT TO AN ACTUAL DEVICE

Marcello Valdatta[(1)], Stefania Toschi[(2)], Jacopo Piattoni[(3)], Antonio Spadanuda[(4)], Federico Romei[(5)], Gian Paolo Candini[(6)], Niccolò Bellini[(7)], Davide Rastelli[(8)], Stefano Naldi[(9)], prof Fabrizio Piergenitli[(10)],

(1) University of Bologna, Aerospace Eningeering, Via Fontanelle, 40, Forlì FC, Italy; Marcello.valdatta@gmail.com
(2) University of Bologna, Metallurgy group, Department of Industrial Engineering, Via Risorgimento 4, Bologna, Italy; ste910@gmail.com
(3) University of Bologna, Aerospace Eningeering, Via Fontanelle, 40, Forlì FC, Italy; jacopo.piattoni@gmail.com
(4) University of Bologna, Aerospace Eningeering, Via Fontanelle, 40, Forlì FC, Italy ; antonio.spadanuda@gmail.com
(5) University of Southhampton,Faculty of Engineering and Envirorment, Astronautic Research Group; University of Southampton, University road, S017 1 BJ, Building 13 +44747681878lfede.pulsar@gmail.com
(6) Instituto de Astrofisica de AndalucíaGlorieta de la Astronomia, s/n 18008 Granada – Spain; gpaolo79@gmail.com
(7) NPC Spacemind, Via enrico Malatesta, Imola (BO) Italy, n.bellini@npcitaly.com,
(8) NPC Spacemind, Via enrico Malatesta, Imola (BO) Italy, d.rastelli@npcitaly.com
(9) NPC Spacemind, Via enrico Malatesta, Imola (BO) Italy, s.naldi@npcitaly.com,
(10) University of Rome "La Sapienza",DIMA department, via Edudossiana 18, 00184 Roma, Italy fabrizio.piergentili@uniroma1.it

ABSTRACT

REDEMPTION (REmoval of DEbris using Material with Phase Transition: IONospherical tests) is an experiment proposed by the former Space Robotic Laboratory (SRL) of the Faculty of Engineering of the University of Bologna ALMA MATER STUDIORUM. The working team was composed by bachelor, master and PhD students which were involved in the SRL's research activities, related to different subjects, such as the design and manufacturing of a Cubesat and Space Debris observation. REDEMPTION was selected by a panel of experts of the ESA (European Space Agency), DLR (German Aerospace Agency), SNSB (Swedish National Space Board) and SSC (Swedish Space Corporation) to fly onboard the sounding rocket REXUS in March 2012 in the framework of the REXUS/BEXUS Program (Rocket and Balloon Experiments for University Students). The experiment is based on a new technology for the Actival Debris Removing. REDEMPTION proposes a new system based on a sprayed foam that solidifies, which can be used as link between satellite and debris or like drag augmentor. This substance is a bi-component poliuretanic foam which expands and becomes rigid. After the flight the research moved ahead. After the mission, the study on the material brings new ideas to its utilization and new concept for space debris mitigation. In particular a variant of the foam was used to develop a concept for a deorbiting sail sutiable for cubesats. This sail was chosen like a payload for the cubesat Eleonora, participating to the CSDC (Canadian Satellite Design Challenge). The payload performed various test including the vibration test at David Florida Laboratory of Canadian Space Agency. Accordign with experience of Eleonora, a simple version of the sail was developed arriving to ARTICA an actual deorbiting device that will be part of the QB50 cubesat Ursa Major of University of Rome

1. SPACE DEBRIS PROBLEM

The exponential increase of satellite launches in the last 50 years has determined the problem of space debris especially in LEO. The remains of past missions are dangerous for both operative satellites and human activity in space . But not only: it has been shown that uncontrolled impacts between space objects can lead to a potentially dangerous situation for people on Earth [1]. In this scenario it is possible to reach a situation of instability where the big amount of debris could cause a cascade of collisions, the so called Kessler syndrome, resulting in the infeasibility of new space missions for many generations [2]. The space debris environment is routinely monitored by radar and optical observation systems [3]. Currently 19000 debris larger than 5 cm are tracked, while 500000 smaller than 1cm are estimated. LEO polar orbit represents the most critical and risky area. In spite of that, the gravity of the situation and of the numbers listed above is offset by the apparent easy solution to the problem: recent studies indicates that to stop the population growth could be enough to remove only 5 big debris a year. Even if it could be appear relatively a little regarding to the big amount of debris, recent technology didn't show yet the feasibility of removal. Many of these are now under study: one of that consists in the use of lasers to give a little impulse to the object and push it in a graveyard orbit or to be destroyed in the atmosphere. Another solution is the use of a satellite to rendezvous with the space junk and then use a net or a robotic arm to capture it and destroy it in

the reentry phase. Using nets or arms, the catching phase is complicated by the possibility of the debris to move freely.

2. FOAM AS ADR MISSION COMONENT

The former Space Robotic Group of the University of Bologna was involved in different research on space debris. One of the studies was to propose a new system for the ADR (active debris remove) technology. During these studies It was identified a potential method in the use of a polyurethane foam to perform the grabbing of the debris. The idea is to use this foam sprayed on the debris (fig1) to incorporate space debris and its catching thanks to its capability to solidify. This method it will be efficient even in case of tumbling of the debris. It is possible to perform two kind of mission [3][4]:

1) Not controlled removal: the two components are designed to react producing a low density, high expanded, spongy foam that incorporates the debris. The A/m ratio of the debris is increased and in this way also the ballistic parameter. As a consequence, the effect of atmospheric drag increases and the orbit life time is reduced.

2) Controlled removal: the reaction of the two components leads to a high density, medium expanded, rigid foam. The idea is to create a link between the satellite and the object: in this case the deorbit is performed by the cleaner satellite propulsion, in a smaller time compared to the first configuration. Several tests and designs are in implemented to achieve the goals of the research

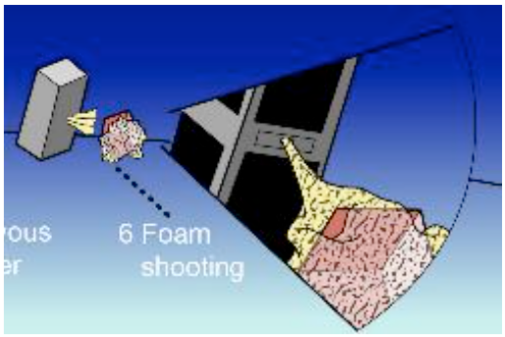


Fig 1. The satellite is spraying the debris

The foam is generated by a chemical reaction of 2 liquid components. The result of reaction is CO2 that allow to inflates the compounds, which expands. After the expansion, start the solidification. The process of foam generation and formation is really rapid, and is completed in some seconds (fig 2).



Fig2 The foam after the solidification

In order to test the capability of the foam to work in vacuum a test was performed. The test consisted in realize the reaction in a vacuum chamber and observe the result (fig 3). The test give two main results. The first one was confirming of the possibility to use the foam in space environment, the second one, unsuspected, was that there is the possibility to modify the reaction to have different level of hardness of the foam, by the regulation of the quantity of gasses produced by the reaction.[4][5]



Fig 3 Vacuum test of the foam during its fomation

The foam is produced by the reaction of two liquids mixed together .The speed of reaction and quality of the foam are influenced by the starting temperature of the reagents: this is why after several tests it has been decided to require 50°C at the moment of the fluid injection. The chemical formulation of the foam has been developed and calibrated by the producer, Duna Corradini Group.
To test the possibility to use the polyurethane foam for grabbing the debris, was performed on adhesion test: The test has been performed on aluminium, the most common material of space debris. Two aluminium beams have been cross-linked together by casting on

them the foam (without incorporating the beams to verify just the adhesion). The link was characterized by an interface surface of about 2000 mm^2. It has undergone subsequent load test, by increasing the suspended mass step by step. As a result, the maximum load supported by the link is about 6,3 kg. It was also performed a thermal test to ensure that the liquids survive to the climatic condition. The two reagent supported without problems the cold/hot cycle, passing from -19°C to 70°. The cycle was repeated 3 times on the same samples and after made them react. The result was a normal reaction. [11]

3. REXUS TEST

To test the foam in space, the foam was boarded on the Rexus sounding rocket, in frame of ESA Rexus/Bexus educational programme. The name of the experiment was REDEMPTIOM ((REmoval of DEbris using Material with Phase Transition: IONospherical tests)). [4] [5] [6] [7] [8] [9]. To test the material was developed a system for release automatically the foam. The system called “test cell”(fig4,5) had a sector in which the piston is actuated by linear springs, a sector containing the tanks of the two liquids with a heating syste,, an electronic valve and an expansion room for the foam.

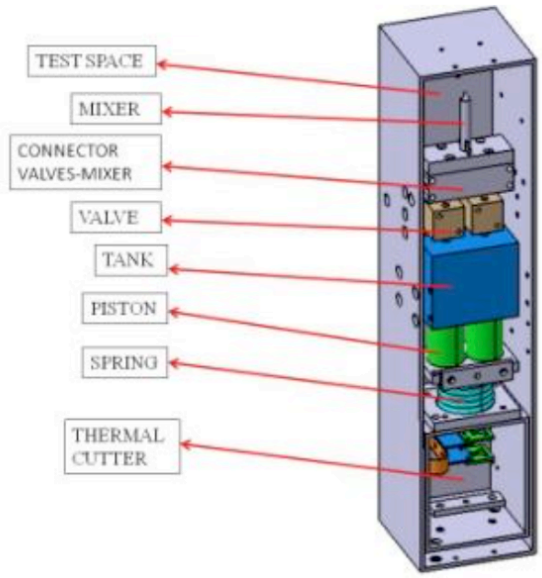


Fig 4 Test cell scheme

The test cell is provided with its own tank, separated from the other ones, consisting in a double syringe (an heating system providing to keep the liquids at the operating temperature): it contains the two reagents in separated bodies, and has a plunger that simultaneously pushes them out. The valves between the tanks and the mixers avoid that the reagents come in contact before the spring release time.

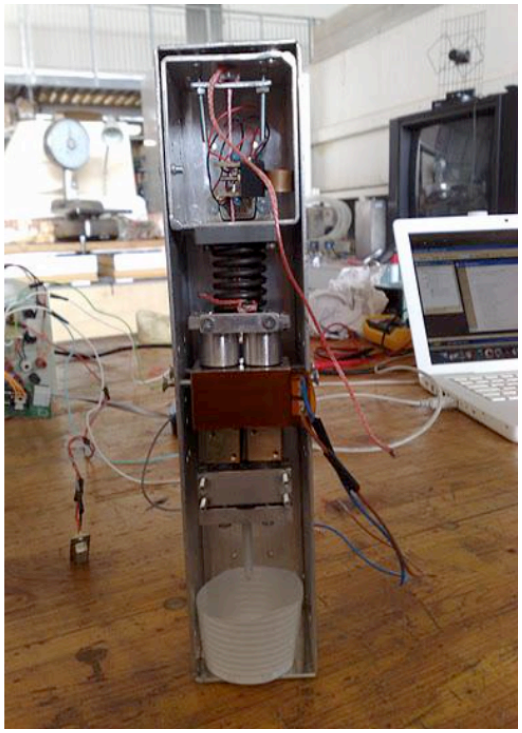


Fig 5 an actual redemption test cell

Redemption experiment flown on board of Rexus12 rocket the 18th march 2012. Unluckily, the rocket, had a malfunction and was not possible to deploy the foam. By the way the foam releasing system, passed, without problem, all the test campaign to be accepted and integrated on the rocket (fig 6,7,8,9). [5][6][7][8][9]

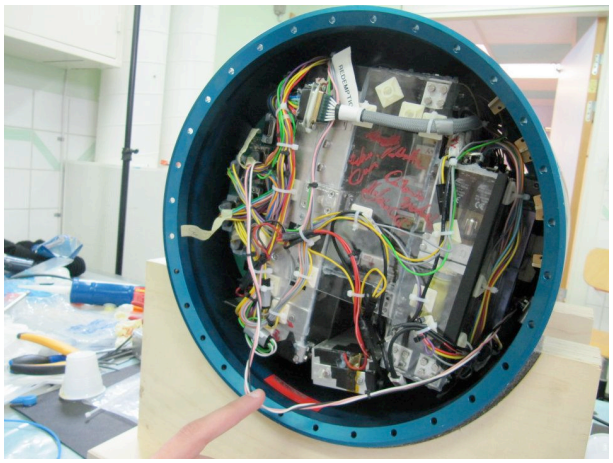


Fig 6 Rexus module ready for the integration



Fig 7 Redemption integrated in the Rexus12 Payload



Fig 8 Rexus 12 fully integrated

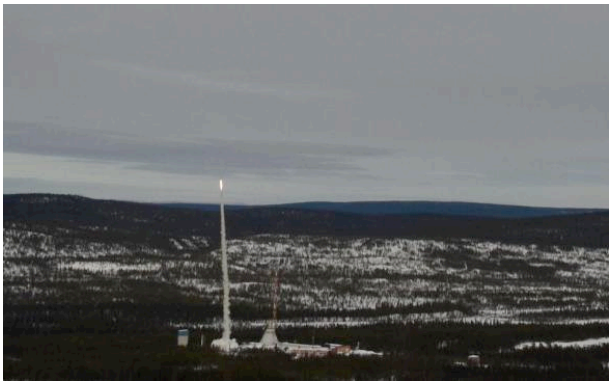


Fig 9 Rexus 12 launch

4. REDEMPTION 2

The team decide to re-submit the experiment to have an other flight opportunity, but with some change. The designed was revised in order to avoid critical issues like the consumption of some important components. The experiment was also resized (fig 10) to have a more chance to be accepted. In other hand even if simplified, the experiment was expanded. In particular was introduced the request to test in flight a new kind of foam in this case an open cell foam already preformed before the flight.

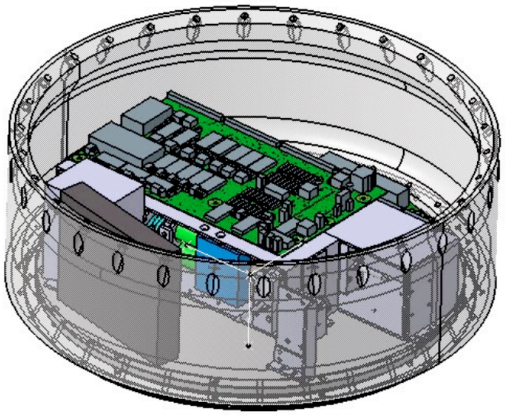


Fig 10 Redemption2 design

This foam in fact, is quite similar to foam-rubber and have the proprieties to recovery its initial shape after a compression (thanks to the elastic proprieties of the material). The idea it was to use this material to extend in space booms. After the pre-formation and pre shaping in ground, it is possible to exploit is propriety of compression (till 50 times after a dedicated calibration) to store in a small space during an eventual launch in space and after deploy it. Everything that need to be deployed in space could use this technology, for this, the test in space of this tehcnology.
Even whit this upgrade REDEMPTION2 was not be selected for the re-launch. Despite this, the team continued to work on this particular idea. An interesting application was identified with the deploy of an deorbiting sail for small satellite

5. SAIL CONCEPT

The effect of a sail is to increase of the aspect mass ratio of the satellite, the drag sail accelerates the deorbiting rate of the satellite, thereby reducing its lifetime in orbit. This drag sail, stored in a standalone box of 0.25U, could be suitable also for a 1U CubeSat, leaving enough free space for a scientific payload. The system is based on the physical principle of increasing the wet surface of the satellite to increase atmospheric drag. The perturbations induced by the drag cause the satellite to lose energy, and switch to a lower orbit. A lower orbit means more speed, and the increase of speed, together with the increased atmospheric density, causes another switch of orbit, and so on. At very low orbits, the atmosphere destroys the satellite.

The analysis of the process begins with the first equation of perturbed motion in orbit. By solving the

equation in relation with the atmospheric drag vector, it is possible to derive Equation 1, which describes the orbit lifetime in relation to several parameters:

$$(t_f - t_0) = \frac{H}{B\sqrt{\mu r}} \frac{1}{\rho_{(r_0)}} \quad (1)$$

$$B = c_d \frac{A}{m} \quad (2)$$

where (tf − t0) is the orbit lifetime, H is the scale height of the parametrization of the atmosphere, μ is the gravitational constant, r is the orbit radius, ρ(r0) is the atmospheric density at the initial altitude and B (equation 2) is the ballistic parameter [8]

Generally the sail need some structural component to be deployed like for example metallic spars or other mechanism. This mechanism has three disadvantages:

1. The system can suffer a failure due to the mechanism complication

2. The extension of a solid and metallic boom can, in case of collision with some debris, originate more microdebris.

3. Sometimes the storage space for mechanism don't make suitable the system for cubesat smaller than 3U or in other case the sail is the payload itself

The system proposed is innovative, with the spars of the sail built with a polymeric memory shape material. The chemical formulation of the material has been studied by the Space Robotic Laboratory in cooperation with several companies in order to make it suitable for the space environment [9]. The memory shape material eliminates the need of mechanical devices inside the "box" of the sail, therefore reducing the space occupied on board of the satellite and the complexity of the system.

The use of flexible material like "passive foam" for the main structure of sail is really important also considering the possible impact with other object [10, 11]: it is interesting to consider that the augmentation of area increases also the possibilities of impact with other object in space (Fig.11). For that it is important that the energy of impact is reduced in order not to create catastrophic disruption of operative satellite: polyurethane structure consists in a low density material able to drastically reduce the energy of impact and keep it under the level of 10-15 J/g defined as the threshold minimum to have a catastrophic collision with an exponential mass distribution. In that way the system is fully compatible with mitigation guidelines for which every deorbiting system should not increase the possibility of creating other debris [11,12].

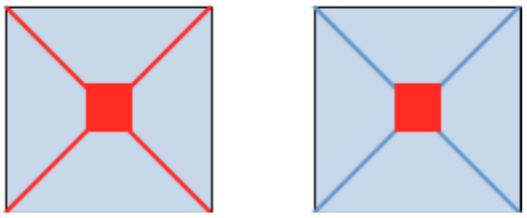


Fig 11 Difference between metallic spars and polymeric spars: the red color indicates High Energy Impact Region that causes debris generation in case of impact. Blue color indicates Low Energy Impact Region

6. DEORBITING SYSTEM DESIGN

After the selection of the dimension of the sail, the design is started form the deployment system of the sail. The box is based on a mechanical opening system that avoid any kind of electric engine. The box is kept closed by a nylon wire and actuated by a thermal cut driven by independent batteries.
The mission profile can be scheduled to open the box after the life time of the spacecraft. In order to achieve that, an electronic computer whit its own power system and a thermal cut will open the box at the predicted time. (fig 12)

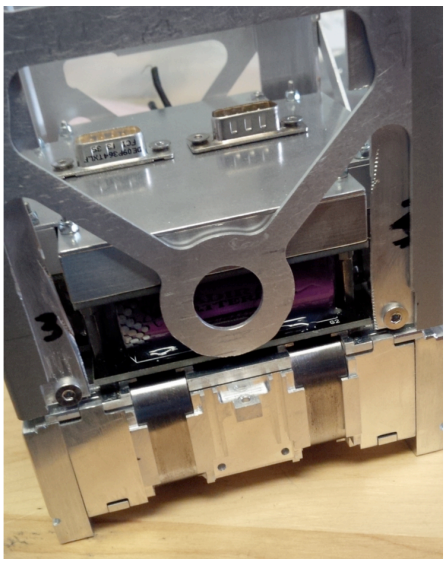


Fig 12 Artica integrated in the bottom of the satellit

The actuator system for the box opening is composed of springs. The system, initially designed to be totally standalone, is properly redundant: in fact, in case of

failure of the battery, an emergency line from the satellite supplies the system. In case of electronic failure, the system will be deployed by the action of the atomic oxygen on the wire, that will erode it. It is not possible to predict the opening time in this case, but it will surely open before the satellite orbit collapses.

7. ELEONORA

Whit the cancel of REDEMPTION2 the concept of the systems needed to be tested in space condition in some other way. The occasion was the partecipations, toghether with the Politechnique of Montreal (EPM) to the Canadian Satellite Design Challenge (CSDC) [13]
The CSDC is an interuniversity design competition aimed at developing professional-level expertise in space technologies among Cana- dian universities. The contest, which is at its second edition, involves the design, assembly and testing of a 3-unit CubeSat over a two-year period. In order to win the competition, teams must plan a one-year mission with one or more self-assigned scientific objectives, and integrate payloads related to these objectives into a 3U CubeSat standard frame

The EPM was developing a 3U cubesat for the CSDC and the former Bologna Team was invited to join the team.
The deorbiting system named ARTICA (Aerodynamic Re-entry Technology In CubeSat Application) was suitable for the mission, as the satellite was in an high orbit (700 km) whiteout the possibility to perform a re-entry manover.
The work with EPM was very useful because allowed the mechanical and electronical integration fro the first time of ARTICA with an actual satellite. Moreover professional vibration test were performed at David Florida Laboratory (DFL) of the Canadian Space Agency (CSA) (fig 13, 14)

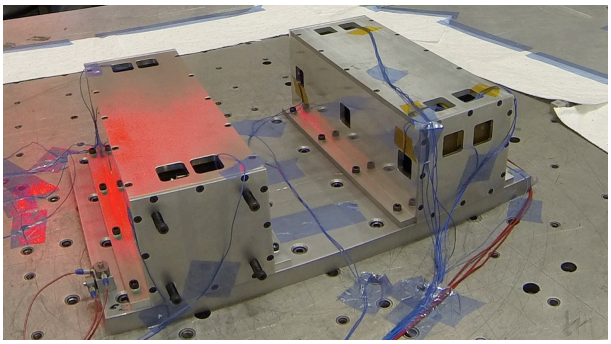


Fig 13 Eleonora/Artica vibration test



Fig 14 Eleonora Satellite

The informations collected during this 20 months program, allowed the team to validate the concept, the hardware and the electronics of the deorbiting system. In particular the system survived to the simulated rocket vibrations and integration with the satellite allow identify some issue in the electronic, now solved. Unluckily the team, even if won the third prize, didn't succeed to won the free launch and the system again couldn't be tested in flight. [14]

8. QB50

An other launch opportunity is QB50. QB50 is an atmospheric research network, where 40 CubeSats are foreseen, with one unit (the 'functional' unit) providing the usual satellite functions and the other unit (the 'science' unit) accommodating a set of sensors for lower thermosphere and re-entry research. Participating CubeSat teams are free to use any space left in the 'functional' unit of the CubeSat for a technology package or a sensor of their own choice.
The University of Rome participate to QB50 with the cubesat "Ursa Major" [15]
A part of the former Bologna's research group is now in Rome and the connection allowed to have the possibility to test the deorbiting system on board of Rome'satellite and integrate Artica on it. (Fig 15)

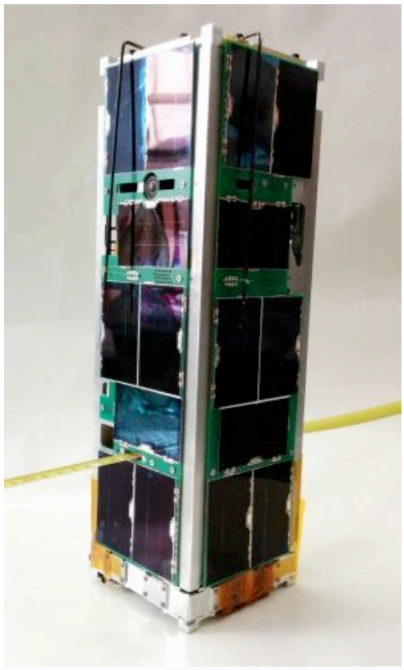


Fig 15 Artica integrated in Ursa Major

Due to the possible incompatibility with the material (as a lot of tests still need to be done and there was not sufficient time to perform them) it was not possible to use the foam sail that had to be replaced with a conventional one.
In other hands the all the architecture of the deploying systems can be considered valid and can fly. It means that will be possible to test in space a large part of the components of the original deorbiting system, and in this way will be possible to obtain fly heritage of these components.
In the meanwhile environment tests on the foam material will be scheduled and execute in order to prepare the foam sail for the next launch opportunity to prove the feasibility of the concept.

9. CONCLUSION

An innovative deorbiting system was presented. The system derived directly from an experiment on space debris active debris removal system, developed by the former Space Robotic group of the University of Bologna.
The evolution of the system is started from a sounding rocket to an actual device that will be tested in flight during the next QB50 mission.
A great part of the ground test is already performed and the flight will allow the system to gain fly heritage that will be necessary in the next flight with the foam sail. This will be important because will allow to exclude these components from an eventually malfunctions and to avoid to test in the same moment multiple components and multiple failure sources

10. REFERENCES

[1]J-C. Liou, N.L.Johnson, N.M.Hill, “Controlling the growth of future LEO debris populations with active debris removal”Acta Astronautica, Volume 66, Issues 5–6, March–April 2010, Pages 648–653.

[2]Kessler, D.J., Cour-Palais, B., “Collision frequency of artificial satellites: The creation of a debris belt”, Journal of Geophysical Research: Space Physics, Volume 83, Issue A6, pages 2637–2646, June 1978.

[3]F.Santoni, R. Ravaglia, F. Piergentili, “Analysis Of Close Approach In GEO Using Optical Measurements”, paper IAC-12,A6,5,22.p1,x14304, 63rd International Astronautical Congress, Naples, Italy, 1-5 October 2012.

[4] Valdatta, Bellini, Rastelli "ADR Mission with small satellite". Unisec 2nd Mission Idea Contest, 4th UN/Nanosatellite symposium - Nagoya 10-14/11/2012 - Published on "Innovative Ideas for Micro / Nano Satellite missions", IAA Books series - Small Satellites, Programs, Missions, Technological and applications. Sandau, Kawashima, Nakasuka, Sellers SKU:B042, ISBN: 978-2-917761-28-1

[5]Valdatta, Bellini, Rastelli, Piergentili, Santoni "Demonstration of feasibility of ADR mission usingc ubesat", IAA-B9-1407P,9th IAA "Smalle Satellites for Earth observation"; IAA Book Series, Small Satellites - Programs Missions, Technologies and Apllications. Editors: Sandau, Roser, Valenzuela ISBN 978-2-917761-32-8

[5]Piergentili F., Candini, J. Piattoni, F. Romei, A. Spadanuda, S. Toschi, M. Valdatta, F. Santoni, “REDEMPTION: a microgravity experiment to test foam for space debris removal” IAC-11-A6,5,7,x11777, 62nd International Astronautical Congress, 3 – 7 October 2011, Cape Town, SA.

[6]. Toschi, Valdatta, Spadanuda, Romei, Piattoni, Candini Santoni, Piergentili "Redemption: a student experiment proposing a solution to Active Debris Removal", IAC-12,E1,9,9,x14722, 63rd International Astronautical Congress, Naples 2012.

[7] Valdatta, Romei, Spadanuda, Toschi, Candini, Piattoni, Piergentili, Sanotni "Inflatable system based on polyurethanic foam",IAC-12,D1,1,12.p1,x15216, 63rd International Astronautical Congress

[8] Rizzitelli, Bellini, Candini, Rastelli, Romei, Locarini, Spadanuda, Valdatta, Bagassi "Active Debris System based on polyurethanefoam". 6th European conference on Space Debris ESA/ESOC 22/ 25 April

2013 Darmstadt , Germany6a.P5 ID:2818781

[9] Valdatta, Romei, Spadanuda, Toschi, Piattoni, Candini, Santoni, Piergentili; "Redemption: an experiment on sounding rocket totest a system for actival debris removal - Rexus12 ".21st ESA Symposium on European Rocket andBallon Programmes and related Research. 9 / 13 June 2013,

[10] Kerry T. Nock, Kim M. Aaron, Darren McKnight, "Removing Orbital Debris with Less Risk", DOI: 10.2514/1.A32286, Journal of Spacecraft and Rockets

[11] U.S. Government Orbital Debris Mitigation Standard Practices, NASA, 2000, http://orbitaldebris.jsc.nasa-gov/library/USG_OD_standard_practices.pdf [retrieved 3 Dec. 2012].

[12] Bellini, Locarini, Naldi,Rastelli, Valdatta, Piergentili; "A space debris cleaner kit based onpolyuretanic foam",IAC-13,A6,P,29.p1,x17013,64thInternational Astronautical Congress, Beijing, China, 2013

[13] Smyth,Bourbeau, Panerati,Bellini,Labbè, Buffet,Guay, Locarini,Naldi, Rastelli, Valdatta; "3U Cubesat for the Canadian Satellite DesignCallange: A Polytechnique of Montreal and University of Bologna cooperation."IAC-13, E2,3-V.4.4x18640,64th International Astronautical Congress, Beijing, China 2013

[14] [1] IAC-15,E1,3,8,x30090 ELEONORA, A 3U CUBESAT FOR THE CANADIAN SATELLITE DESIGN CHALLENGE - Constance Fodé Alexandre Guay, Prescilia Desroches, Mathieu Lalonde, Jacopo Panerati, Mark Smyth, Marcello Valdatta, Niccolò Bellini, Davide Rastelli, Stefano Naldi, Giovanni Beltrame)

[15] Bellini, Naldi, Rastelli, Valdatta "A.R.T.I.C.A. Deorbiting System: the new design and prototype of a compact deorbiting sail on board cubesat Ursa Maior", , IAC-15,A6,IP,30,x30649 IAC Jerusalem 2015

SESSION 4: D - Educational Programs & Strategies 2

(Thursday 10th - 11.30)

Chairman: Prof. Michéle Lavagna

REXUS PROJECT SALINE LIQUIDS AND CONDUCTIVITY IN THE ATMOSPHERE (SALACIA)

Daniel Nilson[1], Elias Krantz[2], Jonah Ekelund[*], Frej Emmoth[*], Johannes Güttler[*], William Höhlund Leuf[*], Linnea Ingeström[*], Aras Jafari[*], Filip Jensen[*], Viktor Lidström[*], Matej Lukanovic[*], Patrik Olsson[*], Marcus Persson[*], Alvaro Soria[*], Martin Svensson[*], and Jessica Ågerlind[*]

[1]*Luleå University of Technology, Kiruna, Sweden* adiino-2@student.ltu.se
[2]*Luleå University of Technology, Kiruna, Sweden* elikra-2@student.ltu.se
[*]*Luleå University of Technology, Kiruna, Sweden,* www.salacia.se

ABSTRACT

An increasing amount of data mainly from the Curiosity Mars Rover indicates that liquid brines might exist on the surface and sub-surface of Mars. As this has the potential of In-situ Resource Utilization as a water reserve on Mars it is of important value to study the processes related to formation of brines on Mars. Several calls from NASA and ESA for scientific instruments on future Mars landers and rovers have resulted in a suggestion by Professor F. Javier Martín-Torres at Luleå University of Technology (LTU) on an instrument where the brines on Mars could be studied further. Prof. Martín-Torres is the PI of the instrument called HABIT (HabitAbility, Brine, Irradiance and Temperature) recently selected by ESA to be part of the European contribution to the ESA/Roscomos Suface Platform ExoMars 2018. After Prof. Marti-Torres′ suggestion we have developed the concept of the experiment SALACIA (Saline Liquids and Conductivity in the Atmosphere). The SALACIA project is a proposed Rexus project developed by students at Luleå University of Technology performing a pre-study on brines and their interaction in a low pressure atmosphere.

The Rexus/Bexus project is a jointly funded program by the German Aerospace Center (DLR) and the Swedish National Space Board (SNSB) which gives university students the possibility to test their ideas in sounding rockets/balloons. In addition to providing a unique test environment for student projects the Rexus/Bexus project introduces the students to ESA standard documentation and design processes that otherwise might be hard to learn in a classroom environment. The Rexus/Bexus projects are finally launched from Esrange Space Centre in Northern Sweden.

The concept of the SALACIA project, expected to be launch in 2017, has been created by 16 students at LTU in Kiruna, Sweden and is currently under review by the Rexus/Bexus committee. The main goal of the project is to examine the behavioural characteristics of the brines and vessels proposed to be sent on ESA′ ExoMars Surface Platform by Professor Martín-Torres. In addition to this, the brines' interactions with a low pressure atmosphere will be examined via continous conductivity measurements thus indicating how much atmospheric water has been absorbed.

Thus, the SALACIA project, through the opportunity created by Rexus/Bexus, has the potential of generating results that might be of essential value in the development of future brine related missions to Mars where both behavioural characteristics of brines during launch and interactions with a low pressure atmosphere should be understood.

Key words: REXUS/BEXUS, SALACIA, brines, Mars, water.

1. INTRODUCTION

Mars is one of the most studied planets in the Solar system, that continues to be of interest for major space agencies around the world.[1][2] However, as master students, testing ideas and concepts related to Martian exploration might pose a challenge. This paper will describe how the REXUS/BEXUS program allow us, students at the Luleå University of Technology, to design a mission planned to be launched on a sounding rocket.

The mission is called SALACIA after the roman Goddess of salt water[3] and is the acronym for Saline Liquids and Conductivity in the Atmosphere. The first part of this paper will begin with a description of the REXUS/BEXUS program in order for the reader to understand how this program is used as a space educational activity. In addition some background fact necessary to understand the SALACIA mission will be presented.

1.1. The REXUS/BEXUS program

On the REXUS/BEXUS website one can read that:[4]

> The REXUS/BEXUS programme is realised under a bilateral Agency Agreement between the German Aerospace Center (DLR) and the Swedish National Space Board (SNSB). The Swedish share of the payload has been made available to students from other European countries through a collaboration with the European Space Agency (ESA).

The REXUS/BEXUS program is thus an opportunity for European students to test their ideas. REXUS, short for Rocket Experiments for University Students, offers the students the possibility to have their payload mounted on a sounding rocket. In addition, BEXUS, short for Balloon Experiments for University Students, allow a stratospheric research balloon to be used as a platform for the payload.[4]

The REXUS rocket is a single stage rocket that allows around 90 seconds of testing in a low gravity environment, if a despin is performed, reaching its apogee at approximately 100 km. In comparison, the BEXUS balloon can reach an altitude of 35 km but provide experiment times of 2-5 hours depending on atmospheric conditions such as wind. Annually, two rockets and two balloons are launched from Esrange in Northern Sweden.[6]

The REXUS/BEXUS process starts around 18 months before launch with a Call for proposals. This gives the students time to get organized and formulate their ideas that are supposed to be submitted 2 months later. The proposals will then undergo a review processes and the teams with ideas deemed potential for selection will get an invitation to a selection workshop at ESTEC. Around 15 months before launch the selected teams will get their acceptance to the REXUS/BEXUS program.[5]

Documentation and reviews similar to the ESA standard is a vital part of the REXUS/BEXUS program in order to prepare the students for a career in the space industry. The teams are asked to submit a proposal with information about their experiment and its goal. When chosen, the students will be asked to provide three important documents: the Student Experiment Documentation, the Campaign Requirements Plan/Flight Requirements Plan and the Flight Report Documentation. In addition to this there are numerous reviews relating to everything from the design to the integration.[5]

The Student Experiment Documentation will provide necessary information about the experiment proposed by the group of students and will be the main documentation of the experiment. Further, the Campaign Requirements Plan/Flight Requirements Plan is created in order to guarantee a successful launch and the requirements are formulated on an individual basis to each team. Lastly the Flight Report Documentation will be a short summary of the performance of the experiment during the flight and the preliminary results. Following a successful launch the students will publish their results and/or attend a seminar where they will present their results from the experiment.[5]

Being able to gather results do however necessitate that the experiment is designed to withstand the environment to which it will be exposed to during the flight. With a peak acceleration of approximately 20 g (around 200 m/s^2) and a landing velocity of around 8 m/s this requires the students to consider harsh situations that are rarely replicated during typical academic classes. In addition, fast temperature and pressure changes also needs to be considered when designing the experiment.[5]

1.2. Brines on Mars

On Mars the average surface pressure is 6 mbar and has a mean temperature of 215 K. It should be noted however that due to several factors, including the planet's eccentricity and low heat capacity due to the low atmospheric pressure, the temperature variations could be up to around 100 K between night and day. The atmosphere on Mars mostly consists of carbon dioxide but also have some other trace species as water vapour.[7]

Mars has been mapped by several orbiters in the last decade and one of the most frequent topics of research has been related to finding water and especially liquid water. However, due to the low pressure combined with the low temperature on Mars, observing liquid water on the surface has been problematic.[7] Further, in April 2015 evidences of liquid water were found during the Martian night were found after the analysis of Curiosity data.[12] These evidences were confirmed later by instruments in the Mars Reconnaissance Orbiter from NASA that in October 2015 detected seasonal variations in several Recurrent Slope Lineae on Mars, suggesting flows of water sustained by brines on the surface and subsurface.[12] Figure 1 depicts the classical idea about the flow of water on Mars. However, with the indications of brines this might have to be changed allowing for the incorporation of a more complex brine-stage for water (see Figure 2).

The presence of salts in the Martian soil is the explanation as to why liquid water is possible to exist at the low pressures on Mars. For example, chloride salts that have been observed on Mars as well as perchlorate salts can lower the freezing temperature of the water on Mars.[9][10] Perchlorate are known to be widespread over the surface on Mars thus increasing the possibility of finding brines all over the planet.[11]

One of the main reasons why liquid water, and by extension: brines, is interesting to study on Mars is because water is a requirement for life as we know it.[13] In addition, future manned missions to Mars could benefit from having access to water reserves if it turns out that there is a subsurface level of liquid brines. Having the possibility

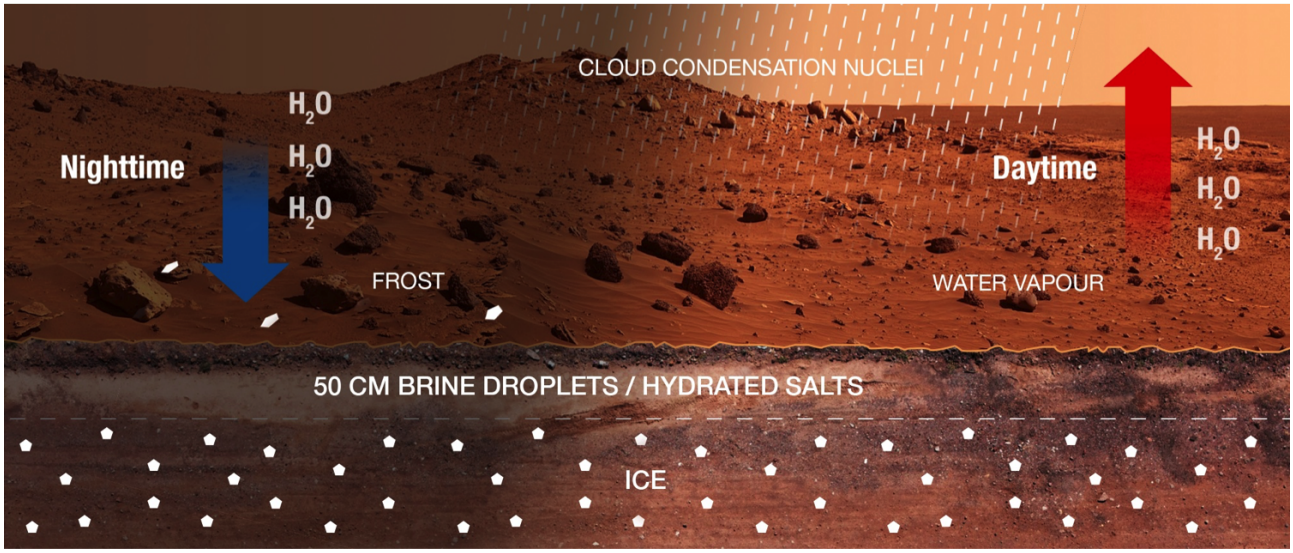


Figure 2. This picture shows the new proposed water cycle on Mars. Credits: Martin-Torres and Zorzano.



Figure 1. The traditional view on how water changes phase on Mars needs to be altered due to the discovery of brines.

of examining brines on Mars would therefore be of high interest.

2. THE SALACIA MISSION

The SALACIA mission[1], full name Saline Liquids and Conductivity in the Atmosphere, is a REXUS mission currently under review and it will hopefully help to provide useful information. The mission started with a brainstorming session to formulate the idea and it will hopefully fly in the beginning of 2017. The following section is summary of the mission including its goals, the current design of the instruments and the expected results.

[1] One can also follow the SALACIA mission at `www.salacia.se`

2.1. Goals of SALACIA

Following a series of discussions with Professor Javier Martín-Torres the interest of brines in the Martian environment was understood and suggestions had been made on how this could be examined. For instance, Professor Javier Martín-Torres and Professor Maria-Paz Zorzano jointly proposed the BOTTLE (Brines Observation Transition to Liquid Experiment) to fly with the next Mars 2020 rover. The BOTTLE experiment included taking brines that are known to exist on the surface of Mars and, through conductivity measurements, examine how much water they could extract from the Martian atmosphere. Later, BOTTLE, as part of the HABIT instrument proposed by Prof. Martin-Torres and Prof. Zorzano has been selected by ESA to be part of the ExoMars Surface Platform 2018.

There are a few challenges though and the SALACIA mission hopes to address these and thus provide a basis for future missions to Mars. Following discussions with Professor Martín-Torres it became obvious that there currently are some problems about how the salts and its containers would behave during a rocket launch. As the BOTTLE experiment propose to take salts aboard the rocket their behaviour during launch is of vital importance. The main goal of the SALACIA mission is thus the following:

> To demonstrate that SALACIA will work after exposed to launch conditions and study the behaviour of the salt during launch and identify mission-critical weaknesses for future missions to Mars.

In addition, a secondary goal from a scientific perspective is:

Characterize the ambient conditions (air temperature, relative humidity) throughout the troposphere, stratosphere and mesosphere. As well as, measure the speed with which the salts can obtain water from the atmosphere and the amount of water obtained during flight conditions.

These goals will thus hopefully help to address some of the challenges faced when designing missions to examine brines on Mars.

2.2. Instrument

In order to achieve the goals for the SALACIA mission an instrument has been developed. The design is an adapted version of the instrument proposed in the BOTTLE experiment in order for the results to be applicable to future Mars missions. Some of the design drivers during the development phase have been:

- The SALACIA instrument shall have vessels that are thermally coupled to Earth's atmosphere and exposed to airflow without the salts being able to leave the vessels. It shall be clean of the Power Supply Unit (PSU) and electronics thermal contamination.
- The SALACIA instrument shall have 5 independent vessels with a volume of 9 cm^3 each, filled with a selection of salts available on Mars. One of the vessels will be left empty to have a base of comparison and minimize measurement errors.
- The SALACIA instrument shall perform measurements on brine conductivities
- The SALACIA instrument shall perform measurements on the air temperature
- The SALACIA instrument shall perform measurements on the vessel temperature
- The behaviour of the salts shall be visually monitored using a camera system
- The salts shall be dehydrated before launch
- The instrument shall be able to operate autonomously and acquire data continuously with high frequency

These are thus the design drivers that have been formulated for the SALACIA mission and they have been of major importance during the design of the instrument. Also, it can be noted that the salts proposed to be used are chloride and perchlorates that have been found on Mars (see previous section). Information about the salts can be found in Table 1.

As said, during the rocket flight the salts will be exposed to a rapid change of temperature, pressure etc. and in order to examine how the salts behave during these conditions the each salt will be place in a 9 cm^3 vessels that will be partially filled with the salts described in table 1. In addition to this, a fifth container will be used for reference and calibration.

In order to prevent the salts from leaving the vessels during launch while still having the salts coupled to the atmosphere allowing atmospheric vapour to be captured by the salts there will be a filter on one of the sides in the vessels. This filter is yet to be selected. The preliminary design of the vessels can be seen in figure 3 where the air is supposed to flow through the middle of the setup.

The top side of the vessels will be covered in a transparent material allowing visual recordings of the salts behaviour during the flight to be made. In addition, a conductivity sensor will be placed inside each of the vessels implying how much atmospheric water vapour the salts have absorbed and if any changes in the hygroscoptic properties occur. Also, a thermometer will be placed in the experiment and with this design the instrument should thus be able to fulfill both the primary and secondary goal.

2.3. The SALACIA team

The following section is dedicated to give a description of the people involved in the SALACIA mission and how the project is structured.

Table 2 shows the students involved in the SALACIA project and several senior scientists at Luleå University of Technology has also offered assistance when needed. These involve Professor F. Javier Martín-Torres Chair of the the Atmospheric Science Group and currently Co-PI of the REMS instrument on the Mars Science Laboratory and has offered to provide scientific and engineering input. Further, Professor María-Paz Zorzano Mier also at the atmospheric group at LTU, who is also a Co-PI of the REMS instrument has offered to, in addition to scientific and engineering input, provide input on the project managing of the SALACIA mission. As mentioned before both are co-PIs of the HABIT instrument.

The SALACIA team is structured in such a way that there is a team leader, Elias Krantz, responsible for the overall workings of the project. He is assisted by the assistant project manager, Johannes Güttler, to whom Krantz is able to delegate tasks. These two people together represent the management group of the SALACIA team.

In addition to this group there are also: economy, electronics, mechanical, payload, PR and software. Due to limited number of people several different people can be a part of more then one group. The economy group is responsible to make sure that we have the sponsors needed for the development of our instrument. Meanwhile, the electronics group are responsible to develop and build the electronics needed for the instruments. The will then be placed in the structural frame built by the mechanical group. The payload group is responsible for the scientific

Table 1. The proposed salts and their properties

Salt	Chemical formula	Melting point (K)	Other	References
Magnesium Perchlorate	$Mg(ClO_4)_2$	251 (decomposition)	Strongly oxidizing	[16]
Sodium Perchlorate	$NaClO_4$	482 (decomposition)	Strongly oxidizing	[16]
Calcium Perchlorate	$Ca(ClO_4)_2$	270 (decomposition)	Strongly oxidizing	[14]
Calcium Chloride	$CaCl_2$	772 (anhydrous)		[15]

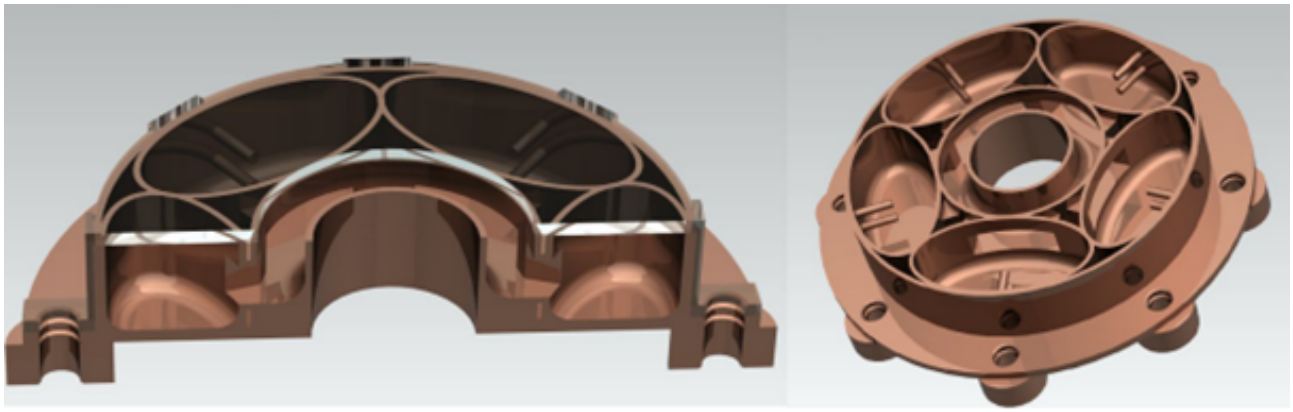


Figure 3. Preliminary design of the vessels. Left: the transparent material on the top will allow visual monitoring of the salts. Right: the airflow duct in the centre can be seen, air will then be directed into the vessels through a filter.

Table 2. A list of the people involved in the SALACIA mission

Name	Role
Elias Krantz	Team leader
Jonah Ekelund	Software Responsible
Frej Emmoth	Hardware testing
Johannes Güttler	Assistant Project Manager
William Höglund Leuf	Software Developer
Linnéa Ingeström	Finance Responsible/Assistant Software Developer
Aras Jafari	Design testing
Filip Jensen	Thermal modelling
Viktor Lidström	Electrical Design Responsible
Matej Lukanovic	Mechanical Design Responsible
Daniel Nilsson	Outreach Responsible/Assistant payload researcher
Patrik Olsson	Mechanical Design Drawing and Modelling
Marcus Persson	Hardware Modelling and Simulation
Alvaro Soria	FEM-modelling
Martin Svensson	Payload Responsible
Jessica Ågerlind	PCB Design and Assembly

background of the experiment providing the other groups with relevant limitations and demands. The PR group is responsible for the communication to the public and the software group is, as the name implies, responsible for the development of the relevant software to the project.

Deciding to structure the team like this was not obvious as concerns where raised about the possibility of these groups would create problems arising form lack of communication. This concern where partially addressed by the introduction of the assistant project manager and the understanding that a major role of the managers would be to guarantee that there was no lack of communication.

This type of structure does provide the opportunity for some benefits though as a lot of work can be made parallel thus saving a lot of time. It is also thought to be beneficial if everyone knows what is expected from them as that will allow time for sufficient research into the topic one is responsible for.

3. DISCUSSION ON THE SALACIA MISSION

The following section will provide a discussion regarding the expected results from the SALACIA mission, its challenges and more. Firstly, it can be noted that the SALACIA mission is expected to provide results that can be used when designing future missions to Mars examining brines. The results from the SALACIA mission should be able to indicate that the design and salts are able to withstand the conditions during launch. If this is not the case, indications of mission-critical weaknesses should be able to be identified. Further, the conductivity measurements and combined with the measured ambient conditions should indicate the salts ability to obtain water from the atmosphere during flight conditions.

This raises a few concerns though. As "mission-critical weaknesses" are hard to predefine measurements have to guarantee the ability to detect several different scenarios. The conductivity measurements will be able to provide indication that there might have been any hygroscopic changes to the salts during the launch while the camera could give indications of mechanical failure.

A post-flight examination of the material would also be beneficial as, for instance, changes in the filters abilities are hard to detect with the previous mentioned method. Following an exhaustive testing period before launch still being developed and formulated by the SALACIA team the areas of interest should be better understood thus dictating, among other things, the location of the camera. It should be expected that the pre-flight tests could affect the final design of the instrument.

One of the tests that have been formulated and are currently being performed involve the conductivity measurements. Each vessel have two probes dedicated to measure conductivity as depicted in Figure 3. Between these probes a conductivity bridge will be created and the ability of the electricity to flow measured. However, due to the vibrations of the rocket this value might change even though the moisture level of the salts remains constant preventing knowledge about how water vapour is absorbed during the flight.

Current testing thus involves doing probe measurements on the salts in a non-humid atmosphere and detecting the error one can expect during vibrations. The results from these tests will indicate if the errors are high enough to create the need for a different measurement technique. Should this be the case, the use of a mesh-grid structure is currently being considered as a viable alternative method.

Moving on, due to the nature of the SALACIA mission several critical stages exists. As an example several of the salts are highly oxidizing and during the REXUS launch guaranties will have to be made clearly showing that they never pose a risk to other experiments or the rocket. Further, in order to achieve the secondary objective of the SALACIA mission it also becomes important to decouple the instrument from the thermal profile of the rocket which might prove to be a challenge. Moreover, even if that is done one would also prefer to have a laminar flow from the surrounding atmosphere which might be hard due to the flight characteristics of the rocket.

In conclusion, the SALACIA mission is, through the REXUS/BEXUS program, able to provide usable results while also offering important experience for all the students involved in the processes. This experience range from a practice of writing proposals and documentations while also giving the students practical experience of project management. The following section will present our thoughts of the REXUS/BEXUS program as a space educational activity.

4. DISCUSSION ON REXUS/BEXUS AS A SPACE EDUCATIONAL ACTIVITY

One of the most beneficial aspects of the REXUS/BEXUS program that has been observed during the SALACIA mission is the practice of writing documentation and getting feedback on areas that needs to be improved. Many of the students involved in the SALACIA mission has experienced this to be one of the main differences to the normal education which has focused more on theories and methods. However, having the ability to practice writing of proposals and documentations is something that has been highly appreciated.

It can be said though, that teaching proposal and documentation writing in a classroom environment is problematic which might be a reason why it is currently not a major part of the education. As the current workings of the space industry require this knowledge however the importance of it should not be underestimated. Further, offering the opportunity for the students to perform the entire spectrum of activities: formulating the idea, designing and building the instrument, testing the instru-

ment and finally launching and analysing the results is very useful.

The REXUS/BEXUS program's ability to offer these kinds of hands-on activities in terms of documentation writing and designing/building of the instruments are something that have been experienced as very rewarding as an educational activity. It gives the student an understanding of the bigger picture as one is able to experience the entire processes of instrument development. This is done while also allowing the students to produce scientific data that might be usable to ongoing research and the REXUS/BEXUS program does therefore have the possibility of creating a life-long interest among the students.

Furthermore, as the students are responsible for the project they are also responsible for budget allocation both in terms of monetary costs and time which doubtless can be considered a useful experience for the future. Communication, both to the public and the scientific community is also something the REXUS/BEXUS teams will have to consider during their projects.

However, it should be noticed that the REXUS/BEXUS program does require a well-designed time budget and have a possibility of having a negative impact on the studies that are carried on in parallel to the program if the time budget should fail. In vain, data on how many REXUS/BEXUS instruments fail to launch and why was researched during the writing of this report but no reliable source was found. It would be interesting however to examine the launch rate of the REXUS/BEXUS program and the most common reason for failure. The SALACIA teams experience indicates that the time consuming nature of the program might be a reason but a more thorough study would be interesting.

Another thinkable reason might be problems related to the project management of the team which was also a new experience for many in the SALACIA team. Being able to practice project management and observe what tools that can be used to simplify the project work as a part of the REXUS/BEXUS program was however also experienced as a very rewarding thing with the REXUS/BEXUS program. Problems with a good scoping of the mission is also a challenge the teams will have to deal with during this program.

5. CONCLUSION

The REXUS/BEXUS program is an opportunity for European students to test their ideas in a sounding rocket or an atmospheric balloon. As a part of this program the SALACIA project was created which is aims to study the behavioural characteristics of brines hoping to contribute to future missions to Mars dedicated to the study of brines. As a space educational activity the REXUS/BEXUS program has been experienced as a valuable coaching experience for a future career in space science.

ACKNOWLEDGEMENTS

The authors would like to thank Professor F. Javier Martín-Torres and Professor María-Paz Zorzano Mier for their help and support.

REFERENCES

[1] European Space Agency, 2015, Cosmic Vision: Space Science for Europe 2015-2025, ESA Brochure BR-247

[2] NASA, 2011, Vision and Voyages for Planetary Science in the Decade 2013-2022

[3] Guerber, H.A., 1993, The Myths of Greece and Rome, Dover Publications

[4] REXUS/BEXUS, 2015, accessed 2015-11-13, available at `http://www.rexusbexus.net/`.

[5] Mawn, S., 2014, Rexus User manual version 7.13, EuroLaunch

[6] Roth, M., REXUS and BEXUS, accessed 2015-11-10, available at `http://www.dlr.de/rd/en/desktopdefault.aspx/tabid-2282/3421_read-10516`.

[7] Pater, I. de, Lissauer, J. J., 2015, Planetary Sciences, Cambridge University Press, 81, 208

[8] Renno et al., 2009, Possible physical and Thermodynamical Evidence for Liquid Water on the Phoenix Landing Site, Journal of Geophysical Research, 114

[9] Leshin, L. et al., 2013, Volatile, isotope and organic analysis of martian fines with the Mars Curiosity Rover, Science 341, 6153

[10] Ming, D. W. et al., 2014, Volatile and organic compositions of sedimentary rocks in Yellowknife Bay, Gale crater, Mars. Science 343, 6169

[11] Archer, P. D. Jr et al., 2013, 44th Lunar Planetary Science Conference 2168 (Lunar and Planetary Institute)

[12] Martin-Torres, J. F., 2015, Transient liquid water and water activity at Gale crater on Mars, Nature Geoscience 8, 357–361

[13] McKay, C. P., 2006, Life as we know it (ed. Seckback, J.) Springer 373–382

[14] Dale, L, P., 2011, Handbook of inorganic Compounds, CRC Press

[15] Ledgard, J., 2007, The preparatory manual of explosives, Jared Ledgard

[16] Schumacher, J.C., 1960, Perchlorates Their Properties, Manufacture and Uses ACS Monograph Series, Reinhold Publishing Corp

AEROSOLS AND CLOUD FORMATION RESEARCH IN A5-UNIBO EXPERIMENT ONBOARD BEXUS 18: LESSONS LEARNED

Encarnacion Serrano Castillo[1], Erika Brattich[2], Riccardo Lasagni Manghi[1], Laura Tositti[2], Fabrizio Giulietti[1]

[1]*Industrial Engineering Department, University of Bologna, Forli (FO), 47121, ITALY, Email: nani.serrano@unibo.it (Presenting author)*

[2]*Department of Chemistry "G. Ciamician", University of Bologna, Bologna (BO), 40126, ITALY, Email: erika.brattich@unibo.it*

Keywords: cloud formation; atmospheric ions; stratospheric balloon; BEXUS

ABSTRACT

A5-Unibo experiment of the University of Bologna has flown in BEXUS18 stratospheric balloon within the REXUS/BEXUS students' programme. The experiment performed several measurements from different instruments and sensors integrated in the system, with the aim to create vertical profiles of different atmospheric parameters involved in cloud formation processes. In addition, it performed an in-situ sampling of stratospheric aerosols for a post-flight analysis. Aerosol is a complex and dynamic mixture of solid and liquid particles suspended in the atmosphere, acting as cloud condensation nuclei for water vapor condensation. The experiment aimed at a better understanding of the proposed link between the major sources of ions (such as radon and cosmic rays) and cloud-particle formation.

The development of the experiment was a challenge for the students involved, who were requested to achieve very specific tasks without previous experiences on this subject. This work will present lessons learned and possible future developments of the experiment as well as a detailed description of the experiment.

1. INTRODUCTION

One of the most important tasks of Space agencies is to inform the public about the latest advances in the space science and technology. Most of these agencies develop Educational programs to inspire young people to pursue careers in aerospace, motivating and enabling their literacy in science and technology, and supporting them in several ways. For example, the REXUS/BEXUS programme realized under a bilateral Agency Agreement between the German Aerospace Center (DLR) and the Swedish National Space Board (SNSB) allows students from universities and higher education colleges across Europe to carry out scientific and technological experiments on research rockets and balloons. The Swedish share of the payload has been made available to students from other European countries through a collaboration with the European Space Agency (ESA), EuroLaunch, a cooperation between the Esrange Space Center of SSC, and the Mobile Rocket Base (MORABA) of DLR, is responsible for the campaign management and operations of the launch vehicles. Experts from DLR, SSC, ZARM and ESA provide technical support to the student teams throughout the project. REXUS and BEXUS are launched from SSC, Esrange Space Center in northern Sweden.

A5- Unibo was developed by a group of students at the Flight Mechanics Laboratory of the University of Bologna. The team was created with the aim to participate in the program, with Prof. Fabrizio Giulietti as supervisor and Encarnación Serrano Castillo, a PhD candidate, as coordinator. A5-Unibo experiment scientific idea was developed starting from the suggestion of Prof. Laura Tositti of the Chemistry Department "G. Ciamician" at the University of Bologna to investigate the cloud and particle formation process through the study of some key atmospheric parameters. In fact, the programme gives a great opportunity to study the atmospheric environment, and our experiment was invented to give a contribution to the study of Earth science, and in particular to atmospheric science. The Flight Mechanics Laboratory provided the engineering background regarding the sensors' acquisition, the system integration, operations, and testing while the department of Chemistry provided the experience concerning the data analysis and interpretation.

1.1 Scientific background

Particulate matter (or aerosol) is generally defined as a complex and dynamic mixture of solid and/or liquid particles suspended in the air. Aerosols may originate from both natural (such as volcanoes, sea-spray or dust) as well as anthropogenic sources (e.g., traffic, heating, energy production, industry). Sources affect aerosol's physical (size, surface, area, and density) and chemical properties.

Atmospheric aerosol is able to affect climate through both a "direct effect" of absorption and scattering of solar radiation as well as "indirect effects" by influencing cloud formation processes [1]. In fact, aerosol particles exhibit a complex interaction with solar radiation depending on their physic-chemical properties: some aerosol particles, such as sulphates, scatter incoming solar radiation reducing its flux to the Earth's surface, while other aerosol components, such as elemental carbon, have a continuous absorbing spectrum extending to the IR. The indirect effects of aerosols include their impact on cloud microphysics (which induces changes

in cloud radiative properties, their frequency, and their lifetimes) [1], since aerosols act as condensation nuclei for water vapor. Aerosols' net effect regarding global radiative forcing, defined as the change in solar irradiance with respect to 1750, includes cloud adjustments and results from the balance of positive forcing, mainly due to black carbon absorption of solar radiation, and a negative forcing of reflecting aerosols. Its value, as calculated in 2011, is estimated to be -0.9 (-1.9 to -0.1) W m^2 which means an overall cooling effect [2].

Aerosols and clouds continue to represent the largest uncertainty in the estimate and interpretation of the Earth's changing energy budget [2], mostly due to our incomplete understanding of the microphysical processes involved in cloud formation.

New particle formation by nucleation has been frequently observed in many different environments [3]: it may take place thermodynamically, kinetically or by the activation of pre-existing nanometer-size clusters [4]. Homogeneous nucleation in the presence of sulphuric acid is an important source of new particles, but is not sufficient alone to explain the observed particle formation [5]. Ternary nucleation involving ammonia [6] and ion-induced nucleation (IIN) [7] have been proposed to explain the gap between observations and models. IIN is thermodynamically advantaged over homogeneous nucleation since it requires a smaller supersaturation of the involved gases. Nevertheless, experiments still do not agree on the relative contributions of ion and neutral nucleation [e.g., 8-10].

Major sources of ions in the atmosphere include radon isotopes, cosmic rays (CR) and terrestrial gamma radiation [4], with a variable relative contribution depending on the altitude and latitude. Possible mechanisms linking the flux of ionizing galactic CR with the global cloud cover have been proposed [11]: the "ion-aerosol clear-air" mechanism and the "ion-aerosol near-cloud" mechanism [12]. The "ion-aerosol clear-air" mechanism stems from the expected enhancement of particle formation and growth due to the presence of ions. The underlying hypothesis of "ion-aerosol near-cloud" mechanism is that variations in cosmic ray ionization might modulate the fair-weather current generated by the electric current flowing into the cloud, leading to a sequence of micro-physical and macro-physical responses in cloud processing [13-14].

Model simulations are still the most convenient source of information regarding these effects, since observations are often incomplete and not conclusive [e.g., 15-17]. For example, the CLOUD experiment at CERN, consisting in a chamber filled with atmospheric gases and crossed by charged pions that simulate ionizing CR's, also aims at investigating of the potential link between CR's and cloud formation. Some preliminary results suggest that indeed IIN is a relevant factor to determine nucleation rates in the upper troposphere [18].

To the aim of a better understanding of cloud formation processes and IIN, the A5-Unibo experiment (Fig. 1), realized by the University of Bologna was flown onboard BEXUS18 stratospheric balloon. The primary objective of the experiment was to acquire vertical profiles of atmospheric parameters involved in these processes (particles size distribution, ion densities, and key atmospheric parameters such as temperature, humidity, and pressure), while the secondary one was the sampling of stratospheric aerosols for a post-flight analysis.

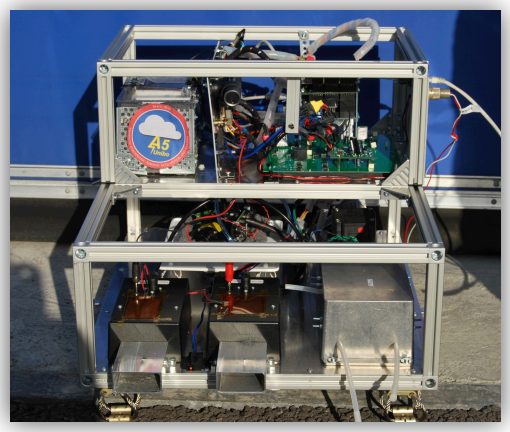


Figure 1. A5-Unibo experiment onboard Bexus 18

2. A5-UNIBO SYSTEM, SUBSYSTEMS and LESSONS LEARNED

REXUS/BEXUS programme has a very strict timeline set by the organization. After the submission of an experiment proposal, the team was pre-selected and asked to present the preliminary idea at the selection workshop. A general concept of the whole experiment was defined and the project was presented to the other teams and to the experts. The panel presentations and feedbacks were essential to give an overview of the next steps required to the team. The internal organization started once the team received the acceptance notification, . The first step was to create a work breakdown structure (WBS), which highlighted the main tasks for each subsystem, and to assign these tasks to the team members, depending on their previous experiences and interests. Since most of the team members were aerospace engineers with only little experience regarding space project development, they were required to acquire new skills and create an expertise in many fields, depending on the roles assigned. Once all the subsystems were covered, individual work could start, while periodic meetings of the whole group were held in order to make the members aware of the progresses and to plan future steps. The presentations at the selection workshop regarding the planning, organization, and realization of a space project were essential to this scope. At that point, the first experiment objectives along with preliminary requirements about flight altitude, duration, payload mass, and recovery information were defined.

The whole system was designed in order to accomplish the primary and secondary scientific objectives established by the team. The primary objective concerned the measurement of different atmospheric parameters and in particular, particles density and size distributions, ionization, and environmental parameters (temperature, pressure and humidity). The secondary objective involved the study of the chemical composition of the stratospheric aerosols collected on filters analysed after the flight. Since all of these parameters are important for a comprehensive study of the phenomenon, we employed a multi-instrument approach. All the different instruments chosen for the experiment were selected by taking into account their ability to work in the

harsh stratospheric environment, and specifically their range of operating temperatures, besides their reduced sizes and weight. Only a few "off the shelf" components did not comply with the thermal requirement, and for this reason an active control of the temperature inside the experiment was implemented with the use of patched foil heaters.

The most complex and critical instrument was the Optical Particle Counter (OPC), a device that exploits back-scattered radiation of a laser diode to measure particle densities and size distribution of aerosols with a size range from 0.3 μm to 100 μm. In parallel to particle size distributions, also ion densities (both positive and negative) were measured during the flight with two Air Ion Counters one for positive ions and the other for negative ions. Vertical profiles of environmental parameters such as temperature, pressure and humidity were also measured environmental parameters to complete the vertical profiles. The process of cloud condensation is in fact a dynamical one that depends not only on the presence of CCNs (such as aerosols), but also on the availability of water vapor for condensation, on the local temperature and on pressure. Only the simultaneous knowledge of all these influencing factors allows for studying and possibly validating theoretical models.

The experiment acquired data every ten seconds: the slow ascending speed of the BEXUS balloon the short sampling time enabled to create detailed vertical profiles of particles, ions and environmental parameters throughout the whole troposphere and stratosphere..

Moreover, once reached the nominal altitude in the stratosphere, an in-situ collection of aerosols was performed with the use of a diaphragm pump. This pump was ideally meant to create an airflow of constant volumetric flow through a special collector called Sioutas Impactor (SI). Under the assumption of having a constant flow of 9 l/min, the SI owns the advantage of sorting the sampled particles by their mass and size, giving the possibility to analyse the chemical composition as a function of particles size..

2.4. Subsystems final design and lessons learned

The overall performance of the experiment is considered a success; however, some issues and criticalities were identified, both in the design and in AIT phase. The final design and these issues will be addressed below.

2.4.1 Power subsystem

2.4.1.1 Design drivers

The power budget was estimated and the design was divided in three power lines (PL), taking into account performance, costs, and reliability of the system: 1) PL1 powered the pump and pinch valves which had the highest power consumption; 2) PL2 fed heaters and OPC; and 3) PL3 fed all the other instruments and the electronics.

The power was provided by two different sources: 1) GONDOLA batteries that powered PL2 and PL3. In particular, two batteries were put in parallel through the power board; 2) A5-Unibo battery pack, which provided power to PL1 and was designed to match the high power request for this line. Each power line was equipped with a current limiter (CL) to prevent overconsumption in case of failure of some instruments, and to ensure the possibility of recovery for the system.

2.4.1.2 Lessons Learned

The power budget was too conservative, and hence the batteries were oversized with respect to their actual use. This led to excessive costs and problems during transportation due to airport safety regulations.

Batteries' discharge voltage was higher than expected when at full charge. This resulted in higher power consumption from the pump, and a slightly different airflow with respect to the nominal one, which caused a reduced performance of the SI.

While an analytic approach based on data-sheet is sufficient during the early phases of the project, detailed and early testing of the batteries performance is a key aspect to be considered during the advancement of the project.

2.4.2 Electronics subsystem

2.4.2.1 Design drivers

A5-Unibo used an Arduino MEGA 2560 microcontroller for OBDH, data acquisition from sensors and instruments and for the direct control of the electro-valves and pump. In order to connect the sensors with Arduino, a hardware interface was created and two stacked boards were designed. The boards exactly fitted with Arduino MEGA 2560 pin schematics, in order to overlap the microcontroller and minimize the space occupied by the electronics.

An Arduino Ethernet Shield was used to connect the Arduino MEGA 2560 board with E-Link, the BEXUS telemetry system. A motor controller board was used to control the speed of the motor pump and in this way to adjust the airflow through the impactor. Other electronic boards were designed for the experiment, namely: 1) A heater board (H-Board) for a direct control of the heaters, which had to turn on in the event a threshold temperature (0ºC) was reached.

The H-Board was divided into two different parts: logic and control function. 2) A power control unit with the three power lines.

2.4.2.2 Lessons Learned

The electronic boards showed different issues during the assembly and integration phase due to our lack of experience in the early design stages. The PCBs had to be manually modified, and still showed a lot of flaws.

The power control from the PCU was poorly handled. The pump and pinch valves were fed by the same power line and this resulted in variable tensions on the Motion Mind motor controller, making an active and precise control of the pump flow impossible.

Pinch valves were supposed to open at the same time, as they did during the testing phase, but during launch campaign operations, an unknown issue with the PCU caused delays in the opening of valves, which could have been critical.

Power lines were supposed to be closed (turning off the experiment) by GS command before the descent. However, the PL that was feeding the electronics, Arduino, the two AIC's and the OPC kept on running, causing in this way a possible safety issue for these instruments.

Harnessing was not efficient, and had to be completed or modified strongly by the attendees during the launch campaign. Mechanical fixing of the boards was hardly considered by the electronic engineer, and its flaws caused many problems during the assembly and testing phase.

It is essential to think of a harnessing strategy since the early stages of the project, and in particular to our experience, around PDR (Preliminary design review). Moreover, in order to avoid late modifications of the boards or unexpected behaviors, the design of the boards should start very early in the project. Once the design is fixed and the components have been received, early prototyping and testing of the whole subsystem are necessary before the assembly of the final boards. Late changes in the board design due to insufficient testing may result in fact in much higher costs and delays in the schedule that could become critical for the mission success.

2.4.3 Ground Station Design

2.4.3.1 Design drivers

All data collected by the on-board unit was sent to the Ground Station and displayed via HID through a graphical interface. These data included sensory data (i.e. ambient data, internal sensory, etc.) together with flags reporting the status of the different components of the system. The interface also allowed the user to manually set some of the system parameters such as heaters, valves, pumps and to turn on and off specific instruments. Ground station was developed using LabVIEW.

2.4.3.2 Lessons Learned

LabVIEW is a great software environment, user-friendly and fit for programming a ground station, being capable of sending commands, receiving and visualizing data,. The team definitely recommends its use for ground station design.

2.4.4 Software design

2.4.4.1 Design drivers

Overall the software was designed to comply with the following requirements:
1) Error handling is necessary to have a reliable on-board software; 2) All processes should be monitored to prevent unpredictable behavior by handling errors, exceptions or bad data; 3) All processes should be supervised regarding the execution time, using timeouts to end a task without creating long delays in the life cycle.

The main parts of the control software were divided into functional groups, one for each of these specific tasks:
1) Monitor status and parameters of the components. 2) Monitor altitude readings (both from GPS and pressure sensor) to control the status of the experiment. 3) Handle communication with GS and store critical data in internal flash memory.

2.4.4.2 Lessons Learned

In principle, altitude should be measured twice, with the most reliable measurement being provided by the GPS, and a second one from pressure readings (Failure Detection, Isolation and Recovery approach). However, some problems arose from the incompatibility of the communication protocols between the GPS and the OPC that forced us to rely only on the barometric pressure readings for altitude determination. Again, early testing of the whole system could have possibly avoided this issue.

Different operating modes were implemented and the mission was divided into different mission states. Each state represented a specific step of the mission and requested its own specific routine to be correctly performed. The successful completion of one state was the essential requirement to pass to the following one. This kind of behavior was the most likely and desired, and proved to work well for the experiment.

2.4.5 Mechanical design

2.4.5.1 Design drivers

The mechanical design had to fulfil the requirements set by the SSC panel according to the vibrational profiles and mechanical loads experienced in the gondola during previous flights. In particular, a ± 10 g vertical static load and a ± 5 g horizontal load were considered. Further constraints were set by the weight and size limit, and by the mounting interface with M-Egon gondola.

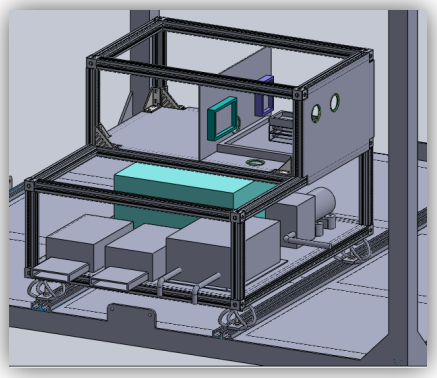


Figure 2. A5-Unibo experiment on-board Bexus 18 gondola

Based on these considerations, the experiment was mounted on 2mm thick aluminum plates, housed in a frame of aluminum extrusions. The whole structure was then fixed on the gondola mounting rails through four compact wire rope springs to reduce the forces experienced at landing.

The structure was modular and divided into three main sections: one containing the scientific instruments, one for the electronics, and one for the batteries, so that each of these sections could be easily accessed during operations (Fig.2).

Each component was bolted directly to the aluminum plates, except for the OPC, which required additional damping due to its fine alignment optics and was therefore mounted on four small springs, and the pump, for which a rubber thickness was used to reduce vibrations.

While in the early stage the design was checked through Finite Elements Method (FEM) simulations, the final setup was tested through both random vibrations and drop tests, and proved adequate during the campaign.

2.4.5.2 Lessons Learned

The mechanical structure worked well, but was far from optimized from the weight and size point of view. The mechanical fixation of most of the instruments was considered only during the last phases of the project and late modifications of the structure were therefore necessary. Moreover, the absence of an early harnessing strategy resulted again in late modifications of the structure and in a tremendous amount of work during the launch campaign in order to fix all the criticalities.

Mechanical fixation and housing of the components, harnessing, interface with the other subsystems, and modularity, are key factors for the mission success, and should be addressed during the early stages of the project in order to reduce the amount of late work and the rising of costs.

2.4.6 Thermal Subsystem

2.4.6.1 Design drivers

The functional requirement for the thermal subsystem was that the experiment had to survive the harsh thermal environment encountered during the pre-flight and flight phases. In particular, a two hours idle phase at a temperature of -15° C, and a three hours floating phase at a temperature of -70° C were considered. A detailed thermal model was developed and implemented through a Matlab script, in order to estimate the temperature evolution of the components.

The external temperature profile recorded during the previous BEXUS 10 flight was used as boundary condition. All environmental thermal fluxes (solar, albedo and planetary) and internal heat losses (due to cold air suction from AICs and Pump) were considered for this model.

Simulations showed temperatures below the operating limit for some of the main instruments and for the batteries, so we decided to implement both passive and active temperature control.

For the former, we employed a polyurethane-foam wall cover, while for the latter we installed a series of five Kapton foil heaters on the most critical components, controlled through a closed loop electronic system (Heaters' board).

EBASS (Esrange Balloon Service System) data showed that the minimum external temperature recorded was -60°C, while the minimum internal temperature measured in the Electronic Control Unit was 15° C, thus confirming the good performance of the thermal control system.

2.4.6.2 Lessons Learned

As already mentioned, the temperature was controlled through a closed loop system of thermistors and heaters, and only one temperature sensor was placed on top of the electronics. This choice was due to simplicity, since it allows for temperature control without the need of GS commands and data recording. However, the absence of data about the internal temperature was also its main drawback, since this latter can represent a key information in case of failure or malfunction of the subsystem. Moreover, this design did not allow adjustments in the case temperature significantly departed from the expected behavior.

Due to the unavailability of suitable facilities, the testing of the thermal subsystem was also not sufficient. This was also one of the main causes for the oversizing of the battery pack, since no a-priori knowledge of the estimated power consumption from the foil heaters was available.

The team suggests the use of a direct control and monitoring of the internal temperature of the system from OBDH and GS in a fault detection strategy. Moreover, detailed but careful testing should be performed to validate the numerical simulations and estimate the power consumption.

2.4.7 Scientific Subsystem

2.4.7.1 Design drivers

The requirements were defined on the basis of the primary and secondary objectives, which were also used for the choice of the scientific instruments.

2.4.7.2 Lessons Learned

No external temperature sensor was implemented, and as a consequence the team had to rely on EBASS data for this information.

The particular kind of AIC chosen was not the best option for this application. The instruments were in fact probably meant for industrial use, and the signal to noise ratio was very low due to the amount of charged particles present in the atmosphere. Moreover, many problems arose in the correct choice of ADC to use for data acquisition of their analogic signal.

In addition, the RH sensor should have been installed outside of the experiment, instead of on top of the electronics board, to obtain more reliable information.

The GPS did not work due to late communication conflicts with the OPC and was therefore removed. As it was not essential for the experiment, it did not become an issue, and EBASS GPS data was used.

Finally, the stringent volumetric flow rate required by the SI resulted in the need of a very complicated control of the diaphragm pump and in a great amount of testing and flow characterization at low pressures. A lot of time and resources were thus allocated to the secondary objective of the sample collection, while a simple change of filtering system or a small downscaling of this latter could have

solved these issues.

Overall, many problems arose from the choice of the instruments due to the lack of communications with the producing companies (from the company's side) and the absence of detailed data sheets about some of the instruments. It is suggested to evaluate not only the performance of an instrument during the design phase, but also the complexity of its interfaces and the cooperation of the company in case of malfunctioning or in the need for modifications.

2.5. Verification and testing

Almost all the tests had positive results and allowed us to validate the correct performance of their assigned subsystems. The process of verification and testing, started after the preliminary design phase and continued throughout the launch campaign, was a key factor for the success of the mission. Some tests highlighted the most critical issues in our design:

1) The first vacuum chamber test for OPC reported a malfunction of the instrument at low pressures (below 50 mbar) that caused a drop of the performance and possibly a hazard for the instrument itself. This forced us to change the selected instrument and to choose the LOAC (Light Optical Aerosol Counter), a small OPC for balloon measurements of the size distribution of atmospheric particles.

2) The Pump characterization test showed that the volumetric flow rate of the pump required by the SI, was not only difficult to achieve with the chosen pump, but also impossible to measure on site, due to its very low dynamic pressure; an active control of the flow rate during the flight was therefore not feasible. Possible future improvements for the experiment would be to choose a different combination of pump and filters, allowing for a direct measurement and control of the flow rate.

3) It was not possible to perform detailed thermal tests and calibrations for the Air Ion Counters (AICs) due to the lack of a suitable testing facility (thermo-vacuum chamber with temperatures down to -60°); for this reason, we were unable to determine a temperature-voltage profile for the offset measurements of the two AICs, required for a correct data acquisition.

2.6. Project management lessons learned

Once A5-Unibo received the acceptance notification, the tasks for every subsystem were defined. Every task was appointed to a specific person, in order to cover all the aspects of the project. Every single member was also part of a working sub-team, where all the information was shared to avoid possible vacancies in the subsystems. This gave also the possibility of replacing team members in the event they were absent or retired from the team.

In order to respect the deadlines and for a better organization of the project, it is important to keep updated the Gantt chart, which gives an outline of the project duration. The chart was updated every week inserting the pieces of information collected during the weekly meetings about the progress of the project.

It is fundamental to start thinking about tests, procedures, and facilities as soon as possible. In fact we met many problems in finding a suitable facility to perform the thermal-vacuum test, and this finally resulted in the impossibility of performing the test itself. However, the thermal environment for the experiment was good due to over-conservatism in both thermal analyses and design.

Fundraising is also a fundamental part of the project, which has to be considered right from the beginning. Possibly, a person should be dedicated entirely to this task, since the preliminary design can change a lot depending on the availability of funds in the early part of the project. Many instruments were bought late in the project due to lack of funds, and many tests had to be postponed because of delays in the delivery of these instruments.

The team should have probably designated one member of the team as mainly responsible for the communication outside the team; in our case, the fact that many people were in charge for the communication with private enterprises resulted sometimes in misunderstandings and/or delays with significant changes to the preliminary schedule.

A tight involvement of every team member at every step of the project/experiment is also required. In our case, internal weekly meetings for updates were often cancelled due to unavailability of team members. This resulted in trivial mistakes in the design that could have been avoided with more communication.

Deadlines are necessary for the group and the single members to keep up with the planned schedule. The difference between working days and holidays should be taken into account when planning a schedule and a safety margin shall always be applied. In addition, exam sessions should be considered.

Electronics and Software subsystems are tightly bound, and prototyping of electronic boards is necessary both to prove the sounding of the chosen design, and to allow the software to be run on a physical support. In our case, a testing for the electronics was possible only after the production of the PCB's, and this resulted in many errors in the design found only at a late stage. However, the team managed to overcome these delays on the software and communication side by using software-in-the-loop simulation for the testing and validation of the code. This left us with only a small number of remaining issues to be solves after the assembly of the entire experiment.

A critical issue during the launch campaign was the shipment and/or delivery of the experiment. Due to delays in assembly and test phase, the experiment could not be shipped on time and had to be disassembled and carried by the attendees in their personal luggage. This represented a huge risk, both due to airport security regulations and to possible damages of the components during the travel. However, all of the tasks were scheduled in detail prior to the launch campaign, and this enabled a more efficient and quick

teamwork, which allowed us to reassemble the experiment and perform all the tests right on time.

3. RESULTS AND CONCLUSIONS

3.1 The flight - Recovery

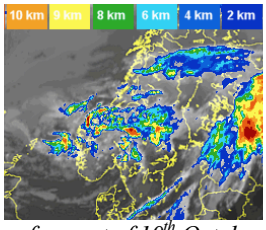


Figure 5. Weather forecast of 10th October 2014 - Bexus 18 flight

The flight had a floating phase of 1h 9min and reached a maximum height of 27.2 km, with an average ascending speed during climbing of 3.5 m/s. Fig. 5 illustrates the weather forecast for the day of the flight, which shows the presence of clouds during the flight, an interesting feature since directly connected to the primary goal of our experiment. The gondola was open on our experiment's side as requested for correct data acquisition and aerosol sampling (Fig. 6.a). This allowed for the introduction of a camera pointing outside of the gondola, and a post-flight visualization of the operations (Fig. 6.b). This was important in order to better understand causes of eventual failures or to identify unexpected events or behaviors. The experiment landed in Finland and the recovery team brought it back safely to the ESRANGE Space center facilities the day after the flight.

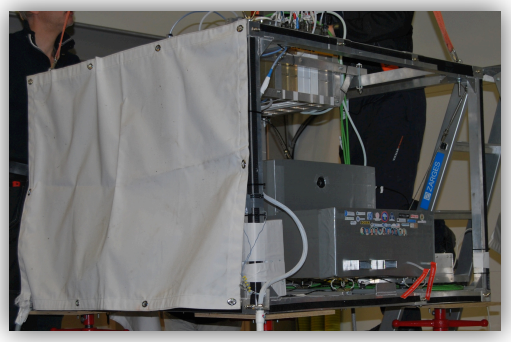


Figure 6.a 10th October 2014 - Bexus 18 gondola ready for flight



Figure 6.b 10th October 2014 - Bexus 18 On-board view camera from A5Unibo

3.2. Data post – processing

Our experiment recorded particles' size distribution, ion densities, pressure and humidity data every ten seconds. External temperature and GPS data were retrieved a-posteriori from EBASS. Prior to analyzing the dataset, the EBASS data (acquired every second) was averaged at the same sampling time of our experiment in order to relate the external temperature profile with the parameters acquired by our experiment. Moreover, before the analysis a number of operations (namely removal of the outliers, subtraction of the offset acquired during the mission at 4 different pressure levels from AIC data, and conversion of OPC data from numerical counts to particles number per unit volume and per size interval) were performed on the raw data acquired during the flight. Statistical analyses of the data-set were successively performed by means of Statistica 7 (Statsoft Inc.), Origin 8 (Origin-Lab Corporation), and R (R Core Team, 2013). Particles size distribution are being processed with a new software in collaboration with the developers of the instrument.

Fig. 7 shows the acquired vertical profiles for atmospheric parameters (pressure, relative humidity, and temperature).

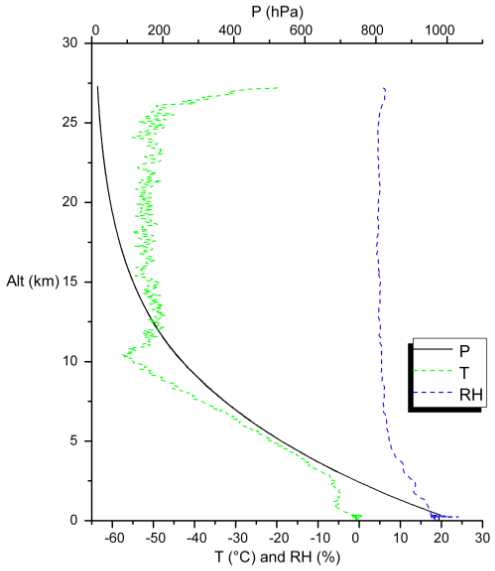


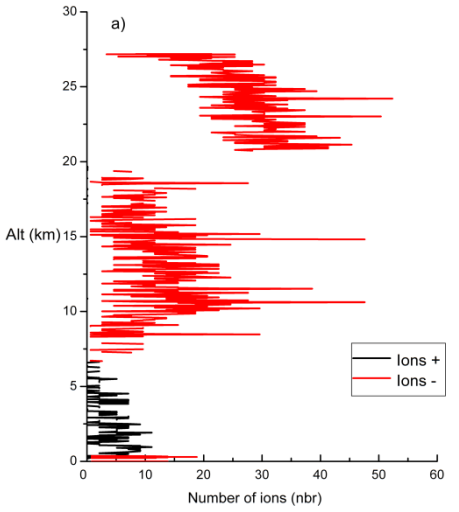
Figure 7. Vertical profiles of pressure (P), ambient external temperature (T), and relative humidity (RH).

The pressure profile (Fig. 7) showed a negative exponential decreasing during the flight, in agreement with theoretical expectations. The temperature profile seems to show a small inversion layer close to ground, and a general positive static stability condition. The tropopause level (i.e., the level where the temperature sounding first becomes an inversion in the upper troposphere) was located at about 11 km and extended up to the height of 25 km, where the temperature profile shows the trend typical of the stratosphere. Ambient air was already dry at ground level; relative humidity decreased until about 5 km, and after that it was more or less constant, with only a minor increase at about 26 km.

In Fig. 8, we report vertical profiles for ion densities and particles size distribution acquired during the flight ascent. From Fig. 8a it can be observed that: 1) when present, there were much more negative ions than positive ions; 2)

charged particles were somehow intermittently present: positive ions were observed up to about 6.5 km, and negative ions were instead observed at ground level and at altitudes higher than 7 km, with a peak at about 22 km. This result is consistent with previous observations, showing that ionization from turbulent transport of radon (positive ions) and gamma radiation (negative ions) prevail near the Earth's surface, whereas ionization from CR (negative ions) dominates away from the continental surface (upper troposphere and above) [4]. The number of positive charges was always very limited, with maxima in the lower troposphere at high pressures and relatively high humidity conditions. Peaks of negative charges appeared in the stratosphere at low pressures, low humidity and low temperatures, while they were not observed at intermediate levels.

Particles size distributions of fine (diameter ≤ 2.0 µm) (Fig. 8b) and coarse particles (having diameter larger than 2.0 µm) (Fig. 8c) peaked at ground level and generally decreased with increasing height. Coarse particles are relatively large airborne particles mainly produced by the mechanical break-up of larger solid particles (such as dust, pollen, spores, fly ash, plant and insect parts); they constitute a large part of the ambient aerosol in terms of weight, but their number is usually very limited, since they are removed soon after their production due to gravitational settling.



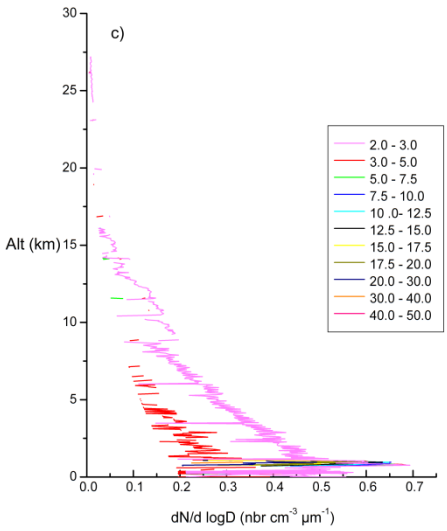


Figure 8 (a,b,c). Vertical profiles of: a) ion densities; b) particles size distribution for particles in the 0.2-3.0 µm diameter range; c) particles size distribution in the 3.0-50.0 µm diameter range.

Vertical profiles of particles size distributions were further analyzed by means of exponential and linear fitting. In fact, the vertical profile of fine particles (up to 1.0-2.5 µm aerodynamic diameter) can be approximated by a negative exponential curve. Coarse particles in the 7.5-10 µm diameter range were observed at ground level and then at tropopause level (about 10 km during the flight) and higher, while they were almost absent in the upper troposphere. Larger particles in the 17.5 – 20.0 µm diameter range linearly increased with height until the height of 1 km, while they were absent at upper heights. Vertical profiles acquired by our experiment are consistent with "theoretical" expectations, with higher concentration of particles at higher pressures, temperatures and humidity.

The existence of inter-relationships between particles size distributions, ion densities and key atmospheric parameters was further investigated by means of correlation analysis, scatterplots, and 3D plots. Fig. 9(a,b) shows the value of the correlation coefficient between the vertical profiles of measured parameters (particle number densities, ion densities, atmospheric parameters). Fig. 8 indicates a positive correlation of particles number density with pressure, temperature, relative humidity, and positive ions, and a slight anti-correlation with negative ions. The correlation coefficient decreases with increasing particle size. Particles in the 17.5-20.0 and 20.0-30.0 µm diameter range were anti-correlated with pressure, temperature, and relative humidity. When considering the whole vertical profile, the particles number density is more correlated with positive charges than with the negative ones. Moreover, the number of particles is more correlated with relative humidity than with temperature (which nevertheless plays a role).

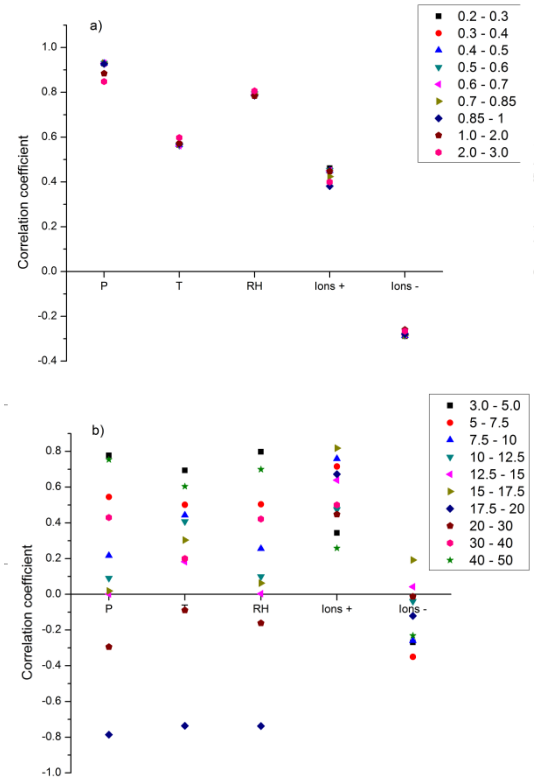


Figure 9 (a,b). Correlation coefficient between vertical profiles of pressure (P), temperature (T), relative humidity (RH), and ion densities with a) fine particles number density; b) coarse particles number density.

Negative ions have been generally observed to have a wider effect in IIN with respect to positive ones [9-11]. Our results for correlation coefficients are potentially biased by the maxima at lower altitudes observed both for positive ions as well as for particles. In fact, when considering only heights above 9 km (upper troposphere/lower stratosphere), the same analysis of correlation coefficients between vertical profiles shows a positive correlation between size distributions of particles in the 0.2-5.0 μm and negative ions.

As a final step of our analysis, a simple multi-linear regression model to estimate particles number profiles on the basis of key atmospheric parameters and ion densities was developed. Tab. 1 reports the values of some parameters indicating the performance of such simple model. A good regression model is one for which the model sum of squares (MSS) is high and the residual sum of squares (RSS) is low (the best the model for the highest value of MSS and the lowest value of RSS). The coefficient of determination (r2) is the ratio between MSS and TSS and represents the estimate of the variance explained by the MLRA model. The multiple correlation coefficient represents instead the linear correlation between experimental response (parameter to be predicted, dependent variable) and predictors of the dependent variable (independent variables, in our case atmospheric parameters and ion densities). A significance of the Fisher's F lower than 0.05 means that the variance explained by the model is not due to the chance and therefore the model is associated to a statistically significant causality. The constant represents the intercept of the regression model.

Table 1. Performance parameters of the MLRA model

	R	r^2	MSS	RSS	TSS	F	Sig	Cost
0.20 - 0.30	1.00	1.00	2.53	0.01	2.54	1748	0.000	-0.10
0.30 - 0.40	1.00	1.00	2.19	0.00	2.19	2739	0.000	-0.06
0.40 - 0.50	1.00	1.00	1.93	0.00	1.94	1729	0.000	-0.09
0.50 - 0.60	1.00	1.00	1.68	0.01	1.69	1072	0.000	-0.13
0.60 - 0.70	1.00	0.99	1.47	0.01	1.48	734	0.000	-0.18
0.70 - 0.85	1.00	0.99	1.20	0.01	1.21	475	0.000	-0.27
0.85 - 1.00	0.99	0.99	0.94	0.01	0.96	296	0.000	-0.32
1.00 - 2.00	0.99	0.98	0.80	0.02	0.82	221	0.000	-0.34
2.00 - 3.00	1.00	0.99	0.38	0.00	0.39	344	0.000	0.07
3.00 - 5.00	1.00	1.00	0.13	0.00	0.13	102	0.075	-1.31

It can be noticed that the performance of the MLRA significantly decreases with increasing particles size. The application of this simple model reveals once more an important effect of pressure, humidity, and number of positive ions on (fine) particles number (significant for particles larger than 0.3 μm). Temperature seems to be an important parameter for particles in the 0.7-2.0 μm diameter range.

4.2 Conclusions

In conclusion, our analyses show a possible role of positive ions in particle formation processes in the lower troposphere and of negative ions in the upper troposphere/lower stratosphere as well as a larger importance of humidity with respect to temperature.

The data collected with the LOAC is currently being analyzed with a new software that will allow a detailed study of the relationship between ions and particles. The results of this new analysis will be published soon in a scientific journal.

4.2.1 Possible future improvements

1) The use of one Air Ion counter which can measure both positive and negative ions simultaneously. 2) The use of a more reliable GPS, compatible with the other instruments,; 3) The optimization of the mechanical design to reduce weight and size; 4) The introduction of an active thermal control, which employs an array of temperature sensors placed near critical components. All the information coming from these sensors should be sent to GS for real-time performance evaluation. The same procedure should be used during the testing phase to validate the thermal simulations; 5) The use of a new and more precise instrument for ion density measurements. In addition, clearness of the data-sheet, and simplicity of calibration and data acquisition should be considered for the choice of this instrument; 6) In case the choice of SIOUTAS sampler as a filter is maintained, a suitable differential pressure sensor should be used in the vacuum chamber for a correct flow determination of the pump at low pressures. In addition, the use of a new pump should be considered. 7) The possible addition of ampere-meters and volt-meters in the electronics for failure detection and the improvement of the power budget calculations; 8) A possible future mission could employ new instruments, such as an Aitken Nuclei counter, which can follow the nucleation process even at smaller scales, and hence give us a complete

overview of the condensation process. 9) The introduction of external sensors for temperature and RH.

5. ACKNOWLEDGEMENTS

This work was designed and developed within the collaboration of the Flight Mechanics Laboratory and the Department of Chemistry of the University of Bologna as main supporters.

Every team member was essential for success of the mission: Encarnación Serrano Castillo (Team Leader and System Engineer), Riccardo Lasagni Manghi (Verification and Testing engineer), Erika Brattich (Data Analysis, Scientific expert), Igor Gai (Ground Station engineer), Danilo Boccadamo (Power engineer), Paolo Lombardi (Mechanics), Alice Zaccone (Software engineer), Abramo Ditaranto (Electronics engineer), Luca Mella (Software engineer), and Marco Didonè (Thermal engineer).



Figure 9. A5Unibo team members representation during IPR

We also acknowledge: a) institutional supporters: DLR, Rymdstyrelsen, SSC, ESA Education Office, EuroLaunch, ZARM; b) private companies and associations: AlphaLab Inc., Boxer, Iacobucci HF Aerospace, Icos, CNA Forlì-Cesena, Dogcam, Gruppo SDS, Società Italiana di Medicina Generale, Plastica Panaro, Bustaplast, Bellini Tiziana, Mascherpa.

6. REFERENCES

[1] Albrecht B.A. (1989). Aerosols, clouds, microphysics, and fractional cloudiness. Science 245(4923), 1227-1230.

[2] Boucher O., and coauthors (2013). Clouds and Aerosols. In: Climate Change 2013: The Physical Science Basis. Contribution of Working Group I to the Fifth Assessment Report of the Intergovernmental Panel on Climate Change. [Stocker T.F., et al. (eds.)] Cambridge University Press, Cambridge, United Kingdom and New York, NY, USA, pp. 571-657.

[3] Carslaw K.S., Harrison R.G., Kirkby J. (2002) Cosmic rays, clouds and climate. Science 298, 1732-1737, doi:10.1126/science.1076964

[4] Dunne, E.M., Lee, L.A., Reddington, C.L., Carslaw, K.S. (2012) No statistically significant effect of a short-term decrease in the nucleation rate on atmospheric aerosols. Atmos Chem Phys 12, 11573-11587

[5] Eisele F.L., and coauthors (2006). Negative atmospheric ions and their potential role in ion-induced nucleation. J Geophys Res 111, D04305, doi:10.1029/2005JD006568

[6] Forster P., and coauthors (2007). Changes in Atmospheric Constituents and in Radiative Forcing. In: Climate Change 2007: The Physical Science Basis. Contribution of Working Group I to the Fourth Assessment Report of the Intergovernmental Panel on Climate Change.[Solomon S. et al. (eds.)] Cambridge University Pess, Cambridge, United Kingdom and New York, NY, USA, pp. 129-234

[7] Hirsikko A., and coauthors (2011) Atmospheric ions and nucleation: a review of observations. Atmos Chem and Phys 11, 767-798.

[8] Kirby, J., and coauthors (2011) Role of sulphuric acid, ammonia and galactic cosmic rays in atmospheric aerosol nucleation. Nature 476(7361), 429-433.

[9] Korhonen, P., and coauthors (1999) Ternary nucleation of H_2SO_4, NH_3, and H_2O in the atmosphere. Journal of Geophysical Research 104(D21), 26349-26353

[10] Kulmala, M., and coauthors (2000) Stable sulphate clusters as a source for new atmospheric particles. Nature 404, 66-69.

[11] Kulmala, M. (2003) How particles nucleate and grow. Science 302, 1000-1001

[12] Kulmala, M., and coauthors (2004) Formation and growth rates of ultrafine atmospheric particles: a review of observations. J Aerosol Sci 35, 143-176

[13] Laakso L., and coauthors (2007). Hot-air balloon as a platform for boundary layer profile measurements during particle formation. Boreal Env. Res. 12, 279-294.

[14] Lee S.H., and coauthors (2003) Particle Formation by Ion Nucleation in the Upper Troposphere and Lower Stratosphere. Science 301, 1886-1889

[15] Manninen H.E., and coauthors (2009). Charged and total particle formation and growth rates during EUCAARI 2007 campaign in Hyytiälä. Atmos. Chem. Phys. 9, 4077-4089.

[16] Pierce, J.R., and Adams, P.J. (2009) Can cosmic rays affect cloud condensation nuclei by altering new particle formation rates? Geophys Res Lett 36, L09820, doi:10.1029/2009GL037946

[17] Raes, F., and Janssens, A. (1986) Ion-induced aerosol formation in a H2O-H2SO4 system-I. Extension of the classical theory and search for experimental evidence.

[18] R Core Team (2013). R: a language and environment for statistical computing. Vienna, Austria: R Foundation for Statistical Computing. [Available at: http://www.R-project.org/]

MICRO-REENTRY-CAPSULE-2 (MIRKA2) REXUS

Wizemann S.[(1)], Ehresmann M.[(1)], Baumann J.-P.[(1)], Behnke A.[(1)] Franz J.[(1)], Gäßler B.[(1)], Galla D.[(1)], Grabi F.[(1)], Koller M.[(1)], Kuhn G.[(1)], Müller N.[(1)], Papanikoloau A.[(1)], Rieser J.[(1)], Schöneich V.[(1)], Seiler H.[(1)], Siedorf M.[(1)], Starlinger V.[(1)], Stier A.[(1)], Tabelander A.[(1)], Pagan A.S.[(2)], Montag C.[(2)], Herdrich G.[(2)], Fasoulas St.[(2)], Klinkner S.[(2)]

[(1)]Small Satellite Student Team University of Stuttgart; Pfaffenwaldring 29, 70569 Stuttgart, Germany
Phone: +49 15 222700266 Email: wizemann@ksat-stuttgart.de
[(2)]Institute of Space Systems University of Stuttgart; Pfaffenwaldring 29, 70569 Stuttgart, Germany
Phone: +49 711 685-62412 Email: herdrich@irs.uni-stuttgart.de

ABSTRACT

The Micro-Re-Entry-Capsule-2-REXUS (MIRKA2-RX) student experiment is a precursor project for the CubeSat Atmospheric Probe for Education (CAPE) at the Institute of Space Systems (IRS) of the University of Stuttgart. CAPE is a CubeSat system, which shall allow a miniature capsule to perform a re-entry to qualify new ablator materials and to assess a respective aerothermodynamic data base. MIRKA2-RX is intended for the validation of the capsule's flight behaviour and to ensure the functionality of the electrical and communication system. The experiment is segmented into three components: The first segment is the capsule, which is a version of the later flight model, containing pressure, temperature, acceleration and radiation sensors. A dummy heat shield will be used, as the expected temperatures will not exceed critical levels during this suborbital return.
The second segment is the newly developed ejection-mechanism. It is designed to perform a reliable and simple ejection of the capsule using pyro cutters.
The third segment is a replica of the electric system of the capsule, which will reside within the experiment in the REXUS rocket during the entire compartment flight. It is used as a backup system in case of communication malfunction and if the capsule is irretrievable. This data can be used to evaluate the performance of the electric system independently.
When the sounding rocket reaches its apogee, the capsule will be ejected. During its return to Earth, it will collect and transmit data generated by the sensors. After its impact, it is attempted to retrieve the capsule and to extract additional data stored on board.

1. INTRODUCTION AND MOTIVATION

The MIRKA2-RX experiment is an experiment executed by students to validate the flight behaviour, the communication and electronic system of the MIRKA2 capsule [1] and the specially developed ejection-mechanism LOTUS (Low Orbit Technical Unit Separator) of the of the nanosatellite project CubeSat Atmospheric Probe for Education (CAPE) [2].
CAPE is an educational project, which helps students develop general system engineering as well as specialized experts skills [3]. The vehicle itself serves as a demonstration and qualification platform for electric propulsion and atmospheric re-entry technology. In addition, its mission scenario (see Fig. 1) provides an excellent basis for a spatial characterisation of Earth's lower thermosphere.

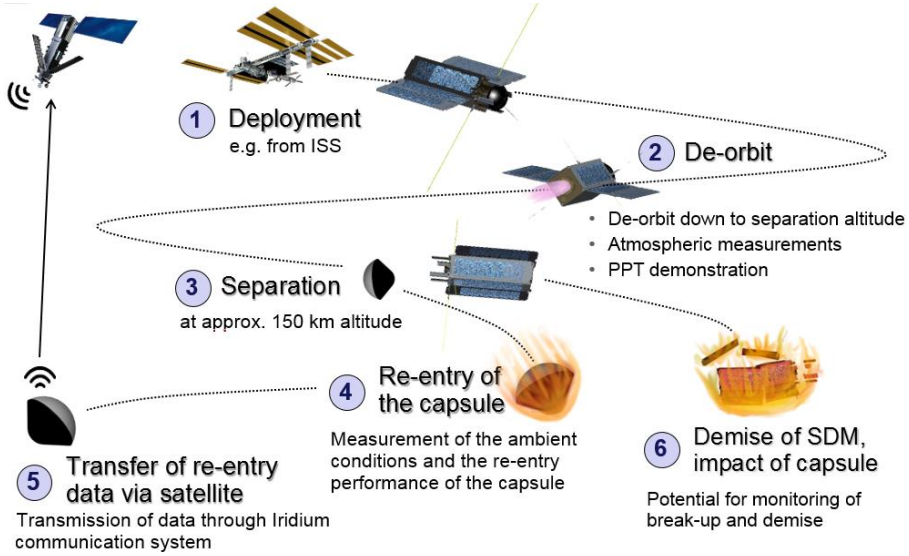


Figure 1. Cape mission scenario

The CAPE system consists of a Service and Deorbit Module (SDM) [4] and the Micro Re-Entry Capsule MIRKA2 (in German: MIkro RückkehrKApsel 2). After the deployment from the ISS at an altitude of 400 km the Pulsed Plasma Thruster (PPT) propulsion system of the SDM reduces the altitude of CAPE down to the separation altitude at 150 km. During the de-orbit manoeuvre, the SDM collects atmospheric data from the lower thermosphere. After the separation of the capsule from the SDM through a separation mechanism, the capsule will perform a re-entry manoeuvre. For the duration of the re-entry, the capsule will collect data of the ambient conditions and the re-entry performance with several sensors. Since no recovery is foreseen, the capsule has to transfer its collected data via the Iridium network to the ground station right after the blackout phase of re-entry. The SDM itself will demise in the atmosphere following the re-entry of the MIRKA2 capsule, which additionally offers an opportunity for monitoring the break-up and demise of the SDM.
Since there is little experience of the flight behaviour of such a small capsule, it is important to validate its in-flight stability and to ensure the functionality of the electrical and communication system.
This validation is conducted by the MIRKA2-RX experiment, which will launch on board REXUS-19 in March 2016 and is described in the following.

2. DESCRIPTION

2.1. Mission Scenario

The Experiment will be carried inside of a standard experiment module of the sounding rocket REXUS. After the lift-off signal, the rocket will rise for 26 seconds until burnout as depicted in Fig. 2. At about 64 seconds, the nose cone and motor separate and a jo-jo despin is performed. After 120 seconds, the experiment module will reach the apogee at 80 - 100 km, where the capsule will be ejected. Right after this separation, the electronic system of the capsule will be activated. A satellite link will be established to the Iridium satellite network to transfer most of the data, which are generated by the sensors to the ground station. During the return, the capsule will collect data related to the inflight stability in low Mach regimes. At the same time, the On-Board Control Unit (OCU) inside of the experimental module of the REXUS rocket will activate the mirror system, which is an almost exact replica of the electronic system of the capsule. It serves as a redundancy system for the verification, in case the data transmission of the capsule fails and a recovery thereof is not possible.
After 800 seconds, the experiment module lands and it will be retrieved thereafter. The capsule will impact beforehand. Because of the small size of the capsule, a recovery will prove to be very difficult. To increase the chances of locating and retrieving the capsule, it features a radio beacon.

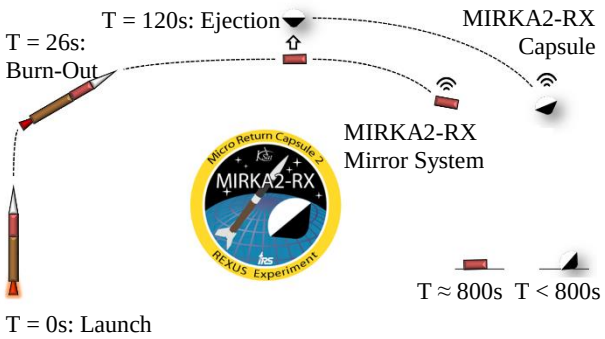


Figure 2. MIRKA2-RX mission overview

2.2. Experimental Setup

As depicted in Fig. 3 the MIRKA2-RX experiment consists of four main sub-systems:

- MIRKA2-RX capsule
- LOTUS ejection-mechanism
- Mirror system of the capsule electronics
- On-board Control Unit (OCU)

The MIRKA2-RX capsule will be placed inside the separation mechanism LOTUS, which is fixed at a mounting structure holding one of the two action cameras as well. This action camera faces directly out of the module and records the separation of the capsule. The second camera is directed to the separation-mechanism itself and records the performance of LOTUS and the separation.
The mirror system and the OCU are mounted inside of the mirror box, which is attached to the base plate of the experimental module. The hatch of the module is fixed by wires. To release the hatch, a pyro cutter, controlled from the rocket itself, will cut the wire and four compression springs will separate the hatch from the experimental module.

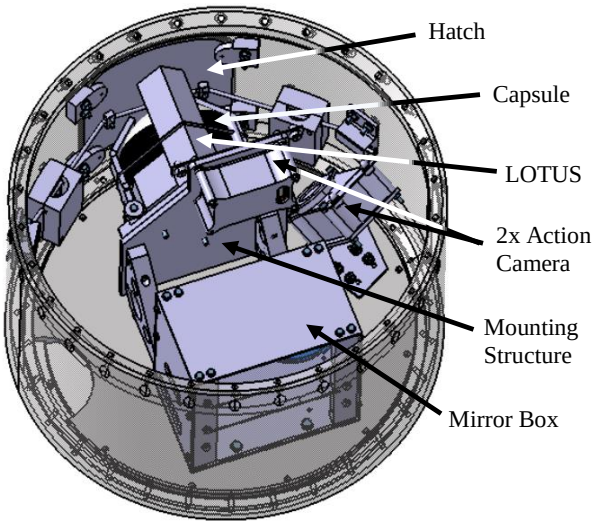


Figure 3. Experimental set-up

Right after the hatch is released, LOTUS will push the MIRKA2-RX vehicle out of the module.
To reduce the cost and development effort, most of the experimental parts are commercial-off-the-shelf components (COTS).

2.3. Capsule MIRKA2-RX

Since the capsule of this experiment is intended to validate the flight behaviour of the MIRKA2 capsule for the CAPE mission, it has the same geometry. The shape is a scaled version of the Re-Entry Breakup Recorder (REBR) [5] with a maximum diameter of 100 mm, in order to fit in one CubeSat Volume Unit (100 x 100 x 100 mm^3). Because of its very compact measurements it has a ballistic coefficient of $\beta = 49\ kg/m^2$ in the continuum flow region [6].
The cross section in Fig. 4 depicts the arrangement of the subsystems inside of the vehicle. They are divided into structure and mechanism, energy system, sensors, communication system and the data-handling system.
The outer structure protects the components inside of the capsule from the loads of the sub-orbital return and provides mechanical stability. It consists of an aluminium tip covered by a dummy heat shield, which stands in for the heat shield material to be used for the MIRKA2 capsule of CAPE. The aft shell is made of the WHIPOX™ ceramic [7] instead of a metallic material to allow for an unobstructed transmission for the GPS- and Iridium transceiver as well as the wildlife tracker. To ensure a stable flight a tungsten alloy weight is placed as close as possible to the nose tip.
In order to guarantee that the capsule will not send any signals during the prelaunch/launch-phase, the deactivation pin pushes the deactivation button to cut of the power supply of the capsule. The pin itself will be pushed by a deactivation rod through a hole in the front cone, which simultaneously serves as a view hole for the thermopile sensor and for the stagnation pressure measurement. To be sure that the capsule is shut down, a buzzer placed inside of the vehicle stops buzzing after the electronics are switched off.

Table 1. Battery service life

		min [h]	nominal [h]	max [h]
Transmitter Off	nominal	3.01	3.78	5.74
	hot case	3.31	4.16	6.32
	cold case	1.68	2.12	3.22
Transmitter On	nominal	1.84	2.01	5.75
	hot case	2.02	5.75	6.32
	cold case	1.03	2.10	3.22

The design of the capsule electronics is depicted in Fig. 5 in the right-hand box. To supply the electronic system with electrical power, the energy system comprise three lithium SAFT LM 17130 primary batteries and a LDO Power Converter. The switch is the deactivation-mechanism mentioned earlier. The batteries are lined up in a serial circuit to generate a voltage of 9V and have a capacity of 0.5Ah each. The LDO Power Converter stabilizes and transform the 9V to 5V. In Tab. 1, it can be seen that for all operational cases the supply duration is far above the total experiment duration of 800s.
To determine the performance of the capsule, it is equipped with several sensors. For the assessment of the flight stability during the separation and the return phase, the IMU (Inertial Measurement Unit) will use an acceleration-, rotation- and a magnetic field-sensor.
A GPS-Receiver is used to track the position of the vehicle and to measure the velocity. Because of the high return velocities of more than 500 m/s and altitudes exceeding 18 km, which are not supported by common GPS devices, a space qualified GPS-Receiver is necessary. Since most space qualified GPS-Modules do

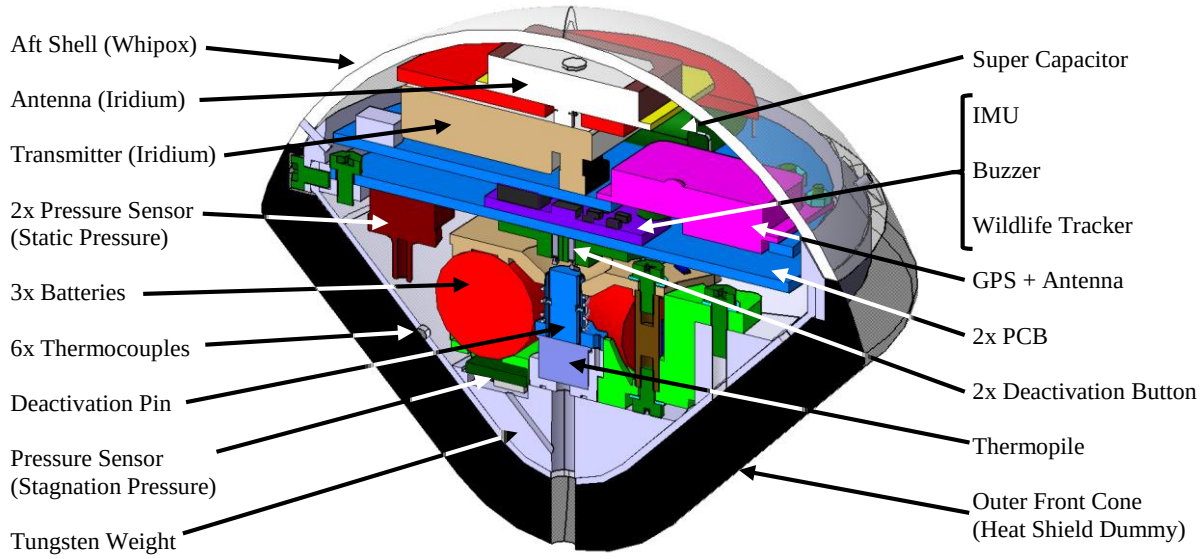


Figure 4. Design of the MIRKA2-RX capsule

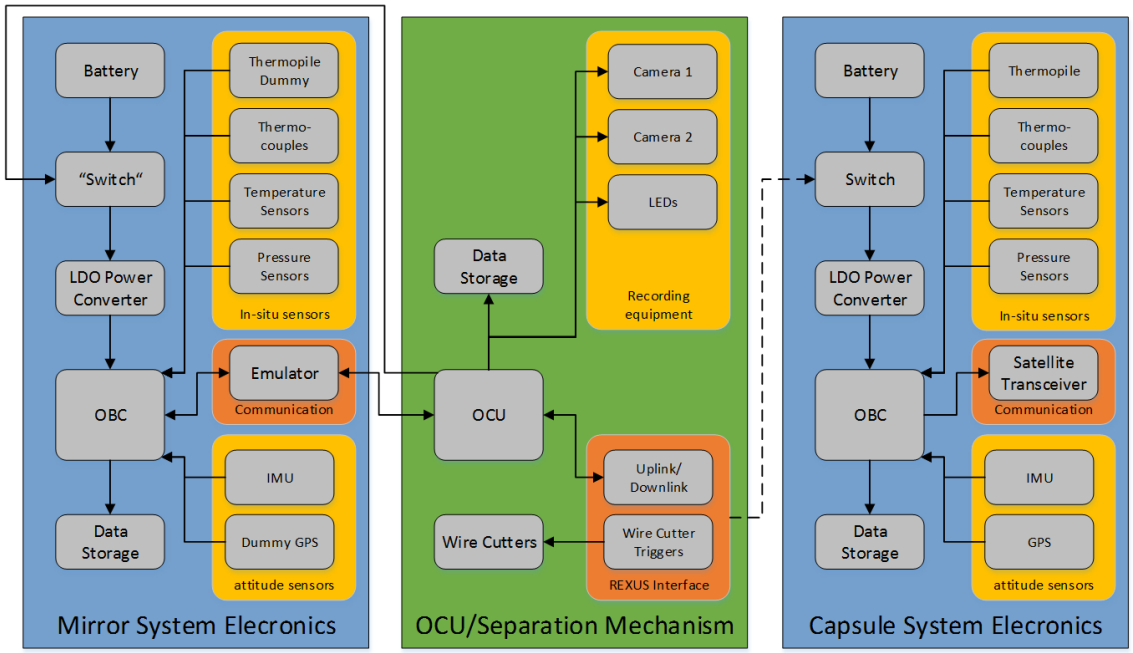


Figure 5. Electronics design overview

not fit inside of the capsule or exceed the budget, the commercially available GPS-Module LS20031 [8] was selected, which is restricted in functionality. Hence, position and velocity measurements are only possible below 18 km altitude.

To analyse the ambient conditions, a pressure sensor, which features an integrated temperature sensor, is placed inside of the capsule. For a wide measurement range, 2 different pressure transductor each adjusted for a specific pressure regime will be operated. In addition there will be a pressure sensor to detect the stagnation pressure at the nose tip.

For the determination of the heat shield performance in the CAPE mission, thermocouples will be placed inside of the ablator in different depths and locations.

Thermocouples are utilized to measure temperatures and heat fluxes through the ablator. The regression rate is indicated through failure of an individual thermocouple. As there no real re-entry manoeuvre is conducted in the MIRKA2-RX project, the thermocouples will only be used to verify the performance of the electronics and the software.

To identify the composition of the plasma and the performance of the ablator for the duration of the re-entry in the CAPE mission, a thermopile detector is placed inside of the deactivation pin and is directed to the hole inside the nose tip.

All the created sensor data will be transmitted via a Quake Iridium 9603 transceiver [9]. It consists of a 1 W transceiver and a patch antenna with 6 dBi gain. To generate the high power required to send the data, a super capacitator is used, which will be charged while the On-Board Computer (OBC) is collecting and preparing the data for the transmission. Since the possibility of a recovery of the capsule is taken into account, an on-board data storage is included to secure all measured values and housekeeping data. This will increase the chance of obtaining sensor information in case the Iridium uplink fails. To help find such a small vehicle, a wildlife tracker is integrated, which will start to send a signal right before it impacts on the ground. To ensure the functionality of the wildlife tracker after the impact, all electronics to run it and an own power source is cast in plastic material for mechanical damping.

The OCB handles all the sensor data and prepares them for transmission with the Iridium transceiver. It consists of three Arduino Nanos [10]. Each of them has a different task, as presented in Fig. 6. The Sensor/SPI Master Board comprises the six thermocouples and the three pressure sensors and manages the SPI (Serial Peripheral Interface) communication of the sensors and the boards. The IMU Board handles the thermopile, IMU, GPS, Buzzer and the storage of the sensor data on the SD-Card. The Communication Board will gather, process and transmit all sensor data to the Iridium satellite constellation.

To overcome uncertain influences such as space radiation on non-space-qualified hardware, a watchdog mechanism is implemented. Any two microcontrollers can reset the third microcontroller, if they agree that the third one is faulty.

Because of the small size of the MIRKA2-RX vehicle, there is not enough volume to integrate three Arduino Nanos and the harness for all individual components. To implement the microcontrollers and all the parts, a specifically designed Printed Circuit Board (PCB) was constructed. The advantage of this configuration is that the required space is reduced, because the stacking of components can be avoided and less cabling is required.

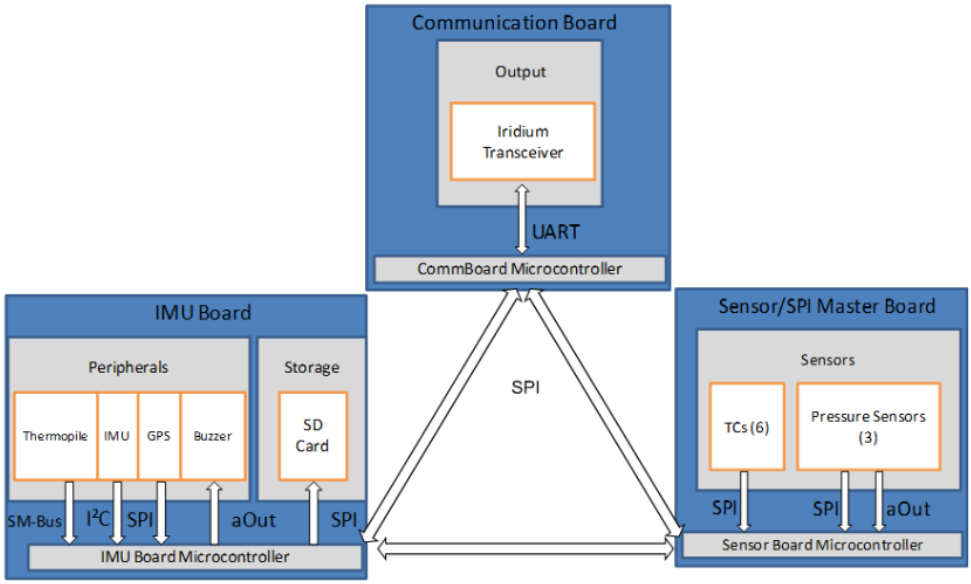


Figure 6. Simplified OBC process overview

This will greatly reduce the complexity of the integration. However, the components can be arranged in any order and the contour of the board is customised to fit the inner volume of the capsule.

2.4. Mirror System

The left-hand box of Fig. 5 illustrates that the mirror system is almost an exact copy of the capsule electronics. Like the capsule, it features its own power source. It only varies in the connection to the electronics of the separation-mechanism, which will send the attained data to the ground station by the REXUS downlink. The Iridium- and GPS-transceiver are replaced by dummy resistors. To simulate an Iridium connection, the OCU emulates the Iridium interface. The activation of the mirror system will be triggered by the OCU, when the experiment starts.

2.5. Separation-mechanism LOTUS

LOTUS is designed to ensure a secure and well-defined separation of the MIRKA2-RX vehicle. It is shown in Fig. 7. It is fixed via a base plate to a mounting structure connected to the bottom plate of the experimental module discussed in chapter 2.2. Two rails are mounted to the base plate in order to fix the position of the carriage and to guide it during the separation phase.
To ensure a good sliding of the carriage Polytetrafluorethylene (PTFE) parts are mounted to the inner side of the rails. The carriage provides a good fit for the nose tip of the capsule and is placed between the two rails. Between the base plate and the carriage, four compression springs are located, which will be held down with the capsule inside of the carriage by two clamps. A wire around LOTUS holds the clamps together until separation. In the centre of the base plate the deactivation rod described in chapter 2.3 is fixed. It runs through a hole in the middle of the carriage into the nose tip of the capsule to maintain the deactivation of its electronic system until it will be ejected.
To eject the capsule, the wire around LOTUS will be cut by a pyro cutter to release the two clamps, which will swing open due to torsion springs. Subsequently, the compression springs push the carriage outward after which the capsule is released. At the same time, the deactivation rod releases the deactivation mechanism and the capsule is switched on.
The electronic design of the separation-mechanism is depicted in Fig. 5 in the green box in the centre. As already mentioned in chapter 2.2, the action cameras will record the performance of the separation. They are intended to be activated when the power supply of the REXUS rocket is switched on. The data of the camera directed towards the hatch will transmit to the ground station via REXUS TV downlink.

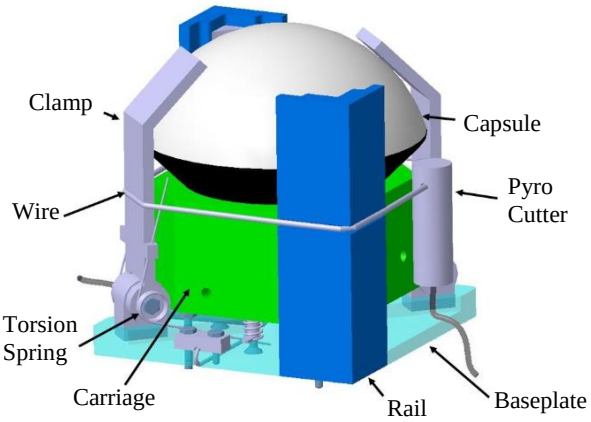


Figure 7. Ejection system in tension state

The data of the second camera directing to LOTUS will be saved on the SD Card located on the OCU, which will be explained in detail in the following section 2.6. The signal to trigger the ignition of the pyro cutter will be generated by a pyro cutter board, which is part of the OCU. The OCU is positioned inside of the mirror box.

2.6. On-Board Control Unit

The OCU consists of one Arduino Mega [12] and one adapter board placed on the top of the Arduino. The Arduino is responsible for the data handling and the transmission of the sensor data of the mirror system as depicted in Fig. 8. To simulate the Iridium transceiver, the sensor data of the mirror system will be acquired with an emulated iridium interface. Subsequently the data will be transmitted via REXUS downlink, to the ground station. The adapter board provides the connections to attach all peripheral components and the D-sub connector from the rocket to the Arduino. In addition, it contains all necessary parts to control the action cameras and to run the LEDs, which will illuminate the module for the cameras.
To be able to provide the high current of 1A to ignite the pyro cutter of LOTUS, a dedicated pyro cutter board was designed. It contains several tantalum capacitors, which provide the needed power. They will be charged by a separate power source consisting of five SAFT lithium batteries. A separate power source is needed to separate it completely from the REXUS energy system, because after the ignition of the pyro cutter a short circuit occurs, which may otherwise damage the power system of REXUS.

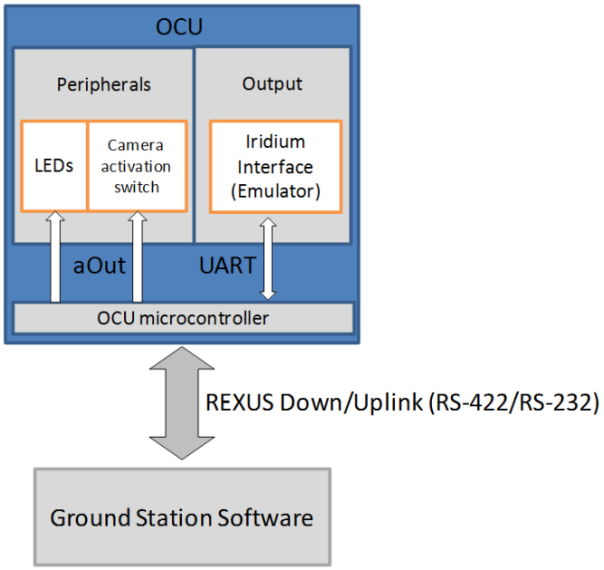


Figure 8. Simplified OCU process overview

3. QUALIFICATION TESTS

Currently, the MIRKA2-RX project is in its qualification phase. Hence, all system elements will be tested for compliance with the requirements.
To qualify the flight stability, a mock-up of the capsule with adjustable centre of gravity was dropped from a crane from a height of 20 m. The movement of the capsule showed that with a centre of gravity at 46% of the capsule's length as seen from the nose tip, the capsule stabilizes itself even if it is dropped with the aft shell pointing downwards.
Furthermore, a vertical wind tunnel test was successfully conducted. Therefore, the capsule was hung inside the wind tunnel and the wind velocity was raised until the capsule started floating. From the moment it began floating it displayed a stable flight behaviour.
The separation mechanism was already successfully tested under gravitational influence without the pyro cutter as well.
Besides the stability tests and the separation test, some of the electronic components such as the wildlife tracker and the Iridium transceiver as well as some software elements were successfully tested.
In order to test the behaviour of the whole system under the extreme conditions of the launch and in space, the following tests will include a shaker test, a thermal vacuum test and an electromagnetic test.

4. CONCLUSION

The experiment MIRKA2-RX is described. Since within this project the whole ejection system as well as the electronics, software, communication and structure of the capsule was developed, the CAPE project will make a major step forward to its completion. Aside of the technical advance, the measurement of the flight stability and the stagnation pressure can be used to improve simulations. Furthermore, the acquired experience will be of great help towards the construction of the SDM of CAPE.
For the involved students it is an excellent opportunity to apply their knowledge and to improve their skills in developing and executing spaceflight projects, in order to be better prepared for future challenges in the space industry. In this aspect, the MIRKA2-RX project stands out for its ambitious aim to integrate more than 20 students alongside their studies, which is enabled through the student society called KSat e.V., a well-structured project management and the support of the Institute of Space Systems (IRS) of the University of Stuttgart, Germany.

5. OUTLOOK

After the experiment, the attained data will be analysed and used to improve the performance of the capsule and the separation system, followed by further experiments to qualify the system and to rise the Technical Readiness

Level. Subsequent to the qualification, the SDM of CAPE will be designed, built and tested. For the qualification process, another REXUS experiment could conceivably be performed.
Should the CAPE mission prove a success, the SDM could also carry other payloads beside the MIRKA2 capsule.

6. REFERENCES

[1] M. Ehresmann, A. Behnke, J.-P. Baumann, J. Franz, D. Galla, B. Gäßler, F. Grabi, F. Hießl, M. Koller, G. Kuhn, N. Müller, R. Müller, A. Papanikoloau, J. Rieser, V. Schöneich, H. Seiler, M. Siedorf, V. Starlinger, A. Stier, A. Tabelander, F. Vardar, S. Wizemann, A. S. Pagan, G. Herdrich, and R. Laufer: *CubSat-sized Re-entry Capsule MIRKA2*. 10th IAA Symposium on Small Satellites for Earth Observation, Berlin, 2015

[2] A.S. Pagan, G. Herdrich, R. Laufer, and the KSat Team: *CubeSat Atmospheric Probe for Education (CAPE)*. 10th IAA Symposium on Small Satellites for Earth Observation, Berlin, 2015.

[3] G. Herdrich, R. Laufer, A. S. Pagan, et al: *Planetary Probe Design Workshop: Collaborative Hands-On Small Satellite Training for Engineering Students*, 10th IAA Symposium on Small Satellites for Earth Observation, Berlin, 2015

[4] V. Schöneich, F.Grabi, H.Seiler, J.-P. Baumann, A. Behnke, M. Ehresmann, J. Franz, D. Galla, M. Koller, J. Rieser, M. Siedorf, R. Tietz, A.S. Pagan, G Herdrich, and R. Laufer: *A Service and Deorbit Module for CubeSat Applications*. 10th IAA Symposium on Small Satellites for Earth Observation, Berlin, 2015

[5] A. Sidor, R. Braun, and D. DePasquale: *RED-Data2 Commercial Reentry Recorder: Size Reduction and Improved Electronics Design*. AIAA Atomospheric Flight Mechanics Conference, 2014 [Online] http://www.ssdl.gatech.edu/papers/conferencePapers/AIAA-2014-1231.pdf (accessed November 2015)

[6] J.-P. Baumann, A. Pagan, and G. Herdrich: *Aerothermodynamik re-entry analaysis of the cubesat-sized entry vehicle MIRKA2*

[7] J. Göhring, S. Hackemann, and B. Kanka: *Whipox®: Ein faserverstärkter oxidkeramischer Werkstoff für Hochtemperatur- Langzeitanwendungen. Mat.-wiss. U. Werkstofftech. (2007), 38: 766-772.doi: 10.1002/mawe.200700191*

[8] LOCOSYS Technology Inc.: GPS_LS20031_datasheet_v1.3. Available online at: http://www.locosystech.com/product.php?zln=en&id=20# (accessed November 2015)

[10] Quake Global, Inc.: Quake Q9602 datasheet. Available online at: http://www.m2mconnectivity.com.au/sites/default/files/brochures/9602_Marketing_Datasheet.pdf (accessed November 2015)

[11] Arduino, LCC: Arduino Nano Data Sheet. Available online at: https://www.arduino.cc/en/uploads/Main/ArduinoNanoManual23.pdf (accessed November 2015)

[12] Arduino, LCC: Arduino Mega Documentation. Available online at: https://www.arduino.cc/en/Main/ArduinoBoardMega2560#documentation (accessed November 2015)

[13] S. Lee: The CubSat Program: *CubeSat Design Specification.* California Polytechnic State University, San Luis Obispo, CA 93407, USA. Technical note - Revision 13 (2014)

THE COSMIC PARTICLE TELESCOPE PROJECT - FIRST RESULTS

Timo A. Stein[*1,2], **Julian Petrasch**[3], **Anton Walter**[4], **Anastasiya Dykyy**[1], **Michael Beermann**[1], **and Lucas Kempe**[5]

[1]*Norwegian University of Science and Technology, 7491 Trondheim, Norway.*
[2]*Integrated Detector Electronics AS, 0484 Oslo, Norway.*
[3]*Freie Universität Berlin, 14195 Berlin, Germany.*
[4]*Beuth Hochschule für Technik Berlin, 13353 Berlin, Germany.*
[5]*Technische Universität Berlin, 10587 Berlin, Germany.*

ABSTRACT

The Cosmic Particle Telescope (CPT-SCOPE) instrument is a technology demonstrator utilised for the study of subatomic particle precipitation in the lower atmosphere. The device has been developed by students from Norway and Germany within the REXUS/BEXUS programme. It combines COTS with custom radiation-hard components to allow for rapid development and low-cost while providing valuable scientific output. CPT-SCOPE was flight-tested aboard BEXUS 20 on October 10, 2015.

The instrument test was successful and produced altitude-dependent particle count rates showing the Pfotzer maximum, temperature and pressure readings as well as positional data. This paper summaries the preliminary scientific and technological findings, states observed issues and the CPT-SCOPE educational programme. Lastly, future steps towards a miniaturised radiation monitor for nano- and picosatellites will be outlined.

Key words: Radiation Monitor, REXUS/BEXUS, Stratospheric Balloon, COTS, BEXUS 20, CPT-SCOPE, Particle Telescope, Rad-hard.

1. INTRODUCTION

1.1. Motivation

The study of primary and secondary cosmic rays in the atmosphere and in space has been carried out over several decades [1, 2]. Nevertheless this field remains an active and dynamic research topic. Taking the space perspective it is important to follow the latest trend of highly miniaturised consumer electronics. Traditional space-rated electronics is of much older technology and usually larger, more expensive with lower performance. The available state-of-the-art electronics should be utilised in space to serve emerging sectors involving nano- and picosatellites such as CubeSats [3]. These platforms have a radically different and simplified philosophy as compared to conventional larger satellites allowing for easier and rapid design and lower overall cost but providing less reliability.

Such inexpensive satellites may be used to build larger constellations. One application for such would be a space weather monitoring service in LEO with a few satellites also placed in other orbits. A first serious step towards space weather monitoring capabilities by CubeSats was taken in 2012 when the CSSWE mission was launched providing valuable scientific data to the community [4]. However, at present there are no standard compact radiation monitoring devices available off the shelf for CubeSats. Either these devices are too large e.g. SREM [5] or NGRM [6], not yet fully space-qualified (HMRM), have only a small number of channels (CSSWE) or are restricted due to export regulations. This project is intended to start a new design of a compact radiation monitor for CubeSats. This is done along-side other on-going European activities such as the HMRM [7, 8]. In the present approach an IDEAS rad-hard front-end integrated circuit (IC) is used in combination with consumer electronics to build a sufficiently miniaturised device capable of delivering valuable scientific data. Such device is becoming increasingly relevant for more sophisticated space infrastructure is build and plans of human space exploration beyond LEO are at hand. An ultra compact radiation monitor may also be used for proposed interplanetary CubeSat missions or personal dosimetry.

When looking at Earth the interaction of cosmic rays with the atmosphere and its effect the our planet's climate is not well understood [1, 9, 10]. In particular the radiation fields and dynamics in the stratosphere lack observational data [11] and are subject to recent studies e.g. by the BARREL team [12].

The CPT-SCOPE project started with a single-channel lab prototype developed within a master thesis [13, 14]. This activity was a spin-off from the Norwegian NUTS CubeSat project [15, 16]. Based on the initial single channel design a team of Norwegian and German students developed a four channel technology demonstrator which is capable to withstand the harsh conditions associated with

[*]corresponding author, e-mail: timo.stein@ideas.no

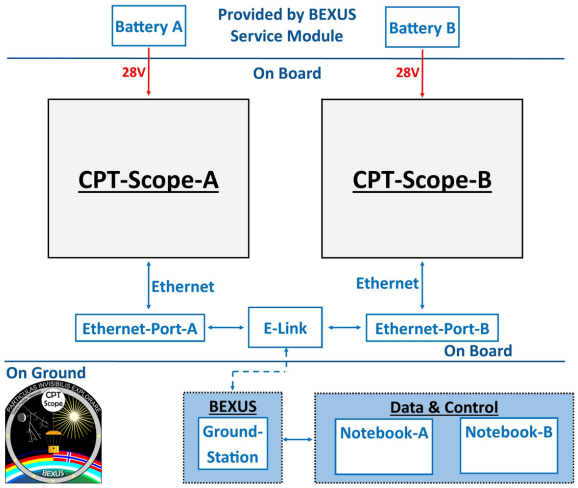


Figure 1. CPT-SCOPE main block diagram.

a stratospheric balloon flight while being able to study the particle precipitation in the tropo- and stratosphere.

The team was selected for the REXUS/BEXUS programme [17] for a flight aboard BEXUS 20, a stratospheric balloon, along-side the Belgium HACORD (directivity of cosmic rays) and German COSPA (microscopic particles) instruments. CPT-SCOPE is the first Norwegian participation for BEXUS. Other radiation detectors have flown previously aboard BEXUS or REXUS mission such as PERDaix [18] or other instrument examples [19, 20, 21, 22]. One common atmospheric feature studied by these missions concerning cosmic rays was the Pfotzer maximum [1]. In regard to CPT-SCOPE the focus of the project was technology development and testing while producing sound scientific data for cosmic rays in the lower atmosphere.

1.2. Instrument Description

The instrument is capable of measuring subatomic particles with energies ranging orders of magnitude of 0.1 MeV to 100 MeV and low-energetic gamma rays of 50 keV to 150 keV. This is achieved with four epoxy-covered, reversed-biased silicon detectors (First Sensor X100-7 THD, 250 μm thickness, 1 cm^2 active surface, biasing voltage: 35 VDC) arranged in an absorber-sensor-stack, also known as particle telescope. The sensors had a p-readout i.e. positive charges were injected into the front-end electronics.

Limited ability to determine the particle species and energy based on individual trigger patterns was planned. However, this feature had to be removed due to resource limitations. A trigger-based, as opposed to an analogue readout, approach was utilised in order to allow for high-count rates and reduced external hardware. The count rates for each channel was recorded instead of more advanced pattern recognition. Redundancy was provided by

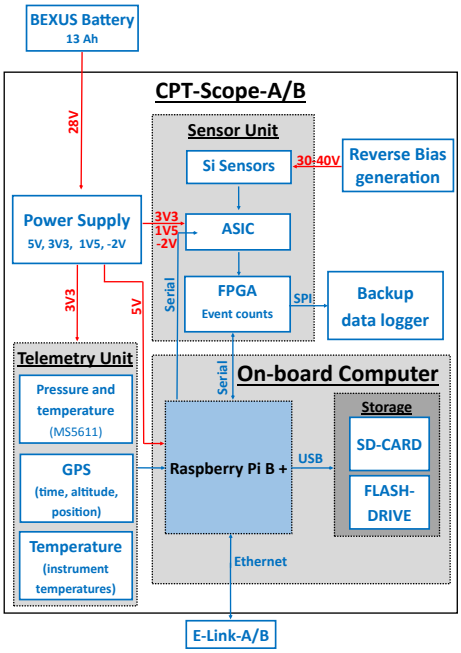


Figure 2. CPT-SCOPE individual instrument system block diagram.

duplicating the hardware, running two devices independently called CPT-A and CPT-B. Each instrument was identical besides the used particle telescope geometry which was optimised for different energy ranges. CPT-A and CPT-B utilised 4 channels with each two triggers (A and B) per channel at different threshold values.

The device implementation used mostly commercial off-the-shelf (COTS) components to allow for rapid development and low cost. These were combined with specialised detector front-end electronics based on a radiation-hard IDEAS VATA465 integrated circuit (IC) [23, 24]. A custom power supply, reverse-bias generation board and two interface cards were designed. The block diagrams for the overall CPT-SCOPE and for the individual instruments CPT-A and CPT-B are shown in Fig. 1 and Fig. 2, respectively. CPT-SCOPE instruments CPT-A and CPT-B were each connected to a BEXUS 28VDC battery and the E-Link system for communication.

A FPGA was used as high-speed counter with a SPI interface. The counter received and processed trigger signals from the VATA465 IC. A Numato Lab Mimas board featuring a Xilinx Spartan-6 FPGA was used and programmed in VHDL. The science payload was configured and readout by an on-board computer (OBC), a Raspberry Pi model B+, running a Linux operating system and storing data on a SD card. In addition to particle count rates, telemetry data was collected by the OBC and telemetry unit such as external pressure and temperature at various locations and position information using a commercial modules. Telemetry modules were readout using either I2C or serial interfaces. Care has been



Figure 3. CPT-SCOPE mounted inside the BEXUS 20 gondola. The black material is the thermal insulation and the red labelled places are access points. Gaffer tape was used to keep the insulation in place.

taken to isolate and shield sensitive analogue electronics such as the sensor head from noisy digital electronics e.g. the OBC. Low-pass filtering has been employed on all sensor-related power rails. The total power consumption for CPT-SCOPE was 7 W. CPT-A and CPT-B (each 3.5 W) were powered from individual batteries and had their own E-Link connection.

The OBC was running multiple threads of Python scripts to control I/O operations, schedule and execute readouts and configurations of subsystems as well as communicating with a ground station control and monitoring software written in Python and Java. UDP was used for down-streaming sensor and telemetry data. Every UDP package used a MD5 checksum to verify the package integrity. Each packet received a unique identifier and system timestamp. The logging thread is controlled by a server thread. The server thread receives commands via E-Link. The commands are transferred with a self-developed protocol based on TCP. The device can also run autonomously.

The finished device had dimensions of 27.9 cm x 29.0 cm x 32.2 cm (LxWxH, including mounting) and a total weight of 4.1 kg. The mechanical structure was made from aluminium sheets. Thermal insulation of approx. 1 cm thickness was used on all sides with the exception of two openings for the particle telescopes, cables and other access points. A picture of the final device mounted inside the gondola is shown in Fig. 3 while the opened CPT-SCOPE instrument exposing CPT-A and CPT-B along with labelled subsystems is provided in Fig. 4. A more detailed overview about CPT-SCOPE was provided in a recent ESA PAC paper [16].

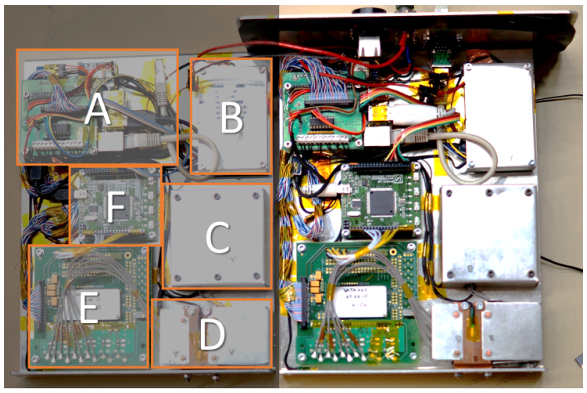


Figure 4. CPT-A (left, labelled) and CPT-B (right) with exposed subsystems before assembly: A - OBC and interface card 1, B - power supply, C - reverse-bias generation, D - particle telescopes, E - front-end electronics and interface card 2, F - counter FPGA.



Figure 5. GPS flight path of BEXUS 20 recorded by the CPT-A telemetry unit. Background map credit: OpenStreetMap.

1.3. Flight Campaign

CPT-SCOPE was launched on October 10, 2015, 09:16:54 UTC from the European Space and Sounding Rocket Range (ESRANGE) in Kiruna, Sweden. The balloon was ascending for 1h 39m with 4.68 m/s till 28.2 km altitude. The float began around 10:54:35 UTC. Its duration was 2h 10min 5s and the float ground range was 171 km at approx. 28 km altitude with a slight decease towards the end. Cut-down occurred at 13:06:03 UTC. The ground was reached around 13:43:04 UTC over Finish territory. The mainly eastwards flight track is shown in Fig. 5.

The ground station was receiving telemetry and science data for the whole flight duration except the last 1,000 m of descend. It was not necessary to change the readout IC's configuration. Therefore, only ping commands were issued to the instruments to check the functionality of the command connection periodically and retrieve near-real time data. After the landing the instrument was running for an additional 19h 54min 28s until the batteries were empty. Hence, the total runtime of instrument CPT-A was 1d 1h 34min 45.41s and 1d 1h 31min 52.99s for CPT-B.

The instrument was returned to ESRANGE on Sunday, October 11, 2015. The instrument remained mounted in

the gondola and was transported back from Finland by truck after being airlifted to the next street using a helicopter. The gondola had a hard landing bending the aluminium frame. From the detailed GPS altitude data the gondola has likely experienced at landing a rapid fall of at least 10 m after impact and shortly after experienced three more falls of at least 1 m each within a four minute window. However, since no separate acceleration data is available the exact events during the landing are not clear. In addition, the gondola was transported loaded sideways causing excessive mechanical stress on the instrument. This is important for our investigation into a minor mechanical failure at the end of this paper.

2. RESULTS AND DISCUSSION

The OBC unit recorded data continuously for over 25 hours 30 minutes starting on October 10, 2015, at 07:53:15 UTC until the supply batteries were drained. This resulted into 53489 and 53679 data packages for CPT-A and CPT-B, respectively. Of these were valid 53477 (>99.9%) for CPT-A and 53568 (>99.7%) for CPT-B and provided useful telemetry and science data. Each package contained a unique ID, system time, ambient pressure, several temperature readings from in- and outside the instrument, GPS location and time, test register readings and the science data i.e. counter register values. The period between packages was 1723 ms and 1732 ms for CPT-A and CPT-B, respectively.

The data analysis was carried out using a Python 2.7 script in combination with libraries Numpy, Pandas and the Matplotlib. The system time of instrument CPT-B had to be manually synchronised to the CPT-A GPS-time due to a failure of the CPT-B GPS-receiver. The science data was re-sampled using Pandas at 4 minute intervals in order to reduce noise by adding registered events within each time bin. The raw data is available on request.

In the following paragraphs we will present the preliminary data and subsystem status retrieved from the recovered instruments CPT-A and CPT-B memory. The data correspondents with the down-linked data (not shown) which was obtained during the flight.

2.1. Technical Data

2.1.1. Subsystem Status

All subsystems have been found operational throughout the flight for both CPT-A and CPT-B. Minor technical issues were observed with the telemetry and on-board computer unit. The FPGA module has always returned proper test register values and was hence functioning properly the entire time. No power cycling was observed from the system indicating full functionality of the power supply. Science data was obtained pre-, during and post-flight. Although the observed noise levels were high at times for individual channels the overall function of the sensor unit (science payload) was complete throughout the entire run. The OBC reported stable core temperature, frequency and voltage (10 °C - 30 °C, 700 MHz, 1.2 V). Network communication through the E-Link system was available throughout the flight and data was recorded continuously. Nevertheless, a small number of packages were lost or corrupted, and several others written to memory delayed or duplicated likely due to internal buffering. This affected below 0.5% of all packages. The GPS-receiver for CPT-B failed before flight already, while unit CPT-A worked without any issue allowing for precise timing and positional data.

No data is available after the instruments shut down on October 11, 2015 at 09:37:24 UTC. When the instrument was taken apart for inspection back at ESRANGE it was observed that the aluminium cap protecting the sensitive readout IC for CPT-B was loose and damaged several wire-bonds. Due to the fact that CPT-B delivered proper science data even after the landing the damage must have occurred during the transport back to ESRANGE. A failed M2.5 screw thread inside the aluminium cap (not shown) in combination with the hard landing and mechanical stress during back transport was identified as cause of the failure.

2.1.2. Telemetry Data

The telemetry unit on both instruments functioned without significant failure. Telemetry data included instrument position and UTC time from GPS satellites, ambient pressure and several temperatures from the in- and outside. Units CPT-A and CPT-B recorded 8 temperature readings per cycle.

The temperature readings for CPT-A (top) and CPT-B (bottom) are shown in Fig. 6 for the duration of the flight.

Internal temperatures: Note that the internal temperature was always within a range of -15 °C and +25 °C while external temperatures varied between approx. -58 °C and +25 °C. Temperature sensitive components such as the FPGA board where mounted close to components with higher heat dissipation to allow for higher operating temperatures. The placement of the external temperature sensors was also important as the gondola slowly rotated in and outside the sun causing variable heating.

External temperatures: The CPT-A ambient, external temperature (right) and pressure (left) profile for the ascend phase is shown in Fig. 7. The altitude is inferred from the GPS positional data collected by the telemetry unit. The ambient temperature on the ground was approx. -1 °C. The temperature decreased to -5 °C by the time an altitude of 1.2 km was reached. The balloon flew then through an inversion layer in the troposphere causing a rise in temperature to +2.5 °C at 2.1 km. The tropopause was reached at an altitude of 12.3 km with minimum

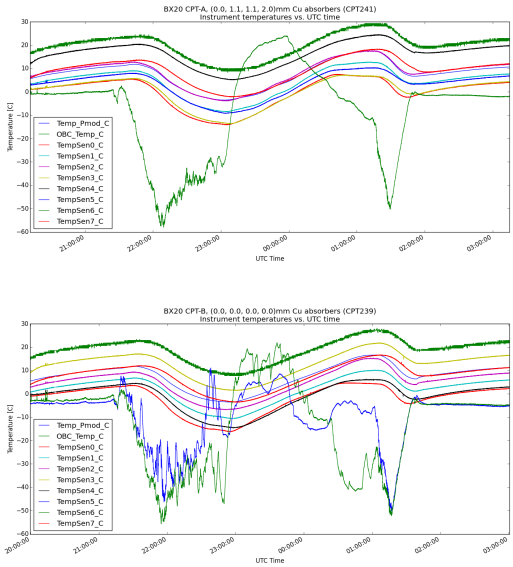


Figure 6. Temperature readings of CPT-A (top) and CPT-B (bottom) shown for the flight of BEXUS 20. The temperature range is from -60 °C to +30 °C (y-axis).

temperature of -58 °C. The temperature then increased steadily within the stratosphere until the float altitude of approx. 28 km was reached with initial temperatures of -32 °C to -27 °C. The variation in the temperature is suspected to be caused by a slow rotation of the gondola in reference to the sun. The external sensor slowly started to warm up to +10 °C before cut-down due to heat dissipation of the instruments and solar irradiation. This leads to the suggestion that no thermal equilibrium was achieved, likely due to too strong thermal insulation. However this allowed to operate all components within tested temperature limits.

Pressure profile: The pressure profile (left) for the ascend of CPT-A as function of altitude is shown in Fig. 7. Note the logarithmic scale for the pressure. The ground temperature was -1 °C at an altitude of 322 m. The decrease in pressure follows approximately the expected exponential decrease over increasing altitude. However, the effect of the varying external temperature is visible as "bending" away from the idealised standard atmosphere at constant temperature. The float altitude was around 28.2 km with external pressure of 11.9 mbar. The readings of the pressure sensor were used in the determination of the interaction depth X for the science data analysis but not for altitude determination.

Altitude profile and positioning: The telemetry unit of CPT-A was able to provide precise positioning data during the BEXUS 20 flight and helped to understand what happened during and after the landing. The altitude profile for the flight is shown in Fig. 8, while the flight path is shown projected onto a map in Fig. 5. The BEXUS 20 flight was already discussed above.

2.2. Science Data

At the heart of the CPT-SCOPE project was the development of a compact radiation monitoring device capable of measuring count rates for energetic subatomic particles in the energy range of several 100 keV to several 10 MeV. Each instrument hosted one particle telescope consisting of each four silicon (Si) detectors stacked on top of each other. While CPT-A had thin copper (Cu) absorbers between the inner sensors, CPT-B had none. Both instruments had the first sensor ("0") exposed facing the top towards the balloon. The thickness of the Cu absorbers for CPT-A were 1.1 mm in front of the second ("1") and third ("2") each and 2.0 mm before the last sensor ("3"). The sensor separation within the particle telescope was approx. 4.0 mm. The particle telescopes were mounted within a 6 mm thick Cu housing closing all sides besides an opening for the PCBs and sensors facing the top. This acted as shield against lower to medium energetic particles not entering from the top.

Due to variable performance of the individual channels the threshold values of the readout IC were set to different values for each channel and A- / B-window trigger. The following values were used for CPT-A: A0 = 30, A1 = 30, A2 = 43 and A3 = 50; B0 = 1, B1 = 1, B2 = 2 and B3 = 2. While CPT-B was configured as follows: A0 = 30, A1 = 30, A2 = 30 and A3 = 30; B0 = 1, B1 = 1, B2 = 1 and B3 = 1.

For every data package the OBC requested from the FPGA the value for each channel's current counter value. This data is available at relatively high time resolution of some 1.7 s. The readout device was automatically reconfigured every 1,000 packages resulting in erroneous counter readouts. These values were easily removed thanks to their repetitive nature as a first step. In the next step the previous counter value was subtracted in order to only deal with new triggers instead of their cumulative number relevant for dosimetry.

At the relatively high readout rate and small detector size only a few triggers are expected per reading. In order to increase the expected number of events, and therefore improving the counting statistics, the raw counter increase values were first summed for fixed time intervals of 240 s using the `resample()` function of the Pandas library in Python. This step does not influence the resulting data analysis but enables to improve noise performance at the cost of a lower temporal resolution, and to deal with missing data points or noise triggers.

In the last step the count rate is determined by dividing the counter increase over the integration time in order to obtain instrument count rates.

In order to display the data in a well-comparable manner the interaction depth X was chosen instead of the altitude. The interaction depth X, calculated from the ambient pressure p, is a measure of how much the air column atop the instrument weights per unit area. This is directly related with the number of possible interaction partners

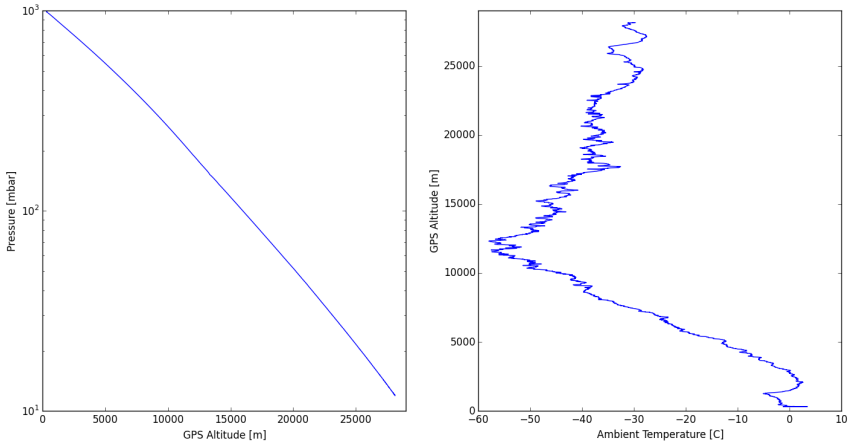


Figure 7. Relevant meteorological flight data for the balloon ascend provided by CPT-A: Logarithmic plot (left) of the ambient pressure over altitude. The external temperature profile (right) over altitude.

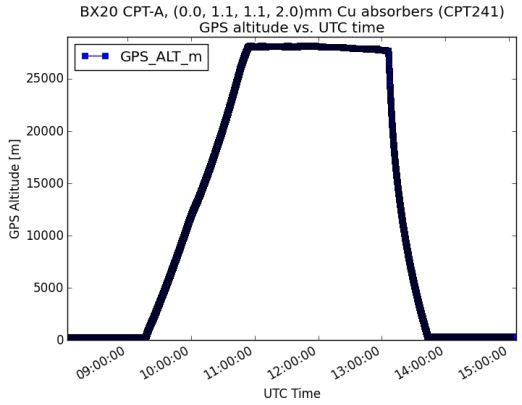


Figure 8. GPS altitude over UTC time for the BEXUS 20 flight.

an energetic particle encounters along its path towards the ground. To first order it is assumed that all particles are coming vertically i.e. perpendicular to the ground. In this way the interaction depth X is easily evaluated as:

$$X = \frac{p}{g}.$$

The local[1] acceleration due to gravity was used for Kiruna, Sweden, namely $g = g_{\mathrm{Kiruna}} = 9.8227\, m\, s^{-2}$. The value of X was approx. 1,000 g cm^{-2} on the ground as compared to some 12 g cm^{-2} during the float phase, a decrease by a factor of almost 100. The resulting instrument count rates - in units of Hz cm^{-2} - are shown for the sensor A-trigger (top) and B-trigger (bottom) in Fig. 10 for CPT-A (Cu absorber) and in Fig. 11 for CPT-B (no absorber). Note that the threshold values for the channels was set to different values (see above). The scaling for these figures is as follows: Interaction depth from 10 to 1,010 g cm^{-2} logarithmic scale for all graphs, and instrument count rate in the range of 0 to 2 Hz cm^{-2} and 0 to 1 Hz cm^{-2} (linear) for the A- (top) and B-trigger (bottom) graphs, respectively.

The general picture is consistent with the expected behaviour [1]: The count rate is lowest but non-zero at ground level (X = 1,000 g cm^{-2}), less than 0.05 Hz cm^{-2} and 0.03 Hz cm^{-2} for A- and B-triggers of CPT-A and CPT-B, respectively.

As the balloon climbs the count rate increases significantly until it reaches a broad maximum with 0.35-0.75 Hz cm^{-2} (0.10-0.60 Hz cm^{-2}) for the B-trigger and 0.80-1.00 Hz cm^{-2} (0.90-1.10 Hz cm^{-2}) for the A-triggers of CPT-A (CPT-B) around an interaction depth $X \approx 40$ g cm^{-2} (equivalent to p = 39.3 mbar, 21.6 km altitude). This likely constitutes the Pfotzer maximum which is to be expected at an $X < 100$ g cm^{-2} [1].

With higher altitude i.e. lower interaction depth X the count rate decreases but less pronounced to 0.30-0.50 Hz cm^{-2} (0.10-0.40 Hz cm^{-2}) for the B-trigger and 0.60-0.80 Hz cm^{-2} (0.55-0.65 Hz cm^{-2}) for the A-triggers of CPT-A (CPT-B).

Please note that the broad spreed is due to the different response and threshold settings of the individual sensors and their placement within the particle telescope. Follow-up tests must be conducted to verify the correct labelling of sensor values. However, a wrong labelling is unlikely. Furthermore, several transient triggers are visible in particular for the A0 triggers of both CPT-A and CPT-B, and in addition the A3 channel of the CPT-B. Such events are also visible in the long-term raw data shown in Fig. 9. The nature of these events is unclear but are likely caused within the instrument itself or due to pick-up from external interference as such behaviour was previously observed in the laboratory as well.

[1]Obtained from the Gravity Information System of PTB: `http://www.ptb.de/cartoweb3/SISproject.php`.

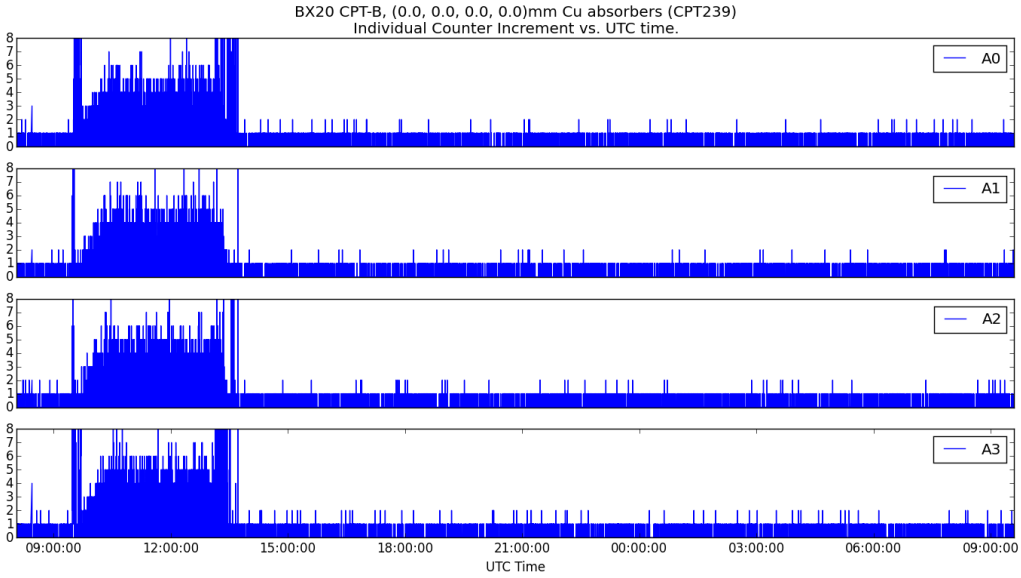


Figure 9. Increment of A-trigger counters for CPT-B (no absorbers) between consecutive package readings as function of time. The data has the periodic erroneous readings due to the device configuration already removed. However, the original sampling rate and the full measurement duration of over 25 hours are shown. Clearly visible are the increased triggers due to increased number of particles at higher altitude during the BEXUS 20 flight (approx. 9:00 and 14:00 UTC). Strong transient noise triggers are are also visible in particular at ascend and descend in channel A0. Note that no significant change in the count rate is observed after landing indicating that the mechanical failure of the readout IC housing occurred during recovery and transport back to ESRANGE.

Further evaluation of the scientific data without detailed simulations and calibration measurements are not possible. These steps shall be further investigated in the following months. It should be noted that CPT-SCOPE is due to time limitations a technology demonstrator and hence emphasis was placed on getting the detector system to work without full pre-calibration. Nevertheless, it should be noted that all channels produce scientific data and the overall shape of the measured instrument count rates follows the expected behaviour. The observed count rate graph is compatible with the preliminary findings of the HACORD instrument, a Geiger-counter-based radiation detector developed by Belgium students also flying aboard BEXUS 20. It will be of interest to compare the HACORD and CPT-SCOPE data once the data analysis is completed for both experiments.

3. EDUCATIONAL AND OUTREACH PROGRAMME

Besides the technical and scientific objectives the CPT-SCOPE project has also a strong outreach component. Its main focus was on education with the development of a secondary and high school curriculum by two science teacher students in Norway. The program consisted of two building blocks for the respective age group. The first module was theoretical and the other practical in order to engage students directly. The goal of both modules was to motivate students for future studies within space research or other natural sciences disciplines. Educational material for teachers was also created and complemented with simple experiments such as floating weights on helium-filled balloons or visualising radioactivity with cloud chambers. Throughout the CPT-SCOPE school programme four sets of educational materials for the use in schools were developed. We also presented our material to some 150 secondary school pupils in seven different presentation at secondary schools in the Trondheim region, Norway. In addition, talks were given at conferences and science outreach days such as the Researcher's Night 2015 in Trondheim. Lastly, a web[2] and Facebook page ("CPTSCOPE-Team") were maintained in English, German and Norwegian.

4. OUTLOOK

Further data analysis and calibration runs will hopefully allow us to properly adjust the instrument trigger rates to obtain true count rates. In this way we will be able to better compare our data with the HACORD results which are expected in early-2016, or previous REXUS/BEXUS radiation detectors. These findings along with other lessons learned will be published in a final SED document [25] and ideally additional articles.

[2]CPT-SCOPE web page: http://www.cpt-scope.com.

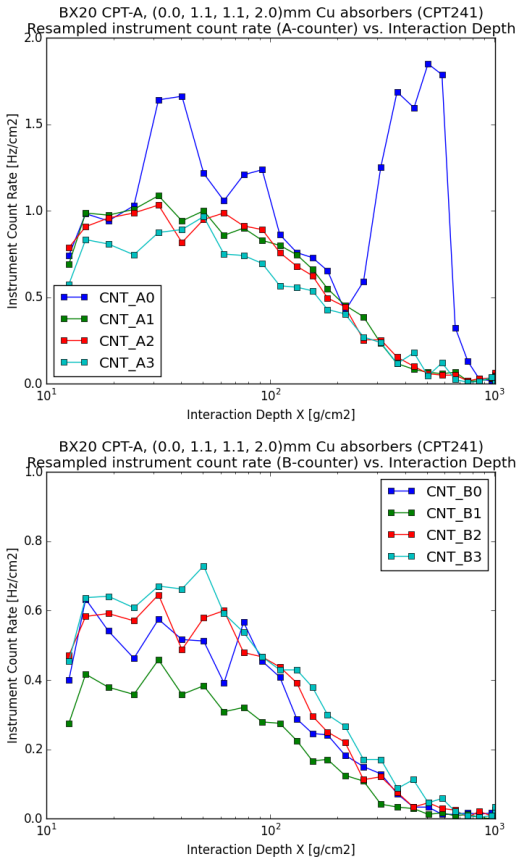


Figure 10. Instrument count rate as function of interaction depth X for CPT-A. The first graph shows the high-gain channel A-triggers, while the second one displays the B-triggers. Note that CPT-A has Cu absorbers between the inner sensors installed.

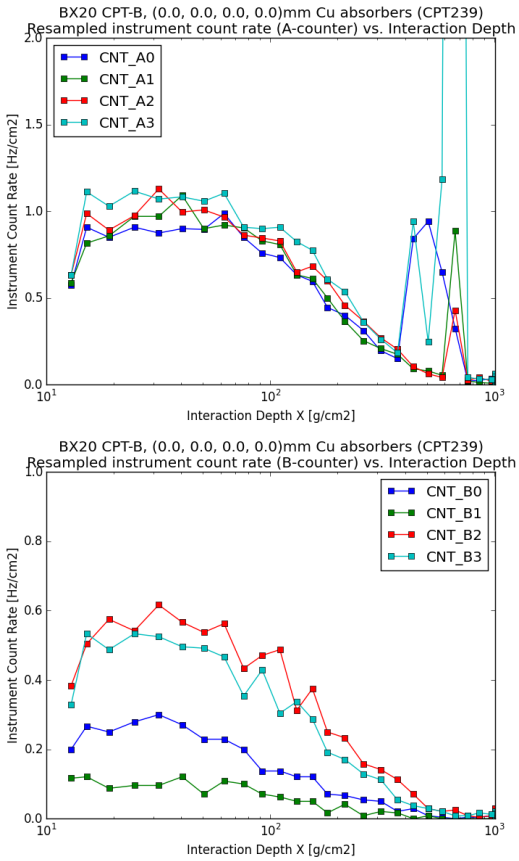


Figure 11. Instrument count rate as function of interaction depth X for CPT-B. The first graph shows the high-gain channel A-triggers, while the second one displays the B-triggers. Note that CPT-B has no absorbers installed.

The educational programme will continue and the Norwegian University of Science and Technology (NTNU) has acquired several cloud chambers for their school lab to visualise radioactivity. Alongside this and our school visits, we hope to have contributed inspiring a new generation of scientists and engineers.

Based on the experience made using an IDEAS VATA465 readout IC with CPT-SCOPE the development of a CubeSat-ready radiation payload will be the next step. For that an updated particle telescope geometry and the latest IDEAS VATA466 readout IC model, designed for the flight to Jupiter aboard the RADEM instrument [26] of the ESA JUICE mission, will be used which is easier to interface and providing better performance and features such as build in counters. This should allow for the development of a functioning prototype within the next three years. Such development could also be useful towards a personal dosimeter for astronauts in human space exploration beyond LEO orbit or for aircrews and passengers on polar routes.

5. CONCLUSIONS

The CPT-SCOPE instrument was successfully flight-tested aboard BEXUS 20. The two instruments CPT-A and CPT-B functioned almost fully with only minor issues. Both telemetry and science data provided valuable information to determine the functionality of the compact radiation monitoring technology demonstrator and towards future improvement. The radiation monitoring payload was able to measure the instrument count rates due to particle precipitation as function of altitude. A clear increase of the count rate with altitude is visible from all radiation data aboard both instruments and channels. The Pfotzer maximum is visible peaking at some $X = 40$ g cm^{-2} (21.6 km altitude). Additional analysis is required to fully calibrate the radiation data and comparing it to the HACORD instrument results. Transient noise triggers, in addition to other minor issues in subsystems, have to be further investigated. The CPT-SCOPE project was done within a short life cycle of less than one year which provided valuable experience. The first Norwegian participation within the BEXUS programme was achieved and in collaboration with German students the project was a big success and important milestone towards our planned compact radiation monitor for nano- and picosatellites.

ACKNOWLEDGEMENTS

CPT-SCOPE is a joint Norwegian-German student project. In addition to the authors, the following students contributed: F. Freyer, P. M. Schönberg, J. Stahn, R. Wenzel and G. H. Wesenberg. We would like to thank the project's endorsing professor, I. Simonsen (NTNU), and the REXUS/BEXUS team and partners. We would like to thank our main sponsor the Integrated Detector Electronics AS (IDEAS). In addition, the project has been supported by Sparebanken Midt-Norge, the Anette og Brynjulf Skaugens Veldedige Stiftelse, NUUG, SNSB / DLR / ESA, NTNU, UiO, CONTAG, Corentium, Hirose Electric, Numato Lab, Ikalogic, Advanced Energy Industries, WIMA, First Sensor AG, Flexitron, Webspace-Verkauf.de, with additional contributions of other sponsors and partners to which we are all grateful. Special thanks go to our families for their patience and support, to our IDEAS co-workers for their help, to SNSB / DLR / ESA for giving us the opportunity to participate in the REXUS/BEXUS programme, to the ESRANGE flight and support crew which allowed us to have a successful flight and stay in Kiruna and to the other REXUS/BEXUS teams of Cycle 8 for the great time.

REFERENCES

[1] P. K. F. Grieder. *Cosmic Rays at Earth: Researcher's Reference Manual and Data Book*. Elsevier Science & Technology, 2001. ISBN 0444507108.

[2] L. Dorman. Discovery and Research of Cosmic Rays on Balloons. In *Proc. "21st ESA PAC Symposium", 9-13 June 2013, Thun, Switzerland (ESA SP-721, October 2013) - ISBN 978-92-9092-285-8*, pages 655–662. European Space Agency, 2013.

[3] P. Fortescue, G. Swinerd, and J. Stark. *Spacecraft Systems Engineering*. John Wiley & Sons, third edition, 2003. ISBN 978-0471619512.

[4] X. Li, Q. Schiller, L. Blum, S. Califf, H. Zhao, W. Tu, D. L. Turner, D. Gerhardt, S. Palo, S. Kanekal, and et al. First results from CSSWE CubeSat: Characteristics of relativistic electrons in the near-Earth environment during the October 2012 magnetic storms. *Journal of Geophysical Research: Space Physics*, 118(10):6489–6499, Oct 2013. ISSN 2169-9380. doi: 10.1002/2013ja019342. URL `http://dx.doi.org/10.1002/2013JA019342`.

[5] A Mohammadzadeh, H Evans, P Nieminen, E Daly, P Vuilleumier, P Buhler, C Eggel, W Hajdas, N Schlumpf, A Zehnder, et al. The ESA Standard Radiation Environment Monitor program first results from PROBA-I and INTEGRAL. *IEEE Transactions on Nuclear Science*, 50(6):2272–2277, 2003.

[6] L. Desorgher et al. ESA Next Generation Radiation Monitor. In *14th European Conference onRadiation and Its Effects on Components and Systems (RADECS)*, pages 1–5, Sept 2013. doi: 10.1109/RADECS.2013.6937362.

[7] E. F. Mitchell, H. M. Arajo, E. Daly, N. Guerrini, S. Gunes-Lasnet, D. Griffin, A. Marshall, A. Menicucci, T. Morse, O. Poyntz-Wright, R. Turchetta, and S. Woodward. The Highly Miniaturised Radiation Monitor. 2014. URL `http://arxiv.org/abs/1401.3533`.

[8] N. Guerrini et al. Design and characterisation of a highly miniaturised radiation monitor HMRM. *Nuclear Instruments and Methods in Physics Research Section A: Accelerators, Spectrometers, Detectors and Associated Equipment*, 731:154–159, Dec 2013. ISSN 0168-9002. doi: 10.1016/j.nima.2013.06.073. URL http://dx.doi.org/10.1016/j.nima.2013.06.073.

[9] K. S. Carslaw, R. G. Harrison, and J. Kirkby. Cosmic rays, clouds, and climate. *Science*, 298(5599):1732–1737, 2002. doi: 10.1126/science.1076964. URL http://www.sciencemag.org/content/298/5599/1732.abstract.

[10] L. Dorman et al. Cosmic Rays and other Space Weather Factors Influenced on the Earth's Climate. In *Proc. "22nd ESA PAC Symposium", Tromsø, Norway, 7-12 June 2015 (ESA SP-730, September 2015) - ISBN 978-92-9221-294-0*, pages 547–554. European Space Agency, 2015.

[11] G. Reitz. Radiation environment in the stratosphere. *Radiation Protection Dosimetry*, 48(1):5–20, 1993. URL http://rpd.oxfordjournals.org/content/48/1/5.abstract.

[12] L. A. Woodger et al. A summary of the BARREL campaigns: Technique for studying electron precipitation. *Journal of Geophysical Research: Space Physics*, 120(6):4922–4935, 2015. ISSN 2169-9402. doi: 10.1002/2014JA020874. URL http://dx.doi.org/10.1002/2014JA020874. 2014JA020874.

[13] T. A. Stein. Development of a compact radiation monitor for space application. Master's thesis, NTNU, 2015. URL http://hdl.handle.net/11250/2352104.

[14] T. A. Stein. CubeSat-ready Radiation Monitor Front-End Electronics. 2014. URL https://www.cubesatsymposium.eu/.

[15] O. Gutteberg and R. Birkeland. Overview of the NUTS CubeSat project. In C. Chappelletti and F. Graziani, editors, *Proceedings of the 2nd IAA Conference of University Satellite Missions & CubeSat Workshop*, volume 2 of *IAA Book Series*. International Academy of Astronautics, 2013.

[16] R. Birkeland, T. A. Stein, M. Tømmer, M. Beermann, J. Petrasch, and A. Gjersvik. The NUTS Cubesat Project: Spin-offs and Technology Development. In *Proc. "22nd ESA PAC Symposium", Tromsø, Norway, 7-12 June 2015 (ESA SP-730, September 2015) - ISBN 978-92-9221-294-0*, pages 649–656. European Space Agency, 2015. URL http://pac.spaceflight.esa.int/proceedings/.

[17] N. Callens et al. REXUS/BEXUS: Rocket and Balloon Experiments for University Students. In *Proc. "21st ESA PAC Symposium", 9-13 June 2013, Thun, Switzerland (ESA SP-721, October 2013) - ISBN 978-92-9092-285-8*, pages 561–568. European Space Agency, 2013.

[18] C. Mai et al. The PERDaix experiment. In *Proc. "20th ESA PAC Symposium", Hyere, France, 22-26 May 2011 (ESA SP-700, October 2011) - ISBN 978-92-9092-264-3*, pages 539–546. European Space Agency, 2011.

[19] M. J. Losekamm et al. AFIS: A New Instrument for Cosmic Radiation Studies on BEXUS 18 and Future Nanosatellite Missions. In *Proc. "22nd ESA PAC Symposium", Tromsø, Norway, 7-12 June 2015 (ESA SP-730, September 2015) - ISBN 978-92-9221-294-0*, pages 377–384. European Space Agency, 2015.

[20] S. Martensen et al. Angular Distribution of Charged Particles on the Atmosphere - Results of the ADAM Experiment on BEXUS 19. In *Proc. "22nd ESA PAC Symposium", Tromsø, Norway, 7-12 June 2015 (ESA SP-730, September 2015) - ISBN 978-92-9221-294-0*, pages 535–538. European Space Agency, 2015.

[21] T. Möller et al. Radiation Measurement on the Stratopsheric Balloon BEXUS13. In *Proc. "21st ESA PAC Symposium", 9-13 June 2013, Thun, Switzerland (ESA SP-721, October 2013) - ISBN 978-92-9092-285-8*, pages 637–640. European Space Agency, 2013.

[22] B. Zabori et al. REM-RED Cosmic Radiation Monitoring Experiment On-board the REXUS-17 Sounding Rocket. In *Proc. "22nd ESA PAC Symposium", Tromsø, Norway, 7-12 June 2015 (ESA SP-730, September 2015) - ISBN 978-92-9221-294-0*, pages 539–546. European Space Agency, 2015.

[23] D. Meier et al. VATA465 Datasheet (Rev. 1.5). 2015. URL http://www.ideas.no/.

[24] D. Meier, S. Azman, J.E. Ramstad, A. Hasanbegovic, J. Talebi, M.A. Altan, H.K.O. Berge, P. Pahlsson, C. Gheorghe, T.M. Johansen, and G. Maehlum. Development of an ASIC for charged particle counting with silicon radiation detectors. In *Nuclear Science Symposium and Medical Imaging Conference (NSS/MIC), 2013 IEEE*, pages 1–5, Oct 2013. doi: 10.1109/NSSMIC.2013.6829764.

[25] T. Stein et al. Student Experiment Documentation (SED) for BEXUS: CPT-SCOPE, version 5.0. 2015.

[26] W. Hajdas et al. Development of radiation hard electron monitor RADEM for ESA JUICE mission. In *Geophysical Research Abstracts (EGU2015-11661)*, volume 17, 2015. URL http://meetingorganizer.copernicus.org/EGU2015/EGU2015-11661.pdf.

MISSUS EXPERIMENT SENSORS DATA ANALYSIS

S. Chiodini[(1)], C. Palla[(2)], G. Colombatti[(1)], S. Debei[(1)]

[(1)]CISAS "Giuseppe Colombo", Via Venezia 15, 35131 Padova (ITALY), Email: sebastiano.chiodini@studenti.unipd.it,
[(2)]Cranfield University, Space Research Centre, College Road, MK430AL Cranfield, Bedfordshire (UK)

ABSTRACT

MISSUS experiment (Meteorological Integrated Sensor SUite for Stratospheric Analysis) is a multi-sensor scientific package dedicated to the characterization of thin atmosphere parameters, such as temperature and pressure, and to the attitude and trajectory reconstruction. In particular, MISSUS temperature sensor is the prototype of MarsTEM the instrument which is part of the DREAMS suite (Dust characterization, Risk assessment, and Environment Analyser on the Martian Surface) on board ESA mission ExoMars 2016. BEXUS stratospheric flight provided a unique opportunity to test MarsTEM sensor prototype in a Mars similar environment, due to low atmospheric pressure and thermal exchange mechanisms.
This paper presents the data collected by MISSUS during BEXUS 15 flight, the experiment logged data continuously for 4 hours and 6 minutes. During the flight MISSUS temperature sensor measured the air stability and experienced strong temperature variations. Moreover, during the whole ascending phase of BEXUS balloon, experiment sensors were exposed to a discontinuous solar radiation, due to the gondola rotation. Direct solar exposure led to an increase of temperature sensor measurements up to 30 °C, this has been observed correlating temperature signal with gondola heading angle. Actually, the gondola heading angle, which has been retrieved by means of a fluxgate tri-axial magnetometer, is geometrically related to sensors sunlight exposure. The whole attitude reconstruction process is then described. Finally, a numerical thermal model of the RTD sensor has been implemented in order to deeply understand the thermal exchanges observed during the flight.
From the MISSUS temperature sensor behaviour during BEXUS 15 flight some useful improvements have been introduced in the design of MarsTEM flight model.

1. INTRODUCTION

The role of meteorological instrumentation is central for planning a surface mission on a planet because the study of the atmosphere allows to go deeply into the dynamics of the atmosphere formation and to investigate the evolution processes of the whole Solar System. The recent ESA programs have focused on Mars for 2016-2018 and beyond, to investigate the environment of the planet, in particular on the research of present and past life traces and demonstrate new technologies for future missions and landings.
From this starting point the need of realizing a meteorological package conceived for applications in Mars-like environments arose. MISSUS experiment, composed of several sensors for the measurement of temperature, pressure, humidity, velocity, magnetic field and attitude, gives a useful contribution in the development of integrated multi-sensors packages for harsh atmospheres exploration. At an altitude of 20-30 km, Earth atmosphere is similar to Mars ground environment concerning the pressure and the thermal exchange mechanisms, whereas differences respect to Mars atmosphere are related to the thermal conductivity and thermal capacity of Carbon Dioxide and the presence of dust [1].
At the moment, CISAS is involved in the testing of DREAMS package, which is part of the payload on Exomars 2016 Mission [2]. MISSUS results constitute a useful input for the mission: the innovative temperature sensor onboard is the prototype of the sensor which will be used to directly measure the temperature profile of Mars atmosphere on the Entry Descent and Landing Demonstrator Module (EDM, Exomars 2016) [3]. From the detailed analysis of the acquired data and the sensor behavior during flight, some useful improvement and modifications have been introduced in the design of the Flight Model of the sensor.

2. EXPERIMENT OVERVIEW

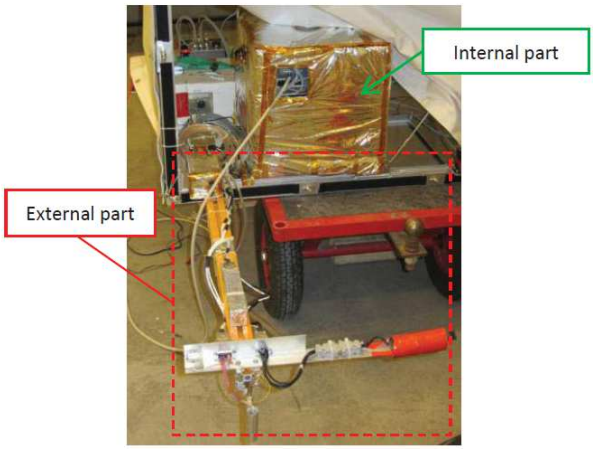


Figure 1. MISSUS experiment onboard BEXUS gondola.

As described above, MISSUS experiment is able to provide both meteorological measurements and attitude and trajectory measurements [4]. The innovation of the experiment is based on the integration of all the sensors and on data-fusion, which has been managed in post-processing: every measurement has been cross-correlated

with the others to increase the accuracy of the results, based on a synergic approach.

The experiment is split in two parts: some sensors have been placed outside the gondola, on a 1.2 meter length aluminium mast attached to the gondola rails, for the meteorological measurements; the other sensors have been placed inside the gondola, together with the electronics, which controlled the sensors, the batteries and the on-board control processor PC104, for the data-sampling, data-handling and transmission to the ground station. The power supply for all the sensors has been provided by two Lithium – Ion batteries through the electronics. Data conditioning and telemetry subsystem collected data coming from sensors and sent part of them to the ground station through BEXUS E-link unit, while the whole data volume has been stored in a solid state memory.

All internal components (sensors, electronics and batteries) have been mounted inside an edged box, (380x360x364) mm^3 volume, close to the external side of the gondola, easily accessible (in order to recharge batteries) and close to the boom (in order to minimize the length of the external cables). The experiment has been provided with the following sensors:

- An innovative resistance temperature sensor, placed on the tip of the external mast, on an Aluminium support, in order to get the temperature of the external environment as a function of the altitude. This sensor is a home-made platinum resistance thermometer with a thin platinum wire wrapped around a PEEK support.
- A second temperature sensor (a Resistance Temperature Device commercial sensor), used as a reference sensor for the innovative temperature sensor and for redundancy reasons; it has been placed next to the innovative temperature sensor.
- A humidity sensor (Honeywell HIH-4000 series), placed on the mast, used for the measurement of humidity during the ascending and descending phases.
- Two USB cameras (Logitech), for the monitoring of the experiment (e.g. to assess the position of the Sun by the observation of the shadows) and for public outreach contribution.
- A fluxgate tri-axial magnetometer (Bartington Mag-03MS1000) for the measurement of Earth magnetic field; it has been placed on the mast, far from the gondola in order to minimize spurious effects due to the magnetic field of the gondola and its subsystems: it contributed to completely reconstruct the gondola attitude.
- An absolute pressure sensors (Freescale MPX-2200 series) and a gage pressure sensor (Honeywell 060MG), placed inside the gondola, near to the electronics, to get the absolute pressure as a function of the altitude.
- A differential pressure sensor (Vaisala PDT101), placed inside the gondola, and connected to the external Pitot tube, placed on the tip of the mast, in order to obtain the descending velocity by detection of the differential pressure.
- An IMU (XSENS MTi-G), provided with GPS receiver, in order to reconstruct the gondola attitude and trajectory;
- A tri-axial accelerometer (Dytran7523A5), specific for shock measurements.

Combining the signals provided by the tri-axial accelerometer, able to measure shocks, and the absolute pressure sensor, a system has been developed to detect the probe impact with the ground. The aim of the system was to demonstrate the feasibility of this technology since one of the most critical issues in stratospheric balloon missions is the separation of the payload from the parachute after probe landing. The parachute may drag the payload for long distances before being recovered, with consequent damage of the instrumentation. The absolute pressure sensor signal is fundamental to measure absolute pressure on ground, avoiding accidental separation during the flight (e.g. when parachute is deployed).

A housekeeping system (e.g. additional temperature sensor) and active thermal control system have been used in order to monitor and control the experiment respectively.

Fig. 1 shows the internal and the external parts of MISSUS with all the sensors integrated.

3. ATTITUDE SENSORS DATA ANALYSIS

TRIAD algorithm [5], [6], has been used for BEXUS 15 gondola attitude determination. Attitude determination with reference to North East Down (NED) frame is necessary in order to show the correlation between temperature measurements and RTD sensor sunlight exposure. The TRIAD algorithm find the rotation matrix between two reference vector and two measured vector. The measured vector are the gravity vector and the Earth's magnetic field vector form a magnetic vector. Both gravity and magnetic vector are known in the NED reference frame. Soft and iron calibration has been performed for the external magnetometer basing on the flight data [7], [8]. Fig. 7 and Fig. 9 show the yaw angle reconstruction, 0° direction point to the geographic North, the rotation is considered positive eastward.

4. TEMPERATURE SENSOR DATA ANALYSIS

Measurements were collected for 4 hours and 6 minutes during BEXUS 15 ESA/SSC/DLR stratospheric balloon mission in September 2012. Fig. 2 shows the atmospheric air temperature measured by MISSUS RTD sensor.

Several events have been highlighted during the whole flight: (1) a drop of atmospheric temperature around 33 min lasting for a least 17 min; (2a-b) relevant increases of temperature at 1 h 31 min and 3 h 57 min.

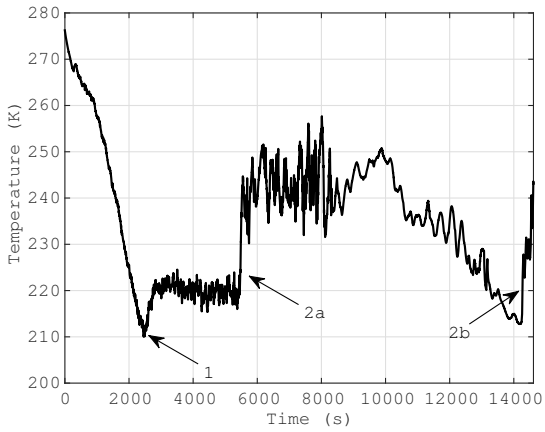


Figure 2. Air temperature measured by MISSUS RTD sensor during BEXUS 15 flight and analyzed events: (1) Temperature drop; (2a)(2b) Temperature increases due to sunlight exposition.

4.1. Temperature drop

Fig. 3 shows the comparison between temperatures provided by MISSUS innovative RTD (black curve), International Standard Atmosphere (ISA) (dot-dashed curve) and NRLMSISE-00 model (dashed curve) [9]. MISSUS RTD sensor is able to measure fast temperature fluctuations, in the experiment configuration it is directly exposed to the atmosphere.

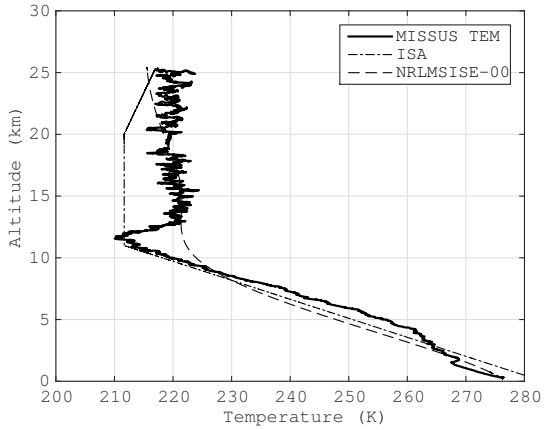


Figure 3. Comparison between measured air temperature as function of altitude (black curve), ISA (dot-dashed curve) and NRLMSISE-00 (dashed curve) models.

The mean slope of measured temperature as function of altitude is similar to ISA and NRLMSISE-00 slopes. Deviations from the model in troposphere zone are due to the adverse meteorological conditions of the day, we can see the presence of clouds and humidity in CALIPSO Vertical Features Mask (VFM) (Fig. 4).

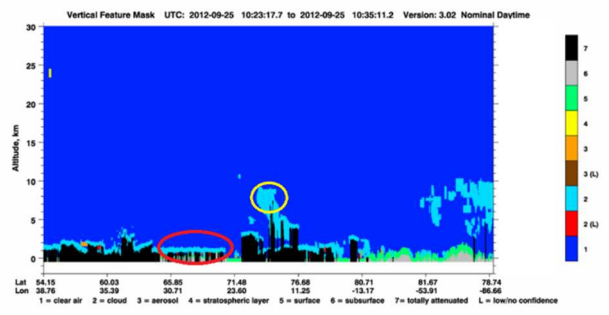


Figure 4. VFM of CALIPSO shows the air profile and clouds, in the circle the low troposphere layer of clouds present during the day of flight. Red circle water clouds, yellow circle icy cirrus clouds.

A drop in the temperature of the atmosphere is evident in the layer between 10 km and 13 km. The same decreasing trend is observed also for the other temperature sensors. This drop is detected on the correspondent foreseen tropopause and a positive not expected lapse rate is observed (see Fig. 3). In the stratosphere layer, the trend of the temperature provided by RTD sensor is compliant with values provided by the NRLMSISE-00 model.

Three scenarios related to the measured temperature drop, have been investigated: clouds, stable cold layers, stronger horizontal winds.

Clouds

The first hypothesis takes into account the possibility that BEXUS gondola crossed a cirrus cloud during its ascending phase. Cirrus clouds temperature is highly variable: at midlatitudes the average temperature is 210 K and at polar latitudes around 200 K. Typically cirrus clouds are observed in the cold upper troposphere and close to the tropopause. The observed vertical distribution of temperature matches the ones detected by [10], [11] over Kiruna during cirrus observations. Cirrus clouds have been observed near BEXUS trajectory by CALIPSO satellite. CALIPSO has been providing nearly continuous measurements of the vertical structure and optical properties of clouds and aerosols from 2006 [12]. CALIOP is the name of the CALIPSO lidar and is an acronym for Cloud-Aerosol Lidar with Orthogonal Polarization. The lidar profiles provide information on the vertical distribution of aerosols and clouds, cloud particle phase, and classification of aerosol size. CALIPSO orbits in formation with other spacecraft in the A-Train satellite constellation, and provides complementary, near-simultaneous, observations with the other active and passive instruments in the

constellation to better understand the effects of clouds and aerosols on climate, weather, and air quality. CALIPSO data revealed clouds in low troposphere layers in a narrow region crossed during BEXUS 15 flight from 10:23 to 10:35 UTC in the Polar area and higher icy clouds around 10 km (see Fig. 4).

Stable cold layer

The second hypothesis considers the presence of a layer of stable cold air. Other temperature profiles during the day have been analyzed: PTU (Pressure Temperature Humidity) probes before launch and during flight measured the same drop. The amplitude of this drop is about 10 K for the first probe before flight, about 6 K for the second one during the flight. The temperature drop is located between 10 km and 13 km for the first and the second PTU.

Stronger horizontal winds

The third hypothesis supposes that the gondola crossed a region where stronger horizontal winds are present. This is confirmed by PTU wind measurements provided by EuroLaunch during the day of flight, between 8-14 km. The drop is observed at the same altitude of winds with higher speed, more than 12 m/s.

A review on cirrus clouds phenomena suggests that during BEXUS 15 flight the region between 10-13 km was crossed by cold cirrus clouds, moreover stronger winds caused increase in convective thermal exchange.

4.2. Floating phase temperature increases

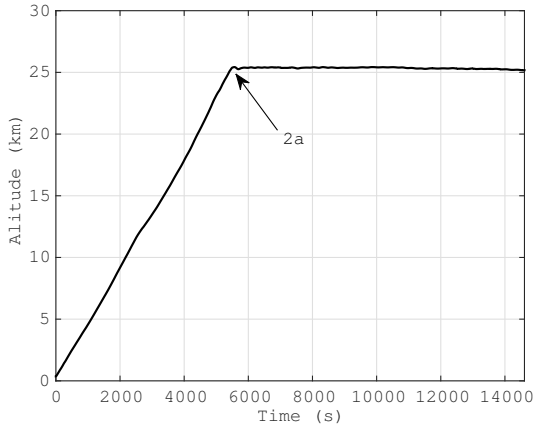


Figure 5 Altitude from GPS and pressure versus time.

A sudden increase in temperature of about 20 °C has been detected at 1h 32 min of the flight, event 2a in Fig. 2, at the beginning of the floating phase (Fig. 5). A second relevant temperature increase has been detected at 3h 53min. Temperature fluctuations of 10 °C have been observed during the whole floating phase. Two possible scenarios have been investigated.

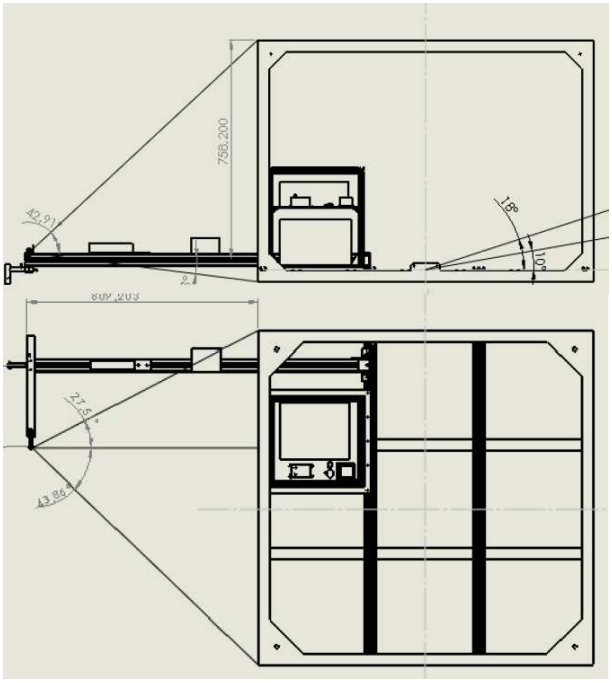


Figure 6 MISSUS in the correct position on the gondola (upper view) and angles that define the RTD sensor shadow zone.

Direct exposure of sensitive element to sunlight.

The evaluation of sunlight influence on RTD temperature measurements has been performed thanks to the estimation of sun relative position during BEXUS 15 flight. The sun position during floating was calculated using the Solar position algorithm for solar radiation application by [13]. The input parameters of the algorithm are: local UTC time, latitude, longitude, altitude. The output parameters are the zenith angle in degrees from the vertical and the sun azimuth in degrees, eastward from the geographic North. During the cruise phase, the azimuth variations are: [207° 242°], while the zenith variations are [72° 80°]. Fig. 6 shows gondola shadow zone: $-43.6° < \psi_{boom} < +27.5°$ taking into account the yaw range (with geographic North as reference), during the cruise phase the thermometer is not illuminated in the following zone: start of floating (UTC TIME=11:49) $344° < \Psi < 54°$, last measurement collected (UTC TIME=14:22) $18° < \Psi < 89.5°$. During the ascent phase, the gondola has a high spin rate that does not allow sun influences on measurements. From 2800s to 4300s the average spin rate is 3 deg/s. When the gondola reaches the floating phase (event 2a Fig. 5.) and its spin rate decrease, the increase of temperature occurs in less than 2 minutes.

After the last complete rotation (around 5500 s) is clearly visible that the increase of temperature occurs in less than 2 minutes, this is compliant with the moving in the illuminated zone (see Fig. 7). The temperature increase of 20°C, in less than 100 s, at t = 14250 s, this is compatible with RTD sensor shift to the zone exposed to the sunlight.

When the sun exposure is maintained also the temperature is higher than that predicted by the atmospheric models (at 25.6 km altitude), this confirms the hypothesis of influences by illumination. Furthermore between 5500 s and 9000 s small rotations (clockwise and counter clockwise) of the gondola around the vertical axis are observed; the temperature trend also shows different oscillations, however the correlation is not well defined. The cooling time is much longer respect to the heating one, around 30 minutes, which corresponds to a slow rotation of the gondola in the dark zone. The cooling of the sensitive wire of the sensor results less clear. Influences of the thermal inertia of the sensor structure and support device are hypothesized. In addition other sources of uncertainty come from the gondola structure and external bodies protruding from the gondola body (other experiments, supports, etc.), which shield the sensor and modify the shadow zone.

The RTD sensitive element thermal model developed by [14], [15], had been improved considering empirical relations for heated wires at low Reynold numbers [16]–[18]. Model shows that the direct exposure to the solar radiation of the sensitive element could lead to increase of temperature of at a maximum of 1.5 °C. A further analysis of the fluid-sensor structure convective exchanges shows that the structure thermal boundary layer could affect temperature measurements.

Sensor structure thermal boundary layer

The second hypothesis is related to the sensor structure thermal boundary layer. A coarse RTD sensor has been placed in proximity of MISSUS fine RTD sensor structure; coarse sensor and structure are insulated by a kapton film. Despite the insulation, coarse RTD temperature is closer to structure temperature. As we can see from Fig. 8 the sensor structure and the coarse RTD sensor are affected by solar heating. Fig. 10 shows CFD analysis results, floating phase conditions have been simulated (p = 2500 Pa, T_{air} = 218 K, $T_{structure}$ = 243 K). A free stream velocity of 0.1 m/s (tangential speed of the sensor) has been considered, we assuming that during the floating phase the gondola speed with reference to an inertial frame is equal to wind speed. CFD simulations show that the measured temperature could be increased up to 236 K when U = 0.1 m/s and rotation is westward, up to 238 K when U = 0.1 m/s and rotation is eastward. The ΔT introduced by the structure thermal boundary layer is about 2 K when the upstream velocity is 1 m/s, this value is compliant with the temperature oscillation observed between 3000 s and 5500 s, when the sensor is alternately exposed to gondola shadow.

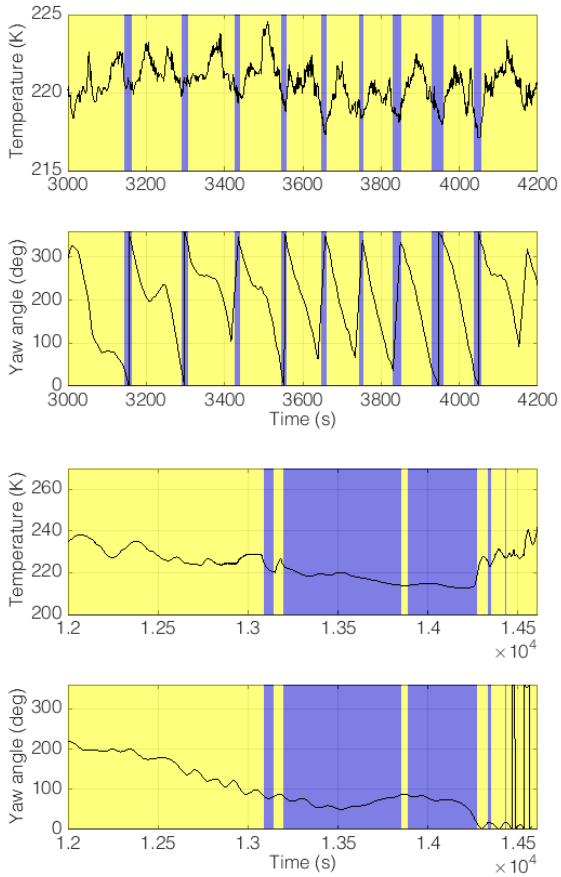


Figure 7. Temperature profile and yaw angle as function of time. (Yellow area: sensor illuminated by sunlight; Blue area: shadow zone). Top image: zoom during the ascending phase, bottom image: zoom during the floating phase.

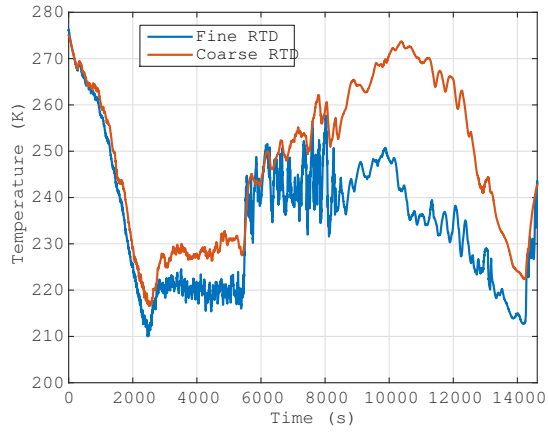


Figure 8. External air temperature measured by Fine RTD and Coarse RTD.

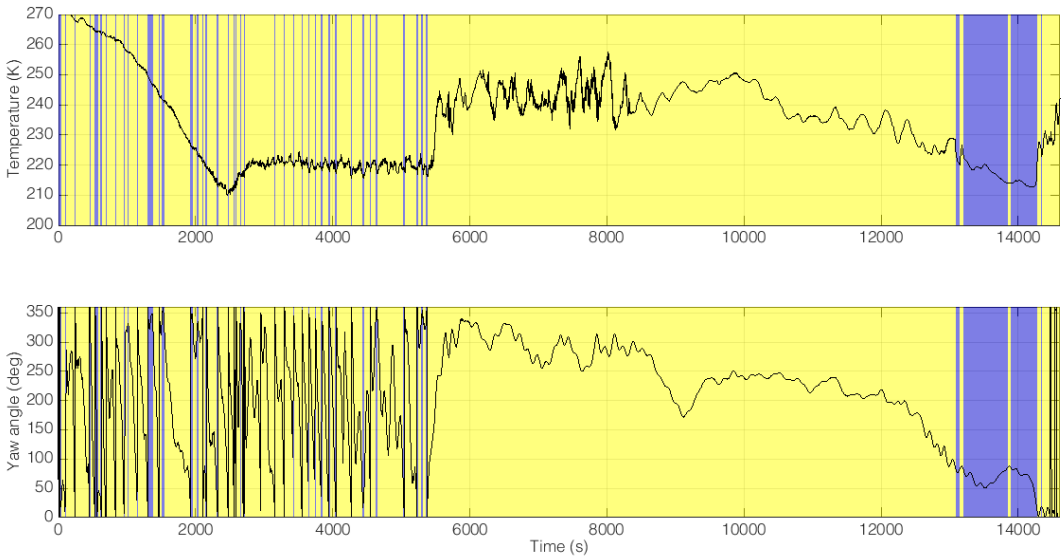


Figure 9. Temperature profile and yaw angle as function of time. (Yellow area: sensor illuminated by sunlight; Blue area: shadow zone)

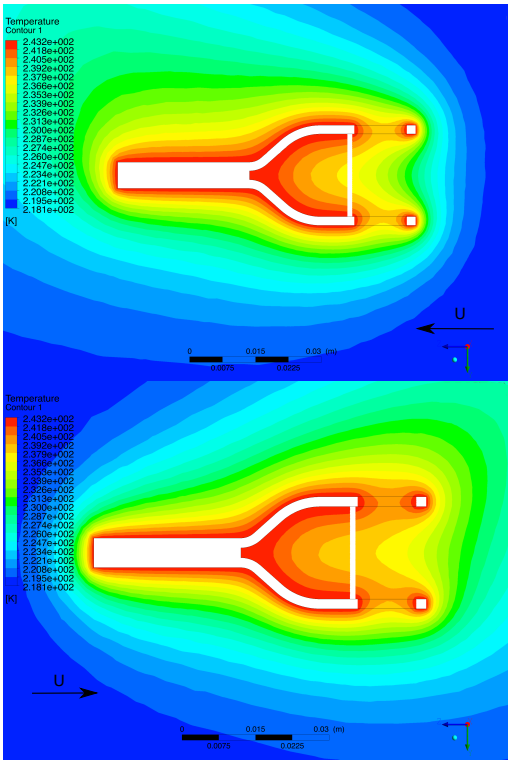


Figure 10. Sensor structure thermal boundary layer for a free stream velocity of 0.1 m/s, for the two rotation directions.

The performed CFD analyses suggest that the increase of temperature observed during the cruise phase is not due to the direct exposure of the sensitive element to the sunlight. The analyzed increases of temperature are probably due to the measurement of the thermal boundary layer of the sensor structure, which is heated by the sun. During the cruise phase the wind speed relative to gondola is equal to zero, from the ascending phase to cruise phase the sensor structure thermal exchanges switch from forced convection to natural convection. The overall effects are shown in Fig. 10.

5. CONCLUSIONS

MISSUS, an integrated sensor suite for meteorological measurement, attitude and trajectory reconstruction has been conceived, designed and realized for stratospheric balloon flights. A great amount of data has been collected during the ascend and cruise phase, allowing the verification and validation of atmospheric models. Thanks to the data fusion approach has been possible to correlate different kind of data in order to obtain a deeper understanding of the observed phenomena. GPS data has allowed to correlate the temperature drop observed during the ascend phase, to satellites cirrus clouds data (CALIPSO), moreover thanks to the attitude reconstruction the RTD temperature signal has been correlated with the direct sensor exposure to the sunlight. BEXUS 15 flight has been a unique opportunity to test the MarsTEM prototype on Mars-like environment. The sensor has been developed and successfully tested during the flight. The analysis of collected data has allowed an

improvement of the sensor design. MarsTEM sensor flight model structure has been modified and improved in order to reduce the structure thermal boundary layer.
Finally, the participation of MISSUS team to the BEXUS/REXUS programme has been a valuable training activity for a young professional team.

6. ACKNOWLEDGEMENTS

Thanks to all the MISSUS team composed by: Francesca Cucciarrè, Giovanni Tovo, Ireneo Vidali, Davide Bettio, Davide Cornale, Veronica Botti, Emanuele De Villa Bais, Marco Didonè.
The experiment realization was possible thanks to the support by CISAS "G. Colombo", Borgoverde S.r.L., Rotary Club International Valle dell'Agno and Ca'Da Mosto S.p.A, Federmanager Venezia, which provided the team with funds needed to manufacture the experiment. In particular University of Padova provided also the facilities and premises needed for the realization and the verification. Professor Massimo Masi made available his expertise and the wind gallery for the calibration of the Pitot tube, whereas Alessio Aboudan and Michele Cesaro gave their constant and effective contribution in the software conception and development.
Antonio Selmo, electronics engineer, designed, manufactured and tested the electronics board and the rack, making available his workshop and supervising the last phases of the experiment realization, also during the launch campaign.
Our gratitude goes to all ESA, SSC, SNSB, DLR staff for the great support during the milestones and the launch campaign.

REFERENCES

[1] A. Spiga, "Elements of comparison between Martian and terrestrial mesoscale meteorological phenomena: Katabatic winds and boundary layer convection," *Planet. Space Sci.*, vol. 59, no. 10, pp. 915–922, 2011.

[2] C. Molfese, F. Esposito, S. Debei, C. Bettanini, I. A. Rodríguez, G. Colombatti, A. Harri, F. Montmessin, C. Wilson, and A. Aboudan, "DREAMS: a payload on-board the ExoMars EDM Schiaparelli for the characterization of Martian environment during the statistical dust storm season," in *EGU General Assembly 2015*, 2015, vol. 17, p. 13647.

[3] G. Colombatti, S. Chiodini, E. Friso, A. Aboudan, C. Bettanini, S. Debei, and F. Esposito, "MarsTEM: The temperature sensor of the DREAMS package onboard Exomars2016," in *2014 IEEE Metrology for Aerospace (MetroAeroSpace)*, 2014, pp. 249–254.

[4] F. Cucciarrè, S. Chiodini, C. Palla, G. Tovo, I. Vidali, D. Bettio, D. Cornale, V. Botti, E. De Villa Bais, M. Didonè, G. Colombatti, and S. Debei, "MISSUS experiment onboard BEXUS 15 : An innovative integrated sensors suite for meteorological measurements in low pressure environments and for attitude reconstruction," in *21st ESA Symposium om European Rocket and Balloon Programmes and Related Research*, 2013, pp. 107–114.

[5] M. D. Shuster and S. D. Oh, "Three-axis attitude determination from vector observations," *J. Guid. Control. Dyn.*, vol. 4, no. 1, pp. 70–77, Jan. 1981.

[6] H. D. Black, "A passive system for determining the attitude of a satellite," *AIAA J.*, vol. 2, no. 7, pp. 1350–1351, 1964.

[7] S. Chiodini, "Progettazione, realizzazione e taratura di una sonda per la misura della velocità di un payload a bordo di un pallone stratosferico e ricostruzione dell'assetto e della traiettoria," Università degli studi di Padova, 2013.

[8] D. Gebre-Egziabher, G. H. Elkaim, J. David Powell, and B. W. Parkinson, "Calibration of Strapdown Magnetometers in Magnetic Field Domain," *J. Aerosp. Eng.*, vol. 19, no. April, pp. 87–102, 2006.

[9] J. M. Picone, A. E. Hedin, D. P. Drob, and A. C. Aikin, "NRLMSISE-00 empirical model of the atmosphere: Statistical comparisons and scientific issues," *J. Geophys. Res.*, vol. 107, no. A12, p. 1468, 2002.

[10] C. Schiller, M. Krämer, A. Afchine, N. Spelten, and N. Sitnikov, "Ice water content of Arctic, midlatitude, and tropical cirrus," *J. Geophys. Res.*, vol. 113, no. D24208, pp. 1–12, 2008.

[11] J. Siebert, C. Timmis, G. Vaughan, and K. H. Fricke, "Letter to the editor A strange cloud in the Arctic summer stratosphere 1998 above Esrange (68 ° N), Sweden," *Ann. Geophys.*, vol. 18, no. 4, pp. 505–509, 2000.

[12] D. M. Winker, C. A. Hostetler, M. A. Vaughan, and A. H. Omar, "CALIOP Algorithm Theoretical Basis Document Part 1 : CALIOP Instrument , and Algorithms Overview CALIOP Algorithm Theoretical Basis Document Part 1 : CALIOP Instrument , and Algorithms Overview," 2006.

[13] I. Reda and A. Andreas, “Solar Position Algorithm for Solar Radiation Applications Solar Position Algorithm for Solar Radiation Applications,” 2008.

[14] I. Vidali, “MarsTem, un termometro per la misura della temperatura atmosferica marziana: progettazione, prototipazione e studio degli effetti dovuti all’autoriscaldamento,” Università degli Studi di Padova, 2012.

[15] C. Palla, “MISSUS experiment on BEXUS programme: Temperature data analysis and correlation,” Università degli studi di Padova, 2013.

[16] S. Chiodini, G. Colombatti, E. Friso, M. Pertile, and S. Debei, “Multiphysics modelling of MarsTEM shield,” in *2015 IEEE Metrology for Aerospace (MetroAeroSpace)*, 2015, pp. 271–276.

[17] D. C. Collis and M. J. Williams, “Two-dimensional convection from heated wires at low Reynolds numbers,” *J. Fluid Mech.*, vol. 6, no. 03, p. 357, Oct. 1959.

[18] L. V. Baldwin, V. A. Sandborn, and J. C. Laurence, “Heat Transfer From Transverse and Yawed Cylinders in Continuum, Slip, and Free Molecule Air Flows,” *J. Heat Transfer*, vol. 82, no. 2, p. 77, 1960.

SCRAT EXPERIMENT: A STUDENT EXPERIENCE

Matteo Duzzi[(1)], Lorenzo Olivieri[(2)], Alessandro Francesconi[(3)]

[(1)]CISAS "Giuseppe Colombo", Via Venezia 15, 35131 Padova (ITALY), matteo.duzzi@gmail.com
[(2)]CISAS "Giuseppe Colombo", Via Venezia 15, 35131 Padova (ITALY), olivieri.lrnz@gmail.com
[(3)]CISAS "Giuseppe Colombo", Via Venezia 15, 35131 Padova (ITALY), alessandro.francesconi@unipd.it

ABSTRACT

S.C.R.A.T. experiment (Spherical Compact Rechargeable Air Thruster) is the technology demonstrator of a cold gas actuator which uses the atmospheric air as a propellant. Its key feature is the "rechargeability": SCRAT is able to collect directly from the surrounding environment the propellant it needs. This solution allows to avoid the on–board gas storage, saving more volume and weight destined to the mission's payload, and to have a rechargeable propulsion system.
SCRAT was developed by a team of university students in 2009-2010 and successfully tested in the extreme environment of a stratospheric flight. The main objective of SCRAT was to measure the thrust delivered by the actuator in terms of maximum thrust and impulse in relation to the altitude at variable conditions of temperature, pressure and disturbances; this goal was achieved thanks to the BEXUS platform, a stratospheric research balloon which allows the payload to reach an altitude of ~25 *km*, with an external pressure of ~25 *mbar* and a temperature close to 200 *K*. The BEXUS projects, within the REXUS/BEXUS educational programme, provides the unique opportunity of fly an experiment of a university students team on board of a sounding rocket (REXUS) or a stratospheric balloon (BEXUS).
This paper presents an overview from the concept and design of the experiment to the launch campaign. The experiment working principle will be illustrated, along with the design and assembly phases following the typical milestones of a real space mission scenario. Studies about new mechanisms, problem solving and backup solutions will be introduced as part of the lessons learned during the entire programme. Qualification tests will be presented for payload qualification and admission to the final launch phase. Particular interest will be given to the BEXUS 10 flight campaign and the integration of the experiment onto the BEXUS' gondola. Finally, the analysis of retrieved scientific results will be showed.

1. INTRODUCTION

Recently, small-scale air systems such as drones and Lighter-than-Air (LTA) vehicles are showing an increasing interest thanks to several technology developments that led to a considerable cost reduction and to an increased utilization in many different scenarios [1]. On Earth, such vehicles are employed in commercial, scientific and military applications, as well as in remote observation of hazardous or inaccessible environments [2]; in parallel, the feasibility of planetary exploration of Earth rocky relatives by means of small aerial vehicles is under evaluation [3-4], as well as the investigation of outer giants moons atmospheres [5-6].
In this context, one of the key technologies to further improve the vehicles autonomy and versatility is the propulsive one, to give them the ability to provide accurate attitude control and manoeuvrability; low-thrust (in the range 10-1000 *mN*) actuators are under investigation, in order to provide reliable, light and compact solutions. While propellers are at today mostly employed in drones and LTAs, cold gas thrusters may represent valuable candidate in particular environmental conditions, thanks to their advantages in simplicity, ease of operations, low-cost and suitability to miniaturization. On the other hand, such actuators main drawbacks are the need of carrying on board the propellant and their low specific impulse.
In this framework, SCRAT (Spherical Compact Rechargeable Air Thruster) student experiment aimed to validate a new-concept cold gas actuator that employs the atmospheric air collected from the surrounding environment as propellant. The primary objectives of SCRAT were (1) to design and develop the novel thruster, (2) to test it in different ambient conditions by means of a stratospheric flight, and (3) to let the student team gain practical experience from a real, small space mission. The experiment was realized in the framework of the REXUS/BEXUS (RX/BX) programme, and flew on board the BEXUS 10 balloon in October 2010.
The REXUS/BEXUS program offers European university students the opportunity to carry out scientific experiments aboard sounding rockets (REXUS, Rocket-borne EXperiments for University Students) or stratospheric balloons (BEXUS, Balloon-borne EXperiments for University Students). It is realized under a bilateral Agency Agreement between the German Aerospace Center (DLR) and the Swedish National Space Board (SNSB). The Swedish share of the payload is been made available to students from other European countries through a collaboration with the European Space Agency (ESA). EuroLaunch, a cooperation between the Esrange Space Center of the Swedish Space Corporation (SSC) and the Mobile

Rocket Base (MORABA) of DLR, is responsible for the campaign management and operations of the launch vehicles. Experts from ESA, SSC and DLR provide technical support to the student teams throughout the project [7]. In more details, the BEXUS flight opportunity consists in the launch on board of a stratospheric balloon with a volume up to 12 000 m^3 (the dimensions are similar to those of a big hot-air balloon) to a maximum altitude of 35 *km*, depending on total experiment mass (ranging from 40 to 100 *kg*) and atmospheric conditions. The flight duration, considering both the ascending and descending phases, is from 2 to 5 hours. During the mission, as the altitude varies, the experiments are exposed to different temperature and pressure conditions, which can reach extreme values as low as -90 *°C* and a few *mbar*.
From selection, students have nine months before launching their experiments on board the BEXUS balloon. During this period, they are subjected to a tight schedule representing the usual space systems development process, approaching the following reviews:

- Preliminary Design Review (3rd month)
- Critical Design Review (5th month)
- Interim Experiment Review (7th month)
- Experiment Acceptance review (9th month)

At each review, they are requested to present updated documentation and (after CDR) hardware, in order to arrive to the launch campaign week with the experiment ready to be integrated on the BEXUS gondola.
This paper presents the development of SCRAT experiment from design to launch, introducing the main results collected during the flight in the Scandinavian skies. The contents focus on the educational outcomes of the experience, presenting the main steps and the lessons learned in the development of the project. Next section introduces the rechargeability concept and the experiment working principle, followed by the description of SCRAT evolution from sketch to a working technology demonstrator (section 3). Section 4 presents the main solutions developed during the experiment life to reach the scientific tasks and to address the main issues of reliability and simplicity; a brief report of the launch campaign follows in section 5, and the main scientific results are presented. Last, the paper focuses on the educational outcomes of the whole experience.

2. CONCEPT

SCRAT is a low-thrust cold gas actuator which uses the air collected by two micro-compressors from the external environment as propellant. Its working principle consists in drawing the air from the surrounding environment and compress it into a two-stages tank. The distribution of the air between the two stages is regulated by two automatic electro-valves. Heaters are used to warm up the gas and thus increase the pressure before the release. When the gas reaches a fixed pressure it is ejected from the second stage through a nozzle at high speed directly into the ambient. The delivered thrust is measured thanks to a torsional load cell on which the nozzle is mounted. Fig. 1 highlights the working principle of SCRAT.

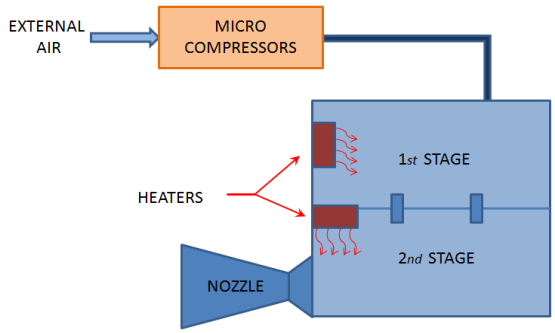


Figure 1: SCRAT working principle. The gas is collected by two micro-compressors from the external environment and compressed into a two-stages tank (CGA). Reached a fixed pressure, the gas is released through a nozzle and the thrust level is measured thanks to a torsional load cell.

The groundbreaking feature of SCRAT lies on its "rechargeability": the gas used as propellant is in fact collected from the external environment. This uncommon peculiarity prevents the issues of storing on-board the propellant, allowing the destination of more free space in terms of volume and weight to the mission's payload. Moreover, it assures the use of an "environmental friendly" rechargeable propulsion system.

3. MILESTONES

The final configuration of SCRAT is the consequence of a long evolution process, which started with the first sketches for the RX/BX proposal and finished with a working technology demonstrator fully operative. Here is a recap of the main milestones followed during the participation at the RX/BX programme, with special focus on the initial idea presented at the proposal and all the improvements/changes made during the whole campaign.

3.1. Proposal

The first idea was to have the experiment divided into two main parts (as can be seen from the preliminary sketches for the RX/BX proposal, Fig.2):

- the CGA (Cold Gas Actuator), which constituted the off-board package together with a Dummy Actuator Assembly (DAA).

- the PB (Proximity Box) which was the on-board package;

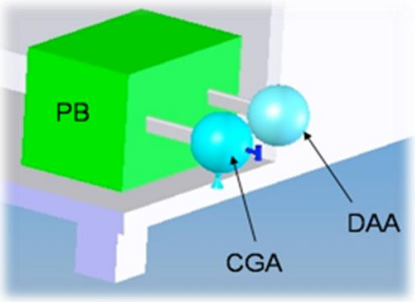


Figure 2: RX/BX proposal, preliminary sketches. The figure shows the on-board package (PB) and the off-board package (CGA & DAA).

The CGA was a hollow spherical structure with a nozzle vertically oriented and pointing towards the Earth. The structure internal volume was split in two chambers (actuator's first stage and second stage): the first stage was separated from the second stage by a calibrated one-way automatic check valve; the second stage and the external ambient were separated by another calibrated one-way automatic check valve which was located within the nozzle (Fig. 3). Pressure and temperature sensors were placed inside each of the two actuator's chambers. A Pitot tube and an additional temperature sensor were fixed outside the CGA, to measure both ambient temperature, static and stagnation pressure.

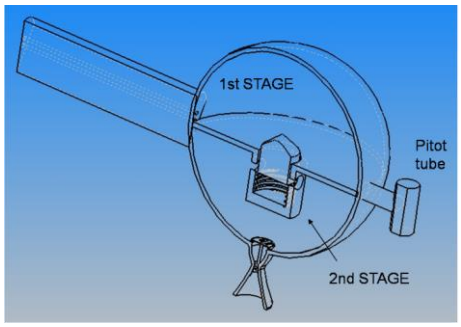


Figure 3: CGA structure. The first and second stages were divided by an automatic check valve. A second check valve, located in the nozzle, separated the second stage from the external environment. A Pitot tube was fixed outside the sphere.

The PB contained the micro-compressor, the batteries, the electronic equipment to condition the sensors output, an AD converter and a PC104 board to store data and to format the stream sent to the balloon telemetry.
The PB (on-board) and the CGA (off-board) were connected by a proper tube which brought into the first stage the air pressurized by the micro-compressor and the wires carrying sensors signals into the box. Moreover, the connecting tube acted as flexural load cell (based on strain gauges) to measure both the drag acting onto the CGA and the thrust level during CGA operations.
The DAA was a dummy assembly (geometrically identical to the CGA) which could not provide thrust. It was used just to provide a measure of the drag force when the CGA was operated (and hence the load cell signal was the sum of the drag force and the thrust generated).

3.2. Selection workshop

At the selection workshop only minor changes were presented. Some numerical gas dynamic (Fig. 4) and thermal control simulations were performed, acquiring crucial information about the mean thrust, peak thrust and total impulse of the actuator. Preliminary satisfying results and information were obtained to characterize the valves requirements.

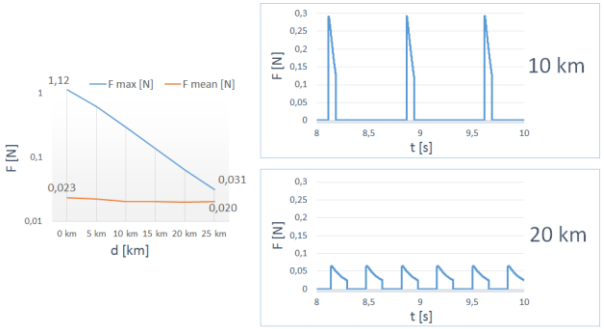


Figure 4: Gas dynamic simulations. Maximum and mean thrust values in function of the altitude (left) and thrust profile (right) at 10 km (top) and 20 km (bottom).

The mechanical design was improved, with a preliminary estimation about the overall volume and weight and the investigation of nominal and peak loads transmitted to the gondola. The experiment structure was refined along with the CGA configuration (Fig. 5).

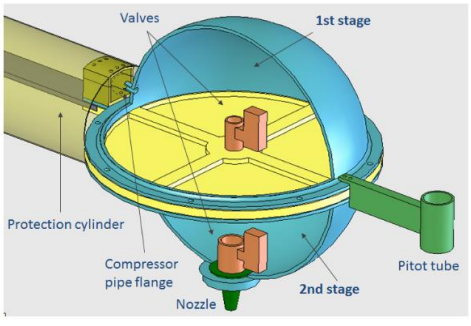


Figure 5: CGA configuration refined. The figure shows the two stages of the CGA and its main components.

Sensors selection and location were made (Fig.6), both to guarantee a real time knowledge about the system status and measure the atmospheric profiles (pressure, temperature and density).

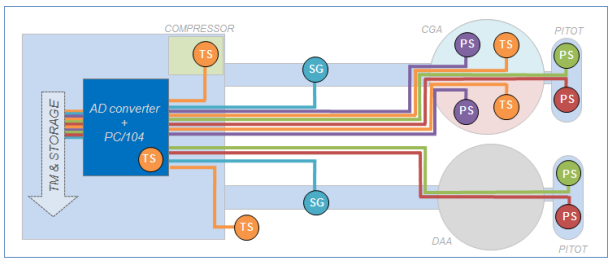


Figure 6: Sensors location. Temperature Sensors (TS), Pressure Sensors (PS) and Strain Gauges (SG).

Storage and data handling were considered to have a preliminary idea about the data volume. The study for an innovative pneumatic valve was initiated and a backup solution was already found. A preliminary outreach program was scheduled.

3.3. Preliminary Design Review (PDR)

The first evolution of SCRAT (Fig. 7) took place with the achievement of the first review, the PDR.

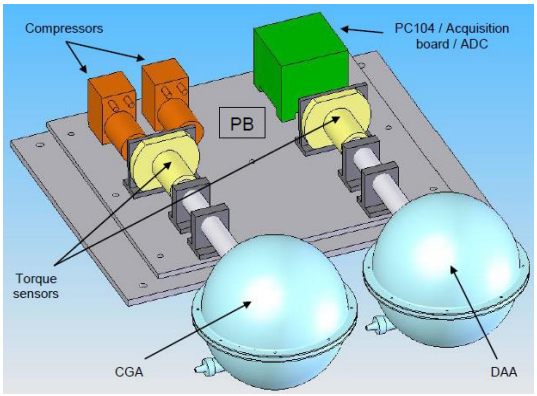


Figure 7: Experiment design. A further compressor was added both for redundancy and performance improvement. New shafts were designed to measure the thrust and support the CGA/DAA.

The main changes for the PDR were:

- the thrust measurement method (from a flexural measure to a torsional one, in which the rotation of the CGA connected to the shaft gave the impulse to the torsional cell, the measuring system of the thrust);
- the use of two compressors in parallel for both redundancy and performance improvement;
- the shaft design, with the double function of transmit the torque generated by the thrust to a custom load cell under development and support the CGA & DAA (designed to withstand peak loads);
- the pitot tube discharge.

Full 3D FEM analysis on the structure were performed along with Simulink models to evaluate the dynamics of the pneumatic valve. Backup solutions of the critical subsystems were considered and the electronic/software design were started.

3.4. Critical Design Review (CDR)

With the CDR the experiment design was subjected to drastic changes due to the higher machining cost, complexity and assembly respect to previous estimations.
First of all, the decision of implementing only one vessel (the CGA) outside the gondola (removing the dummy actuator assembly DAA presented in the first design of SCRAT and used for disturbances calculation) was taken considering that the new measurement system was less sensitive to the external disturbances; this decision leads to mass, volume and cost saving.
The original spherical shape of the vessel was abandoned in favor of the cylindrical shape because the spherical vessel leads to:

- high machining complexity;
- high machining cost;
- high difficulty in machining, assembling and integrating other parts like flanges, nozzle and valves.

Several shapes have been studied, but the cylindrical one with the characteristics described below was considered optimal both for machining and accessibility (Fig. 8).

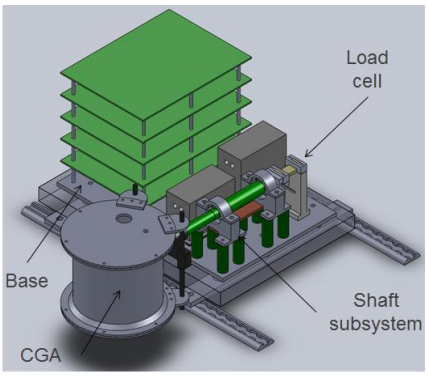


Figure 8: New structure design. The two spherical vessels outside the gondola were replaced with a cylindrical one. The dispositions of the components inside the PB were finally consolidated.

The Aluminum CGA was made of three pieces (Fig. 9):

- the cylinder: it was made from a single piece and it contained the plate which divided the pressure vessel in two stages; there were holes to mount the valves and to permit the air flow;
- the top cover plate (with two little plates, to sustain the CGA), made from a single circular plate; there were holes to permit the electric wiring with the internal components of the first stage, and to permit the air flow coming from the compressors;
- the bottom cover plate (with two little plates), made from a single circular plate; there were holes to permit the electric wiring with the internal components of the second stage, and to permit the air flow to the nozzle and the secure valve.

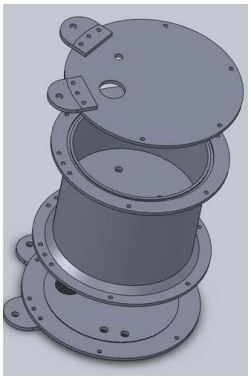


Figure 9: CGA. Single piece cylinder with top and bottom plates.

Secondly, the shaft (made of fiber glass, a resistant non-conductive material, Fig. 9) had to sustain the CGA and transmit the torque to the load cell. It was supported by two steel bearings, which locked all the movements of the shaft except for rotation. Additional fiber glass supports for the bearings' housings were implemented in order to insulate the bearing from the base of the experiment and to keep them as warm as possible.

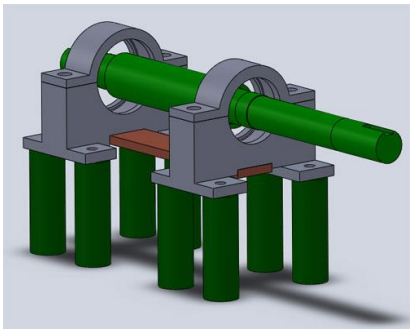


Figure 9: Shaft subsystem. The figure shows the shaft (fiber glass) with the ball bearing housing (steel) and the insulator supports (fiber glass).

The choice of diameter of the shaft has been influenced by several interconnected factors:

- resistance to the peak loads;
- high torsional stiffness, in order to transmit in the best way the torque to the load cell;
- small diameter, in order to have bearings with a starting moment lower than the minimum expected thrust torque;
- resistance of the bearings to the peak loads;
- non-conductive material, to avoid problems with bearing lubricants.

The interactions between these requirements imposed the selection of a compromise solution: the chosen diameter of the shaft where the bearings were mounted was 20 *mm*. This diameter guaranteed optimal mechanical resistance (and thus high torsional stiffness), and a good value of starting moment of bearings.
Finally, a sensitive support (Fig. 10) for the load cell (full bridge configuration) was adopted to measure the thrust and the pneumatic valve design was completed.

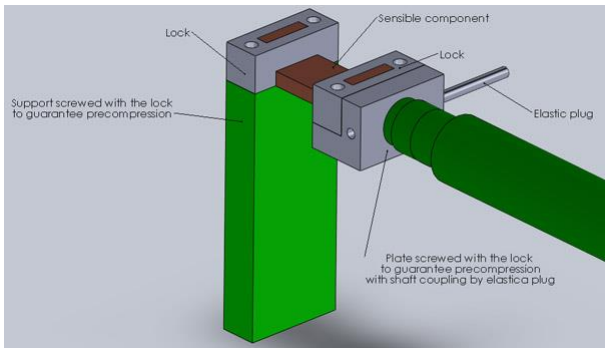


Figure 10: Load cell support: overview design.

Backup solution for the pneumatic valves was ready in case of failure during laboratory testing and pneumatic and thermal simulations were improved to choose the best compromise between active and passive controls. Safety/no-return valves were added to the CGA. The micro-compressors test was performed in order to compare the performances on ground with the producer datasheet. The electronic boards were created with the complete cabling design. Last, the draft flight software was implemented with the communication protocols.

3.5. Interim Experiment Review (IER) & testing

To have a confirmation of the results obtained from the simulations it was necessary to check the real response to vacuum and low temperatures of all the subsystems; a deep experimental investigation through laboratory tests was hence demanded. Before and in correspondence of the standard reviews such as the CDR, the IPR and the EAR, many tests have been carried out to assess the

correct functioning of all the experiment components; in the specific the following tests have been performed:

- Test 1: micro–compressors test, mass flow rate determination (vacuum test sequence, Fig. 11);

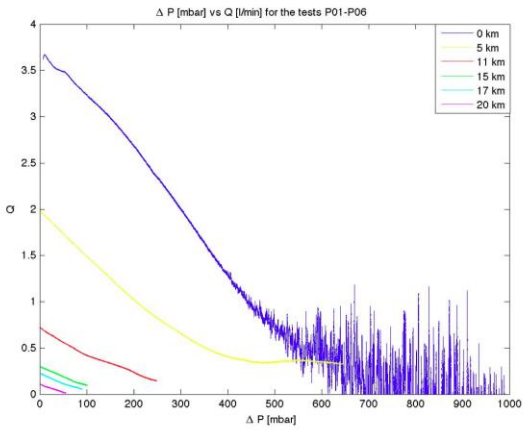


Figure 11: Compressor operative curves ΔP-Q. Direct measure of the pressure in function of the flow rate, tested at different environmental pressure.

- Test 2: electronic valve test (vacuum test sequence);
- Test 3: cold pressure test for CGA (4 bar at 210 *K*, Fig. 12);



Figure 12: Cold pressure test for the CGA.

- Test 4: load static test of the off–board package;
- Test 5: final vacuum test of the complete experiment.

3.6. Experiment Acceptance Review (EAR) & final configuration

At the EAR the experiment was ready and in its final configuration (Fig. 13). Only minor changes were adopted, regarding the base connecting the PB to the gondola and the design of the CGA hook. The original position of the CGA (connected to the shaft) was changed: the vessel was no more connected directly to the shaft but fixed outside the gondola. The pressurized air was delivered to the measuring subsystem (which consisted in a small rotating plate connected to the shaft) through a pipe. This change guaranteed a better thrust measure, lowering the not negligible inertial component due to the CGA presence in the previous measuring system which affected negatively the performances of the actuator.
The assembly was completed and the final tests under development. The pneumatic valve test failed and thus this device was abandoned in favor of the electro-valve backup solution.



Figure 13: SCRAT final configuration. Flight model of the experiment.

4. PROBLEM SOLVING APPROACH: CRITICAL COMPONENTS

During the development of SCRAT, particular attention was made towards backup solutions. Some innovative mechanisms were presented, developed and studied during the campaign. These new solutions could be the principal cause of failure of the experiment, because their validation was performed simultaneously to the advance in the programme: the failure during the acceptance test meant the failure of the mission, if backup solutions were not ready. For these reasons, a problem solving approach was adopted to foresee possible issues.

4.1. Valves

The critical components of the pneumatic subsystem were the valves. Two valves have been used between the first and the second stage and another one between the second stage and the external environment. The design of the valves was not easy, and there were no available COTS that satisfied exactly the hysteresis response required: the reduced opening time was

smaller than the minimum thrust impulse previewed in simulation.
The hysteretic behaviour and the possibility to control the variable opening force at different external pressures were the valve main design drivers.
The design of the valve was produced with a Matlab® Simulink model and the mechanical drawings, followed by the machining of a prototype. Critical problems of this design were the O-rings and the dynamic behavior.
Testing phase of the valve was important to demonstrate its useful and innovative design. Unfortunately, during the acceptance test, an anomalous behavior was spotted: a limited opening of the valve, caused by excessive friction, slowed the operative phases, especially during closing phase.
For this reason, the pneumatic valve was discharged in favor of the back-up solution of the electronic valve.

4.2. Thermal control

Thermal behavior of critical components was studied in order to design the active and passive thermal control of the experiment and find effective and simple solutions.
The active thermal control consisted in four heaters, composed by an electrical resistance. Two heaters, with a total power budget of 5 *W* (each one 2.5 *W*), were implemented on the valves to prevent icing.
Two other heaters were designed to work on the compressors, but their presence did not influence the power budget: they worked when the compressors were switched off, using compressors power alimentation. The heathers were designed to prevent icing and to permit the compressors switch on, and they were not working if compressors temperature was higher than the minimum working temperature.

4.2.1. Compressors

A thermal simulation of the compressors was performed to study their behavior and their worst heating case scenario.
In Fig. 14 is reported a scheme of the thermal model of the compressor; it had been considered:

- a conductive heat transfer through the junctions to the PB base;
- a negligible convective heat transfer: the compressor was in its protective box and the convective effects were negligible;
- an Irradiative flow between the compressor and the box with a shape factor of 100%;
- an Internal Joule heating of the compressor;
- as a worst cold case of the general model, PB and compressor box surfaces at environmental temperature.

The analyses considered the following variable aspects:

- the presence/absence of 5 *W* heaters;
- a variable conduction through the joints;
- a variable irradiative flow;
- a pre-heating operation;

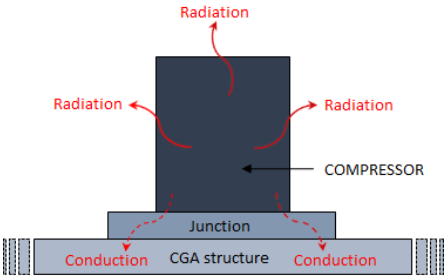


Figure 14: Simplified thermal model of the compressor.

Several analysis were performed, but the most interesting were the worst hot and worst cold cases with the same conditions; the worst hot case was under the hypothesis of an external temperature at least of 240 *K* and the maximum compressor heating of 5 *W*, the worst cold case was with a heating of the compressor of 0.5 *W* for 120 *s* every 10 minutes and an operative temperature of the gondola of 220 *K*.
In the worst hot case temperatures were compatible with the compressor operational range, in the worst cold case there was a final period with a temperature of 266 *K*, very close to the limit temperature but tolerable in the last part of the flight.
According to the model analysis and the test results the better, easier and cheaper solution to control the compressor thermal behavior was a good insulation and a pre-flight heating to minimize the effect of the external environment. Moreover, to prevent any extra heating (for example due to a malfunction), a thermal sensor was placed over the compressor; an automatic software procedure was implemented to interrupt electrical power if measured grew up over the limit of 330 *K*.

4.2.2. Valves

As for the compressors, several simulations were performed on the thermal model (Fig. 15) of the valves to investigate their behaviour; among all, the most relevant were the worst cold and hot cases.

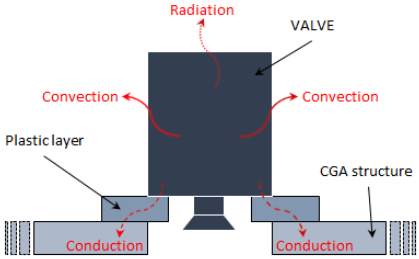


Figure 15: Simplified thermal model of the valve.

The worst cold case considered an external temperature of 220 *K* with the CGA at the same temperature. In this case, considering convection, conduction and radiation, the total amount of heating was of 2.2 *W* and therefore active heaters were designed to work with about 2.5 *W*, assuming a safe factor.
The worst hot case was estimated with the CGA exposed to solar radiation during the whole flight. In this case the temperature could rose to about 350 *K*. The simulations results proved the valve to reach the excessive temperature of about 390 *K*; to prevent extra heating or damages to non-metallic parts (joints or wire protections), a remote control of the heaters was implemented, with a regulating device devoted to the switching off of the heaters.

4.2.3. Ball-bearings

Ball-bearings usually need a specific thermal design to prevent lubricant freezing.
According to preliminary analysis, a thermal model of the ball-bearing was created (Fig. 16) with the following characteristics:

- it was modelled as a steel cylinder of 50 *mm* of diameter and 20 *mm* of depth, with a hole of 30 *mm*;
- the external part of the metallic shaft (near the CGA) was at the temperature of external environment (for convective and radiation effects);
- the supports of the ball-bearings were insulated from the gondola;
- supports and ball-bearings were protected from irradiative heating;

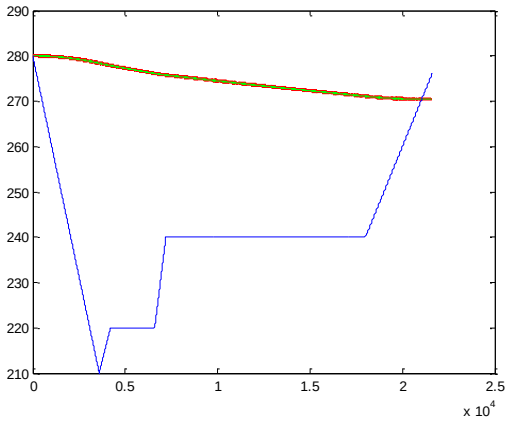


Figure 16: Simulation with a non-conductive shaft. Temperature trend in function of the altitude. The blue line represents the ambient temperature, the red one the temperature of the ball-bearing during a simulated flight.

Using the same profile of temperature from BEXUS09 data and a heater, the results of the simulation demonstrated that to have a good range of temperature the heater should be of about 200 *W*; this solution was therefore not acceptable.
To obtain a better solution it has been considered to reduce the conductive flow through the shaft: the best solution was the implementation of shaft of fiber-glass, with a thermal conductibility of 1.4 *W/mK* which reduced the conductive losses up to 1/100 of the previous case; the result of a new simulation with the non-conductive shaft is visible in Fig. 16.
Another implemented solution was to connect the DC-DC converters of the electronics to the ball-bearings with a copper jumper, in order to warm-up the ball-bearings with the benefit of preventing extra-heating of the converters. The length of the conductive joints was about 0.3 *m*, and with a 120 mm^2 section the equivalent thermal resistance was of 0.15 *W/K*. The presence of this thermal source helped to control the ball bearing thermal behaviour with a stable incoming heat flux of 4±1 *W*.

5. INTEGRATION & LAUNCH

After EAR, SCRAT experiment was shipped to ESRANGE Space Center in Sweden, for the ten-days launch campaign of BEXUS 10 and BEXUS 11. During the first week, all the experiments sharing the gondolas were subjected to final tests, to monitor their response and detect any damage from shipment and to check any interference they could create to their flight companions. SCRAT was the first BEXUS-10 experiment to be installed on the gondola (as visible in Fig. 17), followed before long by CASSE [8] and I-BATE [9].

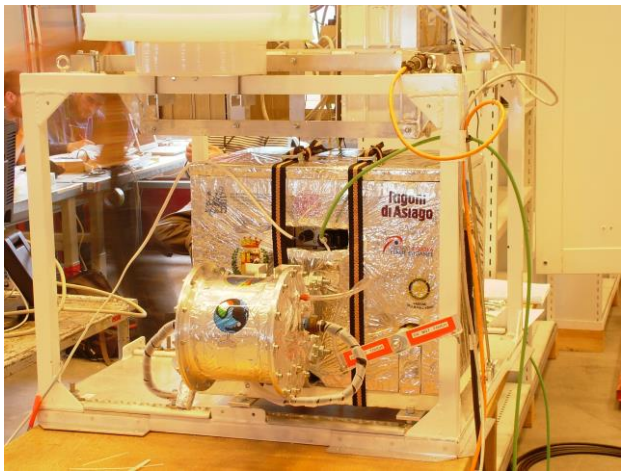


Figure 17: SCRAT integrated on the BEXUS 10 gondola.

After a week of uncertain weather, the first launch attempt was planned for the night of October 7th, but due to gusty winds it was postponed to next evening. Finally, on October 8th at 22.00 (local time) the countdown for launch started, and at 03.07 (01.07 UT) of October 9th the BEXUS 10 balloon took off from the launch pad (Fig. 18) to disappear into the cloudy sky.



Figure 18: BEXUS 10 launch on October 9th, 2010.

6. FLIGHT & DATA ANALYSIS

After the launch, the BEXUS 10 balloon moved upward at mean velocity of 5 *m/s*, reaching the floating altitude (about 24 *km*) after 1*h* 15 *min*. The balloon cut-off command was sent after 4*h* 30 *min*, and the gondola landed in a forest in Finland, about 515 *km* south-east of Esrange.

During the whole flight, SCRAT worked as expected, executing all the planned procedures and communicating preliminary data to ground station. After launch, an unexpected overheating of one compressors was detected, but the on-board software switched-off the component before reaching critical temperatures. After cooling, the compressor was again switched on and worked nominally for the rest of the flight; flight operations were not influenced by this anomaly.

Environmental data allowed to reconstruct atmosphere pressure and temperature profiles, as visible in Fig. 19; Pressure sensor saturated before reaching floating, and more reliable data was obtained by the gondola EBASS system. Pressure dropped to 23 *mbar* and temperature to -71 °*C*; sunrise caused the experiment to heat to about -50 °*C* in the last hour of the flight. Pressure and temperature profiles, as well as data from the descending phase, also allowed to determine the atmosphere density profile [10].

During the flight, a series of 15 cycles were performed, each one composed by 4 minutes of pumping and 1 minute of rest, with the pneumatic subsystem switched off. The on-board software was designed to allow ground station direct control of valves operational profiles. Raw data from the on-board memory was recovered the next day after the experiment rescue from Finland.

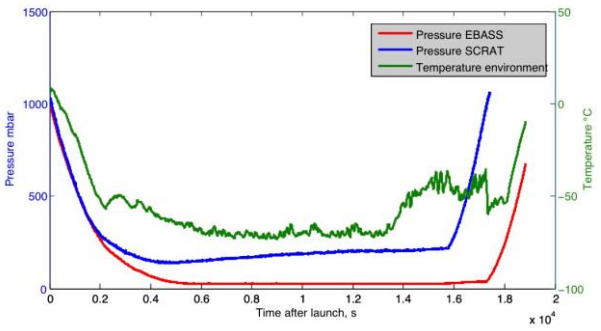


Figure 19: Temperature and pressure profiles during the flight.

In Fig. 20, two thrust profiles are shown, collected at 2 *km* and 10 *km* heights, with red arrows indicating the valves actuation commands. It is interesting to notice the increase of background noise (caused by tropospheric gusts) and the reduction of thrust magnitude with the height.

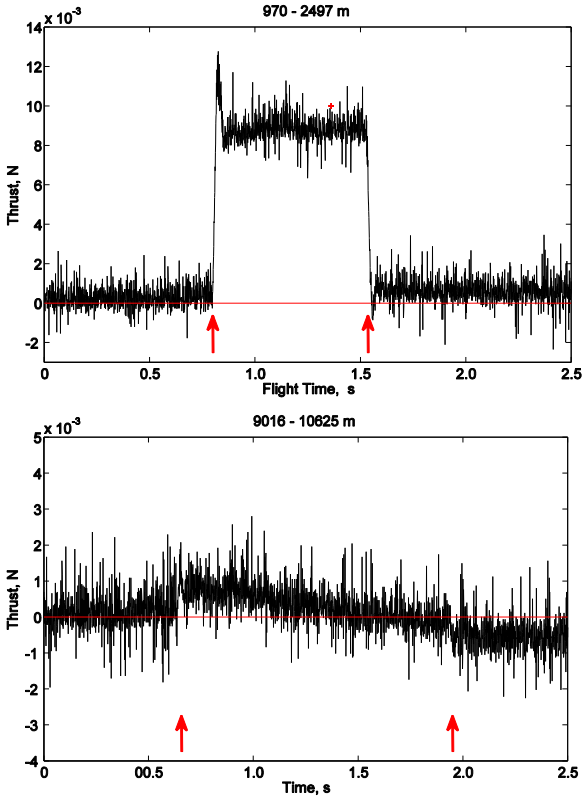


Figure 20: Thrust profiles during the first cycle at about 2 km (up) and the sixth cycle at about 10 km (down), from on board memory raw data. It is interesting to note the change in thrust shape and the increase of background noise in the 10 km data. Red arrows indicate switch-on and switch-off instants.

The preliminary assessment of raw data indicated that a signal processing and filtering was required, as reported

in Fig. 21. First, a complete signal examination was performed, to identify the pulses respect to the background noise at the highest altitudes, with the assistance of the on-board software data log information on the actuation commands. A second phase was dedicated to signal band-pass and notch filtering, eliminating low frequency (wind) and high frequency (vibrations and electric disturbances) noises. Last, deconvolution allowed to reconstruct the thrust profile applying the transfer function of the measuring system.

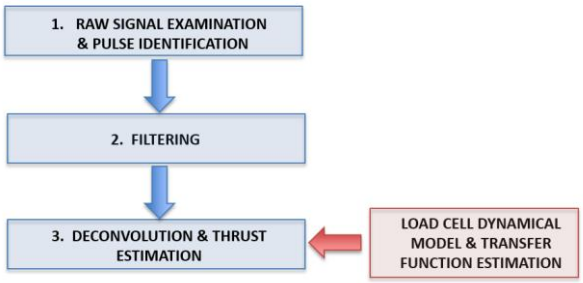


Figure 21: Raw data processing approach.

The transfer function was evaluated by modelling SCRAT measurement system, affecting the thrust profile in dependence on the shaft inertia, the damping coefficient of the ball bearing and the load cell stiffness. A more complete description of the data analysis approach can be found in [11].

7. RESULTS

Data analysis allowed to detect all the 101 thrusts commanded during the flight, with magnitude in the range of 10^{-1}-10^{-4} N; in Fig. 22 a summary comparison between gas dynamic simulations and experimental results can be found. Both the thrust and the total impulse values show a discrepancy of more than one order of magnitude, that was basically related to (1) an underestimation of SCRAT compressors performance at low pressures (later pointed out during laboratory tests) and (2) to friction losses due to the air flow from the CGA vessel to the nozzle (that was not included in the theoretical model).

Post-flight analysis through computational fluid dynamic (CFD) software were then performed, to evaluate the influence of the air pipe and connectors linking the CGA vessel to the nozzle. A series of simulations allowed to calculate internal losses in different environmental conditions (pressure and temperature), and to calculate the outlet velocity. It was therefore possible to evaluate the thrust and the impulse under these different conditions: the results, again reported in Fig. 22, allowed to explain the detected discrepancy, validating the experiment models with the collected data and recognizing the experimental setup limitations and the possible ways to improve it.

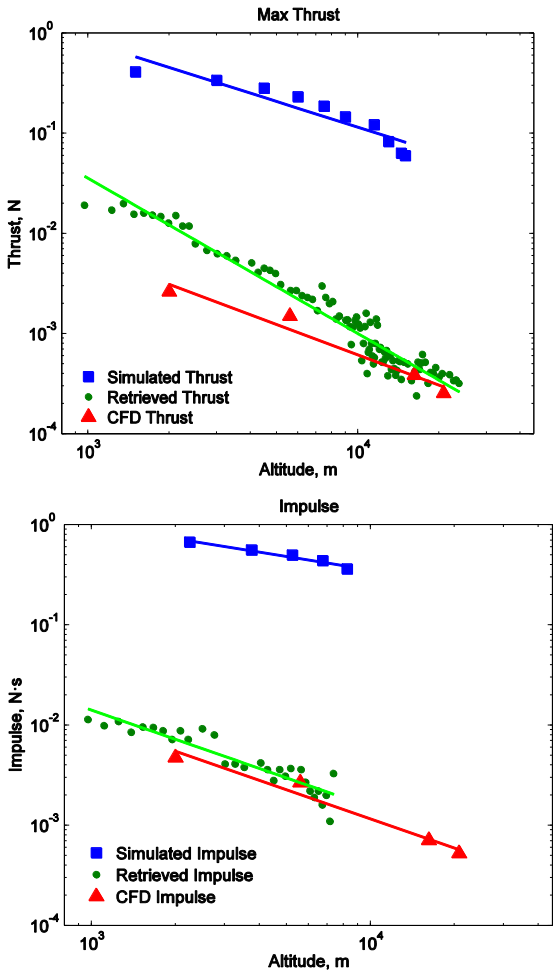


Figure 22: Measured (dots) and predicted (squares) maximum thrusts (up) and impulses (down) for the entire flight; in triangles, post flight CFD analysis.

8. LESSONS LEARNED

Participating to the REXUS/BEXUS programme give students the exciting possibility to participate to a real, little space mission, and to learn all those process and methodologies that are usually not included in academic courses. Furthermore, SCRAT team was motivated by being the ESA first hands-on experiment of the University of Padova: a positive outcome from the experience would give the program good visibility, allowing other students to participate to next BEXUS cycles. In the end, following SCRAT footprints, the next four years four experiments from Padova were selected for BEXUS, respectively ARCADE, MISSUS, ARCADE-R2 and POLARIS.

From the technical point of view, the most important lesson learned is to keep the experiment as simple as possible: a simpler hardware allows a simpler software to be designed and implemented, thus reducing the experiment possible points of failure, and the experiment is more likely to fulfil all its primary and

secondary objectives. In this contest, using COTS is suggested, due to their reduced procuring time and their robustness and reliability respect to custom components.
In parallel, the nine-month program forces students to learn scheduling and organization, thanks to the standard milestones and deadlines comparable to the ones of a real space program. The team had to learn how to divide the group work balancing the tasks delegated to the single members with the need of supporting and involving the members in the most demanding situations. This helped to create a team chemistry that was not limited to the experiment development, but was at the base of the "SCRAT Tuesday evenings" when the team used to meet for dinner and some drinks after work; at today, team members still plan to meet at least once a year, to have party and stay in touch, remembering the experience and the best moments spent all together.
In conclusion, the BEXUS program gave SCRAT team not only a valuable experience for the future and the first hands-on opportunity on space engineering, but also the possibility to aggregate and stay together outside the academic environment; SCRAT was not a simple and forgettable experiment, but an important step in our carrier and personal growth.

9. CONCLUSIONS

This paper presented the evolution of the SCRAT experiment, developed following the typical milestones of a real space mission. After nine months of hard working, SCRAT experiment has been successfully launched on board of BEXUS 10 the 9th of October, 2010 from the Esrange Space Center in Sweden. The experiment worked nominally for the whole flight, which lasted for around five hours. The data retrieved have led to achieve the experiment goals: primarily the estimation of the thruster performance, in terms of maximum thrust and impulse in relation to the altitude; secondarily the atmospheric study in terms of temperature, pressure and density. A total amount of 101 thrusts were detected between 10^{-1} *N* (ground level) and 10^{-4} *N* (20 *km* of altitude), with a total impulse in the range of $10^{-2} – 10^{-3}$ *Nm*. The discrepancy between flight data and the theoretical model was successfully explained considering the load effect induced by air drag into the air pipe used to connect the thruster nozzle to the torsional load cell employed for thrust measurement.
The backup solutions selected worked as expected during the validation process phases, assuring the accomplishment of the mission. All the foreseen precautions adopted during the experiment development were successfully implemented guaranteeing the achievement of the goals.
Beyond the scientific goal of SCRAT experiment, there is the most important goal of space education. The RX/BX Programme introduced us to the real space activities allowing us to gain familiarity and experience with space researches and related discipline in the rich and innovative European contest offered by ESA.

10. ACKNOWLEDGMENTS

The authors would like to thank all the REXUS/BEXUS staff and ESA, DLR, SSC and SNSB expert, in particular ESA Education office and ESRANGE Launch Base personnel.
The SCRAT Experiment was developed by an amazing student team (Fig. 20), that made it possible to participate to the BEXUS-10 launch thanks to their tireless work and enthusiasm: SCRAT was not just an experiment, but a long educational adventure for all of us, and the first taste of real space activities.
Last, thanks to Mr. Antonio Selmo for his support in the design and development of SCRAT electronics.



Figure 20: The SCRAT Team: from left, Matteo Duzzi, Giulio di Donato, Michele Cesaro, Lorenzo Olivieri, Leonardo Barilaro, Marco Chiaradia, Ruggero Comisso, Gabriele Rodeghiero, Federico Spagnolo and Antonio Selmo

11. BIBLIOGRAPHY

[1] K. P. Valavanis, Advances in Unmanned Aerial Vehicles, state of the art and the road to autonomy, Springer, 2007
[2] W. R. Davis Jr., B. B. Kosicki, D.M. Boroson, D. F. Kostishack, Micro Air Vehicles for Optical Surveillance, The Lincoln Laboratory Journal 9-2 (1996) 197-214
[3] A. Colozza, Airships for Planetary Exploration, NASA/CR—2004-213345 (2004)
[4] Jones, Jack A., et al. Montgolfiere balloon missions from Mars and Titan. Pasadena, CA: Jet Propulsion Laboratory, National Aeronautics and Space Administration, 2005.
[5] ESA contribution to the Titan Saturn System Mission, ESA-SRE 4 (2008)

[6] J. Chela-Flores, From the Moon to the Moons: Encedalus and Europa. The Search for Life and Reliable Biomarkers, Journal of Cosmology 5 (2010) 971-981
[7] Fittock M. REXUS/BEXUS: launching student experiments a step towards a stronger space science community, 38th COSPAR Scientific Assembly, July 2010.
[8] Juanes-Vallejo, Clara M., et al., Cranfield Astrobiological Stratospheric Sampling Experiment (Cass. E): Overview of Flight Hardware Configuration, Implemented Planetary Protection and Contamination Control Procedures and Preliminary Post-Flight Results, 20th Symposium on European Rocket and Balloon Programmes and Related Research. Vol. 700. 2011.
[9] Rieber, R. R., Norheim, T., Brodsky, Y., I-BATE: a precursor to space-based air traffic control, 20th Symposium on European Rocket and Balloon Programmes and Related Research. Vol. 700. 2011.
[10] Rodeghiero, G., Olivieri, L., Francesconi, A.: Atmospheric Modeling by SCRAT Experiment During the 2010 ESA BEXUS 10 Flight Campaign, 3rd CEAS Air and Space Conference, Venice, Italy, Oct. 2011
[11] Olivieri, L., Duzzi, M., Rodeghiero, G., Francesconi, A., Data retrieved by SCRAT Experiment during the 2010 ESA BEXUS 10 flight campaign, 65th IAC, Toronto, 29 September – 03 October 2014

POLARIS EXPERIMENT: STRATOSPHERIC FLIGHT OUTCOMES AND EXPERIENCE GAINED FROM THE REXUS-BEXUS PROGRAMME

Davide Paganini[(1)], Riccardo Dalla Vecchia[(1)], Matteo Zorzan[(1)], Francesco Branz[(2)], Lorenzo Olivieri[(2)], Francesco Sansone[(1)], Alessandro Francesconi[(2)]

[(1)] Department of Industrial Engineering, University of Padova, Via Gradenigo 6/a, 35131 Padova, Italy
(Email : dav.paganini@gmail.com, polaris.unipd@gmail.com)
[(2)]) CISAS "G. Colombo", University of Padova, Via Venezia 15, 35131 Padova, Italy

ABSTRACT

POLARIS – acronym for POLymer-Actuated Radiator with Independent Surfaces – is a tech demonstrator, based on a new concept of variable-geometry heat radiator engineered for space and planetary probes.
In detail, the radiator is composed by three overlapped plates, parallel and constrained so that it is possible to separate them or put them in good thermal contact. Taking advantage of this possibility, the radiator changes the way the heat passes through it, from a conductive path to a radiative one. The switching operation, obtained by mean of a linear actuation, is triggered in order to vary the system equivalent thermal resistance and so to control the heat flux dissipated to the environment. Thus, the radiator adaptability is achieved with a simple but very effective solution. In order to test the performance of this new concept of radiator, an experimental setup was designed and built. This experiment has been selected to participate in the REXUS/BEXUS programme (Rocket and Balloon-borne Experiments for University Students), which allows university students to carry out scientific and technological experiments on sub-orbital rockets and stratospheric balloons. POLARIS was launched from the ESRANGE Space Center (Kiruna, Sweden) on-board the BEXUS 18 stratospheric balloon on October 2014. The conditions experienced by the experiment during a BEXUS flight permitted to evaluate the radiator in a realistic context, giving an extraordinary opportunity to characterize its abilities. The experiment studied the radiator performances in variable environmental conditions and aimed to guarantee the thermal steadiness of a dummy payload, through the radiator active control. External environment data, in terms of pressure, temperature and radiation were monitored in order to fully characterize the thermal loads applied to the radiator plates. Post-flight analysis showed the radiator capability to double its equivalent thermal resistance, using a negligible amount of power. Nevertheless, the radiator active thermal control capabilities are not restricted to this performance, which is strongly influenced by the flight setup design, but they could be easily tailored to face different mission environments by modifying drivers as the number of plates, their thickness and thermo-optic properties.
In this paper, POLARIS architecture is described together with the main results obtained from the flight. Moreover, post flight analysis and future development of the radiator concept are presented.

1. INTRODUCTION

On one hand, the design of spacecraft able to tolerate the exposure to the space environment has always thrown hard challenges to engineers. Among these, one is the design of thermal control subsystem (TCS), whose objective is to maintain the temperature of satellite components within operative ranges, avoiding failures due to freezing or overheating. The importance of this subsystem appears clear by examining the limited range of temperatures tolerated by most of spacecraft components along with the temperatures that can be reached due to the heat exchanges with the space environment, depending on attitude and orbital position. Substantially, the TCS aims to manage the equilibrium between two heat fluxes [1]: the first comes from the environment and it is mainly composed by the direct sunlight, the Earth albedo and IR emission, while the second is internally generated by the satellite electronics. This equilibrium is reached exploiting different techniques, combined together to obtain a highly optimized solution that represents the best trade-off between power consumption, mass and development complexity, considering the mission requirements and its thermal environment. Nowadays, the most common solution is a combination of insulating coatings, heaters (on critical components) and heat radiators. These last devices, heat radiators, are essential devices for the survival of a space system: they are usually composed by a bare metal plate conductively connected to payloads, and their task is to dissipate the excessive thermal loads resulting from the spacecraft internal generation. The radiator sizing must be carefully calculated in order to ensure the right dissipation in the worst hot case, namely the one with maximum internal and external heat fluxes. Nevertheless, given that these two fluxes may vary during the mission lifetime (i.e. during electronics switching off, eclipses, attitude variation, and surfaces degradation) the radiator design has to be chosen in order to obtain an opportune flexibility on its performances.

On the other hand, space exploration requires to reduce the mass, sizes and electrical power demand of spacecrafts and probes; this objective could be achieved through the miniaturization of spacecraft subsystems, but this solution is usually constrained by performance requirements, reliability and other system drivers. Therefore, new ways are to be tested, and one of these is the development of new technologies, such as new kind of actuators. Electroactive polymers (EAPs) are a particular class of polymers, widely studied in the last decade, which show a deformation in response to an electric stimulation; this particular behavior encouraged new studies to test their potentialities as actuators. Among EAPs, actuators based on Dielectric Elastomers (DE) exhibit the most promising properties. The natural ease of preparing and shaping such DE materials, coupled with their low mass and large displacements, show that they have the potential to enable new actuation technologies.

In this framework, POLARIS (POLymer-Actuated Radiator with Independent Surfaces) Student Experiment was a technology demonstrator of a new concept of heat radiator, named *multiplate*, which is able to vary its equivalent thermal resistance though a geometry change. This concept enables to obtain a flexible active thermal control by exploiting a linear actuation. A set of EAP actuators (four Rolled DE Actuators[4]), completely manufactured by the students, was included in the experiment as a part of the radiator actuation system.

POLARIS Experiment aimed to study the performances of the radiator in variable environmental conditions. It also aimed to guarantee, through the active thermal control allowed by the radiator, the thermal steadiness of a dummy payload. Lastly, it aimed to verify the correlation between the thermal model used to predict the radiator behavior and the measured data.

The radiator features have application in different space mission scenarios: one of these is certainly the one of planetary probes without an attitude control, exposed to environmental changes. These conditions are close to those of a balloon stratospheric flight: for this reason, in December 2013 the experiment was proposed for the REXUS/BEXUS (RX/BX) Programme, and flew on board the BEXUS 18 stratospheric balloon in October 2014. The REXUS/BEXUS programme offers to European university students the opportunity to carry out scientific experiments aboard sounding rockets (REXUS, Rocket-borne EXperiments for University Students) or stratospheric balloons (BEXUS, Balloon-borne EXperiments for University Students). The Programme is realized under a bilateral Agency Agreement between the German Aerospace Center (DLR) and the Swedish National Space Board (SNSB). The Swedish share of the payload is been made available to students from other European countries through a collaboration with the European Space Agency (ESA). EuroLaunch, a cooperation between the Esrange Space Center of the Swedish Space Corporation (SSC) and the Mobile Rocket Base (MORABA) of DLR, is responsible for the campaign management and operations of the launch vehicles. Experts from ESA, SSC and DLR provide technical

2. RADIATOR CONCEPT

POLARIS experiment is based on a heat radiator with adjustable equivalent thermal resistance, named *multiplate* [2]. In detail, this radiator is composed by three parallel metallic plates, linked together and constrained so that an actuation system can separate them or put them in good thermal contact. Taking advantage of this feature, the nature of the heat path through the radiator is modified, switching between a mainly conductive path and a mainly radiative one.

On one hand, when the radiator is in its closed configuration, the three plates are in contact. The pressure between them can ensure an adequate thermal conductivity coefficient in order to make them work almost as a single plate. In this case, the internally generated heat is transferred through the plates mainly by conduction and then radiated to the environment by the last plate. This condition is favorable to the heat exchange.

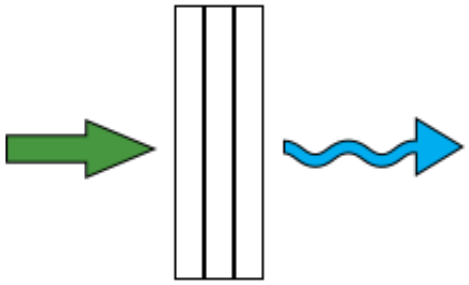


Figure 1: Sketch of the Closed-Plates configuration

On the other hand, when the radiator is in its open configuration, the three plates are not more in contact and the conductive link between them becomes mainly a radiative link. This condition leads to an increase of the system equivalent thermal resistance. In this case, the heat generated by the payload is transferred through the plates and to the environment mainly by radiation. This condition is more unfavorable to the heat exchange.

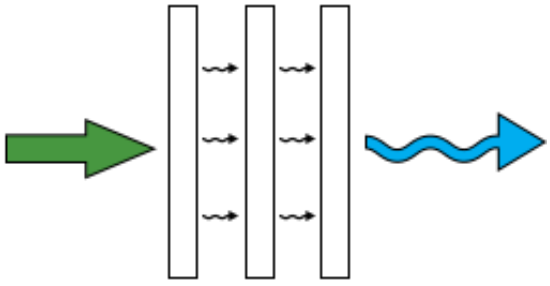


Figure 2: Sketch of the Open-Plates configuration

The switching operation between these two configurations, obtained by means of a linear actuation, varies the system equivalent thermal resistance and so enables to influence the heat exchange towards the environment.

3. EXPERIMENT MILESTONES

POLARIS participated in the 7th cycle of REXUS/BEXUS Programme. Each cycle is roughly one year long and it is structured with a series of milestones recalling the typical space project lifecycle. The programme alternates design phases with reviews from experts in the field, culminates in the launch of the experiments and ends with the publication of the final reports. This section will briefly present the evolution of the POLARIS Experiment from its initial idea to its flight setup.

3.1 Proposal (November '13)

In its first conception, the experiment setup was divided into two main section, one thermally insulated in respect to the other: the On-Board Electronic Box and the On-Board Payload Box. The first contained the PC, the electronics, the data acquisition device and the high voltage power supply for EAPs; the second contained the actuators, the sensors, the dummy payload (bound to the first plate) and the radiator plates (exposed to the environment).

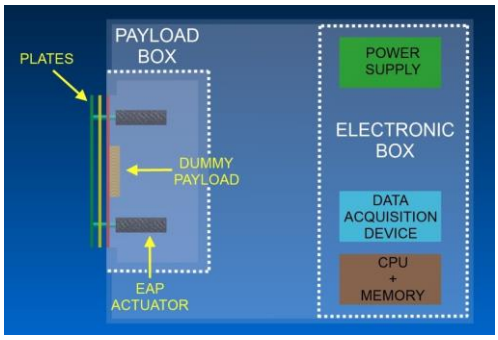


Figure 3: POLARIS Experiment initial scheme

The two radiator configurations were already set, but the mechanism for the radiator actuation was not yet designed: the idea was to connect the EAP actuators to the plates by non-conductive rods. The actuation control was based on a time controlled loop or on a temperature controlled loop. In order to simulate the heat generation of a real payload, a power resistor was connected to the first plate of the radiator as a dummy payload. Sensors to measure the payload and the radiator temperature were taken into account. The setup contained also sensors to monitor the atmospheric conditions, (such as temperature, pressure, wind speed and direction). The power dissipated by the dummy payload was also monitored. Finally, sensors measured the force applied by the EAP actuators and the distance between plates.

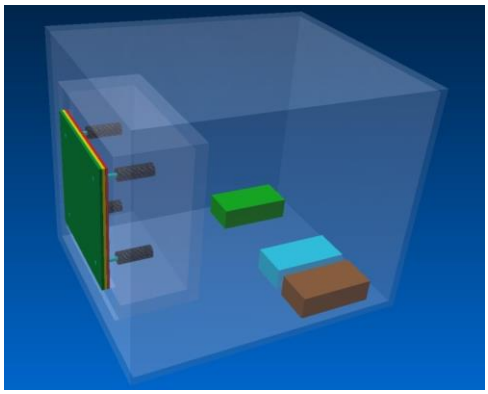


Figure 4: POLARIS Experiment initial 3D view

3.2 Selection Workshop (December '13)

After the application to the RX-BX Programme, the experiment was pre-selected and the team was invited to ESTEC to present a more detailed version of the experiment concept.

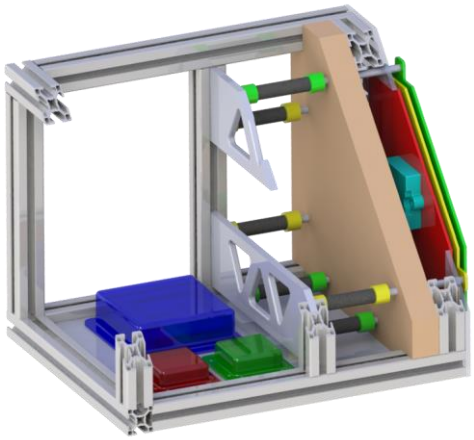


Figure 5: POLARIS Experiment render for the RX-BX Selection Workshop (ESTEC)

The mechanical design, even if largely undefined, was improved: the experiment structure is composed by extruded aluminum bars and the actuation system is now based on 8 Dielectric Elastomers actuators. The sensors and their location were completely defined: they were the same as the proposal, except for wind and force sensors which were substituted by radiometers to measure the incoming visible and infrared radiation. First estimations on the link budget were calculated (22 kbit/s) together with the expected data volume (60 Mbit). Thermal simulations were performed, in order to understand the minimum time of flight required for the radiator characterization.

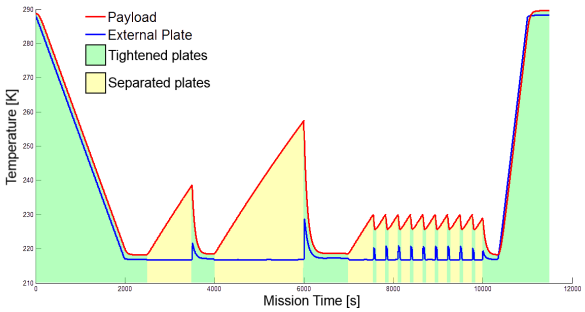


Figure 6: POLARIS Mission simulation (thermal) for the RX-BX Selection Workshop (ESTEC).

3.3 Student Training Week (February 2014)

The first review of the experiment, the Preliminary Design Review (PDR), took place at the ESRANGE Space Centre. The mission objectives were defined along with the system requirements and verification methods.

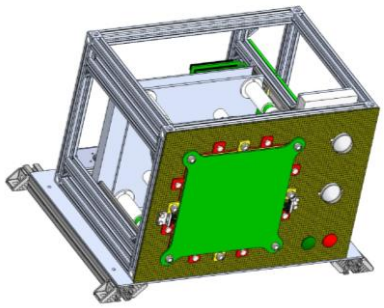


Figure 7: POLARIS Experiment mechanical design for the RX-BX Student Training Week (ESRANGE) [3]

The mechanical design was almost complete, except for some detail regarding the radiator actuation system: the DE actuators manufacturing process was still under development so there were some uncertainty about their final dimensions.

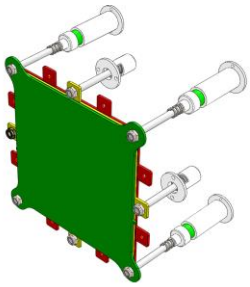


Figure 8: POLARIS Radiator, mechanical design for the RX-BX Student Training Week (ESRANGE)

The radiator actuation system, subjected to major changes since the SW, was finally composed by four DE actuators, coupled with a system of springs. In order to ensure a reliable actuation even in the case of DEs malfunctioning, an electrical actuator was included in the setup; by pulling the base which the DEs were connected to, it could move the actuators and consequently the radiator plates. The first DE actuators were successfully manufactured in the facilities of the University of Padova.

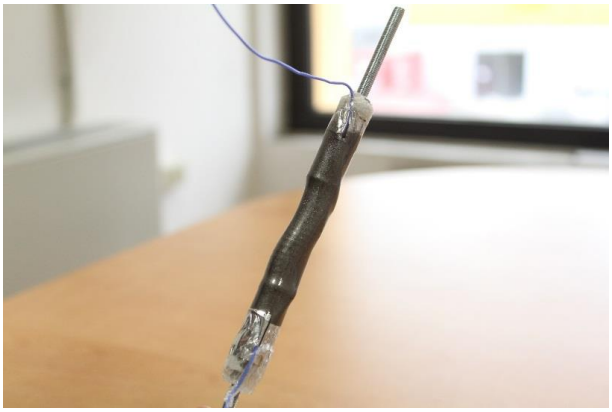


Figure 9: First prototype of DE actuator successfully manufactured, right before RX-BX Student Training Week (ESRANGE)

FEM analysis on the structure were performed along with improved thermal simulations. Electronics and software design were outlined and under development.

3.4 Critical Design Review (May '14)

The second review of the experiment, the Critical Design Review (CDR), took place at ESTEC. The design of the mechanical, electrical and electronic subsystem was completed and ready to support proceeding with manufacturing, assembly, integration and test.

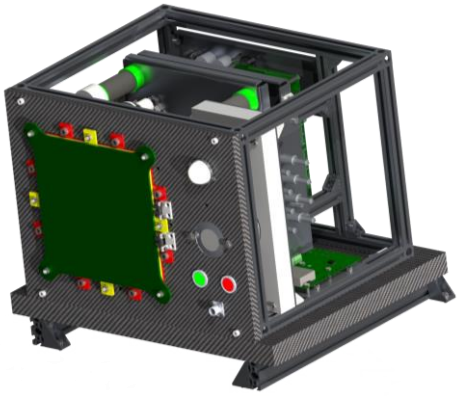


Figure 10: POLARIS Experiment, render for the CDR

The experiment CDR design was just a more detailed version of the PDR one, there were just minor changes.

3.5 Integration Progress Review (July '14)

The third review of the experiment, the Integration Progress Review (IPR), took place at the University of

Padova. At the time, the mechanical integration was in its final phase and the Printed Circuit Boards (PCBs) manufacturing was completed.

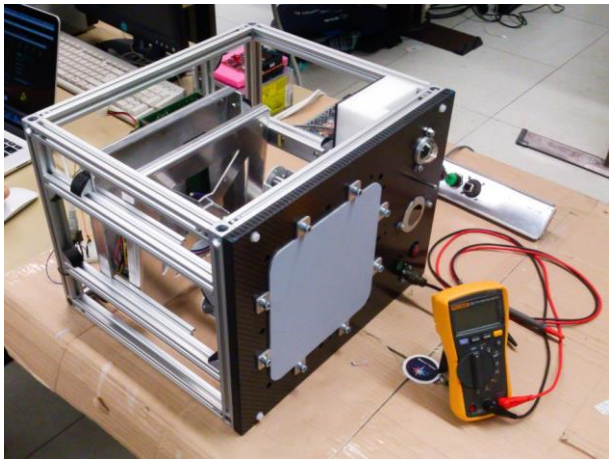


Figure 11: Structure of POLARIS, inner radiator plate mounted, during the IPR

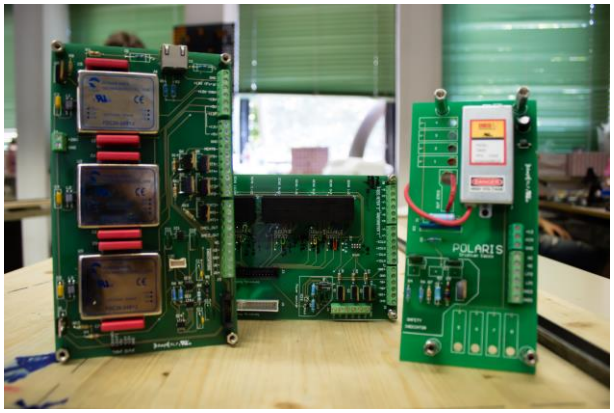


Figure 12: POLARIS PCBs during the IPR, in detail from left: power distribution, data acquisition and high voltage

Experts from ESA and SSC evaluated the state of the experiment, giving important advices on the test planning. The DEs manufacturing was finally standardised and test were performed on the actuators force and deformation, on their manufacturing repeatability, on the DEs response to low pressure, storage and cold environments. At that time started to become established the idea that the DEs performances could not be enough to meet the radiator mechanism requirements, at least not with safety margins. Nevertheless, the backup electrical actuator (included in the setup at the PDR) permitted to proceed without major changes. The only change was to stop considering the DEs as the primary choice for the radiator actuation, but only as another test.



Figure 13: DE actuator mounted on a load cell setup

The software logic was designed and under implementation, as well as the experiment ground station GUI (Graphic User Interface).

3.6 Experiment Acceptance Review (September '14)

The fourth review of the experiment, the Experiment Acceptance Review (EAR), took place at the University of Padova. An expert from SSC evaluated the experiment, ensuring that the experiment was flight ready, and discussed all the information required for the launch campaign preparation. The experiment was fully integrated and functioning.

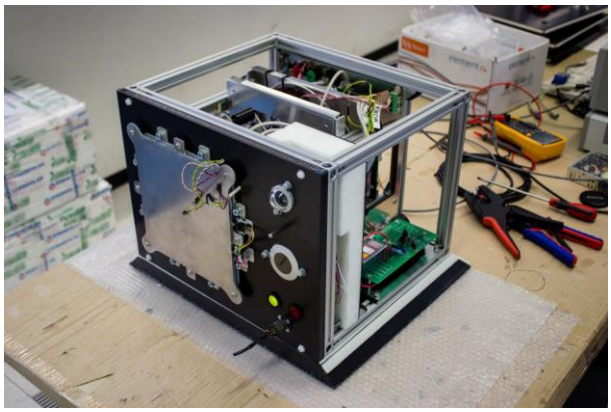


Figure 14: POLARIS (partially open) at the EAR

The software was fully implemented and its response to critic events during the flight was virtually tested. Final system tests were carried out: one complete mission simulation inside a dry ice cold facility (about 220 K) and one complete mission simulation inside a vacuum chamber. After these test, since they did not highlighted particular issues, the experiment was disassembled and shipped to the ESRANGE Space Centre.

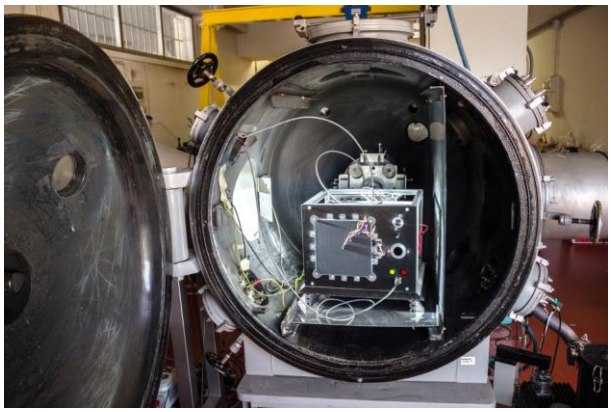


Figure 15: POLARIS (partially open) inside the vacuum chamber

4. FLIGHT DATA

POLARIS Experiment flew on-board the BEXUS18 Balloon in October 2014, from the ESRANGE Space Center (Kiruna, Sweden). During the stratospheric flight, a set of sensors monitored the radiator behaviour in response to the environmental conditions.



Figure 16: POLARIS in stratosphere on board the BEXUS18 Balloon

Table 1: The list of measured data, and the sensors respective position in the POLARIS setup

SPOT	MEASURE
Dummy Payload	Temperature Power dissipation
Inner Radiator Plate	Temperature and its spatial distribution
Outer Radiator Plate	Temperature and its spatial distribution
Plates Supports	Plates position
Environment B.C.	Pressure Temperature Incoming Visible Radiation Incoming Infrared Radiation

The flight duration, starting from launch to the balloon cut down, was 3h 12': 1h 56' of ascending phase and 1h 16' of floating phase in stratosphere. The original flight schedule foresaw at least 3h of floating, but the cut down decision was anticipated due to meteorological issues. The flight altitude profile is presented in Fig.17. This information comes from the pressure sensors, since their measurements have been used to indirectly estimate the altitude using the US Standard Atmosphere model. In Fig.18 it is possible to see the comparison between the pressure measured by POLARIS and the one by the BEXUS18 own service system (named EBASS).

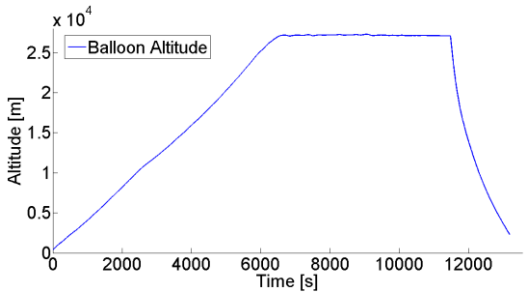


Figure 17: Flight altitude profile

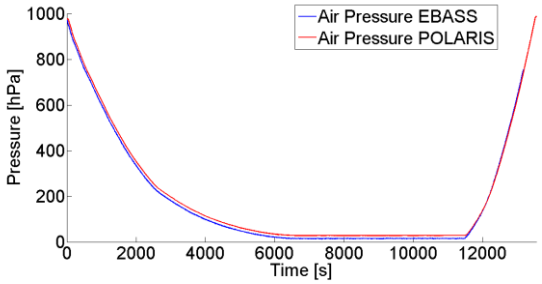


Figure 18: Pressure [hPa] during the flight

During the whole flight the experiment internal temperature stayed within the required values and for most of the mission time the internal heaters were switched off. As shown in Fig.19, the setup thermal control well designed and maintained the experiment internal temperature between 284 - 293 K, even if the external temperature reached 215,5 K (measured by BEXUS18 EBASS[5]).

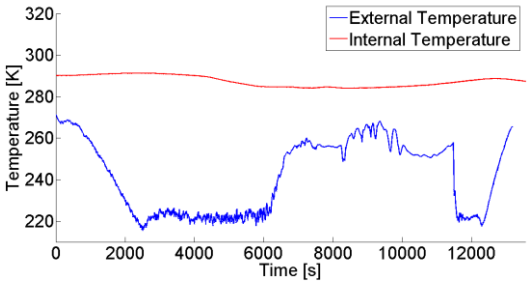


Figure 19: External and Internal Temperature during the flight

Two radiometers provided the exact value of the incoming radiation (both UV and IR), shown in Fig.20.

From this values, it is possible to extrapolate two other parameters: on one hand it is possible to see how the presence of the atmosphere influenced the IR radiation (~300 W/m2 at ground, ~170-200 W/m2 in floating); on the other hand it was possible to extrapolate, through a FFT, the period of the gondola rotation. The system shows a first clear oscillation at 9,9*10-4 Hz, which is the BEXUS rotating period of 1010 s (~17 minutes). No other significant periods were found, this means that all the other fluctuation were mostly random and caused by other pitch and yaw rotations of the gondola respect to the sun.

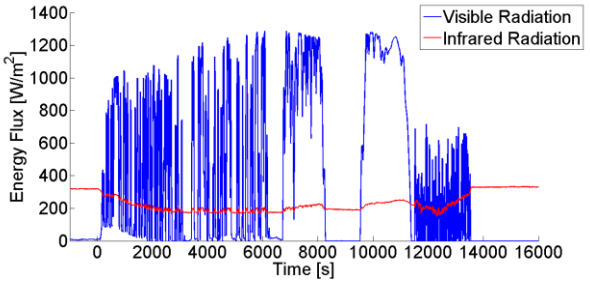


Figure 20: Visible & IR Incoming radiation during the flight

The last data to be inserted in the thermal model in order to estimate the radiator performance is the one regarding the plates temperature. These data are shown in Fig.21.

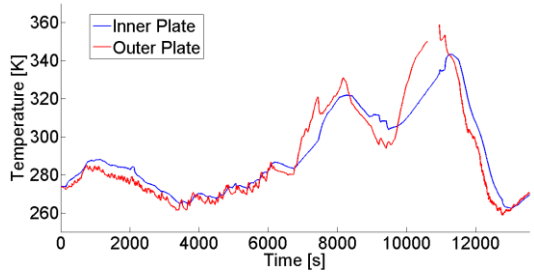


Figure 21: Radiator plates temperature during the flight

Unfortunately, the thermal simulations carried out during the setup preparation, which were used to foresee its behavior during the flight, were badly affected by an incorrect estimation of the air convective heat transfer coefficient in low pressure. This inaccuracy led to design some of the setup characteristics expecting a much colder environment. Moreover, the time of flight has been shortened due to unfavorable wind conditions, becoming too brief to achieve a steady state heat exchange for both the radiator configuration. Due to these unpredictable events, it was not possible to obtain a quantitative characterization of the radiator performance during the flight.

Nevertheless, by cross-checking the environment data with the radiator temperatures measured during the flight, it was possible to estimate a new value for the convection coefficient. This allowed to achieve a far more precise model of the radiator behavior in low-pressure environments. Thanks to this revised thermal model it was possible to compare the multi plate radiator flight behaviour with the one of a simulated, non-actuated multi plate radiator.

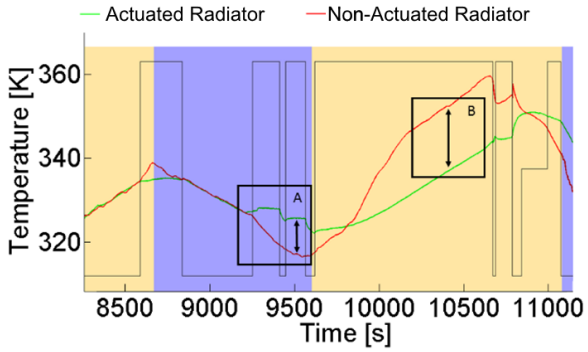


Figure 22: Effects on P/L Temperature of the POLARIS actuation, "non-actuated radiator" is simulated (Yellow represents sunlight exposure, Purple represents shadow exposure, Flat High Black line represents Open plates configuration, Flat Low Black line represents Closed plates configuration)

This comparison used the real conditions encountered in stratosphere as boundary conditions and permits to appreciate qualitatively the multi plate radiator performance (shown in Fig. 22). In order to understand this comparison, it must be stated that the multi plate radiator was designed with a clear purpose: being able to increase payloads temperature when exposed to cold conditions, and insulate payloads when exposed to hot conditions. The two enlighten parts of the Fig.XIX shows that these purposes have been fulfilled:

• Considering the Rectangle A: the radiator is in the shadow (consequent cold conditions) and the three plates are opened two times. It is clear how the opening of the plates strongly increases the payload temperature with respect to the classic radiator.

• Considering the Rectangle B: the radiator is exposed again to sunlight (consequent hot conditions) the three plates are opened. It is clear how the opening of the plates strongly insulates the payload in respect with the classic radiator.

5. LESSONS LEARNED AND CONCLUSIONS

REXUS/BEXUS program gives students the exciting possibility to participate to a real space mission, teaching them how to deal with such a challenging experience. Students do not just learn things, they

develop a full new mindset, both about team work, system engineering methodologies and projects deadlines; this kind of things cannot be learned from academic formation.
During the whole duration of project, the most important lessons learned as a result of the issues encountered were:
• How to deal with the shipment of the experiment components: the experiment manufacturing (and thus all the following phases) should be carefully planned in order to avoid significant shifting of the work schedule due to retailers delays.
• How to deal with the development of new technologies without extensive literature references (i.e. Dielectric Elastomers): the technology development should not be absolutely underestimated; an intensive research work requires a lot more time than we expected, and should be faced with a scrupulousness that we acquired after a long time after the beginning of the BEXUS experience.

During the experiment development, the most important lesson learned as a result of the issues encountered was to keep the design as simple as possible, with accessible components and easy-to-remove parts, since it is not so unusual to repeatedly dismount and remount part of the experiment or one subsystem, due to manufacture errors and assembly inaccuracies. Every experiment should be designed keeping in mind this principle, since the develop a new technology (with the experience of a college student) means frequent errors and design rethinking. More in detail, the team faced the following issues:
• The temperature measurement requirements (accuracy and number of sensors) were initially very demanding, resulting in a lot of time spent to find a way to satisfy them. Later, the team realized it was impossible to achieve this goal with our budget, therefore we agreed to relax the requirements . This was done after performing deep thermal simulations, eventually revealing that the initial accuracy and large number of sensors were not really necessary for the experiment purposes. A better initial investigation of the effective requirements, joint with a budget analysis would have saved a lot of time.
• The team chose the onboard computer before having a clear and definitive view of the sensors and components in the experiment. This resulted in some interfacing issues that could be avoided by choosing a different computer board or components.
• The PCBs had to be redesigned several times due to changes in the experiment design, such as new sensors or functionalities, resulting in a lot of wasted time. It would have been better to wait for a final design before working on the PCBs.
• During the assembly came to light the complexity to fasten some components because of a very compacted design.
• The team overestimated the performances of the DE actuators, due to a lack on literature. Therefore, a lot of time and efforts could have been saved if an electric actuator with know and certified properties was chosen as a primary actuation system; however the team chose to use an electric actuator as a backup solution (which later became the primary option).
Concerning other aspects of the project (i.e. teamwork, planning, testing, documentation, internal team management, time management, communication inside and outside), the team encountered some minor issues which not worth to be mentioned here; clearly also this latter aspect were precious learning experiences for the team members.

Concluding, despite of an unexpected flight condition, it was possible to demonstrate the functionality of this concept of radiator. POLARIS bus was functional during the whole flight: the electronics and the sensors were able to measure almost everything during the flight, never showing a crucial failure that would lose important data. Unfortunately, the DE actuators performances were not high enough to meet the experiment requirements during the flight. Anyway, the developed know-how about the DE actuators manufacturing process will be a useful asset for future projects involving this cutting-edge technology. The structure showed no evidence of failures even though POLARIS landed hitting the front face of the experiment to the ground. In conclusion, the mission on BEXUS18 was an excellent test bench for the whole system because of the extremely variable conditions faced by the experiment.The encouraging data collected confirm the radiator potentialities and allow to state that the mission was a success, both operatively and scientifically speaking.

6. ACKNOWLEDGEMENTS

The authors would like to thank all the REXUS/BEXUS staff and all the ESA, DLR, SNSB and SSC personnel involved in the programme. The experiment realization was possible thanks to the University of Padova (especially the Industrial Engineering Department and the Center of Studies and Activities for Space "G.Colombo") and to private sponsors.

7. REFERENCES

[1] D. G. Gilmore et. al., "Spacecraft Thermal Control Handbook", The Aerospace Press, 2002, pp. 207-222
[2] D. Paganini et al., "A New Concept Variable Resistance Radiator", 65th IAC, Toronto 2014

[3] “Student Experiment Documentation: POLARIS Experiment – BEXUS18”, 2015
[4] R. Zhang, “Development of Dielectric Elastomer Actuators and their Implementation in a Novel Force Feedback Interface”, Swiss Federal Institute Of Technology, Zurich 2007
[5] Olle Persson et al., “BEXUS User Manual”, EuroLaunch, 2011

SESSION 5: E - Atmospheric & Planetary Experiments

(Thursday 10th - 17.00)

Chairman: Prof. Anton Ivanov

Education Activity of Sapienza Space Systems and Space Surveillance Laboratory – S5lab

Federico Curianò[(1)], Lorenzo Arena[(2)], Tommaso Cardona[(3)], Francesco Diprima[(4)], Gioacchino Scirè[(5)], Federica Angeletti [(6)], Alice Pellegrino [(7)], Paolo Marzioli [(8)], Armando Grossi[(9)], Gianluca De Zanet[(10)] , Fabrizio Piergentili[(11)], Fabio Santoni[(12)]

[(1)] Sapienza – University of Rome, Via Eudossiana 18, Rome (Italy), fcuriano@gmail.com
[(2)] Sapienza – University of Rome, Via Eudossiana 18, Rome (Italy), lorenzo.arena@uniroma1.it
[(3)] Sapienza – University of Rome, Via Eudossiana 18, Rome (Italy), tommaso.cardona@uniroma1.it
[(4)] Sapienza – University of Rome, Via Eudossiana 18, Rome (Italy), francesco.diprima@uniroma1.it
[(5)] Sapienza – University of Rome, Via Eudossiana 18, Rome (Italy), giacchino.scire@uniroma1.it
[(6)] Sapienza – University of Rome, Via Eudossiana 18, Rome (Italy), fe.angeletti@gmail.com
[(7)] Sapienza – University of Rome, Via Eudossiana 18, Rome (Italy), ali.pellegrino.92@gmail.com
[(8)] Sapienza – University of Rome, Via Eudossiana 18, Rome (Italy), paolomarzioli@gmail.com
[(9)] Sapienza – University of Rome, Via Eudossiana 18, Rome (Italy), gianluca.dezanet@live.com
[(10)] Sapienza – University of Rome, Via Eudossiana 18, Rome (Italy), armandogrossi91@gmail.com
[(11)] DIMA, Sapienza – University of Rome, Via Eudossiana 18, Rome (Italy), fabrizio.piergentili@uniroma1.it
[(12)] DIAEE, Sapienza – University of Rome, Via Eudossiana 18, Rome (Italy), fabio.santoni@uniroma1.it

ABSTRACT

The S5Lab (Sapienza Space Systems and Space Surveillance Laboratory) is a research laboratory involving two Engineering Departments of Sapienza University of Rome, DIMA and DIAEE. This paper describes the main on-going projects at S5Lab, including research and education programs involving the participation to international student competitions. The main research activities are related to satellite systems and space surveillance systems. S5Lab develops the 3U CubeSat URSA MAIOR (University of Rome la SApienza Micro Attitude In ORbit testing) in the framework of the QB-50 program and is responsible for the development of the EQUO project (Equatorial Observatory for Space Debris) in collaboration with ASI (Italian Space Agency). Its purpose is the set up of two observatories at the Broglio Space Centre in Malindi (Kenya) fully-dedicated to space debris surveillance and tracking. S5Lab Students took and take part in several international contests. In December 2014, a S5Lab team participated to the REXUS/BEXUS pre-selection workshop with IRIDIUM (Investigating Radiation Impact and Damages in UV-sensitive Materials). In 2015 another S5lab student group was selected to participate in December 2015 to the REXUS/BEXUS 2015-16 pre-selection workshop. The experiment is called STRATONAV (STRATOspherical NAVigation) and its main goal is to test the possibility of using the traditional VOR (VHF Omnidirectional Range) navigation system for high-altitude flight navigation.
The main S5Lab facilities open to students for use in their education and research projects are described in the paper.

1. INTRODUCTION

S5Lab (Sapienza Space Systems and Space Surveillance Laboratory) was established as a result of the cooperation activity between DIMA (Department of Mechanical and Aerospace Engineering) and DIAEE (Department of Astronautical, Electrical and Energetics Engineering) of Sapienza Università di Roma. S5Lab main research activities are in satellite systems, including on-board and ground equipment, and space surveillance systems, including optical observation system design and operation, data analysis, orbit determination and active debris removal systems.
The S5Lab team is composed of students at different levels, including PhD, Master's and Bachelor's degree, with different backgrounds, mainly Aerospace Engineering and Astronautics. Many of them are involved in laboratory activities, participating in education and research programs, international contests and student competitions. This allows gaining hands-on and team-working experience, performing key decisions in design, testing and flight operations. S5Lab aims at enhancing the students' education by means of practical work and challenging activities in order to improve their skills and problem solving abilities and their interest and motivation. The entire S5lab educational activity focuses on the training of untrained personnel (i.e. students), considering it as important as – if not more important – the nominal "mission" related to the on-going projects.
One of the main S5Lab ongoing projects related to satellite systems design is the development of the nanosatellite URSA MAIOR (University of Rome la SApienza Micro Attitude In ORbit testing) [1-2]. It will carry the mNLP (multi-Needle Langmuir Probes) science unit designed by the University of Oslo [3] and

will house two scientific experiments: a drag sail deorbiting system made of polymeric material [4] and the MEMS MicroThruster Experiment (MEMIT), a thruster for small satellite attitude control [5].
The activity related to space surveillance systems at S5Lab is presently devoted mainly in the development of the EQUO (EQUatorial Italian Observatory) in cooperation with Italian Space Agency (ASI) in order to establish a fully dedicated observatory for space debris surveillance at the Broglio Space Center in Malindi, Kenya [6-8]. Furthermore, S5Lab students are participating in several competitions and contests worldwide, among which is the REXUS/BEXUS (Rocket&Balloon-borne Experiments for University Students) project with scientific and technological experiments developed and realized at the S5Lab facilities.
The URSA MAIOR and the EQUO projects are described in the following sections, mainly for what concerns the student involvement in these programs.

2. THE CUBESAT URSA MAIOR

URSA MAIOR is a 3U CubeSat developed in the framework of QB50, an FP7 Project, led by the Von Karman Institute for Fluid Dynamics (Belgium). The main goal of QB50 mission is to carry out an atmospheric research within the lower thermosphere, between 200 km and 380 km of altitude, in order to study the least explored layer of the atmosphere. The project has also an educational aim and it is intended for university students who want to deal with the complete realization of a CubeSat, in order to gain experience and become confident with the problems related to a real project. Several PhD and Master students in Space Engineering are involved in the CubeSat design, manufacturing and testing, supported by professors of S5Lab.

2.1. URSA MAIOR OVERVIEW

The URSA MAIOR CubeSat is shown in ***Figure 1***. Its main scientific payloads are the multi-Needle Langmuir Probe (mNLP), the drag sail ARTICA (Aerodynamic Re-entry Technology In Cubesats Application) and the MEMIT (MEMs Micro Thruster). The mNLP was developed at University of Oslo and consists of four cylindrical Langmuir probes, capable of performing absolute electron density measurements without the need to know the spacecraft potential and the electron temperature [3]. The instrument works by measuring the current collected individually by four needle probes, placed on the satellite's shock front. The mNLP provides reasonable data as long as the CubeSat is in a precise attitude configuration: the minimum axis of inertia must be parallel to the velocity vector with the probes facing the direction of motion. This condition can be obtained after a de-tumbling using the magnetorquers and a pitch momentum wheel. ARTICA is a passive and independent deorbiting system for nano-satellites based on a polymeric drag sail designed and manufactured by NPC SpaceMind [4]. MEMIT is a cold gas micro-thruster experiment for nano-satellite attitude control developed at CRAS (Sapienza Aerospace Research Center) whose main goal is testing a new integrated MEMS (Micro Electro Mechanical System) valve-nozzle [5]. The URSA MAIOR attitude determination and control system (ADCS) is provided by the Surrey Space Centre [9]. It uses a combination of MEMS rate sensor, a magnetometer, and sun and nadir sensors to estimate attitude and angular velocity. Attitude control is based upon a pitch momentum wheel and three magnetorquers.
The payloads' operation is managed by two OBDH/OBCs (On-Board Data Handling/On-Board Computers) with PC104 interface completely designed, manufactured and tested in-house. They are based on a redundant microcontroller-FPGA architecture, with hardware and software error mitigation solutions. They have also a latch-up detection scheme with short-circuit and over-current protections. A third PC104 board manages all the telemetry data. ***Figure 2*** shows all the CubeSat PC104 boards during satellite assembly.
The communication system, in the amateur UHF and VHF bands, is based on two commercial space qualified radios.

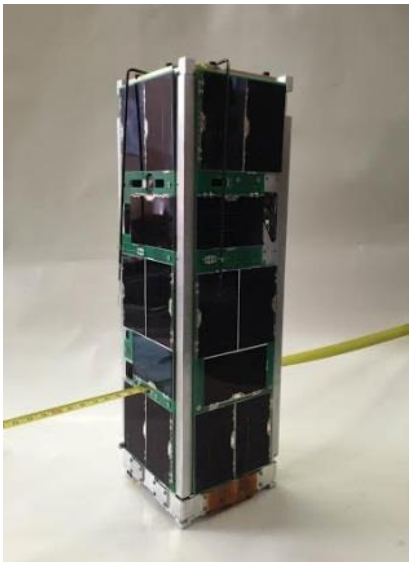


Figure 1 - The Cubesat URSA MAIOR

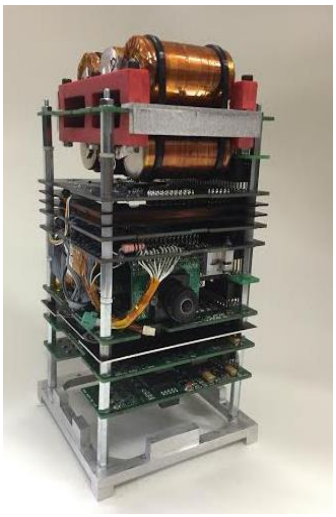


Figure 2 – CubeSat PC104 boards

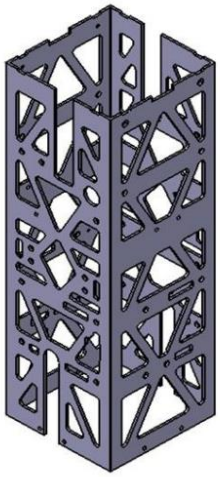


Figure 3 – CAD model of URSA MAIOR structure

2.2. URSA MAIOR STRUCTURAL DESIGN, MANUFACTURING AND TESTING

The nanosatellite structure, providing housing for all the on-board subsystems and withstanding the launch loads, was designed to guarantee accessibility and inspection during the mounting phase and good thermal, mechanic and electric behaviour, while maintaining a low weight. Some of the commercial and custom-designed structures for CubeSats are based on modular panels assembled on load carrying frames. This solution allows a very good accessibility during the mounting phase, by simply removing the outer panels. A possible drawback of frame-based structures is that thermal gradients may arise due to the loss of physical material continuity between consecutive external faces. The thermal behaviour is improved by structure architectures preserving material continuity among all the external faces. Another drawback of frame-based structures is the number of parts to be manufactured and assembled, with related costs. A very low cost solution guaranteeing material continuity and single piece design was implemented in the URSA MAIOR structure, obtained by a single piece of (100x100x2 mm) aluminium square tube profile. This is machined using a small milling available in house, to optimize the weight by removing excess material from the outer surface. A simplified analysis was carried out in order to size the preliminary structural design. The CAD model of the structure is shown in ***Figure 3***. The aluminium square tube profile was properly milled to obtain variously shaped holes in the four faces in order to maximize the stiffness-to-weight ratio while preserving a continuous path for heat conduction and a high degree of accessibility. Several numerical analyses were carried out to validate the structural design. The thermal analysis was performed using a specialised numerical tool to evaluate the heat flux from the Sun, the Earth and the deep space.

The thermal analysis results showed that the temperature range is compatible with the subsystem operations. A FEM model was realized considering the structure with the battery pack, the propulsion system, the drag sail box and the radios. Solid tetrahedral and hexahedral meshes were developed and applied to the parts of the satellite, for a total of 71547 nodes in the entire model. Modal and a PSD spectrum analyses were performed [2]. The results assured that the QB50 requirements are fulfilled [10].

A vibration test campaign was carried out at the Sapienza's Structural Dynamics Laboratory using an electro-dynamic shaker to reproduce the launch dynamic environment. By following the QB50 Guidelines [2-10], two Sine Sweeps and a random vibration test were carried out, validating the structure design. ***Figure 4*** shows the satellite integrated on the vibrating table.

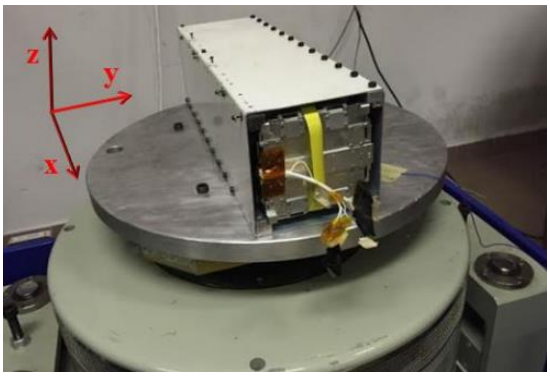


Figure 4 – URSA MAIOR under vibration tests and satellite reference frame

Three single-axis accelerometers were placed on the structure, on the sail and on the MEMIT support. A vibration test of a satellite dummy mock-up was preliminarily performed, showing that no potentially dangerous acceleration peaks for the printed circuit

boards and other internal satellite parts were to be expected. ***Figure 5*** shows the measured accelerations of the structure on X axis, with peaks at 75 Hz, 150 Hz and above 200 Hz. Further analysis showed that the 75Hz peak is not due to the CubeSat, but it is intrinsic to the frequency response of the fixture [10].

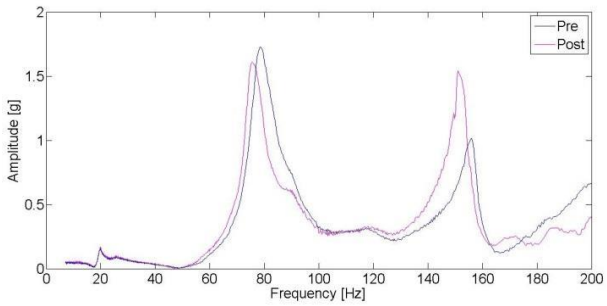


Figure 5 – Pre- and post- random measured acceleration of the structure on X axis with input acceleration on Z axis

3. THE EQUO PROJECT

S5Lab research team is involved in IADC (Inter Agency Space Debris Coordination Committee) observation campaigns for space debris survey and tracking. The need to improve observation capabilities in space debris monitoring and cataloguing is constantly growing, due to the continuous increase of the number of operative satellites in the GEO (Geostationary Earth Orbit) and LEO (Low Earth Orbit). Italy is participating in the European effort to improve space debris environment monitoring and forecast capability, establishing an operational Space Surveillance and Tracking network [11]. The Italian Space Agency (ASI) and the Department of Astronautics, Electrical and Energetic Engineering (DIAEE) of "La Sapienza", University of Rome, have the opportunity to access an equatorial site with all the necessary logistics as well as scientific infrastructures and decided to establish an equatorial observatory settled at the Broglio Space Center (BSC) in Kenya (EQUO–EQUatorial Observatory) in the framework of a more general ASI-Sapienza Agreement for the conduction of scientific activities at the BSC [6-8]. The BSC base is on the coast of the Indian Ocean and consists of two segments, the base camp on the shore and the marine segment including two off-shore platforms in the ocean, at about 6 km from the coast.

The EQUO observatory will consist of two observation sites, one in the BSC base, and one off-shore, located on the San Marco platform, the one used for the launch of several Scout launches from 1967 until 1988. Thanks to its equatorial location, the base offers unique features in complementing observations from mid-latitude sites for Space Surveillance purposes.

The use of two jointly operated observatories in Italy and in Kenya is potentially profitable. Observatories located in Italy and in Kenya are complementary as to the percentage of usability during the year, in terms of cloud coverage and rainfall. Two periods around March and around August are suitable to perform joint observations. Daylight analysis shows that situations exist in which both sites are close to the terminator and could observe a passing LEO object during the same orbit. Seasonal cloud coverage percentage and the average rainfall per month demonstrate the suitability of an observatory located in Malindi during wintertime and of an observatory located in Italy during summertime [6].

The feasibility of establishing this observatory for space debris was demonstrated as a result of the observation campaign performed in September 2010, based on the model of the standard IADC survey campaign in LEO and GEO orbits. Comparing statistical results of the surveys obtained from Malindi observatory with literature data, a good agreement was found, showing that, though operating at sea level, the observatory is suitable for space debris observation. During the three observation weeks several data sets were collected in order to compare achievable results from Malindi sites with the standard survey campaign performed from Northern hemisphere observatories. The average observation time was about 5 hours with more than 1000 pictures collected per night.

3.1 EQUO ARCHITECTURE

The design of the observatory regards the system level analysis and the definition of components to be assembled. The main components of the observatory are the mount, the telescope, the CCDs, the software and the dome. The selected Alt-Az mount is controlled by dedicated software and it is capable to track objects with differential rate on two axes at HEO orbits in order to track fast object such as LEO objects. The selected telescope is a 200mm f/4 telescope. The selection of the CCD was based on an analysis of the state of the art commercial hardware. The mission requirements led to the identification of two different CCD sensors, one for astrometry, due to its large FOV, for photometry, due to larger quantum efficiency and larger pixels despite of a smaller FOV.

The EQUO control software is totally developed by S5Lab research group. The tool is suitable for controlling all the operations needed to perform automatic observation campaigns. Observatory Control is characterized by a simple graphic user interface (GUI) that allows the user to set the principal options in order to perform and observation. It is possible to control the both the mount and CCD sensor and all the necessary features to perform automatic observations are included.

The installation of the observatory at the BSC in Malindi is scheduled in 2016, with the involvement of students who developed their thesis on this subject.

3.2 OBSERVTORY TESTING

A complete observation test campaign was performed in order to evaluate the performance and compliance with requirements. Different observing strategies have been tested at different orbital regimes from the terrace of our department. Multiple observations of GEO operative satellites with updated and precise TLEs (Two Line Element set) data set were carried out in order to validate tracking ability of the whole system. Moreover, non-operative GEO satellites were observed to validate the system with uncontrolled orbiting objects. ***Figure 6*** shows an example or the images acquired during the test campaign

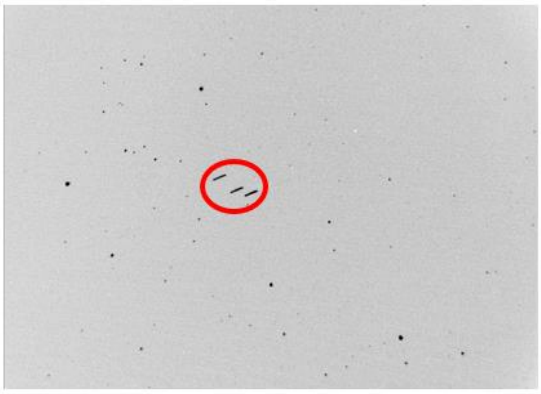


Figure 6 – Eutelsat Hot Bird 13B, 13C, 13D (Sidereal Tracking on with 6 sec exposure time)

4. S5Lab PARTICIPATION IN REXUS/BEXUS

In 2014 a student group from S5Lab participated in the pre-selection workshop for the BEXUS 2014-15 campaign [12], with the IRIDIUM experiment. Its main goal was to the investigate sunlight effects on UV sensitive materials. Moreover, in December 2015 another S5Lab student team will participate in the BEXUS 2015-16 preselection workshop with the STRATONAV (STRATOspherical NAVigation) experiment. Its main scientific goal is to test the traditional VOR navigation system to analyze its possible operational range extension to high-altitude flight through a testing campaign on the BEXUS stratospheric balloon. The technical target is to test COTS (Commercial Off-the-Shelf component) VOR receivers during the whole balloon flight validating their data by comparison with GPS/GLONASS positioning and ICAO (International Civil Aviation Organization) VOR acceptable accuracy and precision. The main possible advantage offered by the experiment is the possibility to use a reliable and available system as a stand-alone positioning system method or as add-on to increase the accuracy of present and future space-borne positioning system.

5. S5Lab FACILITIES

S5Lab facilities are located in two Engineering Departments of Sapienza – University of Rome (DIMA and DIAEE). The main facilities include: (i) low-vacuum (few mbar) vacuum chamber (Figure 7) used for preliminarily testing of satellite subsystems and devices [13], which is also very well suited for stratospheric equipment testing, such as the BEXUS experiment; (ii) 3D Helmholtz coils system, 2.6 meters side, (***Figure 8***) for the reproduction of the orbital magnetic field on the ground, with a spherical testing volume of diameter 60cm (magnetic field uniformity better that 0.1percent); (iii) frictionless air bearing system for attitude dynamics and control testing, which can be installed inside the 3D Helmholtz coil (***Figure 9***); (iv) attitude control testing platform including IMU, magnetometer and a system of four miniature Control Moment Gyros for attitude control ground testing (***Figure 10***) [14]; (v) satellite ground station in the VHF and UHF radio-amateur bands (*Figure* ***11***); (vi) three-axis CNC milling machine (Figure 12); (vii) sun simulator lamp for fast and preliminary solar cell and solar panel testing (***Figure 13***); (viii) remotely operated space debris observatory (***Figure 14***); (ix) electronic laboratory and related equipment (***Figure 15***).

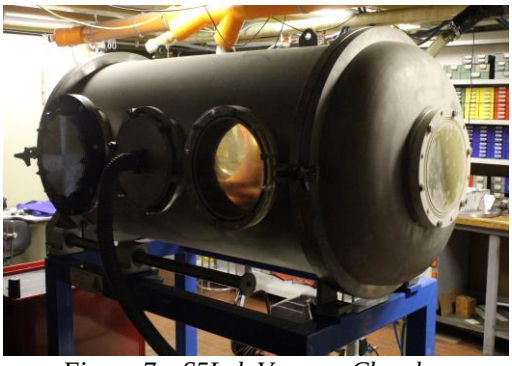


Figure 7 – S5Lab Vacuum Chamber



Figure 8 – S5Lab 3D Helmholtz coil system

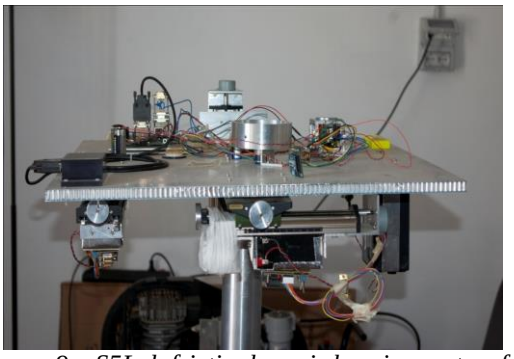


Figure 9 – S5Lab frictionless air bearing system for spacecraft attitude dynamics and control testing



Figure 10 – 3 DoF ADCS test-bed equipped with Control Moment Gyros (CMGs)



Figure 11 – S5Lab satellite ground station



Figure 12 – S5Lab Milling Machine

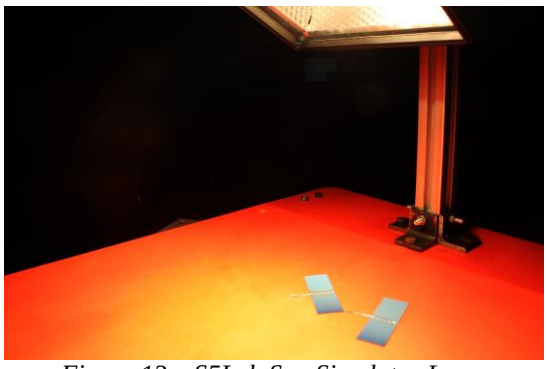


Figure 13 – S5Lab Sun Simulator Lamp



Figure 14 – S5Lab Remotely controlled space debris observatory

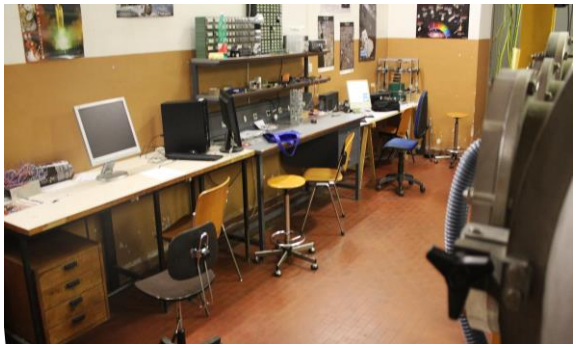


Figure 15 – S5Lab Electronic Laboratory and relate equipment

6. CONCLUSIONS

S5Lab Educational Activity at University of Rome "La Sapienza" plays a key role in the education and training aerospace engineering students. They have the opportunity to participate actively into S5Lab on-going projects related to both satellite systems design and space surveillance systems and to be involved in their phases, from the design to the testing campaign to the final realization. It is a unique opportunity to carry out the theoretical knowledge gathered during academic courses, by getting involved real projects in order to be better prepared for the working future. In fact, this is not only a growing possibility, but also an opportunity to increase the student knowledge in the space field and to cultivate their passions and interests.

Main ongoing projects at S5Lab concern research programs and international competitions. In particular, URSA MAIOR project has entered into the integration phase after the qualification and structural validation of the structure carried out at University of Rome "La Sapienza" facilities. EQUO is currently an on-going project and the S5Lab research group has finished the design and hardware selection of the observation site that will be installed at the Broglio Space Center at the beginning of 2016. Moreover, STRATONAV experiment will participate to the pre-selection workshop for BEXUS 2015-16 flight.

The S5Lab educational activity has been described. Finally, an overview about the Sapienza Space Systems and Space Surveillance Laboratory facilities has been presented in order to illustrate the laboratory equipment and to show its potentialities.

7. ACKNOWLEDGEMENTS

This work was developed in part under the funding granted to S5Lab by the Italian Space Agency (ASI) in the framework of the "Convenzione ASI-Sapienza N. 2013-078-C.0"

8. REFERENCES

1. Piergentili, F., Angeletti, F., Arena, A., Balucani, M., Cardona, T., Coppotelli, G., Curianò, F., De Zanet, G., Gaeta, M., Lamarca, V., Nasuti, F., Panicucci, P., Pellegrino, A., Santoni, F., Design, Manufacturing And Test Of The Cubesat URSA MAIOR, paper IAC-15,B4,2,7,x30886, 66th International Astronautical Congress, Oct. 2015, Jerusalem, Israel.
2. Arena, L., Angeletti, F., Curianò, F., De Zanet, G., Gradini, R., Pellegrino, A., Thermal And Mechanical Design And Test Campign Results Of A Single-Piece Structure For The URSA MAIOR Nanosatellite, paper IAC-15,C2,1,8,x30546, 66th International Astronautical Congress, Oct. 2015, Jerusalem, Israel.
3. T.A. Bekkeng, QB50 m-NLP Science Unit Interface Control Document - QB50-UiO-ID-0001 M-NLP ICD Issue 3.
4. F. Piergentili, M. Balucani, R. Crescenzi, J. Piattoni, F. Santoni, B. Betti, F. Nasuti, M. Onofri, *MEMS Cold Gas Microthruster on URSA MAIOR Cubesat*, paper IAC-13,C4,5,1,x17444, 64th International Astronautical Congress, Beijing, China, 23-27 Sept 2013.
5. Bellini N., Naldi S., Rastelli D., Valdatta M., A.R.T.I.C.A. Deorbiting System: the new design and prototype of a compact deorbiting sail on board cubesat "Ursa Maior", paper IAC-15,A6,IP,30,x30649, 66th International Astronautical Congress, Oct. 2015, Jerusalem, Israel.
6. Piergentili, F., Ceruti, A., Rizzitelli, F., Cardona, T., Battagliere, M.L., Santoni, F., "Space Debris Measurement Using Joint Mid-Latitude and Equatorial Optical Observations". IEEE Transaction on Aerospace and Electronic Systems, IEEE Log No. T-AES/50/1/944815.
7. Santoni, F., Piergentili, P., Arena, L., Cardona, T., Diprima, F., Scirè, G., Spinetti, A., Canu, C., Portelli, C., "EQUO: an equatorial observatory to improve the Italian space surveillance capability", 66th International Astronautical Congress, Jerusalem, Israel.
8. Santoni, F., Piergentili, P., Arena, L., Cardona, T., Diprima, F., Scirè, G., Spinetti, A., Curianò, F., Pellegrino, A., Canu, C., Portelli, C., "Equatorial Italian Observatory For Space Debris Monitoring at the Broglio Space Center" 23rd Conference of the Italian Association of Aeronautics and Astronautics AIDAA2015.
9. Visagie, L., QB50 ADCS Reference Manual.
10. Hunt, T., INMS Acceptance Vibration Test Procedure, QB50-INMS-MSSL-TP-14010 Issue 1
11. http://www.esa.int/Our_Activities/Operations/Space_Situational_Awareness/Space_Surveillance_and_Tracking_-_SST_Segment
12. http://rexusbexus.net/
13. Bellini, Q., Arena, A., A Low Cost Thrust Stand For Testing Of Nano-Satellite Propulsion Systems, paper IAC-15.D1.5.6, 66th International Astronautical Congress, Oct. 2015, Jerusalem, Israel.
14. Arena, L., Delfini, A., Design, Manufacturing and ground testing of a small and cost-effective FPGA-based Control Moment Gyro for the URSA MAIOR nanosatellite, 65th International Astronautical Congress 2014, Toronto, Canada.

SPACE ENGINEERING AND SMALL SATELLITES EDUCATIONAL ACTIVITIES AT UNIVERSITY OF BOLOGNA

Dario Modenini[(1)], Marco Bosco[(1)], Alfredo Locarini[(1)], Paolo Tortora[(1)]

[(1)]University of Bologna, Department of Industrial Engineering, Via Fontanelle 40, 47121 Forli, Italy
Email: dario.modenini@unibo.it, marco.bosco3@unibo.it, alfredo.locarini@unibo.it, paolo.tortora@unibo.it

ABSTRACT

Since 2003, the Alma Mater Microsatellite and Space Microsystems Lab at the University of Bologna carries out research activities on space technology. The laboratory hosted many students from the Aerospace Engineering courses and aims at training them to space systems design through several hands-on projects. The focus is on small satellite platforms that better fit the university budget constraints and the educational outreach, since they represent a cost-effective test-bench where students can learn by doing, having the opportunity to participate in the entire space project lifecycle, including on-orbit operations.
The Lab activities started with the ALMASat-1 project, a microsatellite launched in 2012: more than 60 BSc, MSc and PhD students took part to the entire satellite development.
Building on the success of the ALMASat-1 experience, the laboratory has now a role in support to the Prime Contractor SITAEL (formerly ALMASpace, a spin-off from the University of Bologna), in the development of the European Student Earth Orbiter (ESEO), an ESA Education Office project for the development of a micro-satellite mission to Low Earth Orbit.
This paper details the present projects the laboratory is involved in, along with the updated status of the on-going educational and research activities.

1. INTRODUCTION

The Alma Mater Microsatellite and Space Microsystems Lab activities started with the ALMASat-1 project, a 30x30x30 cm^3 microsatellite (see Fig. 1) launched in February 2012 on board the VEGA maiden flight. The purpose of this mission was to validate the platform technology and the on-board micro-propulsion system [1]. All spacecraft subsystems were developed in-house, as well as several ad-hoc hardware and software tools in support to the design activities. As part of the project, in 2003 an amateur radio ground station for small LEO satellites tracking was design and installed, which is currently being subjected to major upgrades.
ALMASat-1 development represented a huge effort, from and educational view-point, whose main outreach can be summarized as follows:

- First UniBo S/C in orbit.
- ALMASat-1 fully functional at first G/S pass, with all subsystems performing nominally.
- ALMASat-1 telemetry received and decoded by many radio amateurs worldwide.
- More than 60 BSc, MSc and PhD students taking part to a real space project.
- First university microsatellite project in EU managed according to industrial standards (Project and Documentation control, ECSS tailoring, etc.).
- Launch/Integration campaign successfully achieved with full appreciation of Guiana Space Centre personnel.

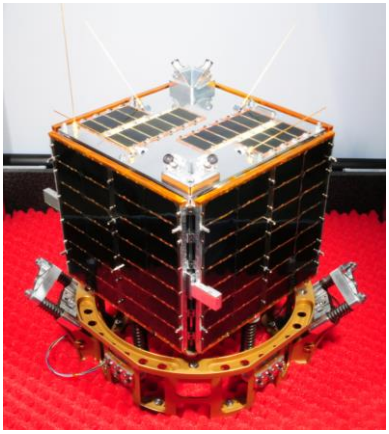


Figure 1. ALMASat-1 on the launcher adaptor/separation system

Most important, it also paved the way to the subsequent space-related activities, as the ongoing efforts of the laboratory within the ESA Educational Office ESEO project, which is led by SITAEL as Prime Contractor.
University of Bologna (UniBo) contribution to ESEO programme covers different areas, namely being a) responsible for the educational activities for the EU students belonging to the ESEO University Network; b) in charge of the development of the GPS-based navigation subsystem; c) responsible for the development of the ground segment and the mission control centre, and d) in support to the development of the cold-gas micro-propulsion subsystem.
Following the industrial re-organization of its former spin-off, the Microsatellites and Space Microsystems Laboratory is now focusing on the following target areas, closely related to, and further developing, the activities within ESEO:

1. GPS based navigation; development of navigation algorithms for GNSS positioning that aim at achieving a sub-meter 3D RMS in-orbit real time accuracy.
2. Ground segment; satellite software-defined radio ground stations and mission control applications, such as telemetry/telecommands handling and satellite passes scheduler, enabling large degree of autonomy for spacecraft monitoring and control.
3. Micropropulsion; development of a monopropellant microthruster fed with high test peroxide for enhancing small spacecraft orbit control capabilities.

The paper is organized as follows: first, a section introducing the ESEO programme with a detailed description of the educational activities will be given. Then, a description of the ongoing activities of the laboratory in the three key areas above will be presented, encompassing both research and educational related aspects.

2. ESEO PROGRAMME

The European Student Earth Orbiter (ESEO) is a project of the Education Office of the European Space Agency (ESA) aimed at providing students with unparalleled hands-on experience to help preparing qualified space engineers for the Europe's future [2]. This is achieved through the design, development, integration and testing of a micro-satellite to be launched in a sun-synchronous low Earth orbit. The objectives of the mission are taking pictures of the Earth and other celestial bodies for educational outreach purposes, providing dosimetry and space plasma measurement and its effects on satellite components and testing technologies for future education satellite missions. SITAEL is the prime contractor and responsible for the ESEO platform and mission implementation whilst the university network (Fig. 2) provides the scientific and technological payloads and develop the ground segment. The University of Bologna coordinates the network of the European universities joining the ESEO project and organises university lecture courses and internship opportunities for 60 students out of about 200 students involved in the ESEO project. For the first time, academic credits (18 ECTS) are granted to students for their participation in hands-on projects of ESA's Education Office.



Figure 2. ESEO University Network and roles

In order to prepare future space engineering professionals, the ESEO project is carried on as a typical ESA project under a strong technical supervision of ESA specialists. Students are required to prepare and timely update the technical documentation describing the requirements, design, test plans, procedures and reports using the ECSS standards as reference. The ESA's Education Office sponsors the participation of students to the co-location meetings of all major project reviews where the state of the project is reviewed by a panel of ESA specialists. In this way, students become familiar with the formal steps of a space project milestone review including the processing of RIDs ('Review Item Discrepancy'), NCRs ('Non Conformance Reports'), and RFW/RFD ('Requests for Waiver/Requests for Deviation').

The ESEO project started in January 2013, the Preliminary Design Review PDR was successfully completed in November 2013 and the Critical Design Review CDR in June 2015. Now the project is in phase D and the launch is foreseen for the second half of 2016.

To facilitate networking for students involved in this international project and provide them with the theoretical knowledge and practical experience in space systems engineering, a series of Lecture and Training Courses and Internships opportunities are organised and conducted at system level at the UniBo and SITAEL premises. Three sessions of courses and internships took place starting in September 2013, February and September 2014. During each session, the students attended:

1. the Lecture Course for 2 weeks;
2. the Training Course for 1 week;
3. the Internship in small groups (typically 5 students each) for 4 weeks.



Figure 3. ESEO lecture courses at Bertinoro University Center

The Lecture course program is scheduled for a total of 77 hours and all lectures are held from well-recognised international professional specialists from academia and aerospace organisations. The topics of the first week of lectures cover Space Environment, Orbital Mechanics, Spacecraft Dynamics and EO Mission Analysis whilst during the second week students get closer to satellite sub-systems design (thermal and power, AOCS, propulsion, communication and ground segment). A mandatory final test grants 9 ECTS credits.

The Training Course allows students to gain both knowledge and practical skills related to the micro-satellite subsystems. A proficient participation together with a successful final test grant students 3 ECTS.

Finally, the Internships allow the students to apply the learned concepts and the gained skills during the previous course to the design, prototyping and integration of payloads for which their university is responsible under the supervision of SITAEL personnel. This is also a good opportunity to enhance the collaboration between the University Network and the System Prime Contractor. At the end of the internship, students are required to write a final report and based on the evaluation of the report, they can gain 6 additional ECTS.

3. GROUND SEGMENT

In the framework of the ESEO project, we are developing ground systems to support micro satellites operations. UniBo is responsible for the design and development of the mission control centre and the primary ground station for telemetry and telecommand (TMTC) operations. The ESEO ground stations network (GSN) is a collaboration with other European universities: the Technical University of Munich, responsible for the downlink of scientific payload data and the University of Vigo as a secondary TMTC ground station. At UniBo, we decided to upgrade our ground station used to support ALMASat-1 operations, introducing a software-defined radio SDR. These radios are becoming every day more popular in amateur and university ground stations for satellite communications. They allow fast and cheap reconfiguration of the ground station for satellite missions using a different modulation scheme, communication protocol and frequency. This is possible thanks to the wide frequency band of RF front-end and because the signal is digitally processed at software level. Moreover, SDR is very beneficial for education purposes: engineering students can simply develop digital communications algorithms on a computer applying their knowledge in communication theory to practical applications minimizing the budget for supplementary expensive hardware (e.g. oscilloscope, spectrum analyser, signal generator, etc.). Moreover, thanks to its versatility, an SDR-based ground station will allow participating to many university satellites GSN easing a beneficial collaboration among universities. The SDR can be programmed using applications, which are usually well known by engineering students like MATLAB/Simulink and LabVIEW. For the ESEO project, we implemented the SDR software in LabVIEW performing the GFSK modulation, Reed-Solomon channel coding, AX.25 packet encoding, signal analysis, display and recording. After a complete code review, we performed compatibility tests with the ESEO on-board transceiver obtaining good results in terms of packet error rate. The SDR device is the USRP N210 model by Ettus Research equipped with an SBX daughterboard (400 – 4400 MHz).

Another important activity is the implementation of a spacecraft S/C monitoring and control (M&C) system to allow S/C operators to handle TMTC. The most important requirement to develop this application were the design of an intuitive and easy-to-use graphical user interface GUI for the selection of the desired commands and the visualization of the satellite TM data and the connection to a database (DB) for the storing of downlinked data and the retrieving of commands and satellite parameters. We implemented this software in LabVIEW because it allows easily coding the GUI and it offers a module for MySQL DB operations. This application can be directly connected to the SDR software for the sending of TCs and receiving of the TM data through an UDP connection as shown in Fig. 4 for the downlink chain and in Fig. 5 for the uplink chain. The mission control system MCS PC can be also connected to SATNet, an application developed by CalPoly University to communicate with a network of ground stations. This option will be used for ESEO operations to exchange data with other ground stations.

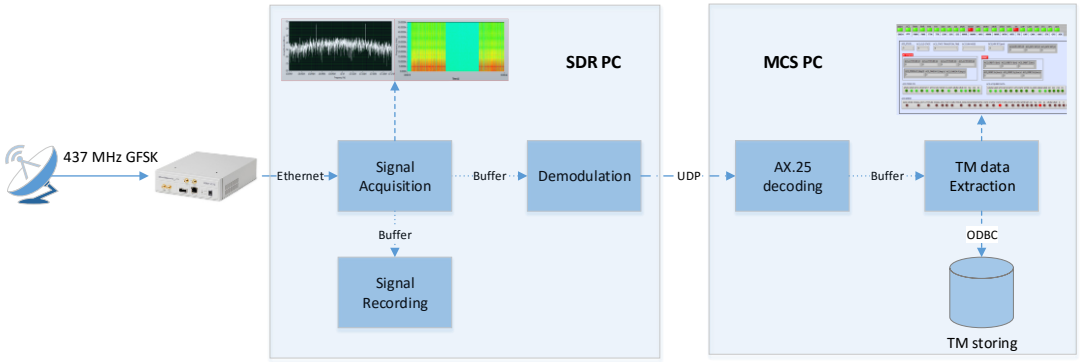


Figure 4. Software functionalities in downlink operations

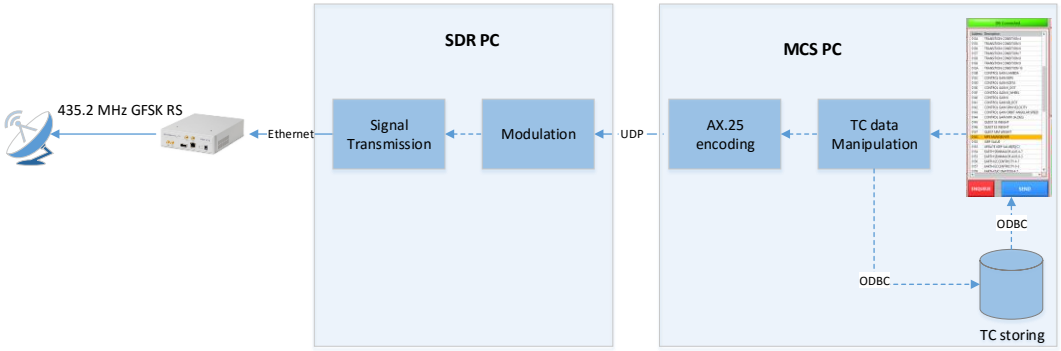


Figure 5. Software functionalities in uplink operations

The mission control center and the ground station of UniBo will soon be moved to a new building, which will host the UniBo Aerospace Engineering laboratories. A room will be completely dedicated to the mission control room furnished with technical equipment. Here, students will learn by following and performing satellite operations. The VHF/UHF (144-146, 430-440 MHz) bidirectional ground station and the S-band (2025-2120, 2200-2300 MHz) bidirectional ground station will be installed at the top of the building as shown in Fig. 6. The Yagi and 3m parabolic dish are pointed to the S/C using an azimuth-elevation rotor mounted on a 3m aluminum trellis.

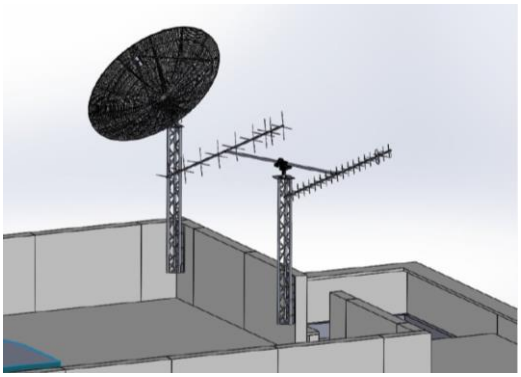


Figure 6. Parabolic and Yagi antennas mounted on the roof of the mission control room

When dealing with a GSN and different satellites, it is essential to plan a conflict-free schedule of satellite passes for maximizing the number of tracked satellites. For this reason, we developed an application named Satellite Passes And Conflicts Engine (SPACE) to compute visibility passes, detect and resolve pass conflicts based on a satellite priority list defined for each ground station. The application is based on a two-line element TLE propagator, which implements the simplified perturbation model SGP4. The application is implemented in Python and can be used through a GUI to choose satellites, ground stations, datetime interval and acquisition of signal (AOS) and loss of signal (LOS) time margins between two consecutive passes. The antenna horizon mask can also be inserted in the application to have results that are more accurate. Results are reported in html pages as tables, plots and Gantt charts (Fig. 7). Students can use this tool to better understand satellite low Earth orbits (LEO), ground station contacts and blind orbit concepts.

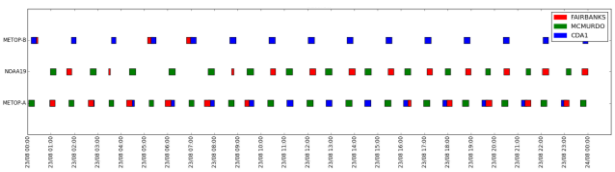


Figure 7. One-day conflict free schedule for three satellites (y-axis) over three ground stations (legend)

4. MICROPROPULSION

The research activity in the field of microsatellite propulsion started in the frame of ALMASat-1 project. The platform carried on-board a cold gas micropropulsion system (Fig. 8), whose core were the 12 silicon MEMS De Laval nozzles fed with pressurized N_2, featuring a throat size of 40 µm and a delivered thrust of about 1 mN at 0.1 MPa of inlet pressure. Thanks to the low impulse-bit achievable, the system was designed for both attitude (three-axis stabilisation) and orbit control, as well as momentum wheel desaturation. The 12 thrusters were arranged in four clusters, each one embedding three thrusters oriented in mutually orthogonal directions, to allow for 6 DoF control.

Several students were involved in the development of the subsystem and related testing equipment. Among these last, it is worth mentioning a high accurate balance for thrust measurement in vacuum in the mN range, based upon the pendulum principle employing a laser optical displacement sensor (Fig. 9).



Figure 8. ALMASat-1 propulsion system tray

Built upon the heritage of the ALMASat-1 micropropulsion system experience, ESEO satellite will also host a cold gas propulsion subsystem, whose design is under SITAEL responsibility. UniBo support is due mainly for the test phase, providing the facilities and testing equipment developed during ALMASat-1 program and afterwards. This will enable full characterization of the nozzles thrust and specific impulse.

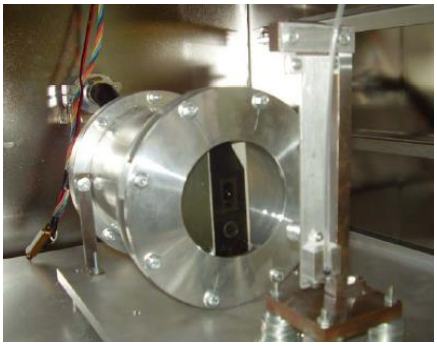


Figure 9. Thrust balance

Recently, in response to the increasing interest in the development of highly capable micro/nanosat platforms, which demands for high performance on-board propulsion technologies to meet orbit control and de-orbiting needs, the focus moved toward warm gas monopropellant systems. In particular, a high test peroxide (HTP) based microthruster is under study, which represents a promising technology, since it offers the highest volumetric specific impulse as compared to other propellants. The research activity is jointly undertaken by a consortium composed by UniBo, Sitael and Fondazione Bruno Kessler (FBK, Trento).

The working principle relies on the exothermic chemical decomposition of the H_2O_2 propellant, induced by a catalytic material, into oxygen and water. Due to the heat of reaction, if the propellant concentration is sufficiently high, the aqueous products vaporize, allowing for a high temperature gas stream at the outlet.

The first thrusters prototypes (Fig. 10), manufactured at FBK premises, consist of silicon MEMS devices, which integrate in a single unit an inlet region, the decomposition chamber and the convergent-divergent nozzle. The decomposition chamber features a dense pattern of staggered pillars upon which a thin layer of metal catalyst is deposited.

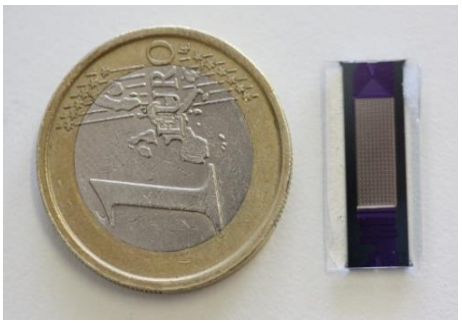


Figure 10. Overall size of the H_2O_2 µthruster prototype

The investigation encompasses several aspects, including numerical modelling, characterization of catalyst performance, device manufacturing and testing.

Focus is placed over miniaturization related issues, such as the effectiveness of catalyst integration over microstructures and thermal management, which affects performance and represents a main driver for the design and manufacturing process.

Currently, a detailed finite element model is under development for analyzing the complex interactions within the chemically reacting-non-isothermal-evaporating flow inside a microchannel, including fluid-solid thermal coupling, to drive the design of the next generation thrusters prototypes.

Available equipment at the Lab allow for in-house distillation of propellant starting from low-concentration H_2O_2 solutions, with a procedure consolidated during a student's final project.

Main laboratory facilities include:

a) a thermo-vacuum chamber;
b) the in-house developed micro-thrust balance;
c) a chemical hood equipped with a fractional distillation system for in-house production of propellant starting from low concentration aqueous peroxide solutions;
d) a high precision mass flow controller for both liquid and gases in the mg/s range;
e) a syringe pump;
f) an optical microscope equipped with a high-speed camera acquisition system (1,000 fps);
g) a refractometer for measuring propellant concentration;

From an educational point of view, the potential of the propulsion related activities above is clear: they allow gathering hands-on experience over several aspects of spacecraft propulsion from propellant manufacturing to design, analysis and testing of thruster assembly.

5. GNSS

A GPS-based navigation sub-system is currently under development as part of the ESEO project. It is one of the payloads carried on-board the ESEO platform and the purposes of this experiment are both the validation in space environment of commercial technologies commonly used in terrestrial GNSS receivers and the development of an embedded sophisticated navigation algorithm, designed to assess the positioning accuracy achievable by commercial receivers in space (Fig. 11).
This sub-system aims to represent the perfect trade-off between a low-cost solution for GPS positioning in space and the capability to provide high quality scientific data, becoming a standard equipment for small satellites missions, due to its fast and cheap manufacturing. This project has been carried out during years by students as part of their BCS, MCS ad PhD thesis and research work.



Figure 11: GPS Payload for the ESEO mission

The Payload is composed of four functional units connected together (Fig. 12):

- Two COTS GPS receivers, model OEM615 from Novatel, in cold double redundancy, which perform GPS signal acquisition, tracking and data demodulation. They provide the raw GNSS measurements together with the GPS satellite broadcasted navigation data.
- A custom on board computer that hosts the navigation algorithm and distributes power to the baseband processor and antenna. It also collects positioning data and distributes them to the other satellite's subsystems.
- A passive antenna from Sensor Systems with flight heritage, model S67-1575-20, mounted on the satellite top panel.
- A Passive Antenna Amplification Stage: custom PCB designed to provide the correct electrical interface between the passive antenna and the based-band processors.

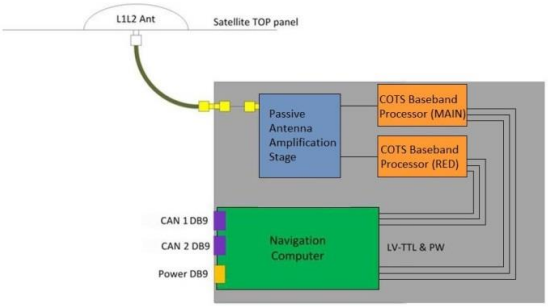


Figure 12: GPS Payload functional architecture

The navigation computer is based on the STM32F407 microcontroller, equipped with single precision FPU, capable of 1.25 DMPIS/MHz, with maximum clock frequency up to 168 MHz. It includes isolated DC/DC converters supported by an overvoltage protection circuit and a current limiter stage the monitors and manages the power request of the two COTS front-ends, avoiding that any damage due to the effect of space radiations could affect the navigation computer.

The navigation computer will host two different algorithms:

- Kinematic solution: a direct computation of the receiver position from the raw observables using a Least Square Algorithm, without including any information about the orbit dynamic model. The provided accuracy is between 10-15 m 3D RMS.

- Reduced dynamic solution: this algorithm is based on an Extended Kalman Filter that performs an integration of the raw observations within an accurate orbit dynamics model. The expected 3D RMS positioning accuracy of this algorithm is between 60 and 80 centimeters. Since the selected receiver only supports L1 frequency, the code and phase measurements are expressed as a ionosphere-free combination called GRAPHIC. The expected 3D RMS

positioning accuracy of this algorithm is between 60 and 80 centimeters, 3D RMS, according to the complexity of the model and to the observations combination.

Several tests has been performed so far on different parts of the device, to validate the software and hardware design. This activity helped students understanding how to design and perform a test campaign following the standard indications of ESA space missions:

- Recursive Filter test: in order to verify the performance of the navigation algorithm in a real scenario, it was implemented and used to process GRACEA raw observations. The off-line processing showed a positioning error of about 80cm 3D RMS when using broadcasted GPS ephemeris and clocks. It is expected that the ESEO positioning error will be worse, due to the lower quality of the receiver oscillator.
- Baseband Processor Test: since one of the main concerns during the preliminary design was the actual functionality in space environment of a GPS receiver designed for ground application, a test was performed on the COTS front end at the ESA/ESTEC facilities. Using a GPS signal simulator, the mission scenario was simulated to verify the functionality with typical space doppler values (Fig. 13). This test demonstrated the need for a forced setting of the receiver's channels to scan and track the GPS signal with a pre-configured frequency offset.

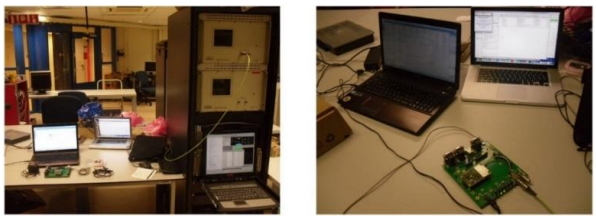


Figure 13: Functional test using a GPS signal simulator

- Communication test: another full functional test was then performed without the GPS signal simulator, and with the payload in "flight configuration", i.e. with the front end connected to the related interfaces on the navigation computer. This test aimed at verifying the correct hardware and software implementation of the communication between the microcontroller of the custom PCB and the COTS front end.
- Thermal test: this environmental test has been performed on the payload in "flight configuration", in order to assess the functionality of both the COTS front end and the custom navigation computer under external thermal conditions close the ones experienced during the operative life. The thermal chamber was set first to the cold scenario (-25°) and then to the warm scenario (70°), and for both the settings an electrical and a functionality tests have been performed. From the results it was clear that no critical degradations of the performances occurred under extreme external conditions.

This project represented for students the opportunity to face directly problems and issues that may rise during the design of subsystems for space missions, covering all aspects of the development of a payload. In particular, since this technology has been developed under the supervision of the ESA technical officers, this experience also trained students to conform their work to the quality standards of ESA missions, thanks to the frequent reviews to which the payload has been subjected.

6. CONCLUSIONS

For more than a decade, the Alma Mater Microsatellite and Space Microsystems Lab at the University of Bologna have been involved in research and educational activities in the field of space technologies.
In this paper, we gave a perspective over the past and present activities, with focus placed upon the educational outreach.
Starting from 2003 and for some years, the efforts were almost entirely devoted to the development of the ALMASat-1 microsatellite, during which many students were trained to space systems design through a "learn-by-doing" approach, encompassing the entire space project lifecycle.
After the foundation of a spin-off of the laboratory, ALMASpace (now SITAEL) the activities of the laboratory narrowed, from the entire platform development, down to some selected areas, namely GPS based navigation, ground segment, and spacecraft micropropulsion. In parallel, the laboratory is being involved in the development of ESEO, a project of the Education Office of the European Space Agency, whose educational aims were deeply discussed.
A short description of the current research activities at the Lab was finally given, along with an outline of their expected short-term evolution.

7. ACKNOWLEDGMENTS

The authors would like to acknowledge the entire ESEO team, in particular Piero Galeone and Antonio de Luca from the Tertiary Education Unit of ESA's Education and Knowledge Management Office, and SITAEL personnel. The micropropulsion related activities are jointly carried out in collaboration with SITAEL and

FBK (Fondazione Bruno Kessler), whose contribution is greatly acknowledged.

8. REFERENCES

1. Tortora P. and Troiani E. *The microsatellite research program at Università di Bologna"*, Acta Astronautica, Volume 56, Issue 7, April 2005, p. 696-704.
2. Bruzzi D., et al. *The ESEO development: merging technical with educational challenges*, Proceedings of the Small Satellites Systems and Services - The 4S Symposium, European Space Agency, Majorca, Spain, 26-30 May 2014.

ON THE STUDENT ROCKET PROGRAM AT ANDØYA SPACE CENTER

Alexander Biebricher[(1)]
Jøran Grande[(1)]

[(1)]*Norwegian Centre for Space-related Education (Norway), alexander@narom.no*

ABSTRACT

In 2011, Norwegian and Canadian institutions of higher education launched the CaNoRock-program. The Norwegian centre for space-related education (NAROM) has been a partner since the beginning, contributing with a one-week student rocket course for university students from Norway and Canada. The program has been a huge success in terms of motivating and giving new opportunities to students interested in space science. NAROM and Andøya Space Center (ASC) together with Norwegian universities intend to expand the cooperation and propose to start a new rocket course open for European countries. This paper will give an overview of the recent development and status of the current student rocket program and make some suggestions for future opportunities within a possible new European student rocket program.

1. INTRODUCTION

Andøya Space Center (ASC) at 69º N latitude includes the world's northernmost permanent rocket launch facility as well as several ground-based remote sensing instruments technology testing sites of different charater, a spaceship simulator and an educational branch aiming to promote space-related topics.

The Norwegian Centre for Space-related Education (NAROM), which was established at ASC in 2000 as a national center of education and school laboratory. As a non-commercial entity it has a mandate from the Norwegian government to work towards increased recruiting to the Norwegian Space industry in particular as well as towards heightened interest for STEM subjects [1].

NAROM's mandate does not include graduation of students. At the same time, NAROM collaborates closely with schools and universities around its teaching and development of teaching. Its location at Andøya Space Center provides NAROM with a unique framework to its teaching, seminars and conferences. NAROM takes part in such activities nationally and internationally. In 2014, about 3500 students and teachers participated in NAROM's activities.



Image 1: Aerial view of the main area at Andøya Space Center. Instrumentation is scattered all over the island of Andøya. (Credit: Andøya Space Center)

2. CaNoRock AND THE STUDENT ROCKET PROGRAM

CaNoRock started with the goal of being a 10-year bilateral student sounding rocket program (2011-2021) with the involved countries being Canada and Norway. The stated goal of the project is to increase motivation in students to increase their knowledge of physics, engineering and electronics connected to sounding rockets and stratospheric balloons such that a possible transition from studies to work in a space-related field may go as smoothly as possible. The program includes working with different platforms such as Unmanned Aerial Systems and Long Duration Balloons. The collaborating parties, i.e. the universities of Oslo, Tromsø, Alberta, Calgary and Saskatchewan also share common research interests in magnetosphere and atmosphere physics. Since each of these institutions approach the subject by means of different experiments, collaboration is paramount for a common research goal. Thus, the path to educational collaboration was a short one.

This educational collaboration is therefore based on science, innovation development and recruiting to knowledge-based industry in the Arctic region. CaNoRock started simultaneously with increased solar activity, thus giving heightened chances of navigation and communication problems in the high North. As the Arctic oceans open up more and more for commercial traffic this concern can already be introduced to the students.

3. TECHNICAL DETAILS OF THE ROCKETS

The first student rocket was launched from ASC was launched in 1998. Since then, around 80 student rockets launched while the concept of student-led rocket campaigns at ASC evolved both technologically and didactically.

At the moment there are two rocket configurations in use.

The first configuration uses a C-14 rocket motor which is normally part of the CRV-7 air-to-ground weapon system [ref]. In only 2.2. seconds of burn time the 5 kg payload is accelerated to a maximum speed of around 800 meters per second. The acceleration is therefore at around 80 times the gravitational acceleration in the rockets direction of propagation. Part of stabilizing this particular rocket is a spin of around 20 times per second on average, with the spin direction changing three times during flight. The flight itself last up to around 90 seconds. This particular behaviour of the rocket itself with unsusal spin development and high acceleration make it already an exciting subject to study for the students.

The steel payload section of the rocket measures in at 700 millimetres. It is shown in Fig. […]. It is equipped with encoder, transmitter and antennas. These parts are fabricated and mounted on the payload by staff at ASC. The transmitter frequency is around 2300 MHz, i.e. in the S-band, such that the telemetry equipment at ASC can be used in the same way as with larger sounding rockets.

[…]

4. COURSE CONTENT

Student rocket courses vary from one week to several months in length. This last version happens during teaching at the local high school where space technology is a special subject. In this article, we focus on the week-long version of the student rocket. During this week the participants are divided into several groups.

A. Rocket Systems Design
B. The Experiments group
C. The payload group
D. The Telemetry group.

The groups work separately in principle but collaborate where necessary (or interesting to do so) in order to prepare all stations for the up-coming launch..

Group A are responsible for the pre-flight modulation and simulation calculations for the rocket in use. With help of several software packages such as Matlab and RockSim [ref] the students model the rocket trajectory and in-flight behaviour based on their own modeling and of that intrinsic to the software by setting basic parameters such as the rocket motor properties and geometry of the rocket. After the flight the rocket data is processed to give a measured rocket trajectory and velocity.

Group B are responsible for the scientific instruments in the payload. The sensors may vary from campaign to campaign, but typically include temperature, pressure, magnetic field, light intensity and acceleration sensors. Part of group work is also calibration and testing of the instruments. The students assemble the sensors for the payload by soldering all the surface-mounted components onto a circuit board. Finally, the group also decoded the signal to display realtime data.

Group C assembles the payload and performs qualification tests before launch. Testing includes spin and stability tests. In group work all sensor boards are integrated. One of the main tasks is to find

out in which way the payload section is mounted best to withstand the enourmous acceleration, both longitudinal and rotational during launch. Once integration is done, the data transmission can be tested.

Group D sets up and operates a mini-version of ASC's main telemetry station. Even though the students do not run the main telemetry station during launch, they still help setting it up. The group tunes receivers, sets up data storage and tests the trajectory tracking systems. During flight the students track the rocket which a process that requires getting used the equipment. As an exercise, the students track a NOAA satellite in the run-up to the launch. They also build a dummy payload with which to test the systems. This dummy acts as the backup payload in case it should be required.

5. RESULTS AND OUTLOOK

[…]

REFERENCES

[…]

SESSION 6: C - Educational Programs & Strategies 1

(Friday 11th - 09.30)

Chairman: Dr. Riccardo Rando

EDUCATIONAL OPPORTUNITIES THROUGH MARS ANALOG RESEARCH

Kartik Kumar [(1)], Reinhard Tlustos [(2)], Gernot E. Grömer [(3)],

[(1)] Delft University of Technology, Kievitsbloem 20, 2631TB Nootdorp, The Netherlands, Email:kartik.kumar@oewf.org
[(2)]Austrian Space Forum, Sillufer 3a, 6020 Innsbruck, Austria, Email: reinhard.tlustos@oewf.org
[(3)] Austrian Space Forum, Sillufer 3a, 6020 Innsbruck, Austria, Email: gernot.groemer@oewf.org

ABSTRACT

Mars analog research encompasses a fundamental effort to build the capabilities, capacity and understanding to conduct future human missions to the Red Planet. In a nutshell, Mars analog missions are geared towards generating a holistic understanding of the factors that will underpin the success of such endeavours, by developing key technologies, processes and workflows. To this end, the Austrian Space Forum (OeWF) has conducted international Mars analog missions in challenging environments, to study human-robotic partnerships for exploration, with a focus on geosciences, astrobiology, engineering and human factors. The OeWF has developed significant experience in this domain and has utilized this position to offer students and young professionals the opportunity to participate in a variety of roles.

In this paper, we canvas the spectrum of educational opportunities that have been established by the OeWF within the framework of Mars analog research. In particular, we analyse the recently concluded AMADEE-15 mission as a case study, the eleventh such activity conducted by the OeWF, and highlight the broad envelope of learning initiatives adopted prior to and during the mission.

Initiatives include the Junior Researcher Program, through which a pilot project was conducted that enabled fifteen carefully selected students to interact with senior researchers during the AMADEE-15 Mars simulation at 3000 meters altitude. The participants were trained as "ambassadors for space exploration" with the intention of providing them with the tools to subsequently communicate their impressions and lessons learned to their respective social environment. The underlying assumption was that direct communication amongst peers offers a higher level of authenticity and hence impact, than a "top-down" approach whereby researchers offer interaction with classrooms directly. Also, due to the significant media attention generated by the mission, the credibility of the students amongst their peers was amplified.

International internships, tele-lectures and classroom visits have provided students with a wide array of insights into missions conducted by the OeWF. In addition, the opportunity to execute science within missions such as AMADEE-15 offers early stage academics the chance to serve as Principal Investigator within a highly dynamic team environment.

We provide a critical analysis of the outcomes of these initiatives and evaluate their success in raising awareness about Mars analog research. We conclude with a set of recommendations to expand upon the current educational program within the OeWF and provide an outlook on the continued positive impact that can be generated.

1. INTRODUCTION

1.1. The Austrian Space Forum

The Austrian Space Forum (OeWF) is a citizen science organisation for space professionals and people with a passion for space. The organisation has the legal status of an association in Austria and works in collaboration with both national and international research institutions, industry and politics.
The OeWF is a volunteer run organisation that initiates, supports and connects careers through student internships, project involvements as well as supervision of academic theses. The Forum enables participation in research and the development of projects. Students, interns and young professionals are an integral part of the OeWF staff and help maintain and expand a multitude of activities conducted by the OeWF. [1]

The OeWF specializes on space sciences, (human) Mars exploration, Earth Observation and Astrobiology. Results are published in peer-reviewed journals, presented at scientific conferences and communicated both to specialists and the public. [2]

The flagship project "PolAres" is an interdisciplinary research program preparing exploration strategies and procedures for future human-robotic Mars surface expeditions. The program focuses on the development and testing of a space suit simulator series "Aouda" (Figure 1), a family of analog Mars surface rovers and a stratospheric balloon series Passepartout. [3]



Figure 1. The Aouda spacesuit simulator: a 45 kg "spaceship to wear"

1.2. Simulated Mars Missions

Since 2006 the OeWF is conducting Mars Simulations with increasing complexity and international involvement. In recent years the missions include analogue sites like Rio Tinto in Spain (2011), the Dachstein ice caves in Austria (2012), the Moroccan desert (MARS2013) and the latest AMADEE-15 mission at the Kaunertaler Glacier in Austria. [3] [4]

These simulations are made up of 3 major groups. The field crew conducts experiments in-situ at the test site, this includes the analog astronaut corps who are operating the space suit simulator. The flight control team staffs the Mission Support Center (MSC) from which the mission is directed. The MSC functions as a hub for communication between the mission and the outside world, eg. Remote Science Support and Media relations. The third group includes external partners and Principal Investigators (PIs) that the provide experiments which are conducted during the mission by the field crew.
Students are involved in most of the operational aspects in an interdisciplinary environment and have the opportunity to learn about the processes involved in conducting such an international endeavour. During the recent missions students also executed their own experiments in conjunction with experiments from senior scientists. [3]

2. STUDENT OPPORTUNITIES

2.1. Internships

The Austrian Space Forum is hosting about 5-10 interns each year, ranging from Austrian high school students with an outstanding motivation to international university students with an exceptional track record in space project engagement. Although only a part of these internships is paid, a well-defined workflow managing expectations on both the side of the intern and the organisation foster a structured career evolution. This starts with a carefully designed and competitive selection process, based upon standard job interview questions and a series of unconventional test questions targeting creativity, resilience and self-reflection. After acceptance, they are introduced into the organisation and included in the team information flow. The participants are provided with recommended reading material and are encouraged to discuss potential internship projects beforehand. After a standardised introductory one-on-one talk during the first week, also documenting their expectations, the interns and their respective supervisors agree on how much time to spend on which type of project, with regular milestones requiring them to self-assess their working capabilities. After the internship, a standardized exit-interview compares the initial expectations with the actual work at the Austrian Space Forum, and ends with a career advice, reflecting on the strengths and weaknesses of the intern. [5]

Since this method was established, the retaining rate of interns who became volunteers afterwards, has more than doubled. This is probably also due to the fact that the interns recognized the work at the Austrian Space Forum as a career step beyond following their respective "space passion". In selected cases, there were a number of episodic cases where not only the career choice was shaped through those internships, but also a success on later job interviews could be traced back to the experiences obtained at the OeWF.

Anecdotal career pathways range from the 15 year old high school student who, after being at the OeWF for more than 10 years, is now a leading engineer for the spacesuit development team, ISS flight controllers, who obtained their first Mission Support duties during OeWF missions, to students who started their academic thesis at the organisation and the follow-up volunteer engagement qualified as professional experience for their later jobs.

Cross Section of Tasks:

- OeWF Space Suit Laboratory
    - Assistance in Analog Astronaut Training
    - Working directly on the Space Suit Simulator hardware
    - 3D printer operation and preparation of print templates
- Marketing research and analysis
- Outreach event planning and implementation
- Conducting tele-lectures
- Preparation for Field Tests and Simulation Campaigns

- Participate in Mars Simulations as part of Mission Support Team
- Preparing and participating in technical visits to partners (eg. industry, ESA) see Figure 2.



Figure 2. OeWF interns and president Dr. Grömer meet ESA Astronaut Samantha Cristoforetti during European Astronaut Center visit in Cologne, Germany

2.2. Academic theses

Within the framework for an academic thesis, internships between 2-24 weeks are possible. The precise task will depend on the professional experience of the applicant. The OeWF has had interns with various backgrounds e.g. physics, biology, media sciences, project management, architecture, informatics etc. with the goal of developing an academic thesis (e.g. seminar, bachelor or master thesis).

In the past 6 years (2009-2015) a total of 8 Bachelor and 7 Master theses were written in the context of an OeWF internship or by members involved in OeWF activities. The topics range from hands on space simulator related work, theoretical works on a concept for surface navigation systems, to Contamination and planetary protection theses. [6]

2.3. Junior Researcher Program

In the framework of the most recent AMADEE-15 Mars analogue mission in August 2015, the OeWF managed the Junior Researcher Program (JRP) in cooperation with PLANSINN GmbH and under contract with the Austrian Federal ministry for Transportation, Innovation and Technology.
This program brought together 13 students from Austria and 2 from Switzerland for two days when they had the chance to join the mission and experience field research first hand. The students were aged between 16 and 20 years. [4]

The participants were familiarized with the AMADEE-15 experiments and each had to "adopt" one experiment. They established contact with the respective PIs and were encouraged to learn as much as possible about the experiments. The overall aim was to get the students in contact with senior scientists on equal footing and help remove the "barrier" that usually exists. This allowed the students a better immersion in the mission and a richer experience.
The JRP participants had the opportunity to accompany the field crew on the glacier, meet an analogue astronaut, visit the base habitat, see most of the experiments and engage in discussions with the PIs in person. Figure 3 shows an example PI and JPR participant interaction.

Additionally, the program included a visit to the Mission Support Center where the setup and operation was explained. The participants also engaged in a special career talk with professionals.

The participants were encouraged to become space ambassadors themselves and share their experiences with a wider audience in their respective social and work environments. Through this the younger generation can be reached and a wider interest in space research in general created.



Figure 3. Dr. Alain Souchier / Association Planete Mars explains the Cliffbot hardware to JRP participants

3. CONCLUSIONS

The opportunities offered by the OeWF provide valuable hands-on experience for both national and international students and young professionals from a large variety of backgrounds.
In the future the OeWF can look towards expanding its student activities and potentially recruit volunteer members from the growing corps of OeWF internship alumni.

4. REFERENCES

[1] Austrian Space Forum Website, English
http://www.oewf.org/en/
(Date accessed: 2015-11-28)

[2] Austrian Space Forum Website, List of Peer Reviewed Publications

http://www.oewf.org/en/polares-science/publications/
(Date accessed: 2015-11-28)

[3] Austrian Space Forum Website, Overview Mars Simulations
http://www.oewf.org/en/portfoliocat/field-simulations-expeditions/
(Date accessed: 2015-11-28)

[4] Austrian Space Forum Website, AMADEE-15 Final Mission Report
http://www.oewf.org/dl/AMADEE-15_FinalReport_PUBLIC_V3.pdf
(Date accessed: 2015-11-28)

[5] Austrian Space Forum Website, Internship Opportunities
http://www.oewf.org/en/become-member/jobs-internships/
(Date accessed: 2015-11-28)

[6] Austrian Space Forum Website, Theses Overview,
http://www.oewf.org/en/polares-science/academic-thesises-at-the-austrian-space-forum/
(Date accessed: 2015-11-28)

THE CANADIAN SATELLITE DESIGN CHALLENGE: BUILDING FUTURE SPACE CAPABILITY IN CANADA

Lawrence Reeves[(1)], Chantal Dubois[(2)]

[(1)]Canadian Satellite Design Challenge Management Society, 5050 Elgin St., Vancouver, B.C. CANADA
E-mail: LReeves@csdcms.ca

[(2)] University of Manitoba, Winnipeg, Manitoba, CANADA
Email:umduboi9@myumanitoba.ca

ABSTRACT

The Canadian Satellite Design Challenge (CSDC) is a Canada-wide competition for teams of university students to design and build a cubesat satellite. The primary objective of the competition is to launch the winning team's satellite, in order to conduct its science mission; however, there are several additional objectives, intended to help build space knowledge and research and development capability at the university level, and to give university students a valuable educational experience which will help them to become future leaders in the space community.

A key element of the CSDC is "hands-on" workshops at which participating students acquire space industry skills in diverse areas of space mission design and development, such as assembling solar panels in a cleanroom, subjecting potential cubesat components to a simulated space radiation environment, and conducting random vibration testing on their finished cubesat prototypes.

The CSDC also has an Educational Outreach component, whereby each team is required to give presentations to a variety of audiences. Specific among these are pre-university (elementary and secondary) students, with the goal of inspiring and motivating them to pursue post-secondary education in science or engineering disciplines. Recently, the CSDC instituted a prize which will be awarded to a team for outstanding effort and contribution their Educational Outreach efforts.

In this paper and presentation, the authors present results from the first three competitions, focusing on results from the "hands-on" workshops and testing activities which help foster new space expertise and capability at Canada's universities, and on Educational Outreach efforts which the teams have dedicated to younger students.

1. INTRODUCTION

The Canadian Satellite Design Challenge (CSDC) is a Canada-wide competition for teams of university students to design and build a 3U cubesat (or "triple cubesat") satellite. The CSDC has the ultimate objective of launching the winning satellite in order to conduct its science mission.

2. COMPETITION STRUCTURE

The CSDC is structured like a real-world space mission; the CSDC management assumes the role of the Customer, and each participating team assumes the role of a Prime Contractor. Teams are issued requirements documents at the beginning of the competition, and have documentation delivery milestones, and a comprehensive Critical Design Review, all of which are reviewed by a panel of experience space industry professionals.

The CSDC also offers "hands-on" workshops, in which the participating students work side-by-side with experienced space missions professionals, benefiting from the mentorship which is transferred to them.

It is hoped, and intended, that the experience and leadership skills they acquire will help them to achieve success in their post-university careers, and benefit equally the organisations at which they pursue their careers.

The CSDC runs over two academic years. The current competition (the third offering to date) started in September, 2014, at the beginning of the Canadian university academic year. The current offering is scheduled to complete in May, 2016. The schedule of events and milestones (e.g., document deliverables) takes into account the requirements of the university academic year (e.g., mid-term or final exams).

3. COMPETITION GOVERNANCE

The CSDC is managed by the CSDC Management Society Inc. (CSDCMS), a registered not-for-profit organisation in Canada. It is entirely volunteer-run, predominantly by the Board of Directors; there are no employees. The Directors are representatives from Canadian Space industry (MDA and UrtheCast), academia, a science and engineering research funding agency, and public education-focussed space centre.

The competition has a relatively modest budget. The CSDC has received grants of US $50,000 from Boeing for each offering, and has received and additional $10,000 to $15,000 from Canadian industry and governmental organisations.

However, added to the financial contributions is an extremely valuable array of in-kind contributions of time, expertise and mentorship, and facility usage, from Canadian space companies and governmental organisations, as well as the members of the Board of Directors.

Each participating team is required to secure contributions (funding or in-kind) from their universities or other sponsors, in order to cover the costs of procuring the spacecraft hardware, and also for some travel-related costs (although travel costs are partially supported by the CSDCMS).

With this format, the Canadian Satellite Design Challenge is able to offer a high-value educational experience to university students (from a broad range of disciplines), at a relatively low cost.

4. SPACE MISSION MANAGEMENT EXPERIENCE

The CSDC is structured and managed like a real space mission project, and gives participating students a simulated experience at managing and working on a real industry space mission.

The schedule of the current competition is shown in **Error! Reference source not found.**; it is a basic schedule of activities and milestones which are a template for many space mission projects.

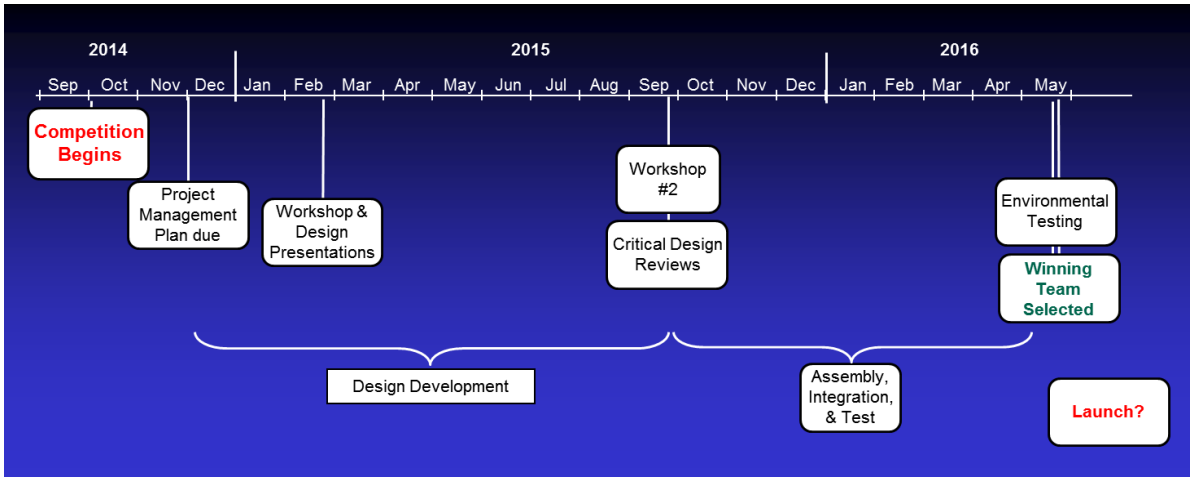


Figure 1. ***The CSDC schedule, a simplified version of a typical space mission schedule of milestones.***

The CSDC management assumes the role of a Customer, with each team being a Prime Contractor. The competition begins with the release of the mission and spacecraft requirements documents, and has required documentation deliverables, and a Critical Design Review which is presented and graded by a panel of experience space mission professionals.

With these elements, the CSDC provides a foundation in project management, which is rarely encountered in a university curriculum. This experience benefits both the students following graduation, as well as the companies which hire them with the added experience which the students bring.

5. HANDS-ON SPACECRAFT ASSEMBLY AND TESTING EXPERIENCE

One of the primary benefits of the CSDC, in comparison with other undergraduate engineering competitions, is that the CSDC organises a series of workshops to provide "hands-on" experience in elements of spacecraft design, assembly, and testing.

In the first two competitions, a solar panel assembly workshop was held for representatives from each team, at a Canadian space mission company (Neptec Design Group, in Ottawa, and MDA Corporation, in Montreal).

At the workshop, the students were given an introduction to spacecraft assembly processes, and a presentation on soldering for spacecraft electronics. Then, working in a clean-room environment (one of the workshops was held in a Class 100,000 spacecraft payload integration room at MDA in Montreal), the students assembled a cubesat solar panel using space-qualified solar cells, adhesives, and materials. At the MDA workshop, the soldering was evaluated by a

senior technician; the results were humbling – and an excellent learning experience - for the students.



Figure 2. Students soldering a string of solar cells.

For the current CSDC competition, team representatives met at the Tri-University Meson Facility (TRIUMF), a nuclear science facility which contains the world's largest cyclotron, at the University of British Columbia, in Vancouver. The teams brought cubesat electronics in order to conduct radiation testing which would simulate the space radiation environment.

The students worked side-by-side with nuclear science researchers, learning about the radiation testing process and the science which governs it, as well as its applications to other sectors (e.g., medicine).

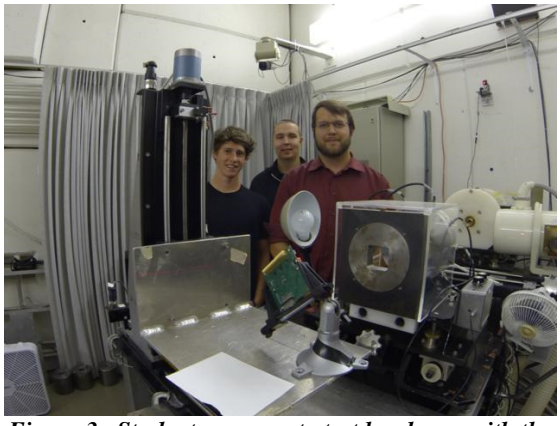


Figure 3. Students prepare to test hardware with the TRIUMF proton beam.

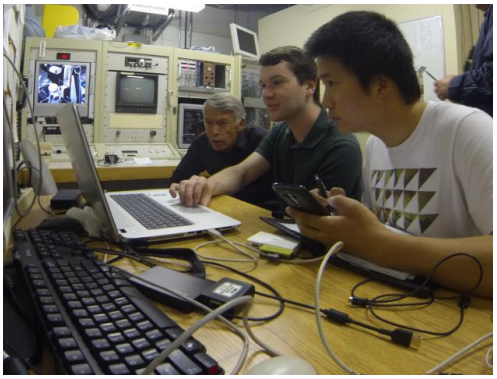


Figure 4. Monitoring the radiation testing remotely from the control room.

6. CRITICAL DESIGN REVIEWS

Approximately 13 months into the competition, each team is required to give a comprehensive 2½-hour Critical Design Review (CDR) presentation about the design of their satellite, in front of a panel of space industry experts. The presentation simulates a real mission CDR by a mission Prime Contractor to its Customer.

The CDR presentations are extremely valuable for the teams, all of which have expressed sincere appreciation for the thorough review, and for providing the "voice of experience" which helped them improve their understanding of their spacecraft and mission design process.

The Critical Design Reviews are also a valuable experience at preparing such a comprehensive design summary, and effectively communicating it; valuable skills for their eventual careers.

7. ENVIRONMENTAL TESTING

The final phase of the CSDC is the environmental testing, during which the cubesats are subjected to launch qualification random vibration testing.

The environmental testing has previously been held at Canada's national spacecraft test facility, operated by the Canadian Space Agency.

This is another excellent educational experience for the students. They are treated as well as any commercial customer, being supported by engineers and technicians during the testing phase. The value of this experience – both from a learning perspective, and as an experience which inspires and motivates them to pursue such interesting and rewarding careers following graduation – is immense.



Figure 5. Preparing for vibration testing.

8. LAUNCH

Since the inception of the CSDC, it has been a goal to launch the winning satellite into orbit in order to conduct its science mission. While this is currently beyond the financial capacity of the competition, the CSDCMS continues to investigate avenues to realise this goal.

The team which won the first competition in 2012, from Concordia University in Montréal, applied to the European Space Agency's "Fly Your Satellite" opportunity, and was one of the six selected teams. Although the teams was unable to complete the qualification process, the experience validated that the CSDC participants are capable of producing flight-worthy hardware, and so the CSDCMS will continue to pursue a launch opportunity for the winning satellite.

Note: The ESA "Fly Your Satellite" programme is planning on launching the satellites to the ISS, and the safety requirements exceeded those that Concordia's satellite was designed to, and could not be accommodated within the allowable schedule. The CSDCMS has subsequently updated the CSDC requirements to envelope the ISS requirements.

9. INTERNATIONAL COLLABORATION

Although intended for Canadian universities, the CSDC has welcomed the opportunity to incorporate international collaboration between Canadian university teams and universities from other countries.

The opportunity first began when the CSDC Manager was approached by students from the University of Bologna at a conference, following a presentation about the CSDC. The University of Bologna students were eventually paired with the team from the École Polytechnique de Montréal, with each group manufacturing a portion of their cubesat entry. What is perhaps most significant about their teaming together is the fact that their working language, English, was the second language for the students on both teams.

International collaboration has continued in the current CSDC, with students from the University of New South Wales in Sydney, Australia, working with the team from the University of Toronto.

These pairings have given each team even broader experience – and, arguably, more realistic, as many current space missions are international collaborative efforts.

10. CREATING OPPORTUNTIES FOR YOUNG LEADERS

Participating in the Canadian Satellite Design Challenge has opened up new opportunities for excellent students. The CSDC has given participants an opportunity to work on an exciting project, and demonstrate their abilities to learn and lead. These qualities have, in many cases already, contributed to new opportunities being created.

- Former participants have been able to secure positions with Canadian space missions companies (MDA and Magellan). The two years of experience that participants acquire in spacecraft and space mission design, as well as the hands-on experience, make them desirable hirees.
- Three CSDC participants have attended the International Space University's Summer Session Programme, one each in 2013 (Linz, Austria), 2014 (Montréal, Canada), and 2015 (Cleveland, Ohio, USA).
- Co-author Chantal Dubois, a CSDC participant, is currently on a three-month placement with the Space Generation Advisory Council.
- CSDC participants have attended and presented at several Canadian and international space conferences, including the International Astronautical Congress (2013 to 2015), and Japan's Nanosatellite Symposium.
- The University of Alberta participated in the Second Space Mission Ideas Contest, organised by the University Space Engineering Consortium (UNISEC) in Japan, and was presented with the prize for the best environmentally-themed mission by the International Academy of Astronautics. Building on their experience in the CSDC, the University of Alberta is now participating in the QB50 initiative, and is preparing for a launch of their satellite in 2016.

11. EDUCATIONAL OUTREACH

An important element of the CSDC - and a significant enhancement over other existing university-level engineering competitions - is the Educational Outreach component.

As a requirement of their participation in the CSDC, each team is required to give presentations about space, space science and engineering, their CSDC projects, and/or space applications, to at least five different audience types (elementary school, secondary school, their university, a professional group or sponsoring company, and the general public) each year.



Figure 6. Educational Outreach to elementary school students.

The objectives of the Educational Outreach component are to:

- motivate and inspire pre-university students to pursue science and engineering educations; and,
- increase public awareness and interest in the applications of satellite missions, and the importance of satellites and space for Canadians.

The Educational Outreach also provides a benefit to the participating university students in that it helps them to become better, more engaging, presenters, a skill which is rarely emphasised for university science and engineering students.

12. SUMMARY

The Canadian Satellite Design Challenge is a challenging competition for predominantly undergraduate students. The competition is organised by volunteers on a relatively modest budget, and presents a significant learning and career development opportunity for the participants, who acquire interdisciplinary technical, teamwork, leadership, and management skills. Not only do the participants gain a wealth of knowledge and experience about spacecraft design and engineering, but also project management.

The value of the competition comes from the many in-kind contributions of expertise and facilities, from Canadian space missions companies and government agencies. Visits to space companies and facilities, working in the facilities, and receiving presentations and mentoring from experienced space mission experts, all create an environment for the students which encourages them to learn and excel, and opens up opportunities for careers or graduate studies in space-related disciplines.

In summary, the Canadian Satellite Design Challenge offers a high-value educational experience for university students (both undergraduate and graduate), at a modest budget. The almost universal appeal of working on a space mission, with the potential of one day seeing it launched into orbit, motivates students to excel – not only in their own chosen disciplines, but to gain a broader understanding and appreciation for many other disciplines which comprise real-world space missions. Even without yet having launched any of the competition's satellites, the CSDC has nonetheless created a valuable educational experience which is developing future space industry leaders, for the benefits of all stakeholders.

About the Authors

Lawrence (Larry) Reeves is the President of the Canadian Satellite Design Challenge Management Society, and main organiser of the competition. He has almost 20 years of experience on Canadian and international space missions projects, and is a Senior Member of the Systems Engineering group at UrtheCast in Vancouver.

Chantal Dubois is a student at the University of Manitoba, in Winnipeg, and is the Director of Business & Outreach for the University of Manitoba Space Applications and Technology Society (UMSATS), which is participating in the CSDC. She is nearing completion of a three-month placement with the Space Generation Advisory Council (SGAC) in Vienna, Austria.

PROVIDING HANDS-ON SPACE EDUCATION BY INVOLVEMENT OF COLLABORATING SELF-RELIANT STUDENT TEAMS

Johannes Gutsmiedl[1]: +49 89 289 16028 / johannes.gutsmiedl@warr.de,
Martin Dziura[2], Martin Langer[2], Martin Losekamm[3], Maria Grulich[1] and Monty Mutschler[1]

[1]Scientific Workgroup for Rocketry and Spaceflight (WARR)
[2]Institute of Astronautics (LRT), Technische Universität München (TUM)
[3]Physics Department E18, Technische Universität München (TUM)

***Abstract*—The Institute of Astronautics (LRT) at Technical University of Munich (TUM) incorporates self-reliant student teams to provide hands-on space education. Organized within the student group WARR almost 200 students are developing space hard- and software supervised by the institute's staff members. The CubeSat project MOVE-II is one of the most challenging ongoing projects. About 40 students are developing a satellite with high requirements in terms of power and data transmission. To qualify the CubeSat's hold-down and release mechanism, a collaborating student team launched a prototype within the REXUS 18 campaign. As a reference payload the Multi-Purpose Active-Target Particle Telescope (MAPT) is developed by a another student team. Once tested on the BEXUS 18 campaign, another qualification flight is planned on BEXUS 22/23. Meanwhile WARR's oldest branch consisting of almost 50 students develops a cryogenic hybrid rocket engine - aiming to brake the European altitude record for amateur rockets with the WARR-EX 3. Successfully launching the hybrid sounding rocket WARR-EX 2 in 2015 in Brazil the team gained important experience.**

I. INTRODUCTION

Providing true hands-on experience in space education without disregarding scientific advances is a challenge for universities. The Institute of Astronautics (LRT) at Technical University of Munich (TUM) incorporates self-reliant student teams as collaborators into research projects to tackle this problem.

The Scientific Workgroup for Rocketry and Spaceflight (WARR) is the biggest sovereign student group at TUM, currently consisting of almost 200 active members. The students create and maintain their own project infrastructure and are working on diverse fields, such as rocket propulsion, satellite technology, the space elevator and studies for interstellar spaceflight.

II. THE CUBESAT PROJECT MOVE-II

The largest educational project currently running at LRT is the CubeSat MOVE-II (Figure 1). It is a follow-on to the First-MOVE mission launched in November 2013.

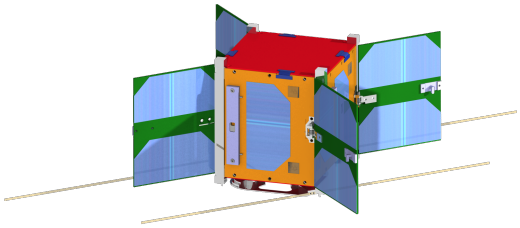


Fig. 1. MOVE-II Concept Drawing

In First-MOVE, students were involved only in the form of theses, while all long-term work was done by LRT employees, similar to educational nanosatellite projects at many other universities. Among the many lessons learned in the mission was the realization that long-term involvement of Bachelor's and Master's students beyond just the few months of a thesis is crucial for a complex multi-year project in order to prevent loss of knowledge, especially since only a single full-time employee is available to work on MOVE-II. From an educational point of view, this also has the advantage of allowing students to experience the full life cycle of a spaceflight project from mission concept to operations instead of just working on one aspect of a subsystem during a specific development phase, as is commonly done in theses. The long experience of the WARR with self-organized student groups greatly simplified the set-up of such a structure for MOVE-II, leading to a collaboration between LRT and WARR and the formation of the WARR Satellite Technology Group.

Work on MOVE-II began in December 2011 and proceeded quickly to a mission concept review in May 2012. Unfortunately, funding from the German Aerospace Center (DLR) could not be obtained until early 2015, pushing back the anticipated launch date to 2018. At the moment, the mission is going through a system definition review before heading into the design

phase. Thanks to the model of allowing students to work on the satellite during their free time, work on MOVE-II never stopped between 2012 and 2015, which now helps to keep the project within the anticipated time frame. In addition, many of the students who started out in the project as undergraduates in 2011 have now been in the program for years and were thus able to gain a lot of experience in their respective subsystems, which is now being passed on to new team members. The project has also produced multiple scientific publications with students as main authors or contributors (e.g. [1]).

After multiple revisions in the funding application process, MOVE-II will now be a single unit CubeSat designed to support a scientific payload, which would be mounted within a second unit stacked on top of the bus. The interface will be as generic as possible in order to allow for many different missions to be fulfilled with the MOVE-II bus. As a reference mission the Multi-Purpose Active-Target Particle Telescope (MAPT), currently under development at TUM's Physics department, was selected. Its high power requirements and the (for a CubeSat) immense amounts of data needing to be downlinked make it a very good "high-end" benchmark. It will not fly on MOVE-II due to lack of funding, but the satellite bus will be fully tested on-orbit. Important features of the satellite include a half-duplex S-Band transceiver for payload data downlink, deployable solar panels for power generation and a novel FPGA-based dependable on-board computer. The satellite will also feature active three-axis attitude control. At the moment, about 40 Bachelor's and Master's students are working on MOVE-II in six subsystem teams.

III. Qualification on REXUS/SMARD

As part of the MOVE-II mission a group of nine students from LRT participated in the Rocket Experiments for University Students (REXUS) program.

REXUS provides an experimental space platform for students onboard a sounding rocket. The REXUS-BEXUS program is realized under a bilateral Agency Agreement between the German Aerospace Center (DLR) and the Swedish National Space Board (SNSB). EuroLaunch and the Mobile Rocket Base (MORABA) of DLR are responsible for the campaign management and operations of the launch vehicles. Each year two sounding rockets carrying about 10 experiments are launched in Kiruna, Sweden. SNSB share their payload capabilities with student teams from other European countries through a collaboration with the European Space Agency (ESA).

This program offers students the possibility to get their hands on a real space project. Within the 18 months' duration the students pass through all stages of reviews, beginning from the selection process to the Critical Design Review (CDR) until the Experiment Acceptance Review (EAR) and the launch. During this program the students gain a lot of experience not only in the technical point of view also in project team work and management. Soft Skills become more and more important and are useful for their future career.

All teams get technical support throughout the project from experts from DLR, SSC; ZARM and ESA.

In the past mostly every two years the LRT had one team successfully participating in the REXUS-BEXUS program. Some of the former participants stayed at the LRT for their PhD. Hence, the former participants tell other students about their experiences during this program and they encourage them to come up with an own experiment. The teams can benefit from the knowledge and experience of the former teams.

Therefore, the LRT encouraged the students within the MOVE-II mission to form a team and to participate in the REXUS-BEXUS-program. The LRT provides the teams with excellent facility infrastructure to built their experiments. The student teams having their own student lab with computers and workplaces. They can also use the LRT workshop abilities including a thermal-vacuum chamber to test the experiment under vacuum conditions.

The last team from the LRT developed the Shape Memory Alloy Reusable Deployment Mechanism (SMARD), a hold- down and release mechanism (HDRM) for the solar panels of a nanosatellite[2]. Usually a single-shot system for such a mechanism is used. The shape memory alloy enables repeatable actuation and the ability to reset quickly. The reusability simplifies testing and reduces the time between tests and the possibility of a potential failure during the assembly procedure.

To ensure a successful operation of the mechanism during MOVE-II's mission, thorough testing of the mechanism in all relevant environments is necessary. With high vibrational stresses and g-loads during launch, as well as the vacuum and milli-gravity environment during the coast phase, a sounding rocket is ideal for this purpose. The experiment was launched on the 18th of March 2015 on board the sounding rocket REXUS 18. As a result of this flight SMARD was successfully qualified for its application.

IV. The reference payload MAPT

The intention to equip the MOVE-II satellite with a scientific payload triggered the formation of a new student group at TUM's Physics Department in early 2012. While researchers at the Institute for Hadronic Structure and Fundamental Symmetries (E18) usually try to solve the mysteries of subatomic particles – using accelerator facilities at CERN and in Japan – the at that time recent discovery of antiprotons trapped in Earth's

radiation belts in the summer of 2011[3] provided the initial idea for a quite different project. When asked about potential CubeSat-sized payloads, the head of the institute, Prof. Dr. Stephan Paul, had the idea to build a miniaturized particle detector that would be able to measure the flux of antiprotons circling the planet while in low-Earth orbit. Although such a device would not be able to directly compete with high-profile experiments like AMS-02 on the space station, it could nevertheless provide new data in the very-low-energy region that is not accessible by any other experiment in orbit today[4]. Inspired by the successful efforts of LRT and WARR to provide hands-on education to young students, Prof. Paul decided to pursue the idea in the form of a student project. Together with one of the authors, he gathered a small team of dedicated undergraduate students eager to gain practical research experience.

The detector design that was conceived by the group builds upon a novel identification principle for charged particles. Most other experiments that aim to identify single particles and reconstruct their kinetic energies rely on a spectrometer-like setup: Incident particles pass through several layers of position-sensitive detectors while being subjected to a strong magnetic field. The field forces them onto a curved path whose radius of curvature is proportional to the particles' charge and mass. Other parts of the setup measure the particles' speed and kinetic energy. Combining these different data sets, scientists can identify the species of each particle and reconstruct their energies. For an unambiguous identification a complete dataset from all the detectors in the setup is needed, a requirement that is impeded by a fundamental property of particles: When passing through matter they lose kinetic energy through interactions with the material's atoms, which slows them down until they eventually stop. If that happens before a particle passes all layers of the detector it cannot be unambiguously identified anymore. Thus, particles must have a minimum kinetic energy to be identifiable. Another drawback of a spectrometer-like setup is that only particles entering through a narrow entrance window under a small angle of incidence can be detected, effectively limiting the detector's field of view to a small patch of space.

Both issues were addressed by the students when designing the Multi-Purpose Active-Target Particle Telescope (MAPT). Its core is made of "active" material – 900 small pieces of scintillating fiber that produce light when a charged particle passes through them. The amount of light created is directly proportional to the energy the particle lost within the fiber. Arranging those pieces of fiber in the right way allows to determine the track of a particle within the core. As the energy-loss profile along the track depends on their species and initial kinetic energy, particles stopping in the core can be unambiguously identified. Even the properties of particles that do not stop but still lose a significant amount of their kinetic energy can be determined using extrapolation algorithms. The design – being able to identify particles incident from all directions – removes the constraint of a fixed entrance window altogether and lowers the minimum kinetic energy a particle needs to have significantly.

To be able to deploy MAPT aboard small satellites, the team had to develop a data acquisition system that can handle 900 detector channels while consuming as little power as possible from scratch. Throughout the project, new components (e.g. silicon photomultipliers and new application-specific integrated circuits) and technologies (e.g. 3D-printing integral parts of the detector's structure) are used, giving the students the chance to be part of leading efforts to utilize ever more compact systems for the exploration of space.

To prove that MAPT's design and particle identification principle are working as intended, the team built a down-scaled prototype that was tested at a particle beam at Paul Scherrer Institute in Switzerland in late 2013. Using newly-developed analysis algorithms, they could show that the system does indeed work and even outperforms expectations in terms of energy resolution[5]. A second, full-scale prototype was subsequently developed and selected to fly aboard the BEXUS 18 stratospheric research balloon in October 2014. During the campaign, the detector was subjected to conditions similar to those in space and did operate stably throughout the whole flight[6].

Initially, the group tried to coordinate their efforts with those of the team around MOVE-II, so they might eventually be able to launch MAPT into orbit as its main payload. As it became clear that because of inadequate funding the detector could not be flown within the MOVE-II mission, the project's focus shifted from measuring the flux of trapped antiprotons in low-Earth orbit to developing a general-purpose radiation detector that can be used to monitor the radiation environment on a multitude of spacecraft. Currently efforts are underway to secure a launch opportunity to the space station and to conduct another test flight on a stratospheric balloon as part of the BEXUS 22/23 campaign.

As intended by Prof. Paul, the project has already given many students the opportunity to gain hands-on experience in the fields of particle physics and space technology. Since 2012, two Master's and four Bachelor's theses were successfully produced, with several Master's and Ph.D. theses ongoing at the time of writing. The group has received funding from the Cluster of Excellence "Origin and Structure of the Universe" – situated at TUM's campus in Garching – twice and has also been sponsored by several commercial businesses.

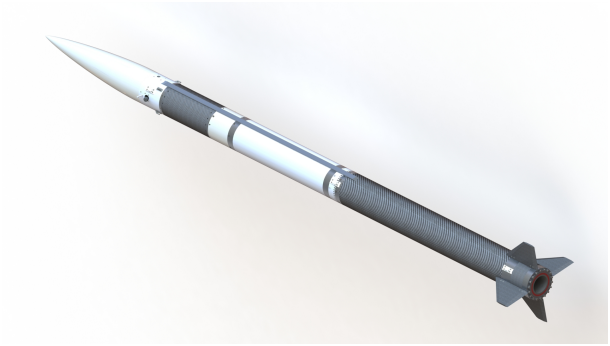


Fig. 2. WARR-EX 3 Concept Drawing

In 2015, the group has been officially named Space Detector Systems (SDS), representing a new interdisciplinary part of TUM's Institute for Hadronic Structure and Fundamental Symmetries.

V. Hybrid rocketry project WARR-EX

The rocketry department is WARR's oldest branch. It was founded by Robert Schmucker in 1962 and is, thus even older than the Institute for Astronautics at TUM. In 1974 WARR launched the first German hybrid rocket - "Barbarella". In the following years work on static liquid engines started with the ultimate goal of building a sounding rocket with a liquid engine. Owed to a small team size and the department moving, the project was ultimately not successful. At the beginning of the 21st century however, WARR Rocketry returned to its old favourites - hybrid rockets. Here the current project is the cryogenic hybrid rocket WARR-EX 3. With its own workshop on the campus, the support of the Institute for Flight Propulsion (LFA) and its 50 highly engaged members, WARR Rocketry is well prepared for various rocket projects.

The WARR-EX 3 (Figure 2) cryogenic hybrid rocket is developed within the Cryosphere project which started in 2013. The project goal is to launch a rocket, developed by WARR, using HTPB and LOX as propellants. The project is supported by the German Aerospace Center (DLR) within their Student Experimental Rockets (STERN) program, which enables student groups of several German universities to build and launch their own rockets. The STERN mission goals were extended by WARR Rocketry. The rocket is to reach an apogee of more than 15 kilometres, thereby reaching at least Mach 2.4. It will be fully recovered and will deliver live telemetry. With the project progression until now, several outputs can already be noted. A cryogenic test infrastructure has been established at the facility within the last years. The heart of this infrastructure is the self-developed oxygen liquefier with a corresponding test rig for different motors and a control box. Several successful tests with a small demonstrator engine and a subscale engine have already been conducted in order to train the crew in handling liquid oxygen. The full scale motor, which will deliver a thrust of 10 kN and a total impulse of 130 kNs, is currently manufactured and will be tested in early 2016. The rocket will be launched at the Esrange site in Kiruna, Sweden.

Ideally, the European altitude record for amateur rockets will also be broken, which proves to be very demanding in recent times, since many European student rocket groups are beginning to develop and launch bigger and more powerful rockets. The goal is to not only be part of this new fascinating movement but to be at the leading edge.

For this reason, WARR Rocketry participates in several international fairs and conferences (e.g. [7]), the most recent and productive being the EASM conference in October 2015 held in Milano. Several student rocketry groups from all over Europe participated and presented their current projects. A very important outcome of the conference is the creation of a European student rocketry competition which is expected to start in early 2016.

The WARR-EX 2 rocket, being the predecessor project, had its maiden flight in spring 2015 in Brazil (Figure 3) on an invitation of the University of Fortaleza. With a length of 2.3 m and a launch mass of 20 kg it is significantly smaller than WARR-EX 3 but also uses a hybrid motor. The propellant combination is HTPB and nitrous oxide. The participating students were not only able to witness a real rocket launch but rather to conduct one on their own. Besides of reaching an apogee of 4.2 kilometres and breaking the sound barrier, this was also the first launch of a hybrid rocket in Brazil. The simulated flight trajectory could be verified using radar tracking by the Centro de Lançamento da Barreira do Inferno (CLBI). After their return, the launch crew shared their experiences with their fellow students which had to remain home.

All in all, WARR Rocketry is on its way to establish a vast portfolio of rockets in different scales and for different areas of application. The WARR-EX 1 solid motor rocket for verification of subsystems of our bigger rockets and training of new crew members. The WARR-EX 2 which, after its successful launch has now its own succeeding project, WARR-EX 2B in which the rocket is improved according to the experience made. And lastly WARR-EX 3 cryogenic rocket as the current flagship and greatest challenge for the student group so far.

It is not only the goal to launch rockets but also to constantly improve the existing rockets and raise the claims with new challenging projects. The core requirement for this broad base in rocketry is a team of highly motivated and well educated students which mostly work on this



Fig. 3. Maiden flight of WARR-EX 2 in Brazil 2015

projects in their free time. Allowing students to make hands on experiences and engage in real problems which expand the theoretical foundations of the lectures is the passion of WARR.

REFERENCES

[1] C. Fuchs, C. Trinitis, and M. Langer, "Enabling dependable data storage for miniaturized satellites," in *29th AIAA/USU Conference on Small Satellites*, Logan, Utah, USA, 2015.

[2] M. Grulich, A. Koop *et al.*, "Smard-rexus-18: Development and verification of an sma based cubesat solar panel deployment mechanism," in *22nd ESA Symposium European Rocket & Balloon Programmes and Related Research*, Tromsø, 2015.

[3] O. Adriani, G. C. Barbarino *et al.*, "The Discovery of Geomagnetically Trapped Cosmic-Ray Antiprotons," *The Astrophysical Journal*, vol. 737, no. 2, p. L29, 2011.

[4] M. J. Losekamm, T. Pöschl *et al.*, "The AFIS Detector: Measuring Antimatter Fluxes on Nanosatellites," in *65th International Astronautical Congress*, 2014.

[5] T. Pöschl, M. J. Losekamm *et al.*, "A Novel CubeSat-Sized Antiproton Detector for Space Applications," in *34th International Cosmic Ray Conference*, The Hague, 2015.

[6] M. J. Losekamm, T. Pöschl *et al.*, "AFIS: A New Instrument for Cosmic Radiation Studies on BEXUS 18 and Future Nanosatellite Missions," in *22nd ESA Symposium European Rocket & Balloon Programmes and Related Research*, Tromsø, 2015.

[7] A. Zeiner, Y. Metsker *et al.*, "Simulation and verification of hybrid propulsion operating behavior," in *63rd International Astronautical Congres*, Naples, Italy, 2012.

SPACE GENERATION ADVISORY COUNCIL'S PROJECT GROUPS: EDUCATION ACTIVITIES IN AN INTERNATIONAL NETWORK

Ana Raposo[(1)], Minoo Rathnasabapathy [(2)]

[(1)]Space Generation Advisory Council, c/o ESPI, Schwarzenbergplatz 6; 1030 Vienna, Austria, Email:ana.raposo@spacegeneration.org
[(2)]Space Generation Advisory Council, c/o ESPI, Schwarzenbergplatz 6; 1030 Vienna, Austria, Email: minoo.rathnasabapathy@spacegeneration.org

ABSTRACT

The Space Generation Advisory Council (SGAC) is a global non-governmental organisation and network which aims to represent university students and young space professionals to the United Nations, space agencies, industry, and academia.
SGAC works on the international, regional and national level to link together university students and young professionals acting as the forum for the next generation of space sector leaders to discuss, debate the current space policy topic and inject the new generation point of view into international space policy creation.
SGAC has created a series of Project Groups to allow its members to carry out activities and debates during the year. This is an opportunity for students and young professionals to broaden their horizons and to deepen their knowledge about a specific topic. This project groups are: Space Exploration (SE), Space Law and Policy (SL&P), Commercial Space (CS), Near-Earth Objects (NEO), Small Satellites (SSPG), Space Safety and Sustainability (SSS), Space Technologies for Disaster Management (STDM) and Youth Promoting Cooperation and Education in GNSS (YGNSS).
These overarching SGAC Project Groups produce papers with input from a broad sample of the members and embodies SGAC's purpose as envisioned in United Nations' UNISPACE III (1999). In this paper, the activities of the Project Groups, from perspectives on space situational awareness and space debris to thoughts on exploration and space workforce issues, will be presented, together with the most important results and recognitions achieved.

1. SPACE EXPLORATION PROJECT GROUP

The Space Exploration Project Group was established in 2014 with the aim of creating an international and interdisciplinary forum formed by students and young professionals in order to approach Space Exploration from a multidisciplinary point of view. More specifically, the group aims to focus on the 8 common goals outlined in the Global Exploration Roadmap (GER) [1]:

- Develop Exploration Technologies and Capabilities
- Engage the Public in Exploration
- Enhance Earth Safety
- Extend Human Presence
- Perform Science to Enable Human Exploration
- Perform Space, Earth, and Applied Science
- Search for Life
- Stimulate Economic Expansion

Despite being the most recent group of SGAC, the team has already presented its work in journals and supported different initiatives within the Space Exploration sector.

1.1. Project – Global Exploration Roadmap (GER) Survey

According to the group's research among SGAC members, aged 18 to 35, 63% of the respondents had previous knowledge of the GER and 81% believed that specific international legal and policy framework should be included in future iterations of the document [2].
Moreover, the survey results indicate that the majority of the respondents believe in the planning of international space exploration at an inter-agency level instead of being conducted by individual governments or the United Nations. Among the different objectives indicated in the GER document, respondents prioritised, in the first place, the utilisation of the International Space Station (ISS), followed by a human mission to Mars, robotic mission to Mars and an asteroid mission [2].
Finally, it is important to note that 97% of the respondents referred the importance of inspiring young people in STEM disciplines as an objective for the GER [2], reinforcing the importance of the group's educational activities, as SGAC as a whole.

1.2. Project – Lunar Mission One

The Space Exploration Project Group (SEPG) has been supporting the Lunar Mission One initiative since the beginning of 2015.
Lunar Mission One is an international unmanned robotic spacecraft aiming to land at an unexplored area of the Moon – the south pole. There, the spacecraft will drill down to 100m in order to collect and analyse lunar rock dating up to 4.5 billion years in age. The mission will therefore assess the south pole's suitability for a future permanently manned lunar base and investigate

the Moon's potential for deep space radio astronomy [3].
By promoting the Lunar Mission One initiative, the group is working towards its educational purpose, providing hands-on experience to group members and contributing to the advancement of space exploration.

1.3. Analog Planetary Operations Group (APO-G)

Recently, the Space Exploration Project Group merged with the APO-G. APO-G is a group, external to SGAC, composed by students and young professionals dedicated to promote, support and conduct analog planetary research, focusing on comparative geology, operational procedures as well as human factors that will affect future crewed missions on planetary surfaces [4].
Considering that analog studies are addressed in the GER as one of the essential preparatory activities to extend human presence further into space, it was considered that both teams would benefit from the merger, increasing the scope of the group's work and pushing it towards new goals and challenges [4].
Elements of both SEPG and APO-G are currently working together in the ESA Moon Challenge. The so called ALCIDES team aim to understand how to efficiently and safely get humans and robots to the dark side of the Moon. Once there, they will both collaborate, gathering valuable data/samples which will play an important role in the advancement of systems/capabilities eventually enabling potential Moon habitats and radio telescopes, as well as further deep-space exploration destinations, such as asteroids, comets, and other solar system planets [5]

2. SPACE LAW AND POLICY PROJECT GROUP

The Space Law and Policy Project Group (SLPPG) was established in 2012 and has six main goals [6]:

- Engage in critical debates about actual legal and policy aspects concerning space activities
- Investigate legal and regulatory challenges faced by the space community
- Propose space-related policy recommendations
- Address potentially emerging questions and issues in the space sector
- Develop research papers regarding trend questions and issues of the space community
- To contribute and collaborate with the space community on multidisciplinary topics.

With around 16 active members, the group has attended 15 events during 2015, including several sessions at the United Nations Committee on the Peaceful Uses of Outer Space (UNCOPUOS) and different presentations at the European Space Policy Institute (ESPI), as well as major annual events within the Aerospace community such as the International Astronautics Conference (IAC) in Jerusalem [7].
The group works closely with the International Association for the Advancement of Space Safety (IAASS), having one of its members to work as contributing writer to the Space Safety Magazine. Moreover, together with the Commercial Space and Small Satellites Project Groups, Space Law and Policy began a project with Swiss Space Systems and is currently preparing a survey on the regulatory and economic aspects of nano-satellites [7].

2.1. Project - Suborbital flights regulation

The group has been recently working together with the UNCOPUOS LSC Working Group on the Definition and Delimitation of Outer Space, reflecting on suborbital flights for scientific missions and/or human transportation [8].
When expressing its view at the UNCOPUOS session, the SLPPG defended the importance of the legal definition of suborbital flights, considering not only the perspectives of States but also other actors within the space sector, such as commercial and other entities relating to air and space activities. Moreover, national and international viewpoints should be considered, while still respecting international law regarding air and space activities [8].
In its statement, the SLPPG proposed several aspects to be considered in the framework of the legal definition of suborbital flight such as

- the difference between passengers, astronauts, and space tourists
- the consideration of air passengers regulation as an example for potential regulation concerning suborbital flight passengers, and
- the obligation for suborbital flights to also follow air regulations or an integrated set instead [8].

2.2. Project – Nano-satellites survey

With the nano-satellite survey, the SLPPG aims to highlight the existence of international space law and its application to the national activities of States that have joined the Space Treaties, to find to what degree nano-satellite developers follow recently formulated national space law, to find differences and similarities in the registration of satellites across the world, to assess the pre-requisites for licensing nano-satellites in each legal regime, to identify best practices in sensitive legal areas such as import/export (especially ITAR in the US) and also IPR, to find out whether the nanosat community realises the importance of adopting safety measures prior to launching (risk assessment) and during operation (debris mitigation), as well as to understand the issues raised by the insurance requirements, the impact of their high costs and the associated liability [9].
Results are expected to be published in 2016.

3. COMMERCIAL SPACE PROJECT GROUP

The Commercial Space Project Group (CSPG) operates under four essential objectives:

- to conduct academic research on the "theory of industrial practice" in the commercial space sector
- to gather a next generation "think-tank" for commercial space
- to make the project influential upon decision-makers and getting the generation's thoughts on commercial space be heard publicly, and
- to equip the young generation with knowledge, tools and network to be active in the realm of commercial space and entrepreneurship [10].

3.1. Space is Business Competition

The group has been organizing the "$pace is Business" competition for the past three years, aiming to promote commercial space among students and young professionals, which usually gain the opportunity to present their work at the IAC [11].

In 2014, the $pace is Business competition accepted papers concerning the "Public/Private Human Access to Space" or "New Space and New Science", including, for instance, the historical or present analysis of human orbital space activities, the identification of benefits/barriers for private organisations to conduct scientific space exploration, or the understanding of opportunities and barriers for the development of a commercial market for human access to orbit [11].

In 2013, the winning paper analysed the impact of microsatellites and microlaunchers in the disruption of the space industry [12]. This work highlighted the importance of a dedicated launcher in order to create more value to microsallites, contrasting with the actual interest of the launching segment, which does not recognise the value of the microsatellite market [12].

3.2. Project - Nano-satellites survey

The CSPG has set its own goals when supporting the nano-satellite survey developed in collaboration with Swiss Space Systems and two other SGAC project groups. Therefore, the group aims to assess the typical investment necessary to launch & operate a nano-satellite, including the typical cost structure, collect best practices / typical ways of funding the development & operation of nanosats, assess whether there are already economic interests behind the development of nanosats, and identify conditions would foster the nanosat development over the upcoming years [9].

Results are expected to be published in 2016.

4. NEAR-EARTH OBJECTS (NEO) PROJECT GROUP

The NEO project group aims to help the worldwide planetary defence community, providing a youth perspective to planetary defence through annual reports, competitions, conference attendance, and public outreach projects related to Near Earth Objects [13].

4.1. "Move an Asteroid" technical paper competition

The "Move an Asteroid" competition has been organised since 2008, responding to the danger posed by a great of asteroids and comets. Although large-enough objects to trigger events capable of causing species extinction on Earth are rare, experts are increasingly concerned about their likelihood and far more common objects between 10 and 100 meters large can cause significant damage and loss of life, making detection and preparedness efforts all the more pressing [14]. Moreover, worldwide interest in missions to NEOs for human and/or robotic exploration and for resource utilization is growing [14].

The competition challenges students and young professionals worldwide to come up with original ideas relating to Near Earth Objects (NEOs) and welcomes technical paper submissions addressing one or more of the following topics [14]:

- Safe deflection of an Earth-bound NEO
- NEO study, characterisation and detection
- Global NEO impact warning system
- NEO resource utilisation
- Proposals and concepts for NEO missions aiming at planetary defence, exploration, and/or resource utilisation
- NEO impact consequences
- NEO education programs and strategies

In 2014, the winner described a tool capable of mapping asteroids ephemeris to impact probability distributions on the surface of the Earth, with the concept and accurate performance of the system being demonstrated with ten asteroids [15].

4.2. "Find an Asteroid" search campaign

Thanks to a partnership with International Astronomical Search Collaboration (IASC) and Minor Planet Centre (MPC), the NEO group has promoted the "Find an Asteroid" campaign with the aim of locating and identifying asteroids, responding to an attempt of minimising the risk posed by these objects [16].

There are 15 slots reserved for SGAC teams, which can apply in order to receive the necessary software to analyse the images, the corresponding instructions, as well as all the necessary information to concerning how to get ready for the search campaign. Teams will typically receive 3 to 5 images per week and are

expected to analyse each image, corresponding to an estimated work load of 1.5 to 2.5 hours/week [16].
This search campaign provides a unique opportunity for students and young professionals to gain hands-on experience in asteroid detection and at the same time contribute to an important mapping and identification of potential threats.

5. SMAL SATELLITES PROJEC GROUP

The Small Satellites Project Group (SSPG) considers three main objectives:

- To provide career and project assistance for young professionals and students already active in the small satellite community.
- To provide the small satellite community with up-to-date information on relevant topics, as well as recommendations regarding the directions to be taken for future research and development and/or policy and legal issues, and
- To attract young professionals and students to the world of small satellites and generally to the world of space exploration [17].

5.1. Project – Nano-satellite survey

The Small Satellites project group defined the following objectives to the nano-satellite survey developed in collaboration with Swiss Space Systems and two other SGAC project groups:

- Collect experience reports from academia and industry, understanding what benefits are involved
- Identify the benefits gained by industry when collaborating with research and academia
- Understand the required balanced between innovation and standardisation [9]

Results are to be published in 2016.

5.2. Project – QB50

The SGAC Small Satellites Project Group discussed with the Van Karman Institute to create an Android-Application showing all public data of all future QB50 satellites. At the time of writing, the project is still in its concept phase and is expected to start its development stage in the first quarter of 2016 [18].

6. SPACE TECHNOLOGIES AND DISASTER MANAGEMENT PROJECT GROUP

The Space Technologies and Disaster Management Project Group (STDM PG) aims to promote awareness of how space technologies contribute throughout the disaster management cycle [19]. Despite the importance of space technologies in disaster management, and the involvement of several national and international organizations in facilitating the use of space for disaster management, it is still a relatively unknown field. Members of academia, industry, governments, and the general public can benefit from addressing this gap, and increasing knowledge of how space is used in preparing for, responding to, and recovering from disaster events.
The main objectives of the STDM group are to inform general public about how space-derived information are valuable in disaster management and to provide a channel for new perspectives for research efforts used in space disaster management as well as an interdisciplinary forum to those who have an interest in disaster management and space activities, and their impact on society [19].

6.1. Project – The Role of Global Navigation Satellite Systems (GNSS) and Earth Observation in Disaster Management" Workshop 2013

The STDM Project Group organised after the 12th Space Generation Congress and prior to the 64th International Astronautical Congress (IAC). With 50 top students and young professionals, it provided the opportunity to meet and exchange views with leaders of the space sector from government, industry, and academia on how GNSS and Remote Sensing technologies is used in disaster management. The event included background presentations, panel discussions, and hands-on training provided by high-level experts from local, international, and multilateral organisations for an international student and young professional audience between the ages of 18-35. The workshop also allowed delegates to explore this key topic, get some interactive hands on experience using key tools, and network with other professionals as well as with GNSS experts [20].

7. YOUTH PROMOTING COOPERATION AND EDUCATION IN GNSS (YGNSS) PROJECT GROUP

The YGNSS group is a team of university students and young professionals who aim to help bring the maximum benefits of the Global Navigation Satellite System, or GNSS, to society. YGNSS supports the International Committee on GNSS (ICG), an international forum for cooperation on Global Navigation Satellite Systems recognized by the United Nations. Two of the primary goals of the project team are to provide input to ICG, particularly on matters related to education and public outreach, and to act as a medium for information dissemination on GNSS. Among other activities, YGNSS conducts promotional activities relating to cooperation in GNSS and GNSS applications and presents the benefits of GNSS at various conferences around the world [21].

7.1. Project – YGNSS Workshop on Interoperability and International Cooperation 2015

The YGNSS organised a workshop on interoperability and international cooperation, taking place in November 2015 [22].
The introduction Galileo, Beidou and new systems in the satellite navigation scene raised a wide and deep discussion on how users can benefit from a multi-system scenario. The navigation community has set up mechanisms of international cooperation (ICG Working Group A, annual meetings of the Interoperability Working Group) towards achieving a cluster of systems that can potentially complement each other. Interoperability is thus a subject that will be of paramount importance in the future, as it is today and will require a mentality of international cooperation. However, since it is not a core topic in a traditional GNSS college course, this workshop indends to fill that gap with compelling lectures, discussions and a hands-on tutorial.
Moreover, it aimed to provide an opportunity for the next generation of GNSS professionals to meet the actors of today, targeting top industry, research and academia [22].

7.2. Project – Presentation to the PNT Advisory Board

The YGNSS group presented the SGAC activities to the Positioning, Navigation, and Timing Advisory Board on the Introduction of Youth for GNSS (YGNSS) and the results from the Space Generation Congress (SGC). The National Space-Based Positioning, Navigation, and Timing (PNT) Advisory Board provides independent advice to the U.S. government on GPS-related policy, planning, program management, and funding profiles in relation to the current state of national and international satellite navigation services [23].

8. SPACE SAFETY AND SUSTAINABILITY PROJECT GROUP

The SSS project group aims to encourage active participation among students and young professionals in space safety and sustainability related debates and activities, create an international space forum to showcase the perspectives of the next generation of space leaders on the safety and long-term sustainability of outer space activities and afford current industry stakeholders access to a pool of young space enthusiasts interested in space safety and sustainability related issues [24].

8.1. Project – Active Debris Removal

During the past few years, several research programs have assessed the current state and future evolution of the Low Earth Orbit region highlighting the urgency for active debris removal (ADR). An Active Debris Removal System should be capable of approaching the selected debris object through a close-range rendezvous, establishing physical contact, stabilizing its attitude and finally de-orbiting the debris object using a type of propulsion system in a controlled manoeuvre.
In this long running project (now in its third year), a novel method was proposed based on modifying a launch vehicle upper stage for the removal of large rocket bodies from polar orbit. The project focused on assessing the feasibility of such a method by analyzing propulsive requirements, technological feasibility and re-entry safety. The groups investigated different methods of approach and de-orbiting (chemical, chemical-EDT) using Analytical Graphics Inc. Systems Tool Kit (STK) and ESA software DRAMA [25].

8.2. Project – Recommendations to the UNCOPUOS

The use of nuclear power for spacecraft has enabled several important missions in the past and it can continue to do so as long as the necessary safety measures are undertaken [26].
For this, the group presented the following recommendations to the UNCOPUOS [26]:

- If a spacecraft will use a nuclear core, it shall carry it to orbit and start the fission reaction only in orbit, as opposed to using nuclear propulsion as a means to reach orbit.
- For all spacecraft using nuclear power, special emphasis shall be placed on the robustness and sturdiness of the nuclear power system. It shall be protected against debris impacts, re-entry stresses, and extreme temperatures.
- Deep space missions carrying nuclear power systems shall use non-direct transfer orbits if possible.
- Upon reaching their end of life, all spacecraft in low Earth's orbit using an RTG system shall be re-entered in a controlled manner and assuring the intact survival of the nuclear power system.
- Upon reaching their end of life, all spacecraft using nuclear reactors or using an RTG in geosynchronous orbit, shall be transferred to a "graveyard" orbit. This graveyard orbit should be selected in such a way as to assure stability (i.e. do not decay or present a collision hazard) for the duration of the nuclear fuel's half-life or until the radiation emitted does not pose a hazard for human populations
- For every mission considering nuclear power, there shall be an independent nuclear safety panel (similar to the USA's Interagency Nuclear Safety Review Panel (INSRP)) to assure that all safety procedures are followed
- Safety efforts must focus on planning and prevention rather than investigation of accidents.

9. CONCLUSIONS

The eight current project groups of SGAC provide valuable hands-on experience opportunities for students and young professionals, promoting the promoting the views of a young generation of space professionals.
In 2015 alone, the 8 project groups have published more than 10 papers and attended the major conferences in their fields, confirming the interest and quality of the work developed by SGAC members.

10. REFERENCES

[1] Space Exploration Project Group Website 2015 http://spacegeneration.org/projects/space-exploration.html

[2] CALZADA, A. et al. 2014, "The Global Exploration Roadmap – A Global Strategy from SGAC's point of view", 65th International Astronautical Conference, Canada

[3] What is Lunar Mission One (website) https://lunarmissionone.com/what-is-lunar-mission-one.html

[4] Analog Planetary Operations Group 2015 https://analogplanetaryoperationsgroup.wordpress.com/2015/10/26/sewg-and-apo-g-announces-merger/

[5] ALCIDES Team Facebook Page https://www.facebook.com/TeamALCIDES/

[6] Space Law and Policy Group Website 2015 http://spacegeneration.org/projects/space-law.html

[7] Space Law and Policy Annual Report 2015 to the Project Coordinator

[8] SGAC response to UN COPUOS Legal Subcommittee Conference Room Paper A/AC.105/1039/Add.4, "Questions on suborbital flights for scientific missions and/or for human transportation"

[9] S3-SGAC, "Objectives of the Survey on the Regulatory and Economic Aspects of Nano-Satellites by S3-SGAC" (internal document), 2014

[10] The Commercial Space Project Group Website http://spacegeneration.org/projects/commercial-space.html

[11] $pace is Business competition website http://spacegeneration.org/projects/commercial-space/103-competitions/965-pace-is-business-2014.html

[12] SERRA, L. et al 2013, "Microsatellites and microlaunchers: the tandem that will disrupt the satellite industry", 64th International Astronautical Congress, Beijing, China.

[13] Near-Earth Project Group Website 2015 http://spacegeneration.org/projects/neo-project-group.html

[14] Move an Asteroid competition website 2015 http://www.spacegeneration.org/component/content/article/103-competitions/1389-move-an-asteroid-2015-competition.html

[15] Rumpf, C. 2014, "Global Asteroid Risk Analysis", SGAC Move an Asteroid competition, available at http://spacegeneration.org/images/stories/Projects/NEO/winning_papers/2014-Clemens%20Rumpf_MAA.pdf

[16] "Find an asteroid" competition 2015, http://spacegeneration.org/component/content/article/103-competitions/1397-find-an-asteroid-2015.html

[17] Small Satellites Project Group website 2015 http://www.spacegeneration.org/projects/small-sats.html

[18] SGAC Small Satellites Project Group Annual Report 2015

[19] Space Technologies for Disaster Management group website 2015 http://spacegeneration.org/projects/space-technologies-for-disaster-mgmt.html

[20] "The Role of GNSS and Earth Observation in Disaster Management" Workshop 2013 http://www.spacegeneration.org/projects/space-technologies-for-disaster-mgmt.html?id=825

[21] YGNSS Project Group website 2015 http://spacegeneration.org/projects/ygnss.html

[22] YGNSS Workshop on Interoperability and International Cooperation 2015 http://spacegeneration.org/zh/event/ygnss-workshop-2015.html

[23] YGNSS Project Group Annual Report 2015 (to the project coordinator)

[24] Space Safety and Sustainability Project Group 2015, http://spacegeneration.org/projects/space-safety-and-sustainability.html

[25] Active Debris Removal Technical Paper, http://www.spacegeneration.org/projects/space-safety-and-sustainability.html?id=1120#ADR

[26] SGAC SSS Group, “National research on space debris, safety of space objects with nuclear power sources on board and problems relating to their collision with space debris”, presented to the UNCOPUOS, 2015 Available at: http://www.unoosa.org/pdf/limited/c1/AC105_C1_2015_CRP08E.pdf

SESSION 7: B - Nanosat Technologies

(Thursday 11th - 11.30)

Chairman: Prof. Anton Ivanov

TOWARDS A COLLABORATIVE DISTRIBUTED GROUND STATION FOR SMALL CUBESAT TEAMS

Lasse Bromose[*], Anders Ellersgaard Kalør[*], and Jesper Abildgaard Larsen[†]

Department of Electronic Systems, Aalborg University, 9000 Aalborg, Denmark
[*]{*lbromo12,akalar12*}*@student.aau.dk*

[†]*jal@space.aau.dk*

ABSTRACT

Most student developed CubeSats are operated from a single ground station, which may become a bottleneck in getting mission science data. This paper presents a distributed ground station system which allows CubeSat teams to collaboratively share their ground station. System requirements are formed based on experience from previous satellite missions and include scalability, robustness and data-link protocol independence. To provide scalability, the connected ground stations use a distributed coordination algorithm for assigning roles during passes. If multiple ground stations receive frames from the same satellite, the frames are merged by the system to reduce the number of bit errors.

A performance evaluation of the system indicates that it can handle more than 140 ground stations without a decrease in performance, and that the system is tolerant to high network latencies and packet loss. Experience from using the system during the AAUSAT5 mission confirms that the ground station works as intended.

1. INTRODUCTION

Over the recent years, the number of nano- and picosatellites developed by university students has increased rapidly. In particular the CubeSat standard, defining a 1 kilogram and $10 \times 10 \times 10$ cm cubic satellite, has attracted attention due to the low cost and the manageable amount of complexity. Since the launch of the first CubeSat, the platform has proven to be capable of carrying advanced payloads and to be well suited for space experiments. For these reasons, the CubeSat platform is often used by universities as an entry point to space engineering, and for carrying out experiments in space.

Most CubeSats are deployed into a low Earth orbit (LEO). This induces a low orbital period, and hence short pass duration. Together with the generally short lifetime of less than a year [Swa13], this significantly limits the effective operational time of CubeSats and hence the possibilities of operating the satellite, and for downloading payload data. Large satellite manufactures usually handle this by using high-coverage ground station networks and high throughput radios. However, these are infeasible options for most university CubeSat teams and in particular for newcomers in space. Therefore, most CubeSat teams operate using a single ground station and may not exploit the full potential of their satellites. During critical phases, such as the Launch and Early Operations phase (LEOP), where the initial signals from the CubeSat are of vital importance, CubeSat teams are often assisted by radio amatures, who voluntarily listen for the CubeSats and report signals. However, reporting the received signals is often a troublesome process and is often limited to CW beacons which do not provide much information to the CubeSat teams.

In this paper, we present a collaborative distributed ground station developed for small CubeSat teams which allows universities, radio amatures and other volunteers to help receiving and providing signals directly to operating CubeSat teams. We discuss the overall requirements derived from experience from CubeSats built by students at Aalborg University, as well as the overall design and implementation. We also present performance evaluation results and discuss future work.

There have been several proposals for a distributed ground station network for student satellites. Most notably is the Global Educational Network for Satellite Operations (GENSO) coordinated and supported by the ESA Education Office [Edu15]. The GENSO project was initiated in 2007 and several universities have participated in the development including several groups of students from Aalborg University [NDK08]. However, the project is currently not active. GENSO was developed to be a system connecting ground stations around the world using the Internet, and thereby allowing operators to communicate with their satellites from all over the world. GENSO aimed to provide several services, including scheduling of uplink sessions and error correction by using several ground stations. These are services which are important for a shared ground station, and therefore we aim to provide the same in the system presented in this paper.

The GENSO ground station consists of three main parts: a Mission Control Client (MCC), a Ground Station Server (GSS), and an Authentication Server (AS). The MCC was used by the satellite team as an interface to the ground station network. The MCC authenticated with the AS, which was controlled by a trusted GENSO administrator. When authenticated, the MCC was allowed to interact with the GSS. This division of responsibilities allows for a secure network while relaxing on the security requirements of the GSSs. This is important since the GSSs are out of the hands of the system operators.

One of the main drawbacks about GENSO is the fact that it was designed exclusively for the AX.25 protocol. While many CubeSats use AX.25, new and more efficient protocols are being developed. For instance, the CubeSat Space Protocol (CSP) [Wik15] developed by Aalborg University and used in AAUSAT3, AAUSAT4 and AAUSAT5, as well as GomSpace satellites, cannot be used with GENSO as it is not compliant with the AX.25 protocol. This is a limitation which we remove in the ground station presented in this paper.

The remainder of the paper is organized as follows. In Section 2 we discuss the background context and the main motivation behind this work. Section 3 introduces the primary system requirements and in Section 4 we introduce the overall system architecture used in our distributed ground station. Section 5 discusses the implementation of the system and in Section 6 we evaluate the performance of the implemented system. Section 7 discusses the results and future work of the distributed ground station. Finally, we summarize our contributions in Section 8.

2. BACKGROUND

A total of four CubeSats have been developed, launched and operated by students at the Electrical Engineering and Information Technology programme at Aalborg University [LN11]. Our first satellite, AAU-CubeSat, was launched in June 2003 and the latest satellite, AAUSAT5, was launched from the International Space Station in October 2015 as part of the ESA Fly Your Satellite from the ISS! programme. From developing and operating the CubeSats, we have gained a significant amount of experience. One example of this is from the mission of AAUSAT3, where the ground station setup was identified as a bottleneck, as the payload, an AIS receiver, was producing more data during a single orbit that the ground station was capable of downloading. This was despite the fact that AAUSAT3 was deployed into a near-polar orbit with daily high elevation passes over our ground stations in Aalborg, Denmark and Thule, Greenland.

For AAUSAT5 the problem was presumed to be even larger as AAUSAT5 was deployed from ISS with an inclination of approximately 52 degrees. AAUSAT5 would never pass Thule, and the quality of the link from our ground station in Aalborg would be limited due to the low elevation. This led us to the desire of expanding our network of ground stations.

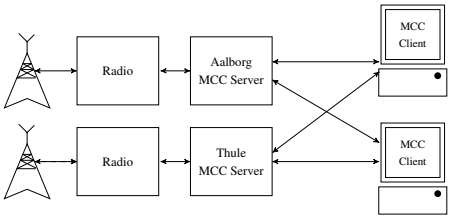


Figure 1: The previous ground station configuration. The client connects through the MCC Client software to a MCC Server, located at the ground station, which controls the radio and rotor.

With the previous ground station system used at Aalborg University, an operator can connect to any of the ground stations from an arbitrary PC and use it for communication (Figure 1). While this approach is manageable for two ground stations, it does not scale well. Furthermore, the ground stations do not collaborate, so the operator must change ground station during the pass if the ground stations overlap. As the passes are of short duration and the operator usually has a tight schedule for each pass, monitoring and switching between several ground stations is an undesired additional task.

After the launch of AAUSAT5 it was found that the downlink signal was weaker than expected. Only with the help from radio-amateurs we managed to get a stable two-way communication link with AAUSAT5. Currently Lars Mehnen (OE3HMW) from Austria and Mike Rupprecht (DK3WN) from Germany are hosting receiving ground stations, and by transmitting from our ground station in Aalborg, we are able to communicate with the satellite. To operate this scenario with the previous ground station system, the operator is required to connect to each of the three ground stations and monitor the transmission and reception on each of them. This is inefficient and increases the risk of making wrong conclusions and decisions while operating the satellite. The distributed ground station system presented in this paper overcomes this problem by autonomously controlling several ground stations.

3. SYSTEM REQUIREMENTS

The overall requirements for the system are based on experience from earlier missions flown by Aalborg University, especially AAUSAT3. The primary requirements are the following:

- Scalability
- Decentralized, fault-tolerant coordination
- Data-link protocol independent

Scalability is the central requirement for the distributed ground station as the main motivation behind the system is the lack of scalability in the previous system. Furthermore, the ISS orbit imposed to AAUSAT5 encouraged us to look for additional ground stations in Central or Southern Europe, and the number of ground stations should not be limited by system capabilities. As part of the scalability aspect, it is desirable for the ground station network to employ decentralized coordination. This is mainly due to a long term desire of inviting radio amateurs to participate in the missions. In this case, the system shall handle sporadic crashes and connect to the network whenever the ground station owner wants to share her resources. In order to fulfill this requirement, fault tolerance must be taken into consideration in the core of the system. AAUSAT5 is designed to use the CubeSat Space Protocol which is fairly new and not so widely used by CubeSats. Therefore, in order to make the system attractive for other CubeSat teams, the distributed ground station is required to be data-link protocol independent. This also allows existing satellites to make use of the system which is important as it allows us to test the system using already launched satellites.

Besides the primary requirements, there are other desired properties of the system. This includes the possibility to correct bit errors by combining frames received by multiple ground stations as well as a resource allocation scheme so that teams know when communication slots are allocated for their CubeSat. While the actual frame combining and the resource allocation are not the main priorities of the initial system design, the ability to support and extend these features is important. Therefore, they are considered important parts of the system.

4. SYSTEM ARCHITECTURE

The developed distributed ground station is divided into two subsystems; the ground station controller (GND CTRL) and the distributed ground station proxy (Client Proxy Server) as shown in Figure 2. The GND CTRL is placed at the individual ground stations and controls the radio and rotor. Furthermore, it is responsible for negotiating pass roles with other spatially close ground stations in order to determine the transmitter ground station. The Client Proxy Server acts as a layer between the client and the ground stations, making the decision made by the distributed ground station invisible to the user. The ground stations connected to the network send and receive data through the Client Proxy Server which is also responsible for detecting duplicate frames received by multiple ground stations. To keep the system independent of data-link protocols, the input and output of the GND CTRL and Client Proxy Server are bit streams of data. However, the radio located at the ground station also puts some limitations to the physical layer of the communication which must be taken into account in the coordination of ground stations.

In the following sections, we describe the main parts

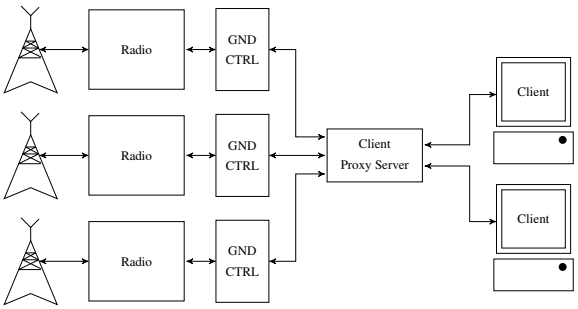


Figure 2: System architecture of the distributed ground station network.

of these two subsystems; the decentralized coordination, performed by the GND CTRLs, and the frame alignment procedure, performed by the Client Proxy Server, which removes duplicate frames received from the ground stations.

4.1. Decentralized coordination

When having multiple ground stations within line-of-sight of the same satellite, a mechanism for coordinating the transmission is required so that only one ground station transmits at a time. In order to handle the scalability requirements placed on the system, we propose a fault-tolerant decentralized coordination algorithm in which spatially close ground stations collectively decides on the transmitter. This approach has several advantages. First, it does not rely on a single node which is important in order to provide a fault-tolerant system. Second, as the coordination complexity increases as the number of ground stations increases, we exploit the fact that an increasing number of ground stations also provides an increasing level of computational power.

From a collection of ground stations, it is reasonable to use the ground station with the best link for transmission. This problem can be considered as a distributed leader election problem where the best candidate is elected as leader. In this system, we use a modified Bully algorithm. Given a set of nodes uniquely identified by an id, the Bully algorithm select the node with the highest id as leader in a fault tolerant way [GM82]. The algorithm assumes that all node ids are known by all nodes, and that crashed nodes recover to an initial state. Furthermore, it assumes that all communication is instant and that every node can communicate with all other nodes. Under these assumptions the algorithm guarantees a worst case of n^2 messages needed, where n is the number of nodes. The election time of the algorithm is independent of the number of nodes, hence election time is constant.

The algorithm is as follows [GM82]:

1. When a node suspects that the current leader has crashed it sends out an ELECTION message to all nodes with an id higher than its own.

2. Nodes with a higher id reply with an OK message and send an ELECTION message to nodes with higher ids than itself.
3. If a node does not receive an OK message, and therefore is the node with the highest id, it sends out a COORDINATOR message to inform the other nodes about the election result.

Due to the assumptions in the Bully algorithm, some modifications are needed to use the algorithm to select the currently best ground station as transmitter. First, as the satellite link quality changes over time, the ranks (i.e. node ids) are not static or known before-hand. Instead, we introduce a cost function using which the ground stations calculate their costs upon each election, and the ground station with the lowest cost becomes the transmitter. The cost function is defined by the current elevation, e, and the remaining time of the pass, t, by the following function:

$$cost(e,t) = \begin{cases} \frac{1}{11}\left(10\left(1-\frac{e}{90}\right)+\left(1-\frac{t}{20\cdot 60}\right)\right) & \text{if } e > 0 \\ 0 & \text{if } e \leq 0 \end{cases}$$

As the cost may not be unique (this is required for the Bully algorithm to terminate) each ground station is assigned an unique 32-bit id, and the ground station id is concatenated to the cost to create a unique cost while keeping the order defined by the cost function. The unique cost is defined as:

$$unique_cost(e,t,id) = cost(e,t) \cdot 2^{32} + id$$

When a ground station initiates an election it will broadcast the ELECTION message to all its neighboring ground stations, as the costs of the other ground stations are unknown. Furthermore, to overcome the assumption of instant communication we have introduced an election timer. If a ground station does not receive an OK message before the timer times out, the ground station assumes that it won the election and sends a coordinator message to all its neighbors. To reduce the message complexity of the modified Bully algorithm a few heuristics are implemented. This includes an exponential back-off period based on the cost so that a ground station with a low cost replies with an OK message faster than ground stations with high costs. In this way, only a fraction of the ground stations transmit OK messages upon an election, and the total number of messages passed per election is reduced.

The election process is implemented as a state machine as shown in Figure 3. The ground station starts in the *Idle* state and goes to the *Election* state when it receives an ELECTION message with a higher cost, or it has AOS from a satellite. If the ground station wins the election it transitions into the *Coordinator* state where it stays until an election is lost or it has LOS from a satellite.

4.2. Frame alignment

Having multiple ground stations listening for the same satellite requires a mechanism for aligning frames so that

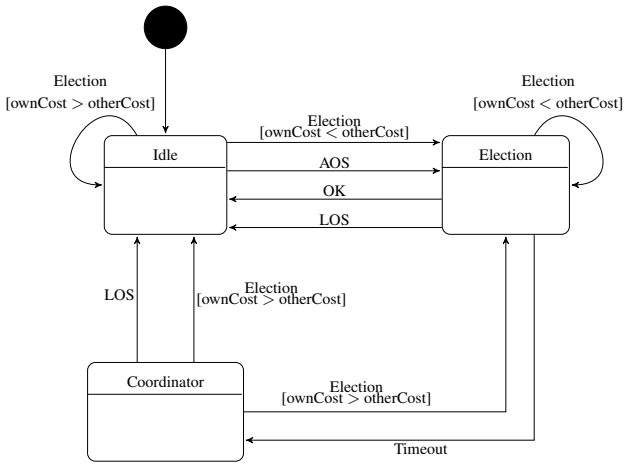


Figure 3: State machine defining the transmitter election algorithm.

the client does not receive the same frame from each receiving ground station. Due to the desire of having a data-link protocol independent system, this functionality cannot be implemented by using frame content such as sequence numbers. Another possibility could be to compare received frames and align identical frames. However, this method has two major drawbacks. First, wireless communication is exposed to noise and hence ground stations may not decode the same frame identically. Second, if two identical frames are intentionally transmitted subsequently but received by to different ground stations, then they will be treated as the same frame. The approach proposed for this project is to use reception time. Although ground stations may receive the same transmitted frame with a small time difference, this is considered to be insignificant compared to the data rates usually used on today's CubeSats. One major drawback of this approach, though, is that the ground stations must be time synchronized. In this paper, we assume that the ground stations are equipped with a GPS disciplined oscillator (GPSDO) as this provides sufficient synchronization. At the time of reception, the ground station assigns a timestamp to the received frame and forwards it to the Client Proxy Server which is in charge of aligning the frames.

For simplicity, we first assume that the Client Proxy Server is aware of all received frames. We merge frames which are received by the ground stations within a certain time frame. Formally, we consider a sequence of frames $\mathcal{F} = \{f_1, f_2, \ldots\}$ with associated timestamps $\mathcal{T} = \{t_1, t_2, \ldots\}$. We are interested in finding set $\mathcal{F}_j \subseteq \mathcal{F}$ containing the same frame received by different ground stations. We do so by letting $\mathcal{F}_j = \{f_i \in \mathcal{F} | t_j - \epsilon < t_i < t_j + \epsilon\}$ for some ϵ depending on the data rate for the satellite of interest.

We now consider the fact that the Client Proxy Server does not know the entire set $\mathcal{F}$ when aligning the frames. This introduces the problem of determining when all frames which should be contained in $\mathcal{F}_j$ are received by the Client Proxy Server as the Client Proxy Server

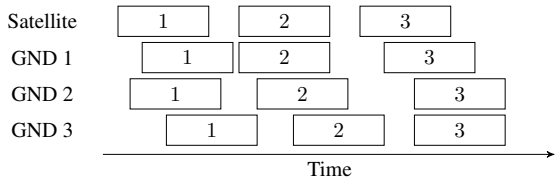


Figure 4: The frame alignment problem: Frames are received by different ground stations at different times.

receives frames delayed from the ground stations. The problem is conceptually depicted in Figure 4. We solve this problem by estimating the latency between the individual ground stations and the Client Proxy Server. By assuming that these follow a specific distribution (e.g. the Shifted Gamma distribution as proposed in [CPS02]), we can estimate the probability that a frame from a ground station should have been received (given by the cumulative distribution function). Let t denote the current time at the Client Proxy Server and let f_j be a frame already received by the Client Proxy Server. Furthermore, let X_i be a random variable denoting the latency between ground station i and the Client Proxy Server. We then perform the frame alignment when one of the following conditions are fulfilled:

1) A frame has been received by all ground stations

2) $P(X_i < t - t_j) > \delta$ for all i for which $f_i \notin \mathcal{F}$

where δ is a confidence parameter which we set to 0.99.

After the frames have been aligned, we perform a bitwise voting to merge the frames and reduce the probability of bit errors (given that more than three frames have been received). This is a very simple approach, and does not consider the fact that some ground stations have better link than others. However, the implementation allows this possibility and is something we highly consider for future work. After aligning and merging the frames, the merged frame is sent to the client who is responsible for decoding etc.

5. IMPLEMENTATION

The distributed ground station has been implemented in Java. Based on the goals of providing a scalable system with a distributed communication model, we have used the Akka toolkit [Typ14] that provides an implementation of the actor model which has proven to be very scalable and fault tolerant [Agh90]. With the actor model we were able to structure our implementation in a highly hierarchical way in which crashes are handled by parent actors. Furthermore, the actor model is consistent with the event-based nature of the system components, e.g. the coordination algorithm, where ground stations send events at AOS, LOS and during passes.

The communication between the Client Proxy Server and the individual ground stations happens through a RabbitMQ [Piv14] instance. This allows the Client Proxy Server to be unaware of the current transmitting ground stations, and greatly simplifies the handover process.

The system keeps track of ground stations and satellites using a MongoDB database [Mon14]. We utilize the built-in support for spatial search queries to discover neighbor ground stations. Storing information about the connected ground stations centrally allows us to provide information about coming passes to the client without the need to request all connected ground stations. Although the database may not be up to date in regard to crashed ground stations, this is deemed to provide sufficient information to the satellite operators.

The Client Proxy Server provides a JSON interface to the user which supports basic operations such as requesting comming passes, and transmitting and receiving bit streams.

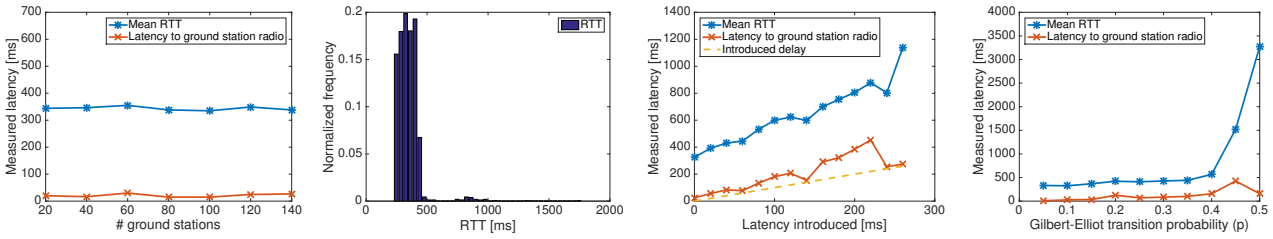
6. PERFORMANCE EVALUATION

In this section we evaluate the performance of the distributed ground station system running in a controlled environment. We first investigate how the system performs as the number of collaborative ground stations increases. Then, we seek the limitations of our system, namely how it reacts to increasing network latency and packet loss.

6.1. Performance metrics

We use latency as a metric in the performance evaluations. There are several reasons for that. First, we believe that any performance issues and crashes will be reflected in higher latencies due to the guarantees provided by the TCP protocol. Second, latency is an important parameter for the alignment algorithm as it is used for determining whether frames received from distinct ground stations are identical.

To get a adequate overview of the performance, we measure the latencies of two paths in the system: round-trip-time (RTT) from the client to the radio and back to the client, as well as the latency between the client and the transmitter radio. In order to obtain these values, we have implemented a TCP radio module which transmits data over TCP to a central server which continuously collects timestamps and replies the frames back to to radio. We are well aware that this adds an additional latency to the system. However, as we are mainly interested in how the latency evolves when varying parameters, this is considered insignificant.



(a) (b) (c) (d)

Figure 5: Performance evaluation results. (a) Latency measurements as the number of ground stations in the network increases. (b) Histogram of the round-trip-times measured as the number of ground stations increases. (c) Latency measurements for various introduced delays. (d) Latency measurements for increasing packet loss probability.

6.2. Number of ground stations

One thing of particular interest is the number of ground stations which can be connected to the distributed ground station system at the same time. The ground stations were executed on three 20 core 2 GHz virtual machines with 64 GB of memory. The Client Proxy Server and the TCP server responsible for collecting timestamps were executed on a dual-core 2 GHz virtual machine with 2 GB of memory. These machines were located in Amsterdam. The client was executed on a 2 GHz dual-core laptop located in Aalborg. The experiment was performed by incrementing the number of ground stations in batches of 20.

Figure 5a shows the average of the measured latencies. There is no significant increase in either the round-trip-time or the latency to the radio as the number of ground stations increase. The high round-trip-time compared to the latency to the radio is due to the delay of 200-400 ms added by the alignment algorithm. The peaks in both latency measurements are due to elections which periodically cause the frames to the radio to be buffered. A histogram of the round-trip-time measurements is shown in Figure 5b. From the histogram it is evident that the measured latencies are generally distributed near the mean, with a small cluster around 800-1000 ms. This is due to elections, which cause the ground stations to pause transmitting until a transmitting ground station is elected.

6.3. Various qualities of service

In this section we apply various qualities of service to the network connecting the ground stations. Identifying the network requirements is of great interest as it allows us to decide whether introducing a new ground station to the network is likely to cause problems. The quality of service parameters are introduced with the KauNet network emulator [GCPB07].

In the first experiment, three ground stations with overlapping coverage are started, and the latency between the ground stations and the remaining system parts is controlled. As previously, frames are sent periodically through the ground station network to the TCP server which replies immediately. The experiment is repeated for various network latencies, incremented with 20 ms between each experiment. The measured mean latencies are shown in Figure 5c. The measurements where the latency to the ground station radio is close to the introduced delay are due to no elections taking place during the measurement period. The latency introduced by elections increases exponentially as the simulated delay increases. This is due to the fact that the election algorithm sends several messages between the ground stations, and the delay is applied for every message. When the introduced delay reached 300 ms the ground stations were no longer able to agree on a coordinator due to the timeout period in the election algorithm, which causes multiple ground stations to become transmitters.

Another quality of service experiment is to examine how the distributed ground station is affected by high packet loss probability. We model the packet loss as a Gilbert-Eliot model depicted in Figure 6 and define the probability of packet loss in state G to be $1 - k = 0.001$ and in state B to be $1 - h = 0.5$. During the test we keep $p + r = 1$ which causes the stationary error rate to be $P(error) = (1 - k)(1 - p) + (1 - h)p$. We initialize $p = 0.05$ and increase it periodically in steps of 0.05. As TCP is used on the transport layer, packet loss will be reflected in increased latency due to retransmissions. The measurements are shown in Figure 5d. With a transition probability $p > 0.4$ the system starts to become unstable. At this point, the stationary error rate is $P(error) > 0.7$. The number of transmissions needed before a packet is received follows a geometric distribution with success probability $P(success) = 1 - P(error)$. The expected number of transmissions before the first successful reception is given by $1/P(success) = 1/(1 - 0.7) = 10/3$. Hence, in average more than two retransmissions are needed. Considering the fact that TCP acknowledgements can also be lost, the actual number of retransmissions is even higher.

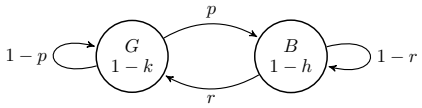


Figure 6: The Gilbert-Elliot model used to model burst packet loss.

7. DISCUSSION AND FUTURE WORK

The performance evaluation indicates that the distributed ground station handles an increasing number of ground stations without any increase in latency, and hence without any noticeable degradation in performance. This suggests that the distributed processing and coordination scheme used in the distributed ground station is indeed scalable, which was one of the main requirements to the system. The performance evaluation also indicates that the system is tolerant to increasing latency and packet loss. The point where the system breaks is above the level of packet loss and latency expected in a real network. This robustness of the system allows the system to be used in areas with various network qualities, and perhaps even using cellular networks. Being able to connect ground stations using a cellular network such as 4G ATE adds a new dimension to the possibilities of deploying a network of ground stations, and investigating these possibilities would be interesting future work.

Although the decentralized coordination algorithm has proven to be very robust during the performance evaluation, it was found that most elections terminate long before the election times out causing resources to be wasted while waiting for the timeout. In other cases, the election timer times out too early, causing more than one ground station to claim the transmitter role. One way of resolving the issue of determining the election timeout could be to estimate the delay between ground stations and wait until the election is completed with high confidence.

Another limitation in the coordination algorithm is that the cost function used to determine the transmitter ground station only uses the location of the ground station. In reality, the quality of the ground stations may vary much based on the equipment and local environment such as background noise and obstacles. However, including signal quality can be difficult, as it may cause the transmitter ground station to change often, hence potentially causing an unstable system. Developing a cost function which includes these parameters and at the same time includes a stability metric would be interesting future work for the system as well.

The fact that the signal quality varies may also be used in the frame merging algorithm, which currently weighs received frames equally. An evident improvement would be to include the signal strength in the merging so that frames received with high signal strength are weighted higher than frames received with low signal strength.

The current system does not contain a sophisticated resource allocation method, but simply allocates ground stations based on the time of AOS. However, this may be an unfair and a sub-optimal use of the available ground stations. Therefore, developing a fair resource allocation algorithm for the ground stations may also be relevant future work.

8. CONCLUSION

This paper described a distributed ground station network developed for small CubeSat teams as part of the AAUSAT projects at Aalborg University. The developed system fulfills the key requirements defined from experience in previous satellite missions, namely scalability, fault-tolerant coordination, and data-link protocol independence. Experiments show that it is able to handle 140 ground stations, and possibly more, without decrease in performance, which allows for the system to be collaboratively shared between small CubeSat teams.

Experience from AAUSAT5 mission indicates that the system works as intended with three ground stations. However, we have a desire to evaluate the system with even more ground stations in the future. To facilitate this, we are currently extending the system to include a GNU Radio interface, which allows any radio to be used in the network. This is something that enables new teams to use the distributed ground station network without having to recompile the system.

ACKNOWLEDGMENTS

The authors would like to thank ESA and the study board of Electronics and IT at Aalborg University for their sponsorships which allowed us to attend this conference.

REFERENCES

[Agh90] Gul Agha. Concurrent object-oriented programming. *Commun. ACM*, 33(9):125–141, September 1990.

[CPS02] Andrew Corlett, DI Pullin, and Stephen Sargood. Statistics of one-way internet packet delays. *53 rd IETF*, 2002.

[Edu15] ESA Education. Global education network for satellite operations. `http://www.esa.int/Education/Global_Educational_Network_for_Satellite_Operations`, 2015. last visited: 11.29.2015.

[GCPB07] Johan Garcia, Emmanuel Conchon, Tanguy Pérennou, and Anna Brunstrom. Kaunet: Improving reproducibility for wireless and mobile research. In *Proceedings of the 1st International Workshop on System Evaluation for Mobile Platforms*, MobiEval '07, pages 21–26, New York, NY, USA, 2007. ACM.

[GM82] Hector Garcia-Molina. Elections in a distributed computing system. C-31(1), 1982.

[LN11] Jesper Abildgaard Larsen and Jens Frederik Dalsgaard Nielsen. *Development of Cubesats in an Educational Context*, volume 1, pages 777–782. IEEE Press, 2011 edition, 6 2011.

[Mon14] MongoDB Inc. Mongodb. http://mongodb.org, 2014. last visited: 12.05.2014.

[NDK08] Jens Dalsgaard Nielsen, Xiangyun Du, and Anette Kolmos. *A Knowledge Building approach for learning engineering: a case study of GENSO (student satellite) project*. Sense Publishers, 2008. Konferenceartikel udkommet på cdr vedlagt "Book of abstracts" ISBN 978-90-8790-571-2.

[Piv14] Pivotal. RabbitMQ - Messaging that just works. http://www.rabbitmq.com/, 2014. last visited: 09.30.2014.

[Swa13] M. Swartwout. The first one hundred cubesats: A statistical look. *JoSS*, 2(2):213 – 233, December 2013.

[Typ14] Typesafe Inc. Akka. http://www.akka.io/, 2014. last visited: 09.30.2014.

[Wik15] Wikipedia. Cubesat space protocol — Wikipedia, the free encyclopedia. https://en.wikipedia.org/wiki/Cubesat_Space_Protocol, 2015. last visited: 11.29.2015.

ICE CUBES – A FAST-TRACK, LOW-COST SERVICE FOR SMALL EXPERIMENTS TO THE ISS

Tom Hoppenbrouwers, [1], **Mauro Ricci** [2], **Thomas Peignier** [3], **Jean-Marc Wislez** [4], **Leonardo Surdo** [5]

[1] *Space Applications Services NV/SA, Belgium, Email:* tom.hoppenbrouwers@spaceapplications.com
[2] *Space Applications Services NV/SA, Belgium, Email:* mauro.ricci@spaceapplications.com
[3] *Space Applications Services NV/SA, Belgium, Email:* thomas.peignier@spaceapplications.com
[4] *Space Applications Services NV/SA, Belgium, Email:* jean-marc.wislez@spaceapplications.com
[5] *Space Applications Services NV/SA, Belgium, Email:* leonardo.surdo@spaceapplications.com

ABSTRACT

The International Commercial Experiment Cubes service (ICE Cubes) will provide rapid, simplified, low cost access to the International Space Station (ISS), creating the opportunity to maximize the use of the remaining lifetime of the ISS. The ICE Cubes service will enable any organisation, public or private entity or individual to perform experiments on the ISS, with a specific focus towards universities, academic programmes and (European or National) Space Agency educational programmes.

Space Applications Services is currently developing, supported by the European Union, the ICE Cubes on-orbit facility, aiming at a launch to and installation in the ISS towards the end of 2017. The ICE Cubes facility will enable accommodation of up to 20 single Experiment Cubes (default size 1U = 10cm x 10cm x 10cm) or a smaller number of multi-unit Experiment Cubes and can be installed in a drawer of an ISS rack. A cross-platform compatible core of the ICE Cubes facility is under development and the facility external interfaces will be completed once the agreements with a Space Agency are finalized. Independently on their dimensions, the Experiment Cubes will adopt standardized physical and operational interfaces. Each Experiment Cube may be equipped with commercial off-the-shelf (COTS) components, significantly reducing the cost and duration of development and allowing for the utilization of the most recent technologies. This standardization approach greatly reduces complexity and allows universities and schools to develop and build experiments for the ISS more easily.

In addition to reducing the complexity to construct experiments for the ISS, Space Applications Services significantly lowers the 'entry barrier' to the ISS by providing an end-to-end service to the users. I.e. the ICE Cubes service fully supports the process of experiment development (if requested) and takes care of the flight acceptance launch manifest and operations of the users' Experiment Cubes. Furthermore, an out-of-the-box installable ground monitoring and control software allows the users to access their Experiment Cubes directly from their premises. In order to initiate and validate the ICE Cubes service, the International Space University (ISU) will become the pilot user: ISU is developing the Experiment Cube #1, to be launched together with the ICE Cubes facility.

The plug-and-play nature of the ICE Cubes experiments in combination with the provided ICE Cubes services will result in a 'cradle-to-orbit' time (Experiment Cube construction, flight acceptance and launch readiness) of one year, fitting very well with academic schedules. Non-standard Cubes and multi-unit Cubes may require a slightly longer period.

1. INTRODUCTION

The International Space Station (ISS) is a great technical achievement, designed as a flexible laboratory able to support the performance of science and education activities in a wide range of disciplines. Now fully assembled and with its Full Operational Capability in place since 2011, there is a major opportunity for Europe and the world to exploit its capabilities to the maximum extent. However, making use of the ISS is still deterrent for the majority of potential users, because of the burden of complex rules, procedures and reviews associated with e.g. development, product assurance, flight qualification, documentation, launch scheduling , operation of equipment on board the ISS. This weighty process translates into many years from initial idea to flying the resulting experiment/payload.

The August 2012 "*Independent Evaluation of ESA's Programme for Life and Physical Sciences in Space (ELIPS)*" report by the European Science Foundation (ESF) makes several recommendations on how science/ELIPS should be improved. The following are excerpts from the ESF recommendations: (1) reaching out to a broader scientific community, (2) mixing direct research with curiosity-driven activities, and (3) reducing the turnaround time (time from the Announcement of Opportunity to actual implementation of an experiment on the ISS).

ESA and the European Commission are now poised to make changes in the way Europe develops payloads and

accesses the ISS providing an opportunity not only for European but also for international customers. Some changes are already underway, such as the use of commercial off-the-shelf (COTS) parts (e.g. CubeSat components) in payload developments, preventing lengthy and costly qualification processes. Other changes are expected to be implemented in the near future, which should simplify the approach to experiments development.
The ICE Cubes service aims at significantly lowering the 'entry barrier' to the ISS and drastically shortening the 'turnaround' or 'cradle-to-orbit' time for small experiments to the ISS.

2. ICE CUBES CONCEPT

2.1. Overall Concept

Space Applications Services will establish the International Commercial Experiment Cubes (ICE Cubes) service, which will provide rapid, simplified, low cost access to the ISS**,** creating the opportunity to maximize its use for the remaining lifetime. The ICE Cubes service will enable any organisation, public or private entity, such as universities, academic programmes, schools, (European or National) Space Agency educational programmes research and development institutions, to perform experiments on the ISS.
Space Applications Services is currently developing, supported by the European Union[1], the ICE Cubes on-orbit facility and the relevant ground infrastructure, aiming at a launch to and installation in the ISS towards the end of 2017. The ICE Cubes facility comprises a Framework that can accommodate up to 20 single Experiment Cubes (default size 1U = 10cm x 10cm x 10cm) or a smaller number of multi-unit Experiment Cubes and can be installed in a drawer of an ISS rack. A cross-platform compatible core of the ICE Cubes facility, making it easily adaptable to different hosting locations in the ISS (different payload racks, centre-aisle locations, etc.) is under development and the facility external interfaces will be completed once the agreements with a Space Agency are finalized. Independently on their dimensions, the Experiment Cubes will have standardized physical and operational interfaces. Each Experiment Cube may be equipped with COTS components, significantly reducing the cost and duration of development and allowing for the utilization of the most recent technologies. This standardization approach greatly reduces complexity and allows universities and schools to develop and build experiments for the ISS more easily.

In addition to reducing the complexity to construct experiments for the ISS, the ICE Cubes service significantly lowers the 'entry barrier' to the ISS by providing an end-to-end service to the users. I.e. the ICE Cubes service fully supports the process of experiment development (if requested) and takes care of the flight acceptance launch manifest and operations of the users' Experiment Cubes. Furthermore, an out-of-the-box installable ground monitoring and control software will allow the customers to access near real-time their Experiment Cubes directly from their premises.
The plug-and-play nature of the ICE Cubes experiments in combination with the provided ICE Cubes services will result in a 'cradle-to-orbit' time (Experiment Cube construction, flight acceptance and launch readiness) of one year, fitting very well with academic schedules. For non-standard Cubes and multi-unit Cubes a slightly longer period is envisaged.

2.2. Accommodation on-board ISS

The accommodation of the ICE Cubes facility on-board the ISS is not defined yet and will be subject to negotiation and agreement with Space Agencies.
In parallel with the design and development of the cross-platform compatible core of the ICE Cubes facility, a partnership with the European Space Agency (ESA) is being proposed in the frame of the Call For Ideas (CFI) *"Space Exploration as a Driver for Growth and Competitiveness: Opportunities for the Private Sector"* about the possibility to accommodate the ICE Cubes facility and exploit the service in the Columbus module of the ISS.
The partnership idea has been selected for consultation by an ESA panel, out of 60 ideas received in response to the CFI.
Following the first consultation meeting, ESA and Space Applications Services are presently assessing the possibility to initiate a pilot phase for reviewing the implementation feasibility of the partnership idea and for jointly maturing the partnership approach.

3. ICE CUBES FACILITY OVERVIEW

The ICE Cubes facility is composed of 1) the Framework, hosting the Experiment Cubes, 2) a Case/Drawer, providing containment and mechanical interface to the ISS, and 3) ancillary parts such as jumper cables for power and data interface from/to the ISS.

[1] The ICE Cubes project has received funding from the European Union's H2020 Program for research, technological development and demonstration under Grant Agreement No. 666815.

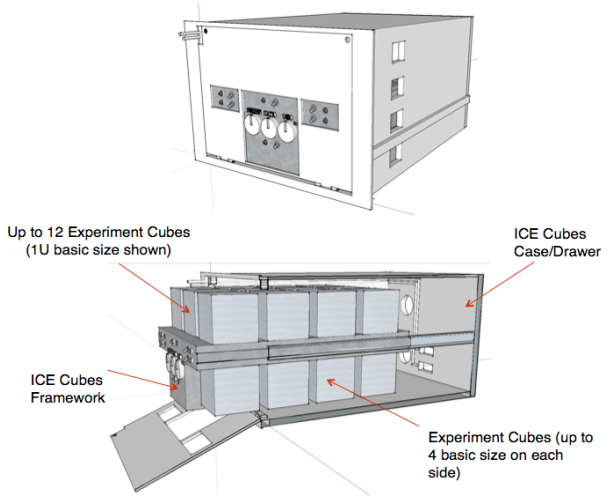


Figure 1. ICE Cubes Framework Facility

The Framework is designed following criteria of simplicity and cross-compatibility with the various possible accommodation platforms on board the ISS. The role of providing external mechanical interfaces is left to the Case/Drawer, whose design will be finalized following the agreement with the Space Agency about the accommodation of the ICE Cubes facility inside the ISS and the associated service.

The Framework is powered by a single feed (10A, 28V, 280W). A LAN port is present for communication to/from the ISS infrastructure and to/from ground. Additional dedicated telemetry (TM) line(s) could be added, e.g. for hardwired temperature monitoring or smoke sensing, depending on the specific accommodation needs. The system is conceived to be monitored and operated from ground. Nominal intervention of the crew is limited to activation of power switches, exchange of Experiment Cubes and collection of scientific data on USB flash drive, if requested.

Experiment Cubes will be connected to the Framework via power and data connectors (utilization of USB Type-C connectors is under study).

The Experiment Cubes can be functionally interconnected via the network offered by the Framework. The facility housekeeping and the scientific data will be stored on a removable hard drive and will be downlinked to ground according to the capabilities offered by the ISS infrastructure. The ICE Cubes service will be, anyway, compatible with the forthcoming ESA-developed Multi-Purpose Computer Communication (MPCC) enhancement system, which will allow for monitoring and control of the experiments, via IP communication protocols, directly from the customer's users' home base.

Different voltages / power profiles will be available for each Experiment Cube location e.g. 5V, 2.0A (10W), and 12V, 3.0A (36W). The power requested by the Framework to support internal and housekeeping functions is kept to a minimum by design optimization. Most of the power remains available for the Experiment Cubes. A minimum amount of power will be guaranteed to each Experiment Cube without restrictions. Higher power allocations will be possible, conditional to a review of the Experiment Cube's operational profile and a stage analysis of the increment.

The Case/Drawer is an aluminium structure providing mechanical interface to the ISS. It also serves as containment for both Framework and Cubes, and contributes to defining the path for internal forced-air circulation used to thermally control the Framework and the Experiment Cubes. Depending on the accommodation on board the ISS and the cooling system offered by the ISS infrastructure, the Case/Drawer will provide inlet/outlet windows for air, fans or air/water heat exchanger.

All the elements of the system will be qualified to comply with the scenario of the possible available launchers. The approach for packaging for launch (and return) shall be soft-stowed in foam/Nomex® and contained in a standard NASA Cargo Transfer Bag (CTB).

The same soft-stowage approach will be adopted for the Experiment Cubes during the service phase, as illustrated in Fig. 2.



Figure 2. Experiment Cubes Soft-Stowed in Foam/Nomex®

4. ICE CUBES SERVICE

The ICE Cubes service will consist of an engineering service, an operations service and a sales service, and will have the following unique advantages:

1) Fast-track, low-cost: the whole service will be provided over a timeframe of one year (from the moment a user signs a contract until the operations of his/her Cube on board the ISS) and for a fixed cost.
2) Complete 'end-to-end service', including payload development support (if needed), interfacing with the Space Agency and Launch Authority, and handling and monitoring the on-board operations.

An overview of the service is illustrated in Fig. 3

4.1. Engineering Service

One of the ICE Cube service's objectives is to open the exploitation of the ISS also to experiments selected, developed and operated with non-Agency funds. The user (e.g. university, school, private entity or national Agency) proposing an experiment for exploitation in ICE Cubes remains the owner of the experiment itself and responsible for the mission success. The ICE Cubes service will submit the experiment data to the Space Agency hosting the facility and to the Launcher Authority for flight certification and integration on the ISS. Certification will be limited to adequacy of the deliverable for flight and operation on the ISS, i.e. adhering to the launch vehicle and ISS safety requirements, while reliability aspects –correct implementation of scientific, functional and performance requirements– will be under the responsibility (and financial risk) of the Cube owner. The users will (obviously) select the topic and define the scientific requirements. They will also design and develop the experiment hardware or purchase it from a third party.

This approach will save a lengthy experiment selection process (as it is common with Announcements of Opportunities and peer-reviewed science) and will avoid numerous design- and safety-related reviews with the Space Agency. Space Applications Services, as service provider, will streamline the processes with the Agency and ideally will work towards one (the Phase III) flight acceptance safety review with the Agency, the Phase 0/I and Phase II steps being run internally. The overall result will be the 'fast-track' implementation of small experiments, i.e. a 'cradle-to-orbit' time of about one year. It has to be mentioned that this approach is especially suitable for "small" experiments (e.g. density ~2kg/dm³ and power up to 36W, depending on the volume).

The ICE Cubes engineering service will:

- Support the Experiment Cube owners / developers / integrators in their payload development (limited support is included by default, more extensive support can be acquired at an additional cost);
- Generate Interface Control Documents (ICDs);
- Generate Safety Data Packages (SDPs);
- Accommodate and handle Safety Reviews with the Space Agency and Launch Authority;
- Interact with the involved organisations and Agencies Payloads, Safety and Operations Teams.

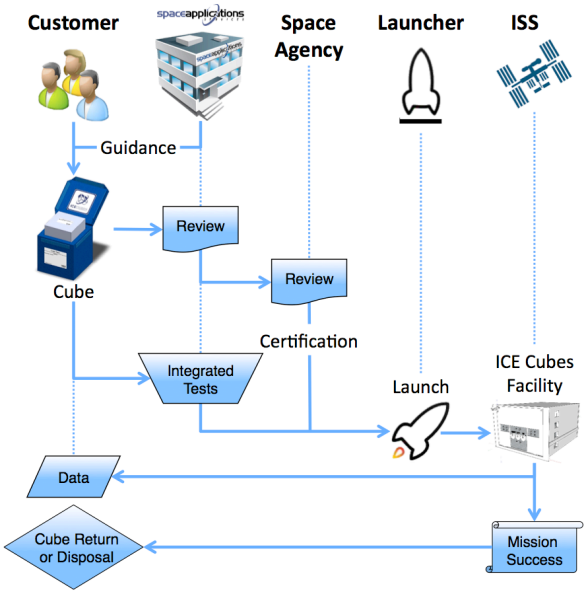


Figure 3. ICE Cubes Service Approach

4.2. Operations Service

The ICE Cubes operations service will:

- Assist in the preparation of the payload operations concept;
- Monitor and control ICE Cubes payload operations from ground (near real-time telemetry and telecommand is the target, as allowed by the communication infrastructure between Ground and ISS made available by the hosting Agency);
- Provide users with an out-of-the box installable ground monitoring and control software to allow access to their Experiment Cubes from their own premises (as allowed by the communication infrastructure between Ground and ISS made available by the hosting Agency);
- Receive and distribute data to the various users.

The operational concept is illustrated in Fig. 4

4.3. Sales Service

The ICE Cubes sales service will:

- Promote and attract experiment developers and foster cross-fertilization between different entities and organizations interested in creating small experiments for the ISS;
- Assist customers in getting flight opportunities with ICE Cubes;
- Ensure/book data uplink and downlink capabilities;
- Ensure/book crew time for Experiment Cubes installation / de-installation and (potentially) data retrieval;

- Handle disposal or book hardware (Cube or USB flash drive) download capability as requested;
- Maintain a web catalogue of miniaturized space proven/qualified off-the-shelf electronics parts and instruments.

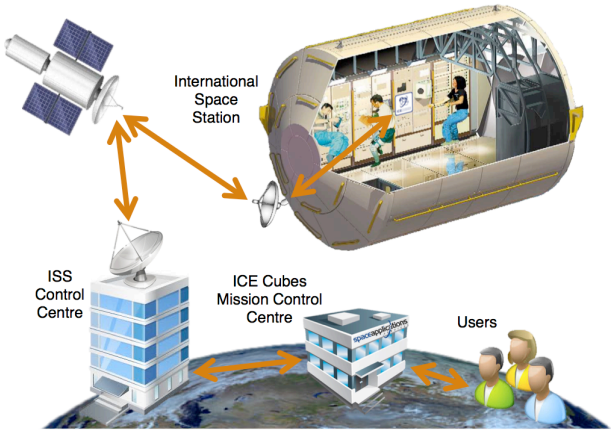


Figure 4. ICE Cubes Operational Concept

5. POTENTIAL USERS

A wide variety of potential users is envisaged, from universities and research centres, over science and industrial communities, to traditional space agency users.

The 'plug-and-play' Experiment Cubes can be very attractive to and can act as a catalyst for universities, high schools and research centres, also from 'developing space-faring nations'. The ICE Cubes service fits perfectly well in the frame of STEM (science, technology, engineering, and mathematics) education activities, in this way supporting hands-on activities, so important in the preparation of the next generation of space scientists and engineers As an example the International Space University (ISU) already committed to develop a first experiment (Experiment Cube #1) and become the pilot user of the ICE Cubes facility. The ISU Experiment Cube will be launched together with the ICE Cubes facility and a functional Cube for commissioning purposes (Cube #0).

Furthermore the ICE Cubes service can be seen as complementary to the Space Agencies Educational Programmes such as ESA's 'Spin your thesis!' (experiments in the large diameter centrifuge at ESTEC), 'Drop your thesis!' (drop tower experiments in Bremen), 'Fly your thesis!' (parabolic flight experiments in cooperation with Novespace), or like the joint DLR's (German Aerospace Centre) and SNSB's (Swedish National Space Board) REXUS / BEXUS programme (sounding rocket and stratospheric balloon experiments launched from Esrange).

The ICE Cubes service will provide a solution to the science and educational community wanting to fly small experiments to the ISS as part of or complementing the programmes already established by the various Agencies. The envisaged users are:

- ESA, for their sponsored scientific and educational payloads;
- Science and educational organisations wanting to perform experimentation for which non-Agency funds are available and a peer review is deemed not necessary;
- National Space Agencies (e.g. ASI, DLR, CNES, but also non-European Space Agencies) sponsoring scientific and promotion payloads.

6. CONCLUSIONS

The ICE Cubes service, developed by Space Applications Services, will allow for rapid, simplified and low cost development and operations of experiments making affordable the access to the International Space Station.

The service will provide a solution to the science community wanting to fly small experiments, which, due to the nature and approach of the previous Agency programmes (e.g. the ESA ELIPS) and to the characteristics of the existing infrastructure may not be so readily accommodated.

Currently under development is the ICE Cubes on-orbit facility, aiming at a launch to and installation in the ISS towards the end of 2017. The ICE Cubes facility comprises a framework that can accommodate up to 20 single plug-and-play Experiment Cubes or a smaller number of multi-unit Experiment Cubes and can be installed in a drawer of an ISS rack. A cross-platform compatible core of the ICE Cubes facility is under development and the facility external interfaces will be completed once the agreements with a Space Agency are finalized.

In parallel to the hardware and software development, the ICE Cubes service itself is being set-up, consisting of an engineering service, an operations service and a sales service. The objectives of the ICE Cube service are to lower the 'entry barrier' to the ISS and to open the exploitation of the ISS also to experiments selected, developed and operated with non-Agency funds. The plug-and-play nature of the ICE Cubes experiments in combination with the provided ICE Cubes end-to-end service will result in a 'cradle-to-orbit' time (Experiment Cube construction, flight acceptance and launch readiness) of one year, fitting very well with academic schedules.

###

HORIZON ACQUISITION FOR ATTITUDE DETERMINATION USING IMAGE PROCESSING ALGORITHMS – HORACE ON REXUS 16 – AN EDUCATIONAL PROJECT

Arthur Scharf, Jochen Barf, Matthias Bergmann, Hakan Kayal, and Thomas Rapp

Team HORACE
Chair of Computer Science VIII – Julius Maximilian University of Würzburg c/o Prof. Dr. Hakan Kayal
Am Hubland, D-97074 Würzburg, Germany
Email of corresponding author: arthur.scharf@horace-rexus.de

ABSTRACT

HORACE is a student project of the University of Würzburg that took part in the REXUS/BEXUS programme. The aim of HORACE, the Horizon Acquisition Experiment, as payload on the REXUS 16 was to prove the concept of a horizon sensor based on image processing algorithms that extract one-axis attitude information from ordinary camera pictures in the visible spectrum. Due to its high robustness we envision the field of application of this sensor to be in the area of attitude determination for satellites in emergency cases such as uncontrolled tumbling or spinning. In addition, we aim the sensor to be applicable for rough attitude determination of small satellites. This paper provides an overview about the overall approach and layout of the experiment and describes the outcome of the project. Furthermore, the project is discussed from an educational point of view. Special attention is paid to the project challenges and achievements as well as to the interconnection between theoretical know-how and its practical application in this particular project. The lessons learned while facing the challenges and applying theoretical knowledge are described in detail.

Key words: HORACE; Horizon Acquisition Experiment; Horizon Sensor; Attitude Sensor; REXUS 16; Hands-On Project; Educational Project; University of Würzburg; Aerospace Information Technology; Space Master .

1. INTRODUCTION

The emerging sector of space technologies and their decreasing costs, due to the commercialisation of space flight, leads to more and more sophisticated technologies used in spacecraft. One of the most essential subsystems of a spacecraft is the Attitude Determination and Control System (ADCS) which is crucial for the viability of a satellite and thus has to be fail-safe and be able to work in unforeseen situations, such as uncontrolled tumbling or spinning. Besides conventional sensors like star trackers, sun sensors etc. new technologies and concepts may be used to determine the spacecrafts attitude thanks to the increasing processing power and miniaturisation of spacecraft systems.
Such a relatively new concept, using ordinary optical sensors sensitive to the visible spectrum of light instead of infrared sensors for sensing the horizon of earth, was evaluated and implemented by a technology demonstration mission, HORACE (Horizon Acquisition Experiment). By using the visible spectrum of light, we envision a future sensor that relies mostly on image processing techniques. Such a sensor might be able to use existing onboard cameras on a spacecraft and thus is weight, volume and cost efficient.
The scope of the REXUS/BEXUS programme, a bilateral agreement between the German Aerospace Center (DLR) and the Swedish National Space Board (SNSB), enabled us to develop an appropriate test platform and image processing algorithms for such a horizon acquisition. In order to validate the concept of such a horizon sensor under space-like conditions, HORACE was launched on board of REXUS 16 on May 28 2014 13:30 (UTC+2) from Esrange Space Center, Sweden. The unguided parabolic flight of the rocket provided conditions to simulate the intended operational environment.
However, even if the technology demonstration was the main objective of HORACE, the educational part of this particular mission played a significant role in the overall project life cycle, especially because it took part within the frame of the REXUS/BEXUS programme. The further sections describe not only the HORACE project itself, but also the challenges, achievements and lessons learned during the project life cycle with emphasis on the educational aspects and the interconnection between theoretical knowledge and practical realisation.

2. EXPERIMENT DETAILS

The flight segment of the experimental setup consists of five main components, further called subsystems:

the *camera*, the *core system*, the *power distribution unit*, the *measurement unit* and the *mechanical structure* (cf. Fig. 1). The following section provides only a rough experiment overview, a detailed description may be found in Barf et al. (2015).

2.1. Mechanical & Electrical Setup

All components used in the flight segment are off-the-shelf-components to reduce costs and time needed for development.

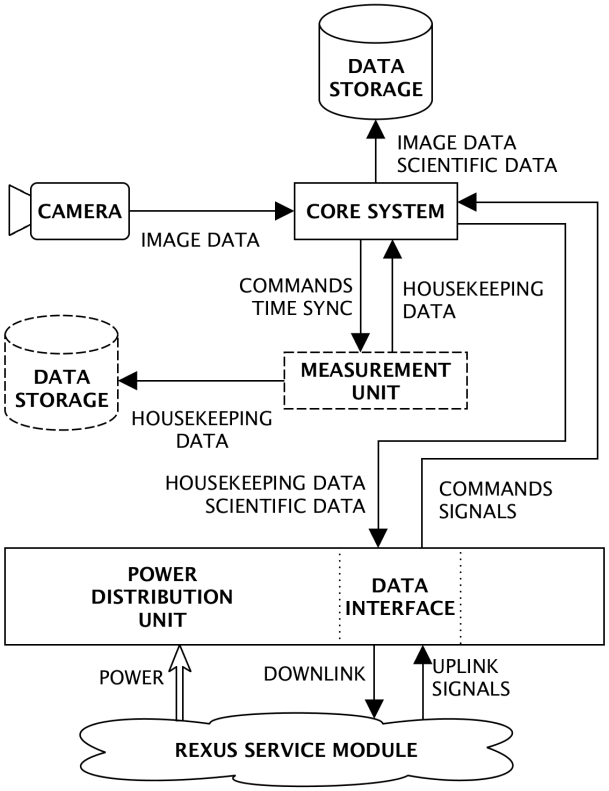


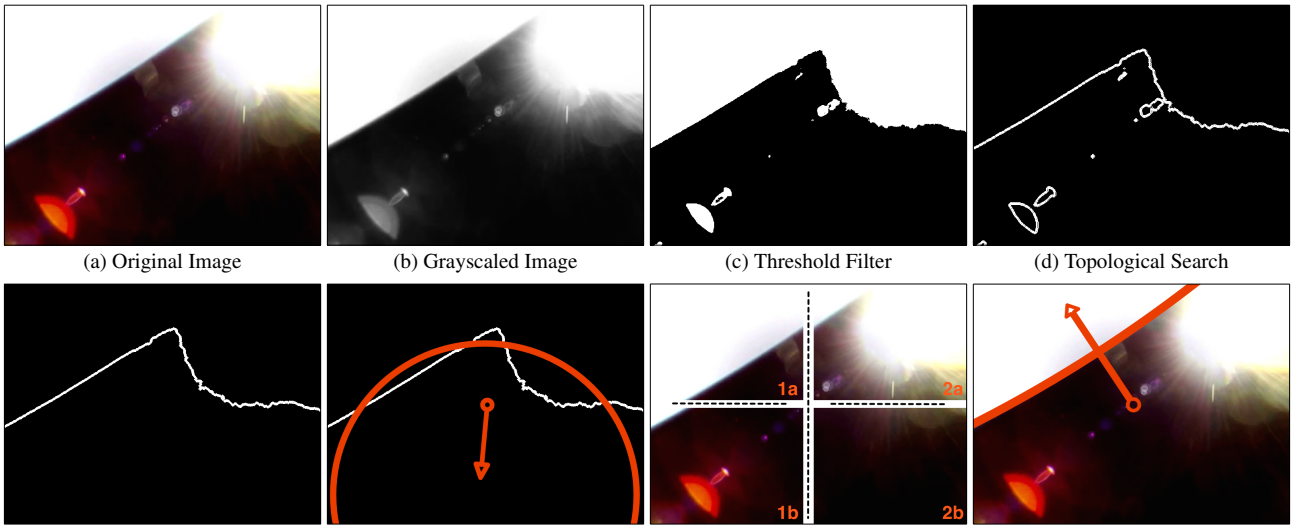
Figure 1: Block diagram of the flight segment. The measurement unit & its data storage (both dashed) are implemented by the master system only. (Barf et al. 2015, Fig. 1)

The camera, mvBlueCOUGAR-X102b, an industrial camera manufactured by Matrix-Vision, is faced perpendicular to the rocket's roll axis, to observe the outer environment. The captured image frames are then fetched by the core system, a industrial single-board computer (MIO-2260) through a GigE-Vision interface using a standard Ethernet cable. The core system then applies the horizon acquisition algorithm on the captured image frames and stores the image frames as well as the calculation data on the SSD attached via an SATA-II connection. In addition, the core system interprets the signals from the REXUS Service Module (RXSM) as well as manages the up- and downlink. For later evaluation a global timestamp is provided as well, which is linked to all data saved to the SSD.
To be able to downlink and save health and telemetry data as current consumption, temperature etc., the core system is connected to the measurement unit via an RS232 connection. The measurement unit itself collects current and temperature sensor readings and forwards them to the core system for downlink. Additionally, the data are saved to a separate SD card with the timestamp provided by the core system. During flight, the data is only stored on the SD card to save downlink bandwidth.
In order to be able to power the systems mentioned above, the power distribution unit is connected to the 28V unregulated power source of the REXUS rocket and takes care of regulating the power using DC/DC converters. All those components are placed in aluminium boxes to protect the electronic circuits from the outer environment and simplifies the replacement of subsystems. For redundancy reasons and to collect more scientific data, two independent, identical flight systems are placed within the same REXUS module (cf. Barf et al. 2015, Sec. 3).

2.2. Software Design

In order to operate the experiment, the core system runs *Arch Linux* (Griffin 2015), a minimal Linux operating system, on which the flight software runs on top. Using an operating system as a basis for the flight software was a specific decision to reduce development time compared to a bare metal implementation. On top of that the groundstation used a Linux derivate as well, which made it possible to use the same communication framework implementation on the groundstation and on the core system. Furthermore, this decision allowed testing in early stages of the software development, but introduced a higher risk of unwanted behaviour of the operating system. By using Arch Linux it was possible to combine the best of both worlds, since the minimal Linux distribution required explicit configuration of every operating system component.
To control the experiment, the flight software implements three different modes, the *standby* mode, the *flight* mode and the *shutdown* mode. The standby mode is executed while the rocket is still on ground. Here the flight system downlinks telemetry consisting of experiment health data to the groundstation and performs several self-checks, for example data storage access and camera connection.

After receiving the lift-off signal the flight software switches to the flight mode, where no housekeeping data but only some basic scientific data are downlinked, since the radio link bandwidth is limited. The detailed algorithm results and measurement unit data, as well as the captured images are stored on the data storages onboard. Ten seconds before being shut off by the RXSM at T+600s the flight software switches to the shutdown mode in order to finish writing data to the data storages and to prevent data corruption during the power cutoff (cf. Mawn et al. 2014; Barf et al. 2015).



(a) Original Image (b) Grayscaled Image (c) Threshold Filter (d) Topological Search

(e) Line Detection (f) Failed Vector Calcuation (g) 3 Divisions (h) Successful Processing of Partial Image 1a

Figure 2: States of Image data during Processing (Barf et al. 2015, Fig. 2)

2.3. Algorithm Design

In order to be able to find the horizon line, the software of the flight system runs a horizon acquisition algorithm which is fed with images in the visible spectrum captured by the camera. The main concept in finding the horizon is using the contrast between deep space and the central body. To cope with disturbances like lens flares, the sun etc. some additional logic is used.
This approach obviously requires the central body to be within the field of view of the camera, which sets some additional constraints for the optical system one may use. In case of HORACE, which was predicted to reach an apogee of approx. 80km, a lens with a field of view of about 18° and a very low maximum distortion of -1.6% (LENSATION 2014) was chosen. This ensured the earth horizon to be visible for at least one camera during the whole flight.

The first step of the algorithm, the *Preprocessing*, is scaling down the image while preserving its proportions to reduce computation time for the further steps and converts the coloured image to a grayscale image (Fig. 2b). If the image exceeds a certain value, e.g. is too dark or too bright, the image gets rejected and is not further processed (cf. Barf 2014, Sec. 2.2.1).
The second step applies a dynamic *Threshold Filter* to the greyscaled image, which means assigning a 1 to bright pixels and a 0 to dark pixels using an experimentally determined threshold factor and the overall brightness of the image.
In the *Line Detection* step, a topological search using an algorithm presented by Suzuki & Abe (1983) is applied to find continuous lines of border pixels and select the longest one (Fig. 2e, note: image was enhanced).
Having found the longest continuous line, the *Vector Calculation* is applied by fitting the line to a circle using the least square method. Thus, the radius of the circle can be checked for validity, since the expected radius range may be calculated if the properties of the optical system are known. Nevertheless, other factors like the atmosphere, the earth's albedo etc. have to be taken into account for tuning the parameters of the radius range calculation to avoid false positives or false negatives (Barf 2014, cf.). If the calculated radius is valid, the vector from the center of the image to the center of the circle is calculated, giving the nadir vector of the 2D projection of the central body.
In case the calculated radius is not valid, e.g. due to image disturbances (Fig. 2f shows a failed vector calculation, note: image was enhanced), a Divide-and-Conquer approach is applied in the *Division* step to divide the image in the middle of the longer side. This is done until the partial images are too small to process and get rejected by the *Preprocessing* or return a valid result. The valid result of a partial image is then extrapolated and the circle may be calculated (Fig. 2h). Therefore this approach can be used even if the primary image is severely disturbed (cf. Barf et al. 2015, Sec. 4).

3. SCIENTIFIC RESULTS

Since the scientific data collected by the experiment during the flight were severely degraded due to a failure of the camera which led to a complete overexposure of most image frames, it was not possible to prove nor to disprove the overall concept of a software-based horizon sensor in space-like conditions (cf. Rapp 2014, Sec. 2.4).

Still, from an operational point of view, the experiment is seen as a success, since all operations went flawlessly during the Launch Campaign. Amongst other things, the developed communication framework as well as the software concept was proven to work nominally during all

critical phases. In addition, the algorithm worked as intended by discarding all unusable image frames, means it processed all the captured frames in a correct manner. Even though no useful footage was captured during flight, it was still possible to test the algorithm and its accuracy using simulations which were created by using a model of the camera and its properties within Cinema4D, a 3D-Simulation Software. Since using simulations made it possible to know the exact relative position to the earth, a comparison between the simulation data and the algorithm output could be done, which showed that the algorithm works with an accuracy of $\pm 0.6^\circ$ in the simulated environment. During the whole simulation not a single false positive was reported and only 10.29% false negatives (cf. Rapp 2014, Sec. 3.5.4).
The disadvantage of using simulations to verify the accuracy is the inaccurate representation of reality, for instance in the simulated environment the atmosphere of the earth could only be modelled roughly.

In addition to the scientific results, some valuable technical insights were gained. During one of the last tests at the Launch Campaign only few days before the launch, it was unveiled that HORACE was disturbing the GPS antenna of the REXUS rocket when the experiment was powered on. Due to the very late discovery, it was not possible to detect the exact cause of this issue prior to launch, and counter-measures like putting ferrite beads around the cables in the HORACE setup did not solve the problem. This led to the decision to fly the REXUS rocket without a GPS signal in-between T-600s and T+600s, since the GPS signal was not vital for other experiments or the rocket itself during the period of time HORACE was powered. This issue was discovered late, because in the system tests before the Launch Campaign, especially during the bench test, the test configurations were different from the real flight configuration. Mainly, the nose-cone of the rocket, where the GPS receiver was located, was not mounted as in the real flight configuration during the tests. Later on, during the post-flight analysis the cause of this issue was narrowed down to three components - the core system, the SSD and the cable connecting those two components. It was not possible to detect the exact component which caused the issue, so the only viable counter-measure would have been to shield all three components (cf. Rapp et al. 2014, Sec. 7.4).

Another anomaly, first detected during the integration week, was an issue concerning the grounding of the experiment. Even though the grounding of the experiment was done compliant to the REXUS user manual, this seemed to cause uncontrolled and indeterministic stray currents which led to occasional, unpredictable crashes of the software on the core system. Since it was not possible to fully understand the cause for the shifted ground potential, the issue could not be resolved properly. Workarounds like replacing the core system and a software solution for restarting the flight software only reduced the probability and severity of the issue to an acceptable level. So far, the only solution to this problem would have been a complete electric isolation from the REXUS rocket (cf. Barf et al. 2015).

4. PROJECT CHALLENGES

During the lifecycle of the project we faced many different challenges, some were more general and could have been encountered at any project and some were very project specific. Since all of the team members were in their second undergraduate year when HORACE was started we had trouble keeping up with the workload of the project in parallel to classes. Especially the review preparation phases (PDR, CDR, etc.) which often coincided with the exam phases forcing us to retake some exams. Also the project management of a team of six people and its resources over a two-year period turned out to be a nontrivial task, especially since we were short on experience concerning teamwork.
Although we studied "Aerospace Information Technology", the knowledge gained during the course of studies had less than expected overlap with the needed knowledge to complete HORACE. That meant that even though we still could apply much of actual class content, we had to acquire a lot of additional knowledge in parallel to the classes. Since we were the first team from our university participating in the REXUS programme we could not rely on previous experience gained in that area. All of us were computer scientists, so we had no mechanical, optical or electrical engineering knowledge which were necessary for the design of the experiment. Especially the formulation of the requirements presented a serious challenge to us.
Of course the software part of HORACE proved to be challenging as well. Besides the classical debugging of software the algorithm had to be designed in a way that it is resistant against disturbances like reflections or the sun in the camera's field of view (cf. Barf 2014). Additionally, since we do not have courses in mechanical engineering at our university we had trouble finding adequate testing facilities. For example to test the reliability at temperatures below -40°C (cf. Rapp et al. 2014, Sec. 5.2) an external company with a cooling chamber had to be contacted, since the thermal-vacuum chamber being available at the chair only allowed temperatures down to -20°C.
Another challenge was the funding of travel expenses and materials. Most materials were sponsored by the manufacturers themselves or paid by the REXUS programme and the university, but travel expenses were only fully covered for four team members.

5. CONNECTION TO ACADEMIC EDUCATION

Regarding the connection between the HORACE project and the participating students' academic education we could identify two main factors: firstly, the aspects of hands-on projects in the field of aerospace in general, which can be found at the University of Würzburg not only in the HORACE project, and secondly, the direct connection of HORACE to specific concepts and methods previously being taught in specific courses at least

some of the participating students had attended. Both factors are discussed in detail in the following.

5.1. Hands-On Projects at University of Würzburg

One experience, which can probably be confirmed by any student who leaves the University and starts to work on concrete technical or scientific projects will be that there is still a lot to learn. In todays world, the education at the university will never be able to give a student all the knowledge, which is needed for a specific task. So the actual aim of a university can not be to just give a complete set of knowledge on every possible problem. It is rather to give students a fundament of specific knowledge but also and more importantly to help students to learn how to systematically develop systems , solve problems and apply appropriate methods, where necessary auto-didactically. This can all be done theoretically. But a better way is to give them the opportunity to be involved in a "real" project before they start working on projects outside the university. Although such an involvement of students is by far not obvious at every university, it is an extremely useful way to inspire and especially motivate young students.
Students at the university of Würzburg, studying in the field of Aerospace (either Bachelor of Aerospace Information Technology or SpaceMaster or Master of Informatics with a focus on Aerospace) have several such opportunities. They can for example work as student co-workers in the frame of real space related projects (e.g. star sensors, autonomous imaging systems, lunar satellites, communications systems), take part in practical work in rocketry or even work in real world problems in the frame of the international space station (ISS). In some cases, they are even allowed to do so in a relative early stage of their studies, namely within the first few semesters of their bachelor studies.
One of the examples of practical work opportunities are the REXUS/BEXUS experiments, which are a very valuable contribution of DLR/SNSB to University education. At the University of Würzburg, we have decided in 2012 to initiate and support such experiments in order to improve education and research by many different means. As described in detail in this paper, the student team worked very hard to achieve their goals and learned a lot by own experience. Even if some of the aspects had been taught beforehand by lecturers, the own experience will be much more unforgettable. As a simple example, students who are involved in space systems design projects learn how to formulate requirements, learn the organisation and management of a space project and design a space system. But to be confronted with the same contents in the frame of an external environment like REXUS, is a different experience. The pressure and willingness of being successful is much higher, than just the need of passing a regular exercise.
This increases the level of maturity of the involved students to a much higher level, which means that the institutions they will work in after the education will benefit from this fact as they will save time on job training.
The specific experience described further in this paper just confirms all of these positive impacts to education. For us, the lesson learned from this is, that the universities should support much more such activities by means of more resources, which are usually very limited.

5.2. Connection to Specific Course Contents

Although, as outlined above, the gain in experience and abstract competences like problem solving in general undoubtedly had the greatest impact regarding the educational aspects of the HORACE project, we succeeded to directly link many contents of theoretical classes to the project challenges (cf. 4). Thus, we could not only face those challenges appropriately, but also gain deeper insight in those topics than it was possible during each and every of the courses.

Besides the basic architecture and the content of *telemetry and telecommand packages* which were taught in space related courses, concepts regarding reliable end-to-end transmission, i.e. error detection and correction, like the *Hamming distance* between code words or *cyclic redundancy check* were part of the "Information Transmission" lecture. Furthermore, especially the concept of *Divide and Conquer*, which was taught during "Algorithms and Data Structures" by the example of sorting algorithms, turned out to be the most important part of the HORACE algorithm to cope with heavy image distortions (cf. 2). In the lecture "Central Avionics", the advantages of common *coding directives* and a simplified example of those broadly used in the aerospace sector were presented and motivated to adapt them to improve the quality of the software. Standardised concepts of abstract modelling of software, like the *Unified Modeling Language*, standard processes and design patterns of software development were taught in the lecture "Software Technology". Applying those standards increased the collaborative productivity within the team and ensured comprehensibility of the abstract models of the software architecture for external partners. Many mathematical concepts and methods were helpful for the development of the HORACE algorithm, the later evaluation as well as to estimate the overall accuracy of the algorithm. This was not only the case for contents of the freshman course "Mathematics for Engineering Students", but also the lecture "Error Analysis" which, for example, introduced the *Least Square Method* applied for the circle fit step of the horizon (cf. 2).

As it can be seen from those various examples, the HORACE project offered the invaluable opportunity to apply the knowledge gained in the scope of our University studies. In many cases this was the very first time to do so out of the pure educational context where the concepts are often studied as isolated problems or by means of very simple examples. This raised the difficulty that, unlike in exercises of University classes, we were not told which set of tools and concepts should be applied, but we had to select, adapt and modify ones, suitable for the

"real world's" problems, from our total set of theoretical knowledge. However, this way we were able to directly link our theoretical knowledge to personal experience and hence learn even more because - as one says - "knowledge gained through experience is far superior and many times more useful than bookish knowledge."

6. PROFESSIONAL SKILLS ACQUIRED

Of course, the theoretical knowledge from university classes mentioned in the previous section was not enough to overcome all challenges and to successfully complete the HORACE project. Hence, several professional skills had to be acquired mostly in an autodidactic manner. Besides the so called "soft skills", i.e. conducting proper team work or preparing good presentations, this includes skills regarding the usage of several professional tools and software-frameworks.
As the HORACE algorithm is based on image processing techniques and as it was neither reasonable nor possible to implement all needed algorithms from scratch, the *OpenCV* library was extensively used. Therefore, the team member charged with the algorithmic development had to acquire deep knowledge not only about its usage but also the underlying algorithms, limitations and disadvantages. Another essential part of the experiment was to implement a proper communication link between the core system and the camera to reliably gather images. Hence, the software developers had to study both the proprietary camera API of MatrixVision and the open and standardised one called *GenICam*. The core system ran with *ArchLinux* (cf. 2). That had the benefits of fast development of the actual HORACE flight software and a very stable and controlled operating system, but required a broad understanding of Linux itself, its configuration from scratch and how to implement applications on top of the operating system. This required of course advanced *C++* and *bash* programming skills. The measurement unit was based on the *Arduino* platform. The beginner friendly platform was easy to use in the beginning. But as the application grew more complex we had to get a deeper insight, especially regarding the restrictions and limitations of the simplified programming language as we were used to more advanced software development and hence also restricted in our thinking and way of problem solving. To test and verify the algorithms, simulations were created with *Cinema4D*. But unlike for some hobby movie project, one could not apply "trial and error" to render the simulations as they had to be as realistic as possible and as internal concepts of the tool, e.g. the internally used coordinate frames, had to be understood in order to numerically verify the HORACE algorithm (cf. 3). Although the emphasis of the project was on software components, of course some hardware was needed to run the software. While electronic components were bought as COTS to a large extend, the mechanical assembly was customised in most parts. Designing the mechanical structure using CAD-Software (*Autodesk Inventor*) was new to all team members as we all had a computer science background (cf. 4). To keep track of the project and ensure proper teamwork especially regarding software development with multiple contributors, several tools like *SVN*, *doxygen*, *Microsoft Project* or *TeamWorkPM* were applied, which of course were not covered by the theoretical university classes. For documentation and publications LaTeXwas used by some team members for the first time in an advanced and productive manner.
Already by now, several of the acquired professional skills helped to get placements for internships, student jobs or master projects and will surely be valuable for our professional careers.

7. PROJECT ACHIEVEMENTS

Even though the ultimate goal of full performance under real-life conditions was missed (cf. 3) the project delivered several valuable partial achievements besides the just mentioned education of students.
First of all, despite the competition of the project schedule with study and exam periods all SED submission, manufacturing, software completion and verification deadlines were met. This enabled us to launch a fully operational experiment. Beforehand, in order to test and verify the function of the algorithm special test videos were rendered. The short clips of a few minutes simulate the view of the experiment's camera as mounted on the tumbling rocket. In these simulations, all parameters of the optical system, the sun, clouds and the movement of the rocket were included although reality can only be approximated. Successive projects might also take advantage of the work done.
With these simulations in addition to real video footage from a previous REXUS experiment (EXPLORE) the performance of the algorithm could be analysed and verified. We managed to develop the mathematical concept and an implementation in *C++* of a horizon sensing algorithm with image processing techniques. This is another valuable outcome for successive projects.

8. LESSONS LEARNED

By facing the project's challenges and dealing with unforeseen events and difficulties, we learned a few lessons. The most unpleasant of them was learned when we missed to perform a late *End-To-End* test at the Launch Campaign. Due to that, we did not discover the overexposure of the camera pictures and as a consequence, let the scientific data become unusable. This would have easily been noticed if the experiment was fully tested outside the laboratory shortly before the mounting onto the vehicle. It would have also been possible to implement a function that allows the operator to take a quick view on the camera pictures even when the vehicle is already mounted on the launcher. This function could then have also been used at many occasions before the assembly and would have revealed the camera failure but was not

considered in the design phase (cf. Rapp et al. 2014, Sec. 7.4.1.4).
Another lesson learned could be named "*Test What you Fly - Fly What You Test*". During Bench Test an error was discovered, causing the core system software to crash completely. In previous testing this error did not occur. In later analysis it turned out that it was caused by a ground shift in connection with the grounding of the experiment structure to the RXSM structure (cf. 3). The ground connection was established the first time at Integration Week and identified as cause of malfunction during Bench Test, so the malfunction was discovered too late in the project cycle and could therefore not be fully eliminated (cf. Rapp et al. 2014, Sec. 7.4.1.2). The same lesson was learned at the Launch Campaign itself when HORACE interfered with the GPS antenna of the RXSM (cf. 3). Again, the cold countdown test was the first time the exact flight configuration was applied, meaning the "GPS antenna mounted inside the mounted nosecone and the cable harness fed through the experiments." (Rapp et al. 2014, Sec. 7.4.1.3).
Here we also had to learn that, while working on urgent problems, one should not neglect the actual important issues. While we were busy trying to install a workaround for the grounding issue in order to prevent software crashes we omitted further End-To-End tests of the whole experiment and thus allowed the camera failure to remain undiscovered as described above.
We also had to learn not to trust the manufacturer naively. The camera software provided by the camera manufacturer MatrixVision was not as flawless as it was assumed. A bug that was corrected in a later version is partially accountable for the overexposure of the camera. Had we validated the functionality of the provided software instead of trusting the manufacturer the error might have shown up before launch.

Besides these technical experiences a lot of lessons in the area of project and team management were learned. Since the University of Würzburg does not offer mechanical or electrical engineering degrees, the team consisted only of students of Aerospace Information Technology. The lack of specialised electrical and mechanical engineers was considered uncritical since no complicated electrical or mechanical components were needed. But without special knowledge in a discipline all work takes a lot more time. In addition, later in the project the need for protective windows to shield the camera from hot air inrush emerged. Especially the design of their mounting was indeed complicated and consumed a lot of time. Furthermore, the communication with the glas manufacturer was challenging and time consuming due to the lack of knowledge in available materials.

Without having a fully equipped laboratory or workshop available, all tools and materials had to be purchased or used from the personal portfolio. The costs for these purchases were completely underestimated in the early periods of the project. Another management variable that was underestimated was the time consumed by outreach activities. Creating websites and preparing presentations was assumed to be done incidentally. It eventually turned out that a proper outreach for a project like HORACE is a one-man full-time job. But outreach was also very rewarding, since it rose awareness and interest in the project. That and the SED preparations also made us practice our abilities to explain complex concepts to outsiders comprehensively. The communication inside the team was quite easy-going, since everybody studied the same subject in the same year and thus was at about the same level of knowledge. In addition, the stable team structure was very beneficial, making everyone available in the whole lifecycle. Although there were rough periods, a project of the complexity of HORACE with its team structure is manageable in parallel to the studies. Not only regular meetings but also a team management software, internal deadlines before the actual deadlines and the distribution of small tasks with short time schedules helped to keep track of all tasks. In this scope it is also advantageous to have supervisors who support the team with resources and knowledge where necessary but do not interfere with the design, manufacturing and verification process.

Writing requirements at the very early phase in the project is very tedious and time consuming. But this work is highly beneficial since every team member has time to make up his mind about the project and to discuss his perception. Furthermore, in the verification phase this work makes it possible to verify every single requirement and thus ensures that all functionalities are available. Another very tedious work is the preparation of procedures, that might never be used. But if they are needed they are extremely helpful. We experienced this when a SD card stopped working after the payload stack of the vehicle was already fully assembled. A procedure to replace the SD card was written beforehand and gave the Payload Manager a complete insight in the work to be done. It also helped us to avoid mistakes in this time crucial phase. A rather important lesson that the we learned is to start software development early, even if the design is not finalised yet. The time for software development is often hard to estimate and can easily exceed expected boundaries. Especially debugging is often very time consuming. Thus, early testing is crucial and can even affect the design. (cf. Rapp et al. 2014, Sec. 7.4)

9. FURTHER WORK & OUTLOOK

After the project HORACE was completed, a Bachelor Thesis (Barf 2014) took the algorithm to the next level by creating a version in *C++* that uses only standard libraries and implements all necessary functions previously used from *OpenCV*. This implementation is currently used by the REXUS Team PATHOS which is the followup project of HORACE. Key objectives of PATHOS are the "miniaturisation of HORACE so it could be part of a satellite, and the enhancement of the efficiency of the horizon-detection and vector-calculation algorithm" (Wagner et al. 2015). Hopefully that team can achieve what HORACE missed: a successful test under space-like conditions.

Furthermore, a setup to evaluate the accuracy and performance in a real application with a reference sensor system as proposed by Rapp (2014, Sec. 5) is a possibility for further development. Rapp also suggests the porting to already existing hardware and the upgrade of the system to provide full attitude information instead of only roll and yaw information. A Master Thesis on this topic is planned for 2016. In the scope of that work a horizon sensor based on the idea of HORACE shall be implemented to improve attitude information from heavily drifting relative attitude sensors on a sounding rocket with sensor fusion.

Thanks to the close cooperation with many space related organisations we got insights into their work and could already make contact with their staff. This already proved advantageous - and will presumably be in future - when searching for internships, thesis works and work places.

10. CONCLUSION

Although the major objective - the demonstration of the horizon detection in space-like conditions - was missed due to the overexposure of all image data, HORACE is still considered a success. This is not only because of valuable engineering outcome but also because of the great experience gained by the participating students.

Regarding the engineering conclusion, we could show that the horizon detection for attitude determination in the visible spectrum is basically possible and works with an accuracy of 0.6° in simulations. The algorithm itself proved to be working on simulated data and on real footage with a reasonable rate of false positives and false negatives. The project did not reveal any reasons why this idea can not be implemented as rough attitude determination system for safe-mode or as attitude determination sensor for small satellites. But there is still some way to go, especially regarding mass, power consumption and sampling time.

In the REXUS/BEXUS programme education plays a huge role throughout the project. In this manner it is save to say that HORACE was a full success. We now have a deep understanding of all phases of a project life-cycle and know how they affect each other, especially how design and verification insufficiencies can lead to what kind of failures. Of course, we faced challenges, made mistakes and even failed but we learned the lessons and are able to apply this experience in all further projects. Apart from the huge amount of technical skills and knowledge we also gained a fair amount of soft-skills especially regarding teamwork. We were also granted a brief insight into the space business and were already able to make first contact with possible future employers. To conclude, we suggest every space engineer to take the opportunity if it is available to take part in the REXUS/BEXUS programme and make all those experiences - good and bad - it is worth the effort.

ACKNOWLEDGMENTS

At first we want to thank our supervisors from the Chair of Aerospace Information Technology at the Julius-Maximilians-University of Würzburg, Prof. Dr.-Ing. Kayal, Dipl.-Inf. Gerhard Fellinger and M.Sc. Oleksii Balagurin not only for their financial support and usage of the chair's facilities and resources, but also for their support with their knowledge. Additionally, we want to thank the DLR (German Aerospace Center) and SNSB (Swedish National Space Board) and all their staff for providing the chance to participate at the REXUS/BEXUS programme and thus to make HORACE possible. Furthermore we want to thank ESA (European Space Agency), ZARM (Centre of Applied Space Technology and Microgravity), MORABA (DLR Mobile Rocket Base) and SSC Esrange (Swedish Space Centre), for all the support and that the professionals are always working on the same level with the students. And finally we want to thank all other sponsors, supporters and partners, whether they are individuals or from the the industry, who supported us in uncountable and valuable ways.

REFERENCES

Barf, J. 2014, Development and Implementation of an Horizon Sensing Algorithm based on Image Processing Technologies (Julius Maximilian University of Würzburg, Am Hubland, D-97074 Würzburg)

Barf, J., Rapp, T., Bergmann, M., et al. 2015, in ESA Special Publication, Vol. 730, Proc. of '22nd ESA Symposium on European Rocket and Balloon Programmes and Related Research', Tromsø, Norway 7-12 June 2015, ed. L. Ouwehand, ESA Communications, ESTEC, Noordwijk, The Netherlands, pp.627–634

Griffin, A. 2015, Arch Linux, https://www.archlinux.org, retrieved: 26 May 2015

LENSATION. 2014, Specification Lensagon BT8020N

Mawn, S., Schmidt, A., Hellmann, H., et al. 2014, REXUS User Manual v7.13, EuroLaunch

Rapp, T. 2014, Development and Post-Flight-Analysis of HORACE the Horizon Acquisition Experiment (Julius Maximilian University of Würzburg, Am Hubland, D-97074 Würzburg)

Rapp, T., Barf, J., Bergmann, M., et al. 2014, HORACE Student Experiment Document v 5.0, this document was written in the context of a REXUS project

Suzuki, S. & Abe, K. 1983, Topological Structural Analysis of Digitized Binary Images by Border Following (Shizuoka University, Hamamatsu 432, Japan)

Wagner, D., Aicher, M., Ehnle, J., et al. 2015, PATHOS Student Experiment Document v 3.1, this document was written in the context of a REXUS project

DEVELOPMENT AND TESTING OF THE ON-BOARD SOFTWARE FOR QB50 NANOSATELLITE IP^{2}SAT

Damien Watremetz [(1)], Thierry Capitaine[(2)], Matteo Emanuelli[(3)], Daniele Emanuele Chiuri[(4)], Rania Toukebri[(5)], Lionel Zieminski[(6)], Maite Compiegne[(7)]

[(1)] Université de Picardie Jules Verne - INSSET, 48, Rue Raspail, 02100, Saint-Quentin, France, damien.watremetz@u-picardie.fr
[(2)] Université de Picardie Jules Verne - INSSET, 48, Rue Raspail, 02100, Saint-Quentin, France, thierry.capitaine@u-picardie.fr
[(3)] Université de Picardie Jules Verne - INSSET, 48, Rue Raspail, 02100, Saint-Quentin, France, matteo.emanuelli@u-picardie.fr
[(4)] Université de Picardie Jules Verne - INSSET, 48, Rue Raspail, 02100, Saint-Quentin, France, daniele.emanuele.chiuri@u-picardie.fr
[(5)] Université de Picardie Jules Verne - INSSET, 48, Rue Raspail, 02100, Saint-Quentin, France, toukebri.raniaa@gmail.com
[(6)] Université de Picardie Jules Verne - INSSET, 48, Rue Raspail, 02100, Saint-Quentin, France, lionel.zieminski@free.fr
[(7)] Université de Picardie Jules Verne - INSSET, 48, Rue Raspail, 02100, Saint-Quentin, France, compiegne.maite@orange.fr

ABSTRACT

The Institut Supérieur des Sciences et Techniques (INSSET) of Saint-Quentin, France, has developed IP^{2}SAT, a 2U CubeSat for the QB50 project. The satellite will specifically study the molecular composition of the thermosphere, which is the penultimate level of the atmosphere before the exosphere, between 380 km and the satellite's demise at 80 km. The CubeSat, due to the initial pressing schedule of the project, has been mainly integrated with commercial off the shelf parts. However, INSSET, employing a team of students supervised by university staff, has developed internally the telecommunication subsystem and the on-board software using the experience acquired in previous non-spatial projects. The development of the telecommunication subsystems and the satellite software has spanned for about 9 months and in this paper the activities, the solutions to the obstacles found on the path, the description of the software functionality and the test performed to validate the software itself are going to be described. It will be also shown the philosophy behind the telecommunication card, mainly focused on creating a board that can deal with different protocols by simply modifying the software. In fact, one of the main issue the design of the on board software had to address has been the compatibility and translation between different protocols. This issue has been specifically between the AX.25 protocol necessary for the communications to ground using the EPFL's Satellite Control Software (SCS) and the internal CubeSat Protocol (CSP) developed by GomSpace ApS, necessary for the internal communications among the different subsystems. The solution identified using only the software and the validation test will be described. A specific code has been also developed to perform and automatise all the necessary functional tests (FFT, TCF, etc.) the satellite had to undergo during the test campaign.

1. INTRODUCTION

The Institut Supérieur des Sciences et Techniques (INSSET) is a branch of the Université de Picardie Jules Verne (UPJV) located in Saint-Quentin (France). The embedded system department of INSSET, led by Professor Thierry Capitaine, has conducted space-related projects since 2003, mainly focused on the development of a ground station and on works related to the first unsuccessful version of the Global Educational Network for Satellite Operations (GENSO) project. In 2012, in conjunction with the request for proposal issued by the QB50 Consortium, the attention shifted from the ground segment to the space segment, aiming to develop and operate a CubeSat.

2. QB50 PROJECT

The QB50 project aims to demonstrate the possibility of launching a network of 50 CubeSats in Low Earth Orbit (LEO). Each of these spacecraft, built by university teams all over the world, embarks a primary scientific payload provided by the consortium to perform first-class science, carrying out multi-point in-situ measurements in the largely unexplored lower thermosphere between 380 km and 80 km[i].
The satellites, initially scheduled to be launched aboard the Ukrainian/Brazilian rocket Cyclone 4 from the Alcântara Launch Centre (Brazil), in January 2016, after

the issues that brought to the cancellation of the Cyclone 4 program[ii], are now scheduled to be launched with the American company Nanoracks from the International Space Station starting from July 2016.



Figure 1 QB50 Project chart outlining the four goals of the project[i]

2.1. Why Participating in QB50?

The participation in the QB50 project with IP^2 SAT CubeSat (Fig. 2) meant for INSSET the possibility of applying years of experience in embedded systems in one of the harshest environment an electronic system could endure: the space environment.
The energetic particles, solar particles emitted from the Sun or cosmic rays can penetrate the interior of a satellite and interact with its electronic circuitry, causing a wide variety of issues, from neglectable ones to problems that can shorten the life of the craft, to even the loss of the entire satellite. Although for bigger satellites it is possible to prevent these problems by using radiation-hardened components, this is not necessary true for nanosatellites since the cost of these components would often be unsustainable for the budget expected in a typical university nanosatellite mission. Moreover, these missions would not exceed few years, with no relevant economic value, making radiation-caused damages a risk that could be taken, without proper actions to mitigate it.
Before applying for QB50, INSSET carried out different scientific researches in collaboration with industrial partners (e.g. Matra Electronique, SEICER) in order to develop "secure" electronic boards with commercial components. The aim has been to develop boards that can withstand errors produced by radiation by using a wise design of the board itself and the software installed. Therefore, the participation in the QB50 project is justified and configured in a larger strategy of research in partnership with the local industry.

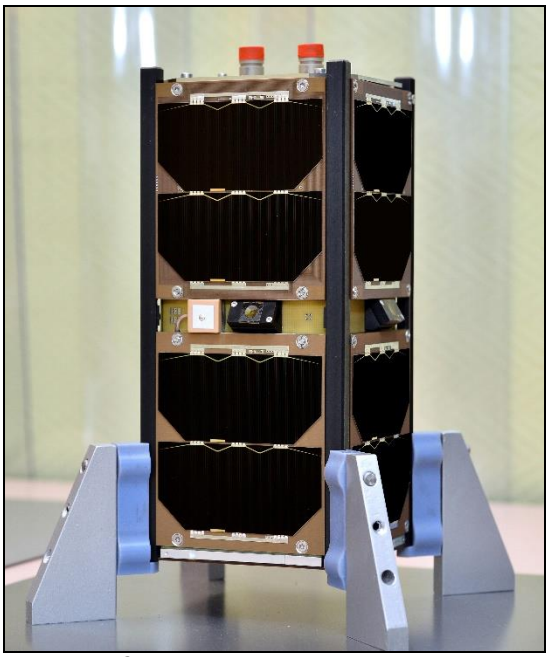


Figure 2 IP^2 SAT, the CubeSat developed by UPJV-INSSET for the QB50 project.

3. IP^2 SAT

IP^2 SAT, the INSSET contribution to the QB50 project, is a 2U CubeSat, based on a hybrid configuration of commercial-off-the-shelf (COTS) components and in-house subsystem. The satellite itself in short is composed by:

- Electrical Power Unit (EPS): Nanopower p31u
- On-Board computer: NanoMind 712D
- Solar Panels: NanoPower P110 series
- ADCS: NanoMind A3200
- Structure: ISIS - Innovative Solutions in Space BV
- TT&C: In-house
- Antenna: ISIS Deployable UHF/VHF 2-monopole Antenna

The CubeSat mounts on in the flight direction the Flux-Φ-Probe-Experiment (FIPEX) payload, developed by Technische Universitat Dresden (TU Dresden) for the the QB50 project and Surface thermal monitors (STM) supplied by Mullard Space Science Laboratory.

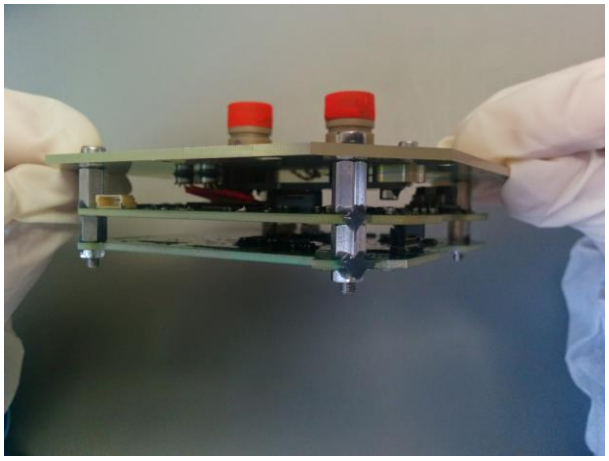


Figure 3 FIPEX during verification

FIPEX is able to distinguish and measure the time-resolved behaviour of atomic oxygen as a key parameter of the lower thermosphere. Atomic oxygen is the dominant species in these regions and therefore its measurement is crucial in the correlation and validation of atmosphere models. Moreover, erosion of spacecraft surfaces due to interaction with atomic oxygen is a serious concern and merits in situ study in its own right. The measurement is based on solid oxide electrolyte micro-sensors. For oxygen-conducting solid-state electrolytes (e.g. yttrium-doped zirconia), the conductivity starts at high temperatures and so the sensor operates at an elevated temperature of 600-700°C, heated by an electrical resistance. Oxygen is "pumped" from one electrode to the other by an applied direct voltage and in accordance with Faradays' law; the measured current is proportional to the mass flux by electrolysis. In order to determine the actual flux, the sensor needs to be in free flow and the attitude of the satellite with respect to its direction of motion needs to be known.

The STM experiment consists of six temperature transducers mounted as follows:

- Five channels are mounted on the CubeSat (on the inner side of solar panels).
- Sixth channel is mounted inside the FIPEX

IP^2 SAT was supposed to mount also a third payload, a test on-board computer developed at INSSET and based on the technology developed in the framework of the industrial project denominated "Secure-OBC". The on-board computer would have to run memory test to recognize and correct memory errors produced by space weather.

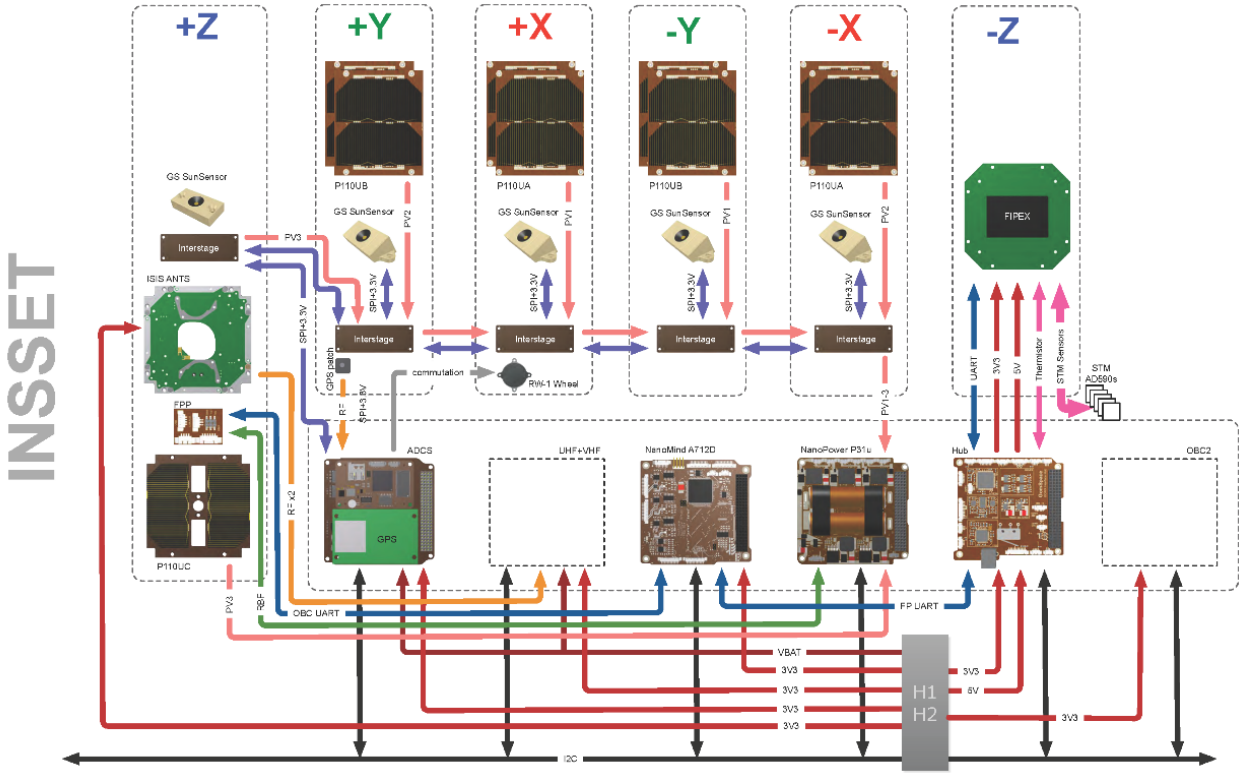


Figure 4 IP2 SAT Diagram

4. ON-BOARD COMPUTER

Although the on-board computer (OBC) has been purchased at GomSpace (NanoMind 712D), the flight software has been developed internally during a period of 1 year. IP²SAT OBC is the centre of the CubeSat, allowing all the information to circulate among the different subsystems and to communicate with the ground. The OBC has been also equipped with flash memory storage of 2 GB, to retain the scientific data on board in case of communication difficulties with the ground stations and to assure the correct operations of the payload using telecommanded scenarios and scripts.
The development of a CubeSat flight software can be approached with two different methodologies:

1. The space segment affects the development ground segment.
2. The ground segment affects the development space segment.

Although the first method is preferable as the ground segment is in general more flexible and inclined to modifications than the subsystems in a CubeSat, the second method becomes more interesting and therefore better when the ground segment is more developed or already in place. The latter undeniably offers advantages when the communication protocols, data structure and commands have been already developed as it offers an efficient framework for the flight software.

4.1. CSP and SCS

IP²SAT has been initially developed following the first methodology, however, when it has been made the decision to use the Satellite Control System (SCS) of the Ecole Polyethnique de Lausanne (EPFL), the point of view had to be shifted. It was decided to use SCS to increase the possibility of contacts, using ground station of other QB50 teams (mounting SCS as well) in case of their availability. However, SCS came with communication protocols and libraries for encapsulation/ de-encapsulation already defined, causing a compatibility problem between the internal communications protocol and the external one. IP²SAT uses the GomSpace's CubeSat Protocol (CSP), which is based on FreeRTOS, to communicate among the different subsystems of the satellite, while the communications with the ground is executed using the SCS protocol. These two protocols are not compatible without being treated accordingly following the command/data reception. Since the majority of the subsystems has been acquired at GomSpace, it was deemed to use CSP to decrease the flight software's developing time. However, it has been noticed that CSP as it is not a "clean" protocol, having different layers of development nested in it. In addition, the maximum length of messages allowed by CSP is only 252 bytes, while SCS would allow a much greater flexibility. The maximum length of messages used internally in IP²SAT is 250 bytes.

```
typedef union {
        uint8_t tab[31];
        struct __attribute__((__packed__)) {
                uint8_t var1;
                uint8_t tab1[8];
                uint32_t var2;
                uint16_t var3;
                uint32_t tab2[4];
        };
} strucTest_t;
```

Figure 5 IP² SAT code example

The code example in Fig. 5 allows solving the problem related to the different communication protocols. Although the standard data packet is 8 bits, the structure may be composed by 16, 32 or more bits. Therefore, it might be difficult to send plainly all the data. The "union" function regroups in 8 bits the structure, allowing the possibility of sending all the data in the structure. This solution makes the transmission of packages easier; however, it leaves some problems due to the static memory.
In order to develop an efficient software, first of all the approaching methodologies should be defined, then the communication protocol must be clearly understood in order to find efficient solutions.

4.2. Operating System

IP²SAT runs an Operating System (OS) based on FreeRTOS. Since the OS uses tasks to operate, in case of any problem to the tasks, it is possible to continue operating the satellite by simply rebooting. In addition, tasks allow assigning different priorities and it is possible to arrange them by functionality or upgrade even later the flight software itself with new tasks. The OS also provides tools (e.g. interrupt software, message queue etc.) for developing the software more efficiently and faster. Moreover, the scheduler, which organises and executes the different tasks, can detect various problems. In smaller scale, it is generally preferable to use OS to develop the flight software than to develop a single application in C or C#, always considering that the hardware has to support to OS itself. Good choices of OS are FreeRTOS itself or Linux.
The OS on IP²SAT allowed managing the communication between the scientific payload, FIPEX and the OBC. In fact, this communication uses two tasks, the first to send a command and the second to receive the response and the sensor data. The OS, allowing queueing, stopping or synchronising these tasks, lets the OBC continue working after the reception.

Although IP²SAT has been designed to be perfectly autonomous even with no communication with ground,

security procedures via FreeRTOS has been designed to connect to the satellite, similar to a Super User, in case, for example, there is the need of updating FIPEX's parameters.
The OBC software contains nine tasks, some of them are cyclical and others are activated only in a specific case with safeguards allowing deactivating or rebooting a single task in case of an error is detected.

5. FUNCTIONAL TEST

Software's testing is obviously important and different functional tests can help detecting failures in advance. The best way to execute a functional test would be to test the satellite as it is supposed to fly, however this, as for IP^{2}SAT case, is not always possible due to time constraint, etc. In such case, it is possible to simulate on ground some situations that can happen in space, testing how software reacts and applying the necessary corrections. The End-to-End (E2E) test is definitely necessary to check and guarantee that the command and data chain is flowing without problems. In order to overcome delays in delivering the payload, End-to-End has been performed with a mix of simulated systems and engineering hardware. The test has taken place with the ground station software on one end and engineering model of the OBC and simulation of FIPEX on the other end. In order to speed up the test, the connection has been established via cable.

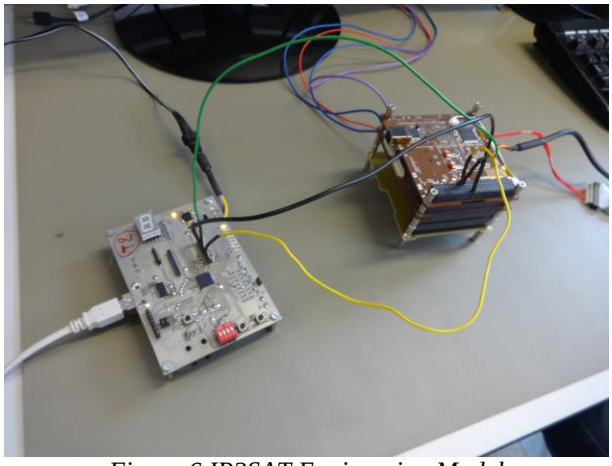


Figure 6 IP2SAT Engineering Model

An oscilloscope has been branched to check all the passages in the communication, allowing a direct verification of the test at all levels.
The End-To-End test for IP^{2}SAT has been conducted over two days together with EPFL team in order to verify the updated version of SCS and it has been the first test of its kind of the QB50 Project.



Figure 7 Oscilloscope visualizing the results of the test

For the vibration (i.e. quasi-static, natural frequencies, sinus, random, shock) and thermo-vacuum tests it has been important to test, before and after, all the main software functionality to find modifications caused by the test itself. This is because, for example, the shock is executed with a mass smashing support where the satellite is fixed while many sensors record the effect on the structure and it can, of course, cause problems.



Figure 8 IP^{2}SAT Shock Test

The results of the software tests are stored in order to compare the situation before and after. All the results need to be compared with a simulation. For example in our satellite, it has been developed an user interface to send commands and see in real time the answer of the system and save all the outputs. If there is an error, it is necessary to verify if it is critical or not and to evaluate if the system can survive it. For example, if the communication between two components fails 3 times and again after a reset, this is a critical problem. To find

critical errors it is just needed to answer the question if it is important or not for the mission. For example, losing a thermistor that is redundant is not dangerous for the mission but if the communication between two board is interrupted it is certainly critical.

Testing is important for the satellite because it helps finding problems beforehand rather than in the worst moment (i.e. anytime since the end of integration).

6. TELECOMMUNICATION CARD

The telecommunication card developed at INSSET (WallCom v1.0) is based on the concept of modularity, where each module (brick) can operate independently on a single task and can, in case, substitute others faulty modules. This approach speeds up the maintenance and the validation. WallCom is built on distributed architecture of Digital Signal Processors (DSP). Each DSP manages external and internal functionalities dedicated to a specific task, enabling simultaneous but independent processing operation (e.g. full duplex transmission and reception).
The DSP "Master" defines globally the state/mode of WallCom board by the propagation to the other DSP, via the local I2C bus, of an event, eventually with the needed configuration parameters. Since each DSP operates as a state machine, the reception of a change mode event launches the execution of a task integrating sub-functions (e.g. Start/Stop, Peripheral initialization and configuration). In addition, two supplementary modes are defined: the "Sleep mode" to reduce the consumption of the functionalities and the associated "WakeUp mode", when it is not generated by the master.



Figure 9 WallCom V1.0 (-Z side in CubeSat Reference)

The data between the DSPs are exchanged via local I2C bus to reduce the charge on the main I2C bus. The mode order change and event management can influence even the main DSP via the following source/event:

- High-level order from another subsystem (including the OBC).
- Event from the slave DSP (e.g. end of task's execution because of new data received, failures or new order from satellite subsystems).

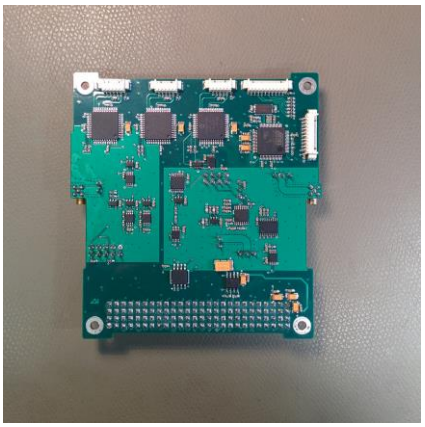


Figure 10 WallCom V1.0 (+Z side in CubeSat Reference

6.1. Master DSP

The Master DSP is in charge of all the data exchange between the telecom subsystem and all the others subsystems. Three slave DSPs are connected to the Masters by the local I2C bus (See fig. 4)
The main characteristics of the Master are:

- Encapsulation and de-encapsulation of the radio frames, sent and received, to be "translated" in CSP protocol
- CSP Router for the ground station
- Transmission of data to the other subsystems via CSP protocol (transparent mode)
- Interact as shell task (command interpreter) connect (virtually) with a terminal operated by one user at the ground station
- Master of the telecom module with the other DSP
- Activation of the Transponder Mode for Ham Radio operators
- Integrate FREE-RTOS operating system.

The system has also embedded storage functionality for the different set of operating parameters.

6.2. Uplink

The receiver module is formed by COTS modules for reception of analog and digital data, allowing a great customisation depending on the needs.
Considering the particular needs of the QB50 projects, one DSP has been dedicated to the reception of AX.25 protocol from the ground station. In addition, the DSP has been configured to extract the message received and

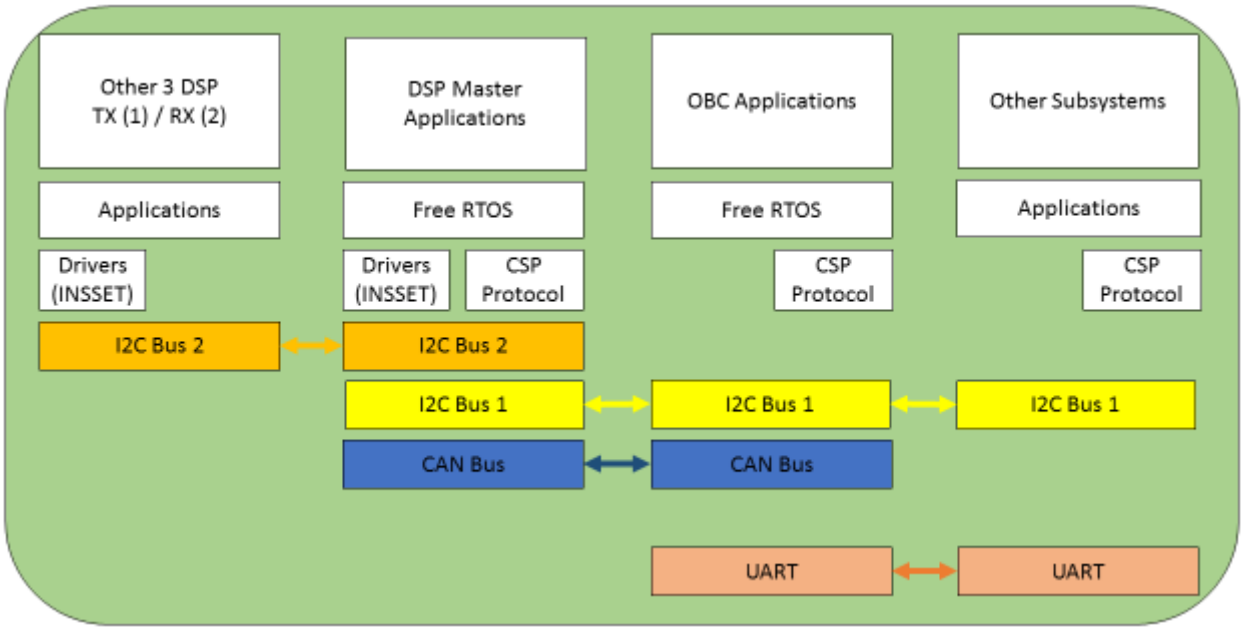


Figure 11 WallCom functional connections (internal &external)

send it to the Master DSP. In order to be able to stop the transmission activities remotely (QB50 requirements) the second DSP has been dedicated solely to the reception of dual-tone multi-frequency (DTMF) signal. The parameters of DTMF DSP can be modified remotely and independently from the other DSPs' parameters.

6.3. Downlink

The last of the three slave DSPs is dedicated to radio frames' transmission in:

- Morse code.
- AX.25 with customised bit rate and tone
- GMFSK 9600 based on the software replacement of a G3RUH hardware modem.

The main function of this DSP is to generate the low-level set of information to encapsulate the data delivered by the Master DSP. The transmission functions are synchronized on a periodic interruption generated by a timer and the modular architecture reduces considerably the charge on the DSP in use.

6.4. G3RUH Generation

In order to fulfil the project's requests, a G3RUH software modem has been designed and implemented in the DSP. The vast majority of the Terminal Node Controllers' (TNC) internal modems are able to provide a standard packet VHF/UHF radio data rate of 1200 b/s. However, QB50 required a higher data rate of 9600 b/s. The G3RUH modem has been designed as a high performance full duplex modem, compatible with most of the Narrow Band FM (NBFM) radios. The main characteristic of a G3RUH modem is the digital generation of the transmitted audio waveform and its tight control.

6.4.1. Transmit Waveform Generator

The waveforms transmitted are stored in EEProm memory in WallCom. The most recent bits used for the lookup table are contained in an 8-bit shift register. 2 bits/sample of sinus go to make up the profile in order to have a lookup table containing four samples of sinus. The transmitted waveform is synthesized from the current bit, all the last preceding 8 bits and the following 8 bits. A Digital-to-Analog Converter (DAC) directly converts every value output from the EEProm to voltage. An analogue low-pass filter removes the clock's harmonics, creating a finite impulse response (FIR) filter

The communication input/output between the DSP and the peripherals is slower than the execution time of necessary for sending and receiving characters (bits). In fact, the time calculated for the sending or reception of an 8-bit character at a flow rate of 9600 bit is more than 1 ms, while a cyclic period of an instruction takes fewer time. FIFO principle has to be used to detect the arrival of data in the bus and their storage, bringing the probability of data loss close to zero; only when the data are stored it is allowed to send new data.

Therefore, the work principle is based on the establishment of a communication buffer managed by the system via interruptions with two communication canals per peripheral (IN/OUT) established.

6.4.2. Transmission filter

The transmission filter is designed using a polyphase structure due to the multiple sampling rate (multirate).

In order to increase the working data of the filter, the system performs zero padding, filtering and decimation. Therefore, the decimator converts 38.400 samples per second with some samples ignored and not calculated. The number of samples has been calculated using the lookup table. This process is called “multirate filtering”.
A polyphase FIR filter is crucial for the 9600-bit/s transmission. The filter has been used without the lookup tables stored in EEProm by direct simple operations implemented in DSP.
The cut-off frequency was set at 4800 Hz and the bit-rate 9600 bit/s. It has been done an oversampling of 4 samples per bit. The FIR’s coefficients are pre calculated via a coefficient table only once.
Four output samples per input bit are calculated (i.e. 38400 samples per second).
The sample’s calculation uses only 8 of the 32 coefficients, therefore the filtering is not expensive in term of CPU’s resources and there is no need of using a lookup table since the DSP can perform easily the operations.
The settings (Timer, Frequency division value) are configured as follow:

- The timer is incremented by 1 at each clock counting from 0 up to the value contained in the register of the frequency division values. When it reaches the value, it goes back to zero and it generates an interrupt, which initialise the data program.
- The value of the clock is a function that can be divided by 4 possible values. So there are in the end 4 power values for the timer.



Figure 12 G3RUH Signal

6.5. Securisation

The hardware functionality implemented in the peripherals are doubled by software functions, which are activated automatically in case of failures of the hardware part. For example, all the modulation signals can be generated by the frequency synthesizer or by software function activated by an internal timer of the processors (Pulse Wave modulation signal).

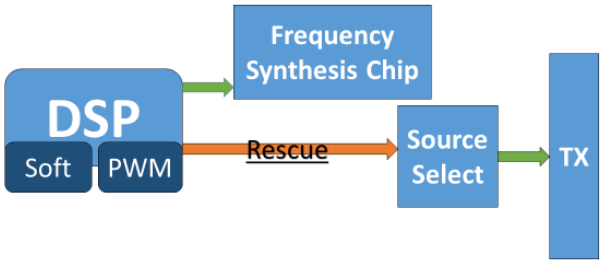


Figure 13 Double securisation on WalCom

In addition, since the modularity conception by (microcontroller, DSP) allows a very low usage of the memory (10%) for the specific task, WalComm has been also provided with a dynamic functional redundancy in case a single module fails.

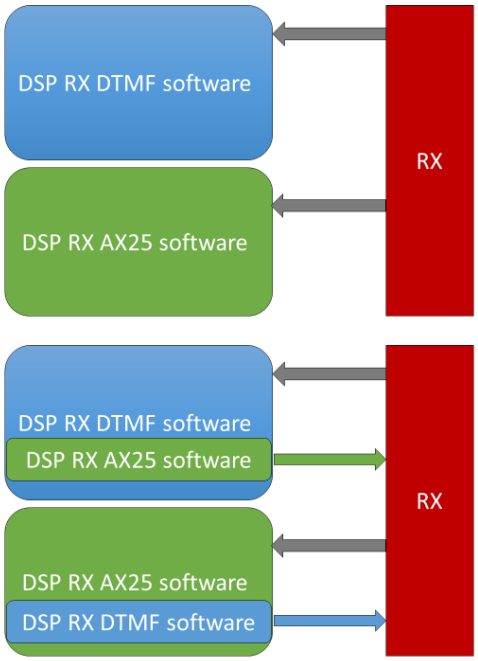


Figure 14 Example of Dynamic Functional redundancy in the modules

7. CONCLUSION & FUTURE WORKS

The main goal of INSSET satellite program is to demonstrate the capacity of building an entire nanosatellite from scratch with resources located in the Picardie region.

Therefore, the work carried out for IP^{2}SAT will be the basis for the development of other satellite subsystems, following the modularity concept and the dynamic functional redundancy, which are INSSET signature and drive.

[i] www.qb50.eu/

[ii] Selding, P. B. (2015, April 16). *Brazil Pulling Out of Ukrainian Launcher Project*. Source Space News: http://spacenews.com/brazil-pulling-out-of-ukrainian-launcher-project/

AUTONOMOUS NAVIGATION FOR DEEP-SPACE CUBESATS

Boris SEGRET[(1)], Jordan VANNITSEN[(2)], Daniel HESTROFFER[(3)], Florent DELEFLIE[(3)], Jiun-Jih MIAU[(2)], Jyh-Ching JUANG[(2)], Kaiti WANG[(2)], Students[(4)]

[(1)] PSL Research University, Observatoire de Paris, LESIA-ESEP, 5 place Jules Janssen
92195 MEUDON Cedex, FRANCE, Email:boris.segret@osbpm.fr
[(2)] National Cheng Kung University, 1 University Road, Tainan, TAIWAN, Email:jordan.vannitsen@gmail.com
[(3)] Institut de Mécanique Céleste et de Calcul des Éphémérides, Observatoire de Paris, 77 avenue Denfert-Rochereau
75014 Paris, FRANCE, Email:daniel.hestroffer@obspm.fr
[(4)] See full list of involved actors in section 8.

ABSTRACT

An on-board function of autonomous navigation for deep-space CubeSats has been developed since 2013. An initial study case is BIRDY, a 3U CubeSat to probe the interplanetary space weather on the way to Mars. BIRDY gets the main delta-V from any host missions to Mars (opportunities every two years). BIRDY is jettisoned at the beginning of the journey and collects data on the solar wind and the cosmic rays. The data are transferred to an orbiter already at Mars. Although the autonomous navigation function is still under feasibility studies, it seems very promising. It requires a ground segment and a flight segment. On ground a "trajectory solver" computes a reference trajectory and the ephemerid of a selection of interplanetary objects as seen from this trajectory. The data are stored on-board before launch. In flight the drift of the CubeSat wrt to the reference trajectory is computed in 3D on the basis of triangulations of objects in foreground of stars. Then the Trajectory Correction Manoeuvres can be performed as necessary with embedded electric propulsion. In 2015 it has appeared that the same concept can be applied for a second mission profile, temporarily named QBDIM, for in situ geodesy of asteroids. QBDIM would be carried and released on sight by a mother-craft that would also provide the data-relay with the Earth. The concept of operations is to run the same sequence of simple measures during multiple flying-legs in the vicinity of the asteroid. Each flying-leg lasts about two days and is prepared on ground with the best up-to-date gravitational and non-gravitational models. This "models-in-the-loop" approach is possible due to orbits reconstruction from radio-science and optical relative navigation. The next flying-legs with the expected trajectories are sent via the mother-craft. The autonomous navigation computes the necessary delta-V from the on-board determination of the relative position. QBDIM was presented before the national space agency that has funded additional studies. To date more than 40 students from France and Taiwan have been involved.

1. INTERPLANETARY 3U CUBESATS?

While in the past CubeSats were only associated to educational goals, they are more and more associated with high scientific payback for a very affordable financial effort. In 1999 the California Polytechnic State University (Cal Poly) and the Stanford University developed the CubeSat specifications to help the universities build their own spacecraft. The CubeSat standard (www.cubesat.org) makes the development of satellites, especially by universities, easier, cheaper and faster than usual space programmes. Paris Observatory is a member of the French PSL Research University and has created its space campus CERES for CubeSats. Various projects are hosted including BIRDY and QBDIM for deep-space science at CubeSat scale. A major partner for BIRDY and QBDIM is the National Cheng Kung University (NCKU) in Taiwan that has been experienced with CubeSats for many years.

A 3-Unit CubeSat (3U), like BIRDY and QBDIM, has a volume of about 10x10x30 cm^3 in its deployment container before launch, and a maximum mass of 4 kg.

To date, never a CubeSat has been launched on an interplanetary mission. A first attempt will be the MarCO mission consisting in two 6-Unit CubeSats to fly with the next INSIGHT mission to Mars and to relay the data to the Earth during the Entry-Descent-Landing phase at Mars. As assessed by Staehle et al. [1], a deep-space CubeSat should be at least a 6-Unit in volume to consider the need of long-range telecommunication, of propulsion for large delta-V needs (solar sail or thrusters) and of large payload. However, with different assumptions, we decided to keep the 3U form factor and to take advantage of the new paradigm of CubeSats in terms of limited size and standardized interface to the host mission. An example of limitation of the CubeSat paradigm will likely remain the use of Commercial off-the-shelf components (COTS) for deep space missions that shall be carefully addressed due to long durations of the missions.

The main assumptions for both BIRDY and QBDIM that keep the spacecraft at 3U form factor are a 1U payload, the delta-V to deep-space provided by the host mission, the short-range datalink and a 0.5U 4-thruster electrical propulsion system.

2. BIRDY FOR INTERPLANETARY SPACE WEATHER

BIRDY stands for "Bleeping Interplanetary Radiations Determination Yo-yo". The science case is to take advantage of any major mission to Mars to prepare a dedicated Earth-Mars-Earth mission that would take part in the space weather understanding. BIRDY's payload is a specialized and miniaturized instrument inspired from an instrument in the Martian MSL-Curiosity mission that was turned on during the cruise to Mars. It can improve the current models of radiations due to the solar wind, the Galactic Cosmic Rays (GCR) and their mutual interactions.

BIRDY Science Case is being assessed by PhD Student Jordan Vannitsen at NCKU Taiwan, with the support of NCKU Master's degree students.

2.1. Lessons learned from the RAD instrument on MSL-Curiosity

To study the radiations, their abundance and their propagation in the interplanetary medium, simultaneous observations at different locations of the solar system are absolutely needed, hence the idea of multiplying low-cost probes inside the solar system. Then dynamic models can be consolidated by observational data.

The science for space weather concerns different kinds of particles in a broad energy range. It addresses major questions in fundamental physics and, notably, the interactions with the Earth atmosphere. It also addresses the interactions with the structure of spacecraft. It contributes to assess the risks of future manned missions by providing the knowledge of the deep space environment. The case of a journey to Mars makes an interplanetary CubeSat relatively easier in many ways. Satellites have already provided some data, for instance the twin probes STEREO A and B, SOHO. Their measurements of radiations are inferred from data produced for primary goals that do not target Space Weather science specifically. Most of the missions studying Space Weather focus on the energy range of a few keV/nucleon to a few tens MeV/nucleon. Also, most of those missions do not try to characterize the energetic particles by ion species.

In 2011-2012, during the Earth-Mars cruise of the Mars Science Laboratory (MSL) Curiosity mission, the Radiation Assessment Detector (RAD, P.I. D. Hassler, 2012, [2]) provided the first observational data of the interplanetary medium on an Earth-Mars trajectory. The availability of additional in-situ data is strategic, at least for the following reasons:

• The interactions between solar wind and GCR are complex and measurements at different phases of the 11-year solar cycle activity are necessary.

• The available radiation measurements in interplanetary medium from any spacecraft are constrained by the primary goal of that spacecraft that is rarely related to Space Weather (OFF mode or no orientation request). A dedicated mission such as BIRDY would get radiations data dedicated to space weather.

• Despite the fact that several space agencies are preparing interplanetary human missions, the radiations in interplanetary space are still not well known. When the radiation risks of a human mission to Mars are assessed, large margins are taken into account in the radiation models for the safety of the astronauts. Then, it leads to the conclusion that a human mission to Mars is too dangerous according to the radiation levels. This is inaccurate if the models have overestimated the radiation levels. NASA has just started reviewing its past assumptions on radiation hazards and counter-measures (e.g., Aerospace America, 03/2014).

It can also be noted that the RAD instrument (Fig.1) is about 25x10x10 cm^3, 1.6 kg and could be miniaturized to fit in a CubeSat providing a sub-selection of the initially targeted particles. Moreover, various new sensors for particles are also being developed, for instance REPTile (in the US, 1.2kg), HMRM (UK, 52g), SREM (CH, 2.5kg) or NGRM (CH, 1kg).



Figure 1. RAD "Radiations Assessment Detector", 1.5Kg © NASA

2.2. Energetic particles of interest

Beyond the Earth's immediate environment, the possible sources of radiations are the Van Allen belts, the Galactic Cosmic Rays (GCR), the Solar Particle Events (SPE) and secondary particles.

• Van Allen belts

The Van Allen belts are made up of particles trapped in the Earth's magnetic field. The outer belt extends until

about 60 000 km. In the case of a manned mission to Mars, the radiation encountered in traversing the Van Allen belts would make a relatively small contribution to the total radiation incurred during the overall mission. They are not considered as a primary objective for BIRDY. However, BIRDY will be turned on as soon as possible after being jettisoned and depending on the time when it will be released, it may also be able to study the radiation belts as a bonus.

• Galactic Cosmic Rays (GCR)

GCR are charged particles that originate from sources beyond our solar system. The GCR are found in the interplanetary space and are comprised of roughly 85% hydrogen (protons), 14% α particles (He), and about 1% high-energy and highly charged ions called HZE (Heavy ion) particles (Jon et al, 2008 [3]). Most of the deleterious effects with regard to health produced by the radiation from the GCR are associated with nuclei in the energy range from several hundred MeV/nucleon to a few GeV/nucleon. A conservative value of 10 MeV/nucleon was proposed (Armstrong, [4]) to define the threshold energy of particles potentially dangerous to humans in space. The current models of GCR disagree with one another especially at energies lower than 1 GeV/nucleon (figure 2). There is a lack of knowledge regarding the solar wind interactions with the GCR. Indeed, it is still not well established which parameters of solar activity and of the solar wind are responsible for the 11-year variation of the isotropic intensity of the GCR. Thus, obtaining in-situ data of the incoming particles due to GCR and solar activity is a key measurement for a better understanding of the solar wind, galactic the cosmic rays and their mutual interactions.

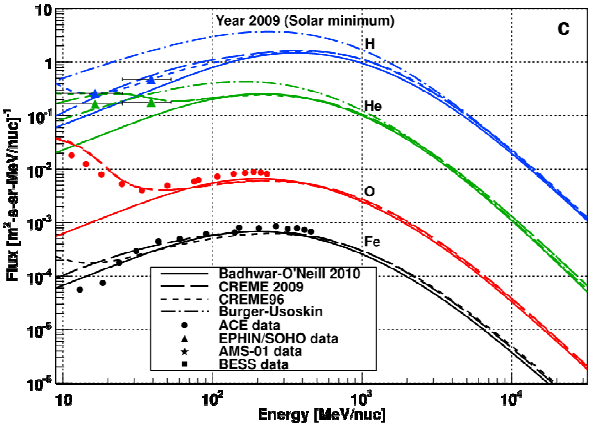


Figure 2: Different GCR models (Mrigakshi, et al., 2012 [5]). Density of ions wrt energy per nucleon. The colors code the different ions, each symbol is associated to a given model

• Solar Particle Events (SPE)

Solar energetic particle events are mostly composed of protons with, in addition, about 10% of He and less than 1% of heavier elements. Solar particle events are rare and occur most often during the solar maximum phase of the 11-year solar cycle (Benton, 2001 [6]). Although SPE are more likely to occur around solar maximum, such events are unpredictable at present (Feynman, 2002 [7]).

The SPE particles get through interplanetary medium along the IMF (Interplanetary Magnetic Field), which describes the so-called “Parker spirals” within the solar system. The typical angle between the IMF lines and Sun's direction is the scientific factor driving the orientation requirement for the payload. Thus, the mission could verify the Hohmann-Parker effect, see [8], which defines that a spacecraft traveling on an Earth-Mars Hohmann trajectory is magnetically connected by the same IMF line coming from Earth or the same IMF line going to Mars (Fig.3). If so, the same SPE flux detected by a space probe could be also detected a few hours earlier nearby the Earth and/or later nearby Mars by other probes. Such a confirmation with BIRDY would be a bonus to contribute in Space Weather awareness.

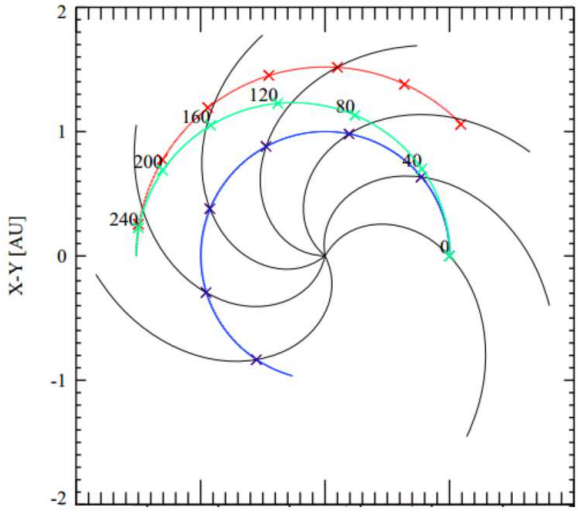


Figure 3: IMF lines (black spirals). Tick marks are successive positions of Earth (blue), of a probe on a Hohmann trajectory (green), of Mars (red). Positions are magnetically connected if the marks are on a same IMF line (Posner, 2013 [8])

• Secondary particles

The secondary particles result from the interaction of SPEs and GCRs particles with matter like the spacecraft itself. In the BIRDY mission, they will not be considered because the CubeSat structure is not representative of a future manned spacecraft structure. These effects could be separately modelled from the measurements of primary particles to implement them in the according high-energy particle transport codes for simulations (Atwell, 2004 [9]). It should be noted that particles due to the CubeSat structure or detector may be mistakenly counted as primary particles with a lower

energy than the actual primary particle. It would result in confusion in the counting of the primary particles. This issue is still under investigation.

2.3. Priority to manned missions

The BIRDY mission has primary scientific and engineering objectives. In addition, it also aims at inspiring people with the deep-space exploration.

The main objective is to take part in the understanding of interplanetary space weather by bringing back in-situ observations to improve the models of radiations. Some arbitration among the possible energetic particles may be necessary to gather useful measurements with a space probe as small as a CubeSat. As there is a huge interest of the public for the manned missions in general and to Mars even more, the priority will be given to the assessment of the manned mission risk.

We also think that the time has come for interplanetary CubeSats. Fortunately, the journey to Mars is easier than other destinations due to launch opportunities every two years. In addition several orbiters are already at destination and could provide data relay for BIRDY. For this reason the mission profile is focussed on missions to Mars and, if demonstrated, could be extended to any opportunity of a planetary mission.

3. BIRDY MISSION PROFILE

The original idea for BIRDY is to take advantage of any flagship missions to be sent to Mars. BIRDY will cruise to Mars and come back to Earth on a so-called "free-return" trajectory as seen in Fig. 4 inspired from Dennis Tito's mission profile for 2018 ([10]). But the trajectory should not necessarily be identical.

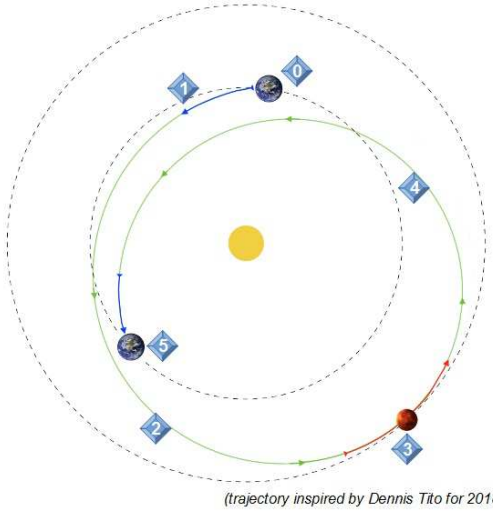


Figure 4: Typical free-return trajectory for BIRDY's mission profile from Earth to Mars and back (inspired by Dennis Tito / Inspiration Mars Foundation and recomputed for BIRDY)

BIRDY is piggy-backed on the host mission to Mars and jettisoned at the beginning of the journey (phase 1 in Fig.4 above) after the Interplanetary Orbit Injection (IOI), thus the delta-V is provided by the host mission. Then it operates in full autonomy, free to spin and without putting any risk on the host mission. It counts energetic particles while rotating its detector's axis in a plane perpendicular to the Sun direction (phase 2 above). During this phase there is not any communication with the Earth. The BIRDY navigation function is an optical "planet tracking" system that relies on a fine ground preparation that yields the data to be stored on-board before the departure (phase 0 above) and a robust on-board computation based on these data and optical measures as detailed in the next sections. It adapts its trajectory to perform the exact flyby at Mars (phase 3 above) that permits to upload the scientific data to a Martian orbiter and to come back to the Earth. Reaching Mars is mandatory to get the data back to the Earth. The flyby at Mars is required to tilt the return orbital plane so there will be an encounter of the return trajectory and the Earth, if achievable. However it is a bonus because a first set of valuable data will have been uploaded already. As said, the collected science data are uploaded in Mars' vicinity (at step 3) and when back to the Earth (at step 5) before crashing in the atmosphere. On the way back (phase 4 above), a second set of scientific data is collected like in phase 2.

Thus, two major engineering objectives have to be taken into consideration:

• to collect and keep the data for a duration as long as an Earth-Mars-Earth free-return trajectory, and to upload these data to a Martian orbiter and to ground stations when back nearby the Earth;

• to autonomously estimate its own position with a Planet Tracker and to adapt its trajectory with an on-board small electric propulsion to allow a free return to Earth.

4. DEEP-SPACE ABSOLUTE NAVIGATION

4.1. Overview of the AOCS

This paper reports the progress of on-going studies mainly performed by students at Undergraduate, Master's and PhD degrees.

For Attitude Control, the Liquid-micro-Pulsed-Plasma-Thruster (LµPPT) configuration shows sufficient performances with ideal sensors (fine models have still to be introduced). The LµPPT also induces residual linear velocity during attitude control that must be included in the Trajectory Correction Manoeuvres (TCM) calculation.

For autonomous navigation, it was demonstrated that LµPPT is sufficient for the necessary TCM after jettisoning from the host mission between Earth and Mars.

The feasibility issue is about the accuracy of the location determination. A software architecture has been developed for intensive testing of many situations in terms of jettisoning delta-V or TCM delta-V applied during the journey. First achievements have been to identify residual inconsistencies in the prototype of the flight software.

4.2. Liquid PPT propulsion for ADCS and TCM

An electrical propulsion system called "LµPPT" in a 4-thruster configuration provides both the attitude actuators (in Attitude Determination and Control System, ADCS) and the trajectory correction actuators (in Trajectory Correction Manoeuvers, TCM). LµPPT is a solution for CubeSats currently at TRL 3 and being developed by the European FP7 funded "LµPPT" consortium. The propellant is made of liquid Teflon and the tank allows an equivalent delta-V of 80 to 100 m/s (delta-V or attitude control).

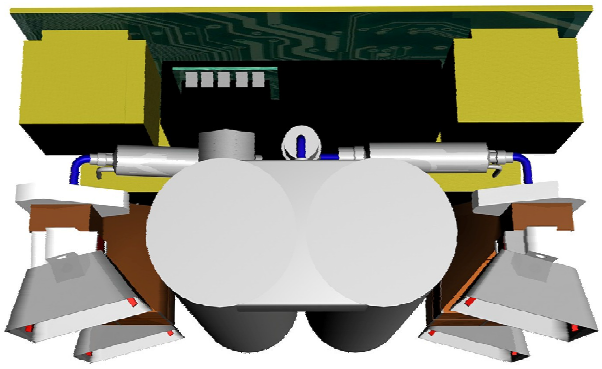


Figure 5: Liquid-µPulsed Plasma Thruster 4-thruster configuration for BIRDY

The functional integration of the propulsion as a full AOCS system for BIRDY and QBDIM is being developed since 10/2015 by PhD Student Gary Quinsac at PSL Research University FRANCE.

For attitude Control, some preliminary control laws have been defined and simulated by undergraduate students at NCKU Taiwan for detumbling, spin, inertial pointing modes. They show an ability to establish the desired mode in a few tens of minutes and less than 10 hours for detumbling with LµPPT only (no reaction wheels).

As a result of the 4-thruster off axis configuration, all modes induce a residual linear velocity. This velocity cannot be neglected in the TCM. The example in Fig. 6 shows an induced linear velocity as great as 7 cm/s while establishing a 0.8 rpm spin), which is a serious amount for deep-space TCM.

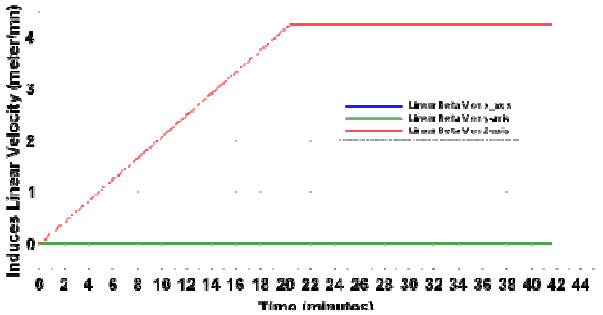


Figure 6: Induced linear velocity on Z-axis by Liquid-µPulsed Plasma Thruster while establishing a 0.8rpm spin about Z-axis.

For trajectory control, preliminary studies have assessed that the propulsion budget available is sufficient to provide the necessary adaptations of the trajectory that will fine-tune the flyby of Mars. The main delta-V for IOI (~8-9km/s) is given by the host mission. After jettisoning, a tiny delta-V (a few m/s) provided by a set of electrical thrusters will change the CubeSat's apocenter by tens of thousands of kilometres.

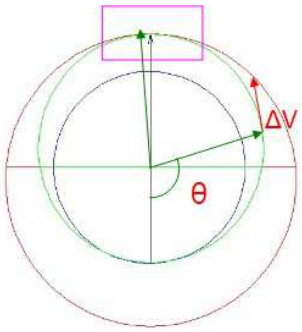


Figure 7: Hohmann trajectory from Earth' orbit to Mars' orbit, prograde delta-V applied at true anomaly θ

The Fig. 8 illustrates the impact on BIRDY's heliocenter in Mars vicinity after a delta-V is applied at true anomaly θ on the Hohmann trajectory between Earth' orbit and Mars' orbit (notations as in Fig.7).

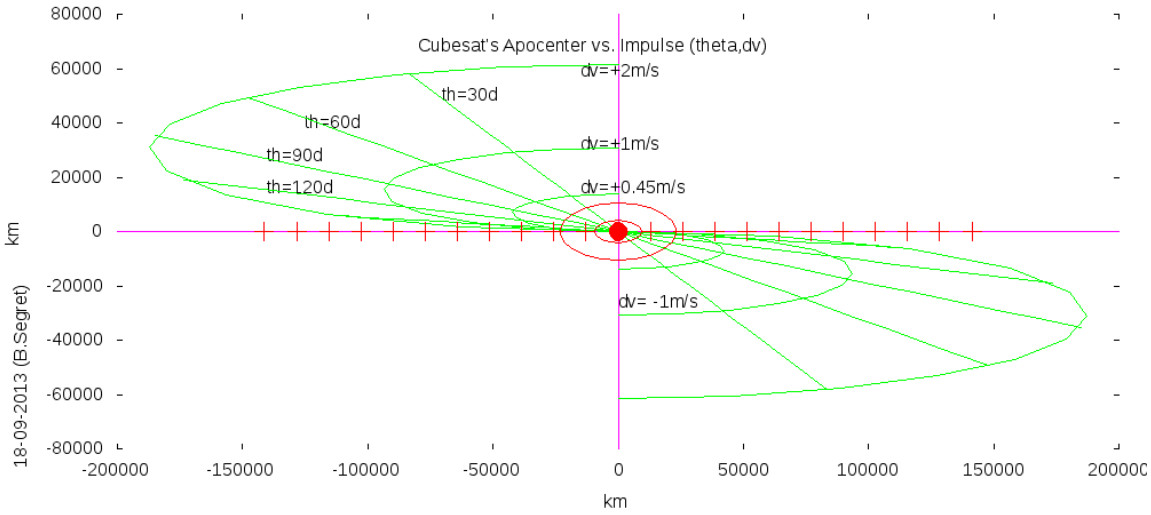


Figure 8: Changed apocenter in green (zoom on the purple area of Fig.7) after a (dv, θ) impulse, drawn for iso-θ (or "th") in [30°; 120°] and iso-dv in [-2m/s; 2m/s] (the Sun is at infinity in -Y direction). Mars and its 2 moons orbits are drawn in red for scale with relative motion on X-axis (1 graduation per hour).

It shows that +2m/s applied in the middle of the journey (θ=100°) will maximize the shift of the heliocenter by 175'000 km and 30'000 km on X-orbit (comparable with Mars' orbit) and Y-orbit (comparable with Sun-Mars radial direction) respectively. This impact of +2m/s has to be considered wrt the ~80m/s delta-V budget of the LµPPT solution.

4.3. Location determination

After jettisoning from the host mission, the CubeSat is fully autonomous. An optical system (Planet Tracker) will provide sky pictures. From those pictures the software will recognise stars and planets directions and compare with the preloaded ones provided by the ground segment. The Autonomous Navigation covers three main functions: the Trajectory preparation (on ground before flight) with a Trajectory Solver, the location determination with a Flight software, and TCM with the LµPPT solution presented above.

Successive versions of the Trajectory Solver, of the Flight software prototype and the testing architecture have been developed by undergraduate, Master's degree and post-Master students in France and in Taiwan under PSL/Paris Observatory's supervision.

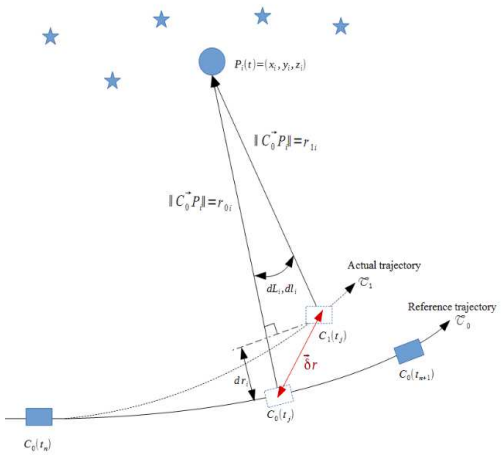
The navigation software consists in estimating the CubeSat's position close to a reference trajectory previously computed on ground by the so-called "Trajectory Solver" and loaded on-board before flight. The initial prototype was written in Free Software SCILAB with CNES library CelestLab for specialized functions in celestial mechanics. The prototype has been migrated to free software Python with the ESA library PyKEP. The major stakes of the Trajectory Solver are:

• to allow easy updates by Paris Observatory's IMCCE (Institut de Mécanique Céleste et de Calcul des Éphémérides, co-author) of the gravitational and non-gravitational models to be considered by the trajectory propagator,

• to quickly and easily assess whether a given launch opportunity allows a mission for BIRDY by providing all necessary analyses to be included in an answer for a Announcement of Opportunity,

• to produce the trajectory of the CubeSat, with the associated ephemeris of foreground bodies as seen from it, with the lightest possible sampling due to on-board storage constraints, taking into account the uncertainty of departure date.

Assuming a reference trajectory is available on-board that provides the expected ephemerid of foreground objects, the theory tells that either multiple images at different dates of a single objet or images of several foreground objects are necessary (Fig.9).



$$\begin{bmatrix} 1 & 0 & 0 & \cos(l_{0i})\cos(L_{0i}) \\ 0 & 1 & 0 & \cos(l_{0i})\sin(L_{0i}) \\ 0 & 0 & 1 & \sin(l_{0i}) \end{bmatrix} \begin{pmatrix} \delta x \\ \delta y \\ \delta z \\ dr_i \end{pmatrix} = \begin{bmatrix} r_{0i}\cos(l_{0i})\sin(L_{0i}) & r_{0i}\cos(L_{0i})\sin(l_{0i}) \\ -r_{0i}\cos(l_{0i})\cos(L_{0i}) & r_{0i}\sin(l_{0i})\sin(L_{0i}) \\ 0 & -r_{0i}\cos(l_{0i}) \end{bmatrix} \begin{pmatrix} dL_i \\ dl_i \end{pmatrix}$$

*Figure 9: Calculation of **δr** in spherical coordinates, assuming the actual trajectory is close from the reference trajectory (Taylor's development at the first order). System of equations: 4 unknowns (δx, δy, δz, dr) and 3 equations, the problem is under-constrained.*

By multiplying measurements from the CubeSat and assuming that the velocity is constant (Fig.10) during a session of measurements the problem can be expressed with 4 measurements in a system of 21 equations and 19 unknowns, thus it becomes over-constrained.

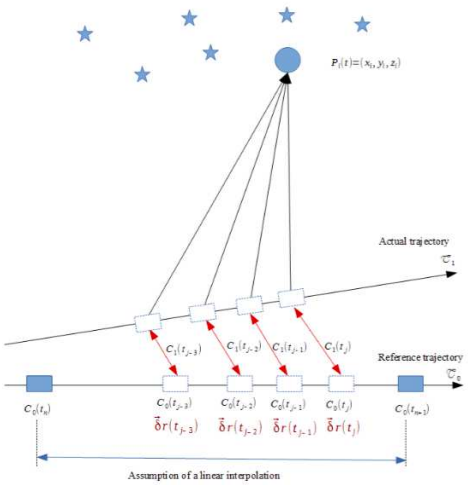


Figure 10: Four measurements (here of the same foreground object at different dates) with assumption of a constant velocity.

The matrix system is expressed in [C].[X]-[Y]=[0], with [X] the state-vector of 19 unknowns, [C] a 21x19 matrix and [Y] a 21-dimension vector. A scalar function χ^2 is defined based on the standard norm in 21-dimension:

$$\chi^2(\vec{X}) = \left\| C.\vec{X} - \vec{Y} \right\|^2 \qquad (1)$$

The problem consists now in finding [X] that best minimizes the χ^2. [X] being a 19-dimension vector, the gradient of χ^2 is a 19-dimension vector and is equal to zero vector at any local minimum. Expressing the analytical form of the gradient being zero yields a linear system of 19 equations on [X] that can eventually be inverted.

$$\vec{X} \,\Big|\, \overrightarrow{\nabla\chi^2(X)} = \left[\frac{\partial \chi^2}{\partial x_i} \right]_{i=1..19} = \vec{0} \quad (2)$$

There are several ways to proceed and three additional requirements:

• the solution must be computed on-board

• the measurements must be made when TCM are still possible with the remaining delta-V budget

• the accuracy on [X] must be sufficient to apply an efficient delta-V.

At a prototyping level in the open source free software OCTAVE we decided to directly invert the matrix in (2) and to analyse the accuracy we can expect on [X]. With our Trajectory Solver we produced an Earth-Mars reference trajectory, say T_0, and its associated ephemerid of Jupiter, say J_0, with a simulated jettisoning of the CubeSat in the Earth vicinity. Then we produced a second trajectory, shifted from T_0, and its associated ephemerid of Jupiter, say T_1 and J_1, with a +1m/s delta-V on a transversal axis at the date of jettisoning the CubeSat at the same location like previously in T_0. We then injected the J_1 as measurements of the foreground object (only one object at different dates) and compared the [X] state-vector as solved with our Flight software prototype with the actual [X] vector as simulated in T_1. The results all over the trajectory were plotted (Fig.11) in terms of transversal and longitudinal errors (reconstructed T_1 along actual T_1).

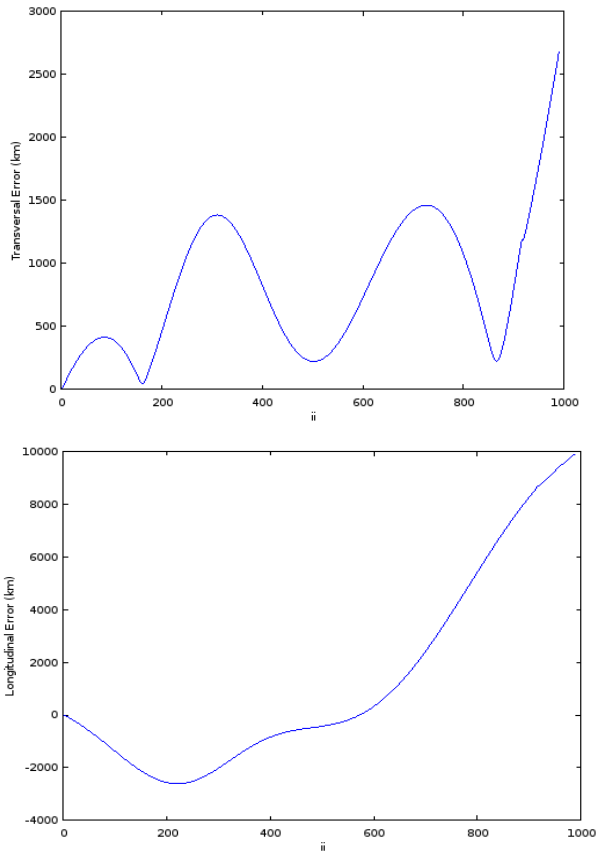


Figure 11: Transversal (top) and longitudinal (bottom) errors of T_1 trajectory as reconstructed compared to the actual T_1. ("ii" axis are the 6-hour timesteps, i.e. the full journey to Mars is about 200 days = 800 timesteps)

Several limitations were introduced in this simulation: the use of only one foreground object (Jupiter) instead of several in the general case, the shift of T_1 wrt T_0 that increases over time and the assumption of a constant velocity during the measurements that could not be optimized here. Considering these limitations, we can conclude that we obtained very promising results: indeed the error in absolute interplanetary location by ~2000 km in the middle of the journey (to be considered with the true anomaly θ=100° in section 4.2 for a most efficient TCM) is very good.

5. APPLICATION TO QBDIM

The studies for QBDIM are just starting, with a financial support by the French agency CNES. Master's degree students shall be involved from January 2016.

5.1. Planetary geodesy at an asteroid

QBDIM was initially proposed as a complementary probe for an ESA's mother-craft mission called AIM (see [11]) to Didymos, a complex double asteroid that will approach the Earth at 0.11 AU in 2022. However QBDIM is not limited to this asteroid and offers a new concept of operations.

Our knowledge of the Solar System formation, its evolution, as for extrasolar planetary system in general relies in part on our knowledge on the dynamical and physical properties of the small bodies of the Solar System (SBSS). One of the - still poorly known - properties of asteroids and small bodies in general are their mass, density, and internal structure. These are somewhat related, and binary asteroids, to that respect, are of prime importance. Indeed observation from ground (generally with large telescopes e.g. ESO's Very Large Telescope, or CARA's W.M. Keck Observatory) or from Earth-bound platforms (e.g. ESA-NASA's Hubble Space Telescope, or ESA's Gaia mission) can generally reveal the total mass of the system. Besides rendezvous missions as in-orbit probes provides the mass from the gravity perturbations.

This applies to any kind of bodies in particular moons in orbit of a primary asteroid or a planet ([12]).

We plan to use radio science, that has demonstrated to be a powerful and well established approach, and optical capabilities on CubeSat to derive the mass and the gravity field information (expected to be very low, [13]), emphasizing the case of a binary / multiple system since in that case one has at disposal two satellites, one moon and one artificial satellite. The relative position of the binary components and the position w.r.t. to stellar background provides the necessary material (scale and orientation) needed to compute all the orbital parameters, and their evolution [14].

By this way we want to enhance our expertise on:
• autonomous navigation, astronautic, radio-science, space astrometry
• planetary geodesy, mass, gravity field, internal structure determination

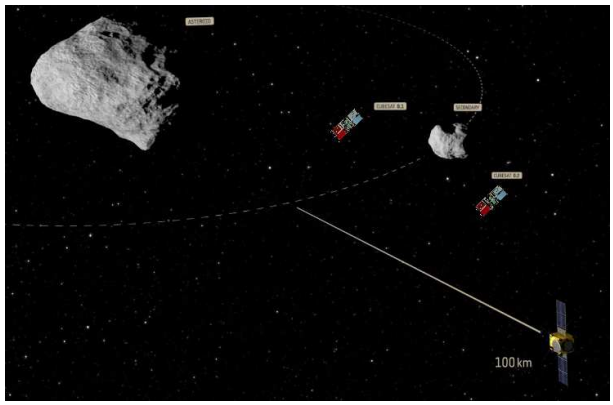


Figure 12: Artist impression of ESA's AIM context at Didymos with 2 CubeSats (background image © ESA)

Interplanetary CubeSats are valuable: approaching the target is worth taking the risk, while it is too risky for the mother-craft to do, and brings supplementary information to the main mission. QBDIM could fly inside the system of a double asteroid (e.g. Didymos in 2022), hover the terrain where a lander has been released (e.g. Philae and Rosetta), fly at close distances to image the surface for proper motion determination, or experience gravitational effects of the explored bodies (e.g. MEX at Phobos or Cassini at Saturn's moons). The CubeSat complementary mission will provide additional data faster and most likely at a higher precision than would be possible using the mother-craft only, for instance, regarding the rotation state, the gravity field and the orbit dynamics. In addition within ESA's AIM mission, an American impactor should impact the small body and there is so an opportunity for CubeSat to perform from multiple angles impact and post-impact observations. Probing the gravity field at various distances yields different frequencies of the harmonic expansion, and different information on the mass distribution. For low- to micro-gravity objects one needs to perform close approach rendezvous.

5.2. QBDIM Concept of Operations

An important assumption is the S-band communication between the mother-craft and the CubeSat to perform a data relay (command and measures) with the Earth. In the particular context of AIM, the full Didymos A-B system is about 1 km in size and the mother-craft would release the CubeSat not closer than 5 km and would then operate from an average distance of 100 km.

Then the concept of operation of QBDIM can be summarized as “Multiple flying legs – One routine sequence”. It consists in commanding successive flying legs within the double system Didymos A & B. One leg is a basic sequence of operations and measurements and lasts a few days. Each leg is commanded by a simple set of data transmitted from the ground via the mother-craft and returns the data gathered in the previous leg. The ground segment can be updated, during the mission with the best available gravitational models by Paris Observatory’s IMCCE and interfaces with the mother-craft mission communication pipeline.

The design includes the LµPPT solution as presented in section 4.2 and Fig.5. The configuration with 4 thrusters provides detumbling, linear and rotational delta-V. It can be assisted with reaction wheels if needed (trade-off), then the LµPPT system would provide the Wheel Off-Loading function.

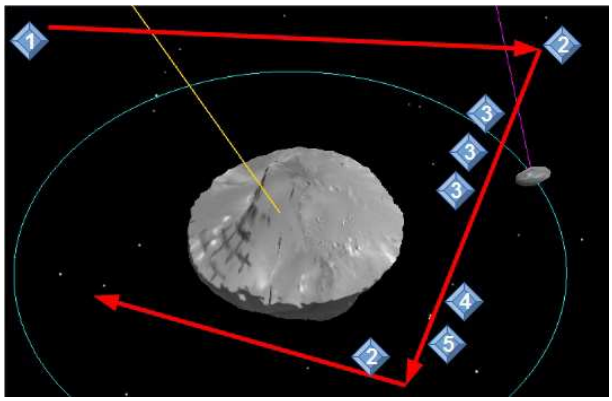


Figure 13: Sequence of operations in each “flying-leg”

After jettisoning and detumbling in a few hours, the CubeSat is sent to one single direction. It takes less than one day for LµPPT to provide 1 m/s (for instance) and ~40 km will have been flown, then it can fly about one more day (~90 km) within the double system Didymos A-B, then a new delta-V, combining previous and next velocity needs, takes another one or two days (marks “2” in Fig.13). As a good magnitude, it can be considered that a single leg lasts about 2 days and flies up to 150 km. The delta-V budget of the LµPPT solution allows 30 to 50 flying legs within about 3 months.

The standard sequence of operations anticipates image data and radio-science (echo or Doppler with multiple targets) at close range (marks “3” in Fig.13) from the asteroid and radio-science (mark “4”) with optical navigation (mark “5”) measurements at long range.

5.3. Re-use of BIRDY studies for QBDIM

As already said, the same electric propulsion for BIRDY at 0.5U is considered for both attitude and orbit controls in QBDIM.

The so-called "Planet Tracker" for BIRDY becomes an “Object Tracker” for QBDIM as foreground objects are not planets anymore but Didymos A-B and possibly the mother-craft as well. COTS accelerometers and COTS sun sensors may also be considered for the attitude determination (trade-off).

The autonomous navigation in QBDIM consists in a relative navigation within the system. The reference trajectory is computed for each flying leg and sent on-board with the S-band data relay. Then the shift of the actually experienced flying leg is reconstructed on-board with the same approach like BIRDY (section 4.3). The shift is taken into account to apply the next TCM. In addition the computed shift, some images of the context (foreground objects with stars) and radio-science data are sent back to the ground and models are improved for the computation of future flying legs.

Two new engineering requirements for this particular context of operations can be expressed:
• anticipate the effect of non-punctual objects on the data reduction of optical measures (with object shapes that will be known very late only)
• provide a very reactive ground segment based on the “models-in-the-loop” approach, with a dedicated team during the operations that should integrate smoothly within the mother-craft mission.

6. PROTO-FLIGHT MODEL IN HEO

The challenges for both deep-space CubeSats BIRDY and QBDIM require an In-Orbit Demonstration around Earth before flying to Deep-Space:

• the functional integration of the LµPPT solution as an Attitude and Orbit control actuator, considering the time needed to establish a measurable change with this kind of propulsion.
• the telecommunication either in S-band at a distance of a few thousands of kilometres (mother-craft at an asteroid or flyby over an orbiter at Mars), or in UHF/VHF at long-range and high velocity with ground stations (while returning to the Earth).
• the autonomous navigation, either in absolute or relative location determination, considering the needed time to make measures of close objects and to compute the location on-board.
• the resilience in an interplanetary radiation environment for a long period of time, in particular for the stored data before uploading them to another spacecraft or to a ground station.

A Proto-Flight Model in Highly Elliptical Orbit (HEO) can demonstrate these functions. However a part of the demonstration could be also provided by other means (sounding rocket above 100 km, non-released payloads on intermediate stages of launchers to GEO…).

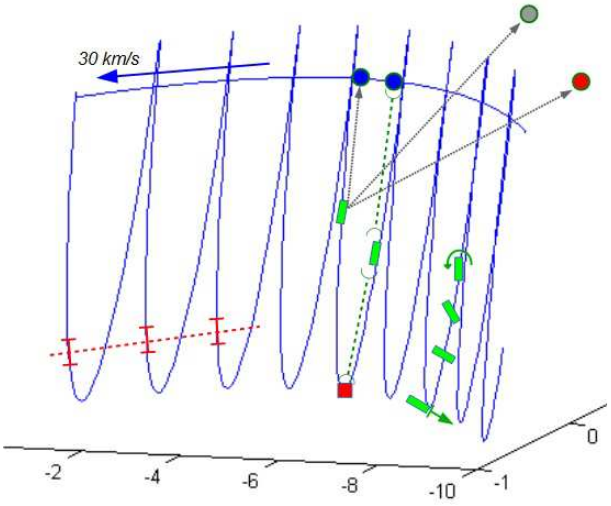


Figure 14: Possible demonstrations in GTO (plotted in Sun-centered reference) with a Proto-Flight Model

As a baseline we expect a Proto-Flight Model could demonstrate the four functions on a HEO that could be a Geostationary Transfer Orbit (GTO). GTO is interesting because it is a relatively frequent opportunity and not too much demanded for CubeSats. It seems that GTO could then allow:

• test the LµPPT solution by measuring on-board received GPS signals while applying some propulsion in the slow motion sections of the orbit (close to apogee), as shown in green on the right of Fig.14.

• test the telecommunications for close to far distances, including intersatellite communications with a satcom in GEO, as shown in green at the center of Fig.14.

• test the autonomous navigation by considering foreground objects like planets and possibly bright satellites in LEO/MEO/GEO, and considering a pseudo-reference trajectory, as shown in red of Fig.14, that could be the parallel of Earth's orbit about the Sun if the measurements are made at a same given true anomaly of the HEO (then the pseudo-velocity between the measures can be assumed constant).

• regarding the radiation environment, the advantage of a GTO is to cross the harsh environment of the Van Allen belts providing so a valuable resilience test. It has been estimated that 15 days at crossing the Van Allen belts on a GTO is equivalent to the total dose that the CubeSat would receive in 1.5 year in interplanetary medium on the Earth-Mars-Earth journey. Then the PFM should have a timeline that could demonstrate all necessary functions within a few days.

7. AKNOWLEDGMENT

All preliminary studies for BIRDY and QBDIM have been made possible with the financial support of the Labex ESEP (www.esep.pro) of PSL Research University and Investissements d'Avenir.

8. LIST OF CONTRIBUTORS

(08/2015)

Students (numbers in brackets refer to the institutions listed below): J.Vannitsen (8), A.Ansart (15,8), Q.Tahan (15,8), M.Agnan (10,8), J.Velardo (10,3), A.Deligny (10,3), G.Quinsac (10,3), A.Porquet (10,3,7), A.Lassissi (10,3), N.Gerbal (15), O.Sleimi (14,8), S.Durand (10,3,4), R.Klajzyngier (18), J.Diby (18), T.Mallet (18), J.Foissaud (18), L.Orsatto (18), E.Colin (18), N.Heim (18), J.Lin (8), A.Tsai (8), A.Chen (8), J.Tsai (8), T.Chang (8), D.Boisseau (15,8), A.Sibué (11), J.Evens (11), A.Schnitzer (10,3), S.Thibault (10,3), H.Poincelin (10.3), S.Delaire (20), I.Berber (20), T.Charoy (20), A.Nirello (20), A.Sabir (20), M.Bougadouha (20), F.Le-coz (20), M.Gonzalez (20), M.Romero-Lopez (20), D.Gonzalez (20), I.Ouattara (8), F.Rizzitelli (8).

Supervisors, experts and sponsors (numbers in brackets refer to the institutions listed below): B.Segret (4,9,3,1), B.Mosser (4,10,11), K.Wang (8), J.C.Juang (8), J.J.Miau (8), C.Koppel (16,17), J.Daniel (1), Y.Desplanques (18), D.LePicart (18), P.Boutin (20), F.Deleflie (7,3,6,12,13), M.Cabane (5,12), M.Dudeck (12), K.L.Klein (4), N.Vilmer (4), R.Heidmann (1), P.Brisson (1,2), D.Coscia (5), G.Cimò (19).

Involved institutions: 1.Association Planète Mars, 2.Mars Society Switzerland, 3.Observatoire de Paris, 4.Laboratoire d'Etudes Spatiales et d'Instrumentation en Astrophysique, 5.Laboratoire Atmosphères, Milieux, Observations Spatiales, 6.Centre National de la Recherche Scientifique, 7.Institut de Mécanique Céleste et de Calcul des Ephémérides, 8.National Cheng Kung University, 9.LabEx Exploration Spatiale des Environnements Planétaires, 10.Centre d'Etudiant pour la Recherche et l'Exploration Spatiale, 11.Research University Paris Sciences Lettres, 12.Pierre and Marie Curie University, 13.Université Lille 1 Sciences et Technologies, 14.Institut Polytechnique des Sciences Avancées, 15.École d'Ingénierie des Sciences Aérospatiales, 16.Consortium Liquid Micro Pulsed Plasma Thruster, 17.KopooS Consulting Ind., 18.Ecole Centrale Lille, 19.Joint Institute for VLBI in Europe, 20.Ecole Centrale Paris

9. REFERENCES

[1] Staehle R., et al. (2013): Interplanetary CubeSats: Opening the Solar System to a Broad Community at

Lower Cost, Journal of Small Satellites, Vol. 2, No. 1, pp. 161-186.

[2] D.M. Hassler, et al., The Radiation Assessment Detector (RAD) Investigation, 2012, Space Sci Rev DOI 10.1007/s11214-012-9913-1.

[3] Jon R., Wenonah V., Barbara J. N., Al K, Space Faring, The Radiation Challenge, NASA, 2008.

[4] Armstrong, T.P., Strategies for mitigation based on increased knowledge of the solar particle radiation hazard en route to/at Mars for spacecraft systems and for astronauts/cosmonauts. In: The Particle Radiation Hazard enroute to and at Mars. Publ. Internat. Acad. Astronautics.

[5] Mrigakshi et al., 2012, Journal of Geophysical Research, 117, . A08109.

[6] Benton, E. R., et al., Space radiation dosimetry in low-Earth orbit and beyond, Nucl. Imm" Method Phys Res., B. vol. I E4 (I - 21, pp.255-294, 2001).

[7] Feynman J., et al., 2002, JPL proton fluence model: an update. J. Atmos. Terr. Phys. 64(1),679–1,686.

[8] Posner A., et al., The Hohmann-Parker effect measured by the Mars Science Laboratory on the transfer from Earth to Mars: Consequences and opportunities, 2013, Planetary and Space Science 89, pp. 127–139.

[9] Atwell W., Saganti P., Cucinotta F.A., Zeitlin C.J., 2003, A space radiation shielding model of the Martian environment experiment (MARIE), Advances in Space Research 33 (2004) 2219–2221.

[10] Tito Dennis, et al., Feasibility analysis for a manned Mars free-return mission in 2018, Aerospace Conference, 2013 IEEE.

[11] Michel et al. AIDA: Asteroid Impact and Deflection Assessment Mission Under Study at ESA and NASA. LPICo 1809, #6008.

[12] Tajeddine et al. 2015. Cassini ISS astrometry of the Saturnian satellites: Tethys, Dione, Rhea, Iapetus, and Phoebe 2004-2012A&A 575, 73. http://cdsads.u-strasbg.fr/abs/2015A%26A...575A..73T

[13] Fujiwara, et al. 2006. The Rubble-Pile asteroid Itokawa as Observed by Hayabusa. Science 312.1330

[14] Kovalenko et al. 2014. Study of binary asteroids with three space missions. COSPAR 40, #1609.

ON DESIGN FOR RELIABILITY OF ELECTRONICS IN NANOSATELLITE

Olga V. Mamoutova, Andrey A. Antonov

Peter the Great St. Petersburg Polytechnic University,
off. 216, 21 Polytechnicheskaya st., St. Petersburg 194021 Russia,
Email: mamoutova@kspt.icc.spbstu.ru, a.a.antonov.aivt@gmail.com

ABSTRACT

One of the current trends in quickly maturing nanosatellite technologies is a dependability concern. The challenge is to keep design for reliability in a nanosatellite project relatively cheap and simple. This paper gives an overview of current approaches to fault tolerant nanosatellite designs, which include topics of component selection, hardware and software architectures, team management decisions, etc. The educational project Polytechnic-Space 101 serves as an example of reliability engineering university course adapted for a nanosatellite design task.

Key words: dependability; nanosatellite; engineering education.

1. INTRODUCTION

Since late 1990[s] university nanosatellite projects have been providing practical education and training for engineers in the field of techniques and rigours of a spacecraft design and construction [29]. With a small mass (from 1 to 10s kg), relatively low cost and short design time a nanosatellite gives an opportunity to implement a complex functionality, which is comparable to the one in a bigger, traditional satellite.

Reliability has not been the major concern for nanosatellites. Designers intentionally use commercial-grade electronic components and exclude costly procedures to shorten the design lifecycle and reduce the mission cost. The traditional reliability analysis and qualification tests are usually omitted. And this was fully acceptable for the early days of nanosatellites.

However, quickly maturing nanosatellite technologies promise longer mission durations, ambitious scientific objectives and commercial profit, and therefore call for reliable solutions that remain easily applicable and comparatively cheap.

The aim of this paper is to investigate state of the art approaches to fault tolerant nanosatellite design from an electronic or computer engineer point of view. Section 2 contains the basis of dependability topic. Section 3 defines the objectives and features of a fault tolerant nanosatellite. Section 4 contains an overview of the state of affairs in the field. And section 5 presents the *Polytechnic-Space 101*, which is the working title of an educational nanosatellite project being developed in Peter the Great St. Petersburg Polytechnic University.

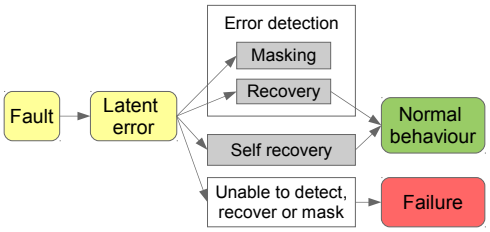


Figure 1. Lifecycle of a fault

2. PRELIMINARIES: DEPENDABILITY AND DESIGN FOR RELIABILITY

Dependability is one of the basic objectives of engineering, along with performance, energy efficiency, cost and design time. A schematic overview of dependability and reliability design issues is shown in Fig. 1. The basic concept of dependability is *fault*. All kinds of faults result from the system environment, components and design process. In presence of vulnerabilities of the system a fault causes changes in the state of the system – an *error*. Occurred errors may lead to a subsequent deviation of delivered behaviour (or service) of the system from the expected one. When the system can no longer fulfil its target function there is a *failure* [2]. So *dependability* can be defined as an evaluated property of the system to deliver the expected behaviour [22].

Dependability is a broad term, which covers availability, reliability, safety, maintainability, security, etc. But usually for a particular system only a certain combination of attributes from the list is applicable. The most common one is *reliability* – the system property to continually provide a service over a period of time.

To address the challenges of dependability the present approaches to *design for reliability* target four areas: fault prevention, fault tolerance, fault removal, and fault forecasting. *Fault prevention* finds and eliminates causes of faults. *Fault tolerance* ensures the continuity of the service in the presence of detected faults. *Fault removal* attempts to recover the system from the detected errors. Also unintended redundancy of the system itself may create *self recovery* effects. *Fault forecasting* includes both design-time and

operation-time estimations of fault occurrence, presence and consequences.

An established armoury of reliability engineering methods and techniques for computing systems includes a broad range of tools from risk analysis approaches, error detection and correction via structural, informational and timing redundancies, strategies for a quality design, verification, simulation and fault injection methods, to dependability benchmarking. And only the proper combination of those means for dependability can result in a successful design with a certain level of confidence in reliability.

3. NANOSATELLITES AND RELIABILITY

3.1. Nanosatellite Definition and Objectives

The history of modern nanosatellites starts from the first launches in 1997. The definition of a nanosatellite (also called a lean satellite) includes the following key features [4], [9]:

1. small mass, from 1 to 50 kg,
2. short development schedule, from 12 to 18 month,
3. extensive utilization of modern technologies that are uncommon for traditional "big" satellites.

The objectives of those projects are educational purposes, technology demonstration, scientific experiments and radio communication. Orbits and mission durations of nanosatellites vary, but a typical nanosatellite would be created for a low Earth orbit with a lifetime around eight months.

The design of a nanosatellite is always severely constrained by limited electrical power, size and weight budgets. Moreover, these constraints result in reduced data rates over a radio channel and reduced resolutions (e.g., optical) of observation instruments. This limits target payload and overall mission objectives.

However, nanosatellites are considered to provide an excellent, cost-effective means for conducting single-purpose missions. Today the nanosatellite technologies have a huge projected growth and a vast potential for civilian space industry [6]. With ever lowering cost of development they continuously move more towards critical missions in the field of space-related scientific and commercial applications. Therefore the reliability of a nanosatellite becomes quite an important subject.

3.2. Nanosatellite Reliability Peculiarities

Foremost, the reliable design starts with a dependability and security specification. It should identify the classes of expected faults, and set the goals for important dependability attributes. Following is a brief overview of the key points of that specification.

Expected faults. There are three major classes of faults: development, physical and interaction. They are common for any system, but their importance depends on the particular system's development and operational environment. The full taxonomy of a fault is multi-dimensional and complex, hence it is important to understand, which faults should be addressed during design and operation phases. Here we offer a description of the fault classes in a manner that is appropriate for a nanosatellite project.

Development faults can occur in the forms of design mistakes or bad design decisions. (We consciously omit malicious design faults from this overview out of presumption about a designer's goodwill.) Both types are highly relevant to nanosatellite designs. First, it is a matter of fact, that every design has *mistakes* in it. Then, the amount of mistakes is jeopardized due to rejection of traditional qualification tests and current inexistence of newly-established test methods and procedures appropriate for nanosatellite designs. On top of that there may be presence of certain poor qualities of the design teams: staff turnover, lack of competence, etc. (which is typical of university-based projects). Second, inherently strict design budgets inevitably result in tradeoffs, which can later manifest themselves as unacceptable system behaviour and turn out to be *bad decisions*. This problem could be addressed with an extensive verification, but again, the lack of simple and easily applicable design methodologies does not allow for elimination of bad design decisions. Addressing development faults requires some expertise in the field of quality design.

Physical faults affect hardware of the system. Physical faults are either development faults in separate components of the system (production defects), or the faults originating from physical deterioration and from the operational (use) environment. Operation in the open space involves the following environmental factors: ionizing radiation, vacuum, varying temperature, strong vibration and g-force acceleration. In summary, occurrence of physical faults mainly depends on the balance between the cost of the mission, the mission lifetime and the use of non space-qualified components. Addressing physical faults requires some expertise in the field of dependability design.

Interaction faults are external faults occurring during the operation phase. Due to inherent autonomy of a spacecraft, the range of possible faults is limited to *reconfiguration faults* made by erroneous commands from the ground stations or from the satellite constellation, and to *malicious intrusion attempts* exploiting flaws of radio-communication protocols. It is noteworthy, that interaction faults depend on development faults, since only the presence of some vulnerability provides a successful propagation of an interaction fault, which then will result in the system failure. Addressing interaction faults requires some expertise in the field of security design.

Dependability goals. A nanosatellite can be considered as a data-critical application, opposed to money- or life-critical applications of traditional reliability engineering. Indeed, the complete or partial failure of a nanosatellite mission would hardly ever directly endanger a human life or significantly reduce one's commercial revenue. However, a failure would lead to loss of valuable data that satellite is supposed to collect, process and transfer back to Earth while successfully operating in orbit.

In any case a nanosatellite should be a fail-controlled system with the desired level of reliability defined by the target mission. For an educational project dependability the requirements can be very loose, while a commercial mission would set a goal of a highly-reliable mission in order to get the best revenue per satellite ratio.

During the development phase budget or schedule failures can happen. Usually they occur from underestimation of the design complexity. Those failures are typical of R&D projects, and are minimized with industrial technologies. So for the nanosatellite technologies, which are approaching their maturity, we can predict almost a complete elimination of those kinds of failures.

For the operational phase of the nanosatellite's lifecycle the severity classes of failures should be defined. Here the spacecraft autonomy again becomes an important factor, as it limits its repairability and maintainability, i.e. a nanosatellite cannot be repaired after deployment and the possibility of external service restoration is confined to remote reconfiguration from the ground station.

Failures are defined as catastrophic or minor in the context of specified nanosatellite's functions. To provide a graceful degradation of functionality in presence of partial failures it is common to define several operation modes, e.g. mission, standby, safe, emergency and coma [20].

In the scope of previously defined fault classes the goals for operational dependability can be attributed with the reliability metrics for major service functions, robustness for particular fault classes, and availability and security for remote communications functionality.

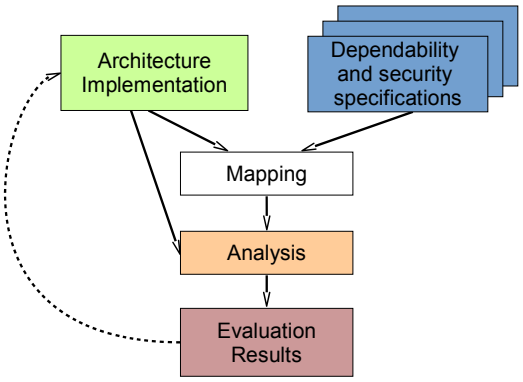


Figure 2. Y-diagram of the design flow from the reliability engineering point of view

Design flow. Virtually any modern design methodology implies an iterative top-down process of specification refinement steps. This is also true for dependability, where another iteration of implementation gives the sources for dependability and security specification updates. Fig. 2 gives an overview of this cycle.

Dependability and security specifications are a set of risk analysis results and failure frequencies and severities analysis results.

A new detailed implementation of the system architecture includes corresponding means of dependability, and initiates a wave of verification, testing, benchmarking and extensive fault injection campaigns. The obtained results of dependability analysis are then included in the next refinement step and will be re-evaluated later.

Fig. 3 gives an overview of all presented terms for design of highly-reliable nanosatellite.

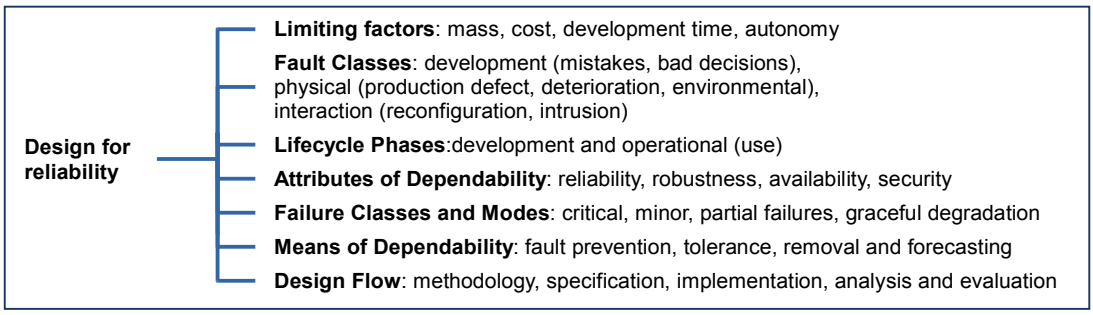


Figure 3. Design for reliability – tree of terms

4. RELIABILITY TRENDS IN NANOSATELLITE ELECTRONICS

Reliability has become the main objective in nanosatellite projects lately. For example, there is a PiCPoT project, where the flight model of a reliable nanosatellite is to be created with less than 25,000€ cost of development [25]. The challenges of creating an operational nanosatellite for a critical mission are thoroughly discussed by Homan and Young [18]. And Hadwin et al. [17] claim, that for next-generation nanosatellites developers must take a vertical approach to design, considering performance, SWaP (size, weight and power) and reliability.

Small satellites in general are less complex hence are expected to be more reliable. Smaller size gives less potential for redundancy implementation, though. Following is a general reliability estimation. Success rate of nanosatellite missions since 2012 is 90% [25]. Reported reliabilities of nanosatellites are less than 30% after 1 y in orbit. The wearout phenomena are not the primary cause of failures in nanosatellites, since infant mortality is much more influential [15], [16]. Meantime, in presence of no statistically meaningful data regarding nanosatellite missions reliability [12], detailed reliability reports are difficult to obtain.

Electronic subsystems make a significant part of a nanosatellite. Those parts perform the power distribution and handle payload data processing, household data and command processing, telemetry, tracking and control support, etc. Failure contribution reports for nanosatellites state that up to 40% of all spacecraft failures relate to telemetry, tracking and control and power supply unit, and up to 15% failures relate to on-board computers and payload [15]. Both for the data-criticality of a nanosatellite mission, and for the control-enabling role of electronics, the reliability of nanosatellite's electronics is crucial for the mission success.

The rest of the section overviews the approaches to reliability that are used for nanosatellites.

4.1. Unreliable components

Commercial- and industrial-grade components substituted space-qualified components and became an enabling technology for nanosatellites by providing higher performance and volumes, and less power dissipation [3]. And those modern commercial components, including microcontrollers, memories and Field Programmable Gate Arrays (FPGA), have proved to be reliable enough to ensure the success of short-lifetime missions.

The remaining concern – radiation – appear as a total ionizing dose and single event effects (SEE). Because of its inevitability these effects are considered as a factor of normal operation and are treated accordingly.

There are two approaches to compensate intolerance of components to radiation. The first one is to use mature components with flight heritage. In this case the cost of the components still remains low, but with time more space-validated nanosatellite-class components will be developed and will become available [18]. The orthogonal approach is to provide fault tolerance via traditional techniques on architecture levels: hardware and software, or a mission level [25].

4.2. Architectures with Redundancy

Nanosatellites with single-string configuration do not suit the needs of critical missions. In such designs, the failure of a single component can result in the mission failure.

Therefore the design of a reliable nanosatellite calls for fault tolerance techniques, which include *structural redundancy* in the form of replicated units with voting, *informational redundancy* in the form of error correcting codes with scrubbing, *timing redundancy* in the form of reboot procedures, check-pointing and roll-back, and *algorithmic redundancy* in the form of watchdog timers and diverse replications of functional chains.

4.3. Distributed Computing and Reconfigurability

One of the emerging trends for nanosatellite architectures is implementation of autonomous or remote reconfiguration. It strongly correlates to the idea of "subsystemless" design [21], which means that there is no strict allocation of traditional satellite functions to physical units. Instead, albeit those traditional functions remain on the logic level, they can be arbitrarily distributed and redistributed across the present multifunctional physical units. This concept comes in a good agreement with the aim for highly-reliable nanosatellite designs.

For example, in Delfi-n3Xt project, implementation of basic computing functions can be delegated to a microcontroller at the primary radio unit [10]. Another great example is described by Ibrahim et al. [19], where SEU protection of FPGAs is achieved with two modes: through software fault tolerance within the majority of the orbit, and through structural redundancy in the minority part of the orbit, where severe SEUs are expected.

In general case, in-flight redistribution of functionality across the units of the system can compensate for failure of a single unit. Moreover, certain units can be switched off and their tasks redistributed on demand according to current flight conditions, or performance and reliability requirements.

Reconfigurability in presence of redundant intersatellite communication media provides an effective elimination of 'single point of failure' vulnerability.

4.4. Generic Modules

Nanosatellites adapted this concept from current small satellite designs with plug-and-play architectures. In essence, modules are designed to be generic, but easily tailored for the specific mission, with (to some extent) arbitrary orbit and target payload. The design concept aims to provide fast and error-free assembly, integration and test process. The greatest advantage of this approach is in reduction of non-recurring engineering costs and reduction of design times, which allows a cost-effective series production.

Existing projects, which utilize this idea, all can be characterized as modular, flexible, scalable, with high-performance and high-reliability. Examples for nanosatellite projects are Multi-Mission Nanosatellite (MMN) platform [26], AraMiS project [28], Reconfigurable Multifunctional Architecture (RMA) with Multifunctional Structural Units (MSUs) [21], distributed multi-computer architecture of the BIRD satellite [3], and low-cost 5kg Generic Nanosatellite Bus (GNB) in CanX project [13].

It is noteworthy, that distributed computing and reconfigurability, which were described earlier, are inherent synergetic qualities of multi-functional designs.

4.5. Efficient Reliable Power

Any gain of functionality and reliability comes at a price of increased power consumption. And we can say, that most designs continue to struggle over this trade-off.

The power subsystem not only should be efficient, it should employ a single-point-failure free implementation, like in the Delfi nanosatellite program [11]. Another example is the PiCPoT satellite with a redundant power management and timing unit, which selects the most charged battery every 60 seconds to power one of functional chains [25].

4.6. Fault Tolerant, but Simple Software

It is known, that fault tolerance is most effective when applied on all levels of system hierarchy. Therefore the flight software of a nanosatellite should also be able to tolerate and isolate faults, recover from errors, and to preserve spacecraft functionality after occurred failures.

An important property of modern satellites is reprogrammability, which supports reconfigurability of multi-functional modular designs. For example, the Fault Protection Engine, described by Jackson [20], is the system-level executive, which serves as a comprehensive fault protection for the satellite and provides modification of fault protection operation on orbit via a software parameters table.

For all that redundancy the software should remain as simple as possible to be power-efficient and easy-to-test. One of the ways to achieve that is to follow the hardware architectures and have a modular, well-structured software architecture [3].

4.7. Security Services

Critical missions of nanosatellites have a risk of malicious attempts to get an unauthorized access and to intercept valuable satellite data. Hence both the uplink and the downlink of the satellite need to be protected.

For that task nanosatellites implement proprietary solutions or inherit standard approaches of traditional satellites. The Consultative Committee for Space Data Systems (CCSDS) protocols and Advanced Encryption Standard (AES) are widely used. Those security services can be implemented either in software [26], or in hardware [30].

4.8. Mission Redundancy

Mission redundancy can compensate limited functionality and fault intolerance of a nanosatellite. Multiple nanosatellites can form a cluster – swarm (when nanosatellites are identical) or a constellation (or satellite network, or formation flight).

A lot of authors investigate this topic. The microspace philosophy [13] states, that to implement redundancy through multiple missions is preferable to multiple components on a single mission. This results in a reduced cost of space missions while increasing mission redundancy and reliability. Jackson and Epstein [21] express the same idea about large nanosatellite constellations: nanosatellites in aggregate have significant capability, the system is inherently fault-tolerant, with reduced recurring cost.

While a nanosatellite itself is complex enough, the nanosatellie constellation can be considered as a system of systems with a complexity of orders of magnitude greater than complexity of a single satellite. Therefore performance and reliability analysis for a constellation becomes a challenging task. To address this problem Engelen et al. [15] developed an analytical model of a nanosatellite swarm in order to evaluate the reliability of the swarm and to show that the spacecraft can be built without any redundant subsystems, if redundancy is provided on a mission level. Another method has been used for the Illinois Observing Nanosatellite (ION) project [1]. To simulate network performance and dependability they have used stochastic activity networks (SANs) in Mobius tool. They show how accumulated radiation dosage affects the functioning of the proposed network, how redundancy and shielding can be profitably used to increase dependability, and how sharing resources through a network could improve communication with the ground.

4.9. Design Methodologies

A lot of effort goes towards development of design methodologies for the nanosatellites. The goal is to have tools and methods, appropriate to the schedule, budget, and risk tolerance of a nanosatellite mission. They imply high speed and low cost of development, common reliability criteria and design approaches, and absence of costly qualification procedures. Current design methodologies vary widely, and certain approaches of different methodologies often contradict with each other.

Firstly, a nanosatellite project needs a general fool-proof design practices. For example, electromagnetic interference control measures, such as component shielding, interface signal filtering, properly designed ground planes, are critical and can help avoid costly corrective repairs during integration phase of design [26], [25]. Designers of ICUBE-1 have developed a programming manual with the programming standards, coding style guides and other established techniques to develop quality codes. Moreover, during the software development process, their software quality assurance team continuously monitors the process as per those guidelines [23]. Busch et al. [7] give a detailed overview about tools and procedures developed for support of robust satellite engineering in the University of Wuerzburgs UWE nanosatellite project. On the same note a microspace philosophy [13] gives general recommendations to focus on good design in consideration of the operating environment and to implement targeted quality assurance approaches.

More specifically a nanosatellite can be considered as a complex system of systems, which needs appropriate systems analysis (or systems engineering) approaches, for example, tools that were created for highly adaptive small satellites (HASS) [14]. Previously mentioned microspace philosophy [13] states, that reliability is related to complexity and that simple satellites are intrinsically more reliable.

The next topic is team-management approaches. Rossoni and Panetta [27] advocate the concurrent engineering team approach for the tightly integrated nanosatellite designs. They state that in order to make optimum gains in integration each discipline engineer will become a “systems level” engineer, concerned of all other disciplines. Eagleson et al. [13] also have chosen to work in small, tightly-knit design teams that focus on cross collaboration rather than on intense documentation.

And towards topic of fault management Brumbaugh and Lightsey [5] proposed a risk management plan for nanosatellites. They have adapted larger-scale risk management plans to the smaller platform with a new set of practices. Based on their work a systems engineer or a mission planner may develop their own risk management plan uniquely suited for their mission.

4.10. Open Technical Standards

For unification of design methodologies several standardization initiatives have been created.

The CubeSat standard is the most commonly used one. It was established in 1999 [8] such that CubeSats could be safely and readily incorporated into the launch vehicle and mission plan without impact to the primary payload. The standard enabled mass production of stock deployment devices and electronic components. With the flight heritage it decreases design, manufacturing and testing costs and provides a certain level of confidence in reliability.

In 2014, an activity at ISO/TC20/SC14 has started with the aim to describe definition and requirements of small satellites.

In 2010 Rogers and Summers [26] introduced a Product Assurance Implementation Plan (PAIP) for nanosatellite missions using the MMN architecture. This is a quality management approach that provides confidence in a mission success. The approach has been developed to be an open nonproprietary standard broadly used by the developer community.

Another big trend is development of testing strategies, appropriate for nanosatellites. The effort for such strategy, which has not resulted in a standard though, has been the part of the AraMiS project [28]. Later, in 2014 an affordable and reliable test standard for nanosatellites has been initiated: ISO/CD/19683 “Design Qualification and Acceptance Tests of Lean Satellites and Units”. It targets satellites in general that utilize untraditional risk-taking development approaches. The aim of the standard is to achieve low-cost and fast-delivery with a small number of team, as well as achieving reliability against infant mortality after satellite launch to orbit [9].

5. STUDY PLAN

Historically the reliability research in the university is devoted to traditional applications. The expertise includes high reliability computing and reliability analysis for complex systems. And application of this experience to the nanosatellite project would be valuable. Hence the educational goal of the project is to give the students an opportunity to apply established reliability practices to a real project. This goal can be achieved by adapting the reliability educational program to a nanosatellite design flow.

The reliability course is taught for master’s degree and PhD students in electronic and computer engineering. The original course has 72 academic hours of theory and practice. The adapted course is complemented with laboratory work and exercises, dedicated to introduce

students to the space reliability applications. The main idea of the course adaptation is to seamlessly integrate it into the nanosatellite design flow: exercises and labs will become the stages of the design flow. The adapted course consists of 5 modules, where each module uncovers reliability aspects relevant to nanosatellite design.

5.1. Module 1 – Basic Terms of Reliability

This module is an introduction into reliability theory, it is taken from the original course almost without changes and consists of:

- Course agenda;
- Basic terms and concepts;
- Classification of reliable systems;
- Analysis of fault sources in technical systems;
- National and international standards on reliability;
- Reliability metrics.

Also this module covers concepts of system lifecycle in general and lifecycle of a nanosatellite.

5.2. Module 2 – Risk analysis

This module is devoted to show the students, which risks can affect the system that they develop. The first important part of risk analysis is the analysis of external environmental factors that have effect on the system. For nanosatellites these factors are:

- radiation environment – Total Ionizing Doze (TID), Single Event Effect (SEE);
- spacecraft charging;
- temperature;
- vibrations.

Students should conceive of physical phenomena behind these factors, which factors are critical for the system that they develop, and which are not. Since radiation is an important concern, an attention is given to radiation effects analysis. Tools like SPENVIS, OMERE and CREME-MC are studied. This part of the module is supported with exercise: students should develop the requirements on robustness to these factors using reference data on influencing factors.

The second part of risk analysis is devoted to the internal risks of the design. Reliability of the overall system is composed of:

- architectural reliability of the design;
- reliability of hardware system components;
- reliability of communication channels and communication protocols;
- user and instrumental software reliability;
- operating system reliability and security.

Students should be able to evaluate these partial reliabilities, analyze the internal risks and understand their influence to overall reliability. The exercise for this part of the module is to develop requirements to system hardware and software components. The practical result of this module for the nanosatellite project are the risk analysis plan and the dependability and security specification, which will be included into the project specification.

5.3. Module 3 – Fault Prevention, Fault Tolerance and Fault Removal

This module starts from the topic of silicon production technologies as a reliability foundation of a final device. Some of the current technologies that target the problem of radiation sensitivity include:

- Silicon on Insulator (SOI) / Silicon on Sapphire (SOS) processes;
- radiation-hardened cell libraries;
- memory on Dual Interlocked Cells (DICE).

At the end of this part of the module the students should become familiar with these technologies and understand their contribution to the overall device reliability. Also an important skill the reliability engineer is to be able to analyze and use reliability reports provided by the components manufacturers (such as FPGA reliability reports). This is especially important in nanosatellite project, where the goal is to build a highly reliable system using commercial-grade components.

The second part of this module introduces the students to architectural solutions that improve the reliability. They can be divided into three categories.

1. Component's native architectural solutions such as SEU mitigation techniques provided by component's manufacturer (generally for FPGA): Error Detection Cyclic Redundancy Check (EDCRC) and scrubbing for embedded configuration and user memory (CRAM, BRAM), partial reconfiguration, TMR solutions provided be EDA tools (Xilinx, Altera).
2. User-defined hardware architectural solutions:

- NMR for control logic and using history-based voting algorithms with adaptation;
- Error Detection And Correction (EDAC) codes for memory controllers, interfaces and protocols: parity check, Hamming, Hsiao, CRC, Golay, Reed-Solomon, etc.;
- System-level redundancy: tightly-coupled processing cores with arbiter;
- Device-level redundancy: hot standby, cold standby.

3. User-defined software solutions:

- System monitoring and ability to perform graceful system degradation with the function redistribution;
- Highly reliable software with recovery logic, rollback and critical code section reexecution;

- Event logging and using that life data to forecast faults and failures during the operational phase.

At the end of this module students should be familiar with all these reliability improving techniques and understand a four-dimensional fault-model with:

- Logic faults;
- Memory faults;
- Communication faults;
- Software faults.

This module includes exercises and labs, which will result in development of fault-tolerant IP-cores, modules and software functions for the target mission of the nanosatellite project.

5.4. Module 4 – Fault Forecasting at Design Phase

This module is devoted to fault forecasting that is performed during design phase – it is a consecutive phase after the risk analysis and should be performed throughout the design process. It includes:

- Hardware reliability analysis;
- Software reliability analysis;
- Complex system reliability analysis.

With the gradual refinement of a system design the results of fault forecasting become more accurate and need different methods for analysis. At the early design stage the methods and tools to perform complex system reliability analysis include:

- Definition of stochastic processes of fault occurrence;
- Boolean algebra methods for reliability calculations;
- Formal verification using temporal logic;
- etc.

At the implementation phase the most convenient way to test the system and to validate its reliability are simulation techniques. In this part of the module students are introduced to simulation using general methods like queuing theory methods, and using EDA-provided simulation tools. Simulation could be performed to hardware/software modules, to satellite sub-systems, to the whole satellite and to the satellite constellation (simulating communications between satellites).

The necessary part of the design flow for fault-tolerant system are fault injection campaigns. They are essential for evaluation of architectural vulnerabilities of the system with regards to implemented reliability improving solutions. Fault injection can be performed with the native fault injection tools provided by hardware components manufacturer (for example, in FPGA EDA tools), or in the form of custom hardware and software fault injection tools.

The concluding part of design validation is reliability and performability benchmarking, therefore some sets of software benchmarks should be developed.

This part of the module contains exercises, focused on creation of test plans, simulation, native and in-house fault injection methods and some on benchmarking. As a result the students will create testbenches for the IP-cores, modules and software developed in the previous module and curate mission-specific benchmarks to analyze performance and reliability of the system in the next module.

5.5. Module 5 – Design for Reliability

This module is devoted to the topic of system design: how to tie all system components into a verified highly reliable system – nanosatellite – which is ready to be launched to the orbit.

Since the project is an embedded team project it is important to introduce the students to the aspects of working in a team:

- Team management;
- Design partitioning for the hardware part of the project;
- Project versioning for the hardware and software parts of the project.

The other important part of every project is documentation – from the specification to lessons learned report. For the highly reliable nanosatellite the importance of having an extensive and well-verified documentation increases dramatically. The first stage of the design flow is creating the project specification, therefore the students will develop a functional specification and dependability and security specification for the target mission, as well as more detailed specifications for modules of the nanosatellite using results from the previous modules. Analysis of dependability specification should lead to understanding of the fact, that simplicity is a key to reliability, and all the complicated fault-prevention, fault-tolerant and fault-removal techniques should be used in moderation and with the integral system design approach in mind. As a result the documented flow-down specification with project requirements will be obtained.

On a special note, since the paradigm of design for reliability strongly relates to Design For Testability (DFT), the students are additionally challenged to use DFT techniques in the project.

In the final module the students will use the knowledge and skills obtained in the previous modules to create a project of their own nanosatellite for the preliminary design review.

6. POLY-SPUTNIK

The project *Polytechnic-Space 101* is a part of a Russian universities nanosatellite constellation plan. Primary objectives of the project are technology demonstration and support of various ongoing research activities, including topics of reliability engineering. Thus the project perfectly suits as a framework to study the presented reliability course: to practice established dependability engineering methods and sense the latest trends of nanosatellite design.

Particular engineering and research goal of the project is to develop a reliable spacecraft bus that will be suitable for a nanosatellite. Our aim is to adapt a platform-based design approach for a command and data handling subsystem (C&DH) of a spacecraft. The idea is to use a unified, parameterized design of C&DH modules, which can be customized for the current payload and desired onboard network architecture of a particular mission. More specifically, we want to adapt a hardware platform architecture for a small satellite bus called Universal Module for Managing the Information (UMOMI) [24], which has been developed for SpaceWire-based Plug-and-Play architectures. Levels of customization of the architecture include parameters of module's components, mixture of optional components and interfaces in the module, and HW/SW partitioning. The resulting solution will be complemented with a middleware, incorporating a function of intersatellite communications for distributed information storage and processing in a nanosatellite constellation.

Some notable secondary coordinated tasks of a project include:

• comparison of IC technologies for on-board computing: SRAM-based FPGA vs flash-based FPGA vs custom-made ASIC vs General Purpose CPU;

• analysis of capabilities of a nanosatellite for testing new ASIC designs for use in space environment (regarding thermal, acceleration, vibration and radiation conditions);

• evaluation of in-house created fault-injection techniques for validation of developed C&DH architecture.

• in-flight evaluation and analysis of in-house created Built-In Self-Test methods of C&DH designs.

The projected result of our initiative is a new distributed, reconfigurable, fault-tolerant C&DH subsystem solution and a cost-effective and simple reliability design paradigm for nanosatellites.

7. DISCUSSION

The goal of this paper is to investigate the topic of dependability in the field of nanosatellite design and to identify the ways to support the educational process throughout the nanosatellite project. Presented overview shows that creation of a fault-tolerant nanosatellite continues to challenge developers to adapt contemporary design practices and to search for trade-offs between cost, functionality, simplicity, and efficiency. This section highlights some important aspects of this task.

1. In the first place, nanosatellite's electronics dependability should not be considered separately from the dependability of the satellite as a whole. It means that dependability should be treated as an integral characteristic and requires a strong cooperation between team members with diverse specialities.

2. The design quality typically results in a significant part of all nanosatellite designs' faults. Hence deliberate design methodologies should be practised, which can be especially critical for a university design team.

3. Autonomy of a spacecraft is a controversial factor in achieving a highly-reliable and secure progress of a nanosatellite mission. On the one hand it limits the ways to recover from failures, since the spacecraft should be able to recover itself or to be recovered by means of a limited remote control from a ground station. On the other hand, vulnerability to malicious attacks is limited as well, which is advantageous to the mission. However, in the light of lately being created nanosatellite constellations the impact of autonomy shifts in both directions.

4. Power budgets of spacecrafts place a strong limit to the objectives of nanosatellite missions: both functionality and resources for redundancy are limited, while the power subsystem itself should not be a single point of failure. Hence a breakthrough in a power supply area can become a next enabling factor for the growth of reliable nanosatellite technologies.

5. Finally, there is a strong need for statistically meaningful results of nanosatellite missions' successes and failures. Hence a life-data collection and analysis functions should be considered imperative in current and future nanosatellite missions.

REFERENCES

[1] Athanasopoulou E., Thakker P., Sanders W. H., 2005, Second Int. Conf. on the Quantitative Evaluation of Systems, 95

[2] Avizienis A., Laprie J.-C., Randell B., et al., 2004, IEEE TDSC 1, 11

[3] Behr P., Bärwald W., Brieß K., et al., 2003, Proc. of DASIA 2003, 76

[4] Bouwmeester J., Guo J., 2010, Acta Astronautica 67, 854

[5] Brumbaugh K. M., Lightsey E. G., 2013, JoSS 2(1), 147

[6] Buchen E., DePasquale D., 2014, 2014 Nano / Microsatellite Market Assessment, SpaceWorks
[7] Busch S., Schilling K., Reichel F., et al., 2013, Automatic Control in Aerospace, 236
[8] Chin A., Coelho R., Brooks L., et al., 2008, AIAA/6th Responsive Space Conf., 4006
[9] Cho M., 2015, International Conference on Space Science and Communication
[10] Cornejo N. E., Bouwmeester J., Gaydadjiev G. N., 2009, Small Satellites for Earth Observation: 7th Int. Symp. of the Int. Academy of Astronautics
[11] De Jong S., Aalbers G. T., Bouwmeester J., 2008, 59th Int. Astronautical Congress IAC 2008
[12] Dubos G. F., Castet J.-F., Saleh J. H., 2010, Acta Astronautica 67, 584
[13] Eagleson S., Sarda K., Mauthe S., et al., 2006, AIAA/USU Conference on Small Satellites
[14] Ekpo S. C., George D., 2013, IEEE Systems Journal 7(4), 642
[15] Engelen S., Gill E., Verhoeven C., 2014, IEEE TAES 50(2), 1027
[16] Guo J., Monas L., Gill E., 2014, Acta Astronautica 98, 97
[17] Hadwin C., Twining D., Strobel D., 2014, CubeSat Developers' Workshop
[18] Homan D., Young Q., 2008, AIAA/USU Conf. on Small Satellites, SSC–08–I–3
[19] Ibrahim M. M., Asami K., Cho M., 2013, IEEE Aerospace Conf., 1
[20] Jackson B., 2014, IEEE Aerospace Conf., 1
[21] Jackson B., Epstein K., 2000, IEEE Aerospace Conf., 185
[22] Laprie J.-C., 1995, Sixth Int. Symp. on Software Reliability Engineering, 2
[23] Mahmood R., Khurshid K., ul Isalm Q., 2013, 6th Int. Conf. on Recent Advances in Space Technologies, 517
[24] Mamoutova O., Fedotov A., Filippov A., et al., 2015, 17TH Conference of Open Innovations Association, 116
[25] Passerone C., Tranchero M., Speretta S., et al., 2008, IEEE Aerospace Conf., 1
[26] Rogers A. Q., Summers R. A., 2010, Johns Hopkins APL Technical Digest 29(3), 283
[27] Rossoni P., Panetta P. V., 1999, Proc. AIAA/USU Conference on Small Satellites, SSC–99–V–3
[28] Speretta S., Reyneri L. M., Sansoe C., et al., 2007, 58th Int. Astronautical Congress, IAC–07–B4.7.09
[29] Underwood C., Crawford M., Ward J., 1998, AIAA/USU Conf. on Small Satellites
[30] Vladimirova T., Banu R., Sweeting M., 2005, MAPLD proceedings

SESSION 8: I - Students Rocketry

(Friday 11th - 15.00)

Chairman: Prof. Michèle Lavagna

SOUNDING ROCKET DEVELOPMENT WITH LIQUID PROPELLANTS WITHIN THE DLR STERN PROGRAMME

C. Bach, J. Sieder, A. Konietzke, and M. Tajmar

Institute of Aerospace Eningeering, Technische Universität Dresden, 01069 Dresden, Germany

ABSTRACT

STERN is a nationwide education programme initiated in 2012 by the German Space Agency DLR to promote young professionals for launcher systems and establish a practical education of students in this field. This paper describes the motivation and objectives of this endeavour as well as its execution. Moreover the eight participating university teams and their student sounding rocket developments are presented. Special focus is laid on TU Dresden's SMART Rockets project that deals with the complex development of a liquid-propellant rocket engine. Also first results of the recently conducted first launch campaign are presented. Since STERN comes to its preliminary end in 2016, this paper concludes and summarises the educational benefits for the various involved parties. Finally an outlook on follow-up activities is given.

Key words: SMART; STERN; sounding; rockets; students; experimental; space; education; DLR; TU Dresden.

1. INTRODUCTION

Initiated and conducted by the German Space Agency (DLR) and funded by the Federal Ministry of Economic and Technology (BMWi), one of Europe's largest space educational activities is found in the programme "STudentische Experimental RaketeN" (STERN), which comprises the efforts of German university teams to develop student sounding rockets. The acronym "STERN", the German word for "star", was chosen for two reasons. "The first reason was to emphasise the idealistic goals of spaceflight providing students with the opportunity to "reach for the stars". The second and most important one was that the programme offers engineering students a practical chance to experience the scope of aerospace and should motivate them to become a new star in this field." [1] The programme logo is shown in figure 1.

STERN was initiated in April 2012 and its completion is foreseen in June 2016. Within this time frame several universities conduct their individual sounding rocket development projects with a duration of three years. As



Figure 1. The logo of STERN

the programme is in its final stage with the first rockets already launched and it comes to an end in the nearby future, this paper aims to summarise the conducted work and present the first results, both with special respect to educational aspects. The second section will therefore state the goals of STERN and how it is executed collaboratively. The participating university teams will be presented in section 3, while the student work within the SMART Rockets project by Technische Universität Dresden is described in greater detail in section 4. The fifth section provides an overview of the first 4 rocket launches from Sweden in October 2015. Section six will summarise the benefits of this programme, before an outlook on further activities is presented in section seven.

2. OBJECTIVES AND EXECUTION OF STERN

"The STERN programme is open for all German universities which offer aerospace engineering lectures and offer students the possibility to develop, build, test and fly their own rockets in university teams." [1] The focus on university students and the development of whole rocket systems including propulsion segments distinguishes STERN from other educational programmes like "Rocket EXperiments for University Students" (REXUS) and the french "Projet Etudiant de Recherche Spatiale Europen Universitaire et Scientifique" (PERSEUS). Latter shares the same goals, which are depicted in the following, but has an even more distributed network, which includes also schools and various small and medium-

sized enterprises (SMEs). Yet the participants conduct smaller sub-projects in shorter time. Therefore these are contributing to several larger projects coordinated by Centre national d'tudes spatiales (CNES) instead of being independent projects on their own. [2, 3]

2.1. Objectives

"To ensure Europe's autonomous and cost-effective access to space for the future, an ongoing development of the Ariane and its successor is necessary. The main requirement for this development are well-educated skilled employees. Responses from the economy, the universities and analyses of the DLR have shown a considerable decrease of young scientific and technical professionals in the field of space transportation." [4] One reason for this development is the attraction of students by small satellite projects, whose number increased massively in the past decade and which today can be found at almost every university of aerospace engineering. Those projects offer practical work and hands-on experiences, while rocketry was mostly bare theory in tertiary education. To counteract this process and to promote young academics in the field of launcher systems is the primary objective of DLR's STERN programme [5]. This goal shall be achieved by fostering a practical education of aerospace engineering students and adjacent fields. Besides elating students for the space transportation subject, STERN wants to motivate universities to increase the lecture activities in the field of launcher and propulsion systems. [4]

2.2. Execution

To achieve these objectives, DLR provides financial and administrative support for the universities to focus on the development of their complete rocket systems within three years. Students have to work project-oriented and in teams to fulfill this task. To ensure a minimum of scientific and engineering effort, some basic requirements have been set: The achievement of a flight altitude of at least $3\,\mathrm{km}$, the achievement of a flight velocity of at least the speed of sound and the implementation of a telemetry payload to transmit flight data that allows a tracking of the rocket. This data shall also be stored on board. Furthermore each rocket has to contain a recovery system.
Besides these basic requirements, one key characteristic of STERN is that the university teams have great freedom to design their sounding rockets as they like. There is no upper limit on the flight altitude or the chosen propulsion concept. "Commercially available solid propulsion motors can be used as well as own developments in liquid-, hybrid- or hot water propulsion." [4] An overview over the systems is given in the next section. But "as in any development program, the students have to pass several reviews in which they have to present and defend their rocket design in front of experts." [1] This practically oriented study shall prepare the students for an employment in industry. The review boards consist of experts from the DLR Space Administration, the DLR Mobile Rocket Base (MORABA) and the DLR Institute of Space Propulsion as well as further experts as required. In addition the teams also have to pass reviews by the launch site providers such as Esrange Space Center in northern Sweden, where most rockets are being launched.
Besides the conduction of reviews, DLR MORABA and the DLR Institute of Space Propulsion accompany the students during the development until the final launch. One key element in this process are special workshops, which offer a platform for exchange of experiences and technical information. It is important to emphasise that despite of the great diversity within the different approaches (cf. section 3), the STERN programme is no competition between the teams. The interaction is far more determined by an atmosphere of collaborative learning and advancing for all participants. Therefore the workshops are a fundamental platform to enable an exchange of ideas and knowledge in order to tackle challenges collaboratively. There are two workshops per year, one is organised by the DLR Institute of Space Propulsion in Lampoldshausen and deals with the engine systems and test activities, while the other is organised by DLR MORABA in Oberpfaffenhofen and focuses on the remaining subsystems like communication and recovery as well as the preparation of the launch campaigns themselves.
Moreover DLR MORABA provides the interface to the launch site providers and arranges all launch campaigns, for which multiple rockets are bundled (cf. section 5). "At DLR site Lampoldshausen the M11.5 test field was erected and came into service in June 2013, at which [...] the STERN student groups can come with their developed rocket combustors and engines to test them. These tests are conducted under the auspices of experienced researches and engineers from the institute. This process of teaching, supervision and exercises shall help the students to get a deeper understanding how a development and test process runs and how to react on occurring difficulties." [4] Above all the DLR Space Administration is responsible for the overall management of STERN and provides corresponding help in all aspects of its implementation.
On the student side, the conducted work is mostly part of project theses, research papers and diploma, bachelor or master theses. But in addition many volunteers support the projects besides their primary studies. The teams can have undergraduate as well as postgraduate students and are coordinated by a supervisor, who pays attention on schedules, milestones and the budget. Not only aerospace engineering is addressed, but also adjacent fields. Thus the teams consist of members from various disciplines, foremost - but not exclusively - the Science, Technology, Engineering and Mathematics (STEM) sector, which includes fields like physics, computer science and electrical engineering. "In order to teach students engineering and science, as well as to put their technical knowledge to the test as early as possible in their studies, they are integrated into courses at their universities, which already deal with various aspects of rocket technology and space research." [1]

Table 1. Overview of the teams participating in STERN and their sounding rockets [6]

University (Team)	Mission	Engine Type	Propellants	Thrust (N)	Apogee (m)
HS Augsburg	HyCOMET	Hybrid	HTPB + N_2O	1.000	5.000
HS Bremen	Aquasonic	Hybrid	PE + N_2O	1.000	6.000
ZARM/Uni Bremen	ZEpHyR	Hybrid	Paraffin + LOX	1.800	10.800
TU Berlin	DECAN	Solid	Al + APCP	3.000	7.500
TU Braunschweig (ERIG)	Leonis	Hybrid	HTPB + N_2O	1.300	5.400
TU Dresden	SMART	Liquid	Ethanol + LOX	500	4.100
TU München (WARR)	Cryosphere	Hybrid	HTPB + LOX	8.000	15.000
Uni Stuttgart	HyEnD	Hybrid	Paraffin + N_2O	10.000	46.000

3. PARTICIPATING UNIVERSITY TEAMS

In total eight university teams participate in the STERN programme. Table 1 gives an overview of the missions, engine types, used propellants as well as the envisaged thrust levels and flight altitudes. It can be seen that most teams develop hybrid rocket engines for their propulsion systems. The combination of solid fuel and liquid or gaseous oxidant is believed to be a good compromise between commercial solid rocket motors and more complex full liquid propellant rocket engines. Yet there is a huge diversity in the mission concepts. Even within the hybrid engines, only a single propellant combination can be found twice. The fuel choice ranges from Hydroxyl-Terminated PolyButadiene (HTPB) to paraffin. While nitrous oxide is the most represented oxidant because of its low price and easy handling, some go for liquid oxygen (LOX) to obtain a better performance on the one hand side and to introduce the students to the handling of cryogenic propellants on the other hand side.
There is also a wide range of envisaged altitudes reaching from 4 up to 46 km, correlating to the engine thrust levels. One reason for this wide spectrum is that all teams started with different preconditions. While TU Braunschweig and TU München have decades of experience with amateur rocketry associations like "ExperimentalRaumfahrt-InteressenGemeinschaft e.V." (ERIG) and "Wissenschaftliche Arbeitsgemeinschaft für Raketentechnik und Raumfahrt" (WARR), other universities like HS Augsburg and TU Dresden probably never launched a rocket before and therefore had no preexisting infrastructure.
The university of Stuttgart develops the most powerful rocket, but has besides its student association "HYbrid ENgine Development" (HyEnD) also the highest number of aerospace engineering students in Germany and close ties to the nearby DLR Institute of Space Propulsion. TU Berlin and HS Bremen had experiences with hot water propelled rockets and originally wanted to use such systems as a first stage for a final two stage rocket. However they both dropped this idea for the first launch campaigns within STERN.
Further differences can be found in the specific objectives of the individual projects. For instance TU Berlin integrated a payload bay for a CanSat in their rocket. This picosatellite is not part of the project itself, but could be provided by any other student group. On the other side HS Augsburg pursues the goal of a rocket which consist out of fibre-reinforced structures to the highest possible extend. And at TU Dresden, a new sensor and communication platform is completely developed in-house, while most other teams fall back on commercial off the shelf (COTS) components.

4. TU DRESDEN'S SMART ROCKETS PROJECT

Since almost all participating universities use various types of hybrid rocket engines, TU Dresden's rocket "Mira" is unique by its implementation of a Liquid-Propellant Rocket Engine (LPRE). In fact it is so far the only full LPRE developed and tested at an European university. The rocket motor uses the "green" propellant combination of LOX as oxidiser and ethanol as fuel.

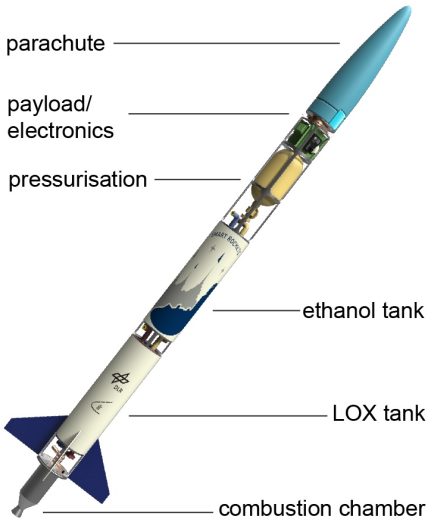


Figure 2. Design and subsystems of TU Dresden's STERN rocket [7]

4.1. Scope of the Project

The overall development philosophy is to use as less COTS components as possible. The students shall experience all project phases from conceptual and detailed design over manufacturing and assembling to verification and testing. This includes all subsystems (cf. fig-

ure 2) like the propulsion system with pressure vessels and thrust chamber, the in-house developed electronic compartment with on-board CPU, sensor and communication platforms and the recovery system, which consists of a drogue and a main parachute. Only the latter subsystem is comprised mainly of COTS components to minimise the relatively high failure rate of recovery systems in general. And besides fluid pipes, valves and the nitrogen pressure tank all components are developed by the students themselves. [8]
This comprises also both the rocket engine test bench, which can be seen active in figure 3 and has been described in detail by Sieder [9], and the whole Ground Support Equipment (GSE). Latter consists of three mobile facilities: the launch pad and two modified freight containers. As elaborated in a previous work [7], one of the two units assures safe transport of the rocket and all other hardware to the designated launch- and test area and serves as an assembly workshop. The second container is equipped as a mobile control room and enables the control of all test / launch processes including communication as well as the record and display of all measured data.

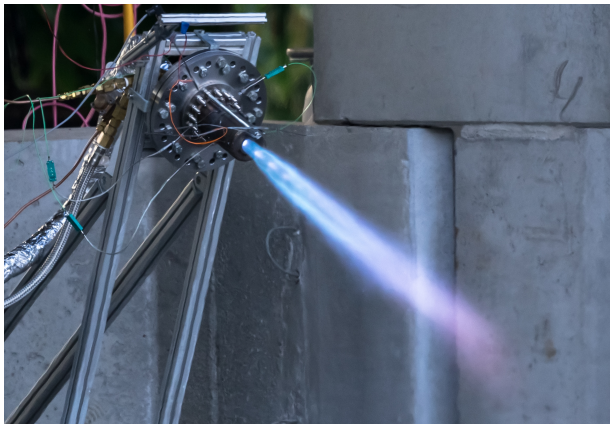


Figure 3. Hot firing of a test combustion chamber on the rocket engine test bench ©Jens Dziewiencki

4.2. Liquid Propelled Rocket Engine

One of the most challenging aspects of the rocket "'Mira"' is its small dimension and thrust of 500 N. With only 120 mm in diameter it is difficult to find parts which fit into the system. In particular LOX compatible COTS parts are oversized and heavy. The engine is a pressure fed system, whose pressure tank is located in the upper part of the rocket (see figure 4). It stores the nitrogen at 250 bar for pressurisation of the propellant tanks. The tank is an off the shelf paint ball tank to avoid the development and the qualification process of high pressure devices. To control the pressure inside the feeding system a pressure regulator is mounted on the nitrogen tank. The pressure level inside the propellant tanks is regulated to almost constant 25 bar. This is necessary to drive the propellants out of the tanks into the combustion chamber, which creates a combustion pressure of 15 bar.
Both propellant tanks are in-house developed aluminum alloy AW EN 6060 vessels. To supply the lower LOX tank with pressurisation gas and the engine with ethanol both propellant tanks have an inner feed through tube. It is possible to check the tank pressure via a pressure sensor on the top of each tank, where also the refilling sockets are mounted. The ethanol fueling can be done far in advance of the launch due to its shelf life. Yet the LOX has to be fuelled shortly before because of its cryogenic nature. An insulation coating is only provided by the service tower with two half shells that will be detached at lift-off. A long down time would lead to the vaporisation of most of the propellant.
From the tanks the propellants are fed to the injector plate, where a coaxial swirl injector (described in detail by Fiore [10]) provides the propellants to the combustion chamber. Next to the injector plate the LOX feeding line has a connection to a flushing line. This line is used to flush the combustion chamber with nitrogen, which will be provided by the service tower via a quick connection that will be pulled off during countdown.
Before the ethanol enters the injector it flows through cooling channels in the back of the face plate. Inside the coaxial swirl injector both propellants are mixed and atomised. One main impact on the coaxial swirl injector design is its recess length, which is the distance between the front sides of ethanol and LOX injector. At a small distance both fluids will not mix sufficiently. A narrow angle of the spray cone will appear at larger recess lengths. However a wide angle is necessary to use the whole combustion chamber efficiently. [9]
To lower the temperature inside the combustion chamber the propellant mixture is fuel rich. In combination with a coaxial swirl injector this configuration produces a positive secondary effect. Unburned ethanol reaches the combustion chamber walls and establishes a film cooling. The combustion chamber walls are made of graphite. To ensure structural integrity of the thrust chamber during the 20 s of the powered ascent, the graphite has an oxide-oxide ceramic matrix composite (OCMC) casing with the ability to withstand high temperatures and thermal shocks

5. FIRST LAUNCH CAMPAIGN OF STERN

The first STERN launch campaign took place from 16. to 30.10.2015 with 3 participating teams, who launched in total 4 rockets successfully from Esrange. Table 2 summarises the achieved flight altitudes and malfunctions, which may have occurred. The very first rocket was the "FAUST" of the Leonis project (see figure 5), the first rocket with a hybrid engine that ever took off from Esrange. However it was not the last one as HyEnD's HEROS followed later the same day. Although subsystems including the recovery system, which also consisted of 2 parachutes, worked flawlessly, a malfunction within the propulsion segment forced the rocket to a non-nominal flight, thus the apogee stayed way below the target altitude of 46 km.

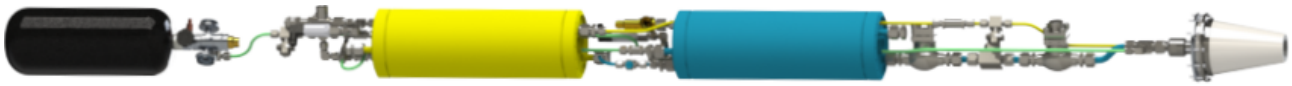


Figure 4. The propulsion system including pressurisation tank (black), ethanol tank (yellow), LOX tank (blue) and OCMC combustion chamber

The DECAN team from Berlin launched even two identical rockets that achieved similar results. Unfortunately one of the rockets could not be recovered. All other rockets have been recovered and meanwhile brought back to Germany. By the time of writing this paper, data evaluation is still being conducted. But the first launch campaign with 4 successful take-offs in only 2 weeks is already seen as a huge success and gives the direction for future launches. The system performance can be optimised yet, especially in case of recovery systems, which are almost impossible to test under relevant conditions on ground. But the conduction of the campaign itself and the collaboration of all participants - universities, DLR institutions as well as the team from Esrange - was a great pioneering accomplishment on its own. The educational aspects were fully met and one can argue that the learning effect is even greater if not everything works out perfectly.



Figure 5. ERIG's "FAUST" right after take-off [11]

6. EDUCATIONAL BENEFITS FOR THE SPACE INDUSTRY

With STERN being conducted for over three years now, it can be concluded that all participating institutions benefit from this programme in numerous ways. Of course most notably the young professionals gather knowledge and experiences they could not gain otherwise. The established practical education enables the students not only to evolve their technical and scientific capabilities, but also to gain project management and social skills. The complex development of a rocket system as a whole fosters interdisciplinary thinking and teamwork. Students are encouraged to put their knowledge to the test as early as possible in their studies. The constant review process and high number of collaborative partners introduces them to the real work of a space engineer. Therefore students also get a better understanding of the space branch and its characteristics like quality assurance, verification processes and documentation. At the end of their studies, the participating students will be better prepared for their professional careers and of higher value for companies that usually want to employ motivated young academics who already have a certain amount of practical experience. [1, 4]

Also "the non-profit research organisations and associations, which are involved in the STERN programme, can obtain different kinds of benefits" [1]. The participating universities are enabled to identify PhD candidates and future research projects. Even more important the funds provided by DLR and BMWi lead to an installation of a lot of laboratory equipment, test benches and other hardware that supports future educational activities also outside of STERN. Hence the general education quality at aerospace engineering universities rises and also students not directly part of the STERN teams benefit through this endeavour.

Student associations like ERIG and WARR get the chance to expand their efforts. An increase of members can be noticed since their participation in STERN. This attracts further young academics for STEM fields and propels activities at the corresponding universities. On top of that the reviews and workshops offer a platform for exchange of information and thus establish and strengthen ties between the research organisations and universities. This leads to a strong and broad network of stakeholders, who can combine their efforts to represent their interests, for instance in the European launcher market.

On the other hand the European commercial space industry benefits not only from well-educated and skilled new employees. Those young professionals, which are trained to meet the industry needs, are the key to secure Europe's access to space through launch vehicles like Ariane 5 and 6. Germany, with DLR's test center for rocket engines and a large number of research an technology development facilities an indispensable partner in the Ariane programme, therefore particularly depends on new generations of professionals. [1]

Furthermore STERN increases public attention to Europe's launcher programmes and associated activities as well as to its importance for space access and Germany's strong contribution to it. This is enabled not only by several contributions to scientific conferences and journals, but also by media coverage in the form of numerous press articles and also short television and radio broadcasts. Up to date about 400 students (volunteers excluded) participated in STERN, the number of theses reaches nearly 200.

Several of the graduates of STERN are now employed in

Table 2. Overview of the first launch campaign within STERN [6, 11]

University Team	Rocket	Apogee (m)	Remarks
TU Braunschweig	FAUST	5.700	Recovery system failed - rocket could still be recovered, but not intact; first hybrid rocket ever launched from Esrange
Uni Stuttgart	HEROS	-	technical malfunction of the engine led to a non-nominal flight of the rocket, all other systems worked as planned
TU Berlin	SHARK I	5500	malfunction of the recovery system, rocket not recovered
	SHARK II	5700	malfunction of the recovery system rocket recovered

research institutes and space companies, where their past engagement in complex rocket development activities is highly appreciated. Yet the transition between university in industry can still be improved. One way to foster the connections between education, research and industry is to involve commercial space companies in the STERN programme. One step in this direction has been taken already with the cooperation between STERN and Esrange, which has proved to be a benefit for both sides. The university teams profit a lot from the expertise and professional work of the Esrange staff. And Esrange has to adapt its launch preparation associated processes to hybrid rockets with radio controlled fuelling and pressurisation, which are very different from the known handling of solid propellants, and therefore gains new capabilities to host commercial payload experiments in the future. [1]

7. OUTLOOK

Due to the success of STERN also other industrial players have a growing interest in participation. Airbus Defense and Space sees the opportunity to use the student sounding rockets for technology demonstration and maturation. In flight tests of newly developed components are challenged by a very limited amount of launch capabilities. The STERN rockets can provide shorter lead times at lower costs, less bureaucratic effort as well as less financial and technological risks. Airbus takes this opportunity and provides two payloads for the upcoming launches of the two Bremen rockets. The experiments will be a technology demonstration for the application of thermoelectric generators (TEGs) in launcher systems. The rocket of Aquasonic and the ZARM Experimental Hybrid Rocket (ZEpHyR) will form the next launch campaign at Esrange, which is scheduled for April 2016.
After this launch campaign the only rockets left for takeoff are provided by Augsburg and München in fall 2016. This will conclude the STERN programme, but a successor is already planned to be started in 2016. After formally closing their projects, the participating universities will have the opportunity to apply for a follow up in STERN II, which could be started as early as June 2016. It is of highest importance to secure a continuation of this programme, because the education of students is an ongoing process. An incredible effort was made so that a huge amount of infrastructure and expertise in executing such a programme has been established, both at the participating universities and the DLR. Yet it is obligatory to perpetuate and intensify this endeavour to expand the initiated network for even higher benefits of all participants.

ACKNOWLEDGMENTS

We appreciate the assistance and support by: The DLR and the BMWi, who fund the project (REF.-Nr.50 RL 1256); Karsten Lappöhn, the manager of STERN; Katharina Schüttauf from DLR MORABA for her support and all the information she provided; and all students contributing to the SMART rockets project.

REFERENCES

[1] Schüttauf K., Stamminger A., Lappöhn K., Ciezki H., and Kitsche W., 2015, 22nd ESA Symposium on European Rocket and Balloon Programmes and Related Research

[2] Hingre H. and Oswald J., 2015, 6th EUCASS

[3] Oswald J., Perrier-Gustin R. and Delpy R., PERSEUS, 2015, Presentation, Dresden

[4] Stamminger A., Ciezki H., Kitsche W., Kobald M., Lappöhn, K. and Schmidt A., 2013, 21st ESA Symposium on European Rocket and Balloon Programmes and Related Research

[5] Lappöhn K., Regenbrecht D., Bergmann D., Schmid M. and Rickmers P., 2012, 61st German Aerospace Congress

[6] Schüttauf K., STERN - STudentische Experimental RaketeN, 2015, Presentation, Dresden

[7] Bach C., Sieder J., Grasselt-Gille S., Przybilski O. and Tajmar M., 2014, 63rd German Aerospace Congress

[8] Bach C., Sieder J., Wehner F., Nürmberger M., Przybilski O. and Tajmar M., 2015, 6th EUCASS

[9] Sieder J., Bach C., Nürmberger M., Voigt N., Przybilski O. and Tajmar M., 2014, 63rd German Aerospace Congress

[10] Fiore G., Bach C., Sieder J. and Tajmar M., 2015, 6th EUCASS

[11] Deutsches Zentrum für Luft- und Raumfahrt, 2015, http://www.dlr.de/dlr/en/desktopdefault.aspx/tabid-10081/151_read-15572/#/gallery/20995

IMPROVING A SOUNDING ROCKET TECHNOLOGY DEMONSTRATOR FOR STUDENT EXPERIMENTAL ACTIVITIES

Matteo Poli[1], Alberto Madonna[2], Mattia Pezzato[3], Filippo Trevisi[3], Eugenio di Iorio[3], Davide Scalzi[3], Nicola Bressanin[4], Niccolò Galiazzo[3], and Diego Martignago[3]

[1]*CISAS (University of Padova)*
[2]*Italian National Institute for Astrophysics (INAF)*
[3]*University of Padova*
[4]*Polar Machines srl*

ABSTRACT

The Nimbus Project team, made of young engineers and university students, has developed a sounding rocket with the main purpose of engineering a reusable, cost-effective test bench. This would make possible to field test many aerospace technologies such as guidance or re-entry systems, and enable airborne atmospheric measurements and high altitude students' experiments with lower production and launch costs. A technology demonstrator has been designed and produced: its modular architecture allows to house different payloads, composite material structures reduce weight, while construction processes and off-the-shelf components provide for lower costs; ease of transportation and usability qualify it as a very versatile platform. The technology demonstrator is scalable to carry heavier payloads, to perform tests in a range of altitudes up to 1000 m and has already flown multiple times. The team's activities are already involving a number of university students in different capacities and this may further develop with growing academic collaboration. In this paper we provide a brief overview of the rocket vector and its subsystems; we illustrate the upgrades introduced since the system first debuted and the opportunities they enable; finally, we analyse the data acquired during the last two rocket launches and evaluate system performance.

Key words: Sounding rocket; Technology Demonstrator; Reusability; COTS; Improvements; Student.

1. INTRODUCTION

Sounding rockets exist from the dawn of rocket science in the thirties-forties, and have been used as research and educational tools in the aerospace field. Typically, experiments follow a 1-2 years development cycle before launch on present day sounding rocket systems [1], [2]. The expendability of rocket motors and structures increases production needs, contributing to high costs per launch and long intervals between launches, which in turn reduce potential requests from research and commercial clients. Launch ranges are situated in remote and difficult to reach locations needed to allow for wide enough reentry area to accommodate the uncontrolled crash landing: these are additional and often overlooked costs. In order to accommodate this market, systems that are both cost effective and simple to operate are required. An easily accessible sounding rocket allows the testing of a huge quantity of products, parts ed experiments: systems and subsystems of more complex experiments, guidance and thrust vectoring algorithms, communication technologies, commercial and aerospace parts subject to dynamic and environmental challenges; moreover, it allows altitude atmospheric measurements and students' experiments.

The Nimbus project team, formed by young engineers and students from the University of Padova, built the technology demonstrator Sagitta to show these goals are achievable. This deliberately cost effective approach is based on COTS (Commercial-Off-The-Shelf) components, a modular architecture and easily manufacturable parts. The whole system is simple and reusable, and can be set up for the next launch within 4 hours or less.

After a first successful test flight, several upgrades were developed over the initial design, ranging from flight software, to fuselage production, to internal components arrangement, to motor configuration. All share the common objective of improving system reliability, performance and flexibility towards a third-party payload.

The project represents a compelling opportunity for students, either as team members or as end users of the Sagitta system. Indeed, a significant number of project participants are university students, seeking to combine lecture room theory with practical knowledge of sounding rocket development.

The rest of the document is structured as follows: Section 2 provides an overview of the Sagitta technology demonstrator and its subsystems; Section 3 details the improvements to the rocket since its debut; Section 4 describes the involvement of students inside the Nimbus Project; Section 5 provides reports and analysis for the two test launches Sagitta performed so far.

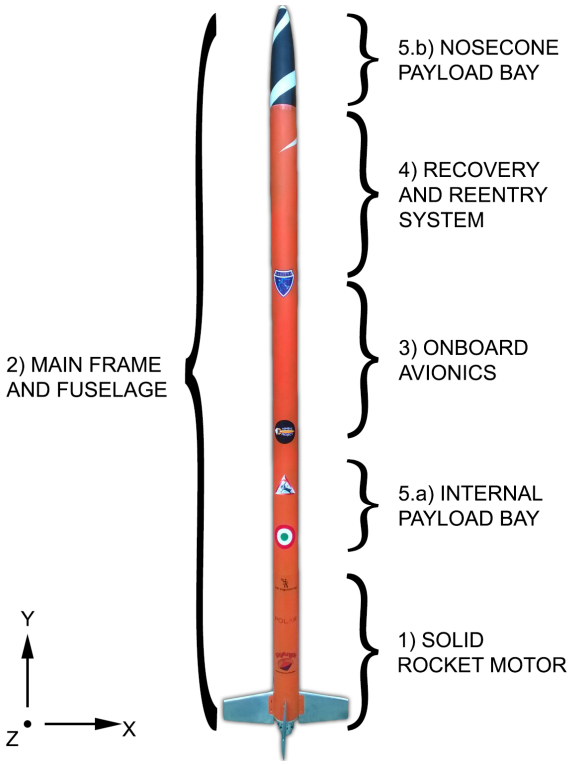


Figure 1: Sagitta's sections.

2. THE SAGITTA SYSTEM

A technology demonstrator called *Sagitta* has been designed, built, tested and launched. Sagitta is used to define and test the production technology in short times and with a high return on investment.

The typical Sagitta mission foresees a payload design time and an integration procedure, testing and preparation phases, launch, telemetry acquisition, re-entry and a subsequent re-preparation for the next launch.

In Figure 1 one can see the Sagitta internal configuration: it is equipped with a solid rocket propellant motor (Section 2.1), main structure and fuselage are made of composite materials (Section 2.2), COTS electronics is based on the open-source Arduino development platform (Section 2.3), a traditional unguided re-entry round parachute (Section 2.4) and two payload bays (Section 2.5).

2.1. Propulsion subsystem

Sagitta is propelled by a solid rocket motor, the Prometheus Version 6 (PR-V6). The propellant loaded is a mixture of potassium nitrate (KNO_3) and sucrose ($C_{12}H_{22}O_{11}$), the thrust profile is neutral and the total impulse can span from 200 Ns to 570 Ns, depending on the amount of propellant. The PR-V6 was subject to a great number of ground tests to validate the theoretical ballistic combustion model in terms of curve shape, thrust

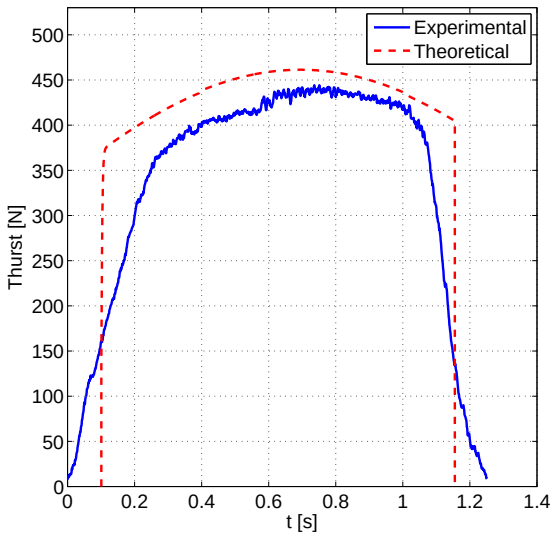


Figure 2: Experimental thrust of the PR-V6 solid rocket motor (blue line) compared to theoretical prediction (red dashed line).

and pressure absolute values. Dynamic loads, generated by thrust fluctuations, have been measured to better define structural loads. Thermal loads have been modelled and measured during the tests at the mechanical interfaces between the motor and the internal components. In Section 2.2 thermal loads are further analysed.

Figure 2 shows experimental and theoretical thrust curves, the latter is derived from a ballistic model of the rocket motor. Measurement accuracy for the thrust curve is $\pm$ 5.4% with a confidence interval of 3σ. From the analysis it is possible to deduce that the total impulse and the maximum thrust peak of the theoretical curve is about 5% higher than measurements. This effect can be explained by combustion and nozzle efficiencies.

2.2. Main structure and fuselage

The main internal structure of Sagitta consists of decks, made of Glass Fiber Reinforced Plastic (GFRP) in single skin or sandwich configuration, and structural rods, made of Carbon Fiber Reinforced Plastic (CFRP). Four rods connect each deck, on which the rocket's subsystems are mounted, to another and transfer the inertial loads. The interfaces between decks and rods are reinforced with bonded joints.

A mock-up of a structural module of Sagitta, composed of a couple of deck and the rods, was subject to different axial quasi-static tests: both compression, that simulates thrust of the motor, and tensile, normally experienced at parachute opening. The first load has been determined with rocket motor ground tests, whereas the latter with over-sizing the parachute expected force at deployment.

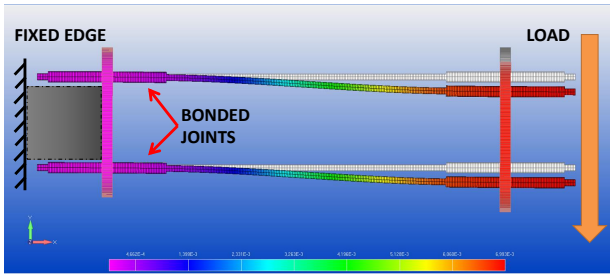


Figure 3: FEA of the structural mock-up subject to lateral load condition.

A structural Finite Element Analysis (FEA) has been carried out and results of the simulations were analysed to verify the test. The load configuration used to validate the FEA is different from the characteristic axial load at launch: the structure can strain much more under bending than under compression or tensile stress, therefore the mock-up was subject to lateral load in order to guarantee the greater sensibility possible on this measurement. The mock-up has been restrained with a fixed edge on one deck, on the other the load has been applied, and the strain measured at the free edge. This configuration can be seen in Figure 3.

Different approaches in the computational modelling of the mock-up have been prospected to find optimal mesh density. The modelling of the bonding joints is critical to determine stiffness. Different lengths of modelled bonding joints have been investigated to fit the FEA stiffness to the tested one; in Figure 4 different load-strain curves are shown: the red line is from experimental results, the yellow, blue and green lines are from FEA data. The yellow line is calculated with bonded joints identical to the tested mock-up, while the green line, without bonded joints, results in a more weak structure. The blue line depicts results with a 30% reduced length of the joints. These analyses have been carried out in a thesis work at the University of Padova [4].

The fuselage is loaded by aerodynamic and inertial forces. It is made of GFRP with VA-RTM process. It is a good compromise between plant, production costs and mechanical properties and repeatability. Aerodynamic loads have been estimated by Computational Fluid Dynamic (CFD) commercial software and custom written code for stability and fins sizing [3].

Temperatures have been investigated at the mechanical interfaces between the motor and composite material parts. The maximum temperature allowed at these interfaces is 80 °C before the employed epoxy resin softens and loses performance. A Thermal Mathematical Model (TMM) of the motor, fuselage and structure has been implemented in the MATLAB environment to predict these temperatures. The TMM takes into account conductive, convective and radiative thermal fluxes, the coefficients used for materials characterization were derived from literature searches. The Nusselt number adopted in the natural convection for horizontal tubes is derived from the

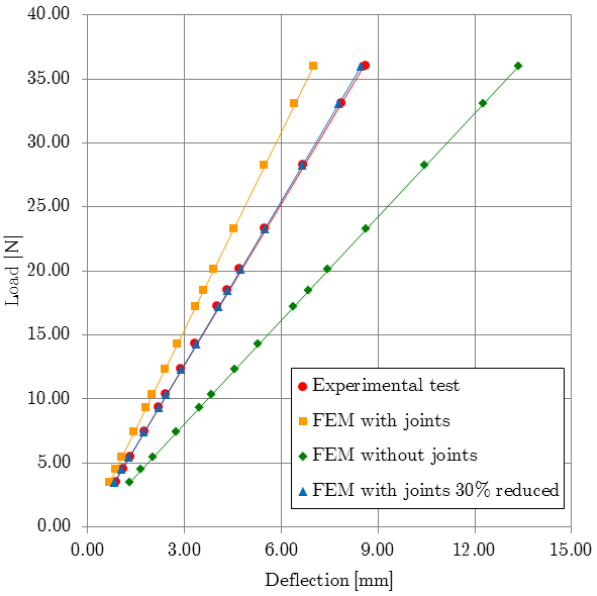


Figure 4: FEA output compared to bending test of the structural mock-up.

Churchill-Chu equation, valid with a Rayleigh number $10^{-5} < \mathrm{Ra} < 10^{12}$ [5].

Results have been compared to temperature profiles acquired during rocket motor ground tests, with fuselage and structure mock-up mounted to reproduce a real configuration. Thermal resistances (PT-100) have been placed in relevant points to measure the local temperature. The plot in Figure 5 shows measured temperatures of Temperature References Probes (TRP) placed on the external surface of the motor case (TRP4 red line) and the fuselage at the interface with the motor (TRP5 green dashed line). The blue dashed line (TRP5 TMM) represents temperature computed through the TMM at the same position of TRP5. The comparison between TRP5 measured and TRP5 TMM is used to validate the model.

2.3. Software and electronics

The flight software structure, outlined in Figure 6, is designed around the usage of a Micro Controller Unit (MCU). It controls rocket housekeeping functionalities, manages the TeleMetry and Tele-Controls (TMTC) systems, the main chute deployment sensors and actuators and the payload bay sensors. The MCU is an Arduino Mega 2560 with an ATmega2560 16 MHz microcontroller. Arduino is an open source development board: ”plug and play”, easy to use, cost-effective and widespread, with software debugging and verification as its main drawback.

During all the launch and flight phases, Sagitta generates housekeeping data to monitor subsystems’ status, e.g. battery charge and motor ignition readiness, while sensors in the internal payload bay send their data to the

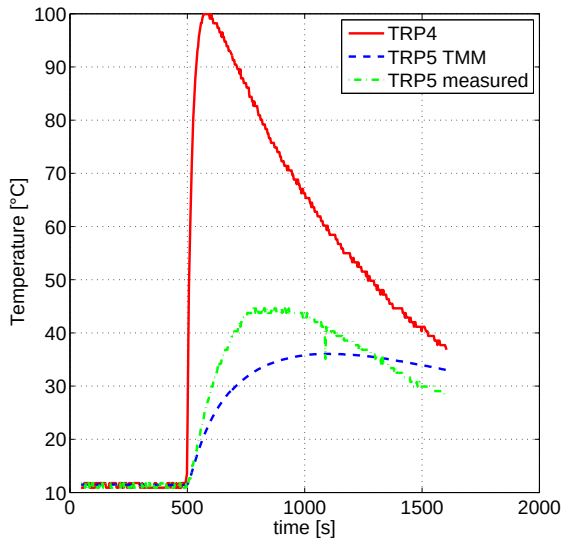


Figure 5: Temperature profiles measured at TRP4 (red) and at TRP5 (green) and theoretical prediction of TRP5 through Thermal Mathematical Model (dashed blue line).

MCU. These data are stored in an internal SD flash memory; before being sent to ground, housekeeping data is analysed on-board to monitor system's health and take actions if necessary. The MCU is loaded with two fundamental algorithms: the Attitude and Heading Reference System (AHRS) and the Flight Altitude Filter (FAF); this strategy has been chosen because of the ATmega2560's computational performance limitations. The AHRS filter operates an optimally weighted combination of attitude data given by accelerometer/magnetometer and gyro, which also serves for apogee recognition. The FAF, a sampling moving average filter algorithm performed on barometric altitude, guarantees the optimal chute deployment timing and prevents accidental deployments caused by barometer noise or pressure fluctuations. The MCU loop duration determines the number of sampled values N needed in the average height Hm_j in Equation 2:

$$Hm_j = \frac{1}{\Delta t} \sum_{i=2}^{N} H(i)\,(t_i - t_{i-1}) \tag{1}$$

$$Hm_j < Hm_{j-1} - THRESHOLD \tag{2}$$

where $H(i)$ is the instantaneous altitude, Δt corresponds to $t_N - t_1$, and the $THRESHOLD$ value is calculated by imposing the maximum speed at main chute deployment. The condition for parachute deployment takes also into account the module of accelerations for safe apogee determination and descent rate calculation.

To validate this conceptual approach to devise the correct parachute deployment condition, a stripped down rocket has been constructed and launched five times. An electronic board, functionally equivalent to the one used in

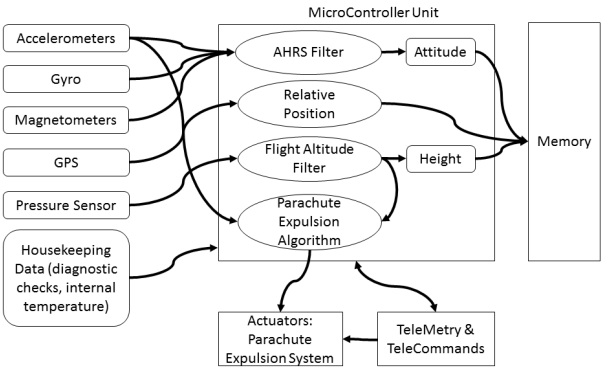


Figure 6: Software structure block diagram.

Sagitta, was loaded with the flight software. Different tests have been performed to verify the optimal threshold of the FAF.

Figure 13 shows the barometric altitude Above Ground Level (AGL) acquired during the ascent phase of the second launch of Sagitta. The mean frequency of the MCU loop is about 17 Hz. The blue continuous line is the raw altitude data from the barometric sensor, the stepped red line is FAF-processed altitude, the dashed pink line is the theoretical altitude computed with a dynamic model. C_D is derived from CFD simulations, thrust of the rocket motor is modelled with initial condition of the flight configurations and through the ballistic model introduced in Section 2.1. The relative difference between theoretical and measured altitude of only the 2.5% showing a good accordance between the dynamic model and Sagitta performances. The vertical blue and black dashed lines are the rocket motor ignition flag and the parachute opening flag respectively. The latter depends directly from the FAF evaluations of the thresholds; the deployment of the parachute was correctly actuated by the filter.

2.4. Re-entry system

Sagitta has a main conventional round parachute provided by SkyAngle and a pilot chute used for extraction of the main. The parachute is deployed through a pneumatic device that pressurizes the parachute bay and ejects the nose cone. The theoretical descending speed is 4.2 m/s.

2.5. Payload

Sagitta is equipped with two payload bays: an internal one in the fuselage and an ejectable one in the nose cone (see Figure 1). During the two launches, acceleration, angular velocities, magnetic field sensors and GPS device have been fitted in the internal payload bay. These sensors are used in the software loop to correctly activate the parachute ejection device (see Section 2.3) and also to determine flight loads and rocket attitude.

3. SYSTEM IMPROVEMENTS

The technology demonstrator, as presented in Section 2, carried out a test flight to validate operation of all subsystems and of the system as a whole (details at Section 5.1). The launch provided valuable data, which were combined with our long-term development program for the rocket to plan the first improvements to the system, enhancing reliability and usability. Some of the developments presented in this Section were already tested during the demonstrator's second launch (Section 5.2), while others are in the final phases of integration.

3.1. Software

The flight software was subject to an extensive review after the first launch. The test flight, specifically, helped to pinpoint a weakness in the parachute deployment algorithm, where certain environmental conditions inside the avionics compartment could cause the premature ejection of the nose cone; conversely, a failure of the barometric pressure sensor could prevent parachute deployment altogether.
To resolve these issues, a new expulsion algorithm has been implemented, taking into account data from the accelerometer and introducing an activation timer. Figure 7 illustrates the flowchart for the new procedure.

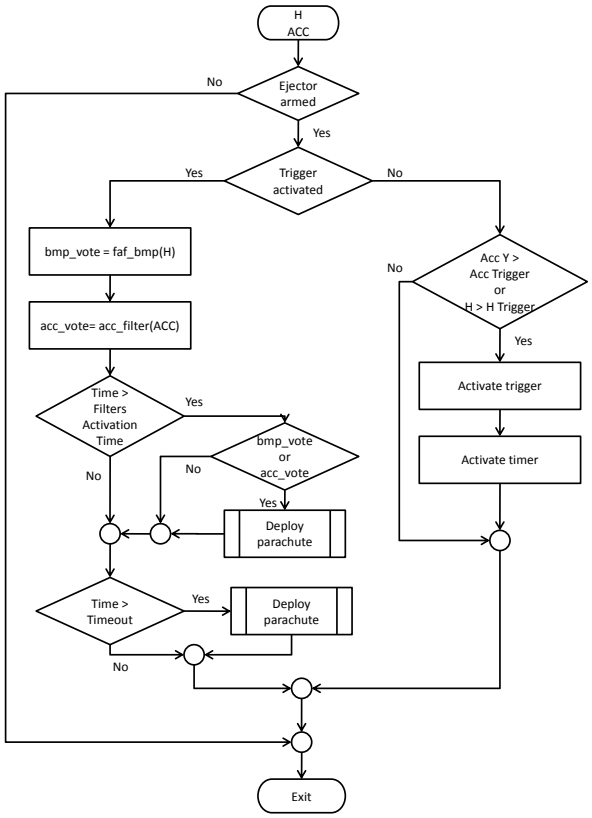


Figure 7: Flowchart for the new ejection algorithm

When the rocket is in the launch pad and all systems are ready for take-off, the ground station sends a command to arm the ejector system. From this point onward, a software trigger monitors altitude and accelerometer data (H and ACC respectively in the flowchart) to determine if the vehicle has left the pad and is ascending in accordance to the mission profile; data from each source have their own activation condition, which is customizable on a per-mission basis. When the trigger detects the conditions have been met, it starts an activation timer and enables two software filters: the first is the FAF already described in Section 2.3; the second is another sampling moving average filter closely derived from FAF, but operating on the magnitude of the acceleration vector, and thus dubbed *Acceleration Filter (AccF)*. Each filter casts a vote regarding parachute deployment. Differently from the FAF, the AccF looks for a positive derivative of the acceleration norm after an absolute minimum near zero (presumably when the rocket reaches apogee conditions). The derivative value must be over a set threshold and the minimum vector norm near apogee must be within a certain tolerance: expecting an exactly null acceleration vector upon apogee is unreliable due to possible eccentric motions and random sensor noise.
The activation timer prevents a premature actuation of the ejection device due to abnormal sensor readings during the first few seconds after take-off. After this brief time has passed, the votes from the filters are evaluated at each MCU loop iteration and, if positive, the parachute deployment is commanded. Should the filters for any reason never return a positive vote, the ejection system is activated anyway upon expiration of a second *timeout* timer, calibrated according to the predicted mission profile and maximum allowed vertical speed for successfully deploying the parachute.
All the described elements are complementary to each other and bring mutual benefits: the Acceleration Filter allows more accurate apogee determination and prevents the sole reliance on the barometric pressure sensor, the timers protect the systems from abnormal or lacking data (by preventing action in the first case and forcing it in the second), and the software trigger safeguards the whole procedure from a motor malfunction resulting in a failed liftoff. The final result is a much more accurate and reliable ejection system, improving the capability to safely recover the rocket.
Integration of other data sources is under consideration to grow this algorithm into a complete sensor outvoting mechanism.

The code review also revealed opportunities to remove some obsolete conditions to pace code execution (originally introduced for debugging purposes), and to optimize I/O performance. Most notably, data are now written to the internal SD storage in raw binary format, providing for faster processing, better numerical value preservation and reducing the required memory. Combining all these small modifications improved the main MCU loop frequency to an average of 36 Hz. This con-

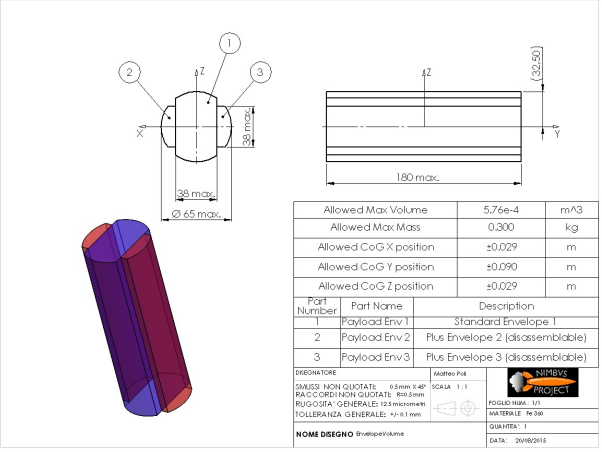


Figure 8: Mechanical interfaces.

tributes to a much greater quality of data gathered and processed in flight (as seen during the second test launch), leading to more accurate and timely actions by the controlling hardware. Finally, the greater quantity of data samples helps to better analyze performance and diagnose problems in the post-processing phase.

3.2. Compacted electronics

Accelerometers, gyroscopes, magnetometer and GPS were originally housed in the internal payload bay (point 5.1 of Figure 1). To save volume inside the rocket, these sensors have been moved directly on the main MCU Shield. A 10DoF IMU has been chosen to replace the MPU-6050, BMP-180 and HMC5883L individual boards with a more compact design. Also, the GPS sensor has been placed on a specifically conceived support. These improvements allow to save room, in particular in the payload bay described in the next Section. Furthermore, they remove cables and other apparatus, reducing the overall mass of the system by 1-2%.

3.3. Payload bay

As a consequence of the room saved by compacting the electronics, the internal payload bay is now free to house third-party payloads. In Figure 8 one can see an extract from the Mechanical Interface Control Document, that defines the maximum allowed volume mass and the position of the Centre of Gravity. A student payload can be loaded in this volume, and it can be electrically powered by the main bus or at 5 V or 3.3 V, granting the maximum grade of flexibility.

3.4. Fuselage

Further analyses have been carried out to optimize fuselage mass. In the first phases of the project the loads at landing were a great unknown because of the difficulty of simulating the landing impact, affecting the first design of the fuselage. Acquiring direct experience of the landing from the first test flight has allowed to laminate a new, lighter fuselage. The mass saved is 14% with respect to the first fuselage. Further improvements can be achieved by substituting glass fiber with carbon fiber as the reinforcing material.

3.5. Motor ignition system

The Motor Ignition System (shortened in SAM from the italian *Sistema Accensione Motore*) is formed by an electronic board and a pyrotechnic device that ignites the solid rocket motor when commanded from the ground station. The main advantage of having the SAM on board is that the rocket is electrically independent from ground and can be operated easily, while the main drawbacks are mass and volume occupied on the rocket. In the perspective of rocket optimization, the SAM is going to be removed, saving around 7% in mass and 3% in volume. This improves the maximum payload mass and volume, moderately increasing the launch complexity. This new configuration is currently being tested and will be effective in the next launches.

3.6. High power motor configuration

The motor flown during the first two test flights was employed in a low-power configuration: total impulse and maximum thrust were intentionally limited to stress electronics and structure components as little as possible. As the overall functionality of the Sagitta rocket has been demonstrated (see launch reports in Section 5), the motor grain configuration has been changed to offer sufficient thrust and burning time to exceed the altitude of 1000 m. The measured thrust of this configuration can be seen in Figure 2. A peak of 650 N has been reached with a neutral burning profile. The predicted theoretical thrust is within 5% of the measurements as mentioned in Section 2.1. The total impulse measured is 560 Ns.

4. STUDENTS INVOLVEMENT

The Nimbus Project team is made of young engineers and students, all from the University of Padova. The team was initially born a few years ago from an idea among some Aerospace Engineering students, all of them keen on space exploration. The main objective was to apply in a practical way the knowledge acquired at the university. Some of the members are now professionals, but their dedication to the project has not changed.
The contribution of new students plays a fundamental role in the project: on one hand it allows an equal work distribution inside the team, on the other it offers the possibility to take part in the various phases of development

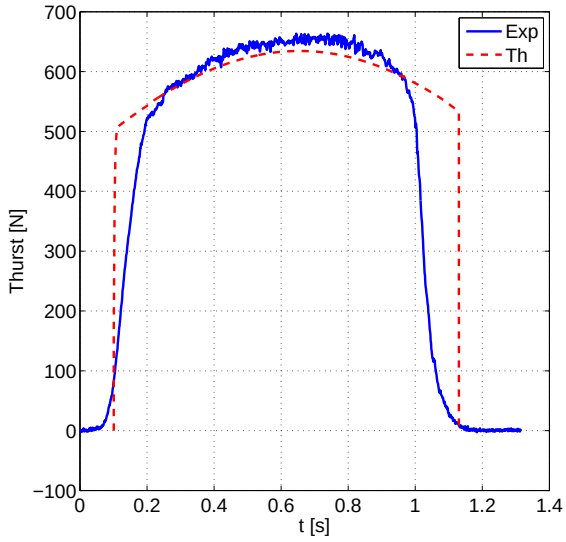


Figure 9: PR-V6 motor experimental and theoretical thrust in high power configuration.

of a sounding rocket, bringing fresh ideas and focusing on the aspects one finds most interesting. The project also offers the opportunity to develop graduation theses about the work carried out inside the team; in particular, two theses have been developed so far. The first is a bachelor's thesis regarding the design and construction of the main structure of the sounding rocket, with the annexed phases of numerical modelling and experimental validation [4]. The latter is a master's thesis focused on the development of a controlled re-entry system for the sounding rocket [6]. Furthermore, additional theses are going to be scheduled as new students join the project. These thesis works are possible thanks to the collaboration of some university professors.

5. LAUNCH REPORTS

Sagitta has a dry mass of 3.3 kg, is 2.1 m long and 74 mm in diameter. The motor currently mounted is capable to carry STD at an altitude of 1000 m AGL with a propellant mass of 400 g. In each of the two launches carried out so far the motor was under-powered to maintain low acceleration levels for structural and electronic verifications.

The current acceleration measured reached a peak of 14 G, while the maximum predicted acceleration with a full-power configuration of the motor is 25 G.

5.1. First launch

The first flight has been made to test all of the subsystems needed to accomplish operation of the sounding rocket technology demonstrator. The first flight used a PR-V6 motor with a reduced propellant load, around 80 % of the nominal load. Therefore the predicted apogee was 678 m. The choice of reducing the motor's thrust has been made to keep accelerations within 15 g and to verify and visually inspect avionics and structural performances and integrity. Figure 10 shows the barometric altitude profile as recorded by the pressure sensor, plus the FAF output used to command the chute deployment. The motor firing flag (vertical dashed line on the left) shows the instant in which the ignition wire is burnt; after that, there's a 1 s delay and then take-off occurs. An unexpected spike of pressure due to a vent of propellant gas can be seen after the ignition.

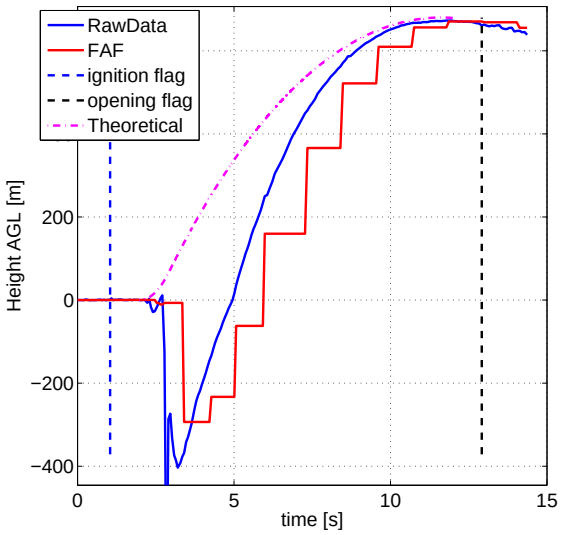


Figure 10: Sagitta measured (Raw Data), filtered and theoretical altitude of the first launch Above Ground Level. Vertical dashed lines are ignition of the rocket motor and parachute deployment signal (blue and black respectively).

In the acceleration graph (Figure 11) linear measured accelerations a_x, a_y, a_z are plotted; the take-off is identifiable at $T = 0.946$ s. The related frame of reference X,Y,Z is visible in Figure 1. The peak acceleration reached during the propelled flight is 14.3 g; when the motor shuts down the minimum acceleration peaks at -1,75 g.

Referring to angular speeds (Figure 12), the spinning rate is generally kept under 0.5 Hz on the Y axis. On the X and Z axes, spinning rates are very low, and especially negligible at the launch pad exit (2°/s oscillations). This shows that deviations caused by out-of-axis thrust are well balanced by the stabilizing fins, and the latter are well aligned to the fuselage.

As the altitude increases, a decrease to zero in both rotational speed and accelerations can be observed until the apogee, when the chute is deployed. The ejection devices worked as planned. However, some problems appeared, thus preventing a correct deployment. Sagitta descended at an higher speed of about 17 m/s landing down hard

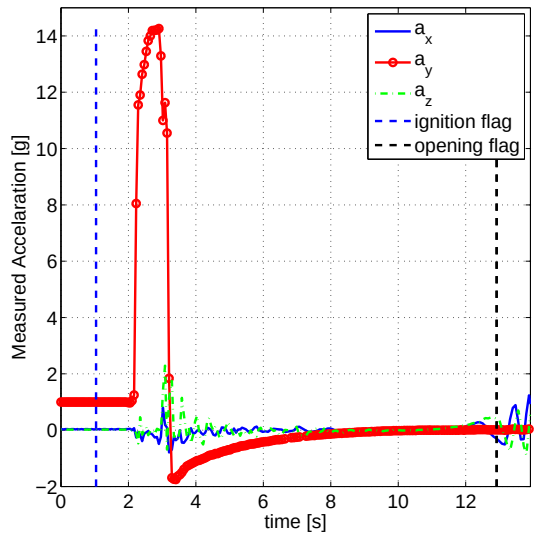


Figure 11: Sagitta measured and theoretical accelerations during the the first flight.

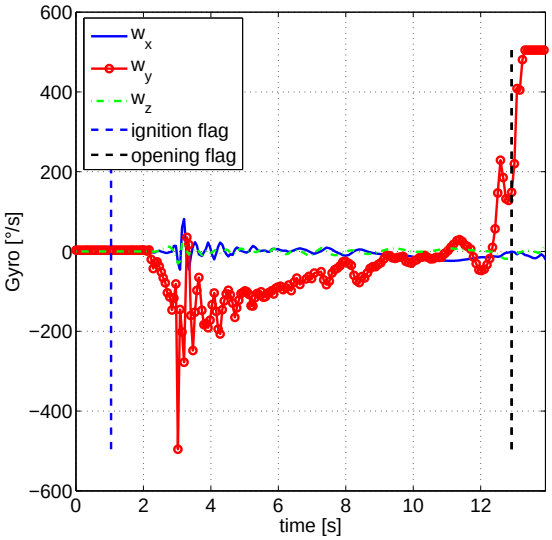


Figure 12: Sagitta measured angular velocity during the first flight.

but without major consequences. Neither avionics nor primary structures suffered functional damage, with light damage affecting secondary structures only. The worst damage has been the rupture of an interface between a stabilizing fin and the fuselage.

5.2. Second launch

The second flight has been made to test the changes done in the motor in order to prevent the vent of propellant gas (a ground test was already done) and verify the correct parachute deployment. The second flight, like the first, used a PR-V6 motor with a reduced propellant load, around 65 % of the nominal load. Therefore the predicted apogee was 515 m. Figure 13 shows the barometric altitude profile as recorded by the pressure sensor, plus the FAF output used to command he chute deployment. The motor firing flag (vertical dashed line on the left), shows the instant the ignition wire is burnt; after a 1 s delay, take-off occurs. No spike of pressure was measured this time. The apogee was 504 m.

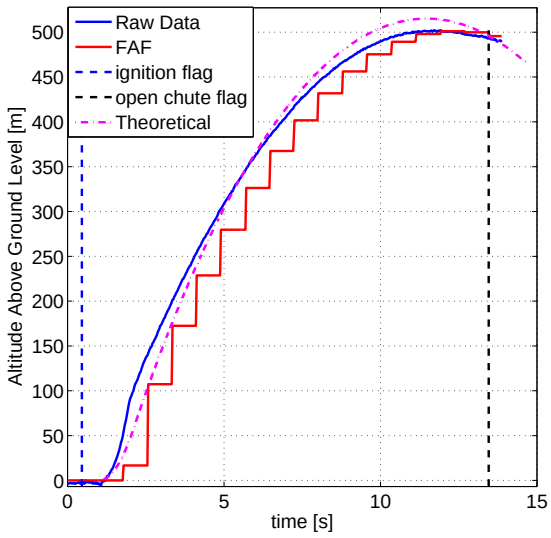


Figure 13: Sagitta measured (Raw Data), filtered and theoretical altitude of the second launch Above Ground Level. Vertical dashed lines indicate ignition of the rocket motor and parachute deployment signal (blue and black respectively).

Linear measured accelerations a_x, a_y, a_z are plotted in Figure 14; the related frame of reference X,Y,Z is visible in Figure 1. The axial acceleration of the rocket is along Y (a_y) and the high positive value generated by motor thrust is clearly visible: maximum acceleration measured is about 13.5 g. Immediately after the burnout, a_y drops down and it's possible to see the aerodynamic drag acting on the rocket. The incrementing profile of acceleration, from a minimum of -0.46 g to nearly zero at the apogee, can be used for drag coefficient estimation. Figure 14 also plots the theoretical a_y acceleration with a dashed pink line: during propelled flight the relative difference between predicted and measured accelerations is about 26%, while during inertial flight the maximum relative error is about 7% with respect to the predicted a_y.

In Figure 15 angular velocities are shown; the most interesting is the spinning velocity w_y. The maximum angular velocity reached is 300 °/s, which is equal to a rotation frequency of about 0.8 Hz.

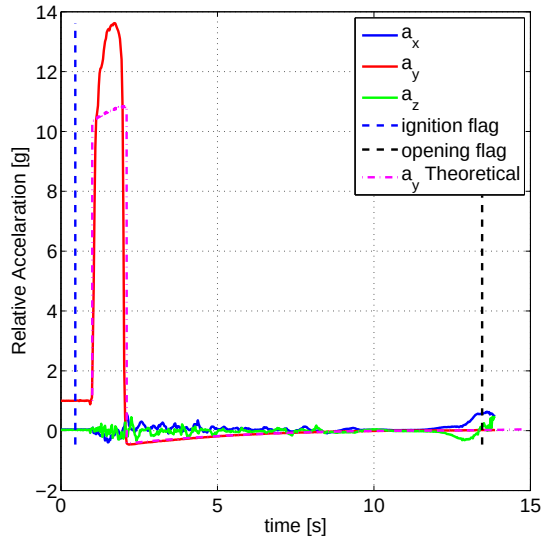


Figure 14: Sagitta measured and theoretical accelerations during the second flight.

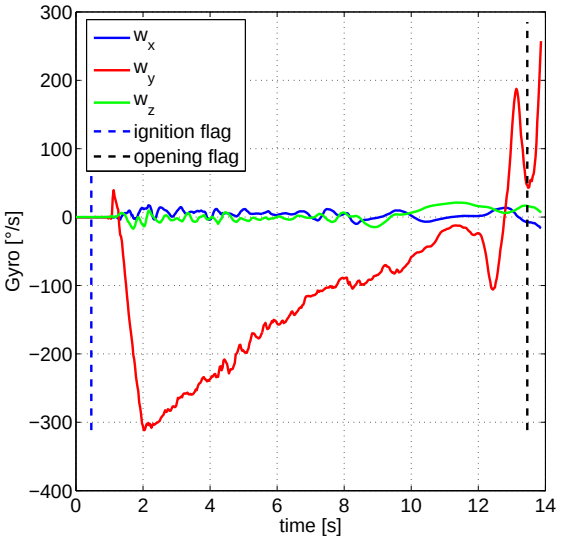


Figure 15: Sagitta measured angular velocity during the second flight.

6. CONCLUSIONS

In this paper we briefly introduced the Sagitta technology demonstrator, an affordable solution for a sounding rocket. The experience and data acquired from its first test flight allowed to develop several improvements to the original design. The flight software features better performance and an enhanced parachute deployment algorithm; compacting the electronic sensing equipment frees room for an internal bay at the complete disposal of third-party payloads; a lighter fuselage and a re-engineered motor ignition system reduce overall weight and increase maximum payload mass; finally, a high-power motor configuration will expand the operating window of the rocket. All these upgrades contribute towards a greater reliability, performance and usability of the whole system.
The limited cost and high versatility of the technology demonstrator make it a suitable vehicle for carrying student payloads or serving as a platform for other educational activities.
Students' involvement is fundamental for the project: most of the team members are university students, and some had the opportunity to write graduation theses about their work on the rocket's development.
Two successful launches proved the effectiveness of the technology demonstrator and showcased its performance.

ACKNOWLEDGEMENTS

We would like to thank CISAS for the support and especially: Prof. Stefano Debei, Eng. Carlo Bettanini, Eng. Mirco Zaccariotto (CISAS, University of Padua). Fulvio Stel, professor of Atmospheric Physics at the University of Trieste, and Alberto Gobbi for supporting us in the atmospheric field. Our thanks also go to Eng. Federico Rodighiero for electronics design assistance, Eng. Andrea Franchini for motor anodization, POLAR for IT support, b2Rocketry for support on the recovery system and Ivan Apolloni. A big thank you to Pololu Electronics for supplying electronic components and Girardi Print Factory for providing stationary and printing support. Last but not least, we thank ACME Italia and Stefano Figini for launch facility support.

REFERENCES

1. *European User Guide to Low Gravity Platforms*, UIC-ESA-UM-0001 Issue 2 Revision 0.

2. *Sounding Rocket Program Handbook*, Goddard Space Flight Center, Wallops Island, Virginia 23337, June 1, 1999.

3. *Design of aerodynamically stabilized free rockets*, American Department of Defence, 17 July 1990.

4. Pezzato M., *Design of the main structure of a sounding rocket: numerical model and experimental validation*, unpublished thesis, University of Padova, February 2015.

5. Churchill S. W., Chu H. H. S., *Correlating equations for laminar and turbolent free convection from a horizontal cylinder*, International Journal of Heat Mass Transfer n°18, p. 1049, 1975.

6. Martignago D., *Paraglider multibody simulation and control electronics proposals for a sounding rocket re-entry system*, unpublished thesis, University of Padova, October 2015.

LOW COST MEMS IMU CALIBRATION FOR AEROSPACE STUDENT ACTIVITIES

A. Rivolta[1], M. Giurato[2], F. Cuzzocrea[2], F. Rovere[2], and S. Farí[2]

[1]*Department of Aerospace Engineering, Politecnico di Milano, Milan, Italy*
[2]*Skyward Experimental Rocketry, Politecnico di Milano, Milan, Italy*

ABSTRACT

Student associations in the aerospace sector are becoming more and more relevant in the education of technical universities and many of those associations are actually building sounding rockets, small satellites and other vehicles. Inertial Measurement Units (IMUs) are golden sensors for determining position, velocity attitude and other quantities; Micro Electro-Mechanical Systems (MEMS) IMUs are simple and low cost sensors that are quite appealing for low budget student practical activities. The main drawbacks of MEMS IMUs are the signal noise and intrinsic parameters: both can be determined through a calibration procedure. Simple techniques coming from computer science and robotics community are quite popular also with hobbyists.

However, in the aerospace sector the simplifications made are in general non-valid: different techniques have to be used. Moreover, for engineering students advanced and rigorous algorithms are more instructional and delivers accurate results for practical applications. In this article is presented the design of a low cost and student-affordable platform for MEMS IMUs calibration as well as a rigorous procedure to obtain intrinsic parameters. The procedure is validated through experimental calibration of some IMUs to be used in sounding rockets attitude and position estimation.

Key words: IMU; Gyroscopes; Accelerometers; MEMS; calibration.

1. INTRODUCTION

Student activities involving rockets have a long history in Europe and recently the number of university students groups developing sounding rockets has increased. Developing sounding rockets embrace engineering fields such as mechanics, propulsion, aerodynamics, control, electronics and many more, requiring the capability to interact with the real world trying to translate paper design into actual rockets. Such activities allow students to gain invaluable experience for the job market covering the latency of purely theoretical classes thought at universities. In countries like Italy, where theoretical study is in general preponderant over practical activity, sounding rockets design and construction became a very important opportunity for students.

There are several disciplines involved in the design of a rocket that would require huge experience and computational power or costly facilities like aerodynamics. Student level understanding of the aerodynamics of a rocket is in general very basic and many wind tunnel available for students may not reach the condition of a supersonic flight regime. The best way to deepen the understanding of such topics is to actually launch the rocket and register data to be interpreted afterward. Such way of proceeding is not trivial and requires precise measurement of dynamical quantities or at least the state of the rocket during the flight.

Common sensors that can be installed on a sounding rocket for such purpose are altimeters, gyroscopes, accelerometers, magnetometers, cameras, etc. Among these sensors altimeters require to have access to the external air, cameras need pointing and clear sky and magnetometers may suffer from interaction with other electronics equipment. The only sensors that have low impact and low requirements from the design point of views are accelerometers and gyroscopes that form IMUs. Students activities usually have low budget, therefore the cheapest IMU usually used in such context are MEMS IMUs.

MEMS IMUs are characterized by low cost, low power request, low mass and unfortunately poor noise performance. In order to gather flight data to be used for post processing or in flight navigation it is mandatory to calibrate and evaluate the noise of these sensors. In this article a review of pre-existing calibration procedures as well as the development of an instructive way of proceeding with the calibration will be presented. Special focus is given to the students capability to prepare experiments and acquire knowledge on the subject in an engineering fashion. For better understanding of the issue and methods like the Allan Variance please refer to [1, 2].

1.1. Sounding rockets applications

Skyward Experimental Rocketry is an active student association operating inside Politecnico di Milano, it was

born in 2012 with the goal of designing and realizing small and medium sized experimental sounding rockets. The first flight of the student built rocket "Rocksanne I-X" was November 2013 and the apogee was 1000 m. The first flight had failures on parachute deployment and gyroscope acquisition. In june 2014 a new Rocksanne I-X rocket was launched twice within 24 hours reaching a maximum apogee of about 1100 m, no failure registered. IMU data from the 2014 launches have been processed and analyzed after the launch to reconstruct the trajectory of the rocket during the ascending phase. The capability of pure IMU reconstruction is comparable with the altitude reconstruction of an altimeter, showing promising use of IMUs in students made sounding rockets [3].

2. IMU MEMS ERROR MODELS

MEMS tri-axial IMU are composed by three single axis accelerometers and three single axis gyroscopes, therefore one source of error is the misalignment of the three axial sensors that form a triads that can cover the whole 3D world measurements [2]. Another common source of error is the static bias, i.e. the constant signal the sensor gives off when it is not affected by motion. Such offset is bound to cause problems in applications where attitude and or position are computed integrating IMU measurements since cause a rapid divergence of the integration. The most problematic aspect is that biases are usually temperature dependent: a calibration performed at a temperature different from the operating temperature may lead to wrong results. Scale factors are usually provided by manufacturers, however each sensor behaves differently and a proper assessment of the sensor is mandatory.

Should be noted that for students sounding rocket applications the long term drift of IMU signal is not an issue due to the short flights. Long term performance might become important if the IMU signal is required also in the descending phase that is characterized by a longer duration with respect to the ascending phase. Basing on flight experience, it is important to stress out that during the parachute descent high rotational velocities are expected.

2.1. Accelerometers

MEMS accelerometers measures body frame accelerations that can be linked with the inertial accelerations $\mathbf{a}_\mathrm{i}$ as follows

$$\mathbf{a}_\mathrm{i} = \mathbf{R}_\mathrm{ib}\mathbf{a}_\mathrm{b} + \mathbf{g} \tag{1}$$

where $\mathbf{g}$ is the acceleration due to gravity force field, $\mathbf{a}_\mathrm{b}$ the accelerations in the body fixed frame without gravity contribution, $\mathbf{R}_\mathrm{ib}$ the rotation matrix to rotate the accelerations from body reference frame to the chosen inertial reference frame. It is easy to see that when a MEMS IMU is not accelerating (force equilibrium) the signal it provides is $\mathbf{a}_\mathrm{b} = -\mathbf{R}_\mathrm{ib}^T\mathbf{g}$, therefore it should give back an acceleration of one g towards the zenith. As a matter of fact the only acceleration an IMU cannot measure is indeed gravity [4].

The ideal measures $\mathbf{a}_\mathrm{b}$ are however affected by noise and other intrinsic parameters due to the sensor manufacturing. These calibration parameters are item dependent and must be determined for each IMU before use. These parameters are the focus of the calibration procedure of this work. The complete measuring model for an accelerometer is

$$\mathbf{a}_\mathrm{b} = \mathbf{R}_\mathrm{mis}\mathbf{T}_\mathrm{a}\mathbf{S}_\mathrm{a}\mathbf{a}_\mathrm{m} + \mathbf{b}_\mathrm{a} + \mathbf{n}_\mathrm{a} \tag{2}$$

where $\mathbf{a}_\mathrm{m}$ is the signal of the sensor, $\mathbf{b}_\mathrm{a}$ is the accelerometer bias vector, $\mathbf{S}_\mathrm{a}$ the diagonal matrix representing the three axis scale factors $\mathbf{S}_\mathrm{a} = \mathrm{diag}\,[\mathrm{s_a}]$, $\mathbf{T}_\mathrm{a}$ a matrix that represents the non orthogonality of the three accelerometer axis, $\mathbf{n}_\mathrm{a}$ the zero mean noise vector (usually assumed to be white noise) and $\mathbf{R}_\mathrm{mis}$ is the rotation matrix that represents the small misalignment of the accelerometer axis with the intended body reference frame.

The non orthogonality is expressed by the following matrix

$$\mathbf{T}_\mathrm{a} = \begin{bmatrix} 1 & -\beta_\mathrm{yz} & \beta_\mathrm{zy} \\ \beta_\mathrm{xz} & 1 & -\beta_\mathrm{zx} \\ -\beta_\mathrm{xy} & \beta_\mathrm{yx} & 1 \end{bmatrix} \tag{3}$$

where the angles β are small angles that relates to the misalignment of each axis to form an orthogonal triad. An extensive explanation of this issue can be found in [2].

2.2. Gyroscopes

MEMS gyroscopes measures the angular velocities of the body the sensor is attached to. With respect to inertial angular velocities the relation is

$$\omega_\mathrm{i} = \mathbf{R}_\mathrm{ib}\omega_\mathrm{b} \tag{4}$$

and the sensor error model is basically the same as for accelerations of Equation (2)

$$\omega_\mathrm{b} = \mathbf{R}_\mathrm{mis}\mathbf{T}_\omega\mathbf{S}_\omega\omega_\mathrm{m} + \mathbf{b}_\omega + \mathbf{n}_\omega \tag{5}$$

The terms included are the same as for the accelerometer. Should be noted that gyroscope behavior may change at high acceleration regimes [5, 6], therefore before practical use should be wiser to test gyroscopes on a vibrating plate to test the influence of the launch acceleration and residual vibrations. Such influence will not be considered

in this work for the sake of simplicity and cost effectiveness.

3. CALIBRATION PLATFORM DESIGN AND REALIZATION

In order to calibrate MEMS IMUs different techniques have been implemented. While some do not use external equipment [2] others rely on platforms that provide a steady reference for accelerations and angular velocities. In [7] it has been used a six degrees of freedom Stewart platform while in [8] a gimbal platform has been suggested. From a student perspective the latter one is easier to implement and control, since two rotations are enough to cover all the possible attitudes and the gimbal platform is able to impose higher angular velocities. The Stewart platform has advantages for applications where small signals in angular velocity and linear motion are expected, but proves to be less adequate to sounding rockets applications where passively stabilized rockets spin quite fast on the longitudinal axis. Stewart platform may reproduce accelerations signals that a gimbal platform cannot provide, however imposing an acceleration in the order of tens of g may prove quite challenging. The gimbal equipment seems the most reasonable choice but cannot provide alone a full testing due to the limited acceleration signal bandwidth.

3.1. Hardware

An automated calibration solution requires that the sensory unit is moved through a range of orientations relative to the Earth's gravitational fields for the calibration of the accelerometers. It must also be able to rotate the sensory unit around its three axes independently for the calibration of the gyroscopes. Different solutions with several architectures can be found in commerce and some documentation about them can be found in literature [7, 8, 9].

The solution here presented is the actuated 3 Degrees Of Freedom (DOF) gimbal shown in Figure 1. For the IMUs calibration the rotational DOF at the base is redundant and is not considered for the experimental activity. The first joint can rotate from -180° up to 180° thanks to a transmission: this must be enforced to cover all the orientations with servo actuators that have a nominal range of 180°. The structural components are made of plywood in order to minimize the magnetic interference for magnetometers (here not considered) and costs. The platform is controlled through an Arduino MEGA, entirely programmed in Simulink environment. The platform is thought to be easily replicable and adaptable for anyone to reproduce the results and incorporate the calibration hardware and procedures. The main requirement found in the design of such equipment is to have at least one joint able to cover a 360° angular span to be able to cover all the orientations and angular velocity profile for the calibration. Depending on the desired accuracy and budget

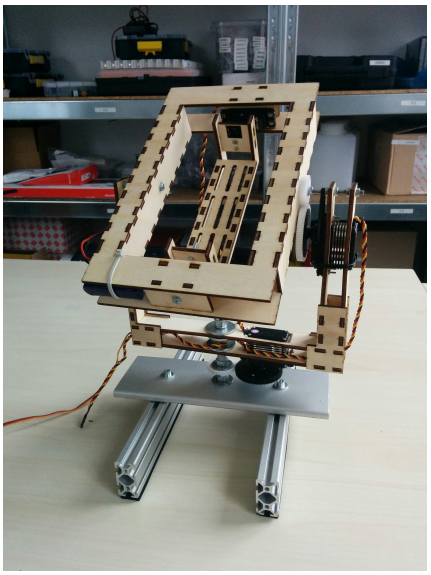


Figure 1. Calibration Platform

limitations it is possible to change the scheme to obtain the desired performances, bearing in mind that low cost MEMS equipment have accuracy limitations (especially noise and variable bias induced effects) for many applications.

Different IMUs have been tested, each one with a custom data logging architecture due to practical limitations. The first IMU used in the calibration experiment is the R2P IMU module, details can be found in [10]. The second model that has been tested is the GY-88 breakout board due to its popularity and low cost. It is composed by three different sensors: an Invensense MPU-6050 triaxial IMU, an HMC-5883L magnetometer and a BOSCH BMP085 barometer. For the purpose of the tests the accelerometer was set with ±2g full-scale range, while the gyro was set with ±250 degrees full-scale range. The GY-88 signals were transmitted using a Arduino Pro Mini and a cheap RF 315 MHz Transmitter-Receiver module in order to fit the testing bay and reduce interference with the platform; an I2C protocol was used. The receiver module was connected to a PC through an Arduino Mega in order to log the IMU output directly in the MATLAB environment.

3.2. Calibration sequence

The calibration platform allows to have a repeatable sequence of rotations in order to test the IMU and gather data usable for the calibration. The sequence of rotations is very important and is deeply connected with the architecture. The platform is commanded through 2 rotations and is capable of spanning the entire vector field, allowing a static calibration of magnetometers and accelerometers. Accelerometers are often used to get an attitude measure when they experience quasi-static motion; this use has often caused the complete misinterpretation of

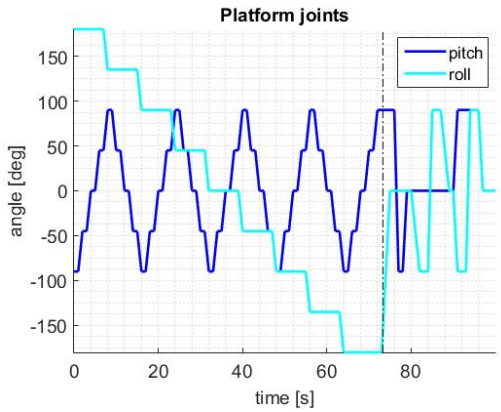


Figure 2. Calibration platform joint sequence

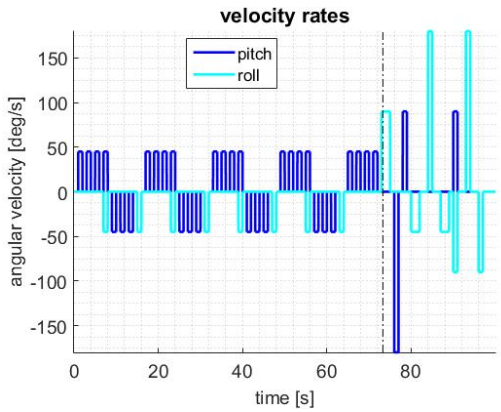


Figure 3. Calibration platform joint velocity

the measure accelerometers provide.

In order to fully calibrate an accelerometer a vibrating plate is usually requested, however for basic uses might be enough a calibration in near static conditions. As a matter of fact in constrained quasi-static motion, the accelerometer measures the reaction force per unit mass that counterbalance the gravity force, meaning that such acceleration has modulus equal to the gravity acceleration but in opposite direction. This means that an accelerometer placed on a table will give a vector signal pointing upwards in the opposite direction of the gravity force. In the hobbyist world the simplest calibration is carried out by placing the accelerometer on each face, thus setting gain and bias with only in 6 different acquisitions. The procedure is simple but not robust or instructive for students. Exploiting the calibration platform it is possible to rotate the sensor and acquire the vector signal spanning through all rotations. This allows to compute the bias and the gain of the accelerometer such that, regardless of its orientation in space, it will measure the same reaction force induced acceleration.

Knowing the sequence of positions and velocity allows also to calibrate the gyroscope. However, due to the inherent reduced velocity of the accelerometer sequence, where quasi-static motion is preferred, it is wiser to design a sequence where the signal of the gyroscopes is higher, therefore an angular velocity constant signal of about 180°/s is preferred. A similar procedure can be found in [8]. To achieve this feat with only two rotation axis it is mandatory to change the attitude of the IMU such that all three axes are excited and a clean signal is registered.

The sequence is presented in Figure 2 where the two angles of the imposed sequence have been highlighted as well as the the point of transition between accelerometer sequence and gyroscope sequence. The angular velocities of the joints, that can be then translated to the signal the gyroscope should measure is presented in Figure 3

Using Denavit-Hartemberg convention and parameters to describe the kinematics of the platform [11] it is possible to determine both linear velocity and angular velocity, therefore getting a reference signal also for the gyroscope.

4. CALIBRATION PROCEDURE

As stated before the platform allows to have reference signals that can be used for calibration. The most exploited way is to use data fitting techniques like the Levenberg-Marquardt [12]. Practical implementations of such methods is not the aim of this article and MATLAB built in functions were used in the development. Here follows two calibration procedures, one for accelerometers and one for gyroscopes, organized with a hierarchical approach.

4.1. Accelerometer

Accelerometer measurements of the IMU shall be confronted with a reference signal computed using the platform attitude. Should be noted that it is needed the computation of the rotation from the accelerometer reference frame to the tip reference frame, which is configuration dependent: mounting different accelerometer may result in different alignments due to installation constraints or product design. In order to provide a good signal to be calibrated it is often necessary to filter as much as possible the noise of the MEMS without losing information. Figure 4 shows an example of the filtering results for the three axis.

A first guess of accelerometer scale factor and biases may be computed taking the first samples where there is actually no motion and considering the maximum value on each axis for the whole sequence. Initial guess of such parameters allows to rapidly visualize data and check for consistency. Once the signal is comparable it is possible to align signal and reference, therefore registering two curves. In many application such registering may be done

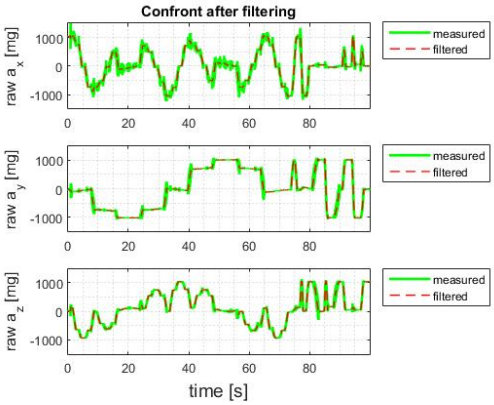


Figure 4. Accelerometer filtering example

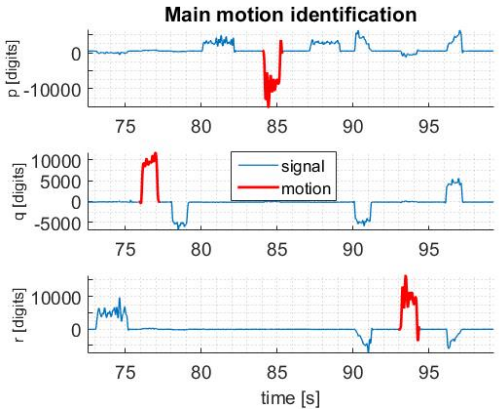


Figure 5. Angular motion identification

by the operator, however it is not very instructive for students. Automatic registration allows to register multiple acquisition with ease, however requires some effort in the programming. Should be noted that unlike general registration problem here the time axis is not altered but just shifted, therefore there is just one parameter for each acquisition that align the accelerations and angular velocities measured by the IMU with the reference signal. Time warping functions are not used and the registration problem becomes a simple time shifting problem [13].

There is, however, one way to refine the bias, scale factor and registration constant in a single swipe. By using a non linear data fitting algorithm it is possible to compute bias $\mathbf{b}_\mathrm{a}$, scale factor $\mathbf{s}_\mathrm{a}$ and time shift Δt by trying to fit the measures with the reference signal $\mathbf{r}$ minimizing a cost function as follows

$$\min_{\mathbf{s}_\mathrm{a},\Delta t,\mathbf{b}_\mathrm{a}} \left(\mathbf{r}\left(t_\mathrm{i}\right) - \mathbf{S}_\mathrm{a}\mathbf{a}_\mathrm{m}\left(t_\mathrm{j}+\Delta t\right) - \mathbf{b}_\mathrm{a}\right) \qquad (6)$$

Data fitting techniques however are usually thought for linear correspondence and not for vector, therefore a proper choice of fitting function is required. Since bias and scale factor are different for each axis it is possible to compute each axis separately, however the time shift factor is a global properties common to all three axis. Grouping the measures together and fitting each axis allows to compute a good solution. Should be noted that with respect to modulus fitting [8] the computation is more precise but slower since the number of equations in the fitting is three times greater than in the other approach.

The result in registration is quite satisfying therefore the registration constant is consolidated and not modified afterward. Then the registered data are fitted on the reference signal component by component and taking into account also the misalignment of the sensor and the non orthogonality. Guess values for scale and bias are taken as the outcome of the previous minimization to speed up the process.

$$\min_{\mathbf{R}_\mathrm{mis},\mathbf{T}_\mathrm{a},\mathbf{s}_\mathrm{a},\mathbf{b}_\mathrm{a}} \left(\mathbf{r} - \mathbf{R}_\mathrm{mis}\mathbf{T}_\mathrm{a}\mathbf{S}_\mathrm{a}\mathbf{a}_\mathrm{m} - \mathbf{b}_\mathrm{a}\right) \qquad (7)$$

The computed misalignment should be analyzed with care since it includes intrinsic misalignment of the sensor and mounting misalignment on the platform. To understand better this parameter, several experiments where the mounting is modified each time should be performed.

Fitting techniques have been used also in [2] and here have been considered using a hierarchical approach. Extending the reasoning, the procedure should seek to determine an increasing number of parameters by adding each time new DOF in the minimization. Usually by adding new states the overall error tends to decrease regardless of the physical implications, therefore a proper comparison between levels allows the operator to find inconsistency if these arises.

4.2. Gyroscope

Gyroscope calibration is also divided in two parts with increasing complexity. First of all the scale factor and bias must be estimated in order to proceed smoothly with the determination of all parameters. To this end, the second part of the calibration platform motion is exploited. Since the angular velocities on the three axes are maximum in correspondence of such motion it is easy to locate the maneuvers. More complex is the registration process where beginning and end of motion are automatically computed. Here has been used a simple and effective procedure without seeking complex algorithms. From the located peaks the algorithm takes a symmetric window larger than the duration of the motion in order to catch the flat signal before and after. Then from the first instants a search on the initial point is made comparing the mean of preceding samples with the mean of the following 10 samples, when a user defined threshold is reached, then the starting point of the maneuver is found. The ending point is computed as the point following the peak where the signal has the same value as the identified motion start.

Figure 5 shows the gyroscope measures for the second part of the calibration sequence. The main motion have been highlighted in red and the image shows a good extraction of the sequences.

Then the relative angular motion is precisely computed from the reference attitude of the platform. By design such motion is about 180 degrees, however by computing it each time it is possible to obtain a more refined evaluation of the angular displacement and recognize the axes of rotation. Bias can be estimated using the values of the gyroscopes at the end of the sequence, where for few seconds the platform is fixed and not moving. Taking the mean of the signals over this period (i.e. the mean of gyroscope output from a time t_a to a time instant t_b when the platform is not moving) allows to compute the bias as function of the signal and scale factor as follows

$$\mathbf{b}_\omega = -\mathbf{S}_\omega \left\langle \omega_\mathrm{m}|_{t_\mathrm{a}}^{t_\mathrm{b}} \right\rangle \tag{8}$$

Considering only scale factor and bias, the body angular velocities from Equation (5) can be expressed as

$$\omega_\mathrm{b} = \mathbf{S}_\omega \left(\omega_\mathrm{m} - \left\langle \omega_\mathrm{m}|_{t_\mathrm{a}}^{t_\mathrm{b}} \right\rangle \right) + \mathbf{n}_\omega \tag{9}$$

Then, knowing the angular displacement for the three axes $\Delta\vartheta$ and the beginning and end of each axis sequence it is possible to compute the scale factor. The time extremes of the integration are denoted with t_1 and t_2 using a compact notation, however should be clear that the values of such time instants varies from axis to axis and the computation is decoupled. The result is

$$\mathbf{s}_\omega \simeq \left(\mathrm{diag} \left[\int_{t_1}^{t_2} \omega_\mathrm{m} dt - \mathrm{diag}\left[t_2 - t_1\right] \left\langle \omega_\mathrm{m}|_{t_\mathrm{a}}^{t_\mathrm{b}} \right\rangle \right] \right)^{-1} \Delta\vartheta \tag{10}$$

Such procedure allows to have an estimation of the scale factors using a relevant signal and the static behavior of the sensor. Should be noted that in Equation (10) the integral $\int_{t_1}^{t_2} \omega_\mathrm{m} dt$ includes also the noise $\mathbf{n}_\omega$, therefore the estimation is affected by the random walk due to the integration of a white noise. In order to filter out such behavior and determine misalignment parameters a further step is necessary.

The second step is exactly the same as for the accelerometer, therefore enforcing Equation (5) in Equation (7) with the reference taken as the angular velocity computed using joints velocity and the platform model. Unlike for accelerometers the misplacement of the IMU on the platform does not influence the signal, therefore no regular residual motion is expected. Possible variation from the reference signal to the real motion are expected due to the nature of the step motors used for the motion of the platform.

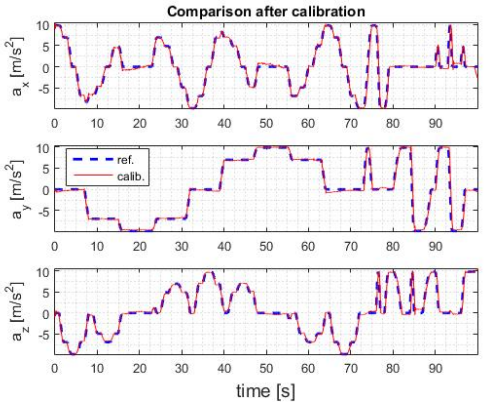


Figure 6. R2P accelerometer calibration results

5. EXPERIMENTS AND CALIBRATION RESULTS

Several experimental acquisition have been performed with different hardware.

5.1. R2P IMU test

Figure 6 presents the calibration results of a R2P accelerometers set using the presented technique. It is possible to appreciate the matching of the calibrated accelerometer and computed reference in the first part, while some visible differences arises in the second part where huge rotations occurs. This is mainly due to the high angular velocities causing apparent accelerations since the sensor is not perfectly aligned with the center of rotation. This behavior can be seen also in small transition areas in the first sequence, however the algorithm is capable of ignoring such inconsistency since are smaller with respect to the expected motion.

The calibration of gyroscopes is presented in Figure 7 for a small portion of the accelerometer sequence to highlight better the good matching. The fitting of the gyroscopes on the second sequence are shown in Figure 8. Small visible differences in the second sequence are due to the effective rotation profile imposed by the joints, thus hardware related errors. Even with a low cost students made platform results are quite encouraging and support the use of IMU for students sounding rocket applications.

Table 1 reports the output of the hierarchical calibration of R2P IMU. Misalignment and non-orthogonality angles are measured in degrees; the misalignment rotational matrix has been computed using the exponential mapping of Lie algebra for computational efficiency. It is possible to appreciate the consistency of the first and second step,

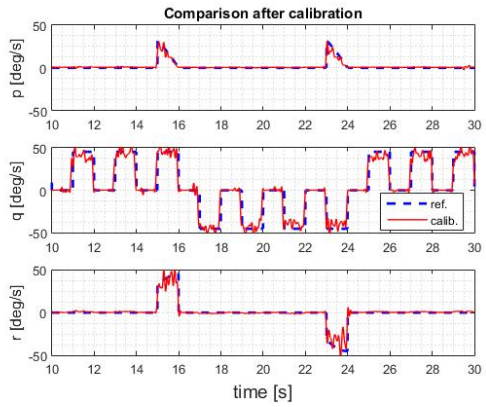


Figure 7. R2P gyroscopes calibration

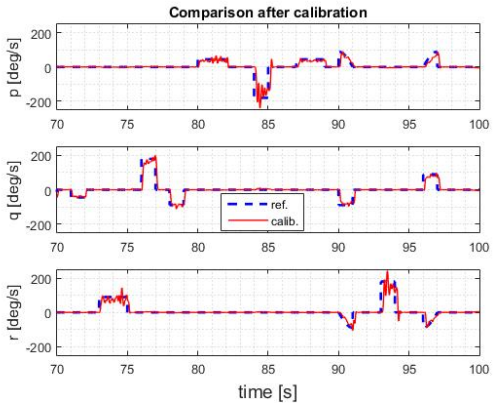


Figure 8. R2P gyroscopes calibration - high angular velocities

Table 1. Hierarchical calibration R2P IMU

	Accelerometer		Gyroscope	
	I	II	I	II
b	0,0510 0,1981 -0,5826	0,0392 0,2078 -0,5731	-9,1172 2,8568 1,4009	-7,2092 2,5896 1,4516
S	0,0094 0,0096 0,0098	0,0094 0,0096 0,0098	0,0184 0,0181 0,0180	0,0154 0,0169 0,0148
$\mathbf{R}_{\text{mis}}$		0,8428 0,9181 0,7541		-2,5954 3,0167 -0,9857
T		-0,5593 -0,6859 -0,3369 0,2214 -1,3349 0,4020		-1,8419 1,8162 -3,7902 -0,3968 2,2555 2,5878
Error	0,0114	0,0109	0,2347	0,2236

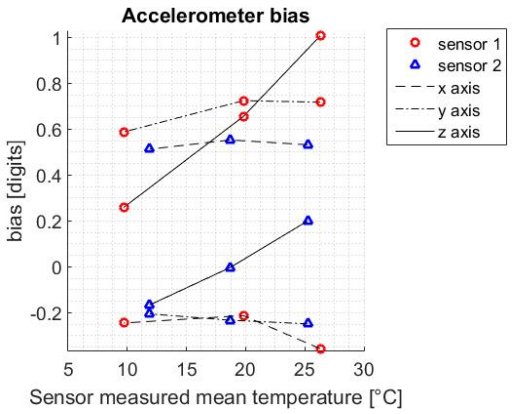


Figure 9. GY88 accelerometer bias variation with temperature

especially in the accelerometer calibration. The overall norm of the error is not decreasing much from one iteration to the next, however it is lowering. The variation in scale and bias, the most important parameters, is reduced, as expected. Only in the gyroscope calibration is possible to appreciate a variation in the bias, remembering that the values for that are digits, i.e. dependent on the order of magnitude of the digital output of the sensor. The difference lies also in the fact that the I iteration of gyroscope is quite different from the other since it uses small portion of the signal to get the first true estimation of the signal. To check consistency between gyroscopes and accelerometers it has been performed two separate registration that yielded the same results, assuring that it is not necessary to repeat the alignment operations.

5.2. GY-88 IMU test

Extensive measurements were taken with different units of GY-88 to test temperature variability and consistency of the calibration. For the consistency three trials on three different GY-88 sensors were taken and calibration results were compared. Considering very small temperature variation between the trials it has been noticed that the estimated bias and scale factors are within few percentage points and the misalignment and non orthogonality angles differ at most by half degree.

Test with varying temperature have been performed without a calibrated reference temperature but using the internal measured temperature. This is not rigorous for a calibration however is closer to a real sounding rocket application where temperature compensation is carried out with the same sensor. This test was meant to show the variability of some quantities with the measured temperature rather than obtain a fine calibration of the sensors since huge data acquisition campaign should be performed. During the tests temperature varied approximately from 5 to 25 °C and two different GY-88 sensors were used.

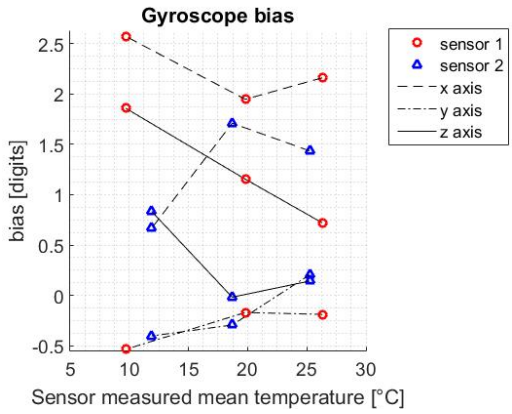


Figure 10. GY88 gyroscope bias variation with temperature

Test have shown that the accelerometer scale factors change with temperature is almost negligible, while its bias and the gyroscope bias and scale are much more affected by temperature variation. In order to be used for closed loop stability control system or similar applications, bias are usually the most problematic error to be faced. Figures 9 and 10 presents the variation of the IMU bias as function of the temperature. A clear trend is not easily found and each axis behaves differently, suggesting to carry out a calibration of the IMU bias with temperature through extensive tests in order to have better flight performance. Should be noticed that in some cases could be necessary or better performing to have a temperature control of the sensor during the flight.

6. CONCLUSION

In this article it has been presented a hierarchical preliminary calibration procedure for MEMS IMUs to be used for sounding rocket students activities. Simplicity, low cost and students education were the key focus of the development of the equipment and methodology. The use of a reference signal proves to be effective in covering all the possible calibration parameters determination and offers useful insights to understand the behavior of such popular sensors. The experimental activities showed the capability of the developed method to calibrate sensors for sounding rockets as well as providing students with real engineering problem experience.

Further works will focus on acquiring more data to correlate temperature and biases and high acceleration tests for the gyroscopes. More functional data analysis will be included in the following works in order to achieve better accuracy and highlighting more the sensors behavior and suggesting new calibration and compensation methods.

REFERENCES

[1] M. Vágner, P. Beneš, and Z. Havránek, "Experience with allan variance method for mems gyroscope performance characterization," in *Instrumentation and Measurement Technology Conference (I2MTC)*, pp. 1343–1347, IEEE, 2012.

[2] A. P. David Tedaldi and E. Menegatti, "A Robust and Easy to Implement Method for IMU Calibration without External Equipments," in *IEEE International Conference on Robotics and Automation (ICRA)*, pp. 3042–3049, IEEE, 2014.

[3] R. Di Battista and A. Rivolta, "Mission analysis integrated project team final report," tech. rep., 2015.

[4] M. S. Grewal, L. R. Weill, and A. P. Andrews, *Global positioning systems, inertial navigation, and integration*. John Wiley & Sons, 2007.

[5] J. B. Bancroft and G. Lachapelle, "Estimating mems gyroscope g-sensitivity errors in foot mounted navigation," in *Ubiquitous Positioning, Indoor Navigation, and Location Based Service (UPINLBS)*, pp. 1–6, IEEE, 2012.

[6] L. Iozan, J. Collin, O. Pekkalin, J. Hautamäki, J. Takala, and C. Rusu, "Measuring the earthâĂŹs rotation rate using a low-cost mems gyroscope," in *Proceedings of the 2010 Symposium Gyro Technology, Karlsruhe, Germany*, vol. 2122, 2010.

[7] Ø. Magnussen, M. Ottestad, and G. Hovland, "Calibration Procedure for an Inertial Measurement Unit Using a 6-Degree-of-Freedom Hexapod," in *International Conference on Unmanned Aircraft Systems (ICUAS)*, 2012.

[8] S. Madgwick, "Automated calibration of an accelerometer, magnetometers and gyroscopes - A feasibility study," tech. rep., sep 2010.

[9] J. J. Hall, R. L. Williams II, and F. van Graas, "Inertial measurement unit calibration platform," *Journal of Robotic Systems*, vol. 17, no. 11, pp. 623–632, 2000.

[10] A. Bonarini, M. Matteucci, M. Migliavacca, and D. Rizzi, "R2p: An open source hardware and software modular approach to robot prototyping," *Robotics and Autonomous Systems*, vol. 62, no. 7, pp. 1073 – 1084, 2014. Reconfigurable Modular Robotics.

[11] J. Denavit, "A kinematic notation for lower-pair mechanisms based on matrices.," *Trans. of the ASME. Journal of Applied Mechanics*, vol. 22, pp. 215–221, 1955.

[12] H. Gavin, "The Levenberg-Marquardt method for nonlinear least squares curve-fitting problems," *Department of Civil and Environmental Engineering, Duke University*, 2011.

[13] J. O. Ramsay and B. W. Silverman, *Applied functional data analysis: methods and case studies*, vol. 77. Springer New York, 2002.

ACTIVE MODEL ROCKET STABILIZATION VIA COLD GAS THRUSTERS

Danylo Malyuta[1], Xavier Collaud[1], Mikael Gaspar[1], Gautier Rouaze[1], Raimondo Pictet[1], Anton Ivanov[1], and Nikolay Mullin[2]

[1]*Space Engineering Center (eSpace), EPFL, Station 11, 1015, Lausanne, Switzerland.*
[2]*Bauman Moscow State Technical University, ul. Baumanskaya 2-ya, 5, Moscow 105005, Russia.*

ABSTRACT

This paper describes the development and testing of a reaction control system (RCS) for a model rocket named FALCO-4. The rocket uses cold gas jets to keep itself perfectly vertical at low speeds. We first describe the mechanical layout of FALCO-4 and the characteristics of the cold gas propulsion system. We then propose a dynamical model of the rocket and a control scheme based on decoupled PID regulators for roll, pitch and yaw. The control scheme is then evaluated based on MATLAB® simulation and flight data collected over 4 test flights that showed the RCS to work well even though vertical orientation was only partially achieved due to insufficient thrust from the cold gas thrusters. Finally, the present approach is evaluated and improvements are suggested.

Key words: model rocket; active stabilization; PID control; vertical landing.

1. INTRODUCTION

Traditionally, rockets are built as expendable systems. Today, however, there is a growing trend towards designing partially or fully reusable rocket systems [1] [2] [3], spurred by the prospect of massive cost reductions (up to 100 times [1]) and the need for such systems in future manned planetary exploration. It is likely that all future rockets will include some reusability aspect. As such, the present project is an effort to accustom engineering students to the "reusable rocket" paradigm and the challenges that it entails.

Our team aims to design a cheap and accessible model rocket featuring all the necessary technology to be a plug-and-play platform for testing rocket landing algorithms. The present paper discusses the first step in this project – the design and validation of a cold gas reaction control system for maintaining a vertical attitude at low speeds. The mission for this paper is to maintain a vertical attitude around apogee.

This paper is organized as follows: Section 2 describes the mechanical layout of the rocket and the characteristics of the cold gas reaction control system. Section 3 develops the dynamical model of the rocket and the control scheme used. Section 4 presents the results from four test flights. Finally, Section 5 evaluates the effectiveness and suggests improvements over the present system.

2. MECHANICAL DESIGN

2.1. Rocket Structure

The final design, shown in Figure 1, contains the following major components:

1. LV-Haack (minimum drag) nose cone ($C = 1/3$).
2. Fiberglass tube (avionics compartment).
3. Fiberglass tube (RCS compartment).
4. Fiberglass tube (parachute and propulsion compartment).
5. Tapered, swept flat-plate fins (fiberglass-reinforced lemonwood).
6. Plywood (1 [mm]) and balsa (8 [mm]) sandwhich mounting bar.
7. Raspberry-Pi 1 Model B+ [4] (with USB ports removed).
8. 3D-printed cowling (ABS plastic) for Raspberry Pi Spy Camera [5].
9. DC/DC boost converter [6].
10. Tube coupler and RCS nozzle ring (pine).
11. RCS valves [7].
12. Pressure tubing [8].
13. Pressure regulator [9].
14. CO_2 cartridge [10].
15. CO_2 cartridge retainer (pine).
16. Horizontal CMOS camera [11].
17. Tube coupler (pine).
18. Parachute (drogue and main).
19. Engine mount tube (cardboard).

20. Centering ring (pine).
21. Pressure sensors [12].
22. Power electronics and MSP430G2553 slave microcontroller.
23. RCS activation alarm and debugging LEDs.
24. LiPo battery storage [13].
25. Engine nozzle.

Weighing 2560 [g], the rocket is 1.36 [m] long, 7.62 [cm] in diameter and is composed of two bodies that separate after apogee for parachute deployment. The fuselage length is determined by the size of the RCS and avionics compartments as well as a static stability requirement. The final static margin is 6.08 calibers between the center of mass and center of pressure, offering sufficient aerodynamic stability at lift-off. The diameter was dictated by the available tubing serving as a mold.

For propulsion, the Aerotech RMS H-238 reusable motor with 175 [Ns] specific impulse was chosen in order to obtain an off-launchrod velocity of 15-18 $\left[\frac{\text{m}}{\text{s}}\right]$ required for passive stabilization by the fins. The burn time is less than 1 [s] during which the rocket undergoes an acceleration of up to 78.9 $\left[\frac{\text{m}}{\text{s}^2}\right]$ and reaches a maximum speed of about 59 $\left[\frac{\text{m}}{\text{s}}\right]$. The maximum altitude is approximately 187 [m].

Finally, Figure 2 shows a top-level overview of the avionics that flew aboard the rocket. In addition, all software source code in MATLAB® and C is available at [14].

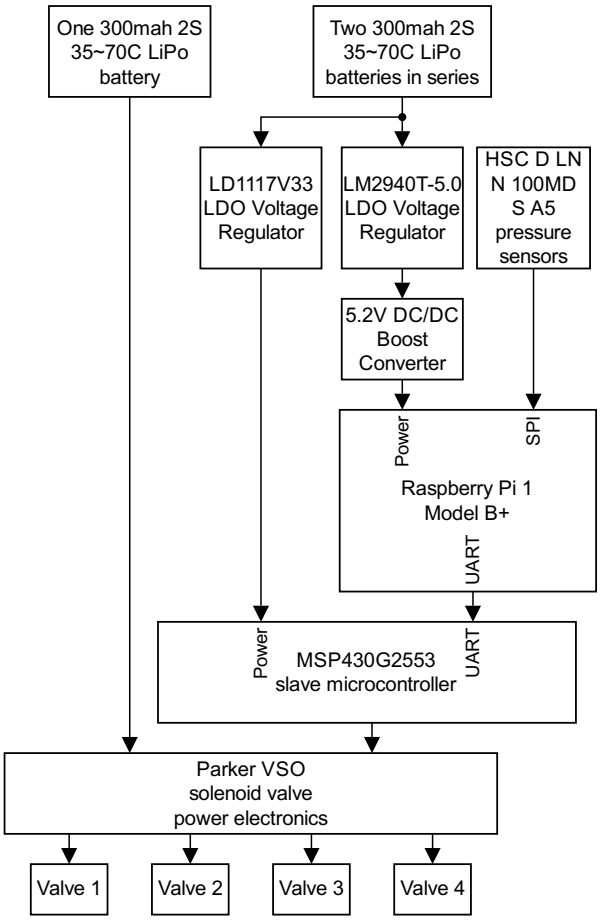


Figure 2. High-level layout of the rocket avionics.

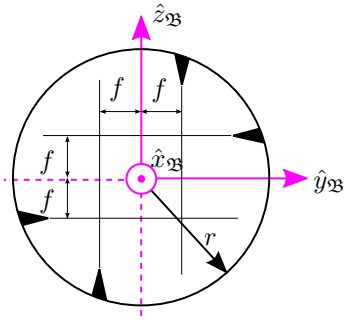


Figure 3. Layout of the RCS (top view). $f = 5$ [mm], $r = 3.81$ [cm].

2.2. Reaction Control System

The cold gas reaction control system is composed of a cartridge of 68 [g] of liquid CO_2 pressurized at $p_0 = 60$ [bar], a pressure regulator to $p_1 = 6$ [bar] and a set of pressure tubes leading to four proportional solenoid valves that expell gas in their respective directions. Figure 3 shows the geometric nozzle layout. The entire RCS assembly weighs 834 [g].

We now discuss the valve thrust calculations that drive the selection of these components in view of minimal weight and a 1 [N] thrust per valve requirement (this thrust was not achieved by the final RCS). We use numerical values relating to the aforementioned RCS components, however the following calculations have been done for several component candidates in order to select the present combination.

We assume CO_2 to be an ideal gas and the flow through the valve to undergo an isenthalpic throttling process. The flow conditions upstream are determined by the pressure regulator (see the layout schematic in Figure 4) and are set to the following values:

$$\begin{cases} T_1 = 273 \text{ [K]}, \\ p_1 = 6 \text{ [bar]}. \end{cases}$$

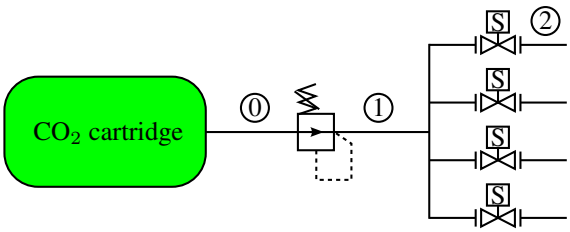


Figure 4. Pressure connections schematic for the RCS.

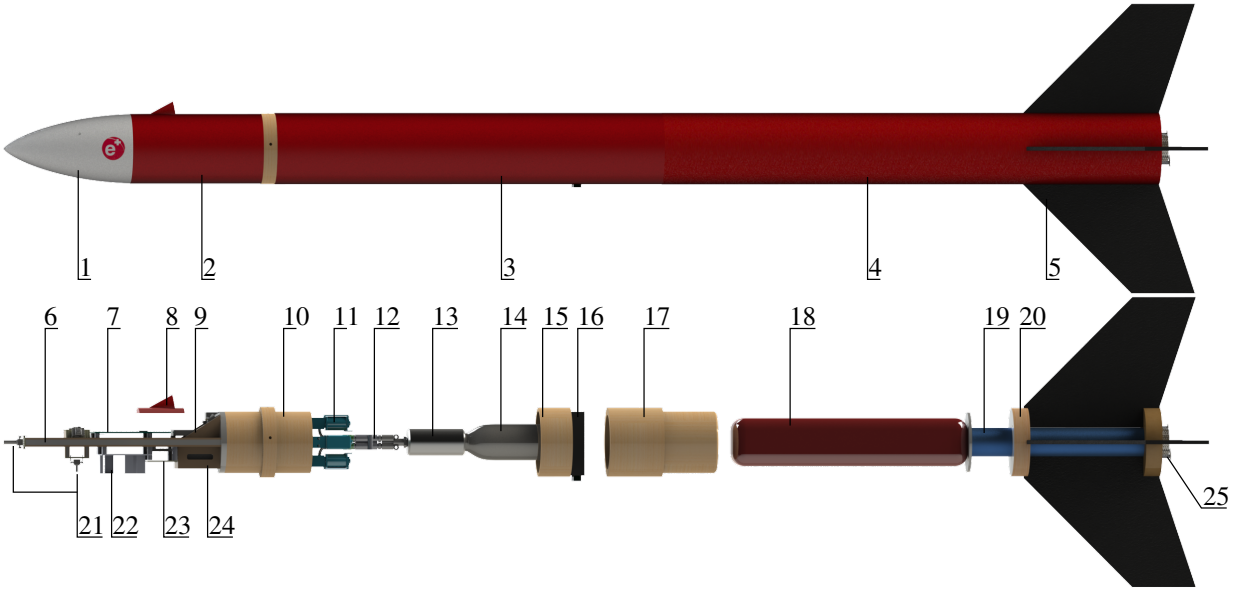


Figure 1. Structural layout of FALCO-4.

Where the indices refer to the locations of corresponding circled numbers in Figure 4. It is further assumed that $p_2 = p_{\text{atm}} = 101325$ [Pa]. It is then possible to compute the temperature of the flow after the valve by making the isentropic flow assumption:

$$T_2 = T_1 \left(\frac{p_2}{p_1}\right)^{\frac{\gamma-1}{\gamma}} \approx 184.48 \text{ [K]}, \tag{1}$$

where the CO_2 specific heat ratio γ is 1.28. We check for sonic conditions at the valve orifice, assumed to be the narrowest part of the flow:

$$p_{\text{cr}} = \left(\frac{2}{\gamma+1}\right)^{\frac{\gamma}{\gamma-1}} p_1 \approx 329620 \text{ [Pa]} > p_2. \tag{2}$$

Therefore the flow downstream of the valve orifice is equal to the speed of sound. The nozzle exit velocity is therefore:

$$U_2 = \sqrt{\gamma R T_2} \approx 211.56 \left[\frac{\text{m}}{\text{s}}\right], \tag{3}$$

where the CO_2 gas constant R is 189 $\left[\frac{\text{J}}{\text{kg}\cdot\text{K}}\right]$. We now use the isenthalpic throttling process assumption to compute the mass flow rate through the valve:

$$\dot{m}_{\max} = c_d A \frac{p_1}{\sqrt{RT_1}} \sqrt{\gamma \left(\frac{p_{cr}}{p_1}\right)^{\frac{\gamma+1}{\gamma}}} \approx 1.7069 \left[\frac{\text{g}}{\text{s}}\right]. \tag{4}$$

Note that (4) gives the maximum mass flow rate since the maximum valve opening area A is used for the calculation. Finally, the maximum thrust is:

$$F_{\max} = U_2 \dot{m}_{\max} \approx 0.3611 \text{ [N]}. \tag{5}$$

Note that this value is very close to experimental measurements, for which maximum thrust varied between 0.32 and 0.37 [N]. In the future, maximum thrust could be increased by using de Laval nozzles instead of ejecting gas directly from the tube.

3. CONTROL SYSTEM DESIGN

3.1. Dynamical model

In this section, the dynamical attitude model of the rocket is developed using Euler-Lagrange formalism. Because only rocket attitude is controlled, translational dynamics are not modelled under the assumption that translational and rotational motions are decoupled about the center of mass. Furthermore, as the control system is turned on *after* engine cutoff, rocket mass is assumed to be constant.

The Lagrangian of a system is defined as:

$$\begin{aligned} \mathscr{L}(\boldsymbol{q}, \dot{\boldsymbol{q}}) &= \mathscr{K}(\boldsymbol{q}, \dot{\boldsymbol{q}}) - \mathscr{U}(\boldsymbol{q}) \\ &= \frac{1}{2}\dot{\boldsymbol{q}}^T M(\boldsymbol{q})\dot{\boldsymbol{q}} - \mathscr{U}(\boldsymbol{q}), \end{aligned} \tag{6}$$

where $\mathscr{K}(\boldsymbol{q}, \dot{\boldsymbol{q}}) \in \mathbb{R}$ is the kinetic energy, $\mathscr{U}(\boldsymbol{q}) \in \mathbb{R}$ is the potential energy, $M(\boldsymbol{q}) \in \mathbb{R}^{n\times n}$ is the inertia matrix and $\boldsymbol{q} \in \mathbb{R}^n$ is the vector of generalized coordinates. In this case, $\boldsymbol{q} = [\varphi \quad \theta \quad \psi]^T \in \mathbb{R}^3$ and the Tait-Bryan Euler angle convention is used with (ψ, θ, φ) representing respectively (yaw, pitch, roll).

The Euler-Lagrange equation that describes the system dynamics is:

$$\frac{\text{d}}{\text{d}t}\left(\frac{\partial \mathscr{L}(\boldsymbol{q}, \dot{\boldsymbol{q}})}{\partial \dot{\boldsymbol{q}}}\right) - \frac{\partial \mathscr{L}(\boldsymbol{q}, \dot{\boldsymbol{q}})}{\partial \boldsymbol{q}} = \mathscr{F}(\boldsymbol{q}), \tag{7}$$

where $\mathscr{F}(\boldsymbol{q}) \in \mathbb{R}^n$ is the vector of generalized forces and torques acting on the rocket. [15] shows that substituting (6) into (7) gives:

$$M(\boldsymbol{q})\ddot{\boldsymbol{q}} + C(\boldsymbol{q}, \dot{\boldsymbol{q}})\dot{\boldsymbol{q}} + \boldsymbol{G}(\boldsymbol{q}) = \mathscr{F}(\boldsymbol{q}), \tag{8}$$

where $C(\boldsymbol{q}, \dot{\boldsymbol{q}}) \in \mathbb{R}^{n\times n}$ is the Coriolis and centrifugal force matrix and $G(\boldsymbol{q}) \equiv (\partial \mathscr{U}(\boldsymbol{q})/\partial \boldsymbol{q}) \in \mathbb{R}^n$ is the gra-

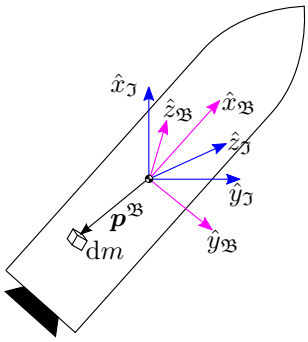


Figure 5. Infinitesimal element kinematics.

dient of potential energy with respect to the generalized coordinates.

The $C(\boldsymbol{q},\dot{\boldsymbol{q}})$ matrix is computed using the Christoffel symbols of the first kind:

$$c_{ij} = \sum_{k=1}^{n} \left\{ \frac{1}{2} \left(\frac{\partial m_{ij}}{\partial q_k} + \frac{\partial m_{ik}}{\partial q_j} - \frac{\partial m_{kj}}{\partial q_i} \right) \dot{q}_k \right\}, \quad (9)$$

where c_{ij} and m_{ij} are the elements at row i and column j of the $C(\boldsymbol{q},\dot{\boldsymbol{q}})$ and $M(\boldsymbol{q})$ matrices respectively. Given that $C(\boldsymbol{q},\dot{\boldsymbol{q}})$ depends on $M(\boldsymbol{q})$ via (9), we must only find the $M(\boldsymbol{q})$, $\boldsymbol{G}(\boldsymbol{q})$ and $\mathscr{F}(\boldsymbol{q})$ in order to obtain the full attitude dynamics.

3.1.1. Finding the $M(\boldsymbol{q})$ matrix

Equation (6) implies that the $M(\boldsymbol{q})$ matrix may be found by rewriting the kinetic energy in quadratic form. Let us consider an infinitesimal element of mass $\mathrm{d}m$ on the rocket as shown in Figure 5. The element's position vector $\boldsymbol{p}^{\mathfrak{B}}$ (expressed in the $\mathfrak{B}$ frame) is fixed in the $\mathfrak{B}$ frame as the rocket is assumed to be a rigid body. The kinetic energy, however, must be written in the $\mathfrak{I}$ (inertial) frame. We can write:

$$\boldsymbol{p}^{\mathfrak{I}} = R^{\mathfrak{I}}_{\mathfrak{B}} \boldsymbol{p}^{\mathfrak{B}}, \quad (10)$$

where $R^{\mathfrak{I}}_{\mathfrak{B}}$ is the rotation matrix from the $\mathfrak{B}$ frame to the $\mathfrak{I}$ frame. From the Tait-Bryan convention we have:

$$R^{\mathfrak{B}}_{\mathfrak{I}} = R_\varphi R_\theta R_\psi, \quad (11)$$

$$R^{\mathfrak{I}}_{\mathfrak{B}} = (R_\varphi R_\theta R_\psi)^T = R_\psi^T R_\theta^T R_\varphi^T. \quad (12)$$

Now that we know an infinitesimal element's position in the $\mathfrak{I}$ frame, its velocity in the $\mathfrak{I}$ frame can be found by differentiating (10):

$$\dot{\boldsymbol{p}}^{\mathfrak{I}} = \dot{R}^{\mathfrak{I}}_{\mathfrak{B}} \boldsymbol{p}^{\mathfrak{B}} + R^{\mathfrak{I}}_{\mathfrak{B}} \dot{\boldsymbol{p}}^{\mathfrak{B}}. \quad (13)$$

As the position of the infinitesimal element is fixed, $\dot{\boldsymbol{p}}^{\mathfrak{B}} = \boldsymbol{0}$. To further develop (13), define the skew-symmetric matrix $S(\boldsymbol{\omega})$:

$$S(\boldsymbol{\omega}) = \begin{bmatrix} 0 & -\omega_z & \omega_y \\ \omega_z & 0 & -\omega_x \\ -\omega_y & \omega_x & 0 \end{bmatrix}. \quad (14)$$

The rotation matrix has the property:

$$\dot{R}^{\mathfrak{I}}_{\mathfrak{B}} = R^{\mathfrak{I}}_{\mathfrak{B}} S(\boldsymbol{\omega}^{\mathfrak{B}}_{\mathfrak{B}\mathfrak{I}}), \quad (15)$$

where $\boldsymbol{\omega}^{\mathfrak{B}}_{\mathfrak{B}\mathfrak{I}}$ is the angular velocity of the $\mathfrak{B}$ frame with respect to the $\mathfrak{I}$ frame, written in the $\mathfrak{B}$ frame. Combining (13), (15) and the property $S(\boldsymbol{a})\boldsymbol{b} = -S(\boldsymbol{b})\boldsymbol{a}$ yields:

$$\dot{\boldsymbol{p}}^{\mathfrak{I}} = -R^{\mathfrak{I}}_{\mathfrak{B}} S(\boldsymbol{p}^{\mathfrak{B}}) \boldsymbol{\omega}^{\mathfrak{B}}_{\mathfrak{B}\mathfrak{I}}. \quad (16)$$

Consider now the kinetic energy of the infinitesimal element in Figure 5:

$$\mathrm{d}\mathscr{K} = \frac{1}{2} \left(\left(\dot{\boldsymbol{p}}^{\mathfrak{I}}\right)^T \dot{\boldsymbol{p}}^{\mathfrak{I}} \right) \mathrm{d}m. \quad (17)$$

Substituting (16) into (17) and using the property $(R^{\mathfrak{I}}_{\mathfrak{B}})^T R^{\mathfrak{I}}_{\mathfrak{B}} = I$, we get:

$$\mathrm{d}\mathscr{K} = \frac{1}{2} \left[\left(\boldsymbol{\omega}^{\mathfrak{B}}_{\mathfrak{B}\mathfrak{I}}\right)^T S^T(\boldsymbol{p}^{\mathfrak{B}}) S(\boldsymbol{p}^{\mathfrak{B}}) \boldsymbol{\omega}^{\mathfrak{B}}_{\mathfrak{B}\mathfrak{I}} \right] \mathrm{d}m. \quad (18)$$

To obtain the kinetic energy of the entire rocket, we simply integrate over the mass of the rocket. Since $\mathrm{d}m = \rho\,\mathrm{d}V$, we get:

$$\mathscr{K} = \frac{1}{2} \left(\boldsymbol{\omega}^{\mathfrak{B}}_{\mathfrak{B}\mathfrak{I}}\right)^T \left[\int_V \rho S^T(\boldsymbol{p}^{\mathfrak{B}}) S(\boldsymbol{p}^{\mathfrak{B}})\,\mathrm{d}V \right] \boldsymbol{\omega}^{\mathfrak{B}}_{\mathfrak{B}\mathfrak{I}}. \quad (19)$$

We identify the integral in (19) as the inertia tensor J of the rocket, expressed in the $\mathfrak{B}$ frame. This integral is not trivial given the multitude of elements inside a rocket – electronics, parachutes, coupling rings, engine casing, etc. However, J is directly obtained from any CAD package (in this case, Solidworks®) if each part of the CAD model is assigned the correct mass properties.

Note that a mapping exists from the Euler angle time derivatives to the angular velocity of the rocket [16]:

$$\omega^{\mathfrak{B}}_{\mathfrak{B}\mathfrak{I}} = W_\eta(\boldsymbol{q})\dot{\boldsymbol{q}}, \quad (20)$$

$$W_\eta(\boldsymbol{q}) = \begin{bmatrix} 1 & 0 & -\sin(\theta) \\ 0 & \cos(\varphi) & \sin(\varphi)\cos(\theta) \\ 0 & -\sin(\varphi) & \cos(\varphi)\cos(\theta) \end{bmatrix}. \quad (21)$$

Substituting (20) into (19) and replacing the integral with the inertia tensor J:

$$\mathscr{K} = \frac{1}{2} \dot{\boldsymbol{q}}^T W_\eta^T(\boldsymbol{q}) J W_\eta(\boldsymbol{q}) \dot{\boldsymbol{q}}. \quad (22)$$

Based on (6) and (22), the inertia matrix $M(\boldsymbol{q})$ can finally be identified:

$$M(\boldsymbol{q}) = W_\eta^T(\boldsymbol{q}) J W_\eta(\boldsymbol{q}). \quad (23)$$

3.1.2. Finding the $\boldsymbol{G}(\boldsymbol{q})$ vector

The discussion for (8) yields:

$$\boldsymbol{G}(\boldsymbol{q}) = \frac{\partial \mathscr{U}(\boldsymbol{q})}{\partial \boldsymbol{q}}. \quad (24)$$

For a rigid body rocket:

$$\mathscr{U}(\boldsymbol{q}) = Mg \begin{bmatrix} 0 \\ 0 \\ z \end{bmatrix}, \quad (25)$$

where M is the rocket mass, $g = 9.81\ \left[\frac{\mathrm{m}}{\mathrm{s}^2}\right]$ is the gravitational acceleration and z is the distance along the $\hat{z}_{\mathfrak{I}}$ axis *from* the $\mathfrak{I}$-frame origin *to* the $\mathfrak{B}$-frame origin, taken as

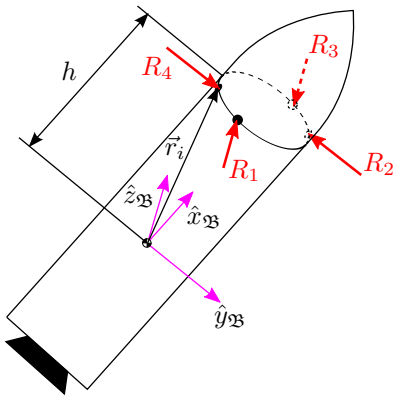


Figure 6. Free-body diagram for the RCS.

positive in that direction. However, we only consider *attitude*, so from (25) we conclude that $\mathscr{U}(\boldsymbol{q})$ is independent of the generalized coordinates $\boldsymbol{q}$. Therefore:

$$\boldsymbol{G}(\boldsymbol{q}) = \boldsymbol{0}. \tag{26}$$

3.1.3. Finding the generalized torque vector $\mathscr{F}(\boldsymbol{q})$

$\mathscr{F}(\boldsymbol{q})$ is composed of control torques, $\boldsymbol{T}^*(\boldsymbol{q})$, from the RCS and aerodynamic torques, $\boldsymbol{A}^*(\boldsymbol{q}, \dot{\boldsymbol{q}})$, from the aerodynamic moments acting about the rocket's center of pressure:

$$\mathscr{F}(\boldsymbol{q}) = \boldsymbol{T}^*(\boldsymbol{q}) + \boldsymbol{A}^*(\boldsymbol{q}, \dot{\boldsymbol{q}}). \tag{27}$$

Finding $\boldsymbol{T}^*(\boldsymbol{q})$. The most general control that can be applied on the rocket is a torque vector $\boldsymbol{\tau}^{\mathfrak{B}} = [\tau_x^{\mathfrak{B}} \ \tau_y^{\mathfrak{B}} \ \tau_z^{\mathfrak{B}}]^T$, expressed in the $\mathfrak{B}$-frame and positive according to the right-hand rule. To find $\boldsymbol{T}^*(\boldsymbol{q})$, we apply the principle of virtual work. Because we consider the rocket as a *single* rigid body, the virtual work principle degenerates to:

$$\delta W = \left(\boldsymbol{\tau}^{\mathfrak{B}}\right)^T \delta \boldsymbol{r} = \left(\boldsymbol{T}^*\right)^T \delta \boldsymbol{q}, \tag{28}$$

where $\delta \boldsymbol{r}$ is an infinitesimal change in the position vector of the body (expressed in the same frame as $\boldsymbol{\tau}^{\mathfrak{B}}$, i.e. the $\mathfrak{B}$ frame) and $\delta \boldsymbol{q}$ is an infinitesimal change in the generalized coordinates. To find $\delta \boldsymbol{r}$ we "integrate" (20). Note that because $\boldsymbol{\omega}^{\mathfrak{B}}_{\mathfrak{B}\mathfrak{I}}$ is not integrable [17], this approach only works thanks to the infinitesimal change assumption. Therefore:

$$\delta \boldsymbol{r} = W_\eta(\boldsymbol{q}) \delta \boldsymbol{q}. \tag{29}$$

By substituting (29) into (28), the generalized control torques are expressed:

$$\boldsymbol{T}^*(\boldsymbol{q}) = W_\eta^T(\boldsymbol{q}) \boldsymbol{\tau}^{\mathfrak{B}}. \tag{30}$$

However, $\boldsymbol{\tau}^{\mathfrak{B}}$ can be related to the thrust forces generated by the four RCS nozzles of the rocket. For this, consider Figures 3 and 6. Noting that $f \ll r$, calling $\vec{r}_i$ the position vector of the i-th nozzle and keeping in mind that thrusts (R_1,R_3) and (R_2,R_4) are parallel to the $\pm\hat{z}_{\mathfrak{B}}$ and $\mp\hat{y}_{\mathfrak{B}}$ axes respectively, we find the relation between RCS thrusts and the control torque vector:

$$\boldsymbol{\tau}^{\mathfrak{B}} = \begin{bmatrix} -f & f & -f & f \\ -h & 0 & h & 0 \\ 0 & -h & 0 & h \end{bmatrix} \begin{bmatrix} R_1 \\ R_2 \\ R_3 \\ R_4 \end{bmatrix} := B\boldsymbol{R}, \tag{31}$$

where we call B the "mapping" from RCS thrusts to control torques. In summary, substituting (31) into (30):

$$\boldsymbol{T}^*(\boldsymbol{q}) = W_\eta^T(\boldsymbol{q}) B \boldsymbol{R}. \tag{32}$$

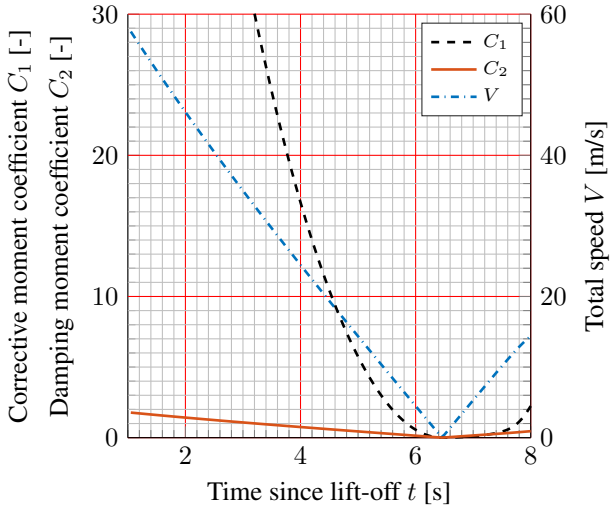


Figure 7. Evolution of C_1 and C_2 based on OpenRocket® simulation data.

Finding $\boldsymbol{A}^*(\boldsymbol{q}, \dot{\boldsymbol{q}})$. We only consider the corrective and damping moment coefficients for the aerodynamic torques acting on the rocket, denoted as C_1 and C_2 respectively. These are given by [18]:

$$C_1 = \frac{1}{2}\rho A_{ref} V^2 C_{N\alpha}(Z - W), \tag{33}$$

$$C_2 = \frac{1}{2}\rho A_{ref} V \sum_{i=1}^{n_c} \left\{C_{N\alpha,i}(Z_i - W)^2\right\}, \tag{34}$$

where $A_{ref} = \pi r^2$ is the nose cone base area, V is the speed, $C_{N\alpha}$ is the total normal force coefficient derivative, $C_{N\alpha,i}$ is the i-th structural component's normal force coefficient derivative, Z is the distance from the nose to the rocket center of pressure, Z_i is the distance from the nose to the i-th structural component's center of pressure, W is the distance from the nose to the center of mass, α is the angle of attack (in radians) and n_c is the total number of components of the rocket (FALCO-4 has one nose cone, four body tubes and one set of four fins).

The rocket was modeled in OpenRocket®, whose technical documentation [19] [20] provides a method to evaluate (33) and (34). Thus, a plot of C_1 and C_2 for FALCO-4 is produced in Figure 7.

For test flights, the RCS control is activated from the 4th second of flight onwards in order to conserve CO_2

pressure for the low speed flight near apogee. Therefore, based on Figure 7, the control must be able to deal with the following range of aerodynamic coefficients:

$$\begin{cases} C_1 \in [0, 17], \\ C_2 \in [0, 0.75]. \end{cases} \tag{35}$$

Since C_1 and C_2 depend on speed, the attitude-only dynamical model of the rocket has no state available to compute these coefficients. Therefore, the corrective and damping moments are considered as disturbances that the RCS must be able to counteract in order to keep the rocket vertical. We assume that the corrective and damping moments act through the yaw (ψ) and pitch (θ) Euler angles. In reality, these moments would act about the axis $((R^{\mathfrak{I}}_{\mathfrak{B}}\hat{x}_{\mathfrak{B}}) \times \hat{x}_{\mathfrak{I}})$, but unfortunately the orientation of this axis degenerates when the rocket is perfectly vertical, i.e. when $R^{\mathfrak{I}}_{\mathfrak{B}}\hat{x}_{\mathfrak{B}}$ is parallel to $\hat{x}_{\mathfrak{I}}$. Note that zero aerodynamic roll moment is assumed. Therefore, the aerodynamic moments are expressed as:

$$\begin{cases} A^*_\varphi = 0, \\ A^*_\theta = -C_1(\theta - \theta_o) - C_2(\dot{\theta} - \dot{\theta}_o), \\ A^*_\psi = -C_1(\psi - \psi_o) - C_2(\dot{\psi} - \dot{\psi}_o), \end{cases} \tag{36}$$

where $\{\theta_o, \psi_o\}$ accounts for the "pitch" and "yaw" of the local wind vector in case of side wind. Note that the rocket passively stabilizes about the local wind vector, not $\hat{x}_{\mathfrak{I}}$. The local wind vector has no "roll", so $\varphi_o = 0$. In matrix notation, (36) is written as:

$$\boldsymbol{A}^*(\boldsymbol{q}, \dot{\boldsymbol{q}}) = A_1(\boldsymbol{q} - \boldsymbol{q}_o) + A_2(\dot{\boldsymbol{q}} - \dot{\boldsymbol{q}}_o), \tag{37}$$

with:

$$A_1 = \begin{bmatrix} 0 & 0 & 0 \\ 0 & -C_1 & 0 \\ 0 & 0 & -C_1 \end{bmatrix}, A_2 = \begin{bmatrix} 0 & 0 & 0 \\ 0 & -C_2 & 0 \\ 0 & 0 & -C_2 \end{bmatrix}. \tag{38}$$

3.1.4. The dynamical equations

In summary, the following dynamical equations for the rocket attitude were obtained:

$$M(\boldsymbol{q})\ddot{\boldsymbol{q}} + C(\boldsymbol{q}, \dot{\boldsymbol{q}})\dot{\boldsymbol{q}} + \boldsymbol{G}(\boldsymbol{q}) = \boldsymbol{T}^*(\boldsymbol{q}) + \boldsymbol{A}^*(\boldsymbol{q}, \dot{\boldsymbol{q}}),$$

with

$$\begin{cases} M(\boldsymbol{q}) = W_\eta^T(\boldsymbol{q}) J W_\eta(\boldsymbol{q}), \\ \boldsymbol{G}(\boldsymbol{q}) = \boldsymbol{0}, \\ \boldsymbol{T}^*(\boldsymbol{q}) = W_\eta^T(\boldsymbol{q}) B \boldsymbol{R}, \\ \boldsymbol{A}^*(\boldsymbol{q}, \dot{\boldsymbol{q}}) = A_1(\boldsymbol{q} - \boldsymbol{q}_o) + A_2(\dot{\boldsymbol{q}} - \dot{\boldsymbol{q}}_o), \end{cases} \tag{39}$$

where $C(\boldsymbol{q}, \dot{\boldsymbol{q}})$ is given by (9), $W_\eta(\boldsymbol{q})$ is given by (21), $J \in \mathbb{R}^3$ is the rocket inertia tensor in the $\mathfrak{B}$-frame, $\boldsymbol{0} \in \mathbb{R}^3$ is a zero vector, B and $\boldsymbol{R}$ are given by (31) and finally A_1 and A_2 are given by (38).

3.2. Open-loop simulation

Using (39) we can develop a non-linear Simulink® model (Figure 8) that is used for simulation. For control system design, this plant is linearized about the rocket's vertical orientation (i.e. $\boldsymbol{q} = \boldsymbol{0}$). Using this plant we can simulate the attitude of a rocket when it is flying quickly (Figure 9) or slowly (Figure 10) with zero side wind in both cases. A side wind can also be simulated.

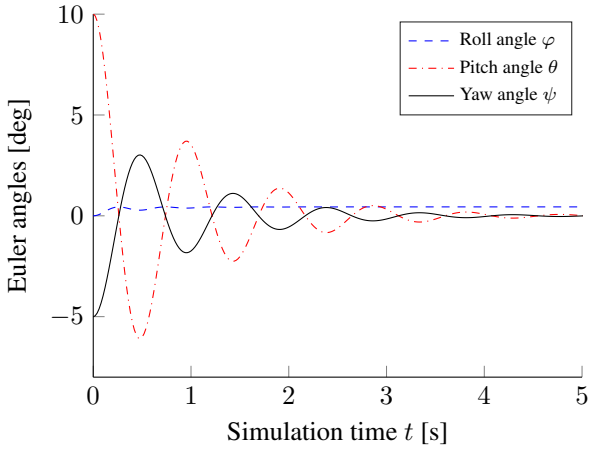


Figure 9. Euler angles evolution for a fast-moving rocket with $C_1 = 16$ and $C_2 = 0.75$ (i.e. 4 seconds into the flight moving at ≈ 24 [m/s]).

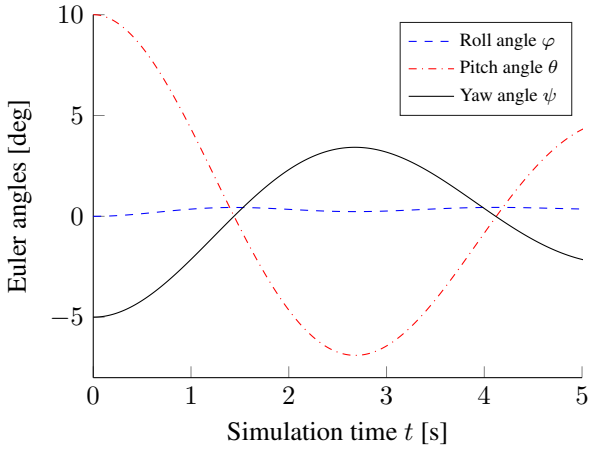


Figure 10. Euler angles evolution for a fast-moving rocket with $C_1 = 0.5$ and $C_2 = 0.1$ (i.e. 6 seconds into the flight moving at ≈ 4 [m/s]).

In our application a restoring aerodynamic moment is only beneficial in the absence of side wind. When side wind is present, the local velocity vector would be off the geometric vertical (axis $\hat{x}_{\mathfrak{I}}$) and the control would have to work against the aerodynamic moments. As the absence of side wind cannot be guaranteed, a neutrally stable rocket ($C_1 = C_2 = 0$) would be optimal for our application. However, for safety and due to the presence of body lift and other aerodynamic effects, a certain passive stability was built into the FALCO-4 by the four tail fins discussed in Section 2.1. However, at low speeds (e.g around apogee) aerodynamic effects become smaller (see Figure 7), for which reason the control was designed for the case of small aerodynamic coefficients $C_1 = 0.5$ and $C_2 = 0.1$ (see Figure 10).

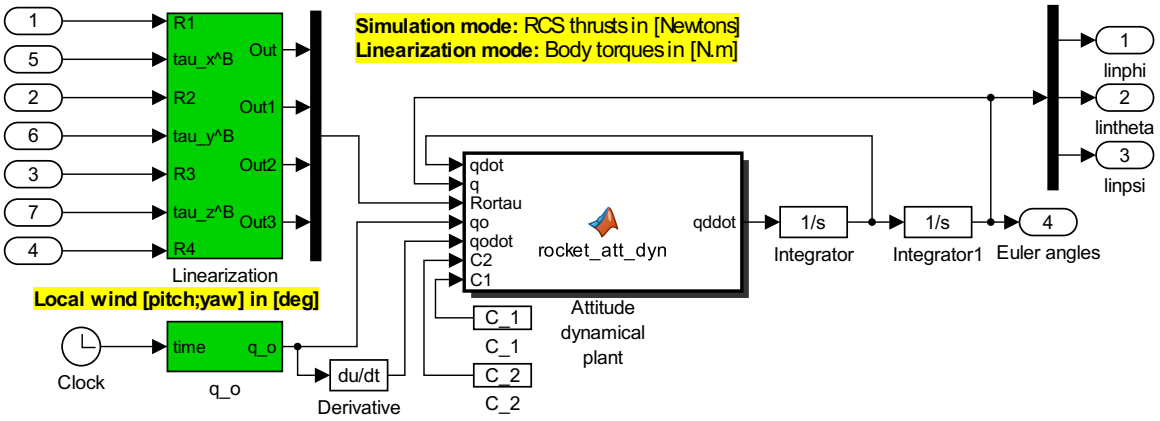


Figure 8. Simulink® block diagram of the rocket plant.

Now that the non-linear plant has been created, it is possible to develop and test a control scheme for vertically stabilizing the rocket.

3.3. Control scheme

3.3.1. Plant linearization

Physically, the system inputs are the four RCS thrusts. However, it is easier to control in three torques $[\tau_x^{\mathfrak{B}}\ \tau_y^{\mathfrak{B}}\ \tau_z^{\mathfrak{B}}]^T$ than in the four thrusts $[R_1\ R_2\ R_3\ R_4]^T$. This is because $W_\eta^T(\boldsymbol{q})$ in (30) is simpler than $W_\eta^T(\boldsymbol{q})B$ in (32). Figure 8 handles this via the green `Linearization` block which, using switches, selects four RCS thrusts $\{R_1, R_2, R_3, R_4\}$ for simulation or three torques $\{\tau_x^{\mathfrak{B}}, \tau_y^{\mathfrak{B}}, \tau_z^{\mathfrak{B}}\}$ for linearization.

Using MATLAB®'s `linmod` to linearize the Simulink® plant model for Figure 10's conditions, we obtain:

$$\begin{cases} \ddot{\varphi} = 337.8378\tau_x^{\mathfrak{B}}, \\ \ddot{\theta} = -1.3901\theta - 0.2780\dot{\theta} + 2.7802\tau_y^{\mathfrak{B}}, \\ \ddot{\psi} = -1.3901\psi - 0.2780\dot{\psi} + 2.7802\tau_z^{\mathfrak{B}}. \end{cases} \tag{40}$$

The coefficients above result from FALCO-4's geometric and dynamic properties, such as its inertia tensor values. Converting (40) into state space form, it can be shown that each axis (roll, pitch and yaw) is controllable using RCS torques $[\tau_x^{\mathfrak{B}}\ \tau_y^{\mathfrak{B}}\ \tau_z^{\mathfrak{B}}]^T$ as inputs.

Notice that each equation in (40) is *decoupled*. Therefore, decoupled PID controllers for roll, pitch and yaw can be designed (at least in the linear case). Since the pitch and yaw dynamics of (40) are identical, they are assigned identical PID controllers.

3.3.2. Pitch control design

Figure 11 shows the implemented feedback control scheme.

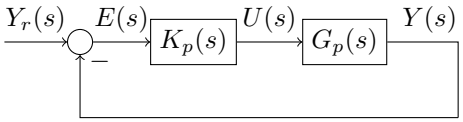


Figure 11. Yaw control block diagram.

From (40), the pitch transfer function is:

$$G_p(s) = \frac{2.7802}{s^2 + 0.2780s + 1.3901}. \tag{41}$$

A PID controller of the following form is sought:

$$K(s) = K\big(1 + \frac{1}{T_i s} + T_d s\big). \tag{42}$$

In order to obtain the coefficients in (42), Ziegler-Nichols tuning rules are applied to $G_p(s)$:

$$\begin{cases} K &= 1.4197, \\ T_i &= 0.8565, \\ T_d &= 0.2141. \end{cases} \tag{43}$$

However, subsequent hardware-in-the-loop testing revealed that the integral term caused persistent saturation due to sensor noise, fast nature of rocket dynamics and the limited thrust of the final RCS. As a result, the integrator term was removed.

Manual tuning of the remaining proportional and derivative terms gives the final pitch controller architecture:

$$\begin{cases} K &= 5, \\ T_d &= 3, \\ K_p(s) &= K + T_d s. \end{cases} \tag{44}$$

A Bode plot of the loop transfer function $K_p(s) \cdot G_p(s)$ is shown in Figure 12. K was tuned by hardware-in-the-loop testing to avoid excessive saturation in the control signal. T_d was chosen to place a zero after the resonance frequency in Figure 12 so as to prevent the -180 degree drop in phase, therefore stabilizing the system.

The lack of an integrator means that a steady-state offset is present in the response. However, for a 10 degree disturbance, this offset is only 2.6 degrees in simulation. This is within our tolerated precision. For this reason,

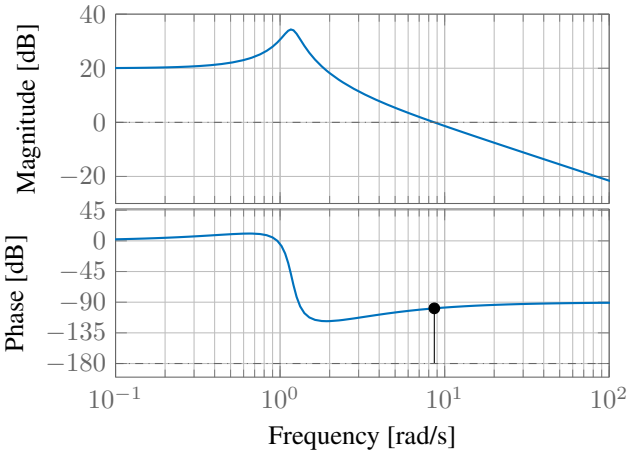


Figure 12. Bode plot of $K_p(s) \cdot G_p(s)$.

the PD controller was chosen as a satisfactory alternative to the aforementioned PID. It was also chosen over a loop-shaping approach for implementation simplicity. Finally, as can be seen from Figure 12, the controller offers infinite gain margin and 81 degrees of phase margin. Such robustness is important as we cannot measure the exact final parameters of the rocket to a great precision. Also, the coefficients C_1 and C_2, and thus the dynamical model, are bound to change during flight.

For final implementation, (44) is discretized using backwards Euler difference (i.e. substituting $s = \frac{z-1}{zT_s}$):

$$K_p(z) = K + T_d \frac{1 - z^{-1}}{T_s}, \tag{45}$$

where T_s is the sampling time. The coefficients K and T_d therefore remain the same. Note, that θ and $\dot{\theta}$ were Kalman filtered prior to being passed into the controller.

3.3.3. Roll control design

The scheme from Figure 11 is also used for roll control. However, unlike pitch and yaw where we desire to control *angles*, we only wish for the rocket to have zero roll *rate* – we do not care what "roll angle" the symmetric rocket has. Therefore the roll equation of (40) can be written as a first-order relation in roll rate:

$$\dot{\omega}_\varphi = 337.8378 \tau_x^{\mathfrak{B}}. \tag{46}$$

Taking $\tau_x^{\mathfrak{B}}$ as input, the transfer function for roll is:

$$G_r(s) = \frac{337.8378}{s}. \tag{47}$$

Since (47) contains an integrator, an interator in the controller is not needed for zero steady-state offset. As such, a proportional controller is deemed to be sufficient for roll control. The proportionality constant is chosen according to the equation:

$$K = \frac{\max(\tau_x^{\mathfrak{B}})}{\max(\omega_\varphi)}, \tag{48}$$

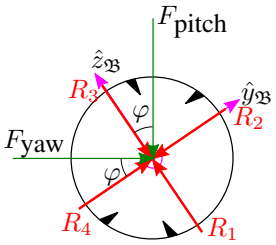


Figure 13. Roll-mapping of the RCS thrusts.

where $\max(\tau_x^{\mathfrak{B}}) = 2fR_{\max}$ and $\max(\omega_\varphi)$ is the roll rate deemed to be so large as to make us want to saturate the RCS in trying to reduce it. This situation may arise after, for example, an accident during launch that induces a severe spin in flight. We chose $\max(\omega_\varphi) = 100$ [deg/s]. Lastly, $R_{\max} = 0.36$ [N] is the maximum thrust that an individual RCS nozzle can produce. Therefore the final (both continuous and discrete time) roll controller is:

$$K_r(z) = 0.002063. \tag{49}$$

This gives an infinite gain margin and a 90 degree phase margin – which, again, offers good stability.

3.3.4. Optimal thrust allocator

To develop the controllers, we replaced the RCS thrusts with net torques about the rocket's center of mass. Now, a combination of $\{R_1, R_2, R_3, R_4\}$ to produce these net torques must be found. As an infinite number of such combinations exist – and as this allocation problem is linear – linear programming is used to find the *optimal* $\{R_1, R_2, R_3, R_4\}$ combination. On-board, this is implemented as the Simplex algorithm [21].

The idea is to use a "mapping" which eliminates roll from the pitch and yaw stabilization: as the rocket rolls, we want to re-distribute the thrusts amongst the four RCS nozzles in order to continue yaw and pitch stabilization in the same direction. Using Figure 13, we can write:

$$\begin{cases} F_{\text{yaw}} = -R_1 S_\varphi - R_2 C_\varphi + R_3 S_\varphi + R_4 C_\varphi, \\ F_{\text{pitch}} = -R_1 C_\varphi + R_2 S_\varphi + R_2 C_\varphi - R_4 S_\varphi, \\ \tau_x^{\mathfrak{B}} = -R_1 f + R_2 f - R_3 f + R_4 f, \end{cases} \tag{50}$$

where:

$$\begin{cases} F_{\text{yaw}} = \tau_z^{\mathfrak{B}}/h \\ F_{\text{pitch}} = \tau_y^{\mathfrak{B}}/h \\ S_\varphi = \sin(\varphi) \quad \text{and} \quad C_\varphi = \cos(\varphi) \end{cases} \tag{51}$$

The optimal thrust allocation problem is then:

$$\begin{aligned} &\min\left(R_1 + R_2 + R_2 + R_4\right) \\ &\text{subject to} \\ &\begin{cases} -R_1 S_\varphi - R_2 C_\varphi + R_3 S_\varphi + R_4 C_\varphi = \tau_z^{\mathfrak{B}}/h, \\ -R_1 C_\varphi + R_2 S_\varphi + R_2 C_\varphi - R_4 S_\varphi = \tau_y^{\mathfrak{B}}/h, \\ -R_1 f + R_2 f - R_3 f + R_4 f = \tau_x^{\mathfrak{B}}, \\ R_1, R_2, R_3, R_4 \geq 0. \end{cases} \end{aligned} \tag{52}$$

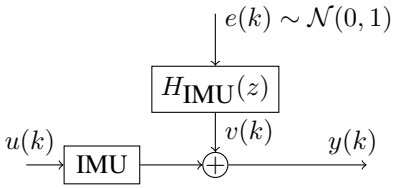


Figure 14. Additive noise model for the IMU.

On-board, (52) is solved using the Simplex algorithm [21] at a frequency of 50 [Hz].

3.3.5. Sensor noise model

An important part of control system design is modeling the feedback dynamics – i.e. the sensors. Here the IMU dynamics are ignored (assume it is a unit gain), however we do model sensor noise according to Figure 14.

To identify $H_{\text{IMU}}(z)$, the IMU was placed on a steady surface and the output angle signals were measured for one minute. A Discrete Fourier Transform of the output signal was then taken in MATLAB®. Assuming white Gaussian noise $e(k) \sim \mathcal{N}(0,1)$ as the input, the following transfer function was obtained by fitting and then discretizing a second-order model to fit the blue noisy empirical transfer function in the top plot of Figure 15:

$$H_{\text{IMU}}(s) = K_{IMU} \cdot \frac{\omega_1^2}{s^2 + 2\omega_1\zeta s + \omega_1^2} \cdot \left(1 + \frac{s}{\xi}\right). \quad (53)$$

Figure 15 shows the visual match between our measurements and the identified noise filter $H_{\text{IMU}}(z)$. Finally, a first-order extended Kalman filter was used to filter $y(k)$ before passing it to the pitch, yaw and roll controllers (and can be consulted in the GNC source code [14]).

3.4. Closed-loop simulation

Using (45) as the pitch and yaw controller, (49) as the roll controller and (39) as the dynamical plant, Figure 18 shows the master view of the Simulink® diagram used for simulation. Figures 16 and 17 show results for a simulation where the rocket is nearing apogee ($C_1 = 0.5$, $C_2 = 0.1$) with the initial attitude $\{\varphi_0, \dot{\varphi}_0, \theta_0, \dot{\theta}_0, \psi, \dot{\psi}_0\} = \{0, 30, -7, 0, 7, 0\} \cdot \pi/180$.

Figure 16 shows the evolution of rocket attitude after RCS activation at $t = 1$ [s]. Note that prior to $t = 1$ [s], the Kalman filter converges to the true rocket attitude. Noise is effectively being filtered and the rocket is maintained reasonably vertical by the RCS, however wind disturbances after about 4 [s] have little hope of being corrected. This is because real tests of the RCS show the compressed CO_2 container to lose pressure rather quickly. This phenomenon was taken into account as an exponential decrease in RCS thrust saturation level after 1 second of allowed full-thrust operation – see top of Figure 17. This simple model allows to simulate the effect

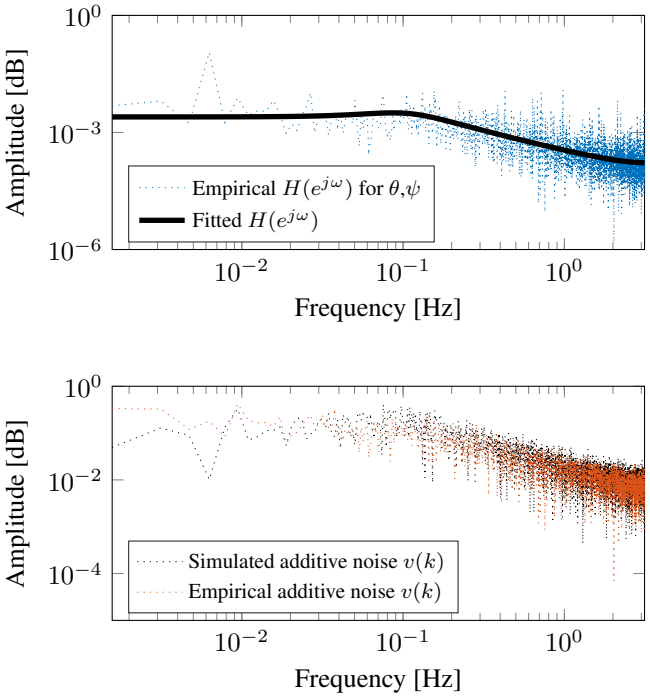


Figure 15. Identification of the IMU noise filter.

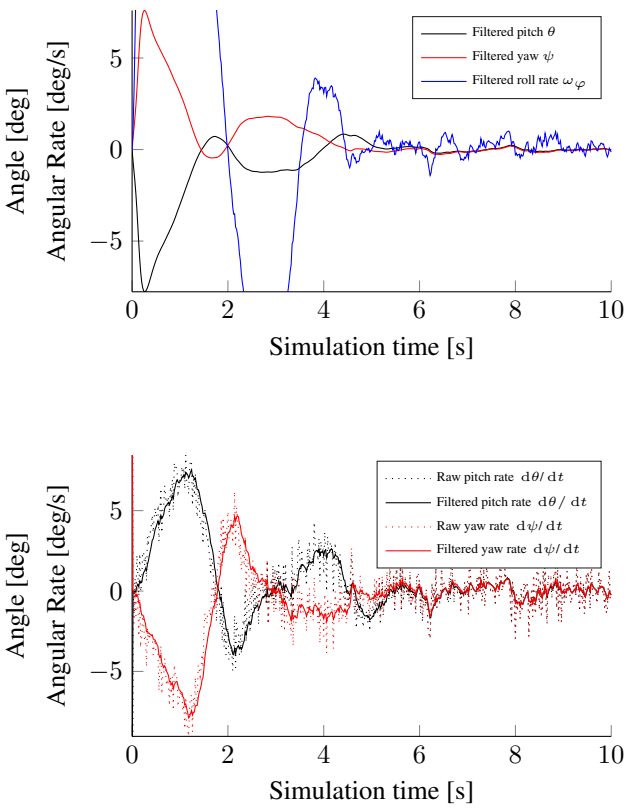


Figure 16. Closed-loop simulation angle and angular rate evolution.

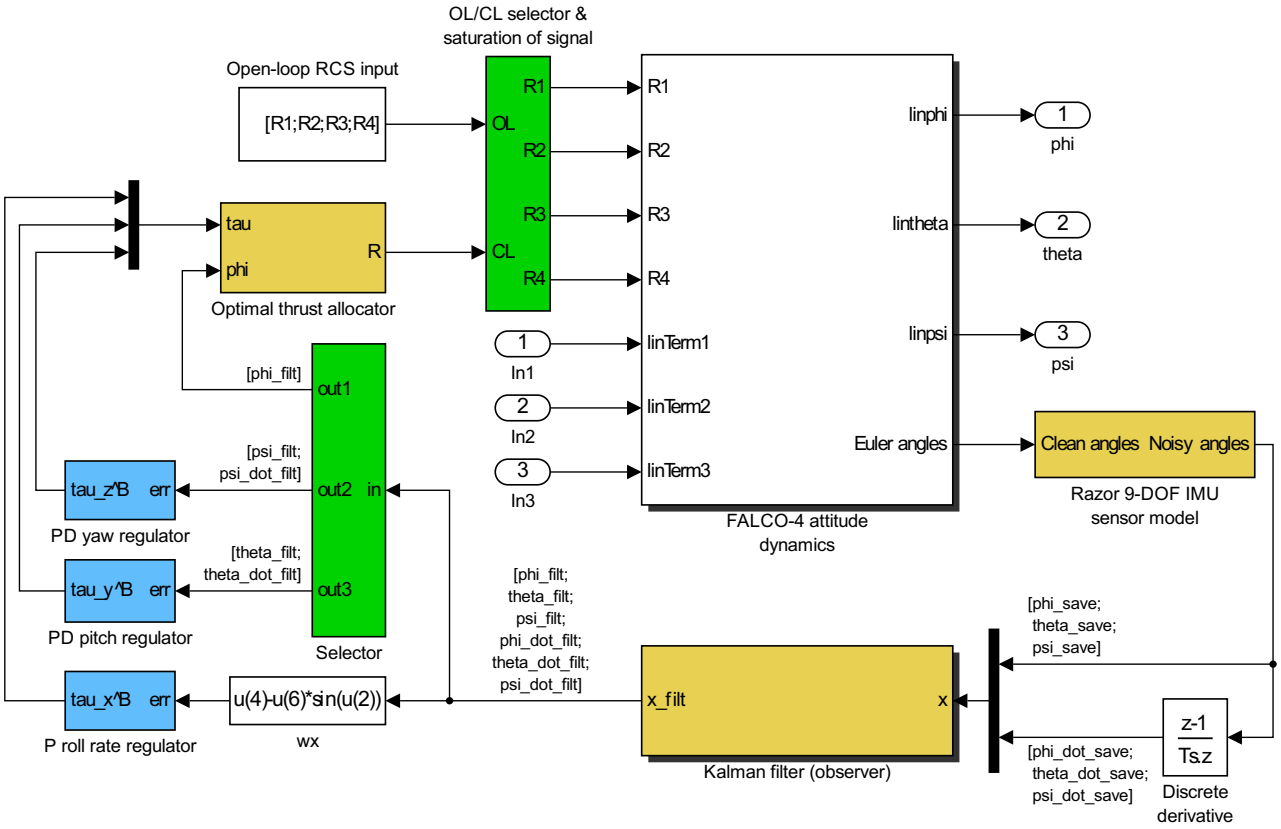


Figure 18. Attitude control system overview. Green – selectors; orange – computations; blue – controllers.

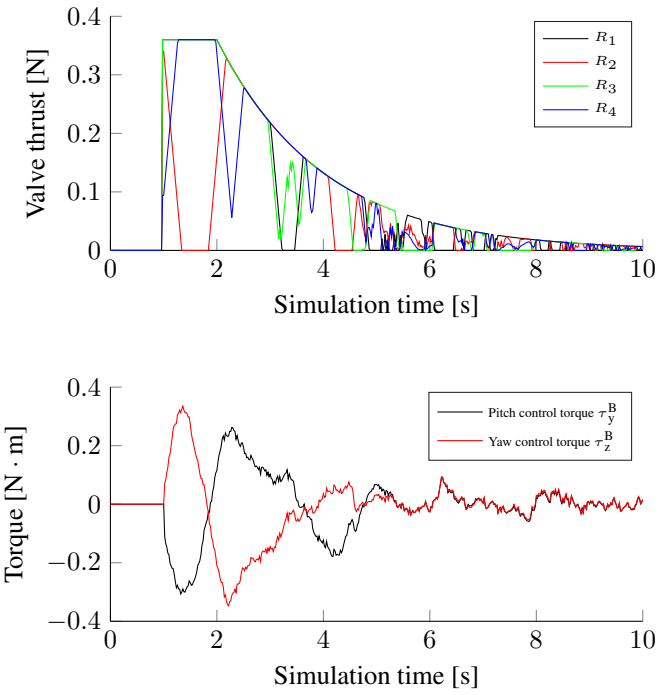


Figure 17. Closed-loop simulation of control torques and RCS thrusts mapped by (52).

of a decreasing thrust level and predicts that after a short time the RCS is only be able to resist (rather than completely correct) rocket deviation from the vertical. The next section describes how test flight data confirms these simulation results.

4. EXPERIMENTAL RESULTS

On June 6, 2015, five test flights were conducted with the objective of recording the difference in the rocket's deviation from the vertical between the controlled and uncontrolled configurations. Initially, three controlled and three uncontrolled flights were planned. However, a limited CO_2 cartridge supply made only one controlled launch possible due to an extra ground test using one cartridge and a valve malfunction forcing the first flight to be uncontrolled, during which a hard landing ruptured the RCS pressure tubing and thus emptied a second cartridge. Nevertheless, four uncontrolled flights were made – of which the last could not be used for data analysis due to corrupted accelerometer data at lift-off.

Figure 19 summarizes the main result of flight data analysis. It shows the angles between the $\hat{x}_{\mathfrak{B}}$ and $\hat{x}_{\mathfrak{I}}$ axes – i.e. the angle by which the rocket attitude deviates from the vertical. For the uncontrolled flights, the graphs are very similar with about 90 degree deviation from the ver-

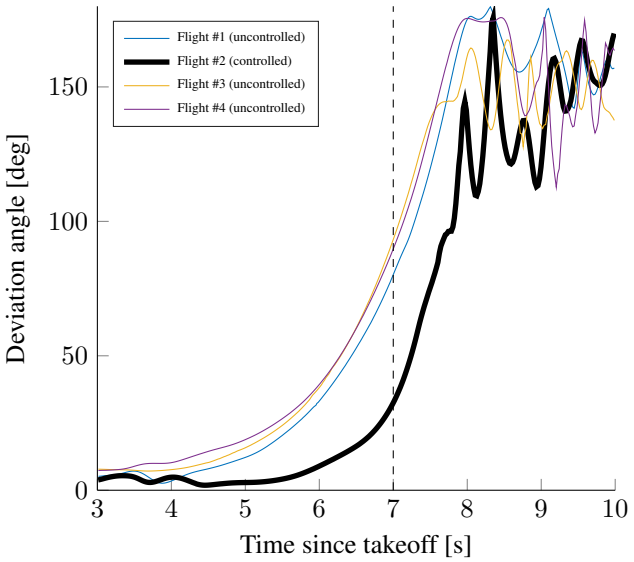


Figure 19. Deviation angle between rocket longitudinal axis and the vertical (test flight data).

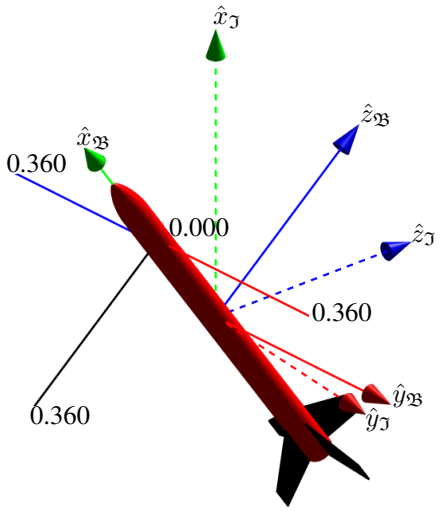


Figure 21. Attitude and RCS thrusts at $t = 7.035$ [s] (flight #2 data).

tical at the approximate moment of apogee (shown by the dashed vertical line in Figure 19). Meanwhile, the controlled flight's deviation angle is almost 3 times smaller – i.e. ≈ 30 degrees at apogee. Note that parachutes open at $t \approx 8$ [s], so the deviation angle thereafter is meaningless. These results are visually confirmed by on-board video recordings of each flight.

It is worth noting that the RCS was turned on 4 seconds into the flight. Correspondingly, in Figure 19 there is a drop in deviation angle at 4 seconds with almost no deviation up to about 5 seconds, while the deviation angle for all three uncontrolled flights steadily increases. This suggests that the RCS was doing its job very well while the CO_2 tank pressure was high and thus valve thrust was sufficient. However, after the first second of operation the dropping pressure in the CO_2 cartridge rendered the RCS unable to fully cancel the flight moments. As a result, the RCS could only *resist* rather than *remove* vertical deviation for the remainder of the flight up to apogee – which is what Figure 19 shows.

Figure 20 shows the commanded RCS thrusts by the onboard computer for the controlled flight. Note that Figure 20 shows the *expected* RCS thrusts. These were not actually measured in flight. The valves were calibrated in open-loop on the ground, so a value in the graph simply indicates the value that the controller assigned to that valve and not the one that was actually output. As previously noted, after ≈ 5 [s] CO_2 pressure began droppping and the open-loop PWM-to-thrust mappings no longer held.

Figure 21 allows to visualize Figure 20 at $t = 7.035$ [s] (the same color scheme for RCS thrusts is used). As the rocket tipped at apogee, the RCS saturated trying to push it back to the vertical orientation. This is the "resistance to deviation" effect discussed for Figure 19.

5. DISCUSSION AND CONCLUSION

The experimental results closely match what was predicted through simulation. The initial goal of maintaining a vertical alignment via cold gas thrusters was partially achieved. The control works as expected, the only shortcoming being a drop in RCS gas pressure. Nevertheless, the results show that vertical attitude can be maintained throughout the controlled flight if sufficient thrust is achieved.

The following is a non-exhaustive list of improvements to make in future vehicles of this type:

1. Close the loop on valve thrusts (i.e. measure thrust levels). This will allow to implement cascade control and better interpret flight data.
2. Account for CO_2 pressure drop – e.g. by increasing CO_2 cartridge volume.
3. Change the IMU to give angles at a higher frequency – the 50 [Hz] limitation of [22] may be a limiting factor for future development.

In conclusion, this paper and the flight software [14] should help individuals interested in learning and helping advance rocket vertical landing efforts.

ACKNOWLEDGMENTS

This work was kindly sponsored by the Space Engineering Center at the École Polytechnique Fédérale de Lausanne.

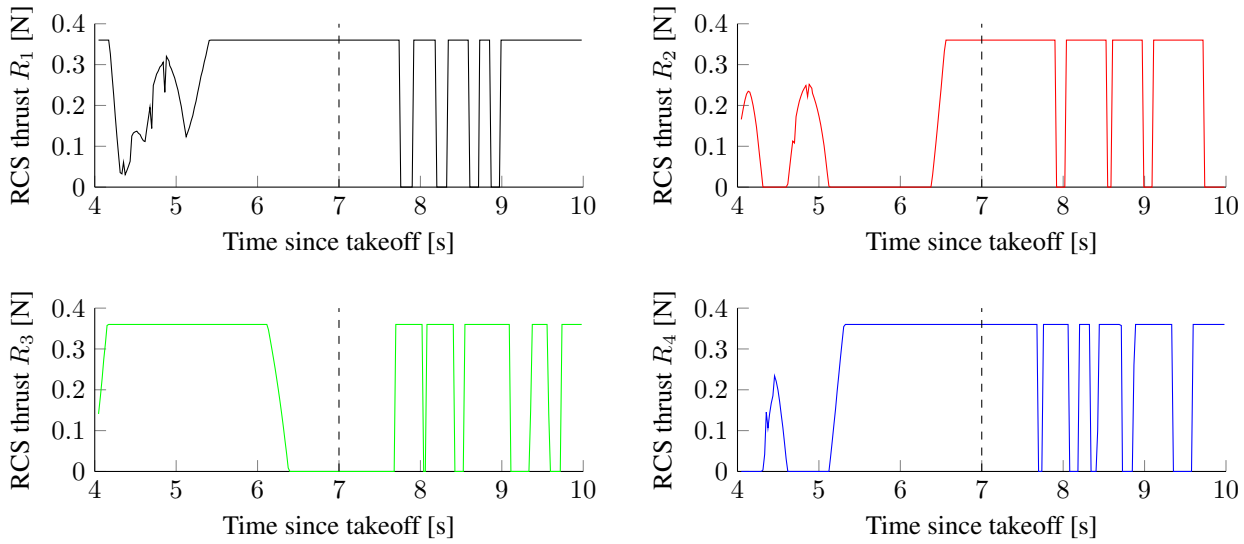


Figure 20. Commanded RCS thrusts (flight #2 data).

REFERENCES

[1] SpaceX. Reusability: The Key to Making Human Life Multi-Planetary. http://www.spacex.com/news/2013/03/31/reusability-key-making-human-life-multi-planetary, 2015.

[2] Spaceflight Now. ULA chief explains reusability and innovation of new rocket. http://spaceflightnow.com/2015/04/14/ula-chief-explains-reusability-and-innovation-of-new-rocket/, 2015.

[3] Space.com. Airbus' Adeline Project Aims to Build Reusable Rockets and Space Tugs. http://www.space.com/29620-airbus-adeline-reusable-rocket-space-tug.html, 2015.

[4] Adafruit. Raspberry Pi Model B+ 512MB RAM. http://www.adafruit.com/products/1914, 2015.

[5] Adafruit. Spy Camera for Raspberry Pi. https://www.adafruit.com/products/1937, 2015.

[6] Adafruit. PowerBoost 500 Basic - 5V USB Boost at 500mA from 1.8V+. https://www.adafruit.com/products/1903, 2015.

[7] Parker. VSO Miniature Proportional Valve. http://ph.parker.com/us/12051/en/vso-miniature-proportional-valve, 2015.

[8] SMC Pneumatics. http://www.smcpneumatics.com/.

[9] Leland Gas Technologies. Fixed Pressure Regulator, NR-10. http://www.lelandltd.com/regulating_valves_prd.htm, 2015.

[10] Leland Gas Technologies. 68 gram 1/2 threaded CO2. http://www.lelandltd.com/small_high_pressure.htm, 2015.

[11] HobbyKing. HD Wing Camera 1280x720p 30fps 5MP CMOS. http://hobbyking.com/hobbyking/store/__17200__HD_Wing_Camera_1280x720p_30fps_5MP_CMOS.html, 2015.

[12] Honeywell. HSC D LN N 100MD S A 5 temperature-compensanted pressure sensor. http://sensing.honeywell.com/honeywell-sensing-trustability-hsc-series-high-accuracy-board-mount-pressure-sensors-50099148-a-en.pdf, 2015.

[13] HobbyKing. Turnigy nano-tech 300mah 2S 35 70C Lipo Pack. http://hobbyking.com/hobbyking/store/uh_viewItem.asp?idProduct=36220, 2015.

[14] Danylo Malyuta. Falco-4 open source code database. https://github.com/DanyloMalyuta/FlyARocket_GNC.

[15] Guilherme Vianna Raffo. *Robust Control Strategies for a Quadrotor Helicopter*. Doctoral thesis, Universidad de Sevilla, Escuela Técnica Superior de Ingeniería, 2011.

[16] Warren F. Phillips. *Mechanics of Flight*. Wiley, second edition, 2010.

[17] Herman Bruyninckx. Robot kinematics and dynamics. http://people.mech.kuleuven.be/~bruyninc/tmp/HermanBruyninckx-robotics.pdf, 2010.

[18] George J. Caporaso Mandell, Gordon K. and William P. Bengen. *Topics in Advanced Model Rocketry*. MIT, 1973.

[19] Sampo Niskansen. *OpenRocket technical documentation For OpenRocket version 13.05*, 2015.

[20] The Sky Dart Team. Open Rocket: Dynamic Stability Characteristics. https://sites.google.com/site/theskydartteam/openrocket\#TOC-Corrective-Moment-Coefficient, 2015.

[21] Jean-Pierre Moreau. Linear Programming in C/C++. http://jean-pierre.moreau.pagesperso-orange.fr/c_linear.html, 2014.

[22] Sparkfun. 9 Degrees of Freedom – Razor IMU. https://www.sparkfun.com/products/10736, 2015.

PRIMO: AN ULTRALIGHT LAUNCH VEHICLE FOR NANO AND MICROSATELLITES

Giovanni Pandolfi[(1)]

[(1)]*Leaf Space Srl, Viale Luigi Majno 28 - 20129 Milano (Italy), Email: giovanni.pandolfi@leafspace.eu*

ABSTRACT

The market of nano and microsatellites has seen a huge worldwide expansion during the last five years, moving from research and academics purposes to commercial ones. The lack of dedicated launch vehicles, leading to long booking time and the impossibility to get to the desired orbit, considerably limits a further expansion of the capabilities of this class of satellites. Primo is an ultralight two-stage hybrid launch vehicle, specifically designed to solve this problems of the nano and microsatellites market. This paper deals with Primo's preliminary design.

1. Introduction

This paper presents the work done in the past months by the author for a preliminary design of Leaf Space's ultralight launch vehicle Primo. A different design approach has been used, where the method to reduce the costs is not linked to the GLOW (Gross Lift-Off Weight) but to the overall production technology and methodology. Economics and reliability of the selected technologies are placed before the pure performances, in order to lowering the manufacturing and operating costs of the launch vehicle.
This method has been used in the last years by companies such as Space Exploration Technologies (SpaceX), RocketLab, FireFly and others.
This paper contains the starting point for the thesis for the Master Degree in Space Engineering at Politecnico di Milano of the author.

2. MISSION REQUIREMENTS

The project of Primo has started, differently from the major part of launch vehicles projects, from the market Leaf Space is interested in. Since the major part of microsatellites expected to be launched until 2020 has a mass comprised between 1 and 50 kg, Leaf Space has decided to set this range of payload as primary requirement for launch vehicle Primo.
A higher payload mass would lead to a considerably higher GLOW and therefore to a higher complexity, longer development time and higher costs. In addition, having a higher payload mass, would lead to the possibility to have a high number of microsats on board, not solving so much the problems highlighted in the abstract.
A smaller payload mass would preclude a substantial part of the market and decrease the reliability of the launch vehicle due to the lower admitted error margin.
Analysing the orbits in which microsatellites has been launched from 2000 and 2014, it can be shown that the major part have altitudes between 150 km and 700 km, inclinations ranging from equatorial to sun-synchronous orbit, and different eccentricity. For these reasons, an altitude of 700 km has been selected as design point. Then, a 700 km radius polar orbit has been selected as the worst orbit configuration to achieve with a 50 kg payload
In order to take advantage of mass production, in terms of both costs and reliability, a minimum flight rate of 20 launches per year has been imposed.
After a first preliminary analysis, a two-stage configuration has been selected, in order to have a simpler design and a lower number of separation events. Therefore, this kind of configuration makes easier to recovery a great part of the launcher (the first stage), feature that could lead in the future to a partially reusability of the vehicle.
Thanks to Leaf Space internal know-how, it has been decided to use hybrid propulsion technology in order to decrease development time and costs and to increase safety requirements with respect to liquid and solid propellant engines. This facts have been proven by AMROC with the development of the Aquila launch vehicle that costed about 10 M$ until the first flight test that suffered a main valve failure. This test highlighted the enhanced safety of hybrid propulsion, since the rocket did not explode and the launch pad damage costs were about 2 k$.
Another major requirement has been imposed: to minimize development, production, operation and disposal costs, and also to minimize the environmental impact of production, operation and disposal of the launch vehicle.

2.1. Flight Constraints

Analysing former manned and unmanned launch vehicles, some typical flight constraints have been selected:

- Maximum longitudinal acceleration: 65 m/s^2;
- Maximum dynamic pressure: 35 kPa;
- Take Off T/W: 1.4.

3. DELTA-V BUDGET

In order to place a 50 kg payload on a 700 km polar circular orbit, a total delta-v of 9.72 km/s is needed. The different contributions and their relative amounts are listed in Table 1.

Table 1 - Delta-V Contributions.

DV contributions	Amount
Orbital Velocity (200 km)	7.79 km/s
Hohm. Trans. 200-700 km	0.28 km/s
Gravity loss	1.3 km/s
Drag loss	0.2 km/s
Steering losses	0.05 km/s
Performance margin	1%
Total	**9.72 km/s**

Gravity, drag and steering losses are typical values taken from (Osborne, 1967).

4. VEHICLE CONFIGURATION

In order to sustain the requirement of minimizing costs, the launch vehicle configuration has also to minimize the number and types of subsystems. Therefore, the same hybrid rocket motor on both stages will be used (with a different nozzle), in single on the second stage and in cluster configuration on the first stage. In this way, the same systems will be implemented on both stages (oxidizer feed, pumps, igniters injectors, TVC), enhancing reliability, due to mass production and increasing the available data on the motor during each flight.
Previous analysis made by the author, shows that the best cluster configuration for the first stage, from a geometrical and volumetric filling point of view, is the one with seven motors disposed with a central one and the others around. This configuration has also a better load distribution with respect to a non-cylindrical configuration as has been demonstrated by Space Exploration Technologies (SpaceX) with the transition between Falcon9 v1.0 and v1.1 launch vehicles.
In order to perform a mass budget, the first things to know are the specific impulses of the engines for each stage.

4.1. Specific impulses

The specific impulse of a propulsive system strictly depends on the propulsive technology and the propellants. Since the technology has already been imposed, the only variable remains the propellants. Hybrid rocket motors have, generally, a liquid oxidizer and a solid fuel (inverse hybrid motors have been developed but have shown lower performance). In the following subsections different oxidizer and fuel will be compared.

4.1.1. Solid fuels

One of the toughest problem of a hybrid rocket motor is the low fuel regression rate that limits its thrust, and a low combustion efficiency (92-95% when liquid rocket engines achieve 97-99%). During his ten years of research conducted at Politecnico di Milano, Matteo Boiocchi (CRO at Leaf Space) has studied several fuels with different properties. A chemical, thermal, mechanical and ballistic investigation of paraffin-based solid fuels strenghtened with an elastomer and filled with different energetic fillers, such as metallic hydrides, was presented in several publications.
The most promising are a family of paraffin based fuels able to reach regression rates at least four times higher than typical polymer fuels (HTPB), and a higher combustion efficiency (with suitable design features). For further information see: (Galfetti, Merotto, Boiocchi, Maggi, & DeLuca, Ballistic and rheological characterization of parafin-based fuels for hybrid rocket propulsion., 2011), (Galfetti, Merotto, Boiocchi, Maggi, & DeLuca, Experimental investigation of paraffin-based fuels for hybrid rocket propulsion., 2013), (Merotto, et al., 2011), (Karabeyoglu, Cantwell, & Altman, Development and testing of paraffin-based hybrid rocket fuels., 2001), (Karabeyoglu, Hybrid rocket propulsion with liquefying fuels., 2012). Therefore, thanks to its combustion properties and the internal experience gained during last years, a paraffin based fuel has been chosen for the launch vehicle.

4.1.2. Liquid Oxidizers

The requirements on costs and environmental impact set to not use hypergolic or toxic oxidizers, which, even if in some cases they enhance the performances, commonly are more expensive to buy and handle. Therefore, only three oxidizers will be compared in order to choose the one that better fulfils the requirements and performance needed.
Table 2 shows some important characteristics of these oxidizers that influence the overall launch vehicle design.

Table 2 - Liquid oxidizers characteristics.

Feature	LOX	N_2O	H_2O_2 (98%)
Density [kg/m^3]	1141	743.9 (56.6 bar/ 25°C)	1440
Boiling point [K]	90.19	Pressure dependant	423
Cost [€/kg]	< 0.2	< 5	< 1.7
Oxidizer power	1	0.36	0.94
Self-pressurizing	No	Yes (not for high mass flow rate)	No

Storable	No	Yes	Yes (slightly degradation)
Catalyst need	No	Yes (only for high mass flow rate)	Yes
Theoretical Specific Impulse with paraffin based fuel [s]	370	320	320
Ignition system need	Yes	Yes	No
Equivalent TNT detonation power	0	ND	1
Availability	High	Medium	Very low

Nitrous oxide has a low density and a low oxidizer power (meaning bigger tanks), but it is storable and has the capability to pressurize itself, but only for low mass flow rate, so it need a pressurization system for high thrust motors (like this case).

High Test Peroxide (H_2O_2 with 98% concentration) has a high density (higher than LOX) and a high oxidizer power (meaning small tanks). It is storable, even if for at most 2 years, and, since it need catalytic decomposition, no ignition system is needed, allowing for multiple restarts. HTP has two main disadvantages: it is difficult to find large quantities on the market (quality required to allow high flight rate), and above all, at higher concentration than 95% it has the same detonation power as an equivalent mass of TNT (Fernando de Souza Costa, 2010). The latter disadvantage implies higher handling cost to prevent detonation and injuries in general.

Liquid Oxygen has a slightly lower density than HTP but, obviously, a higher oxidizer power. It has a slightly capability to self-pressurize using an expander cycle. Its cryogenic nature implies the use of insulating layers but its higher theoretical specific impulse (when used with paraffin fuels) allows lower propellant mass to achieve mission goals and therefore lower cost of tanks materials. Further, LOX is commonly produced around the world and has a really low cost. All this features leads to choose LOX as oxidizer for both stages (using different propellants on each stage will lead to high development and handling costs).
The optimal OF ratio for paraffin LOX hybrid rocket motor can be found on (Arif Karabeyoglu, 2011), this value is 2.7.

4.1.3. Values

From literature, a range of specific impulse values for hybrid rocket motors with paraffinic fuel and LOX as oxidizer (this is the actual base propellant configuration) can be found. Typically, for booster stages, specific impulse varies from 260 s and 300 s, and from 290 s to 330 s for upper stages. The values contained in Table 3. has been selected in order to have a conservative sizing of the launch vehicle.

Table 3 - Specific impulse values.

Symbol	Output	Value
I_{sp1}	First stage specific impulse	270 s
I_{sp2}	Second stage specific impulse	310 s

4.2. Structural mass

Structural mass fraction is commonly defined as:

$$\varepsilon = \frac{M_s}{M_0 - M_{pl}} \quad (1)$$

where:

- M_s is the structural mass (including all launch vehicle, payload mass and propellant mass excluded);
- M_0 is the initial mass;
- M_{pl} is the payload mass (for first stage it is equal to second stage gross mass).

From literature common structural mass fractions for a stage ranges from 0.08 to 0.12. Since for small launch vehicle is more difficult to achieve extremely low value of structural mass fraction, a value of 0.1 for both stages has been selected (
Table **4**).

Table 4 - Structural mass fraction.

Symbol	Output	Value
ε_1	First stage structural mass fraction	0.1
ε_2	Second stage structural mass fraction	0.1

These values are quite in the range of typical structural mass fraction of several launch vehicles as can be seen from (Gaspar, 2014). For micro launch vehicle is certainly more difficult to achieve low structural mass fraction, but as the example of the Electron rocket

developed by RocketLab, these values are achievable with the use of composite materials.

4.3. Stages delta-V

The delta-V amount for each stage has to be selected in order to have a first stage propellant mass seven times the second stage propellant mass, this way ensures to use the cluster configuration on the first stage and use the same rocket motor for each stage. A constrain on first stage delta-v has to be added in order to limit its maximum altitude, maximum velocity and consequently limiting heating and downrange distance for a future improvement as a partially reusable launch vehicle. These limitations also ensure an easier and then cheaper recovery of the first stage (the first stage will have a recovery system with parachutes).
The delta-v evaluation for each stage has been made iteratively using the imposed requirements in order to remain in the constraints. The "stage_deltav_evaluator" Octave code developed by the author has been used with a tolerance of 1 kg, a delta-v step of 0.1 m/s and an iterations maximum number of 10000. The results can be seen in Table 5.

Table 5 - Delta-V values.

Symbol	Output	Value
ΔV_1	First stage delta-v	4.025 km/s
ΔV_2	Second stage delta-v	5.695 km/s

4.4. Mass Budget

In the following tables the mass budget for the entire launch vehicle and its stages are presented. Those value has been evaluated using "launcher_sizing_comp" Octave code developed by the authors. The code calculates first the initial mass of the second stage imposing the outputs previously shown, and therefore the first stage initial mass using second stage initial mass as payload. The following expression for initial mass, derived from Tsiolkowski's equation, has been used:

$$M_i = \frac{M_{pl}(1-\varepsilon)e^A}{(1-\varepsilon e^A)} \quad (2)$$

$$A = \frac{\Delta V}{I_{sp} g_0} \quad (3)$$

The total initial mass, comprising the payload mass, can be found in Table 6.

Table 6 - Total initial mass.

Symbol	Output	Value
M_i	Initial mass (w/ payload)	6360 kg

4.4.1. First stage

First stage initial mass, without the second stage initial mass (defined as first stage payload mass), propellant mass and structural mass can be seen in Table 7.

Table 7 - First stage mass breakdown.

Symbol	Output	Value
M_{i1}	First stage initial mass (w/o payload)	5530 kg
M_{p1}	First stage propellant mass	4975 kg
M_{s1}	First stage structural mass	555 kg

4.4.2. Second stage

Second stage initial mass, without the payload mass, propellant mass and structural mass can be seen in Table 8.

Table 8 - Second stage mass breakdown.

Symbol	Output	Value
M_{i2}	Second stage initial mass (w/o payload)	790 kg
M_{p2}	Second stage propellant mass	710 kg
M_{s2}	Second stage structural mass	80 kg

4.5. Thrust

Knowing the stages initial a final mass, and knowing the requirements on maximum longitudinal acceleration and on take-off TWR, the thrusts and throttling capabilities needed for both stages can be evaluated.
To evaluate the initial thrust the following expression has been used:

$$T_i = TWR(M_i g_0) \quad (4)$$

Where:

- TWR is the Thrust to Weight Ratio;
- M_i is the initial mass of the stage of reference;

- g_0=9.8065 m/s^2 is the standard gravity acceleration at sea level.

Attention has to be taken on the fact that a cluster will be mounted on the first stage therefore, the initial thrust has to be divided by the number of motors. Since on both stages the same motor has to be mounted, the second stage initial thrust will be equal to the first stage single motor initial thrust.

To evaluate the final thrust the following expression has been used:

$$T_f = M_f a_{max} \quad (5)$$

Where:

- a_{max} = 65 m/s^2 is the maximum longitudinal acceleration;
- M_f is the final mass of the stage of reference.

Therefore, taking these values into account the thrusts included in Table 9 can be evaluated.

Table 9 - Thrust values.

Symbol	Output	Value
T_{i1tot}	First stage total initial thrust	87500 N
T_{i1}	First stage initial thrust (single motor)	12500 N
T_{i2}	Second stage initial thrust	12500 N
T_{f1}	First stage final thrust	87500 N
T_{f2}	Second stage final thrust	8350 N
ΔTh	Motor Throttability	40 %

The first stage do not exceed the maximum longitudinal acceleration constraint during its operation, therefore the motors do not need to be throttle down.

4.6. Propellant mass

Since the OF ratio is 2.7, the fuel and oxidizer mass can be evaluated. These masses for first and second stage can be seen on Table 10.

Table 10 - Propellant mass breakdown.

Symbol	Output	Value
M_{1fuel}	First stage fuel mass	1345 kg
M_{1ox}	First stage oxidizer mass	3630 kg
M_{2fuel}	Second stage fuel mass	190 kg
M_{2ox}	Second stage oxidizer mass	520 kg

5. HARLOCK HYBRID ROCKET MOTOR

Harlock is a hybrid rocket motor that has to ensure high safety and reliability standards, great maneuverability, restart capability and low environmental impact. It will power both Primo's stages using liquid oxygen (LOX) as oxidizer and an internally developed paraffin-based fuel. Its relative small size overcomes scaling and instability problems typical of bigger hybrid rockets (Story, 2006), making it suitable for high production rate and small development costs. Some parameters are shown in Table 11.

Table 11 - Harlock motor parameters.

Symbol	Output	Value
M_{fg}	Fuel grain mass	190 kg
T_{b1}	Burning time (first stage)	184 s
T_{b2}	Burning time (second stage)	211 s
MF_{LOX}	Oxidizer mass flow rate	2.9 kg/s
L_{cc}	Combustion chamber length	1.6 m
D_{cc}	Combustion chamber diameter	0.4 m

As can be seen the grain dimensions are similar to other hybrid rocket motor grains developed in the past (Arif Karabeyoglu, 2011), underlining the feasibility of the production.

In order to maintain the structural mass at low levels, the use of an ablative combustion chamber has been taken into account. Previous studies and testing made by Microcosm Inc. and Sierra Nevada Corporation (J.A. Muss, 2005) of an ablative liquid rocket motor suggest that the use of this technologies also for hybrid rocket motors is feasible (Figure 1).



Figure 1 - Scorpius silica phenolic combustion chambers.

Besides the weight decrease, using silica phenolic composites is also really good for lowering costs and simplify the mass production using filament winding or automatic tape placement machines.
This technology is born to build expandable motors, but it can be used also for reusable engines in the case the economical feasibility of this approcah will be confirmed in the future.

The use of carbon fiber enables the use of an innovative TVC approach with nozzle gimbaling that Leaf Space is developing. This system will ensure low mass and low power needed to control the thrust, compare to classical approaches.

5.1. Feed line

Hybrid rocket motors are generally fed with pressure feed systems, with sporadic cases of turbo-pumps example (Aquila Launch Vehicle). The lack of a liquid fuel makes the pump-fed system a complex choice since the mass saved by decreasing the tank pressure is earned by the need of an external liquid fuel and all the relative components needed. Therefore, the pressure-feed systems are still the favourite choice for this kind of engines.
With the development of new lighter electric motors and high efficiency lithium-based batteries, the electric motor driven pump-feed systems are now a feasible choice.
Pavlov (Pavlov, 2012) highlight the competitiveness of these systems with regard to pressure-feed and turbo-pump systems for liquid rocket engines. In order to compare the different systems the considered masses has to be underlined:

- pressure-feed:
  - pressurant mass;
  - pressurant-tank mass;
  - pressurant feed-line mass;
  - propellant tanks added mass to resist the high pressure.
- turbo-pump:
  - turbo-pump mass;
  - turbo-pump feed-line mass.
- electric-pump:
  - electric motor mass;
  - batteries mass;
  - inverter mass.

This work shows that electric-pump systems are always lighter than pressure-feed systems (tipically one third of the weight) and lighter than turbo-pumps for long burning times (tipically 20% lighter).
The great advantage to use such a technology is the low development cost compared to turbopump systems, that commonly are the major part of a liquid engine cost. Electric-pump systems are also less prone to failure than turbopumps (remind the Antares failure accured on 28/10/2014), and of course more simple to design and build. Electric motor and battery cell technologies currently under development could also extend the proposed feed system convenience. In addition, the electric motor is really simple to control and adjust both during development than operation, making easier to change operational parameters of the rocket motor.
An application of this technology on a hybrid rocket motor concept is explained in (L. Casalino, 2010).

A further analysis has been done by the author on the different types of Lion-based batteries with varying parameters. These parameters are:

- LOX mass flow rate;
- tank internal pressure;
- burning time.

The following masses have been taken into account:

- tank mass;
- electric motor mass;
- pump mass;
- batteries mass;
- inverter mass.

The pump, motor and inverter masses are driven by the pump power needed to put the required LOX mass flow rate into the motor. All the following efficiencies and power densities are typical values of commercial available items.
Therefore the pump power is evaluated with:

$$P_p = \frac{\dot{m}_{lox}(p_{ds} - p_{tk})}{d_{lox}\eta} \qquad (6)$$

where:

- P_p is the pump power;
- LOX mass flow rate: m_{lox}=20 kg/s;
- Discharge pressure: p_{ds}= 25 bar;
- tank pressure: p_{tk};
- LOX density: d_{lox} = 1141 kg/m^3;
- overall efficiency: η = 0.65.

The pump energy is defined as:

$$E_p = P_p t_b \tag{7}$$

where:

- P_p is the pump power;
- t_b is the burn time expressed in hours.

The pump mass has been evaluated using the following formula:

$$M_{pu} = \frac{P_p}{d_p \eta_p} \tag{8}$$

with:

- pump efficiency: $\eta_p = 0.68$;
- pump power density: $d_p = 22$ kW/kg.

The electric motor mass has been evaluated with the following formula:

$$M_{em} = \frac{P_p}{d_{em} \eta_{em}} \tag{9}$$

with:

- electric motor efficiency: $\eta_{em} = 0.8$;
- electric power density: $d_{em} = 3.8$ kW/kg.

The inverter mass has been evaluated with the following formula:

$$M_{inv} = \frac{P_p}{d_{inv} \eta_{inv}} \tag{10}$$

with:

- inverter efficiency: $\eta_{em} = 0.8$;
- inverter power density: $d_{em} = 60$ kW/kg.

The batteries mass are driven alternatively by the pump power and the pump energy depending on whether the bottleneck is the battery power density or energy density. Three Lithium based batteries has been analysed:

- Li-Po;
- Li-Ion;
- Li-S.

Typical values of power densities are:

- Li-Po: 6 kW/kg;
- Li-Ion: 2 kW/kg;
- Li-S: 1.2 kW/kg.

Typical values of energy densities are:

- Li-Po: 130 Wh/kg;
- Li-Ion: 220 Wh/kg;
- Li-S: 350 Wh/kg.

As can be seen the Li-Po has the highest power density, so it is more suited for high power load for a reduced period of time. Instead, the Li-S has the highest energy density, therefore, it is more suited for low power loads for a long period of time.

In Figure 2, Figure 3 and Figure 4 the mass trend of the first stage, depending on the oxidizer mass flow rate, tank internal pressure and burning time can be seen. The tank sizing has been made with a Tsai-Hill resistance method, for a cylindrical tank with elliptic bulkheads, setting the external diameter to 1 m and the oxidizer volume. The safety factor is 1.5. Although the tank mass could seem low, these values are confident with other cryo-composite tanks developed by Microcosm Inc., RocketLab and others.

As can be seen the Li-Po tends to be the better solution in terms of mass saving for every configuration. It is worth to note that the decrease in pump power and then decrease in electric motor mass and so on, due to an increased tank pressure is heavily counterbalanced by the increase of mass tank. Therefore, is better to have the lowest possible tank internal pressure (however the structure has to not collapse during handling and shipping), and make the electric pump responsible of the major part of the pressure increase.

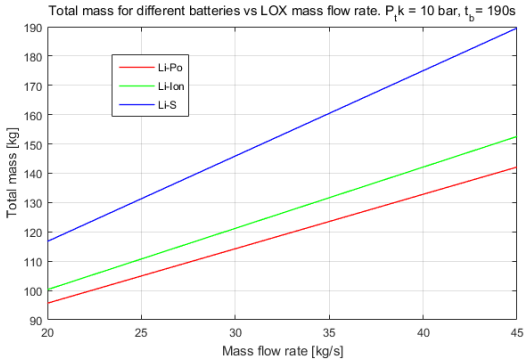


Figure 2 - Electric-pump total mass vs LOX mass flow rate.

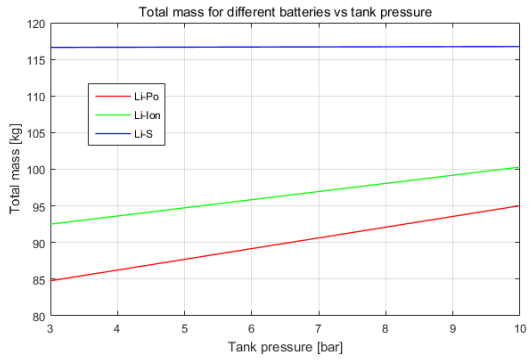


Figure 3 - Electric-pump total mass vs tank internal pressure.

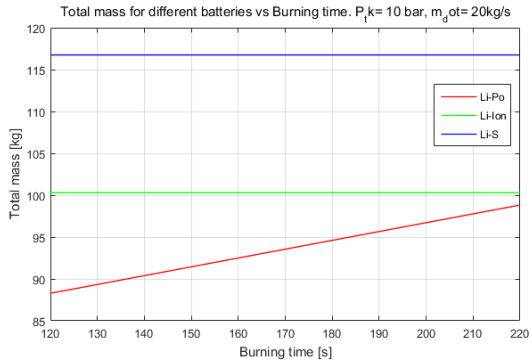


Figure 4 - Electric-pump total mass vs burning time.

The use of electrically driven oxidizer pump is already taking place around the world, one of the best example is surely the Rutherford liquid rocket engine developed by RocketLab for its Electron launch vehicle.



Figure 5 - RocketLab's Electrically powered Rutherford engine.

The easy of oxidizer flux control enables the possibility to do TVC changing instantaneously the thrust of each motor on the first stage. This solution is obviously not adoptable on the second stage where a single motor is mounted.

6. INERT MASS BREAKDOWN

An inert mass breakdown has been made taking into account previously evaluated data and literature data taken from (Hammond, 1999) (Karabeyoglu, Stevens, Geyzel, & Cantwell, 2011) (Gaspar, 2014) (Casalino & Pastrone, 2010) (Ley, 2008).
The results of this procedure are summarized in Table 12. All values have a 20% margin.

Table 12 - Inert mass breakdown.

Output	Value [kg]
Fairing	10
Payload adapter	2 – 10
Second stage avionics and cabling	10
Second stage power system	2
Second stage pressurization system	2
Second stage tank	20
Second stage electric-pump	6
Second stage feed-line	5
Second stage motor	15
Second stage TVC system	2
Second stage miscellaneous	6
Second stage total inert mass	**80**
Interstage and separation system	30
Payload/First stage recovery system	30
First stage avionics	20
First stage power system	10
First stage pressurization system	10
First stage tank	120
First stage electric-pump	40
First stage feed-line	40
First stage motors	105
First stage TVC system	30
First stage miscellaneous	135
First stage total inert mass	**555**

7. FLIGHT SIMULATION

A simple flight simulation has been conducted with a 3 DOF simulator developed in Octave by the author. The simulation stops once the launch vehicle has reached a near null flight path angle at an altitude of 200 km. The simulator also do an iteration process to find the best values of pitching rate for both stages in order to reach the wanted final conditions. The launch site is set on the equator launching in a polar orbit, as required. As can be seen from the graphs the final velocity is slightly higher than the circular orbital velocity for a 200km orbit, that is because the simulator is built to burn all the propellant of the second stage in a single fire, without restart capability (this feature will be added soon). The surplus velocity is the one needed to make the hohmann transfer into a 700 km circular orbit. The gravity loss is quite lower than the value taken from literature, but this difference is compensated by the higher drag loss. Further analysis with optimized trajectory and more accurate drag data will be done in the near future.

As can be seen the staging happens at about 90 km at a velocity of about 2.8 km/s. These are typical values if compared with other launch vehicles (Hammond, 1999) (Gaspar, 2014).

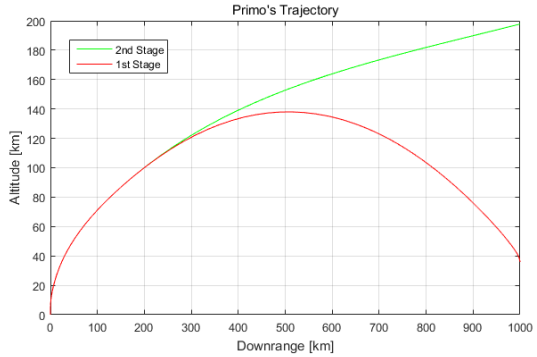


Figure 6 - Trajectory.

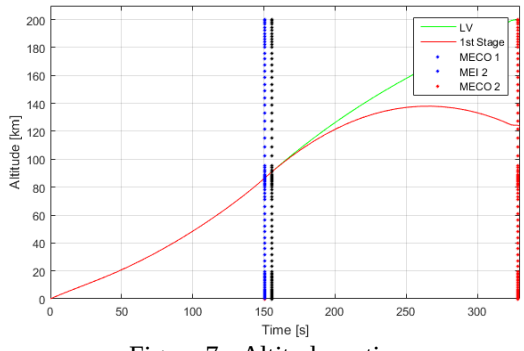


Figure 7 - Altitude vs time.

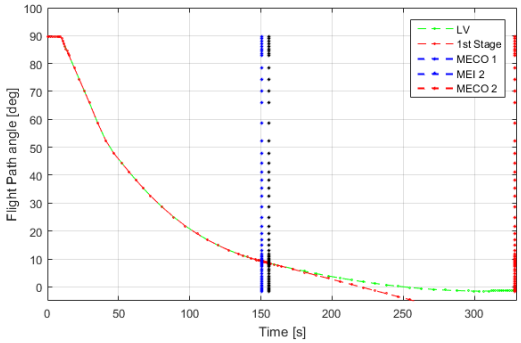


Figure 8 - Flight path angle vs time.

8. PAYLOAD

In order to be able to transport different configurations of payload the fairing can be modified for every need. The typical configuration is shown in Figure 9 and it is big enough to store a washing machine.

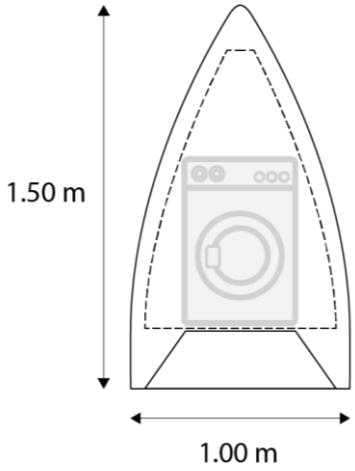


Figure 9 - Fairing accomodation.

Without changing the fairing the launch vehicle can accommodate a single microsatellites of 50 kg, up to 10 3U cubesats and hybrid solution with a microsatellite and few cubesats. The restart capability of the second stage make feasible to launch different payloads in the same orbit plane (a good solution for cubesats constellation) or in slightly different planes and altitudes.

The different capabilities for a wide range of orbits and payload are shown in Figure 10.

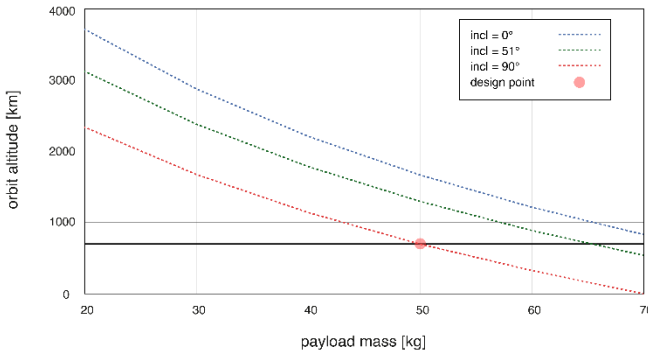


Figure 10 - Payload capabilities.

As can be seen Primo can perform different kind of missions without change its configuration. It is worth to note that the change in velocity needed to deorbit the second stage has already been taken into account. Adding a kick motor as a third stage, Primo will be able to put a little payload in lunar orbit or deep space trajectory.

9. PRIMO CONFIGURATION

The final configuration is shown in Figure 11. The vehicle has been designed to be shipped inside a classical 12m naval container (with detached stages). This is due to make the shipping and handling of the rocket easy and reduce the logistics costs. The great safety typical of hybrid rockets, and the absence of pyrotechnic devices, permits to ship the vehicle everywhere without the need of dedicated transport and security staff.

The payload integration in the fairing can be done in a relatively small clean room thanks to the small dimensions of this stage.

Performing the final assembling and second stage integration on a horizontal configuration inside an expandable 12m container, lowers the need of dedicated facilities, further lowering the costs and enabling much faster operations.

Its high performance margins permits to Primo to be launched from different sites around the world, be those terrestrial or marine.

The major advantages of an air-launched vehicle (responsiveness, orbit coverage, low cost) are satisfied by Primo thanks to its easy of handling and the possibility to be launched from different sites, with the advantage of the land-launch strategy. In fact, Primo does not need an airplane, can be safely tested on ground just before the launch, its payload can be recovered in case of failure of the first stage and the facilities needed on ground are really limited.

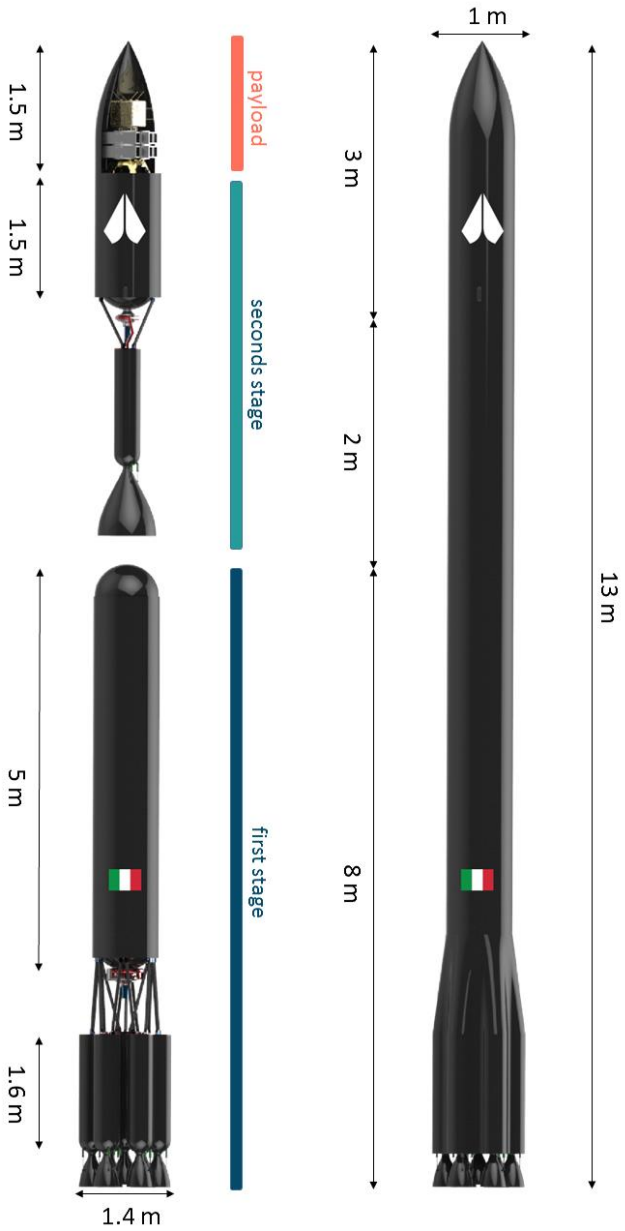


Figure 11 - Launch vehicle configuration.

10. CONCLUSIONS

This paper contains just a part of the work that has been done by the author as a base for its master degree thesis in Space Engineering at Politecnico di Milano. Future works will be focused on a more accurate mass and power budget for all the systems, with particular attention to the study of the TVC and control systems. In addition, a more complex flight simulator will be developed in order to study all the different missions Primo has to accomplish, refining the design parameters.

11. ACKNOWLEDGEMENTS

This work would never been done without the help of Michele Messina, Jonata Puglia, Matteo Boiocchi, Chiara Mirani, Francesco Iervese, Luca di Pancrazio, Antonio Lamonarca, Prof. Airoldi, Prof. Lavagna, Prof. Galfetti and, of course, my parents.

12. REFERENCES

Casalino, L., & Pastrone, D. (2010). Optimization of a hybrid rocket upper stage with electric pump feed system. *AIAA*.

Costa, F. S., & Vieira, R. (2010). *Preliminary analysis of hibryd rockets for launching nanosat into LEO*. Journal of the Brazilian Society of Mechanical Sciences and Engineering.

Costa, R. F. (2010). Preliminary analysis of hybrid rockets for launching nanosat into LEO. *Journal of the Brazilian Society Of Mechanical Sciences and Engineering*.

Galfetti, L., Merotto, L., Boiocchi, M., Maggi, F., & DeLuca, L. (2011). Ballistic and rheological characterization of parafin-based fuels for hybrid rocket propulsion. *AIAA: Joint propulsion conference*.

Galfetti, L., Merotto, L., Boiocchi, M., Maggi, F., & DeLuca, L. (2013). Experimental investigation of paraffin-based fuels for hybrid rocket propulsion. *EUCASS: Progress in propulsion physics*.

Gaspar, D. (2014). *A tool for preliminary design of rockets.* Técnico Lisboa.

Hammond, W. (1999). *Space Transportation: a system approach to analysis and design.* AIAA.

Karabeyoglu, A. (2011). High performance hybrid upper stage motor. *AIAA*.

Karabeyoglu, A. (2012). *22-inch hybrid rocket test media briefing.* Space Propulsion Group Inc.

Karabeyoglu, A. (2012). *Hybrid rocket propulsion design issues.* Department of Aeronautics and Astronautics - Stanford University.

Karabeyoglu, A. (2012). *Hybrid rocket propulsion with liquefying fuels.* Department of Aeronautics and Astronautics - Stanford University.

Karabeyoglu, A., Cantwell, B., & Altman, D. (2001). Development and testing of paraffin-based hybrid rocket fuels. *AIAA*.

Karabeyoglu, A., Stevens, J., Geyzel, D., & Cantwell, B. (2011). *High Performance Hybrid Upper Stage Motor.* AIAA.

Ley, W. (2008). *Handbook of Space Technology.* Wiley.

Merotto, L., Boiocchi, M., Mazzetti, A., Maggi, F., Galfetti, L., & DeLuca, L. (2011). Characterization of a family of paraffin-based solid fuels. *EUCASS*.

Muss, J., Chakroborty, S., & Leyva, I. (2005). *Development of the Scorpius LOX/Kerosene engine family.* MIcrocosm Inc. - Sierra Engineering Inc.

Osborne, B. (1967). *Space Vehicle Dynamics.* Oxford University Press.

Pavlov, P. (2012). *Electric feed systems for liquid propellant rockets.* Universidad de Buenos Aires.

SpaceFlight 101. (2015). Tratto da Launch Vehicle Library: http://www.spaceflight101.com/launch-vehicle-library.html

Story, G. (2006). *Large-Scale hybrid motor testing.* NASA.

Sutton, G. (2001). *Rocket Propulsion Elements.* Wiley.

Zilliac, A. G. (2006). Hybrid rocket fuel regression rate data and modeling. *AIAA 2006-4504*.

DESIGN, SIMULATION AND ANALYSIS OF AN AIR LAUNCH ROCKET FOR HUNTING LOW EARTH ORBIT SPACE DEBRIS

Hamed Gamal[(1)], Mohamed G. Abdelhady[(2)], Essam Omar [(3)]

[(1)] Cairo University, Gamaa St. – Giza, Egypt, Email:hamedgamal@hotmail.com
[(2)]Cairo University, Gamaa St. – Giza, Egypt, Email: m_gag@outlook.com
[(3)] Cairo University, Gamaa St. – Giza, Egypt, Email: essam.omar.95@hotmail.com

ABSTRACT

This paper introduces the progress work done on a segment of a new simple launch concept aiming to reduce the dangers of space debris in the low Earth orbit, This project is mainly focused on the debris falling back to Earth's surface unburnt in the outer atmosphere which highly risk human lives on Earth.

Using a combined system of a High Altitude Balloon (HAB) with an attached rocket, we will be presenting in this paper the technologies and developments done on the rocket segment from the point of view of the design analysis, simulations, control and aerodynamic algorithms and recovery testing aspects, we will be considering the Preliminary design of the rocket's wing, control surfaces, aerodynamics with the flow simulations and recovery system design and testing.

Also discussing the rocket mathematical model and simulation results. Optimizing the hunting trajectory by nonlinear programming and collocation is introduced and enhanced by a time varying LQR control policy. The robustness of this trajectory is tested under different conditions.

1. INTRODUCTION

The basic objective of the Combined Launch System (CLS) [2] is to offer a reliable, efficient and cheap access to delivering scientific payloads and experiments to the low earth orbit. Consisting of a High Altitude Balloon (HAB) and a Controlled High Powered Air Launched Rocket, one of the most important applications of such a system is to deliver the space debris hunting probes to their functioning orbit, in this paper we will discuss the design and analysis of the concept of an air launched rocket with an explosive charge to hunt the low earth orbit space debris falling back to Earth that don't completely burn up during their re-entry.

Using an Air Launch Rocket to shoot or break down space debris into pieces may sound a naive solution to a problem that is causing a headache to all the highly qualified space industries and technologies community, However checking the latest studies about the amount of unburnt space debris from the outer atmosphere falling back to Earth and hitting farms, beaches and even houses gives a simple alert that this is a matter of human's security on their own planet not just a matter for technological or engineering aspects, it is an alarm of a disaster that can happen at any time and anywhere, having a manmade object which was basically made to serve humanity eventually being the source of destruction and harm to its creator is completely not acceptable.

During the last decade, the amount of space debris has a significant rise in the low earth orbit, as shown in Fig. 1 [1], Introducing active debris removing technology always included new innovative concepts which may seem promising but mostly sophisticated designs. Either depending on a long term developing scheduled plans or on a highly cost design requirements, we decided to get back to developing the very basic concepts of air defence systems, rockets. A ground launched rocket is the simplest idea to face the fear of ballistic missiles and objects falling from the skies, However the expenses of targeting space debris from sea level or low altitudes would cost a lot and add much more complexities as moving the rocket launchers will be logistically not applicable. One more problem, there is no guarantee that there will be enough time to do so.

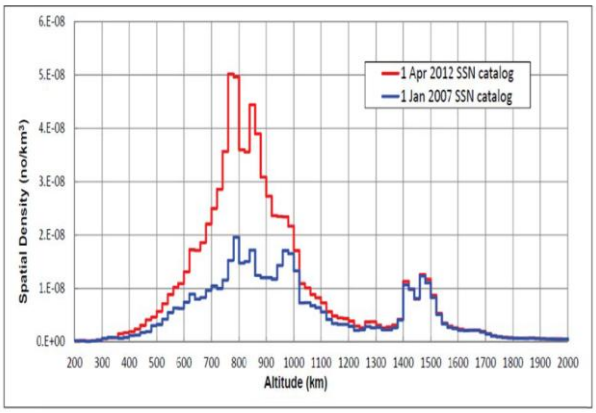


Figure 1: The growth of the debris amount in the low earth orbit

An air launched rocket would require less fuel therefore less cost and would be easier to locate and reach its target as its already hanged up there in the atmosphere.

Due to the Earth's curvature, reaching the target will take less time and an easier approach than an earth launch, those two advantages are main keys to work on this concept.
The main aspects that concerns the key design parameters through this project is to reduce the costs of the system, complexities and offer a reasonable plan to implement a prototyping model in the near future as a proof of concept and how to develop the technologies we have nowadays to reach an optimum design that could end up this fear from the skies.

2. MISSION DESIGN

The CLS consists of two segments with a simple operational design, the High Altitude Balloon will be responsible to lift the rocket to an altitude ranging between 25 to 30 km. Launching the rocket at such an altitude will save many complexities to the design, the density of air at such an altitude offers less aerodynamic drag and therefore less fuel and energy losses. Also this saves the efforts done to establish a ground based launch facility in addition to the advantage of being a portable platform that can be deployed and launched from any place.

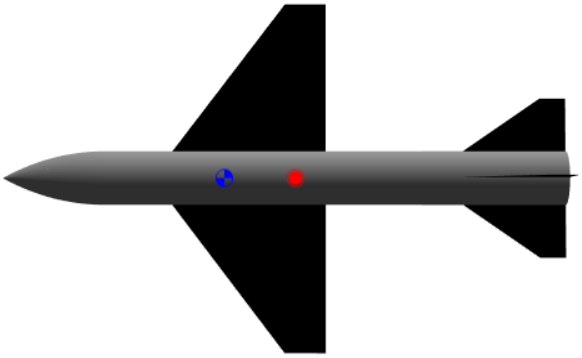


Figure 2: Rocket CAD preliminary design

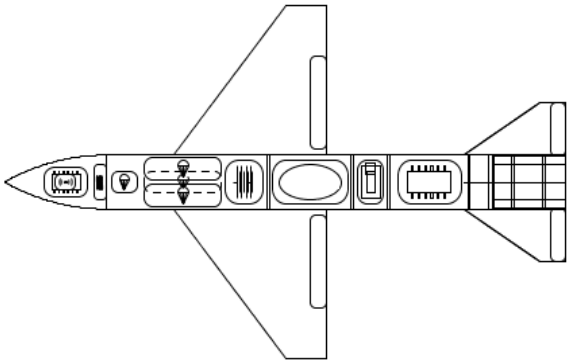


Figure 3: Rocket schematic sectional view

Upon reaching the desired altitude, the separation system will separate the rocket from the high altitude balloon to experience a guided free fall using the aerodynamic forces and stabilizing control surfaces in addition to the thrust vectoring mechanism of the propulsive unite – the rocket motor – to maintain the rocket's balance, the rocket motor will ignite allowing the rocket to gain thrust over its weight and climbing up its trajectory to reach its target.
Using the thrust vectoring, the rocket will reach its target and eject its explosive charge into it. Bringing the debris into smaller pieces will make it easier to those pieces to be burnt in the atmosphere, removing the threat of those objects to fall back unburnt or partially burnt to Earth's surface and demolish any threat to the human lives or infrastructure from falling space debris.

This won't cause the destruction of the whole rocket, only the war head will engage with the target, the rest of the rocket will fall back to the nearest safe location where it can be retrieved, recovered and set ready for another use. The reusability of the system is conducted using a recovery system of parachutes, the rocket will glide first using it's active stabilizing systems then upon reaching the landing site the parachute will open offering a smooth and easy landing, recovering all the hardware is so essential to guarantee the low cost and efficiency of this system.

3. PRELIMINARY ROCKET DESIGN

A Preliminary study was done to size the overall design parameters of this concept, this sizing also aimed to help meeting the requirements with the available components and parts in market that can be used as a prototype to illustrate this concept.

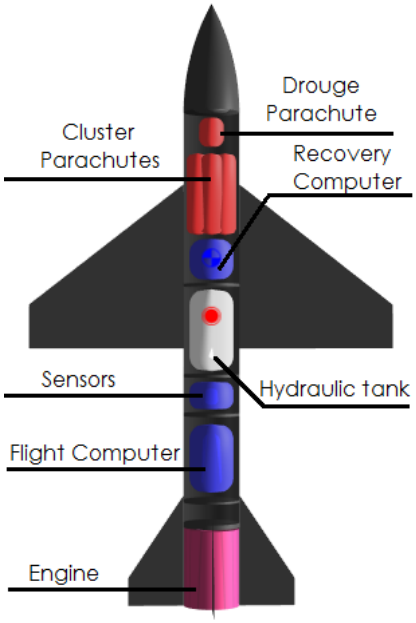


Figure 4: Detailed rocket configuration

3.1. Engine Selection

The rocket motor chosen upon our design requirements was the ORION 38 developed by ATK Launch Systems

Group. The ORION 38 was developed as a low-cost, high-performance third
stage for the Pegasus launch vehicle, and incorporates a ± 5-deg vectorable nozzle.



Figure 5: ORION 38 rocket motor

It also functions as the standard third-stage motor for other launch vehicles such as the Pegasus XL, Taurus, Taurus XL, and Taurus Lite launch vehicles; and as the fourth stage of the Air Force's Minotaur vehicle. However due to our air launch and significant light payloads, this motor will be our primary and only stage. This motor has performed successfully in 44 flights in over a decade of use.

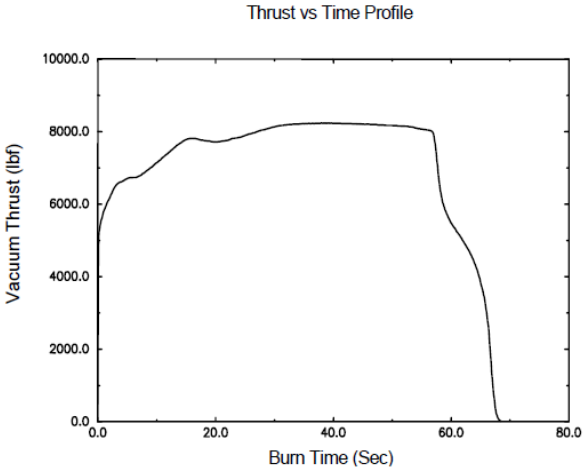


Figure 6: Thrust vs Time profile for the ORION 38 rocket motor

The 800 kg motor will produce approximately 32 KN of thrust in 67.7 seconds, with a total impulse of about 215 kg.sec and a ± 5-deg vectorable nozzle the rocket will be guided to its trajectory successfully and offering a powered till the rocket reach its target.

3.2. **Aerodynamics**

During our approach to design and calculate the aerodynamic forces, two separate methods from rocketry literature were used for estimating an aerodynamic coefficient using the rocket's geometry. The first is for estimating the normal force coefficient C_N and the second is for estimating the coefficient of drag C_D.

The equations for estimating the normal force, and the location of the centre of pressure have been proposed by Barrowman and others [3] [4] [5] while developing the Theoretical Aerodynamic Derivatives computer program (TAD) for computing the aerodynamics of rockets for NASA Goddard Space Flight Center. While the equations for estimating the coefficient of drag force on a rocket are done using the United States Air force Stability and Control Datcom Method, the equations used were developed by Mandell [6] who followed Barrowman's method.

Determining the Aerodynamic derivatives was an essential part in our research in order to allow the required information and data needed to design the control systems and algorithms, also a numerical analysis was done to confirm our calculations and offer more data about the overall performance in a detailed form.

3.3. **Wing and Fins Design**

It's known that adding a wing above the center of mass destabilizes the rocket regular vertical ascending. However, the wing has a significant role in the re-entry and gliding to a retrieval location after ejecting the explosive charge. So it is designed to this mission specifically.

Before losing the motor power, the rocket flies nearly horizontally and the wings control surfaces moves to have a positive angle of attack with flow preparing to glide after finishing the motor burn time. The wing make this gliding possible by having the center of mass between the wing and the fins and providing enough left to prevent the fast diving noze down in regular rockets.

4. NUMERICAL SOLUTION AND ANALYSIS

The numerical analysis was conducted using Ansys software engineering package, beside solving using the Barrowman solution proposed [2,3] we could compare the results to reach the most accurate design.

As follows the results of the latest iteration for solving the rocket in the climbing phase.

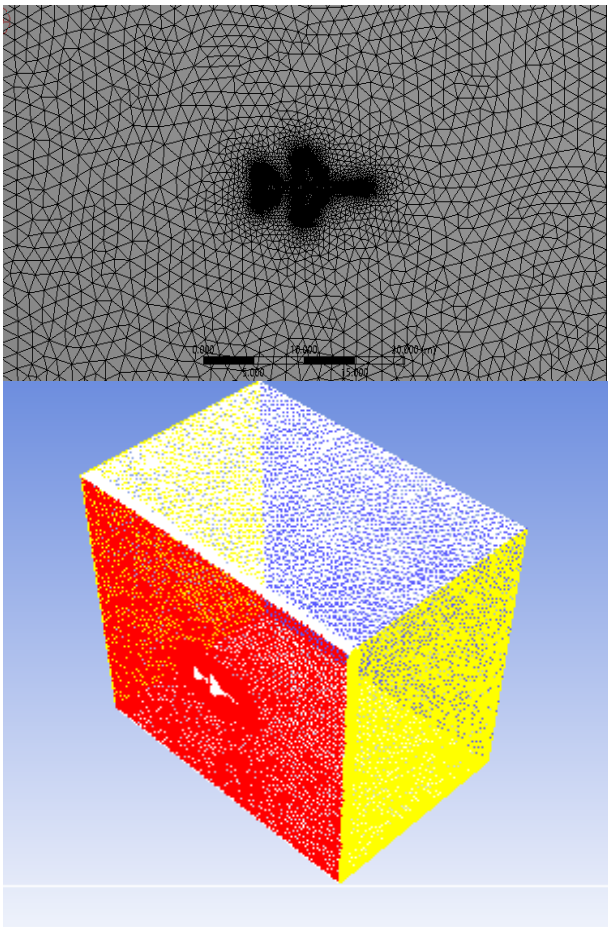


Figure 7: Meshing using Fluent Ansys package

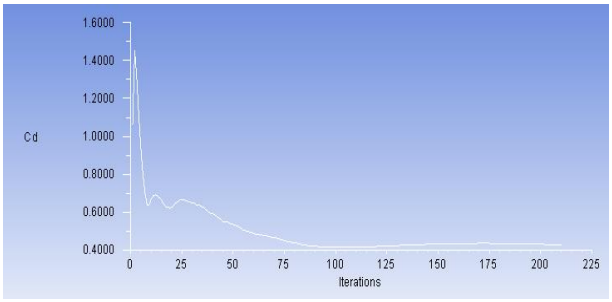


Figure 8: C_D convergence with Iterations solved

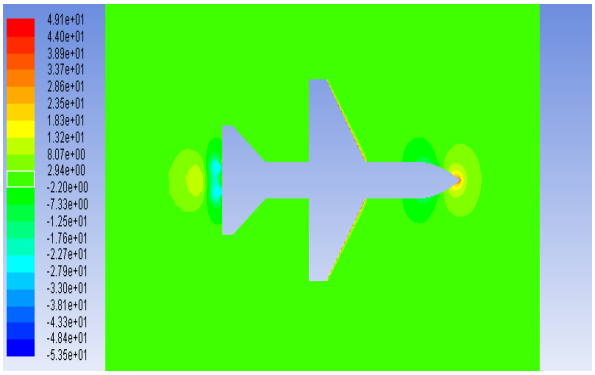


Figure 9: Pressure distribution around the rocket

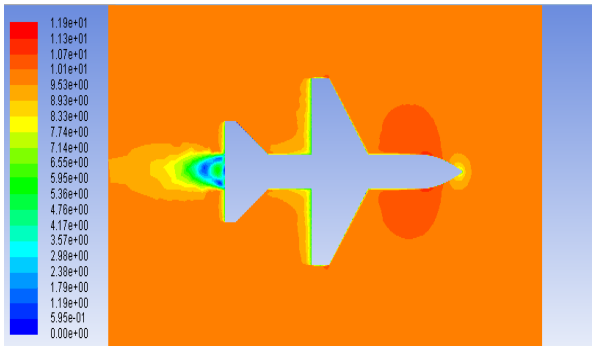


Figure 10: Velocity distribution around the rocket

5. CONTROL ALGORITHM DESIGN

The rocket is controlled by two angles of thrust vectoring to adjust the rocket trajectory. Control algorithm in this paper is restricted to a segment of the mission that starts after detaching the rocket from the balloon until the rocket ejects the explosive charge in the facing direction of the falling debris with enough velocity to collide. The other segment in the mission is meant to guide the rocket trajectory to a landing location using the remaining thrust and control surfaces in the wing. This paper discusses a solution to the first segment only.

The first subsection develops the rocket mathematical model and compares results from launching this rocket passively without control to test the selected design parameters. The second subsection deals with the trajectory optimization problem with all constraints of the initial and final conditions. Stabilizing this trajectory requires time-varying linear quadratic regulator TV-LQR on different linearization points on the trajectory. The trajectory stabilization is discussed in the third subsection.

5.1. Mathematical Model

The model is the equations of motion of a varying mass body with three sources of forces and moments: gravity, thrust and aerodynamics. The only control inputs in this part of the mission are thrust vectoring two angles.

Kinematics and mass calculations

The inertial frame of reference $\{i\}$ is fixed on the balloon as a relative inertial frame. The second frame is a fixed-body frame $\{B\}$ aligned as illustrated in Fig.11 and its origin is fixed at the rocket center of mass.

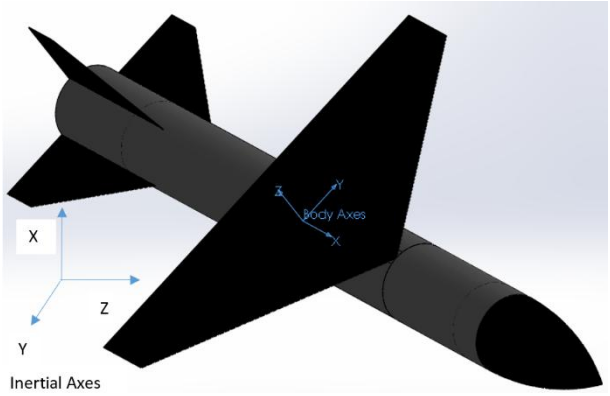


Figure 11. the frame of reference attachment

The state vector is:

$$S = \left[\underline{X}^i \ \underline{V}^B \ \underline{\Theta} \ \underline{\omega}^B \ \underline{\delta}\right] \quad (1)$$

Where the position of center of mass is:

$$\underline{X}^i = [x, y, z]^T \quad (2)$$

Orientation vector of Euler ZYX angles is defined as:

$$\underline{\Theta} = [\phi, \theta, \psi]^T \quad (3)$$

The rotation matrix from frame {B} to {i} in Euler ZYX order is defined as follows:

$${}^i_B R = R_z \, R_y \, R_x \quad (4)$$

The velocity vector

$$\underline{V}^B = [u, v, w]^T = {}^i_B R \, \frac{d}{dt_i} (\underline{X}^i) \quad (5)$$

The angular velocity vector:

$$\underline{\omega}^B = [p, q, r]^T = I \, [\phi^o, 0, 0]^T + R_x^T \left[0, \underline{\theta}^o, 0\right]^T + \\ + R_x^T R_y^T \left[0, 0, \underline{\psi}^o\right]^T \quad (6)$$

The thrust vectoring angles:

$$\underline{\delta} = \left[\underline{\delta}_1 \, , \underline{\delta}_2\right]^T \quad (7)$$

The control inputs are the angular velocities of the rotating angles in thrust vectoring system. The nozzle movement is assumed to be constant angular velocities as follows:

$$U = [\tau_1, \tau_2]^T \quad (8)$$

$$\delta_1' = \tau_1 \ \& \ \delta_1' = \tau_2 \quad (9)$$

All mass parameters are variant during the flight according to the fuel burning rate as follows:

The system mass m(t) is defined by

$$m(t) = m_s + m_f\big(1 - r(t)\big) \quad (10)$$

$$r(t) = \frac{\int_0^t thrust \, dt}{Total \ Impulse} \quad (11)$$

The structure mass is m_s and m_f is the fuel mass. The center of mass is defined as follows:

$$X_{cg}(t) = \frac{X_{cg_s} m_s + X_{cg_f} m_f\big(1 - r(t)\big)}{m(t)} \quad (12)$$

The structure mass center is X_{cg_s} and X_{cg_f} is fuel center of mass. Each of them is measured from the rocket base. The moment of inertia is changing during the fight as defined in equations (5.13)

$$\begin{aligned} I_{xx} &= I_{xx_s} + 2I_2 \\ I_{yy} &= I_{yy_s} + I_1 + I_2 \\ I_{zz} &= I_{zz_s} + I_1 + I_2 \\ I_{xy} &= I_{xz} = I_{zy} = 0 \end{aligned} \quad (13)$$

The moments of inertia about the body axes are $I_{xx}, I_{yy}, I_{zz}, I_{xy}, I_{xz}, I_{zy}$ and $I_{xx_s}, I_{yy_s}, I_{zz_s}$ are the moments of inertia of the structure without fuel. The fuel contribution is defined as:

$$\begin{aligned} I_1 &= m_s\big(X_{cg}(t) - X_{cg_s}\big)^2 \\ &+ m_f(t)\left(\frac{r_f^2}{2} + \big(X_{cg}(t) - x_f\big)^2\right) \end{aligned} \quad (14)$$

$$I_2 = m_f(t)\frac{3\,r_f^2 + h_f^2}{12} \quad (15)$$

Where $r_f \ h_f$ are the fuel dimensions assuming the fuel radius and height are constants.

Dynamics

The equations of motion are written in Newton-Euler form and all forces and moments are calculated in the center of mass as follows:

$$\begin{aligned} \sum \underline{F}^B &= \frac{d}{dt}|_i \big(m \, \underline{V}^B\big) \\ &= m' \underline{\mathrm{V}}^{\mathrm{B}} + m \underline{V}'^B + \underline{\omega}^{\mathrm{B}} \times (\mathrm{m} \, \underline{\mathrm{V}}^{\mathrm{B}}) \end{aligned} \quad (16)$$

$$\begin{aligned} \sum \underline{M} &= \frac{d}{dt}|_i \left(I \, \underline{\omega}^B\right) \\ &= I' \, \underline{\omega}^B + I \, \underline{\omega}'^B + I \times (I \, \underline{\omega}^B) \end{aligned} \quad (17)$$

Where: $\sum \underline{F} = \underline{F}_{gravity} + \underline{F}_{thrust} + \underline{F}_{aerodynmics}$

$$\sum \underline{M} = \underline{M}_{thrust} + \underline{M}_{aerodynamics}$$

Gravitational and Thrust Forces and Moments
The weight force is:

$$\underline{F}^{B}{}_{gravity} = {}^{B}_{i}R[-mg, 0,0]^{T} \quad (18)$$

Thrust is unaligned with body x axis after using thrust vectoring by the two angles δ_1 & δ_2 as follows:

$$\underline{F}^{B}{}_{thrust} = thrust * [c\delta_2\, c\delta_1\, , s\delta_2\, c\delta_1\, , -s\delta_1]^{T} \quad (19)$$

$$\underline{M}^{B}{}_{thrust} = thrust\, X_{cg}[0\, , -s\delta_1, -s\delta_2\, c\delta_1\,]^{T} \quad (20)$$

The system inputs are the angular velocities of the rotating nozzle in thrust vectoring system. The nozzle movement is assumed to be constant angular velocities as follows:

$$\delta_1' = \tau_1\ \&\ \delta_1' = \tau_2 \quad (21)$$

Aerodynamic forces and moments
The aerodynamic coefficients are simplified in [7],[15]. But it is useful to represent these forces in the rocket frame of reference.

- Body and Fins:

The two forces are the axial force F_A and the normal force F_N acting in the center of pressure X_{cp} as measured from the rocket base.

$$\underline{F}^{B} = [-F_A\, , -F_N\, s\theta\, , -F_N\, c\theta]^{T} \quad (22)$$

$$\underline{M}^{B} = (X_{cg} - X_{cp})[0\, , -F_N\, c\theta\, , F_N\, s\theta]^{T} \quad (23)$$

Where: $\theta = atan2(v, w) \in [-pi\, , pi]$

- Wing:
  Similarly the two forces are the axial force and the normal force acting in the wing center of pressure as measured from the rocket base.

$$\underline{F}^{B} = \left[-F_{A_{wing}}\, , 0\, , -F_{N_{wing}}\, \right]^{T} \quad (24)$$

$$\underline{M}^{B} = (X_{cg} - X_{cp_{wing}})\left[0\, , -F_{N_{wing}}\, , 0\right]^{T} \quad (25)$$

Running this model on Simulink to test the preliminary design parameters. In Fig. 12 the summary of the mathematical model written on Simulink.

The next Fig. 13 is for the altitude simulation in two different initial conditions: from the earth surface and from the balloon altitude 30 km. This plot is the Simulink Model response. The launch from the balloon altitude saves the power waste to overcome the aerodynamic forces, so the rocket can ascend twice the altitude it can reach from earth surface.

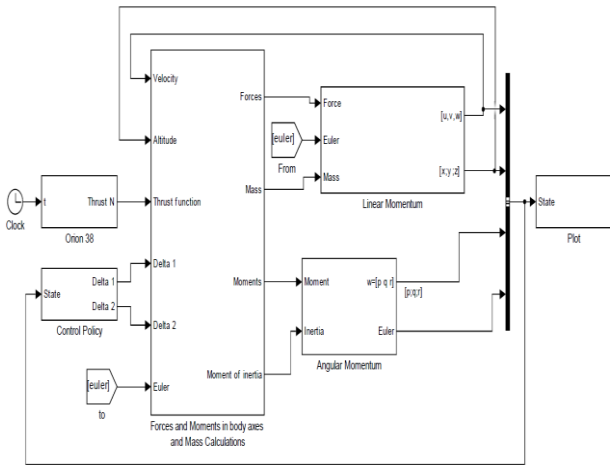


Figure 12. Simulink Model of the Rocket

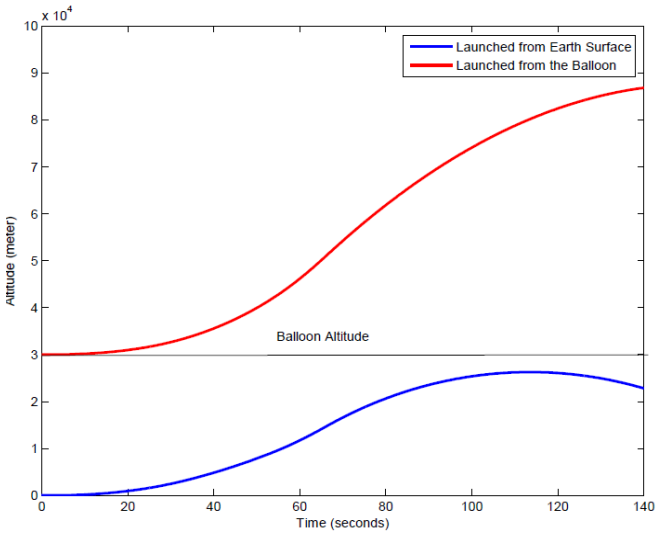


Figure 13. Altitude simulation for launch from Earth Surface and From the Balloon

5.2. **Trajectory Optimization**

The rocket detaches from the Balloon with initial orientation to fall under the balloon and ignite the motor after reaching a certain distance. The trajectory starts from these initial conditions and ends by reaching a steady state where the rocket is moving exactly in the opposite direction of the falling debris to eject the explosive charge. After the ejection the rocket leaves this trajectory flying with another trajectory to a landing location using the remaining thrust and control surfaces in the wing.

Several trajectory optimization algorithms have been surveyed to end up with Direct Trajectory Optimization Algorithm Using Collocation and Nonlinear Programming [9],[11]. This algorithm reduces the state variables to piecewise cubic polynomials and employs piecewise linear interpolation to control inputs. The

dynamics has to be satisfied at every node between the piecewise polynomials and collocation points at the half distance between the nodes. Thus, the optimization problem is formulated as follows:

Decision parameters for N nodes:

$$\underline{D} = [S_1\ S_2\ \dots S_N\ U_0\ U_1\ \dots U_N], \qquad (26)$$

As State vector:

$$S = \left[\underline{X}^i\ \underline{V}^B\ \underline{\Theta}\ \underline{\omega}^B\right] \qquad (27)$$

And input vector:

$$U = [\tau_1\ \tau_2] \qquad (28)$$

Decision parameters are chosen to minimize a cost function:

$$\min_{\underline{D}} \sum_{i=0}^{N-1} g(S_i, U_i) \qquad (29)$$

Such that $\forall i$
The rocket dynamics at the nodes:

$$S_i' = f(S_i, U_i) \qquad (30)$$

And the dynamics at the collocation points:

$$S_c' = f(S_c, U_c) \qquad (31)$$

With boundary constraints on the states and inputs:

$$D_l \le D \le D_u \qquad (32)$$

The inequality constraints on the decision parameters enable searching for optimal trajectory over the limits on the states and control inputs like the initial or final conditions, in addition to the actuators saturation. It is more than constraints on the initial or final conditions, so it can be on any state in between to force the trajectory to pass through.

For instance, hunting a vertically falling debris at position:

$$\underline{X}_{target} = [50e3, -400, 400]^T$$

$$\underline{V}_{target} = [-C, 0, 0]^T$$

We can solve this feasibility problem i.e. without objective function that has the following constraints:

- Initial constraints:

$$\underline{X}_0 = [30e3, 0, 0]^T,\ \underline{\Theta}_0 = [0, -45^0, 0]^T,$$

$$\underline{v}_0 = [-u_i, 0, 0]^T,\ \underline{\omega}_0 = [0,0,0]^T \text{ and } \underline{\delta}_0 = [0,0]^T$$

- Final constraints:

$$\underline{X}_f = [30.5e3, -400, 400]^T,\ \underline{\Theta}_f = [0,0,0]^T,$$

$$\underline{v}_f = [u_f, 0, 0]^T \text{ and } \underline{\omega}_f = [0,0,0]^T$$

- States limits along the trajectory (the thrust vectoring limits):

$$-5^0[1,1]^T \le \underline{\delta} \le 5^0[1,1]^T$$

- Inputs limits along the trajectory:

$$-2[1,1]^T \le \underline{\tau} \le 2[1,1]^T \quad \text{RPM.}$$

This example is solved by a sequential quadratic programming solver implemented in MATLAB and using an open source code Drake System [12] ,[10]. The results are shown in Fig. 14

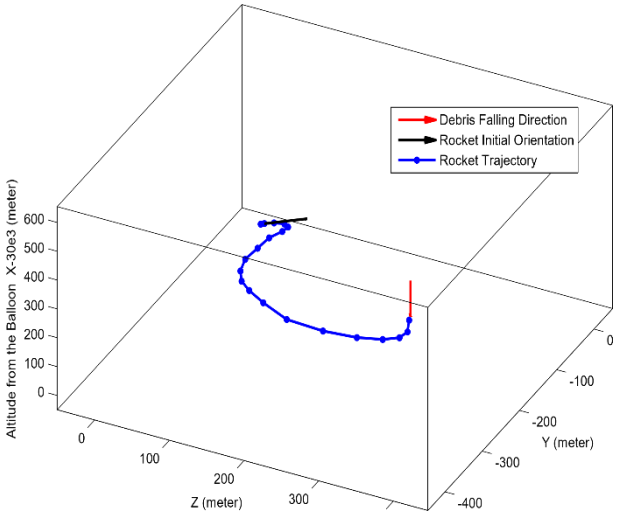


Figure 14. The trajectory produced by direct trajectory optimization using collocation and nonlinear programming

5.3. **Trajectory Stabilization with time- varying LQR**

The model used to optimize trajectories is simplified to a non-variant mass and thrust system. This simplification reduces trajectory optimization time on a personal computer to about 30 seconds. However the process of trajectory optimization produces an open loop policy for control inputs. Thus, the trajectory of the variant mass and thrust model diverges from the nominal trajectory. Surprisingly, designing linear feedback policy along the trajectory can deal with disturbances from mass and thrust varying. Moreover, this policy forces trajectories that start from other initial

conditions near to the nominal trajectory to converge to the final objective.

The feedback policy used is a time varying linear quadratic regulators tv-LQR. The collocation direct trajectory optimization algorithm produces a nominal trajectory of states and inputs: $[S_{nom}\ , \mathrm{U_{nom}}]$. The plan is to linearize the dynamics along this nominal trajectory $[S_{nom}\ , \mathrm{U_{nom}}]$ to have a time varying linear model that can be used to tune a time varying LQR controller along the nominal trajectory as follows:
Linearize the nonlinear dynamics $S' = f(S, U)$ along the nominal trajectory so,

$$S' = f(S_{nom}, U_{nom}) + \frac{\partial f(S_{nom}, U_{nom})}{\partial S}(S - S_{nom}) + \frac{\partial f(S_{nom}, U_{nom})}{\partial U}(U - U_{nom}) \quad (33)$$

Thus,

$$\bar{S'} = A(t)\,\bar{S} + B(t)\,\bar{u} \quad (34)$$

The objective of LQR is to minimize the quadratic cost function:

$$\min_{\bar{u}} \int_0^{tf} (\bar{S}^T\ Q(t)\ \bar{S} + \bar{u}^T\ R(t)\ \bar{u}\ )\ dt + \bar{S}^T\ \ Q_f(t)\ \ \bar{S} \quad (35)$$

Where the matrices $Q = Q^T \succcurlyeq 0\ ,\ R = R^T \succ 0\ , Q_f = Q_f^T \succcurlyeq 0$ are chosen as tuning gains. This cost has a closed form solution: Riccati differential equation [10],[14] That can be solved numerically to get:

$$U = U_{nom} - k(t)\,(S - S_{nom}) \quad (36)$$

For instance, choosing $Q, R\ , Q_f$ to tolerate certain accepted error as follows:

Q: is a $R^{14\times14}$ diagonal matrix with the following weights on the diagonal: $\left[\frac{1}{2^2}, \frac{1}{2^2}, \frac{1}{2^2}, \frac{1}{6^2}, \frac{1}{6^2}, \frac{1}{6^2}, \frac{1}{0.0785^2}, \frac{1}{0.0785^2}, \frac{1}{0.0785^2}, \frac{1}{0.0524^2}, \frac{1}{0.0524^2}, \frac{1}{0.0524^2}, \frac{1}{0087^2}, \frac{1}{0087^2}\right]$

R: is a $R^{2\times2}$ diagonal matrix with the following weights on the diagonal: $\left[\frac{1}{0.0013^2}, \frac{1}{0.0013^2}\right]$

Q_f: is a $R^{14\times14}$ diagonal matrix with the following weights on the diagonal: $\left[\frac{1}{0.5^2}, \frac{1}{0.5^2}, \frac{1}{0.5^2}, \frac{1}{6^2}, \frac{1}{6^2}, \frac{1}{6^2}, \frac{1}{0.0175^2}, \frac{1}{0.0175^2}\ , \frac{1}{0.0175^2}, \frac{1}{0.0524^2}, \frac{1}{0.0524^2}, \frac{1}{0.0524^2}, \frac{1}{0087^2}, \frac{1}{0087^2}\right]$

Fig.15 shows the response of the mass and thrust time varying response due to the nominal input trajectory and the response to the feedback control policy. The robustness of the TV-LQR with trajectory optimization is impressive to suppress the perturbations from parameters varying. Moreover, in Fig. 16 the trajectory is robust even for different starting point.

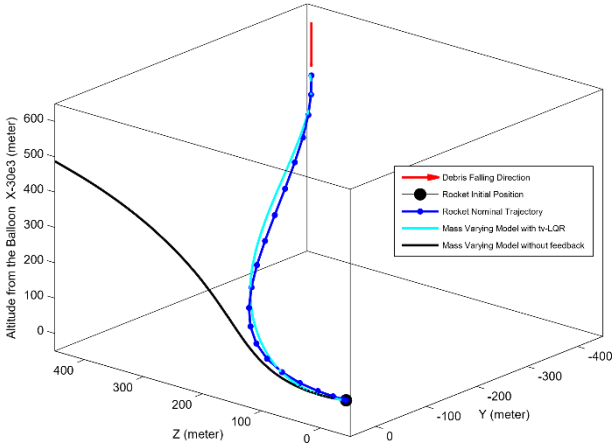


Figure 15. Comparison between the mass and thrust variant model response for by feedback and without

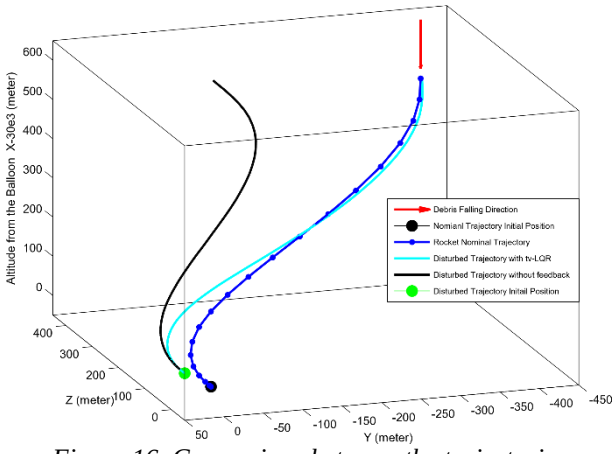


Figure 16. Comparison between the trajectories disturbed from initial point of the optimized trajectory

All trajectories start from certain space of initial conditions can be proved to converge to the nominal trajectory [14]. Out this region of attraction the rocket may lose robustness and convergence to the debris. In the future work this region of attraction will be obtained as a measure to robustness and stability.

6. RECOVERY SYSTEM

Once approaching the landing site, the gliding control surfaces will work on getting the rocket in an aerodynamic stall, this will increase the turbulence therefore slowing down the rocket's horizontal velocity and get it ready to deploy the parachutes.

As we can't guarantee the horizontal velocity will decay till it approaches zero, dual deployment technique will be implemented. The dual deployment technique is widely used in sounding rocket's recovery parachutes and even sky diving parachutes, this technique depends

on using two parachutes, a drogue parachute which is relatively small in size and simple in design is ejected first with a high decent rate, this parachute has a smaller area therefore won't produce that much drag, however this is the main design point as it will be deployed at high velocities which a conventional parachutes would be torn apart if deployed at such conditions.

Drogue parachutes may also be used to help stabilize direction of flight, the drogue parachute is often used to gain control of very fast descents, also one of the main advantages of this technique is to avoid drifting before opening the main parachute. Side winds could cause drifting and change the landing site causing extensive damage to the rocket or parachutes.

The first event – drogue parachute deployment – occurs at the moment the rocket approaches the landing site rocket falls down fast and there is no large drag due to the small drogue parachute area that wind can push into, also the drift is low by then. Once the rocket reaches the predetermined altitude a main parachutes will be deployed.

Due to our simple design and to avoid using a large parachute, we will be using also a Parachute cluster system as our main recovery parachute. Parachute clusters system is developed to avoid the use of excessively large single canopies. A practical limit for the utility of single round canopies is approached, a cluster of parachutes have a number of benefits over a large single canopy, this include the ability to rig and manufacture the system. Clusters also have the advantage of backup protection, this is evident when a single cluster parachute failure is considered. The system under a smaller subset of the canopies still has a lower impact velocity than a free fall.

Clustering permits use of the same type of parachute for a large range of weights in addition to providing a stable descent system even when using individual, high-drag, unstable parachutes, parachute cluster has a shorter filling time than a single large parachute.

After the second event occurs – cluster parachutes deploy – the rocket will reach its decent velocity which is safe enough for landing all the rocket components in a ready to fly condition. The drift rate during this phase is significant but as the rocket is already at a very low altitude the overall drift does not presents a significant problem for the rocket recovery. However working on a solution for this problem we have been analyzing and calculating the specific time needed for a the parachutes to fully extend and start functioning to limit the decent time with a fully extended parachutes as much as we can to avoid any drift and allowing us to land even in extreme high wind conditions.

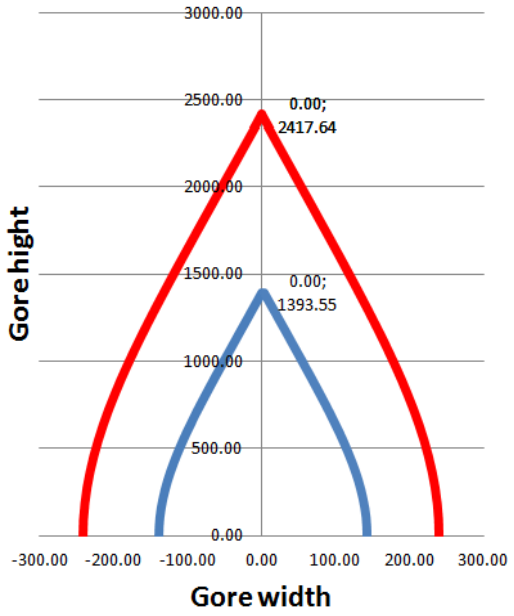
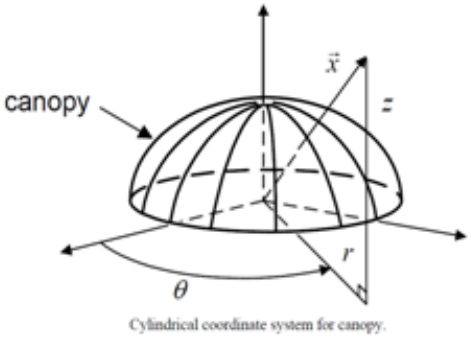


Figure 17: Cluster parachute (in blue) gore dimensions compared to one main parachute (in red) gore dimensions.

Parachutes design:

The net vertical external force for a descending rocket F is equal to the difference between the drag D and the weight W.



Cylindrical coordinate system for canopy.

Figure 18: Canopy design

$$F = D - W \quad (6\text{-}1)$$

Where $$D = C_D \, \rho \, v^2 \, \frac{A}{2} \quad (6\text{-}2)$$

The required parachute area which achieve the required decent rate determined from

$$S = \frac{2\,m\,g}{\rho\ C_d\ V^2} \quad (6\text{-}3)$$

$$D = 2\sqrt{\frac{S}{\pi}} \quad (6\text{-}4)$$

Where, D is the parachute diameter, S is the area of the parachute g is the acceleration due to gravity, m is the mass of the rocket and parachutes, ρ (Greek letter "rho") is the density of air at current, C_D is the coefficient of drag which is dependent on the chute and V is the descent rate.

Each canopy in the cluster will experience less than the drag that would be experienced by the equivalent single canopy at the same descent velocity. This reduction in drag is attributable to the shape about which clustered parachute systems oscillate. Each canopy in the cluster is most often positioned at some angle of attack to the trajectory path of the system, which reduces the drag produced by each canopy. The optimization of a cluster configuration can result in a trade-off between the overall height of the system, which affects the opening time, etc., to the lengths used for the risers.

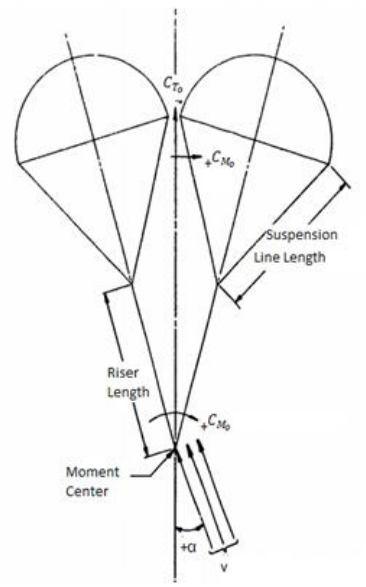


Figure 19:Parachute cluster design

Effective cluster line length (L_{e_c}) is calculated as follows

$$L_{\theta c} = D_o\sqrt{n} \quad (6\text{-}5)$$

Where n is the number of parachutes in the cluster.

In equilibrium descent, parachutes descend at a constant dynamic pressure q

$$q = \frac{\rho\ v^2}{2} \quad (6\text{-}6)$$

For velocity given in indicated air speed, dynamic pressure q can be calculated to

$$q = \frac{v^2}{x} \quad (6\text{-}7)$$

Where x =1013.1 for velocity in km/h dimensions.

Tangential force coefficient (C_{T_o}):

$$C_{T_o} = \frac{mg}{q(\sum_{i=1}^{n} S_{O_i})} \quad (6\text{-}8)$$

Moment coefficient (C_{M_o}):

$$C_{M_o} = \frac{M}{nq(\sum_{i=1}^{n} S_{O_i})\,(\sum_{i=1}^{n} D_{O_i})} \quad (6\text{-}9)$$

the drag coefficient (C_{D_o}):

$$C_{D_o} = \frac{W}{q(\sum_{i=1}^{n} S_{O_i})} \quad (6\text{-}10)$$

$$S_o = \frac{\pi\,{D_o}^2}{4} \quad (6\text{-}11)$$

Where S_o = canopy surface area

For a given system weight, W_T. a required rate of descent, V the required nominal parachute diameter is

$$D_o = \sqrt{\frac{2.547\ W_T}{C_{D_o}{v_e}^2\rho}} \quad (6\text{-}12)$$



Figure 20: Parachute CAD

Gore design

As a more efficient and proper parachute is one where the deployed canopy takes on the shape of a hemisphere. To form a parachute that deploys as a hemisphere, it is necessary to take the desired three dimensional hemispherical shapes and divide it into a number of two dimensional panels, called gores. Each gore is individually cut to a specific shape so that when re-assembled it will form a hemisphere upon deployment.

$$H = \text{height up the gore plan.} = (\pi \ D \frac{x}{360}) \quad (6\text{-}13)$$

$$W = \text{gore width} = (\pi \ \frac{D}{N} \ \cos(x)) \quad (6\text{-}14)$$

Where,
D = diameter, N = number of gores, x= any value between 0 and 90 where zero is the bottom edge of the gore and 90 is the point.[8]

In practice, because there are a finite number of shrouds under tension and the fact that the shroud lines converge at a common central point directly below the canopy this means that the parachute canopy that results will still not be quite a perfect hemisphere since it comprises a relatively small number of two dimensional gores. A closer to perfect result can be achieved by constructing a parachute with more gores. However more gores equals more sewing for assembly and for purposes true perfection in the parachute canopy profile is not absolutely required

Parachute stability

Parachute stability is enhanced if a hole is provided in the top of the parachute canopy. The disconcerting hole in the top of the parachute canopy is called an apex vent. Before the apex vent, the only way that the air trapped underneath the parachute could escape was to spill out from one edge of the canopy, thereby tilting it and throwing the hapless parachutist to one side.
As the canopy swung back, more air would spill out from the opposite side, setting up a regular, pendulum-like oscillation. As you can imagine, hitting the ground during a downswing was understandably hazardous, especially if it was also a windy day.

The apex vent, by allowing the air to leak slowly out of the top of the parachute canopy, prevents this wild oscillation and makes for much safer landings. Another benefit of the apex vent is that it slows down the opening of the parachute. Without the vent, air inflates the canopy much more abruptly, and it can damage the parachute, of course too large a hole will reduce the drag to a low level negating the purpose of having the parachute in the first place.

Stability is also noticeably enhanced if the shroud lines are made longer below the canopy and conversely stability is reduced if they are shortened. A good starting point for shroud line length is for the shroud length below the lower perimeter of the canopy to be at least equal to the diameter of the deployed parachute canopy.



Figure 21: Parachute and shroud lines design and Parachute model test using a sounding rocket

Clustered parachute systems have excellent stability characteristics compared to most single-canopy systems. This is partly because of the terminal descent shape of multiple bluff bodies versus a single bluff body. There are some undesirable features of parachute clusters, which include the difficulty in obtaining a time-sequenced opening of all canopies together. This phenomenon is known as "lead lag," in which one canopy opens quicker than the next canopy. This generally forces the individual parachutes in the cluster to be stronger than would be needed for a consistent opening of all canopies together. Another disadvantage of parachute clusters is that Parachute clusters in which individual parachutes have long reefing times, Parachute clusters experience a reduction in drag because of interference and systems geometry.

Dynamic contact phenomena that can be experienced in parachutes and parachute clusters present an important challenge and current barrier in parachute modeling efforts. Contact can occur between gores in a single canopy and between different canopies in a Parachute cluster. In each situation, contact algorithms are necessary to prevent penetration between surfaces in our parachute structure.

7. CONCLUSIONS AND FUTURE WORKS

The paper presents the design, simulations and analysis of the rocket segment of the Combined Launch System, the overall mission concept is illustrated including a detailed design of the rocket with sizing of all the components including the engine study and choice and

the control system detailed analysis in addition to the trajectory study and optimization.

The rocket is supposed to carry an explosive charge to target unburnt space debris that is not desirable to fall back to Earth, such components like rocket nozzles and fuel tanks are made from special material that won't burn upon re-entry, also being mostly toxic and falling at very high speeds is making their destruction a must before they approach the Earth's surface.

From a Research and Development prospective the true benefit from this concept lies on eliminating a danger of a falling object from space and also at a very low cost compared to other space platforms. The reusability of the rocket introduces a great budget reduction that will help opening a new simple aspect of reaching higher altitudes in general, The rocket is a part of a system that aims to reach the near-space at the lowest costs for various scientific applications.

Developing this concept and improving the design performance will continue in the future, with an experimental fluid analysis to verify the computational results and more investigations for the required components and adapting the design to fit the concepts of simplicity of both manufacturing and operation. Also we are in the process of refining our solutions and improving its quality to make sure we reach the best results before our test flight.

8. REFERENCES

[1] Anon, Orbital Debris Quarterly News, vol. 16, p. 8, April 2012.

[2] Hamed Gamal, " Combined Launch System: a new concept to reduce the launch costs for Micro (Cube) Satellites and Debris hunting probes", 5th CEAS Air & Space conference, September 7-11, 2015, Delft, Netherlands.

[3] Barrowman, J. S., Fan, D. N., Obosu, C. B., Vira, N. R., and Yang, R. J., "An improved Theoretical Aerodynamic Derivatives computer program for sounding rockets", Sounding Rocket Technology Conference, 5th, Houston, Tex., March 7-9, 1979, Technical Papers. (A79-25751 09-12) New York, American Institute of Aeronautics and Astronautics, Inc., 1979, p. 111-120.

[4] Barrowman, J. S., "The practical Calculations of the Aerodynamic Characteristic of Slender Finned Vehicles", M.S. Dissertation, The Catholic University of America, March 1967.

[5] Pitts, W. C., Nielsen, J. N., and Kaattari, G. E., "Lift and Center of Pressure of Wing-Body-Tail Combinations at subsonic, Transonic, and Supersonic Speeds". NACA Report 1307,1959.

[6] Mandell, Gordon K, Caporaso, George J and Bengen, William P. Topics in Advanced Model Rocketry. s.l. : MIT Press, 1973.

[7] Box, Simon, Bishop, Christopher M and Hunt, Hugh. Estimating the dynamic and aerodynamic parameters of passively controlled high power rockets for flight simulation.

[8] Kenji Takizawa "Multi-scale methods for gore curvature calculations from FSI modelling of spacecraft parachutes"

[9] Hargraves, C., and S. Paris. "Direct trajectory optimization using nonlinear programming and collocation." Journal of Guidance, Control, and Dynamics 4 (1986): 121.

[10] Russ Tedrake. "Underactuated Robotics: Algorithms for Walking, Running, Swimming, Flying, and Manipulation" (Course Notes for MIT 6.832). Downloaded in Fall, 2014 from http://people.csail.mit.edu/russt/underactuated/

[11] Betts, John T. "Survey of numerical methods for trajectory optimization." *Journal of guidance, control, and dynamics* 21.2 (1998): 193-207.

[12] Russ Tedrake. "Drake: A planning, control, and analysis toolbox for nonlinear dynamical systems",2014 http://people.csail.mit.edu/russt/underactuated/

[13] Tewari, Ashish. *Advanced control of aircraft, spacecraft and rockets*. Vol. 37. John Wiley & Sons, 2011.

[14] Moore, James, and Russ Tedrake. "Control synthesis and verification for a perching UAV using LQR-Trees." *Decision and Control (CDC), 2012 IEEE 51st Annual Conference on*. IEEE, 2012.

[15] S. Box, C. Bishop, and H. Hunt. Estimating the dynamic and aerodynamic properties of small rockets for flight simulations. Technical Report, available online at http://cambridgerocket.sourceforge.net/, 2009.

SESSION 9: H - Students Research

(Friday 11th - 17.30)

Chairman: Prof. Alessandro Francesconi

CONVECTIVE HEAT TRANSFER MEASUREMENTS AT THE MARTIAN SURFACE

A. Soria-Salinas[1], **M.-P. Zorzano**[1,2], **and J. Martn Torres**[1,3]

[1]*Division of Space Technology, Department of Computer Science, Electrical and Space Engineering, Luleå University of Technology, 98128 Kiruna, Sweden*
[2]*Centro de Astrobiologa (INTA-CSIC), 28850 Madrid, Spain*
[3]*Instituto Andaluz de Ciencias de la Tierra (CSIC-UGR), 18100 Granada, Spain*

ABSTRACT

We present a new sensing method to characterize the convective wind activity on the surface of Mars. This method is based on the use of three rods that monitor the air temperature, and can provide information about the wind speed, direction and temporal oscillations. The sensor monitors the heat transfer coefficient h of the sensing element, on a Mars surface spacecraft. This sensing method will be implemented in the HABIT (HabitAbility: Brines, Irradiance and Temperature) instrument which has been included as scientific payload for the future ExoMars 2018 (ESA-Roscosmos) Surface Platform.

The method is based on the use of three Air temperature Sensors (ATS) placed at three different positions with different orientations. Each ATS consist of a rod with three Resistance Temperature Thermodetectors (RTD) which measure the temperature of this fin at 3 different locations along the axial direction. The thermal profile of this fin depends on the convective heat transfer with the Martian atmosphere and on the exposure to the local wind. It also depends on the temperature and density of the fluid. Under certain approximations the thermal profile of each fin can be analytically solved. By measuring simultaneously the three temperatures of the rod, the method retrieves the fluid temperatures T_f and an average adimensional parameter. This method has already been used on the Rover Environmental Monitoring Station (REMS) that has been operating now for three years on board the Mars Science Laboratory, on the surface of Mars. In this work we show in which way the m parameter is related to the heat transfer coefficient h. Given that h is dependent on the local forced convection, it can be used to characterize the Mars surface wind.

In this preliminary study a computational fluid dynamics code is used to illustrate the method. We obtain numerical results of the convective heat transfer h and m parameter for different wind speeds. The results are compared with the predictions based on theoretical calculations. The different values of each ATS when exposed to the same wind flow can be used to retrieve information about the orientation of the wind.

Key words: Mars; HABIT; Heat Transfer.

1. INTRODUCTION

Over the last fifty years the exploration of Mars has been an strategic research field of the space exploration programs. It was in the 60s when the first soviet probes and the successful NASA probe *Mariner 4* were sent to the red planet. In 1975 the NASA missions *Viking 1* and *Viking 2* achieved the first steps into the search of organic life on the Martian surface through the landers *Viking I* and *II* respectively.

Nowadays, and in continuation of the search for habitability on Mars, on board the NASA *Mars Science Laboratory* (MSL), the *Rover Environmental Monitory Station* (REMS) instrument is designed to characterize the environment of the Martian boundary layer. This station has now been on operation for more than three years. It consists of a Wind Sensor (WS), Ground Temperature Sensors (GTS), Air Temperature Sensors (ATS), Relative Humidity Sensor (RHS), Ultraviolet Sensor (UVS) and a Pressure Sensor (PS).

In the near future there is a new mission to Mars: the ESA-Roscosmos *ExoMars* program, which will consist on two missions, the *ExoMars 2016* and the *ExoMars 2018*. While the first one will consist of the *Trace Gas Orbiter* (TGO), and the *Entry, Descent and Landing Demonstrator Module* (EDM); the second one will carry a *rover* inside a *lander* to the Mars surface, becoming the first ESA mission which achieve landing on Mars surface.

Just recently, the HABIT (*HabitAbility: Brines, Irradiation and Temperature*) project has been approved as scientific payload for the *Surface Platform* of *ExoMars 2018*. This project has the aim of characterizing the habitability of the Martian surface in terms of temperature, UV irradiation and water availability. In order to complete this task, the instrument includes three ATS sensors similar to ones already implemented on REMS, six UVS, and the BOTTLE (*Brine Observation Transition To Liquid Experiment*).

The use of the ATS sensors as a proxy for wind activity is a novel application, and it is based on the use of an intermediate value that is measured by each ATS, the *m* parameter.

In this work we show in which way the m parameter is related to the heat transfer coefficient h. Given that h is dependent on the local forced convection, it can be used to characterize the Mars surface wind.

In this preliminary study a computational fluid dynamics code is used to illustrate the method.

2. M-MODEL

In this section we shall first present the architecture of the ATS sensors located on the HABIT instrument. The governing equations describing the physical problem are then presented and finally, the assumptions and approximations of the problem are described.

2.1. ATS sensors

Each of the three HABIT-ATS sensors consists of a rod made of FR4. This material has a low thermal conductivity which minimizes the thermal contamination from the platform and computing unit of HABIT. At the same time, the rod presents three Minisens RTD Thermistors, a type of PT-1000 Class A, bonded to it, which makes possible to measure the temperature at three different points. The measurements are taken at the base T_b (which is supposed to be in equilibrium with the HABIT structure temperature), an intermediate point T_{Ln} along the rod, and the extreme of the last one, T_a. These thermistors have been selected due their robustness, accuracy and excellent time response. Each ATS fin consists a FR4 rod of 35 mm long with a cross-section of 2 x 3 mm whose three points of measurement allow for obtaining the temperature profile along them as well as the fluid temperature T_f around by using these three known temperatures. Given the HABIT configuration, the three ATS sensors are located in a horizontal plane, two of them in the same line and opposite direction, and the third one perpendicular to this line.

2.2. The governing equations and assumptions

In order to approximate the ATS geometry and model the problem, the sensors are considered as horizontal cylindrical rods. It simplifies the analysis without losing generality on it. Regarding the energy balance equations, it has also been considered that the rod is length enough to disregard the heat loss from the tip. The temperature at each cross section along the rod is considered uniform, which gives as a result that the heat transfer along the rod is one dimensional.

The cylindrical rods considered, which emulate the ATS sensors, have their bases coupled to the HABIT structure at a constant temperature T_b and are exposed to a fluid (the Martian air) current with a temperature of T_∞ in the far field of the rod surface. The steady-state equation describing the heat flux balance along a differential element of the rod with one dimensional conductive heat transfer, and convective and radiative heat transfer on the envelope of the rod, can be written as (1).

$$\underbrace{\dot{Q}_x - \dot{Q}_{x+dx}}_{conduction} \quad \underbrace{-d\dot{Q}_{loss}}_{convection+radiation} = 0 \qquad (1)$$

By using the expressions for each of the heat transfer modes, the equation (1) results (2):

$$\underbrace{\frac{d}{dx}\left(\kappa A_c \frac{dT}{dx}\right)}_{conduction} \underbrace{- h_c \frac{dA_s}{dx}(T - T_\infty) - \varepsilon\sigma \frac{dA_s}{dx}(T^4 - T_\infty^4)}_{convection+radiation} = 0 \qquad (2)$$

where h_c is the convective heat transfer coefficient, κ the rod conductivity, A_c the rod cross-section area, A_s the lateral surface area of the rod, ε the emissivity of the rod and σ the Stefan-Boltzmann constant. Let us mention that h_c, ε and κ are not constant along the rod length. In this study both the conductivity κ and emissivity ε are considered as constant values with no temperature dependencies. The h_c coefficient depends on the local surface temperature. Later on, an average value will be derived.

By assuming that the radiative term could be expressed in a similar way to the convection term, the total heat transfer coefficient for both radiation and convection h can be written as follows (3):

$$h = h_c + h_r = h_c + \varepsilon\sigma(T^2 + T_\infty^2)(T + T_\infty) \qquad (3)$$

where h_r would be the radiative equivalence of the convective heat transfer coefficient. Including this total coefficient to the heat flux balance equation, (1) can be expressed as (4):

$$\frac{d^2\theta}{d^2\chi} - m_\chi^2(\chi, \theta, T_f)\theta = 0 \qquad (4)$$

where $\theta = T_x - T_f$ is the difference between the temperature at a position x of the rod, T_x, and the temperature of the fluid, T_f; $\chi = x/L$ the dimensionless axial coordinate of a rod of length L; $m_\chi = L\sqrt{4h_\chi/\kappa D}$. Here h_χ is the total heat transfer coefficient at χ and D the diameter of the cylinder whose cross-section area is equal to 2 x 3 mm , D = 2.76 mm .

The two boundary conditions are also needed to define the thermal profile along each one of the ATS sensors. The temperature at the rod base is known, given that it is considered in equilibrium with the HABIT structure to which is bonded (5).

$$\theta|_{\chi=0} = \theta_b \tag{5}$$

Finally the boundary condition at the tip of the rod is defined by the energy balance at this point. However, due to the small rod cross-section compared to its longitude, it can be assumed that the heat flux through the tip is negligible in comparison with that one presented along the rod surface. Consequently, the second boundary condition results (6):

$$\frac{d\theta}{d\chi}|_{\chi=1} = 0 \tag{6}$$

The analytical solution to this problem is exact and it is given by the following expression (7):

$$\theta(\chi) = \theta_b \frac{cosh(m(1-\chi))}{cosh(m)} \tag{7}$$

It has to be emphasized that here, both the total heat transfer coefficient and the parameter $m = \sqrt{4h/\kappa D}$ represent average values over the length of the rod. The shape of this thermal profile in the absence of forced convection, under Earth ambient conditions, has been experimentally confirmed using a long conducting bar, fixed to a controlled temperature and exposed to ambient conditions (in the limit $m \to \infty$, i.e. when either $L \to \infty$ or $h \to \infty$ or $\kappa \to 0$) [1].

2.3. Retrieval method

The retrieval method proposed is based on the application of this boundary-value problem to each one of the three ATS sensors located on the HABIT instrument. Furthermore, this measuring process has been implemented and validated on the REMS-ATS. In this sensor as in HABIT, measurements are taken at 1 Hz ratio during 5 minutes at the beginning of each hour.

Using the analytical solution previously obtained, and given that the three thermistors located at each ATS provides simultaneously and in real time the temperatures at the base of the rod, T_b, at an intermediate point at $x = L/n$, T_{Ln} (where n is a number of subdivisions of the rod), and at the free extreme, T_a, then the following system of equations applies (8, 9):

$$(T_a - T_f) = (T_b - T_f) \frac{1}{cosh(m)} \tag{8}$$

$$(T_a - T_f) = (T_b - T_f) \frac{cosh(m(1-\frac{1}{n}))}{cosh(m)} \tag{9}$$

Using the three simultaneous temperature measurements T_b, T_{Ln} and T_a, this system of two equations with two unknowns, T_f and m, can be solved. This gives the fluid temperature and an m parameter. This m varies in time, depending on the action of the air and wind and it represents an average over the length of the rod of all the physical processes exposed above.

The validity of this model under forced convection and Martian atmospheric conditions will be verified at the wind tunnel facility at Luleå University of Technology.

3. NUMERICAL CALCULATION

In this preliminary study a computational fluid dynamics code is used to illustrate the method. We shall obtain numerical results of the convective heat transfer h and m parameter for different wind speeds. The results are compared with the predictions based on theoretical calculations. Here we will show how the different values of each ATS when exposed to the same wind flow can be used to retrieve information about the orientation of the wind. This study has been performed with ANSYS 16.0, including the *Design Modeler*, *Workbench Meshing*, *Fluent* and *CFD-Post* modules.

3.1. Geometry model

With the purpose of achieving a model for the ATS sensors scenario on Mars surface onboard the $SurfacePlatform$ of the $ExoMars2018$ mission, the numerical simulation has started with a geometry model which locates the HABIT in one of the lander legs (one of the two locations proposed). The leg has been simplified as a vertical pole, in order to reduce the mesh complexity. This does not affect the results of this study. The fluid flow has been investigated with different angles of incidence in relation to the HABIT axial orientation. As the ATS model are concerned, they have been designed with a diameter $D = 5\ mm$ and a longitude $L = 42\ mm$. A general view of the configuration can be visualized at the Figure 1.

3.2. Physical model

A correct modeling of the Mars surface atmospheric conditions is crucial to have a realistic description of the heat transfer process.

- **Fluid model**

  Regarding the modeling of the fluid dynamics problem, there are three dimensionless numbers that

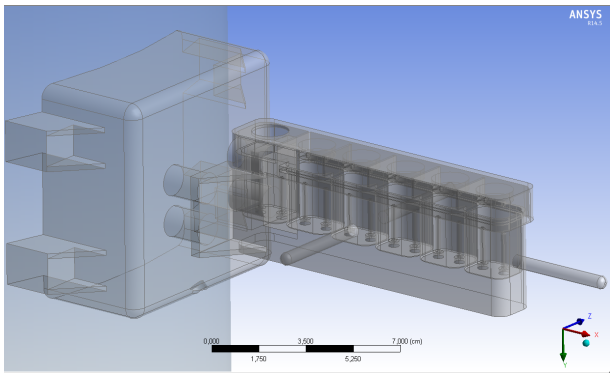


Figure 1. Geometrical configuration of the HABIT instrument, Design Modeler module, ANSYS 16.0.. The three ATS are placed at the front, and at each of the sides of the body of HABIT.

have to be specified. First of all, for the hydrodynamics of the flow around de ATS sensors, the Prandtl Number has to be concreted (10).

$$Pr = \frac{C_p(T)\mu}{\kappa_f(T)} \tag{10}$$

It quantifies the ratio between the viscous and thermal diffusion effects and depends on the CO_2 properties. In particular it depends on the temperature dependent heat capacity $C_p(T)$, the temperature dependent thermal fluid conductivity $\kappa_f(T)$, and the viscosity μ.

Equally important is the dimensionless Reynolds number, which quantifies the ratio between the convective and viscous terms (11).

$$Re = \frac{\rho v_{wind} L_c}{\mu} \tag{11}$$

In this case, the dimensionless number depends on the characteristic longitude under consideration within the fluid dynamic problem which is named L_c; the density of the fluid, ρ; and its viscosity and wind speed velocity, μ and v_{wind}. In this study we assume a wind with a given incidence angle within a horizontal plane β. For this case the longitude L_c is defined at this point as $L_c = D/cos(\beta)$. Given that the forced convection is analyzed over a cylinder exposed to an external flow, the reference for the characteristic longitude is the major axis of the elliptical section of the ATS cylindrical sensors. Regarding the air density, the flow is considered to be composed of pure CO_2 and its density is retrieved from the ideal gas equation. In addition, due to the low velocity studied, $v_{wind} = 1\ m \cdot s^{-1}$, the Mach number M is low enough ($M = 4.016 \cdot 10^{-3}$) to consider CO_2 as incompressible ideal gas. The density for the present simulations is taken as $\rho = 1.482 \cdot 10^{-2} kg \cdot m^{-3}$, which has been taken from the values measured by REMS on the Martian surface. The pressure will be also considered constant and equal to $720Pa$, as measured on sol 45 of the MSL mission.

Coefficient	Value
a_1	$4.45247158 \cdot 10^{2}$
a_2	1.69739101
a_3	$-1.34580010 \cdot 10^{-3}$
a_4	$4.64595961 \cdot 10^{-7}$
a_5	$-2.71480543 \cdot 10^{-11}$

Table 1. Coefficient for the CO_2 heat capacity polynomial form $C_p(T) = a_1 + a_2 \cdot T + a_3 \cdot T^2 + a_4 \cdot T^3 + a_5 \cdot T^4$ valid for a range of temperatures $T(K) \epsilon [200, 1000]$, and low pressures $P(mbar) \epsilon [1, 10^4]$ in $[J \cdot Kg^{-1}]$.

Finally, the third dimensionless number required to complete the fluid general characterization is the Nusselt number, Nu, which quantifies the ratio between the convective and conductive heat transfer through the fluid (12).

$$Nu = \frac{h_c L_c}{\kappa_f(T)} \tag{12}$$

As it can be appreciated, this dimensionless number depends on the convective heat transfer coefficient, an unknown of the problem exposed. For this reason, an experimental expression for a cylinder exposed to a normal fluid current [5] is going to be used. This is applicable to a wide range of Re and Pr numbers (13) as long as $Pr \cdot Re > 0.2$.

$$Nu = 0.3 + \frac{0.62 Re^{1/2} Pr^{1/3}}{\left[1 + \left(\frac{0.4}{Pr}\right)^{2/3}\right]^{1/4}} \left[1 + \left(\frac{Re}{282000}\right)^{5/8}\right]^{4/5} \tag{13}$$

Next the fluid parameters of heat capacity $Cp(T)$, conductivity κ_f and viscosity μ are defined. The heat capacity $C_p(T)$ and conductivity κ_f have been modeled with a temperature dependant polynomial form. Their respectives expressions and coefficients are shown in Table 1 [6] and Table 2 [7].

On the other hand, the viscosity μ has been modeled for a low pressure and temperature regime through the *Chapman-Enskog*'s Kinetic Theory [8], having been demonstrated to be a truly suitable approximation for polyatomic gases in this conditions.

Next the resulting values for a fluid temperature of $T_f = 250K$ are summarized in (Table 3).

- **Heat transfer**

  The problem modeled takes into account the conductive, convective and radiative heat transfer within the volume control analyzed.

Coefficient	Value
a_1	$-7.215 \cdot 10^{-3}$
a_2	$8.015 \cdot 10^{-5}$
a_3	$5.477 \cdot 10^{-9}$
a_4	$-1.053 \cdot 10^{-11}$

Table 2. Coefficient for the CO_2 conductivity polynomial form $\kappa_f(T) = a_1 + a_2 \cdot T + a_3 \cdot T^2 + a_4 \cdot T^3$ valid for a range of temperatures $T(K)\epsilon[185, 1670]$ and low pressures $P(mbar)\epsilon[1, 10^4]$ in $[W \cdot m^{-1} \cdot K^{-1}]$.

Coefficient	$C_p(T)$	$\kappa(T)$	μ
Unit	$[Jkg^{-1}K^{-1}]$	$[Wm^{-1}K^{-1}]$	$[\ Pa\ s\ ]$
Value	792.64	$1.300 \cdot 10^{-2}$	$1.297 \cdot 10^{-5}$

Table 3. Transport parameters values for a CO_2 current flow at $T_f = 250K$ and $P = 720Pa$.

As the conductive heat transfer is concerned, the structure has been divided in two solids in order to model the different conductivities that are representatives of the scenario. The structure has been separated into one part conformed by the Surface Platform leg and HABIT. For these simulations we assume an aluminium structure. The three ATS sensors are then modeled with FR4 material. In both cases, it has been taken into account the low pressures and temperatures characteristic of Mars surface. In addition to this, the Martian ground surface has been emulated with carbonate properties (emissivity, albedo, etc) , such as those that can be found on certain sites of Mars.

The convective heat transfer has also been included. The convective heat transfer coefficient h_c is calculated as follows (14):

$$h_c = \frac{\dot{q}_c}{T_s - T_\infty} \tag{14}$$

where $\dot{q}_c$ is the convective heat flux between the solid and fluid domains and T_s is the temperature at the solid surface.

Finally, for some cases, the radiative heat transfer has been included for comparison. It has been modeled taking only into account the IR region, which following the Wien lay has been enclosed in a representative $0.4 - 0.7\mu m$ band. The solar load has not been included in the study which is representative of a night-time scenario. Regarding the emissivity and absortibity of the surface platform and HABIT they have been modeled as covered by a standard space qualified white paint. The values for each type of surface used are showed in Table 4.

Surface	Emissivity ε	Absortivity α_r
Space Paint	0.88	0.2
FR4	0.9	0.3
Dolomite	0.9	0.5

Table 4. Radiative parameters for the radiative heat transfer model.

As the m parameter definition at (4) is concerned, this expression is the result of an averaged integration along a rod with a circular section. In the real case however, for the study of forced convection with a flow of arbitrary direction, there is an influence of the deviation angle β of the fluid flow. Because of this the fin cross section is, in general, elliptical. For this reason, the effect of this angle has been introduced in its definition as expressed in (15).

$$m_\chi = L\sqrt{\frac{[3(1 + cos(\beta)) - \sqrt{(3 + cos(\beta))(1 + 3 \cdot (cos\beta))}]h}{D\kappa}} \tag{15}$$

3.3. Study cases

After having exposed in general lines the physical model of the problem, this one has been numerically solved with different input parameters in order to compare them with the theoretical approximation. In other words, next we shall compare the convective heat transfer coefficients provided by the numerical solution with the ones derived from the fluid dynamics approximation which is based on the Nusselt number. The goal is to demonstrate that the values are of the same order of magnitude, and that they change with wind speed and orientation as expected. Several cases have been simulated with and without radiative heat transfer for a horizontal fluid flow at $T_\infty = 250K$ with a deviation angle of $\beta = 45^o$ and a range of inlet velocities v. The results are exposed in the next section.

4. RESULTS AND DISCUSSION

The summary of results obtained from the numerical solution of the problem is showed in Table 5. This study considers a range of inlet velocities where the laminar flow hypothesis is applicable. This is a requirement for the application of this theoretical expresion of the Nusselt number. The following notation has been chosen: the left sensor is that one which is orientated following $+Z$, and the right one, $-Z$ (see Figure 1).

Case	$v\ [ms^{-1}]$	ATS	$h_c\ [Wm^{-2}K^{-1}]$	m
		Left	2.7375	1.2559
1	0.5	Frontal	3.4820	1.4164
		Right	0.6860	0.6287
		Left	3.5745	1.4351
2	1.0	Frontal	4.7835	1.6602
		Right	0.9335	0.7334
		Left	3.5745	1.4351
3	1.5	Frontal	4.7835	1.6602
		Right	0.9335	0.7334
		Left	3.5745	1.4351
4	2.0	Frontal	4.7835	1.6602
		Right	0.9335	0.7334
		Left	5.3980	1.7636
5	2.5	Frontal	7.4055	2.0656
		Right	1.8675	1.0370
		Left	5.5980	1.7959
6	3.0	Frontal	7.4105	2.0663
		Right	2.2410	1.1363
		Left	6.3345	1.9104
7	3.5	Frontal	8.6765	2.2359
		Right	2.6205	1.2288
		Left	6.7390	1.9705
8	4.0	Frontal	9.2360	2.3068
		Right	2.9330	1.2999

Table 5. Summary of the results obtained from the numerical simulation for a incident wind flow with at $T_\infty = 250$. The radiative heat transfer is not included.

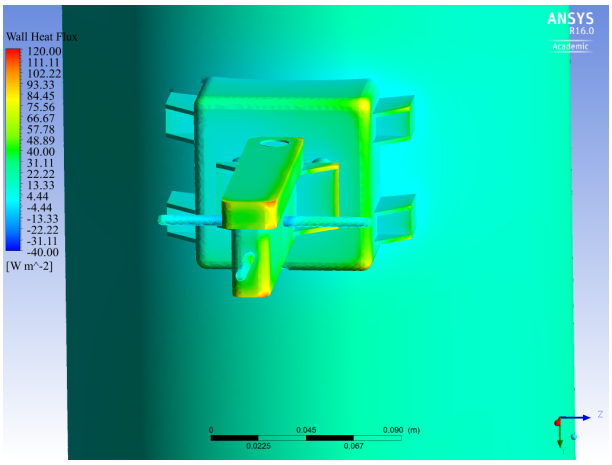


Figure 2. Solution for the convective heat fluxes distribution over the solid surfaces at the case 2 without radiative heat transfer. The minus sign indicates fluxes entering the solid from the fluid.

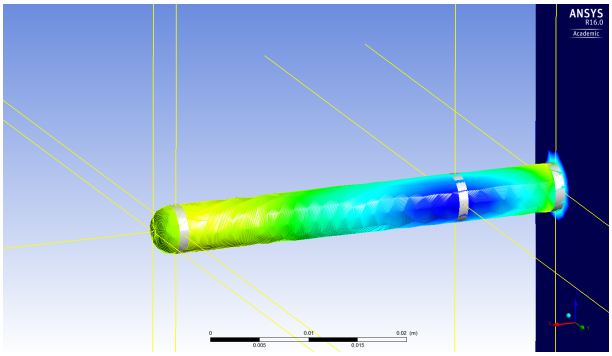


Figure 3. Ring section along each ATS rod. This sections are used to average the temperature and obtain the temperature that would be measured by an RTD placed there. The yellow cross marks the RTD locations at the base of the ATS fin, $1/4$ and tip .

Figure 2 shows the convective heat flux distribution over the surface of the solids for case 2 (without radiative heat transfer).

The heat transfer coefficients exposed in the Table 5 have been calculated taking into account the hypothetical temperature measurements that the RTD thermistors should provide as well as their locations. This is illustrated in Figure 3.

Consequently, each ATS provides three temperatures, T_b, $T_{1/4}$ and T_a, where the second one correspond to the point $\chi = 1/4$ of the rod length from its base and the last one has been located 2 mm before the end of the rod in order to better fit the ATS geometry. For this reason, the calculation of the convective heat transfer coefficient over each ATS sensor has been done by using these three points of measurement. In summary three measurement surfaces have been defined along the sensors, each one consisting of a ring in contact with the ATS sensor sur-

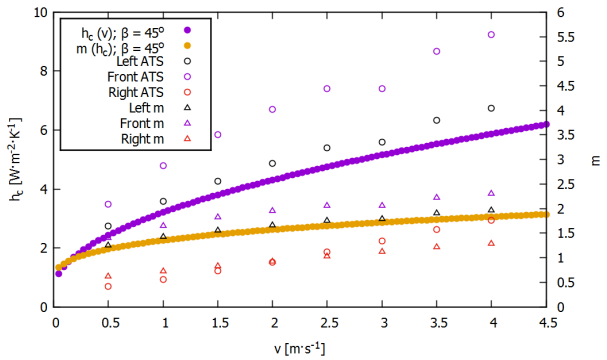


Figure 4. Variation with the incident air wind speed of the theoretical hc coefficient, m parameter and their respective numerical results for a deviation angle $\beta = 45^o$.

faces of $1\ mm$ long following the axial direction, in order to quantify the convective heat flux through them. The heat fluxes and surface temperatures of each location h_{ci} and T_{si} have been averaged over each surface ring. After that, in case of h_c coefficients, the values provided by Table 5 for each ATS are the average value between the $1/4$ point ring and the tip ring (i.e. the average of those that are exposed to the fluid flow). The same procedure has been followed for the m parameter.

Figure 4 shows the comparison between the theoretical h_c coefficient and the numerical solution for a range of wind speeds of the incident flow (with the same angle of incidence). The variation of the m parameter is also included for comparison.

As it can be appreciated, both the numerical result and the theoretical model increase similarly with wind speed flow. In addition each ATS shows a different value, which depends on its position with respect to the incoming flow of air. In particular the ATS that is hidden, behind the HABIT box, shows the smallest convective heat coefficient (and m parameter). The order of magnitude of the numerical simulations and the theoretical model are also comparable.

As the convective heat transfer coefficient is concerned, the averaged value for each ATS sensor is represented together with h_c derived from the Nusselt number.

The differences can be mostly attributed to the assumptions of the model. It has to be noticed that the h_c coefficient has been obtained from a Nusselt number experimental expression conceived for a cylinder exposed to a normal and external flow. However, at the studied case, there is a deviation angle between the current direction and the ATS axial directions, which obviously make the approximation worse. For this reason, the reference dimension for the Re number and h_c coefficient has been the diameter of the elliptical cross section resulting. In addition to this, the derived h_c coefficient is a circumferentially averaged value, and not a surface averaged value, as previously mentioned. This has not been evaluated at the film temperature, which is unknown, but at the fluid

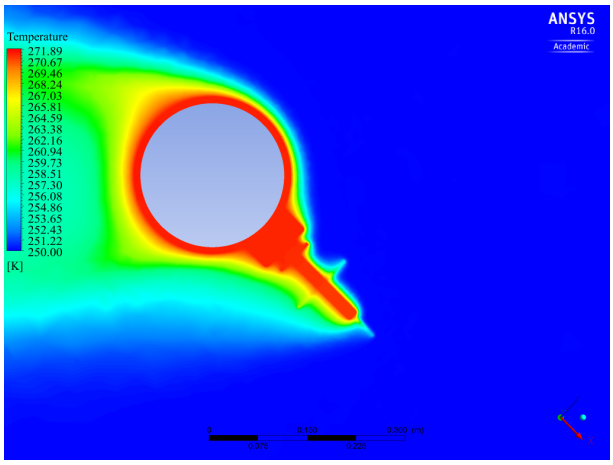


Figure 5. Horizontal section of the thermal wake for the case 2 without radiative heat transfer.

temperature instead.

On the other hand, from the numerical solution point of view, there are other hypothesis that add up. In this context, the h_c coefficient has firstly been averaged through surfaces that clearly do not present an uniform heat flux distribution. The strongest simplification is thus that the ATS heat flux problem is not actually one-dimensional and that furthermore many properties vary along the rods, and also in the other spatial directions. In addition to this, the method to estimate the h_c in each ATS from only two measurements is also a strong approximation, given that the evolution of the h_c coefficient over the rods is not linear, as can be seen in Figure 7.

In spite of all these assumptions, the results summarised in Figure 4, suggest that the h_c coefficient estimated for the left sensor is quite similar to the theoretical approximation. In other words, this ATS is better exposed to the ideal flow of free Martian air, which cannot be said from the other sensors. For the left ATS sensor, the current flow arrives without having been disturbed before, cooling the sensor in a close way to the ideal one. As the front sensor is concerned, it should be cooled in a similar way to the left one, maybe with a high h_c consequence of the lower temperatures at its further base from the platform. Nevertheless, in this case the fluid finds also the frontal HABIT surface, which is an obstacle that it must go around. It probably makes that the current is accelerated near the $1/4$ point increasing the heat flux locally and consequently incrementing the averaged heat transfer coefficient. Finally, for the right ATS sensor, it can be clearly observed that the tendency of its h_c coefficient is always lower than the one of the other sensors, confirming that it is not exposed to the flow of the wind. This ATS is located inside the thermal wake. Actually this sensor is not being affected by a fluid current with a $\beta = 45^o$, given that it is in the wake and therefore the theoretical model is not applicable to this configuration. In the Figure 5 can be observed the thermal wake in a horizontal section of all the solid and fluid domains in case 2.

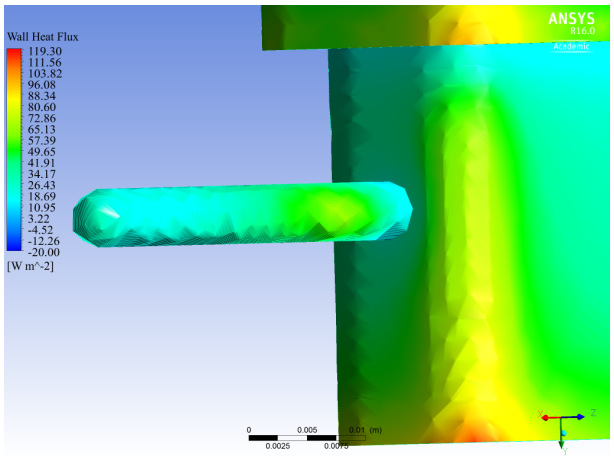


Figure 6. Detail view of convective heat flux distribution along the front ATS sensor in case 2 without radiative heat transfer.

χ	$T_{average}[K]$	$h_{caverage}\ [Wm^{-2}K^{-1}]$
0	270.953	0.332
1/4	263.820	1.545
1	254.806	5.604

Table 6. Temperature and h_c profile along the left ATS sensor for a velocity inlet $v = 1\ m \cdot s^{-1}$, $\beta = 45^o$ and $T_\infty = 250K$ (case 2).

As it can be appreciated, the wake is strongly affecting almost the entire right ATS sensor surface, which agrees with the h_c distribution results. Following with the temperature and h_c distribution along each ATS, in the Table 6 are exposed their profiles for the left sensor in case 2 without radiation, where is easy to confirm that both the temperature and h_c tendencies are absolutely not linear and however the first approximation here introduced still being a simple average between two values. To complete this view, the respective temperature and h_c profiles for each ATS sensor has been represented for the same studied case in the Figure 7. Observing carefully the h_c coefficient profiles it can be confirmed the increment for the front ATS sensor $1/4$ h_c coefficient and, consequently, the artificial growth of the convective heat flux through the forced convection at this point mentioned before. If this local disturbance did not happen, the tendency of this curve would be probably similar to the left ATS sensor one, as it occurs in temperature profiles. A detail view of this local effect can be seen in the Figure 6 for the case 2 without radiation.

In addition to this, as the temperature profiles are concerned, here is clearly represented the thermal wake previously commented and shown in Figure 5 through the evolution of the right ATS sensor profiles.

Resuming the Figure 4, the m parameter variation has

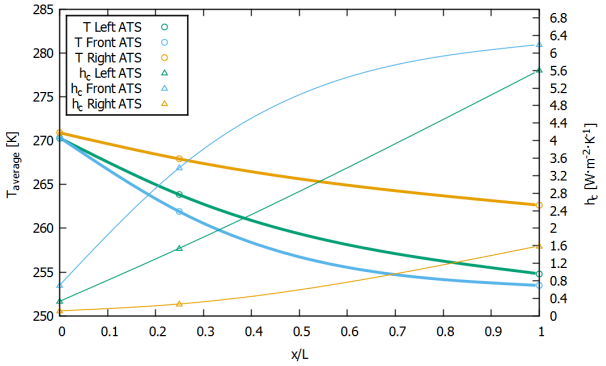


Figure 7. Temperature and h_c coefficient distribution along the ATS sensors in case 2 without radiative heat transfer. Lines are interpolated from points.

also been included together with is numerical solution for each one of the cases mentioned. As it was specified for the h_c coefficient, this parameter should include also the h_r coefficient, which in this case has not been introduced within its formulation. At this point, despite the close location between the respective numerical results and theoretical points, the tendencies of the last ones are not similar to the first one. This is a consequence of the artificial definition of the parameter without radiation contribution.

Finally, it has to be also added that until now, the results exposed and discussed correspond to numerical solutions in which the radiative heat transfer has not be taken into account, it means, $h_r = 0$. Given that the main purpose has been to compare the h_c coefficients, whose correctly evaluation is the key for the retrieval method, the radiative term has been first neglected. However, it will be truly relevant when the m parameter estimation gains importance.

In the following study we summarise a comparison between the two coefficients, h_c and h_r, along the ATS sensors. It is worth noting that the last one remains almost constant along the rods with no dependency from the inlet velocity to the fluid volume. Table 7 shows the values for the h_c and h_r coefficients for each ATS sensor in cases 2 and 8, with inlet velocities of $1\ m \cdot s^{-1}$ and $4\ m \cdot s^{-1}$ respectively.

While the convective heat transfer coefficient grows with the increment of the inlet velocity into the volume, the h_r coefficient remains almost constant both over each RTD thermistor and ATS sensor.

5. CONCLUSIONS

This preliminary study has served as numerical validation of a new retrieval method which shall be used for the three ATS sensors of HABIT instrument on board the $ExoMars2018\ SurfacePlatform$. This method

Case	ATS	$h_c\ [Wm^{-2}K^{-1}]$	$h_r\ [Wm^{-2}K^{-1}]$
2	Left	1.6760	3.4710
	Frontal	2.2320	3.4355
	Right	0.6245	3.5590
8	Left	3.0705	3.3990
	Frontal	3.8740	3.3575
	Right	1.8110	3.4355

Table 7. Comparation of h_c and h_r between case 2 and case 8 including radiative heat transfer.

is sensitive to the wind orientation and speed and can be used in real time to monitor the wind activity and heat fluxes at the boundary layer in the vicinity of the platform.

The numerical results are in agreement with the first order theoretical approximation of the heat balance problem. This probes the robustness of the method in spite of the relatively simple analytical model and the highly simplified and limited numerical model. We conclude from this study that:

- The ATS that is exposed to the free flow of wind shows a convective heat transfer coefficient that is in agreement with those expected from the model. The ATS that is in the wake of the HABIT box has a lower convective term as it is not exposed to the forced convection of wind.
- For the same atmospheric conditions, the convective heat term (and m value) increase with the wind speed as expected.
- The different value of the m's as retrieved from each ATS can be used as a proxy for wind orientation and wind speed.

ACKOWLEDGEMENTS

The work of Alvaro Soria-Salinas has been partially funded by a SNSB fellowship for attendance to this conference.

REFERENCES

[1] D.W. Mueller Jr., H.I. Abu-Mulaweh, *Prediction of the temperature in a fin cooled by natural convection and radiation*, 2006, J. Applied Thermal Engineering 26, 1662-1668.

[2] Casey A. Moore, John E. Moores, Mark T. Lemmon, Scot C.R. Rafkin, Ryamond Francis, Jorge Pla-Garca, Robert Michael Haberle, Mara-Paz Zorzano, Francisco Javier Martn-Torres, John R. Burton, The MSL Team, *A full Martian Year of Line-of-Sight Extinction within Gale Crater, Mars as Acquired by the MSL Navcam through sol 900*, Icarus.

[3] *ANSYS FLUENT Theory Guide*, Release 14.5, October 2012, ANSYS Inc.

[4] Gómez-Elvira et al., *REMS: The envornomental sensor suite for the Mars Science Laboratory rover*, Space Sci. Rev., 170, 583-640, doi: 10.1007/s11214-012-9921-1, 2012.

[5] G. Nellis; S. Klein. *Heat Transfer*. Cambridge University Press, 2009. ISBN 978-0-521-88107-4.

[6] Bonnie J.McBride; Sanford Gordon; and Martin A. Reno. *Coeffcients for Calculating Thermodymanic and Transport Properties of Individual Species*. National Aeronautics and Space Administrations, 1993. NASA TM-4513.

[7] Miller; J.W. Jr.; P.N. Shah; and C.L Yaws. *Chem. Eng. 83*. 1976. 515, 516.

[8] Bird, Stewart, and Lightfoot. *Transport Phenomena*. Wiley, 2002. 2^{nd} edition.

[9] Smith A., Jones B., 1996, A&A 555, 999
G. Nellis; S. Klein. Heat Transfer. Cambridge University Press, 2009. ISBN 978-0-521- 88107-4.
Bird; Stewart; and Lightfoot. Transport Phenomena. Wiley, 2002. 2nd edition.

ROBOTIC REFUELING SYSTEM FOR ON-ORBIT SERVICING

Lorenzo Bucci[1], Marco Brizioli[1], Andrea Bellanca[1], and Michèle Lavagna[2]

[1]*M.S. Student, Politecnico di Milano, Aerospace Science and Technology Department, via La Masa 34, 20156, Milan, Italy*

[1]*Corresponding e-mail: lorenzo.bucci@mail.polimi.it, andrea.bellanca@mail.polimi.it*

[2]*Associate Professor, Politecnico di Milano, Aerospace Science and Technology Department, via La Masa 34, 20156, Milan, Italy*

ABSTRACT

In an average year almost 20 GEO satellites are retired when the propellant supply is exhausted, even if no failures in payload or other subsystems occur. This results in large costs and in a bad exploitation of the real potential of many spacecrafts. The On-Orbit Refueling (OOR) seems to be a very promising solution to mitigate these expenses and optimize the already in orbit space segments exploitation.

The paper reports the results of a robotic system design, devoted to transfer fuel from a servicer to a client spacecraft. The study has been performed in a concurrent design environment, by a team of 12 Master students in Space Engineering at Politecnico di Milano, as part of the Space System and Mission Design course. The study focused on the interface definition and sizing, to autonomously berth the client and connect to its propellant feed system, and on the development of a transfer strategy for the fuel. Xenon is here assumed as the fuel to be transferred, largely used in the most promising electric thrusters well suited for GEO station keeping tasks; however, the study results can be easily generalized and turn useful even if different fuel is considered. In particular, the proposed design well fits also for the Carbon Dioxide utilization, currently under investigation in the specialists community as green propellant towards a cleaner future for space propulsion. The paper discusses the proposed solutions and results, exploited to better investigate the OOR requirements definition. The results about the dynamics obtained by coupling the effects of the orbital motion and fluid exchange while the feeder and the receiver are connected are also preliminarily presented, to better motivate the requirements which shall drive the structural design and the stack station keeping synthesis.

A set of characterization and verification tests are also proposed to fix the obtained sizing results and enhance the technology readiness level. In particular, both the fluid transfer model validation and the flexible connection between the two orbiting bodies sizing verification are proposed as the most relevant to be run experimentally. Eventually, an In Orbit Demonstration mission (IOD) for the OOR feasibility assessment and bottleneck identification is suggested, scaled on microsatellites.

Key words: on-orbit servicing; refueling; robotic space systems.

1. INTRODUCTION AND MISSION SCENARIO

The paper presents some results of a feasibility study [1] performed by a group of M.S. students in Space Engineering from Politecnico di Milano, in a concurrent design environment. It was carried out as a part of the Space Mission Analysis and Design Course, during a period of 4 months. The study results correspond to the Phase A of the system design life cycle.

1.1. Overview

The project analyses the design of a robotic tug, able to refuel geostationary satellites through fully automated interfaces. Importance and effectiveness of on-orbit servicing (OOS) is proved in many studies [2, 3] and recent advancements in the field are collected in a wide literature review by Flores-Abad et al. [4]. Some missions [5, 6] served as technology demonstrators for OOS.

The following high-level requirements were set for the study:

- Capability to refuel at least 3 GEO satellites;
- Launch in the year 2020;
- Use of European launchers preferred.

These requirements led towards the final configuration; the presented system, although designed for a GEO-operating platform, can be easily transferred to other operational orbits, with little modifications.

Two main reasons dictated the selection of Xenon as a payload:

- Future and near-future spacecraft tend to become fully electric, using Hall-effect or gridded ion engines for primary propulsion and station keeping, as well as attitude control; the most promising fuel is Xenon, since it yields the best performances among noble gases;
- The designed spacecraft relies on Hall-effect engines for primary propulsion, using Xenon as fuel; the usage of the same gas both as payload and as fuel simplifies the design of the system as well as allows the possibility of cross-feed in case of failures.

1.2. Paper content

The results here presented focus on the design of the robotic system, the fuel storage and transfer issues, and on the proposed experimental test that could serve as a validation of the used model, underlining all the assumptions used during the study. The orbital dynamics of the coupled chaser-target configuration is also briefly introduced, in order to assess the effects of the flexibility of the robotic arm.

Section 2 describes the sizing of the robotic system and of the fuel transfer system, presenting the assumptions, the used models and the results, together with the preliminary study of the stack dynamics; Section 3 presents the proposed experiments and validation tests, which could be able to assess the feasibility of the designed mission.

2. FUEL TRANSFER AND ROBOTIC SYSTEM

In space applications, for electric propulsion systems, Xenon is usually stored at temperature and pressure greater than the critical point (~ 289.7 K and ~ 6 MPa), in order to guarantee gaseous state for the fuel [7]. Pressure values can go up to ~ 15 MPa in order to increase the quantity of stored propellant [8].

The simplest and basic idea to transfer fuel is to exploit the pressure difference between servicer and serviced tanks. The easier solution would be a free expansion, in which fuel flows from a full vessel to the serviced one until balance of pressure is achieved. A drawback of this method is the impossibility to transfer all the fuel [9]; to solve this problem, it is possible to make use either of a pressurant gas (He), to maintain a constant pressure inside the servicer tank, or of an active machine, able to keep a given pressure difference between the two reservoirs. The first solution is the most appealing, since it allows to transfer the whole fuel payload, it demands less power and it is more reliable [10]; the use of a machine (e.g. a compressor) introduces also vibrations and fatigue issues undesirable for space operations.

2.1. Models and assumptions

The model adopted for the study considers two vessel, one initially full and the other empty, that exchange fluid mass by means of a hose. The tanks can release or receive heat power to and from the external environment, whereas the hose is designed as adiabatic. These design conditions reflect the actual feasibility of such features, since an external hose is easily insulated, while tanks can be heated up by heater or cooled through active or passive techniques.

The evolution of the thermodynamic variables, during the transfer of fuel, can be described in mathematical form using mass and energy conservation laws, together with appropriate state equations. Xenon state equations are implemented using a NIST formulation [11, 12]. Since a single phase fluid is taken into account, the system is fully resolved when two thermodynamical variables are known, according to Gibbs' phase rule [13]. The mass flow rate is assumed to be kept constant, to have a better control on the quantity of transferred fluid and on the evolution of the thermodynamic variables in general. The following choice of variables was performed:

- For the servicer pressure P and internal energy u are used, since the pressurant gas, together with Xenon's self-pressurized nature, keeps the pressure constant;
- For the customer the choice is to use density ρ and internal energy u; the volume of the tank is constant, while pressure neither temperature can be assumed to be so.

The set of equations for the two tanks is then (A and B indicate respectively the servicer and the receiving system)

$$\begin{cases} \dot{U}_A = \dot{m}_A h_A + \dot{Q}_A \\ h_A = h_A(P_A, u_A) \\ T_A = T_A(P_A, u_A) \\ \rho_A = \rho_A(P_A, u_A) \end{cases} \qquad \begin{cases} \frac{dm_B}{dt} = \dot{m}_B \\ \dot{U}_B = \dot{m}_B h_A + \dot{Q}_B \\ h_B = h_B(\rho_B, u_B) \\ T_B = T_B(\rho_B, u_B) \\ P_B = P_B(\rho_B, u_B) \end{cases} \tag{1}$$

with the following use of symbols:

U	Total internal energy (J)
u	Specific internal energy (J/kg)
m	Mass (kg)
$\dot{m}$	Mass flow rate (kg/s)
h	Specific enthalpy (J/kg)
$\dot{Q}$	Heat power (W)

Since the mass exchange is only between the two vessels the following identity holds

$$\dot{m}_B = -\dot{m}_A = \dot{m} \tag{2}$$

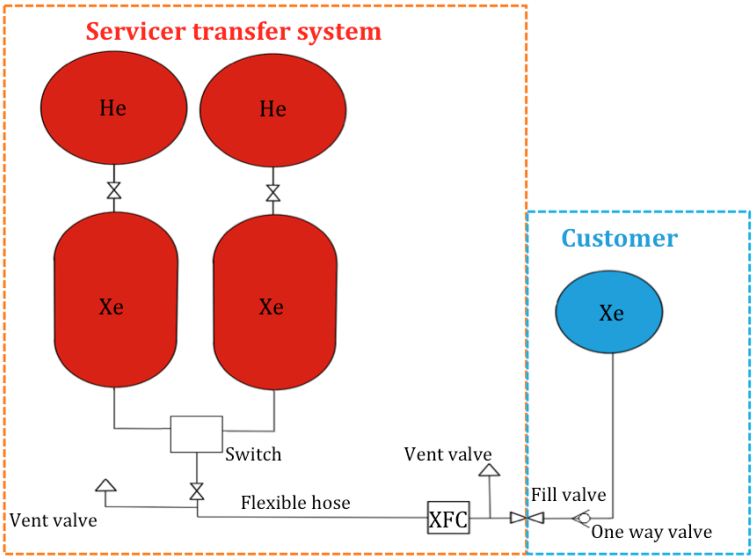


Figure 1: Xenon transfer and storage system

2.2. Hardware description

The suggested configuration considers two tanks, in order to guarantee full redundancy of the storage system, as depicted in Figure 1; different lines are connected to switches and to the final interface valve. The servicer can be connected to the feeding line by means of a coupler element at the end of a flexible hose.

A main element is the Xenon Flow Controller (XFC), that is composed of a flow restrictor valve controlled by an electronic circuit, connected to a mass flow sensing device. Thanks to this component, the mass flow rate can be regulated. The coupler is an already existing component in the electric propulsion systems, but it works with different mass flow rates [14, 15]; an adaptation is then necessary for the present application. Both the coupler and the XFC can be located on the end-effector of the manipulator. In order to control the temperature and the pressure, sensors should be provided in the system, at suitable locations; heaters and a thermal control system are necessary to give heat power and keep the correct Xenon condition, according to the selected mass flow rate.

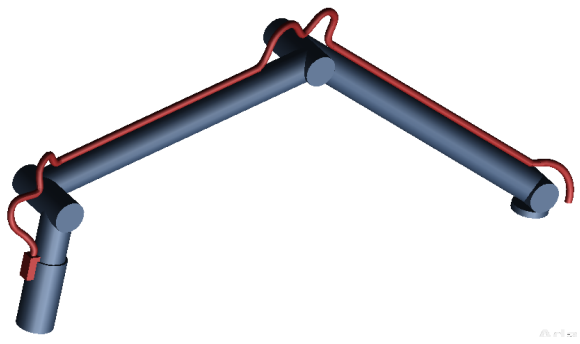


Figure 2: Manipulator

A robotic arm (Figure 2) brings the flexible hose, connected to the end-effector which carries the coupler element, to the fill valve of the customer spacecraft, and ensures the engagement of it. This manipulator is equipped with a camera and photodiodes to illuminate the field of view. The arm is operated as follows:

1. Since the approximate location of the valve is known, the manipulator follows a preset path to arrive in proximity;
2. The camera and the CPU are activated, taking pictures and processing them to obtain data about the correct valve position;
3. A path is autonomously planned up to the final engagement.

In the proposed mission architecture two robotic arms are present, in order again to guarantee a fully redundant system. Simultaneous operation is not considered, but could be exploited in future studies to increase the servicing capabilities.

The most critical component of the robotic system is the end effector, needing to be designed *de novo* since no device exists for the presented purpose. It is composed of many elements, mechanical, electrical and fluidic. The architecture and preliminary design are pictured in Figure 3. This component is in charge of:

- Ensure and maintain the correct engage between customer's valve and coupler, using mechanical fingers that close around the valve;
- Bring the coupler back to the initial position in case of malfunctioning through a spring back safety mechanism, located on the actuator;

- Empty itself once the refueling operation is completed, to avoid drop permanence in the hose, using a vent valve properly open when the fuel transfer ends.

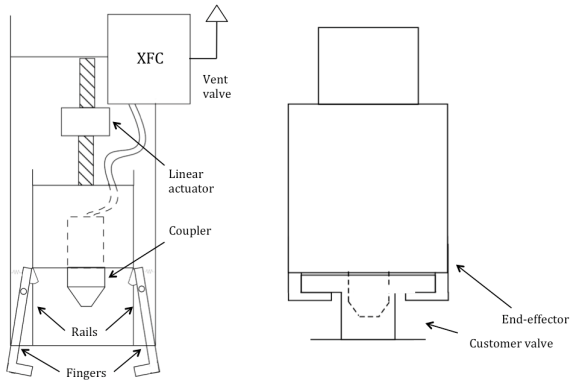


Figure 3: End-effector architecture

The coupler element has the task of creating the fluidic connection between the hose and the tank to be refilled. It is able to translate along rails pushed by a linear actuator; during this operation a mechanism is activated allowing the closure of three fingers around the customer valve. Along these lines the end-effector is fixed on the customer and the linear motor can provide the required force for the dis/engagement, above 350 N.

2.3. Effects of the flexible connection

The robotic arm, once the structural connection is accomplished, is naturally subject to small vibrations due to the elasticity of the material. These vibrations could encounter coupling with the frequency n of the orbital motion, leading to undesired excitations.

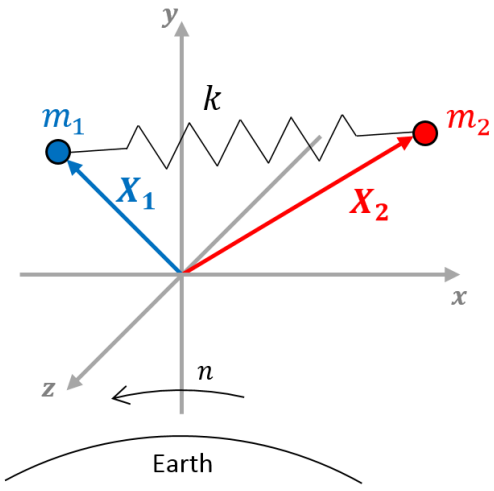


Figure 4: Stack in the orbital frame

A lumped-mass approach is used to face the problem, assuming the two spacecraft as point masses and the connection as a linear spring, with an equivalent stiffness k. This rough approximation is in turn useful to find the first natural frequency of the assembly, which varies in time due to the mass transfer. Figure 4 depicts the framework.

Linear analysis shows that no couplings arise if the structural frequencies are much higher than the orbital motion's ones, i.e. $k \gg n^2 m$, where m is the reduced mass of the system. This happens for any reasonable value of k, corresponding to structural stiffness; cases of very flexible or nearly loose interfaces could in turn show orbit-excited structural vibrations.

The first fundamental frequency can then be studied analyzing the small vibrations of two masses, variable in time. Once the time history of this frequency is known (typical behavior shown in Figure 5), the system can be designed in order to avoid excitation of the structural modes of one of the spacecraft. It is note that the driving parameter is the mass flow rate, dictating how fast the masses changes and influencing the natural frequency with an inverse-square behavior.

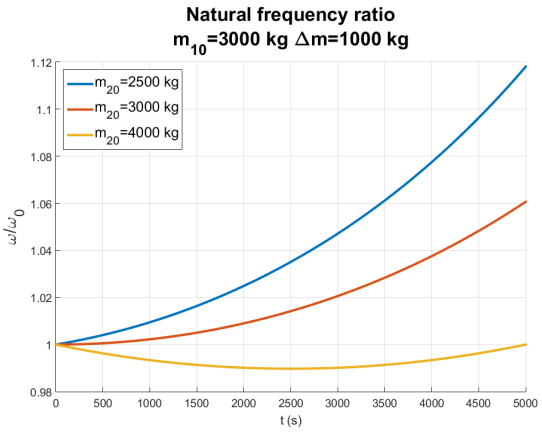


Figure 5: Fundamental frequency variation

3. PROPOSED EXPERIMENTAL VALIDATION

This Section presents some possible experiments, designed to validate and verify those aspects of the project with low TRL and few literature background.

3.1. Fuel transfer system

3.1.1. Validation tests

The behavior of Xenon was modeled with numerical tools, implementing the cited NIST formulation [11]. This model is based on some assumptions:

- Single-phase flow
- Smooth behavior (no discontinuities)
- Viscous stresses neglected
- Constant mass flow rate

These hypotheses simplify the analysis process, being suitable for a preliminary design, but the system shall be experimentally verified to assess the validity of such model.

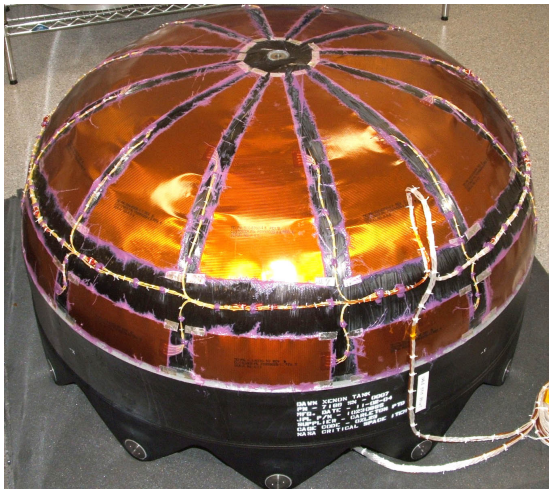


Figure 6: Commercial Xenon tank

A basic test should suffice for the purpose: a fluid transfer from a tank A to a tank B, with a the proposed transfer system. Tank A shall be connected to the pressure regulation system, and posses a temperature feedback control system thanks to thermistors, heaters and heat pipes. Tank B could be a standard Xenon container as shown in Figure 6, that is used to store fuel in the client spacecraft. These tanks are usually insulated by MLI and provided with some heaters, so the experiment shall re-create these conditions.

The fluidic link is a stainless flexible hose, it has to bear high pressure and it has to be completely adiabatic in order to avoid any exchange of heat with the outside environment. The model consider a valve that can regulate the mass flow rate, which shall be built and designed for the purpose.

These validating tests could be performed on ground, in vacuum environment (Figure 7) to avoid any heat exchange by convection as for space habitat. As a first approximation, the use of vacuum can be avoided, if a temperature-controlled test environment is used, and convective heat exchange is kept as low as possible.

In order to have a complete and meaningful set of statistical data, tests has to be accomplished for various combination of initial servicer tank temperature and different mass flow rates, measuring in temperatures and pressures along the line. The numerical result of the model



Figure 7: Example of vacuum chamber

(Figure 8) are based on the worst case of customer tank (the smallest class existing), therefore other tests could be made, changing the customer tank with bigger ones.

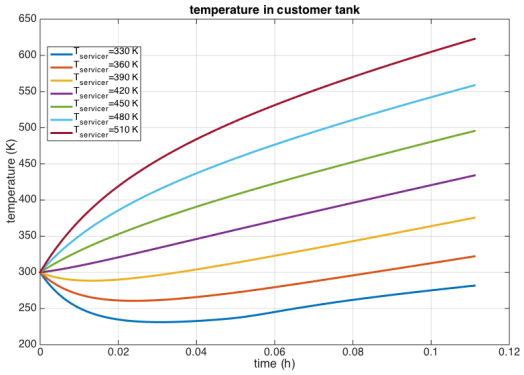
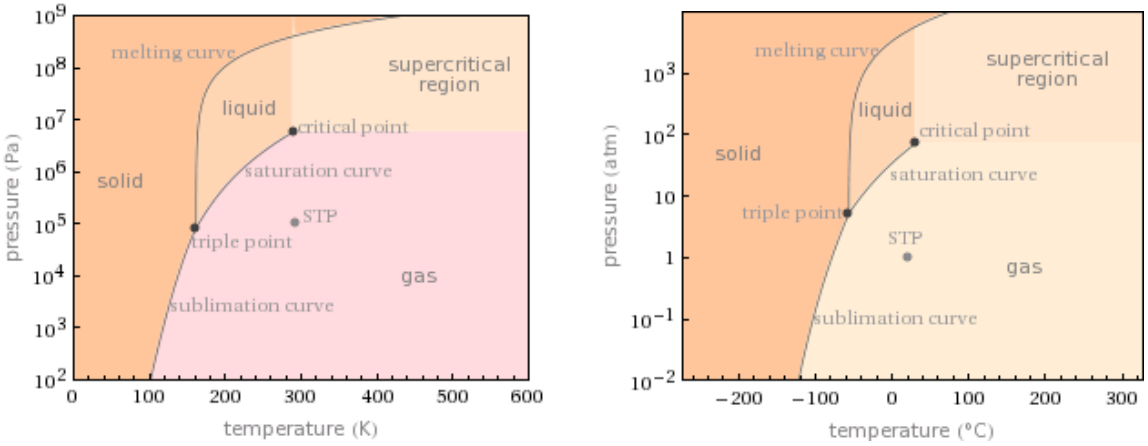


Figure 8: Xenon temperature sensitivity to initial conditions

3.1.2. Validation Assumptions

Keeping the mass flow rate constant during the transfer is a simplifying hypothesis, but with an active control of the flow is possible to not have significant effects on fluid-dynamics, especially sonic blockages along the conduct; furthermore, if the mass flow rate is very low (few grams per second), the temperature gradient in the customer tank is more easily under control. Therefore, on the same test session described, it could be useful to remove the mass flow regulator valve, letting the system to freely expand, and interrupt the flow when the tank reaches the nominal final pressure. This test can validate and assess how strong the constant mass flow rate assumption is, noticing whether such effects are truly negligible.

Considering an adiabatic hose is a strong but realistic assumption, and due to the slow mass flow rate we can consider it as an extension of the volume of the servicer tank. The hose has been designed to be covered with MLI, but for long period of exposition to Sun the thermal exchange could be non-negligible.It could be then useful to analyze



(a) Xe *phase diagram* (b) CO_2 *phase diagram*

Figure 9: Phase diagrams

the temperature along the hose during a transfer with a simulated solar radiation in a vacuum chamber, and compare data without solar radiation to check if significant changes in the results appear, quantifying the error under the adiabatic assumption. Eventually a transfer without MLI could be performed, to understand if the protection is strictly necessary.

For the present analysis, the customer tank has been considered as non-dimensional, neglecting spatial and transition phenomena inside it. Nevertheless, as soon as a fluid is injected in the tank, two fluids at different state conditions coexist. The thermochemical interaction could rise the presence of two phase fluid. This does not provoke any significant issue on the system if the fluid is an ideal gas, but Xenon behavior is not so deducible with the classical laws. The variation of pressure and temperature in all the volume could be different. These effects could facilitate the transfer, because the phase change absorbs energy form the system, probably reducing the enthalpy content of the overall fluid mass and so the increase of temperature due to compression.

3.1.3. Observations

These kind of tests will be expensive, due to the high cost of Xenon and due to the size of the plant. The theoretical model considers the tanks without dimensions, with equal thermodynamic values in all the tank at a given time instant. Therefore the system could be scaled, maintaining pressure and density at the same values; this would reduce the system cost and test time.

All the presented tests should use Xenon, since is the fuel considered for the project, on the other hand its cost goes beyond thousand dollars for kilo. This experimental setup could be adapted to Carbon Dioxide gas, far cheaper, but new equations and numerical models shall be implemented, possibly leading to a substantial re-design of the system which could not represent the aim of the test. A new trade off for the components would be necessary, especially for the hose and flow controller valve, since carbon-dioxide has a critical temperature 20 K greater than Xenon and critical pressure of 7 MPa, 2 MPa greater, as shown in Figure 9. If CO_2 is to be used as a fuel for space applications, it would be convenient at this point to re-design a system tailored on the use of such fluid.

3.2. Robotic connection

To analyze and test the robotic system it is suggested to split it up in its principal components: manipulators, path controller and the end effector.

3.2.1. Manipulators

The robotic arms are similar to existing and flight-proven designs; the TRL is between 6 and 7 so test and validations need to be performed to check the operations before flight. It has to be proven that hose and the components in charge to refuel the target don't hinder the manipulator's operations. Tests able to prove that the manipulator can cover a wide operative area can to be made in controlled environment on ground.

As shown in Figure 10 the manipulator needs to be able to reach the green region (determined numerically) during the mission, hence possible paths and configurations for the robotic system have to be tested using to a mock-up of the chaser and target in stack configuration, to validate the numerical analysis. An important aspect it is to understand how much the hose's stiffness impacts on the movement capacity of the robotic arm. Strain gauges, embedded into the joints, can measure angular displacements induced by fuel flowing through the hose.

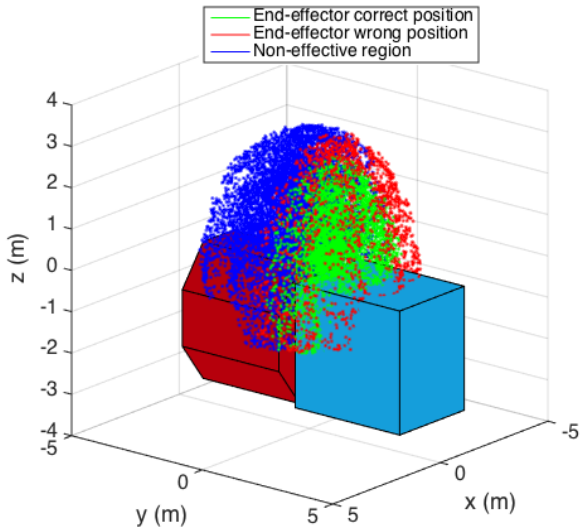


Figure 10: Workspace.

3.2.2. Path controller

The tests have to ensure the capability of the system to correctly process the images, to identify the valve and at to generate a suitable path for the manipulator, according to the elaboration of the correct instructions for the actuators, in order to obtain engagement between valve and end effector.

Different illumination conditions could be tested, simulating various operative scenarios and proving the capability of the system to correctly identify the valve, using its photodiodes to control the illumination. Figure 11 shows a similar configuration for the test [16].

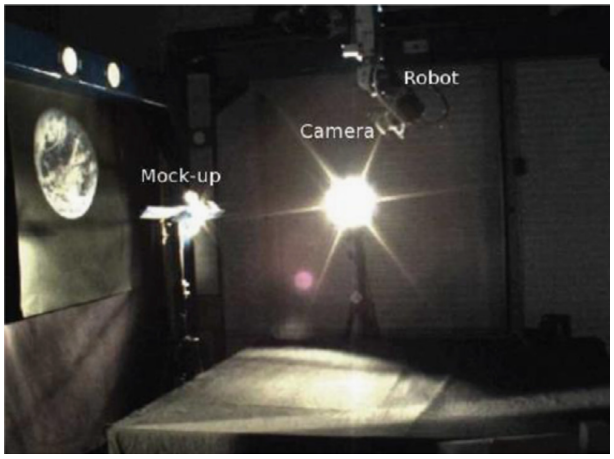


Figure 11: Path controller test

Contact sensors embedded into the valve ensure a feedback signal of the correct engagement between the two parts. As shown in Figure 12 they are able to generate an electrical signal while physical contact happen, and are distributed on the surface of the valve.

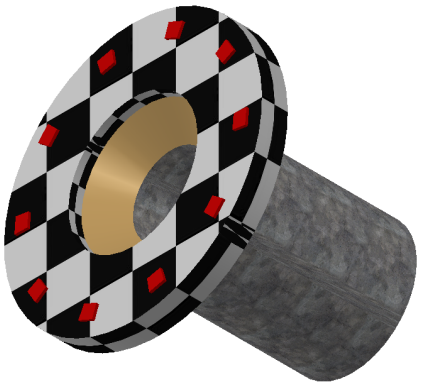


Figure 12: Customer valve with contact sensors

Moreover, it is possible to test the correct alignment between valve and coupler, using optical sensors during the test.

3.2.3. End effector

All the functionalities the end effector is in charge of have to be tested on ground separately and jointly, in order to confirm an high level of reliability. Tests have to confirm the closure of the three fingers around the customer valve. Starting with the valve supported on the end effector, as shown in Figure 13, providing a linear incremented force below the valve, through a load cell, displacement occurs in direction of the coupler until its head is inside the valve as shown in Figure 14.

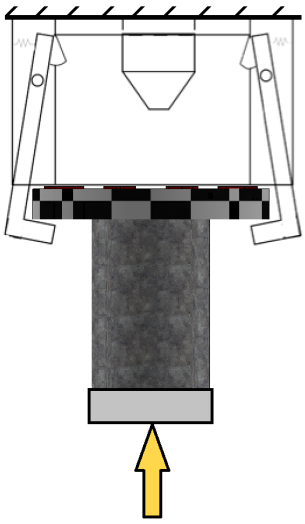


Figure 13: Fingers closure test

Strain gauges on the rails verify the expected displacement. This involves to have no forces exchanged between the end-effector itself and the robotic arm, avoiding disturbances for the attitude of the coupled system and allowing to keep forces (350 N) only on the linear actuator.

In order to verify the correct behavior of the safety

springs a load cell can be used; keeping the system at zero displacement and with no force applied, non-zero measurement of the load cell means that pre-load correctly exists in the springs.

Testing the complete component is the last step. It is mandatory to verify its capacity to get the perfect engagement over fuel transfer phase and the no-force exchange with robotic arm during fuel venting time. Figure 14 shows the end effector configuration for the tests. Thanks to a fixed pressure into the hose driven by a flow controller, measured by sensible pressure sensors at the opposite part of the connection, the test is able to check if no losses of fuel occur during the transfer. Moreover, accelerations and displacements are measured by accelerometers and strain gauges located on the surface between customer valve and end effector. While the vent valve empties the system, load cell on linear actuator must measure values greater than or equal 350 N throughout the test, in order to satisfy the condition to hold the correct engagement between customer valve and end effector, avoiding unexpected disengagement potentially harmful for the system.

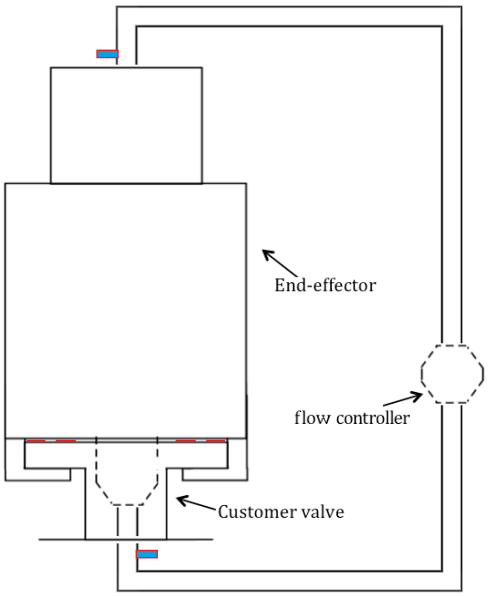


Figure 14: Fuel transfer test

3.3. In-orbit demonstration

An In-Orbit Demonstration would surely be the best way to test the designed system and assess its correct operation in space environment, rising the TRL to 8. Among the actually flown mission, Orbital Express [6] proved fuel transfer between two spacecraft, while NASDA's ETS-VII proved the operations of robotic manipulators for OOS [5, 17]. The following considerations arise for a preliminary design of an IOD:

- The dimensions of the system shall be scaled, in order to contain the costs and assembly time; scaling on Cubesats is suggested, to attain a standardized and portable interface;
- Use of as many COTS as possible (e.g. joints, actuators, tanks) greatly simplifies the mission design, allowing to focus on the complex components (mainly the end-effector) manufacturing and assembly;
- The operational orbit can be scaled to LEO, reducing launch costs; atmospheric drag shall be avoided, since the stresses on the robotic arm could hinder its performances; it is noted anyway that a trade-off can be performed if such aspect is considered, since designing a robotic arm able to bear drag stresses could be cheaper than launching in higher orbits;
- The working fluid can be changed to others (e.g. CO_2), both for economical and for environmental reasons; it is noted, as previously mentioned, that each fluid behaves very differently in critic region, and the system could face complete re-design processes if the fluid must be changed.

ACKNOWLEDGMENTS

The authors would like to acknowledge their student's team, with whom a full Phase A study was performed. In alphabetical order: Andrea Aurini, Maria Chiara Berva, Andrea Capannolo, Nicolò Carletti, Francesco Cavenago, Simone Ceccherini, Luca Ferella, Jonathan Pergoli, Lorenzo Voli. The results presented in this paper are the authors' work, but no goal could have been achieved without the collaboration of all the team components.

Great acknowledgment is due to Prof. M. Lavagna, who provided constant support to all of us throughout the whole project development.

REFERENCES

[1] A. Aurini, A. Bellanca, M. C. Berva, M. Brizioli, L. Bucci, A. Capannolo, N. Carletti, F. Cavenago, S. Ceccherini, L. Ferella, J. Pergoli, and L. Voli. *ERMES feasibility study*. Politecnico di Milano, DAER, July 2015. Internal report.

[2] D. M. Waltz. *On-orbit servicing of space systems*. Krieger Pub. Co., 1993.

[3] N. Davinic, S. Chappie, A. Arkus, and J. Greenberg. Spacecraft modular architecture design study - cost benefit analysis of on-orbit satellite servicing. In *International Astronautical Congress, 48 th, Turin, Italy*, 1997.

[4] A. Flores-Abad, O. Ma, K. Pham, and S. Ulrich. A review of space robotics technologies for on-orbit servicing. *Progress in Aerospace Sciences*, 68:1–26, 2014.

[5] G. Visentin and F. Didot. Testing space robotics on the japanese ETS VII satellite. *ESA bulletin*, 99:61–65, 1999.

[6] R. B. Friend. Orbital Express program summary and mission overview. In *SPIE Defense and Security Symposium*, pages 695803–695803. International Society for Optics and Photonics, 2008.

[7] O. Sifner and J. Klomfar. Thermodynamic properties of xenon from the triple point to 800 K with pressures up to 350 MPa. *Journal of physical and chemical reference data*, 23(1):63–152, 1994.

[8] R. P. Welle. Propellant storage considerations for electric propulsion. In *22nd International Electric Propulsion Conference, AIAA-91-2589*, 1991.

[9] F. Olmos and V. I. Manousiouthakis. Gas tank fill-up in globally minimum time: Theory and application to hydrogen. *International Journal of Hydrogen Energy*, 39(23):12138–12157, 2014.

[10] P. Bravais, R. Salome, and C. Gelas. Improved xenon loading equipment with loading capacity up to 1200 kg for Alphabus. CNES.

[11] NIST Digital Library of Mathematical Functions. http://webbook.nist.gov/, retrieved June 10, 2015.

[12] P. J. Linstrom and W. G. Mallard. *NIST Standard Reference Database Number 69*. National Institute of Standards and Technology, 2011.

[13] P. Atkins and J. De Paula. *Physical Chemistry*. W. H. Freeman, 2009.

[14] J. Bejhed, K. Jonsson, T. A. Gronland, and P. Rangsten. Advanced flow control devices based on MEMS technology for electric propulsion. In *The 33rd International Electric Propulsion Conference*.

[15] E. D. Bushway III, P. T. King, C. Engelbrecht, and L. Werthman. A xenon flowrate controller for Hall current thruster applications. In *International Electric Propulsion Conference Paper*, pages 01–315, 2001.

[16] A. Petit, E. Marchand, and K. Kanani. Vision-based space autonomous rendezvous: A case study. In *Intelligent Robots and Systems (IROS), 2011 IEEE/RSJ International Conference on*, pages 619–624. IEEE, 2011.

[17] T. Kasai, M. Oda, and T. Suzuki. Results of the ETS-7 mission-rendezvous docking and space robotics experiments. In *Artificial Intelligence, Robotics and Automation in Space*, volume 440, page 299, 1999.

MODELING A NEW CONCEPT OF TETHER DEPLOYER WITH RETRIEVABLE CAPABILITY FOR SPACE APPLICATIONS

Gilberto Grassi[1] **and Riccardo Mantellato**[2]

[1]*Master's Student, Aerospace Engineering, University of Padova, via Venezia 1, 35131, Padova, Italy*
[1]*+39 338 6741973, gilberto.grassi@studenti.unipd.it*
[2]*Post Doctoral Fellow, Department of Industrial Engineering, University of Padova, via Venezia 1, 35131, Padova, Italy*
[2]*+39 049 8276795, riccardo.mantellato@unipd.it*

ABSTRACT

In this paper, two mechanical systems intended to carry out the deployment and retrieval of a tethered probe in space are presented, modeled and compared. The systems are two variations deriving from a common concept - the adaptation of a fixed-spool reel, a technology widely used by traditional industry, to the space environment. The tether is modeled as a varying-length dumbbell, whilst at the far end of the tether is a tip point mass, to represent the probe/tool being deployed and retrieved. The deployment will be initiated by a spring-based ejection system. The first solution presents a dedicated active brake mechanism, whose aim is to control the tether tension during deployment, while an electric micromotor is used for retrieving the tip mass once the brace is locked to the tether. In the second solution the brace is always locked, and the control of the tether tension during deployment is directly performed by the electric motor, this by taking advantage of the parasitic torque induced by the counter-electromotive force. Deployment control is operated, in both cases, by means of a feedback control law, whereby the control variables are the instantaneous tether length and length rate. A reference trajectory for the control variables is *a priori* optimized and then fed forward to the controller during numerical integration. Tether tension profiles during deployment of the two systems are observed and compared, so as to pinpoint the pros and cons of each solution and to determine what types of utilization are better suited for each solution. The results of this study shows that the applied control law is effective in delivering the tip mass in the desired position for both the solutions, but that the latter is more complicated than the first in terms of system design, handling and testing, in addition to some critical issues proper of the system.

Key words: tether space system, space tether deployment, retrievable tether deployer.

NOMENCLATURE

b = motor viscous friction constant

d = brake rollers relative distance

e = orbit eccentricity

I = total rotor inertia

i = instantaneous current (motor electric circuit)

J = motor inductance

k_p = proportional gain (control)

k_d = derivative gain (control)

k_v = motor back-emf constant

k_t = motor torque constant

l = instantaneous tether length

m = tip mass

p = brake rollers radius

r = spool radius

R = motor terminal resistance

T = tether tension

V = control voltage

x = instantaneous middle brake roller shift

α = angle underlying tether-brake rollers contact length

θ = instantaneous tether in-plane libration angle

λ = tether/brake sliding friction coefficient

ρ = tether linear mass density

τ = mechanical load (torque) acting on motor shaft

ψ = brace/motor shaft rotation angle

ω = orbital mean motion

1. INTRODUCTION

The deployment of a space tether has always been a critical issue in the past space tether missions. What emerges from literature and heritage in this field is that a successful employment of space tether requires extremely good mechanical design of deployers and brakes, as well as highly robust and adaptive control strategies. For example, the NASA-ASI TSS-1 deployment failed due to a blockage in the tether leveling system of the deployer [1], and the tether was eventually retrieved. This is, at the time of writing, the sole known mission where a successful tether retrieval was performed. The deployment hardware was, in that case, extremely massive and complex and cannot be applied to smaller-scale mission. In parallel to TSS-1, an example of partial control system malfunction was in the ESA YES2 mission. In that occasion a 32-km tether was successfully deployed but the control dynamics was off nominal [2]. Against this, however, a compact and reliable spooling mechanism was designed for YES2 deployment, which behaved successfully. Other missions worth mentioning are SEDS-I and -II, for which a dedicated, simple and lightweight hardware and a robust control strategy were designed [3][4]. Both these NASA missions were fully successful in deploying a 20-km tether with a swinging maneuver. Finally, in 2013 the ESTCube-1 was put into a LEO orbit by a VEGA launcher as the first Estonian satellite [5]. It carried two different payloads, a camera and a tether system that was meant to test the electric solar wind sail concept. The cubesat successfully used its onboard camera to take pictures of its home country but was not able to deploy the 10-m tether due to a possible failure of the deployer, even though there is not an official confirmation of this fact yet.

The main goal of this paper is to introduce a new concept of space tether deployer with retrievable capability presenting the following main characteristics: *a*) compactness and lightness, *b*) simplicity, *c*) reliability. More specifically, the system is presented here with two variations that derives from a common concept, i.e., the fixed-spool reel. In both the solutions presented in this paper, the deployment is initiated by a spring-based launch system. This is a classical solution in thrustless systems, such as SEDS and YES2. The first variation, which from now on will be named *low-inertia* (cf. Figure 1), has a dedicated active brake mechanism, whose aim is to control the tether tension during the deployment, whilst an electric micromotor has the task to retrieve the tip mass once the deployed tether has been seized by a dedicated locking mechanism (*brace*). More specifically, the tether prior to deployment is wound up around a fixed spool, and it is free to flow out from the system with minimal inertia (hence the system name). In this way, there is negligible opposition to the tether acceleration (the mere tether inertia) and the tether exit motion can sustain the relatively high acceleration imparted by the springs. The tip mass is driven along the desired path by means of the tether tension, that is controlled by the brake mechanism. In this study, a simple roller-based linear brake was chosen, in opposition to the classical systems (like barber-pole brakes used in SEDS and YES2 missions), since the deployment of short tethers do not require high control authority. During the retrieval phase, the tether is first engaged by the brace, so that the tether is no longer free to flow. The tether is eventually wound up around the spool by means of an electric micromotor mechanically coupled with the brace. In the second variation (the *inductive brake* system, Figure 2), the brace is always engaged to the tether, and the control of the tether tension during deployment is done by the electric motor by taking advantage of the parasitic currents inside the motor coils induced by the counter-electromotive forces. The retrieval takes place in the same manner of the low-inertia solution. Deployment control is carried out, in both cases, by means of a PD feedback control law, whose control variables are the instantaneous tether length and length rate. The results of this study shows that the applied control law is effective in delivering the tip mass in the desired position for both the solutions, but that the inductive brake variation is more complicated in terms of system design, handling and testing, in addition to some critical issues proper of the system.

One possible utilization of a space tether system like the one proposed in this study could be the delivering, by a servicing spacecraft, of small packages to other spacecrafts already in orbit, this for different purposes, such as de-orbiting of non-cooperative objects (e.g., end-of-life satellites), or extending the life of operational satellites, upgrading their performances or increasing the mission flexibility. This can be accomplished through in-situ operations such as repairing, refueling, reboosting, refurbishing, etc., that are commonly known as On-Orbit Servicing (OOS) [6]. The tethered package could then serve simply as a docking interface[1], or could be utilized as a small "expendable de-orbit package", containing autonomous de-tumbling and de-orbiting hardware that would be attached to the object to-be-deorbited. All these packages should imply grappling systems such as claws, nets or electro-magnetic systems [7][6]. To accomplish this task, a servicing spacecraft should perform a phasing manoeuver in order to bring itself in close proximity of the selected object.

The natural relative motion in orbit between two objects (e.g., the servicing spacecraft and an ejected mass) is essentially a epicycloidal motion depending on the initial conditions. Instead, the motion of two masses connected by tether is of different nature because of the presence of the tether. The motion of a dumbbell system (i.e., two masses connected by a rigid rod) in orbit and its stability has been extensively studied in the literature [8]. As is well-known, a dumbbell system has two equilibrium position, one where the rod is aligned with the local vertical, the other along the local horizontal. Only the first one is stable, hence, a tether deployment performed along the local vertical could take advantage of the motion stability. However, this kind of deployment has a drawback: the relative velocity between the servicing spacecraft and

[1]This is the *soft-docking* concept, i.e., the chaser ejects a tethered probe that eventually docks with a receiving interface on the target; the tether allows then to mate chaser and target by rewinding it, after the two-bodies dynamics has been stabilized [6].

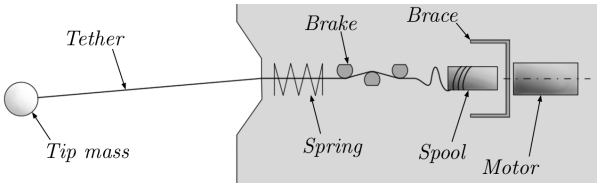


Figure 1: *The* low-inertia *system, during deployment phase.*

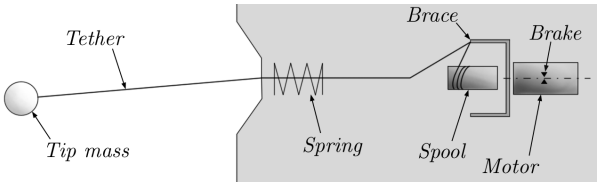


Figure 2: *The* inductive brake *system, during deployment phase.*

the target object is dependent on their relative distance along the radial direction (local vertical). In other words, the more distant along the local vertical the target is, the higher its velocity relative to the servicing spacecraft. For this reason, a docking probe deployed far from the mother spacecraft along the local vertical would have a high rendezvous velocity with respect to the target. This situation should clearly be avoided due to safety requirements. On the other hand, a servicing spacecraft placed on an orbit with semi-major axis similar to that of the target will have very small velocity relatively to the target. As a consequence, a probe deployed along the local horizontal, intended to perform a rendezvous in such configuration, does not suffer from the previously-identified problem. Consequently, in this study we analyze deployment scenarios that take place along the local horizontal. It is also desirable that the tethered probe has small residual libration and length rates at the end of deployment. The chosen scenario is represented in Figure 3.

Finally, we spend a few words on the retrieval capability of the deployer system, even if the problem will not be faced in this study. The retrieval capability enlarges the system reliability, since it provides the possibility to abort an off nominal deployment manoeuver. The deployment manoeuver can, in this way, be attempted again. Besides, in soft docking tasks be-like this capability is a mission requirement. The motion during tether retrieval is generally unstable [9], and, for this reason, classical studies suggest that this maneuver should be taken along the local vertical, where the gravity gradient effect is stabilizing. A schematic example of *abort-and-retrieval* manoeuver is reported in Figure 4.

The paper is organized as follows: in the second paragraph are reported the mathematical models used to predict the tether/probe system behavior, for both the low-inertia and inductive brake systems. In the third paragraph are described the control problem and the numerical implementation. Finally, the implementation results and comparison between the two models are carried out in the fourth paragraph.

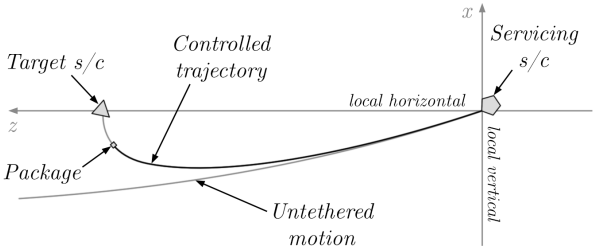


Figure 3: *Deployment scenario.*

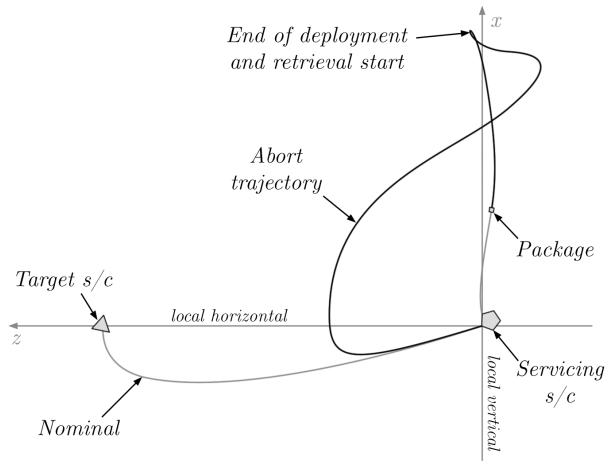


Figure 4: *Deployment abort and tether retrieval manoeuver.*

2. MODELS

The idea at the basis of this work is to design a concept for a tether deployer that is as small and simple as possible. For this reason, a relatively small size was selected, with tether lengths of the order of 10-100 m (as opposite to long multi-km tethers typically treated in literature). A small size was chosen also because a short deployment does not need to be thrust-aided, hence, the achievable total deployed length is limited by the internal friction. Another assumption we have made is that the mother spacecraft and the target are in circular and coplanar orbits. This assumption allows to considerely simplify the relative motion equations.

During tether motion, the forces/accelerations involved are: *a*) Coriolis acceleration, *b*) gravity gradient, *c*) brake-force, and *d*) launching-spring acceleration. Since the deployment is effected along the local horizontal, the gravity gradient force is small. In parallel, a low deployment velocity is preferable due to safety issues. For this reason, the Coriolis force's magnitude is relatively small compared to that of the launching spring's force and the tether tension. Following these assumptions, the maximum velocity experienced by the tip mass will happen at the egress instant from the spring. From this point of view, we can say that the launch spring must necessarily provide the initial velocity required to complete the deployment and, consequently, the launch spring stiffness is directly related to the deployment length and the deploy-

ment friction. Long, thrustless, tether deployments along the local horizontal would require high initial velocities (of order tens of m/s), with negative consequences on safety requirements.

In order to investigate the system dynamics, the tether was modeled as a varying-length dumbbell. Tether attitude is described by means of two variables: *a*) tether length l and *b*) in-plane libration angle θ. The out-of-plane libration motion was ignored because of its negligible influence on tether attitude when the tether is deployed in the orbital plane. θ and l are defined with respect to an LVLH frame of reference $O(x, y, z)$ as follows (cf. Figure 5): the x-axis is directed along the local vertical; the z-axis is directed towards flight direction, in the orbital plane; the y-axis completes the right-handed frame. In-plane libration θ is measured from the x-axis. The mother/servicing spacecraft is positioned at the frame origin (O), and it is assumed to have a much higher mass than the tether/probe system, so that the system center of mass is located at the reference frame origin. The mother spacecraft is orbiting Earth with mean motion $\omega = \sqrt{\frac{\mu}{a^3}}$, with μ the Earth's gravitational parameter and a the semi-major axis of the mother spacecraft's orbit.

The equations of free tether motion, with the mother spacecraft placed in a circular orbit, are reported in Eqq. (1) and (2):

$$\ddot{l} = -\frac{\rho \dot{l}^2}{2(m+\rho l)} + l\frac{2m+\rho l}{2(m+\rho l)}\left[\left(\omega+\dot{\theta}\right)^2 + \ldots \right. \\ \left. \ldots + 3\omega^2\cos^2(\theta)\right] - \frac{T}{m+\rho l} \tag{1}$$

$$\ddot{\theta} = -3\frac{2m+\rho l}{3m+\rho l}\left(\omega+\dot{\theta}\right)\frac{\dot{l}}{l} - 3\omega^2\sin(\theta)\cos(\theta) \tag{2}$$

where m is the tip mass, ρ is the tether linear density and T is the tether tension. In this model, the tether is assumed perfectly rigid. The simplification in this term is justified by the fact that a short tether is indeed stiff. For the derivation of the equations, see Ref. [10]. Since the tether is assumed infinitely rigid, the angle swept by the rotor is directly proportional to the deployed length, i.e., $l = r\psi$, with r the spool radius and ψ the brace rotation angle. The equation means that the tether length is equal to the effectively deployed length. Under these assumptions, the tether tension is directly determined by the brake system; in a similar way, the force applied on the tip mass is the launching-spring force, to yield:

$$T = T_{\text{brake}} + T_0 \tag{3}$$

with T_0 the constant friction term. This term is explicative of the system inner friction, and it is a consequence of the interactions between the tether and the system mechanics. Both terms depend on the system design. Clearly, the better is the system design, the smaller this parameter is.

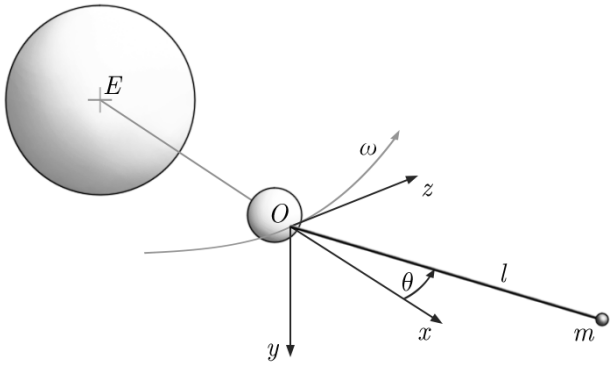


Figure 5: *LVLH frame of reference.*

2.1. *Low-inertia*

In the low-inertia configuration the braking action occurs by means of the interaction between the tether and the brake rollers. This interaction causes friction, the latter tensing the tether in deployment. The friction intensity is controlled by varying the brake rollers relative position. A scheme of the brake geometry is reported in Figure 6.

The variables that describes the tether-roller contact length is the angle α underlying this length. Contact length control can be achieved by opportunely varying the middle roller shift (x coordinate). The law that correlates roller shift x to angle α is Eq. (4):

$$x(\alpha) = d\tan(\alpha) - 2p\frac{1-\cos(\alpha)}{\cos(\alpha)}. \tag{4}$$

Eq. (4) has been expanded in a Taylor series[2]. By comparison of trends (cf. Figure 7), the 1st order approximation was chosen. The inverse function $\alpha = \alpha(x)$ is, consequently, very simple and is reported in equation (5):

$$\alpha(x) = \frac{x}{d} \tag{5}$$

this also brings easy numerical integration. For the specified geometry ($d = 0.09$ m, $p = 0.03$ m), the error deriving by doing this approximation is relatively small for roller shift values up to approximately 9 cm. This is a good upper limit also due to mechanical encumbrance issues. In a more general point of view, by fixing the aspect ratio d/p equal to 3, we can affirm that the linear approximation found by truncation of Taylor expansion at the first term, brings to small error for values of angle α up to approximately 1 rad ($\approx 57°$). The tether tension, due to tether-roller shear friction, becomes equation (6):

$$T_{\text{brake}} = 4\frac{\lambda p}{d}x \tag{6}$$

were it has been assumed a tension behavior directly proportional to the contact length ($T = 4p\alpha\lambda$). p is the rollers' radius and λ is the sliding friction constant. The

[2] $x(\alpha) = d\alpha - p\alpha^2 + \frac{d}{3}\alpha^3 + O(\alpha^4)$

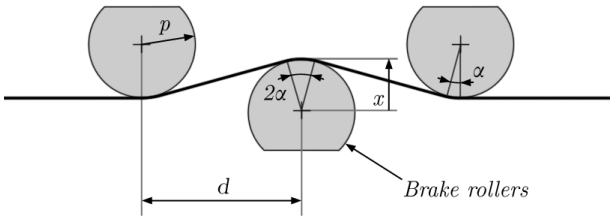


Figure 6: *Low-inertia brake model scheme.*

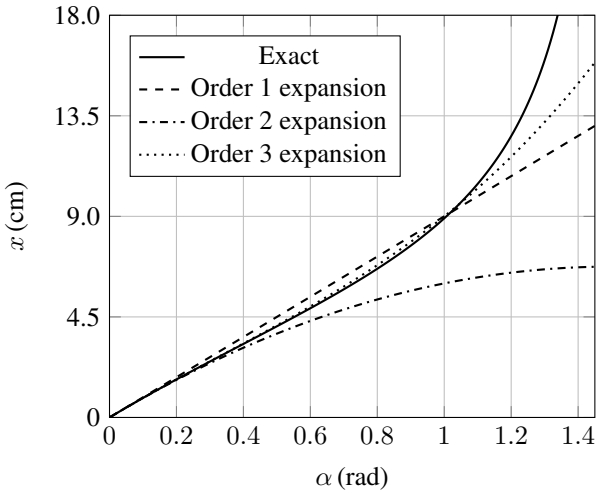


Figure 7: *Middle brake roller shift against angle underlying tether-brake rollers contact length* α*, for* $d = 0.09$ *m and* $p = 0.03$ *m.*

equations of motion of the whole *low-inertia* system are Eqq. (7) and (8):

$$\ddot{l}(m+\rho l) + \frac{\rho}{2}\dot{l}^2 + l\left(m+\frac{\rho}{2}l\right)\left[\left(\omega+\dot{\theta}\right)^2 + \dots \right. \\ \left. \dots + 3\omega\cos^2(\theta)\right] = -4\frac{\lambda p}{d}x - T_0 \tag{7}$$

$$\ddot{\theta} + 3\frac{2m+\rho l}{3m+\rho l}\left(\omega+\dot{\theta}\right)\frac{\dot{l}}{l} + 3\omega^2\sin(\theta)\cos(\theta) = 0 \tag{8}$$

with a state vector of the system defined as follows: $\mathbf{x}_{zi} = (l, \dot{l}, \theta, \dot{\theta})$.

2.2. *Inductive brake*

In the inductive brake solution, the brace is always locked to the tether and control takes place via the torque exploited by the electric motor. The electric motor equations are Eqq. (9) and (10):

$$J\frac{\partial i}{\partial t} + Ri = V - k_v\dot{\psi} \tag{9}$$

$$I\ddot{\psi} + b\dot{\psi} = \tau + k_t i \tag{10}$$

where the term $k_v\dot{\psi}$ is the counter-electromotive force, the $k_t i$ term is the current-induced torque acting on the

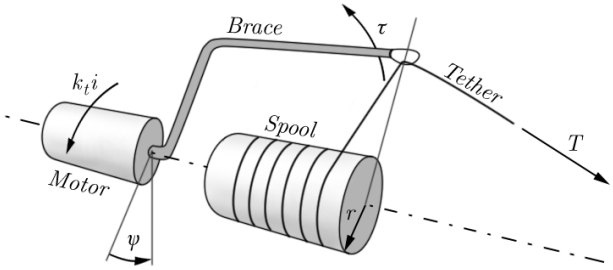


Figure 8: *Sign conventions for the inductive brake system.*

motor shaft, b is the viscous friction constant, I is the rotor inertia, J is the motor inductance and V is the electric tension applied to the statoric circuit of the motor. τ is the mechanical load acting on the motor shaft, an is thus equal to $\tau = Tr$, where $T = T_{\text{brake}} + T_0$ is the tether tension. A scheme illustrating the sign conventions is shown in Figure 8. Combining the models, the equations of motion for the inductive brake system are Eqq. (11), (12), (13):

$$J\frac{\partial i}{\partial t} + Ri = V - k_v\dot{\psi} \tag{11}$$

$$\ddot{\psi}\left[\frac{I}{r} + r(m+\rho r\psi)\right] + \dot{\psi}\left(\frac{b}{r} + \frac{\rho}{2}r^2\dot{\psi}\right) + \dots \\ \dots - \psi r\left(m+\frac{\rho}{2}r\psi\right)\left[\left(\omega+\dot{\theta}\right)^2 + \dots \right. \\ \left. \dots + 3\omega^2\cos^2(\theta)\right] = -\frac{k_t}{r}i - T_0 \tag{12}$$

$$\ddot{\theta} + 3\frac{2m+\rho\psi r}{3m+\rho\psi r}\left(\omega+\dot{\theta}\right)\frac{\dot{\psi}}{\psi} + \dots \\ \dots + 3\omega^2\sin(\theta)\cos(\theta) = 0 \tag{13}$$

with the state vector $\mathbf{x}_{ib} = (i, \psi, \dot{\psi}, \theta, \dot{\theta})$.

3. NUMERICAL IMPLEMENTATION

3.1. Control law

Deployment control is operated, in both systems, by means of a feedback control law. In-plane libration θ and libration rate $\dot{\theta}$ cannot be used as control variables, since a *state observer* system would not be possible to imply because of the high demand in terms of on board resources, such as OBDH, mass and encumbrance, that such a device would require with respect to the whole deployer system. The NASA SEDS-2 mission successfully demonstrated that a small final libration amplitude and libration rate are achievable with a closed loop control law [3], which control variables are the instantaneous tether length and length rate. These variables are easily measurable by appropriate sensors.

The solution of the control problem is a reference trajectory, in the form of l-$\dot{l}$. Specifically, the derivation of

the control trajectory requires solving a two-point boundary value problem. The control is then taken by means of a local linear-feedback controller for a linear-time-varying (LTV) system. The solution of the boundary problem is, in fact, a brakeforce time profile $T = T(t)$, whom drives the tethered probe along the reference trajectory towards the desired final state. Since the dynamics equations of motion are strongly non-linear and mutually coupled, a linearized study is not applicable and a numerical optimization of trajectories must be carried out. For this study, the RETRO software was utilized. The software essential functioning is based on the Nelder-Mead algorithm [11], and tries to minimize the multi-dimensional cost function $\mathcal{F}$ reported in Eq. (14):

$$\mathcal{F} = C_1 \left(l_{\text{end}} - l_{\text{goal}}\right)^2 + C_2 \left(\dot{l}_{\text{end}} - \dot{l}_{\text{goal}}\right)^2 + \dots$$
$$\dots + C_3 \left(\theta_{\text{end}} - \theta_{\text{goal}}\right)^2 + C_4 \left(\dot{\theta}_{\text{end}} - \dot{\theta}_{\text{goal}}\right)^2 \quad (14)$$

where C_i are constant weights, the *goal* parameters are decided *a priori* (in particular, the values of $\dot{l}_{\text{goal}}$ and of $\dot{\theta}_{\text{goal}}$ have always been kept equal to 0) whereas the values for l_{goal} have been varied throughout the simulations (see later). The value for θ_{goal} has been fixed to $90°$. The *end* parameters are the results of an integration of the system equations of motion for a particular brake profile. The integration of the equations of motion has been carried out by means of a 4^{th}-5^{th} order Runge-Kutta integrator. By doing this, the algorithm minimizes the cost function by iteratively varying the brake profile, which is defined by a series of pivot points, which are interpolated by means of cubic splines. The software output is strictly related to the initial pivot points, the boundary conditions (i.e., the tip mass ejection velocity $\dot{l}_0$ and direction θ_0) and the cost function weights. For this reason, being the deployment carried out along an instability position, most of the tried initial position did not bring to convergence the trajectories to the desired final state, i.e., a state vector in the form $\mathbf{x}_{\text{goal}} = (l_{\text{goal}}, 0, \theta_{\text{goal}}, 0)$ for the low-inertia or $\mathbf{x}_{\text{goal}} = (0, \psi_{\text{goal}}, 0, \theta_{\text{goal}}, 0)$ for the inductive brake. A detailed explanation of RETRO functioning can be found in Ref. [10]. An example of the trajectory optimization process is reported in Figure 9.

The control law is a proportional-derivative law based, thus, on the instantaneous tether length and length rate:

$$\mathcal{C} = k_p \left[l_{\text{ref}}(t) - l(t)\right] + k_d \left[\dot{l}_{\text{ref}}(t) - \dot{l}(t)\right] \quad (15)$$

where $\mathcal{C}$ is the control variable. In the two different systems, the control variable is, respectively, the electric tension V applied to the statoric circuit for the inductive brake solution and the middle brake roller shift x for the low-inertia system.

The idea at the basis of the control system is to remove the adequate amount of energy from the system, in order to accompany the probe to the final in-plane libration value. All the optimized trajectories show, moreover, a negative libration rate value, since the deployed dumbbell tends to move towards a stable equilibrium position. The length rate is always decreasing, since the gravity gradient does not exert a relevant force on the deploying probe,

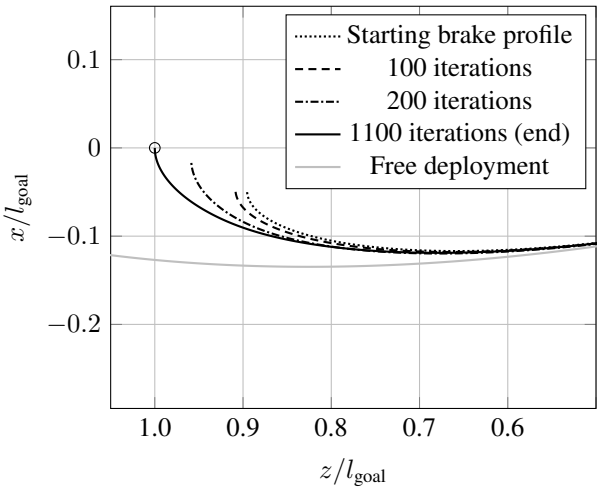


Figure 9: *Example of the optimization process, for an attempt starting brake profile (dotted trajectory). The circle marks the desired final position.*

and, clearly, because the tether cannot be "pushed" by the braking system. A typical trajectory in cartesian coordinates consequent to optimization is reported in Figure 10. The related length, length rate, libration, libration rate, tension rate trends are reported in Figures 11, 12 and 13.

3.2. Boundary conditions

As before described, the servicing spacecraft should be placed in an orbit with a semi-major axis as close as possible to that of the target spacecraft. For this reason we decided to put the two spacecrafts on the same orbit, with no relative velocity. Three post-deployment configurations were considered (Table 1). These cases have in common, clearly, that the deployment is taken along the local horizontal. The launch spring stiffness coefficient has been varied in different simulations, in general keeping it as low as possible, in order to have the lowest spring mass. Anyhow, for the sake of clarity, we decided to report only the probe launch velocity. Also the launch angle θ_0 was varied, depending on the desired final deployed length. As before explained, since the deployment takes place along an unstable equilibrium position, the deployed dumbbell tends to move towards a stable equilibrium position. Moreover, a probe being deployed in the velocity direction will gain an amount of orbital energy that will place it on a higher orbit than that of the mother spacecraft. Therefore, the probe tends to follow a trajectory that will bring her upward. Taken this behavior into account, the launch angle θ_0 must always be greater than the goal angle (i.e., $90°$). The choosing criterion for θ_0 is reported in Eq. (16):

$$\theta_0 = \theta_{\text{goal}} - \bar{\dot{\theta}} t_{\text{end}} \quad (16)$$

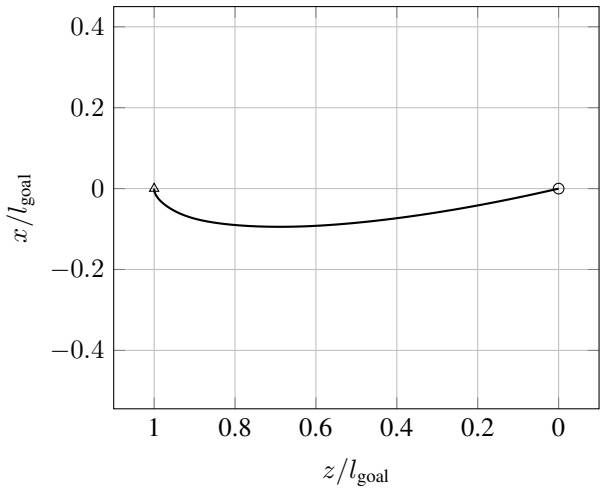


Figure 10: *Typical trajectory in the LVLH frame result of trajectory optimization. The circle marks the start of deployment, the triangle the end of deployment. Positive z/l_{goal} means that the deployment is exerted in the velocity verse.*

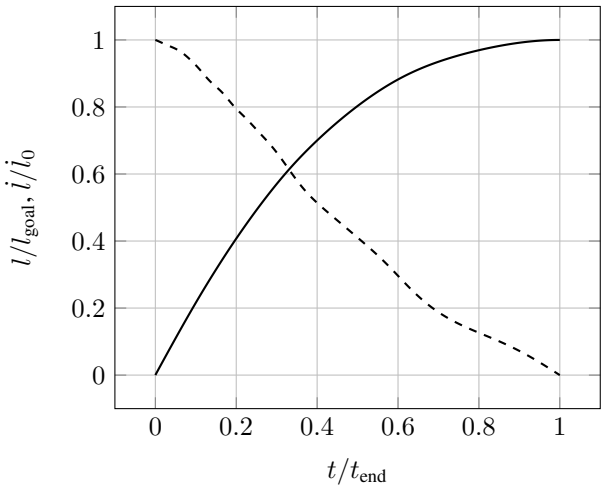


Figure 11: *Typical length (solid) and length rate (dashed) result of trajectory optimization.*

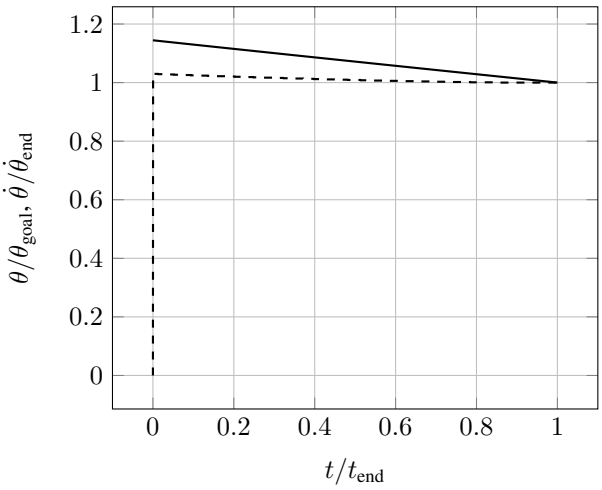


Figure 12: *Typical libration (solid) and libration rate (dashed) result of trajectory optimization.*

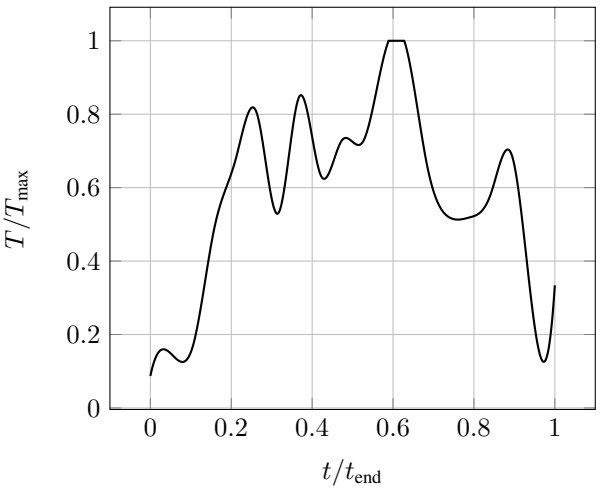


Figure 13: *Typical tension trend result of trajectory optimization.*

l_{goal} (m) $\rightarrow$ $\dot{l}_0$ (m/s) $\downarrow$	50	100	200
0.50	103°	115°	134°
0.75	99°	107°	123°
1.00	96°	101°	114°
1.50	95°	98°	108°
1.75	94.5°	97°	105°
2.00	94°	96°	102°

Table 1: *Chosen launch angles for the considered deployment scenarios. θ_{goal} is always equal to* 90°.

with $\bar{\dot{\theta}}$ the mean angular velocity. $\bar{\dot{\theta}}$ is calculated as reported in Eq. (17):

$$\bar{\dot{\theta}} = -\omega \left(1 + \frac{12}{5}\frac{\omega}{\dot{l}_0}\theta_{\text{goal}} l_{\text{goal}}\right) \tag{17}$$

It is important to underline that $\bar{\dot{\theta}}$ and t_{end} are fictitious values, roughly extimated only for the purpose to yield an initial value for θ. In order to perform this estimation, it has been observed that, for these tether deployment scenarios, $\ddot{\theta}$ is on the average null, so $\dot{\theta} \approx$ const. Equation (17) was derived from Eq. (2) with the hypothesis of $\ddot{\theta} \rightarrow 0$, $\theta \rightarrow \theta_{\text{goal}}$, $\bar{l} = \frac{4}{5} l_{\text{goal}}$, $\bar{\dot{l}} = \frac{\dot{l}_0}{2}$, $\rho l \rightarrow 0$. Moreover, assuming uniformly accelerated motion, we can write $\dot{l}(t) = \dot{l}_0 + \bar{\ddot{l}}t$, that yields[3] Eq. (18):

$$t_{\text{end}} = -\frac{\dot{l}_0}{\bar{\ddot{l}}} \tag{18}$$

where $\bar{\ddot{l}}$ is a fictionous mean acceleration. $\bar{\ddot{l}}$ is estimated as in Eq. (19):

$$\bar{\ddot{l}} = -T_0 - \bar{F}_{\text{friction}} \tag{19}$$

where $\bar{F}_{\text{friction}}$ is the mean hypothesized friction value performable by the braking system. Clearly, the greater the goal length, the larger the initial angle θ_0.

In order to choose a θ_0 value for each simulation scenario, a reasonable choice of initial velocity values has been carried out. In Figure 14 are reported the minimal values for the initial velocity as a function of the goal deployment length, assuming an uniformly accelerated motion under the influence of the sole internal friction. The initial velocity values must clearly stand above the curves reported in Figure 14. The following values for $\dot{l}_0$ have thus been chosen: $\{0.50, 0.75, 1.00, 1.50, 1.75, 2.00\}$ m/s. In Table 1 are reported the related θ_0 values. As a comparison, SEDS-II system deployed a 26 kg tethered mass with a launch velocity of 1.64 m/s [3].

4. MODEL COMPARISON

It has been observed that excessively big goal lengths require a very high initial spring force. In this fashion, the

[3] $\dot{l}(t_{\text{end}}) = 0$

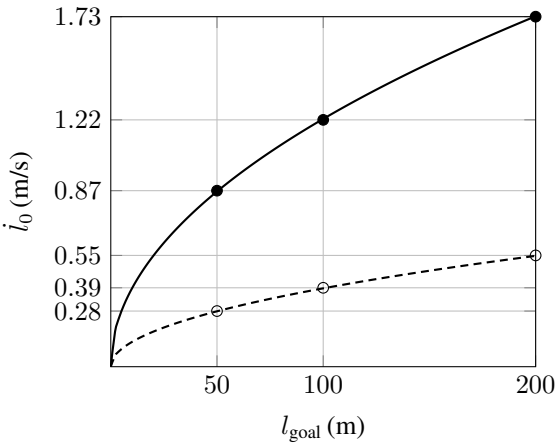


Figure 14: *Lower limit values for $\dot{l}_0$, for low-inertia (dashed) and inductive brake (solid), in the simplified case of uniformly accelerated motion.*

Parameter	Value	Unit
b	$3 \cdot 10^{-6}$	Ns/rad
d	$9 \cdot 10^{-2}$	m
e	0	1
I	$17 \cdot 10^{-7}$	kg m^2
J	$3.65 \cdot 10^{-4}$	H
k_v	$4.05 \cdot 10^{-3}$	Vs/rad
k_t	$3.8675 \cdot 10^{-2}$	Nm/A
p	$3 \cdot 10^{-2}$	m
r	$15 \cdot 10^{-2}$	m
R	2.98	Ω
$T_{0,\text{li}}$	$15 \cdot 10^{-3}$	N
$T_{0,\text{ib}}$	$150 \cdot 10^{-3}$	N
m	20	kg
λ	0.5	N/m
ρ	$1.35 \cdot 10^{-3}$	kg/m
ω	$1.0382 \cdot 10^{-3}$	rad/s

Table 2: *System parameters values.*

l_{goal} (m) $\rightarrow$ $\dot{l}_0$ (m/s) $\downarrow$	50		100		200	
	LI	IB	LI	IB	LI	IB
0.50	●	⊖	●	⊖	⊖	⊖
0.75	⊕	⊖	●	⊖	●	⊖
1.00	⊕	●	⊕	⊖	●	⊖
1.50	⊕	●	⊕	●	⊕	⊖
1.75	⊕	●	⊕	●	⊕	⊖
2.00	⊕	●	⊕	●	⊕	●

Table 3: *Schematic results of the conducted simulations. Successful simulations are marked with the filled circle (●).*

system parameters were fixed to the values reported in Table 2. Constant friction levels ($T_{0,\text{li}}$ for low-inertia, $T_{0,\text{ib}}$ for inductive brake) are estimations based on past hardware studies, such as [3]. The inductive brake constant friction value is significantly higher because of the more sliding parts in the deployment hardware, and the more acute angles drove by the tether. The electrical data is based on commercial off-the-shelf similar-class-hardware.

A total of 36 simulations have been carried out. The results of the conducted simulations are schematically reported in Table 3, whereas the results of the successful simulations are reported in detail in Tables 4 and 5. It is worth remembering that the desired final state vector is equal to $\mathbf{x} = (l_{\text{goal}}, 0, \theta_{\text{goal}}, 0)$, where the 0s means that null final length rate and libration rate are desired. It is also important to point out here that a completely null final libration rate has been proved impossible to achieve, since the equilibrium position along which the deployment was being taken is unstable. For this reason, it has been considered successful a deployment with a final libration rate in the order of 10^{-2} deg/s. Follows a description of the encountered cases (cf. Table 3).

(●) Deployment control was successful and goal state vector achieved.

(⊕) Goal state vector was *not* achieved due to insufficient brake authority control.

(⊖) Goal state vector was *not* achieved due to insufficient initial velocity.

What emerges from the simulations is that the behaviors of the two systems are very different, in the sense that they do acquire similar final state vectors, but by starting from different initial conditions. The following considerations have consequently been taken.

Among all, it is clear that a deployment along the local horizontal is extremely sensitive to initial conditions (being an unstable equilibrium position). In other words, we can say that to obtain a certain profile of deployment is necessary to determine with extreme accuracy the initial conditions of the probe launch. If the initial speed is not correctly determined, the tether-probe system tends to walk away from the equilibrium position, and to align along the local vertical. Conversely, if the deployment had been carried out along the local vertical, shooting approximately around the equilibrium position, the motion would always be stable [10].
The low-inertia system has proven to be easier to design and handle, in both cases of trajectory optimization and numerical integration. Besides, integration time of the low-inertia system is dramatically shorter than that of the inductive brake system. The low-inertia system would thus be preferable at ground test phase.

The error at the end of deployment, for both optimized trajectory and the trajectory obtained by integration with a controller is always less than 0.1% of the desired final position. Deployment time is always in the order of minutes.

The inductive brake system was more authoritative than the low-inertia, since it has achieved a greater number of successful simulations. Anyhow, in some cases high peak current, in the order of 1 A, are reached. For example, in the case of $l_{\text{goal}} = 50$ m, $\dot{l}_0 = 2.00$ m/s, where the highest control authority is needed, we reach a peak current value of approximately 1.5 A. This values may break the security constraints. In fact, in these cases the DC motor was fed to a limit of 24 V (a typical upper limit for COTS DC micromotors).

The limit of the low-inertia is the stroke of the central roller. In this case it has been fixed equal to 9 cm, for encumbrance considerations. This is of obvious pratical consequences: if more control authority is needed, it would be necessary to enlarge the limit, this leading to increased volume encumbrance. In case, the designer should consider a different type of dedicated braking hardware (e.g., classical barberpole brakes).

Other important considerations should be taken about the internal friction value. The friction influence on the tether motion is absolutely relevant in predicting system performances and its value should be determined with extreme accuracy. What we can affirm from this study is that the friction parameter that we estimated strongly penalizes the inductive brake system, which needs a significantly higher launch force, with consequently higher masses in the launch system. Besides, this gap would be strongly enhanced on a smaller-scale platform, e.g., CubeSat application. Care must also be taken when the controller is designed: the system should be worst-case-error-tolerant and capable to handle out of boundaries friction values. We can also say on this point that the low inertia solution could be more tolerant on hardware design inaccuracies, since it has less sliding parts and a considerably lower internal friction parameter. This could lead to less possible system deviation from the nominal condition. In particular, we draw attention on the launch instant, where in the low inertia the tether is free to flow out of the system, whilst in the inductive brake solution the tether/probe motion must accurately be synchronized to that of the brace. If the design has critical issues at this point, the deployment would clearly fail. Further studies are needed on this points, both on worst case error tolerance and on internal friction value determination.

More studies must be carried out also on sensor choice and sizing. The inductive brake solution has only one operating regime (i.e., with the brace always locked to the tether), whereas, conversely, the low inertia has two. This implies the need of more types of sensor for the latter solution and, consequently, more encumbrance, mass and OBDH resources. In particular, the measure of the deployed length in the low-inertia system is not an easy task, since the tether is not mechanically coupled to any rotating device. The measures should, in fact, be taken via optical way.

Finally, post deployment analysis must be carried out, in cases of softdocking following tether deployment, tip mass retrieval and abort-and-retrieval manoeuver.

Low-inertia	
$l_{\text{goal}} = 50$ m $\dot{l}_0 = 0.50$ m/s	$\lvert l_{\text{end}} - l_{\text{goal}} \rvert = 3.6 \cdot 10^{-3}$ m $\lvert \theta_{\text{end}} - \theta_{\text{goal}} \rvert = 6.6 \cdot 10^{-3}$ deg $\dot{l}_{\text{end}} = -0.2 \cdot 10^{-3}$ m/s $t_{\text{end}} = 222.6$ s
$l_{\text{goal}} = 100$ m $\dot{l}_0 = 0.50$ m/s	$\lvert l_{\text{end}} - l_{\text{goal}} \rvert = 0.2 \cdot 10^{-3}$ m $\lvert \theta_{\text{end}} - \theta_{\text{goal}} \rvert = 3.8 \cdot 10^{-3}$ deg $\dot{l}_{\text{end}} = 0.9 \cdot 10^{-3}$ m/s $t_{\text{end}} = 450.6$ s
$l_{\text{goal}} = 100$ m $\dot{l}_0 = 0.75$ m/s	$\lvert l_{\text{end}} - l_{\text{goal}} \rvert = 0.3 \cdot 10^{-3}$ m $\lvert \theta_{\text{end}} - \theta_{\text{goal}} \rvert = 0.4 \cdot 10^{-3}$ deg $\dot{l}_{\text{end}} = 0.9 \cdot 10^{-3}$ m/s $t_{\text{end}} = 295.2$ s
$l_{\text{goal}} = 200$ m $\dot{l}_0 = 0.75$ m/s	$\lvert l_{\text{end}} - l_{\text{goal}} \rvert = 1.3 \cdot 10^{-3}$ m $\lvert \theta_{\text{end}} - \theta_{\text{goal}} \rvert = 0.0 \cdot 10^{-3}$ deg $\dot{l}_{\text{end}} = 0.0 \cdot 10^{-3}$ m/s $t_{\text{end}} = 629.4$ s
$l_{\text{goal}} = 200$ m $\dot{l}_0 = 1.00$ m/s	$\lvert l_{\text{end}} - l_{\text{goal}} \rvert = 0.3 \cdot 10^{-3}$ m $\lvert \theta_{\text{end}} - \theta_{\text{goal}} \rvert = 4.8 \cdot 10^{-3}$ deg $\dot{l}_{\text{end}} = 0.2 \cdot 10^{-3}$ m/s $t_{\text{end}} = 430.4$ s

Table 4: *Detailed results of the successful simulations (●), for the low-inertia system.*

5. CONCLUSIONS

This paper treats the issue of delivering a tethered probe to a desired position in space, by means of a new kind of tether deployer. The the two studied variations of the system design take advantage of a closed-loop controlled brake system. The system could have a number of different applications in tethered missions in space. The control strategy involves the use of a feed-forward reference trajectory and a feedback proportional-derivative control law. A family of length-velocity reference trajectories that guarantee a correct deployment of tethers with total length of 50 m, 100 m and 200 m were found utilizing the Nelder-Mead numerical optimization algorithm. Since the deployment is carried out along an instable equilibrium position, the tip mass ejection angle is dependent on each case goal length. The final error for both optimized trajectories and numercally integrated motion is always less than 0.1%. What emerges from the simulations is that the behaviors of the two systems are very different. The low-inertia system has proven to be easier to design and handle, in both cases of trajectory optimization and numerical integration. Conversely, the inductive brake was the more authoritative solution, even if some critical issues are observed in it. The inner friction strongly penalizes the inductive brake system. Further studies are needed on worst case error tolerance, on internal friction value determination, sensor choice and sizing and on different deployment scenarios.

Inductive brake	
$l_{\text{goal}} = 50$ m $\dot{l}_0 = 1.00$ m/s	$\lvert l_{\text{end}} - l_{\text{goal}} \rvert = 2.9 \cdot 10^{-3}$ m $\lvert \theta_{\text{end}} - \theta_{\text{goal}} \rvert = 1.9 \cdot 10^{-3}$ deg $\dot{l}_{\text{end}} = -0.4 \cdot 10^{-3}$ m/s $t_{\text{end}} = 101.2$ s
$l_{\text{goal}} = 50$ m $\dot{l}_0 = 1.50$ m/s	$\lvert l_{\text{end}} - l_{\text{goal}} \rvert = 1.2 \cdot 10^{-3}$ m $\lvert \theta_{\text{end}} - \theta_{\text{goal}} \rvert = 0.7 \cdot 10^{-3}$ deg $\dot{l}_{\text{end}} = 0.0 \cdot 10^{-3}$ m/s $t_{\text{end}} = 84.3$ s
$l_{\text{goal}} = 50$ m $\dot{l}_0 = 1.75$ m/s	$\lvert l_{\text{end}} - l_{\text{goal}} \rvert = 1.3 \cdot 10^{-3}$ m $\lvert \theta_{\text{end}} - \theta_{\text{goal}} \rvert = 2.5 \cdot 10^{-3}$ deg $\dot{l}_{\text{end}} = -1.7 \cdot 10^{-3}$ m/s $t_{\text{end}} = 75.8$ s
$l_{\text{goal}} = 50$ m $\dot{l}_0 = 2.00$ m/s	$\lvert l_{\text{end}} - l_{\text{goal}} \rvert = 8.8 \cdot 10^{-3}$ m $\lvert \theta_{\text{end}} - \theta_{\text{goal}} \rvert = 13.2 \cdot 10^{-3}$ deg $\dot{l}_{\text{end}} = 3.2 \cdot 10^{-3}$ m/s $t_{\text{end}} = 67.6$ s
$l_{\text{goal}} = 100$ m $\dot{l}_0 = 1.50$ m/s	$\lvert l_{\text{end}} - l_{\text{goal}} \rvert = 82.0 \cdot 10^{-3}$ m $\lvert \theta_{\text{end}} - \theta_{\text{goal}} \rvert = 11.7 \cdot 10^{-3}$ deg $\dot{l}_{\text{end}} = 0.0 \cdot 10^{-3}$ m/s $t_{\text{end}} = 135.6$ s
$l_{\text{goal}} = 100$ m $\dot{l}_0 = 1.75$ m/s	$\lvert l_{\text{end}} - l_{\text{goal}} \rvert = 0.6 \cdot 10^{-3}$ m $\lvert \theta_{\text{end}} - \theta_{\text{goal}} \rvert = 0.2 \cdot 10^{-3}$ deg $\dot{l}_{\text{end}} = -0.1 \cdot 10^{-3}$ m/s $t_{\text{end}} = 118.3$ s
$l_{\text{goal}} = 100$ m $\dot{l}_0 = 2.00$ m/s	$\lvert l_{\text{end}} - l_{\text{goal}} \rvert = 15.9 \cdot 10^{-3}$ m $\lvert \theta_{\text{end}} - \theta_{\text{goal}} \rvert = 2.4 \cdot 10^{-3}$ deg $\dot{l}_{\text{end}} = -0.6 \cdot 10^{-3}$ m/s $t_{\text{end}} = 101.2$ s
$l_{\text{goal}} = 200$ m $\dot{l}_0 = 2.00$ m/s	$\lvert l_{\text{end}} - l_{\text{goal}} \rvert = 0.8 \cdot 10^{-3}$ m $\lvert \theta_{\text{end}} - \theta_{\text{goal}} \rvert = 5.4 \cdot 10^{-3}$ deg $\dot{l}_{\text{end}} = 1.6 \cdot 10^{-3}$ m/s $t_{\text{end}} = 204.7$ s

Table 5: *Detailed results of the successful simulations (●), for the inductive brake system.*

REFERENCES

[1] Dobrowolny, M., and Stone, N.H., "A Technical Overview of TSS-1: the First Tethered-Satellite System Mission", Il Nuovo Cimento C, Vol. 17, No. 1, Jan.-Feb. 1994, pp. 1-12.

[2] Kruijff, M., Van Der Heide, E.J., and Ockels, W.J., "Data Analysis of a Tethered SpaceMail Experiment", Journal of Spacecraft and Rockets, Vol. 46, No. 6, Nov.-Dec. 2009, pp. 1272-1287.

[3] Lorenzini E.C., Bortolami S.B., Rupp C.C., Angrilli F., "Control and Flight Performance of Tethered Satellite Small Expendable Deployment System-II", Journal of Guidance, Control, and Dynamics, Vol. 19, No. 4, 1996, 1148-1156.

[4] Carroll, A.J., "SEDS Deployer Design and Flight Performance", Proceedings of AIAA Space Programs and Technologies Conference and Exhibit, Sept. 1993.

[5] Slavinskis A., Pajusalu M., Kuuste H., Ilbis E., Eenmae T., Sunter I., Laizans K., Ehrpais H., Liias P., Kulu E., Viru J., Kalde J., Kvell U., Kutt J., Zalite K., Kahn K., Latt S., Envall J., Toivanen P., Polkko J., Janhunen P., Rosta R., Kalvas T., Vendt, R., Allik, V., Noorma M., "ESTCube-1 In-Orbit Experience and Lessons Learned", Aerospace and Electronic Systems Magazine, IEEE, Vol. 30, Issue 8, August 2015.

[6] Olivieri L., Mantellato R., Branz F., Sansone F., Cavinato A., Gaino M., Petrillo D., Francesconi A., Lorenzini E.C., "Cubesat Mission Concept for Tethered Electromagnetic Docking Demonstration", Tartu Conference on Space Science and Technology, 2014.

[7] Bonnal C., "Active Debris Removal: Current Status of Activities in CNES", IAF Workshop on Space Debris Removal – UN, Vienna – February 11th, 2013.

[8] Peláez J. and Andres Y.N., "Dynamic Stability of Electrodynamic Tethers in Inclined Elliptical Orbits", Journal of Guidance, Control, and Dynamics, Vol. 28, No. 4, 2005, pp. 611-622.

[9] Misra, A.K., Modi, V.J., "A Survey on the Dynamics and Control of Tethered Satellite Systems", NASA, AIAA, and PSN, International Conference on Tethers in Space, Arlington, VA, Sept. 17-19, 1986, Paper. 54 p.

[10] Mantellato R., Valmorbida A., and Lorenzini E.C., "Thrust-Aided Librating Deployment of Tape Tethers", Journal of Spacecraft and Rockets 52:5, 2015, 1395-1406.

[11] Nelder, J.A. and Mead, R., "A Simplex Method for Function Minimization", The Computer Journal, Vol. 7, pp. 308-313, 1965.

LARGE DEPOT TO SERVICE MANNED MARS MISSIONS

M. Baiguera[1], M. Magnani[2], S.F. Rafano Carnà[3], A. Serboli[4], A. Tiwari[5], and M. Lavagna[6]

[1]*Email: matteo.baiguera@mail.polimi.it Tel:+39 328 0269059*
[2]*Email: marco.magnani1@mail.polimi.it Tel:+39 334 1734557*
[3]*Email: simone.rafano@mail.polimi.it Tel: +39 348 13248794*
[4]*Email: alessandro.serboli@mail.polimi.it Tel: +39 338 8961476*
[5]*Email: anurag.tiwari@mail.polimi.it Tel: +39 351 1355616,*
[1,2,3,4,5]*Politecnico di Milano, Space Engineering MS students, Aerospace Science and Technology Department, via La Masa 34, 20156, MILAN, ITALY*
[6]*Politecnico di Milano, Associate Professor, Aerospace Science and Technology Department, via La Masa 34, 20156, MILAN, ITALY, Email: michelle.lavagna@polimi.it Tel: +39 02 2399 8364*

ABSTRACT

A 3 months study is proposed, developed during the Space Mission Analysis and Design course at Politecnico di Milano, performed with a concurrent design strategy by a team of 13 graduated students in Space Engineering. The name given to the mission is ARDENT, acronym of: Aided Refueling DEpot NeTwork. The challenging study aims to assess the feasibility of a long term propellant depot to support fast and recurrent manned mission to Mars, to enhance the human spaceflight frontiers and develop on-orbit large structures. The numerous multidisciplinary trade-offs have been performed with a multicriteria decision making approach, including cost, mass timeliness and reliability. The comprehensive analysis run to fix the baseline mission phases, timeline and operations, strongly affected by the selection of the depot location in space and the limiting launchable mass constraint, is here discussed in details.

Key words: On-orbit Refuelling Network; On-orbit Staging; Modular structures; Cluster of trusses; Cryogenic hydrogen storage; CR3BP..

1. INTRODUCTION

When speaking about human space flights outside the terrestrial magnetic field, the exposure to solar and cosmic radiations is always a crucial problem in order to guarantee crew health. This work assesses the feasibility of a solution which aims at reducing at most the duration of a deep-space journey to Mars constraining it within 250 days of crew permanence in space. As a consequence, this choice leads to face further challenges to design the mission: extremely expensive interplanetary manoeuvres require the introduction of propulsive units with very high specific impulse, but also high thrust level, such as nuclear propulsive systems. Despite the high specific impulse of these propulsive hardware, the extremely short time of the mission duration requires also customized structures able to host huge fuel tanks and systems capable of performing in-space refuelling. Analysing the Porkchop plot in fig.1, it is clear that a window for a trip to Mars opens up about each 26 months. In order to exploit as many transfer windows to Mars as possible, it is necessary to develop a configuration which is really flexible and capable of adapting to the strongly varying cost in terms of Δv among the different windows. The ISS European module Columbus has been taken as a reference for the engineering budgets of the manned living vehicle. In particular, a payload mass of 10 tons has been considered as minimum capacity for the return trip. On the contrary, all the others vehicles and subsystems needed to make feasible the full mission have been developed and studied with the highest level of detail compatible with the TRL of the specific element. The strategy proposed consists in assembling all the mission's vehicles in Halo orbit around the first Lagrangian point of the Earth-Moon system (EML1) and transferring in advance the fuel in orbit around Mars for the return of the manned mission. In particular, the propulsion units are assembled in EML1 together with some support structures using a robotic arm and subsequently refuelled with modular tanks of different sizes. All components (structural elements, propulsive units and fuel-tanks) are relocated in EML1 exploiting a multi-launches strategy imposed by the launchers maximum mass or envelope limitations. A brief overview of the mission scenario is reported below, with particular focus on the mission phases (fig.2) and on the developed vehicles. A more detailed analysis can be found in ref.[1] and ref.[2], including the description of the assembly and refuelling operations as well as the mission analysis.

Mission Phases:

1. *Robotic core launch to EML1*: a robotic S/C equipped with a robotic arm is launched to EML1

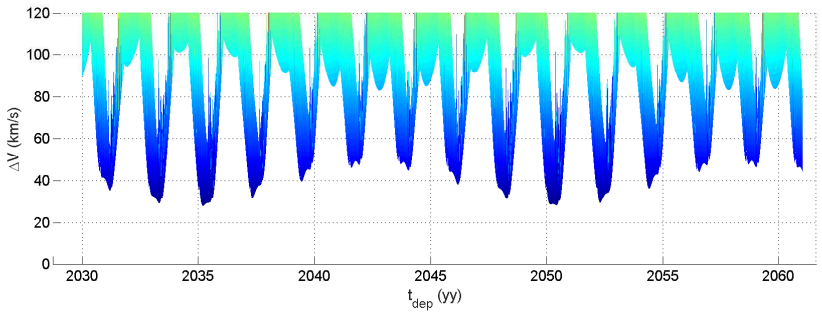


Figure 1. Porkchop plot for the Mars round-trip.

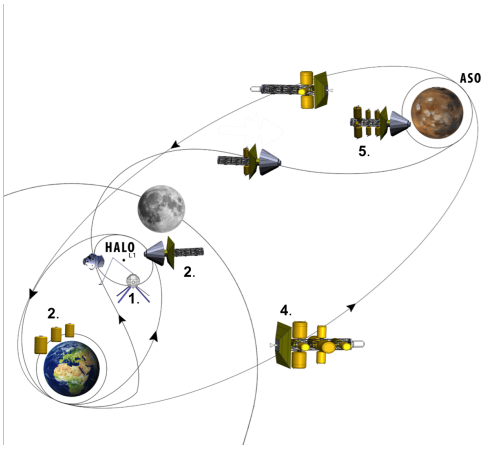


Figure 2. ARDENT mission: strategy overview

2. *Mars depot assembly and refuelling*: structural elements and a continuous thrust propulsion unit are sent to EML1 and assembled together using a robotic arm. Once the main body of the Mars depot is completed, fuel tanks are sent from Earth. Such fuel tanks will properly feed the propulsion unit of the Mars depot, but they will also constitute the fuel-reservoir for the return leg of the manned S/C (refuelling operations occurring around Mars). Once the Mars depot is completely assembled and refuelled, it starts its travel from EML1 to Mars lasting approximately 3 years.

3. *Manned S/C assembly and refuelling*: thanks to the robotic arm, also main structure of the manned S/C is assembled in EML1 (propulsion unit + structural elements + Columbus-like module). The fuel tanks needed to perform the first leg of the round-trip are launched and docked to the main structure of the manned S/C.

4. *Departure*: only when the Mars depot reaches the desired orbit around Mars: the Areostationary Orbit (ASO), the crew is sent to EML1 with a dedicated launch. The crew moves from the Crew Transfer Vehicle (CTV) to the Habitable Module (Columbus-like module) and finally the travel to Mars starts.

5. *Human mission on Mars and manned S/C refuelling*: the human crew executes the planned mission on Mars. In the meanwhile, the tanks carried by the Mars depot undock and are transferred on the manned S/C. Once refuelling operations are concluded and the crew is again on-board, the return travel starts.

6. *Manned S/C return*: when reaching the proximity of Earth, another braking manoeuvre is performed, allowing the manned S/C to decrease its energy and to park again on the operational halo orbit. The crew move back to Earth with the dedicated module and the manned S/C waits in orbit to be refuelled in sight of the next mission.

7. *Mars depot return to EML1*: also the Mars Depot slowly comes back to the proper parking halo orbit around EML1, ready to serve the next mission to the Red planet.

The previously illustrated operational phases are aimed to start an iterative-loop of missions to Mars (starting from phase-2). Once the manned S/C and the Mars depot's main structures have been assembled for the first time, only re-sizing operations are required, performed by means of the robotic arm. Indeed, because of the extremely variable ΔV cost depending on the launch window, the Mars depot and the manned S/C main structures have to be modified in order to host the correct number of fuel tanks to perform the n-th mission. This avoids to size the vehicles accordingly with the most demanding window with the consequence of useless augmented dry mass and fuel waste.

Mars Depots: ARES

It has the task to carry liquid hydrogen tanks in ASO, in order to provide the manned s/c with the fuel needed to perform the impulsive manoeuvres of Mars escape and Earth capture. It is propelled by Magneto Plasma Dynamic (MPD) thrusters and implements a thermal shield for the tanks. A nuclear reactor, equipped with a radiator, deliver the required power to the MPD engine. A CAD representation of the ARES vehicle is given in fig.3.

Manned spacecraft: DIOMEDE

Its main structure is an assembly of truss-structures, as many as needed to support the required number of tanks

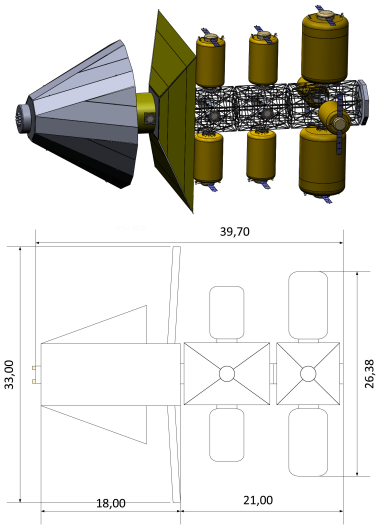


Figure 3. Representation of the ARES vehicle. On the top a 3D visualization is given, on the bottom the dimensions (in meters) are reported in a 2D schematic view

of fuel. The propulsion unit is the ANERVA (a nuclear thermal propulsive system [3]). Its mission is to carry the crew (hosted in the habitable module located at the tip in image 4) during the round-trip to Mars. It uses a thermal shield to protect from Sun irradiation the tanks of liquid hydrogen. A CAD representation of the DIOMEDE vehicle is given in fig.4.

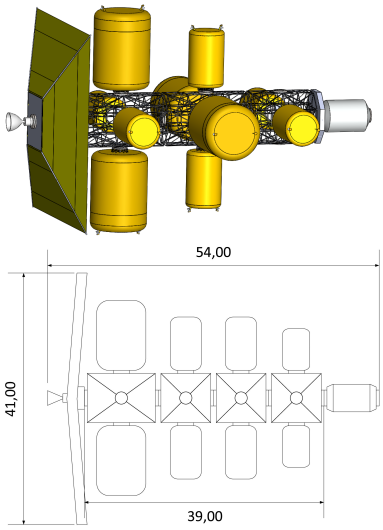


Figure 4. Representation of the DIOMEDE vehicle. On the top a 3D visualization is given, on the bottom the dimensions (in meters) are reported in a 2D schematic view

Service module: ICARUS
All the standardized components (truss elements, propellant tanks and propulsive units) are meant to be brought to EML1 directly by the launchers. However an AOCS unit, named ICARUS, is necessary in order to successfully complete the rendezvous and docking to the main structures of ARES or DIOMEDE.

CORE and Robotic Arm
A robotic arm, mounted on a proper spacecraft called CORE, is used to perform the assembly of the main structures of DIOMEDE (the manned spacecraft) and ARES (the Mars depot). Once the main body of DIOMEDE and ARES is assembled by jointing axially all the truss elements and the propulsive modules, propellant tanks will be docked radially to the main body in a second time. The CORE has available four docking ports, whose usually two are used to accumulate unused truss elements. A CAD representation of the CORE vehicle is given in fig.5.

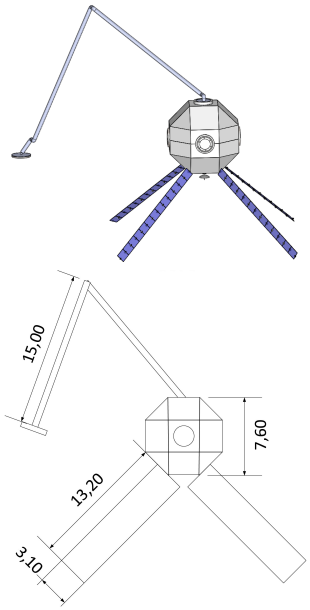


Figure 5. Representation of the CORE vehicle. On the left a 3D visualization is given, on the bottom the dimensions are reported in a 2D schematic view

2. STRUCTURAL SUBSYSTEM

Tanks
The distinctive trait of this mission is the usage of large structures: this is mainly dictated by the need of carrying a large amount of propellant. According to an optimal staging approach tanks of hundreds of tons might be required for the worst case conditions. Of course this necessity must be mitigated by the maximum launch capacity in EML1 of the future launchers: in this case the maximum is fixed by the Space Launch System (SLS) which is able to launch in EML1 a payload of about 40 tons. The low density of hydrogen gives rise to the need of huge tanks: $8m$ of diameter for an height of $11m$. Three different sizes of tanks has been designed in order to approximate the optimal staging without manufacturing tanks with many different sizes. Table 1 shows the size of each tank with the corresponding mass of hydrogen. These

Table 1. Tank dimensions

Tank	*Diameter [m]*	*Height [m]*	*H2 mass [tons]*
T-40	8	11.4	35
T-13	5	8.7	11.3
T-8	4.4	6.8	7

tanks have to bear all the launch loads and respect the frequency constraint of the launcher. To overcome this issue, an extremely high modulus carbon/epoxy material has been selected. Tank mounting is a key factor in the design of the tank, since all static and dynamic loads imposed on the tank are transferred through the mount to the tank shell. For this reason, a truncated cone made of carbon/epoxy has been designed in order to fix the tank circumferentially to the launcher. The skin of the tank is made of sandwich structure with two external layers of carbon composite and an internal core of honeycomb in order to increase the bending stiffness. The shape of the tank is suitable for filament winding technique which constitutes a great opportunity to increase the fibre percentage within the composite. The circular attachment line on the tank is reinforced with a stiffening ring made of Carbon/Epoxy which provides also the opportunity to install explosive bolts for the detachment phase. A finite element model is built up (figure 6) in order to verify that frequency constraints are satisfied, whereas as regards the static loads, since the material of the tank is anisotropic, Tsai-Wu failure criterion has been chosen in order to verify the strength. In table 2 are summarized all the components for the T-40 tank. The FEM results are resumed in table 5 for the three different assemblies.

Table 2. FEM: T-40 assembly

Component	*Mass* $[kg]$	*Material*	*FEM element*
Tank	3700	Nomex Sandwich	S4R
ICARUS-40	180	Al-Li alloy	S4R
Fuel (MMH)	770	-	R3D4
Oxydizer (N_2H_4)	1280	-	R3D4
Pressurant (He)	40	-	R3D4
Solar arrays	20	-	Point mass
Thrusters	45	-	Point mass
Stiffening ring	55	carbon/epoxy	B31
Skirt	2000	carbon/epoxy	S4R

Trusses

The trusses are the main structural components of DIOMEDE and ARES spacecraft. They have the task to host all the tanks needed to perform the round-trip to

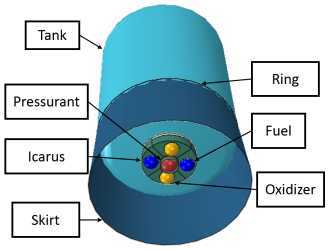


Figure 6. Finite element assembly

Table 3. FEM results for the Tanks

Tank	*Tsai-Wu criterion*	*First bending [Hz]*	*First axial [Hz]*
Tank 40	0.5	16	71
Tank 13	0.35	22	77
Tank 8	0.3	24	82

Mars with a minimal structural mass: for this reason a truss is preferred with respect to a monocoque structure. The main driver for the design of the trusses is the mass. This because the trusses constitute the dry mass of the human flight of DIOMEDE and of the ARES transfer. A second design driver comes from the launch configuration. Due to the large diameter of the Truss, SLS launcher is required in any case, even if the payload mass is far below the maximum limit of the launcher. In order to not exceed the annual launch capacity, it has been chosen to launch two truss elements together, one attached on the top of the other. This of course might cause a problem in terms of bending stiffness: it has been decided to avoid the launch configuration of two beam of 12 m long, so the worst case is represented by 12m+9m beam configuration. This launch configuration gives rise a problem in terms of frequency requirements. This represents the second main driver for the design of the truss: stiffness. These two requirements combined together leads to the selection of Boron/Epoxy composite. An octagonal shape of 3 meters allows to fulfil these requirements and to exploit and optimize the fairing volume of the SLS. The assembly submitted for the analysis is resumed in table 4 and it is shown in figure 7. Table 5 shows that the maximum stress is far below the limit of boron/epoxy composite, which is one of the highest among the aerospace materials. Also the maximum compression load is far below the critical for buckling. In addition the frequency requirements are satisfied with a margin of safety of at least 2.

CORE

The CORE is the permanent structure in charge of assembling the trusses for ARES and DIOMEDE spacecraft. The main drivers for the design are essentially geometric: the CORE has to be compatible with the trusses and has to guarantee a margin in terms of distance when the

Table 4. FEM assembly for Truss-12 + Truss-9

Component	*Mass* $[kg]$	*Material*	*FEM element*
Truss 12	2200	Boron/epoxy	B33
Truss 9	2000	Boron/epoxy	B33
ICARUS 13	270	Al-Li	S4R
Fuel (MMH)	270	-	R3D4
Oxydizer (N_2H_4)	440	-	R3D4
Pressurant (He)	30	-	R3D4
Solar arrays	25	-	Point mass
CMG	200	-	Point mass
Docking port	100	-	Point mass

Table 5. FEM: results for Trusses

Configuration	*Truss 9+ Truss 12*	*Truss 9 + Truss 9*
Max Von Mises (MPa)	22	18
Max Compression Load (kN)	45	40
First bending [Hz]	16	20
First axial [Hz]	82	86

assembly phases take place. The resulting shape is a regular octagonal section of 3m side which allows to satisfy the constraints and also to reduce the total mass. The material selected is Al-Li alloy which constitutes the main structure (central cylindrical monocoque with 4 stiffening panels) reinforced with boron/epoxy stringers in order to avoid resonance of the panels at launch. The complete assembly submitted to finite element analysis is represented in figure 8. Table 7 summarizes the results.

Robotic Arm

The robotic arm is the main mechanism the CORE is equipped with. The main requirement it has to satisfy

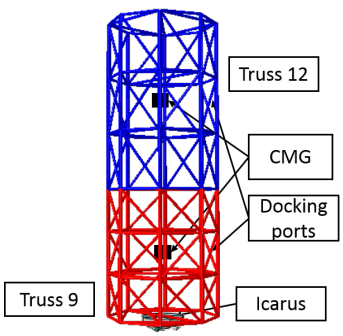


Figure 7. Finite element assembly

Table 6. FEM assembly: CORE

Component	*Mass* $[kg]$	*Material*	*FEM element*
CORE	3000	Al-Li	B31
Stringers	400	Boron/epoxy	B31
Folded arm	650	Boron/epoxy	B31
Cable	25	Carbon Fibre	Spring
Hydrazine	600	-	R3D4
Solar arrays	110	-	Point mass
CMG	200	-	Point mass
Docking port	100	-	Point mass

Table 7. FEM: CORE results

	Max Von Mises (MPa)	*First bending [Hz]*	*First axial [Hz]*
CORE	22	22	142

is in terms of length: in order to correctly assemble the trusses for DIOMEDE and ARES spacecraft the robotic arm must be capable of reaching the second truss, which is at least 25 m apart. According to the standardized manoeuvres, the robotic arm has to accomplish, 4 degrees of freedom are sufficient, nevertheless a fifth one is added in order to face unusual orientations such as erroneous alignment of the truss with respect to the CORE. Finally the maximum handling capacity is dictated according to the highest load it has to carry, which in this case is represented by the nuclear reactor for the MPD engine. The main features of the ARDENT Robotic Arm are listed in table 8.

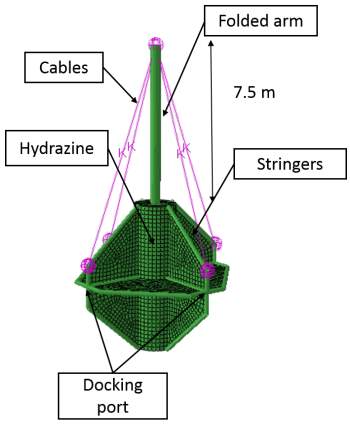


Figure 8. CORE: assembly

Table 8. FEM: CORE results

ARDENT Arm	
Length	30 m
Structural mass	650 kg
Material	Boron/Epoxy
Diameter	50 cm
DOF	5 (2 shoulder, 1 elbow, 2 wrist)
Mass handling capacity	50 tons
Speed of operations	13 cm/s unloaded 3 cm/s loaded

3. PROPULSIVE SUBSYSTEM

ANERVA

The NTP system is used on the manned mission, in order to allow fast transit times thanks to the high thrust and providing at the same higher specific impulse compared to traditional chemical propulsion systems. The following data are required as input for the described preliminary sizing procedure (ref.[4]):

- reactor power density P in $\frac{W}{m^3}$
- desired gravimetric specific impulse I_{sp} in s
- thrust T in kN

The following data, on the contrary, have been assumed:

- chamber pressure: 35 atm
- chamber temperature: 3100 K

The reactor power density required to heat hydrogen at 3100K is equal to $P = 50.27W/m^3$, while the burn time has been conservatively estimated with the following relationship:

$$t_b = TWR_{goal}\Delta V_{max}N_{trips} \tag{1}$$

where $\Delta V_{max} = 36km/s$, the total number of trips to be accomplished is $N_{trips} = 10$ and $TWR_{goal} = 0.09$. Using these conservative values (a lower than expected thrust-to-weight ratio TWR and the worst encountered ΔV) ensures that enough fuel is available to accomplish the mission for all the windows. Assuming a gravimetric specific impulse value of $I_{sp} = 1000s$ (ref.[3]) the mass flow rate $\dot{m}$ assumes a value around $21\frac{kg}{s}$. Then, using the data in ref.[5], the reactor specific power density P can be estimated, assuming a chamber temperature of 3100K and the use of hydrogen as propellant. Therefore, the total core power P_C is computed:

$$P_C = P\dot{m} \tag{2}$$

Assuming an Uranium-fuelled reactor, the quantity of fuel used can be estimated:

$$E_C = P_C t_b \tag{3}$$

For a NERVA-type reactor with a reflector, the final design equation can be formalized as follows:

$$\left(R_C^2\right)^3 - \left(\frac{BV_C}{\pi^2}\right)^2 \left(R_C^2\right) + \left(\frac{2.405V_C}{f_{refl}\pi^2}\right)^2 = 0 \tag{4}$$

where f_{refl} is the reflection coefficient which take values between 1.1 and 1.2, B is the material buckling parameter, R_C and V_C are the radius and the volume of the core, respectively. The chosen reactor power level lies under 1290MW by a small margin, necessitating a reflector, for which a reflection coefficient of $f_{refl} = 1.1$ is assumed. A shadow shield has been considered, which does not completely enclose the reactor but limits itself to provide a "shadow" protecting the rest of the spacecraft. The results obtained are presented in table 9.

Table 9. ANERVA reactor sizing results

P_C (MW)	R_C (m)	H_C (m)	M_C (kg)	M_{shield} (kg)
1095	0.54	0.78	1604.55	3142.38

MPD

The power of the MPD engine is dictated by the heaviest launchable reactor, which, with a mass of 39 tons, limits the electrical power available to 9.895 MW. Due to lifetime constraints (maximum engine lifetime limited to 2000 hours) more than one thruster is needed, but these multiple engines have to be used one at a time, so that the single engine guarantees the specified acceleration. This preliminary design is based on the study and the findings reported in ref.[6]. Knowing the required thrust from mission analysis and the geometry of the propulsive system (internal and external radius of the duct) the current required is easily computed. According to ref.[6], a quite conservative value of specific impulse to take into account is $I_{sp} = 5000\ s$. Therefore, the ideal kinetic power associated to the thrust can be obtained as

$$P_T = \frac{1}{2}\dot{m}v_e^2 = \frac{b^2k^*}{2}J^2 \tag{5}$$

where J is the electrical current, $k*$ is the critical mass flow rate. The evaluation of the mass, due to the very poor availability of data, is carried on using the same power-to-weight ratio as the one obtained in the Pegasus project (ref.[7]). In this study a 7-thrusters assembly mass of $M_{PEG} = 700kg$ and an overall power $P_{PEG} = 6.5\ MW$ are used. These data give as a mass-to-power ratio for the single thruster of:

$$(M/P)_{PEG} = 16.67kg/kW \tag{6}$$

Knowing the input power and this ratio, the mass can be esteemed as (adding a safety margin of $M_{sm} = 20\%$):

$$M_{MPD} = \frac{P_{input}}{(M/P)_{PEG}}(1 + M_{sm}) \tag{7}$$

A final consideration must be made: from the available resources, it is known that these systems have a limited operative lifetime of about 2000 h (ref.[8]), leading to the need to have multiple thrusters to be used one after the other in order to reach the target total lifetime of $1000 days$. The total engine mass is the computed as

$$M_{engine} = N_{engines} M_{MPD} \tag{8}$$

Table 10. MPD preliminary sizing results

b_{time} $(days)$	$lifetime$ $(hours)$	$N_{engines}$	T (N)	M_{eng} (kg)	P_{eng} (MW)
1000	2000	12	121	2375	9.9

4. ELECTRICAL POWER SUBSYSTEM

The challenge in the design of the Electrical Power System (EPS) for the ARDENT mission is represented by the ARES vehicle. Indeed, the extremely high power demand of the MPD thrusters (9.895 MW), installed on it, force the use of a nuclear reactor as power source. Nuclear technologies for space were poorly researched in the last decades, apart from RTG systems. Last important projects in this field were developed in the 90s and only in recent years nuclear reactors had been considered again as power generator for large electric thrusters. In order to perform a preliminary sizing of the nuclear system, a regression law is obtained from all the nuclear reactors sized for space, both with static conversion (thermocouples) and dynamic conversion (turbines, pistons). These data are reported in ref.[1].
The regression law resulting by the comparison is:

$$m_{sys}(kg) = 0.63551[Q_{in}(W)]^{0.62604} \tag{9}$$

where m_{sys} is the overall mass of the system and Q_{in} is the thermal power produced by the nuclear reactor. Q_{in} is afterwards the input of the power conversion system which converts it in the requested electrical power L_{out}, with a certain amount of dissipated power Q_{out} as function of its efficiency. For this specific application, the *dynamic* power conversion is selected because of its higher conversion efficiency and despite its higher complexity. Among the dynamic power conversion methods only the Brayton cycle is ideal for space. Firstly, its simplicity decreases the possibility of mechanical failure. Any rotating shaft can be supported on working fluid gas compliant foil bearings that are noncontacting except for a

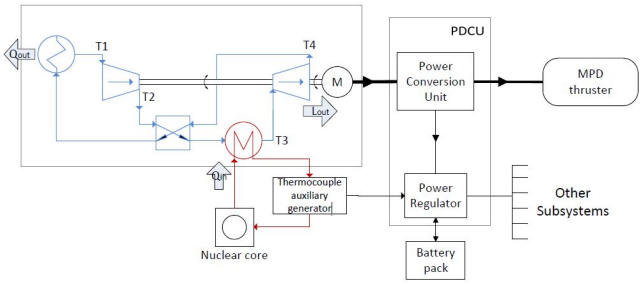


Figure 9. Schematic representation of ARES EPS diagram

brief start-up period. Secondly, a Brayton cycle has significant power scaling advantages and can be used from low kilowatt to multi-megawatt ranges, with the possibility of using a recuperator to increase the efficiency. A scheme of the EPS system for the ARES vehicle, including the Brayton cycle, is reported in fig.9. A mixture of Helium and Xenon with molecular weight of 83.8 g/mol is selected as working fluid and preferred to the use of supercritical fluids. The choice is strongly driven by the high corrosivity of the supercritical fluids, which are not suitable for long space missions and their low TRL (3-4), despite their extremely high efficiency. On the contrary, the He-Xe mixture has higher endurance and absence of corrosion, good efficiency and well-known behaviour (TRL 5-6) of ideal gas with respect to supercritical fluids. The goal of the design is to find a compromise between the overall mass of the system m_{sys}, which has to be launched, and the radiator area A_{rad} needed to dissipate in outer space Q_{out}, reducing thus the deployment related problems. By fixing pressure at compressor inlet P_1 and the temperature at the turbine inlet T_3, it is possible to express all the quantities as function of the pressure ratio β of the Brayton cycle. Indeed, using eq.10 and selecting the compressor inlet temperature T_1 that minimize A_{rad} (since a single value of T_1 exists that satisfies this condition), it is possible to correlate the radiator area A_{rad} to the dissipated power Q_{out} and consequently to the Brayton cycle efficiency η and finally to the pressure ratio β.

$$Q_{out} = \frac{1}{T_4' - T_1} \int_{T_1}^{T_4'} \sigma \varepsilon A_{rad} T^4 dT \tag{10}$$

Similarly, using eq.9, also the total mass of the system becomes a function of η and therefore of β. In this way, a one by one relation is obtained between the mass of the system and the radiator area, which is plotted in fig.10. The largest launchable mass in EML1 is around 40 tons and, as it can be seen, the radiator area increases rapidly when the mass is reduced below this threshold. As a consequence, it has been decided to fix the system mass to the maximum possible of 39 tons in order to get a reasonable value for the radiator area of 1000 m^2. All the other parameters of the cycle are consequently computed and collected in tab.11.

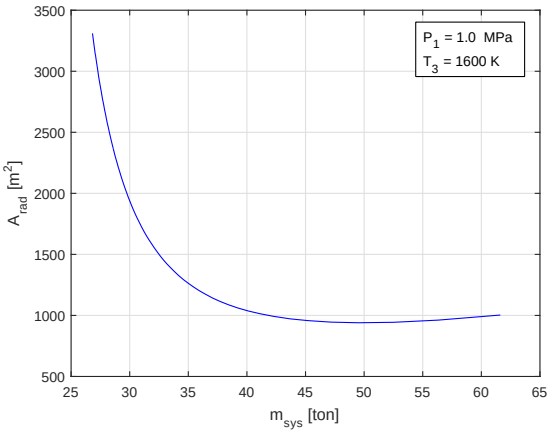


Figure 10. Radiator area over overall mass of the nuclear power generator system

Table 11. Brayton cycle and nuclear power generator system selected parameters

Parameter	*Value*
Compressor inlet temp. T_1	547 K
Compressor inlet press. P_1	1.0 Mpa
Turbine inlet temp. T_3	1600 K
Overall mass m_{sys}	40 T
Radiator area A_{rad}	1000 m^2
Pressure ratio $\beta = P_2/P_1$	2.6
Brayton cycle efficiency η	31 %
Oversizing margin	12 %
Radiator emissivity ε	0.92 -

5. THERMAL CONTROL SUBSYSTEM

The use of cryogenic propellants is crucial for the ARDENT mission because of the extremely high specific impulse they can give. Consequently, the thermal control subsystem has to face the challenging task to guarantee long term storage of the propellants at the cryogenic liquid state. A powerful technique to achieve this goal is to sub-cool the propellants below the boiling point. This operation is intended to be done *on ground* before the launch at atmospheric pressure. Indeed, cryogenic propellants such as liquid hydrogen have very large heat capacities. This characteristic implies the necessity of a large amount of heat to increase the temperature from the sub-cooled point to the boiling point. Thus, reducing efficiently the amount of power that leaks into the tank, it is possible to make the heating period to last for months and even years. The Thermodynamic Cryogenic Subcooler (TCS) (ref.[9]) is the name of the technique proposed to get this result, using a conceptually simple thermodynamic process. The hydrogen that is being sub-cooled, is extracted from the tank. Some of this extracted hydrogen passes through a Joule-Thomson (J-T) valve that isenthalpically expands it, decreasing its pressure and temperature and becomes a two-phase flow. Since the hydrogen in two-phase state is at a lower temperature ($\sim$15k) than the hydrogen in the single-phase state ($\sim$20.4k), it can extract heat from the hydrogen in the single-phase state and thus sub-cool the propellant. During the heat exchange, the two-phase hydrogen increases in vapour quality and is vented to a flare stack through a compressor system when it is totally vaporized. All the process is performed on the launchpad just before the launch and all the components (the heat exchanger, the pump, the compressor, the J-T valve and the insulation system) have not to be launched decreasing in this way at minimum the mass. In addition to the TCS technique, other two tools have been used to keep the hydrogen temperature below the boiling point: covering the tanks with Multi-Layer Insulation (MLI) and equipping DIOMEDE and all the ARES vehicles with a thermal shield. In particular, 30 MLI layers are used for the small tanks (because of their lower mass and so lower heat capacitance) and 20 for medium and large tanks, resulting in 285 kg, 228 kg and 436 kg of MLI mass, respectively. The thermal shield is intended as additional 10 MLI layers to be used as an umbrella during the non-thrusting phases, keeping a Sun point attitude. The thermal shield helps in decreasing the solar power that reaches the tanks but increases the vehicle mass of 500 kg. The worst condition along the ARDENT mission is surely the ARES travel from EML1 to ASO, because ARES cruise includes a long phase nearly at 0.8 AU from the Sun, that results in a high increase of the heat received by the tanks. The analysis has been carried on using the single node approximation, considering Sun irradiation as heat source and space radiation as heat sink and neglecting planets albedo and radiation (because of the large altitude of the considered orbits) and components heat dissipation. In tab.12, all the phases of the ARES travel are listed and for each of them the final temperature inside the small tank (worst case) is computed. As it can be seen, the boiling temperature of 20.45k is reached only at the end of the final phase, when the tank is embarked on DIOMEDE and used. Considering in addition that several conservative approximations have been introduced in the computation, it is possible to conclude that the requirement of keeping the hydrogen in liquid cryogenic state all along the mission is totally met.

6. TELEMETRY, TRACKING AND COMMANDS SUBSYSTEM

TMTC requirements for the ARDENT mission include various sources like type of signals (status and health data mainly), link capacity, coverage area & ground site locations, link signal strength (BER), connectivity (crosslinks, direct links), link availability and lifetime (mission duration). In particular, for Earth-ICARUS, Earth-CORE and Earth-ARES links, Earth atmosphere and deep space environments are to be considered and

Table 12. Temperature of the hydrogen inside the small tank all along the ARES travel.

Location	Functionality	Distance from the sun	Duration	Shield	T Reached $[K]$
EML1	Assembly	$1AU$	6 months	Yes	15.51
Earth Manifold	Earth escape	$1AU$	1.5 years	Yes	17.02
Continuous Thrust	First part	$1AU$	3 months	No	17.30
Phase	Second part	$0.8AU$	1 year	No	19.05
	Third part	$1AU$	3 months	No	19.33
Mars Manifold	Mars insertion	$1AU$	2 years	Yes	20.24
Mars ASO	Waiting DIOMEDE	$1AU$	4 months	Yes	20.31
Between Mars and Earth	DIOMEDE usage	$1.2AU$	4 months	Yes	20.45

for CORE-ARES and DIOMEDE-ARES links only the effects of deep space environment are relevant.

Telecommunication phases
TMTC design has five main phases which have been reported in tab.13 and discussed further.

1. **Launch phase**: use of launcher telecommunication system.
2. **Post launch and cruise phase**: there are 2 cruise phases for the ARDENT mission.
   - *First*: when the launcher releases the payload, LGA could be used to transmit telemetry data. The LGA is a part of the ICARUS service module, which controls the motion of the payload, starting from the separation point from the launcher and up to the docking with the target vehicle (CORE, ARES or DIOMEDE).
   - *Second*: ARES travel from EML1 Halo orbit to ASO. Use of HGA (main), one for each phase for sending and receiving data at high rates. The HGA must be pointed accurately and is therefore steered using the gimbal mechanism.
3. **Orbital motion**: orbiting of ARES around Mars in ASO and waiting for the arrival of DIOMEDE for the purpose of refuelling.
4. **Orbit insertion**: occurs during the spiralling phase performed by ARES for the ASO closure. An HGA is needed.
5. **Docking phases**: this phase occurs in different scenarios: when ICARUS interacts with the CORE, ARES or DIOMEDE (refuelling and assembling in EML1), when the CORE interacts with ARES or DIOMEDE (truss re-sizing) and when ARES interacts with DIOMEDE (refuelling in ASO).An HGA is needed to transmit the information to Earth.

Ground network and radio-frequency
Operation at X-band rather than S band is suggested as far more spectrum is available at X-band than at S-band. Furthermore, there is no performance loss in going to X-band for telemetry; in fact, if an HGA is used on the spacecraft, performance at X-band improves by more than an order of magnitude over that at S. The Deep Space Network (DSN) by NASA have been selected. The Deep Space Network's 34-m HEF antennas can provide nearly all tracking coverage. The 34-m BWG antennas (4-kW instead of 20-kW X-band transmitters) may also be used in case of scheduling conflicts with other projects.

Table 13. TMTC Mission Phases

Phases	Event rate (kbps)	Data band	Antenna (to Earth)
1.Launch	-		Launcher
2. Cruise	1. ICARUS		
	a) Near earth	10	LGA
	b) Far earth	10	MGA
	2. ARES	25	HGA
3. Orbit insertion	ARES orbit Insertion	25	HGA
4. Orbital motion	ARES ASO closure	25	HGA
5. Docking	a)ICARUS-CORE	44	HGA
	b)ICARUS-ARES	44	HGA
	c)ICARUS-DIOMEDE	44	HGA
	d)CORE-ARES	44	HGA
	e)CORE-DIOMEDE	44	HGA
	f)ARES-DIOMEDE	80	HGA

*Frequency band: X

Link design
The basic equation used in sizing a digital data link is:

$$\frac{E_b}{N_o} = \frac{P_t L_l G_t L_s L_a G_r}{k T_s R} \tag{11}$$

The link budget is performed in order to grant the minimum signal to noise ratio that allows the reception of a clean signal, an assumption is done considering a BER (10^{-7} to 10^{-6}). Misalignment losses are evaluated considering a pointing accuracy needed and a requirement on the ADCS is introduced. If this requirement cannot be satisfied a gimballing mechanism could be introduced to grant it. The link budget for different mission phases has been performed and the results are tabulated in 14. Assumed that distance between Earth and ARES is same as between Earth and Mars when ARES is in ASO orbit.

Table 14. ARDENT vehicles link budget

Item	Units	ICARUS	CORE	ARES
Frequency	GHz	8.0	8.8	10
Tx Power	dBW	13.01	13.01	14.77
Peak Tx Antenna Gain	dBi	18	41.27	42.38
Tx Antenna Gain(net)	dBi	15.6	40.07	41.18
EIRP	dBW	29	51.10	53.95
Total loss	dB	-220.74	-221.77	-242.6
Peak Rx Antenna Gain(net)	dBi	46.46	68.27	68.9
Rx Antenna Gain	dBi	46.19	65	65
System Noise Temperature	K	650	700	800
Data Rate	bps	20e3	50e3	90e3
Noise power	dBW	-155.33	-147.8	-144
Power received	dBW	-145.57	-102.41	-119.46
E_b/N_o (a)	dB	14.62	47.32	26.68
Required E_b/N_o (b)	dB	8.6	11	11
Implementation Loss (c)	dB	-2	-3	-3
Margin(a-b+c)	dB	4.03	33.32	12.68
Channel capacity	bps	3.43e4	2.76e5	4.21e5

7. ATTITUDE DYNAMICS AND CONTROL SUBSYSTEM

The main challenges faced in the design of the control system of the large structures (ARES and DIOMEDE) involved in the mission are:

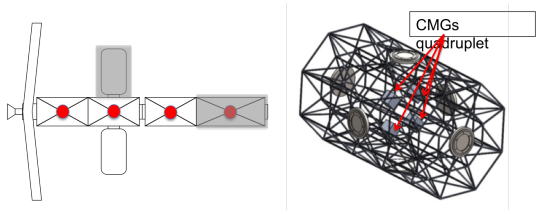


Figure 11. On the left: variable configuration of DIOMEDE vehicle. Shadowed areas represent components that are added in a second time to the assembly . Each red spot represents a CMGs quadruplet mounted inside each truss element. On the right: CMGs location inside the 12m truss structural-element.

- fitting the mission requirements considering that the inetia moments involved are in the order of magnitude of $O(10^7 : 10^8)kg \cdot m^2$
- developing a control strategy capable of adapting on the extremely variable sizes and inertia moments of the mission vehicles. In fact, the length of ARES and DIOMEDE main structures depends on the considered launch window. Furthermore, the fuel tanks are docked one per time to the main structural support and consequently the inertia properties continously change during the assembly operations.

The adopted solution consists in a set of 4 identical Control Moment Gyros (CMG) in a regular tetrahedron disposition that are meant to be mounted inside each beam element (Truss-9,Truss-12). Thus, both DIOMEDE and ARES main structures can be increased in length in order to satisfy the mission requirements and the vehicle attitude is always controllable. The selected CMGs are characterized by the performances, mass and power demand collected in tab.15. The attitude control of DIOMEDE

Table 15. Actuator set selected to be mounted inside each structural element (Truss-9 and Truss-12)

Component	Mass	Power	Maximum torque
Single CMG	$54.12kg$	$30W$	$51.37Nm$
Qudruplet	216.48	$120W$	$63.49Nm$

and ARES can be easily managed by the previously illustrated actuators system during refuelling operations at EML1 and during the cruise from Earth to Mars. Anyway, in order to allow the desaturation of the CMGs (the saturation angular momentum of the CMGs quadruplet is equal to:$H_s = 971.69Nms$) and to enhance manoeuvring capability, both ARES and DIOMEDE must be equipped with a thruster control system. Once all the environmental perturbations have been correctly modelled (according with the mission profile and the vehicles inertia properties), the number of desaturation(n_s) can be estimated by integrating in time the disturbances

torques (M_p) along each principal inertia axis and dividing the obtained result by the saturation angular momentum of the CMGs quadruplet. The integration has been performed numerically, keeping into account all the different perturbation entities (solar pressure, gravity gradient) relative to the different mission phases and pointing requirements. A safety factor of 2 has been taken into account in the final computation of the propellant mass (m_f) needed for the desaturation operations:

$$n_{s_i} = \frac{\int_0^{t_f} Mp_i dt}{H_s} \quad i = 1, 2, 3 \tag{12}$$

$$m_f = \sum_i^3 2n_{s_i} \frac{H_s}{L_i I_{sp} g_0} \tag{13}$$

where L_i represents the lever arm of the thruster from the center of mass of the vehicle (along i-axis) and I_{sp} is the specific impulse of the selected RCS thruster. In accordance to the mission profile for both ARES and DIOMEDE in full configuration, it is required to guarantee at least two manoeuvres around the maximum axis of inertia(I_max), yielding to the following formulation for the control torque required to the thrusters:

$$M_t = 4\Delta\theta \frac{I_{max}}{t_m^2} \tag{14}$$

where $\Delta\theta$ and t_m represent the manoeuvring angle and time, respectively. The additional amount of propellant needed for the manoeuvres is straightforward computed from the previous equation. It is important to remark the fact that, even modifying the manoeuvre time, the $\Delta\theta = \pi$ manoeuvre cannot be accomplished by the CMGs system both for DIOMEDE and ARES in full configuration, since the stored angular momentum is always higher than the angular momentum of saturation of the system. The selected thrusters-system performances are reported in table 16 and it is meant to be mounted at the bottom (upstream with respect to the engines and protected by the Sun shield) and at tip of DIOMEDE/ARES main structures in order to maximize the lever arm along each axis (Li). The amount of propellant needed to accomplish 5 consecutive round-trips to Mars has been estimated equal to $m_f = 320kg$ for ARES and $m_f = 40kg$ for DIOMEDE (in the worst configuration). Therefore, the RCS-thrusters propellant tanks can be launched to EML1 directly mounted on the tip/bottom truss element and they are enough for several servicing. Pointing requirements of the ADCS might change if an increase in temperature is detected inside some of the propellant tanks carried by ARES. In fact, since ARES exploits a continuous thrust trajectory, the attitude is constrained by the thrust direction vector and it can not be possible to direct the Sun-shield during the most part of the cruise. The proposed solution consists in spinning the structure along the minimum inertia axis (as shown in figure 12). In this way, the time that any tank is exposed with maximum surface to solar radiation can be reduced by an half. It is still under investigation if the previously illustrated control strategy would be adequate to fit this additional requirement. By the way, it is important to remark the fact that liquid hydrogen is meant be preserved from boil-off even without this additional expedient.

Table 16. Each set of RCS thruster is characterized by 6 identical nozzles (3 couples working for one axis each with opposite thrust-vector direction), the performance are here reported.

Propellant *type*	I_{sp}	Thrust
$UDMH/N_2H_4$	268s	200N

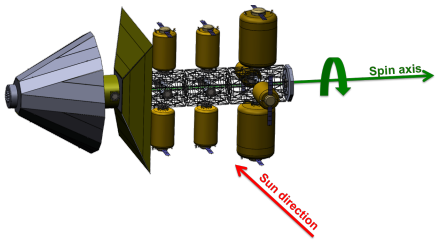


Figure 12. In order to halve the incident radiation on each tank a spinning motion around the minimum inertia axis can be given to the S/C.

8. GUIDANCE, NAVIGATION AND CONTROL SUBSYSTEM

From the navigation and guidance point of view the most critical operation in the mission configuration consists in the docking phase occurring both during the assembly and refuelling operations. Since the delay in communication from EML1 to ground an vice versa is about 3s, all docking operations are meant to be performed unmanned with authority from ground for go-no go decisions at critical steps of docking operations. ATV-5 constituted the main reference in sensors selection. Therefore, in addition to a standard IMU unit, the visual sensors collected in tab.17 are mounted on-board for the rendezvous operations, [10]. Particular attention has been posed in estimating the computational cost due to the visual-based guidance algorithm. The autonomous guidance software size (working from 3.5 km to the final target) has been estimated by analogy with on board software developed for autonomous guidance of military rocket [11], taking into account that EML1 dynamics is considerably slower. In RAM size estimation, the made assumption is that 10 images of the docking port, representing all the possible orientations, contained into $\pm 1^o$ at a given distance are simultaneously processed to determine relative position between chaser and target. The usage of markers can enhance the performances of the algorithm reducing computational cost and increasing accuracy and reliability. Accordingly with current literature [12], by means of 3 different markers the relative distance and spatial orientation can be fully determined (ref.[13]) if compared with

Table 17. Visual sensors

Sensor	Number	Resolution	Frame rate (aq/s)
Laser Imaging Detection and Ranging	1	128×128	3
Visible camera	1	1360×1024	1
Infra-red camera	2	640×480	1

Table 18. Autonomous docking SW size

MIPS	*MFLOPS*	*RAM*
100	60	32MB

docking port captured pictures on ground.

For what concerns the final approach, telegoniometers (TGM) and videometers (VDM) are suitable sensors for proximity operations once the target has been properly guided in the neighbourhood of the correct state (relative velocity and attitude) for the final docking (ref.[14] and [15]). All the sensors previously illustrated are used at different distances between the chaser (Tanks) and the target (DIOMEDE/ ARES partial assembly) in order to achieve ranging and state measurement: The previously sensor-systems are meant to be mounted on the Tank structure upper part, close or directly integrated in the docking port.

9. ACKNOWLEDGEMENTS

The authors thank all the other 8 members of the ARDENT team for their fundamental contribution and commitment to this work: Leela Balasubramanyam, Fabrizio Sassi, Matteo Romano, Edoardo Dell'Aglio, Riccardo Misani, Lorenzo Baroni, Jovan Ardalic, Alberto Napoli.

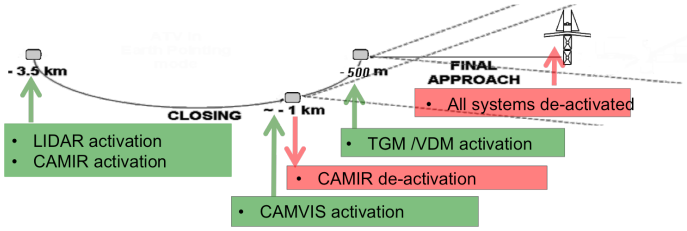


Figure 13. Sensor's system recapitulation

REFERENCES

[1] ARDENT team *Final Report* Politecnico di Milano, Internal use document, Michéle Lavagna project coordinator.

[2] Simone Flavio Rafano Carnà, Alessandro Serboli, Matteo Baiguera, Michèle Lavagna, AIDAA Conference Torino, 2015, *Earth Mars fuel depots to support fast and heavy manned mission to Mars*

[3] Taraba, Zwintz, Bombardelli et al, 2005, *Dual-mode reactor and ANERVA: Project M3-a study for a manned Mars mission in 2031*

[4] Ronald W. Humble, Gary N. Henry, Wiley J. Larson, 1995, *Space Propulsion Analysis and Design*

[5] Ronalwd W. Humble, Gary N. Henry, Wiley J. Larson, 1995, page 462, figure 8.9, *Space Propulsion Analysis and Design*

[6] Mariano Andrenucci, 2010 *Magnetoplasmadynamic Thrusters*

[7] , Edmund P. Coomes, Judith M. Cuta, Brent J. Webb (Battelle Northwest Laboratory, Richland, WA), David Q. King (Jet Propulsion Laboratory, Pasadena, CA), Mike J. Patterson, Frank Berkopec (NASA Lewis Research Center, Cleveland, OH), 1986, *A Multi-Megawatt Nuclear Electric Propulsion System*

[8] Roger M. Myers and James E. Parkes (Sverdrup Technology, Inc. Lewis Research Center Group Brook Park, OH), Maris A. Mantenieks (National Aeronautics and Space Administration Lewis Research Center Cleveland, OH), 1992 *Multimegawatt MPD Thruster Design Considerations*

[9] S. Mustafi , E. Canavan, AIAA 2009-6584

[10] John A. Christian,West Virginia University, Morgantown, WV 26506,Scott Cryan,NASA Johnson Space Center, Houston, TX 77058, *A Survey of LIDAR Technology and its Use in Relative Navigation*

[11] Wookey, Cathy, Nicholson, Bruce, 1996, *A/RD imaging processing"*

[12] David P. Miller and Anne Wright (MITRE Corporation) *Autonomous spacecraft docking using multicolor targets*

[13] *http://www.newtonlabs.com/cognachrome/docking.html*

[14] *www.jena-optronik.de/en/news/reader/items/ATV5-en.html*

[15] Alain Donnard,1st Workshop on Laser solutions for Orbital Space Debris April, 27-28th 2015, *LIRIS: A Lidar and Infrared experiment on-board ATV*

DICKE-SWITCHED MICROWAVE RADIOMETRY USING ETTUS USRP AND GNU RADIO

Simon Olvhammar

Department of Earth and Space Sciences, Chalmers University of Technology, Sweden

ABSTRACT

The Ettus USRP platform has been established as the front runner in software-defined radio (SDR) systems. Together with interfaces such as GNU Radio and Python reliable, cheap and high performing radio systems are now at hand opening up for a whole new set of possibilities. GNU Radio is a software tool-kit providing a clean and dynamic way of implementing signal processing. The vast community as well as a free and open source policy makes GNU Radio an attractive choice.
Dicke-switching, where both the source and a reference are repeatedly observed, is a widely adopted technique for eliminating gain variations in microwave radiometer systems. The observation method is commonly used by radio-astronomers, e.g for studies of the 21 cm hydrogen line. The dexterity of Dicke-switching also makes it suitable for radio-aeronomy applications, such as retrieving vertical profiles of atmospheric O_3 and CO from spectral measurements of the microwave emission from these molecules.
This study focuses on an implementation of a Dicke-switched receiver back-end using the Ettus USRP. The fundamental problem boils down to extracting the right samples that corresponds to the signal and reference state of the received Radio Frequency (RF). The Ettus USRP platform and the GNU Radio program is described as well as how a final spectrum is obtained for analysis. The solution presents new opportunities for scientists and even amateurs of making quality Dicke-switched measurements for different kinds of microwave spectra.
Measurements of mesospheric O_3 at 110.84 GHz and CO at 115.26 GHz is presented using a front-end designed at Onsala Space Observatory, OSO, in Sweden. The results show that a cheap, compact and high performance spectrometer can be achieved using the Ettus USRP and GNU Radio. This can be especially useful for the radio-aeronomy society in its endeavour to build a global network of ground-based stations for microwave remote-sensing of atmospheric gases, where many, reliable, low cost and compact radiometer systems are needed.

1. INTRODUCTION

Software defined radio (SDR) was initially introduced by J.Mitola in 1995 [1]. It can be described as a radio that can change it's physical characteristics through modifications in software. Since the work of Mitola SDRs has obtained a key role in the development of new radio systems [2] which is in part motivated by the high flexibility and cost effectiveness that a digital solution yields [3].
The main supplier for SDRs today is the Ettus Research and National Instruments company (NI) providing the Universal Software Radio Peripheral (USRP) as the SDR product line [4]. The SDR platform essentially provides a front-end for discretization of the signal as well as a Digital Down Donverter (DDC) chain through the usage of a Field-Programmable Gate Array (FPGA) [5]. The strength and flexibility of the USRP is exposed when combined with software interfaces such as GNU Radio and NI-LabView, providing digital domain signal processing [6].
Studies of microwave spectral emission from different kinds of molecules is fundamental in the fields of Astronomy and Aeronomy. Hydrogen is the most common substance in the Universe thus making the transition at 21 cm of central interest to astronomers, e.g. for studies of galactic spiral arms or Search for ExtraTerrestrial Intelligence (SETI) observations. Microwave radiation is also abundant from different gases in the atmosphere, both CO, O_2, H_2O and O_3 exhibit rotational transitions below 150 GHz thus providing a way to study the concentration and distribution of these gases in the atmosphere [7]. The technique most commonly used, for these kinds of studies and observations is Dicke-switching, first introduced by physicist Robert H. Dicke. Dicke-switching is a method that eliminates gain variations in receiver systems by rapidly comparing signals, often labelled signal and reference. The reference can be a source of known temperature, another part of the sky or by defining a reference through mixer tuning. The techniques are referred to as load, sky and frequency-switching respectively [8].
The purpose of this article is to investigate the viability of the SDR platform for usage in Radio Astronomy and Aeronomy applications by implementing a general purpose Dicke-switched Fast Fourier Transform (FFT) spectrometer back-end using the Ettus USRP and GNU Radio. The goal is to achieve a simple, reliable and high

performing solution that can be a part of new systems as well as replace existing back-ends with minimal effort and investments.
Section 2 outlines a basic overview of the Ettus USRP SDR platform and the software interface GNU Radio is described. Section 3 propose a general purpose Dicke-switch implementation in GNU Radio. Measurements of mesospheric ozone (O_3) at 110.8 GHz and carbon-oxide (CO) at 115.26 Ghz is presented in section 4 using a double sideband heterodyne receiver front-end designed at the Onsala Space Observatory (OSO) ($57.4°N$, $11.9°E$) in Sweden.

2. THE ETTUS USRP PLATFORM

Ettus Research and the National instruments company provides a broad product line of SDR platforms with e.g different frequency coverage and bandwidths [4]. The Ettus USRP X3x0 series is currently the most high performing platform and would be the most suitable for radio systems with high demands on bandwidth and accuracy. The provided General Purpose Input Output (GPIO) interface in the x3x0 series also makes implementations of Dicke-switching an easier task. A general USRP architecture is provided in Fig. 1, specifics may vary depending on the model [5].

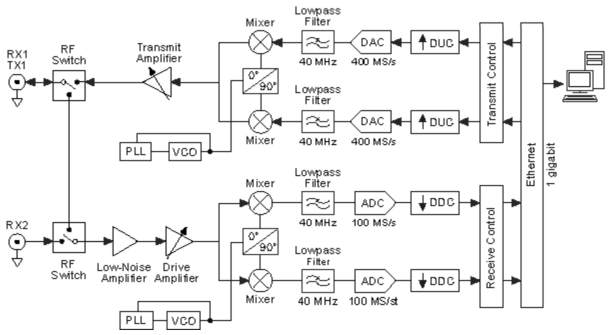


Figure 1. A general Ettus USRP architecture demonstrating the signal chain and processing performed. Based on the Ettus N210 with daughterboard WBX [5].

The first part of the receiver (RX) chain consist of a fundamental Low Noise Amplifier (LNA) with variable attenuation exposed in software e.g GNU Radio. The signal is further modulated into inphase and quadrature signals I and Q. Analog and Digital (A/D) converters handles the discretization of the RF providing a bandwidth determined by the daughterboard i.e the front-end of the Ettus USRP [2]. The onboard FPGA down converts the signal to base-band by an DDC implementation providing fine-frequency tuning and filters for decimation. The data is subsequently exposed to the host computer through Ethernet or PCIe interfaces. The samples produced by the Ettus USRP can be considered raw and further processing is required to achieve the desired result.

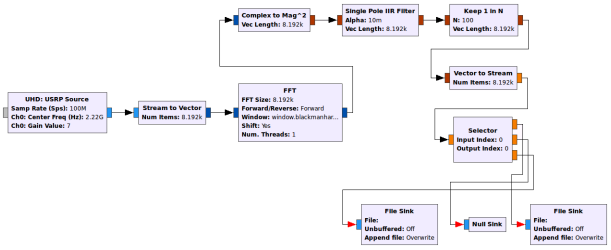


Figure 2. GNU Radio flow graph describing a general purpose FFT Dicke-switched solution for usage with front-ends implementing sky, load or frequency switching.

2.1. GNU Radio

The software interface GNU Radio performs signal processing through the use of dedicated blocks, e.g. infinite impulse response filters (IIR) or FFT calculations, designed in C++. The signal processing blocks can be linked to perform the desired computations in the GNU Radio Companion (GRC) Graphical User Interface (GUI) or directly through the use of a programming language such as Python. GNU Radio provides a vast library of signal processing blocks that can easily be modified to custom specifications.
GNU Radio stands out among other similar interfaces such as NI-LabView, where the open source policy is one of the main motivations, thus making the program free to use and modify [6]. The open source policy and simplicity of GNU Radio has also attracted a large community and new blocks and tools is designed on a regular basis, making GNU Radio a very attractive choice for SDR implementations.

3. A GENERAL PURPOSE DICKE-SWITCHED APPLICATION IN GNU RADIO

Implementing a Dicke-switched FFT back-end that can be used together with front-ends optimized for one of the three Dicke-implementations, frequency-switching, load-switching and sky-switching is possible due to the great configurability of SDR-platforms [2][3].
Frequency-switching can be performed in several ways using the Ettus USRP and GNU Radio. The first alternative is to tune the Ettus USRP front-end i.e set different center-frequencies at a tune rate corresponding to the Dicke-frequency and as such define signal and reference states. An other alternative is to tune an external mixer and send state signals to the SDR i.e. square waves where e.g. high corresponds to signal state and low corresponds to reference state. The same principle of state signals can be applied for implementations of sky and load-switching.
The fundamental problem is to sync GNU Radio with the states, signal or reference, in order to extract the right samples. Interface, bus and processing delays must be accounted for where the group delay of signal processing blocks in GNU Radio is the predominant factor [6].

Depending on block setup this is usually in the order of milliseconds for a standard FFT averaging solution. By combining the transition state of the RF i.e. the transition from signal to reference, with the expected GNU Radio group delay, the amount of discarded FFT frames during a Dicke period is minimized.
A general purpose Dicke-switched application in GNU Radio is proposed in Fig. 2. The Ettus USRP platform is exposed in the GNU Radio flow graph in Fig. 2 labelled UHD:USRP Source. The block provides the stream of samples from the USRP platform through a bus e.g. Ethernet or PCI-e. The signal processing blocks up to Selector is the bulk FFT computations and averaging and can be viewed as a total power measurement of the received RF.
The selector block is fundamental for the Dicke implementation. The selector allows the stream of samples to be directed towards the desired output for data storage, transition states can be directed to a null sink i.e where no FFT data is stored. The Selector is controlled using Python which is in turn synced with the state of the RF signal by utilizing the GPIO ports of the Ettus USRP X3x0 series, alternatively by sending tune commands to the SDRs internal LO. The result is a simple application that can react and direct streams of samples corresponding to different RF states.

3.1. Host load and performance

The hosts limited processing power can become an issue if high sampling rates is desired [2]. Write speed limitations is one of the main reasons for host side overflows, where the host is unable to process all samples [5]. One way to solve the problem is by in stream averaging e.g. Infinite Impulse Response (IIR) filters in GNU Radio, however this puts more stress on the CPU as well as introducing delays. The software defined IIR filters are configurable so a good trade-off between CPU load, delay and write speed can be achieved. Write speed limitations can also be solved by utilizing a ram disk alternatively moving the GNU Radio application or an equivalent application to the FPGA of the Ettus USRP.
FPGA porting in GNU Radio has recently been exposed through a new and innovative software package i.e. RF Network on Chip (RFNoC) [6].

3.2. Data analysis

With the FFT computations and bulk averaging (IIR filters) performed in GNU Radio only a small set of FFT frames remains to be averaged in software. This is implemented by determining the amount of FFT frames contained in a data file and averaging it accordingly. Further, the Dicke operation (Signal - Reference) is required for all N spectra. Division with reference normalizes the gain and is thus also an appropriate proceeding.

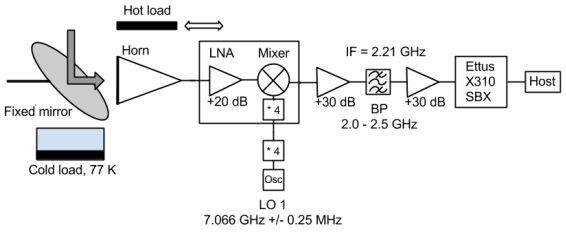


Figure 3. Flow graph describing the receiving chain i.e. a front-end optimized for CO and O_3 retrieval [8]. The back-end consists of the Ettus USRP with host software interface GNU Radio providing a general purpose Dicke-switched FFT analyzer.

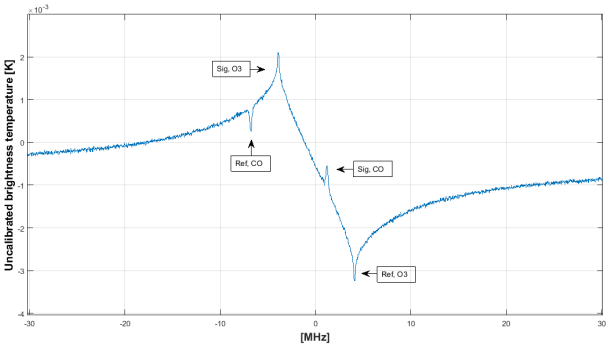


Figure 4. Uncalibrated frequency-switched measurement of CO at 115.27 GHz and O_3 at 110.84 GHz using Ettus USRP and GNU Radio as back-end.

4. RESULTS

A double side band heterodyne receiver front-end designed at Onsala Space Space Observatory, optimized for retrieval of mesospheric O_3 and CO, is used to test the GNU-Radio and Ettus USRP Dicke-switched back-end. An overview of the full receiver chain is provided by the flow graph in Fig. 3. Details of the receiver front-end and it's performance is outlined in [8].
The back-end consist of the Ettus USRP X310 with the SBX daughterboard and a host computer providing the GNU Radio interface. The system is used in frequency-switched mode where the external LO 1 in Fig. 3 is rapidly switched, approximately 1 Hz, between two frequencies corresponding to the signal and reference states. A sync bus transmits signals to the GPIO of the Ettus USRP X310 indicating the state of the received RF, signal or reference, as well as the transition state of the RF.
Fig. 4 shows uncalibrated spectral data of a simultaneous measurement of frequency switched O_3 at 110.84 GHz and CO at 115.27 GHz averaged over approximately one week. The bandwidth is 60 MHz with a resolution of about 15 kHz and the frequency throw between signal and reference is 8 MHz. The O_3 line corresponds to the lower side band of the IF-output and the narrow CO line corresponds to upper side band.
The vertical distribution of the observed mesospheric CO and O_3 can be retrieved by applying the Optimal Estima-

tion Method (OEM) described in [7]. A Hot/Cold calibration procedure is outlined and described in [8].

5. DISCUSSION

The results show that a high performing Dicke-switched back-end can be achieved using the Ettus USRP and a simple GNU Radio application based on free and open source software. The back-end can easily be integrated in existing front-ends as shown in the results where a state of the art COO_3 front-end was combined with the back-end. Thus providing both the radio-aeronomy and astronomy society a back-end that is easily integrated in new or existing systems with minimal efforts and investments. With simple, cost effective and high performing solutions, like the one proposed, a greater distribution of microwave radiometer systems performing quality Dicke-switched measurements can be expected. This opens for e.g atmospheric monitoring on a whole new scale. Due to the simple and elegant nature of SDR platforms the back-end solution would also serve as a great educational resource and thus be a part in spreading the knowledge and importance of atmospheric and interstellar measurements, something that is absolutely crucial for an environmental aware and curious new generation.

ACKNOWLEDGMENTS

First of all I would like to thank Peter Forkman and Gunnar Elgered at the Department of Earth and Space Sciences, Chalmers University of Technology, for making the project possible and supporting me at all times. Lars Pettersson and Eskil Varenius, at the Department of Earth and Space Sciences, have provided me with wonderful insights and a foundation to build upon which I am very greatful for.

REFERENCES

[1] J. Mitola, The software radio architecture, IEEE Commun. Mag., vol 33, no 5, pp. 26-38, May 1995

[2] P. Kildal, A. Hussain, B. Einarsson, MIMO OTA testing of a communication system using SDRs in a reverberation chamber, IEE Antennas Propag. Mag., vol 57, no 2, pp. 44-53, April 2015

[3] P. Cruz et al., Designing and testing software-defined radio, IEEE Microwave Mag. , vol 11, no 4, pp. 83-94, June 2010.

[4] National Instruments Corporation, Austin, TX, USA. [Online]. Available: http://www.ni.com

[5] Ettus Research, a National Instruments Company. [Online]. Available: http://www.ettus.com

[6] GNU Radio Website. [Online]. Available: http://www.gnuradio.org

[7] P. Forkman et al., Six years of mesospheric CO estimated from ground-based frequency-switched microwave radiometry at 57° N compared with satellite instruments, Atmos. Meas Tech., 5, 2827-2841, 2012.

[8] P. Forkman et al., A compact receiver system for simultaneous measurements of mesospheric CO and O_3, Geosci. Instrum. Method. Data syst. Discuss., 5, 311-361, 2015.

Poster Session (Thursday 10th - 15.00)

ANALOG PLANETARY RESEARCH AS A TOOL FOR EFFECTIVE SPACE EDUCATION

Hettrich, S.*[1,2,3], Akinsanmi, B.[1,4], Alizade, A.[1], Ghasemzadeh, L.[1], Ghassabian, H.[1], Karmakar, S.[1], Lawniczak-Wanslaw, M.[1,5], Salteri, E.[1,6], Takla, M.[1], Wojciechowska, M.[1,7], Wojciechowski, I.[1,7], and the SGAC SEPG/APO-G team[1]

Corresponding author, Email: sebastian.hettrich.apog@gmail.com

[1]*Space Generation Advisory Council – Space Exploration Project Group/Analog Planetary Operations Group, Vienna, Austria*
[2]*German Federal Office for Radiation Protection, Ingolstädter Landstraße 1, 85764 Oberschleißheim, Germany*
[3]*Ludwig Maximilian University of Munich – Meteorological Institute, Theresienstraße 37, 80539 Munich, Germany*
[4]*National Space Research and Development Agency, Nigeria*
[5] *Adam Mickiewicz University, Poznan, Poland*
[6]*Democritus University of Thrace, Greece*
[7]*University of Lodz, Poland*

ABSTRACT

Early space exploration was largely driven by political rivalries and was performed by a few large national agencies. Nowadays there are many more players, including many commercial and private companies and organizations. With a more open space sector, many more people are involved in space research and especially in Analog Planetary Research (APR). APR, the testing of space hardware, software, procedures and operations on Earth under space-like conditions has been important for spaceflight since the early days of space exploration. Analogs are also used for conducting human factor studies and training. Space exploration has been inspiring students to study science and engineering for generations, motivating them to become researchers and extend the borders of human knowledge. These space missions not only delivered important scientific data, but have been used to bring science to life for students showing how it can be used. With the advent of a variety of voluntary organizations for students and young professionals we are now able to move from studying previous missions in the classroom to providing hands-on experience.
This paper presents the potential for APR, and especially space analog missions, to contribute to current space research and provide an opportunity for involving students in research, both in and out of the classroom. Analog missions can be used as case studies to teach students about science and space exploration and can offer an opportunity for students from a range of disciplines (such as engineering, science and medicine) to get actively involved and gain hands-on experience in missions.

1. THOUGHTS ON EDUCATION

Throughout history, writers, philosophers, and educators have sought to understand the process of education and find the ultimate and most effective teaching approaches. Students all over the world seem to require more attention from educators now than in past times. Learning techniques and strategies have transformed the role of the educator from someone who doles out information to someone who devises new methods to facilitate student learning in many ways.
As early as 450 B.C., Confucius claimed that one cannot learn to do something only by hearing and seeing it done; one must do it to learn it [1]. Following that thought in 1938, John Dewey, who popularized the concept of 'Experiential Education' claimed that "there is an intimate and necessary relation between the process of actual experience and education."[1]. This idea set the course for a new approach to understanding and advancing education [1]. His research at the Northern Illinois University confirmed the greater benefits of a student-centered learning-by-doing experience (including practical classes, media learning, inquiry-based learning, group discussion learning, etc.) over instructor-centered knowledge-transfer [1].
Here we describe a new approach to involve students in real-life practical and research-based learning (referred to as Learning-by-doing) in the field of space science [1]. By involving students in ongoing research they stand at a vantage point of learning while gaining an insight into what a future career in the field of space science and technology will entail.

2. ANALOG PLANETARY RESEARCH

Analog Planetary Research (APR) is the development and testing of scientific, technical, operational, social and medical procedures in simulated space or planetary environments for application to crewed and robotic space exploration missions [2].
APR aims to serve as a low-cost, low risk basis to prepare all kinds of applicable strategies for future planetary missions [2]. It uses familiar conditions and

properties of terrestrial or Earth-orbit environments that resemble the conditions on the targeted planetary body [2]. Artificial laboratory environments or space stations and natural analogs such as deserts and cave systems are used to simulate certain geological features that are expected for a space mission [3].
Analog studies and analog technological solutions have been widely used by space agencies and companies as an important stage of mission planning and design [4]. Analog Planetary Research includes robotic analog missions where the activities and simulations are carried out without the presence of human beings (e.g. a sample return mission and the testing of exploration rovers). In these cases analog research facilitates testing of structures, control systems, procedures and communications architectures [4].

2.1. APR in National Space Agencies

National space agencies use analog planetary research for various purposes ranging from plant cultivation in space to astronaut training. For example:

- EDEN (Evolution and Design of Environmentally-closed Nutrition sources) is a research initiative from the German Aerospace Centre (DLR) that focuses on Bio-regenerative Life Support Systems (BLSS), especially greenhouses. Its goal is to adapt the latest cultivation technologies to space-related applications [5].
- NEEMO (NASA Extreme Environment Mission Operations) is a National Aeronautics and Space Administration (NASA) project that sends groups of astronauts, engineers and scientists to live in Aquarius, the world's only undersea research station, for up to three weeks at a time. The Aquarius habitat and its surroundings provide a convincing analog for space exploration [6].

2.2. APR in Private Space Companies

In some cases national space agencies fund private institutes to conduct APR. One example is the result of a joint collaboration between NASA and the University of Hawaii at Mānoa, the HI-SEAS. It is an analog habitat for human spaceflight to Mars, located in an isolated position on the slopes of the Mauna Loa volcano on the island of Hawai'i. This project aims for a detailed study of space-flight crew dynamics, behaviors, roles and performance, especially for long-duration missions [7].

2.3. APR in Volunteer Organizations

In the last decade volunteer projects have become more and more popular and in some cases even outranged companies or agencies. Volunteer organizations such as Mars Without Borders (MWOB), the Mars Society, and the Space Generation Advisory Council (SGAC) work to advance science, technology, engineering and mathematics, to raise public awareness and engagement in space exploration, and to educate students and young people. These efforts have the goal of advancing space exploration toward settlement of the Moon, Mars, and other worlds.
A prominent example of analog studies and space education outreach is the Mars Desert Research Station in Utah, which is used by research groups, professionals as well as volunteers, to simulate human Mars exploration in a terrestrial analog.
In robotic APR there are various competitions focusing on space analog tasks, such as NASA's Lunabotic Mining Competition, Google's Lunar XPrize, the Mars Society's University Rover Challenge, the European Rover Challenge, and others that are directly related to the development of planetary exploration rovers.

3. ANALOG PLANETARY MISSIONS

Analog Planetary Research provides opportunities for volunteers and especially students to get hands-on experience in space science and space technologies. Although less common, Analog Planetary Missions are another excellent tool for space education.

3.1. Definition and Description of Analog Planetary Missions

Analog Planetary Missions are the simulation of parts of or entire human, robotic or human-robotic space missions in terrestrial environments that are an analog to the real space environment. These missions allow participants to study hardware, software, operations and human factors in order to obtain valuable data and experiences that might be crucial to future space missions.

3.2. Preparing and Conducting an Analog Planetary Mission

Analog missions are planned in conditions similar to ones in real space missions, yet are conducted on shorter timescales due to the reduced amount of mission elements (e.g. launch, transfer phase, etc.).
An analog mission starts with identifying the scientific objectives of the mission [8]. Primary mission objectives may include questions or study cases that alone justify the conduction of such an analog mission, and have the highest priority throughout the mission. Secondary mission objectives may be study cases that come as a by-product of the primary objectives and are rated at a lower priority [8].
Once the mission objectives are identified, the mission architecture framework is decided on. This includes the mission duration, the mission location, the number of analog astronauts (for a human mission), the communications framework (real-time or delayed

communication), and any other necessary elements [8]. The mission architecture is not only driven by the scientific objectives, but also by financial constraints. For example, a longer mission involving more astronauts will cost more to conduct.
The third step is the selection of experiments to serve the mission objectives and which are reasonable within the framework of the mission architecture.
In a human mission, analog astronauts need to be selected and trained on handling tools and experiments well before the start of the analog mission [9]. Medical and psychological supervision must also be arranged for the astronaut crew.
Another major aspect in the preparation of an analog mission is gathering the necessary funding to conduct the mission. This must be done early in the process before contracts are negotiated. Analog mission preparation also involves obtaining resources for the mission, planning and scheduling mission tasks, outlining emergency procedures, sorting out legal issues, establishing a mission control team, conducting outreach, and organizing any other infrastructure [9][10].
Even though mission duration is usually only in the range of a few days or weeks, the proper preparation time is around one year (in the case of a volunteer organization). Although the workload during a mission will be intense, most of the work takes place before the start of the mission. Afterwards, the gathered data is analyzed and evaluated, and finally published in scientific publications and at conferences.

3.3. Multidisciplinarity of Analog Planetary Missions

A wide variety of personnel from multidisciplinary backgrounds gather to assemble the Mission Control Center (MCC) of each analog mission. The different backgrounds of the personnel are essential for the success of every analog mission, as the experiments conducted there can vary from biology to psychology to material testing. Therefore, a very wide spectrum of specialists is required to monitor and guide the analog astronauts during the experimentation phase. Additionally, during the daily in-mission scheduling phase of the day – whether it is a real-time mission, a 1-day-schedule mission or a 3-days-schedule mission – other specialists such as project managers, data analysts, IT experts etc. are needed to create a fully operational MCC [11].
A number of Mars analog missions have been carried out the last couple of year by various volunteer organizations. During each analog mission, experts from around the world and from every major discipline gathered to formulate the MCC. A mission conducted in 2013 exemplified the high rates of successful experiments owed to the interdisciplinary MCC, who are responsible for planning, guidance and monitoring throughout the mission[10].
In recent analog planetary missions, multidisciplinary teams that formed the MCCs tended to have many young scientists and students as participants. These kinds of missions are a good way to provide young scientists and especially students opportunities for hands-on experiences on real missions. Besides the research work that needs to be done before every analog mission, the MCC team needs to be prepared for sudden emergencies and to adapt at an intensive pace as new data emerges in the mission [11][12]. This provides valuable experience to the participants that can be applied to future analog missions and prepare them for future careers.

4. THE EDUCATIONAL POTENTIAL OF ANALOG PLANETARY MISSIONS

The future of aviation and aerospace education (and therefore also the future of space research and technologies) lies in responding to international, national, state, and local educational needs [13]. According to Dr. C. Elaine McCoy, aviation requires the development of skills ranging from technical aspects to those of human interaction and decision-making [13]. Successful educational programs should therefore teach students these skills and offer them opportunities to practice them by applying relevant concepts and skills to real problems [13].
Analog missions hold a great potential to contribute to space education in both ways, passive and active.

4.1. Passive Space Education

Analog missions of course can serve as demonstration material for educators, teachers, or professors in the classroom or lecture hall. The experiences and knowledge gained during an analog mission can be presented there with real examples and applications of scientific or engineering theories. This can transform a traditional theoretical lecture into something more relatable and thereby more motivating for students.
According to NASA, increasing interest in science and technology among students by providing them with opportunities and experiences is important for the future of space research and exploration [14]. Analog mission planners can allocate ‘student days’ during the mission, giving students the opportunity to explore and experience unique space and aeronautic content; interact with analog astronauts, engineers, and scientists; and observe mission operations [14].

4.2. Active Space Education

While the passive educational aspect of analog space missions presents an interesting and motivating teaching alternative, analog missions also provide active space education that that has the potential to significantly enhance students’ understanding of science and technology, especially space science.

The European Space Agency (ESA) conducts this kind of active education, offering many opportunities for students to learn, gain experience, meet other students and make professional connections [15]. In this case the level of study ranges from kindergarten to doctoral programs [15]. NASA also provides many such opportunities for students starting at a very young age. They aim to inspire their engineers and encourage young people to participate in the future of space exploration [16].

But these space agency programs usually support only one individual or one team of students at any time. Only the most appealing ideas and concepts get consideration by the program managers, neglecting all other applicants who are just as committed and motivated as the selected students.

This is where credible volunteer organizations are able to contribute, involving everyone who is interested in space research, whether student or not, no matter their professional or cultural background. In volunteer organizations such as the Space Generation Advisory Council (SGAC) for example, young people can come together to work on space-related topics [17]. Within the SGAC, the Space Exploration Project Group (SEPG) / Analog Planetary Operations Group (APO-G) conducts analog research in line with the General Exploration Roadmap (GER) [18]. It offers students and young professionals of various professions interested in space exploration the opportunity to gain hands-on experience in a Mars analog mission, to take place in autumn 2016 [19].

Regardless of past experience, participants are involved in the project from beginning to end. They learn about all aspects of space missions, carrying part of the responsibility for leading the whole mission to success. This is effective 'learning by doing', or 'experiential learning' [1].

5. THE BASICS OF EXPERIENTIAL LEARNING

There are numerous theories concerning methods of effective learning. Many researchers have been dealing with this issue for decades in order to find the best way of optimizing the learning process [20]. Most of them agree that a greater active engagement of the learner also provides a better outcome [20].

Gordon Allport proposed the so-called biographical learning theory, which consists of three levels of participation in learning [20]. The first one deals with active attention and intention to learn, meaning basically that one has to make some effort by concentrating his or her attention to learn something [20]. The second level concerns the engagement of the learner in doing things closely connected to the subject of learning [20]. Participating in activities evokes stronger neurophysiological involvement, which enables a better understanding [20]. The final stage of this theory is personal relevance. This notion applies to being interested in the subject of learning, feeling that it involves one personally [20]. Through numerous connections to the ego, things are more easily remembered [20]. This concept favors the idea of creating opportunities for learners to gain and use their knowledge.

Another notable researcher, David Kolb, proposed the Experiential Learning Theory which describes learning as a process of creating knowledge by transforming experience gathered through the interaction of individuals with the environment [21]. In this model knowledge is considered not only as memorizing new elements and information, but also as its constant verification and modification. This process is well presented by the D. Kolb's Cycle of Learning shown in figure 1 [21].

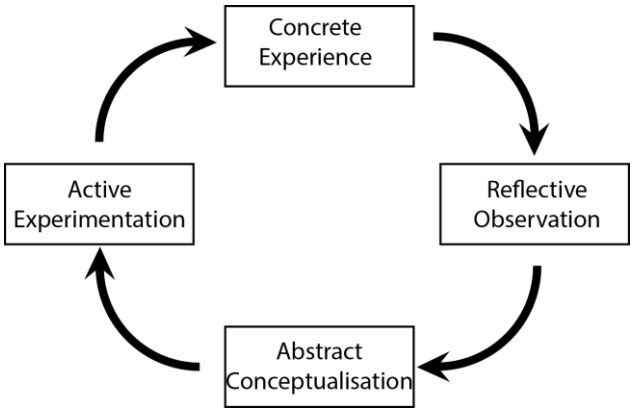


Figure 1. Experiential Learning Cycle [21]

According to this theory, the process of learning starts from experiencing certain situations that are then reviewed and evaluated in the phase called Reflective Observation [21]. Conclusions formed here lead to planning and modifying future experiences, resulting in the transformation of previous knowledge to create theories. This in turn increases knowledge by adding analyzed conclusions from past experience [21]. The last described stage changes the pattern of behavior in certain situations, demanding experimenting and applying new information to verify their applicability [21]. These stages may circulate endlessly, for every single experiment generates new experience, which changes or embeds one's beliefs. The cycle is not reflected in traditional ways of learning, in which students first gain some basic knowledge and then only sometimes gain hands-on experience [21].

This approach, favoring hands-on experience as a more effective method of learning may improve students' performance, since they become acquainted with the subject matter, giving it personal relevance and making it easier to remember and apply.

APR and especially analog planetary missions are in line with this school of thought, and are an ideal way of providing people with space education. Put into practice, even complex science, engineering and management problems become easily understandable and are internalized as personal experience.

6. CONCLUSION

There are currently many ways for people, and especially children and students, to learn about space science and technology in passive ways. These include the introduction of real life examples of space missions and space analog missions into the lecture hall, or vice-versa; bringing the students to view ongoing operations. However, decades of education research show that the learning effect is higher when the student not only hears and sees, but also gets some real hands-on experience. Volunteer organizations such as the SGAC provide easy and free access to these experiences, complementing and adding to space agencies' limited student programs. In a volunteer organization participants can be as involved as they want and have opportunities not only to gain theoretical experience, but also to become actively involved in the process of creating something. Analog planetary missions, for example SGAC's proposed Mars mission simulation, can bring together a multitude of participants from different professional and cultural backgrounds, learning from each other and moreover learning by performing tasks themselves that in the end contribute to a scientific purpose. These programs not only add valuable knowledge to the scientific questions that motivate these missions; they also effectively trigger a deep learning experience and create in participants the motivation to continue contributing to space science and space technology, fostering the space explorers of tomorrow.

7. ACKNOWLEDGEMENTS

The authors would like to especially thank Ms. Kate Arcless Gray and Ms. Kate Howells for their support in spell and grammar checking of this article.

8. REFERENCES

[1] Northern Illinois University, 2015, *Experiential Learning*, Northern Illinois University Faculty Development and Instructional Design Center, www.niu.edu/facdev, 815.753.0595, retrieved 21st Nov 2015.

[2] Hettrich, S., Napier, L., Felix, C.V., Kolodziejczyk, A., Perakis, N., Elorza, I.M., Alizade, A., Ghasemzadeh, L., Khan, M.S., Pfeil, I., & the APO-G team, 2015, *The Importance of Analog Planetary Research for the Success and Safety of Human and Robotic Space Missions*, "Space Safety is no Accident – The 7th IAASS Conference", pp 285-293, Springer International Publishing, DOI: 10.1007/978-3-319-15982-9_34.

[3] Craig, J.O.D., Gresham, E., Hay, J., Graham, R., Graham, L., Williams-Byrd, J., Herrmann, N., Mullins, C., Graham, R., Callahan, J. & Reeves, J.D., 2011, *NASA's Analogs Missions Paving the way for Space Explorations*, NP-2011-06-395-LaRC, Langley Research Center, Hampton, USA.

[4] Sasiadek, J., 2015, "Aerospace Robotics II", Springer International Publishing, DOI: 10.1007/978-3-319-13853-4.

[5] http://www.dlr.de/irs/en/desktopdefault.aspx/tabid-9327/14668_read-39524/, viewed on 21st Nov. 2015.

[6] www.nasa.gov/mission_pages/NEEMO/index.html, viewed on 21st Nov. 2015.

[7] Binsted, K.A., Hunter, J.B., 2013, *HI-SEAS (Hawaii Space Exploration Analog and Simulation) as an opportunity for long-duration instrument/protocol testing and verification*, http://www.hou.usra.edu/meetings/analogs2013/pdf/4044.pdf, retrieved 21st Nov 2015.

[8] Larson, Wiley J. & Wertz, James R., 1999, "Space mission analysis and design", 3rd edition, Microcosm Press & Springer, New York.

[9] Hettrich, S., 2012, *Human-Robotic Mars Science Operations: Itinerary Optimisation for Surface Activities*, Master thesis, Leopold-Franzens-University of Innsbruck.

[10] Hettrich, S., Dinkelaker, A.N., Sejkora, N., Pfeil, I., Scornet, Q., Moser, L., Boyd, A., Terlevic, R., Luger, U., 2014, *Efficiency Analysis of the MARS2013 Planning Strategy*, Astrobiology Volume 14 No. 5, DOI: 10.1089/ast.2013.1076.

[11] Hettrich, S., Dinkelaker, A.N., Alizadeh, A., Lupu, E.S., Pfeil, I., Ghazemzadeh, L., Salteri, E., Felix, C.V., Kauerhoff, T., McArthur, J.L., Marien, G., Rieser, A., Sejkora, N., Scornet, Q., 2014, *Planning Strategies for Mars (analog) missions: real time, 3-days-in-advance and 1-day-in-advance planning*, 13th International Conference on Space Operations 2014, American Institute of Aeronautics and Astronautics, DOI: 10.2514/6.2014-1891.

[12] Marquez J. and Newman D., 2006, *Mission Planning and Re-planning for Planetary Extravehicular Activities: Analysis of Excursions in a Mars-Analog Environment and Apollo Program*, SAE, 2006-01-2297.

[13] Fleezer-Ryan, P., 1993, *Aviation & Aerospace Education: A Positive Impact on the 21st Century*, Journal of Aviation/Aerospace Education & Research, Volume 3, No 4, JAAER Summer 1993.

[14] Marks, S., *NASA Aerospace Education Services Project*,http://www.nasa.gov/pdf/229741main_2007_ESE_AESP.pdf, retrieved on 22nd Nov. 2015.

[15] ESA at the Forefront of Space Education, http://www.esa.int/Education/ESA_at_the_forefront_of_space_education, retrieved on 15th Nov. 2015.

[16] NASA Astro Camp, http://education.ssc.nasa.gov/astrocamp.asp, retrieved on 15th Nov. 2015.

[17] Space Generation Advisory Council, http://www.spacegeneration.org/, retrieved on 21st Nov. 2015.

[18] SGAC Space Exploration Project Group, http://www.spacegeneration.org/projects/space-exploration.html, retrieved on 21st Nov. 2015.

[19] SGAC Analog Planetary Operations Group, http://www.analogplanetaryoperationsgroup.wordpress.com, retrieved on 22nd Nov. 2015.

[20] Łaguna, M.,2004, *Szkolenia.* Gdańsk: Gdańskie Wydawnictwo Psychologiczne (Polish only).

[21] Kolb, A.Y., Kolb, D.A., 2009, *Experiential Learning Theory: A Dynamic Holistic Approach to Management Learning*, Education and Development, 'The SAGE handbook of Management Learning, Education and Development', Sage Publications, ISBN 978-1-4129-3539-5.

SEARCHING FOR LIFE FINGERPRINTS IN THE LABORATORY

Marco Sergio Erculiani[(1,2)], Riccardo Claudi[(2)], Diego Barbisan[(3)], Lorenzo Cocola[(3)], Nicoletta La Rocca[(4)], Nicola Trivellin[(5)], Bernardo Salasnich[(2)], Giancarlo Farisato[(2)], Tomas Morosinotto[(4)], Sabrina Masiero[(2)], Luca Poletto[(3)], Matteo Meneghini[(3)]

[(1)] CISAS-"G.Colombo", Centre of Studies and Activities for Space, Padova, Italy; sergio_erculiani@libero.it
[(2)] INAF-Astronomical Observatory of Padova, Italy; riccardo.claudi@oapd.inaf.it
[(3)] LUXOR- Photonics and Nanotechnology Institute- CNR Padova, Italy; barbisan@dei.unipd.it
[(4)] Department of Biology Vallisneri, Padova, Italy; nicoletta.larocca@unipd.it
[(5)] Department of Information Engineering- DEI, University of Padova, Italy; nicola.trivellin@light-cube.com

ABSTRACT

At the Astronomical Observatory of Padova we are performing laboratory experiments aiming at twofold results. At first we want to understand how photosynthetic biota, once present on an Earth-like planet orbiting in the habitable zone of a star of different spectral type than the sun, can modify its atmosphere. In particular we study how the O_2-CO_2 balance would differ from the terrestrial one.
An ancillary output is to understand if the feature of the "red edge" reflecting property and both the pigment composition and concentration of photosynthetic organisms would be influenced by the extended undergoing to a different radiation spectrum. Studying the different reflectance spectra of the pigments inside organisms grown in different light conditions allow to understand these bio-physical properties.
In these experiments we'll use photosynthetic organisms like the bacteria *Synechococcus sp*. strain PCC 7002, *Halomicronema hongdechloris*, *Acaryochloris marina* and *Chlorogloeopsis fritschii* as well as the microalgae *Chlamydomonas reinhardtii*, *Ostreobium quekettii* and the moss (*Physcomitrella patens*), We will analyze their gaseous productions with a laboratory set up miming the exoplanetary surface temperature and radiation conditions.
With this aim we developed a starlight simulator that reproduce the stellar spectrum in the wavelength range (365-940 nm) overlapping the photosynthetic active range (PAR) (280-850 nm).
These measurements could be useful to translate and understand the spectral data coming from the future space missions, in particular the ones dedicated to the study of exoplanetary atmospheres and in general exoplanet characterizations: CHEOPS, PLATO and ARIEL.

1. INTRODUCTION

Recently, a lot of extrasolar planets have been discovered in any direction of the Galaxy and some of them have been found in the habitable zone of their host stars. Our research will focus on terrestrial-type planets orbiting around F, G, K, and M stars because these stellar types are long-lived enough to support an habitable zone (HZ) capable of evolve and keep liquid water[1,2] and maybe the life.
In particular planets orbiting around M stars are very interesting because of their high statistic density and because of their capability of hosting earth-like planets. In this framework, "Atmosphere in a Test Tube", a project started at Astronomical Observatory of Padua, simulates exoplanetary environmental condition in order to understand how and how much the behavior of photosynthetic bacteria in different planetary/star scenarios can modify the planet atmosphere. The particular case of an habitable planet orbiting an M dwarf star is under study for the time being. In fact, the irradiation of an M star on its planets, due to its lower photospheric temperature, is very different in quality and quantity by the irradiation of a star like our Sun. Their dimness shorten the habitable zone of the host star closer, such that planets may become tidally locked, leading, in exterme cases, one side constantly facing the star[3]. The different radiation regimes of F, K, and M stars lead to different atmospheric photochemistry[4] as well as a much different photon density. This feature can strongly impact with the metabolic cycle of photosynthetic organisms. In the following of the paper a description of the experiment and of its aim is given.

2. SCIENTIFIC REQUIREMENTS

In order to simulate exoplanetary conditions it is useful to know the temperature and the processes that build the chemical composition of its atmosphere.
The temperature interval itself depends by the pressure of the atmosphere and is dependent on the greenhouse effect, that can maintain the superficial temperature of the planet high enough so as to keep the water in liquid state. This feature is obviously lead by the distance of the planet from the host star[5,6]. For example, for a super Earth orbiting an M star, using both the "Venus" and

"Mars" criterion[6] the habitable distance range is enclosed between 0.47 and 0.88 AU and corresponds respectively to 216 K, (the first condensation of CO_2) and 373 K (the water loss limit). The pressure and the gaseous mixture can regulate the atmospheric dynamics[7, 8, 9] and shift back and forth the Habitable Zone (HZ) limits. Understanding how organisms can photosynthesize on M star planets and how the metabolic processes can be influenced by different types of radiation is the topic of this work. This goal will be achieved by means of a ladder composed of different steps. In the first one, in order to avoid expensive laboratory infrastructure and simplify the work, we consider super Earths well inside the HZ of the host star with temperatures between 288 K and 310 K.

Photosynthetic bacteria are the organisms chosen for this experiment and the key to understand how a hot, inhospitable planet can became a safe green and life friendly planet.

In fact photosynthetic organisms produce gases, like O_2, nitric oxides like N_2O_2 and other molecules formed from the breakdown of organic matter like NO_X, CH_3Cl or COS that can have contribute to modify exoplanetary atmospheres in ancient time and can be detected from Earth.

Some of them are called biomarkers because they can outline the presence of biotic. Biomarker measurements are affected by the problem of false positives, that is the abiotic production of gases that can mimic a biotic output. This is the case of O_2 abiotic generation due to photolysis and effects of carbon burial and hydrogen escape.

So, the presence of O_2 only can't prove the presence of life. It is crucial that these data are cross checked with the presence of other reduced gases, (as for example CH_4) that can be explained only with biotic processes capable to maintain a stable chemical disequilibrium[10].

Detectability of photosynthetic bio-products depends on biotic productivity, which depends itself by several factors, like: light, minerals, availability of liquid water, nutrients and electron donors. During the photosynthetic process, light impacts on photo-receptive organisms called antennae whose task is to split water molecules and produce proton gradients and energy useful for the cells.

Finally, O_2, O_3 and CH_4 can be defined as the main biomarkers[11], as well as NH_3 and N_2O.

Not all bacteria respond equally to irradiation, but all of them have a typical response to light spectrum. The theoretical unicellular lower light photosynthetic limit, estimated by Raven (1984)[12] is 0.1 μmol of photons/m^2/s (6 x 10^{16} photons/m^2/s). As the upper limit of photon flux density concerns, Wolstencroft and Raven (2002)[13] found that the theoretical tolerance for land plants against photo damage is 6–9 mmol of photons/m^2/s (3.6–5.4 x 10^{21} photons/m^2/s) over the standard PAR, well above the flux that impinge on Earth's surface [2 mmol photons/m^2/s (1.2x10^{21} photons/m^2/s)], though Wolstencroft and Raven conjectured a theoretical upper limit for land organisms living on Earth-like planets in general, to be 10 mmol of photons/m^2/s (6x10^{21} photons/m^2/s).

Living organisms can adapt to specific environmental niches, like cryptoendolithic organisms that can live under rocks or aquatic organisms that can live shielded under water, being able to proliferate under high surface photon flux[14].

Light-harvesting photo-pigments are the tools that photosynthetic organisms use to metabolize light. They are, among others, chlorophylls like Chl a that occurs in the core antenna, or other Chls, Chl b, c and d, that provide other light harvesting roles. Chl d, recently discovered in cyanobacteria[15,16,17], may replace Chla in some cyanobacteria that live in environments with little visible light[18,19].

Chl d has its absorbance peak in the NIR at 720 nm[19,20]; and thus oxygenic photosynthesis is being performed in the NIR[14]. Recently Chl f has been discovered to be able to capture light energy in the infrared spectrum, with an absorption peak at 706 nm.

In non oxygenic bacteria, BChls play a primary role in electron donor and their peak can extend through the NIR part of the spectrum. Though, anoxygenic bacteria have a productivity far less abundant than oxygenic ones. Other photo pigments present in photosynthetic organisms are carotenoids and phycobilines. The first ones operate in the blue and green part of the spectrum and protect organisms against photo-oxidative stresses, high temperatures and the toxic presence of O_2. Phycobilines, that can be found in cyanobacteria and red algae, work in the green and yellow spectral regions. Other living organisms, such as green bacteria, purple bacteria and heliobacteria, can exploit solar light in slightly extended spectral regions or in ecological niches, such as the near-infrared. For example, purple bacteria have absorbance peak in the 1.013-1.025 μm range using BChl b like *Blastochloris viridi* or *Rhodopseudomonas viridis* (that absorbs at 0.96 μm) and other bacteriochlorophylls in the range 0.7-0.9 μm[21]. They don't use water as electron donor, and then don't release oxygen as byproduct. Photosynthetic Active Radiation (PAR) on planets orbiting around M stars can be lower than the average terrestrial one even by an order of magnitude[22]. Nevertheless this could not represent a problem because several marine organisms on Earth evolved to use only 5x10^{-4} times the average flux received at the Earth's surface, like sulfur bacteria that embed a large antenna complex, the chlorosome, that permit to use only small fractions of light intensities[23]. In these regions radiation is dominated by red or IR radiation. In Table 1 are resumed the previous said data.

Inner and outer M star HZ limits	216-373 K
Life temperature range limits	288-310 K
Biomarkers	O_2, O_3 , CH_4 ,NH_3, N_2O.
Unicellular lower light photosynthetic limit	0.1 µmol of photons/m^2/s (6 x 10^{16} photons/m^2/s)
Theoretical tolerance for land plants against photo damage	6–9 mmol of photons/m^2/s (3.6–5.4 x 10^{21} photons/m^2/s)
Earth radiation tolerance limit	10 mmol of photons/m^2/s (6x10^{21} photons/m^2/s)
Flux that impinge on Earth's surface	2 mmol photons/m^2/s (1.2x10^{21} photons/m^2/s)
Photopigments of oxygenic of bacteria	Chl a, Chl b, Chl d, Chl f, carotenoids and phycobilines
Photopigments of anxygenic bacteria	BChls, carotenoids

Table 1. Overview of the main physical parameters

3. PHOTOSYNTHETIC ORGANISMS

In order to perform our experiment we consider both model organisms like moss *Physcomitrella patens*, the green micro alga *Chlamydomonas reinhardtii* and the cyanobacterium *Synechococcus* PCC 7002 and atypical photosynthetic organisms. All of them are characterized by the presence of chlorophylls (chlorophyll a or a and b) with an in vivo absorption major peak in the red, around 680 nm. In figure 1 are shown different images of these species.

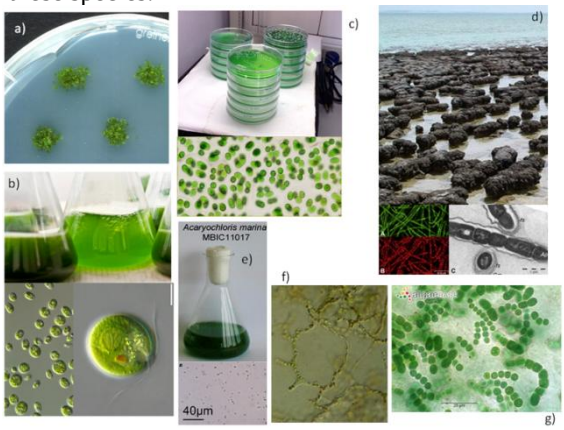


Figure 1: In figure we can see samples of (a) "Physcomitrella growing on agar plates" by Sabisteb - Anja Martin from the Ralf_Reski lab., (b) Chlamydomonas reinhardtii, (c) Synechococcus sp. strain PCC 7002, (d) Halomicronema hongdechloris[24], (e) Acaryochloris marina, (f) Ostreobium quekettii and (g) Chlorogloeopsis fritschii

Physcomitrella patens (Figure 1a) is an early colonist moss that can grow on exposed mud and earth around the edges of pools of water. It only lives in temperate parts of the world, with the exception of South America. *Physcomitrella* contains Chl a and b.

Chlamydomonas reinhardtii (Figure 1b) is a single-cell green alga about 10 micrometers in diameter, widely distributed worldwide in soil and fresh water. It has an "eyespot" that senses light and the organism is able to swims due to the presence of two flagella. *Chlamydomonas reinhardtii* is an especially well studied biological model organism, partly due to its ease of culturing and the ability to manipulate its genome. When illuminated, *C. reinhardtii* can grow photoautotrophically, but it can also grow in the dark if supplied with organic carbon. It contain Chl a and b.

Synechococcus sp. strain PCC 7002 (Figure 1c) is a unicellular (3-4 µ of diameter), euryhaline cyanobacterium. It is a model organism for studies of cyanobacterial metabolism. It exhibits an exceptional tolerance of high-light irradiation and shows very rapid growth. The habitats from which this and closely related strains were isolated are subject to changes in several environmental factors, including light, nutrient supply, temperature, and salinity. It contains Chla.

For this research, we also selected a series of other peculiar photosynthetic microorganisms able to extend their in vivo absorption to the NIR, around 710 nm, due to the presence of other chlorophyll forms like chlorophyll d and f. Members of this second group of organisms are the cyanobacteria *Acaryochloris marina*, *Halomicronema hongdechloris* and *Chlorogloeopsis fritschii*. *Halomicronema hongdechloris* (Figure 1d) is the first reported filamentous cyanobacterium containing Chl f together with Chl a[24]. It was isolated from a stromatolite cyanobacterial community. Its extremely slow growth rate has hindered research on this newly isolated cyanobacterium and the investigation of chlorophyll f-photosynthesis. Chlf is reported to be a "red-light-induced" chlorophyll with increased amount when *H. hongdechloris* is cultured under far-red light (Chen et al., 2012) [24].

Acaryochloris marina (Figure 1e) is a cyanobacterium containing Chlorophyll d, instead of Chlorophyll a allowing it to utilize far-red light, at 710 nm wavelength. It is a species leaving in symbiosis with invertebrate marine organisms or free in the oceans.

Acaryochloris marina could use Chlorophyll d, rather than Chlorophyll a, to perform oxygenic photosynthesis on exoplanets orbiting red dwarf stars (which emit much less light than the Sun). Because approximately 73 percent of the stars in the Milky Way galaxy are red dwarfs[25], the existence of *Acaryochloris marina* implies that oxygenic photosynthesis may be occurring on far more exoplanets than astrobiologists initially thought possible.

Ostreobium sp. (Figure 1f) is a green alga. Chloroplasts are small, spherical or polyhedral to reticulate with no presence of pyrenoids. Cell walls are thin and undifferentiated to thick and lamellose. Their reproduction is by quadriflagellate zoospores known only *Ostreobium quekettii*. It is widely distributed in tropical to temperate areas, growing primarily in calcified substrata including corals, calcified red algae and old mollusc shells. *Ostreobium* is among the deepest growing macro algae in both temperate and tropical regions. Physiological studies on in situ photosynthesis by *Ostreobium* confirm low levels of light requirements and an ability to utilize near infra-red light greater than other green algae. A modified photosystem I reaction centre was hypothesized to account for this.

Chlorogloeopsis fritschii (Figure 1g) is a terrestrial cyanobacterium that can grow in hot springs.

In 2014 the production of chlorophyll f and chlorophyll d in the cyanobacterium *Chlorogloeopsis fritschii* cultured under near-infrared and natural light conditions was reported. *C. fritschii* produced chlorophyll f and chlorophyll d when cultured under natural light to a high culture density in a 20 L bubble column photobioreactor.

In laboratory measurements, the ratio of one of its pigments, Chl f, to Chl a have been reported to change from 1:15 under near-infrared light exposure, until an undetectable level of Chl f under artificial white light.

4. THE EXPERIMENT

The first part of the experiment, consists of three steps[26]. In the first step, called the fiduciary experiment, measurements of photosynthetic bio-products taken in terrestrial conditions. Here will be tested the amount of O_2 produced by the organisms at first in an atmosphere mimicking the terrestrial one, and composed by 15% CO_2 and 85% N. Oxymeter productivity tests will be made to have a reference for the measurements. Bacteria will be lodged in an environment chamber described in 4.1. At first, the pressure will be kept constant at 1.013 bar at about 300 K, a suitable temperature for oxygenic photosynthetic bacteria. The irradiation can reproduce the solar spectrum as by means of a tunable led stellar-light simulator The stellar simulator is a multiple LED matrix cooled by means of air fan technology.

The main aim of the radiation source is to reproduce the spectrum of stellar spectral types ranging from F to M.

In order to endow it with modularity this device is be composed by a mosaic of circuit boards arranged in a pie-chart shape, on the surface of which will be welded the LEDs. The device can be driven by a PC to raise or lower the intensity of both each LED and the lamp, in order to simulate as close as possible a portion of the star spectrum. The wavelength intervals (365 nm to 940 nm) almost overlaps the limits of photosynthetic pigment absorption range (280-850 nm). The reason why we chose a higher outer limit is that M stars have the emission peak at about 1000 nm and we want to study the effects of low-light radiation on bacterial vitality[26,27]. It is well described in section 4.2.

Before and during sample irradiation measurements of gas composition will be taken, expecting a peak of gas concentration variations at the end of bacteria metabolic and photosynthetic process. The measurements of gas concentrations inside the cells will be done with a Tunable Diode Laser Absorption Spectroscopy setup (TDLAS) and is based on absorption energy following Beer's law. This measurement method provides a Vertical Cavity Surface Emitting laser (VCSEL) source shot through the cell environment and to a photodiode diode laser tuned to a particular narrow emission band[28]. The source wave number is selected in order to match a single absorption line on a molecule of interest and the laser emission is scanned several times across the whole spectral width of the absorption feature. Usually, the line width of the laser emission is much smaller than the molecular absorption line width allowing the instrument to be selective among components of a gas mixture and have no interferences from other gases, especially at low pressure (the absorption lines are narrower). The sensitivity of the analyzer is dependent on the absorption strength of the line chosen and on the absorption path length[29].

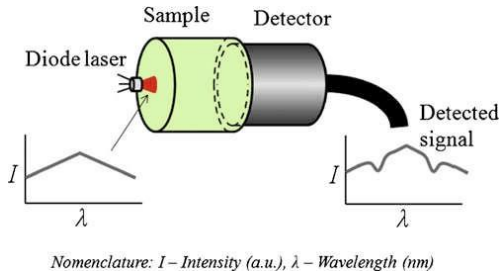
Many gases of biological interest can be sensed in this way (See table 2).

Gas	Detection limit
HF	0.2 ppm.m
H_2S	20.0 ppm.m
NH3	5.0 ppm.m
H_2O	1.0 ppm.m
CH_4	1.0 ppm.m
HCl	0.15 ppm.m
HCN	1.0 ppm.m
CO	40.0 ppm.m
CO_2	40.0 ppm.m
NO	30.0 ppm.m
NO_7	0.2 ppm.m
O_2	50.0 ppm.m

Table 2. Gas detection limits

A Wavelength Modulation Spectroscopy scheme will be used to improve detection of weak absorptions from the low concentrations obtained. The measurement setup will be based on a PC with a DAQ card for synchronous modulation and demodulation of the WMS waveforms

as well as for fitting the absorption signals. In figure 3 is shown a scheme of TDLAS measurement set up[30].



Nomenclature: I – Intensity (a.u.), λ – Wavelength (nm)

Figure 2. Working scheme of the gas detector.

The second step of the experiment will consist to change the irradiation source to simulate an M star. M star spectra have strong absorbance lines, so it is difficult to reproduce exactly it as they are not good black body emitters. Finally, in the third step we will change even the gas mixture inside the cells, keeping the irradiation source as in the previous step. The gas composition will come by theoretical simulation of super earths atmospheres. Measurements of bacterial vitality will be made by means of a Pulse-Amplitude Modulation (PAM) imaging system, that measure the fluorescence of the bacteria in order to know their vitality.

4.1. The incubator chamber

The incubator chamber is a stainless steel main body topped with a Borofloat window. On the lateral surface will open four wedge windows that will be used to probe the gas content, in particular O_2 and CO_2 . The two elbow connectors will need for the gas flowing, in order to select the desired gas mixture inside the cell. In figure 3 is shown an exploded view of the cell. The temperature inside the chamber is kept constant by means of four 60W peltier cells driven by a Thermo Electric Cooler (TEC) controller.

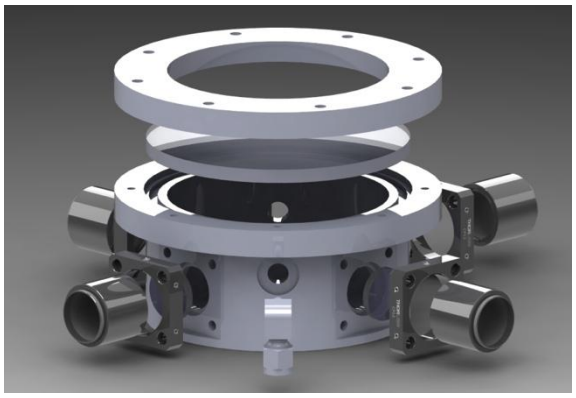


Figure 3. Inner steel cells for bacterial lodging

4.2. The radiation source

The radiation source is a multiple LED matrix cooled by means of air cooling technology. In order to generate a dynamical spectrum we evaluated different kind of radiation sources, but LEDs have been chosen instead of lamps because they are cheap, very small and dynamic. This feature can allow a non-static characteristic of this novel radiation source, that can be tuned by a PC The light emitted by this source is in the wavelength intervals between 365nm and 940nm.
The idea of modularity led us to a multi-plate system shaped in the form of annuli, with mosaic of circuit boards arranged in a pie-chart shape, on the surface of which the LEDs are welded. Dividing the tool in plates, future implementations can be allowed, such as to reproduce other spectral types of stars just changing some kind of LEDs without building a lamp *ex-novo*. In figure 4 and 5 is shown the concept design of the radiative system made with solid works.

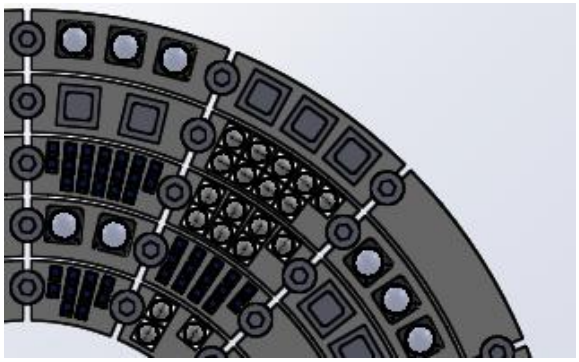


Figure 4. Main radiative system design

The fluxes will be uniformed by means of a reflective silver plated cylinder with 98% reflecting power shown in figure 5.

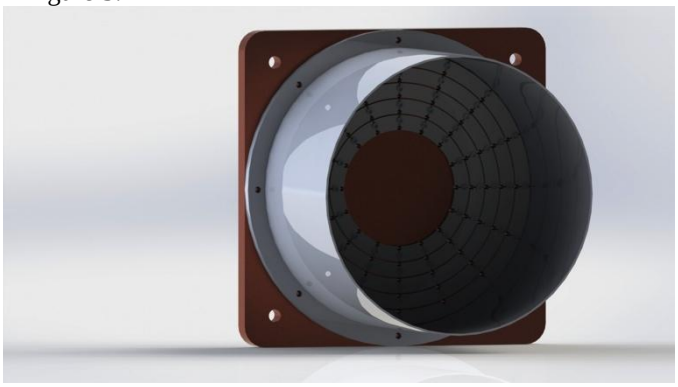


Figure 5. Radiative system design complex

On the back of the lamp will be fixed a copper plate (Figure 6) used to join the main body with the cooling system. The power emanated from the radiation source will be 106.22 W while the thermal power will be 434.05 W. The excess of heat is dissipated with an external fan.

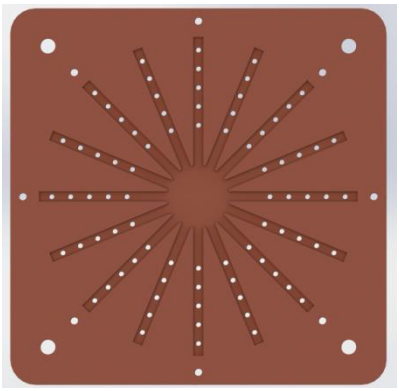


Figure 6. Copper plate design

In figure 7 is shown an example of the radiation source making-of.



Figure 7. Example of the radiation source making-of.

In order to control the radiation source by a PC we chose a 15 channels expandable up to 63 DALI RS232 channel multiplier from Tridonic Labs (Figure 8).
Each channel can support a maximum of 45 V. In order to check the output spectrum of the illuminator an STS-VIS spectrograph from Ocean Optics with cosine corrector is used. This spectrograph has a spectral range falling between 380 and 900 nm, an integration time varying from 1 ms and 10 s and a SNR of 2000:1. It has a dedicated diffraction grating with 600 rows/mm and a linear CMOS ELIS1024 with 1024 elements (figure 9).
In figure 10 is shown an example of spectrum fitting simulation with the radiative source in order to generate the spectrum of an M star on the top of the surface of a terrestrial planet at the moist greenhouse distance.



Figure 8. DALI RS232 channel multiplier from Tridonic Labs and buck led drivers.



Figure 9: STS-VIS spectrograph from Ocean Optics

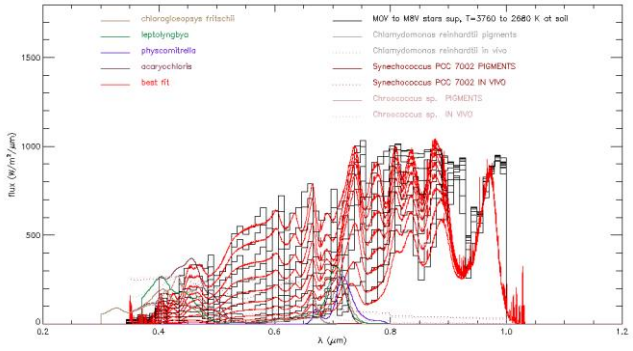


Figure 10: spectrum fitting simulation with the radiative source in order to generate the spectrum of an M star on the top of the surface of a terrestrial planet at the moist greenhouse distance

5. OTHER APPLICATIONS

The astronomical aim of the proposed research has several other applications. The radiation source can be used in different fields:

1) In the field of photo-bioreactors as a reference test bench for the choice of the wavelength to be used in order to maximize the production rate of the bacteria.

2) Microscopy. In fact it can be used as a dynamic light source to irradiate samples at different wavelengths and to study their features at different wavelengths without changing the source.

3) Yeasts growth research could be a good field of application, because these organisms need precise wavelengths to evolve.

4) Transistors quantification, studying the trap states and their behavior at different wavelengths.

5) Finally, a pioneering study has linked the evolution of magnetic metallorganic structures with the cell behavior. Our device will help to better understand the link of these structures with the wavelength radiation.

Other uses of this research are:

1) For university the stellar simulator could represent a new facility for the next experiments, especially for multi-field studies.

2) A radio podcast is under study to reach a wider slice of people. It has been thought as a sort of "pills", a short time space inside which treat an argument of life outside the solar system.

3) Lessons for students could be made with the outputs of this research. For the target 8 and 17 years could be made experiments with shadows.

Each lesson consists of a general science background (information necessary to teach the lesson and answer any questions the children might have), learning objectives (the knowledge and skills the students should acquire during the lesson), a list of teaching materials, and a full description (a step-by-step guide that the teacher can follow to introduce the subject and teach the lesson).

5.1. An app for Android

A useful application of this work is an app for Android capable to see, through the cell phone, the spectrum that an exoplanet explorer could see if walking on its surface. This feature is achievable thanks to the simulations made for this research, in order to understand what spectra could impact on different planets around F, G, K and M stars. With this App the user could change the air-mass of the atmosphere, a raw chemical composition and the incident stellar spectrum. Through digital filters the image will change in real time showing different colors corresponding to the different intensities of wavelength impacting on the planet's surface. There will be even an eye-mode. As our eye is not sensible to NIR and IR light, the image could be filtered through the eye's optical response, letting we see images, through the smartphone, as we were looking directly with our eyes. This App has a good educational potential, both for schools and enthusiasts users.

5.2. Enquiry-based learning

Enquiry-based learning is a powerful means for students to learn both scientific content and scientific reasoning together.

The power of an inquiry-based approach to teaching and learning is its potential to increase intellectual engagement and foster deep understanding through the development of a hands-on, minds-on and 'research-based disposition' towards teaching and learning. Inquiry honors the complex, interconnected nature of knowledge construction, striving to provide opportunities for both teachers and students to collaboratively build, test and reflect on their learning.

A framework for describing enquiry in is[31]:

Student learning is motivated by investigating the answer to a question.

The learning activity is focused on developing learners' competency with practices of doing and thinking about science and astronomy (as described in the list above).

The learning activity is focused on foundational physics and astronomy concepts.

Learning practices and concepts is intertwined: students use scientific practices to gain conceptual understanding, and conceptual understanding motivates the use of scientific practices.

Students have ownership over their learning and gaining competency.

Students use evidence to develop explanations.

The learning activity mirrors authentic scientific research[31].

5.3. Example of lesson

Your shadow on a planet with two suns: how the color of your shadow changes if you live on a planet with two suns of different colors.

AGE: 10-12

BACKGROUND SCIENCE: If you watch the color of your shadow on a sunny day you will realize it is dark. The shadow being the total absence of light, whatever the color of the lamp (or the star) that shines on your body the shadow that will appear will be always dark. If you switch on a red light bulb and place yourself between the light bulb and a screen, the color of your shadow will still be dark, no matter the color of the light bulb you choose.
Now if instead of that you choose two light bulbs, red and blue, say, your shadow will then show colors! Since the two light bulbs are not positioned in the same place, they will produce shadows in different places. When the blue light shines on the dark zone created by the shadow of the red light, it will color the shadow blue. When the red light shines on the dark zone created by the blue light, it will color it red. This is what will happen on a planet lit by two stars--one red, and the other blue.

LEARNING OBJECTIVES: Understanding and reasoning out how your shadow changes if two stars of different colors are up in the sky. Adult supervision recommended.

MATERIALS: Red and blue light bulbs, 1 white screen (or a stretched sheet)

DESCRIPTION:

1. Set the white screen in a room. Place yourself in front of the screen and have the adult turn off the room's lights, then switch on the red light bulb in front of you.
2. After switching on the red light bulb, the adult must switch the blue bulb located close to the red one.
3. Now look behind you. What color is your shadow?

6. Conclusions

In this work we have described the ongoing project of an experiment focused on the study of biosignatures in the atmosphere of a super Earth orbiting an M star well inside its habitable zone. We have underlined the scientific requirements and choice of the bacteria. We have therefore analyzed the aspects of hardware customizing and the development of a source of irradiation as well as the possible educational aspects of the research.

Acknowledgements

We specially thanks Dr. Rosanna Sordo of INAF-Astronomical Observatory of Padova for the stellar synthetic spectra.

7. BIBLIOGRAPHY

[1] Hart, M., H., "The evolution of the atmosphere of the Earth", ICARUS, 1978, 33-23-39

[2] Kasting, J.F., Whitmire, D.P., and Reynolds, R.T. (1993), Habitable zones around main sequence stars. *Icarus* 101, 108–128.

[3] Joshi, M.M., Haberle, R.M., and Reynolds, R.T. (1997) Simulations of the atmospheres of synchronously rotating terrestrial planets orbiting M dwarfs: conditions for atmospheric collapse and the implications for atmospheric habitability. *Icarus* 129, 450–465.

[4] A., Kasting, J.F., Meadows, V., Cohen, M., Scalo,J., Crisp, D., Butler R.A.H., and Tinetti, G. (2005) Biosignatures from Earth-like planets around M dwarfs. *Astrobiology* 5(6), 706–725.

[5] Kasting, J.F., Whitmire, D.P., and Reynolds, R.T., " Habitable zones around main sequence stars." Icarus 101, 108–128 (1993)

[6] Selsis, F.: "Habitable planets around the star Gl 581?." Astronomy and Astrophysics *476 (3): 137-1387* (2007)

[7] Joshi, M., " Climate model studies of synchronously rotating planets." *Astrobiology* 3(2), 415–427 (2003)

[8] Joshi, M.M., Haberle, R.M., and Reynolds, R.T., " Simulations of the atmospheres of synchronously rotating terrestrial planets orbiting M dwarfs: conditions for atmospheric collapse and the implications for atmospheric habitability." *Icarus* 129, 450–465 (1997)

[9] Edson, A.; Lee, S.; Bannon, P.; Kasting, J., F., Pollard, D., "Atmospheric circulations of terrestrial planets orbiting low-mass stars", Icarus, Volume 212, Issue 1, p. 1-13 (2011)

[10] Kiang, N.Y., Segura, A., Siefert, J., Tinetti, G., Govindjee, Blankenship, R.E., Cohen, M., Siefert , J., Crisp, D., and Meadows, V.S., "Spectral signatures of photosynthesis II. Coevolution with other starts and the atmosphere on extrasolar worlds." *Astrobiology* 7(1), 252–274 (2007).

[11] Lammer, H.; Bredehöft, J. H.; Coustenis, A.; Khodachenko, M. L.; Kaltenegger, L.; Grasset, O.; Prieur, D.; Raulin, F.; Ehrenfreund, P.; Yamauchi, M.; Wahlund, J.-E.; Grießmeier, J.-M.; Stangl, G.; Cockell, C. S.; Kulikov, Yu. N.; Grenfell, J. L.; Rauer, H., "What makes a planet habitable?" The Astronomy and Astrophysics Review, Volume 17, Issue 2, pp.181-249 (2009)

[12] Raven, J.A., "A cost-benefit analysis of photon absorption by photosynthetic unicells." *New Phytol*. 98(4593–625 (1984)
[13] Wolstencroft, R.D. and Raven, J.A., "Photosynthesis: likelihood of occurrence and possibility of detection on Earth-like planets." *Icarus* 157(2), 535–548 (2002)
[14] Kiang, N. Y., J. Siefert, Govindjee, R. E. Blankenship and V. S. Meadows "Spectral signatures of photosynthesis I: Review of Earth organisms." Astrobiology, 7(1) 222-51 (2007)
[15] Miyashita, H., Ikemoto, H., Kurano, N., Adachi, K., Chihara, M., and Miyachi, S. "Chlorophyll d as a major pigment." Nature 383(6599), 402 (1996)
[16] Miller, S.R., Augustine, S., Olson, T.L., Blankenship, R.E., Selker, J., and Wood, A.M., "Discovery of a free-living chlorophyll d-producing cyanobacterium with a hybrid proteobacterial cyanobacterial small-subunit rRNA gene." Proc. Natl. Acad. Sci. U S A 102(3), 850–855 (2005)
[17] Mielke, S. P., Kiang, N. Y., Blankenship , R. E., Gunner , M. R., Mauzerall, D.: Efficiency of photosynthesis in a Chl d-utilizing cyanobacterium is comparable to or higher than that in Chl a-utilizing oxygenic species. Biochim Biophys Acta. 1807(9): 1231–1236 (2011)
[18] Chen, M., Telfer, A., Lin, S., Pascal, A., Larkum, A.W.D., Barber, J., and Blankenship, R.E., "The nature of the photosystem II reaction centre in the chlorophyll d containing prokaryote, *Acaryochloris marina.*" *Photochem.Photobiol. Sci*. 4(12), 1060–1064 (2005)
[19] Larkum, A.W.D. and Kühl, M., "Chlorophyll d: the puzzle resolved." Trends Plant Sci. 10(8), 355–357 (2005)
[20] Manning, W.M. and Strain, H.H. "Chlorophyll d: a green pigment in red algae." *J. Biol. Chem*. 151(1), 1–19 (1943)
[21] Scheer, H., The Pigments. Light-Harvesting Antennas in [Photosynthesis] Kluwer, Dordrecht, The Netherlands (2003)
[22] Heath, M.J., Doyle, L.R., Joshi, M.M., and Haberle, R.M., "Habitability of planets around M dwarf stars.", *Orig. Life Evol. Biosph.* 29, 405–424 (1999)
[23] McKay, C.P.,"Thickness of tropical ice and photosynthesis on a snowball Earth." Geophys. Res. Lett. 27, 2153–2156. (2000)
[24] Chen, M., Li,Y., Birch, D., Robert, D., Willows,R.D. (2012) "A cyanobacterium that contains chlorophyll f – a red- absorbing photo pigment." FEBSLetters 586: 3249-3254
[25] Dole, Stephen H. *Habitable Planets for Man* 1965 Rand Corporation report
[26] R. Claudi, M. S. Erculiani, G. Galletta, D. Billi, E. Pace, D. Schierano, E. Giro and M. D'Alessandro, "Simulating Super Earth atmospheres in the laboratory", International Journal of Astrobiology. 05/2015, DOI: 10.1017/S1473550415000117
[27] Erculiani, M. S., Claudi, R., Cocola, L., Poletto, L., Barbisan, D., Bonato, M., Meneghini, M., Trivellin, N., Farisato, G., Giro, E., Salasnich, B., "A tunable integrated system to simulate colder stellar radiation", Proc. SPIE 9626, Optical Systems Design 2015: Optical Design and Engineering VI, 96262D (September 23, 2015); doi:10.1117/12.2189053
[28] P. Werle, F. Slemr, K. Maurer, R. Kormann, R. Mucke, and B. Janker, "Near- and mid-infrared laser-optical sensors for gas analysis," Opt. Las. Eng. 37(2–3), 101–114 (2002)
[29] Bowling, D. R., Sargent, S.D., Tanner, B.D., and Ehleringer, J.R.:"Tunable diode laser absorption spectroscopy for stable isotope studies of ecosystem–atmosphere CO_2 exchange", Agricultural and forest meteorology, 118, 1-19
[30] Erculiani, M. S.,Claudi, Riccardo U.,Giro, Enrico,Galletta, Giuseppe,D'Alessandro, Maurizio, Farisato, Giancarlo,Lessio, Luigi,Micela, Giuseppina,Billi, Daniela, "Interpreting EChO's future data: biological laboratory extimates under M star's planetary surface conditions", Proceedings of the SPIE, Volume 9143, id. 914355 12 pp. (2014)
[31] Hunter L., Metevier A.J., Seagroves S., Kluger-Bell B., Inquiry Framework and Indicators, (Santa Cruz, USA: Institute for Scientist & Engineer Educators, 2014) http://isee.ucsc.edu/projects/inquiry-framework.html

"So… you want to leave the earth?" – The necessity of astronauts psychosocial support

Zoe Lola- *Social Worker, Graduate from Department of Social Management with a specialty in Social Working in the Democretion University of Thrace*
Student of Psychology, Department Of Psychology, European University of Cyprus, Cyprus
Tel: 0030 6970381850
Address: Kentauron 2, Larissa, Thessaly Province, Greece
ZIP code: 41222
Email: zoelola@windowslive.com

Abstract

Considering the radical space technology progress during the recent years, there is an overgrowing need of studying the issues of space missions' human resources and their mental health. The present study is an effort to shed light on some basic issues on this field. Taking into account the enormous physical and psychological pressure, experienced by cosmonauts during a space mission, it is crucial to study issues linked with the mental factors that play a key role to its success. This includes: the stress factor during extreme isolation situations, the correct choice of the space crew members based on their psychological profiles, the space team cohesion, issues related with the leadership and the administration of the space missions, the necessity of counseling, psychological support and psychotherapy of the astronauts and their families in earth, as well. Basis has also to be given on Earth's youth population familiarization with space exploration experience through artistic expression, an educational and artistic tool that will cultivate the space culture during an individual's childhood and adolescent years, enabling youth psyches to embrace the space issues with greater comfort and easiness during the upcoming decades. More specifically, as far as the stress factor is concerned, it is acknowledged why it constitutes an aggravating factor during space missions. Ways are proposed in order to predict its provoking conditions before its emergence, and recognise stress, if and when it appears, so it can be countered with an immediate and discreet intervention, in order to remove any hazardous situation. Additionally, the most suitable adaptation of the astronauts can be ascertained and balanced through their participation into recreative and artistic activities. Felicitous choice of the space crew, a precondition of a mission's success, has to correspond to certain basic personality characteristics, which can be reflected on respective psychometric evaluations. Furthermore, team cohesion issues are related to culture differences, sex issues, personalities and most importantly, the way that human resources are handled and administered. The careful choice of the most suitable leadership drastically ensures the mission's progress. Consequently, its advisement is the cornerstone of Space Psychology. The basis of the present study is the astronauts' mental health, which plays a tremendous part in order to diminish the imponderable factors that can jeopardize a space mission and can facilitate the astronauts' adaptation to space and during their return to homeland Earth.
Keywords: *Space Psychology, astronaut, space education, mental health*

1. INTRODUCTION

This paper attempts to touch different aspects of Space Psychology with an emphasis on the improvement of our understanding on mental health needs of astronauts and cosmonauts, and promoting space culture. Regarding our first objective, in reference to weighty issues such as the meaning of Space Psychology and the reasons we deal with this, what are the factors affecting their lives in space (stress, radiation, difficulties in performance), psychosocial conditions of astronauts and cosmonauts (vast distance from home, crew diversity etc.), psychological tests and difficulties faced by them and finally issues concerning Leadership and Management (scheduling). Regarding the second objective, we are presenting an educational program scheduled from the writer of this essay that focuses on the space culture cultivation to young people through art and fee proposals promoting mental health through art to members of a space mission.

1.1 What is Space Psychology?

Space Psychology is the psychological field which is associated with life in space. It contains parts of the areas of social, clinical, cognitive and experimental psychology, organizational psychology and human factor management. Science also has provided major contribution to the development of this sector similarly to engineering, architecture, biology, medicine, anthropology and sociology (Contemporary Research in Historical Perspective - The NASA History Series, 2011 p.15). The reason that this academic field is so crucial to the study of the human factor role during space missions is because the space mission positive outcome on its own is certainly based on this. And that becomes even more obvious especially when we are dealing with long-term missions (Holland, 2000).

1.2 Factors affecting life in space

There are many factors causing stress during space mission. On the physical aspect we can mention the temperature, acceleration, microgravity, ionizing radiation, meteoroid impacts and the light/ dark cycles. These result in physiological function alteration on the following body symptoms such space sickness, vestibular problems, loss of the 24-h light/ dark cycle which can result in circadian disruption and sleep disturbances, bodily fluid shifts, bone loss and hypercalcemia provoking difficulties in performance (Nick Kanas, Dietrich Manzey). The group size, gender, culture, education, age and previous experience are key actors in adapting to space (G. M. Sandal Z G. R. Leon Z L. Palinkas, 2006).
According to Palinkas (PSYCHOSOCIAL ISSUES IN LONG-TERM SPACE FLIGHT: OVERVIEW, p.25) there are 3 different areas which influence astronauts' behavior. The first area contains the circumstances that affect an individual level the person (such as personal characteristics and resistance to extreme stress conditions). The second relates to interpersonal issues that may hinder the group cohesion (e.g. multinational crew, crew- ground communication). The third factor concerns organizational issues such as leadership and each organization's issues linked with culture.

1.3. Astronaut Selection

According to surveys presented in Palinkas and colleagues (2001) reported that prolonged stay in space or other respective situation- isolated and confined extreme environments (ICE) carries the possibility of a healthy population that has successfully passed the original psychiatric and psychological screening experience criteria to manifest a DSM-IV disorder (such as mood disorder and sleep disorder). In the US space program followed a "select-out " process during the screening and selection of any crew member that have a diagnosed mental illness or there is a possibility of developing one. At the "select-in" process the space crew is chosen from more people that can successfully cope under pressure and perform in team spirit. (Nick Kanas, Vyacheslav Salnitskiy, Ellen M. Grund, Daniel S. Weiss, Vadim Gushin, Alan Bostrom, Olga Kozerenko, Alexander Sled, and Charles R. Marmar, 2001, p.26)
For this reason before any mission takes place, it is essential that candidate astronauts and cosmonauts go through certain tests. There are several psychometric suitability tests which indicate whether a person could be included in a space mission based on the extreme physical and psycho-emotional conditions it encounters in the course of the mission, but also because of the weakness of a sudden exit from it. Experts exclude from the outset someone with a diagnosed mental disorder (Nick Kanas, Dietrich Manzey).

Apart from the right choice there is one other factor that should be mentioned. This concerns the appropriate choice of the crew based on the compatibility among each other. In other words, the crew should have some compatibility between them. (Nick Kanas, 2001)

Through the Personal Characteristics Inventory (PCI) (developed by Helmreich et al) as the NEO Personality Inventory (NEO-P) (developed by Costa and Mc Crae) can clarify the criteria for selecting the appropriate space crew. Through the PCI, candidates are divided into three categories and are evaluated as "Right Stuff ", "Wrong Stuff " and "No Stuff ". PCI test focuses on two expressions of personality: the Instrumentality (associated with one's ability to focus on achieving the objective) and Expressivity (associated with one's interpersonal skills). Other features that are evaluated are verbal aggressiveness, negative instrumentality (negative motivation for goal seeking, arrogant, dictatorial), mastery (master in new and challenging activities), work orientation (desire for hard work), competitiveness, achievement strivings (responsibility towards work), impatience / irritability. (Matthias Rauterberg, Mark Neerincx, Karl Tuyls, Jack van Loon) Through this test the future attitude of someone during the mission can be predicted. The "Right Stuff" presents an ideal personality profile of astronaut combination of the following properties: high levels of instrumentality and expressivity with low levels of interpersonal aggressiveness. The " Wrong Stuff " bears a personality profile people of comparatively inferior performance or because of low achievement motivation or even the attitude of competition, hostility and aggression expressing at the group level. The "No Stuff " includes personality elements which express as main features low positive instrumentality (focus on goal and interpersonal interest) and high levels of verbal aggression. (David M. Musson, Gro. M. Sandal, and Robert. L. Helmreich)

1.4. The psychosocial conditions faced by astronauts and cosmonauts

The key psychosocial barriers faced by the space crew could enlist: Crew heterogeneity, personal conflicts, crew size, leadership issues. Stressors are isolation, confinement, communication difficulties due to linguistic barriers both on cultural differences and scientific terms (ACTA ASTRONAUTICA, DECEMBER 2012). Especially in recent decades that crews are characterized by interculturalism and diversity, many opportunities for conflict appear

between crew members which may endanger the mission. (Contemporary Research in Historical Perspective - The NASA History Series, 2011)
More importantly, if there is a different sociocultural background among the members, their training must take place and focus on those situations that may face between each other. Also crew monitoring is necessary for discreet surveillance and immediate intervention in case of personal boundaries non- respect (Holland, 2000). Among the members of a mission with different cultures, misunderstanding phenomena appear very often, which may endanger the mission. Issues of cultural differences have become visible in relation to the personality, strength psychological pressuring situations, adaptation, execution of complex tasks in periodical (weekly) and organizational issues. The way that a culture perceives a situation can considerably differ from another. In space missions with a multicultural crew layer, situations that occur often may bring permanent cases that threaten the group cohesion (Cultural Differences in Crewmembers and Mission Control Personnel During Two Space Station Programs, p. 532). However, contact with people of other cultures can reduce the feeling of boredom, an opportunity celebrating unaccustomed holidays and acquire a different vision of things. (Peter Suedfel, Kasia E. Wilk, Lindi Cassel)
The difficulties encountered in interpersonal level (Space Psychology and Psychiatry-
Nick Kanas, Dietrich Manzey, p. 2) showing intensity on the group context, withdrawal behaviors and territorial behavior, lack of privacy, scapegoating and internal anger transfer among the crew on mission control personnel. More specifically, "scapegoat ' use can be applied as a means of maintaining the internal balance and peace among the members of the group at the cost of a selected person that becomes the target of intra- group hostility and aggression. (Sandal, Leon, Palinkas).
According to Russian investigators, both in space missions and in the corresponding isolated environments on Earth, in cases where the crew does not externalize and resolve negative feelings that exist between them and are associated with lack of support and hostility among them, are carried to the monitoring personnel, which may be accused of lack of empathy by them. This displacement of negative emotions could bring hazards and communication disruption. These are key issues that endanger the mission (Crewmember and Mission Control Personnel
Interactions During International Space
Station Missions, p.602 & Psychosocial interactions during ISS Missions - ACTA ASTRONAUTICA, February 2007). Possible tensions between the crew and the control personnel can usually arise because the first feel a sense of “taking automatic responses” from the second. Difficulties increase the longer the delay because of the communication time lag in interplanetary missions, such as Mars for example which exceeds 37 min. lag. (ACTA ASTRONAUTICA
DECEMBER 2012, p.590)
Crew’s consistency and good communication are necessary in order to maintain a good psychological state. One means of increasing the group cohesion would be activities with Amusement games. (Peldszus, Dalke).Sense of team spirit, interdependence and mutual friendship feelings can influence group cohesion in a protective manner. (Tafforin, 2015)

1.5. Astronauts and cosmonauts psychological challenges

During a space mission, the astronaut is not only removed from his family and his country but from his own planet. Given this, we can reasonably conclude that the man who will be exposed to extreme isolation in a hostile environment will experience high levels of stress. At the same time it is considered necessary to have the ability to handle complex tasks at relative ease and execute orders efficiently. Therefore, the required features are the composure, the concentration capability and mental clarity under pressure, tolerance to high levels of psychological stress etc. (Holland, 2000).

Rohrer conducted a review on Antarctic and submarines missions which describes the three stages that astronauts confront on a space mission. The first concerns the initial anxiety of what would face during the mission; the second is characterized by depressed mood, which usually occurs in the middle of the mission, deriving from the departure from the familiar environment of the family. The third is characterized by feelings of euphoria and immature behavior. (Crewmember and Mission Control Personnel
Interactions During International Space
Station Missions - Nick A. Kanas, Vyacheslav P. Salnitskiy, Jennifer E. Boyd, Vadim I. Gushin, Daniel S. Weiss, Stephanie A. Saylor, Olga P. Kozerenko, and Charles R. Marmar, p. 601)
In any case it is very important during the in- flight period that the crew makes the correct decision. The role of decision making in space is important because in emergency situations involving risk potential, it is crucial to make the right decisions. Therefore external factors must be taken into account that may affect the correct decision making. These may relate to external environmental factors that affect the proper functioning of parts of the brain, hence leading to decision making. Human cognitive and perceptual motor performance deteriorates under stress and among them the central postural functions, the speed, the accuracy, the attention etc (ACTA ASTRONAUTICA - DECEMBER 2012).
For astronauts’ better adaptation they have to be tested

and trained in similar environmental conditions to the mission's destination before their flight commences. The corresponding environmental conditions in which they can be tested could be divided into: 1) laboratory and simulation 2) natural, physical environment and 3) constructed environment. (Source 3).
In the adjustment difficulties experienced by astronauts, interventions concerning the field of habitability in the spaceship vary and are necessary for the normal life of the crew. This can involve everything aiming to ensure the highest possible quality standards of life even in conditions outside the Earth. This may involve spaceship spatial planning, colors, hygiene, cleanliness, comfort, entertainment etc. (Review Report
By Chiu-Pih Tan, 2007)

The success of a mission is based, to a large extend, on education to be taken by members. It is necessary both the crew members and mission moderators to receive mission control training. The latter would be optimal to train on the empathy skill towards the crew because, as mentioned before, either because of there the distance or because of the delay in communicating tension created, the first ones may think that the latter cannot sense the difficulties they face . Therefore, the pre-fight training is very important. Training and preparation received can be divided into three phases: basic, advanced and mission specific (Holland, 2000).

During the flight (in-flight period) the monitoring and support to the crew are necessary actions to achieve the mission (ACTA ASTRONAUTICA- OCTOBER 2008). Through voice processing the levels of stress can be identified in order to ensure the prompt intervention. Also communication with families on earth lowers stress levels and astronauts are much more focused on the objective of the mission. Also in cases of psychological stress events contribution counseling and psychotherapy to the members of a crew with a psychologist, is very useful and it is carried out via individual sessions made remotely (Kanas, Manzey). But even in cases that this is not feasible, the use of programs of cogno- behavioral type or self-help can operate effectively in the management of mild anxiety and depression (Hennes, Tuyls, Neerincx, Rauterberg). In Psychological Support and Countermeasures phase, well-known standardized psychometric measures used are: The Profile of Mood States (POMS), the Group Environmental Scale (GES) and the Work Environment Scale (WES) (Crewmember and Mission Control Personnel Interactions During International Space Station Missions). Also during in-flight monitoring and care psychometric tools in use such as Space flight Cognitive Assessment Tool (S-CAT), assesses the cognitive performance and neuropsychological status. Also, of great use is the Space flight Behavioral Assessment Tool (S-BAT) which controls levels and distribution of stress during in flight period. (PSYCHOSOCIAL ISSUES IN SPACE: RESULTS FROM SHUTTLE/MIR, 2001) Other space cognitive test and batteries used are the following: MINICOG, the AGARD (Advisory Group for Aerospace Research and Development, STRES (Standarized Tests for Research with Environmental Stressors), The Spaceflight Cognitive Assessment Tool for Windows (winSCAT) and Vigilance Test (PVT). (ACTA ASTRONAUTICA- DECEMBER 2012)
In many cases one of the crew members may be confronted with the emergence of a mental disorder. A severe problem which often occurs is the 'Asthenization'. This title describes a situation experienced by many astronauts and cosmonauts and sensations associated with fatigue, reducing the energy and some activities, irritability, sleep and eating disorders. During her appearance may be a disruption to the team, withdrawal and reduced profitability on the tasks of the mission. (Crewmember and Mission Control Personnel Interactions During International Space Station Missions**)**
The phenomenon of asthenia is a common disease according to the Russians, although not find the same acceptance the American psychiatric community and is not included in the DSM. In this disease there is no agreement between space agencies (ACTA ASTRONAUTICA- DECEMBER 2012). Psychiatric disorders that may occur related to the appearance adjustment disorders, somatoform disorders, mood disorders, schizophrenia and other thought disorders. Due to the delay in communication and appropriate assistance finding difficulty, the crew should be trained in managing the occurrence of psychiatric disorders (ACTA ASTRONAUTICA- DECEMBER 2012), (Space Psychology and Psychiatry - Kanas, Manzey).
The third quarter phenomenon is a situation that many researchers claim to arise within the crew during the mission. It is described as a form of relief emanated by the crew, because they walked half the mission's distance. Nevertheless, feelings of despair follow, realizing that they still have as much way to go until they are back with their families. Therefore, it is considered a pressuring feeling that can affect the crew negatively (ACTA ASTRONAUTICA- FEBRUARY 2007), (Sandal, Leon, Palinkas- 2006)
Even after the mission's ending and their return to earth, psychological care is necessary for the crew. The necessity arises from the fact that the person has been away from earth too long and definitely needs a period of readjustment to their previous lifestyles. Additionally, many researchers mention that the experience called "view on earth" has caused them considerable changes in their personalities and so, a longer period of time may be required in order to

readjust themselves in their new reality (Kanas, Manzey).

It is considered as necessary by all the mission agencies that there should be a well organized psychological help and normal life retaining module for astronauts and cosmonauts. Protection and stability preservation on the side of the family is of utmost importance and for this reason the Family Support and Pre-flight, in-fight and post-flight modules have been founded. The more assured a crew member is that their family sustains their normal function and stability during their absence, the more productive the members and more focused on their mission goals and duties they will be. For this reason, the three stages of family care should be examined:

Pre-flight support includes the astronaut's psychological training process they are chosen and during their training period. In this stage, many changes are about to happen, both in psychological and financial aspects that are going to affect both the astronauts and their families (Review Report by Chiu-Pih Tan, 2007). Both the astronaut and their family must be updated on how long the astronaut is going to be away for their mission, the possible dangers and the communication choices they have, so that feelings of abandoning are developed. The astronaut should also make certain decisions as far as loss of a person is considered, be it parents of children and whether they would like to be informed of it while in the mission or after it is completed and the mission organizers should be aware of these decisions (Kanas, Manzey).
During in-flight support, predestined communication appointments should exist, as well as package sending or email use. Also, psychological assistance should be provided to the wives and children of the astronauts' as far as psychological and social matters are concerned. It is usually helpful that astronauts convey their unease about how well their family is faring rather than express the amount of pressure they feel.

In post flight support, attention is given in the astronaut's welcoming, as well as bonding again with their families. Socio-psychological help may be still needed then (Kanas, Manzey).

1.6 Leadership and Management

Leadership aspects differ with each mission. An effective leader should be flexible and able to adjust to all kinds of situations. They should have mentoring skills such as: providing direction, information, feedback and encouragement when needed. Respect to the hierarchy should be present at all times and they should be able to manage the workload that needs to be done in a methodic way, while being focused on the most important duties (Space Psychology and Psychiatry, p.181). The process of scheduling and workload should be distributed to the crew in terms of effectiveness but not encumbrance and systematic control can be a helpful tool to the above (Evaluating Human Performance and Advanced Technology Design in Extreme Environments, 2003, p.34). Workload can affect mood, energy levels, stress ad socio-psychological interaction between crew members, so it is important that some variety to duties is existent, leisure time and rest (Holland, 2000).

Space mission researchers and other isolation environments claim that to types of leadership roles are necessary, task role and support role. The one leading the mission should be aware of how to act, depending on the phase the mission is at. During the initial stages, clear orders and direction need to be given and an organization leadership model that focuses on duties and prioritizing is needed. On the contrary, in less energetic periods, like the one when the crew is returning to earth, where the crew members show feelings of loneliness and isolation, support leadership may be the case. Therefore, the main characteristics of which leadership should be comprised are effectiveness, flexibility, condition awareness and adjusted response to these conditions. (Crewmember and Mission Control Personnel Interactions During International Space Station Missions)

1.6 Space travelling familiarizing program for kids through creative activities

The aim of this program is the familiarization of kids with space exploration. Taking for granted that science evolution of a civilization traces its roots in well organized upbringing, we are attempting to prepare the next generation through appropriate methods. We aim for kids' space culture and we use creative methods so that kids and teenagers are interested, so that they embrace space matters. As a result, space discoveries of the next decades will be performed in a much easier way and will also be integrated in our everyday life.

The present plan could be brought to life with its school activity integration in the subject of Environmental Training and it is based on manuals of educative scheduling and operating programs (karyda 2006, 23). The choice of subject and the means to bring it to life can be decided on par with its financial stakeholders.

1.7 Plan of intervention- program Phases

1st Phase

- Program Design
- Subject selection: "The familiarization of kids/teenagers with Space Exploration through art."
- General aims and scopes:

- Cognitive (Badic Astronomy, Human Space discovery History, Stakeholders that promote Space Exploration, Planet Characteristics, Importance of Science, Professions of the Future etc.)
- Emotional (the fact that man has crossed the Earth's boundaries)
- Psychokinetic (team play, planet observation through telescope, educational excursions to planetariums, astronomy towers and museums where they can interact with spaceship emulators- like the one located in the Cosmonaut Museum in Moscow, Russia.)

- Description of Parameters related to the subject (Ecological, Environmental, Political, Cultural, National, Historical, Scientific)

2nd Phase

- Determination of the basic parameters in sections

Section A

Getting to know space exploration through movie material, mass media and the use of NASA and ESA websites.

Section B

Getting to know space exploration via the theater

Role playing games co-ordination and small plays with scientific material in the classroom.

Section C

Getting to know space exploration through music-poetry

Contact with songs that are related to space (like Holst's planets, team poem construction for space and setting to music with hand-made musical instruments made in the class from everyday material like dry fruits, rice and carton boxes).

Section D

Getting to know space through painting

Getting in touch with well-known works of art that depict the mystery of space for man, playing through painting while the students construct small paintings depicting the planet or asteroid that they liked most).

Section E

Getting to know Space exploration through photography

Astronaut photo show, such as cosmonaut Valentin Lebedev, who in his diary, in 1988, informed about ways to keep one's body bosy during his Salyut 7 mission. Photographic activities were included that the cosmonaut planned to show and explain in order to set that experience as a key role in his professional career after returning to Earth

Section F

Getting to know Space exploration through art collage

Collage construction from students, under the subject "How do you imagine your life in space".

The aim is the creation of an artistic exhibition that can include art material created by students and that will be exhibited at the end of the program.

3rd Phase

- Organizing and teaching activities according to previous section- Team making and role distribution. This section is the interactive counterpart of kids being separated into groups of 7, where each team is assigned to travel to a planet in a creative way.
- With the help of the team coordinator, each member decides the role they choose to have inside a spaceship (mission leader, mechanic, communication manager, doctor or psychologist, astronauts, etc).
- The team members with decide how to name their mission.
- The team members must construct their flag.
- The team members must compose the team's hymn.
- The team members must construct their uniform with simple material and fabric and can also construct the cards they will be wearing, depicting the mission name, their name and role.
- The team members need to decide the rules of conduct.
- The team members must make their own crew diary on which they will write about their experience and feelings during the game.
- For their better support, it would be advised to visit libraries so they can find printed material for the planet of their choice, or visit the internet if allowed.

The aim is the creation of a short small play from each team which can be presented by the end of the program.

4th Phase

Students getting in touch with space science through the sections of phase 1 of the program (e.g., Space exploration- Historical review etc). The program methods will include printed and visual material that will be shown to all students, along with visits to be made to space-related stakeholders.

The aim is that students are to be divided to team and choose one of the most popular space missions and make an assignment for the mission's history with paintings and collage, along with its analytical description. The assignment can be presented at the end of the program.

5th Phase

Scientific parameters are to be examined. A presentation of all the science fields that are participating in Space exploration is to be held and analyzed as to how each one evolved.

Each child chooses one of the above sciences in order to create a presentation with images and sound of its choosing at the end of the program to the rest of the participants as a scientist of this field, explaining how life will be in 20 years from now with the help of the chosen scientific field. This phase will hold posters of each assignment at the end of the program.

6th Phase

This phase includes the listing of stakeholders and partners that contributed to the program. Detailed listing of the data of each partner and the object/service that helped the program.

7th Phase

Intervention plan design. Child individual assignment folder creation. Special area for the posters, paintings, diaries and photographic material to be assigned and decorated. Promotion of the event to the community may be possible, where the theatrical plays and the remaining creative material can be presented to parents, schools and other stakeholders. Finally, people from space industry could be present in such an event, such as astronauts, so that kids can interact directly with them.

7. A program based to artificial activities for astronauts

As mentioned at the beginning of the present study, its aim is the preservation of a healthy psychological state among the astronauts that participate in space missions. Other studies show that when the crew has a "meaning of life" attitude, its mental well being can be easily retained, especially in long-term missions. (ACTA ASTRONAUTICA- DECEMBER 2012 p. 590) At this point, it would be useful to mention the salutogenesis phenomenon. According to studies, lots of astronauts are experiencing changes in their conscience and personality, which are positive for their mental health. We refer to health promoting and growth enhancing effects of spaceflight. Salutogenesis is a concept that refers to the ability of a person to develop health-related behaviors that manifest under extreme mental pressure conditions (Sandal, Leon, Palinkas, 2006).
Changes in everyday life, the feeling of satisfaction and personal development, new possibilities, stronger religious beliefs, better understanding for others, development of new interests, better understanding for human relationships, an attitude to handle their own life in a better way, a greater interest for the possibility of life on other planets, creative inspiration, extrasensory experiences interest, like telepathy, better understanding of the earth and its fragility, better understanding of the human species and its unity, are some of the changes that may be experienced and may transform an astronaut's personality, leading them to cope in extreme conditions. The study of these people is meaningful so we can figure out ways of mental enforcement for astronauts and cosmonauts (Ihle, Ritsher, Kanas)

In this context of supporting astronauts, artistic programs could be used for their mental enforcement. The aim of those activities is to help them let off some steam in terms of conflicting situations and their creative resolution through art. This program also functions as a form of communication when someone lacks the skills to do it verbally. Also, it promotes social admittance and teamwork. The correct expression of stressful feelings even by this means serves the timely recognition, analysis and support providing. Some suggestions of artistic activities in space are mentioned below:

- Amateur space photography to support children with special health issues (the photos can be sent to earth in order to be used for financial support of these children. This way, space industry shows its humane aspect to the world.)
- Emailing with children who aspire to be astronauts. (this activity can also be linked to the familiarization program mentioned in the previous section).
- Amateur videos of everyday life in space as a means of educating the next generation. (this activity makes the astronauts understand their contribution to history,

shaping them as better people. Mental protection is ensured from feelings of isolation, loss of meaning of life and depression.)

- With the support of the stakeholders undertaking the space mission, intercultural events can be held, with the participation of musicians and movie shows, in order to help the better understanding of the culture each team member comes from (eg Americans and Russians etc).
- Keeping a journal with the experiences of each day (with the possibility of financial support through publication).
- Painting and card making, which can be sent to earth, family members and as a means of Space Tourism promotion.)

2. CONCLUSION

It appears that the science of space psychology is moving along with the evolution of space technology and that it is supportive to it. The well-organised study of factors that affect life in space, the selection of the most suitable human participants that can cope under extreme mental conditions, as well as the training and support given in an individual, socio-psychological and organization scale pose subjects to be considered by space agencies and industry in the upcoming decades, especially in long-term missions, such as the one programmed to Mars.

3. BIBLIOGRAPHY

1. PSYCHOSOCIAL ISSUES IN SPACE: RESULTS FROM SHUTTLE/MIR
Nick Kanas, Vyacheslav Salnitskiy, Ellen M. Grund, Daniel S. Weiss, Vadim Gushin, Alan Bostrom, Olga Kozerenko, Alexander Sled, and Charles R. Marmar
1Department of Psychiatry, University of California, San Francisco (UCSF), and VA Medical Center, San Francisco CA; 2Institute for Biomedical Problems, Moscow, Russia; 3Department of Social and Behavioral Sciences, UCSF
Gravitational and Space Biology Bulletin 14(2) June 2001

2. Psychology of Space Exploration
Contemporary Research in Historical Perspective
The NASA History Series
National Aeronautics and Space Administration Office of Communications History Program Office
Washington, DC2011
NASA SP-2011-4411
Edited by Douglas A. Vakoch

3. Journey to the Unknown: Human/ Social Science in Antarctica for Outer Space
(GCAS) 2007/ 2008
University of Canterbury
Review Report
By Chiu-Pih Tan
December 2007

4. Mars-105 Study: Time-courses and relationships between coping, defense mechanisms, emotions and depression
Nicolas Sandal Weiss & Yusupova
ARTICLE in JOURNAL OF ENVIRONMENTAL PSYCHOLOGY · DECEMBER 2013
Impact Factor: 2.4 · DOI: 10.1016/j.jenvp.2013.05.001

5. Comparison of Spatiotemporal Adaptive Indicators in Isolated and Confined Teams during the Concordia Stay, Tara Drift and Mars-500
Experiment
Carole Tafforin
Journal of Human Performance in Extreme Environments
Published online: 5-20-2015

6. MICRO-SCALE SOCIAL NETWORK ANALYSIS FOR ULTRA-LONG SPACE FLIGHTS
D. Hennes, K. P. Tuyls, M. A. Neerincx, and G. W. M. Rauterberg
1Eindhoven University of Technology, P.O. Box 513, 5600 MB Eindhoven, The Netherlands
2Delft University of Technology, P.O. Box 5031, 2600 GA Delft, The Netherlands

7. Design for the Psychological Habitability of Spacecraft on Extended Exploratory Missions
Regina Peldszus, Hilary Dalke
Kingston University London, Design Research Centre/ Astronautics & Space Systems Group

8. Mitigating the Negative Effects of Stress in Space Flight: ATransactional Approach
Haydee M. Cuevas
University of Central Florida
Published online: 10-1-2003

9. Flying with Strangers: Postmission Re!ections of Multinational Space Crews
Peter Suedfel, Kasia E. Wilk, Lindi Cassel

10. Entertainment Computing in the Orbit
Matthias Rauterberg, Mark Neerincx, Karl Tuyls, Jack van Loon
1 Eindhoven University of Technology, The Netherlands
2 TNO Human Factors & TU Delft, The Netherlands
3 DESC Space Flight/Microgravity & ACTA Free University Amsterdam, The Netherlands

11. Personality Characteristics and Trait Clusters in Final Stage Astronaut Selection
David M. Musson, Gro. M. Sandal, and Robert. L. Helmreich

12. PSYCHOSOCIAL ISSUES IN LONG-TERM SPACE FLIGHT: OVERVIEW
Lawrence A. Palinkas
Department of Family and Preventative Medicine, University of California, San Diego, La Jolla CA

13. Future perspectives on space psychology: Recommendations on psychosocial and neurobehavioural aspects of human spaceflight
ARTICLE in ACTA ASTRONAUTICA
DECEMBER 2012

14. Crewmember and Mission Control Personnel Interactions During International Space Station Missions
Nick A. Kanas, Vyacheslav P. Salnitskiy, Jennifer E. Boyd, Vadim I. Gushin, Daniel S. Weiss, Stephanie A. Saylor, Olga P. Kozerenko, and Charles R. Marmar

15. Cultural Differences in Crewmembers and Mission Control Personnel During Two Space Station Programs
Jennifer E. Boyd, Nick A. Kanas , Vyacheslav P. Salnitskiy, Vadim I. Gushin, Stephanie A. Saylor, Daniel S. Weiss, and Charles R. Marmar

16. Psychosocial interactions during ISS Missions
ARTICLE in ACTA ASTRONAUTICA
FEBRUARY 2007

17. Psychology of Spaceflight
Albert W. Holland
NASA Johnson Space Center
Journal of Human Performance in Extreme Environments
Volume 5 | Issue 1
Published online: 10-1-2000

18. Positive Psychological Outcomes of Spaceflight: An Empirical Study
Eva C. Ihle, Jennifer B. Ritsher, and Nick Kanas

19. Space Psychology and Psychiatry
Nick Kanas, M.D., Dietrich Manzey, Ph.D.

20. Problems and possibilities of astronauts—Ground communication content analysis validity check
ARTICLE in ACTA ASTRONAUTICA
OCTOBER 2008

21. Evaluating Human Performance and Advanced Technology Design in Extreme Environments
Brill, J. Christopher; Mouloua, Mustapha; Hancock, Peter A.; and Kennedy, Robert S. (2003) "Evaluating Human Performance and Advanced Technology Design in Extreme Environments," *Journal of Human Performance in Extreme Environments*: Vol. 7: Iss. 2, Article 7

22. Human challenges in polar and space environments
G. M. Sandal Z G. R. Leon Z L. Palinkas
Published online: 28 July 2006

23. Design Curriculum - New Trends
Gerogiannis Con., Dr. Sociology, Pedagogical Institute
Bouras Ant., PhD Teaching, University of Peloponnese

24. Spatial Design and activities implementation for environmental school education, health education, culture and artistic competitions.
Karydas Eleni
Publishing P. Kyriakidis, Athens

BENEFITS AND CHALLENGES OF STUDENT DRIVEN SPACE PROJECTS: A SURVEY ON HANDS-ON EDUCATION AT TU BERLIN

Cem Avsar and Klaus Briess

Technische Universität Berlin, Department of Aeronautics and Astronautics, Marchstrasse 12, 10587 Berlin, Germany

ABSTRACT

Engineering education faces many challenge and requirements in the ever changing branch of space engineering. This paper shows observations and analyses made on hands-on projects that have been conducted at TU Berlin. The results can lead to an increase of future projects' efficiency regarding risks, costs, schedule and students learning intensity. Students develop satellites, sounding rockets, planetary rovers and CanSats during their studies and take part in experimental campaigns like e.g. parabola flights. In this academic environment, data and experiences were collected on projects which have been conducted with the involvement of altogether over 200 students.

The paper shows approaches from example project to organizing student driven projects regarding team structures and work models. The main challenges, potentials and lessons learned in university space missions are illustrated from the perspectives of students and academic staff. Projects and students can profit from the high potential of student driven space projects. The hands-on approach in education gives students a unique opportunity for gaining disciplinary knowledge, personal and interpersonal skills and competencies in the areas of conceiving, designing and operating a space system.

Key words: TU Berlin; Space engineering; Hands-on education.

1. INTRODUCTION

Reports show that the number of university class satellites is increasing significantly [1]. New countries are joining the space community every year by launching their own spacecraft. This leads to an increased interest in methods for successfully planning and conducting small satellite missions, but also for educating prospective space engineers. The range of small satellite mission types is manifold, but the missions have in common that hands-on education is either a primary or a secondary objective. The strong involvement of students inherits benefits for all parties, but also challenges that can be critical to a space mission. Faculty of universities newly entering the field of space technologies are facing challenges in projects for which a number of methods and lessons learned have been established over the past ten years.

A plain theoretical approach to learning engineering does not reflect the reality in a curriculum. The disciplinary knowledge, interpersonal skills and engineering skills can only be developed to a professional degree, if students are confronted with practice [2]. Students should be involved in as much as possible real space projects during their studies and gain experience in the whole project life-cylce. To be able to outline a curriculum and set up tailored projects to achieve the goals, the requirements of the main stakeholders should be collected at first.

There is large number of diverse hands-on projects and courses conducted at the Chair of Space Technology. Of course, the environment and opportunities have to be given or created for students to be able to provide a satisfactory learning experience and to create valuable outcomes for research. The experiences gained from the number of projects conducted are a good foundation to analyse good practices in hands-on education.

2. THE CHAIR OF SPACE TECHNOLOGY AT TU BERLIN

The Chair of Space Technology at TU Berlin provides an outstanding environment for staff members and students to perform research and education. It is the first chair of its kind in Germany and was established in 1963. The curriculum has evolved over many decades and has been influenced by the large number of space missions. TU Berlin is amongst the leading universities in terms of the number of satellites in orbit. Already 10 satellites have been launched and currently seven are being developed. The spacecraft missions with their main objectives are displayed in Figure 1.

Although the focal point of research at the chair is to miniaturize components and satellite busses for space applications, the activities range from planning and operations of space missions, developing launch vehicles and planetary rovers to fundamental space technology research. The facilities available at the chair allow staff and

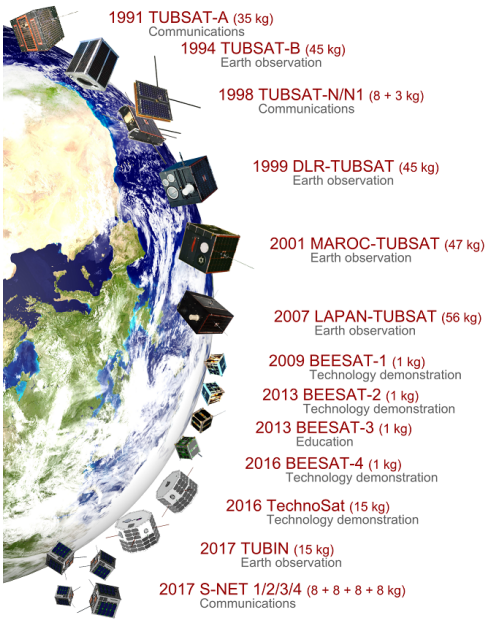


Figure 1. Satellite missions at TU Berlin.

students to work and learn in a professional environment. An impression on the satellite laboratories, the mission control center, the ground station and equipment for qualification and test are given in Figure 2.

The Chair of Space Technology holds two study programs. The German Master's study program in Aerospace Engineering covers a complete curriculum for a Master's degree with specialization in astronautics. In parallel, the international Master of Space Engineering (MSE) program which is taught entirely in English offers a complete 120 ECTS Master's degree. A strong emphasis is given on hands-on experience during the studies. A large portion of the courses are project-oriented and provide projects on mission design, hardware/software development and the participation in national and international space challenges.



Figure 2. Facilities at the Chair of Space Technology.

3. REQUIREMENTS ON SPACE ENGINEERING EDUCATION

The Chair of Space Technology aims to educate prospective space systems engineers who are able to cope with the future challenges in astronautics. To fulfill this objective, the requirements for the curriculum have to be defined. The requirements on educating engineers can be derived from a number of stakeholder groups. These are students, industry, university faculty and society [2].

The term systems engineer has evolved from space flight and describes the application of technical and scientific methods for the system configuration in all phases of a project life-cycle under regard of all constraints.

The leading companies in the space industry have similar views on the function and educational path of a space systems engineer. A systems engineer candidate shall have a broad knowledge in all disciplines of space engineering imparted in a Master's study, about five years of work experience as development engineer in at least two specific disciplines and an additional five years of experience in different positions in the V-logic. Most interestingly, the desired attributes for a graduate are less connected with technical knowledge. Rather a good understanding of engineering fundamentals, system thinking, communications skills, critical thinking and a multi-disciplinary perspective are of more interest.

Surveys on the expected level of proficiency show that the agreement among faculty, industry and alumni are significant. Engineering reasoning, personal attributes, communications and design are consistently the most important skills that should be promoted [2].

4. CHALLENGES OF SPACE ENGINEERING EDUCATION

The main challenges of space engineering education can be divided into general challenges of engineering education and specific challenges related to the field of space engineering.

In general, the learning activities and assessments of them within a curriculum should be aligned with the learning outcomes which the program is intended to deliver [3]. The challenge is to develop an integrated curriculum, that is, to find innovative ways to make double duty of teaching time so that students develop a deeper working knowledge of technical fundamentals while simultaneously learning personal, and interpersonal skills; and product, process, and system building skills [3]. The integrated curriculum is mainly organized around engineering disciplines which are shown to be connected and not isolated.

By integrating a number of hands-on courses, the learning outcomes can be achieved. However, there are limitations which are given either by the complexity and costs of space projects and by students capabilities. For example, planning a space mission in the phases 0, A and B in lecture courses can be achieved with almost no costs. Students are able perform well on an abstract level. Although a Phase C approach would also be possible without expenditures, the level of depth in engineering disciplines like e.g. electronics, mechanics and programming is too high for students. In addition, the space-proven design, verification and launch mostly cannot be fully realized in scope of a student project.

The following requirements are relevant according to [2]:

- Learning outcomes for design-implement experiences need to distinguish between product performance and learning performance.
- The task of the design-implement experience must be sufficiently complex, yet limited in scope, to ensure successful outcomes for students.
- Design-implement experiences require teaching and assessment practices that are different from traditional instruction.
- Few instructors are prepared to assume responsibility for technically challenging projects.
- Design-implement experiences need to be cost-effective.

To be able to perform in a practical project, students should be provided with professional work spaces. These work spaces should provide a flexible and curriculum-oriented environment with space, break-out areas and professional equipment for fabrication of hardware. Of course, the expanded access, safety concerns and maintenance are issues that have to be dealt with by the staff.

5. APPROACHES FOR SPACE ENGINEERING EDUCATION AT TU BERLIN

In both Master's programs at the Chair of Space Technology, a large number of project-oriented lecture courses with a rich variety are offered. The objective is to impart technical knowledge, application of skills in a near-to-reality project and training of interpersonal skills at simultaneously. The experiences are either connected to a certain discipline, interwoven between multiple disciplines or extraordinary and shall be described further.

Problem-based lecture courses at the chair give students a deep insight into a specific field of space engineering. For example, a group project jointly conducted in the lecture courses Space Electronics and Spacecraft Dynamics and Control allow students to apply their knowledge and skills from both disciplines. The goal is to design and develop a system that is able to perform one-axis attitude control on an air-bearing test-bed. The setup for the test-bed and a sun simulator are given to the students. Their objective is to design a complete system consistent of sensors, actuators, electronics, mechanics, software and communications to comply with requirements like e.g. performing a sun-pointing maneuver with certain accuracy in a given time-frame. In groups of five to six students, the students are confronted with several technical and interpersonal problems that they would face in industry projects.

Project-oriented lecture courses allow students to process the entire life-cycle of a space project in one or more semesters. Typical examples are the development and launch of CanSats, CubeSats and sounding rockets. There are a number of challenges lecturers are faced with when conducting a complex project with students. Amongst them are the fluctuation of students over the semesters, diverse capabilities and interest of students and different complexities of the work packages.

Mission design courses usually set a focus on conducting a phase A study for a sophisticated space mission. The mission type can be any current topic interesting for society or faculty and reaches from ocean color imaging and small satellite formation flying to planetary sample return.

Additionally, there are other extraordinary activities for students like sounding rocket experiments, zero gravity experiments or the participation in national and international space challenges.

6. EXAMPLE PROJECTS AT TU BERLIN

For the different types of approaches to hands-on engineering, selected examples of projects conducted at the Chair of Space Technology shall be discussed to outline the main challenges, teaching methods, results and lessons learned.

6.1. SEAR

SEAR (Small Exploration Assistant Rover) shown in Figure 3 is a planetary rover project which has been conducted mainly by integrating students in the development process. The project was initiated in 2013 for participation in the DLR SpaceBot Cup 2013, a national space robotics contest organized by the German Aerospace Center (DLR). The tasks in this contest were autonomous navigation and object manipulation on a terrain with obstacles, acclivities and different surfaces. The contest was conducted on Earth on a large field, but with constraints typical for a space mission like e.g. delayed communication, no direct view and no use of GPS.

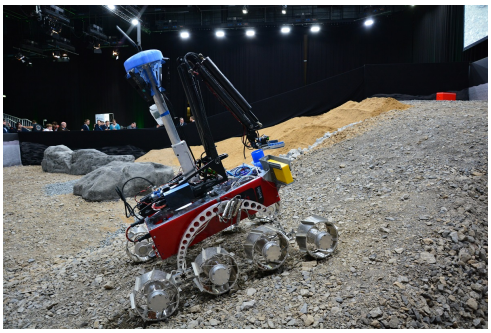


Figure 3. Rover SEAR during transport of two semi-autonomously grasped objects at the DLR SpaceBot Camp 2015.

The funding for the development time of approximately half a year was limited to 50.000 Euros. The funds were used to cover the hardware costs and to employ three student assistants to form a core team. The detailed work was performed by students in project-oriented lecture courses and in theses. In the first course, ca. 20 students have participated in the development. Without background knowledge in the development of complex software for autonomous robots, the students managed to quickly familiarize themselves with the open-source framework ROS (Robot Operating System). Each student was assigned to pre-defined work packages in the areas of mechanics, electronics and software development.

The main challenges in this project can be listed as follows.

- The complexity of developing an autonomous system from scratch without background knowledge and experience.
- Motivating students to continue and share knowledge after they have passed a lecture course.
- Creating awareness of roles and responsibilities in the team for self-dependent work only with little support of staff.
- Creating results at an early stage to avoid high workloads towards the final project stage.
- Creating a continuous work-flow and control mechanisms even during the lecture free periods.

The results of all teams in the DLR SpaceBot Cup 2013 were very much below expectations. Due to the short development time and the lack of focus on providing reliable basic functions, no robotic system was even able to fulfill a fraction of the given tasks. DLR decided to call for a SpaceBot Camp 2015 in which the teams had the opportunity to rework their systems. With the lessons learned from the first attempt and the increased development time, many teams and team SEAR were able to show successfully that they are capable of performing a major portion of the tasks autonomously.

The measures that have been taken to overcome the main challenges were as follows.

- A solid core team of student assistants and experienced students was formed to manage the work from a systems engineering perspective.
- The software framework ROS was a key enabler for easily setting a step into software development. Additional learning videos created by experienced students for upcoming team members simplified the access to certain topics.
- Weekly meetings on the work progress were conducted.
- Students had to write an application to work on a specific work package.
- Initial tasks with a short deadline helped to push the progress in the beginning of the project.
- The students were also motivated by promising them the active participation in the final contest.

The project is a great success for students, the faculty an DLR. Over 50 students have actively participated in the project and had the opportunity to collect practical experiences in a funded research project. The faculty has profited from the students who have gained engineering experience and technical knowledge with participation in the project. Most of the students who worked on SEAR were able to contribute to other projects, e.g. in the development of software for satellite missions. Students in the team valued the experience of the participation in the contest Figure 4 and the contacts made with experts during the time.

6.2. BEESAT-3

In the project BEESAT-3 (Berlin Experimental and Educational Satellite) as seen in Figure 5, a CubeSat mission was developed by students and launched in 2013. The basic idea behind the DLR funded project was to spread the development phases according to the ECSS standards to



Figure 4. Team SEAR during the qualification for the SpaceBot Camp 2015.

a number of semesters. A phase A study was conducted in one semester, a phase B in the second and so on. The main challenges were basically similar to the challenges listed for project SEAR. In addition, the aspect of developing a spacecraft to be qualified and launched into orbit inherited some difficulties.

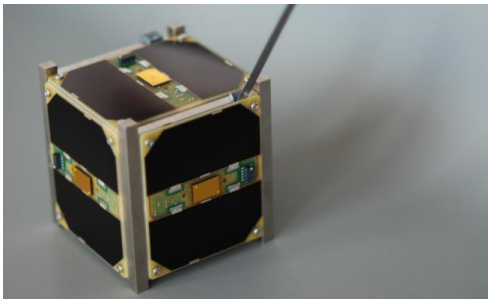


Figure 5. Flight model of Berlin Experimental and Educational Satellite 3.

The experiences made in the first two semester, conducting Phase A/B studies, were quite satisfying. In the third semester, when it was envisaged to start with the detailed design, it was discovered that the progress in most work packages did not exceed beyond the level of detail conducted in the Phase B study. Many students did not have the skills to either design mechanical, electrical or software components of a real satellite within a short time-frame, even though the requirements have been downgraded compared to research satellite missions at the chair.

To push the progress in the project, some countermeasures were taken. These included setting up a small core group of staff and outstanding students to execute and coordinate the works on the satellite. Students with special skills were involved by giving out theses on certain aspects of the satellite mission like e.g. printed-circuit-board design, software development and structural design. In the further lecture courses, the focus was set on higher-level aspects of the mission like e.g. mission operations scenarios.

6.3. DECAN

In the project DECAN, a two-staged sounding rocket for CanSat ejection is developed by students over a number of semesters. The rocket shall be launched in Kiruna to altitudes above 10 km. Compared with the project SEAR and BEESAT-3, additional challenges are linked with safety, since solid propellant is being used. Each semester, students have the opportunity to work on certain aspects of the rocket. Each stage consists of elements to be designed and manufactured. A great emphasis is given on testing parts seperately. For example, newly developed electronics are tested by launching them on smaller rockets and rocket motors are burned in testing facilities.

The project has been a great success for students and faculty for many semesters. Students are facing the challenges of developing a real rocket and the setbacks that naturally come with it. This experience is of great value and some graduates working on rockets like e.g. the Ariane appreciate the opportunities that they were provided with during their studies. Figure 6 shows the launch of a DECAN rocket in Kiruna.



Figure 6. Launch of DECAN-SHARK I in Kiruna.

6.4. CanSats

Even though hardware and software has to be developed in CanSat projects that are conducted in hands-on lecture courses, the activities at TU Berlin set less focus on the technical development, rather than undergoing the whole project life-cycle of a space mission in a singular semester. There are a number of sophisticated CanSat missions that range from collecting telemetry to fly-back which have been conducted as seen in Figure 7. Over a period of three months, students in groups of five to six

have to plan and execute each phase of the project life cycle, starting from A (Feasibilty) to F (Disposal). Each phase is closed-out by a review that is held before faculty staff.

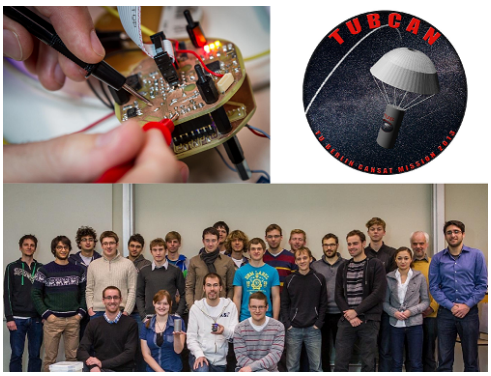


Figure 7. Student group with CanSats.

The challenge for the self-organized student groups lie in the planning and interpersonal communication. The technical aspects are demanding with respect to the short development time, but they are not too complex when comparing them with the technical aspects of real spacecraft.

The costs for conducting CanSat missions are comparably low and no funding is necessary. The ratio of benefits with respect to effort and costs is the largest when comparing CanSat projects with projects like e.g. SEAR, BEESAT-3 and DECAN. However, the CanSat projects cannot reflect certain aspects of real space missions, e.g. verification and space-proven design.

6.5. Attitude control project

Some hands-on projects at TU Berlin focus on certain engineering disciplines. For example, a joint project between the lecture courses Space Electronics and Spacecraft Dynamics and Control is conducted to impart skills in both fields. The goal is to design and develop a system that is able to perform one-axis attitude control on an air-bearing test-bed. The setup for the test-bed and a sun simulator are given to the students. Their objective is to design a complete system consistent of sensors, actuators, electronics, mechanics, software and communications to comply with requirements like e.g. performing a sun-pointing maneuver with certain accuracy in a given time-frame. In groups of five to six students, the students are confronted with several technical and interpersonal problems that they would face in industry projects.

Besides developing a system from scratch within a group whereat facing interpersonal challenges, the students have to design a sophisticated electrical system and algorithms for attitude control. The main challenges for the staff are to harmonize the lecture courses in terms of contents and time schedule and to give students some time to spend on the project. The specific learning outcomes are satisfying for students and even staff can profit from these types of projects. For example, new components for attitude determination or actuation developed at the chair are provided to the students and tested by them. The feedback is valuable for the advancement of the technologies and students feel that they are involved in real research activities, rather than just dealing with a fictional task.

6.6. DEPLiX

Another pillar of educational activities is based on Phase A studies conducted in context of real space missions. One example is DEPLiX, a German-Polish satellite formation flying mission that was envisaged in 2012. Before proposals for funding are being prepared, the key parameters of a mission have to be outlined in good detail. Basically, each proposal for a space mission contains a phase A study. Student groups in lecture courses have found to be a very good source for conducting such studies. Students are motivated when their results are used for research and staff profits from the detailed analyses conducted by the students. The main challenges for lecturers lie in steering the developments in the right direction, ensuring a good quality of the documentation and in scheduling the activities synchronous to the faculty's time schedule.

6.7. TUPEX

The TUPEX (TU Berlin Pico- and Nanosatellite Experiments) series inherits outstanding activities for students and shall also be mentioned here. Many components in TU Berlins satellite fleet are developed in-house with the help of students. Space components development involves extensive functional and environmental verication processes. In the TUPEX series, students have the chance to participate in a sounding rocket campaign to test novel miniaturized components.

The REXUS/BEXUS program allows students from Europe to y an experimental payload on a high altitude balloon or a sounding rocket. It is sponsored by the German Aerospace Center (DLR) and the Swedish National Space Board (SNB) in collaboration with the European Space Agency (ESA). TU Berlin participated three times in a sounding rocket campaign with diverse experiments. Other space-related experiments involve ights in reduced gravity aircraft. These kinds of activities address fewer students than mission design courses, but the intense education provided to a handful of students in conducting a real experiment, reects in a very deep practical knowledge and experience at the end. In most cases, the students write their theses about the related project, since a sounding rocket campaign runs over a period of approximately one and a half years. [4]



Figure 8. Students preparing a zero gravity experiment.

6.8. Conclusion

In conclusion, projects and students profit from the high potential of student driven space projects. The hands-on approach in education gives students a unique opportunity for gaining disciplinary knowledge, personal and interpersonal skills and competencies in the areas of conceiving, designing and operating a space system. Surveys on student satisfaction and impacts on career confirm the positive effect compared to a theoretically driven learning approach. Alumni especially highlight that they appreciate the experience of presenting in front of many review boards during their studies, which gives them an outstanding appearance compared to their competitors.

From the projects perspective, high challenges and risks arise due to the study constraints, e.g. leading to a strong fluctuation in the team structure over the semesters. Results far beyond expectations can be achieved though by implementing a tailored organizational structure for a student driven project, based on proven methodologies.

ACKNOWLEDGMENTS

Special thanks go to the German Aerospace Center for initiating and promoting space projects that are paying a major contribution to high quality hands-on education at the Chair of Space Technology for several years now. Thanks go to the project leaders and lecturers who are passionate about uniting research and educational activities. Thanks go also to the dedicated students who have spent long nights working on projects at our chair.

REFERENCES

[1] Swartwout M., Attack of the cubesat: A statistical look, in Proceedings of the 25th Annual AIAA/USU Conference on Small Satellites, Logan, UT, USA, August 2011

[2] Crawley E. F., et al., Rethinking Engineering Education, 2014, Springer-

[3] Goodhew P., Teaching Engineering, 2015, Royal Academy of Engineering

[4] Avsar C., et al., Journal of Automation, Mobile Robotics & Intelligent Systems, 2014, Vol 8, No 1

ZERO ROBOTICS: A LAUNCHING RAMP FOR HIGH SCHOOL STUDENTS TO STEM UNIVERSITY FACULTIES

Renato Macchietto Pinotto
LICEO SCIENTIFICO STATALE "E.FERMI", C.SO V.EMANUELE II, 50 - 35123 PADOVA (ITALY)),
Email: r.macchietto@alice.it

ABSTRACT

The Zero Robotics High School competition (from now on ZR) is focused on programming and driving SPHERES in a zero gravity environment. The SPHERES (Synchronized Position Hold Engage and Reorient Experimental Satellite) are small satellites inside the ISS that NASA and MIT's scientists use to study the possibilities of robots' self-organization in a practical and economical manner. In the near future robot satellites will be used in space activities such as maintenance activities and/or recovery of disused satellites or their parts, space debris collection, preparation of large-scale experiments[1]. MIT and NASA give high school students the opportunity of working with these SPHERES and face with real space challenges[2]. Some teams of Liceo Scientifico "E.Fermi", Padova, have participated since 2010, reaching excellent results (two first places and one second place in the European finals). Our school experience shows that such activities help students to convalidate their choice of University career path in science faculties.

1. THE ZERO ROBOTICS CHALLENGE

SPHERES (Fig.1) are sphere-shaped mini robots equipped with twelve carbon dioxide thrusters for autonomous propulsion that allow precise manoeuvring in the zero gravity environment; an ultrasound

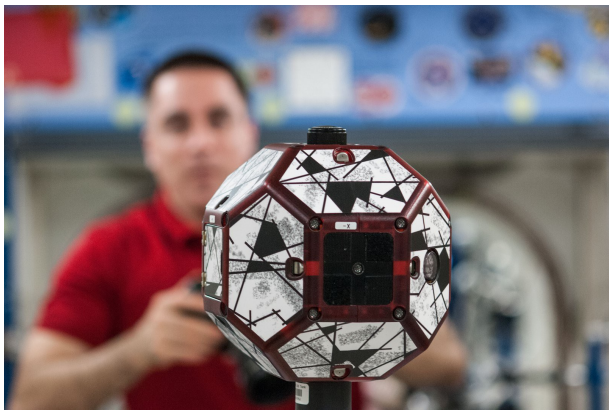


Figure 1. Chris Cassidy with a SPHERE (Aug. 2013)

system to collect kinetic data from the beacons installed in the test area inside the ISS' Japanese module wich is activated periodically by the SPHERES by means of an infrared impulse; a wireless link to a laptop that controls the SPHERES' processor[3].

Since 2009 MIT organises a competition where two SPHERES face in a defined virtual scenario, with set objectives to be achieved within definite time and space limits (time = 180s; space = 1.3m x 1.6m x 1.3m). The SPHERES are guided by a code that students can develop in C ++ language on an IDE platform provided by MIT, using the API set prepared for the game by MIT's ZR staff (composed itself mainly of students of Astronautics).

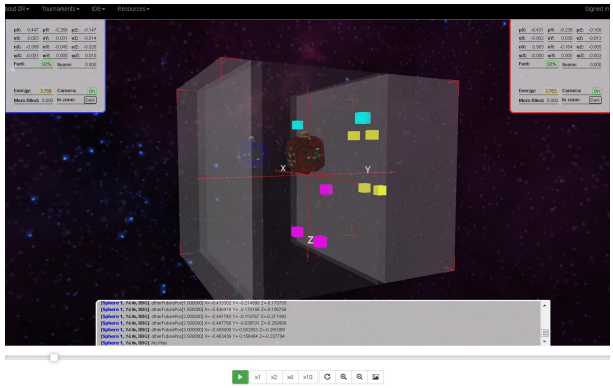


Figure 2. Virtual playground on MIT web platform

The race, originally aimed at the US teams, is rapidly expanding all over the world (in 2010 towards European nations affiliated to ESA, last year to Russian teams and this year to the Australians). The tournament runs from September to December with monthly selection stages and, until the first week of December, it takes place in a simulated environment (Fig. 2). Only the 14 best codes will actually be installed on the true SPHERES on the ISS, in January, where they will play in a final mini-tournament under the supervision of the astronauts-referees (Fig.3-4).

The educational aim of the competition is to involve as many students as possible to face and solve problems with unconventional methods typical of scientific research and encourage an informed and positive attitude towards space activities. Teams are formed of 3 to 20 students, led by a teacher-mentor. Matches are played daily in a win/lose format and the leader board is updated according to the Whole-History Rating (WHR) method, a method to estimate the time-varying strengths

when many players are involved in paired encounters.



Figure 3. Astronaut Samantha Cristoforetti as referee of ZR challenge (Jan. 2015) with two SPHERES

After an initial phase in which they play individually, teams must continue regrouping in international alliances of three teams each (not all from the same continent or country) encouraging cooperation between teams from different countries while maintaining a high number of students involved. The teams that do not pass the selections are still invited to continue in a parallel simulation challenge.

2. ZR IMPACT ON STUDENTS' UNIVERSITY CHOICES

The challenge is exciting both for students and for teachers, but the reason why it takes a special role for the students' University choices is that it requires working abilities similar to real scientific research. It develops skills not only suited to completing a specific task, but also excellent in facilitating coordination required to achieve the objectives.
In particular, we can recognize:
- teamwork, with task sharing and cooperation capabilities;
- ability to collaborate and provide mutual support between teams in the game (by means of the dedicated forum, for example), but at the same time to maintain a certain degree of competitiveness. The aspect of competition between teams, nations, continents is naturally present, but always in an environment that encourages collaboration.
- coordination and work with foreign groups, in final alliances;
- technical skills of different kinds : mathematics, physics, programming, communication in English;
- problem solving skills;
- ability to adapt to changes (e.g. of the rules of the game; of new opponent strategy to face with);
- ability to face with unexpected events and to consider the troubles of life as a part of the problem (server downtime, class assignments; sickness; computer malfunctions) without forgetting the objectives;
- ability to work with the ZR staff to manage the structure of the game itself (e.g. bug reports; propose changes to game rules)
- the need to choose between different options;
- ability to meet deadlines.

With these characteristics (technical, strategic, organizational, communicational) the activity appears to be already a high-level approach to scientific research. Students learn to lose the suspicion typical of the teacher-student relationship to take a problem-oriented approach where the aspect of cooperation becomes primary. They do suffer from some stress, but appreciate the dynamism and the overall cultural quality. Even the teachers' search for funds to attend the live-transmitted finals at MIT in Boston, USA, or at ESA-ESTEC in Noordwijk, Netherlands, is a very similar problem to that of University research groups!). The result is a positive attitude towards scientific research in general, and space becomes a much more familiar environment.
Although our school's students are already oriented to a scientific career, their choices are often aimed at more common faculties or those considered to be the most reliable for future employment. The so-called "hard" science faculties or the more specialized engineering courses, such as Aerospace Engineering, are still regarded with some suspicion. But in the case of students attending excellence activities, like the Zero Robotics challenge, this attitude is very much softened. If once we did not have students choosing Aerospace Engineering, in recent years students with ZR experience have started to choose it. Furthermore, other students in the school, perhaps following their mates engaged in this activity, have changed their attitude and now consider this choice as a viable option.

Tab.1 University faculty attended by ex-Zero Robotics students (since 2011)

	Faculties							
	Engineering				**Math**	**Physics**	**others**	**Tot**
students	Aerospace	Mech	IT	others				
attending Master courses on	1	1	1	2	-	-	-	**5**
attending Bachelor courses on	2	1	3	2	4	2	2	**16**
Tot	**3**	**2**	**4**	**4**	**4**	**2**	**2**	**21**

3. WHAT STUDENTS SAY

As seen in Table 1, the choices of students engaged in the ZR project are strongly characterized: a significant percentage of students (3/21) has chosen the Aerospace specialization; some of them were convinced to choose it just as a result of their participation in the ZR competition.

Here follow some significant statement. Giacomo Scomparin (3rd year Bachelor degree in Aerospace Engineering, Padova Univ.) said: *"Zero Robotics was really a great experience for me. It gave me an idea of what working in a team means and made me think in a different way about mathematics, physics and programming, since I had the opportunity to apply them to real-world problems. After the challenge I was 100% sure that I wanted to work in the space field"* and Giacomo Mingardo (1st year of Master in Science Aerospace Engineering at TU, Delft): *"ZR has been the starting point to choose Aerospace Engineering, from which I then achieved my current specialization in Flight Performance and Propulsion"*.

Even students who have chosen other specializations maintained special attention to space activities. Isabel Naranjo De Candido (1st year Master in Mechanical Engineering, Pisa Univ.) attended a summer internship at JPL; she said *"Zero Robotics has been a great opportunity for me. It made me become fascinated with space exploration history and current space programs. It has been very interesting because it was about putting together some maths and programming knowledge with soft skills like game theory and smart reasoning. [...] This summer I had an internship at Jet Propulsion Laboratory that made me confirm the interest in space and engineering research, started with the Zero Robotics experience"*. Stefano Fogarollo (2nd year of Bachelor degree in Information Engineering, Padova Univ.) is a member of the Padova University Morpheus Team whose task is to build a fully functional rover[4].

But this experience changed the way of thinking also of many students who have made different choices: Izat Baybusinov (3rd year of Bachelor Degree in Physics, Università La Sapienza, Rome): *"Exciting experience. It got me in contact with the difficulties of space exploration and changed my view on applied maths and physics"*; Silvio Galesso (1st year Master in Computer Science Engineering): *"It was an exciting experience, which involved challenges from many technical and scientific fields, and showed us a superb MIT's software project"*; Emilio Corso (1st year Master in Mathematiques Fondamentales, Université Paris 13, Institut Galiléè): *"It was surely the most challenging and exciting teamwork experience I had in my life. It played a decisive role in my following decision to pursue a scientific career"*.

Therefore the major impact of this high-school activity on these students' University choices cannot be denied.

4. ZR IMPACT ON LINKS BETWEEN OUR HIGH SCHOOL AND UNIVERSITY.

Thanks to the four-year experience of Zero Robotics, many students and teachers were convinced to take part in different robotic competitions. For example, this year we have 3 teams involved in the 2015 Zero Robotics challenge and last May another team of our students won the first prize (awarded with a 60cm tall humanoid robot called NAO) at the NAO Italian Challenge 2015. At present, this group of students is involved in a University project for the use of the NAO robot in pediatrics for the assistance of young children waiting for major operations, or just after them, during the convalescence period[5]. This project with NAO robots has also been noted by Microsoft, and the CEO Satya Nadella himself wanted to meet these guys, hobnobbing with them for several minutes at the Microsoft meeting *"Future Decoded"* (Rome, November 2015)[6].

With ZR and NAO activities on robotic control, in two years our students have been selected to participate in the *Maker Faire*, Rome, the biggest fair of innovation in Europe.



Figure 4. A final match running on ISS under surveillance of Samantha Cristoforetti, Elena Serova e Barry Wilmore (Jan 2015)

5. THE NEXT STEPS?

If five years ago there were only one teacher and a dozen of kids, now there are 5 teachers and about 40 students of Liceo "Fermi" involved in these activities. Robotics is entering more and more into the education, projects and programs of many schools. But we are convinced that it is also particularly suitable as a linking field between high school activities and University research, and we believe that it is possible to find many collaboration areas, maybe also among some of those proposed in this Symposium. We are thinking, for example, about the possibility to collaborate on data collection and analysis, simulation, construction of small mechanical and electronic equipment.

For this purpose it would be useful to have a more precise dissemination of this sort of University activity in schools, providing detailed information on the work that could be done by the students together with their teachers or tutors, as it was at the beginning of our ZR experience, in 2010, when we were contacted by Prof. Enrico Lorenzini (at that time responsible for P.H.D. courses in Aerospace Engineering, University of Padova, Italy). Prof. Lorenzini and Prof. Leonardo Reyneri (Electronic Department, Politecnico di Torino, Italy) had accepted a MIT invitation to seek Italian and other European high school teams to be entered in

competition. Lorenzini and his staff then provided ussome first infos and hints on how to approach the SPHERES programming and how to manage the web platform, putting the formed teams in a condition to go ahead autonomously. Now the Italian ZR organization is entrusted to a Guidance Committee chaired by prof. Reyneri (and composed of Politecnico di Torino, Università degli Studi di Padova, Istituto Italiano di Tecnologia IIT@POLITO, Rete Robotica a Scuola, Ufficio Scolastico Regionale per il Piemonte, Agenzia Spaziale Italiana) and involve many Italian schools, so that the number of Italian teams in the competition is the highest, after that of the US, and require a pre-selection to meet the limit of 25 teams for each European country. Furthermore, since 2014, there is also an Italian Zero Robotics challenge for those teams that didn't qualify to the international competition. In four years, Italian teams reached excellent results (always at first place) and the number of players, and their quality, is growing year by year.

For those reasons ZR may be considered a model of a really working collaboration between University and High School. Of course, the planning of these educational activities should be developed with the involvement of some interested teachers and would require a minimum of dedicated resources.

6. CONCLUSIONS

The Liceo Scientifico "Enrico Fermi" experience in the field of robot control in a space environment suggests that a better connection between high school and University research projects could be extremely useful in order to spread among high-school students an interest for high-level scientific topics and drive the students' choices towards "hard" science faculties and eventually produce a targeted selection of the experts of tomorrow.

References:

[1] The history of SPHERES
http://www.nasa.gov/spheres/history.html

[2] MIT's website for Zero Robotics:
http://zerorobotics.mit.edu/

[3] Main SPHERES characteristics and complete list of articles on SPHERES on
http://www.nasa.gov/spheres/satellites.html.
Other technical info on http://ssl.mit.edu/spheres/

[4] Website of Morpheus Project:
http://roverunipd.wix.com/morpheusteam

[5] Roberto Mancin (Servizi Informatici del Centro d'Ateneo di Ricerca e Servizi per la Disabilità, la Riabilitazione e l'Integrazione, University of Padova), "Baby-Goldrake@pediatria.unipd.it: a study about Pediatric Robots (Social & Educational Robots)" , https://www.facebook.com/notes/10155605655715444/, 2015.

[6] Experience and informations reported on fb pages of Liceo Fermi team:
https://www.facebook.com/Nao-BabyGoldrake-Liceo-Fermi-Padova-768153083220918/?fref=nf

(last websites visit, Nov 28, 2015)

A study and approach to use regolith for 3D printing in microgravity environment.

Avishek Ghosh [(1)], Jean Jacques Favier [(2)]

[(1)]International Space University, 1 Rue Jean-Dominique Cassini, 67400 Illkirch-Graffenstaden, France. Email:avishek.ghosh@community.isunet.edu
[(2)]International Space University, 1 Rue Jean-Dominique Cassini, 67400 Illkirch-Graffenstaden, France, Email: jean-jacques.favier@isunet.edu

ABSTRACT

Man has not walked on the lunar surface since 1972 but has the dream to return lives. Efforts are being made to return to the moon within the next few decades but with much longer duration than any manned mission planned ever. For that reason, extensive research to build habitable architectures are necessary, logistically using natural resources (*IN-SITU*) available on the lunar surface and with the help of additive manufacturing technology. Future manned missions to the moon will require the capacity to assemble structures utilizing the moon's *IN-SITU* resources. Geoploymer is a development material that comprises of up to 98% lunar regolith, radically decreasing the measure of material that must be transferred from the Earth in the occasion of lunar development.

This paper investigates the conceptual design and feasibility study of using 3D printer for building habitat for astronauts on the lunar surface. In the initial phase of the study, the mechanical behavior and chemical properties of regolith simulant (JSC-1) and terrestrial regolith were assessed with respect to structural strength, and bonding of layers under gravitational environment. The preliminary stage of this experiment is to determine a perfect ratio or proportion to combine the materials in order to achieve a good Regolith polymer. According to NASA Kennedy Space Centre, it is possible to stabilize regolith by mixing with granular minerals with polymers, clays, sulfur and low melting point metals such as fusible alloy which can reduce the required temperature. It is assumed that the combination of 50% Regolith, 20% Sulphur, 20% Silicon dust, 10% White Cement could reduce the melting temperature, however it would be challenging to melt the entire mixed materials or regolith but if a certain portion of mixture is melt down then the paste product would be worthy enough to print structures. The combined compound of Sulphur and silicon will melt down and compensate to the whole mixture to crate additive bond throughout the whole system.

At present situation, it is necessary to reinvent the technique or pursue applications considerably different than the applications of general 3D manufacturing techniques in industry. It is interesting to find out how this technology can enhance ability to create a unique device which is capable of printing instrument and components to be useful for operating in space. Many space organizations like NASA, ESA and Private Companies are involved developing new concepts of robotic arm 3D printing techniques for space applications into the final frontier.

1. INTRODUCTION

Thus, we need to go to the Moon. Why? Since the Moon is a nearest place in space to accumulate suitable resources outside of the Earth's gravitational field. From the Moon we can send missions into deep space and transport materials for settlement on Mars. For whatever reason, to keep up a vicinity, assembling a base on this little dusty neighbor, is significant. In any case, where might we live? How would we be able to get by on this unfriendly scene? This is the place where basic architects will venture in, to plan and construct, the greatest natural surroundings ever considered. This investigation mission includes establishing a maintained human neighborhood on the Moon, an expansive mission that will oblige various controls to make advancements, considering contemporary issues and forecast new ones. One issue that has been distinguished from the past Apollo missions is the issue of dust relief to secure individuals. This paper portrays examinations of 3D printing techniques for balancing out the lunar regolith for dust moderation and paving the lunar surface acting as a preventive factor for human, materials and equipment from dust effects. The physical 3D printing innovation has created whole structures of visualizing an object practically, heading towards the future space exploration, The modern group is working on feasibilities that lunar resources are comparatively be utilized to construct a lunar living space. According to NASA, 3D printing offers a potential method for encouraging lunar settlement with decreased logistics from Earth. The new conceivable outcomes

from this work then can be considered by global space offices as a major aspect of the present improvement of a typical investigation system. Kept an eye on missions to Mars take up a considerable measure of the spotlight seeing that colonization endeavors are concerned, so it about time a few center is gone for the progressing and set up ideas for colonization of the Moon. We presently have a method for arriving and our innovation is adequately exceptional to maintain life in space, the following step is to start building habitat using IN-SITU resourses. At this initial stage of building a base on lunar surface, we take a glance at the prompt issues confronting architects when arranging territories on a lunar surface. In spite of the fact that this is an oversimplification of the amortization of Apollo programs' costs, it gives us to an extent appraisal for the expense of lunar surface investigation. Understanding these costs can enhance lunar investigation. The preceding thought of Moon colonization began far prior to the period of real space investigation, as the Moon is Earth's common outpost. Recent discoveries of extensive measures of *IN-SITU* resources on lunar surface as well as the need to upgrade space investigation for the resources usability makes this opportunity more concrete and engaging. However the foundation of a kept an eye on human settlement on the Moon will require some type of framework to protect the space travelers and logical instrumentation from an extremely challenging environment. As mankind hopes to come back to the Moon in a more managed way, lunar surface investigation frameworks will need to develop from a framework intended for transient forays to a more adaptable framework equipped for investigating more extensive ranges for more lengths of time. The theoretical outline introduced in this paper is situated inside of the connection of the up and coming era of lunar investigation.

2. OBJECTIVES

Initially, when the toolroom method of manufacturing come in the scenario, the domain of machining represents a commonly subtractive method of manufacturing such as filing and turning through milling and grinding process. In Additive manufacturing process most primitive applications have been on the toolroom end of the manufacturing scale. For example, the purpose of additive manufacturing is one of the earliest alternatives and its operation is implemented to reduce the time and cost to develop prototypes of different parts and devices. It was earlier done with slowly and expensive subtractive toolroom methods. However, the time lapse has brought us in a new frontier with the help continually technological advancement. Additive manufacturing methods are affecting further into the production end of manufacturing. In recent years, there is a growing interest in rapid prototyping technologies in the space industry for their vision to build habitat on moon with *IN–SITU* resources on lunar surface. A few 3D printing innovations and technologies have the capability to utilize sand or dust materials to print structures. This feature is especially attractive for the space industry for manned space exploration. A general study program by National Aeronautics and Space Administration (NASA) suggests 3D printing technology as a potential method to fabricate natural resources to construct habitat on the Moon utilizing lunar regolith. The main objective of this investigative inspection is to show that structures could be assembled utilizing *IN-SITU* resources. For example, the regolith soil that are normally found on planetary surfaces e.g. Earth's Moon. Although it is considerable that difficulties still exists in regards to the formation of a material with satisfactory and repeatable properties for the development of structures under the vacuum and microgravity. However it is the promising begin that scaling of the structures could be delivered in a bigger size. The issues experienced have been recognized and the researchers at NASA Kennedy Space Center is effectively looking for arrangements with collaborators from NASA Marshall Space Flight Center, the University of Southern California and the Pacific International Space Center for Exploration System (PISCES). The objective is to make extensively bigger and complex structures, of numerous types, on lunar surface that are suitable for protecting human and automated equipment.

3. EXPERIMENTAL PLAN

The purpose of this experiment is to investigate the feasibility of using regolith in 3D printing technology for building "Lunar Habitat" for astronauts on the lunar surface. In addition to a "Lunar Habitat", this regolith-3D printing technology can be used to build other lunar outpost structures, storage facilities, paving the ground etc. Using the local resources will dramatically simplify such a lunar mission, reducing the overall costs, time between Earth-resupply, and complexity of launching a large amount of mass.

3.1 Method and approach

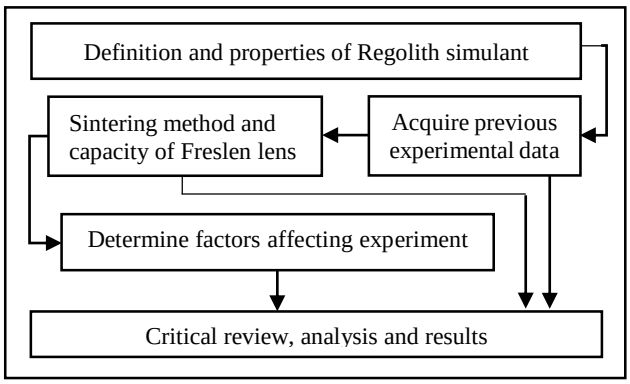


Figure 1: Flow diagram of methodical approach

Regolith is a terrestrial term, likewise utilized for the Moon. It is naturally made out of a few components and mixes in differing fixations. The carbon, hydrogen, and nitrogen found in the dirt are completely dry because of implantation by the sun powered winds. Lunar Regolith is not at all like most Earth soils *(see table 1),* the lunar soil has high convergences of Sulphur, iron, magnesium, manganese, calcium, and nickel. A significant number of these components are found in oxides, for example, FeO, MnO, MgO etc. even Ilmenite (FeTiO3) are the best source of in-situ oxygen.

Grain Size (mm)	**%Weight**
10 - 4	1.67
4 – 0.5	9.6
0.5 - 0.090	27.45
0.090 - 0.020	34.43
less than 0.020	26.85

Table 1: Lunar dust composition

Numerous space research organizations are continuing experiment with the regolith material to find better solution. As the regolith and a large portion of the lunar material melts in high-temperature (1100°C) and could be utilized as a part of glassmaking. Most Lunar materials melt at temperatures over 1100°C. The cooling rate additionally focus precious stone size. Slower cooling rate conveys bigger precious stones keeping in mind the end goal to continue with lunar base development. A unique lunar regolith simulant has additionally been created, which precisely imitates the qualities of the actual regolith. Significantly lunar simulant (JSC-1A) is considered as construction materials in this experiment for their mechanical behavior and properties.



Figure 2: Regolith simulant (JSC-1), NASA

The regolith simulant (JSC-1) (*see figure 2*) is a mixture or blend of silicon, aluminum, calcium, iron and magnesium oxides. Intended to imitate the properties of the Regolith found on the moon, the fine material had a molecular structure looking like that of earthenware production. The substances, such as oxides of silicon, aluminum, calcium, iron and magnesium are added to produce the artificial moon dust. In any case, this innovation is still in its original stage. 3D printers that process lunar Regolith could save money on resupply costs for a kept an eye on base on the moon, which NASA apparently been considering as a conceivable door to destinations more remote in space. The lunar regolith simulant was the same material used in NASA's Lunar Regolith Centennial Challenge. Exploration needed to discover an answer to use this regolith found on non-physical surfaces reinforce it by blending with material dust such as silicon, sulphur, and white cements in an extent so that it could be utilized as a building material. An examination done by KSC on chose laser heating using an infrared laser as the most noticeable system to convey sufficient amount of energy into a little quantities that will allow granular regolith components to fuse together.

Organization	**Method and material**	**Result**
Planetary Geosciences Institute, University of Tennessee	Microwave (2.4 Ghz) sintering on JSC-1A with Titanium dust (Ti)	Rapid heating rate (1750 ° C/) and faster diffusion rate. Glass formed in regolith mixture
Washington State University (WSU)	Laser (50 Watt) applied on moon rock simulant (JSC-1AC)	Melted like wax and printed solid objects.

Table 2: Experimental data on regolith simulant

3.2 Sun based sintering

Sintering is a strategy in which free particles are warmed, yet not completely melted, until they attach together and form a resilient structure. The microwave sintering is apparently useful to create microstructures and blocks for habitat. Sintering is the process by which dust granules are transformed into cognizant solids at temperatures below their melting point. During this process, the powder particles are fused together by softening with the help of certain temperature and following to addition of some mechanical quality. It actually brings density in the mixture and turns into processed solid. Sun based sintering is the method to process sun beam energy through lens and spot on a particular region. The special lens called Fresnel lens, which has this capability to concentrate the energy covered by large area then concentrate and focus on a single point. In this entire process, a sun based concentrator is applied to use energy and heat for melting the dust and powdery grains. The shape changing phenomena observed at interspace

among the sintering particles. There are two stages of sintering, the local bonding stage between adjacent particles, and a pore rounding following to shrinkage stage.

We are living in a world where space exploration is increasingly concerned with queries of energy production and shortage of raw material, this project explores the potential of manufacturing in abundance of nuclear or chemical energy and material. In this experiment, sunlight and regolith simulant (JSC-1) are used as raw energy and material to print objects using a 3D printing process which includes a large size freslen lens which acquires natural sun energy. Solar-sintering aims to rise potential in future space exploration in aspect of 'outer space' manufacturing with full utilization of IN-SITU resources with the most efficient energy resource - the sun. In order to find the definitive answer, this experiment aims to provide a point of initial stage of further space exploration. There are several factors associated with sun based sintering (See Table 3).

Parameters	Conditions	Outcomes
Temperature & Time	The higher the sintering temperature, reduces the sintering time.	Common sintering conditions are: 15 - 30 min at 1050 ℃ – 1250 ℃
Geometrical Structure of Dust particle	Fine dust grains are more difficult to sinter than coarse powder.	The size of the particles considered in commercial iron powders for printing structural parts are usually ≤ 150 μm
Composition of the mixture	For two different powders, alloying takes place simultaneously in the process.	Alloying process of copper and iron mixture could be accelerated by forming liquid phase in the mixture.

Table 3: Factors affecting sun based sintering

3.3 Solar Concentrator: Fresnel lens

A Fresnel lens is an optical module which has refractive capabilities designed with some surface curvature or concentering rings. It has this capability to concentrate the energy covered by large are and focusing the concentrated energy into a single point. The Fresnel lens used in this experiment can focus sunlight transforming it to a beam, creating temperatures between 1400 ℃ to 1600 ℃

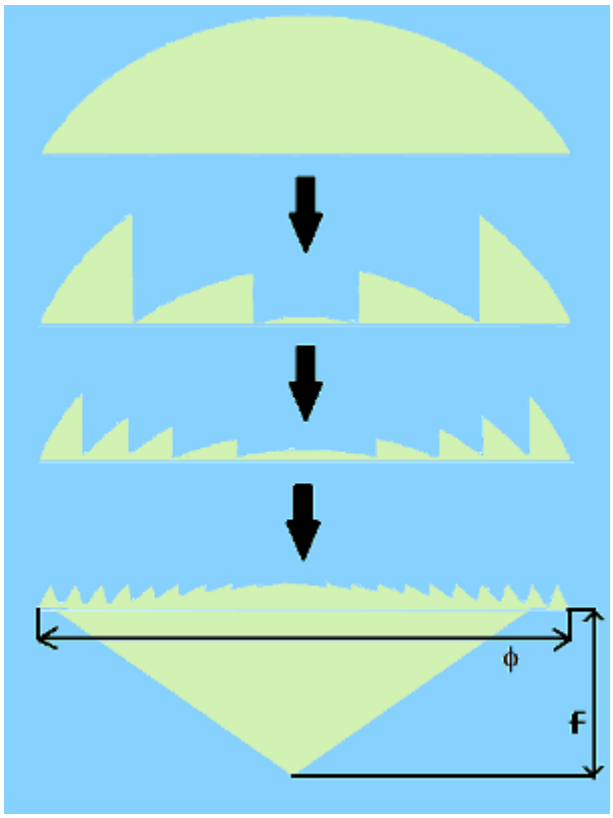


Figure 3: Working principle of freslen lens



SIZE	39H X 28W
POWER EST.	9.2
BEAM	SPOT
BEAM SIZE	4 INCH (2.7" OUTER AREA 900 F)
FOCAL LENGTH	29 INCHES
MAX TEMP. CLIMB	1950 F IR THERMOMETER
MAX TEMPERATURE	2107F
MATERIALS TESTED	
ZINC	MELTS 14 GRAMS - 10 SEC.
GLASS	MELTS 1" GLASS 15 SEC.
CONCRETE	GLOW 15 SEC.MELT 29 SEC.

Figure 4: Specification of Freslen lens used for the experiment

4. RESULT

After conducting several experiments and attempts it is observed that lunar regolith simulant was successfully melted with Fresnel lens (see fig 30). There are some factors caused variations in temperature affecting melting time such as intensity of sunlight and lens inclination angle. The average angle is 45-60 decrees in front of sunlight. However, it is necessary to have proper adjustments to achieve optimum temperature to melt regolith in less time (see table 4).

Regolith simulant (JSC-1)	**Melting Time**
5 grams (approx.)	10-15 seconds
50 grams (approx.)	30-45 seconds
100 grams (approx.)	60 seconds

Table 4: Time variation melting regolith



Figure 3: (a) Initial phase of melting regolith simulant, (b) object after solidified.

5. DISCUSSION

The fundamental goal was to melt regolith in order to print substantial structures. With a specific end goal to warm the regolith enough to stick together and transform into a strong shape, it should be sintered at every layer of material that is laid. Due to the propensity of regolith soil, it can be hard to control utilizing in 3D printer head. So based on some assumptions and previous experiments, it is observed that the experiment can be re-framed with an on-interest fabrication technique to make specially designed framework. For the new study, it is important to bolster the basic simulant powder on a moving bed of a 3D printer, heating the material to high temperatures by focusing freslen lens, utilizing beam energy and printing out in millimeter scale of layers to frame little irregular shapes with no particular



Figure 6: Printed objects with freslen lens

interruptions. The structures that left on the printer bed spoke the truth as hard as it ran like the melting wax candle. The regolith was a great deal when no other substances or the dissolvable were not applied, but distinctive proportion of regolith is utilized and warmed at somewhat shifting temperatures for fluctuation of time. The sintered regolith has delivered an expected but surprising result as it left some objects (see fig.) on the printing bed.

According NASA KSC, an experiment done on regolith polymer. A sunlight based concentrator with a 1 m 2 gathering territory has been developed for field testing at KSC. The sunlight based concentrator comprises of a huge Fresnel lens mounted on an edge that permits the lens to move and take after the sun. The point of convergence of the lens is guided descending toward take into account reinstating over a surface. The most noteworthy measured temperature created by the sunlight based concentrator has been 1350°C, higher than is important to liquefy JSC-1A lunar simulant. Sun based sintering is a promising method since it gets its energy from the sun (1380 W/m), can be lightweight, is modest and is a moderately straightforward innovation. (Mueller, 2015). The last picked proportion was 25% polystyrene polymer to 75 % regolith simulant. A 30g block of this

powder was totally liquefied and solidified in a stove at 250°C in around 30-45 minutes, importance around 1-1.5min/g. In expansion to the polystyrene powder utilized as a part of the blend, powder was produced using Styrofoam compartments that were utilized as a manageability exertion.

According to recent research done at NASA Kennedy Space Centre, there are possibilities to stabilize regolith by mixing with other granules such as sulfur, fusible alloy which can reduce the required temperature. White cement is made from raw materials such as Fe, Mn, Cr and Ti, high-grade limestone and MnO, TiO which is identical in mixture as regolith simulant (JSC-1)

Experiments	Conditions	Outcomes and cost
WSU	Applied laser (50W) but requires high technological process to melt regolith mixture	Takes several hours and need maintenance of electrical and electronic equipment. Hazardous equipment such as laser device are involved. Very expensive experiment
Planetary Geosciences Institute, University of Tennessee	Microwave sintering (2.4 Ghz) Temperature 1750°C	Hazardous equipment and electronic devices involved, requires high temperature
Current Experiment with freslen lens	Applied Freslen lens (41 inches length x 31 inches height)	Melted in regolith in less temperature (1100 °C) Low cost and easy to operate

Table 5: Comparison of current and previous experiments

6. APPLICATION

The general is objective is to add substance for the development of regolith but Space is an unpleasant place for people where they must be shielded from nature for better protection. The assurance is required from electromagnetic space radiation, vast temperature swings and exceptionally wide temperature range, dust particles, vacuum, parting force plant radiation, impact of ejection from rocket at take-off or landing, and even moonquake. This concludes that planetary surface needs to be securely accommodated at whatever point space investigation missions will plan to last considerably for long duration.

There have been various late papers portraying and indexing dust issues among the Apollo missions that relate to human safety and operations. Dust ejection from a rocket crest can influence perceive ability amid landing, dissolve close-by covered surfaces and get into mechanical congregations close to the arrival site. Features taken amid arriving of later Apollo missions, show regolith disintegration on the arrival procedure and space explorers have seen a lot of regolith scattering on takeoff and landing of the Apollo 12 arrival, perceive ability of the nearby geography was obscured to the point that worry the lander could have touched down on a rock or pit. Dust disintegration amid landing can bring about harm to adjacent base, as demonstrated by the recuperation of Surveyor 3 lander parts. The Apollo 12 lander handled 183 m far from the robot lander. There was impressive dust gathering on the specialty and confirmation of sandblasting and setting, as a consequence of dust ejecta amid arriving, on the returned tubing and optics.

Dust transport has been brought on by other human exercises other than the dispatch and landing. There have been reports of dust being kicked up by the rovers. At the point when riding the Lunar Roving Vehicle with a harmed fender, dust was kicked up so seriously that it instantly started to influence the space suits. Dust was additionally watched around the lower legs of the space travelers subsequent to strolling. The dust is to a great degree relentless and holds fast to all surfaces. Dust brought on some intense safety issues for the space travelers. Instances of eye, nose and sinus aggravation were accounted for a few missions. The dust made it into the group modules and brought on issues with space suits and seals, and different instruments. Zippers, connectors and protective caps all accomplished some level of dust-brought about glitch.

7. CONCLUSION

Since regolith is broadly accessible in any area on lunar surface, there are additionally encouraging physical applications for this innovation. The worldwide approach for research has involves the trillions of US dollars investment per annum. However, the real integration of the modern and advance additive technologies into commercial and space production is essentially a matter of further research. It is predicted by some additive manufacturing advocates that this technological development will change the nature of space exploration. Predictions for the future of commercial manufacturing depends upon feasibilities and availabilities of resources. Modern 3D printers are capable of providing output with different colour and multiple materials. It will continue to improve up to a certain to a point where functional products made by *IN-SITU* resources could be delivered with the effects on energy use, waste reduction, and customization. Future lunar missions are thought to be similar in capacity and degree to the late Apollo missions. Instead of the vast pressurized roving vehicles and perpetual base imagined under the interplanetary program, this paper assume sortie missions with an

unassuming increment in landing mass and surface length of time contrasted with the late Apollo missions. Rather than past lunar living space outlines, for occurrence the Lunar Stay Time Extension Module, this framework is intended to drastically increment experimental abilities with a humble increment in Apollo system outlines. There is an expectation for intensifying better technology in future space exploration. Arising 3D printing technology is not confined to Earth but it has opened another corridor for Space. Many space organizations like NASA, ESA and Private Companies are involved developing new concepts of 3D printing techniques into the final frontier. By carrying out analysis and testing, the lab scale is the evidence that the research work has demonstrated that the idea of 3D Additive Construction utilizing *IN-SITU* resource is attainable. Finally, the use of *IN-SITU* resources with the help of the most advanced technology still needs to be studied. The composition of the base material plays a minor role in the working principles of the additive manufacturing process is under evaluation.

REFERENCES

1. *McKay, D. S. et al. in* Lunar Sourcebook *(eds Heiken, G., Vaniman, D. & French, B.) (Cambridge Univ. Press, 1991).*

2. Bowell, E.L.G. "Surface of the Moon." The Earth and Its Satellite, ed. John Guest, New York, pp. 100-111, 1971.

3. *Ceccanti F, D. E. 3D Printing technology for a Moon outpost exploiting lunar soil. International Astronautical Federation, (2010).*

4. Dhingra, D. Copernicus crater: compelling science exploration target waiting for future missions. Annual Meeting of the Lunar Exploration Analysis Group. (2014).

5. Giovanni , C. Building components for an outpost on the Lunar soil by means of a novel 3D printing technology. Acta Astronautica. (2014).

6. Kennedy, J. K., Toups, L. D., & Rudisill, M. Constellation Architecture Team-Lunar Scenario 12.0. NASA Johnson Space Center, (2010).

7. Mackay, D. S. Minerological and chemical properities of Lunar regolith. NASA Johnson Space Center. Houston, Texas.(1989).

8. Montes, C. Evaluation of lunar regolith geopolymer binder as a radioactive shielding material for space exploration applications. Elsevier. (2015).

9. Schreiner, S. S. An overnight habitat for expanding lunar surface exploration. Acta Astronautica. (2015).

10. Stern, A. Where the Lunar Winds Blow Free. Astronomy, (1993).

11. *Taylor, J. G. The Environment at the Lunar Surface." , ed. D. W. Ming and D. L. Henninger,Madison, WI,. Lunar Base Agriculture: Soils for Plant Growth,(1989).*

12. *Balla, V. K., Roberson, L. B., O'Connor, G. W., Trigwell, S., Bose, S., and Bandyopadhyay, A. (2012) "First demonstration on direct laser fabrication of lunar regolith parts." Rapid Prototyping J., 18 (6), 451-457.*

13. Ramachandran, N. A. Gale, Space colonisation, Aerosp. Am. 46 (12) (2008).

14. Woodcock, G.R. Re-thinking Human Space Exploration, AIAA Space 2009 Conference and Exposition, Pasadena, CA (United States), September, (2009).

15. Raval S., Exploration colonization resource extraction and utilization of Moon and Mars (ECROMM), in: Proceedings of the 62nd International Astronautical Congress IAC, Cape Town (South Africa) (2011).

16. Burelle, A. Mining the Moon: a first step in harnessing extraterrestrial resources, in: Proceedings of the 61th International Astronautical Congress IAC 2010, Prague, Czech Republic, October (2010).

17. H.L. Litaker Jr., R.D. Archer, R. Szabo, E.S. Twyford, C.S. Conlee, R.L. Howard, Human habitation field study of the Habitat Demonstration Unit (HDU), Acta Astronautica (2013).

18. B. Sherwood, Decadal opportunities for space architects, Acta. Astronaut.(2012).

19. Zeolite Crystal Growth, NASA website article, (2014).

20. E.Roeder, Use of Lunar Materials in space Construction, Space Solar Power Review,(1981)

21. Temperature in Space, NASA Website Journal Article, (2004).

22. Kenneth G. Cooper I, James E. Good, Layered Metals Fabrication Technology Development for Support of Lunar Exploration, NASA Marshal Space flight Centre, (2014).

23. Hammond, MS., Good, J.S., Gilley, S.D., and Howard, R.W., "Developing Fabrication Technologies to Provide On-Demand Manufacturing for Exploration of the Moon and Mars," 44'" AIAA Aerospace Sciences Meeting and Exhibit, Reno, NV, (2006).

24. Lindhe, U., Harrysson, O., "Rapid Manufacturing with Electron Beam Melting (EBM) - A Manufacturing Revolution?" Society of Manufacturing Engineers Technical Paper, August (2003).

25. Bodiford, M.P., Gilley, S.D., Howard, R.W., Kennedy, J.P., Ray, J.A., "Are We There Yet? Developing In Situ Fabrication and Repair (ISFR) Technologies to Explore and Live on the Moon and Mars" IS' Space Exploration Conference: Continuing the Voyager of Discovery, Orlando, Florida, (2005).

26. Cooper, K.G., "Extending Rapid Prototyping Past the Horizon: Applications in Outer Space", Society of Manufacturing Engineers Technical Paper, (2002).
Cooper, K.G., "Microgravity Manufacturing Via Rapid Prototyping Techniques", Georgia

27. Tech Rapid Prototyping and Manufacturing Symposium, (2001).

28. NASA Turns to 3D Printing for Self-Building Spacecraft, J. Hsu, Space.Com September, (2012).

29. Gholipour, B. 3D Printing on Mars Could Be Key for Martian Colony, Space.com, (2013).

30. J. Billingham, W. Gilbreath, and B. O'Leary, eds., Space Resources and Space Settlements, NASA SP 428, NASA Ames Research Center, Houston, (1979).

31. Hintze, P. E. Lunar Surface Stabilization via Sintering or the use of Heat. 47th AIAA Aerospace Sciences Meeting Including The New Horizons Forum and Aerospace Exposition. (2009).

32. Mueller, R. P. Additive Construction using Basalt Regolith Fines. Kennedy Space Centre. (2015).

esa

→1st Symposium on Space Educational Activities